

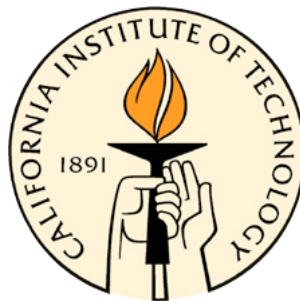
FORAYS INTO THE SYNTHESIS OF ZOANTHENOL: INTRIGUING PATTERNS IN  
REACTIVITY AND SELECTIVITY

Thesis by

Jennifer L. Stockdill

In Partial Fulfillment of the Requirements for the Degree of

Doctor of Philosophy



California Institute of Technology

Pasadena, CA

2009

(Defended 5 December 2008)

© 2009

Jennifer L. Stockdill

All Rights Reserved

## DEDICATION

*To my parents, Dave and Lucy Stockdill,  
who have sacrificed so much for me.*

*To my sister and brother,  
Teresa Barth and Jon Stockdill,  
who have been role models to me all of my life.*

*To my eighth grade science teacher,  
Mary Alice Robinson,  
who sparked a passion that has not died.*

*Finally, to my nieces and nephews,  
Hudson Barth, Deirdre Stockdill,  
Landen Barth, Jonah Stockdill, and Zoe Barth,  
who have provided the extra motivation to finish my Ph.D.*

## ACKNOWLEDGEMENTS

...It is impossible to start....

It cannot be argued with that the most influential person in my graduate career has been my advisor, Brian M. Stoltz. Brian's passion, guidance, and discipline have been indispensable to my growth as a scientist and as a person over these past five and a half years. I am especially grateful to Brian for his devotion to his students' education and success. I have not heard of another professor who goes so far out of his/her way to make sure students are prepared for whatever the next step in their journeys may be. Also, Brian introduced me to my best friend EVER, TLC. After all, it is the fastest, cheapest, easiest way to obtain meaningful information about what's going on in your reaction flask!

I am especially indebted to my thesis committee members, who have been simply unreal. Dennis Dougherty, my committee chair, has done a surprising job of keeping Harry in line, not to mention the insights he has provided in discussing my ideas and the depth to which he forces me to think. Harry Gray has been a constant source of support that has proven to be truly invaluable over the past two years when life has seemed so overwhelming. Bob Grubbs, the most recent addition to my committee has been asking me regularly how my research is going for years (I always regret not having a more cheerful reply, but the inquiries have meant a lot to me), and he always remembers to tell me when he's going climbing and I have to stay in lab! In all seriousness, all of my committee members have been very gracious and generous with their time, ideas, and recommendation letters. Thank you so much to all of them.

I have had the great pleasure of working on my project with Dr. Doug Behenna and Dr. Andy McClory. Doug was the single most influential person on my development as a

bench chemist. He taught me everything from what a TBS group is, to how to run a column, to the true meaning of scale-up. His hard work and friendship over the past years have been critical. I am grateful to Andy for helping me to learn that there is more than one way to approach a problem. He is a brilliant scientist, and I am sure he will be an amazing professor.

The various members of the Stoltz group have provided a diverse, if occasionally tumultuous, environment that has not only shaped me as a chemist, but also as a person. Through all of the ups and downs of the 72+ hours/week that we spend together, I wouldn't replace *any* of the people I have had the opportunity to work with in the lab. The early lab members were instrumental to me in learning techniques and in how to think about chemistry. I am especially grateful to Eric Ashley, Eric Ferreira, Doug Behenna, and Raissa Trend for their advice in my early years. Toward the middle and through the end of my graduate career, I had the great fortune of becoming close friends with Dave Ebner and Ryan McFadden, who were both willing to talk endlessly with me about my chemistry and who always tried the ideas that I suggested for their work. They, of course, have both ditched me, and I miss them dearly. (Congratulations to RMAC on the birth of his son, Nathan!! And Dave...you can't escape! I'll be in NYC soon.) I am more and more grateful to Dan Daspi every day as I write my thesis. Dan is so thoughtful in always trying to make the annoying parts of lab life run more smoothly. He has created a macro for everything you might need to do with a spectrum, and I think I'd still be trying to figure out how to get the things into my thesis right now if it weren't for him. My classmates are an awesome crew. I'm grateful to JT, who is a fountain of info from what's the deal with my NMR or the pKa of chemical X to what's the last step of the Rubik's cube algorithm. (Congratulations to JT on the birth of his daughter, Marie!!) Mike Krout always has what I'm looking for, whether it be a reagent or a procedure, and his generosity with both is appreciated. Also, I've always been grateful to

him for being so nice during group sports...I suck at most of them, and he is always patient. Mike Meyer has been a great friend over the years, and he will always hold a special place in my heart. Which brings me to Jenny Roizen...Jenny, I'll put your part at the end. The fou...fifth years are an eclectic bunch, that I have loved having around for the past four years. Nat Sherden has always been good to me, from bringing my mail in that ended up at his house to walking out of his way to walk me home when it's late at night, to apologizing when *I* have done something wrong, his kindness is overwhelming. Also, the emails...I *love* the emails. I hope I don't get taken off the group list right away because I will miss the misspelled sarcasm-rich frustrations. John Enquist is one of the most dedicated people I've known. It has been fun trying to break through his wall of seriousness (the trick is mint-chip ice cream!), and his dry sense of humor really gets me laughing sometimes. I have really enjoyed Kevin Allan's company as a baymate (briefly) and on years of coffee runs. I will always cherish the memory of late night flash columns listening to Ok Go, and I really admire his enthusiasm in the lab. Also, thanks for the cookie. Sandy Ma is one of the more unusual (in a good way) characters I've met. (DOGGIE!) She always makes me laugh and has the most quotable quotes. Brinton Anna Seashore-Ludlow was a fun baymate and is a great friend. I have missed her often since she moved to Sweeden. I've enjoyed getting to know Pam Tadross better over the past 9 months or so, and I'm sad that it took so long. She is a really thoughtful person and devoted friend. Chris Gilmore has always cracked me up. He's a great person to talk about life with, and lately I've enjoyed talking Obama with him as well. It's been awesome to have Hosea in the lab. He has such a different perspective from the status-quo, it's always fun to see what he thinks. I've really enjoyed Narae's company over the past few years. She is a genuine and sweet person, and I've grown to expect her in lab on Saturday over the past 6 months. I always thought she was joking when she said her hobby was sleeping, but she seems to be in lab the rest of the time! :P I've grown to

really enjoy having Allen Hong in 264, and it will be really sad to say goodbye. I'm thankful for all the candy and especially for his concern...he always wants to know how you're doing when he asks. Of course, I'll miss my secret admirer, aka Hahvard, aka Matt Winston. Matt has been a great cheerleader in my thesis effort and his support is really appreciated. Also, he cheers Jenny up, which cheers me up! The first years in the group are a hilarious bunch, and I regret that I won't have the opportunity to get to know them better. Nathan Bennett, my newest baymate, always has something nice to say, and he is very encouraging, even to himself... "Alright, self..." Jonny Gordon is just too cool for school (but he comes anyway). I dig the purple sweatband and the blue glasses. Alex Goldberg is our newest member, and he seems to share my sarcastic sense of humor. Finally, there are the postdocs. There have been many...I'm especially grateful to Amanda Jones, who has been a really good friend, and is always a pleasure to have in lab, but most importantly, hosts the poker night (no boss allowed!). Jan Streuff has been a fun companion over the past year, and I will miss him when he goes back to Deutschland. Also, Corinne Baumgartner has been a fun exercise buddy, and Christian Defieber always tried to speak German with me. If it weren't for Nolan McDougal, I would not be able to say that I've walked from campus to Roscoe's, or worse, I might not know how to properly eat bread at a nice dinner! I'm grateful to him for the fun memories and for introducing me to scallops. I mentioned Andy McClory briefly, but I need to mention here that he is one of the more loyal friends a person could ask for, and I really enjoyed his friendship. A recent addition to the lab, Chris Henry, has fast become one of my closest friends, and I am very thankful to have met him. Thanks also to Xiaoqing Han (X-Dog), Andy Harned, Haiming Zhang, and Kousuke Tani for their kindness and advice.

I need to make a separate paragraph here for my baymates. Eric Ashley was my first baymate, and I am ever grateful to him for all that he taught me those first few years.

Also, I wouldn't know important things like "what ever happened to a good old fashioned passionate \*%&-whuppin', getting your shoes, coat and your hat tooaken." Brinton Seashore-Ludlow is one of those people that you just love right away. We had lots of fun hiking and going to yoga, and of course running collumm-collummns!! Enough cannot be said about Thomas Jensen, who among other things was the first baymate I had who liked *all* the same music as me. We had a blast jammin' in the lab and talking chemistry. Not to mention playing 10:1 with Dave!

I would like to thank Thomas Jensen, Dave Ebner, Chris Henry, and Brian Stoltz for proofreading *all* of my thesis. Amanda Jones, Doug Behenna, Kevin Allan, Jenny Roizen also edited chapters. Jenny, thanks for doing it at the last minute with no notice. I am especially grateful to Chris Henry for his help with numbering compounds and to Dave Ebner for making my table of contents and list of figures. Dave is also the only person who proofread my whole thesis twice (or was it three times?). He must be really bored over in New Jersey waiting to start his postdoc! ;) Thank you all so much. This document would be a mess without you.

In addition to the outstanding members of the Stoltz group, I have been warmly welcomed by the Grubbs, Bercaw, Gray, Dougherty, and Reisman labs. To thank each of the people in these groups would be overwhelming, but they are all truly appreciated, and I look forward to seeing them in the future.

Amazingly, I managed to meet some people outside of the department, and it turns out that many of them have been among my most critical and constant supporters. I would not be the same person without the friendships of Justin Bois, Raviv Perahia, Hernan Garcia, Tristan Smith, Anna Folinsky, Erin Koos, Nhat Vu, Nate Bode, Vikram Deshpande, Eric Peterson, Lucia Cordiero, Heidi Privett, Crystal Shih, Jeff Byers, Steve Baldwin, Dan Grin and Harmony Gates. You guys have all been truly amazing friends, and I am so thankful for all the times you've scraped me off the ground and reassembled

me into a human again. My move to the West Coast would not have been conceived of without Joe Polidan, and my last year of college would have definitely not been as fabulous without Sheila (a.k.a. Pony 2) Gradwell. Boo Shan Tseng and Hari Shroff were indispensable companions in Argentina/Chile. Likewise, Mike Olsen was a blast to have along in Costa Rica. It was a pleasure spending two weeks with each of them in paradise.

Those memories bring me to Tristan Ursell, who was my companion for three of the most challenging, yet adventure-packed years of grad school. Tristan remains one of my closest friends, and I cannot thank him enough for everything that we shared. I will always treasure our many memories in some of the most beautiful places in the world. Tristan also helped me to learn a lot about myself and ultimately led me in the direction of actually paying attention to what's happening in the world. He taught me to look deeper into myself and to become the person I wanted to be instead of wishing things were different.

I've put this off for awhile now, but it comes time to try to thank Jenny Roizen. There aren't words to express my gratitude to Jenny. For the first three years of grad school, Jenny was my roommate, labmate, and friend. We did everything together. I could not possibly have gotten through some of the rougher times of the past five and a half years without Jenny's constant love and support. I have grown to really appreciate her direct candor with me about everything. To put it briefly, Jenny rocks. I'm so sad to be leaving her in the lab without me. I know that she will get through everything fine, but I wish I could be here to support her, as she has so devotedly supported me over this thesis journey.

Most people are lucky to have one friend as constant and close to their heart as Jenny is to mine. I have had the great fortune during my graduate career of having developed two such friends. Professor Dr. Jen Dionne has become a critical appendage over the years. To lose her would be like losing an arm. I am left frustrated again with the

English language for not having the appropriate words to match the quality and magnitude of Jen's friendship. She has become like a twin sister to me, which is exciting because I never had a twin sister! I will just say to both Jen and Jenny, I love you. You are irreplaceable.

Finally, to thank the people who shaped me into who I am. Becky (Doyal) Orrock and Aimee (Dudash) Ketner have been my best friends since I can remember, and it has been awesome watching each other grow from little girls ogling at cute boys at the beach to grown women, ogling at cute boys at the beach. ☺ Sally, I am glad you moved to Virginia. It's been nice having some extended family nearby, and I always enjoy our phone calls, surprisingly also often relating to ogling at boys at the beach! Grandma Stockdill, it has been fabulous visiting with you more often over the past ten years. I'm glad you were persistent about calling. Your support has been treasured. Grandma Vorlicek, I wish I could see you more, but I wanted to take this chance to thank you for working so hard to keep the family together over the years. I know it was challenging raising 8 kids as a single mom, and I'm amazed that you managed to do it so successfully. Teresa and Jon, thanks for all that you have done for me over the years. I have always looked up to you, and I continue to be awed by your talents as you raise your families. You have the 5 coolest kids in the world. I can't wait to be back with you and with them. Mom and Dad, I love you both and I wish you all the happiness and adventure that you have ensured that I had the opportunity to experience. You have all contributed irreversibly to the person I have become. I cannot thank you enough.

## ABSTRACT

The zoanthamine family of alkaloids has attracted the attention of synthetic chemists for over two decades, beginning with the first report of their isolation in 1984. Not only are these stereochemically dense polycyclic compounds structurally fascinating, but they also display interesting and important biological activities. Foremost among these is the potent anti-osteoporotic effect of norzoanthamine. To date, norzoanthamine remains the only member to have succumbed to total synthesis, by Miyashita and coworkers in 2004. Our studies began by targeting zoanthenol, a structurally similar natural product that possesses the key stereochemical challenges of norzoanthamine, while offering unique opportunities for strategic development as compared to the other family members.

The synthetic work described herein focuses on approaches to the tricyclic core of zoanthenol, specifically employing an approach by which the stereochemical complexity of the C ring, marked by the challenging vicinal all-carbon quaternary centers, is addressed early in the synthesis. These functionalized C ring synthons are then tethered to an aromatic A ring synthon, and methods to form the final bond of the B ring are explored. Special attention is given to the acid-mediated Friedel-Crafts cyclization approach. In addition to the acid-mediated cyclization approach, an alternative cyclization method is discussed wherein the A ring is substituted with a halogen in order to enable generation of a radical. This radical then undergoes a 1,4-addition into a fully substituted enone to close the B ring and provide the desired stereochemistry both of the two new stereocenters that are generated in the cyclization.

In these efforts, we have learned a great deal about the factors governing selectivity and reactivity in these systems. For each case, stereochemical models are discussed and key structural requirements for future investigations are outlined.

## PROLOGUE

### The Importance of Natural Products Synthesis

This prologue is primarily for the benefit of readers outside of the field of chemistry, who may not be familiar with the nuances of the field of total synthesis, and thus, the impact of the research described in this thesis.

Natural products are complex molecules that have been isolated from a natural source, such as a tree bark, a fungus, a bacterial species, or even a marine creature. The study of natural products synthesis is essential to the advancement of organic chemistry, as well as to society as a whole. A natural product synthesis involves looking at a structure that has been isolated from nature, and then finding a way to make it from much smaller starting materials. As such, it is an ideal platform for the discovery of new reactions because every natural product presents a unique array of bonds that have likely not been made before. In order to make some of these bonds, new chemistry must be invented. These new reactions are typically applied to related molecules of varying levels of complexity, leading to the development of a new reaction methodology. Thus, total synthesis fuels the discovery of new methodology, while new methodology simultaneously allows for the completion of total syntheses.

The broader impact of these studies is realized largely through the pharmaceutical industry. Although pharmaceutical companies invest a great deal of time and money into their own research programs, they are generally very focused on a specific goal such as finding a drug for breast cancer. This is a large enough problem on its own that the company cannot invest their own man-hours into synthesizing natural products from scratch. Thus, they turn to academic groups for key information about what bonds were the most challenging to make and what disconnections lead to the shortest and most modular synthesis of a compound. Short syntheses are important to pharmaceutical

companies because even if every step of a 30-step synthesis of a compound proceeds with 90% yield (this is not typical), the overall yield for the process is  $(.9)^{30}$  or 4%. If the company is going to conduct testing on the compound, they cannot afford to waste 96% of their original materials. Thus, it is important for academic groups to discover as many different types of reactions and ways to disconnect natural products as possible. It is also important to have a modular synthesis, so that analog compounds can be made and tested. In many cases, the best pharmaceutical agents are modified versions of natural products. Natural products offer the great advantage of having already been compatible with at least one living system, the one from which they were isolated. If that creature was able to survive with this compound inside it, it is more likely that a human will be able to tolerate the compound than for a molecule that has been 100% designed. Some important drugs that are natural products or derivatives include the antibiotics penicillin and vancomycin, contraceptives (+)-norgestrel and  $17\alpha$ -ethynylestradiol, the anti-inflammatory agent indomethacin, and the ovarian, breast, and small lung cancer drug paclitaxel (taxol).

The research presented herein centers around the synthesis of a marine alkaloid, zoanthenol, isolated off the coast of the Canary Islands from polyps of the genus *Zoanthus*. A number of very similar compounds were also isolated from the zoanthids, and they comprise a family of natural products called the zoanthamines. As a family, the zoanthamines offer a range of biological activities including inhibition of inflammation in mouse ears, cytotoxicity against murine leukemia cells, broad-spectrum antibacterial activity, and activity against human platelet aggregation. Perhaps the most exciting biological activity is the excellent anti-osteoporotic activity demonstrated by norzoanthamine. In ovariectomized mice, a good model for post-menopausal osteoporosis, treatment with norzoanthamine hydrochloride prevented the loss of bone mass and strength. Additionally, bone strength can be restored in ovariectomized mice

by treatment with norzoanthamine hydrochloride without any observed uterine atrophy, a side effect of treatment with  $17\beta$ -estradiol, the current standard in this type of therapy. This difference points to the possibility of a different mechanism of action than estrogen therapy, making the zoanthamines an important family of natural products to target for synthesis.

# TABLE OF CONTENTS

Dedication.....	iii
Acknowledgements .....	ix
Abstract.....	xi
Prologue .....	xii
Table of Contents.....	xv
List of Figures .....	xx
List of Schemes.....	xxxiii
List of Tables.....	xl
List of Abbreviations .....	xliii
CHAPTER 1: THE BIOLOGY AND CHEMISTRY OF THE ZOANTHAMINE ALKALOIDS.....	1
1.1.1 Introduction .....	1
1.2 The Zoanthamine Natural Products.....	3
1.2.1 Isolation and Structural Characterization of the Zoanthamine Natural Products.....	3
1.2.2 Biosynthesis of the Zoanthamine Natural Products.....	6
1.2.3 Reactivity Studies of Norzoanthamine.....	11
1.3 Biological Activities of Zoanthamine Alkaloids .....	13
1.3.1 Anti-Osteoporotic Activity .....	13
1.3.2 Miscellaneous Biological Activities.....	15
1.4 Synthetic Approaches Toward the Zoanthamine Natural Products.....	17
1.4.1 General Remarks .....	17
1.4.2 Miyashita's Synthesis of Norzoanthamine.....	18
1.4.3 Tanner's Diels-Alder Approach to the Zoanthamine ABC Ring System.....	22

1.4.4	Uemura's Approach to the Norzoanthamine ABC Ring System.....	28
1.4.5	Williams's Approach to the Norzoanthamine AB and EFG Ring Systems .....	28
1.4.6	Theodorakis's Annulation Approach to the Norzoanthamine ABC Ring System.....	31
1.4.7	Kobayashi's Synthesis of the Heterocyclic CDEFG Zoanthamine Ring System.....	33
1.4.8	Hirama's Strategy for the Zoanthenol ABC Ring System.....	34
1.5.1	Summary and Outlook .....	38
	<i>References</i> .....	40
	CHAPTER 2: EARLY EFFORTS TOWARD THE SYNTHESIS OF ZOANTHENOL.....	43
2.1.1	Introduction and Retrosynthetic Analysis .....	43
2.2.1	Synthesis of the A Ring Synthon.....	45
2.2.2	Synthesis of the C Ring Synthon.....	45
2.2.3	Synthesis of the Tricyclic Core of Zoanthenol.....	47
2.3.1	Enantioselective Synthesis of the DEFG Synthon .....	53
2.4.1	Summary of Early Synthetic Work .....	55
2.5.1	Materials and Methods.....	56
2.5.2	Preparation of Compounds .....	58
	<i>References</i> .....	85
	<i>Synthetic Summary</i> .....	89
	APPENDIX A: SPECTRA AND X-RAY CRYSTALLOGRAPHIC DATA: EARLY EFFORTS TOWARD THE SYNTHESIS OF ZOANTHENOL .....	92
	CHAPTER 3: ACID-MEDIATED CYCLIZATION APPROACHES TO THE DENSELY SUBSTITUTED CARBOCYCLIC CORE OF ZOANTHENOL.....	181

3.1.1	Revised Retrosynthetic Analysis.....	182
3.2	Toward a Vicinal Quaternary Center-Containing C Ring Synthon .....	182
3.2.1	Synthesis and Desymmetrization of a <i>meso</i> -Anhydride .....	182
3.2.2	Elaboration of the Half-Ester.....	186
3.3.1	Toward a Lactone-Derived C Ring Synthon .....	187
3.3.2	Acid-Mediated Cyclizations of Lactone-Derived A–C Ring Systems .....	188
3.4.1	Functionalization of Allylic Alcohol <b>248</b> .....	190
3.5.1	Toward a 7-Membered Acetal-Derived C Ring.....	191
3.5.2	Acid-Mediated Cyclization of the 7-Membered Acetal Substrate.....	193
3.6.1	Synthesis of a Homologated C Ring Synthon .....	194
3.6.2	Acid-Mediated Cyclizations of the Homologated A–C Ring System.....	195
3.7.1	Modification of the Homologated A–C Ring System .....	196
3.7.2	Acid-Mediated Cyclizations of Carboxylic Acid-Derived A–C Ring Systems .....	196
3.8.1	Mechanistic Hypotheses.....	197
3.8.2	Mechanistic Summary and Substrate Requirements.....	201
3.9.1	Summary of Brønsted Acid Cyclization Efforts .....	202
3.10.1	Materials and Methods.....	203
3.10.2	Preparation of Compounds .....	205
	References .....	240
	Summary Schemes .....	243

#### APPENDIX B: SPECTRA AND X-RAY CRYSTALLOGRAPHIC DATA: ACID-MEDIATED

##### CYCLIZATION APPROACHES TO THE DENSELY SUBSTITUTED CARBOCYCLIC

CORE OF ZOANTHENOL .....	248
--------------------------	-----

CHAPTER 4: RADICAL CYCLIZATION APPROACHES TOWARD THE TRICYCLIC CORE OF ZOANTHENOL .....	366
4.1.1 Introduction .....	366
4.2.1 Synthesis and Cyclization of a Lactone-Derived Precursor .....	368
4.3.1 Synthesis and Cyclization of a Homologated Nitrile-Derived Cyclization Precursor .....	370
4.4.1 Synthesis and Cyclization of a Homologated Ester-Derived Cyclization Precursor .....	371
4.5.1 Synthesis and Cyclization of a 7-Membered Acetal-Derived Cyclization Precursor .....	372
4.6.1 Substrate Requirements and Limits of System .....	373
4.7.1 Summary .....	376
4.8.1 Materials and Methods.....	377
4.8.2 Preparation of Compounds.....	378
References .....	389
Summary Schemes .....	390
 APPENDIX C: SPECTRA AND X-RAY CRYSTALLOGRAPHIC DATA: RADICAL CYCLIZATION APPROACHES TOWARD THE TRICYCLIC CORE OF ZOANTHENOL .....	 392
 APPENDIX D: CURRENT AND FUTURE INVESTIGATIONS TOWARD ZOANTHENOL .....	 417
D.1 Introduction .....	417
D.2 Proposed Methods for the Utilization of Tricycle <b>192</b> .....	417
D.3.1 Development and Cyclization of a 6-Membered Acetal-Derived A–C Ring System with Inverted C(10) Stereochemistry .....	419
D.3.2 Advancement of Cyclopentylidene-Derived C Ring Synthons for	

Acid-Mediated Cyclization .....	421
D.3.3 Advancement of Cyclopentylidene-Derived C Ring for Radical Cyclization .....	422
D.4.1 Alternative Approaches to the Tricyclic Core of Zoanthenol.....	423
D.4.2 Allylation/Diels-Alder Approach.....	424
D.4.3 $\alpha$ -Arylation Approach.....	427
D.5.1 Precedence for Planned Late-Stage Side Chain Couplings.....	429
D.5.2 Alkyne Addition into Enantiopure Lactam Synthons.....	430
D.5.3 Synthesis of a Horner-Wadsworth-Emmons Reagent for Side Chain Synthesis.....	431
D.6.1 Summary .....	431
D.7.1 Materials and Methods.....	432
D.7.2 Preparation of Compounds .....	433
<i>References</i> .....	454

#### APPENDIX E: SPECTRA AND X-RAY CRYSTALLOGRAPHIC DATA: CURRENT AND FUTURE

INVESTIGATIONS TOWARD ZOANTHENOL .....	456
Comprehensive Bibliography .....	509
Notebook Cross-references.....	518
About the Author.....	527

## LIST OF FIGURES

## CHAPTER 1

Figure 1.1.1	Representative zoanthids.....	1
Figure 1.1.2	Natural products isolated from zoanthids.....	3
Figure 1.2.1	Zoanthamine natural products isolated by Rao.....	4
Figure 1.2.2	Zoanthamine natural products isolated by Uemura and Clardy.....	5
Figure 1.2.3	Zoanthamine natural products isolated by Norte.....	6
Figure 1.3.1	IC <sub>50</sub> values for the inhibition of IL-6 production in Uemura's SAR study.....	15
Figure 1.3.2	IC <sub>50</sub> values for the inhibition of IL-6 dependent cell growth.....	15
Figure 1.4.1	Miyashita's retrosynthetic analysis of norzoanthamine.....	18
Figure 1.4.2	Tanner's retrosynthetic analysis of zoanthamine.....	22
Figure 1.4.3	Uemura's retrosynthetic analysis of norzoanthamine.....	28
Figure 1.4.4	Williams's retrosynthetic analysis of norzoanthamine.....	29
Figure 1.4.5	Theodorakis's retrosynthetic analysis of norzoanthamine.....	31
Figure 1.4.6	Hirama's retrosynthetic analysis of zoanthenol.....	34

## APPENDIX A

Figure A.1	<sup>1</sup> H NMR (300 MHz, CDCl <sub>3</sub> ) of compound <b>172</b> .....	93
Figure A.2	Infrared spectrum (thin film/NaCl) of compound <b>172</b> .....	94
Figure A.3	<sup>13</sup> C NMR (75 MHz, CDCl <sub>3</sub> ) of compound <b>172</b> .....	94
Figure A.4	<sup>1</sup> H NMR (300 MHz, CDCl <sub>3</sub> ) of compound <b>174</b> .....	95
Figure A.5	Infrared spectrum (thin film/NaCl) of compound <b>174</b> .....	96
Figure A.6	<sup>13</sup> C NMR (75 MHz, CDCl <sub>3</sub> ) of compound <b>174</b> .....	96

Figure A.7	$^1\text{H}$ NMR (300 MHz, $\text{CDCl}_3$ ) of compound <b>173</b> .....	97
Figure A.8	Infrared spectrum (thin film/ $\text{NaCl}$ ) of compound <b>173</b> .....	98
Figure A.9	$^{13}\text{C}$ NMR (75 MHz, $\text{CDCl}_3$ ) of compound <b>173</b> .....	98
Figure A.10	$^1\text{H}$ NMR (300 MHz, $\text{CDCl}_3$ ) of compound <b>175</b> .....	99
Figure A.11	Infrared spectrum (thin film/ $\text{NaCl}$ ) of compound <b>175</b> .....	100
Figure A.12	$^{13}\text{C}$ NMR (75 MHz, $\text{CDCl}_3$ ) of compound <b>175</b> .....	100
Figure A.13	$^1\text{H}$ NMR (300 MHz, $\text{CDCl}_3$ ) of compound <b>168</b> .....	101
Figure A.14	Infrared spectrum (thin film/ $\text{NaCl}$ ) of compound <b>168</b> .....	102
Figure A.15	$^{13}\text{C}$ NMR (75 MHz, $\text{CDCl}_3$ ) of compound <b>168</b> .....	102
Figure A.16	$^1\text{H}$ NMR (300 MHz, $\text{CDCl}_3$ ) of compound (+)- <b>177</b> .....	103
Figure A.17	Infrared spectrum (thin film/ $\text{NaCl}$ ) of compound (+)- <b>177</b> .....	104
Figure A.18	$^{13}\text{C}$ NMR (75 MHz, $\text{CDCl}_3$ ) of compound (+)- <b>177</b> .....	104
Figure A.19	$^1\text{H}$ NMR (300 MHz, $\text{CDCl}_3$ ) of compound (-)- <b>177</b> .....	105
Figure A.20	Infrared spectrum (thin film/ $\text{NaCl}$ ) of compound (-)- <b>177</b> .....	106
Figure A.21	$^{13}\text{C}$ NMR (75 MHz, $\text{CDCl}_3$ ) of compound (-)- <b>177</b> .....	106
Figure A.22	$^1\text{H}$ NMR (300 MHz, $\text{CDCl}_3$ ) of compound <b>178</b> .....	107
Figure A.23	Infrared spectrum (thin film/ $\text{NaCl}$ ) of compound <b>178</b> .....	108
Figure A.24	$^{13}\text{C}$ NMR (75 MHz, $\text{CDCl}_3$ ) of compound <b>178</b> .....	108
Figure A.25	$^1\text{H}$ NMR (300 MHz, $\text{CDCl}_3$ ) of compound <b>169</b> .....	109
Figure A.26	Infrared spectrum (thin film/ $\text{NaCl}$ ) of compound <b>169</b> .....	110
Figure A.27	$^{13}\text{C}$ NMR (75 MHz, $\text{CDCl}_3$ ) of compound <b>169</b> .....	110
Figure A.28	$^1\text{H}$ NMR (300 MHz, $\text{CDCl}_3$ ) of compound (-)- <b>170</b> .....	111
Figure A.29	Infrared spectrum (thin film/ $\text{NaCl}$ ) of compound (-)- <b>170</b> .....	112
Figure A.30	$^{13}\text{C}$ NMR (75 MHz, $\text{CDCl}_3$ ) of compound (-)- <b>170</b> .....	112
Figure A.31	$^1\text{H}$ NMR (300 MHz, $\text{CDCl}_3$ ) of compound (+)- <b>180</b> .....	113
Figure A.32	Infrared spectrum (thin film/ $\text{NaCl}$ ) of compound (+)- <b>180</b> .....	114

Figure A.33	$^{13}\text{C}$ NMR (75 MHz, $\text{CDCl}_3$ ) of compound (+)- <b>180</b> .....	114
Figure A.34	$^1\text{H}$ NMR (300 MHz, $\text{CDCl}_3$ ) of compound <b>183</b> .....	115
Figure A.35	Infrared spectrum (thin film/ $\text{NaCl}$ ) of compound <b>183</b> .....	116
Figure A.36	$^{13}\text{C}$ NMR (75 MHz, $\text{CDCl}_3$ ) of compound <b>183</b> .....	116
Figure A.37	$^1\text{H}$ NMR (300 MHz, $\text{CDCl}_3$ ) of compound <b>184</b> .....	117
Figure A.38	Infrared spectrum (thin film/ $\text{NaCl}$ ) of compound <b>184</b> .....	118
Figure A.39	$^{13}\text{C}$ NMR (75 MHz, $\text{CDCl}_3$ ) of compound <b>184</b> .....	118
Figure A.40	$^1\text{H}$ NMR (300 MHz, $\text{CDCl}_3$ ) of compound <b>187</b> .....	119
Figure A.41	Infrared spectrum (thin film/ $\text{NaCl}$ ) of compound <b>187</b> .....	120
Figure A.42	$^{13}\text{C}$ NMR (75 MHz, $\text{CD}_2\text{Cl}_2$ ) of compound <b>187</b> .....	120
Figure A.43	$^1\text{H}$ NMR (500 MHz, $\text{CDCl}_3$ ) of compound <b>188</b> .....	121
Figure A.44	Infrared spectrum (thin film/ $\text{NaCl}$ ) of compound <b>188</b> .....	122
Figure A.45	$^{13}\text{C}$ NMR (125 MHz, $\text{CDCl}_3$ ) of compound <b>188</b> .....	122
Figure A.46	$^1\text{H}$ NMR (300 MHz, $\text{CDCl}_3$ ) of compound <b>189</b> .....	123
Figure A.47	Infrared spectrum (thin film/ $\text{NaCl}$ ) of compound <b>189</b> .....	124
Figure A.48	$^{13}\text{C}$ NMR (75 MHz, $\text{CDCl}_3$ ) of compound <b>189</b> .....	124
Figure A.49	$^1\text{H}$ NMR (300 MHz, $\text{CDCl}_3$ ) of compound <b>191</b> .....	125
Figure A.50	Infrared spectrum (thin film/ $\text{NaCl}$ ) of compound <b>191</b> .....	126
Figure A.51	$^{13}\text{C}$ NMR (75 MHz, $\text{CDCl}_3$ ) of compound <b>191</b> .....	126
Figure A.52	$^1\text{H}$ NMR (300 MHz, $\text{CDCl}_3$ ) of compound <b>192</b> .....	127
Figure A.53	Infrared spectrum (thin film/ $\text{NaCl}$ ) of compound <b>192</b> .....	128
Figure A.54	$^{13}\text{C}$ NMR (75 MHz, $\text{CDCl}_3$ ) of compound <b>192</b> .....	128
Figure A.55	$^1\text{H}$ NMR (500 MHz, $\text{C}_6\text{D}_6$ ) of compound <b>193</b> .....	129
Figure A.56	Infrared spectrum (thin film/ $\text{NaCl}$ ) of compound <b>193</b> .....	130
Figure A.57	$^{13}\text{C}$ NMR (125 MHz, $\text{C}_6\text{D}_6$ ) of compound <b>193</b> .....	130
Figure A.58	$^1\text{H}$ NMR (500 MHz, $\text{CDCl}_3$ ) of compound <b>194</b> .....	131

Figure A.59	Infrared spectrum (thin film/NaCl) of compound <b>194</b> .....	132
Figure A.60	<sup>13</sup> C NMR (125 MHz, CDCl <sub>3</sub> ) of compound <b>194</b> .....	132
Figure A.61	<sup>1</sup> H NMR (500 MHz, CDCl <sub>3</sub> ) of compound <b>195</b> .....	133
Figure A.62	Infrared spectrum (thin film/NaCl) of compound <b>195</b> .....	134
Figure A.63	<sup>13</sup> C NMR (125 MHz, CDCl <sub>3</sub> ) of compound <b>195</b> .....	134
Figure A.64	<sup>1</sup> H NMR (500 MHz, CDCl <sub>3</sub> ) of compound <b>196</b> .....	135
Figure A.65	Infrared spectrum (thin film/NaCl) of compound <b>196</b> .....	136
Figure A.66	<sup>13</sup> C NMR (125 MHz, CDCl <sub>3</sub> ) of compound <b>196</b> .....	136
Figure A.67	<sup>1</sup> H NMR (300 MHz, CDCl <sub>3</sub> ) of compound (–)- <b>210</b> .....	137
Figure A.68	Infrared spectrum (thin film/NaCl) of compound (–)- <b>210</b> .....	138
Figure A.69	<sup>13</sup> C NMR (75 MHz, CDCl <sub>3</sub> ) of compound (–)- <b>210</b> .....	138
Figure A.70	<sup>1</sup> H NMR (300 MHz, CDCl <sub>3</sub> ) of compound (–)- <b>211</b> .....	139
Figure A.71	Infrared spectrum (thin film/NaCl) of compound (–)- <b>211</b> .....	140
Figure A.72	<sup>13</sup> C NMR (75 MHz, CDCl <sub>3</sub> ) of compound (–)- <b>211</b> .....	140
Figure A.73	<sup>1</sup> H NMR (300 MHz, CDCl <sub>3</sub> ) of compound (–)- <b>212</b> .....	141
Figure A.74	Infrared spectrum (thin film/NaCl) of compound (–)- <b>212</b> .....	142
Figure A.75	<sup>13</sup> C NMR (75 MHz, CDCl <sub>3</sub> ) of compound (–)- <b>212</b> .....	142
Figure A.76	<sup>1</sup> H NMR (300 MHz, CDCl <sub>3</sub> ) of compound <b>213</b> .....	143
Figure A.77	Infrared spectrum (thin film/NaCl) of compound (–)- <b>213</b> .....	144
Figure A.78	<sup>13</sup> C NMR (75 MHz, CDCl <sub>3</sub> ) of compound (–)- <b>213</b> .....	144
Figure A.79	<sup>1</sup> H NMR (300 MHz, CDCl <sub>3</sub> ) of compound <b>214</b> .....	145
Figure A.80	Infrared spectrum (thin film/NaCl) of compound <b>214</b> .....	146
Figure A.81	<sup>13</sup> C NMR (75 MHz, CDCl <sub>3</sub> ) of compound <b>214</b> .....	146
Figure A.82	<sup>1</sup> H NMR (300 MHz, CDCl <sub>3</sub> ) of compound <b>215</b> .....	147
Figure A.83	Infrared spectrum (thin film/NaCl) of compound <b>215</b> .....	148
Figure A.84	<sup>13</sup> C NMR (75 MHz, CDCl <sub>3</sub> ) of compound <b>215</b> .....	148

Figure A.85	$^1\text{H}$ NMR (300 MHz, $\text{CDCl}_3$ ) of compound <b>215a</b> .....	149
Figure A.86	Infrared spectrum (thin film/ $\text{NaCl}$ ) of compound <b>215a</b> .....	150
Figure A.87	$^{13}\text{C}$ NMR (75 MHz, $\text{CDCl}_3$ ) of compound <b>215a</b> .....	150
Figure A.88	$^1\text{H}$ NMR (300 MHz, $\text{CDCl}_3$ ) of compound <b>203</b> .....	151
Figure A.89	Infrared spectrum (thin film/ $\text{NaCl}$ ) of compound <b>203</b> .....	152
Figure A.90	$^{13}\text{C}$ NMR (75 MHz, $\text{CDCl}_3$ ) of compound <b>203</b> .....	152
Figure A.91	$^1\text{H}$ NMR (500 MHz, $\text{CDCl}_3$ ) of compound <b>168</b> .....	153
Figure A.92	Infrared spectrum (thin film/ $\text{NaCl}$ ) of compound <b>168</b> .....	154
Figure A.93	$^{13}\text{C}$ NMR (125 MHz, $\text{CDCl}_3$ ) of compound <b>168</b> .....	154
Figure A.94	Representation of Lactone <b>184</b> .....	155
Figure A.95	Representation of Acid <b>187</b> • $\text{CHCl}_3$ .....	164
Figure A.96	Representation of Diketone <b>196</b> .....	173
 CHAPTER 3		
Figure 3.2.1	Known <i>meso</i> -anhydride desymmetrization substrates .....	184
Figure 3.8.1	Requirements for future acid cyclization substrates.....	202
 APPENDIX B		
Figure B.1	$^1\text{H}$ NMR (500 MHz, $\text{CDCl}_3$ ) of compound <b>225</b> .....	241
Figure B.2	Infrared spectrum (thin film/ $\text{NaCl}$ ) of compound <b>225</b> .....	242
Figure B.3	$^{13}\text{C}$ NMR (125 MHz, $\text{CDCl}_3$ ) of compound <b>225</b> .....	242
Figure B.4	$^1\text{H}$ NMR (500 MHz, $\text{CDCl}_3$ ) of compound <b>226</b> .....	243
Figure B.5	Infrared spectrum (thin film/ $\text{NaCl}$ ) of compound <b>226</b> .....	244
Figure B.6	$^{13}\text{C}$ NMR (125 MHz, $\text{CDCl}_3$ ) of compound <b>226</b> .....	244
Figure B.7	$^1\text{H}$ NMR (500 MHz, $\text{CDCl}_3$ ) of compound <b>242</b> .....	245
Figure B.8	Infrared spectrum (thin film/ $\text{NaCl}$ ) of compound <b>242</b> .....	246
Figure B.9	$^{13}\text{C}$ NMR (125 MHz, $\text{CDCl}_3$ ) of compound <b>242</b> .....	246

Figure B.10	$^1\text{H}$ NMR (300 MHz, $\text{C}_6\text{D}_6$ ) of compound <b>247</b> .....	247
Figure B.11	Infrared spectrum (thin film/ $\text{NaCl}$ ) of compound <b>247</b> .....	248
Figure B.12	$^{13}\text{C}$ NMR (75 MHz, $\text{C}_6\text{D}_6$ ) of compound <b>247</b> .....	248
Figure B.13	$^1\text{H}$ NMR (500 MHz, $\text{CDCl}_3$ ) of compound <b>247a</b> .....	249
Figure B.14	Infrared spectrum (thin film/ $\text{NaCl}$ ) of compound <b>247a</b> .....	250
Figure B.15	$^{13}\text{C}$ NMR (125 MHz, $\text{CDCl}_3$ ) of compound <b>247a</b> .....	250
Figure B.16	$^1\text{H}$ NMR (500 MHz, $\text{CDCl}_3$ ) of compound <b>248</b> .....	251
Figure B.17	Infrared spectrum (thin film/ $\text{NaCl}$ ) of compound <b>248</b> .....	252
Figure B.18	$^{13}\text{C}$ NMR (125 MHz, $\text{CDCl}_3$ ) of compound <b>248</b> .....	252
Figure B.19	$^1\text{H}$ NMR (300 MHz, $\text{CDCl}_3$ ) of compound <b>250</b> .....	253
Figure B.20	Infrared spectrum (thin film/ $\text{NaCl}$ ) of compound <b>250</b> .....	254
Figure B.21	$^{13}\text{C}$ NMR (75 MHz, $\text{CDCl}_3$ ) of compound <b>250</b> .....	254
Figure B.22	$^1\text{H}$ NMR (300 MHz, $\text{CDCl}_3$ ) of compound <b>251</b> .....	255
Figure B.23	Infrared spectrum (thin film/ $\text{NaCl}$ ) of compound <b>251</b> .....	256
Figure B.24	$^{13}\text{C}$ NMR (75 MHz, $\text{CDCl}_3$ ) of compound <b>251</b> .....	256
Figure B.25	$^1\text{H}$ NMR (300 MHz, $\text{CDCl}_3$ ) of compound <b>251a</b> .....	257
Figure B.26	Infrared spectrum (thin film/ $\text{NaCl}$ ) of compound <b>252</b> .....	258
Figure B.27	$^{13}\text{C}$ NMR (75 MHz, $\text{CDCl}_3$ ) of compound <b>252</b> .....	258
Figure B.28	$^1\text{H}$ NMR (300 MHz, $\text{CDCl}_3$ ) of compound <b>252</b> .....	259
Figure B.29	Infrared spectrum (thin film/ $\text{NaCl}$ ) of compound <b>252</b> .....	260
Figure B.30	$^{13}\text{C}$ NMR (75 MHz, $\text{CDCl}_3$ ) of compound <b>252</b> .....	260
Figure B.31	$^1\text{H}$ NMR (300 MHz, $\text{CDCl}_3$ ) of compound <b>253</b> .....	261
Figure B.32	Infrared spectrum (thin film/ $\text{NaCl}$ ) of compound <b>253</b> .....	262
Figure B.33	$^{13}\text{C}$ NMR (75 MHz, $\text{CDCl}_3$ ) of compound <b>253</b> .....	262
Figure B.34	$^1\text{H}$ NMR (300 MHz, $\text{CDCl}_3$ ) of compound <b>255</b> .....	263
Figure B.35	Infrared spectrum (thin film/ $\text{NaCl}$ ) of compound <b>255</b> .....	264

Figure B.36	$^{13}\text{C}$ NMR (75 MHz, 255) of compound <b>255</b> .....	264
Figure B.37	$^1\text{H}$ NMR (500 MHz, $\text{CDCl}_3$ ) of compound <b>256</b> .....	265
Figure B.38	Infrared spectrum (thin film/ $\text{NaCl}$ ) of compound <b>256</b> .....	266
Figure B.39	$^{13}\text{C}$ NMR (75 MHz, $\text{CDCl}_3$ ) of compound <b>256</b> .....	266
Figure B.40	$^1\text{H}$ NMR (500 MHz, $\text{CDCl}_3$ ) of compound <b>257</b> .....	267
Figure B.41	Infrared spectrum (thin film/ $\text{NaCl}$ ) of compound <b>257</b> .....	268
Figure B.42	$^{13}\text{C}$ NMR (125 MHz, $\text{CDCl}_3$ ) of compound <b>257</b> .....	268
Figure B.43	$^1\text{H}$ NMR (300 MHz, $\text{CDCl}_3$ ) of compound <b>258</b> .....	269
Figure B.44	Infrared spectrum (thin film/ $\text{NaCl}$ ) of compound <b>258</b> .....	270
Figure B.45	$^{13}\text{C}$ NMR (125 MHz, $\text{CDCl}_3$ ) of compound <b>258</b> .....	270
Figure B.46	$^1\text{H}$ NMR (300 MHz, $\text{CDCl}_3$ ) of compound <b>259</b> .....	271
Figure B.47	Infrared spectrum (thin film/ $\text{NaCl}$ ) of compound <b>259</b> .....	272
Figure B.48	$^{13}\text{C}$ NMR (75 MHz, $\text{CDCl}_3$ ) of compound <b>259</b> .....	272
Figure B.49	$^1\text{H}$ NMR (300 MHz, $\text{CDCl}_3$ ) of compound <b>260</b> .....	273
Figure B.50	Infrared spectrum (thin film/ $\text{NaCl}$ ) of compound <b>260</b> .....	274
Figure B.51	$^{13}\text{C}$ NMR (75 MHz, $\text{CDCl}_3$ ) of compound <b>260</b> .....	274
Figure B.52	$^1\text{H}$ NMR (300 MHz, $\text{CDCl}_3$ ) of compound <b>261</b> .....	275
Figure B.53	Infrared spectrum (thin film/ $\text{NaCl}$ ) of compound <b>261</b> .....	276
Figure B.54	$^{13}\text{C}$ NMR (75 MHz, $\text{CDCl}_3$ ) of compound <b>261</b> .....	276
Figure B.55	$^1\text{H}$ NMR (300 MHz, $\text{CDCl}_3$ ) of compound <b>262a</b> .....	277
Figure B.56	Infrared spectrum (thin film/ $\text{NaCl}$ ) of compound <b>262a</b> .....	278
Figure B.57	$^{13}\text{C}$ NMR (75 MHz, $\text{CDCl}_3$ ) of compound <b>262a</b> .....	278
Figure B.58	$^1\text{H}$ NMR (300 MHz, $\text{CDCl}_3$ ) of compound <b>262b</b> .....	279
Figure B.59	Infrared spectrum (thin film/ $\text{NaCl}$ ) of compound <b>262b</b> .....	280
Figure B.60	$^{13}\text{C}$ NMR (75 MHz, $\text{CDCl}_3$ ) of compound <b>262b</b> .....	280
Figure B.61	$^1\text{H}$ NMR (300 MHz, $\text{C}_6\text{D}_6$ ) of compound <b>263</b> .....	281

Figure B.62	Infrared spectrum (thin film/NaCl) of compound <b>263</b> .....	282
Figure B.63	<sup>13</sup> C NMR (300 MHz, C <sub>6</sub> D <sub>6</sub> ) of compound <b>263</b> .....	282
Figure B.64	<sup>1</sup> H NMR (300 MHz, CDCl <sub>3</sub> ) of compound <b>264</b> .....	283
Figure B.65	Infrared spectrum (thin film/NaCl) of compound <b>264</b> .....	284
Figure B.66	<sup>13</sup> C NMR (75 MHz, CDCl <sub>3</sub> ) of compound <b>264</b> .....	284
Figure B.67	<sup>1</sup> H NMR (300 MHz, CDCl <sub>3</sub> ) of compound <b>265</b> .....	285
Figure B.68	Infrared spectrum (thin film/NaCl) of compound <b>265</b> .....	286
Figure B.69	<sup>13</sup> C NMR (75 MHz, CDCl <sub>3</sub> ) of compound <b>265</b> .....	286
Figure B.70	<sup>1</sup> H NMR (300 MHz, CDCl <sub>3</sub> ) of compound <b>266</b> .....	287
Figure B.71	Infrared spectrum (thin film/NaCl) of compound <b>266</b> .....	288
Figure B.72	<sup>13</sup> C NMR (75 MHz, CDCl <sub>3</sub> ) of compound <b>266</b> .....	288
Figure B.73	<sup>1</sup> H NMR (500 MHz, CDCl <sub>3</sub> ) of compound <b>270</b> .....	289
Figure B.74	Infrared spectrum (thin film/NaCl) of compound <b>270</b> .....	290
Figure B.75	<sup>13</sup> C NMR (125 MHz, CDCl <sub>3</sub> ) of compound <b>270</b> .....	290
Figure B.76	<sup>1</sup> H NMR (500 MHz, CDCl <sub>3</sub> ) of compound <b>272</b> .....	291
Figure B.77	Infrared spectrum (thin film/NaCl) of compound <b>272</b> .....	292
Figure B.78	<sup>13</sup> C NMR (125 MHz, CDCl <sub>3</sub> ) of compound <b>272</b> .....	292
Figure B.79	<sup>1</sup> H NMR (300 MHz, CDCl <sub>3</sub> ) of compound <b>273</b> .....	293
Figure B.80	Infrared spectrum (thin film/NaCl) of compound <b>273</b> .....	294
Figure B.81	<sup>13</sup> C NMR (75 MHz, CDCl <sub>3</sub> ) of compound <b>273</b> .....	294
Figure B.82	<sup>1</sup> H NMR (300 MHz, CDCl <sub>3</sub> ) of compound <b>274</b> .....	295
Figure B.83	Infrared spectrum (thin film/NaCl) of compound <b>274</b> .....	296
Figure B.84	<sup>13</sup> C NMR (75 MHz, CDCl <sub>3</sub> ) of compound <b>274</b> .....	296
Figure B.85	<sup>1</sup> H NMR (300 MHz, C <sub>6</sub> D <sub>6</sub> ) of compound <b>276</b> .....	297
Figure B.86	Infrared spectrum (thin film/NaCl) of compound <b>276</b> .....	298
Figure B.87	<sup>13</sup> C NMR (75 MHz, C <sub>6</sub> D <sub>6</sub> ) of compound <b>276</b> .....	298

Figure B.88	$^1\text{H}$ NMR (300 MHz, $\text{CDCl}_3$ ) of compound <b>278</b> .....	299
Figure B.89	Infrared spectrum (thin film/ $\text{NaCl}$ ) of compound <b>278</b> .....	300
Figure B.90	$^{13}\text{C}$ NMR (75 MHz, $\text{CDCl}_3$ ) of compound <b>278</b> .....	300
Figure B.91	$^1\text{H}$ NMR (300 MHz, $\text{CDCl}_3$ ) of compound <b>279</b> .....	301
Figure B.92	Infrared spectrum (thin film/ $\text{NaCl}$ ) of compound <b>279</b> .....	302
Figure B.93	$^{13}\text{C}$ NMR (75 MHz, $\text{CDCl}_3$ ) of compound <b>279</b> .....	302
Figure B.94	$^1\text{H}$ NMR (500 MHz, $\text{CDCl}_3$ ) of compound <b>280</b> .....	303
Figure B.95	Infrared spectrum (thin film/ $\text{NaCl}$ ) of compound <b>280</b> .....	304
Figure B.96	$^{13}\text{C}$ NMR (125 MHz, $\text{CDCl}_3$ ) of compound <b>280</b> .....	304
Figure B.97	$^1\text{H}$ NMR (500 MHz, $\text{CDCl}_3$ ) of compound <b>281a</b> .....	305
Figure B.98	Infrared spectrum (thin film/ $\text{NaCl}$ ) of compound <b>281a</b> .....	306
Figure B.99	$^{13}\text{C}$ NMR (125 MHz, $\text{CDCl}_3$ ) of compound <b>281a</b> .....	306
Figure B.100	$^1\text{H}$ NMR (500 MHz, $\text{CDCl}_3$ ) of compound <b>281b</b> .....	307
Figure B.101	Infrared spectrum (thin film/ $\text{NaCl}$ ) of compound <b>281b</b> .....	308
Figure B.102	$^{13}\text{C}$ NMR (125 MHz, $\text{CDCl}_3$ ) of compound <b>281b</b> .....	308
Figure B.103	$^1\text{H}$ NMR (300 MHz, $\text{CDCl}_3$ ) of compound <b>282</b> .....	309
Figure B.104	Infrared spectrum (thin film/ $\text{NaCl}$ ) of compound <b>282</b> .....	310
Figure B.105	$^{13}\text{C}$ NMR (75 MHz, $\text{CDCl}_3$ ) of compound <b>282</b> .....	310
Figure B.106	$^1\text{H}$ NMR (300 MHz, $\text{CDCl}_3$ ) of compound <b>269</b> .....	311
Figure B.107	Infrared spectrum (thin film/ $\text{NaCl}$ ) of compound <b>269</b> .....	312
Figure B.108	$^{13}\text{C}$ NMR (75 MHz, $\text{CDCl}_3$ ) of compound <b>269</b> .....	312
Figure B.109	$^1\text{H}$ NMR (300 MHz, $\text{CDCl}_3$ ) of compound <b>283</b> .....	313
Figure B.110	Infrared spectrum (thin film/ $\text{NaCl}$ ) of compound <b>283</b> .....	314
Figure B.111	$^{13}\text{C}$ NMR (75 MHz, $\text{CDCl}_3$ ) of compound <b>283</b> .....	314
Figure B.112	Representation of Allylic Alcohol <b>248</b> .....	315
Figure B.113	Representation of Allylic Alcohol <b>253</b> .....	323

Figure B.114	Representation of Bisacetoxycetal <b>256</b> .....	338
Figure B.115	Representation of Tetracycle <b>269</b> .....	347

## APPENDIX C

Figure C.1	$^1\text{H}$ NMR (500 MHz, $\text{CDCl}_3$ ) of compound <b>255a</b> .....	393
Figure C.2	Infrared spectrum (thin film/ $\text{NaCl}$ ) of compound <b>255a</b> .....	394
Figure C.3	$^{13}\text{C}$ NMR (125 MHz, $\text{CDCl}_3$ ) of compound <b>255a</b> .....	394
Figure C.4	$^1\text{H}$ NMR (500 MHz, $\text{CDCl}_3$ ) of compound <b>255b</b> .....	395
Figure C.5	Infrared spectrum (thin film/ $\text{NaCl}$ ) of compound <b>255b</b> .....	396
Figure C.6	$^{13}\text{C}$ NMR (125 MHz, $\text{CDCl}_3$ ) of compound <b>255b</b> .....	396
Figure C.7	$^1\text{H}$ NMR (500 MHz, $\text{CDCl}_3$ ) of compound <b>315</b> .....	397
Figure C.8	Infrared spectrum (thin film/ $\text{NaCl}$ ) of compound <b>315</b> .....	398
Figure C.9	$^{13}\text{C}$ NMR (125 MHz, $\text{CDCl}_3$ ) of compound <b>315</b> .....	398
Figure C.10	$^1\text{H}$ NMR (500 MHz, $\text{CDCl}_3$ ) of compound <b>317</b> .....	399
Figure C.11	Infrared spectrum (thin film/ $\text{NaCl}$ ) of compound <b>317</b> .....	400
Figure C.12	$^{13}\text{C}$ NMR (125 MHz, $\text{CDCl}_3$ ) of compound <b>317</b> .....	400
Figure C.13	$^1\text{H}$ NMR (300 MHz, $\text{CDCl}_3$ ) of compound <b>320</b> .....	401
Figure C.14	Infrared spectrum (thin film/ $\text{NaCl}$ ) of compound <b>320</b> .....	402
Figure C.15	$^{13}\text{C}$ NMR (75 MHz, $\text{CDCl}_3$ ) of compound <b>320</b> .....	402
Figure C.16	$^1\text{H}$ NMR (300 MHz, $\text{CDCl}_3$ ) of compound <b>322</b> .....	403
Figure C.17	Infrared spectrum (thin film/ $\text{NaCl}$ ) of compound <b>322</b> .....	404
Figure C.18	$^{13}\text{C}$ NMR (75 MHz, $\text{CDCl}_3$ ) of compound <b>322</b> .....	404
Figure C.19	$^1\text{H}$ NMR (500 MHz, $\text{CDCl}_3$ ) of compound <b>323</b> .....	405
Figure C.20	Infrared spectrum (thin film/ $\text{NaCl}$ ) of compound <b>323</b> .....	406
Figure C.21	$^{13}\text{C}$ NMR (125 MHz, $\text{CDCl}_3$ ) of compound <b>323</b> .....	406
Figure C.22	$^1\text{H}$ NMR (500 MHz, $\text{CDCl}_3$ ) of compound <b>324</b> .....	407

Figure C.23	Infrared spectrum (thin film/NaCl) of compound <b>324</b> .....	408
Figure C.24	<sup>13</sup> C NMR (125 MHz, CDCl <sub>3</sub> ) of compound <b>324</b> .....	408
Figure C.25	Representation of Alcohol <b>324</b> .....	409

## APPENDIX E

Figure E.1	<sup>1</sup> H NMR (500 MHz, CDCl <sub>3</sub> ) of compound <b>341</b> .....	457
Figure E.2	Infrared spectrum (thin film/NaCl) of compound <b>341</b> .....	458
Figure E.3	<sup>13</sup> C NMR (125 MHz, CDCl <sub>3</sub> ) of compound <b>341</b> .....	458
Figure E.4	<sup>1</sup> H NMR (300 MHz, CDCl <sub>3</sub> ) of compound <b>342</b> .....	459
Figure E.5	Infrared spectrum (thin film/NaCl) of compound <b>342</b> .....	460
Figure E.6	<sup>13</sup> C NMR (125 MHz, CDCl <sub>3</sub> ) of compound <b>342</b> .....	460
Figure E.7	<sup>1</sup> H NMR (500 MHz, CDCl <sub>3</sub> ) of compound <b>343</b> .....	461
Figure E.8	Infrared spectrum (thin film/NaCl) of compound <b>343</b> .....	462
Figure E.9	<sup>13</sup> C NMR (75 MHz, CDCl <sub>3</sub> ) of compound <b>343</b> .....	462
Figure E.10	<sup>1</sup> H NMR (500 MHz, CDCl <sub>3</sub> ) of compound <b>344</b> .....	463
Figure E.11	Infrared spectrum (thin film/NaCl) of compound <b>344</b> .....	464
Figure E.12	<sup>13</sup> C NMR (125 MHz, CDCl <sub>3</sub> ) of compound <b>344</b> .....	464
Figure E.13	<sup>1</sup> H NMR (500 MHz, CDCl <sub>3</sub> ) of compound <b>346</b> .....	465
Figure E.14	Infrared spectrum (thin film/NaCl) of compound <b>346</b> .....	466
Figure E.15	<sup>13</sup> C NMR (125 MHz, CDCl <sub>3</sub> ) of compound <b>346</b> .....	466
Figure E.16	<sup>1</sup> H NMR (500 MHz, CDCl <sub>3</sub> ) of compound <b>347</b> .....	467
Figure E.17	Infrared spectrum (thin film/NaCl) of compound <b>347</b> .....	468
Figure E.18	<sup>13</sup> C NMR (125 MHz, CDCl <sub>3</sub> ) of compound <b>347</b> .....	468
Figure E.19	<sup>1</sup> H NMR (300 MHz, CDCl <sub>3</sub> ) of compound <b>348a</b> .....	469
Figure E.20	Infrared spectrum (thin film/NaCl) of compound <b>348a</b> .....	470
Figure E.21	<sup>13</sup> C NMR (125 MHz, CDCl <sub>3</sub> ) of compound <b>348a</b> .....	470

Figure E.22	$^1\text{H}$ NMR (500 MHz, $\text{CDCl}_3$ ) of compound <b>348b</b> .....	471
Figure E.23	Infrared spectrum (thin film/ $\text{NaCl}$ ) of compound <b>348b</b> .....	472
Figure E.24	$^{13}\text{C}$ NMR (125 MHz, $\text{CDCl}_3$ ) of compound <b>348b</b> .....	472
Figure E.25	$^1\text{H}$ NMR (300 MHz, $\text{CDCl}_3$ ) of compound <b>348c</b> .....	473
Figure E.26	Infrared spectrum (thin film/ $\text{NaCl}$ ) of compound <b>348c</b> .....	474
Figure E.27	$^{13}\text{C}$ NMR (125 MHz, $\text{CDCl}_3$ ) of compound <b>348c</b> .....	474
Figure E.28	$^1\text{H}$ NMR (500 MHz, $\text{CDCl}_3$ ) of compound <b>364</b> .....	475
Figure E.29	Infrared spectrum (thin film/ $\text{NaCl}$ ) of compound <b>364</b> .....	476
Figure E.30	$^{13}\text{C}$ NMR (500 MHz, $\text{CDCl}_3$ ) of compound <b>364</b> .....	476
Figure E.31	$^1\text{H}$ NMR (500 MHz, $\text{CDCl}_3$ ) of compound <b>365</b> .....	477
Figure E.32	Infrared spectrum (thin film/ $\text{NaCl}$ ) of compound <b>365</b> .....	478
Figure E.33	$^{13}\text{C}$ NMR (125 MHz, $\text{CDCl}_3$ ) of compound <b>365</b> .....	478
Figure E.34	$^1\text{H}$ NMR (500 MHz, $\text{CDCl}_3$ ) of compound <b>366</b> .....	479
Figure E.35	Infrared spectrum (thin film/ $\text{NaCl}$ ) of compound <b>366</b> .....	480
Figure E.36	$^{13}\text{C}$ NMR (125 MHz, $\text{CDCl}_3$ ) of compound <b>366</b> .....	480
Figure E.37	$^1\text{H}$ NMR (500 MHz, $\text{CDCl}_3$ ) of compound <b>368</b> .....	481
Figure E.38	Infrared spectrum (thin film/ $\text{NaCl}$ ) of compound <b>368</b> .....	482
Figure E.39	$^{13}\text{C}$ NMR (125 MHz, $\text{CDCl}_3$ ) of compound <b>368</b> .....	482
Figure E.40	$^1\text{H}$ NMR (500 MHz, $\text{CDCl}_3$ ) of compound <b>379</b> .....	483
Figure E.41	Infrared spectrum (thin film/ $\text{NaCl}$ ) of compound <b>370</b> .....	484
Figure E.42	$^{13}\text{C}$ NMR (XXX MHz, XX) of compound <b>379</b> .....	484
Figure E.43	$^1\text{H}$ NMR (300 MHz, $\text{CDCl}_3$ ) of compound <b>380</b> .....	485
Figure E.44	Infrared spectrum (thin film/ $\text{NaCl}$ ) of compound <b>380</b> .....	486
Figure E.45	$^{13}\text{C}$ NMR (75 MHz, $\text{CDCl}_3$ ) of compound <b>380</b> .....	486
Figure E.46	$^1\text{H}$ NMR (300 MHz, $\text{CDCl}_3$ ) of compound <b>387</b> .....	487
Figure E.47	Infrared spectrum (thin film/ $\text{NaCl}$ ) of compound <b>387</b> .....	488

Figure E.48	$^{13}\text{C}$ NMR (75 MHz, $\text{CDCl}_3$ ) of compound <b>387</b> .....	488
Figure E.49	$^1\text{H}$ NMR (300 MHz, $\text{CDCl}_3$ ) of compound <b>388</b> .....	489
Figure E.50	Infrared spectrum (thin film/ $\text{NaCl}$ ) of compound <b>388</b> .....	490
Figure E.51	$^{13}\text{C}$ NMR (75 MHz, $\text{CDCl}_3$ ) of compound <b>380</b> .....	490
Figure E.52	$^1\text{H}$ NMR (300 MHz, $\text{CDCl}_3$ ) of compound <b>389</b> .....	491
Figure E.53	Infrared spectrum (thin film/ $\text{NaCl}$ ) of compound <b>389</b> .....	492
Figure E.54	$^{13}\text{C}$ NMR (75 MHz, $\text{CDCl}_3$ ) of compound <b>389</b> .....	492
Figure E.55	$^1\text{H}$ NMR (300 MHz, $\text{CDCl}_3$ ) of compound <b>391</b> .....	493
Figure E.56	Infrared spectrum (thin film/ $\text{NaCl}$ ) of compound <b>391</b> .....	494
Figure E.57	$^{13}\text{C}$ NMR (75 MHz, $\text{CDCl}_3$ ) of compound <b>391</b> .....	494
Figure E.58	$^1\text{H}$ NMR (500 MHz, $\text{CDCl}_3$ ) of compound <b>392</b> .....	495
Figure E.59	Infrared spectrum (thin film/ $\text{NaCl}$ ) of compound <b>392</b> .....	496
Figure E.60	$^{13}\text{C}$ NMR (125 MHz, $\text{CDCl}_3$ ) of compound <b>392</b> .....	496
Figure E.61	$^1\text{H}$ NMR (500 MHz, $\text{CDCl}_3$ ) of compound <b>393</b> .....	497
Figure E.62	Infrared spectrum (thin film/ $\text{NaCl}$ ) of compound <b>393</b> .....	498
Figure E.63	$^{13}\text{C}$ NMR (125 MHz, $\text{CDCl}_3$ ) of compound <b>393</b> .....	498
Figure E.64	$^1\text{H}$ NMR (300 MHz, $\text{CDCl}_3$ ) of compound <b>396</b> .....	499
Figure E.65	Infrared spectrum (thin film/ $\text{NaCl}$ ) of compound <b>396</b> .....	500
Figure E.66	$^{13}\text{C}$ NMR (75 MHz, 75) of compound <b>396</b> .....	500
Figure E.67	Representation of Allyl ketone <b>366</b> .....	501

## LIST OF SCHEMES

## CHAPTER 1

Scheme 1.2.1	Hypothetical polyketide precursor .....	7
Scheme 1.2.2	Potential mechanism for cyclization of polyketide precursor <b>22</b> ...	8
Scheme 1.2.3	Proposed biosynthesis of norzoanthamine.....	9
Scheme 1.2.4	Structure of zooxanthellamine .....	10
Scheme 1.2.5	Equilibria between lactone and enamine isomers of norzoanthamine.....	12
Scheme 1.2.6	Anomalous reduction of norzoanthamine .....	12
Scheme 1.4.1	Miyashita's Diels-Alder construction of the ABC core.....	19
Scheme 1.4.2	Functionalization of the ABC core.....	20
Scheme 1.4.3	Attaching the southern sidechain.....	21
Scheme 1.4.4	The completion of norzoanthamine .....	22
Scheme 1.4.5	Tanner's approach to a model ABC ring system.....	23
Scheme 1.4.6	Model cyclizations of compounds derived from (-)-carvone.....	24
Scheme 1.4.7	Mechanism for formation of undesired products .....	25
Scheme 1.4.8	Tanner's approach to the functionalized ABC ring system.....	26
Scheme 1.4.9	Mechanism for formation of by-product <b>95</b> .....	26
Scheme 1.4.10	Diels-Alder cyclization and cycloadducts advancement .....	27
Scheme 1.4.11	Uemura's approach to norzoanthamine .....	28
Scheme 1.4.12	Williams's early efforts toward the norzoanthamine AB rings .....	29
Scheme 1.4.13	Williams's recent efforts toward the norzoanthamine AB rings .....	30
Scheme 1.4.14	Williams's synthesis of a model EFG ring system.....	31

Scheme 1.4.15	Theodorakis's approach to the ABC ring system.....	32
Scheme 1.4.16	Theodorakis's installation of the C(9) quaternary center.....	33
Scheme 1.4.17	Kobayashi's sulfone approach to the CDEFG ring system.....	34
Scheme 1.4.18	Hirama's Heck strategy for the zoanthenol ABC ring system .....	35
Scheme 1.4.19	Hirama's alternative assembly of the B ring.....	36
Scheme 1.4.20	Hirama's installation of the C(9) methyl group .....	36
Scheme 1.4.21	An alternate approach by Hirama .....	37
Scheme 1.4.22	Hirama's synthesis of the fully functionalized ABC core of zoanthenol.....	38

## CHAPTER 2

Scheme 2.1.1	Retrosynthetic analysis of zoanthenol .....	44
Scheme 2.2.1	Synthesis of the A ring synthon .....	45
Scheme 2.2.2	Racemic synthesis of the C ring synthon .....	46
Scheme 2.2.3	Decarboxylative alkylation enables enantioselective synthesis.....	47
Scheme 2.2.4	Diastereoselective Grignard addition.....	47
Scheme 2.2.5	Discovery of an unusual acid-mediated cyclization .....	48
Scheme 2.2.6	Other substrates for cyclization.....	49
Scheme 2.2.7	A proposed mechanism for the S <sub>N</sub> ' cyclization .....	50
Scheme 2.2.8	Deoxygenation of the A ring .....	50
Scheme 2.2.9	Refunctionalization of the C(20)-C(21) olefin .....	51
Scheme 2.2.10	Plan for the elaboration of the tricyclic core.....	52
Scheme 2.2.11	Attempts to enolize at C(9) .....	53
Scheme 2.3.1	Retrosynthetic analysis of the DEFG synthon.....	53
Scheme 2.3.2	Jacobsen hetero-Diels-Alder cycloaddition.....	54

Scheme 2.3.3	Conjugate addition and Mitsunobu reaction provide key intermediate.....	54
Scheme 2.3.4	Conversion of the $\delta$ -lactone to the $\epsilon$ -lactam synthon.....	55
Scheme 2.3.5	Vinylation of the $\epsilon$ -lactam to access the enone synthon .....	55
SUMMARY SCHEMES		
Scheme S2.1	Retrosynthetic Analysis of Zoanthenol .....	89
Scheme S2.2	Synthesis of the A Ring Synthon .....	89
Scheme S2.3	Racemic Synthesis of the C Ring Synthon .....	90
Scheme S2.4	Enantioselective Synthesis of C Ring Methyl Ketone <b>177</b> .....	90
Scheme S2.5	Fragment Coupling and Acid-Mediated Cyclization of the A and C Rings .....	90
Scheme S2.6	Deoxygenation of the A Ring and Refunctionalization of C(20) ...	91
Scheme S2.7	Enantioselective Synthesis of DEFG Synthon .....	91
CHAPTER 3		
Scheme 3.1.1	Revised retrosynthesis of zoanthenol .....	182
Scheme 3.2.1	Synthesis of vicinal all-carbon quaternary centers .....	183
Scheme 3.2.2	Mechanism of <i>meso</i> -anhydride desymmetrization by cinchona alkaloids .....	183
Scheme 3.2.3	C ring functionalization: iodolactonization and displacement .....	187
Scheme 3.3.1	Synthesis of a lactone-derived C ring synthon .....	188
Scheme 3.3.2	Grignard addition to synthon <b>252</b> .....	188
Scheme 3.3.3	Lactone-derived A–C ring system cyclizations.....	189
Scheme 3.4.1	Lactone reduction and triol differentiation .....	190
Scheme 3.5.1	Synthesis of a 7-membered acetal-derived C ring .....	191

Scheme 3.5.2	Grignard addition and oxidation to access cyclization substrates .....	192
Scheme 3.5.3	Cyclization of allylic alcohol <b>265</b> .....	192
Scheme 3.5.4	Cyclization of 7-membered acetal-derived enone substrate.....	193
Scheme 3.6.1	Synthesis of a homologated C ring synthon.....	195
Scheme 3.6.2	Fragment coupling and cyclization of the nitrile-derived A–C system .....	195
Scheme 3.7.1	Synthesis of an acid-derived A–C ring system .....	196
Scheme 3.7.2	Cyclization of carboxylic acid-derived tethered A–C ring systems .....	197
Scheme 3.8.1	Proposed mechanism for formation of bis-lactone <b>256</b> .....	198
Scheme 3.8.2	Proposed mechanism for formation of acetal <b>270</b> .....	199
Scheme 3.8.3	Proposed mechanism for formation of tetracycle <b>269</b> .....	200

## SUMMARY SCHEMES

Scheme S3.1	Revised retrosynthetic analysis .....	243
Scheme S3.2	Access to a meso anhydride .....	243
Scheme S3.2	Desymmetrization and elaboration of a meso anhydride.....	244
Scheme S3.3	Synthesis of a lactone-derived C ring synthon .....	244
Scheme S3.4	Fragment coupling and cyclization of the A and lactone-derived C rings .....	244
Scheme S3.5	Elaboration of lactone <b>248</b> .....	245
Scheme S3.6	Synthesis of a 7-membered acetal-derived C ring synthon .....	245
Scheme S3.7	Fragment coupling and cyclization of the A and 7-membered acetal derived C rings .....	245
Scheme S3.8	Synthesis of a homologated nitrile-derived C ring synthon .....	246

Scheme S3.9	Fragment coupling and cyclization of the A and homologated nitrile-derived C rings .....	246
Scheme S3.10	Synthesis, fragment coupling, and cyclization of the A and homologated carboxylic acid-derived C rings.....	247
CHAPTER 4		
Scheme 4.1.1	Failed methods for cyclization of tethered A–C ring systems .....	367
Scheme 4.1.2	Radical-induced cyclization of a tethered A–C ring system .....	368
Scheme 4.2.1	Synthesis of lactone-derived radical cyclization precursor .....	369
Scheme 4.2.2	Attempted cyclization of lactone-derived A–C ring system .....	369
Scheme 4.3.1	Synthesis of homologated nitrile-derived radical cyclization precursor .....	370
Scheme 4.3.2	Attempted cyclization of nitrile-derived A–C ring system .....	371
Scheme 4.4.1	Synthesis of homologated ester-derived radical cyclization precursor .....	371
Scheme 4.4.2	Attempted cyclization of ester-derived A–C ring system .....	372
Scheme 4.5.1	Synthesis of 7-membered acetal-derived radical cyclization precursor .....	372
Scheme 4.5.2	Cyclization of 7-membered acetal-derived A–C ring system .....	373
Scheme 4.6.1	3D representations of cyclization products .....	375
Scheme 4.6.2	Structural requirements for future radical cyclization products.....	376
SUMMARY SCHEMES		
Scheme S4.1	Synthesis of brominated radical cyclization precursors .....	390

Scheme S4.2	Radical cyclization of a 7-membered acetal-derived cyclization precursor .....	391
-------------	--	-----

## APPENDIX D

Scheme D.2.1	Plan for functionalization of C(9) .....	417
Scheme D.2.2	Deuteration to functionalize C(9) by allylation .....	418
Scheme D.2.3	Thermodynamic deprotonation to functionalize C(9) by acylation .....	418
Scheme D.3.1	Common intermediate for acid-mediated and radical cyclizations .....	419
Scheme D.3.2	Toward an optimal C ring synthon .....	420
Scheme D.3.3	Preparation of a C ring synthon with inverted C(10) stereochemistry .....	421
Scheme D.3.4	Acid-mediated cyclization of cyclopentylidene-derived C ring synthon .....	422
Scheme D.3.5	Radical cyclization of cyclopentylidene-containing precursor .....	422
Scheme D.3.6	Radical cyclization of C(19)-substituted cyclization precursor .....	423
Scheme D.4.1	Revised retrosynthesis for allylation/Diels-Alder approach .....	424
Scheme D.4.2	Palladium-catalyzed alkylation of lactone <b>366</b> .....	425
Scheme D.4.3	Allylation of a cyclopentylidene-containing ketone .....	425
Scheme D.4.4	Alternative alkylation and advancement of ketone <b>347</b> .....	427
Scheme D.4.5	Revised retrosynthesis for $\alpha$ -arylation approach .....	428
Scheme D.4.6	Synthesis of aryl bromide <b>379</b> .....	428
Scheme D.4.7	$\alpha$ -Arylation to form A-C ring adduct <b>380</b> .....	429

Scheme D.4.8	B ring closure of $\alpha$ -arylation product <b>380</b> .....	429
Scheme D.5.1	Side chain functionalization of a model ketone.....	430
Scheme D.5.2	Horner-Wadsworth-Emmons coupling strategy.....	431

## LIST OF TABLES

## CHAPTER 1

Table 1.3.1	Cytotoxicity of the zoanthamine alkaloids.....	16
Table 1.3.2	Summary of antibacterial activities.....	16

## APPENDIX A

Table A.1	Crystal data .....	153
Table A.2	Atomic coordinates.....	155
Table A.3	Full bond distances and angles (for deposit).....	155
Table A.4	Anisotropic displacement parameters .....	159
Table A.5	Hydrogen atomic coordinates.....	160
Table A.6	Crystal data .....	162
Table A.7	Atomic coordinates.....	164
Table A.8	Full bond distances and angles (for deposit).....	165
Table A.9	Anisotropic displacement parameters .....	167
Table A.10	Hydrogen atomic coordinates.....	168
Table A.11	Hydrogen bonds .....	169
Table A.12	Crystal data .....	171
Table A.13	Atomic coordinates.....	173
Table A.14	Full bond distances and angles (for deposit).....	174
Table A.15	Anisotropic displacement parameters .....	176
Table A.16	Hydrogen atomic coordinates.....	177

## CHAPTER 3

Table 3.2.1	Optimized synthesis and desymmetrization of a C ring <i>meso</i> -anhydride .....	183
-------------	--	-----

## APPENDIX B

Table B.1	Crystal data .....	369
Table B.2	Atomic coordinates.....	371
Table B.3	Full bond distances and angles.....	372
Table B.4	Anisotropic displacement parameters .....	373
Table B.5	Hydrogen atomic coordinates.....	374
Table B.6	Hydrogen bond distances and angles .....	375
Table B.7	Crystal data .....	377
Table B.8	Atomic coordinates.....	379
Table B.9	Full bond distances and angles.....	381
Table B.10	Anisotropic displacement parameters .....	386
Table B.11	Hydrogen atomic coordinates.....	388
Table B.12	Hydrogen-bond distances and angles .....	390
Table B.13	Crystal data .....	392
Table B.14	Atomic coordinates.....	394
Table B.15	Full bond distances and angles.....	395
Table B.16	Anisotropic displacement parameters .....	397
Table B.17	Hydrogen atomic coordinates.....	398
Table B.18	Hydrogen bond distances and angles .....	399
Table B.19	Crystal data .....	401
Table B.20	Atomic coordinates.....	403
Table B.21	Full bond distances and angles.....	405

Table B.22	Anisotropic displacement parameters .....	409
Table B.23	Hydrogen bond distances and angles .....	411

## APPENDIX C

Table C.1	Crystal data .....	454
Table C.2	Atomic coordinates.....	456
Table C.3	Full bond distances and angles.....	458

## APPENDIX E

Table E.1	Crystal data .....	547
Table E.2	Atomic coordinates.....	549
Table E.3	Full bond distances and angles.....	550
Table E.4	Anisotropic displacement parameters .....	552
Table E.5	Hydrogen atomic coordinates.....	553

## LIST OF ABBREVIATIONS

$[\alpha]_D$	specific rotation at wavelength of sodium D line
Ac	acetyl
ACN	acetonitrile
Ad	adamantyl
add'n	addition
AIBN	2,2'-azobis( <i>iso</i> -butyronitrile)
app.	apparent
aq	aqueous
Ar	aryl group
atm	atmosphere
<i>B.</i>	<i>Bacillus</i>
BBN	borabicyclo[3.3.1]nonane
BHT	2,6-di- <i>tert</i> -butyl-4-methylphenol
BINAP	2,2'-Bis(diphenylphosphino)-1,1'-binaphthyl
bm	broad multiplet
Bn	benzyl
Boc	<i>tert</i> -butoxycarbonyl
BOM	benzyloxymethyl
bp	boiling point
br	broad
BRSM	based on recovered starting material
bs	broad singlet
BSA	<i>N,O</i> -bis(trimethylsilyl)acetamide
Bu	butyl

<i>n</i> -Bu	<i>n</i> -butyl
<i>t</i> -Bu	<i>tert</i> -butyl
Bz	benzoyl
<i>c</i>	concentration for optical rotation measurement
<sup>13</sup> C	carbon 13, isotope
/C	supported on activated carbon
°C	degrees Celsius
cat.	catalytic
calc'd	calculated
CAM	ceric ammonium molybdate stain
CAN	ammonium cerium(IV) nitrate
Cbz	benzyloxycarbonyl
CCDC	Cambridge Crystallographic Data Centre
CDI	1,1'-carbonyldiimidazole
<i>c</i> -Hex	cyclohexyl
comb.	combined
comp.	complex
CSA	camphorsulfonic acid
conv	conversion
COSY	correlation spectroscopy
Cy	cyclohexyl
d	doublet, deuterium, diameter, or day(s)
Δ	heat
δ	chemical shift in parts per million
DA	Diels-Alder
dba	dibenzylideneacetone

DBU	1,8-diazabicyclo[5.4.0]undec-7-ene
DCC	1,3-dicyclohexylcarbodiimide
DCE	1,2-dichloroethane
DCM	dichloromethane or methylene chloride
DDQ	2,3-dichloro-5,6-dicyano- <i>p</i> -benzoquinone
DEAD	diethyl azodicarboxylate
decomp.	decomposes
DIBAL	diisobutylaluminum hydride
DIBAL-H	diisobutylaluminum hydride
DIOP	2,3- <i>O</i> -isopropylidene-2,3-dihydroxy-1,4-bis(diphenylphosphino)butane
DIPA	diisopropyl amine
DIPEA	diisopropylethylamine
DMA	<i>N,N</i> -dimethylacetamide
DMAP	4-dimethylaminopyridine
dmdba	3,5,3',5'-dimethoxydibenzylideneacetone
DMDO	dimethyldioxirane
DME	1,2-dimethoxyethane
DMF	dimethylformamide
DMP	Dess-Martin periodinane
DMPU	<i>N,N'</i> -dimethyl propylene urea
DMS	dimethylsulfide
DMSO	dimethylsulfoxide
DNA	deoxyribonucleic acid
dppb	1,4-bis(diphenylphosphino)butane
DPPE	1,2-bis(diphenylphosphino)ethane

dppp	1,3-bis(diphenylphosphino)propane
dr	diastereomeric ratio
D.-S.	Dean-Stark conditions
ee	enantiomeric excess
<i>E</i>	entgegen olefin geometry
<i>E.</i>	<i>Escherichia</i>
EI	electrospray ionization
equiv	equivalent(s)
Et	ethyl
FAB	fast atom bombardment
g	gram
GC	gas chromatography
Grubbs II	Grubbs second-generation metathesis catalyst
[H]	reduction
h	hour(s) or height
h $\nu$	light
<sup>1</sup> H	proton
<sup>3</sup> H	tritium
HMBC	heteronuclear multiple bond correlation
HMDS	hexamethyldisilazide or hexamethyldisilazane
HMPA	hexamethylphosphoramide
HPLC	high-performance liquid chromatography
HRMS	high-resolution mass spectroscopy
HSQC	heteronuclear single quantum coherence
Hz	hertz
$\eta^n$	eta; n = number of atoms coordinated to metal

<i>i</i>	iso
IBX	2-iodoxybenzoic acid
IC <sub>50</sub>	concentration required for 50% growth inhibition
IL	interleukin
IMDA	intramolecular Diels-Alder
imid.	imidazole
Imid.	imidazole
IR	infrared spectroscopy
<i>J</i>	coupling constant
k	kilo
<i>k<sub>n</sub></i>	rate constant, n refers to various reactions, negative n indicates reverse reaction
kcal	kilocalories
KHMDS	potassium hexamethyldisilazide
L	liter
$\lambda$	wavelength
LAH	lithium aluminum hydride
LDA	lithium diisopropylamide
LD <sub>50</sub>	Lethal Dosage to kill 50% of test population
LiHMDS	lithium hexamethyldisilazide
LITA	lithium tantalate
lut.	lutidine
<i>m</i>	meta
m	multiplet, meter, or milli
$\mu$	micro
M	mega, metal, or molar

<i>m/z</i>	mass to charge ratio
<i>m</i> -CPBA	<i>meta</i> -chloroperbenzoic acid
Me	methyl
( <i>R,R</i> )-Me-DUPHOS	(-)-1,2-Bis((2 <i>R</i> ,5 <i>R</i> )-2,5-dimethylphospholano)benzene
MEK	methyl ethyl ketone
MH-6o	mouse myelohybridoma cells
MIC	minimal inhibitory concentration
min	minute(s)
mol	mole(s)
mol%	percentage used based on moles
MOM	methoxymethyl
( <i>R</i> )-MOP	( <i>R</i> )-(+)-2-(Diphenylphosphino)-2'-methoxy-1,1'-binaphthyl
mp or m.p.	melting point
Ms	methanesulfonyl
MS	molecular sieves
M.S.	molecular sieves
MTPA	$\alpha$ -methoxy- $\alpha$ -(trifluoromethyl)phenylacetic acid
MVK	methyl vinyl ketone
N	normal
<i>n</i>	<i>normal</i>
n	nano
NBS	<i>N</i> -bromosuccinimide
NMP	<i>N</i> -methylpyrrolidinone
NMR	nuclear magnetic resonance
nOe	nuclear Overhauser effect

NOESY	2D nuclear Overhauser effect spectroscopy
NR	no reaction
<i>o</i>	ortho
[O]	oxidation
<i>p</i>	para
PCC	pyridinium chlorochromate
PDC	pyridinium dichromate
PG	prostaglandin
Ph	phenyl
pH	hydrogen ion concentration in aqueous solution
PhH	benzene
PhMe	toluene
PHOX	phosphinooxazoline
Phth	phthalamidyl
Piv	pivaloyl
PMA	phorbol myristate acetate
PMB	<i>p</i> -methoxybenzyl
PMBM	<i>p</i> -methoxybenzyloxymethyl
<i>p.o.</i>	administered orally
ppm	parts per million
PPTS	pyridinium <i>p</i> -toluenesulfonate
Pr	propyl
<i>i</i> -Pr	isopropyl
psi	pounds per square inch
Py, py or Pyr	pyridine
q	quartet

QUINAP	( <i>R</i> )-(+)-1-(2-diphenylphosphino-1-naphthyl)isoquinoline
R	alkyl group
<i>R</i>	rectus (configurational)
Rearr.	Rearrangement
Red-Al	sodium bis(2-methoxyethoxy)aluminum hydride
$R_f$	retention factor
RNA	ribonucleic acid
ROESY	rotational nuclear Overhauser effect spectroscopy
s	singlet
<i>S</i>	sinister (configurational)
<i>S.</i>	<i>Salmonella</i> or <i>Staphylococcus</i>
SAE	Sharpless asymmetric epoxidation
SAR	structure activity relationship
sat.	saturated
sept.	septet
$S_N'$	allylic nucleophilic substitution
$S_N1$	unimolecular nucleophilic substitution
$S_N2$	bimolecular nucleophilic substitution
<i>sp.</i>	<i>species</i>
stoich.	stoichiometric
t	triplet
<i>t</i>	<i>tertiary</i>
$t_{1/2}$	half-life
TBAC	tetrabutylammonium chloride
TBAF	tetrabutylammonium fluoride

TBAI	tetrabutylammonium iodide
TBAT	tetrabutylammonium triphenyldifluorosilicate
TBDPS	<i>tert</i> -butyldiphenylsilyl
TBS	<i>tert</i> -butyldimethylsilyl
temp	temperature
TEA	triethylamine
TES	triethylsilyl
Tf	trifluoromethanesulfonyl
TFA	trifluoroacetic acid
THF	tetrahydrofuran
TIPS	triisopropylsilyl
TLC	thin-layer chromatography
TMEDA	tetramethylethylenediamine
TMS	trimethylsilyl
TOF	turnover frequency
TON	turnover number
TPAP	tetrapropylammonium perruthenate
TROC	trichloroethoxycarbonyl
Ts	<i>p</i> -toluenesulfonyl or <i>p</i> -toluenesulfonic
UV	ultraviolet
Vis	visual wavelength
v/v	volume per volume
wt%	percent by weight
w/v	weight per volume
X	halide or trifluoromethanesulfonate
Z	zusammen olefin geometry

# CHAPTER ONE

## The Biology and Chemistry of the Zoanthamine Alkaloids

### 1.1.1 Introduction<sup>1</sup>

Marine species comprise a vast repository for natural products isolation. In this chapter, we will focus on the biology and chemistry of the zoanthamine alkaloids, isolates from marine zoanthids. The order zoantharia consists of an intriguing group of marine polyps, morphologically classified into at least a dozen genera. Species in this order are widely dispersed throughout the temperate and tropical regions of the Indian, Pacific, and Atlantic Oceans, and these vibrant soft corals are generally aggressive colonizers of reef environments. In the wild, these stunning organisms (Figure 1.1.1) reproduce both sexually and asexually.<sup>2</sup> Recently, analysis of their respective mitochondrial DNA has elucidated the relationships between them.<sup>3</sup>



**Figure 1.1.1** Representative zoanthids.

The polyps have a tube-shaped body and are radially symmetrical. Atop the body are tentacles that guide food to the central orifice for digestion. When alarmed, the polyps contract their tentacles inward, and some species also expel a stream of water laden with powerful toxins from their bodies as a means of defense from predators. For

example, the zoanthids from which the zoanthamines were isolated release a severe eye-irritant when disturbed.<sup>4</sup> Zoanthids frequently contain symbiotic microalgae, which provide additional energy via photosynthesis. These dinoflagellate algae are thought to play an important role in the biosynthesis of some of the secondary metabolites isolated from the zoanthids.<sup>5</sup>

Diverse natural product archetypes have been isolated from species in the order zoantharia (Figure 1.1.2). Zoanthamine (**1**) is a member of the *Zoanthus* alkaloids, the subject of this chapter. Zoanthusterone (**2**) is an ecdysteroid isolated from a *Zoanthus* sp.<sup>6</sup> Prostaglandins like PGA<sub>2</sub> (**3**), isolated from *Palythoa kochii*, stabilize microtubules in a manner similar to paclitaxel.<sup>7</sup> A family of more than a dozen natural products based on the zoanthoxanthin (**4**) skeleton has been isolated from *Parazoanthus axinellae*.<sup>8</sup> A related structure, parazoanthoxanthin A, shows anticholinesterase activity.<sup>9</sup> Perhaps the best-known isolate from these marine organisms is palytoxin (**5**). Isolated from *Palythoa* sp. in the Hawaiian islands, palytoxin is one of the most toxic compounds known, with an LD<sub>50</sub> of 15 µg/kg in mice.<sup>10</sup> The palytoxin structure was determined by Kishi, Uemura, and Hirata, and later synthesized by Kishi.<sup>11</sup>

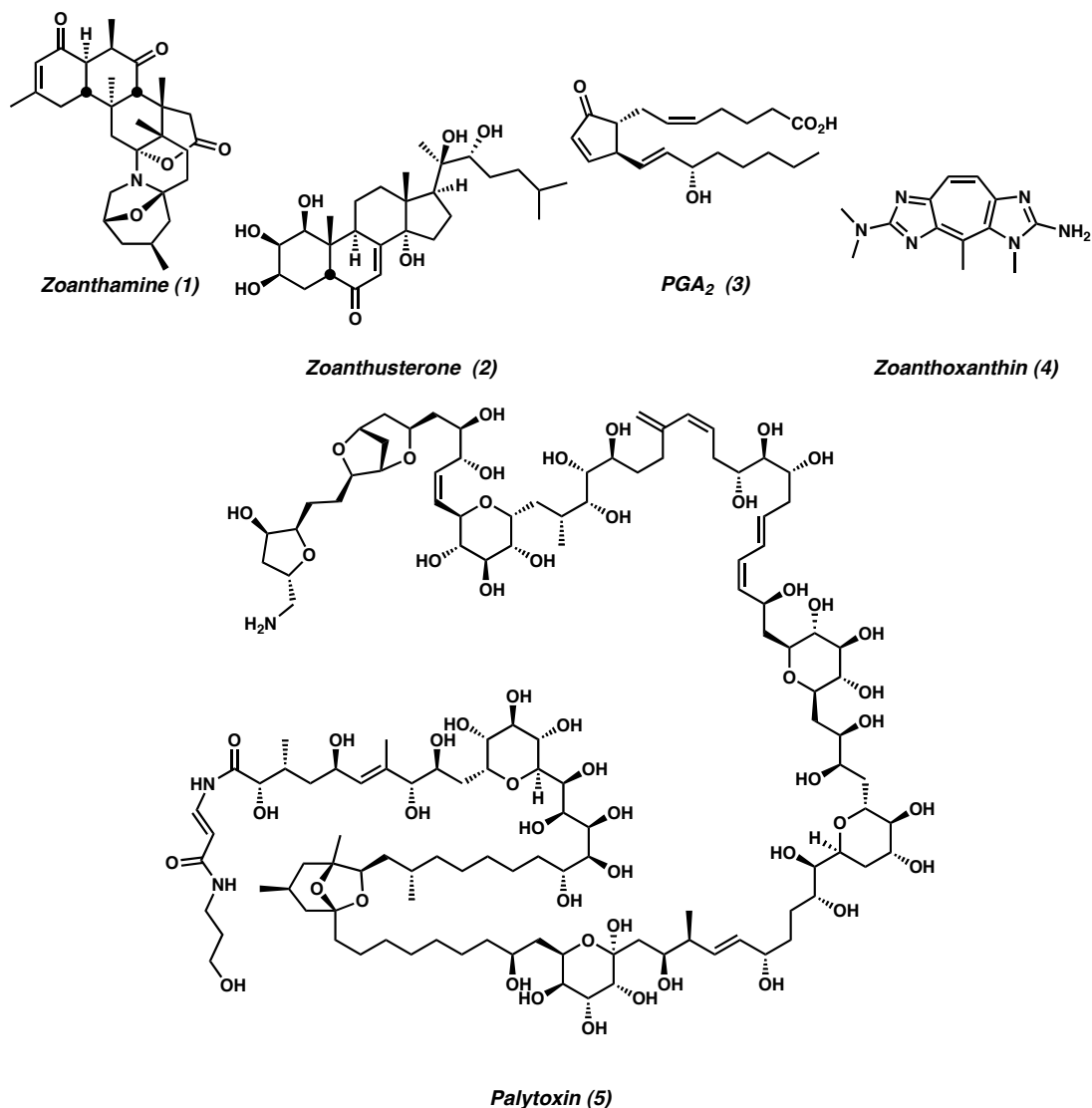


**Figure 1.1.2** Natural products isolated from zoanthids.

## 1.2 The Zoanthamine Natural Products

### 1.2.1 Isolation and Structural Characterization of the Zoanthamine Natural Products

In 1984, Rao and coworkers disclosed the isolation of the natural product zoanthamine (**1**) from a species of the genus *Zoanthus* off the Visakhapatnam coast of India.<sup>4</sup> The connectivity and relative stereochemistry of the previously unknown alkaloid skeleton was unambiguously determined by single-crystal X-ray diffraction.<sup>4</sup> Throughout this thesis, carbon numbering and ring naming will refer to that of

zoanthamine (Figure 1.2.1). The initial isolation effort also afforded the related natural products zoanthenamine (6) and zoanthenamide (7), which were reported in 1985.<sup>12</sup> In 1989, Rao and coworkers isolated 28-deoxyzoanthenamine (8) and 22-*epi*-28-deoxyzoanthenamine (9) from a *Zoanthus* species in the Bay of Bengal.<sup>13</sup> Structures 6–9 were deduced by comparison with zoanthamine's spectroscopic data. Although these isolation efforts were undertaken in search of a known eye irritant produced by the *Zoanthus* species, all five of the isolated alkaloids showed inhibition of phorbol myristate acetate (PMA)-induced inflammation in mouse ears.<sup>4,12</sup>

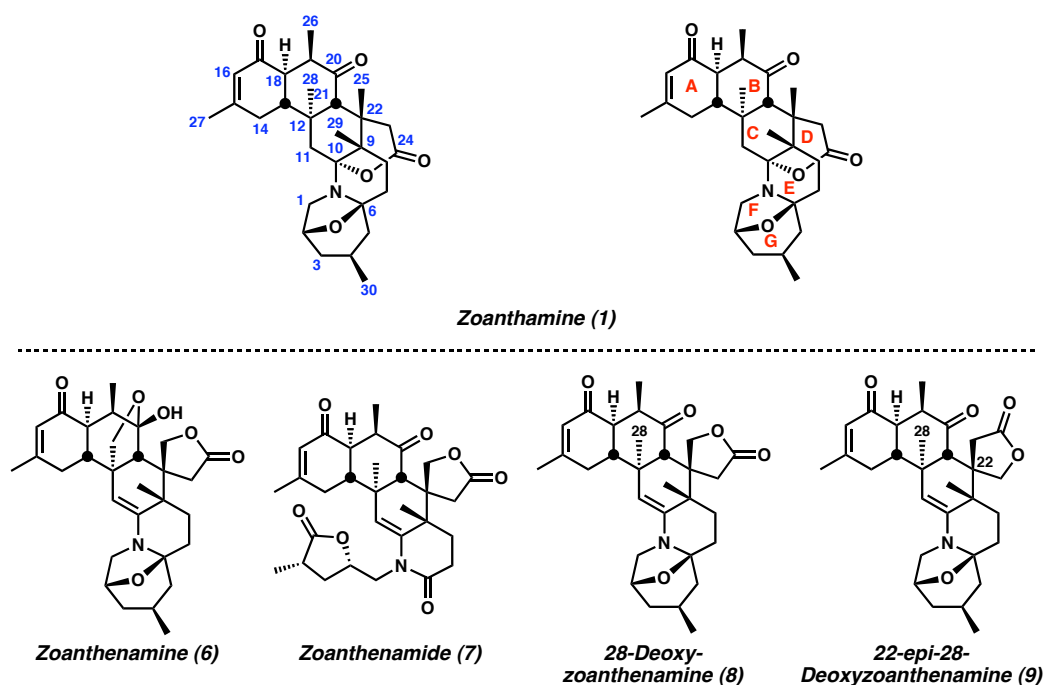


**Figure 1.2.1** Zoanthamine natural products isolated by Rao.

In 1995, Uemura identified five new zoanthamine natural products isolated from a *Zoanthus* species collected off the Ayamaru coast of the Amami Islands south of Japan.<sup>14</sup> These isolates displayed structural variations including compounds lacking functionality at C(19) such as norzoanthamine (10) and norzoanthenamine (11), which is also oxidized at C(11). Oxyzoanthamine (12) is unique in displaying C(26) oxidation (Figure 1.2.2). The relative configuration of norzoanthamine was confirmed by X-ray



result of the structural change, extensive HMBC and ROESY correlation experiments were performed to confirm its structure and relative stereochemistry.<sup>18</sup>

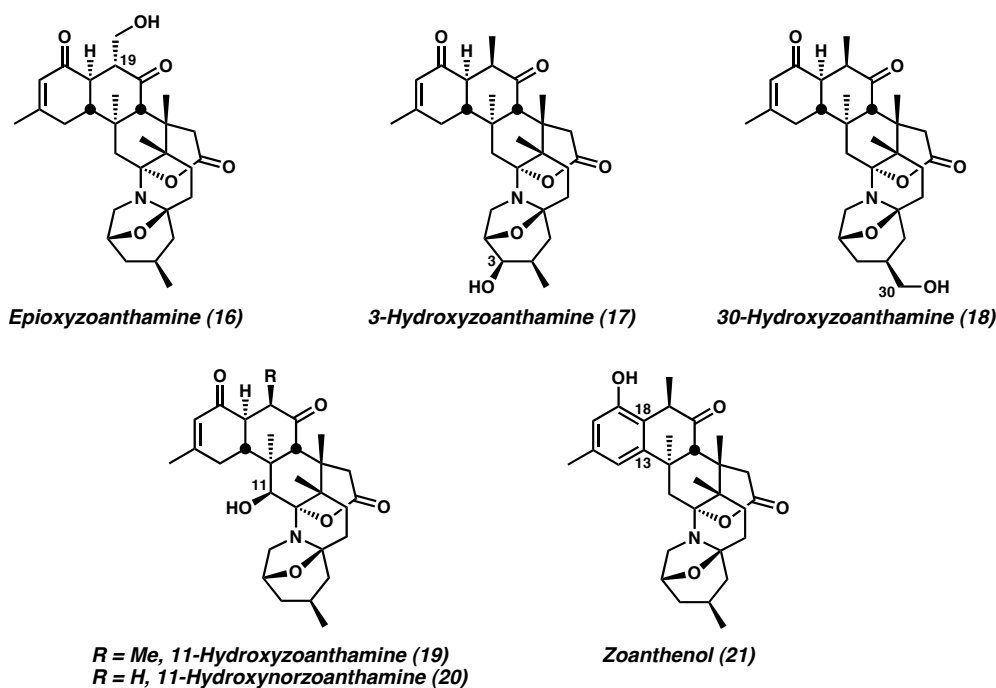
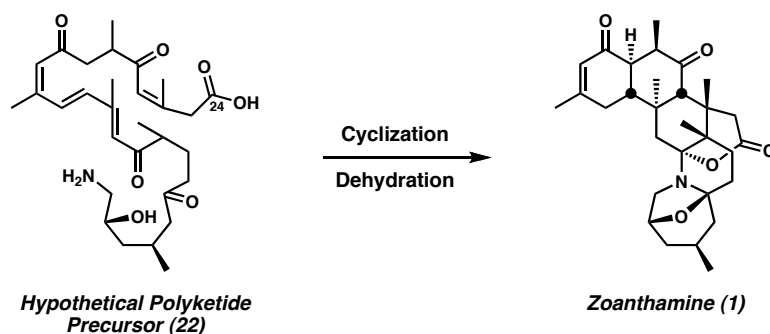


**Figure 1.2.3** Zoanthamine natural products isolated by Norte.

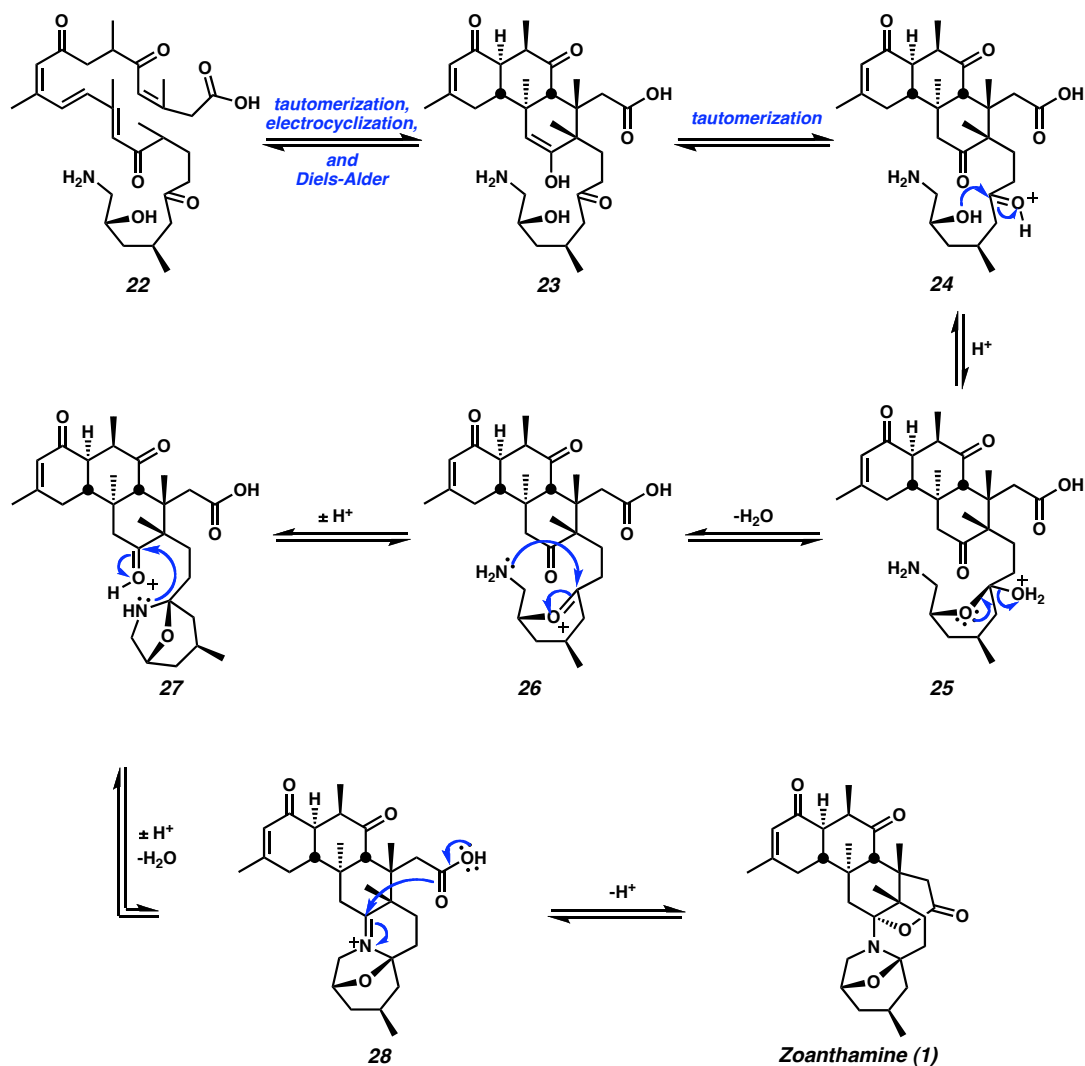
### 1.2.2 Biosynthesis of the Zoanthamine Natural Products

Despite their history of more than 20 years, relatively little is known about the biosynthesis of the zoanthamine natural products. Rao and coworkers noted in 1985 that elements of the 30-carbon zoanthamine skeleton suggest a triterpene origin, however they were unable to identify normal head-to-tail linkages to account for the zoanthamine skeleton.<sup>4</sup> More recently, Uemura has proposed that the zoanthamines may arise from polyketide precursor **22** (Scheme 1.2.1)<sup>15,19</sup> beginning at C(24) with a glycine unit,<sup>5</sup> but he does not further describe the pathway. Nevertheless, proposed intermediate **22** accounts for most of the oxygenation found in the zoanthamines, and it does readily lead to the zoanthamine structure following standard organic reaction mechanisms (Scheme 1.2.2).



**Scheme 1.2.1** Hypothetical polyketide precursor.

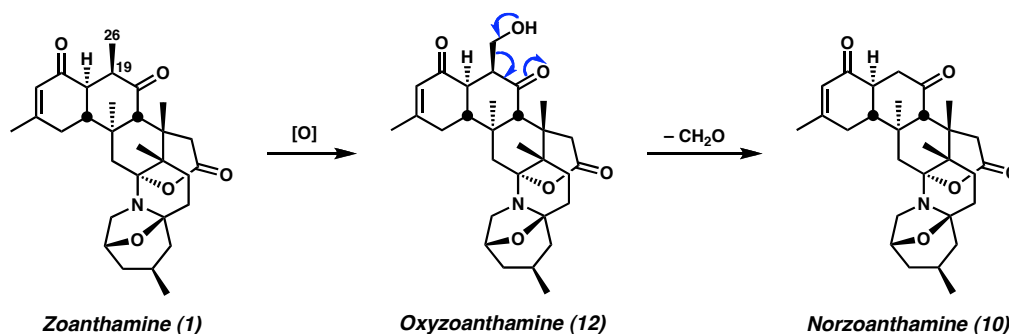
The conversion of **22** to **1** begins with tautomerization, electrocyclization, and Diels-Alder steps to form intermediate **23**. Tautomerization and carbonyl activation of **23** yield **24**, which undergoes 6-*exo* alcohol attack and protonation to form intermediate **25**. Oxocarbenium formation with loss of water gives **26**. Subsequent amine attack and proton transfer leads to intermediate **27**. Iminium formation provides **28**, then carboxylic acid attack and deprotonation provides zoanthamine (**1**). The reversibility of each step in the formation of the DEFG ring system allows formation of the thermodynamically favored product, a fact that will become important for synthetic efforts discussed later in this chapter.



**Scheme 1.2.2** Potential mechanism for cyclization of polyketide precursor **22**.

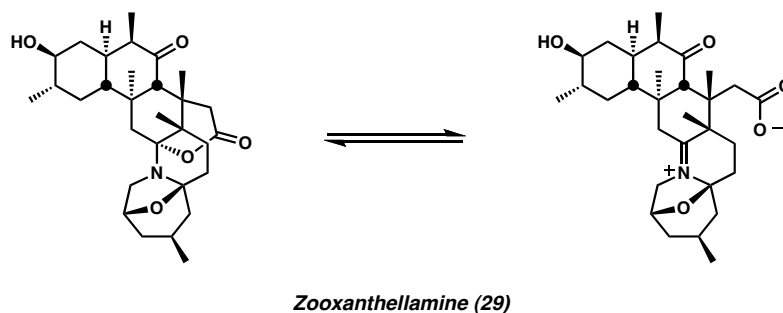
In addition to his polyketide proposal for zoanthamine, Uemura addresses the potential origin of the norzoanthamine-type alkaloids, which do not possess a methyl group at C(19). The isolation of oxyzoanthamine (**12**) prompted Uemura to propose an oxidative mechanism for the demethylation of zoanthamine (Scheme 1.2.3). Direct oxidation of zoanthamine at C(26) to the intermediate oxyzoanthamine, which is poised to undergo a retro-aldol reaction, formally releases formaldehyde and norzoanthamine (**10**).<sup>14</sup> It is unclear why Uemura does not propose substitution of an acetate unit for the relevant propionate unit proposed in Scheme 1.2.1. Such a modification would allow

quicker access to the zoanthamines lacking C(26), such as norzoanthamine (**10**), while direct oxidation of C(26) itself could still explain oxyzoanthamine (**12**).



**Scheme 1.2.3** Proposed biosynthesis of norzoanthamine.

Another factor complicating the understanding of zoanthamine alkaloid biosynthesis is the role of the symbiotic dinoflagellate algae that are commonly contained in zoanthids. Algae of the genus *Symbiodinium* have been isolated from zoanthids of the genus *Zoanthus*.<sup>20</sup> Although such symbiotic strains are difficult to culture in isolation, Nakamura and coworkers have been able to produce quantities of *Symbiodinium sp.* free of zoanthids.<sup>5</sup> While the algae produced different distributions of metabolites depending on the media used, significant experimentation with culture conditions allowed Nakamura's group to isolate a new C<sub>30</sub> alkaloid they named zooxanthellamine (**29**). Zooxanthellamine exists as a mixture of lactone and zwitterionic iminium forms (Scheme 1.2.4). Its structure and relative configuration were established by extensive NMR studies. Zooxanthellamine has the same sense of absolute configuration as the zoanthamine alkaloids, as demonstrated by NMR comparison of its MTPA esters.<sup>5</sup>



**Scheme 1.2.4** Structure of zooxanthellamine.

The remarkable similarity between zooxanthellamine and zoanthamine has called into question the role of the zoanthids in producing the zoanthamine natural products.<sup>21,22</sup> It may be that the zoanthids play only a small role in the biosynthesis, such as adjusting the oxidation state of the completed zoanthamine skeleton. The subtle variations in the alkaloids' structures could be determined by factors in the marine environment or by the host zoanthid species. Alternatively, different species of algae may be involved in the production of different zoanthamines.

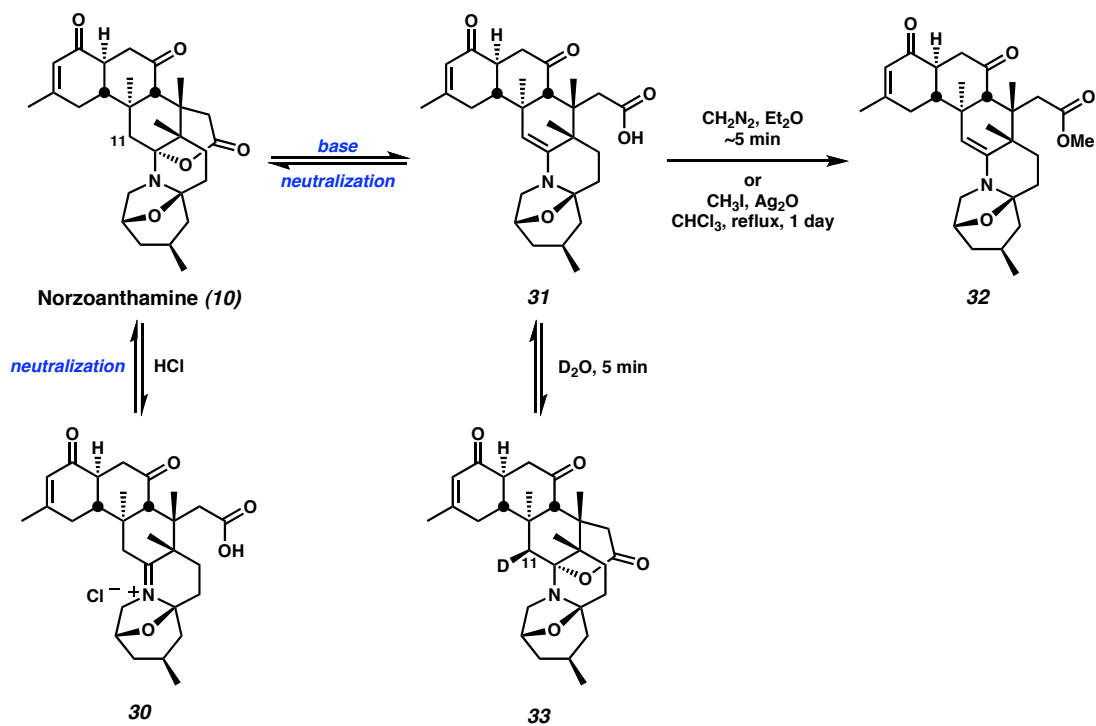
To date, there has been only one published attempt at a study directed toward the elucidation of the biogenesis of the zoanthamines. Norte and coworkers conducted a feeding study, during which labelled sodium acetate, glycine, and glucose were fed to small colonies of *Zoanthus* sp.<sup>8</sup> Although levels of incorporation of the labelled atoms were higher than 10% for all cases, the incorporation appeared to be random, leaving the question of the zoanthamines' biosynthesis unanswered.

Perhaps the clearest insight offered by these biosynthetic proposals is that there is a definite need for further experimental studies elucidating the biogenesis of these compounds. Without such experimental data, biosynthetic proposals cannot be either soundly supported or rationally refuted.

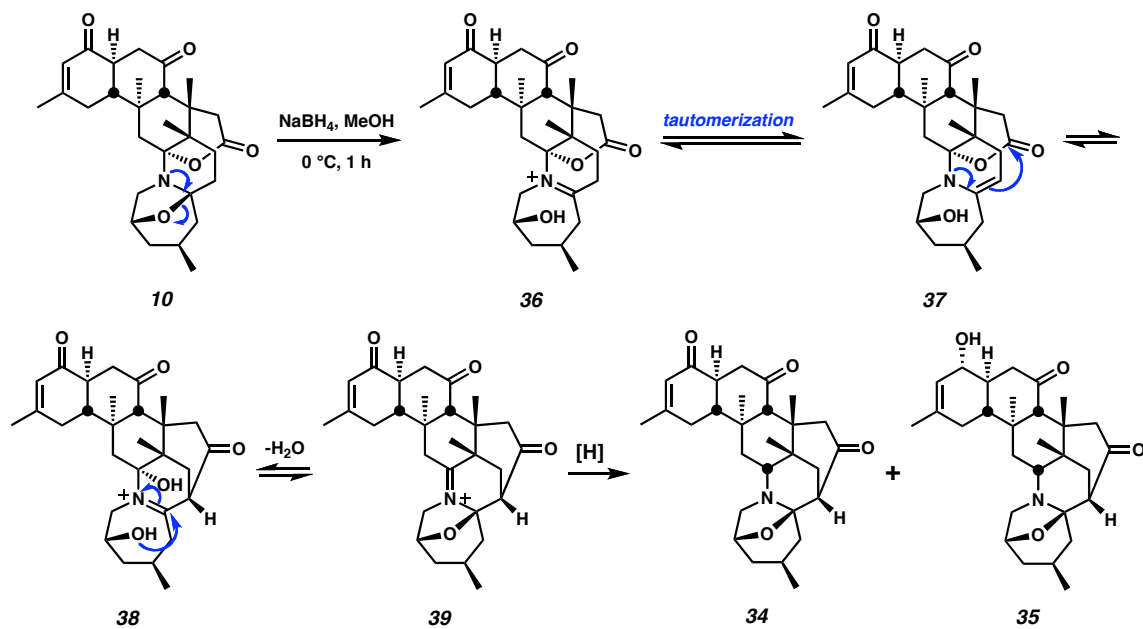
### 1.2.3 Reactivity Studies of Norzoanthamine

Following its isolation, norzoanthamine was subjected to a number of reaction conditions to aid in the formation of hypotheses about its mechanism of action for various biological activities. Fluxion between lactone and iminium isomers, similar to the equilibration observed with zooxanthellamine (Scheme 1.2.4), has been demonstrated in several zoanthamine natural products (Scheme 1.2.5). Norzoanthamine forms iminium **30** under acidic conditions and reverts upon neutralization.<sup>19</sup> Under neutral to basic conditions, elimination occurs to form enamine **31**. The equilibrium between norzoanthamine and enamine **31** was demonstrated by the conversion of norzoanthamine to methyl ester **32** in minutes upon exposure to diazomethane.<sup>19</sup> Furthermore, NMR spectra of norzoanthamine in D<sub>2</sub>O show specific and complete deuterium incorporation at the 11 $\beta$  position to give deuteride **33** in minutes.<sup>17,18</sup> Similar rates of deuterium incorporation were observed with zoanthenol, 3-hydroxy-norzoanthamine, and 30-hydroxynorzoanthamine. In contrast, the 11 $\beta$ -hydroxy-zoanthamines did not show significant deuterium incorporation, suggesting that the elimination to an enamine is inaccessible.<sup>18</sup> This fluxional behavior in aqueous media at physiologically relevant pH may play an important role in determining the bioactivities of these molecules.

The hemiaminal region of the zoanthamine alkaloids also shows intriguing reactivity under reductive conditions. Treatment of norzoanthamine with sodium borohydride generates two anomalous products, enone **34** and allylic alcohol **35** (Scheme 1.2.6).<sup>15,19</sup> The formation of these products may be explained by opening of the hemiaminal to form iminium **36**. Deprotonation leads to enamine **37**, which is believed to attack the lactone in an intramolecular fashion to afford keto-iminium **38**. Dehydration generates iminium **39**, which undergoes reduction to give enone **34**. Further reduction affords allylic alcohol **35**.



**Scheme 1.2.5** Equilibria between lactone and enamine isomers of norzoanthamine.



**Scheme 1.2.6** Anomalous reduction of norzoanthamine.

### *1.3 Biological Activities of Zoanthamine Alkaloids*

#### *1.3.1 Anti-Osteoporotic Activity*

Perhaps the best-studied and most well known biological activity of the zoanthamine alkaloids is the anti-osteoporotic effect first reported by Uemura in 1996.<sup>23</sup> Osteoporosis is a loss of bone mineral density that often results when osteoclasts reabsorb bone tissue at a rate faster than it is regenerated.<sup>24</sup> Norzoanthamine and its hydrochloride salt have been shown *in vivo* to prevent the symptoms of osteoporosis in ovariectomized mice, a pharmaceutical model for postmenopausal osteoporosis.<sup>23</sup> Ovariectomized mice, inherently deficient in estrogen, quickly lose bone mass and strength. However, at doses of 0.4 and 2.0 mg/kg/d (five days a week for 4 weeks, *p.o.*) of norzoanthamine hydrochloride, these mice retained femur weight at statistically higher rates than the untreated ovariectomized mice. With doses from 0.016–0.4 mg/kg/d of norzoanthamine hydrochloride, the femurs of ovariectomized mice maintained strength, measured by failure load at nearly comparable levels to nonovariectomized control mice. Finally, mice treated with norzoanthamine hydrochloride possessed cortical bone that is significantly thicker than that found in the control animals.<sup>25</sup>

In analogy to estrogen replacement therapy in postmenopausal women, treatment with 17 $\beta$ -estradiol rescues ovariectomized mice from the effects of osteoporosis. However, treatment with norzoanthamine hydrochloride shows interesting differences from estrogen therapy. 17 $\beta$ -Estradiol causes a dose-dependent increase in uterine weight in treated mice, while mice treated with norzoanthamine hydrochloride did not exhibit this side effect.<sup>25</sup>

The origin of norzoanthamine's anti-osteoporotic effect may lie in its ability to suppress the production of interleukin 6 (IL-6). IL-6 is involved in stimulating the generation of osteoclasts, which reabsorb bone tissue. Estrogen thus derives its anti-osteoporotic properties from the inhibition of IL-6 production.<sup>26</sup> Norzoanthamine and

its hydrochloride salt (**24**) suppress the excretion of IL-6 from preosteoblastic cells at respective concentrations of 13 and 4.6  $\mu\text{g}/\text{mL}$  in vitro.<sup>27</sup> However, in vitro studies with norzoanthamine hydrochloride showed no effect on osteoclast formation. Also, suppression of IL-6 secretion has not yet been demonstrated in vivo.<sup>25</sup> These last two points, along with the lack of uterine weight gain in ovariectomized mice, suggest that the zoanthamine alkaloids may act by a mechanism distinct from estrogen therapies.<sup>28</sup> Thus, they may offer treatments for post-menopausal osteoporosis that induce fewer side effects.

The need to find nonestrogen osteoporosis therapies has spurred considerable effort to define a structure activity relationship (SAR) for norzoanthamine's anti-osteoporotic effects. Via semi-synthesis, Uemura and coworkers produced and tested a number of norzoanthamine derivatives (Figure 1.3.1).<sup>19,27</sup> It should be noted that all of the derivatives assayed were significantly less efficacious (higher  $\text{IC}_{50}$  values) in limiting IL-6 production than norzoanthamine.<sup>29</sup> The studies revealed that the removal of the olefin (ketone **41** and diol **42**) caused some loss in activity. Furthermore, disruption of the lactone/hemiaminal functionality (carboxylic acid **43** and ester **32**) resulted in a significant drop in activity as well.<sup>19</sup>

More recently, Hirama and coworkers have conducted an SAR study of zoanthamine-related molecules to determine the structural features needed to inhibit the growth of IL-6 dependent MH-60 cells (Figure 1.3.2).<sup>30</sup> In their assays, the zoanthamine hydrochloride salts **30** and **44** showed the greatest inhibition of MH-60 cell growth with  $\text{IC}_{50}$  values of 13 and 26  $\mu\text{M}$ , respectively. A mimic of zoanthenol's "northern" carbocyclic region **45** and a mimic of the zoanthamine "southern" heterocyclic region **46** both showed very poor activity. However, iminium **47**, demonstrated activity approaching that of the zoanthamine hydrochlorides. This result provides further support for two trends: (a) the hydrochloride salt form of a zoanthamine-related

molecule is typically a more active inhibitor of IL-6 production than the natural product, and (b) the heterocyclic portion of the molecule likely is important in the pharmacophore for IL-6 inhibition.

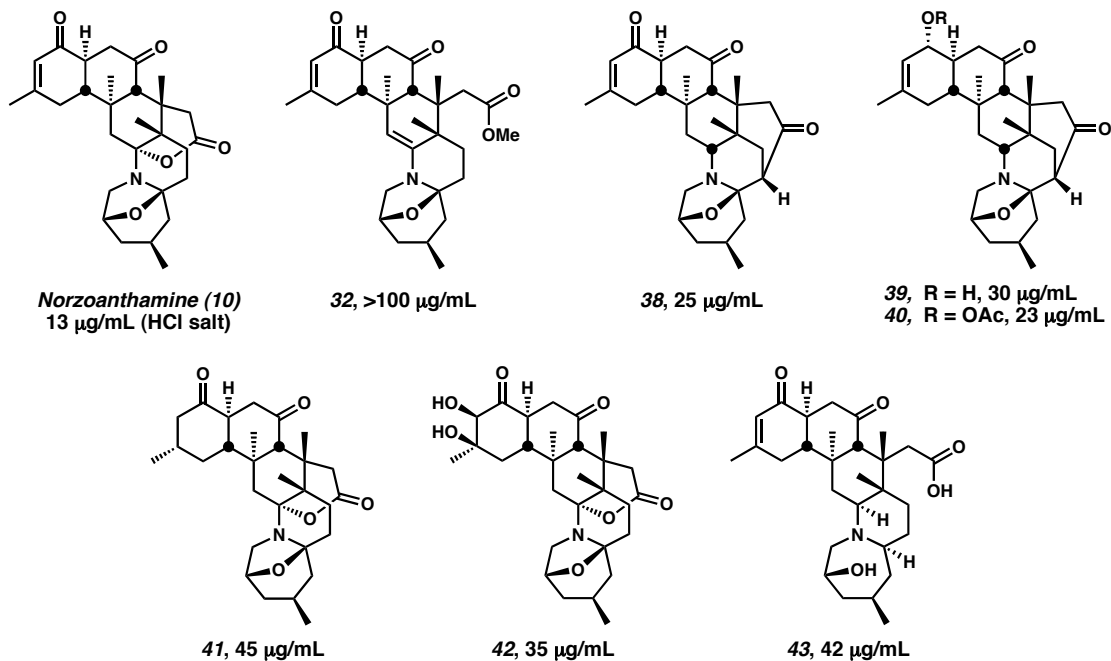


**Figure 1.3.1**  $\text{IC}_{50}$  values for the inhibition of IL-6 production in Uemura's SAR study.

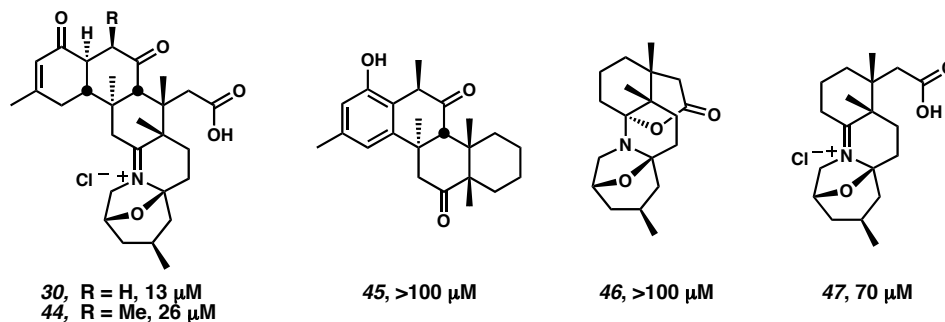


**Figure 1.3.2**  $\text{IC}_{50}$  values for the inhibition of IL-6 dependent cell growth.

### 1.3.2 Miscellaneous Biological Activities

A variety of other biological activities have been reported for molecules in the zoanthamine family. As previously mentioned, zoanthamine (**1**), zoanthenamine (**6**), and zoanthenamide (**7**) were found to be inhibitors of PMA-induced inflammation in

mouse ear.<sup>4,12</sup> Uemura and coworkers reported that norzoanthamine (**10**), norzoanthaminone (**11**), oxyzoanthamine (**12**), cyclozoanthamine (**14**), and epinorzoanthamine (**15**) display significant cytotoxicity against P388 murine leukemia cells (Table 1.3.1).<sup>14</sup> The most potent cytotoxicity was displayed by norzoanthaminone.

### Cytotoxicity

Compound	IC <sub>50</sub> (μg/mL) for Inhibition of P388 Murine Leukemia Cells
Norzoanthamine ( <b>10</b> )	24.0
Norzoanthaminone ( <b>11</b> )	1.0
Oxyzoanthamine ( <b>12</b> )	7.0
Cyclozoanthamine ( <b>14</b> )	24.0
Epinorzoanthamine ( <b>15</b> )	2.6

**Table 1.3.1** Cytotoxicity of the zoanthamine alkaloids.

The antibacterial properties of zoanthamine and several of its reduced derivatives have also been investigated.<sup>31</sup> In disk susceptibility experiments, the zoanthamine alkaloids showed activity against both Gram negative and Gram positive bacteria (Table 1.3.2).

### Antibacterial Activity

Compound	Inhibition Zone (diameter in mm)			
	Gram Negative		Gram Positive	
	<i>S. typhimurium</i>	<i>E. coli</i>	<i>B. sphaericus</i>	<i>S. aureus</i>
Zoanthamine ( <b>1</b> )	6	6	8	7
<b>48</b>	12	6	8	10
<b>49</b>	7	6	8	10
<b>50</b>	6	7	7	9

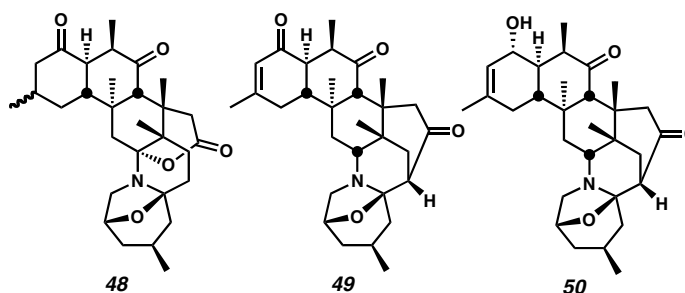


**Table 1.3.2** Summary of antibacterial activities.

More recently, the effect of zoanthamine alkaloids on human platelet aggregation has been investigated.<sup>32</sup> These experiments showed that at concentrations of 0.5 mM, 11 $\beta$ -hydroxyzoanthamine (**19**) and related methyl ester **32** inhibit platelet aggregation caused by collagen, arachidonic acid, and thrombin. Oxyzoanthamine (**12**) and zoanthenol were highly selective inhibitors, showing inhibition of aggregation in the presence of collagen at 0.5 mM, but showing almost no activity in the presence of arachidonic acid or thrombin. Such selective activity is important in the potential treatment of cardiovascular disease. Formation of a thrombus due to abnormal platelet aggregation can lead to obstruction of a vein or artery, causing a cardiovascular event.<sup>33</sup> Several antithrombotic agents are already in use as cardiovascular disease treatments; however, their efficacy is limited by weak antithrombotic effects at the administered dosage and/or deleterious side effects such as the inhibition of haemostasis, leading to significant abnormal bleeding.<sup>34</sup> Experimental and clinical evidence indicate that a selective collagen receptor antagonist will result in only a very small change in haemostasis, meaning a safer, yet still potent drug.<sup>34</sup>

## *1.4 Synthetic Approaches Toward the Zoanthamine Natural Products*

### *1.4.1 General Remarks*

The intriguing diversity of biological activities and the densely functionalized structures of the zoanthamine alkaloids have inspired a host of synthetic chemistry groups to publish strategies toward the total syntheses of these molecules. Many researchers have focused their efforts on the synthesis of the tricyclic ABC ring system, which poses a significant synthetic challenge due to its stereochemical density. For example, the C ring contains three quaternary stereocenters in vicinal and nonvicinal relationships. In addition to the difficulty of synthesizing quaternary centers, their steric bulk also renders even routine transformations on nearby functionality troublesome.

Other researchers have focused on the synthesis of the heterocyclic DEFG rings. The DEFG ring system presents the challenge of forming the heterocycles with the correct hemiaminal connectivity and stereochemistry.

#### 1.4.2 Miyashita's Synthesis of Norzoanthamine

Twenty years after the isolation of the first zoanthamine alkaloids, Miyashita and coworkers reported the first and, as yet, only completed total synthesis of a zoanthamine alkaloid with their synthesis of norzoanthamine.<sup>35</sup> The general synthetic plan is illustrated in Figure 1.4.1. This impressive 41-step effort included several creative solutions to problems that arose during the execution of the synthesis. Their Diels-Alder strategy for the construction of the ABC ring system of norzoanthamine was disclosed in 2002 (Scheme 1.4.1).<sup>36</sup>

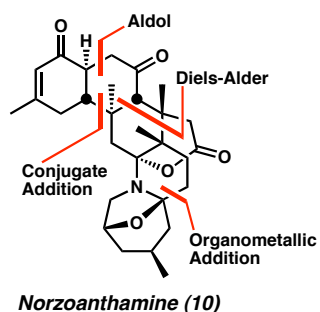
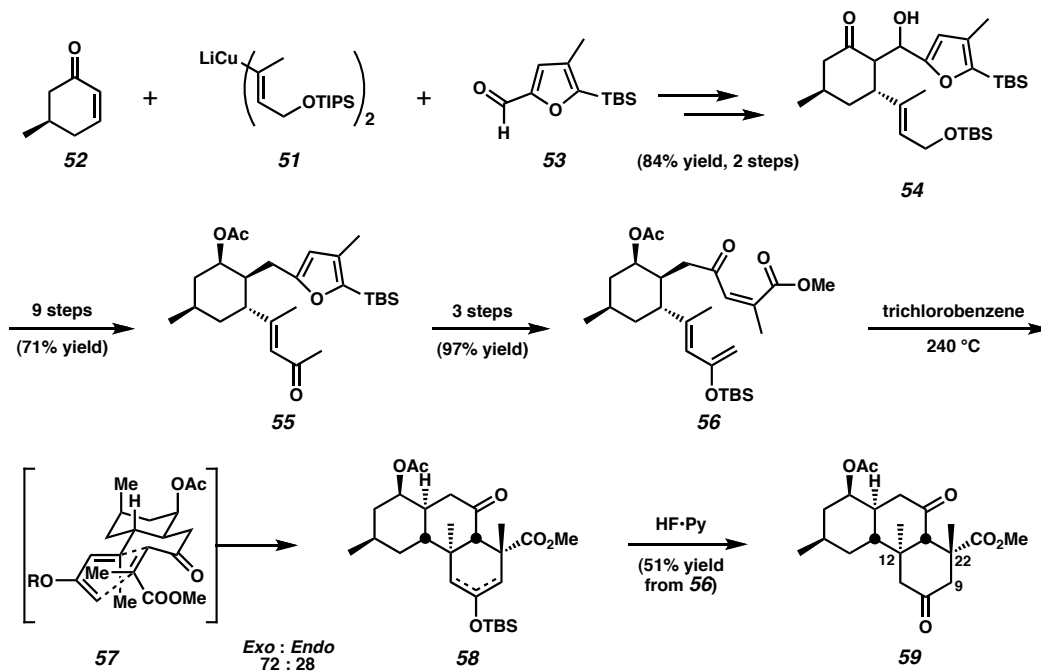


**Figure 1.4.1** Miyashita's retrosynthetic analysis of norzoanthamine.

The synthesis begins with addition of cuprate **51** to enantiopure enone **52**, followed by an aldol reaction with aldehyde **53** to provide ketone **54**. This efficient sequence set the absolute stereochemistry at C(13), from which the remaining stereocenters were derived. Following several functional group manipulations, furan **55** was photochemically oxidized using Katsumura conditions. Subsequent silyl enol ether formation provided Diels-Alder substrate **56**. Upon heating to 240 °C, the Diels-Alder reaction proceeded predominantly through the desired exo transition state **57** to a mixture of silyl enol ether isomers **58**. After silyl cleavage, diastereomerically pure

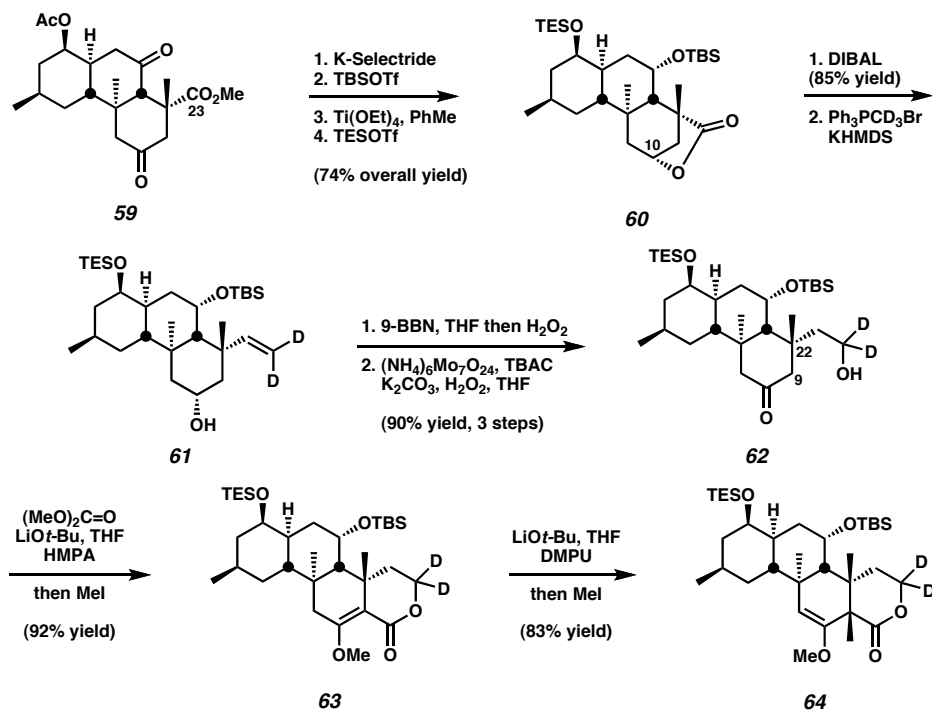
ketone **59** was isolated in 51% yield over the two steps. This Diels-Alder reaction sets both the C(12) and C(22) quaternary centers of norzoanthamine with the correct absolute stereochemistry.



**Scheme 1.4.1** Miyashita's Diels-Alder construction of the ABC core.

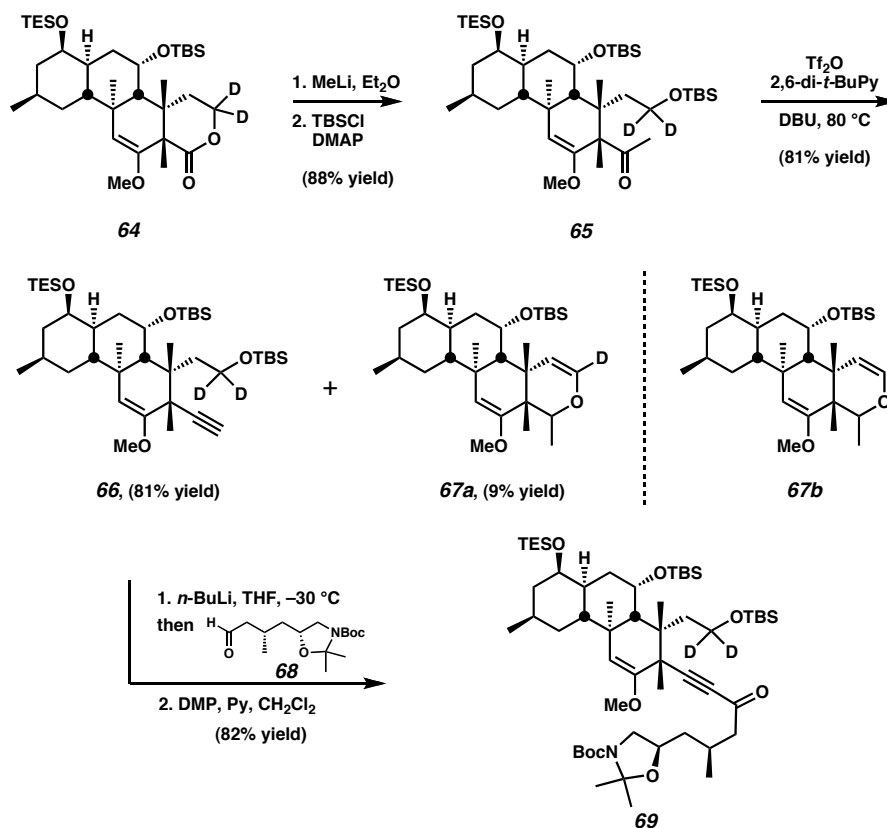
At this point, a number of functional group manipulations were undertaken to allow homologation at C(23) and installation of the final quaternary center at C(9) (Scheme 1.4.2). Diastereoselective reduction of both ketones in **59** was accomplished by K-selectride addition from the convex face, resulting in the desired lactone formation at the C(10) hydroxyl. Silylation with TBSOTf, acetate cleavage, and TES protection afforded protected lactone **60**. Reduction of the lactone to the lactol followed by Wittig reaction provided bis-deutero olefin **61**. Hydroboration and oxidation provided ketone **62**, which was poised for formation of the C(9) quaternary center. To that end, acylation of ketoalcohol **62** with dimethyl carbonate and lithium *tert*-butoxide proceeded regioselectively, presumably due to initial alcohol acylation and subsequent lactone formation by C-acylation of the enolate. This series of events was followed by quenching

with methyl iodide to give lactone **63**. Upon treatment with lithium *tert*-butoxide and methyl iodide in DMPU, lactone **63** underwent C-alkylation to give quaternized  $\delta$ -lactone **64**. Impressively, this difficult transformation provided a single diastereomer in 83% yield.



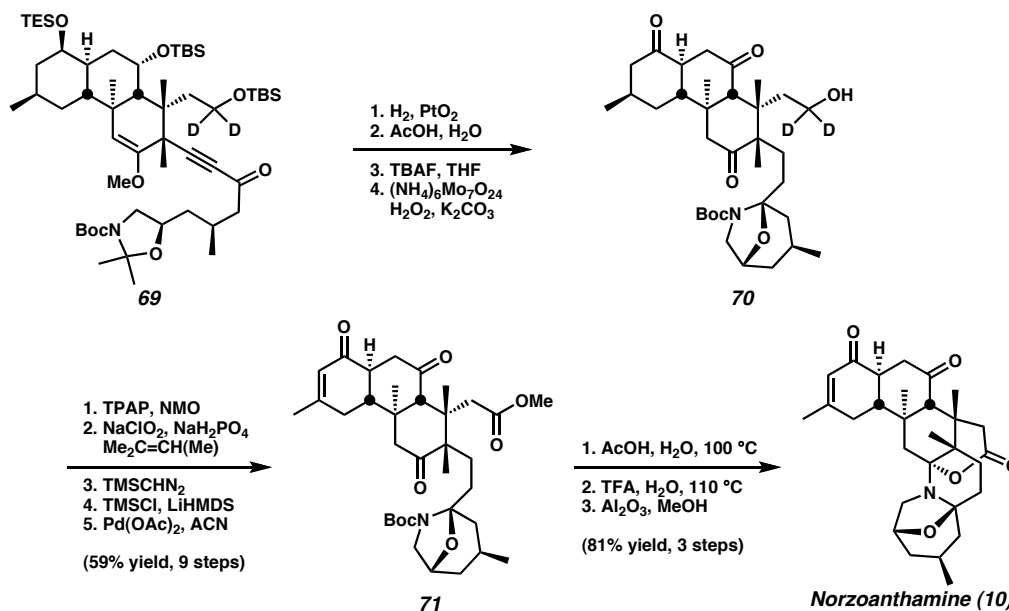
**Scheme 1.4.2** Functionalization of the ABC core.

The synthesis of the southern portion of norzoanthamine began with conversion of the C(8) lactone to an alkyne followed by side chain addition (Scheme 1.4.3). Monoaddition of methyl lithium into lactone **64** then silyl protection provided methyl ketone **65**, which was converted to alkyne **66** by treatment with triflic anhydride and DBU. This conversion was accompanied by formation of a small amount of by-product **67a**. In the corresponding non-deuterated substrate, the by-product **67b** was formed in 30% yield, reducing the yield of the desired alkyne to 66%. The carbon skeleton of norzoanthamine was completed by the addition of aldehyde **68** to the lithium salt of alkyne **66** and oxidation of the resulting alcohol to ynone **69**.



**Scheme 1.4.3** Attaching the southern side chain.

Completion of the target required a further twelve steps of deprotection, oxidation state adjustment, and dehydration (Scheme 1.4.4). From **69**, alkyne reduction, acidic enol ether cleavage and acetal removal, global desilylation, and secondary alcohol oxidation provided **70**. Sequential oxidation of the primary alcohol provided the carboxylic acid, which was esterified with TMS-diazomethane. Saegusa-Ito oxidation installed the A ring enone, yielding **71**. Treatment of **71** with hot aqueous acetic acid resulted in carbamate cleavage and iminium formation. Upon being subjected to aqueous TFA at 110 °C, the methyl ester added into the iminium ion, forming the TFA salt of norzoanthamine. The salt was treated with basic alumina in methanol to reveal the natural product. In addition to the impressive synthetic accomplishment, this synthesis also served to unambiguously confirm the absolute stereochemistry of norzoanthamine, which had previously been deduced from NMR experiments.



**Scheme 1.4.4** The completion of norzoanthamine.

#### 1.4.3 Tanner's Diels-Alder Approach to the Zoanthamine ABC Ring System

Tanner and coworkers also chose to assemble the ABC rings via a Diels-Alder approach (Figure 1.4.2). A Stille coupling was planned for the synthesis of the Diels-Alder precursor, and the synthesis would begin with perillyl alcohol (**72**), both enantiomers of which are available. The stereochemistry of all the remaining stereocenters would then be set by diastereoselective chemistry.

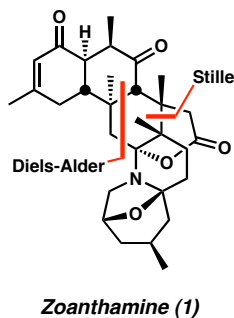
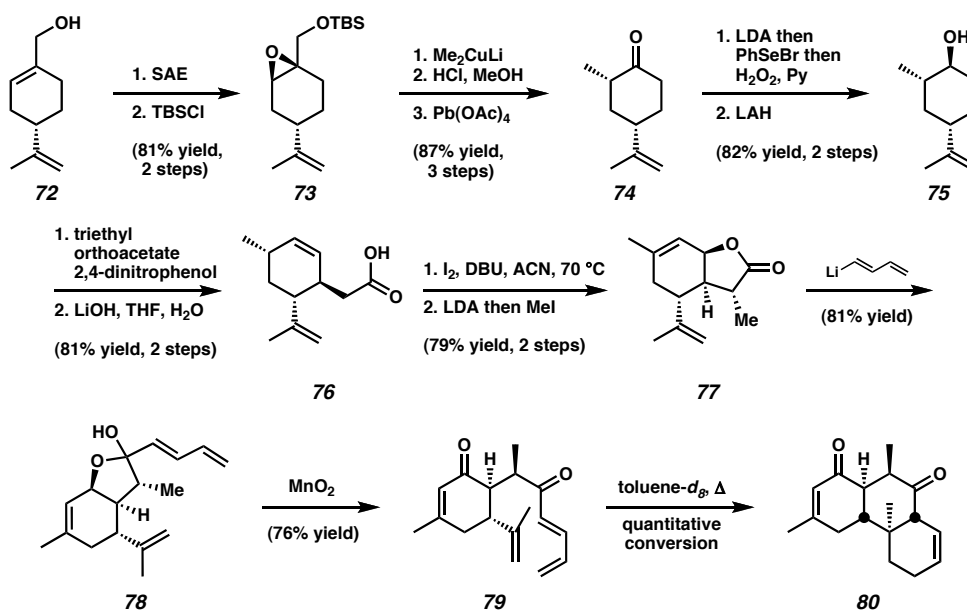


**Figure 1.4.2** Tanner's retrosynthetic analysis of zoanthamine.

Tanner's synthesis began with Sharpless asymmetric epoxidation of known perillyl alcohol (**72**) followed by silylation to provide epoxide **73** (Scheme 1.4.5).<sup>37</sup> The C(15)

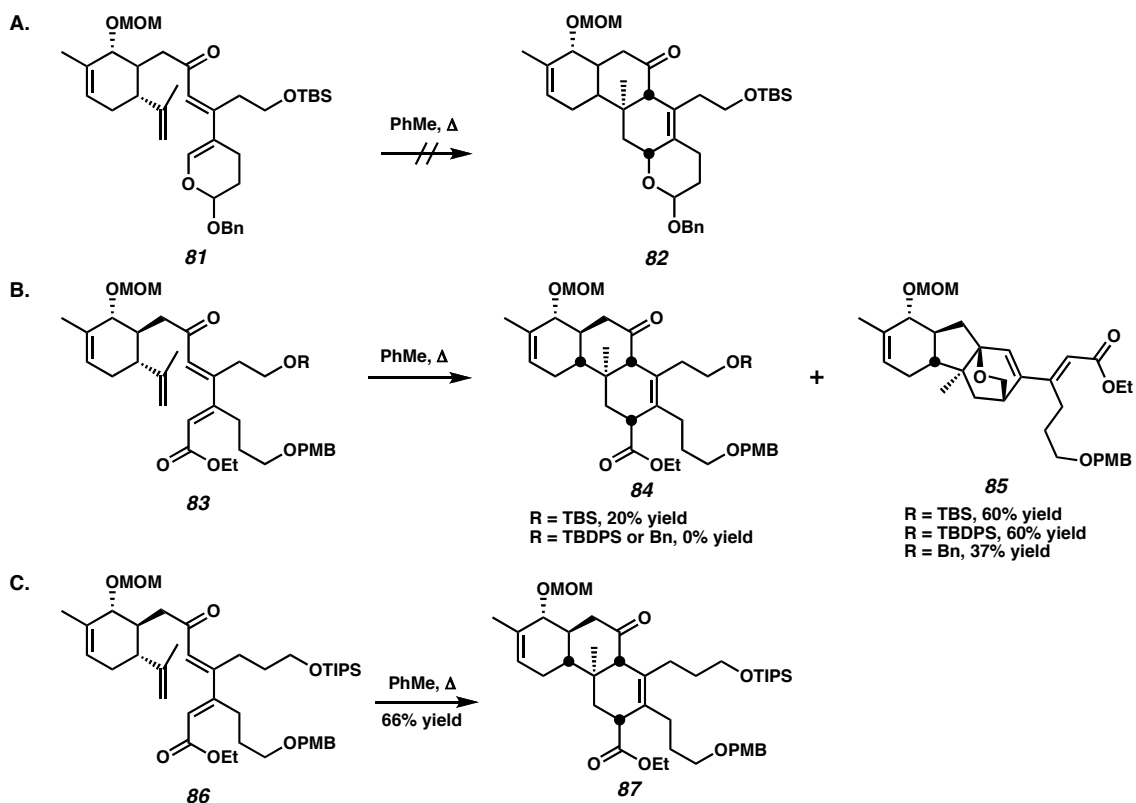
methyl group was installed by diastereoselective addition of Gilman's reagent into the epoxide. Removal of the silyl group and subsequent treatment with lead tetraacetate led to desired methyl ketone **74**. Trapping of the kinetic enolate with PhSeBr and peroxide oxidation allowed for enone installation, and subsequent LAH reduction led to allylic alcohol **75** as a single diastereomer. Alkylation with Claisen rearrangement was affected using triethyl orthoacetate and catalytic 2,4-dinitrophenol. This was followed by saponification with LiOH to form **76**. Iodolactonization occurred to give a mixture of 5- and 6-membered iodolactones that equilibrated upon heating. With DBU in the reaction mixture, the thermodynamically favored product was irreversibly trapped by elimination of HI. Diastereoselective alkylation of this enol lactone with MeI provided **77**, which was subjected to lithiobutadiene yielding hemiacetal **78**. Manganese dioxide oxidation provided Diels-Alder precursor **79**, and heating this intermediate in *d*<sub>8</sub>-toluene provided quantitative conversion of **79** to tricycle **80**.



**Scheme 1.4.5** Tanner's approach to a model ABC ring system.

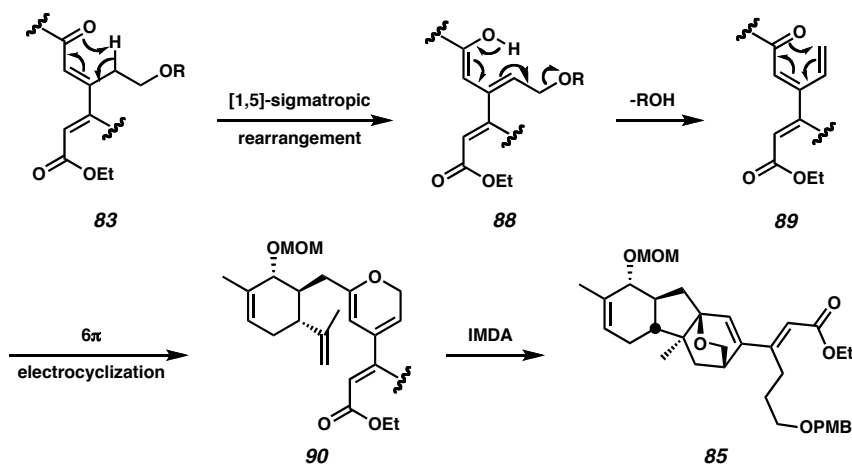
Encouraged by the success of this model Diels-Alder cycloaddition, the Tanner group set out to synthesize a more functionalized precursor. In order to more readily probe the

limitations of the reaction, a number of model substrates were synthesized from (-)-carvone. The first model substrate (**81**, Scheme 1.4.6) led to a disappointing, but critical, discovery. Upon heating in toluene for several days, no reaction was observed. It was determined that the extra electron density in the diene was rendering the desired inverse-electron demand Diels-Alder cycloaddition ineffective. Thus, DA substrate **83** (R = TBS) was synthesized. Upon heating, two products were observed: desired DA adduct **84** and an unusual side product **85**. Upon varying the nature of the protecting group (R), **85** was the sole product observed. However, a one-carbon homologation of the chain at C(22) (**86**) was sufficient to avoid the formation of the side-product, providing a 66% yield of **87** with the correct stereochemistry for the synthesis of zoanthamine.



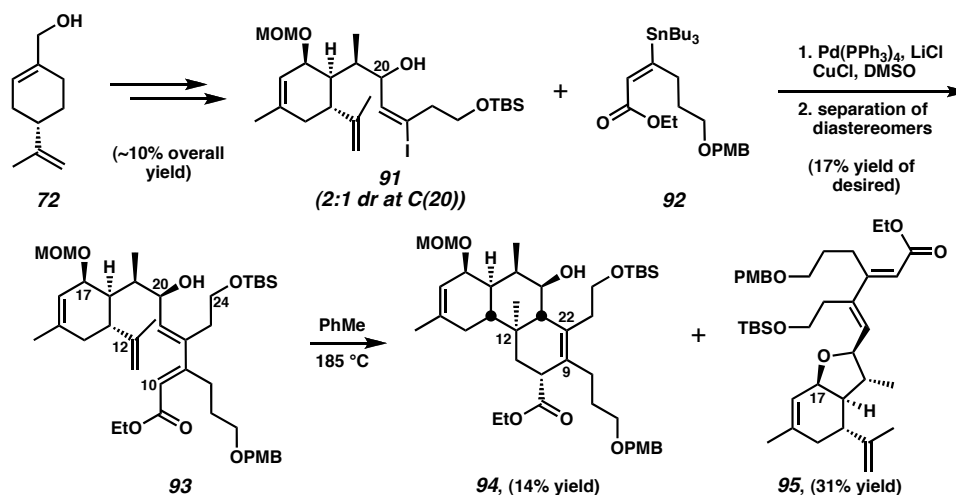
**Scheme 1.4.6** Model cyclizations of compounds derived from (-)-carvone.

This final modification confirmed the mechanistic hypothesis illustrated in Scheme 1.4.7. From the DA substrate (**83**), a 1,5-sigmatropic rearrangement leads to extended enol **88**. Loss of ROH (R = TBS, TBDPS, Bn) then gave terminal olefin **89**. A  $6\pi$  electrocyclicization provided pyran **90**, which then underwent intramolecular Diels-Alder reaction to form the side product **85**.



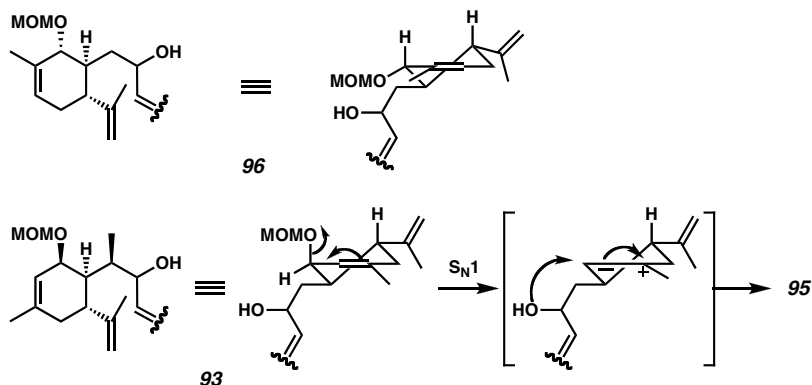
**Scheme 1.4.7** Mechanism for formation of undesired products.

Armed with this information, perillyl alcohol was converted to vinyl iodide **91** (Scheme 1.4.8).<sup>38</sup> Stille coupling with stannane **92** proved difficult and required special conditions reported by Corey to afford reasonable yields of the Diels-Alder substrate **93**.<sup>39-41</sup> Diels-Alder cyclization proceeded with high diastereoselectivity to afford  $\beta,\gamma$ -unsaturated ester **94**, albeit in a modest 14% yield. The major product, tetrahydrofuran **95**, was isolated in 31% yield.



**Scheme 1.4.8** Tanner's approach to the functionalized ABC ring system.

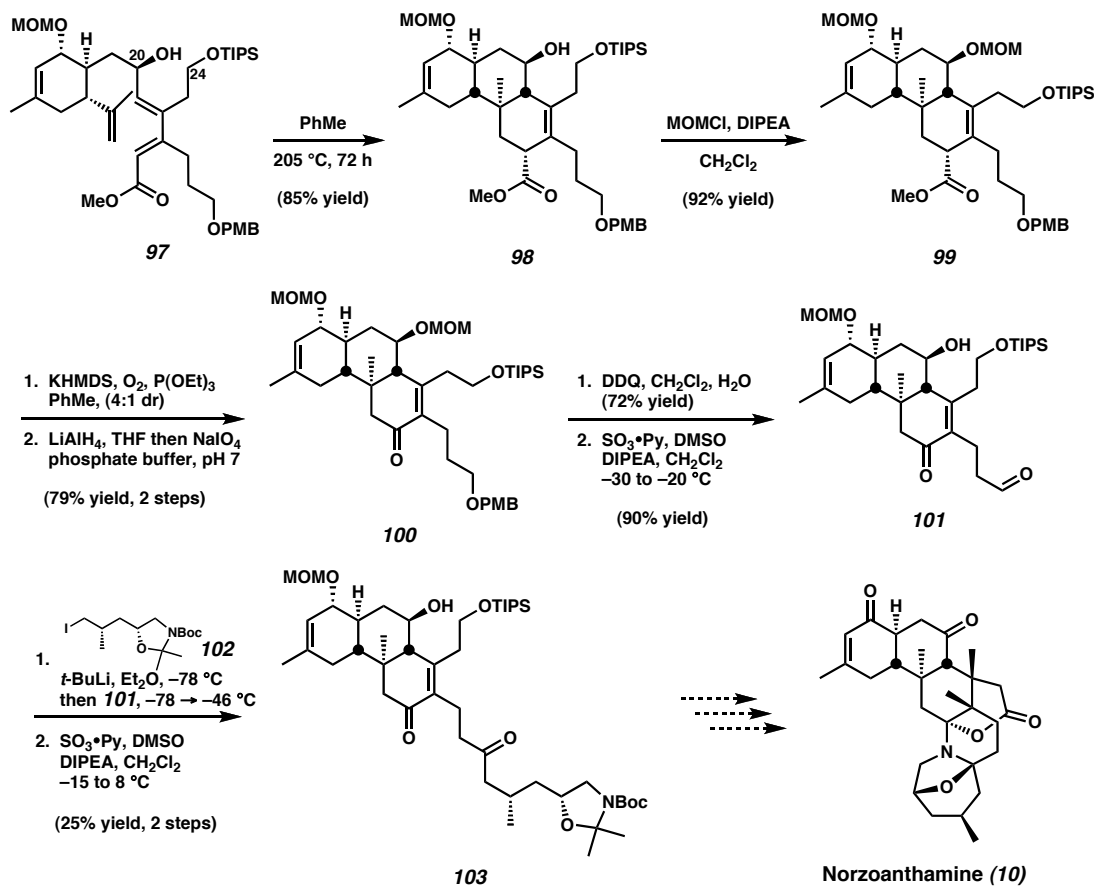
Upon examining the differences between this perillyl alcohol-derived substrate and the corresponding carvone-derived substrate (reaction not shown), Tanner and coworkers noted that the allylic MOM-protected alcohol was arranged in a pseudo-axial orientation in DA precursor **93**, whereas the model substrate (**96**) possesses a pseudo-equatorial MOM ether (Scheme 1.4.9). It is believed that this difference allows for  $S_N1$ -type displacement and cyclization to form tetrahydrofuran **95**.



**Scheme 1.4.9** Mechanism for formation of by-product **95**.

Based on this rationale, a new Diels-Alder substrate (**97**) was synthesized and cyclized by treatment with toluene at 205 °C (Scheme 1.4.10).<sup>42</sup> Gratifyingly, the Diels-Alder proceeded smoothly through an exo transition state to provide tricycle **98** in 85% yield. Protection of the C(20) alcohol as the MOM-ether (**99**) was followed by an

oxidative cleavage sequence to afford enone **100**. Subsequent PMB-ether removal and oxidation provided aldehyde **101**. At this point, side chain **102** was treated with *t*-butyllithium, aldehyde **101** was added, and the resulting alcohol was oxidized to afford advanced intermediate **103**.



**Scheme 1.4.10** Diels-Alder cyclization and cycloadduct advancement.

While this Diels-Alder strategy nicely established the quaternary center at C(12), it will require the formation of the difficult vicinal C(9) and C(22) quaternary centers at a late stage in the synthesis. The Tanner group is poised to begin their installation, which they hope to achieve by Michael addition and alkylation. Once the quaternary centers are installed, only oxidation at C(24) and cyclization of the side chain to form the DEFG rings remain to complete the total synthesis of norzoanthamine.

#### 1.4.4 Uemura's Approach to the Norzoanthamine ABC Ring System

Recently, Uemura and coworkers have reported a synthetic strategy based on their biosynthetic hypothesis, which purports that the zoanthamine alkaloids arise from a linear polyketide skeleton, which then undergoes numerous pericyclic cyclizations.<sup>43</sup> To support this hypothesis, they endeavored to synthesize and cyclize polyene **104** en route to the natural product (Figure 1.4.3).

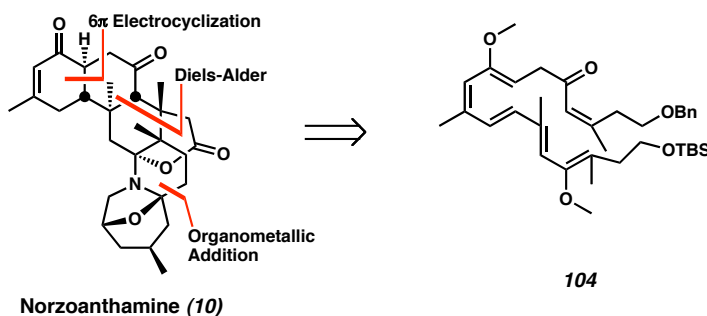
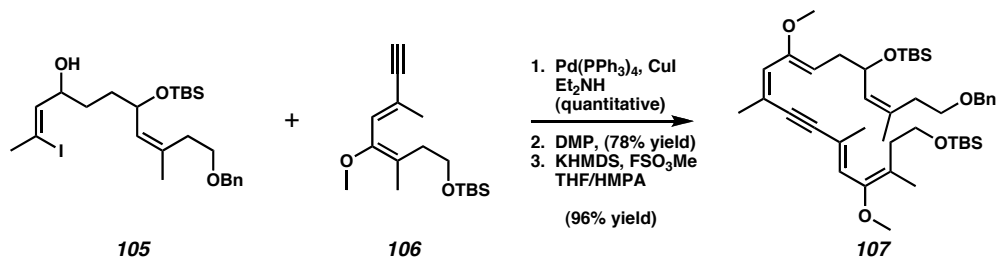


**Figure 1.4.3** Uemura's retrosynthetic analysis of norzoanthamine.

Vinyl iodide **105** and alkyne **106** were efficiently assembled then united by Sonogashira coupling.<sup>44</sup> Conversion to enyne **107** was completed by oxidation and methylation (Scheme 1.4.11). To date, no report has appeared on the selective reduction of enyne **107** to the linear polyene **104** or on attempts to cyclize either **104** or **107**.



**Scheme 1.4.11** Uemura's approach to norzoanthamine.

#### 1.4.5 Williams's Approach to the Norzoanthamine AB and EFG Ring Systems

Williams and coworkers have explored approaches to the synthesis of both the carbocyclic AB rings and the heterocyclic EFG rings of norzoanthamine and zoanthenol.

Their Diels-Alder strategy constructs the AB rings, which will be followed by appending the C ring (Figure 1.4.4).<sup>45</sup> The EFG ring system is formed by conjugate addition of an enamine into a functionalized linear enone then cyclization to form the stereochemistry and connectivity observed in the natural products.

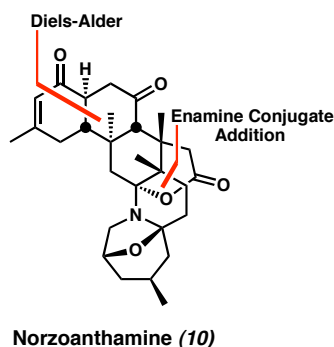
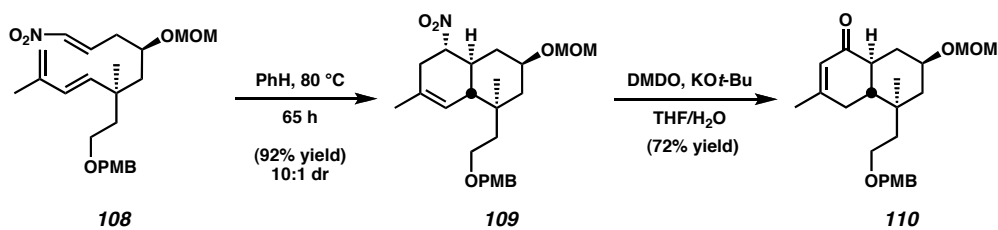


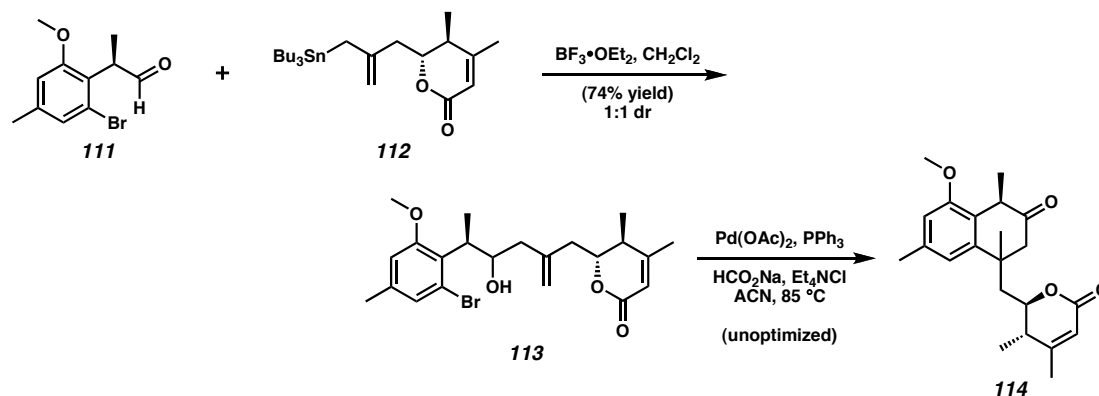
**Figure 1.4.4** Williams's retrosynthetic analysis of norzoanthamine.

In the key Diels-Alder reaction, nitro-alkene **108** underwent reaction in benzene at reflux via an endo transition state to afford decalin **109** in good yield and 10:1 dr (Scheme 1.4.12). A Nef reaction<sup>46</sup> converted the nitro moiety to the desired ketone and facilitated olefin migration. The product enone (**110**) has the necessary stereochemistry and functionality to begin C ring annulation.



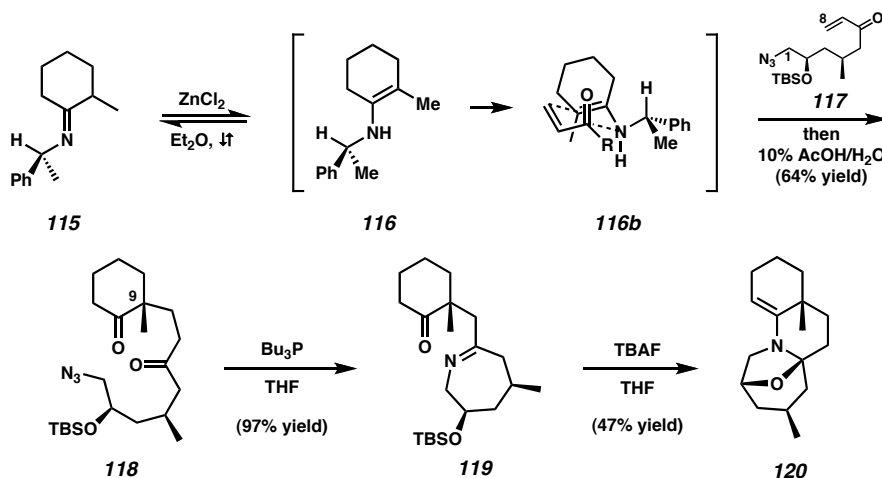
**Scheme 1.4.12** Williams's early efforts toward the norzoanthamine AB rings.

The Williams group has recently published an interesting approach to the zoanthenol AB rings involving allylation of aldehyde **111** with stannane **112** (Scheme 1.4.13).<sup>47</sup> Upon treatment with  $\text{BF}_3$  etherate, a 1:1 mixture of diastereomers of alcohol **113** was formed. Though the conditions remain unoptimized, the desired product of Pd insertion and intramolecular Heck coupling (**114**) has been isolated with good recovery of unreacted starting material.



**Scheme 1.4.13** Williams's recent efforts toward the norzoanthamine AB rings.

In addition, the Williams group demonstrated an efficient strategy to append the C(1)–C(8) (EFG) fragment to the ABC ring system and stereospecifically establish the C(9) quaternary center.<sup>48</sup> When heated with zinc (II) chloride, chiral imine **115** generates a significant amount of enamine **116** at equilibrium (Scheme 1.4.14). The enamine undergoes conjugate addition into enone **117** from the  $\beta$  face over the smaller methyl group of the energy-minimized conformation depicted in **116b**.<sup>49</sup> Enone **117** was prepared in enantioenriched form using Evans chiral oxazolidinone chemistry.<sup>50</sup> Hydrolysis of the intermediate iminium affords diketone **118** with excellent diastereoselectivity (22:1). Staudinger reduction of azide **118** provides imine **119**. Treatment with TBAF cleaves the silyl ether. The resultant alcohol attacks the imine and condenses onto the ketone to give the EFG model enamine **120** after dehydration.



**Scheme 1.4.14** Williams's synthesis of a model EFG ring system.

#### 1.4.6 Theodorakis's Annulation Approach to the Norzoanthamine ABC Ring System

Theodorakis and coworkers propose a unique annulation strategy that begins with an intact B ring and sequentially appends the C and A rings (Figure 1.4.5).<sup>51</sup> The unifying theme of the Robinson annulation is applied for the synthesis of both rings.

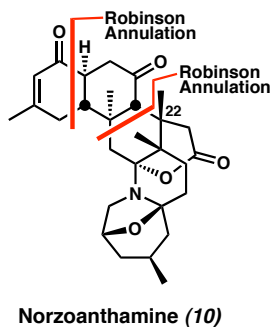
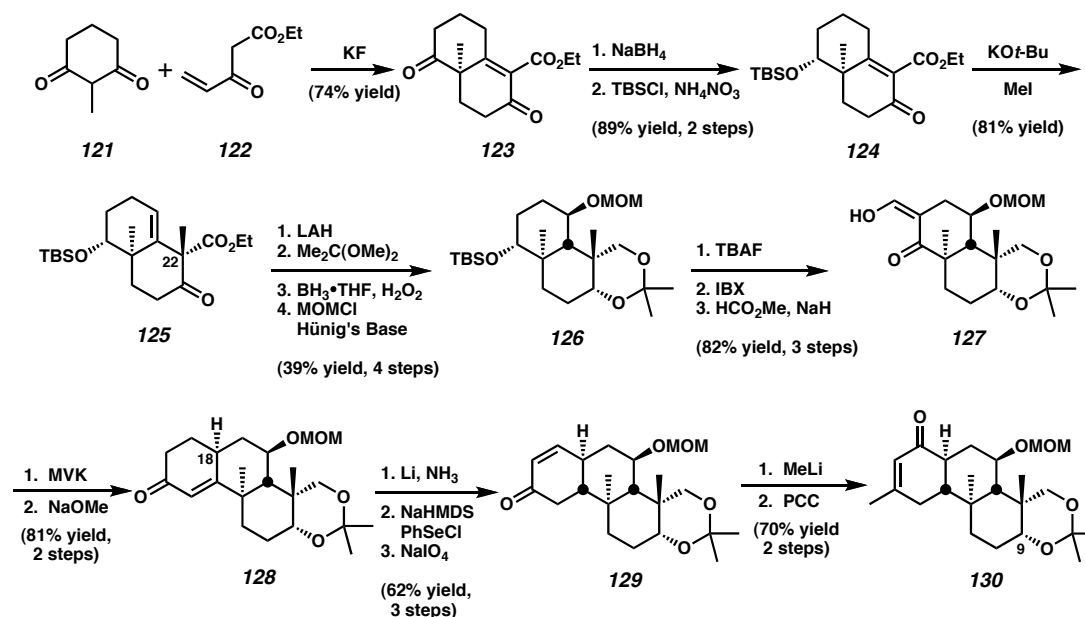


**Figure 1.4.5** Theodorakis's retrosynthetic analysis of norzoanthamine.

The synthesis commences with condensation of meso-diketone **121** and ketoester **122** with potassium fluoride conditions to afford enone **123** (Scheme 1.4.15).<sup>52</sup> Sodium borohydride reduction and silylation provided **124**. Treatment of  $\alpha,\beta$ -unsaturated ketoester **124** with potassium *tert*-butoxide and methyl iodide produced the quaternized ketoester **125** with complete diastereomeric control. Exhaustive reduction with LAH produced a diol, which was then protected as the acetonide. Hydroboration and

oxidation followed by MOM-ether formation provided **126**. Desilylation, oxidation, and alkylation with methyl formate provided hydroxyenone **127**. A two-step Robinson annulation<sup>53</sup> protocol gave enone **128** as a single isomer. Enone **128** was then reduced to the corresponding ketone, and olefin installation provided **129**. Methyl lithium addition and PCC oxidation afforded the transposed enone **130**, which contained all the functionality and stereochemistry in the AB rings.

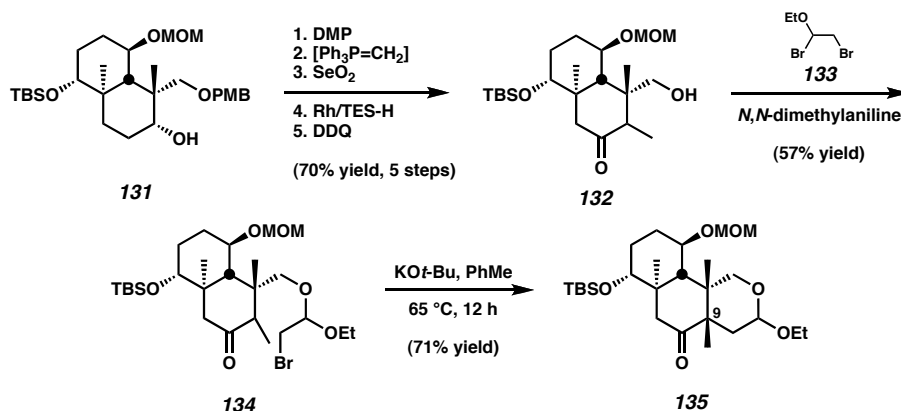


**Scheme 1.4.15** Theodorakis's approach to the ABC ring system.

In a related study, Theodorakis demonstrated that the installation of the difficult C(9) quaternary center was possible from selectively protected alcohol **131** (Scheme 1.4.16).<sup>54</sup> Oxidation to the corresponding ketone and olefination, followed by allylic oxidation provided an exocyclic enone. Conjugate reduction and PMB ether cleavage then provided methyl ketone **132**. Acetal formation between Stork's dibromo-acetal reagent **133**<sup>55</sup> and the alcohol moiety of methyl ketone **132** produced bromide **134**. Exposure of bromide **134** to base gave intramolecular alkylation product **135** in 71% yield. The efficiency of this protocol is impressive given the difficulty of establishing

vicinal quaternary centers. Additionally, the alkylation gave complete selectivity for the desired C(9) epimer of acetal **128**, as confirmed by X-ray structure determination.

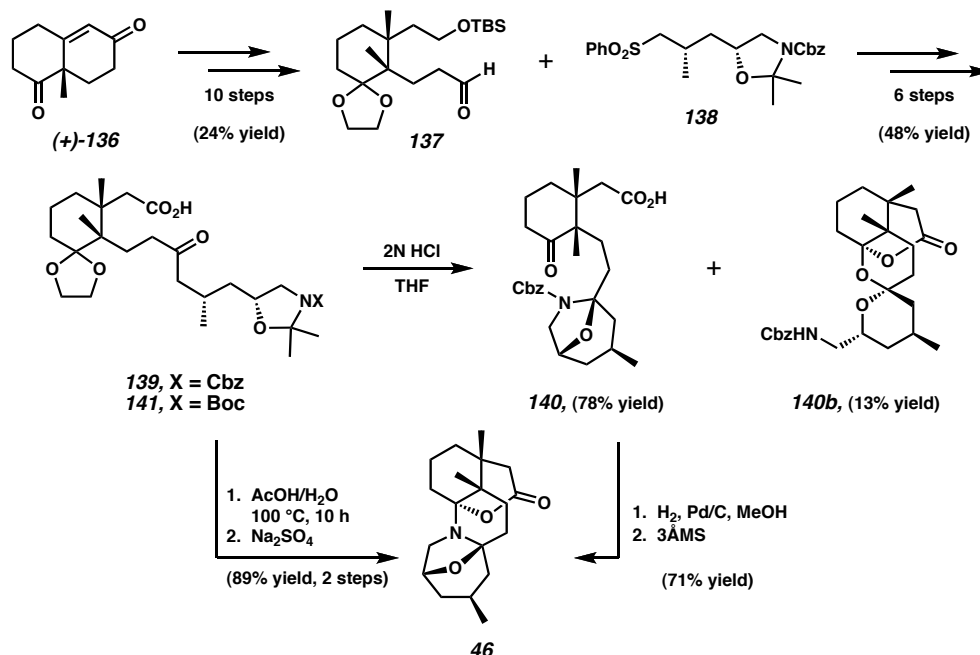
Taken in conjunction with Theodorakis's other work, this strategy solves the difficult problem of generating all three of the C ring quaternary centers and produces a norzoanthamine ABC ring system well poised for the completion of the total synthesis.



**Scheme 1.4.16** Theodorakis's installation of the C(9) quaternary center.

#### 1.4.7 Kobayashi's Synthesis of the Heterocyclic CDEFG Zoanthamine Ring System

In 1998, Kobayashi and coworkers disclosed an enantioselective route to the CDEFG ring system.<sup>56</sup> The Wieland-Miescher ketone (**136**)<sup>57</sup> served as the starting material to produce aldehyde **137** (Scheme 1.4.17). The coupling of the lithium salt of sulfone **138** to aldehyde **137** and oxidation state adjustment completed the Cbz-protected cyclization substrate **139**. Treatment with hydrochloric acid removed the acetonide and formed the FG rings in good yield (**140**), but was accompanied by the formation of an acetal by-product **140b** in 13% yield. Resubjection of this by-product to acidic conditions did not form an aminal-containing product. Tricyclic intermediate **140** was hydrogenolyzed and dehydrated to furnish pentacyclic hemiaminal **46**. A single-flask protocol for cyclization was subsequently investigated using Boc-protected substrate **141** in acidic conditions and gave an excellent yield of hemiaminal **46**.<sup>58</sup>



**Scheme 1.4.17** Kobayashi's sulfone approach to the CDEFG ring system.

#### 1.4.8 Hirama's Strategy for the Zoanthenol ABC Ring System

The strategy proposed by Hirama and coworkers is specifically geared toward the synthesis of zoanthenol's ABC ring system. The key Heck<sup>59</sup> disconnection of the C(12)–C(13) bond relies on the aromatic A ring unique to zoanthenol (Figure 1.4.6). Addition of a stannane into an enone was envisioned for the formation of the C(20)–C(21) bond.

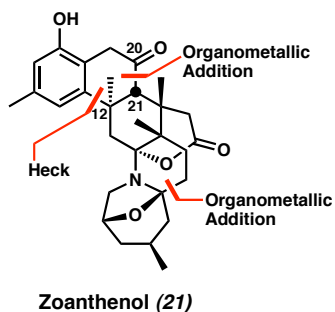
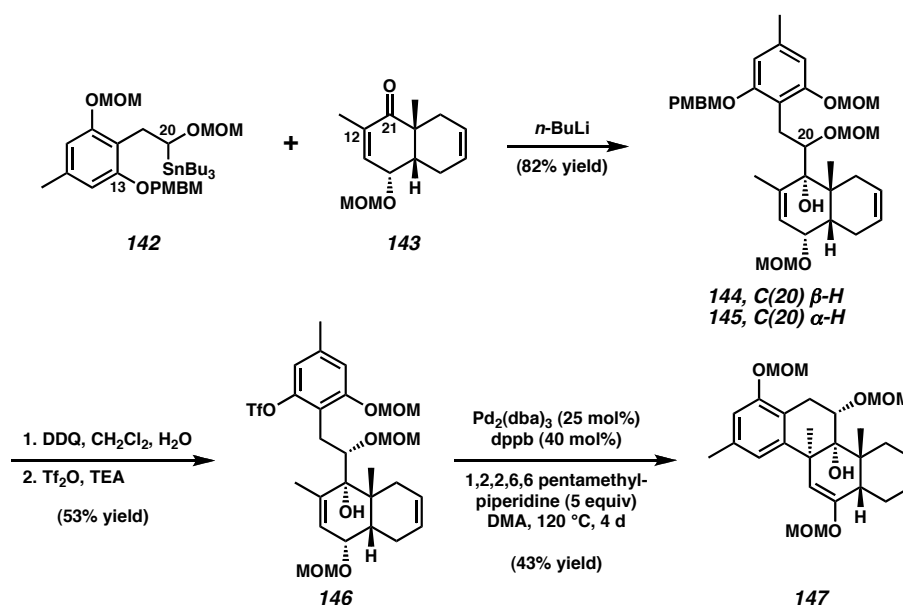


**Figure 1.4.6** Hirama's retrosynthetic analysis of zoanthenol.

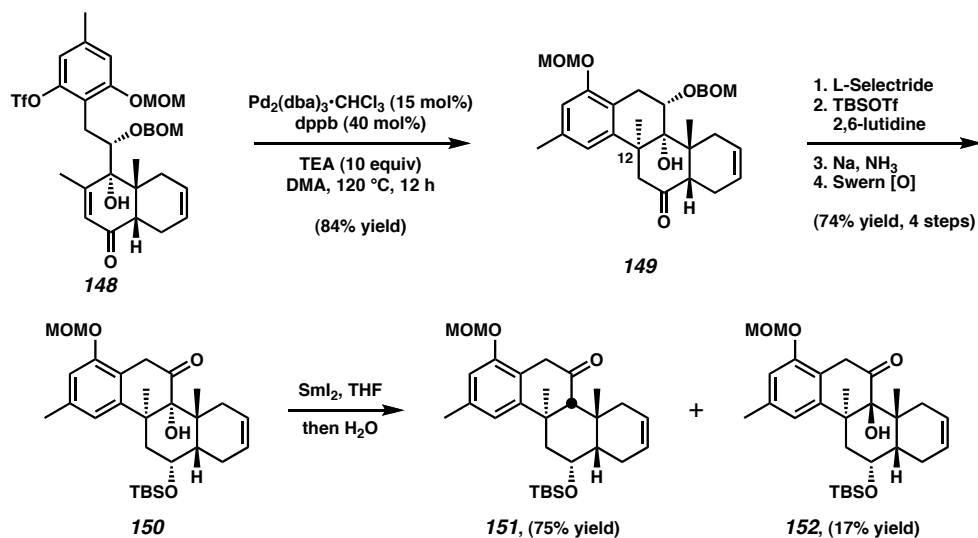
Transmetalation of stannane **142** and addition into enone **143**, derived from an asymmetric quinone Diels-Alder reaction,<sup>60</sup> afforded tertiary alcohols **144** and **145** as a mixture of diastereomers at C(20) (Scheme 1.4.18). PMB ether cleavage followed by

triflate formation provided aryl triflate **146** and allowed for the investigation of the key intramolecular Heck reaction. After significant optimization, conditions were developed to produce the desired enol ether **147** in modest yield.<sup>61</sup> Though the reaction did proceed with excellent diastereoselectivity, it had several drawbacks, including high palladium loading, long reaction times, and side products from simple reduction of the triflate substrate.



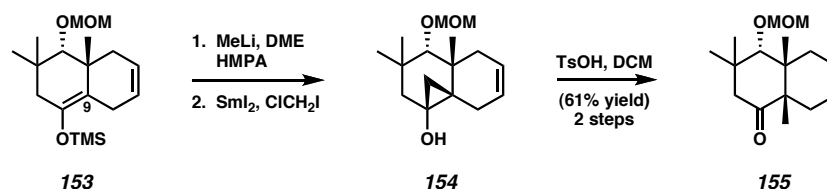
**Scheme 1.4.18** Hirama's Heck strategy for the zoanthenol ABC ring system.

Heck substrate **146** was altered to increase the electrophilicity of the accepting olefin. As shown in Scheme 1.4.19, exposure of enone **148** to reductive Heck conditions produced ketone **149** in excellent yield. With the difficult C(12) stereocenter established, the C ring ketone was selectively reduced with L-Selectride, and the resulting alcohol was then silylated. The next goal was the reduction of the tertiary alcohol moiety of ketone **149**. BOM ether reduction and oxidation provided **150**, which was treated with samarium(II) iodide to give the reduced ketone **151** in good yield as a single diastereomer as well as epimeric alcohol **152**, produced in 17% yield.<sup>62</sup>



**Scheme 1.4.19** Hiram's alternative assembly of the B ring.

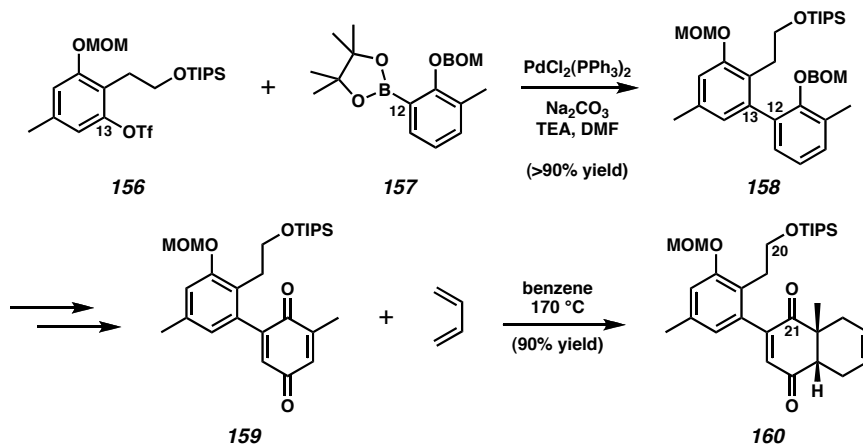
The largest challenge that remains in Hiram's synthesis is the establishment of the C(9) quaternary stereocenter. However, his group has already demonstrated a highly diastereoselective methylation of silyl enol ether **153** as a model of methylation at C(9) (Scheme 1.4.20).<sup>63</sup> The methylation was achieved by samarium(II) iodide-promoted cyclopropanation and acid-mediated ring opening to give methyl ketone **155** and its C(9) epimer with a favorable 3:1 dr.



**Scheme 1.4.20** Hiram's installation of the C(9) methyl group.

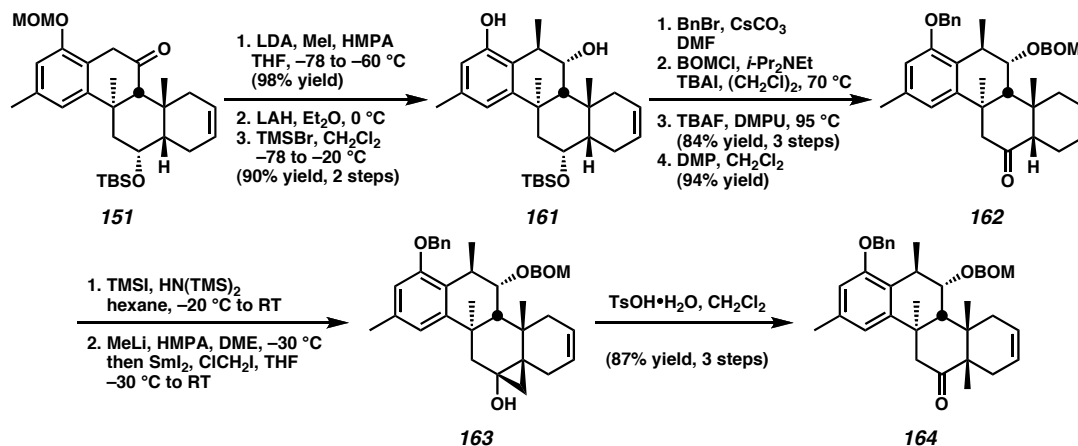
Hiram and coworkers have also disclosed an alternate strategy for the assembly of zoanthenol's ABC ring system. This approach reverses the order in which the B ring bonds are formed.<sup>64</sup> As depicted in Scheme 1.4.21, Suzuki coupling of aryl triflate **156** and borane **157** unite the A and C ring synthons via the C(12)–C(13) bond to yield biaryl **158**. BOM removal and oxidation provided quinone **159**, which was heated with butadiene to form **160**. Upon the elaboration of Diels-Alder adduct **161**, the final B ring

bond, C(20)–C(21), could be constructed by an organometallic addition analogous to the synthesis of tertiary alcohols **144/145** and **148** or by a pinacol-type coupling of the C(20) aldehyde.



**Scheme 1.4.21** An alternate approach by Hirama.

Recently, Hirama and coworkers published the synthesis of the fully functionalized ABC rings of zoanthenol.<sup>65</sup> From intermediate ketone **151**, enolization and trapping with methyl iodide afforded the desired methylated B ring in excellent yield (Scheme 1.4.22). Subsequent ketone reduction and MOM ether cleavage provided phenol **161**. Benzylation and BOM ether formation were followed by desilylation and oxidation to form C ring ketone **162** in 79% yield over four steps. At this point, the quaternary methyl installation modeled above was executed. Ketone **162** was converted to the thermodynamic silyl enol ether, the lithium enolate was formed by treatment with methyl lithium, and the enolate was cyclopropanated under radical conditions yielding cyclopropyl alcohol **163**. Reformation of the ketone occurred with concomitant cyclopropane cleavage upon treatment with toluenesulfonic acid monohydrate to provide the fully functionalized tricyclic core of zoanthenol.



**Scheme 1.4.22** Hirama's synthesis of the fully functionalized ABC core of zoanthenol.

### 1.5.1 Summary and Outlook

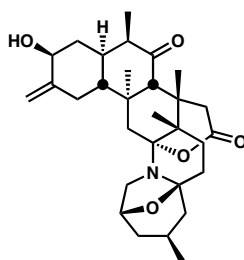
The zoanthamine alkaloids are a structurally unique family of natural products. Though they are isolated from soft coral of the order zoantharia, it may be that symbiotic algae play a large role in the biosynthesis of these secondary metabolites. Their biosynthesis is believed to involve a polyketide pathway, but no specifics of the route are known. The benefit of these complicated natural products to the producing organisms is unknown, but the isolation of various zoanthamine alkaloids in the Indian, Pacific, and Atlantic Oceans suggests that these widespread metabolites may have an important function. Anti-osteoporotic, antibiotic, anti-inflammatory, and cytotoxic biological activities have been observed in various zoanthamines. As a result, these molecules have garnered increasing attention from synthetic chemists.

As synthetic targets, the zoanthamine alkaloids are a challenge to current synthetic methods and an inspiration for the creation of new reactions. In the contemporary era, it is common for newly isolated natural products of interesting structure or biological significance to succumb to total synthesis within one to two years of the isolation. By comparison, twenty years passed between the isolation of zoanthamine and Miyashita's total synthesis of norzoanthamine in 2004. Any successful synthesis of these alkaloids

requires expertise in both carbocyclic and heterocyclic chemistry. Construction of the carbocyclic ABC rings is hindered by the stereochemical density of this region of the molecule. In particular, the three quaternary centers of the C ring present a formidable challenge. This architecture has inspired a number of creative annulation strategies utilizing Diels-Alder, Heck, Friedel-Crafts, and Robinson annulation reactions. The heterocyclic DEFG rings are topographically complex and contain a number of sensitive functional groups. Pioneering syntheses of the heterocyclic region of these molecules have determined the feasibility of different cyclization strategies. For over two decades, the novel bioactivities and synthetic challenges of the zoanthamine natural products have generated a significant body of research. With many questions yet unanswered, interest in the zoanthamine alkaloids is likely to increase for the foreseeable future.

## References

1. Portions of this chapter have been published: Behenna, D. C.; Stockdill, J. L.; Stoltz, B. M. *Angew. Chem. Int. Ed.* **2008**, *47*, 2365–2386.
2. a) Ono, S.; Reimer, J. D.; Tsukahara, J. *Zool. Sci.* **2005**, *22*, 247–255. b) Ryland, J. S. *Invert. Rep. Develop.* **1997**, *31*, 177–188.
2. Sinniger, F.; Montoya–Burgos, J. I.; Chevaldonné, P.; Pawlowski, J. *Mar. Biol.* **2005**, *147*, 1121–1128.
4. Roa, C. B.; Anjaneyulu, A. S. R.; Sarma, N. S.; Venkateswarlu, Y.; Rosser, R. M.; Faulkner, D. J.; Chen, M. H. M.; Clardy, J. *J. Am. Chem. Soc.* **1984**, *106*, 7983–7984.
5. Nakamura, H.; Kawase, Y.; Maruyama, K.; Muria, A. *Bull. Chem. Soc. Jpn.* **1998**, *71*, 781–787.
6. a) Suksamrarn, A.; Jankam, A.; Tarnchompoo, B.; Putchakarn, S. *J. Nat. Prod.* **2002**, *65*, 1194–1197; b) Shigemori, H.; Sato, Y.; Kagata, T.; Kobayashi, J. *J. Nat. Prod.* **1999**, *62*, 372–374.
7. Han, C.; Qi, J.; Shi, X.; Sakagami, Y.; Shibata, T.; Uchida, K.; Ojika, M. *Biosci. Biotechnol. Biochem.* **2006**, *70*, 706–711.
8. Fernández, J. J.; Souto, M. L.; Daranas, A. H.; Norte, M. *Curr. Top. Phytochem.* **2000**, *4*, 106–119.
9. Sepcic, K.; Turk, T.; Macek, P. *Toxicon* **1998**, *36*, 93–940.
10. R. E. Moore, P. J. Scheuer, *Science* **1971**, *172*, 495–498.
11. For structure determination, see: Cha, J. K.; Christ, W. J.; Finan, J. M.; Fujioka, H.; Kishi, Y.; Klein, L. L.; Ko, S. S.; Leder, J.; McWhorter, W. W.; Pfaff, K.-P.; Yonaga, M.; Uemura, D.; Hirata, Y. *J. Am. Chem. Soc.* **1982**, *104*, 7369–7371. For total synthesis, see: Suh, E. M.; Kishi, Y. *J. Am. Chem. Soc.* **1994**, *116*, 11205–11206.
12. Roa, C. B.; Anjaneyula, A. S. R.; Sarma, N. S.; Venkateswarlu, Y. *J. Org. Chem.* **1985**, *50*, 3757–3760.
13. Roa, C. B.; Roa, D. V.; Raju, V. S. N. *Heterocycles* **1989**, *28*, 103–106.
14. Fukuzawa, S.; Hayashi, Y.; Uemura, D. Nagatsu, A.; Yamada, K.; Ijuin, Y. *Heterocyc. Commun.* **1995**, *1*, 207–214.
15. Kuramoto, M.; Hayashi, K.; Fujitani, Y.; Yamaguchi, K.; Tsuji, T.; Yamada, K.; Ijuin, Y.; Uemura, D. *Tetrahedron Lett.* **1997**, *38*, 5683–5686.
16. Atta–ur–Rahman; Alvi, K. A.; Abbas, S. A.; Choudhary, M. I.; Clardy, J. *Tetrahedron Lett.* **1989**, *30*, 6825–6828.
17. Daranas, A. H.; Fernández, J. J.; Gavín, J. A.; Norte, M. *Tetrahedron* **1998**, *54*, 7891–7896.
18. Daranas, A. H.; Fernández, J. J.; Gavín, J. A.; Norte, M. *Tetrahedron* **1999**, *55*, 5539–5546.
19. a) Kuramoto, M.; Hayashi, K.; Yamaguchi, K.; Yada, M.; Tsuji, T.; Uemura, D. *Bull. Chem. Soc. Jpn.* **1998**, *71*, 771–779. b) Uemura, D. *Chem. Rec.* **2006**, *6*, 235–248.
20. Trench, R. K. *Pure Appl. Chem.* **1981**, *53*, 819–835.
21. Also in this study, a molecule closely related to palytoxin, zooxanthellatoxin, was isolated. See ref 5 for details.
22. A similar natural product, loboanthamine, was recently isolated from soft corals of the genus *Lobophytum*:



- Fattorusso, E.; Romano, A.; Tagliatalata-Scafati, O.; Achmad, M. J.; Bavestrello, G.; Cerrano, C. *Tetrahedron Lett.* **2008**, *49*, 2189–2192.
23. Kuramoto, M.; Arimoto, H.; Hayashi, K.; Hayakawa, I.; Uemura, D.; Chou, T.; Yamada, K.; Tsuji, T.; Yamaguchi, K.; Yazawa, K. Symposium Papers, 38th Symposium on the Chemistry of Natural Products **1996**, 79–84.
  24. T. J. Chambers, *J. Cell Sci.* **1982**, *57*, 247–260.
  25. Yamaguchi, K.; Yada, M.; Tsuji, T.; Kuramoto, M.; Uemura, D. *Biol. Pharm. Bull.* **1999**, *22*, 920–924.
  26. Bodine, P. V. N.; Harris, H. A.; Komm, B. S. *Endocrinology* **1999**, *140*, 2439–2451.
  27. Kuramoto, K.; Yamaguchi, K.; Tsuji, T.; Uemura, D. in *Drugs from the Sea*, (Ed.: Fusetani, N.), Karger, Basel, **2000**, pp. 98–106.
  28. For other descriptions of this activity, see: a) Kuramoto, M.; Arimoto, H.; Uemura, D. *J. Synth. Org. Chem. Jpn.* **2003**, *61*, 59–65; b) Kuramoto, M.; Arimoto, H.; Uemura, D. *Mar. Drugs* **2004**, *1*, 39–54; c) Kita, M.; Uemura, D. *Chem. Lett.* **2005**, *34*, 454–459; d) Yamada, K.; Kuramoto, M.; Uemura, D. *Recent Res. Devel. Pure & App. Chem.* **1999**, *3*, 245–254.
  29. The IC<sub>50</sub> values are for inhibition of IL-6 production from preosteoblastic MC3T3-E1 cells stimulated by parathyroid hormone (see ref 26).
  30. Hirai, G.; Oguri, H.; Hayashi, M.; Koyama, K.; Koizumi, Y.; Moharram, S. M.; Hiramama, M. *Bioorg. Med. Chem. Lett.* **2004**, *14*, 2647–2651.
  31. Venkateswarlu, Y.; Reddy, N. S.; Ramesh, P.; Reddy, P. S.; Jamil, K. *Heterocycl. Commun.* **1998**, *4*, 575–580.
  32. Villar, R. M.; Gil-Longo, J.; Daranas, A. H.; Souto, M. L.; Fernández, J. J.; Peixinho, S.; Barral, M. A.; Santafé, G.; Rodríguez, J.; Jiménez, C. *Bioorg. Med. Chem.* **2003**, *11*, 2301–2306.
  33. Benowitz, N. L. *Progress in Cardiovascular Diseases* **2003**, *46*, 91–111.
  34. Jackson, S. P.; Schoenwalder, S. M. *Nature Reviews* **2003**, *2*, 1–15.
  35. a) Miyashita, M.; Sasaki, M.; Hattori, I.; Sakai, M.; Tanino, K. *Science* **2004**, *305*, 495–499. b) Miyashita, M. *Pure Appl. Chem.* **2007**, *79*, 651–665.
  36. Sakai, M.; Sasaki, M.; Tanino, K.; Miyashita, M. *Tetrahedron Lett.* **2002**, *43*, 1705–1708.
  37. Tanner, D.; Anderson, P. G.; Tedenborg, L.; Somfai, P. *Tetrahedron* **1994**, *50*, 9135–9144.
  38. a) Tanner, D.; Tedenborg, L.; Somfai, P. *Acta Chem. Scand.* **1997**, *51*, 1217–1223; b) Nielsen, T. E.; Tanner, D. *J. Org. Chem.* **2002**, *67*, 6366–6371.
  39. Nielsen, T. E.; Le Quement, S.; Juhl, M.; Tanner, D. *Tetrahedron* **2005**, *61*, 8013–8024.
  40. Han, X.; Stoltz, B. M.; Corey, E. J. *J. Am. Chem. Soc.* **1999**, *121*, 7600–7605.
  41. Juhl, M.; Nielsen, T. E.; Le Quement, S.; Tanner, D. *J. Org. Chem.* **2006**, *71*, 265–280.
  42. Juhl, M.; Monrad, R.; Søtofte, I.; Tanner, D. *J. Org. Chem.* **2007**, *72*, 4644–4654.
  43. Irifune, T.; Ohashi, T.; Ichino, T.; Sakia, E.; Suenaga, K.; Uemura, D. *Chem. Lett.* **2005**, *34*, 1058–1059.

44. Sonogashira, K.; Tohdo, Y.; Hagihara, N. *Tetrahedron Lett.* **1975**, *16*, 4467–4470.
45. Williams, D. R.; Brugel, T. A. *Org. Lett.* **2000**, *2*, 1023–1026.
46. For a review of Nef reactions, see: Pinnick, H. W. *Org. React.* **1990**, *38*, 655–792.
47. Williams, D. R.; Ihle, D. C.; Brugel, T. A.; Patanaik, S. *Heterocycles*, **2006**, *70*, 77–82.
48. Williams, D. R.; Cortez, G. A. *Tetrahedron Lett.* **1998**, *39*, 2675–2678.
49. a) d'Angelo, J.; Desmaële, D.; Dumas, F.; Guingant, A. *Tetrahedron: Asymmetry* **1992**, *3*, 459–505; b) Hickmott, P. W. *Tetrahedron* **1984**, *40*, 2989–3051.
50. For a review of Evans aldol methodology, see: Ager, D. J.; Prakash, I.; Schaad, D. R. *Aldrichimica Acta* **1997**, *30*, 3–12.
51. Ghosh, S.; Rivas, F.; Fischer, D.; González, M. A.; Theodorakis, E. A. *Org. Lett.* **2004**, *6*, 941–944.
52. a) Ling, T.; Chowdhury, C.; Kramer, B. A.; Vong, B. G.; Palladino, M. A.; Theodorakis, E. A. *J. Org. Chem.* **2001**, *66*, 8843–8853; b) Ling, T.; Kramer, B. A.; Palladino, M. A.; Theodorakis, E. A. *Org. Lett.* **2000**, *2*, 2073–2076.
53. For a review of Robinson annulations, see: Gawley, R. E. *Synthesis* **1976**, 777–794.
54. Rivas, F.; Ghosh, S.; Theodorakis, E. A. *Tetrahedron Lett.* **2005**, *46*, 5281–5284.
55. The use of dibromide **92** for radical cyclizations was explored by Stork. See: a) Stork, G.; Mook, R.; Biller, S. A.; Rychnovsky, S. D. *J. Am. Chem. Soc.* **1983**, *105*, 3741–3742; b) Stork, G.; Sher, P. M. *J. Am. Chem. Soc.* **1983**, *105*, 6765–6766.
56. a) Hikage, N.; Furukawa, H.; Takao, K.; Kobayashi, S. *Tetrahedron Lett.* **1998**, *39*, 6237–6240; b) Hikage, N.; Furukawa, H.; Takao, K.; Kobayashi, S. *Tetrahedron Lett.* **1998**, *39*, 6241–6244.
57. a) Weiland, P.; Miescher, K. *Helv. Chim. Acta* **1950**, *33*, 2215–2228; b) For enantioselective preparation, see: Buchschacher, P.; Fürst, A.; Gutzwiller, J. *Org. Synth.* **1985**, *63*, 37–43.
58. Hikage, N.; Furukawa, H.; Takao, K.; Kobayashi, S. *Chem. Pharm. Bull.* **2000**, *48*, 1370–1372.
59. a) Heck, R. F.; Nolley, J. P. *J. Am. Chem. Soc.* **1968**, *90*, 5518–5526; b) Heck, R. F. *Acc. Chem. Res.* **1979**, *12*, 146–151. c) Heck, R. F. *Org. React.* **1982**, *27*, 345–390.
60. Moharram, S. M.; Hirai, G.; Koyama, K.; Oguri, H.; Hiramama, M. *Tetrahedron Lett.* **2000**, *41*, 6669–6673.
61. Hirai, G.; Oguri, H.; Moharram, S. M.; Koyama, K.; Hiramama, M. *Tetrahedron Lett.* **2001**, *42*, 5783–5787.
62. Hirai, G.; Koizumi, Y.; Moharram, S. M.; Oguri, H.; Hiramama, M. *Org. Lett.* **2002**, *4*, 1627–1630.
63. Hirai, G.; Oguri, H.; Hiramama, M. *Chem. Lett.* **1999**, *28*, 141–142.
64. Moharram, S. M.; Oguri, H.; Hiramama, M. *Egypt. J. Pharm. Sci.* **2003**, *44*, 177–193.
65. Sugano, N.; Koizumi, Y.; Oguri, H.; Kobayashi, S.; Yamashita, S.; Hiramama, M. *Chem. Asian J.* **2008**, *3*, 1549–1557.

## CHAPTER TWO

### Early Efforts Toward the Synthesis of Zoanthenol

#### Discovery of an Unusual Acid-Catalyzed Cyclization and Development of an Enantioselective Route to a Synthone for the DEFG Rings<sup>†</sup>

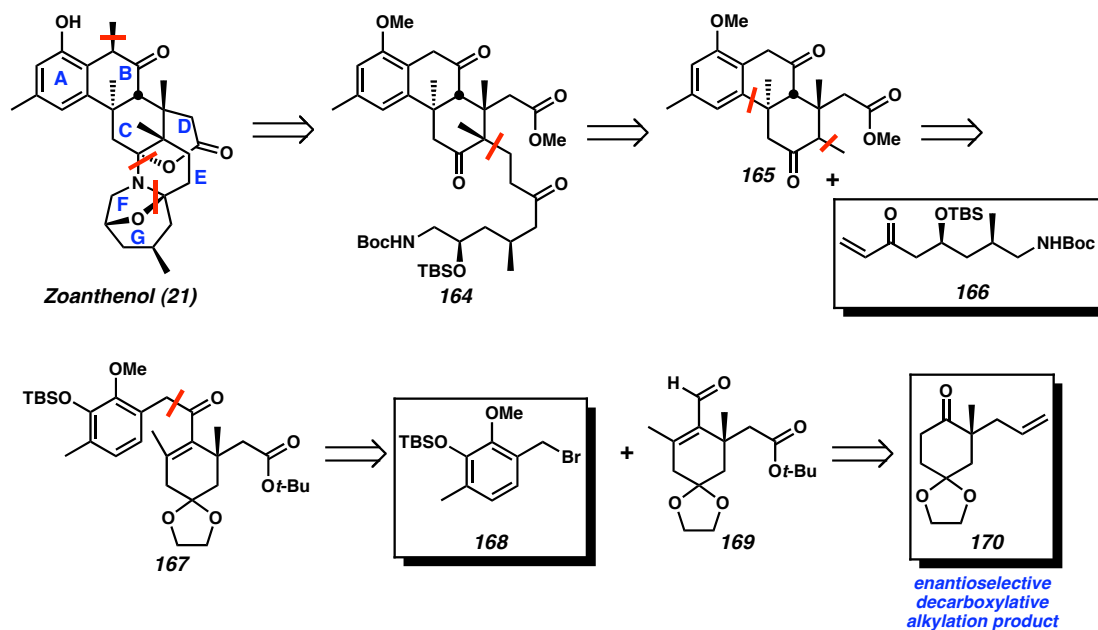
##### *2.1.1 Introduction and Retrosynthetic Analysis<sup>†</sup>*

In Chapter 1, we highlighted the range of biological activities and structural features presented by the zoanthamine family of alkaloids. When we began our efforts toward the synthesis of this intriguing family of natural products, we were drawn to zoanthenol (**21**) as an initial synthetic target because it retains the major stereochemical challenges of the zoanthamines, while its aromatic A ring offers the opportunity to explore unique retrosynthetic possibilities.<sup>2</sup> It was our hope that the challenges encountered during the synthesis of zoanthenol would guide our future synthetic efforts toward the remaining family members. With seven rings and nine stereocenters confined to a 30-carbon framework, zoanthenol is a densely functionalized, topographically complex target molecule. The C ring poses the greatest stereochemical challenge with five contiguous stereocenters, three of which are all-carbon quaternary centers. Our overarching strategy was to generate one quaternary center in an enantioselective fashion and then derive the remaining stereocenters diastereoselectively. A convergent union of the A and C rings by a 2-carbon tether and subsequent closure of the B ring was another design feature. We planned to introduce all the functionality of the heterocyclic C(1) to C(8) fragment in a single operation (i.e., **164**  $\Rightarrow$  **165** + **166**). Previous work by the Kobayashi and Williams groups demonstrated that the complicated hemiaminals forming the DEFG

---

<sup>†</sup> The work described in this chapter was performed primarily by former graduate students in the Stoltz group, Dr. Douglas C. Behenna (Carbocyclic Core) and Dr. Jeffrey T. Bagdanoff (DEFG Synthone), prior to my arrival at Caltech.

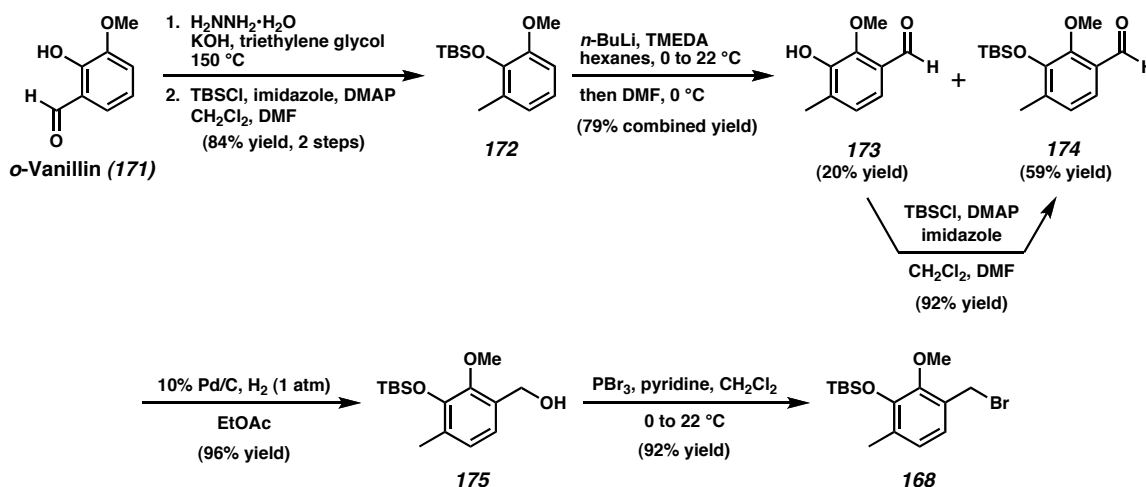
rings were thermodynamically favored.<sup>3</sup> Thus, the DEFG heterocycles could be retrosynthetically unraveled to give triketone **164** (Scheme 2.1.1). Disconnection of the C(8)-C(9) bond and removal of the C(9) and C(19) methyl groups could afford ketone **165** and enone **166**. We envisioned the cleavage of the tricyclic core structure **165** by scission of the C(12)-C(13) bond employing an intramolecular conjugate addition of the A ring into a C ring enone (i.e., **166**).<sup>4</sup> We reasoned that this type of intramolecular Friedel-Crafts reaction would require a highly electron-rich arene for effective cyclization; therefore, oxygenation was incorporated at C(16) of enone **167** to increase the nucleophilicity of the A ring. Enone **167** could arise from 1,2-addition of a Grignard reagent derived from bromide **168** into enal **169**, which in turn could be derived from  $\alpha$ -quaternary allyl ketone **170**, which was accessible in enantioenriched form as the product of an enantioselective decarboxylative alkylation reaction.<sup>5</sup>



**Scheme 2.1.1** Retrosynthetic analysis of zoanthenol.

### 2.2.1 Synthesis of the A Ring Synthon

The A ring synthon could be readily accessed in five steps from *o*-vanillin (**171**, Scheme 2.2.1). Wolff-Kishner reduction of **171** followed by silylation provided arene **172** in 84% yield over two steps. *Ortho*-lithiation was directed by the C(17) methoxy group, and quenching with *N,N*-dimethylformamide provided a mixture of aldehyde **174** and the corresponding desilylated aldehyde **173**. Resilylation of **173** proceeded smoothly under standard conditions to provide **174**. Aldehyde reduction was accomplished by treatment with 10% Pd/C under a balloon of hydrogen to afford benzylic alcohol **175** in 96% yield.<sup>6</sup> Treatment of this benzylic alcohol (**175**) with phosphorus tribromide and pyridine led to benzyl bromide **168** in 92% yield after distillation. This approach to the A ring synthon was efficient and highly scalable, allowing production of 20–25 g of benzyl bromide **168** per batch.

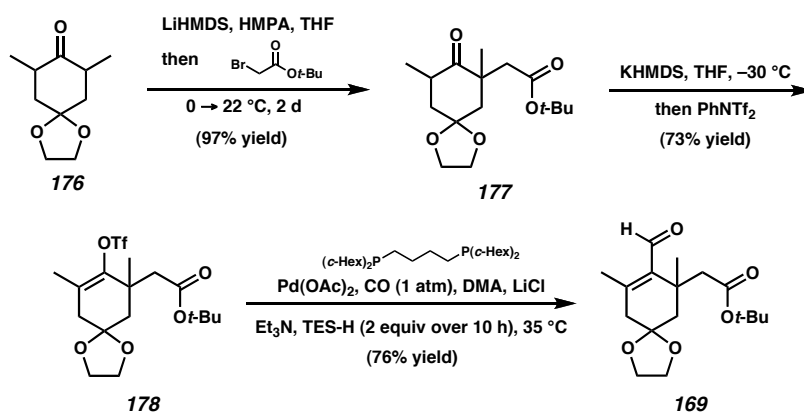


**Scheme 2.2.1** Synthesis of the A ring synthon.

### 2.2.2 Synthesis of the C Ring Synthon

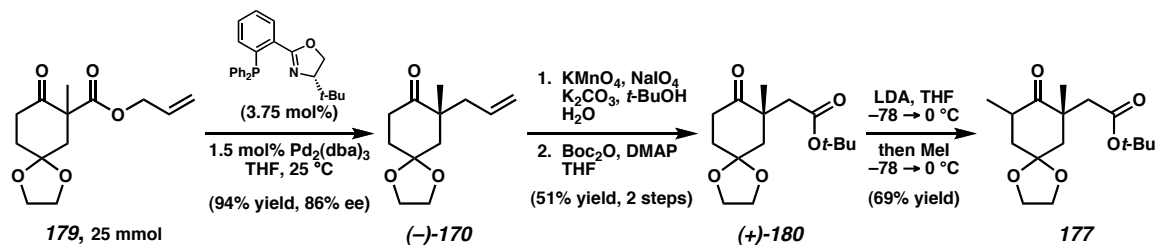
In order to determine the feasibility of the 6-*exo* conjugate addition, the target enal was synthesized as a racemate (Scheme 2.2.2). Known 1,6-dimethyl ketone **176**<sup>7</sup> was deprotonated and alkylated to give ketoester **177** in excellent yield as a mixture of

diastereomers. Deprotonation of methyl ketone **177** and quenching with  $\text{PhNTf}_2$  afforded enol triflate **178**. After significant optimization to accommodate the steric challenges of the substrate, an efficient one-step reductive carbonylation of triflate **178** was developed. Treatment of triflate **178** under an atmosphere of CO with  $\text{Pd}(\text{OAc})_2$ , 1,4-bis-(dicyclohexylphosphino)butane as a ligand, and TES-H as a reducing agent afforded the desired enal **169** in good yield. To our knowledge, this is the first time that such a hindered vinyl triflate has been carbonylated directly to the enal oxidation state.<sup>8</sup>



**Scheme 2.2.2** Racemic synthesis of the C ring synthon.

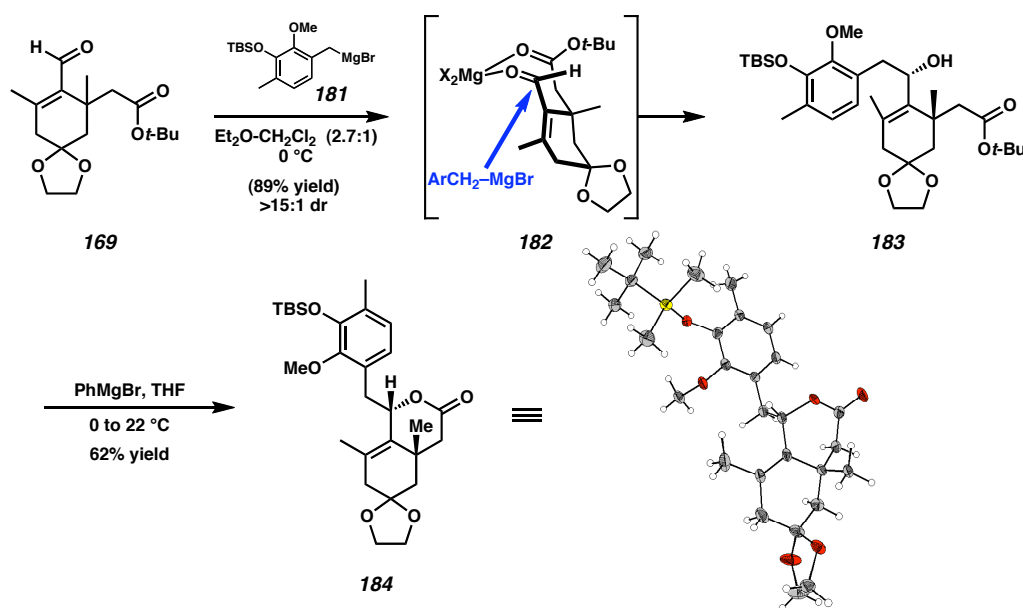
Although racemic material was useful for exploratory studies, our goal from the outset was an asymmetric synthesis of zoanthenol. Toward this end, we were delighted to find that our recently developed asymmetric decarboxylative alkylation methodology<sup>5</sup> was a reliable and efficient method to convert allyl  $\beta$ -ketoester **179** to  $\alpha$ -quaternary ketone (–)-**170** in excellent yield and high ee on 25 mmol scale (Scheme 2.2.3). Oxidative olefin cleavage and esterification gave *t*-butyl ester (+)-**180** in 51% yield over two steps. Subsequent methylation provided a good yield of methyl ketoester **177**, an intermediate in our C ring synthesis, allowing entry into a catalytic enantioselective synthesis of zoanthenol.



**Scheme 2.2.3** Decarboxylative alkylation enables enantioselective synthesis.

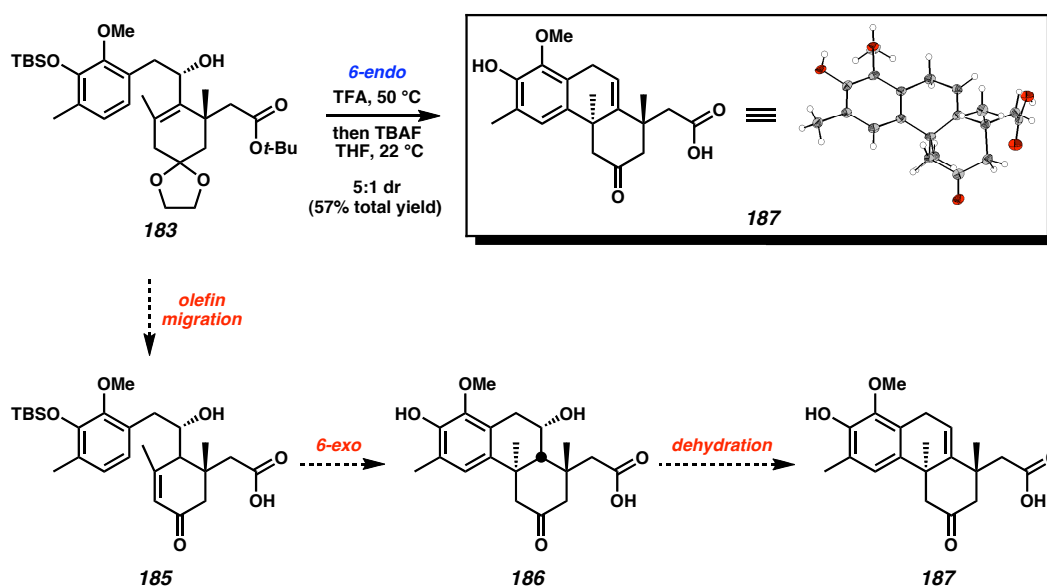
### 2.2.3 Synthesis of the Tricyclic Core of Zoanthenol

Addition of Grignard reagent **181**, derived from A-ring synthon **168**, to enal **169** produced allylic alcohol **183** in high yield and diastereoselectivity (Scheme 2.2.4). Use of methylene chloride as a co-solvent for the addition reaction was critical. We hypothesize that the addition of this noncoordinating solvent encourages the chelation of Mg between the aldehyde and the *t*-butyl ester, resulting in selective attack of the *Re* face of the aldehyde by the incoming Grignard reagent (**182**). This stereochemistry was confirmed by formation of lactone **184** and examination of a single crystal by X-ray structure analysis.



**Scheme 2.2.4** Diastereoselective Grignard addition.

With the A and C rings joined, we could begin to investigate the 6-*exo* cyclization by exposing allylic alcohol **183** to TFA at reflux (Scheme 2.2.5). We anticipated that loss of protecting groups and olefin migration would afford enone **185**, which would undergo 6-*exo* conjugate addition to form keto-alcohol **186**. To our delight, the major product contained a single aromatic C-H peak by  $^1\text{H}$  NMR, as well as two isolated aliphatic  $\text{CH}_3$  groups, signaling that the reaction generated a product containing the two desired quaternary centers. However, the spectrum also possessed an olefinic resonance. Upon standing in  $\text{CDCl}_3$ , the major product formed crystals suitable for X-ray diffraction. Interestingly, cyclization of allylic alcohol **183** had occurred, but via 6-*endo*  $\text{S}_{\text{N}}'$  cyclization to give acid **187**.<sup>9,10</sup> Additionally, the solid-state structure confirmed the anti disposition of the methyl groups at C(12) and C(22) in **187**.

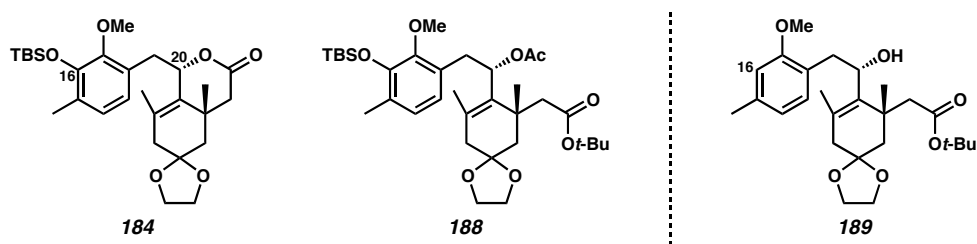


**Scheme 2.2.5** Discovery of an unusual acid-mediated cyclization.

The  $\text{S}_{\text{N}}'$  Friedel-Crafts reaction to produce carboxylic acid **187** achieved the important goal of generating the C(12) quaternary stereocenter with the desired relative configuration. In order to better understand the reaction pathway, a number of parameters were evaluated. The choice of acid in the reaction is crucial, as trifluoroacetic acid was unique in promoting  $\text{S}_{\text{N}}'$  cyclization. Both stronger acids (e.g.,

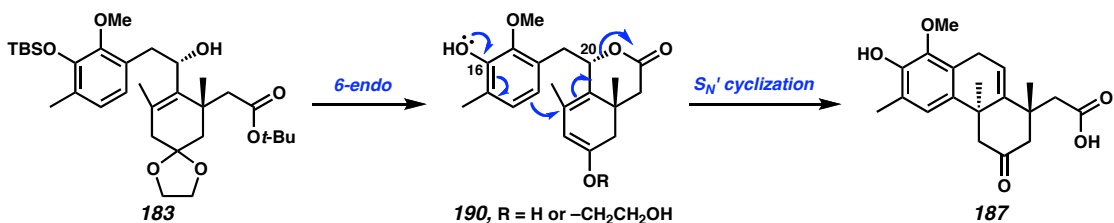
triflic acid) and weaker acids (e.g., acetic acid) failed to produce tricycle **187**. Even the dilution of neat TFA with methylene chloride, benzene, or acetic acid caused the cyclization to fail.

Interestingly, both lactone **184** and allylic acetate **188** underwent cyclization in TFA to give acid **187** with similar yields and diastereoselectivities (Scheme 2.2.6).<sup>11</sup> Furthermore, C(16) des-oxy arene **189** failed to generate any cyclized products, confirming the importance of the nucleophilicity imparted by C(16) oxygenation. Finally, the allylic alcohol substrate epimeric at C(20) does not undergo cyclization.<sup>12</sup>



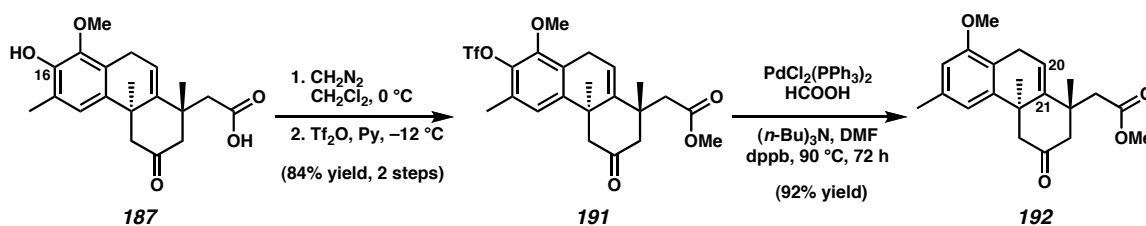
**Scheme 2.2.6** Other substrates for cyclization.

The unique ability of TFA to mediate the reaction suggests that its properties as a strong acid and a dehydrating agent are important to the reaction mechanism. The selectivity of the system indicates that all three substrates (**183**, **184**, and **185**) may proceed through intermediate lactone **190** (i.e., allylic alcohol **183** and acetate **188** may be converted to the lactone in situ), and that the reactions proceed via a partially concerted displacement relying on the directing ability of a carboxylate leaving group and not via a full allylic cation (Scheme 2.2.7).



**Scheme 2.2.7** A proposed mechanism for the  $S_N'$  cyclization.

With an efficient route in hand to construct a zoanthenol carbocyclic ring system containing two of the three quaternary stereocenters, we turned our attention to the completion of our proposed intermediate **165**. Following diazomethane-mediated esterification, deoxygenation of the C(16) phenol was accomplished by formation of aryl triflate **191** and subsequent treatment with  $\text{PdCl}_2(\text{PPh}_3)_2$  and formic acid to form **192** in 92% yield (Scheme 2.2.8).<sup>13</sup>

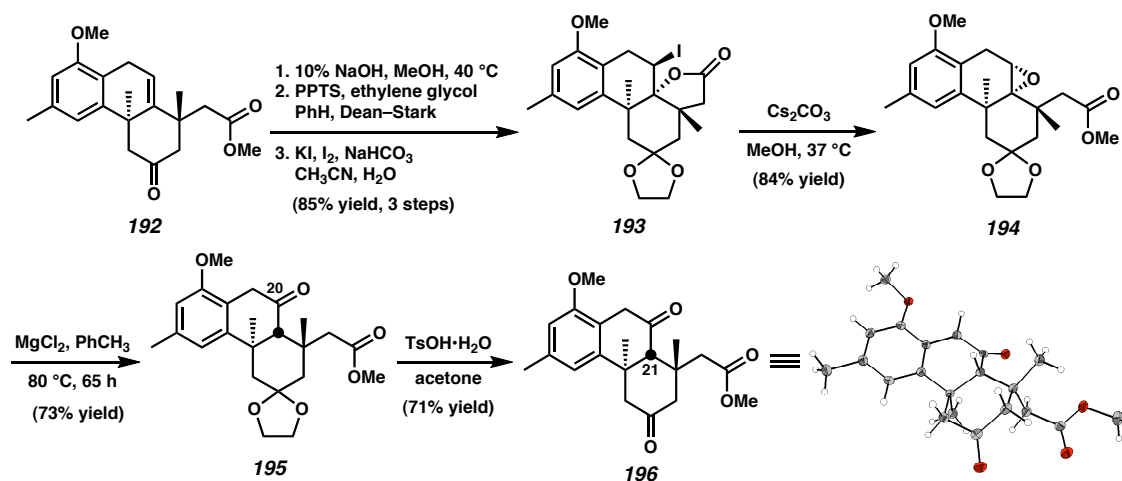


**Scheme 2.2.8** Deoxygenation of the A ring.

Due to our serendipitous discovery of the  $\text{S}_{\text{N}}'$  reaction, we had not anticipated the reoxygenation of the olefin in our retrosynthetic planning. As such, significant experimentation was required to find a synthetic strategy to convert the C(20)–C(21) olefin of ketoester **192** into the desired C(20) ketone.<sup>14</sup> The X-ray structure in Scheme 2.2.5 illustrates the pseudo-axial nature of the methyl groups surrounding the olefin, which partially block the  $\pi$  bond and hinder the approach of typical oxidants.

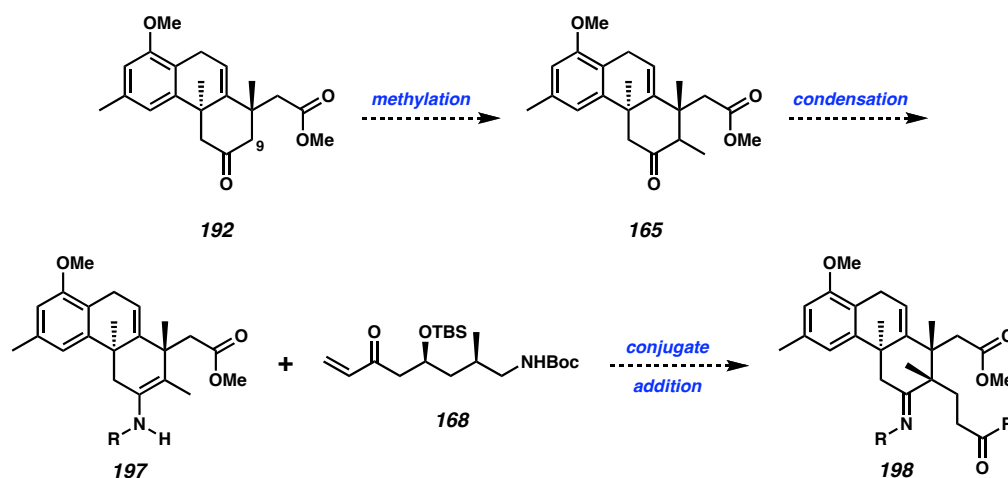
Thus, we chose to pursue an alternative, intramolecular method of olefin oxygenation. Our approach began with saponification of ketoester **192** followed by ketalization (Scheme 2.2.9). Treatment of the crude product with KI,  $\text{I}_2$ , and base gave iodolactone **193** in 85% yield over three steps after recrystallization. Lactone methanolysis under basic conditions afforded smooth conversion to epoxide **194**. Hydride migration from C(20) was accomplished by heating epoxide **194** in toluene with  $\text{MgCl}_2$ ,<sup>15</sup> resulting in smooth conversion to rearranged ketoester **195** in 73% yield. Treatment of ketoester **195** with *p*-toluenesulfonic acid produced diketone **196**, which

was characterized by X-ray crystallography. The solid-state structure confirmed that the desired C(21) stereochemistry was obtained from the hydride shift.



**Scheme 2.2.9** Refunctionalization of the C(20)-C(21) olefin.

Having completed the synthesis of the carbocyclic core, we turned our attention to the installation of the C(9) methyl group and side chain attachment. As illustrated in Scheme 2.2.10, methylation of tricycle **192** would be followed by condensation with a primary amine to form enamine **197**. Conjugate addition of this enamine into enone **168** would then provide readily hydrolyzable imine **198**.

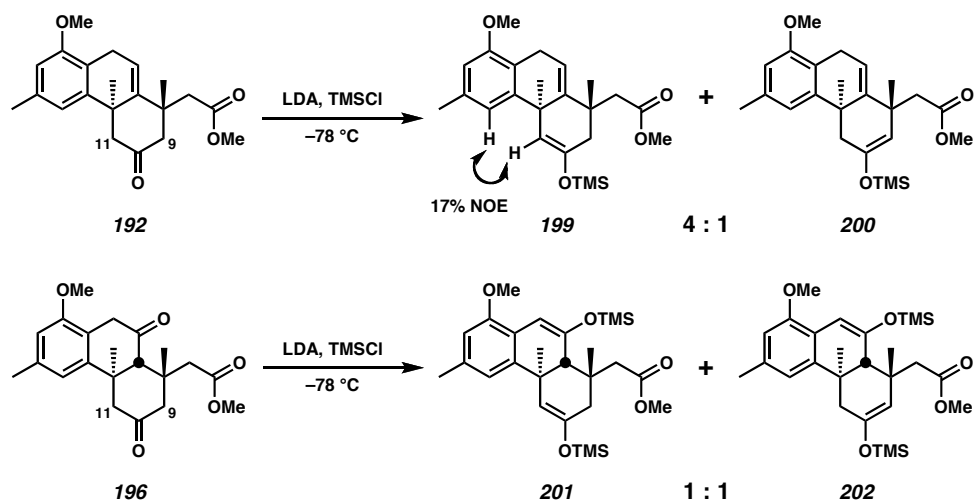


**Scheme 2.2.10** Plan for elaboration of the tricyclic core.

Initial conditions tested seemed to favor enolization at C(11) rather than C(9). In order to solidify the nature of the system's behavior without the complication of

diastereomers, silyl enol ethers were generated under kinetic and thermodynamic conditions (Scheme 2.2.11). Interestingly, when tricycle **192** was treated with kinetic enolization conditions, a 4:1 ratio of silyl enol ethers (**199**:**200**) was observed. The major product of the inseparable mixture of enol ethers was identified as **199** via 1D nOe experiments. Given our uncertainty about the cause of the selectivity in this system, we also tested tricycle **196**. In this case, a 1:1 ratio of silyl enol ethers was observed. This improvement was promising, though certainly not viable at this stage of the synthesis.<sup>16</sup> Despite efforts to improve the selectivity of these alkylations, we were unable to improve the ratio beyond a 1:1 mixture. Ketoester **196** was treated under thermodynamic enolization conditions and nearly exclusive enolization was observed at C(11).<sup>17</sup>

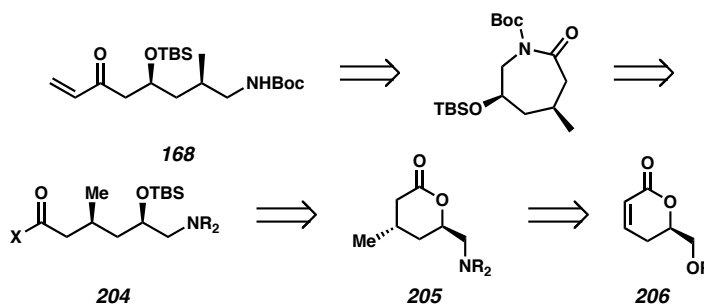
In addition to the challenges faced in the methylation step, we found that a very simple system modeling the conjugate addition step was unreactive.<sup>18</sup> Thus, we considered other options for the installation of this quaternary center. We examined a cyclopropanation approach similar to Hirama's strategy (see Chapter 1)<sup>19</sup> and a Tsuji alkylation-based approach.<sup>20</sup> Ultimately, we chose to alter our synthetic strategy to include the vicinal all-carbon quaternary centers from an early stage, as will be discussed in Chapter 3.



**Scheme 2.2.11** Attempts to enolize at C(9).

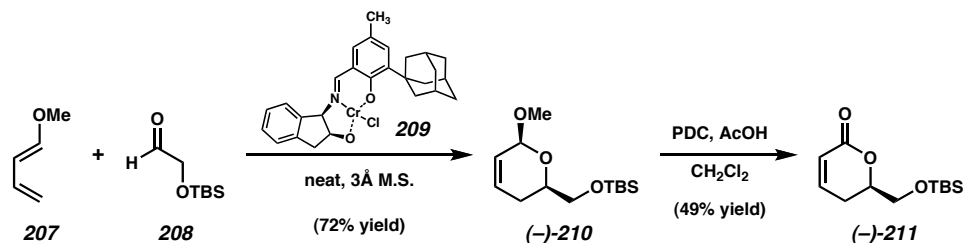
### 2.3.1 Enantioselective Synthesis of the DEFG Synthon

Once we access a suitable carbocyclic core structure, we will need to couple it to an appropriately functionalized side chain in order to form the heterocyclic DEFG ring system of zoanthenol. Our initial target for such a synthon was  $\alpha,\beta$ -unsaturated ketone **166** (Scheme 2.3.1). We envisioned that enone **166** could be accessed from caprolactam **203**, which we disconnected across the amide C–N bond to reveal amine **204**. This amine, in turn, could be derived from  $\delta$ -lactone **205**, accessible from  $\alpha,\beta$ -unsaturated lactone **206**.



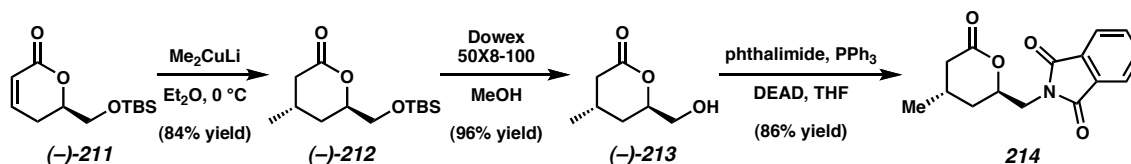
**Scheme 2.3.1** Retrosynthetic analysis of the DEFG synthon.

To access **206** in enantioenriched form, we initially investigated an approach beginning with a glycol, which required oxidation to a lactone as well as the removal of superfluous oxygenation.<sup>21</sup> Additionally, we could access either racemic or enantioenriched material from ( $\pm$ )-glycidol or (*S*)-glycidol.<sup>22</sup> Ultimately, we employed an efficient and enantioselective method developed by Jacobsen and coworkers for the synthesis of  $\alpha,\beta$ -unsaturated lactone **211**.<sup>23</sup> In their work, diene **207** and aldehyde **208** were treated with hetero-Diels-Alder catalyst **209** (Scheme 2.3.2), which facilitates cycloaddition reactions between electron-rich dienes and aldehydes. The desired dihydropyran was isolated in 72% yield and could be converted to the necessary lactone using acidic pyridinium dichromate conditions.



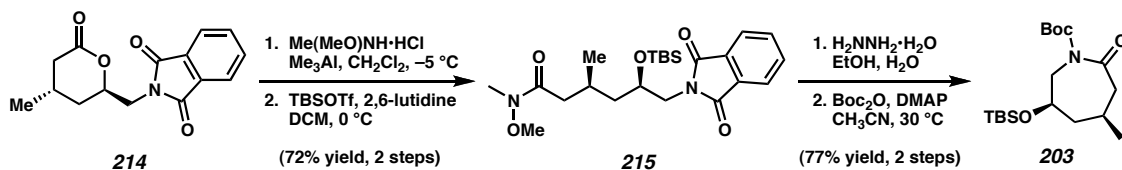
**Scheme 2.3.2** Jacobsen hetero-Diels-Alder cycloaddition.

At this point, a selective 1,4-addition was accomplished by treatment of **211** with Gilman's reagent to afford **212** as a single diastereomer (Scheme 2.3.3). Treatment with an acidic resin induced desilylation to provide alcohol **213**, and subsequent Mitsunobu reaction provided phthalimide derivative **214**.



**Scheme 2.3.3** Conjugate addition and Mitsunobu reaction provide key intermediate.

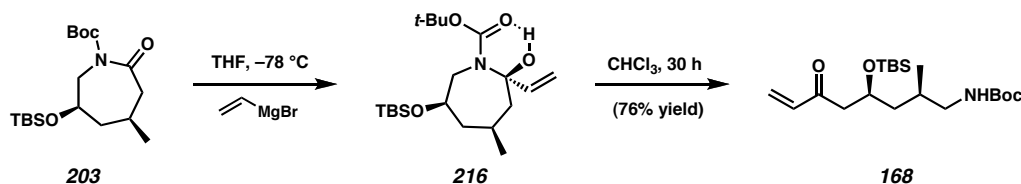
The chiral lactone was then treated under standard Weinreb amide formation conditions, and the intermediate alcohol was immediately trapped by addition of TBSOTf and 2,6-lutidine to yield Weinreb amide **215** (Scheme 2.3.4). Treatment of **215** with hydrazine hydrate in refluxing ethanol revealed the free primary amine, which spontaneously cyclized with the Weinreb amide to form a caprolactam. Carbamate formation with Boc anhydride provided key caprolactam **203**.



**Scheme 2.3.4** Conversion of the  $\delta$ -lactone to the  $\epsilon$ -lactam synthon.

The final step in accessing synthon **166** was to add a single vinyl equivalent to the Boc-protected caprolactamate. Thus, treatment of **203** with vinyl magnesium bromide provided the isolable Grignard adduct **216** (Scheme 2.3.5). The chelation of Mg between

the Boc carbonyl and the amide carbonyl encourages addition of a single equivalent of the nucleophile, and we anticipate that a similar hydrogen-bonding event slows the collapse of hemiaminal **216**. Upon standing in  $\text{CHCl}_3$ , desired enone **166** is produced. Additionally, because we had observed this exquisite selectivity for a single addition, we were ultimately able to employ caprolactam **203** as our DEFG synthon in an alternative route.



**Scheme 2.3.5** Vinylation of the  $\epsilon$ -lactam to access the enone synthon.

#### 2.4.1 Summary of Early Synthetic Work

In conclusion, a concise method for the construction of the zoanthenol carbocyclic skeleton was developed. This approach is highlighted by an unusual diastereoselective  $\text{S}_{\text{N}}'$  cyclization of allylic alcohol **183** producing tricycle **187** bearing all-carbon quaternary centers at C(12) and C(22) in the desired anti configuration. This key step in our route is flanked by a number of novel transformations. Most notably, we demonstrate an unusual palladium-catalyzed formylation of a hindered vinyl triflate, a highly diastereoselective Grignard addition to a congested enal, and an iodolactonization and subsequent epoxide rearrangement utilizing the pendant C(24) carboxylate to incorporate the C(20) ketone. Gratifyingly, application of our catalytic asymmetric decarboxylative alkylation methodology allows ready access into an enantioselective synthesis of zoanthenol. Our studies have also encompassed the synthesis of a fully functionalized, enantiopure DEFG synthon for late-stage coupling with our carbocyclic core structures. The synthesis of this synthon features a Jacobsen enantioselective hetero-Diels-Alder followed by a selective conjugate addition. Additionally, selective

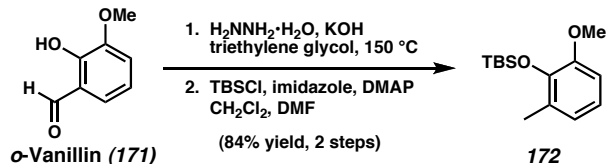
ring opening and ring closing events allow for an elegant elaboration of the key  $\alpha,\beta$ -unsaturated lactone. Namely, Weinreb amide formation with immediate trapping enables the conversion of a  $\delta$ -lactone to a linear intermediate, which upon phthalamide decomposition immediately closes again to a caprolactam. The carbamate produced upon Boc protection is then critical in allowing selective mono-addition of organometallic species into the caprolactam.

### 2.5.1 Materials and Methods

Unless otherwise stated, reactions were performed at ambient temperature (typically 19–24 °C) in flame-dried glassware under an argon or nitrogen atmosphere using dry, deoxygenated solvents. Solvents were dried by passage through an activated alumina column under argon. TMEDA, HMPA, TEA, DIPA, and pyridine were freshly distilled from CaH. KHMDS (95%) was purchased from Aldrich and stored in a glovebox until use. Trifluoroacetic acid (99%) was purchased from Aldrich. Tf<sub>2</sub>O was freshly distilled from P<sub>2</sub>O<sub>5</sub>. Magnesium chloride (~ 325 mesh, < 1.5% H<sub>2</sub>O) was purchased from Aldrich. All other commercially obtained reagents were used as received. Reaction temperatures were controlled by an IKAmag temperature modulator. Thin-layer chromatography (TLC) was performed using E. Merck silica gel 60 F254 precoated plates (0.25 mm) and visualized by UV fluorescence quenching, anisaldehyde, KMnO<sub>4</sub>, or CAM staining. ICN silica gel (particle size 0.032–0.063 mm) was used for flash chromatography. Optical rotations were measured with a Jasco P-1010 polarimeter at 589 nm. <sup>1</sup>H and <sup>13</sup>C NMR spectra were recorded on a Varian Mercury 300 (at 300 MHz and 75 MHz respectively), or a Varian Inova 500 (at 500 MHz and 125 MHz respectively) and are reported relative to Me<sub>4</sub>Si ( $\delta$  0.0). Data for <sup>1</sup>H NMR spectra are reported as follows: chemical shift ( $\delta$  ppm) (multiplicity, coupling constant (Hz), integration). Multiplicities are reported as

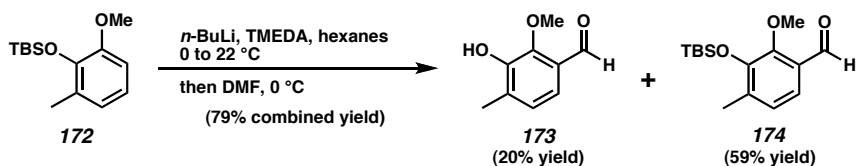
follows: s = singlet, d = doublet, t = triplet, q = quartet, sept. = septet, m = multiplet, comp. m = complex multiplet, app. = apparent, bs = broad singlet, bm = broad multiplet. IR spectra were recorded on a Perkin Elmer Paragon 1000 spectrometer and are reported in frequency of absorption ( $\text{cm}^{-1}$ ). High-resolution mass spectra were obtained from the Caltech Mass Spectral Facility. Crystallographic analyses were performed at the California Institute of Technology Beckman Institute X-Ray Crystallography Laboratory. Crystallographic data have been deposited at the CCDC, 12 Union Road, Cambridge CB2 1EZ, UK, and copies can be obtained on request, free of charge, from the CCDC by quoting the publication citation and the deposition number (see Appendix B for deposition numbers).

## 2.5.2 Preparation of Compounds



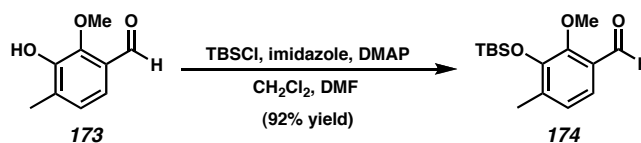
**Arene 172.** To a warmed solution (110 °C for 45 min) of *o*-vanillin (**171**, 60.0 g, 0.394 mol, 1.00 equiv) and  $\text{NH}_2\text{NH}_2\cdot\text{H}_2\text{O}$  (53.6 mL, 1.10 mol, 2.79 equiv) in triethylene glycol (320 mL) in a 1 L round bottom flask was added KOH (132 g, 2.37 mol, 6.02 equiv) (*Caution: gas evolution and exotherm*) in portions over 20 min. The reaction mixture was maintained at 150 °C under a reflux condenser for 5 h, cooled to ambient temperature, and poured into  $\text{H}_2\text{O}$  (750 mL), ice (200 g), and 6 M HCl (500 mL). The mixture was further acidified to pH 2 with 6 M HCl, then extracted with  $\text{CHCl}_3$  (7 x 200 mL), dried ( $\text{MgSO}_4$ ), and evaporated to give a green solid (~ 60 g) that was immediately used in the next step without further purification.

To a solution of this crude solid in DMF (300 mL) and  $\text{CH}_2\text{Cl}_2$  (300 mL) were added imidazole (53.6 g, 0.788 mol, 2.00 equiv), DMAP (62.5 g, 0.512 mol, 1.30 equiv), and TBSCl (62.1 g, 0.414 mol, 1.05 equiv). After 4 h at ambient temperature, the reaction mixture was poured into  $\text{H}_2\text{O}$  (1.3 L), extracted with  $\text{CH}_2\text{Cl}_2$  (3 x 150 mL), and the combined organic layers were washed with cold 0.25 M HCl (2 x 250 mL), 1 M NaOH (250 mL), and brine (2 x 200 mL). Evaporation of the organics gave an oil, which was purified by distillation at reduced pressure (~ 2 mmHg) to give arene **172** (83.6 g, bp 120–127 °C at 2 mmHg, 84% yield over 2 steps) as a colorless oil:  $R_f$  0.74 (10% EtOAc in hexanes);  $^1\text{H}$  NMR (300 MHz,  $\text{CDCl}_3$ )  $\delta$  6.83–6.69 (comp. m, 3H), 3.78 (s, 3H), 2.24 (s, 3H), 1.01 (s, 9H), 0.18 (s, 6H);  $^{13}\text{C}$  NMR (75 MHz,  $\text{CDCl}_3$ )  $\delta$  150.0, 143.1, 129.6, 122.8, 120.5, 109.1, 54.8, 26.1, 18.9, 17.1, -3.9; IR (Neat film NaCl) 2955, 2930, 1488, 1280, 1251, 1233, 1086, 920, 781  $\text{cm}^{-1}$ ; HRMS (FAB+)  $[\text{M}+\text{H}]^+$  calc'd for  $\text{C}_{14}\text{H}_{24}\text{SiO}_2+\text{H}^+$ :  $m/z$  253.1624, found 253.1633.

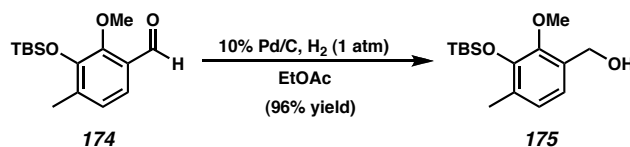


**Benzaldehyde 174 from arene 172.** To a cooled (0 °C) solution of arene **172** (30.0 g, 119 mmol, 1.00 equiv), and TMEDA (25.1 mL, 166 mmol, 1.40 equiv) in hexanes (200 mL) was added *n*-BuLi (2.25 M in hexanes, 63.4 mL, 142 mmol, 1.20 equiv) in a dropwise manner over 15 min. After 1 h at 0 °C, the reaction mixture was allowed to warm to ambient temperature for 6 h. The reaction mixture was cooled (0 °C) again and DMF (15.6 mL, 202 mmol, 1.70 equiv) was added dropwise over 10 min. After an additional 1 h at 0 °C, saturated aqueous NH<sub>4</sub>Cl (100 mL) was added, and the mixture was allowed to warm to ambient temperature overnight. The mixture was poured into H<sub>2</sub>O (200 mL) and Et<sub>2</sub>O (200 mL), then extracted with Et<sub>2</sub>O (2 x 100 mL). The aqueous layers were then acidified with 2 M HCl to pH 1, and further extracted with Et<sub>2</sub>O (5 x 150 mL). The combined organic layers were washed with brine (50 mL), dried (Na<sub>2</sub>SO<sub>4</sub>), and evaporated to give an oil that was purified by gradient flash chromatography on silica gel (2 to 20% EtOAc in hexanes) to give benzaldehyde **174** (19.7 g, 59% yield) as a colorless oil: *R<sub>f</sub>* 0.67 (20% EtOAc in hexanes); <sup>1</sup>H NMR (300 MHz, CDCl<sub>3</sub>) δ 10.28 (s, 1H), 7.36 (d, *J* = 7.5 Hz, 1H), 6.98 (d, *J* = 8.1 Hz, 1H), 3.81 (s, 3H), 2.28 (s, 3H), 1.03 (s, 9H), 0.20 (s, 6H); <sup>13</sup>C NMR (75 MHz, CDCl<sub>3</sub>) δ 189.7, 154.2, 147.2, 138.4, 128.1, 126.4, 120.7, 62.5, 26.0, 18.6, 17.9, -4.1; IR (Neat film NaCl) 2957, 2932, 2859, 1691, 1464, 1273, 1255, 838 cm<sup>-1</sup>; HRMS (FAB+) [M+H]<sup>+</sup> calc'd for C<sub>15</sub>H<sub>24</sub>SiO<sub>3</sub>+H<sup>+</sup>: *m/z* 281.1573, found 281.1572 and phenol **173** (3.9 g, 20% yield) as a white solid: mp 90.0–91.0 °C; *R<sub>f</sub>* 0.25 (20% EtOAc in hexanes); <sup>1</sup>H NMR (300 MHz, CDCl<sub>3</sub>) δ 10.18 (s, 1H), 7.27 (d, *J* = 8.1 Hz, 1H), 7.01 (d, *J* = 8.1 Hz, 1H), 6.02 (bs, 1H), 3.95 (s, 3H), 2.32 (s, 3H); <sup>13</sup>C NMR (75 MHz, CDCl<sub>3</sub>) δ 189.4, 148.4, 147.5, 132.8, 126.7, 126.5, 121.3, 63.8, 16.3; IR (Neat film NaCl)

3410, 2938, 2857, 1686, 1466, 1261, 1061, 782  $\text{cm}^{-1}$ ; HRMS (FAB+)  $[\text{M}+\text{H}]^+$  calc'd for  $\text{C}_9\text{H}_{10}\text{O}_3+\text{H}^+$ :  $m/z$  167.0708, found 167.0708.

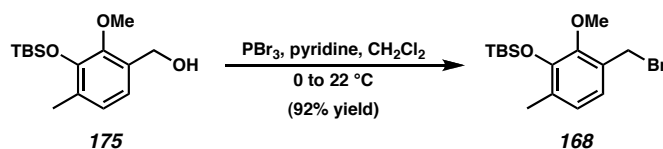


**Benzaldehyde 174 from phenol 173.** To a solution of phenol **173** (10.0 g, 60.2 mmol, 1.00 equiv) in DMF (60 mL) and  $\text{CH}_2\text{Cl}_2$  (60 mL) were added imidazole (8.20 g, 120 mmol, 2.00 equiv), DMAP (9.55 g, 78.3 mmol, 1.30 equiv), and TBSCl (11.7 g, 78.3 mmol, 1.30 equiv). After 36 h, the reaction mixture was quenched with  $\text{H}_2\text{O}$  (200 mL) and  $\text{CH}_2\text{Cl}_2$  (200 mL), and extracted with  $\text{CH}_2\text{Cl}_2$  (3 x 50 mL). The combined organics were washed with  $\text{H}_2\text{O}$  (200 mL) and then brine (100 mL), dried ( $\text{MgSO}_4$ ), and concentrated to an oil, which was purified by flash chromatography on silica gel (2% EtOAc in hexanes) to provide benzaldehyde **174** (15.5 g, 92% yield).

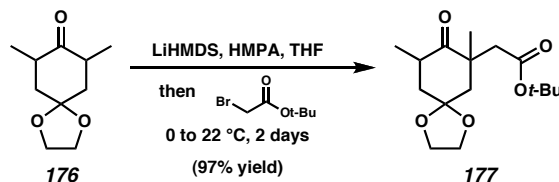


**Benzyl alcohol 175.** A flame-dried 100 mL round bottom flask was charged with 10% Pd/C (270 mg), EtOAc (55 mL), and benzaldehyde **174** (2.0 g, 7.13 mmol, 1.00 equiv) under an  $\text{N}_2$  atmosphere. The reaction mixture and headspace were sparged with  $\text{H}_2$  (5 min) and stirred vigorously under an atmosphere of  $\text{H}_2$  (balloon) for 3 h. Immediately following the completion of the reaction, as indicated by TLC, the reaction mixture was sparged with  $\text{N}_2$  for 15 min then concentrated to an oil, which was purified by flash chromatography on silica gel (10 to 15% EtOAc in hexanes) to provide benzyl alcohol **175** (1.93 g, 96% yield) as a colorless oil:  $R_f$  0.33 (20% EtOAc in hexanes);  $^1\text{H}$  NMR (300

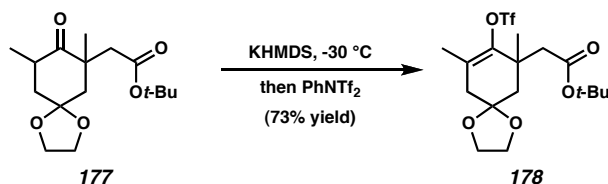
MHz, CDCl<sub>3</sub>) δ 6.88 (d, *J* = 7.5 Hz, 1H), 6.83 (d, *J* = 8.1 Hz, 1H), 4.65 (d, *J* = 6.3 Hz, 2H), 3.75 (s, 3H), 2.25 (t, *J* = 6.3 Hz, 1H), 2.21 (s, 3H), 1.03 (s, 9H), 0.18 (s, 6H); <sup>13</sup>C NMR (75 MHz, CDCl<sub>3</sub>) δ 149.4, 147.0, 132.4, 130.6, 126.1, 121.1, 61.7, 60.5, 26.0, 18.6, 17.2, -4.2; IR (Neat film NaCl) 3340, 2956, 2931, 2859, 1464, 1420, 1285, 839, 782 cm<sup>-1</sup>; HRMS (FAB+) [M+H-H<sub>2</sub>]<sup>+</sup> *m/z* calc'd for [C<sub>15</sub>H<sub>25</sub>SiO<sub>3</sub>]<sup>+</sup>: 281.1573, found 281.1564.



**Benzyl bromide 168.** To a cooled (0 °C) solution of benzyl alcohol **175** (16.0 g, 56.7 mmol, 1.00 equiv) and pyridine (4.36 mL, 53.9 mmol, 0.95 equiv) in CH<sub>2</sub>Cl<sub>2</sub> (200 mL) was added PBr<sub>3</sub> (4.84 mL, 51.0 mmol, 0.90 equiv) in CH<sub>2</sub>Cl<sub>2</sub> (50 mL) over 30 min. After stirring an additional 30 min at 0 °C, the reaction mixture was allowed to come to ambient temperature and stirred for a further 2.5 h. The reaction mixture was diluted with CH<sub>2</sub>Cl<sub>2</sub> (300 mL), brine (500 mL), and H<sub>2</sub>O (250 mL), then extracted with Et<sub>2</sub>O (2 x 150 mL), dried over Na<sub>2</sub>SO<sub>4</sub>, and concentrated. The resulting oil was passed through a plug of silica gel (10 cm h x 5.5 cm d) (1:1 hexanes:CH<sub>2</sub>Cl<sub>2</sub>), concentrated, and the resultant oil was purified by distillation at reduced pressure (~ 2 mmHg) to provide benzyl bromide **168** (27.4 g, bp 146–147 °C at ~ 2 mmHg, 92% yield) as a colorless oil: *R<sub>f</sub>* 0.50 (2.5% EtOAc in hexanes); <sup>1</sup>H NMR (300 MHz, CDCl<sub>3</sub>) δ 6.91 (d, *J* = 8 Hz, 1H), 6.87 (d, *J* = 8 Hz, 1H), 4.56 (s, 2H), 3.83 (s, 3H), 2.23 (s, 3H), 1.04 (s, 9H), 0.18 (s, 6H); <sup>13</sup>C NMR (75 MHz, CDCl<sub>3</sub>) δ 149.7, 147.2, 131.9, 129.6, 126.2, 123.2, 60.4, 28.8, 26.0, 18.6, 17.3, -4.2; IR (Neat film NaCl) 2957, 2931, 2859, 1464, 1421, 1289, 1259, 1239, 1072, 840, 782 cm<sup>-1</sup>; HRMS (FAB+) [M+H]<sup>+</sup> *m/z* calc'd for [C<sub>15</sub>H<sub>25</sub>SiBrO<sub>2</sub>+H]<sup>+</sup>: 345.0885, found 345.0885.

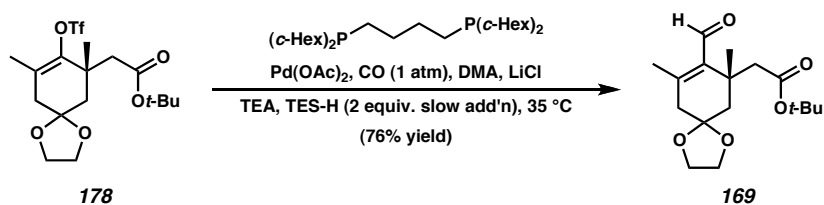


**Ketoester 177.** To a cooled (0 °C) 1.00 M LiHMDS (52.2 mL, 52.2 mmol, 1.20 equiv) solution in THF was added ketone **176** (8.00 g, 43.5 mmol, 1.00 equiv) in THF (50 mL) in a dropwise manner over 30 min. After an additional 30 min at 0 °C, HMPA (8.31 mL, 47.8 mmol, 1.10 equiv) was added and maintained at 0 °C for 1 h. *t*-Butyl bromoacetate (10.6 mL, 69.5 mmol, 1.60 equiv) was added in portions over 1 h and after a further 2 h at 0 °C, allowed to warm to ambient temperature. After 48 h, the reaction mixture was poured into H<sub>2</sub>O (300 mL), extracted with Et<sub>2</sub>O (6 x 150 mL), dried (MgSO<sub>4</sub>), and concentrated to an oil, which was purified by flash chromatography on silica gel (7 to 10% EtOAc in hexanes) to provide ketoester **177** (12.5 g, 97% yield) as a pale yellow oil (as a ~ 3:1 mixture of diastereomers). See below for full characterization of both methyl diastereomers, synthesized in enantioenriched form via asymmetric alkylation.



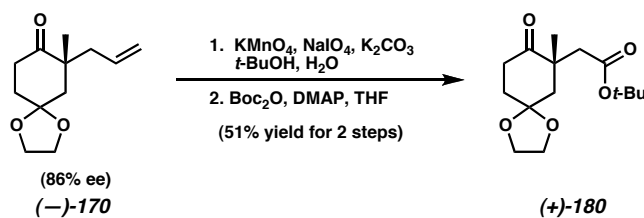
**Triflate 178.** To a cooled (-30 °C) solution of KHMDS (4.41 g, 22.1 mmol, 1.20 equiv) in THF (35 mL) was added ketoester **177** (5.50 g, 18.5 mmol, 1.00 equiv) in THF (30 mL) in a dropwise manner over 10 min. After 5 h at -30 °C, PhNTf<sub>2</sub> (7.20 g, 20.2 mmol, 1.09 equiv) in THF (30 mL) was added, maintained for an additional 30 min at -30 °C, and warmed to 0 °C for 2 h. The reaction mixture was diluted with Et<sub>2</sub>O (200 mL), poured into a mixture of brine (150 mL), H<sub>2</sub>O (150 mL), and 1 M NaOH (50 mL), and extracted with Et<sub>2</sub>O (3 x 50 mL). The organic layers were washed with 1 M NaOH (6 x 50 mL),

H<sub>2</sub>O (50 mL), and brine (3 x 50 mL), dried (Na<sub>2</sub>SO<sub>4</sub>), and concentrated to an oil, which was purified by flash chromatography on silica gel (7 to 10% EtOAc in hexanes and 0.5 % TEA) to provide triflate **178** (5.74 g, 73% yield) as a pale yellow oil: *R<sub>f</sub>* 0.63 (35% EtOAc in hexanes); <sup>1</sup>H NMR (300 MHz, CDCl<sub>3</sub>) δ 4.02–3.92 (comp. m, 4H), 2.71 (d, *J* = 14.5 Hz, 1H), 2.45 (s, 2H), 2.42 (d, *J* = 13.5 Hz, 1H), 2.30 (d, *J* = 14.7 Hz, 1H), 1.78 (s, 3H), 1.70 (d, *J* = 13.8 Hz, 1H), 1.42 (s, 9H), 1.32 (s, 3H); <sup>13</sup>C NMR (75 MHz, CDCl<sub>3</sub>) δ 170.2, 146.9, 124.5, 118.7 (q, *J*<sub>C-F</sub> = 319 Hz), 106.2, 80.5, 64.4, 64.3, 43.1, 42.0, 41.9, 39.2, 28.0, 25.0, 17.8; IR (Neat film NaCl) 2980, 2935, 2888, 1726, 1403, 1212, 1142, 1007, 862 cm<sup>-1</sup>; HRMS (FAB+) [M+H]<sup>+</sup> *m/z* calc'd for [C<sub>17</sub>H<sub>25</sub>SF<sub>3</sub>O<sub>7</sub>+H]<sup>+</sup>: 431.1351, found 431.1365.



**Enal 169.** A solution of flame-dried LiCl (600 mg, 14.2 mmol, 2.69 equiv), Pd(OAc)<sub>2</sub> (156 mg, 0.695 mmol, 0.132 equiv), and 1,4-bis-(dicyclohexylphosphino)butane (314 mg, 0.695 mmol, 0.132 equiv) in DMA (16 mL) was sparged with CO and warmed to 90 °C until a color change from red/orange to pale yellow was observed, at which point, the reaction mixture was cooled to 35 °C. To the homogenous reaction mixture was added TEA (2.60 mL, 18.6 mmol, 3.53 equiv) and enol triflate **178** (2.27 g, 5.27 mmol, 1.00 equiv) in DMA (16 mL). A solution of Et<sub>3</sub>SiH (1.47 mL, 9.28 mmol, 1.76 equiv) in DMA (8.5 mL) was added by syringe pump to the reaction over 10 h. After an additional 14 h at 35 °C, the reaction mixture was cooled to ambient temperature, KF•2H<sub>2</sub>O (2.00 g) was added, the mixture was stirred for 45 min, and then poured into ice water (200 mL). This mixture was extracted with 1:1 Et<sub>2</sub>O:hexanes (5 x 100 mL). The combined organic layers were washed with brine (2 x 100 mL), dried (Na<sub>2</sub>SO<sub>4</sub>), and concentrated to give an

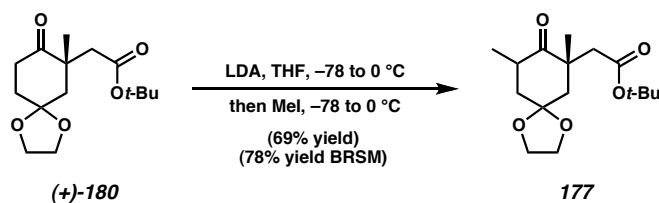
oil, which was purified by gradient flash chromatography on silica gel (10 to 20% EtOAc in hexanes) to give enal **169** (1.24 g, 76% yield) as a pale yellow oil:  $R_f$  0.42, 0.41 (35% EtOAc in hexanes, 20% EtOAc in hexanes developed twice);  $^1\text{H}$  NMR (300 MHz,  $\text{CDCl}_3$ )  $\delta$  10.13 (s, 1H), 4.00–3.90 (comp. m, 4H), 3.04 (d,  $J = 14.4$  Hz, 1H), 2.54 (app. dt,  $J = 1.0, 19.2$  Hz, 1H), 2.37 (dd,  $J = 1.8, 18.9$  Hz, 1H), 2.34 (d,  $J = 14.7$  Hz, 1H), 2.15 (d,  $J = 13.6$  Hz, 1H), 2.12 (s, 3H), 1.53 (dd,  $J = 2, 13.6$  Hz, 1H), 1.35 (s, 9H), 1.33 (s, 3H);  $^{13}\text{C}$  NMR (75 MHz,  $\text{CDCl}_3$ )  $\delta$  191.0, 171.3, 152.8, 137.4, 106.5, 79.8, 64.3, 64.0, 44.7 (2C), 42.4, 38.3, 28.0, 26.5, 19.3; IR (Neat film NaCl) 2977, 2932, 2884, 1721, 1673, 1368, 1161, 1141, 1079  $\text{cm}^{-1}$ ; HRMS (FAB+)  $[\text{M}+\text{H}]^+$   $m/z$  calc'd for  $\text{C}_{17}\text{H}_{26}\text{O}_5+\text{H}^+$ : 311.1858, found 311.1849.



**(+)-*t*-Butyl ester 180.** A solution of ketone (-)-**170** (1.00 g, 4.76 mmol, 1.00 equiv) and  $\text{K}_2\text{CO}_3$  (987 mg, 7.14 mmol, 1.5 equiv) in *t*-BuOH (60 mL) was treated (slight exotherm) with a premixed (30 min) solution of  $\text{NaIO}_4$  (8.14 g, 38.1 mmol, 8.00 equiv) and  $\text{KMnO}_4$  (113 mg, 0.714 mmol, 0.15 equiv) in  $\text{H}_2\text{O}$  (100 mL) and stirred in a room temperature bath for 3 h. The reaction mixture was diluted with  $\text{CH}_2\text{Cl}_2$  (100 mL) and  $\text{H}_2\text{O}$  (100 mL), extracted with  $\text{CH}_2\text{Cl}_2$  (6 x 50 mL), dried ( $\text{MgSO}_4$ ), and concentrated to an oil, which was used immediately in the next step.

A solution of the above crude carboxylic acid in THF (40 mL) was treated with  $\text{Boc}_2\text{O}$  (3.40 g, 15.6 mmol, 3.27 equiv) and DMAP (200 mg, 1.64 mmol, 0.344 equiv). After 12 h, additional  $\text{Boc}_2\text{O}$  (2.00 g, 9.16 mmol, 1.93 equiv) and DMAP (175 mg, 1.43 mmol, 0.30 equiv) were added, and the reaction was stirred for a further 3 h. The reaction mixture

was concentrated and purified by gradient flash chromatography on silica gel (5 to 25% Et<sub>2</sub>O in hexanes) to give (+)-*t*-butyl ester **180** (688 mg, 51% yield) as a colorless oil: *R<sub>f</sub>* 0.27 (10% EtOAc in hexanes developed twice); <sup>1</sup>H NMR (300 MHz, CDCl<sub>3</sub>) δ 4.03–3.94 (comp. m, 4H), 2.70 (d, *J* = 15.9 Hz, 1H), 2.63 (d, *J* = 6.6 Hz, 1H), 2.60 (d, *J* = 6.0 Hz, 1H), 2.49 (d, *J* = 15.9 Hz, 1H), 2.22 (dd, *J* = 1.4, 14.0 Hz, 1H), 2.20–2.08 (m, 1H), 2.04–1.92 (m, 1H), 1.78 (dd, *J* = 2.4, 14.1 Hz, 1H), 1.40 (s, 9H), 1.20 (s, 3H); <sup>13</sup>C NMR (75 MHz, CDCl<sub>3</sub>) δ 212.7, 170.7, 107.6, 80.7, 64.4, 64.2, 46.0, 44.7, 44.5, 35.6, 33.9, 28.0, 25.1; IR (Neat film NaCl) 2976, 2935, 2885, 1725, 1714, 1368, 1157, 1120, 1074 cm<sup>-1</sup>; HRMS (EI) [M]<sup>+</sup> *m/z* calc'd for [C<sub>15</sub>H<sub>24</sub>O<sub>5</sub>]<sup>+</sup>: 284.1624, found 284.1633; α<sub>D</sub><sup>26</sup> +45.63 (c 1.89, CH<sub>2</sub>Cl<sub>2</sub>, 86% ee).

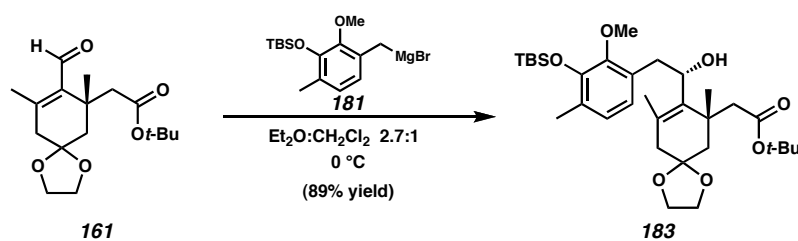


**Methyl ketones 177a and 177b.** A solution of LDA in THF was prepared by dropwise addition of 2.45 M *n*-BuLi solution in hexanes (787 μL, 1.93 mmol, 1.4 equiv) to diisopropylamine (290 μL, 2.07 mmol, 1.5 equiv) in THF (20.7 mL) at 0 °C, followed by stirring for 1 h. Upon cooling the solution to -78 °C, a solution of (+)-*t*-butyl ester **180** (392 mg, 1.38 mmol, 1.00 equiv) in THF (2.00 mL) was added in a dropwise manner, and the reaction mixture was stirred at -78 °C for 1 h, then 0 °C for 1 h. After cooling again to -78 °C, the reaction mixture was treated with MeI (258 μL, 4.13 mmol, 3.00 equiv), allowed to warm to ambient temperature slowly over 5 h, and stirred for an additional 12 h at ambient temperature. The reaction mixture was quenched with saturated aqueous NaHCO<sub>3</sub> (10 mL), extracted with CH<sub>2</sub>Cl<sub>2</sub> (6 x 30 mL), dried (MgSO<sub>4</sub>), and concentrated to an oil, which was purified by gradient flash chromatography on

silica gel (3 to 10% EtOAc in hexanes) to give diastereomeric methyl ketones **177a** and **177b** (284 mg, 69% combined yield) as colorless oils and recovered (+)-*t*-butyl ester **180** (43.2 mg, 11% yield).

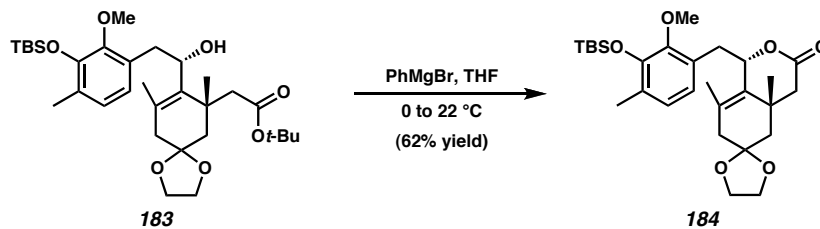
**High  $R_f$  diastereomer 177a:**  $R_f$  0.43 (10% EtOAc in hexanes developed 2 times);  $^1\text{H}$  NMR (300 MHz,  $\text{CDCl}_3$ )  $\delta$  4.10–3.90 (comp. m, 4H), 2.89 (app. d of sept.,  $J = 1.2, 6.6$  Hz, 1H), 2.73 (d,  $J = 16.5$  Hz, 1H), 2.36 (d,  $J = 13.8$  Hz, 1H), 2.16 (d,  $J = 16.2$  Hz, 1H), 2.06–1.96 (comp. m, 1H), 1.93 (d,  $J = 13.5$  Hz, 1H), 1.85 (dd,  $J = 3.3, 13.8$  Hz, 1H), 1.42 (s, 9H), 1.29 (s, 3H), 1.07 (d,  $J = 6.9$  Hz, 3H);  $^{13}\text{C}$  NMR (75 MHz,  $\text{CDCl}_3$ )  $\delta$  214.0, 170.9, 107.5, 80.4, 64.6, 64.0, 46.0, 44.5, 44.3, 41.9, 38.0, 28.1, 26.4, 14.7; IR (Neat film NaCl) 2976, 2932, 2880, 1726, 1710, 1367, 1146, 1080  $\text{cm}^{-1}$ ; HRMS (EI)  $[\text{M}]^+$   $m/z$  calc'd for  $[\text{C}_{16}\text{H}_{26}\text{O}_5]^+$ : 298.1780, found 298.1791;  $\alpha_{\text{D}}^{26} +45.13$  (c 1.06,  $\text{CH}_2\text{Cl}_2$ , 86% ee).

**Low  $R_f$  diastereomer 177b:**  $R_f$  0.32 (10% EtOAc in hexanes developed 2 times);  $^1\text{H}$  NMR (300 MHz,  $\text{CDCl}_3$ )  $\delta$  4.10–3.85 (comp. m, 4H), 3.21 (d,  $J = 14.7$  Hz, 1H), 3.09 (app. d of sept.,  $J = 1.5, 6.6$  Hz, 1H), 2.32 (d,  $J = 14.4$  Hz, 1H), 2.14–2.00 (comp. m, 2H), 1.76 (d,  $J = 14.7$  Hz, 1H), 1.68 (app. t,  $J = 14.0$  Hz, 1H), 1.36 (s, 9H), 1.08 (s, 3H), 1.03 (d,  $J = 6.3$  Hz, 3H);  $^{13}\text{C}$  NMR (75 MHz,  $\text{CDCl}_3$ )  $\delta$  213.8, 170.4, 107.2, 80.8, 64.6, 64.0, 46.8, 46.1, 45.2, 43.9, 37.7, 27.9, 23.0, 14.4; IR (Neat film NaCl) 2976, 2933, 2884, 1726, 1717, 1457, 1367, 1232, 1160, 1141, 1084, 979  $\text{cm}^{-1}$ ; HRMS (EI)  $[\text{M}]^+$   $m/z$  calc'd for  $[\text{C}_{16}\text{H}_{26}\text{O}_5]^+$ : 298.1780, found 298.1775;  $\alpha_{\text{D}}^{26} -25.44$  (c 1.17,  $\text{CH}_2\text{Cl}_2$ , 86% ee).

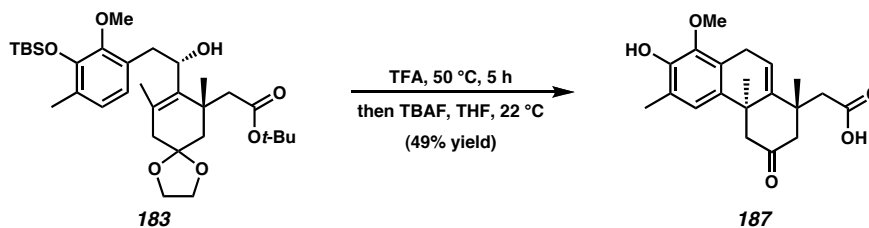


**Allylic alcohol 183.** A flame-dried two-neck round bottom flask equipped with a reflux condenser and septum was charged with magnesium turnings (9.00 g, 370 mmol,

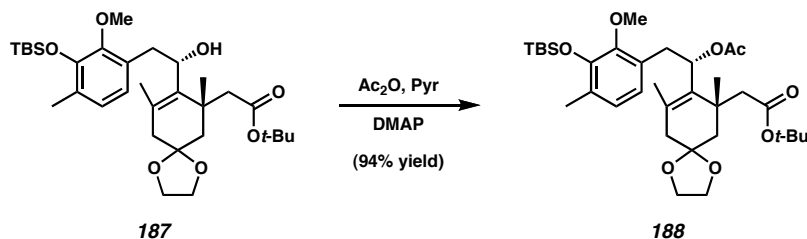
34.6 equiv) and Et<sub>2</sub>O (120 mL) under an N<sub>2</sub> atmosphere and heated to reflux. To this mixture was added 1,2-dibromoethane (1.53 mL, 17.8 mmol, 1.66 equiv) in a dropwise manner. (*Caution: gas evolution!*) When gas evolution ceased, a solution of benzyl bromide **168** (5.91 g, 17.1 mmol, 1.60 equiv) in Et<sub>2</sub>O (50 mL) was added in a dropwise manner over 30 min and heating was continued for an additional 30 min. The Grignard reagent was then cooled (0 °C), and added to a cooled (0 °C) solution of enal **169** (3.32 g, 10.7 mmol, 1.00 equiv) in Et<sub>2</sub>O (100 mL) and CH<sub>2</sub>Cl<sub>2</sub> (100 mL). After 1 h, the reaction mixture was quenched with H<sub>2</sub>O (200 mL) and saturated aqueous NH<sub>4</sub>Cl (100 mL), extracted with Et<sub>2</sub>O (3 x 200 mL), dried (MgSO<sub>4</sub>), and concentrated to an oil, which was purified by gradient flash chromatography on silica gel (7.5 to 20% EtOAc in hexanes) to give allylic alcohol **183** (5.51 g, 89% yield) as a thick syrup: *R*<sub>f</sub> 0.59 (20% EtOAc in hexanes developed twice); <sup>1</sup>H NMR (300 MHz, CDCl<sub>3</sub>) δ 6.83 (s, 2H), 4.43 (dd, *J* = 2.1, 9.9 Hz, 1H), 4.04–3.90 (comp. m, 4H), 3.68 (s, 3H), 3.22 (bs, 1H), 3.17 (dd, *J* = 9.9, 13.8 Hz, 1H), 2.84 (dd, *J* = 3.3, 13.8 Hz, 1H), 2.64 (d, *J* = 13.5 Hz, 1H), 2.31 (d, *J* = 17.4 Hz, 1H), 2.24–2.04 (comp. m, 3H), 2.19 (s, 3H), 2.07 (s, 3H), 1.57 (dd, *J* = 2.3, 13.8 Hz, 1H), 1.40 (s, 9H), 1.12 (s, 3H), 1.02 (s, 9H), 0.18 (s, 3H), 0.16 (s, 3H); <sup>13</sup>C NMR (75 MHz, CDCl<sub>3</sub>) δ 172.1, 149.6, 147.0, 136.7, 131.3, 130.5, 128.7, 125.7, 123.5, 107.6, 80.9, 70.6, 64.2, 63.9, 59.9, 46.4, 43.3, 42.0, 41.3, 36.6, 28.0, 26.8, 26.0, 21.1, 18.6, 17.0, -4.1 (2C); IR (Neat film NaCl) 3499, 2957, 2931, 2896, 2859, 1706, 1462, 1419, 1368, 1286, 1075, 840 cm<sup>-1</sup>; HRMS (FAB+) [M+H]<sup>+</sup> *m/z* calc'd for [C<sub>32</sub>H<sub>52</sub>SiO<sub>7</sub>+H]<sup>+</sup>: 577.3561, found 577.3543.



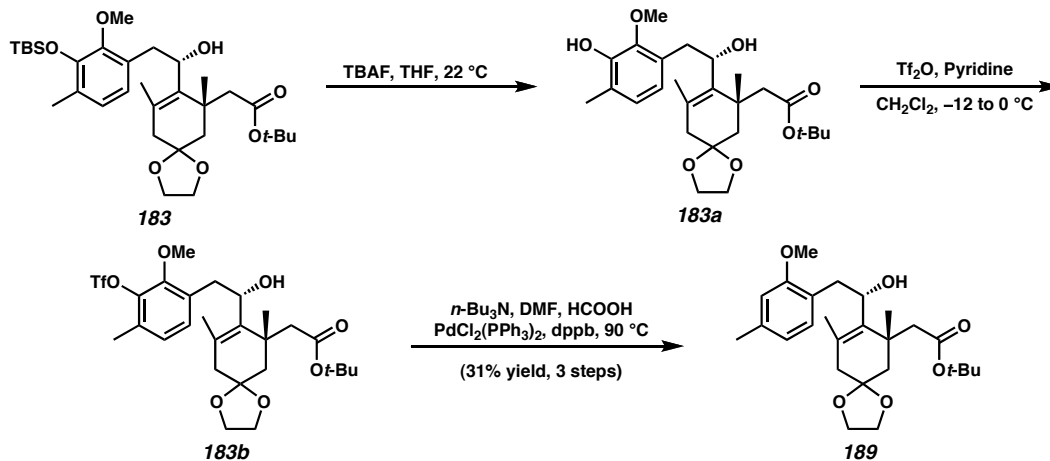
**Lactone 184.** To a cooled (0 °C) solution of allylic alcohol **183** (108 mg, 0.187 mmol, 1.00 equiv) in THF (12 mL) was added 3.0 M PhMgBr in Et<sub>2</sub>O (68.6 μL, 0.206 mmol, 1.10 equiv). Additional 3.0 M PhMgBr in Et<sub>2</sub>O (85.0 μL, 0.255 mmol, 1.36 equiv) was added in portions over 4 h. The reaction mixture was quenched into H<sub>2</sub>O (30 mL) and EtOAc (30 mL), acidified to pH 2 with 0.1 M HCl, extracted with EtOAc (3 x 20 mL), dried over Na<sub>2</sub>SO<sub>4</sub>, and concentrated to an oil, which was purified by gradient flash chromatography on silica gel (10 to 20% EtOAc in hexanes) to give lactone **184** (58.5 mg, 62% yield) as white solid. Crystals suitable for X-ray analysis were obtained by crystallization from hexanes at ambient temperature: mp 139–140 °C (hexanes); *R<sub>f</sub>* 0.40 (35% EtOAc in hexanes); <sup>1</sup>H NMR (300 MHz, CDCl<sub>3</sub>) δ 6.83 (d, *J* = 7.8 Hz, 1H), 6.66 (d, *J* = 8.1 Hz, 1H), 5.40 (d, *J* = 9.0 Hz, 1H), 4.08–3.95 (m, 2H), 3.95–3.86 (m, 2H), 3.67 (s, 3H), 3.07 (dd, *J* = 3.5, 14.3 Hz, 1H), 2.75 (dd, *J* = 10.2, 14.4 Hz, 1H), 2.48 (s, 2H), 2.43 (s, 2H), 2.19 (s, 3H), 1.82 (d, *J* = 13.2 Hz, 1H), 1.71 (d, *J* = 13.2 Hz, 1H), 1.71 (s, 3H), 1.22 (s, 3H), 1.03 (s, 9H), 0.18 (s, 3H), 0.15 (s, 3H); <sup>13</sup>C NMR (75 MHz, CDCl<sub>3</sub>) δ 171.4, 149.7, 147.0, 131.2, 129.8, 128.1, 126.0, 125.5, 123.5, 107.8, 80.0, 64.4, 63.6, 60.0, 45.7, 44.1, 43.4, 38.2, 35.9, 26.0, 25.9, 19.0, 18.5, 17.1, -4.2 (2C); IR (Neat film NaCl) 2957, 2931, 2886, 2859, 1751, 1463, 1419, 1251, 1237, 1078, 841 cm<sup>-1</sup>; HRMS (FAB+) [M+H]<sup>+</sup> *m/z* calc'd for [C<sub>28</sub>H<sub>42</sub>SiO<sub>6</sub>+H]<sup>+</sup>: 503.2829, found 503.2809.



**Acid 187.** A solution of allylic alcohol **183** (5.50 g, 9.53 mmol, 1.00 equiv) in TFA (240 mL) was warmed to 50 °C for 5 h. The reaction mixture was concentrated and the resulting residue was dissolved in THF (100 mL) and 1.0 M TBAF (12.0 mL, 12.0 mmol, 1.26 equiv) in THF was added. After 1 h, the reaction mixture was concentrated to ~ 25 mL, quenched with H<sub>2</sub>O (100 mL), brine (100 mL), and 3 M HCl (100 mL), and extracted with EtOAc (6 x 100 mL). The organic layers were concentrated to an oil, which was purified by flash chromatography on silica gel (1:1 CH<sub>2</sub>Cl<sub>2</sub>:CHCl<sub>3</sub> + 1% AcOH) to give acid **187** (1.62 g, 49% yield) as a white foam. Crystals suitable for X-ray analysis were obtained by crystallization from CDCl<sub>3</sub> at ambient temperature: mp 112–113 °C (CDCl<sub>3</sub>); *R<sub>f</sub>* 0.32 (1:1 CH<sub>2</sub>Cl<sub>2</sub> : CHCl<sub>3</sub> + 3% MeOH developed twice); <sup>1</sup>H NMR (300 MHz, CDCl<sub>3</sub>) δ 6.76 (s, 1H), 6.05 (dd, *J* = 1.8, 6.3 Hz, 1H), 5.63 (bs, 1H), 3.78 (s, 3H), 3.58 (dd, *J* = 6.6, 20.7 Hz, 1H), 3.47 (d, *J* = 17.7 Hz, 1H), 3.17 (d, *J* = 18.3 Hz, 1H), 3.11 (d, *J* = 17.4 Hz, 1H), 2.93 (d, *J* = 15.9 Hz, 1H), 2.76 (d, *J* = 17.4 Hz, 1H), 2.50 (d, *J* = 15.6 Hz, 1H), 2.34 (d, *J* = 17.1 Hz, 1H), 2.24 (s, 3H), 1.24 (s, 3H), 1.17 (s, 3H); <sup>13</sup>C NMR (75 MHz, CD<sub>2</sub>Cl<sub>2</sub>) δ 210.8, 176.8, 146.0, 145.4, 143.9, 137.6, 125.3, 123.1, 121.6, 120.6, 61.2, 50.1, 49.2, 46.2, 39.5, 39.0, 33.3, 30.7, 24.9, 16.0; IR (Neat film NaCl) 3500–2500, 2963, 2926, 1707, 1489, 1461, 1422, 1360, 1295, 1228, 1071, 955, 711 cm<sup>-1</sup>; HRMS (FAB+) [M+H]<sup>+</sup> *m/z* calc'd for [C<sub>20</sub>H<sub>24</sub>O<sub>5</sub>+H]<sup>+</sup>: 345.1702, found 345.1709.



**Allylic acetate 188.** To a solution of allylic alcohol **187** (88.0 mg, 0.153 mmol, 1.00 eq) in pyridine (250  $\mu$ L) and acetic anhydride (3.00 mL) was added DMAP (28.0 mg, 0.229 mmol, 1.50 equiv). After 2 h, the reaction mixture was concentrated to an oil, which was purified by gradient flash chromatography on silica gel (5 to 10% EtOAc in hexanes) to give allylic acetate **188** (89.3 mg, 94% yield) as a colorless oil:  $R_f$  0.68 (20% EtOAc in hexanes developed twice);  $^1\text{H}$  NMR (500 MHz,  $\text{CDCl}_3$ )  $\delta$  6.76 (d,  $J = 7.5$  Hz, 1H), 6.69 (d,  $J = 7.5$  Hz, 1H), 5.73 (dd,  $J = 2.8, 10.8$  Hz, 1H), 4.12–4.04 (m, 1H), 4.00–3.90 (comp. m, 3H), 3.70 (s, 3H), 3.07 (app. t,  $J = 12.5$  Hz, 1H), 2.97 (dd,  $J = 3.3, 13.8$  Hz, 1H), 2.66 (d,  $J = 15.0$  Hz, 1H), 2.57 (d,  $J = 14.5$  Hz, 1H), 2.38 (d,  $J = 17.5$  Hz, 1H), 2.26 (d,  $J = 13.0$  Hz, 1H), 2.24 (d,  $J = 17.5$  Hz, 1H), 2.18 (s, 3H), 1.97 (s, 3H), 1.80 (s, 3H), 1.48 (d,  $J = 14.5$  Hz, 1H), 1.42 (s, 9H), 1.28 (s, 3H), 1.03 (s, 9H), 0.19 (s, 3H), 0.14 (s, 3H);  $^{13}\text{C}$  NMR (125 MHz,  $\text{CDCl}_3$ )  $\delta$  171.8, 169.3, 150.0, 146.9, 135.0, 131.1, 129.3, 129.2, 125.3, 123.4, 107.3, 79.7, 71.5, 64.3, 63.9, 59.9, 43.5, 40.7, 39.9, 35.9, 28.2, 26.2, 26.1, 21.3, 21.0, 18.5, 17.1,  $-4.2, -4.4$ ; IR (Neat film NaCl) 2958, 2931, 2896, 2860, 1740, 1463, 1419, 1368, 1287, 1235, 1147, 1079, 1014, 854, 841, 783, 734  $\text{cm}^{-1}$ ; HRMS (FAB+)  $[\text{M}+\text{H}-\text{H}_2]^+$   $m/z$  calc'd for  $[\text{C}_{34}\text{H}_{53}\text{O}_8\text{Si}]^+$ : 617.3510, found 617.3487.

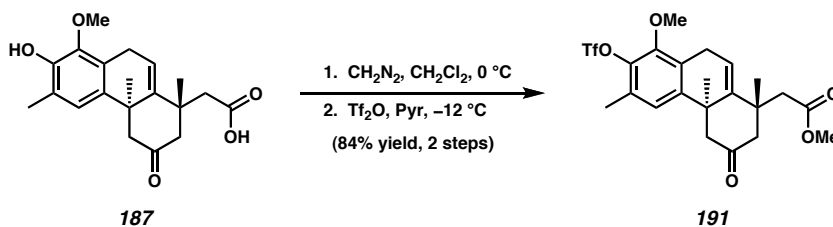


**Arene 189.** To a solution of allylic alcohol **183** (554 mg, 0.962 mmol, 1.0 equiv) in THF (10 mL) was added 1.00 M TBAF in THF (1.50 mL, 1.50 mmol, 1.56 equiv). After 5 min, the reaction mixture was concentrated to ~ 5 mL and was purified by gradient flash chromatography on silica gel (20 to 40% EtOAc in hexanes) to give phenol **183a** (223 mg, 52% yield).

To a cooled (-12 °C) solution of phenol **183a** (202 mg, 0.438 mmol, 1.00 equiv) and pyridine (142 μL, 1.75 mmol, 4.0 equiv) in CH<sub>2</sub>Cl<sub>2</sub> (5 mL) was added Tf<sub>2</sub>O (74.3 μL, 0.526 mmol, 1.2 equiv). After 2 h, additional Tf<sub>2</sub>O (10.0 μL, 0.071 mmol, 0.16 equiv) was added. After a further 2 h, the reaction mixture was quenched into a mixture of H<sub>2</sub>O (10 mL), brine (10 mL), and CH<sub>2</sub>Cl<sub>2</sub> (10 mL), then extracted with CH<sub>2</sub>Cl<sub>2</sub> (3 x 10 mL). The combined organic layers were dried (Na<sub>2</sub>SO<sub>4</sub>), and concentrated to an oil, which was purified by gradient flash chromatography on silica gel (15 to 25% EtOAc in hexanes + 1% TEA) to give triflate **183b** (193 mg, 75% yield).

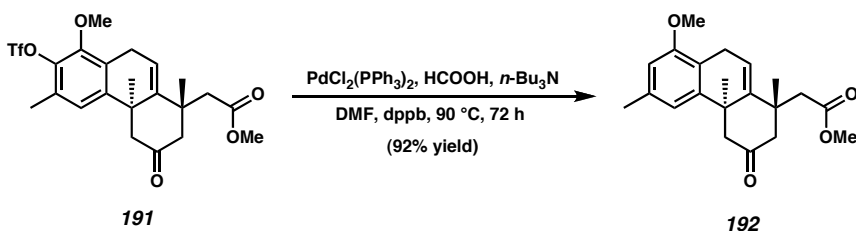
A flame-dried 25 mL Schlenk flask was charged with triflate **184b** (193 mg, 0.325 mmol, 1.00 equiv), PdCl<sub>2</sub>(PPh<sub>3</sub>)<sub>2</sub> (27.3 mg, 0.0389 mmol, 0.12 equiv), 1,4-bis-(diphenylphosphino)butane (40.2 mg, 0.0974 mmol, 0.30 equiv), DMF (4 mL), *n*-Bu<sub>3</sub>N (650 μL, 2.73 mmol, 8.40 equiv), and HCOOH (61.3 μL, 1.62 mmol, 5.00 equiv) under an Ar atmosphere and heated to 90 °C. After 22 h, the reaction mixture was quenched with

H<sub>2</sub>O (40 mL), extracted with Et<sub>2</sub>O (5 x 15 mL), dried (MgSO<sub>4</sub>), and concentrated to a residue, which was purified by gradient flash chromatography on silica gel (10 to 15% acetone in hexanes) to give arene **189** (117 mg, 80% yield) as a white solid: mp 135–136 °C; *R<sub>f</sub>* 0.50 (35% EtOAc in hexanes); <sup>1</sup>H NMR (300 MHz, CDCl<sub>3</sub>) δ 7.15 (d, *J* = 7.5 Hz, 1H), 6.73 (d, *J* = 7.5 Hz, 1H), 6.68 (s, 1H), 4.46 (dd, *J* = 2.3, 10.1 Hz, 1H), 4.02–3.90 (comp. m, 4H), 3.80 (s, 3H), 3.08 (dd, *J* = 10.2, 13.8 Hz, 1H), 3.07 (s, 1H), 2.94 (dd, *J* = 3.0, 13.8 Hz, 1H), 2.65 (d, *J* = 13.5 Hz, 1H), 2.33 (s, 3H), 2.30–2.10 (comp. m, 3H), 2.07 (s, 3H), 1.58 (dd, *J* = 2.1, 13.8 Hz, 1H), 1.40 (s, 9H), 1.16 (s, 3H); <sup>13</sup>C NMR (75 MHz, CDCl<sub>3</sub>) δ 172.1, 157.3, 137.3, 136.8, 131.4, 130.3, 125.1, 121.0, 111.2, 107.6, 80.8, 69.5, 64.2, 63.9, 55.0, 46.4, 43.3, 42.0, 41.3, 36.7, 28.0, 26.7, 21.5, 21.1; IR (Neat film NaCl) 3501, 2974, 2934, 1705, 1368, 1259, 1155, 1126, 1080, 1042 cm<sup>-1</sup>; HRMS (FAB+) [M+H]<sup>+</sup> *m/z* calc'd for [C<sub>26</sub>H<sub>38</sub>O<sub>6</sub>+H]<sup>+</sup>: 447.2747, found 447.2749.



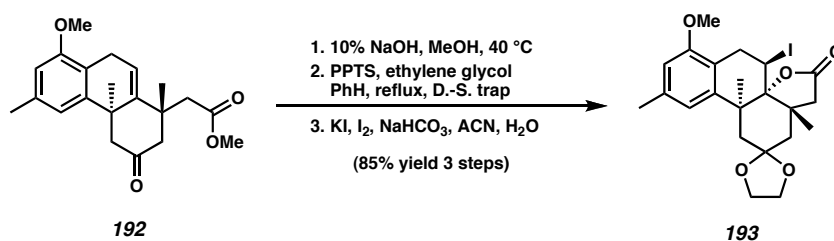
**Triflate 191.** To a cooled (0 °C) solution of acid **187** (994 mg, 2.88 mmol, 1.00 equiv) in CH<sub>2</sub>Cl<sub>2</sub> (30 mL) was added a cooled (0 °C) solution of CH<sub>2</sub>N<sub>2</sub> in Et<sub>2</sub>O (~ 0.2 M, 18.7 mL, 1.30 equiv) in a dropwise manner over 10 min. After 20 min, TLC analysis indicated complete consumption of the starting material and the reaction mixture was concentrated *in vacuo*. To a cooled (-12 °C) solution of the crude reaction mixture and pyridine (2.45 mL, 28.8 mmol, 10.0 equiv) in CH<sub>2</sub>Cl<sub>2</sub> (50 mL) was added Tf<sub>2</sub>O (1.01 mL, 7.20 mmol, 2.50 equiv) in a dropwise manner over 5 min. After 30 min, additional Tf<sub>2</sub>O (1.01 mL, 7.20 mmol, 2.50 equiv) was added. After a further 1 h at -12 °C, the reaction mixture was allowed to warm to 0 °C, stirred for 1 h, and quenched with saturated

aqueous NaHCO<sub>3</sub> (30 mL). The reaction mixture was poured into half-saturated aqueous NaHCO<sub>3</sub> (60 mL), extracted with CH<sub>2</sub>Cl<sub>2</sub> (5 x 30 mL), dried over K<sub>2</sub>CO<sub>3</sub>, and concentrated to an oil, which was purified by gradient flash chromatography on silica gel (10 to 25% EtOAc in hexanes) to give triflate **191** (1.18 g, 84% yield) as an off-white solid: mp 123–125 °C (decomp.) (benzene); *R*<sub>f</sub> 0.45 (35% EtOAc in hexanes); <sup>1</sup>H NMR (300 MHz, CDCl<sub>3</sub>) δ 6.89 (s, 1H), 6.03 (dd, *J* = 2.0, 6.5 Hz, 1H), 3.82 (s, 3H), 3.67 (s, 3H), 3.66 (dd, *J* = 6.3, 21.0 Hz, 1H), 3.50 (d, *J* = 17.7 Hz, 1H), 3.17 (app. d, *J* = 21.9 Hz, 1H), 3.09 (d, *J* = 17.4 Hz, 1H), 2.91 (d, *J* = 15.3 Hz, 1H), 2.76 (d, *J* = 17.4 Hz, 1H), 2.46 (d, *J* = 15.6 Hz, 1H), 2.34 (s, 3H), 2.33 (d, *J* = 17.4 Hz, 1H), 1.29 (s, 3H), 1.16 (s, 3H); <sup>13</sup>C NMR (75 MHz, CDCl<sub>3</sub>) δ 210.1, 171.5, 148.5, 146.0, 144.7, 140.0, 129.4, 127.6, 121.9, 119.7, 118.6 (q, *J*<sub>C-F</sub> = 318 Hz), 61.0, 51.5, 49.3, 48.8, 45.9, 39.4, 38.5, 33.1, 30.3, 24.3, 16.5; IR (Neat film NaCl) 2960, 1735, 1715, 1417, 1210, 1138, 1072, 903, 856 cm<sup>-1</sup>; HRMS (FAB+) [M+H]<sup>+</sup> *m/z* calc'd for [C<sub>22</sub>H<sub>25</sub>SO<sub>7</sub>F<sub>3</sub>+H]<sup>+</sup>: 491.1351, found 491.1363.



**Ketoester 192.** A flame-dried 250 mL Schlenk flask was charged with triflate **191** (azeotroped from PhH solution, 1.150 g, 2.34 mmol, 1.00 equiv), PdCl<sub>2</sub>(PPh<sub>3</sub>)<sub>2</sub> (198 mg, 0.282 mmol, 0.12 equiv), 1,4-bis-(diphenylphosphino)butane (290 mg, 0.704 mmol, 0.30 equiv), DMF (20 mL), *n*-Bu<sub>3</sub>N (4.70 mL, 19.7 mmol, 8.40 equiv), and HCOOH (443 μL, 11.7 mmol, 5.00 equiv) under an N<sub>2</sub> atmosphere and heated to 90 °C. After 72 h, the reaction mixture was quenched with H<sub>2</sub>O (150 mL) and Et<sub>2</sub>O (40 mL), extracted with Et<sub>2</sub>O (6 x 50 mL), dried (MgSO<sub>4</sub>), and concentrated to a residue, which was purified by gradient flash chromatography on silica gel (5 to 10% acetone in hexanes) to give

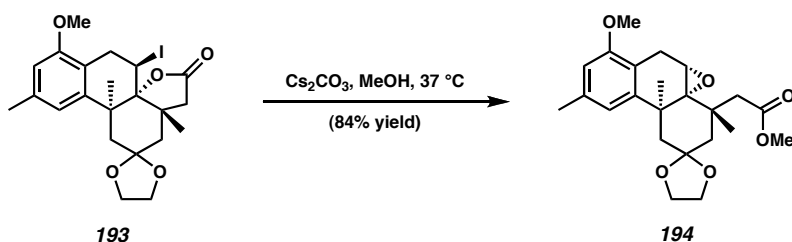
ketoester **192** (735 mg, 92% yield) as a colorless oil:  $R_f$  0.53 (35% acetone in hexane);  $^1\text{H}$  NMR (300 MHz,  $\text{CDCl}_3$ )  $\delta$  6.68 (s, 1H), 6.57 (s, 1H), 6.04 (dd,  $J = 1.8, 6.3$  Hz, 1H), 3.83 (s, 3H), 3.66 (s, 3H), 3.64 (dd,  $J = 6.3, 21.8$  Hz, 1H), 3.47 (d,  $J = 17.4$  Hz, 1H), 3.14 (d,  $J = 17.7$  Hz, 1H), 3.02 (app. d,  $J = 21.6$  Hz, 1H), 2.89 (d,  $J = 15.6$  Hz, 1H), 2.77 (d,  $J = 17.4$  Hz, 1H), 2.46 (d,  $J = 15.6$  Hz, 1H), 2.35 (s, 3H), 2.32 (d,  $J = 17.4$  Hz, 1H), 1.28 (s, 3H), 1.17 (s, 3H);  $^{13}\text{C}$  NMR (75 MHz,  $\text{CDCl}_3$ )  $\delta$  211.2, 171.6, 156.1, 146.0, 144.0, 136.9, 120.8, 119.7, 116.3, 108.4, 55.3, 51.4, 49.6, 49.1, 46.2, 39.2, 38.5, 33.2, 30.9, 24.1, 21.9; IR (Neat film NaCl) 2956, 1735, 1711, 1584, 1462, 1314, 1198, 1134, 1064  $\text{cm}^{-1}$ ; HRMS (FAB+)  $[\text{M}+\text{H}]^+$   $m/z$  calc'd for  $[\text{C}_{21}\text{H}_{26}\text{O}_4+\text{H}]^+$ : 343.1909, found 343.1894.



**Iodolactone 193.** A solution of ketoester **192** (200 mg, 0.581 mmol, 1.00 equiv) in MeOH (13 mL), and 10% w/v aqueous NaOH (13 mL) was heated at 40 °C for 10 h. The reaction mixture was cooled to ambient temperature, poured into brine (50 mL) and H<sub>2</sub>O (10 mL), acidified with 3 M HCl to pH 0, extracted with EtOAc (6 x 20 mL), dried ( $\text{Na}_2\text{SO}_4$ ), concentrated, and used in the next step without further purification.

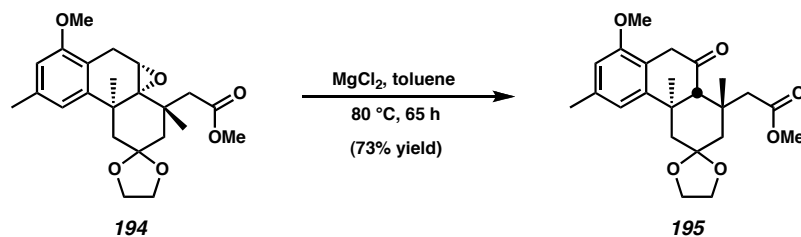
A solution of the above crude carboxylic acid, ethylene glycol (500  $\mu\text{L}$ , 8.97 mmol, 15.4 equiv), and pyridinium *p*-toluenesulfonate (500 mg, 1.99 mmol, 3.42 equiv) in benzene (50 mL) was fitted with a Dean-Stark apparatus and refluxed at 100 °C for 2 h. The cooled (0 °C) reaction mixture was diluted with H<sub>2</sub>O (25 mL), brine (25 mL), and  $\text{CH}_2\text{Cl}_2$  (50 mL), and extracted with  $\text{CH}_2\text{Cl}_2$  (6 x 30 mL). The combined organics were dried ( $\text{Na}_2\text{SO}_4$ ), concentrated, and used immediately in the next step without further purification.

To a solution of the crude ketal and  $\text{NaHCO}_3$  (68.4 mg, 0.814 mmol, 1.4 equiv) in  $\text{H}_2\text{O}$  (5 mL) and acetonitrile (5 mL) was added KI (125 mg, 0.756 mmol, 1.3 equiv) and  $\text{I}_2$  (192 mg, 0.756 mmol, 1.3 equiv). The reaction mixture was stirred in the dark for 30 h and quenched with saturated aqueous  $\text{Na}_2\text{S}_2\text{O}_3$  (10 mL),  $\text{H}_2\text{O}$  (20 mL), and brine (20 mL). The reaction mixture was extracted with EtOAc (8 x 20 mL), dried ( $\text{Na}_2\text{SO}_4$ ), concentrated, and recrystallized (15% acetone in hexanes, ~ 25 mL, from 80 to  $-20$  °C) to give iodolactone **193** (247 mg, 85% yield) as a white solid: mp 155–160 °C (decomp.) (acetone/hexanes);  $R_f$  0.37 (35% EtOAc in hexanes);  $^1\text{H}$  NMR (500 MHz,  $\text{C}_6\text{D}_6$ )  $\delta$  6.92 (s, 1H), 6.22 (s, 1H), 5.29 (app. t,  $J = 10.0$  Hz, 1H), 3.75 (dd,  $J = 10.0, 19.3$  Hz, 1H), 3.52–3.34 (comp. m, 3H), 3.34–3.26 (comp. m, 2H), 3.24 (s, 3H), 3.01 (d,  $J = 18.0$  Hz, 1H), 2.76 (d,  $J = 16.0$  Hz, 1H), 2.49 (d,  $J = 16.0$  Hz, 1H), 2.45 (d,  $J = 18.0$  Hz, 1H), 2.12 (s, 3H), 1.54 (d,  $J = 14.5$  Hz, 1H), 1.13 (s, 3H), 0.98 (d,  $J = 14.5$  Hz, 1H), 0.95 (s, 3H);  $^{13}\text{C}$  NMR (125 MHz,  $\text{C}_6\text{D}_6$ )  $\delta$  173.5, 156.9, 143.6, 138.1, 121.2, 117.6, 109.4, 107.2, 87.2, 64.5, 64.2, 55.1, 46.1, 45.8, 45.4, 43.2, 42.6, 36.5, 30.9, 30.8, 25.2, 22.2; IR (Neat film NaCl) 2964, 2881, 1790, 1461, 1229, 1203, 1071, 1023  $\text{cm}^{-1}$ ; HRMS (FAB+)  $[\text{M}+\text{H}]^+$   $m/z$  calc'd for  $[\text{C}_{22}\text{H}_{27}\text{IO}_5+\text{H}]^+$ : 499.0982, found 499.0986.



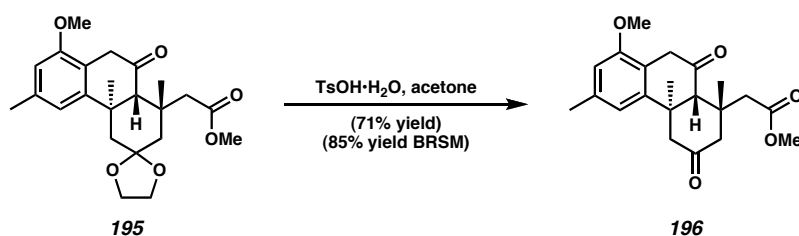
**Epoxide 194.** To a solution of iodolactone **193** (75.0 mg, 0.151 mmol, 1.00 equiv) in MeOH (15 mL) was added  $\text{Cs}_2\text{CO}_3$  (981 mg, 3.01 mmol, 20.0 equiv). The reaction mixture was warmed to 37 °C and vigorously stirred for 19 h. The reaction mixture was cooled to ambient temperature, diluted with  $\text{H}_2\text{O}$  (20 mL), brine (20 mL), and  $\text{CH}_2\text{Cl}_2$  (20 mL), extracted with  $\text{CH}_2\text{Cl}_2$  (5 x 20 mL) and EtOAc (5 x 25 mL), dried ( $\text{Na}_2\text{SO}_4$ ), and

concentrated. The resulting residue was purified by flash chromatography on silica gel (15% EtOAc in hexanes + 1% TEA) to give epoxide **194** (51.0 mg, 84% yield) as a colorless oil:  $R_f$  0.54, 0.28 (35% EtOAc in hexanes, 10% EtOAc in hexanes developed 3 times);  $^1\text{H}$  NMR (500 MHz,  $\text{CDCl}_3$ )  $\delta$  6.72 (s, 1H), 6.45 (s, 1H), 4.12–4.08 (m, 1H), 4.06–4.01 (m, 1H), 3.94–3.86 (comp. m, 2H), 3.78 (s, 3H), 3.66 (s, 3H), 3.58 (d,  $J = 2.5$  Hz, 1H), 3.24 (d,  $J = 19.5$  Hz, 1H), 2.90 (dd,  $J = 3.5, 20.0$  Hz, 1H), 2.80 (dd,  $J = 1.0, 14.5$  Hz, 1H), 2.79 (d,  $J = 14.5$  Hz, 1H), 2.37 (d,  $J = 14.0$  Hz, 1H), 2.31 (dd,  $J = 1.0, \sim 15$  Hz, 1H), 2.30 (s, 3H), 2.03 (d,  $J = 15.0$  Hz, 1H), 1.72 (d,  $J = 15.0$  Hz, 1H), 1.63 (s, 3H), 1.11 (s, 3H);  $^{13}\text{C}$  NMR (125 MHz,  $\text{C}_6\text{D}_6$ )  $\delta$  172.8, 157.5, 144.9, 136.6, 120.4, 116.1, 108.9, 108.2, 65.7, 64.8, 63.7, 57.1, 55.2, 51.1, 48.8, 43.4, 41.7, 39.7, 38.3, 27.5, 26.7, 24.4, 22.2; IR (Neat film NaCl) 2950, 1734, 1590, 1462, 1360, 1196, 1135, 1075, 1017  $\text{cm}^{-1}$ ; HRMS (FAB+)  $[\text{M}+\text{H}]^+$   $m/z$  calc'd for  $[\text{C}_{23}\text{H}_{30}\text{O}_6+\text{H}]^+$ : 403.2121, found 403.2113.



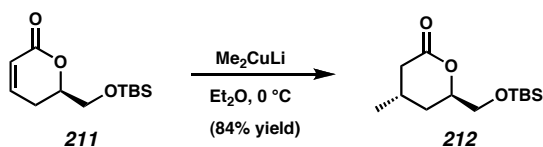
**Ketone 195.** A solution of epoxide **194** (49.0 mg, 0.122 mmol, 1.00 equiv) in toluene (30 mL) in a flame-dried Schlenk flask under an  $\text{N}_2$  atmosphere was treated with magnesium chloride (2.00 g, 21.0 mmol, 172 equiv) and heated to 80  $^\circ\text{C}$  for 65 h. After cooling to ambient temperature, the reaction mixture was filtered and the filter cake was washed with toluene (2 x 25 mL). The filter cake was partitioned between EtOAc (20 mL) and ice cold water (20 mL), and further extracted with EtOAc (3 x 20 mL). The combined organics were dried ( $\text{Na}_2\text{SO}_4$ ), and concentrated to an oil, which was purified by gradient flash chromatography on silica gel (10 to 20% EtOAc in hexanes) to give ketone **195** (36.0 mg, 73% yield) as a colorless oil:  $R_f$  0.55, 0.33 (35% EtOAc in hexanes,

10% EtOAc in hexanes developed 3 times);  $^1\text{H}$  NMR (500 MHz,  $\text{CDCl}_3$ )  $\delta$  6.73 (s, 1H), 6.57 (s, 1H), 4.15–4.05 (m, 2H), 4.00–3.88 (m, 2H), 3.80 (s, 3H), 3.67 (s, 3H), 3.64 (d,  $J = 22.5$  Hz, 1H), 3.47 (dd,  $J = 1.5, 14.5$  Hz, 1H), 3.34 (d,  $J = 22.0$  Hz, 1H), 3.23 (d,  $J = 14.5$  Hz, 1H), 2.58 (dd,  $J = 2.5, 14.5$  Hz, 1H), 2.56 (s, 1H), 2.45 (dd,  $J = 2.5, 13.5$  Hz, 1H), 2.35 (s, 3H), 2.13 (d,  $J = 13.0$  Hz, 1H), 1.30 (s, 3H), 1.21 (s, 3H), 1.14 (dd,  $J = 1.5, 14.5$  Hz, 1H);  $^{13}\text{C}$  NMR (125 MHz,  $\text{CDCl}_3$ )  $\delta$  209.0, 173.9, 156.4, 149.4, 137.6, 117.3, 116.1, 108.7, 108.3, 65.2, 63.0, 62.8, 55.3, 50.9, 46.4, 42.5, 42.3, 40.0, 36.0, 35.6, 28.9, 25.6, 21.9; IR (Neat film NaCl) 2953, 2885, 1731, 1713, 1586, 1462, 1360, 1193, 1065  $\text{cm}^{-1}$ ; HRMS (EI)  $[\text{M}]^+$   $m/z$  calc'd for  $[\text{C}_{23}\text{H}_{30}\text{O}_6]^+$ : 402.2042, found 402.2027.



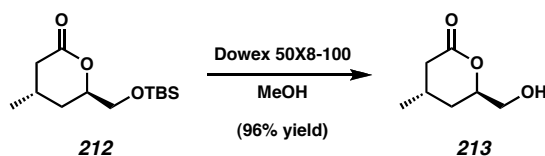
**Diketone 196.** A solution of ketone **195** (29.3 mg, 0.728 mmol, 1.00 equiv) in acetone (10 mL) was treated with  $\text{TsOH}\cdot\text{H}_2\text{O}$  (100 mg, 0.526 mmol, 7.22 equiv) and stirred at ambient temperature for 4 h. The reaction mixture was poured into saturated aqueous  $\text{NaHCO}_3$  (25 mL), extracted with  $\text{CH}_2\text{Cl}_2$  (6 x 15 mL), dried ( $\text{Na}_2\text{SO}_4$ ), and concentrated to an oil, which was purified by gradient flash chromatography on silica gel (7.5 to 12.5% EtOAc in hexanes) to give starting ketone **164** (4.6 mg, 16% yield) and diketone **196** (18.6 mg, 71% yield) as a white solid. Crystals suitable for X-ray analysis were obtained by crystallization from acetone/heptanes at ambient temperature: mp 184–186  $^\circ\text{C}$  (acetone/heptanes);  $R_f$  0.40 (35% EtOAc in hexanes);  $^1\text{H}$  NMR (500 MHz,  $\text{CDCl}_3$ )  $\delta$  6.61 (s, 1H), 6.59 (s, 1H), 3.82 (s, 3H), 3.71 (d,  $J = 22.0$  Hz, 1H), 3.69 (s, 3H), 3.46 (dd,  $J = 1.5, 14.5$  Hz, 1H), 3.39 (d,  $J = 22.5$  Hz, 1H), 3.08 (s, 1H), 2.99 (dd,  $J = 2.3, 12.8$  Hz, 1H), 2.93 (dd,  $J = 2.3, 12.8$  Hz, 1H), 2.89 (d,  $J = 12.5$  Hz, 1H), 2.36 (s, 3H), 2.33 (d,  $J = 14.5$  Hz,

1H), 2.21 (d,  $J = 12.5$  Hz, 1H), 1.36 (s, 3H), 1.16 (s, 3H);  $^{13}\text{C}$  NMR (125 MHz,  $\text{CDCl}_3$ )  $\delta$  208.7, 207.8, 171.9, 156.6, 147.6, 138.2, 117.1, 115.5, 109.3, 62.7, 55.4, 53.6, 52.2, 51.4, 45.7, 40.1, 39.5, 37.6, 28.0, 26.6, 21.9; IR (Neat film NaCl) 2953, 1732, 1713, 1586, 1462, 1331, 1194, 1063, 731  $\text{cm}^{-1}$ ; HRMS (EI)  $[\text{M}]^+$   $m/z$  calc'd for  $[\text{C}_{21}\text{H}_{26}\text{O}_5]^+$ : 358.1780, found 358.1774.

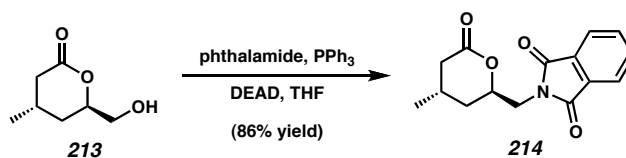


**Lactone 212.** MeLi (1.3 M in ether, 5.8 mL, 7.56 mmol) was added to a stirring slurry of CuI (714 mg, 3.89 mmol) in diethyl ether cooled to  $-78$   $^\circ\text{C}$ . The vessel was warmed to  $0$   $^\circ\text{C}$  for 15 min, then cooled again to  $-78$   $^\circ\text{C}$ . A solution of the  $\alpha,\beta$ -unsaturated lactone **211** (471 mg, 1.95 mmol) in diethyl ether (4 mL) was then carefully added along the cooled inner walls of the reaction flask. After 1 h, the reaction mixture was quenched by the slow addition of saturated aqueous ammonium chloride (15 mL) at  $-78$   $^\circ\text{C}$ . The reaction flask was gradually warmed to ambient temperature for 30 min, then diluted with ether (30 mL). The biphasic mixture was transferred to a separatory funnel and shaken vigorously to dissolve solids. The organic layer was washed with saturated aq ammonium chloride (2 x 20 mL), then brine (1 x 10 mL), dried over magnesium sulfate, and concentrated. The resulting material was purified by flash chromatography over silica gel (25% EtOAc:hexane eluent) to yield  $\delta$ -lactone **212** (422 mg, 84% yield) as a clear oil:  $R_f$  0.20 (25% EtOAc:hexanes);  $^1\text{H}$  NMR (300 MHz,  $\text{CDCl}_3$ )  $\delta$  4.47–4.40 (m, 1H), 3.70–3.73 (m, 2H), 2.55 (dd,  $J = 16.3, 5.1$  Hz, 1H), 2.18–2.29 (m, 1H), 2.12 (dd,  $J = 16.4, 8.9$  Hz, 1H), 1.90–1.99 (m, 1H), 1.52–1.60 (m, 1H), 1.05 (d,  $J = 6.6$  Hz, 3H), 0.87 (s, 9H), 0.06 (s, 6H);  $^{13}\text{C}$  NMR (75 MHz,  $\text{CDCl}_3$ )  $\delta$  171.7, 77.8, 65.1, 38.1, 31.7, 26.2, 24.1,

21.4, 18.6, 5.00; IR (Neat film NaCl) 1743  $\text{cm}^{-1}$ ; HRMS (FAB+)  $[\text{M}]^+$   $m/z$  calc'd for  $[\text{C}_{13}\text{H}_{26}\text{O}_3\text{Si}]^+$ : 201.0947, found 201.0950;  $\alpha_{\text{D}}^{20}$   $-25.027^\circ$  ( $c=1$ ,  $\text{CDCl}_3$ ).

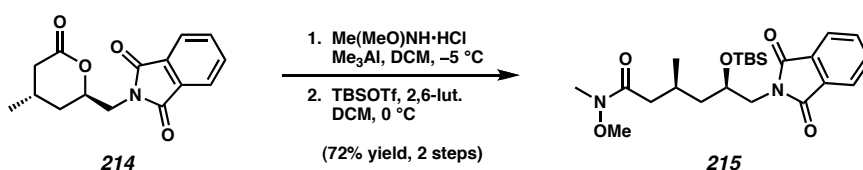


**Alcohol 213.** Lactone **212** (100 mg, 0.39 mmol) was dissolved in methanol (5.0 mL) and added to a reaction flask equipped with Dowex 50X8-100 cation exchange resin (1.0 g). The mixture was stirred at ambient temperature for 3 h, then filtered. The resin was washed with methanol (2 x 5 mL) and the combined organics were concentrated. The crude material was dried overnight under high vacuum to yield alcohol **213** (53 mg, 96% yield) as a clear oil:  $R_f$  0.18 (80% EtOAc:hexanes);  $^1\text{H}$  NMR (300 MHz,  $\text{CDCl}_3$ )  $\delta$  4.47–4.52 (m, 1H), 3.75 (dd,  $J = 12.3, 3.6$  Hz, 1H), 3.66 (dd,  $J = 12.1, 5.8$  Hz, 1H), 2.69 (bs, 1H), 2.53–2.58 (m, 1H), 2.13–2.23 (m, 2H), 1.88–1.97 (m, 1H), 1.49–1.57 (m, 1H), 1.08 (d,  $J = 6.0$  Hz, 3H);  $^{13}\text{C}$  NMR (75 MHz,  $\text{CDCl}_3$ )  $\delta$  172.3, 78.2, 65.1, 37.8, 31.1, 24.3, 21.4; IR (Neat film NaCl) 1722  $\text{cm}^{-1}$ ; HRMS (FAB+)  $[\text{M}]^+$   $m/z$  calc'd for  $[\text{C}_7\text{H}_{12}\text{O}_3]^+$ : 144.0786, found 144.0787;  $\alpha_{\text{D}}^{20}$   $-162.147^\circ$  ( $c=1$ ,  $\text{CDCl}_3$ ).



**Phthalimide 214.** To a stirred solution of alcohol **213** (1.48 g, 10.28 mmol) in tetrahydrofuran (30 mL) was added triphenyl phosphine (2.83 g 10.79 mmol), then phthalimide (1.59 g, 10.76 mmol). Once all reagents had dissolved, the reaction mixture was cooled to 0  $^\circ\text{C}$  and DEAD (1.707 mL, 10.79 mmol) was added dropwise to the stirred solution. The reaction flask was then warmed to 30  $^\circ\text{C}$  for 12 h, then concentrated. The

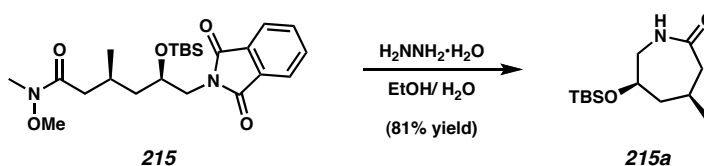
concentrated reaction mixture was flashed over silica (4:1 hexanes:EtOAc). The resulting solid was recrystallized from dichloromethane to provide phthalimide **214** (2.42 g, 86% yield) as a white solid: m.p. 118–120 °C;  $R_f$  0.16 (40% EtOAc:hexanes);  $^1\text{H}$  NMR (300 MHz,  $\text{CDCl}_3$ )  $\delta$  7.82–7.88 (m, 2H), 7.71–7.76 (m, 2H), 4.74–4.83 (m, 1H), 4.04 (dd,  $J = 15.0, 8.3$  Hz, 1H), 3.78 (dd,  $J = 15.0, 5.5$  Hz, 1H), 2.63 (dd,  $J = 16.6, 5.4$  Hz, 1H), 2.28 (m, 1H), 2.16 (dd,  $J = 16.5, 9.1$  Hz, 1H), 1.86 (m, 1H), 1.66 (m, 1H), 1.09 (d,  $J = 6.9$  Hz, 3H);  $^{13}\text{C}$  NMR (75 MHz,  $\text{CDCl}_3$ )  $\delta$  170.9, 168.1, 134.4, 132.0, 123.7, 74.1, 41.9, 37.9, 32.8, 24.0, 21.5; IR (Neat film NaCl) 1774, 1716  $\text{cm}^{-1}$ ; HRMS (FAB+)  $[\text{M}+\text{H}]^+$   $m/z$  calc'd for  $[\text{C}_{15}\text{H}_{15}\text{NO}_4+\text{H}]^+$ : 274.1079, found 274.1076;  $\alpha_D^{20} -68.6255^\circ$  ( $c=1, \text{CDCl}_3$ ).



**Weinreb Amide 215.** Trimethylaluminum (2.0 M in toluene, 10.32 mL, 20.64 mmol) was slowly added to a cooled ( $-10$  °C) solution of *N,O*-dimethylhydroxylamine hydrochloride (2.01 g, 16.80 mmol) in dichloromethane (40 mL). The solution was stirred for 20 min before the dropwise addition of the Mitusunobu adduct **214** (2.26 g, 8.23 mmol) in dichloromethane (10 mL). The reaction was stirred at  $-10$  °C for 30 min before the addition of sat. aq  $\text{NaHCO}_3$  (20 mL). The reaction mixture was then allowed to warm to room temperature. The crude reaction mixture was diluted with dichloromethane (30 mL) and brine (20 mL). The aqueous layer was extracted with dichloromethane (2 x 30 mL). The combined organic layers were washed with brine (30 mL), then dried and concentrated to a volume of 10 mL over a rotovap bath temperature of 15 °C.

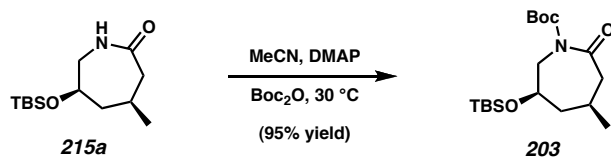
The crude amide was diluted with dichloromethane (20 mL) and cooled to 0 °C. To the cooled, stirred solution was added TBSOTf (3.79 mL, 16.51 mmol) followed by 2,6-

lutidine (1.442 mL, 12.38 mmol). The solution was maintained at 0 °C for 20 min, then quenched by addition of saturated ammonium chloride (20 mL). The biphasic mixture was allowed to warm to room temperature while stirring vigorously, then transferred to a separatory funnel. The organic layer was separated and the aqueous layer was extracted with dichloromethane (2 x 20 mL). The combined organics were washed with sat. aq NaHCO<sub>3</sub> solution (1 x 15 mL) and water (1 x 15 mL), then dried over MgSO<sub>4</sub> and concentrated. The crude product was flashed over silica gel (20% EtOAc:hexanes) to provide Weinreb amide **215** (2.58g, 72% yield) as an oil: *R<sub>f</sub>* 0.30 (40% EtOAc:hexane); <sup>1</sup>H NMR (300 MHz, CDCl<sub>3</sub>) δ 7.82 (dd, *J* = 5.4, 3.1 Hz, 2H), 7.70 (dd, *J* = 5.6, 2.9 Hz, 2H), 4.05–4.14 (m, 1H), 3.68–3.78 (m, 2H), 3.65 (s, 3H), 3.14 (s, 3H), 2.38–2.45 (m, 1H), 2.18–2.29 (m, 1H), 1.51–1.60 (m, 1H), 1.38–1.47 (m, 1H), 1.03 (d, *J* = 6.3 Hz, 3H), 0.76 (s, 9H), -0.01 (s, 3H), -0.20 (s, 3H); <sup>13</sup>C NMR (75 MHz, CDCl<sub>3</sub>) δ 168.5, 134.1, 132.3, 123.3, 68.3, 61.5, 44.0, 43.7, 39.7, 32.3, 26.9, 26.0, 20.8, 18.1, -4.3, -4.4; IR (Neat film NaCl) 3473.5, 2955.4, 2857.3, 1774.2, 1714.5, 1660.3 cm<sup>-1</sup>; HRMS [M+H]<sup>+</sup> *m/z* calc'd for [C<sub>23</sub>H<sub>36</sub>N<sub>2</sub>O<sub>5</sub>Si+H]<sup>+</sup>: 449.2472, found 449.2470; α<sub>D</sub><sup>20</sup> -29.7° (c=1, CDCl<sub>3</sub>).

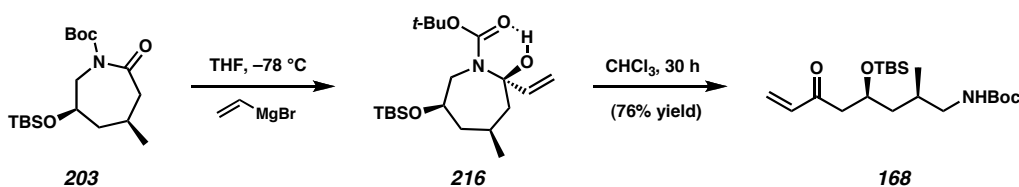


**Caprolactam 215a.** To a solution of **215** (2.848 g, 6.55 mmol) in absolute ethanol was added hydrazine monohydrate (1.75 mL, 32.77 mmol) and deionized water (0.39 mL). The solution was heated to 90 °C for 4 h. The reaction was then cooled in an ice bath and the thick cottony solids were filtered. The filtrate was then concentrated to a solid. The crude solid was taken up in EtOAc (50 mL), cooled in an ice bath, and filtered over a pad of Celite, rinsing with portions of EtOAc (2 x 20 mL). The organics were then dried

over sodium sulfate, and concentrated. The crude solid was subjected to chromatography over silica gel (30% EtOAc:hexane eluent) to yield the unprotected caprolactam **215a** (1.633g, 81% yield) as a white solid: m.p. 79–81 °C;  $R_f$  0.22 (50% EtOAc:hexane)  $^1\text{H NMR}$  (300 MHz,  $\text{CDCl}_3$ )  $\delta$  6.27 (bs, 1H), 3.56–3.65 (m, 1H), 3.18–3.28 (m, 1H), 3.01–3.10 (m, 1H), 2.38 (dd,  $J = 13.7, 11.0$  Hz, 1H), 2.25 (dd,  $J = 12.1, 1.7$  Hz, 1H), 1.96–2.04 (m, 1H), 1.83–1.93 (m, 1H), 1.36 (q,  $J = 11.8$  Hz, 1H), 1.04 (d,  $J = 6.9$  Hz, 3H), 0.86 (s, 9H), 0.05 (s, 6H);  $^{13}\text{C NMR}$  (75 MHz,  $\text{CDCl}_3$ )  $\delta$  177.3, 71.0, 49.7, 48.9, 44.2, 28.6, 26.1, 24.8, 18.4, -4.2, -4.4; IR (Neat film NaCl) 3239.9, 2929.8, 2857.6, 1673.1  $\text{cm}^{-1}$ ; HRMS (EI<sup>+</sup>)  $[\text{M}+\text{H}]^+$   $m/z$  calc'd for  $[\text{C}_{13}\text{H}_{27}\text{NO}_2\text{Si}+\text{H}]^+$ : 242.1576, found 242.1576;  $\alpha_D^{20} -15.0^\circ$  ( $c=1, \text{CDCl}_3$ ).



***N*-Boc-caprolactam **203**.** To a solution of **215a** (853 mg, 3.313 mmol) in acetonitrile (40 ml) was added *t*-butyl carbonate anhydride (1.81 g, 8.28 mmol). After the *t*-butyl carbonate anhydride had completely dissolved, *N,N*-dimethylamino pyridine (1.01 g, 8.28 mmol) was added in several small portions. The resulting dark-brown solution was stirred for 10 min at ambient temperature, then warmed to 35 °C. After 5 hours, the reaction was quenched by addition of water (20 mL). The mixture was transferred to a separatory funnel and extracted with EtOAc (4 x 30 mL). The combined organics were washed with brine (1 x 30 mL), dried over sodium sulfate, and concentrated to give a brown waxy solid, which was purified by flash chromatography over silica (10% EtOAc:hexanes) to provide *N*-Boc-caprolactam **203** (1.314 g, 95% yield) as a waxy solid: m.p. 77–78°;  $R_f$  0.22 (10% EtOAc:hexanes);  $^1\text{H NMR}$  (300 MHz,  $\text{CDCl}_3$ )  $\delta$  4.11 (dt,  $J = 14.8, 1.8$  Hz, 1H), 3.63 (tdd,  $J = 22.0, 4.9, 2.2$  Hz, 1H), 3.33 (dd,  $J = 15.0, 9.5$  Hz, 1H), 2.56 (dd,  $J = 14.1, 10.9$  Hz, 1H), 2.41 (d,  $J = 14.3$  Hz, 1H), 1.96–2.03 (m, 1H), 1.87–1.94 (m, 1H), 1.51 (s, 9H), 1.27–1.39 (m, 1H), 1.04 (d,  $J = 6.6$  Hz, 3H), 0.87 (s, 9H), 0.09 (s, 3H), 0.07 (s, 3H);  $^{13}\text{C NMR}$  (75 MHz,  $\text{CDCl}_3$ )  $\delta$  174.1, 152.5, 83.4, 70.4, 52.4, 47.7, 47.0, 28.4, 28.1, 26.1, 24.5, 18.4, 4.3, 4.4; IR (Neat film NaCl) 2932.4, 1710.2, 1645.1  $\text{cm}^{-1}$ ; HRMS  $[\text{M}+\text{H}]^+$   $m/z$  calc'd for  $[\text{C}_{18}\text{H}_{35}\text{NO}_4\text{Si}+\text{H}]^+$ : 358.2414, found 358.2426;  $\alpha_D^{20} -48.0^\circ$  ( $c=1, \text{CDCl}_3$ ).

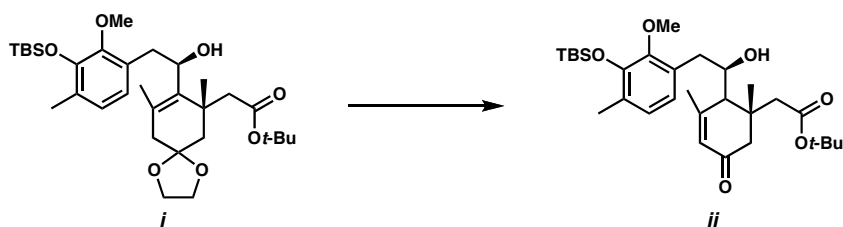


**Enone **166**.** To a stirred solution of *N*-Boc-caprolactam **203** (1.0 g, 2.79 mmol, 1.00 equiv) in THF (10 mL) at -78 °C was added a 1.0 M solution of vinyl magnesium bromide (3.35 mL, 3.35 mmol, 1.2 equiv) dropwise. The solution was stirred at -78 °C for 1 h then

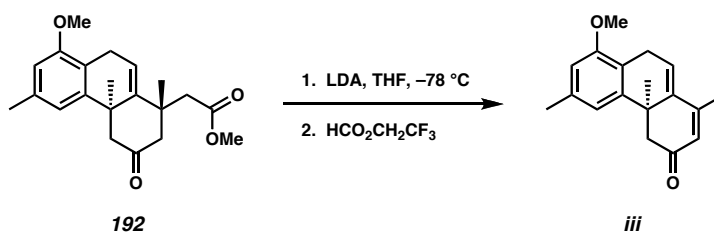
quenched with saturated  $\text{NH}_4\text{Cl}$  (5 mL) at  $-78\text{ }^\circ\text{C}$ . The mixture was allowed to warm to ambient temperature then diluted with  $\text{H}_2\text{O}$  (10 mL) and  $\text{Et}_2\text{O}$  (20 mL). The layers were separated, and the aqueous layer was extracted with  $\text{Et}_2\text{O}$ . The combined organic layers were washed with water then brine and dried over  $\text{Na}_2\text{SO}_4$  and concentrated to give a crude oil, which was purified by flash chromatography (10%  $\text{EtOAc}$ / $\text{Hexanes}$ ) to provide a mixture of **216** and **166**. A solution of the purified product in  $\text{CHCl}_3$  (0.15 M) was prepared and allowed to stand at ambient temperature for 30 h before concentrating to afford enone **166** (818 mg, 2.121 mmol, 76% yield) as a clear oil:  $^1\text{H}$  NMR (300 MHz,  $\text{CDCl}_3$ )  $\delta$  6.35 (dd,  $J = 17.6, 10.2$  Hz, 1H), 6.20 (dd,  $J = 17.6, 1.5$  Hz, 1H), 5.80 (dd,  $J = 10.2, 1.5$  Hz, 1H), 4.78 (bm, 1H), 3.81 (m, 1H), 3.29 (bm, 1H), 3.01 (dt,  $J = 13.8, 6.1$  Hz, 1H), 2.57 (dd,  $J = 15.8, 5.6$  Hz, 1H), 2.39 (dd,  $J = 15.8, 7.9$  Hz, 1H), 2.13 (m, 1H), 1.52–1.28 (m, 2H), 1.44 (s, 9H), 0.94 (d,  $J = 6.7$  Hz, 3H), 0.87 (s, 9H), 0.06 (d,  $J = 3.2$  Hz, 6H);  $^{13}\text{C}$  NMR (125 MHz,  $\text{CDCl}_3$ )  $\delta$  200.1, 156.0, 136.7, 128.0, 69.5, 47.3, 45.8, 42.3, 28.4, 26.0, 25.8, 20.3, 18.0,  $-4.6$  Hz; IR (Neat film NaCl) 3379, 2957, 2930, 2858, 1714, 1705, 1505, 1366, 1253, 1173, 836, 776  $\text{cm}^{-1}$ ; HRMS (FAB+)  $[\text{M}+\text{H}]^+$   $m/z$  calc'd for  $[\text{C}_{20}\text{H}_{39}\text{NO}_4\text{Si}+\text{H}]^+$ : 386.2727, found 286.2713.

## References

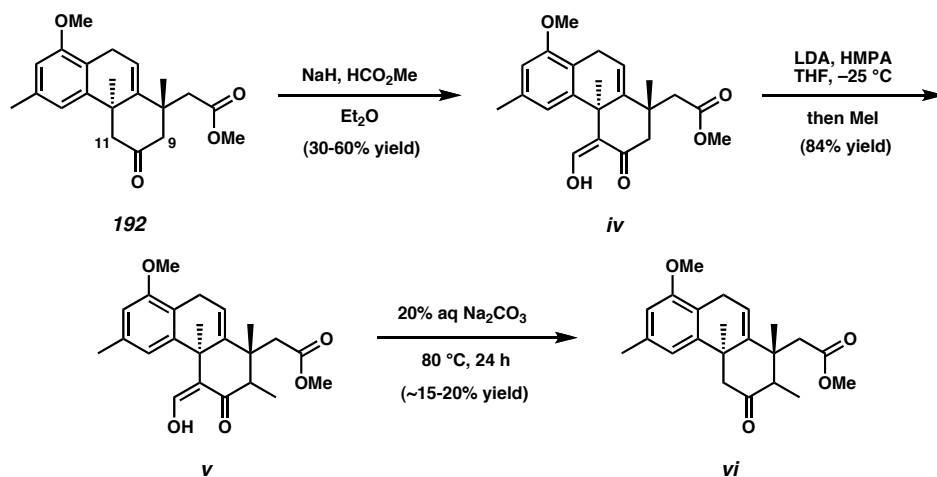
1. Portions of this chapter have been published: Behenna, D. C.; Stockdill, J. L.; Stoltz, B. M. *Angew. Chem. Int. Ed.* **2007**, *46*, 4077–4079.
2. Daranas, A. H.; Fernández, J. J.; Gavín, J. A.; Norte, M. *Tetrahedron* **1999**, *55*, 5539–5546.
3. a) Hikage, N.; Furukawa, H.; Takao, K.; Kobayashi, S. *Tetrahedron Lett.* **1998**, *39*, 6237–6240; b) Hikage, N.; Furukawa, H.; Takao, K.; Kobayashi, S. *Tetrahedron Lett.* **1998**, *39*, 6241–6244; c) Williams, D. R.; Cortez, G. A. *Tetrahedron Lett.* **1998**, *39*, 2675–2678.
4. a) Matsumoto, T.; Ohmura, T. *Chem. Lett.* **1977**, 335–338. b) Liebeskind, L. S.; Chidambaram, R. Nimkar, S.; Liotta, D. *Tetrahedron Lett.* **1990**, *31*, 3723–3726; c) Schmidt, C.; Thazhuthaveetil, J. *Can. J. Chem.* **1973**, *51*, 3620–3624; d) Matsumoto, T.; Usui, S.; Morimoto, T. *Bull. Chem. Soc. Jpn.* **1977**, *50*, 1575–1579; e) Matsumoto, T.; Usui, S. *Chem. Lett.* **1978**, 897–900; f) Stevens, R. V.; Bisacchi, G. S. *J. Org. Chem.* **1982**, *47*, 2396–2399.
5. a) Behenna, D. C.; Stoltz, B. M. *J. Am. Chem. Soc.* **2004**, *126*, 15044–15045; b) Mohr, J. T.; Behenna, D. C.; Harned, A. M.; Stoltz, B. M. *Angew. Chem. Int. Ed.* **2005**, *44*, 6924–6927; c) McFadden, R. M.; Stoltz, B. M. *J. Am. Chem. Soc.* **2006**, *128*, 7738–7739; d) Mohr, J. T.; Nishimata, T.; Behenna, D. C.; Stoltz, B. M. *J. Am. Chem. Soc.* **2006**, *128*, 11348–11349; e) Keith, J. A.; Behenna, D. C.; Mohr, J. T.; Ma, S.; Marinescu, S. C.; Oxgaard, J.; Stoltz, B. M.; Goddard, W. A., III *J. Am. Chem. Soc.* **2007**, *129*, 11876–11877; f) Mohr, J. T.; Stoltz, B. M. *Chem. Asian J.* **2007**, *2*, 1476–1491; g) White, D. E.; Stewart, I. C.; Grubbs, R. H.; Stoltz, B. M. *J. Am. Chem. Soc.* **2008**, *130*, 810–811; h) Marinescu, S. C.; Nishimata, T.; Mohr, J. T.; Stoltz, B. M. *Org. Lett.* **2008**, *10*, 1039–1042; i) Enquist, J. A., Jr.; Stoltz, B. M. *Nature* **2008**, *453*, 1228–1231; j) Seto, M.; Roizen, J. L.; Stoltz, B. M. *Angew. Chem. Int. Ed.* **2008**, *47*, 6873–6876.
6. If alcohol **175** was allowed to persist under the reaction conditions for several additional hours after the consumption of benzaldehyde **174**, significant over-reduction was observed.
7. a) Franck-Neumann, M.; Miesch, M.; Barth, F. *Tetrahedron* **1993**, *49*, 1409–1420 b) In our experience, dimethyl ketone **176** was best prepared by iodobenzene diacetate oxidation of 2,6-dimethylphenol in ethylene glycol to give a quinone monoketal product, which was readily reduced to the ketone with Pd/C under hydrogen (60 psi).
8. Barnard, C. F. *J. Organometallics*, **2008**, *27*, 5402–5422 and references therein.
9. For related cyclizations, see: Ma, S.; Zhang, J. *Tetrahedron Lett.* **2002**, *43*, 3435–3438.
10. We were uncertain at this point whether the observed product had resulted from dehydration of intermediate **186** or from a 6-endo S<sub>N</sub>'-type cyclization to form **187** directly from **183**. Thus, **185** was synthesized independently and subjected to the reaction conditions. No cyclization products were observed, implying that the 6-endo S<sub>N</sub>' cyclization pathway was operative.
11. The analogous trifluoroacetate also underwent cyclization in TFA to give yields and diastereoselectivities comparable to allylic alcohol **183**.
12. This alcohol diastereomer did not produce cyclized products. Rather, deketalization and olefin migration were observed.



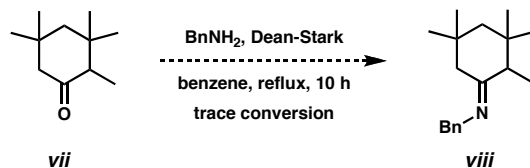
13. These conditions were specifically designed for highly congested aryl triflates, see: Saá, J. M.; Dopico, M.; Martorell, G.; García-Raso, A. G. *J. Org. Chem.* **1990**, *55*, 991–995.
14. Typical epoxidation conditions such as *m*CPBA, dimethyl dioxirane, urea hydroperoxide, iron(III) acetylacetonate and hydrogen peroxide, hexafluoroacetone and hydrogen peroxide, potassium permanganate and copper(II) sulfate, and methyltrioxorhenium and hydrogen peroxide gave oxidation at the benzylic C(19) position or no reaction. Hydroboration was also unsuccessful.
15. a) Treatment with  $\text{BF}_3 \cdot \text{Et}_2\text{O}$  gave the desired hydride shift with concomitant deketalization; however, the yields were lower than the 2–step protocol. b) Naqvi, S. M.; Horwitz, J. P.; Filler, R. *J. Am. Chem. Soc.* **1957**, *79*, 6283–6286.
16. Under other kinetic enolate trapping conditions, fragmentation of ketoester **192** occurred to give the extended enone **iii**.



17. The ability to selectively deprotonate at C(11) led us to pursue a strategy to “protect” C(11). Ketoester **192** was condensed with methyl formate at C(11) to provide **iv** and then successfully methylated at C(9) to give **v**. Unfortunately, despite extensive experimentation, no reagents could be found that were capable of removing the hydroxymethylene from methyl ketone **vi** in greater than ~ 20% yield.

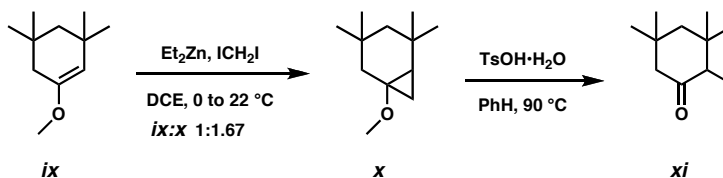


18. Known ketone **vii** was treated with Dean–Stark dehydration conditions in the presence of benzyl amine, but afforded only trace amounts of what appeared to be desired imine **viii**.

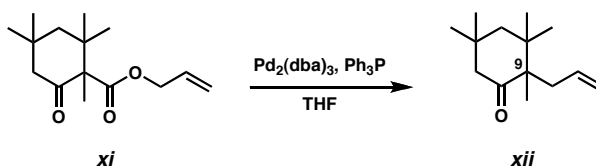


19. a) Sugano, N.; Koizumi, Y.; Oguri, H.; Kobayashi, S.; Yamashita, S.; HIRAMA, M. *Chem. Asian J.* **2008**, 3, 1549–1557.

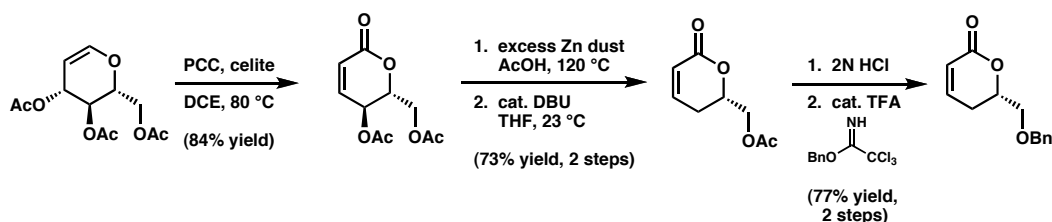
b) Since selective enolization had proved difficult, we hoped to separate the isomers and cyclopropanate the C(9)–C(10) enol ether. To that end, cyclopropanation of steric model methyl enol ether **ix** was attempted with diethyl zinc and diiodomethane. Treatment with *p*-toluenesulfonic acid in benzene opened the cyclopropane **x** to the desired methyl ketone **xi**. However, in our hands it was difficult to drive the reaction to more than ~ 60% conversion under optimized conditions.



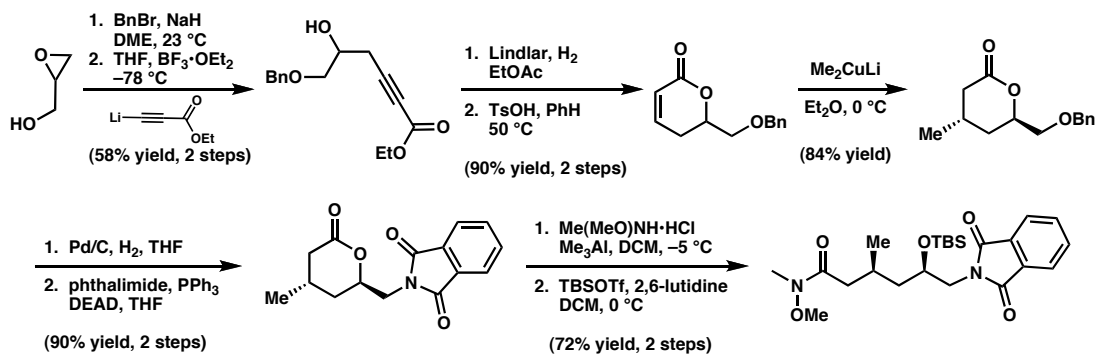
20. We were delighted to find that pentamethyl  $\beta$ -ketoester **xi** underwent alkylation selectively at the more substituted  $\alpha$ -site with Tsuji's conditions to provide **xii**. We envisioned this method as a late-stage means to install the C(9) quaternary stereocenter in the presence of the other C ring quaternary stereocenters. In this case, chiral ligands may have been used to override the inherent diastereoselectivity of the alkylation. These alkylation methods have the additional advantage of forming quaternary centers at room temperature in a few hours or less under neutral conditions.



21. To minimize cost, initial synthetic investigations were conducted using (*D*)-glucal.



## 22. Synthetic route from glycidol.



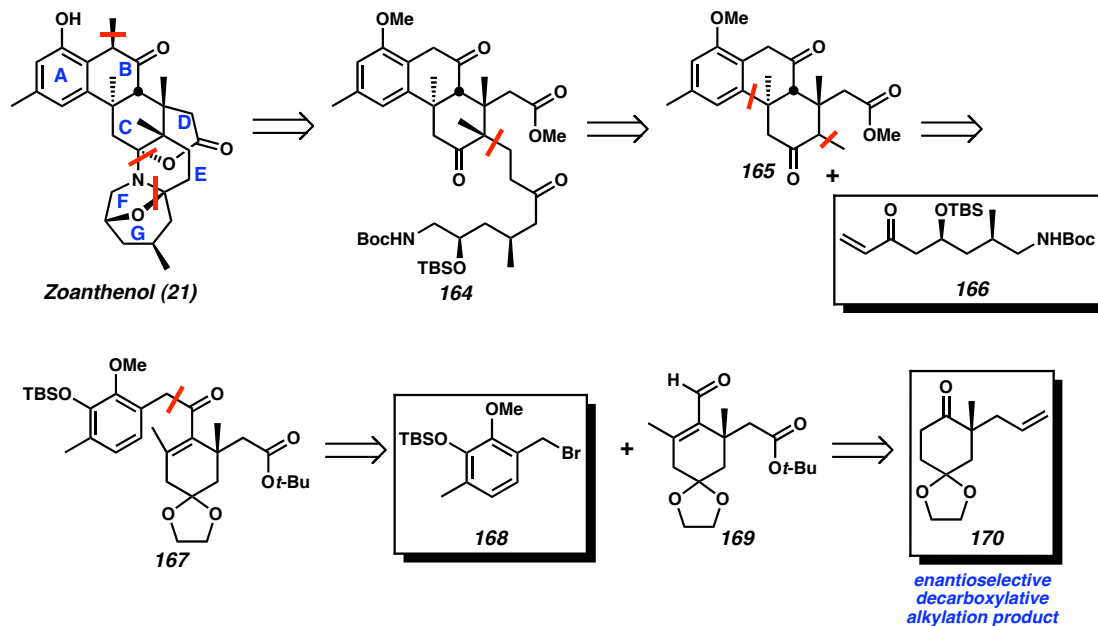
23. Dossetter, A. G.; Jamison, T. F.; Jacobsen, E. N. *Angew. Chem. Int. Ed.* **1999**, *38*, 2398–2400.

## SYNTHETIC SUMMARY

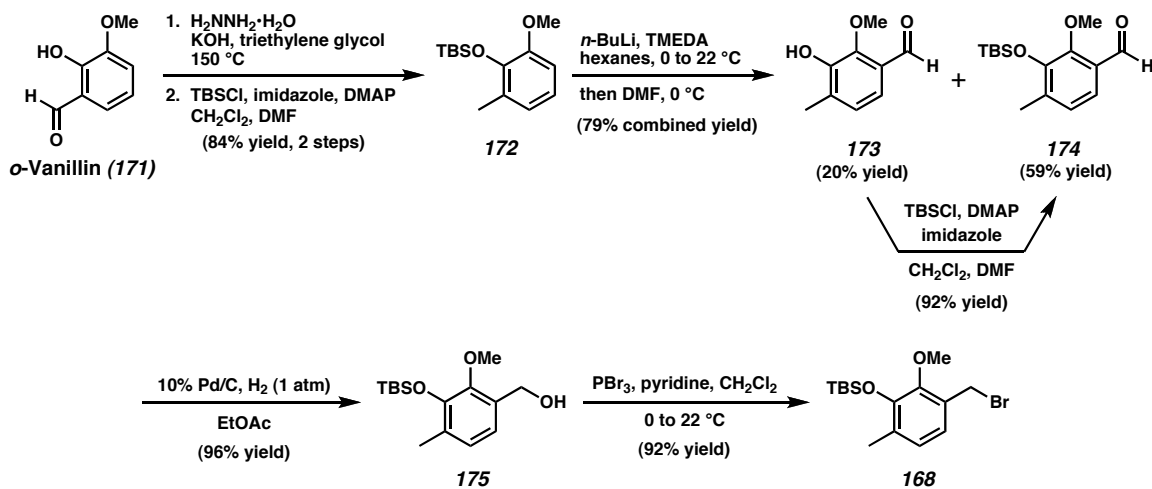
## Early Efforts Toward the Synthesis of Zoanthanol

Discovery of an Unusual Acid-Catalyzed Cyclization and  
Development of an Enantioselective Route to a Synthon for the DEFG Rings

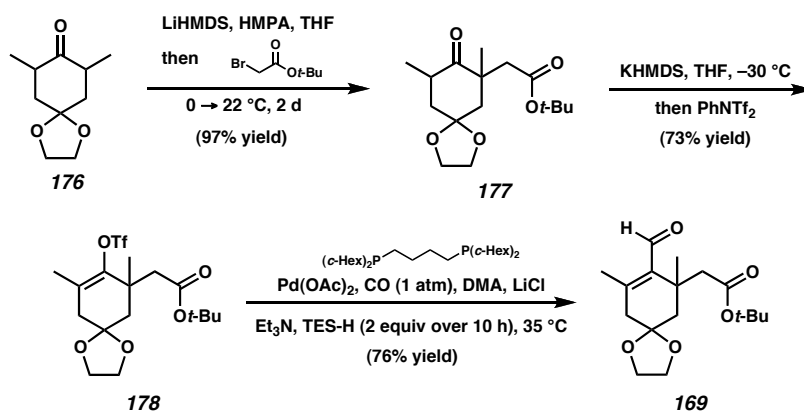
Scheme S2.1 Retrosynthetic Analysis of Zoanthanol



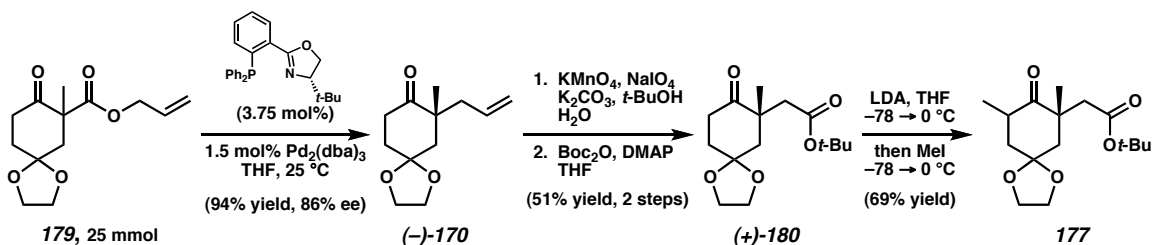
Scheme S2.2 Synthesis of the A Ring Synthon



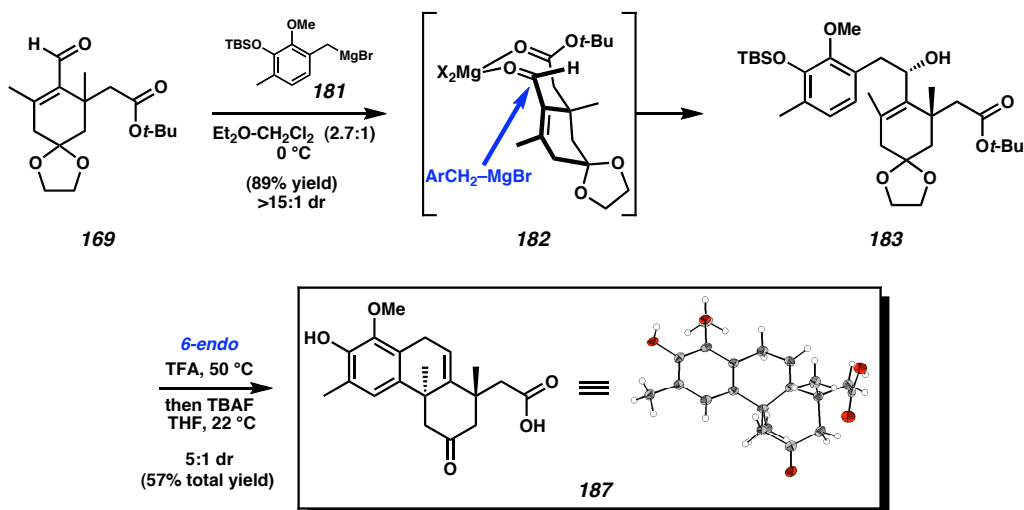
## Scheme S2.3 Racemic Synthesis of the C Ring Synthon



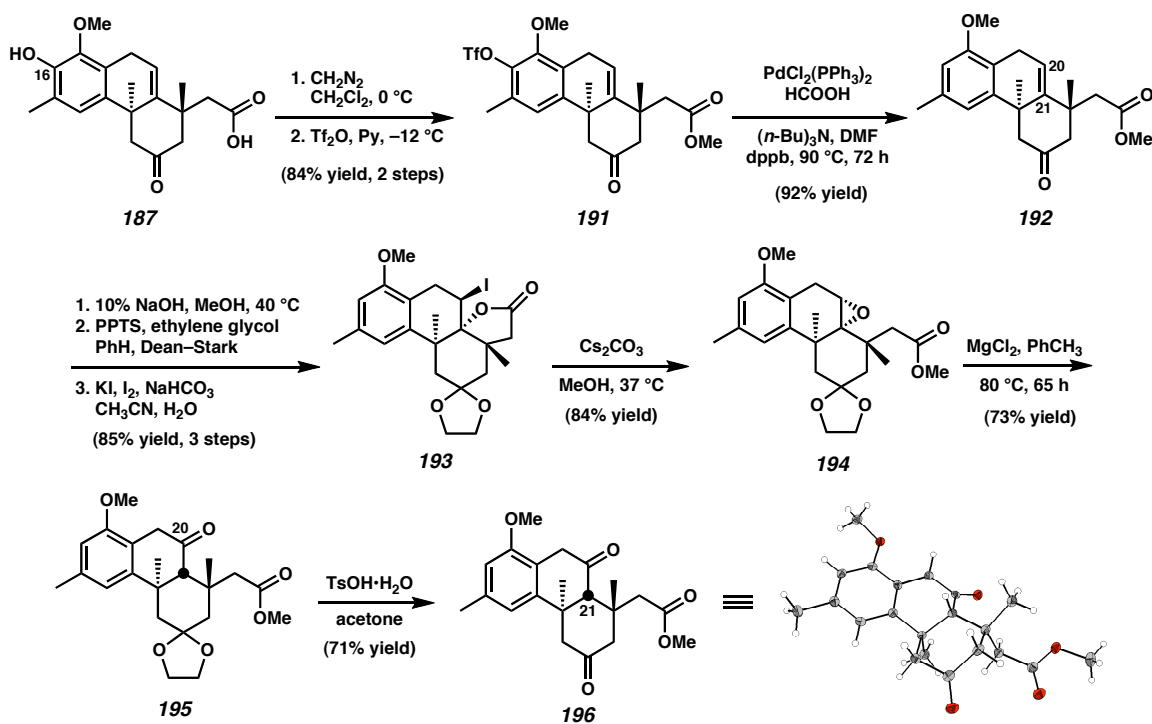
## Scheme S2.4 Enantioselective Synthesis of C Ring Methyl Ketone 177



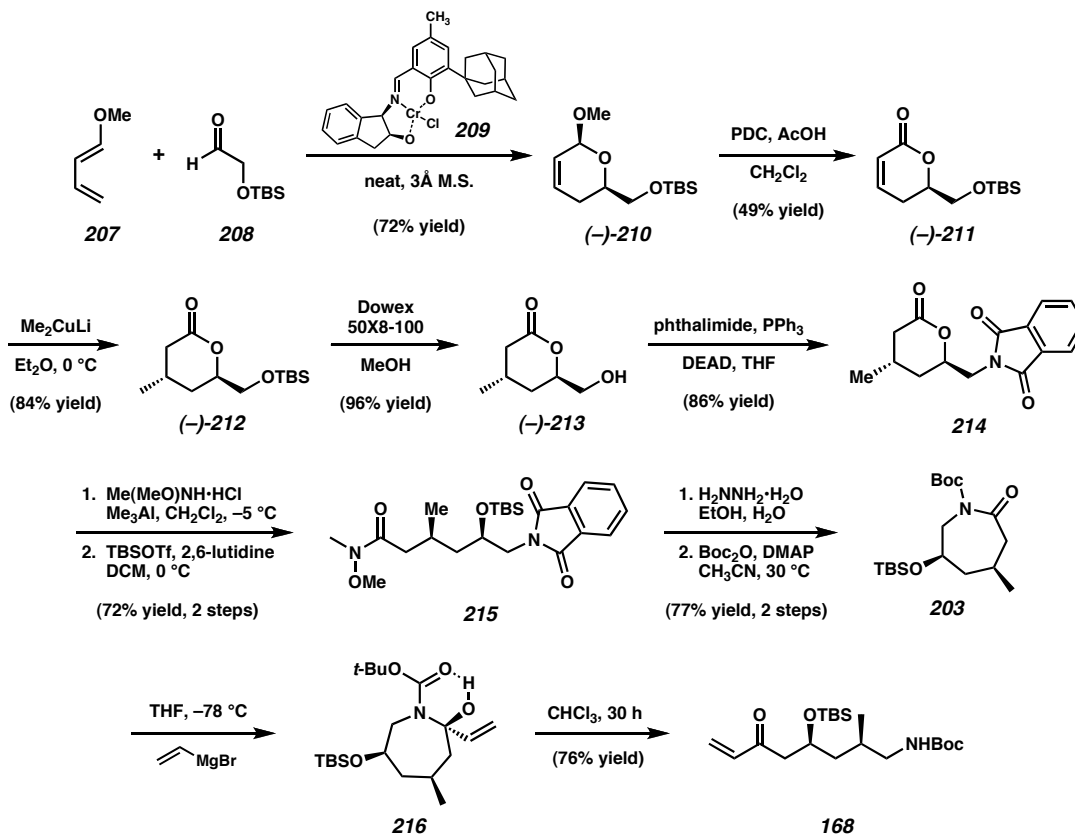
## Scheme S2.5 Fragment Coupling and Acid-Mediated Cyclization of the A and C Rings



## Scheme S2.6 Deoxygenation of the A Ring and Refunctionalization of C(20)



## Scheme S2.7 Enantioselective Synthesis of DEFG Synthone



## APPENDIX A

Spectra and X-Ray Crystallographic Data:  
Early Efforts Toward the Synthesis of Zoanthenol

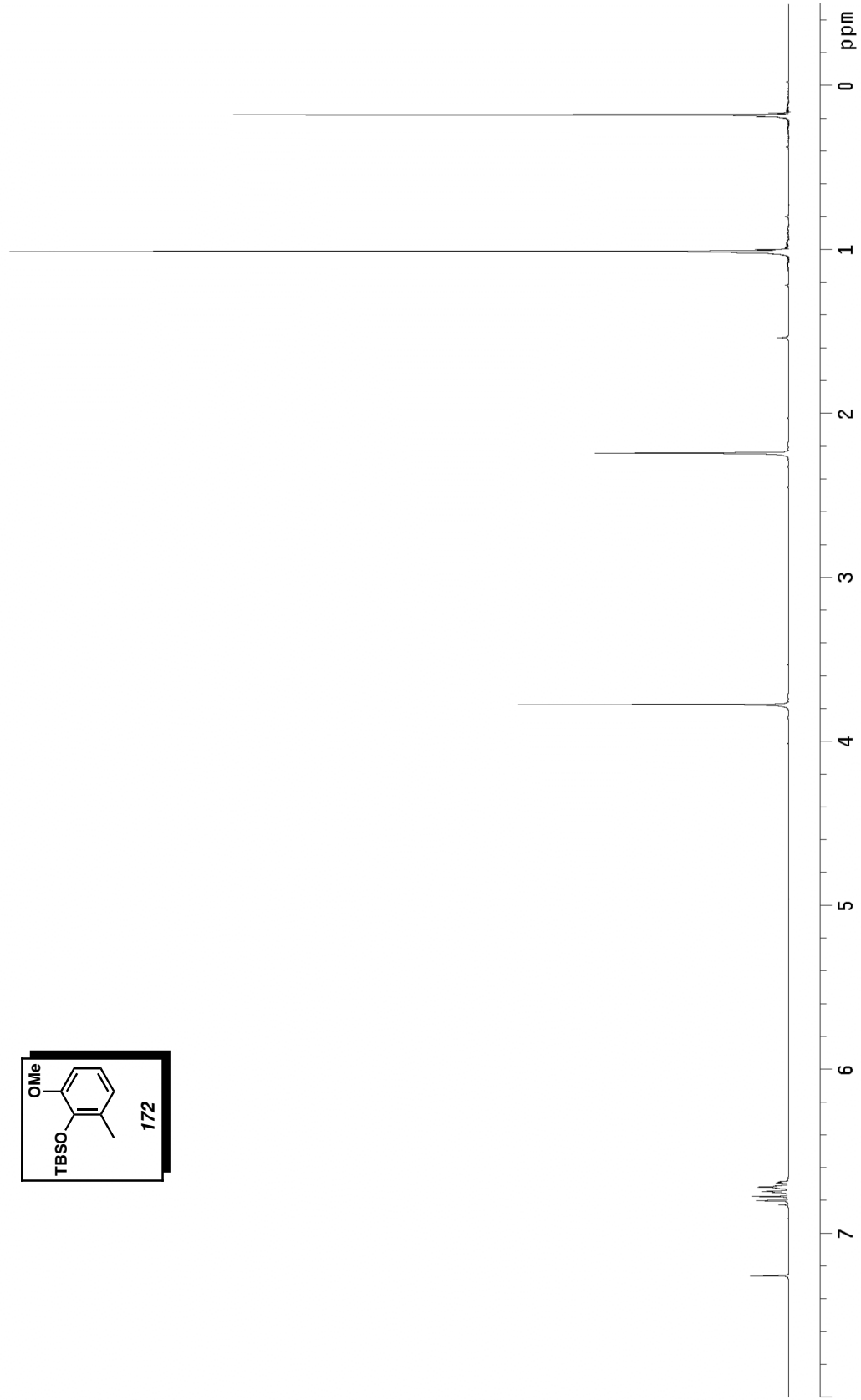
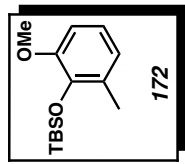


Figure A.1  $^1\text{H}$  NMR (300 MHz,  $\text{CDCl}_3$ ) of compound **172**.

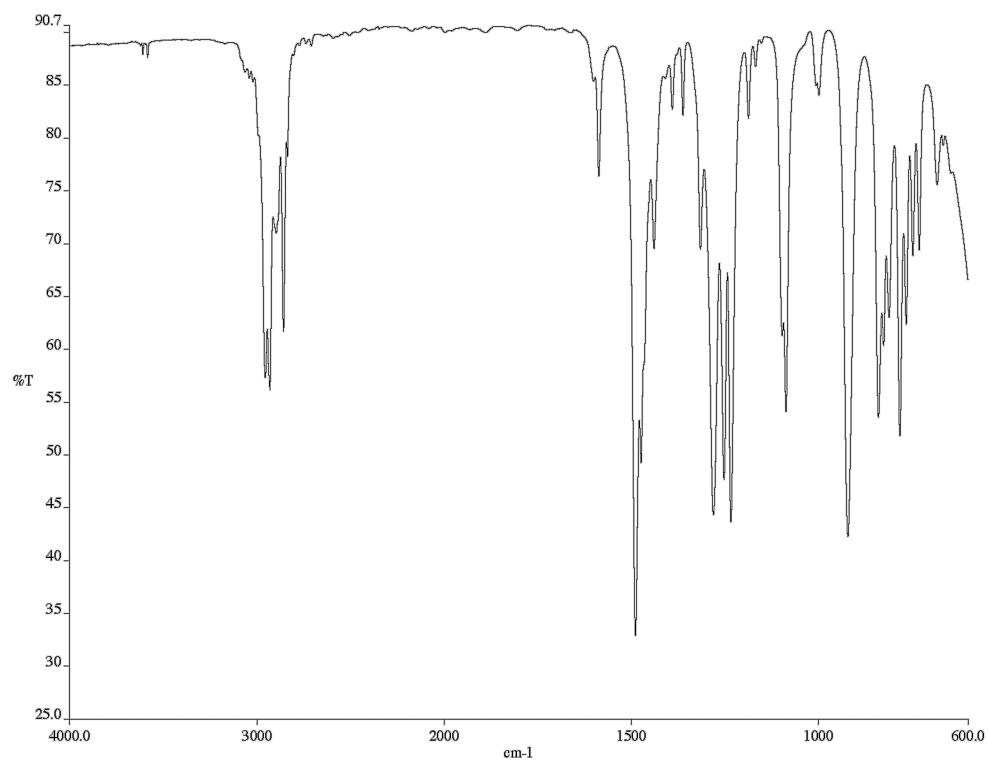


Figure A.2 Infrared spectrum (thin film/NaCl) of compound **172**.

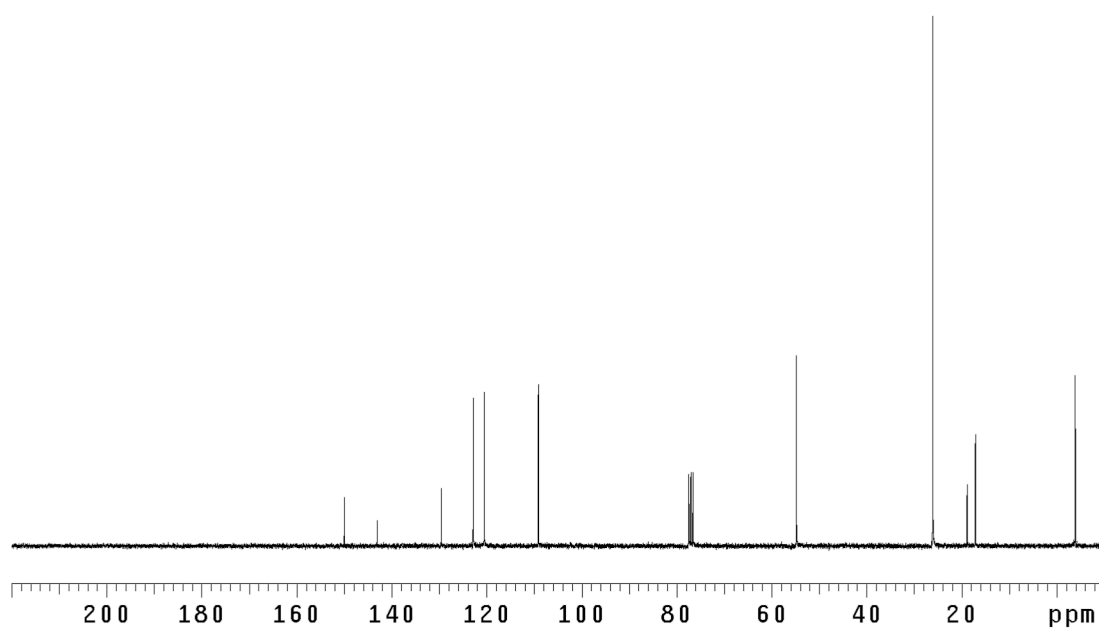


Figure A.3 <sup>13</sup>C NMR (75 MHz, CDCl<sub>3</sub>) of compound **172**.

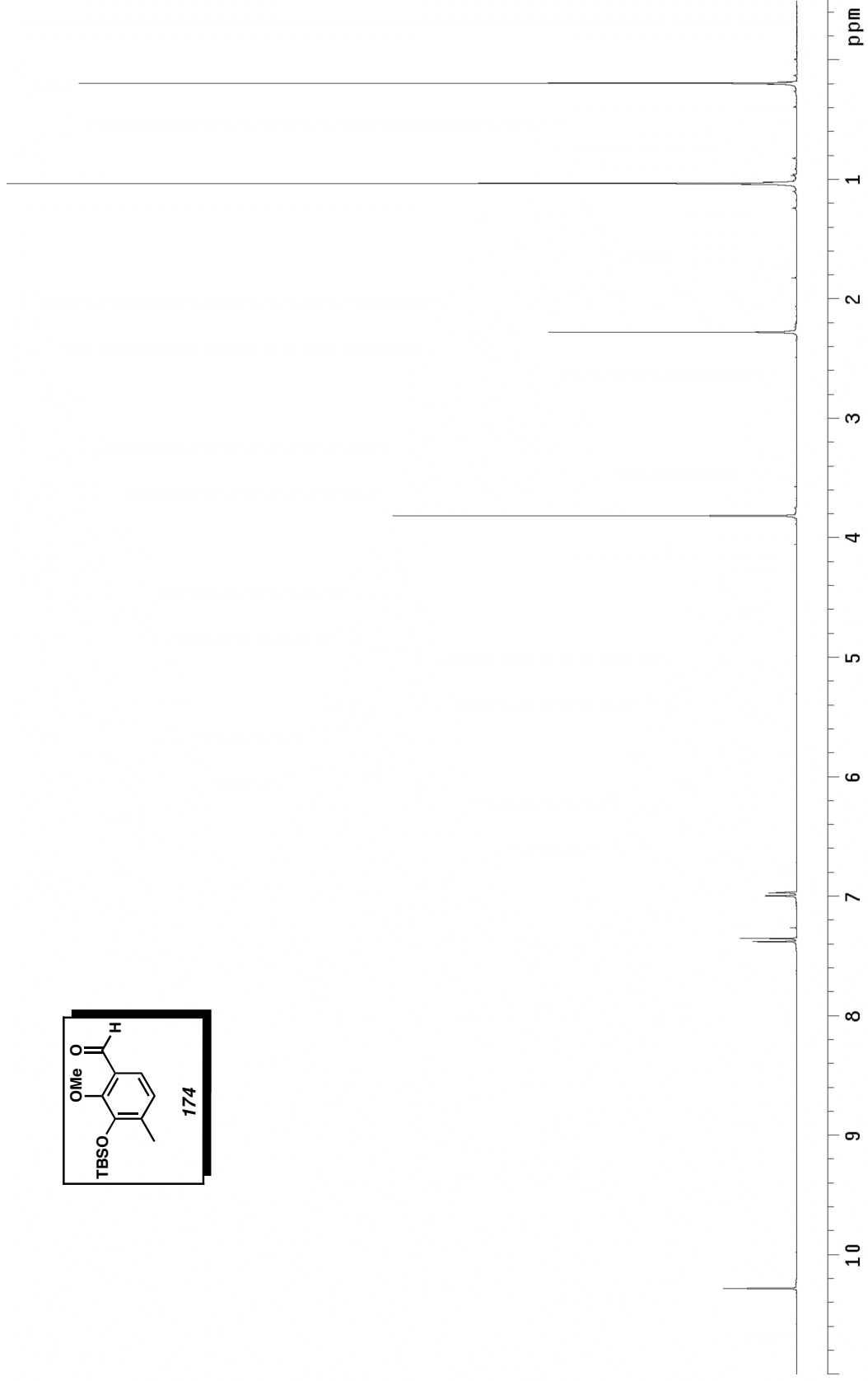
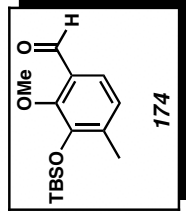


Figure A.4 <sup>1</sup>H NMR (300 MHz, CDCl<sub>3</sub>) of compound **174**.

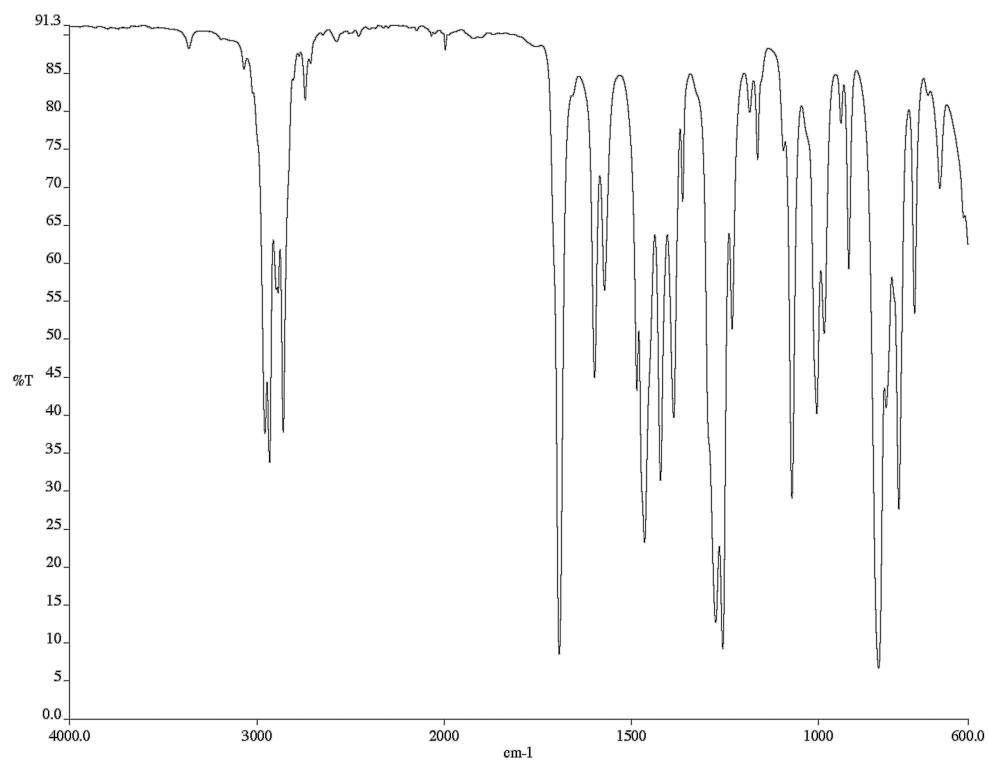


Figure A.5 Infrared spectrum (thin film/NaCl) of compound **174**.

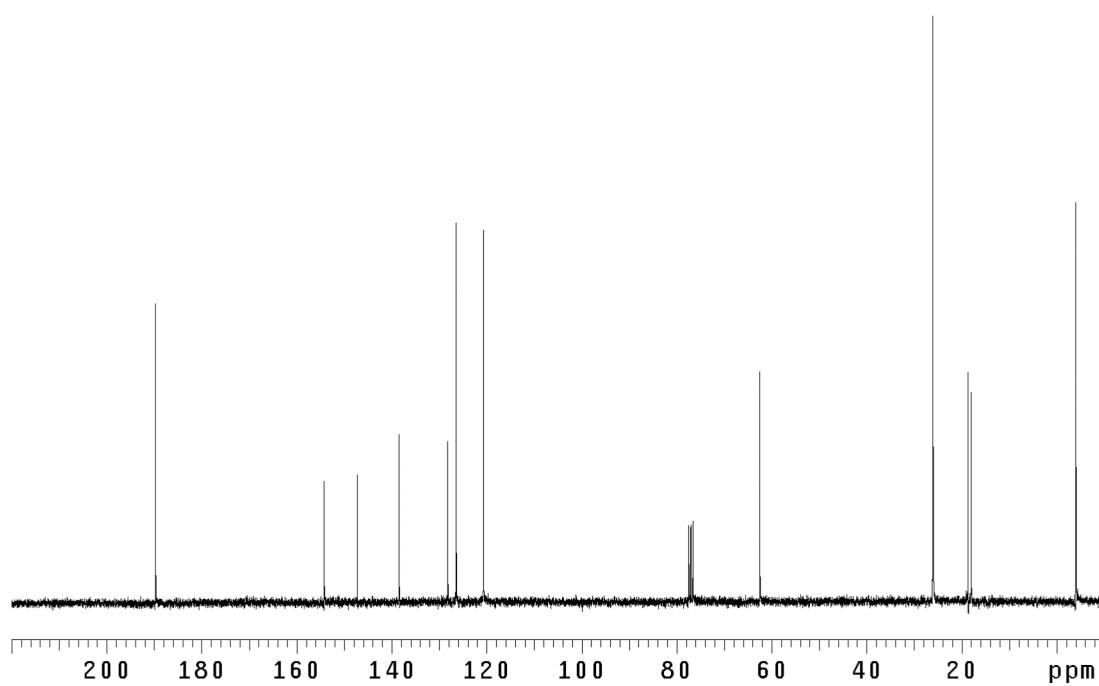


Figure A.6 <sup>13</sup>C NMR (75 MHz, CDCl<sub>3</sub>) of compound **174**.

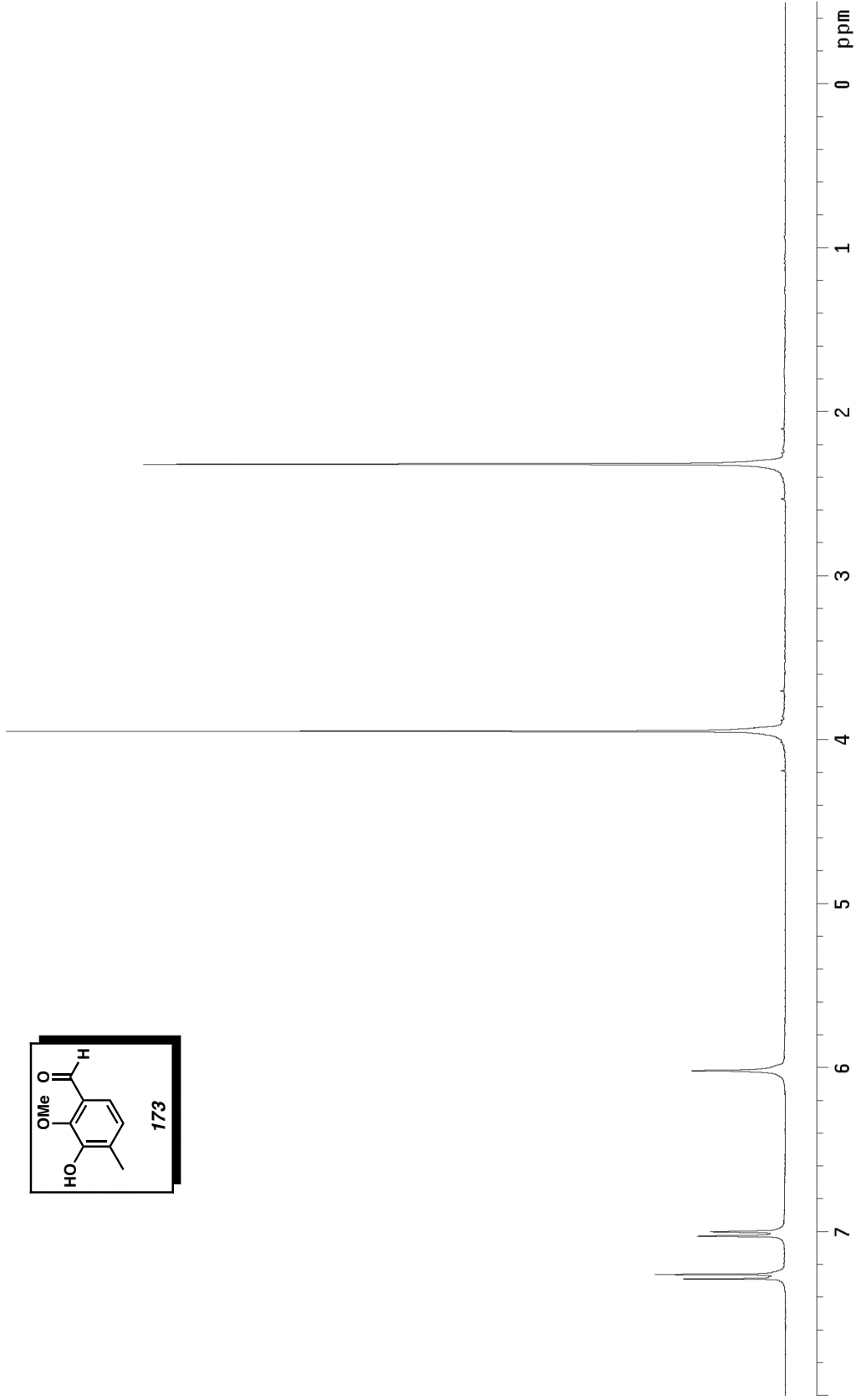
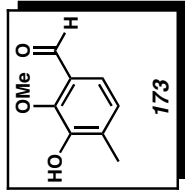


Figure A.7 <sup>1</sup>H NMR (300 MHz, CDCl<sub>3</sub>) of compound **173**.

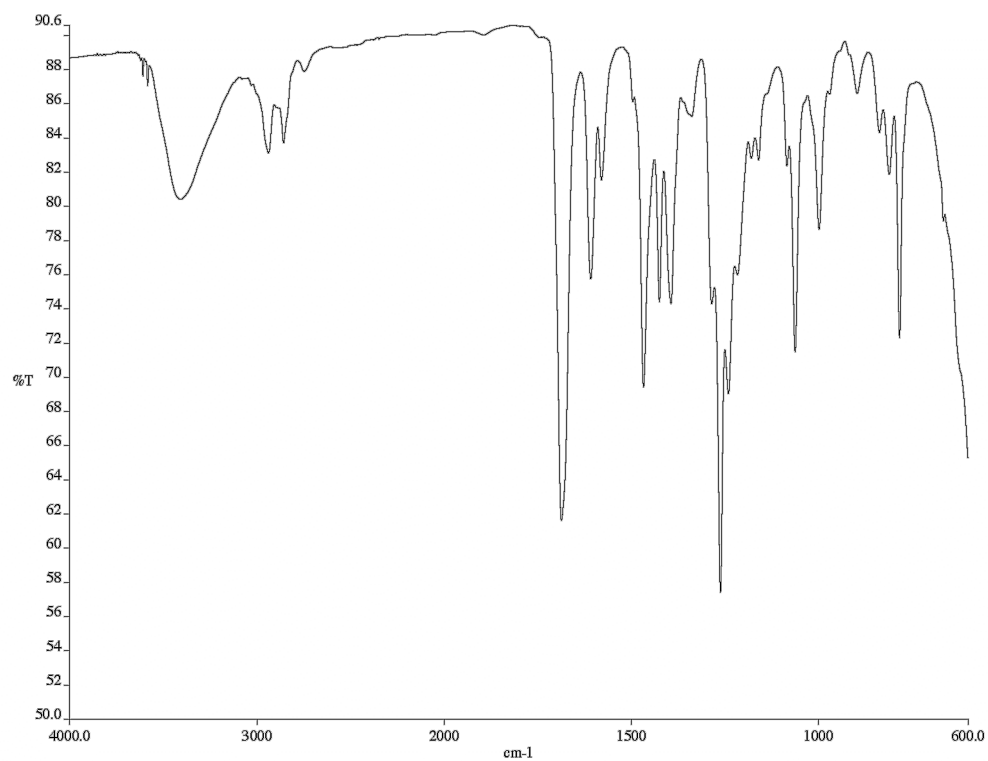


Figure A.8 Infrared spectrum (thin film/NaCl) of compound **173**.

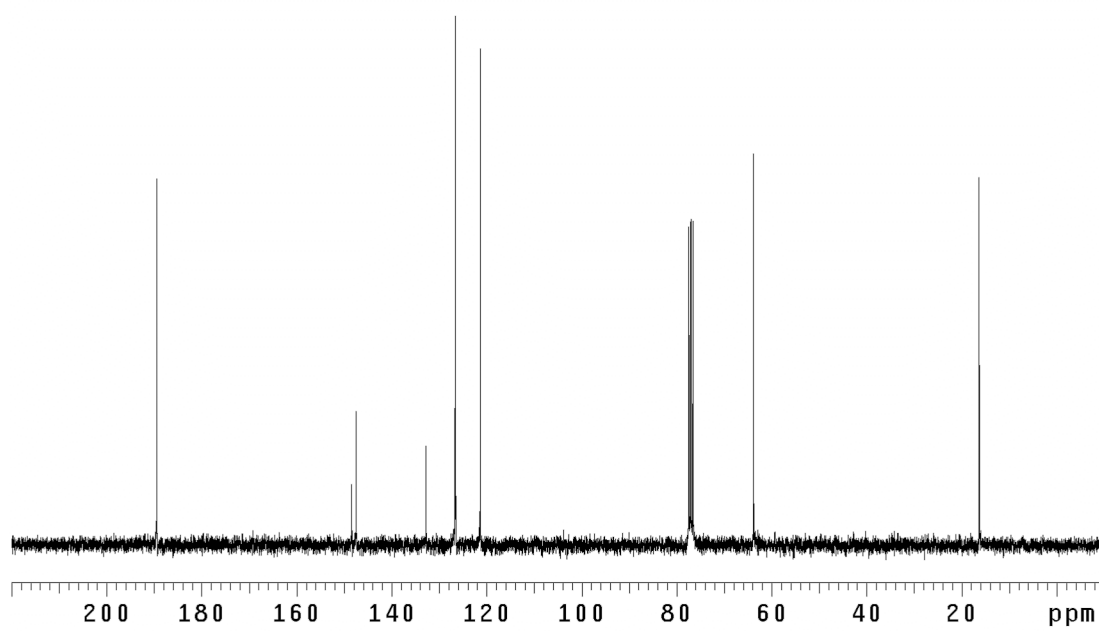


Figure A.9 <sup>13</sup>C NMR (75 MHz, CDCl<sub>3</sub>) of compound **173**.

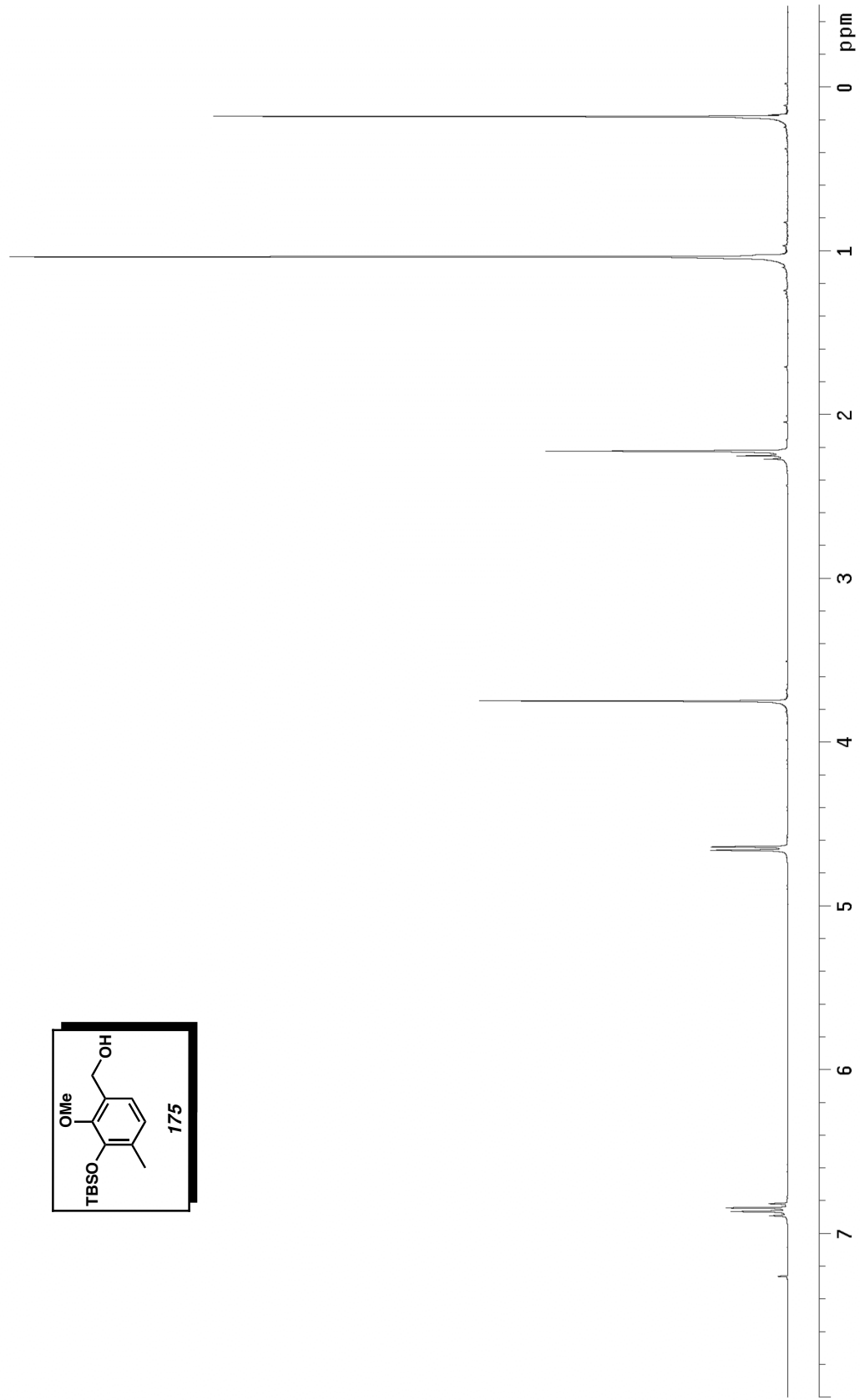
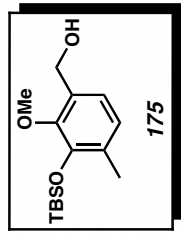


Figure A.10 <sup>1</sup>H NMR (300 MHz, CDCl<sub>3</sub>) of compound 175.

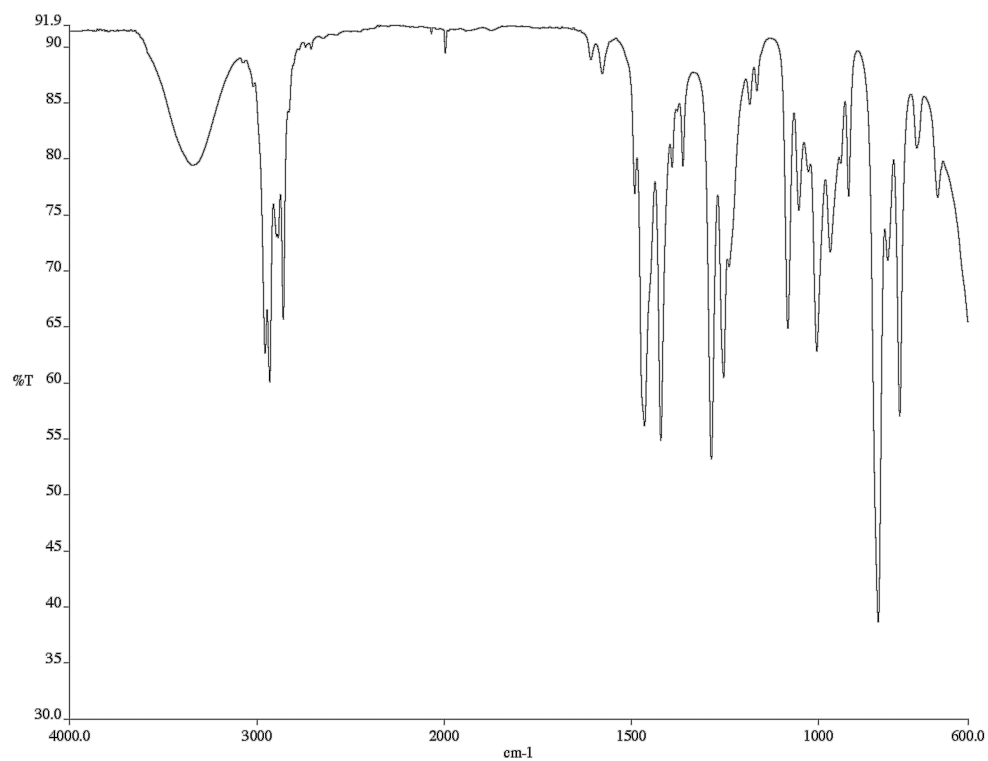


Figure A.11 Infrared spectrum (thin film/NaCl) of compound **175**.

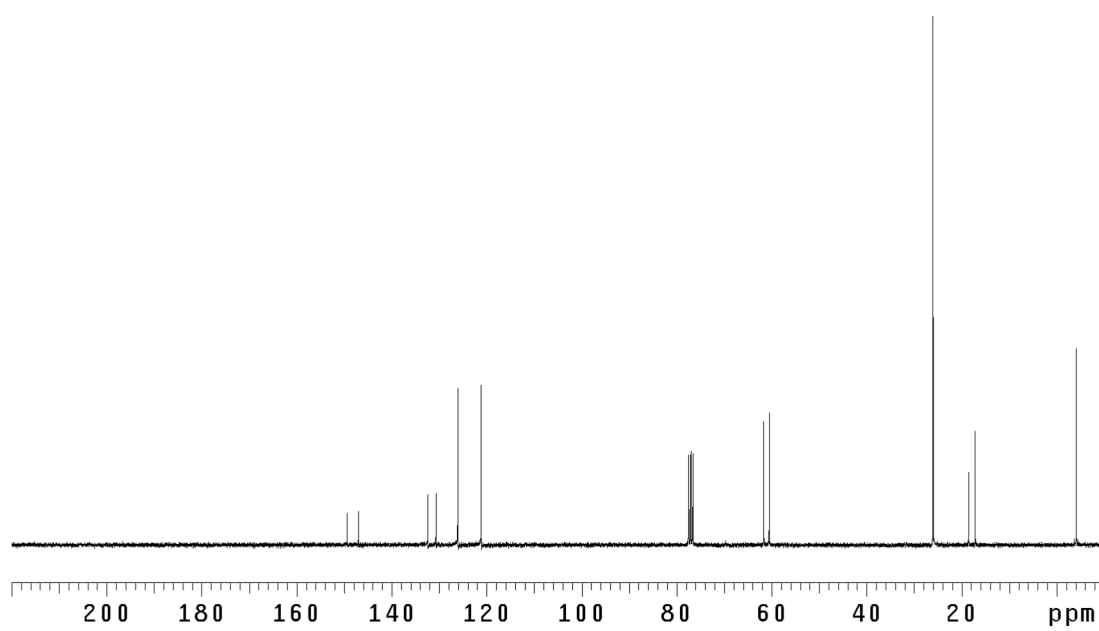


Figure A.12 <sup>13</sup>C NMR (75 MHz, CDCl<sub>3</sub>) of compound **175**.

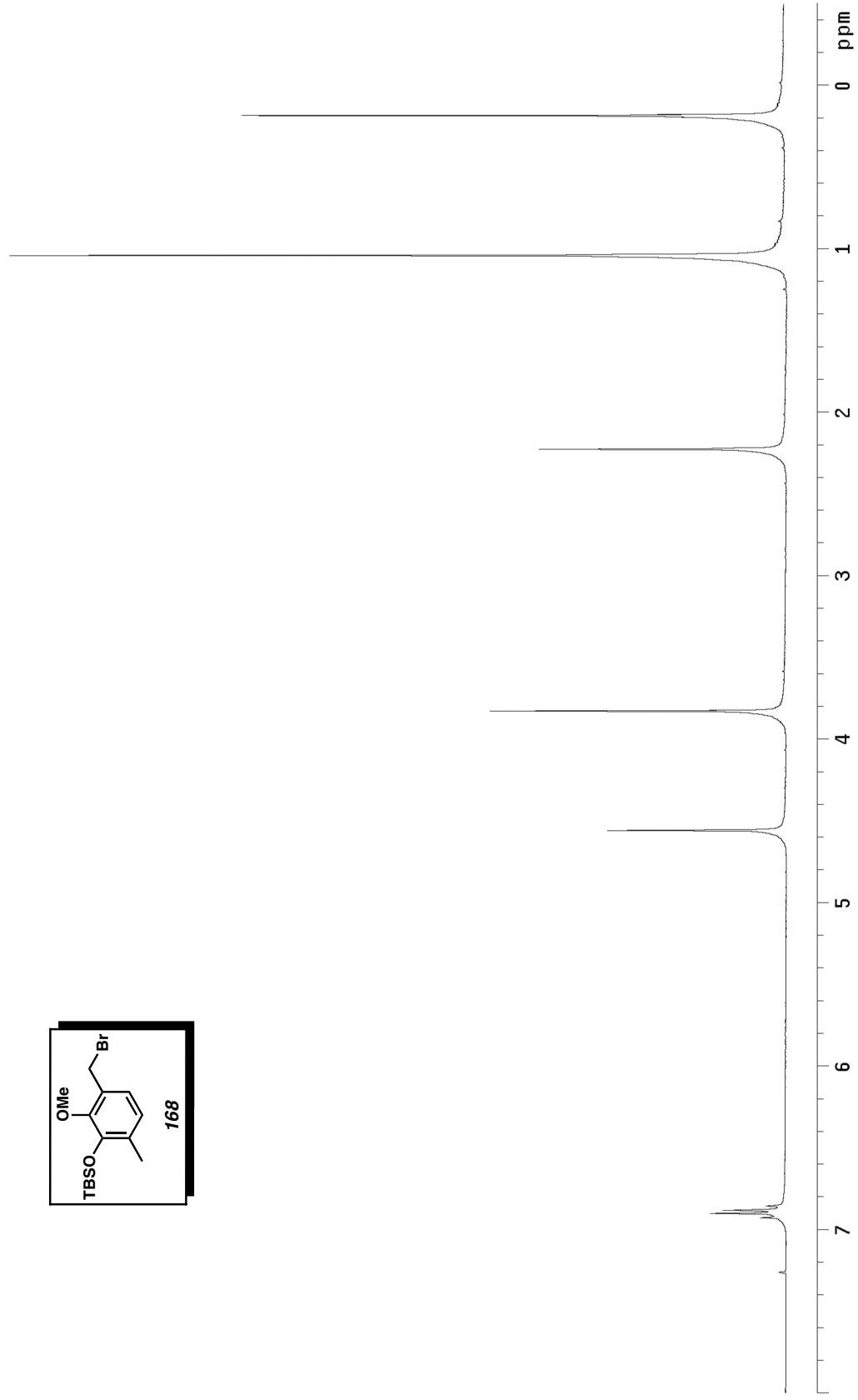
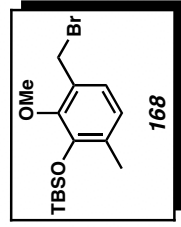


Figure A.13 <sup>1</sup>H NMR (300 MHz, CDCl<sub>3</sub>) of compound **168**.

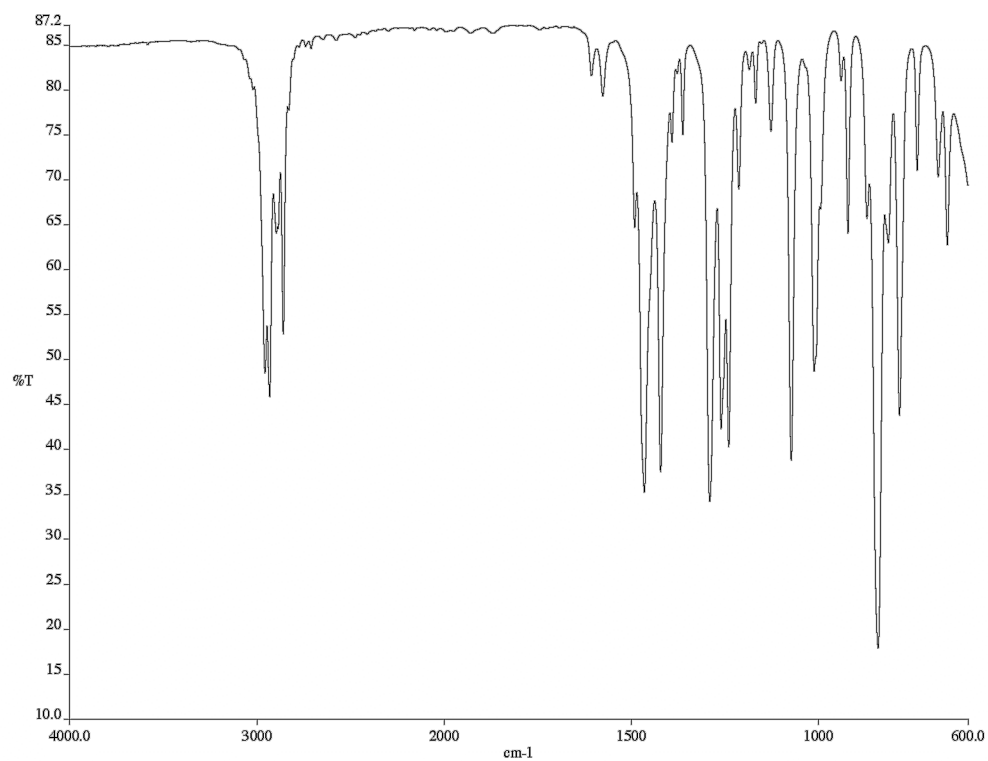


Figure A.14 Infrared spectrum (thin film/NaCl) of compound **168**.

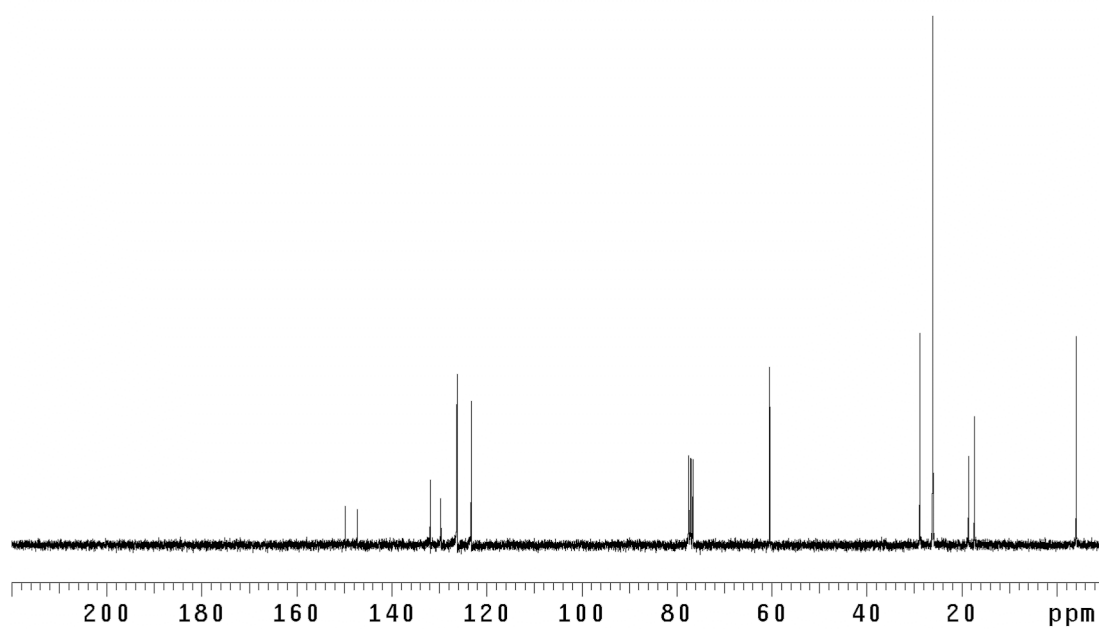


Figure A.15 <sup>13</sup>C NMR (75 MHz, CDCl<sub>3</sub>) of compound **168**.

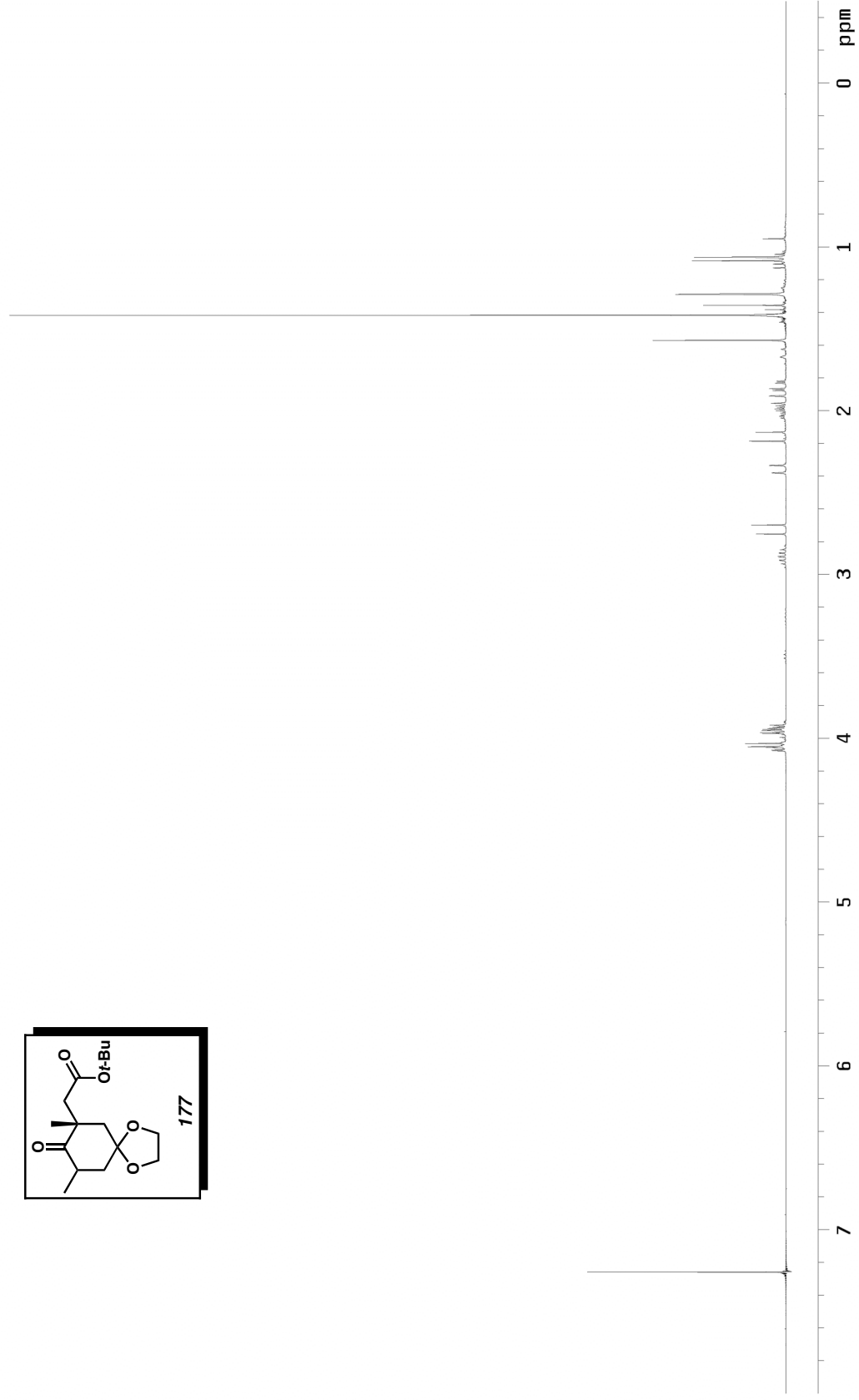
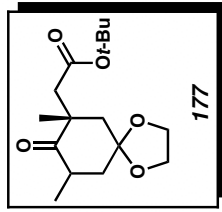


Figure A.16  $^1\text{H}$  NMR (300 MHz,  $\text{CDCl}_3$ ) of compound (+)-177.

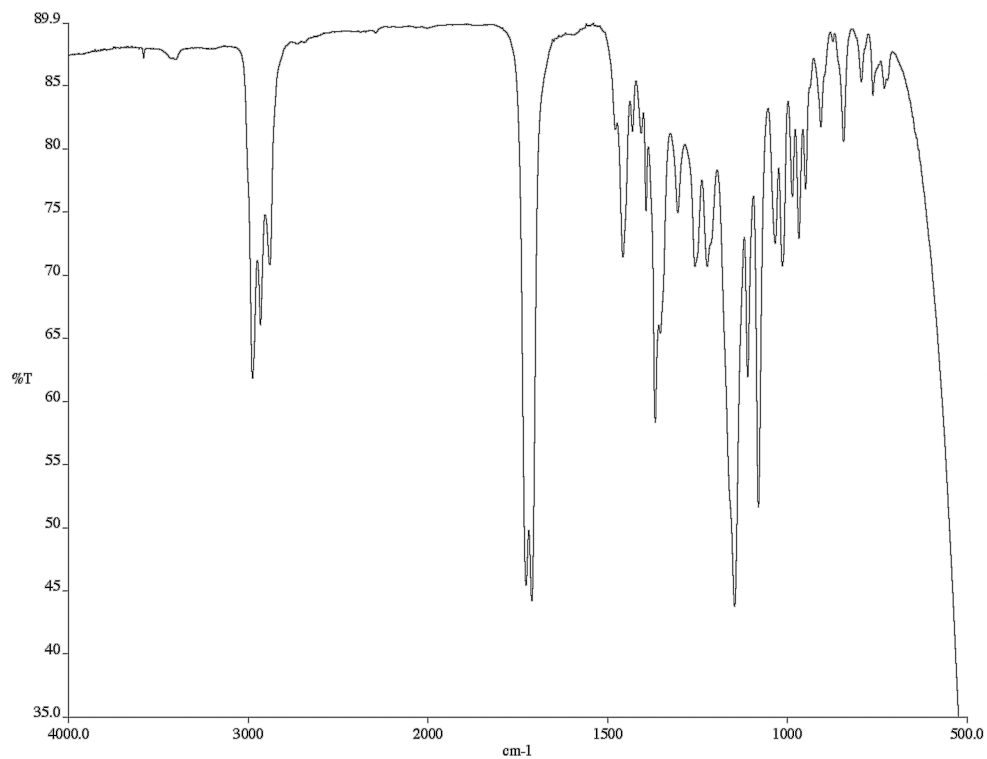


Figure A.17 Infrared spectrum (thin film/NaCl) of compound (+)-**177**.

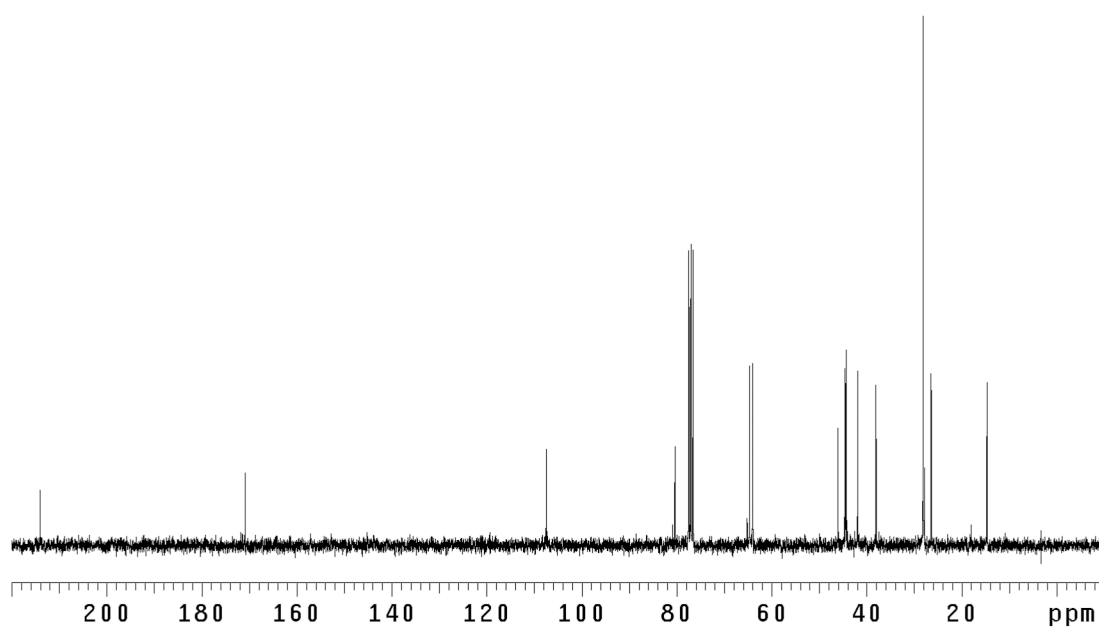


Figure A.18 <sup>13</sup>C NMR (75 MHz, CDCl<sub>3</sub>) of compound (+)-**177**.

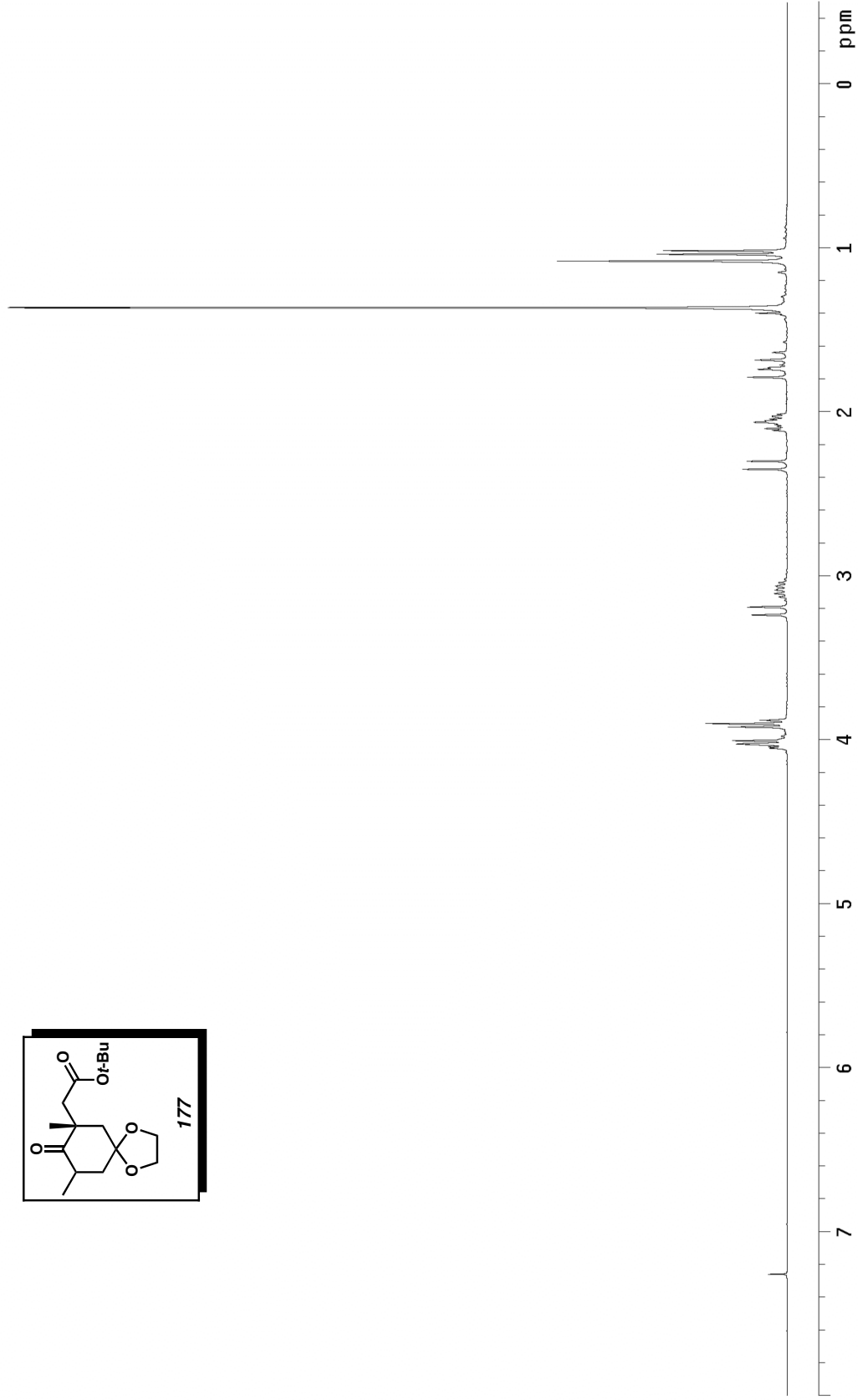
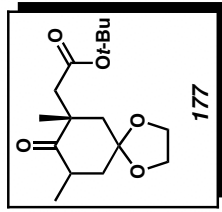


Figure A.19  $^1\text{H}$  NMR (300 MHz,  $\text{CDCl}_3$ ) of compound (-)-177.

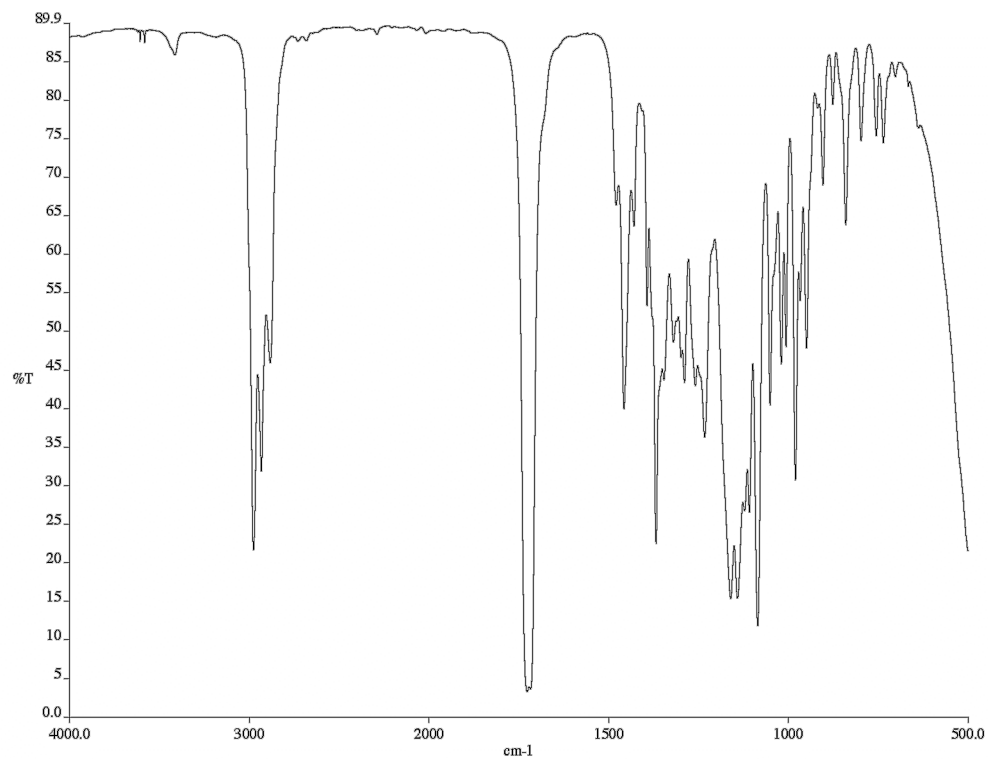


Figure A.20 Infrared spectrum (thin film/NaCl) of compound (-)-**177**.

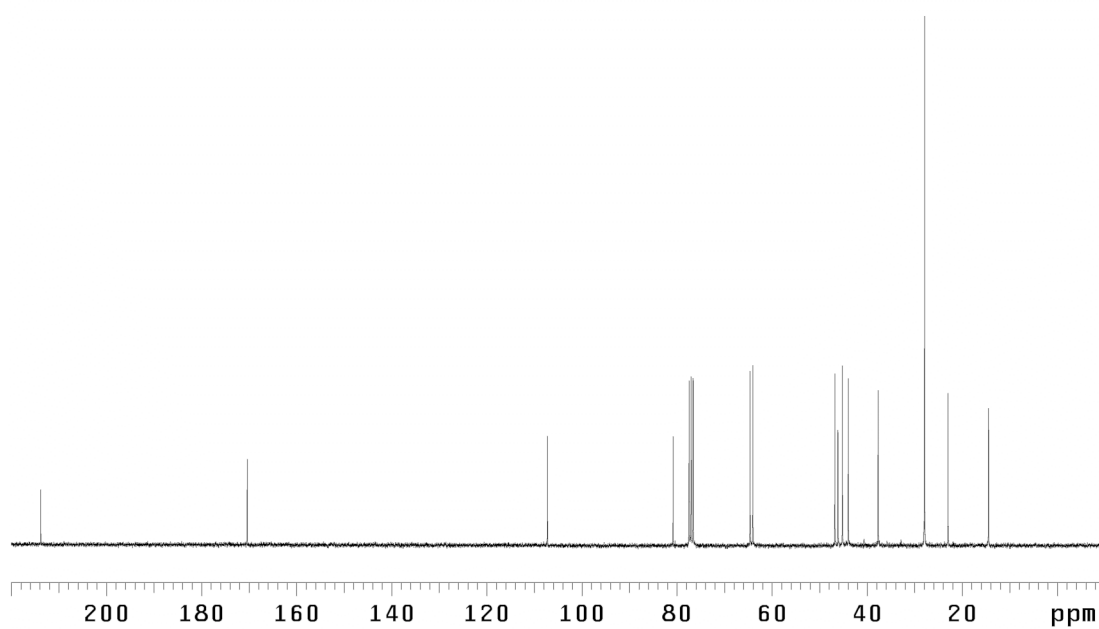


Figure A.21 <sup>13</sup>C NMR (75 MHz, CDCl<sub>3</sub>) of compound (-)-**177**.

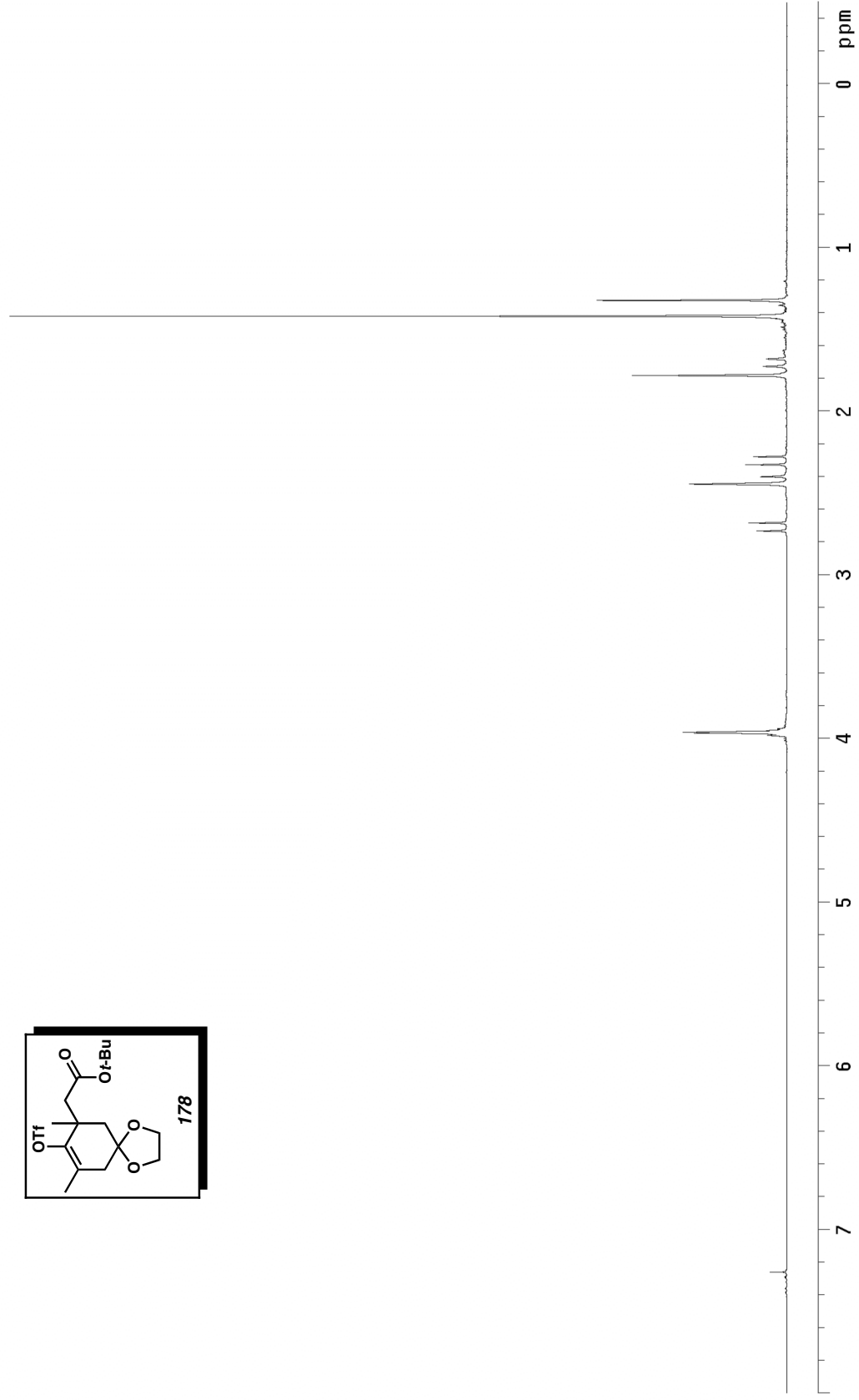
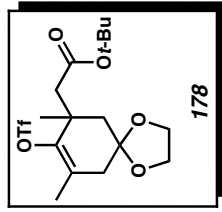


Figure A.22  $^1\text{H}$  NMR (300 MHz,  $\text{CDCl}_3$ ) of compound **178**.

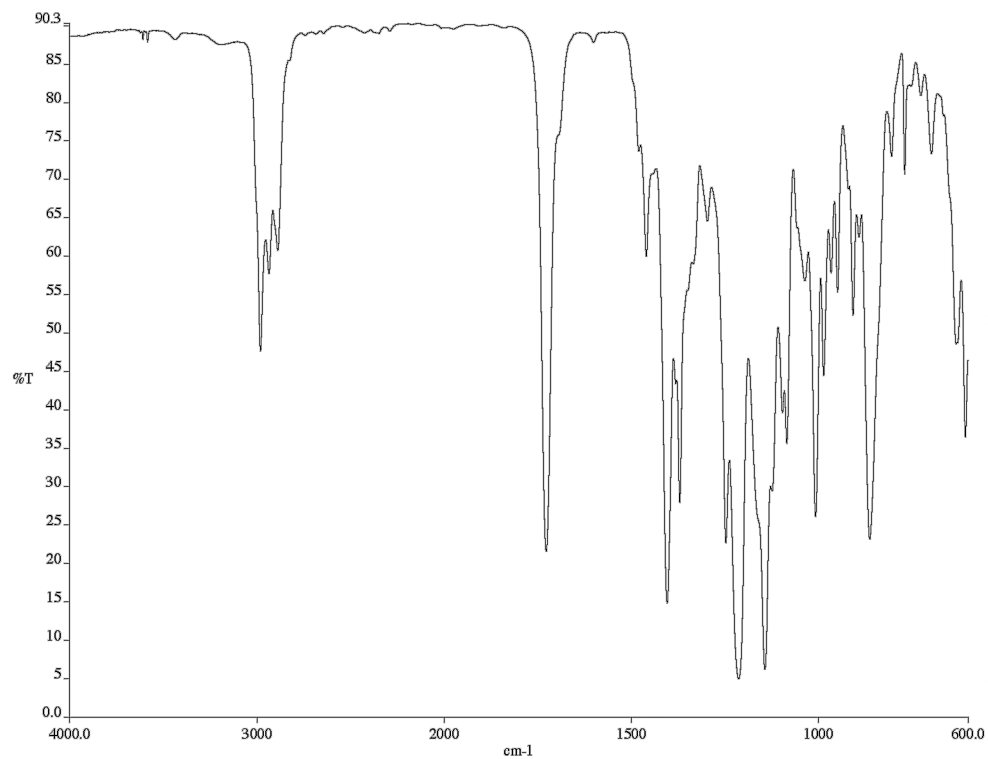


Figure A.23 Infrared spectrum (thin film/NaCl) of compound **178**.

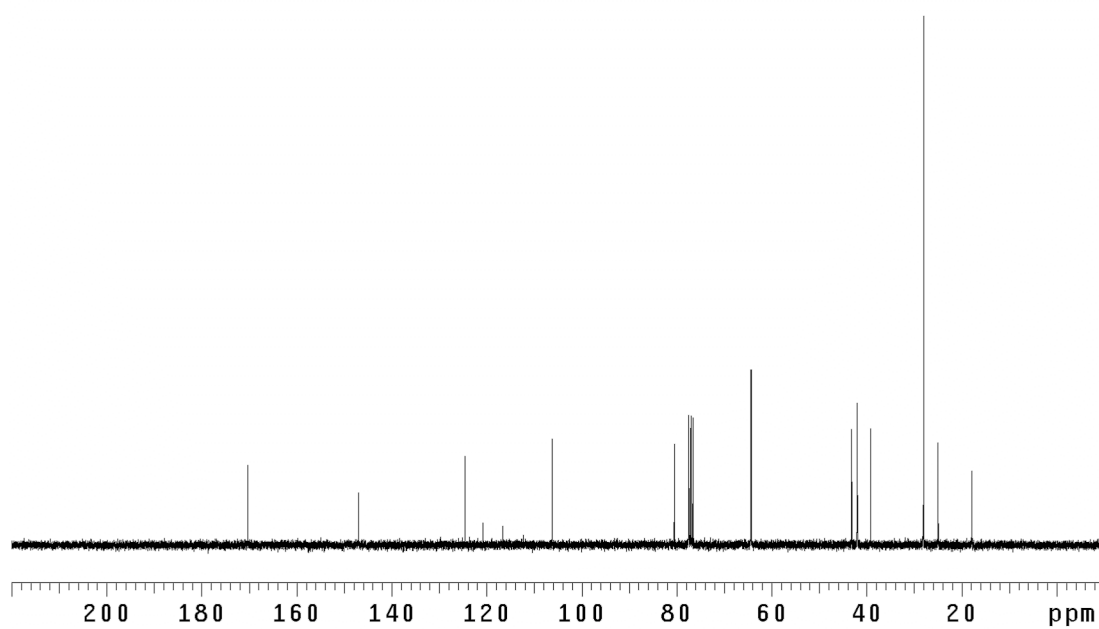


Figure A.24 <sup>13</sup>C NMR (75 MHz, CDCl<sub>3</sub>) of compound **178**.

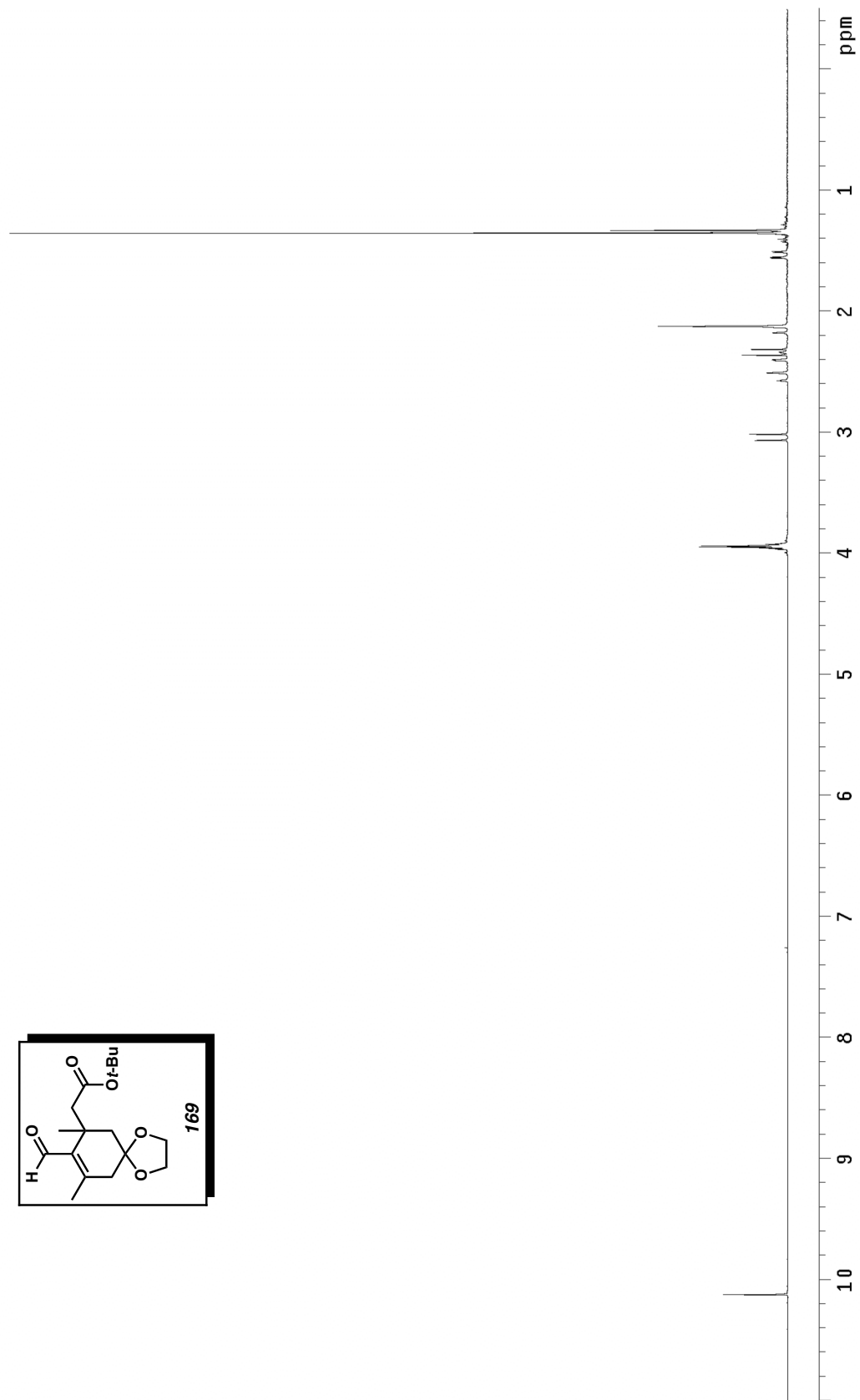
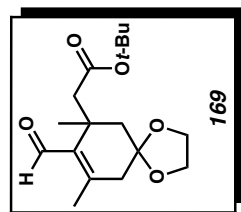


Figure A.25 <sup>1</sup>H NMR (300 MHz, CDCl<sub>3</sub>) of compound **169**.

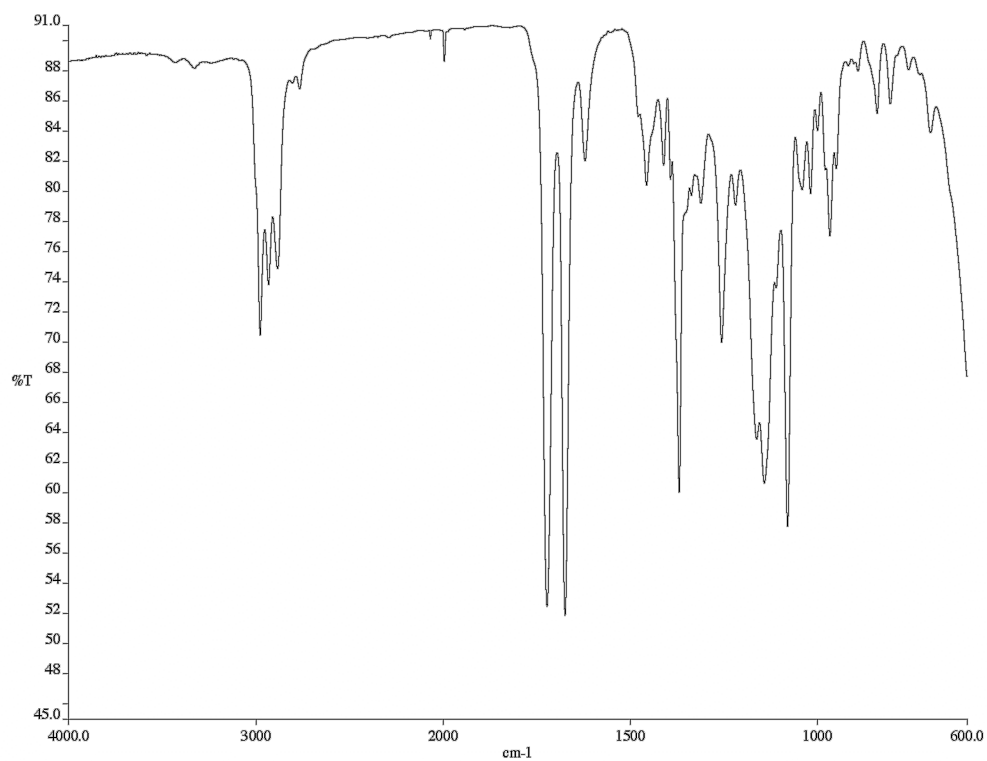


Figure A.26 Infrared spectrum (thin film/NaCl) of compound **169**.

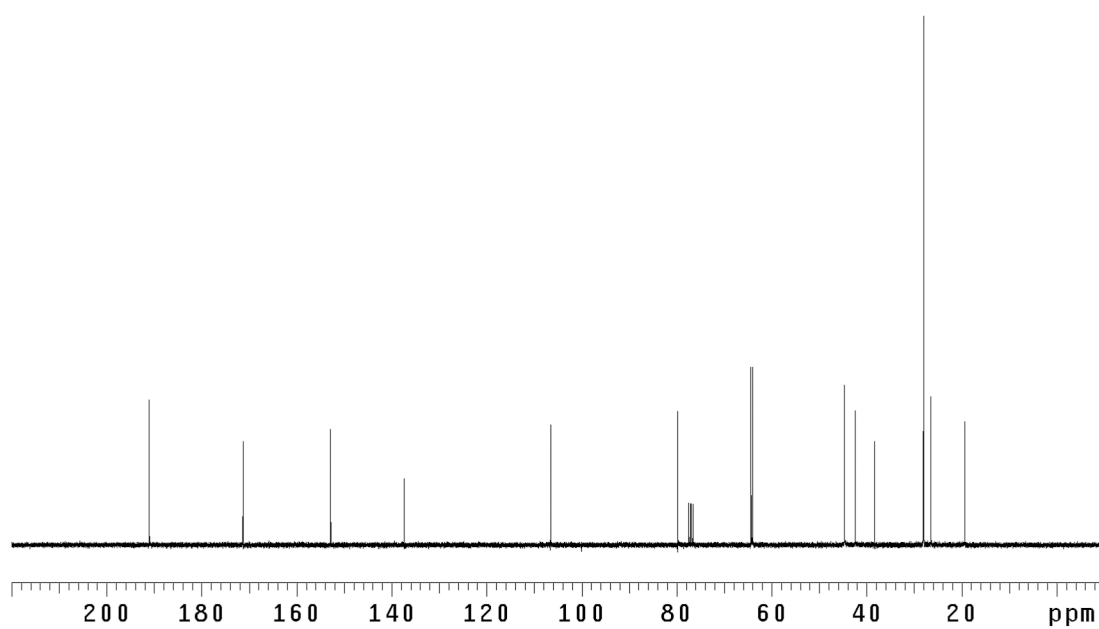


Figure A.27 <sup>13</sup>C NMR (75 MHz, CDCl<sub>3</sub>) of compound **169**.

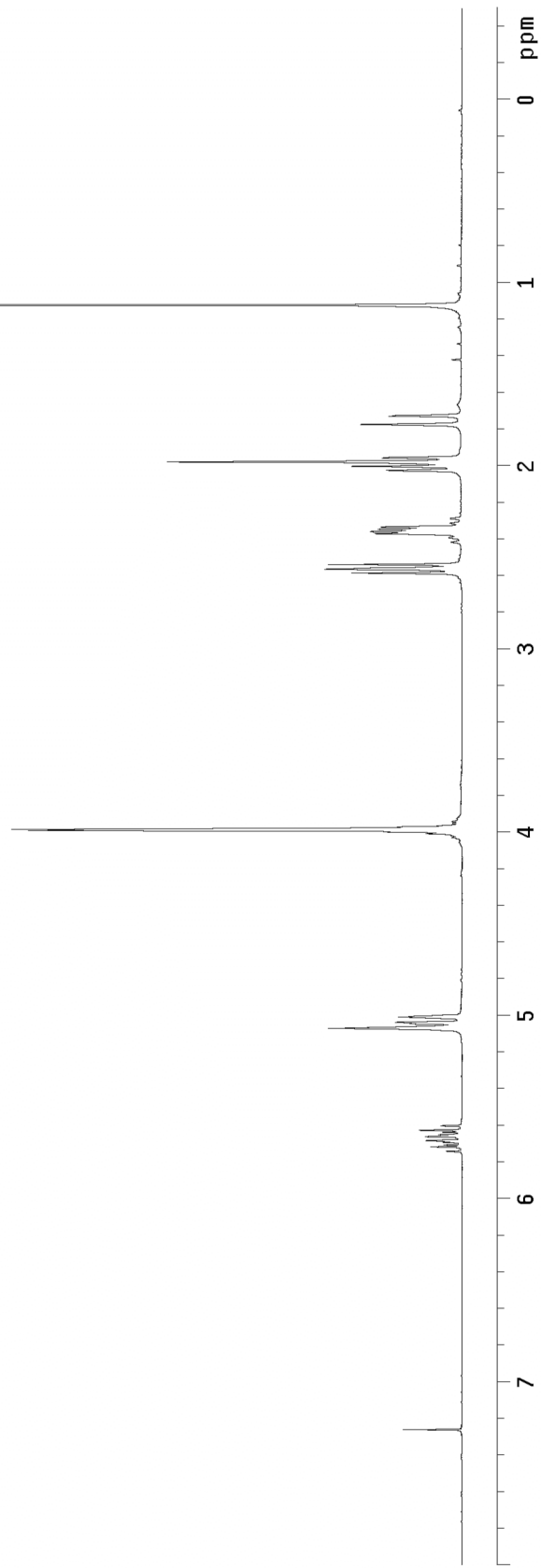
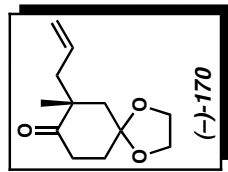


Figure A.28 <sup>1</sup>H NMR (300 MHz, CDCl<sub>3</sub>) of compound (-)-170.

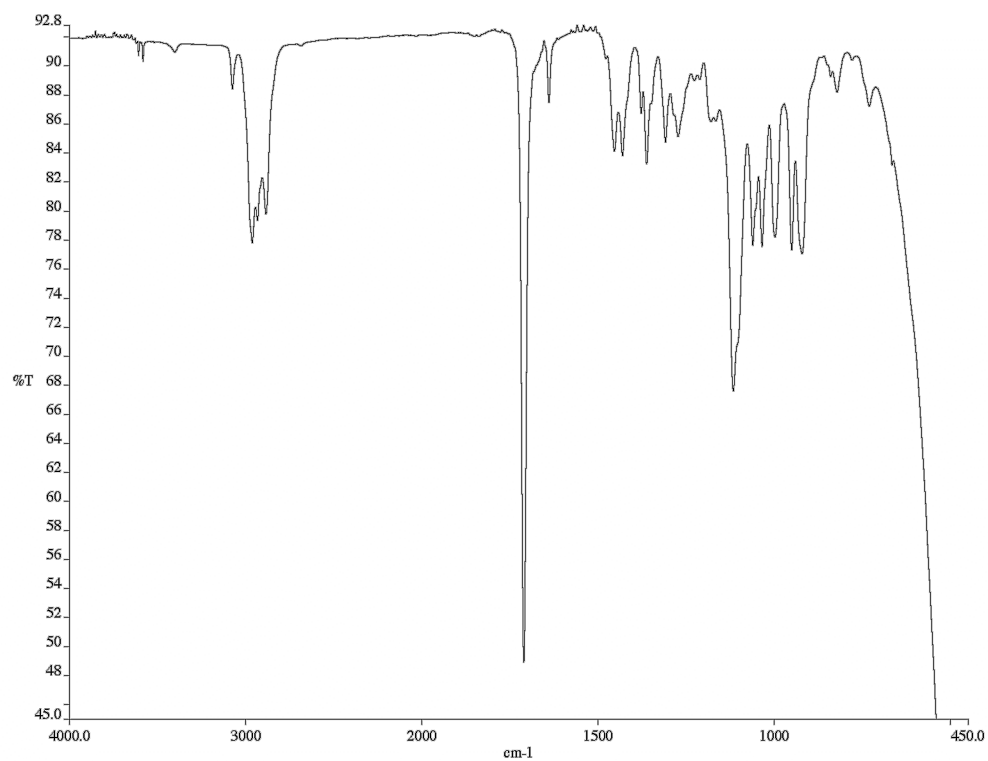


Figure A.29 Infrared spectrum (thin film/NaCl) of compound (-)-**170**.

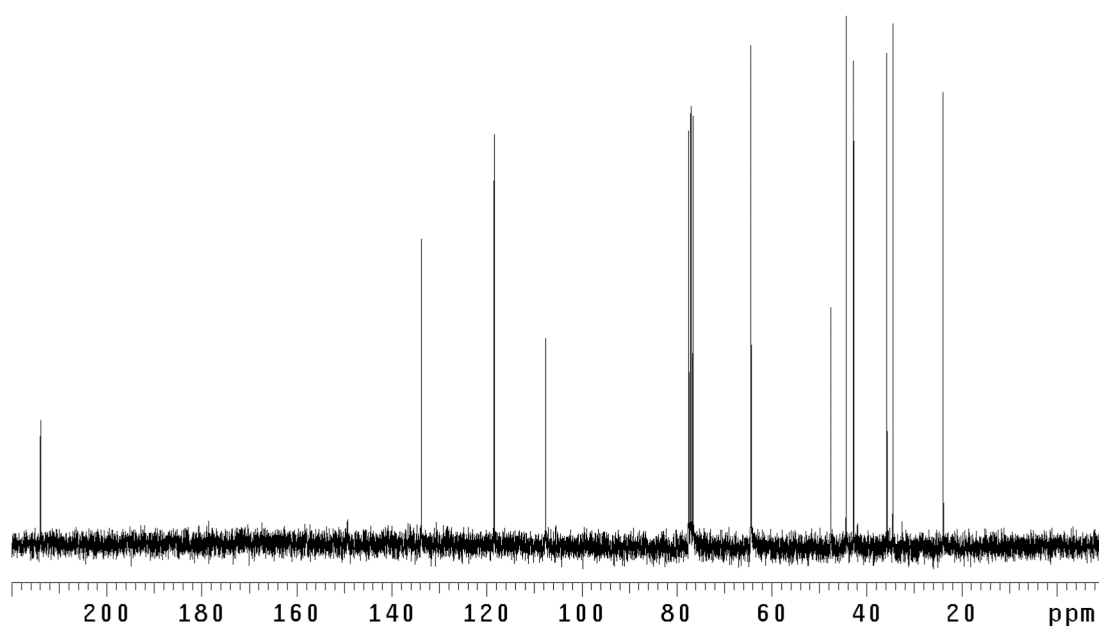


Figure A.30 <sup>13</sup>C NMR (75 MHz, XX) of compound (-)-**170**.

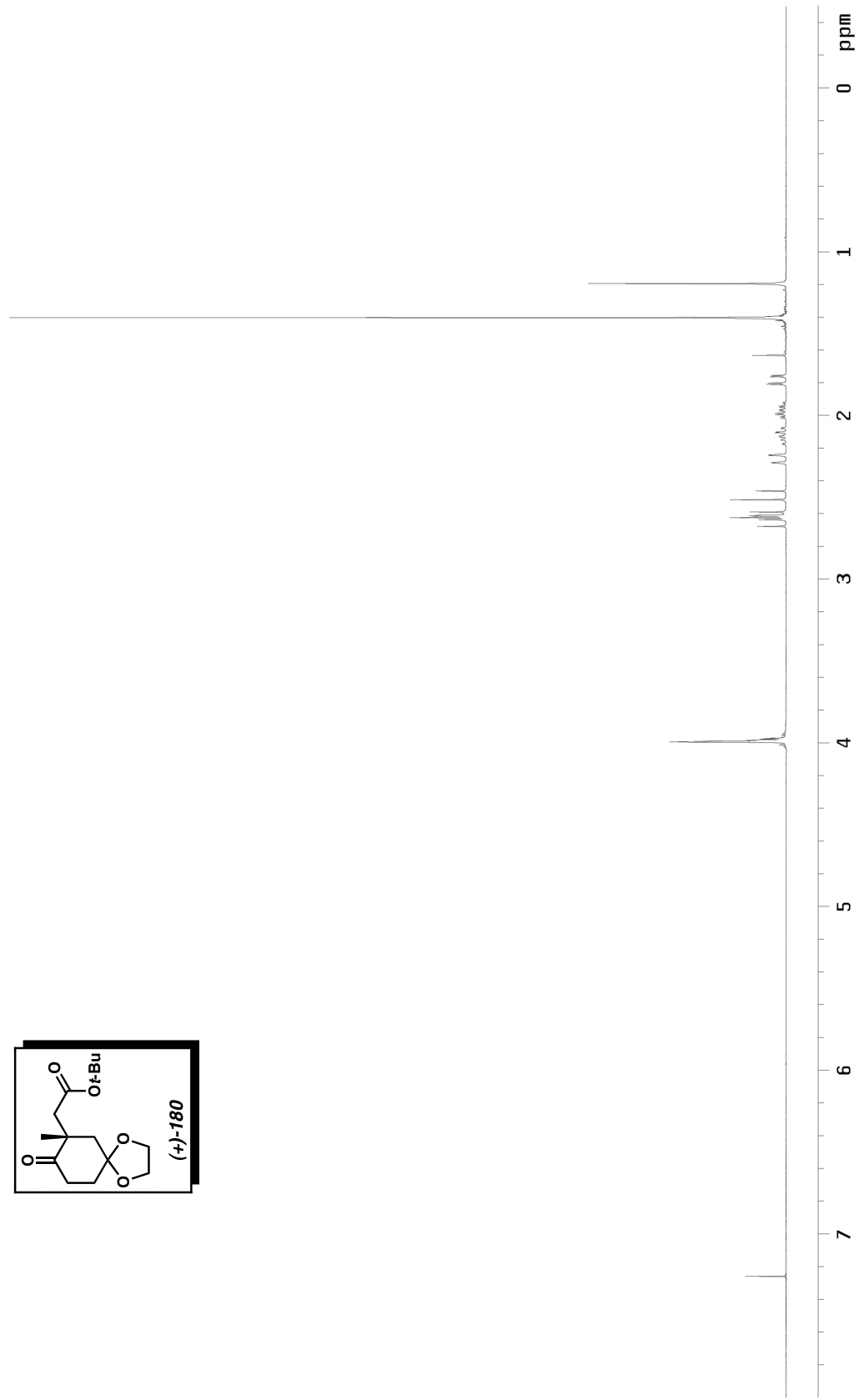
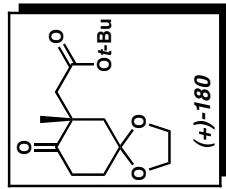


Figure A.31 <sup>1</sup>H NMR (300 MHz, CDCl<sub>3</sub>) of compound (+)-180.

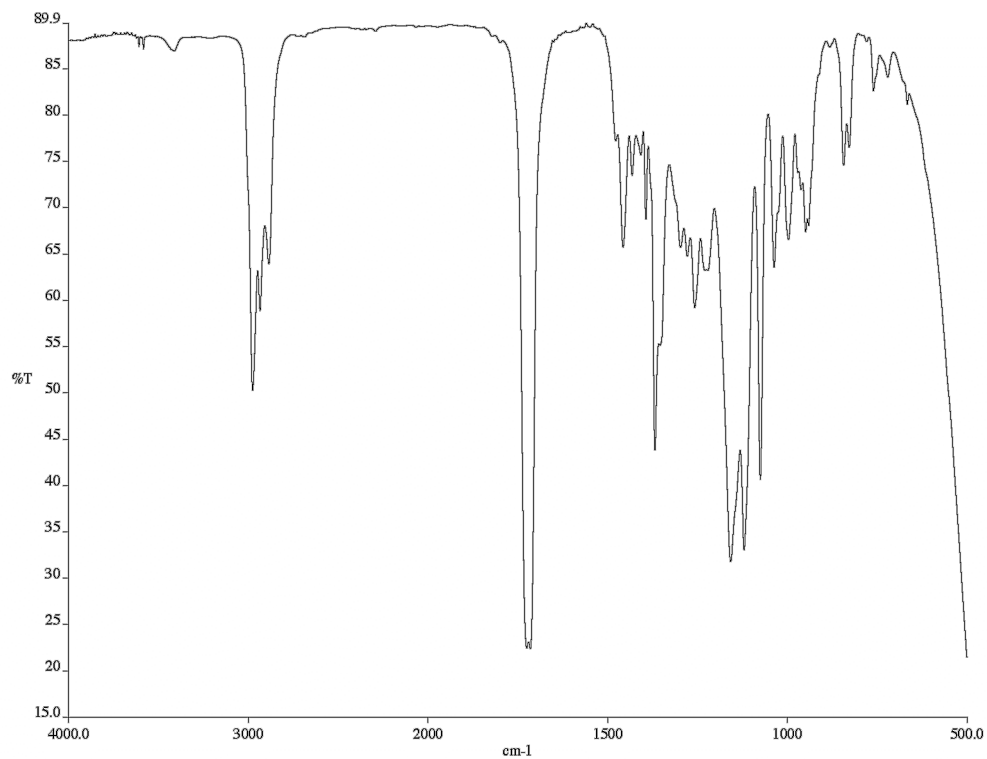


Figure A.32 Infrared spectrum (thin film/NaCl) of compound (+)-**180**.

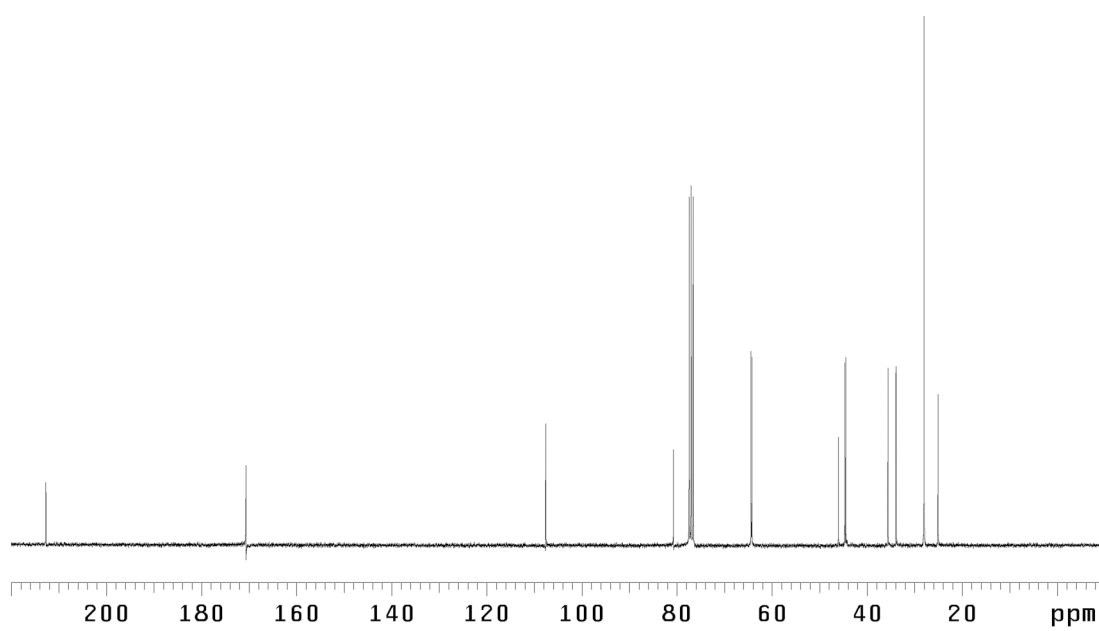


Figure A.33 <sup>13</sup>C NMR (75 MHz, CDCl<sub>3</sub>) of compound (+)-**180**.

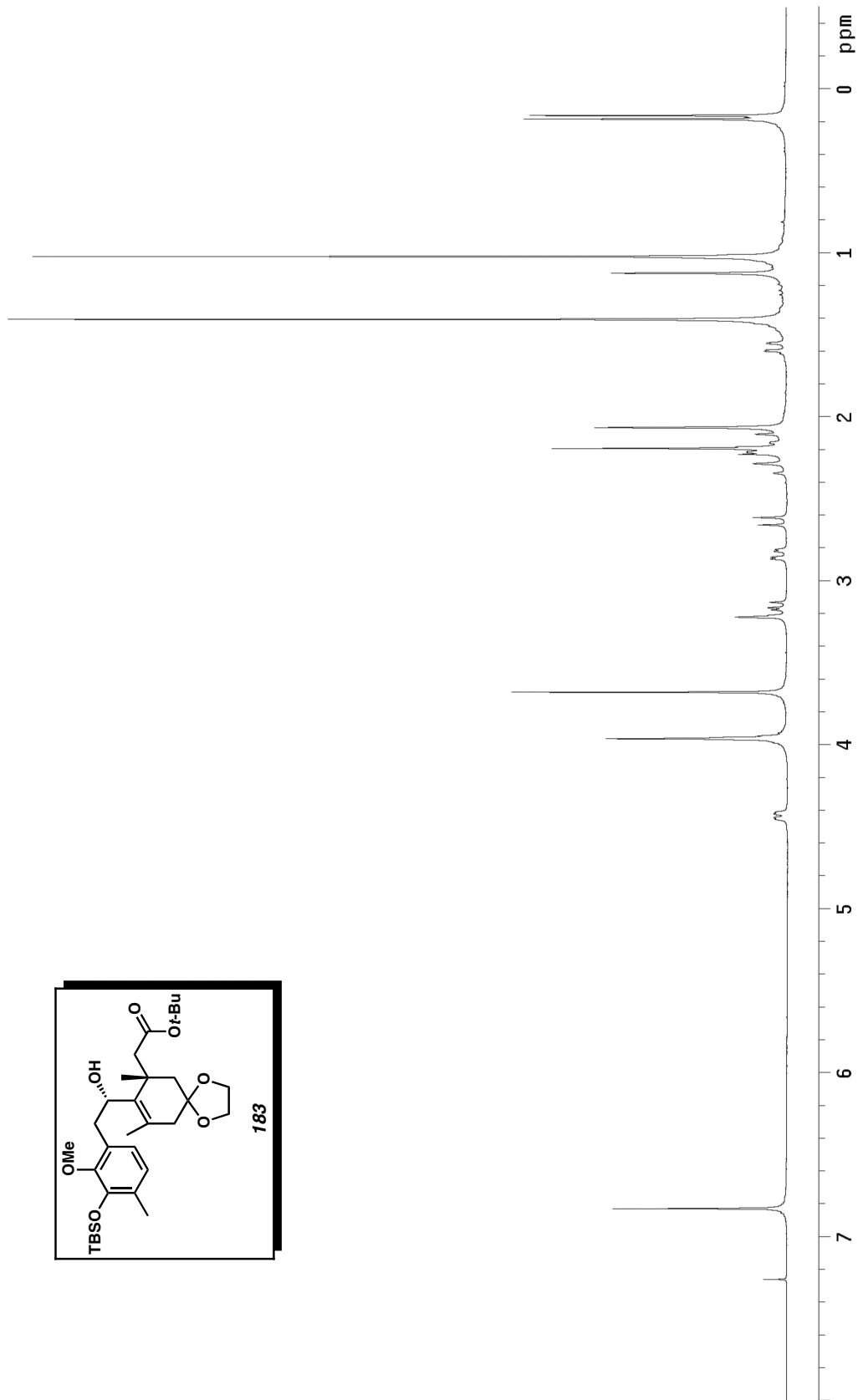
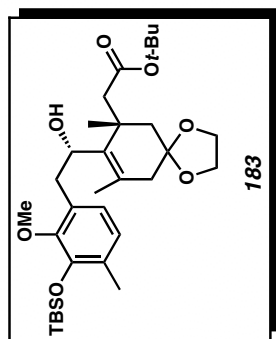


Figure A.34  $^1\text{H NMR}$  (300 MHz,  $\text{CDCl}_3$ ) of compound **183**.

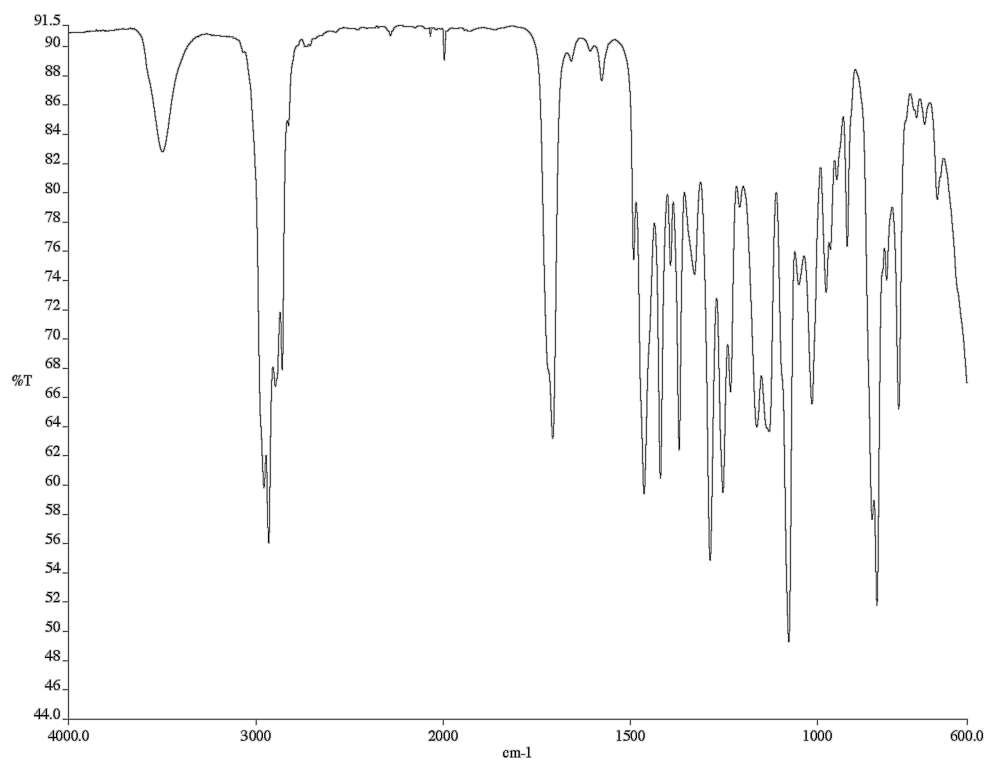


Figure A.35 Infrared spectrum (thin film/NaCl) of compound **183**.

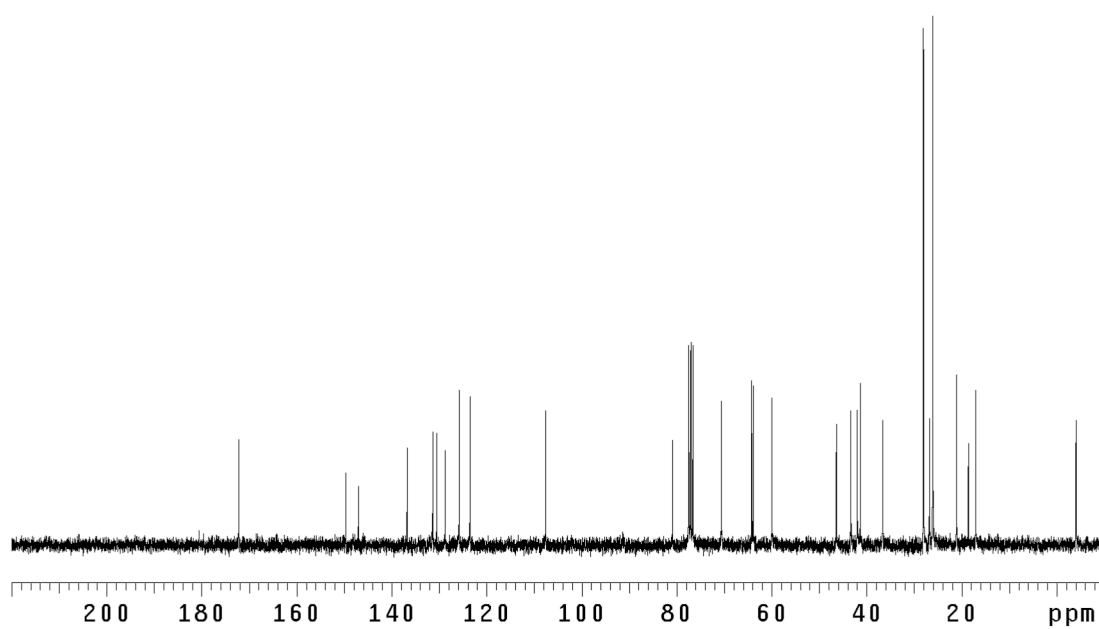


Figure A.36  $^{13}\text{C}$  NMR (75 MHz,  $\text{CDCl}_3$ ) of compound **183**.

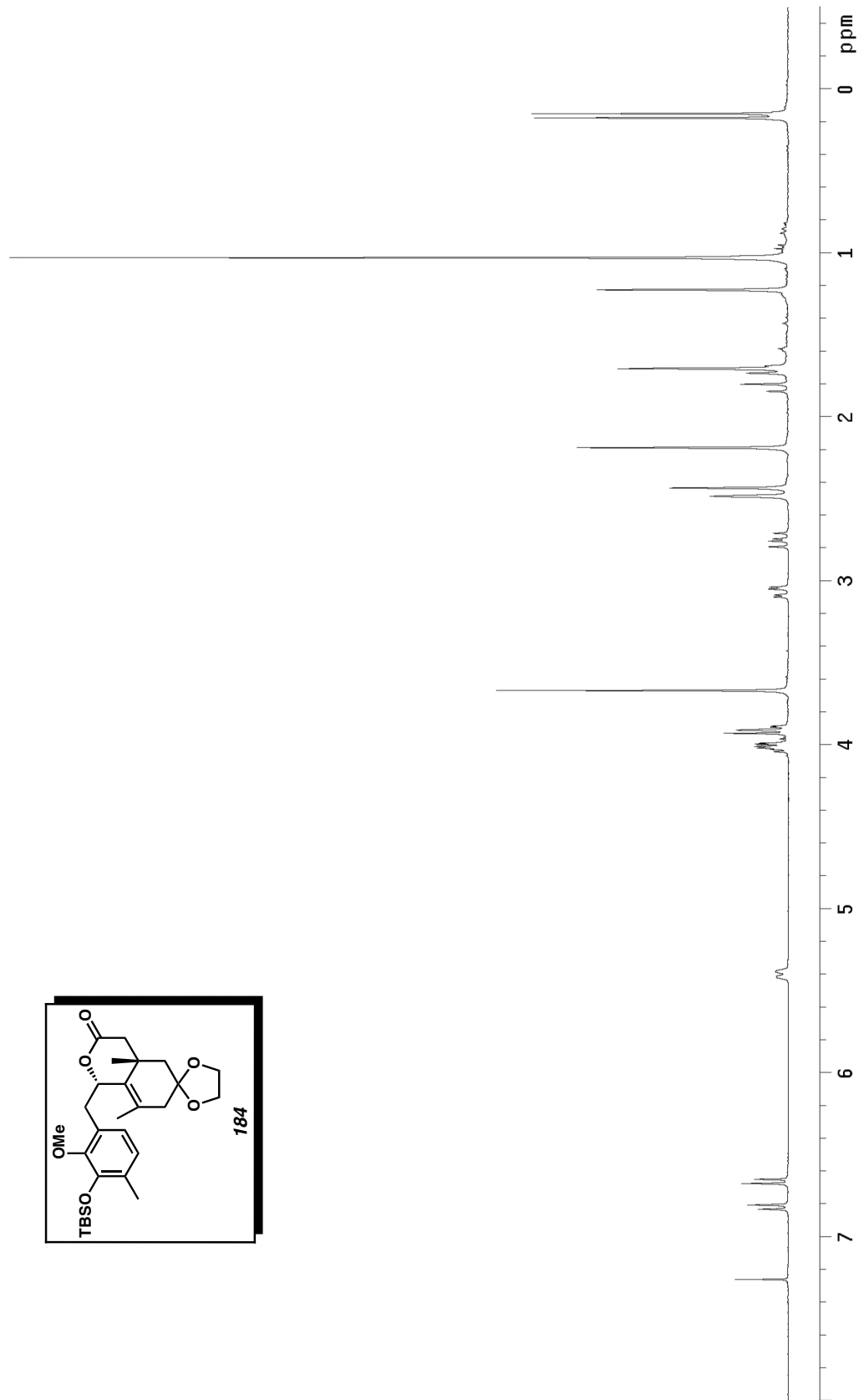
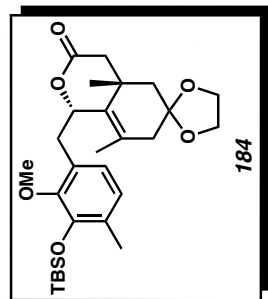


Figure A.37  $^1\text{H}$  NMR (300 MHz,  $\text{CDCl}_3$ ) of compound **184**.

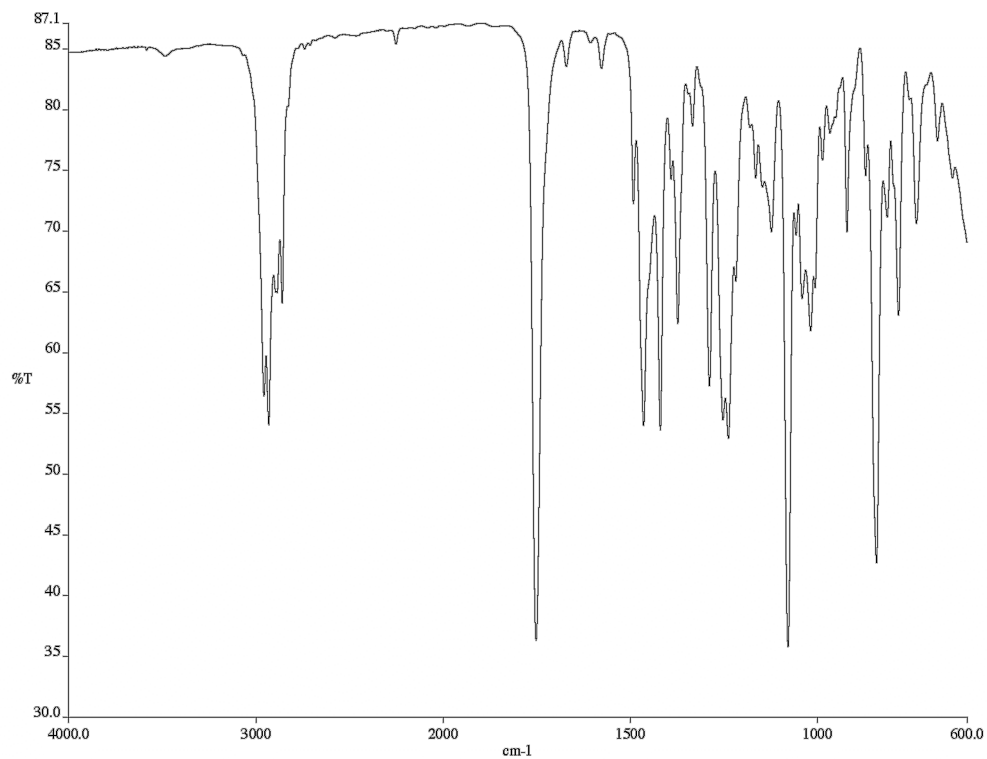


Figure A.38 Infrared spectrum (thin film/NaCl) of compound **184**.

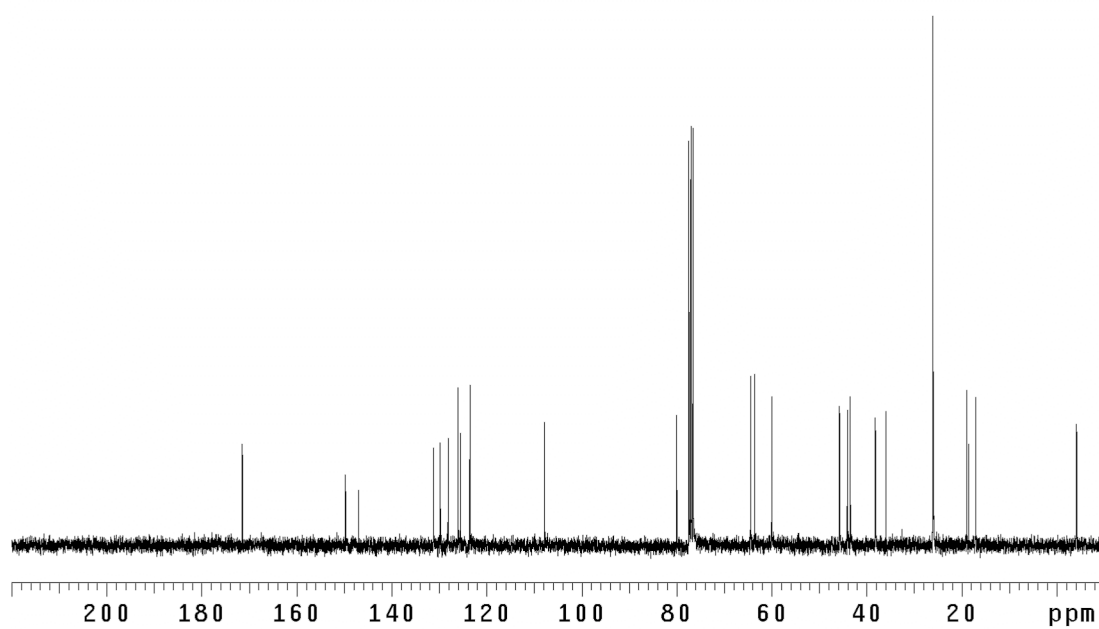


Figure A.39 <sup>13</sup>C NMR (75 MHz, CDCl<sub>3</sub>) of compound **184**.

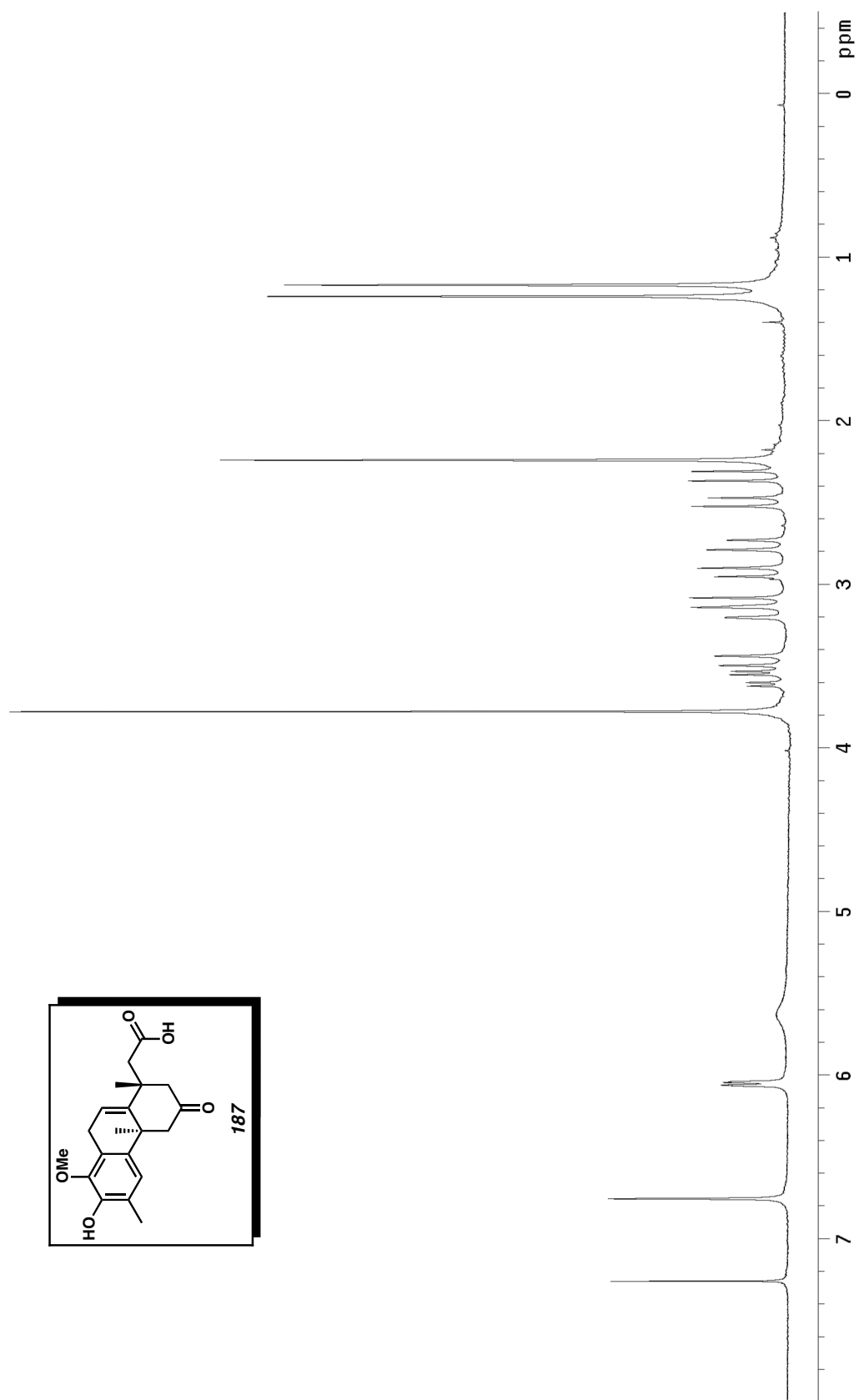


Figure A.40 <sup>1</sup>H NMR (300 MHz, CDCl<sub>3</sub>) of compound **187**.

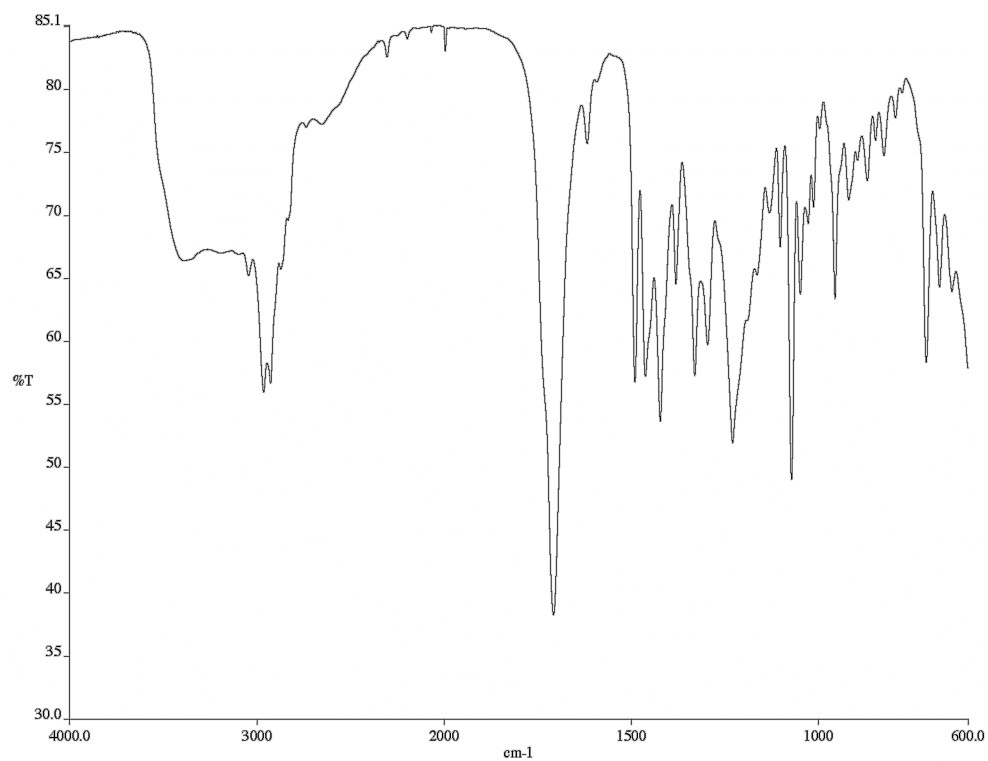


Figure A.41 Infrared spectrum (thin film/NaCl) of compound **187**.

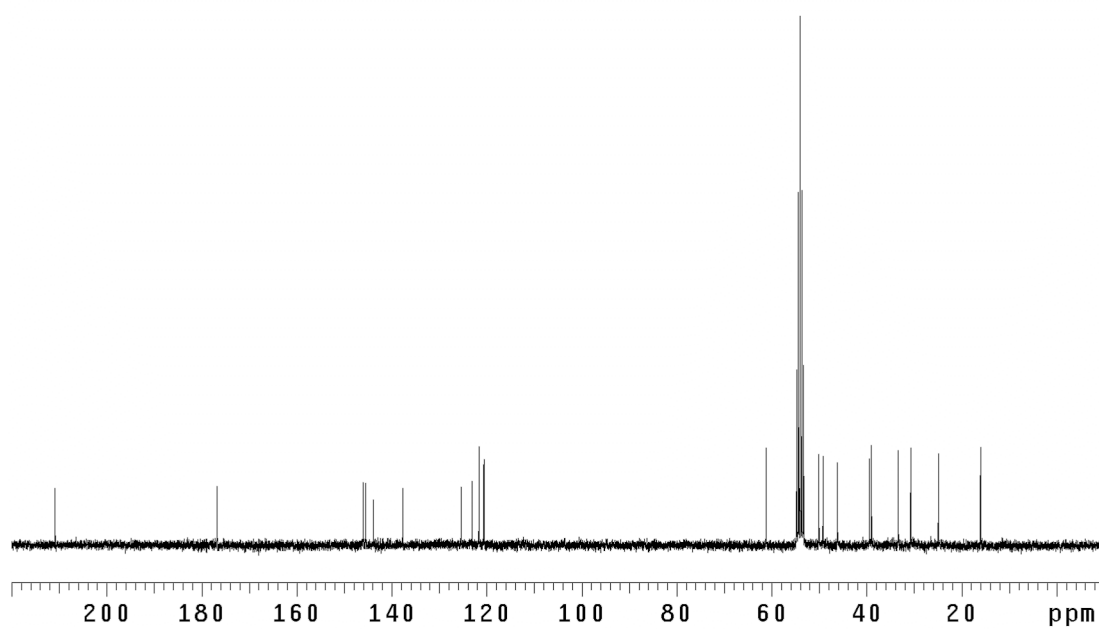


Figure A.42 <sup>13</sup>C NMR (75 MHz, CD<sub>2</sub>Cl<sub>2</sub>) of compound **187**.

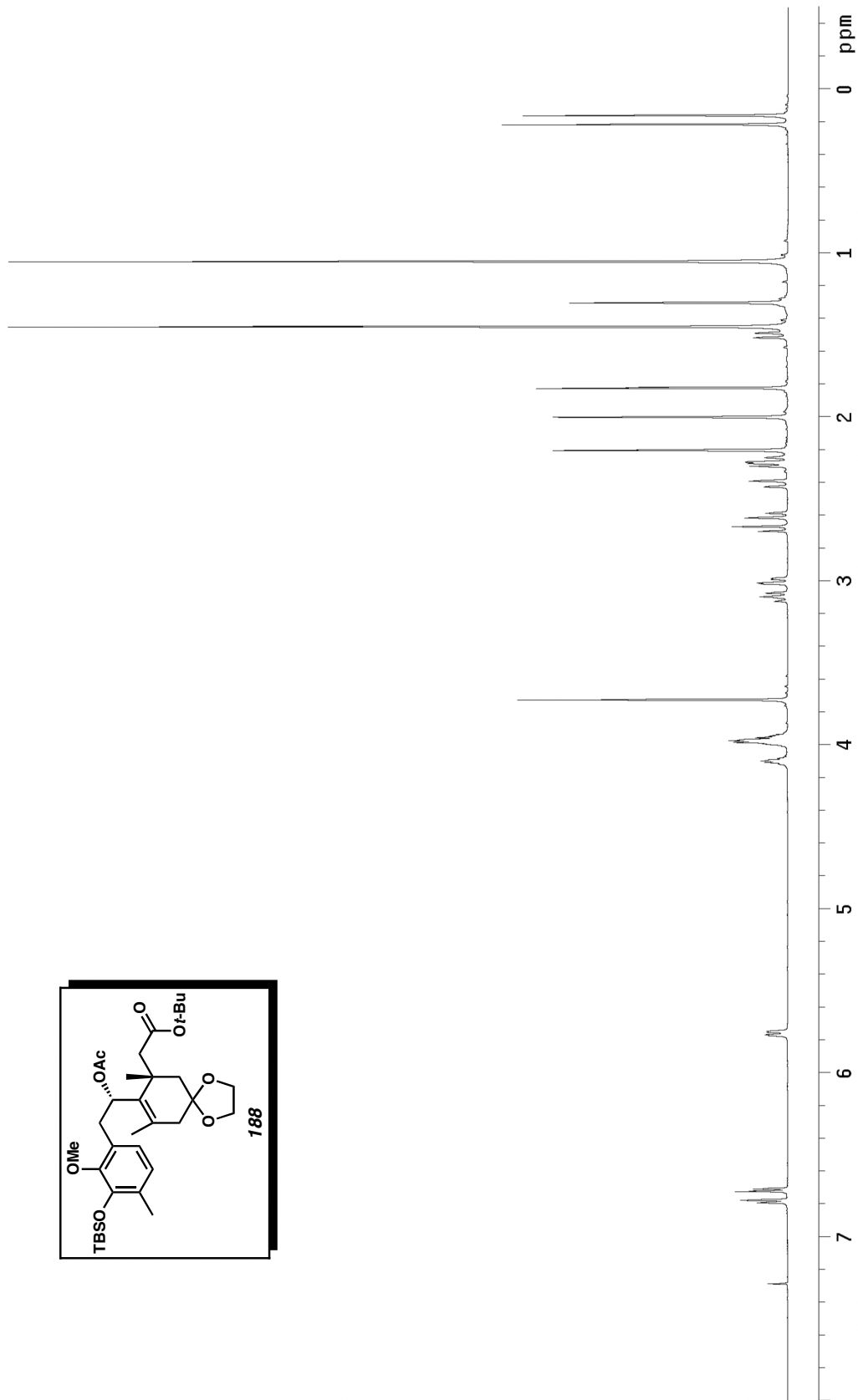
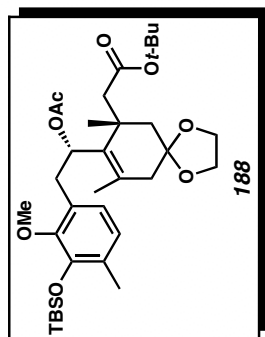


Figure A.43  $^1\text{H NMR}$  (500 MHz,  $\text{CDCl}_3$ ) of compound **188**.

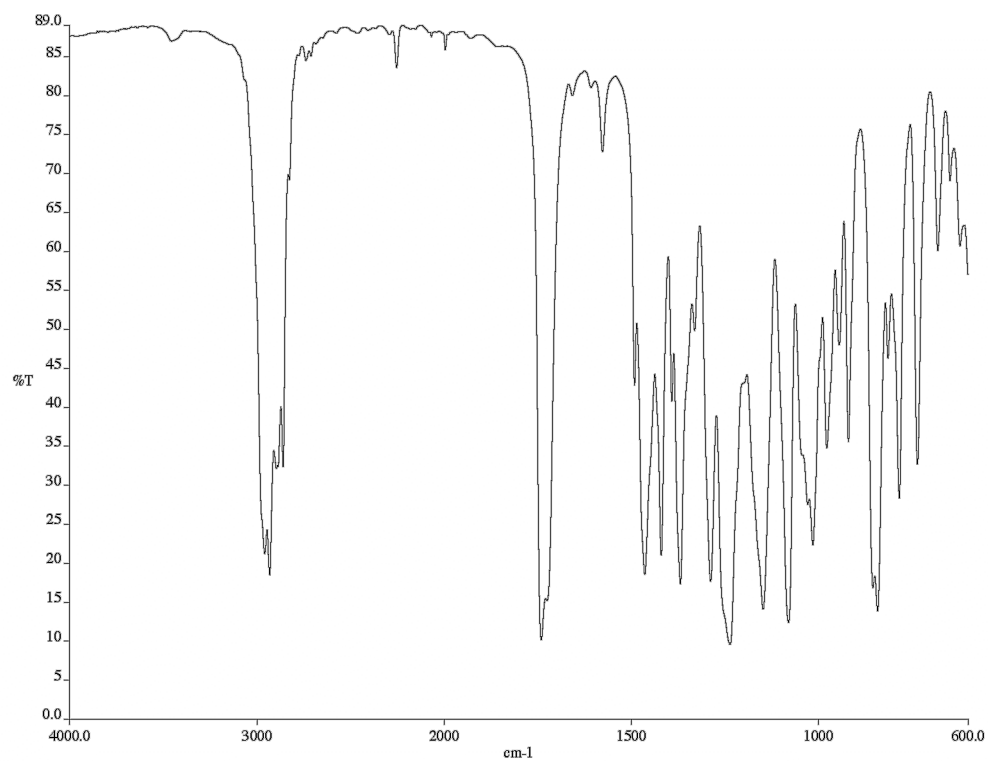


Figure A.44 Infrared spectrum (thin film/NaCl) of compound **188**.

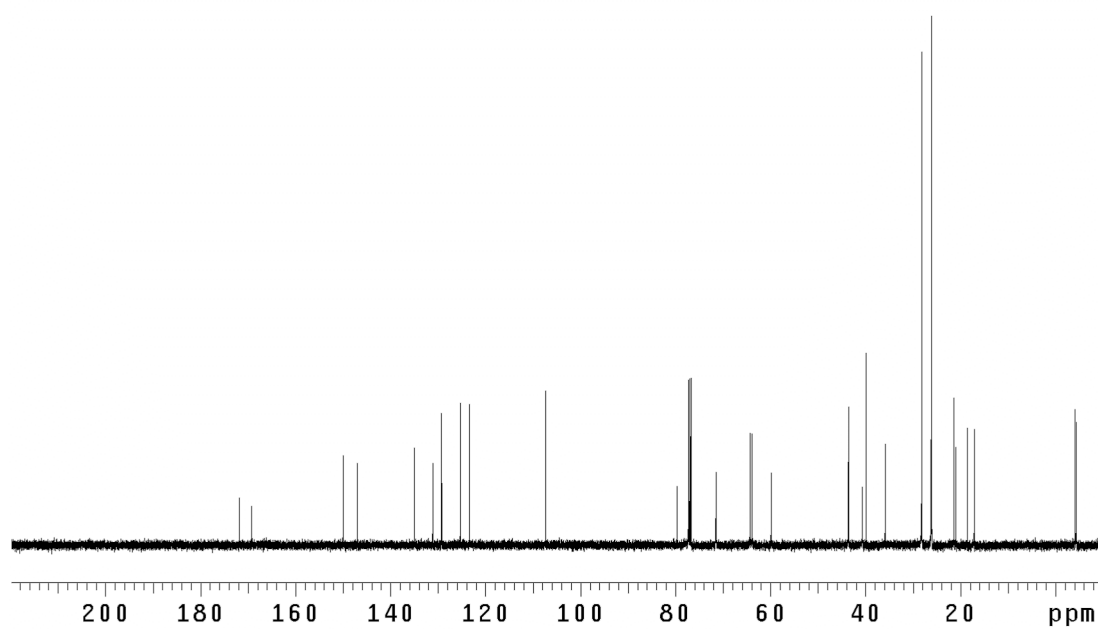


Figure A.45 <sup>13</sup>C NMR (125 MHz, CDCl<sub>3</sub>) of compound **188**.

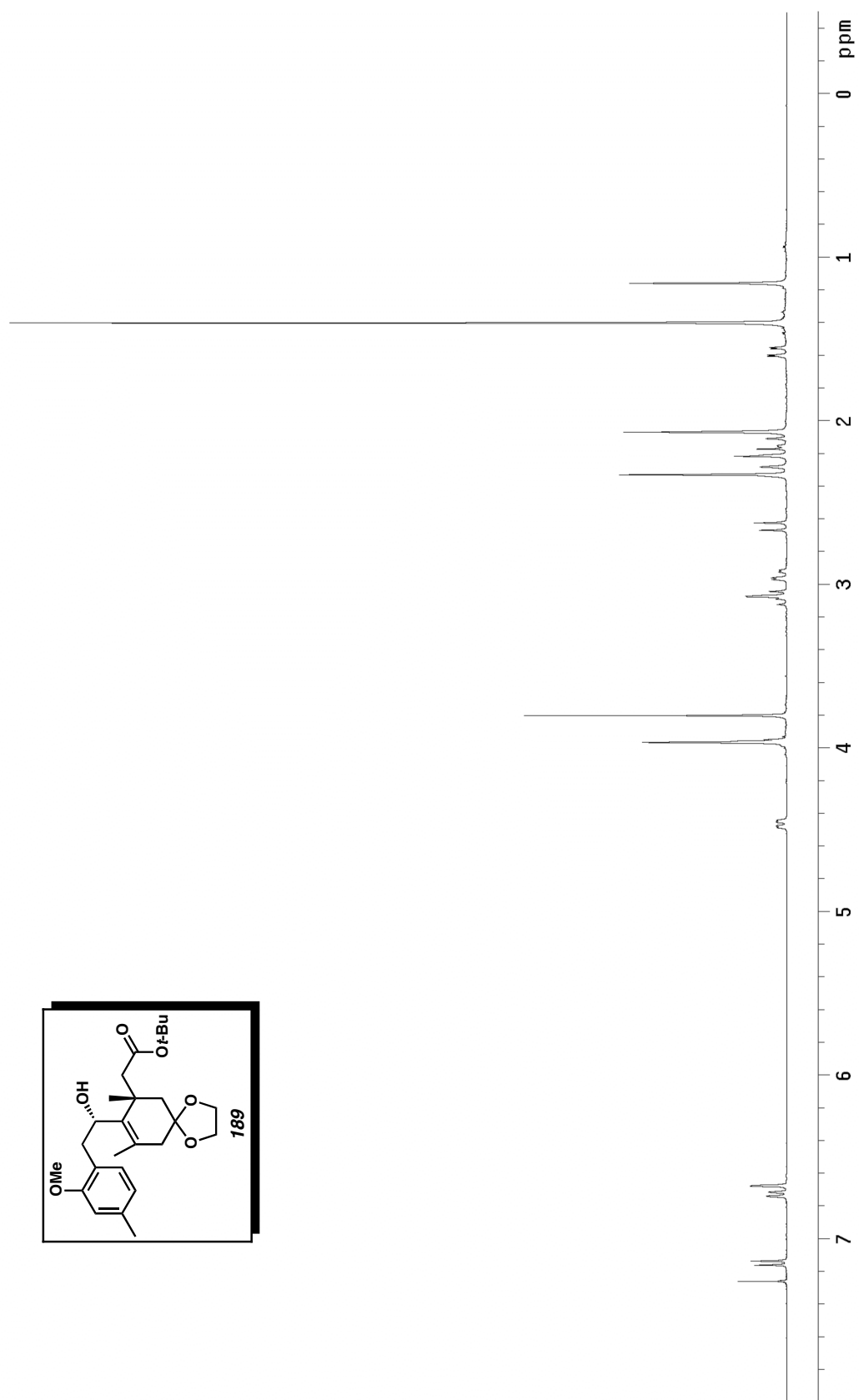
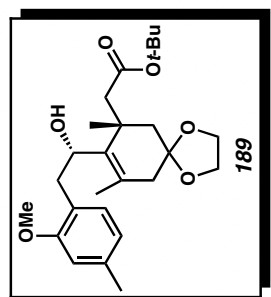


Figure A.46  $^1\text{H}$  NMR (300 MHz,  $\text{CDCl}_3$ ) of compound **189**.

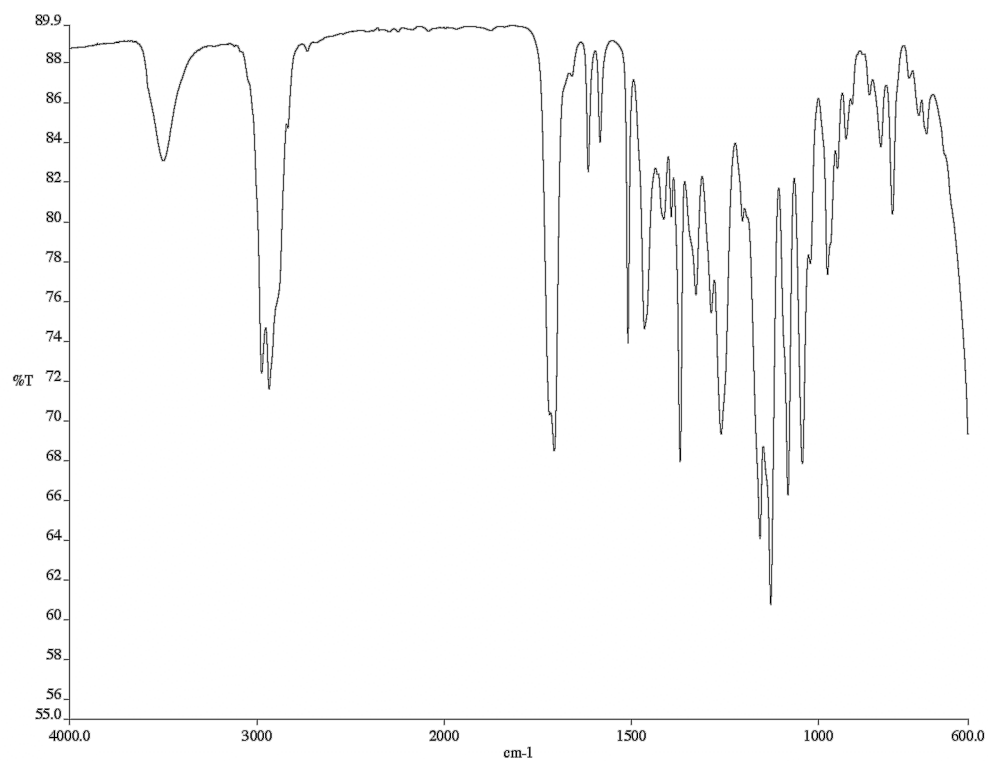


Figure A.47 Infrared spectrum (thin film/NaCl) of compound **189**.

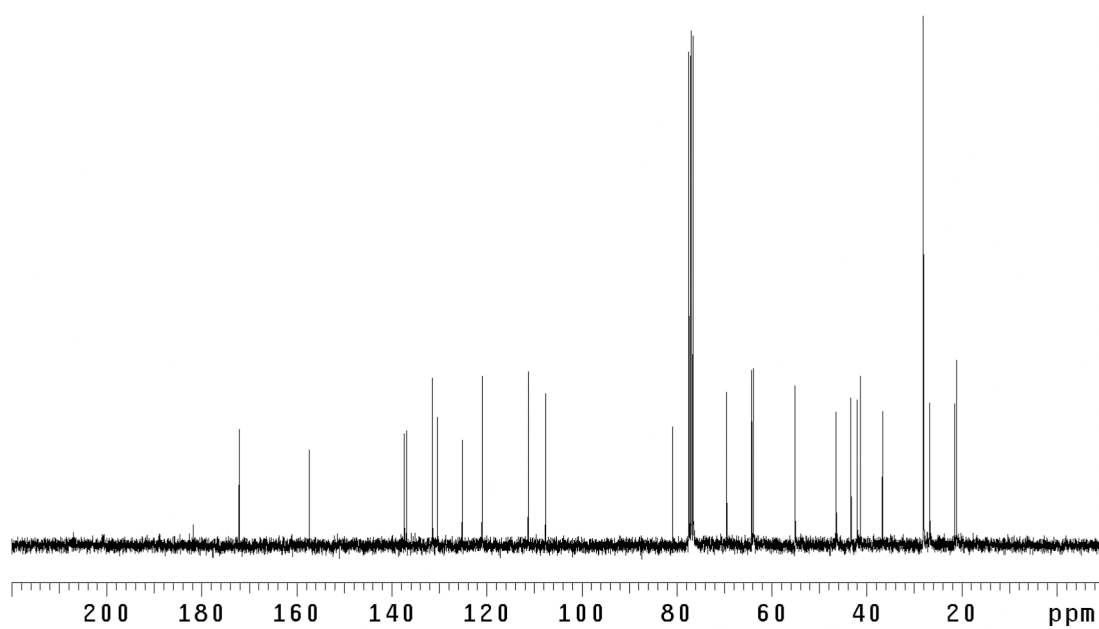


Figure A.48 <sup>13</sup>C NMR (75 MHz, CDCl<sub>3</sub>) of compound **189**.

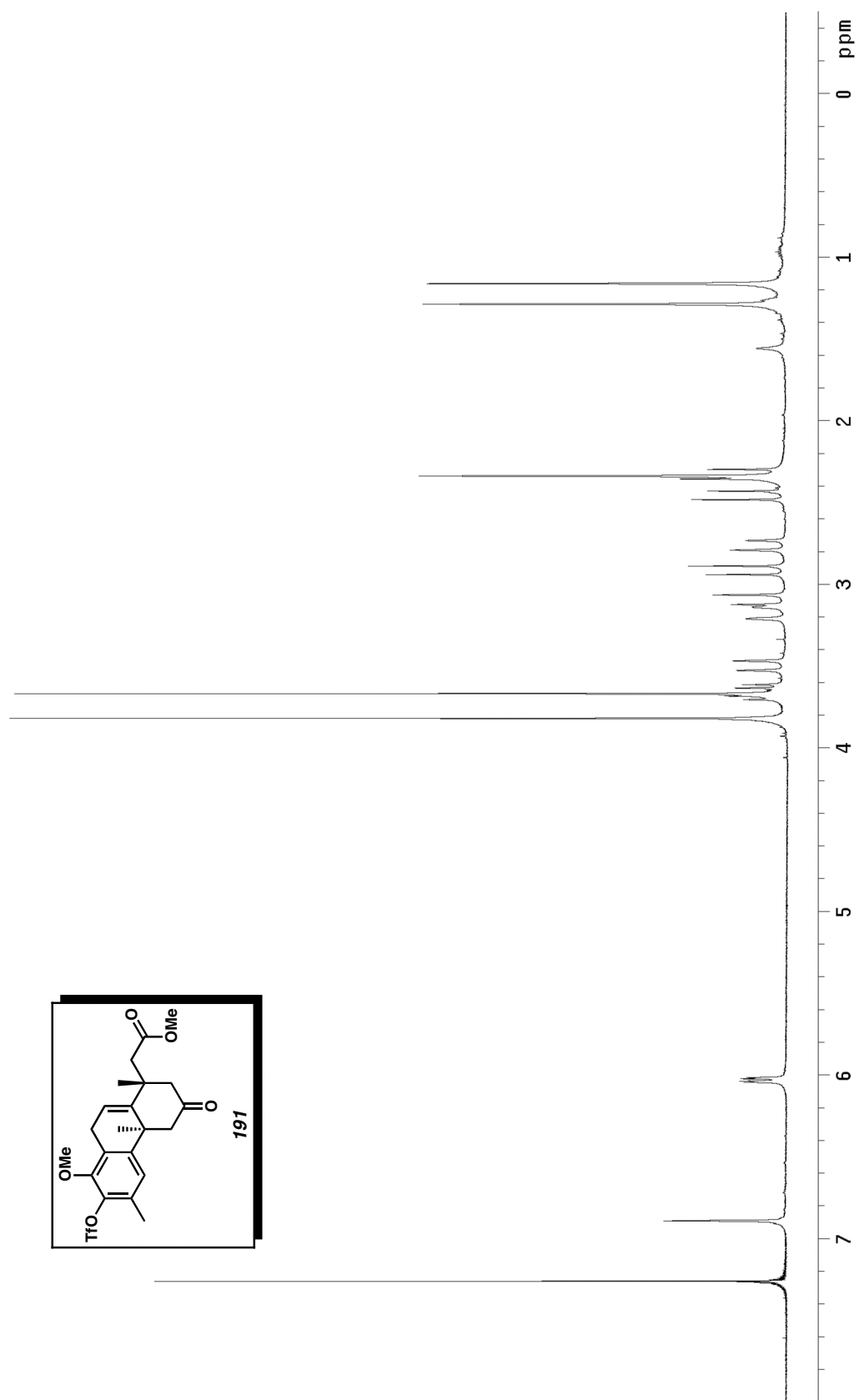


Figure A.49 <sup>1</sup>H NMR (300 MHz, CDCl<sub>3</sub>) of compound 191.

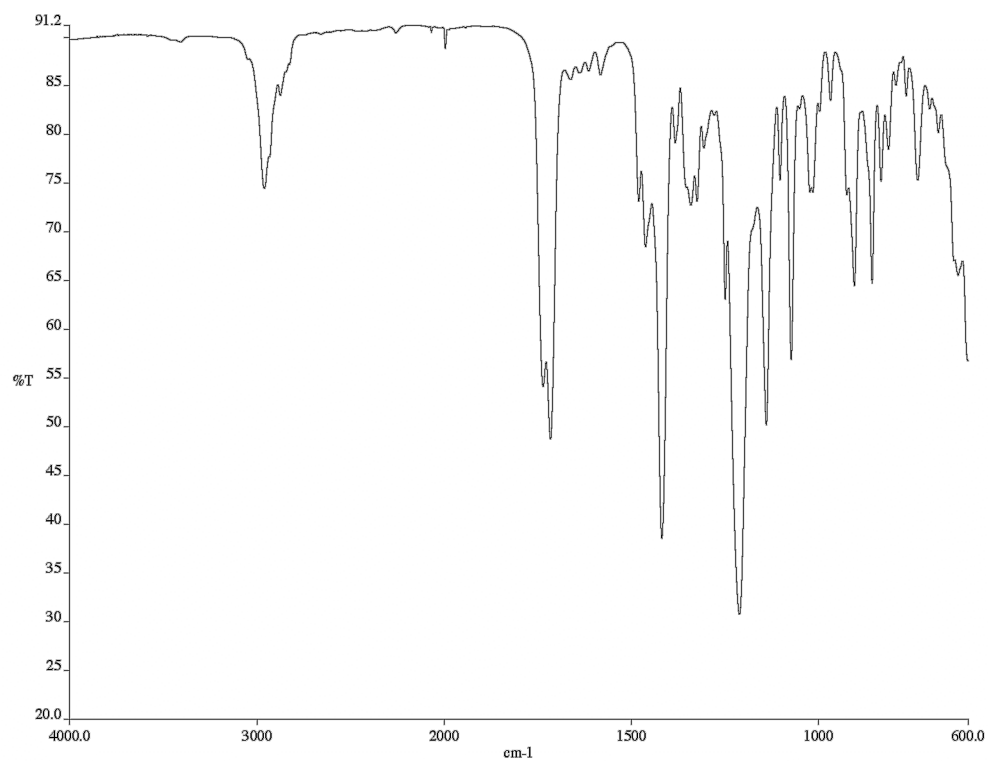


Figure A.50 Infrared spectrum (thin film/NaCl) of compound **191**.

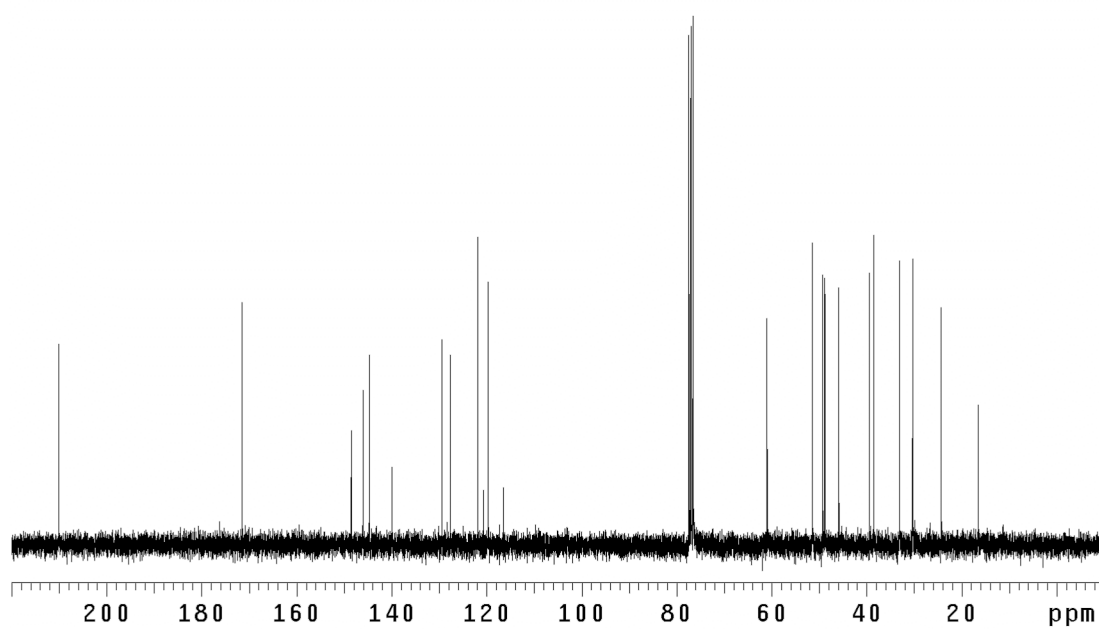


Figure A.51 <sup>13</sup>C NMR (75 MHz, CDCl<sub>3</sub>) of compound **191**.

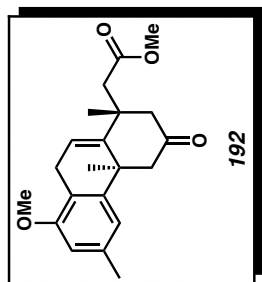
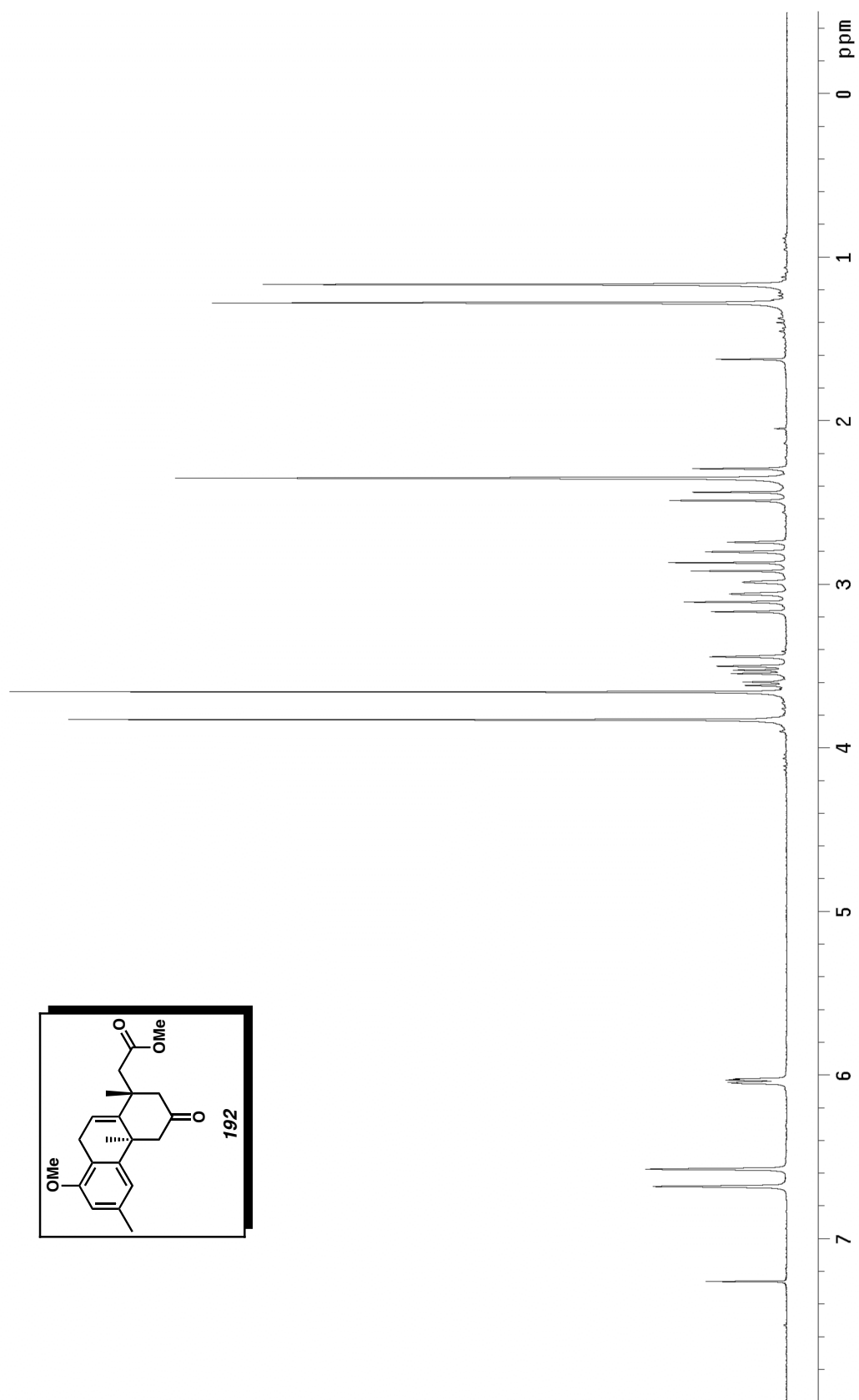


Figure A-52 <sup>1</sup>H NMR (300 MHz, CDCl<sub>3</sub>) of compound 192.

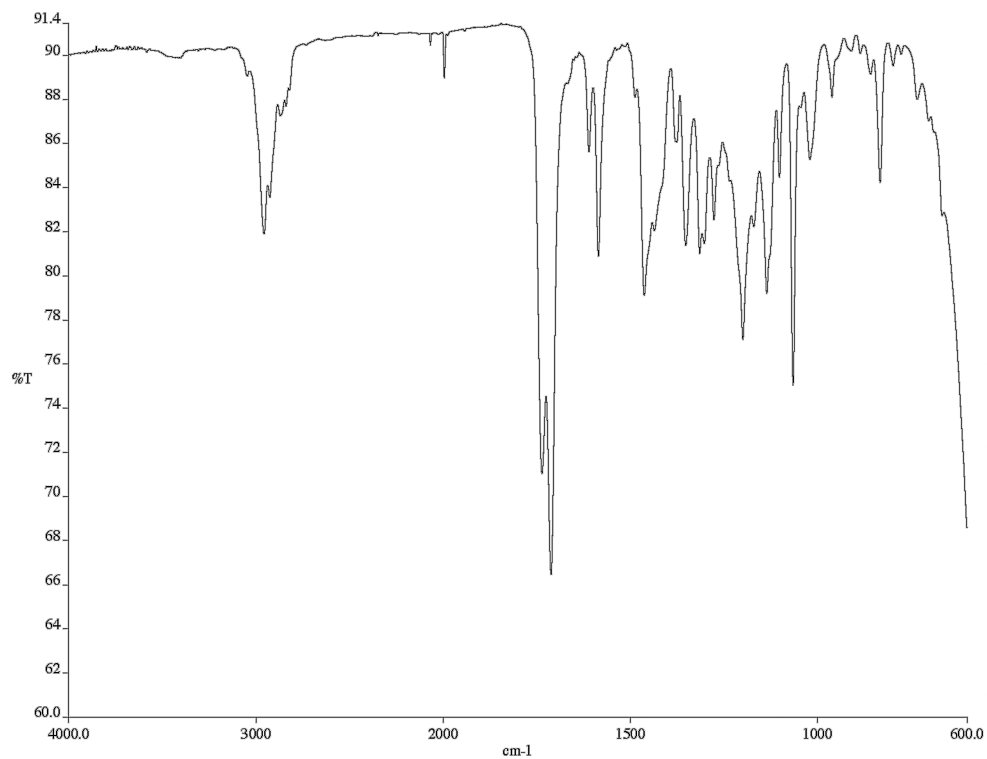


Figure A.53 Infrared spectrum (thin film/NaCl) of compound **192**.

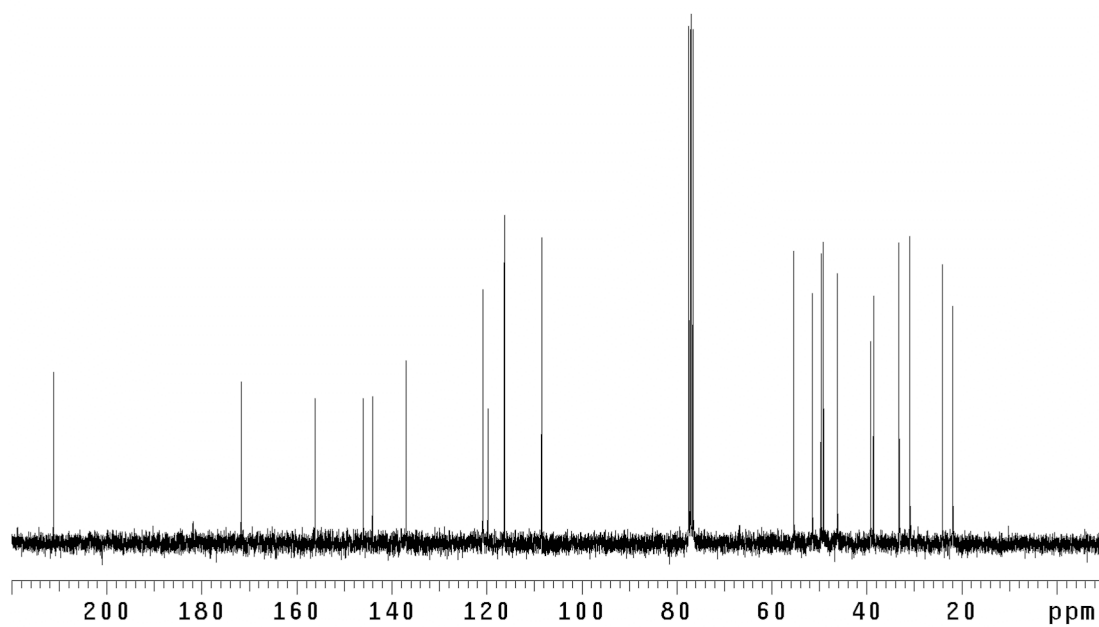


Figure A.54 <sup>13</sup>C NMR (75 MHz, CDCl<sub>3</sub>) of compound **192**.

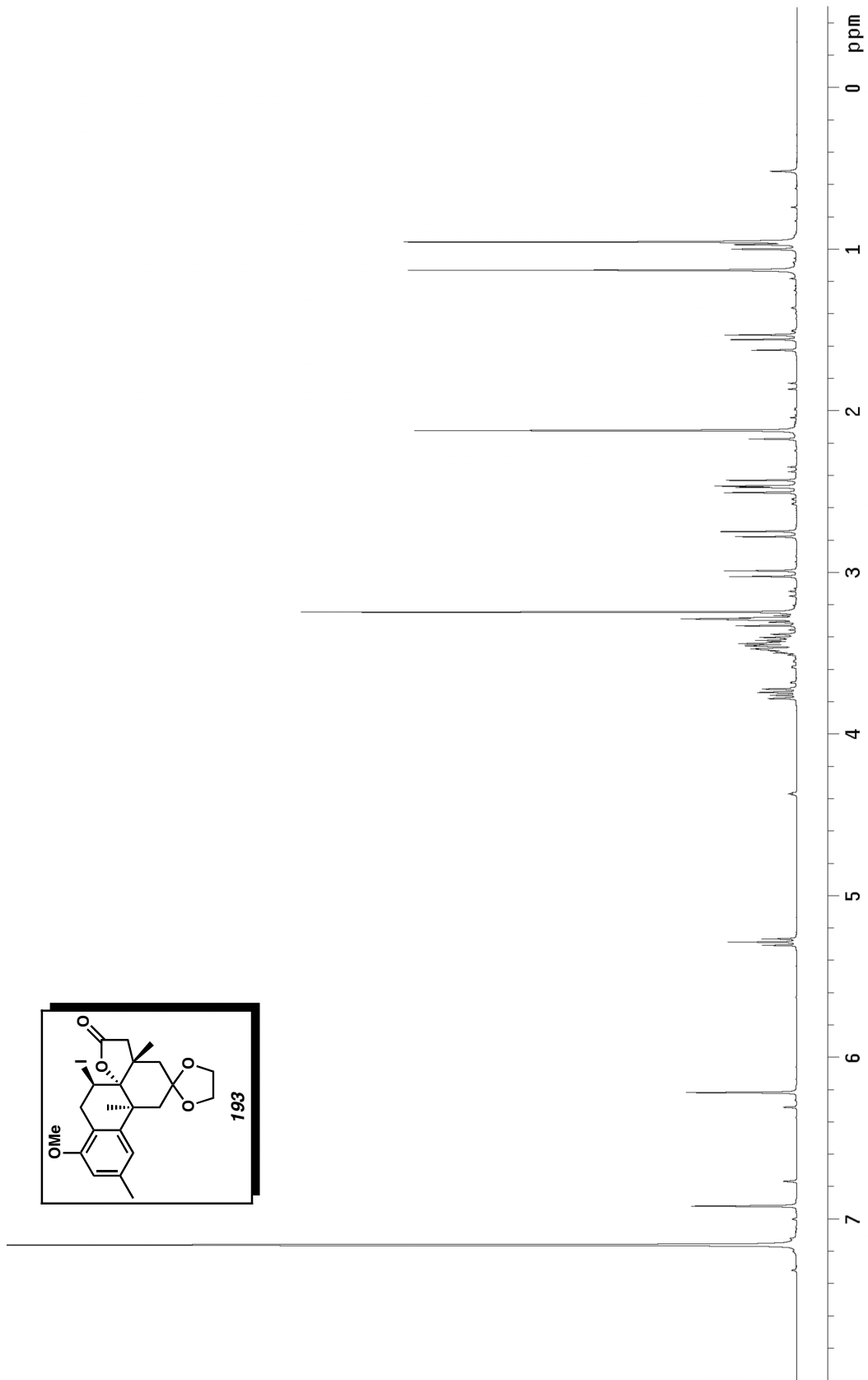


Figure A.55  $^1\text{H}$  NMR (500 MHz,  $\text{C}_6\text{D}_6$ ) of compound **193**.

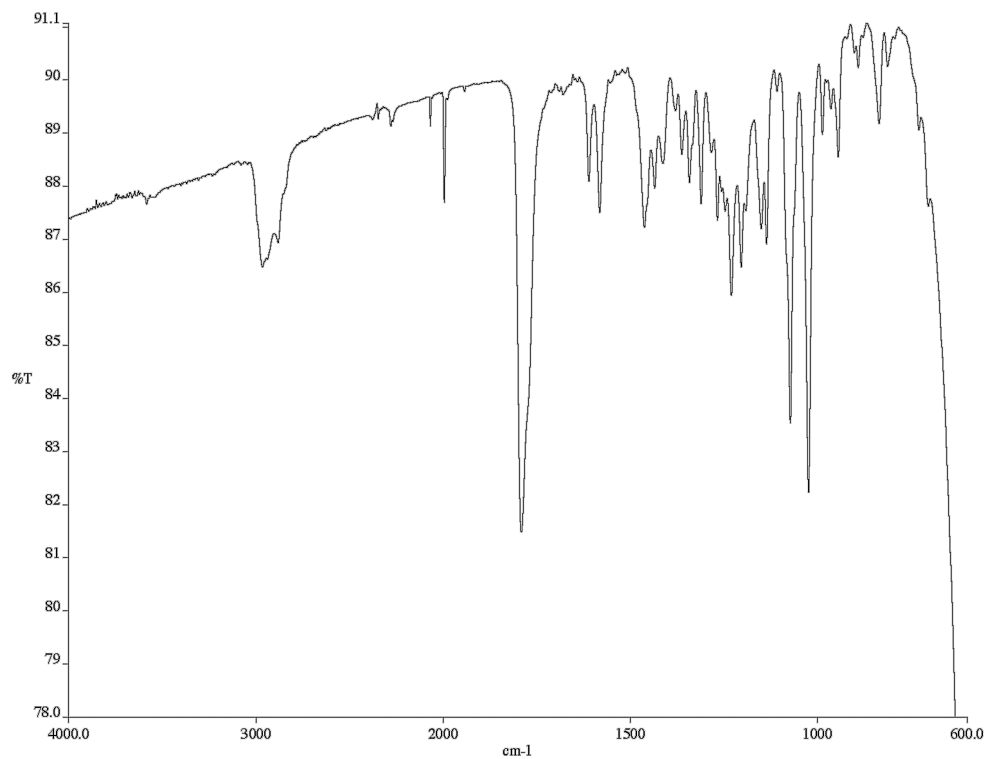


Figure A.56 Infrared spectrum (thin film/NaCl) of compound **193**.

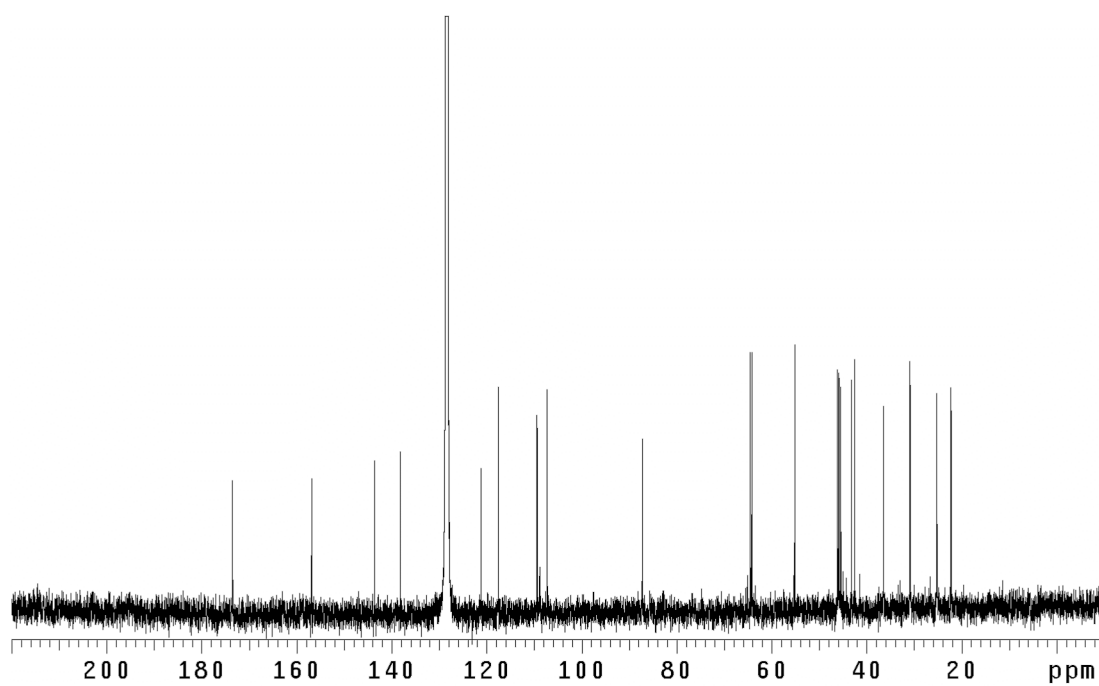


Figure A.57 <sup>13</sup>C NMR (125 MHz, C<sub>6</sub>D<sub>6</sub>) of compound **193**.

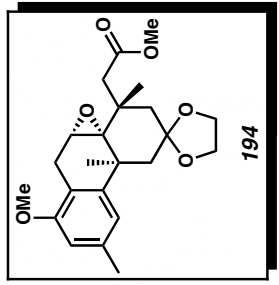
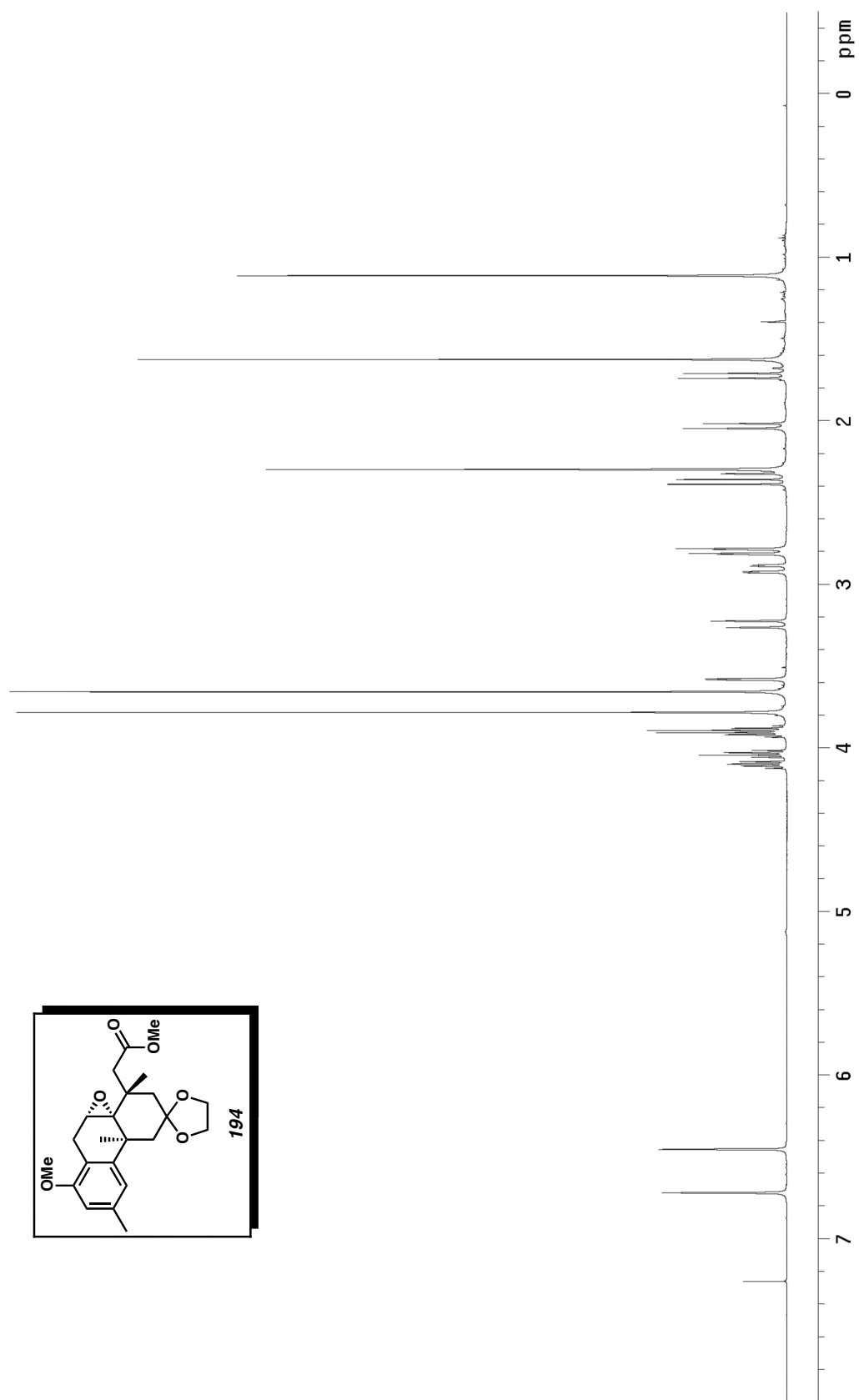


Figure A-58 <sup>1</sup>H NMR (500 MHz, CDCl<sub>3</sub>) of compound **194**.

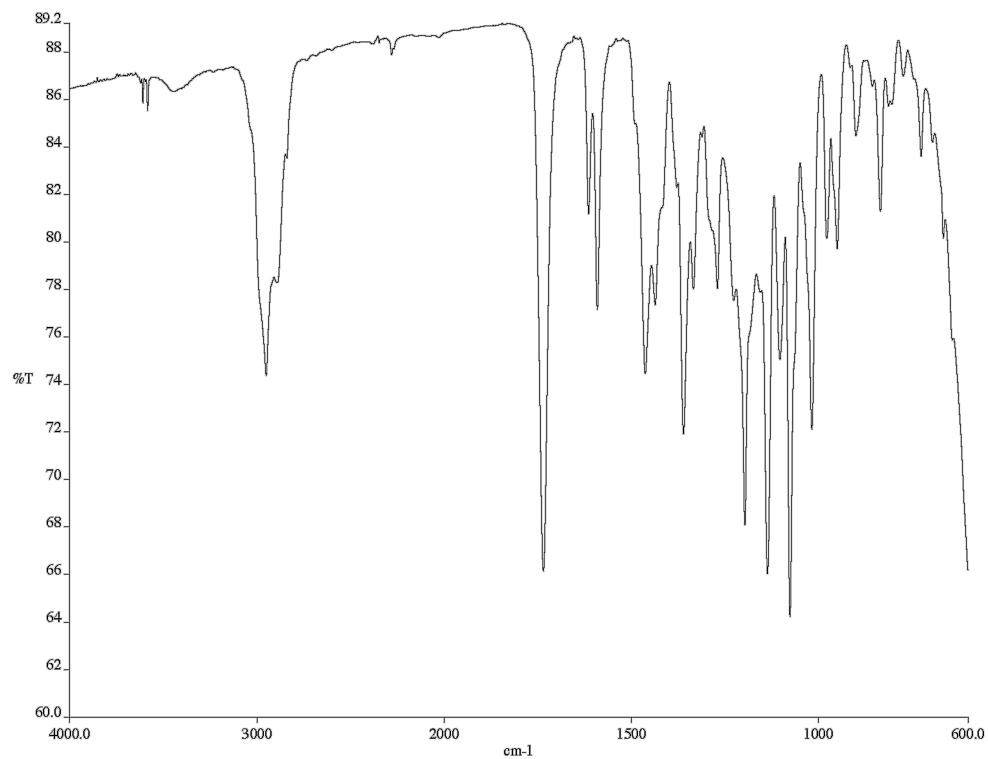


Figure A.59 Infrared spectrum (thin film/NaCl) of compound **194**.

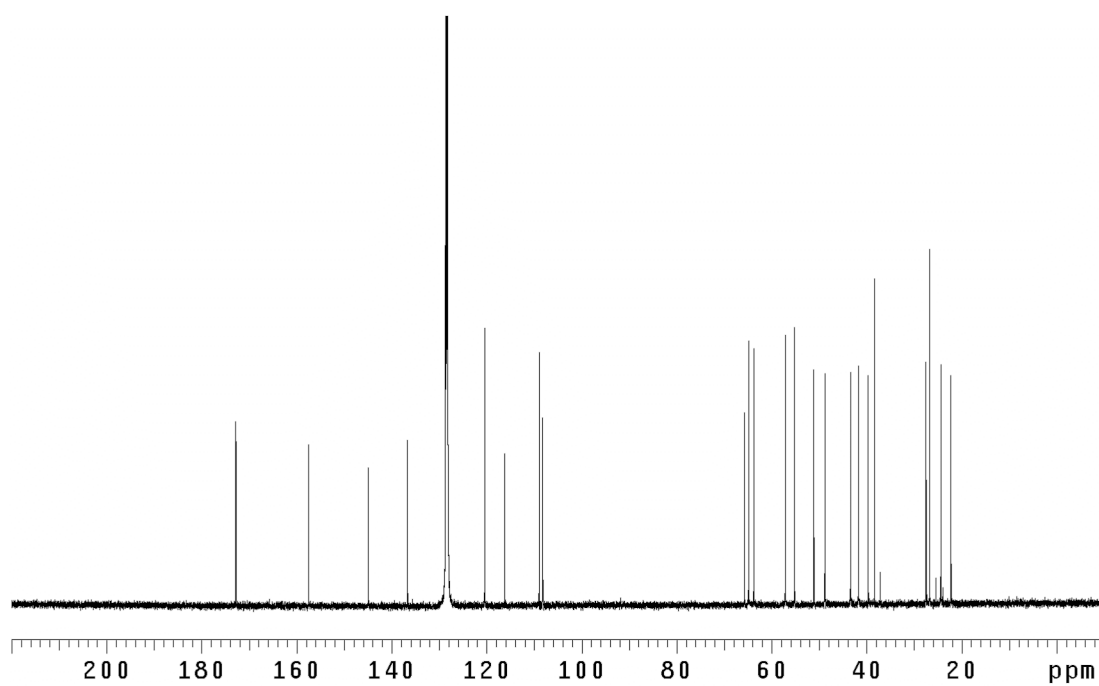


Figure A.60  $^{13}\text{C}$  NMR (125 MHz,  $\text{CDCl}_3$ ) of compound **194**.

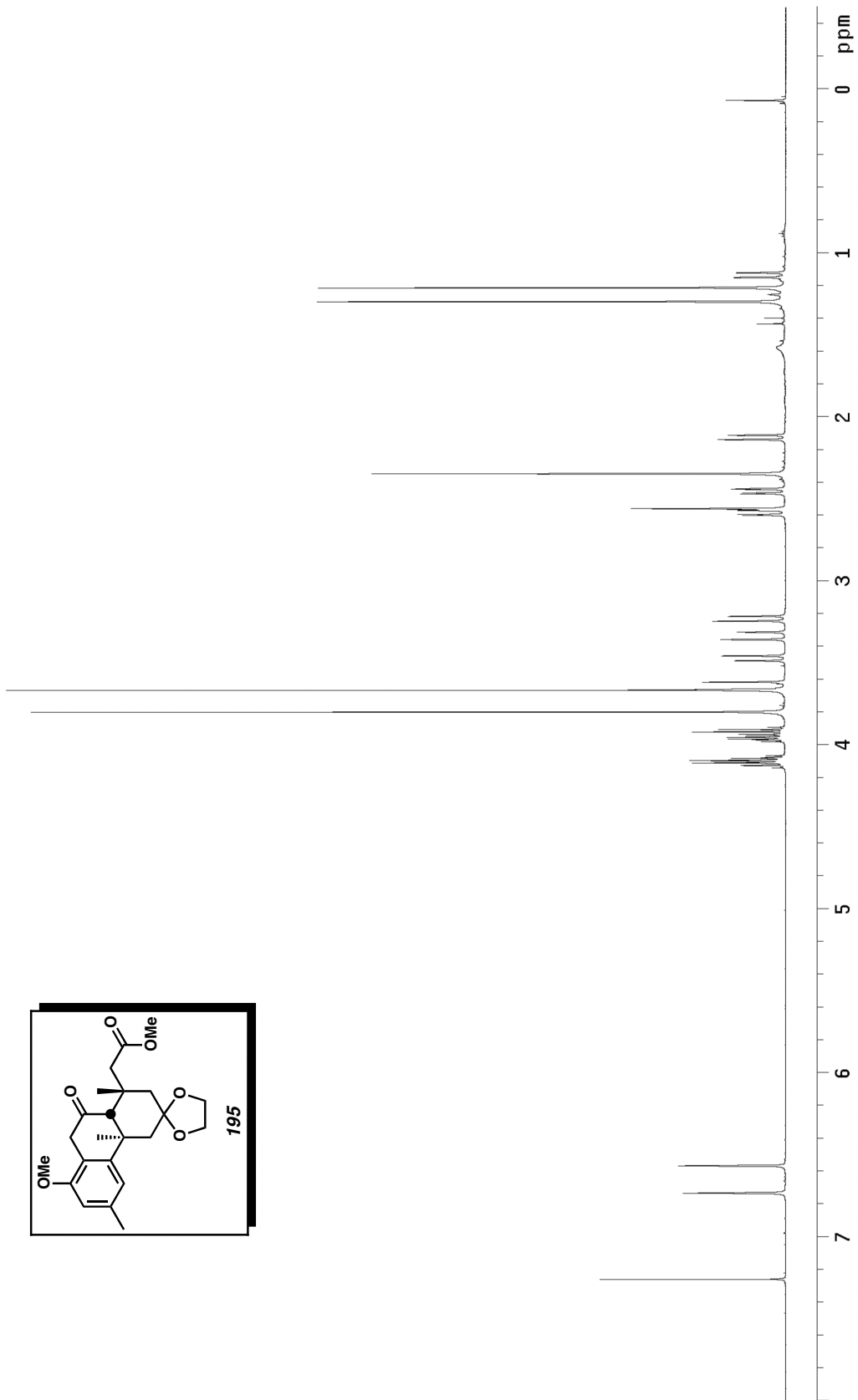
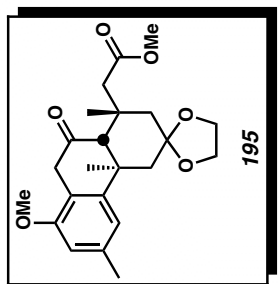


Figure A.61  $^1\text{H NMR}$  (500 MHz,  $\text{CDCl}_3$ ) of compound **195**.

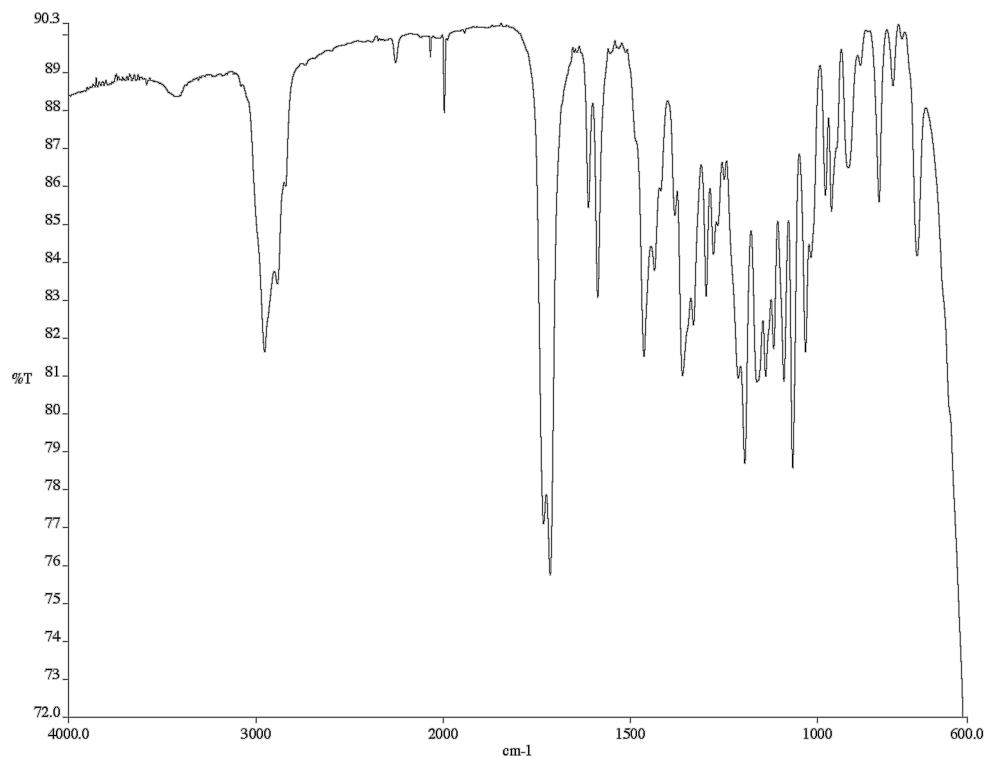


Figure A.62 Infrared spectrum (thin film/NaCl) of compound **195**.

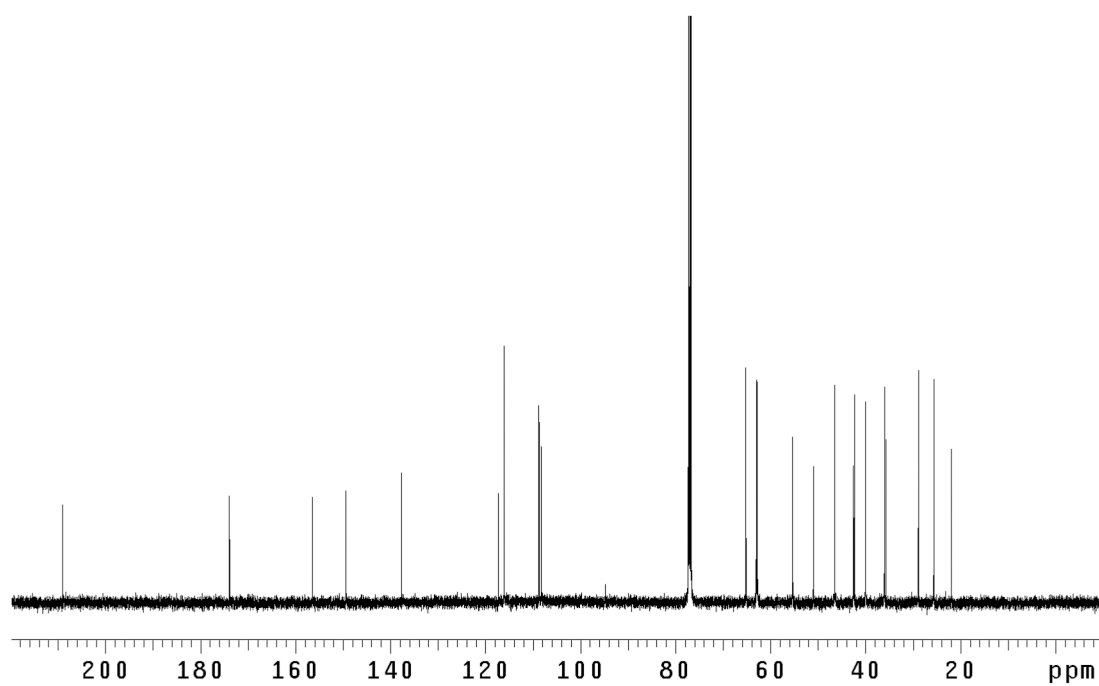


Figure A.63 <sup>13</sup>C NMR (125 MHz, CDCl<sub>3</sub>) of compound **195**.

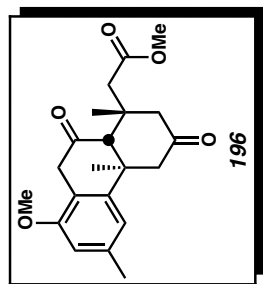
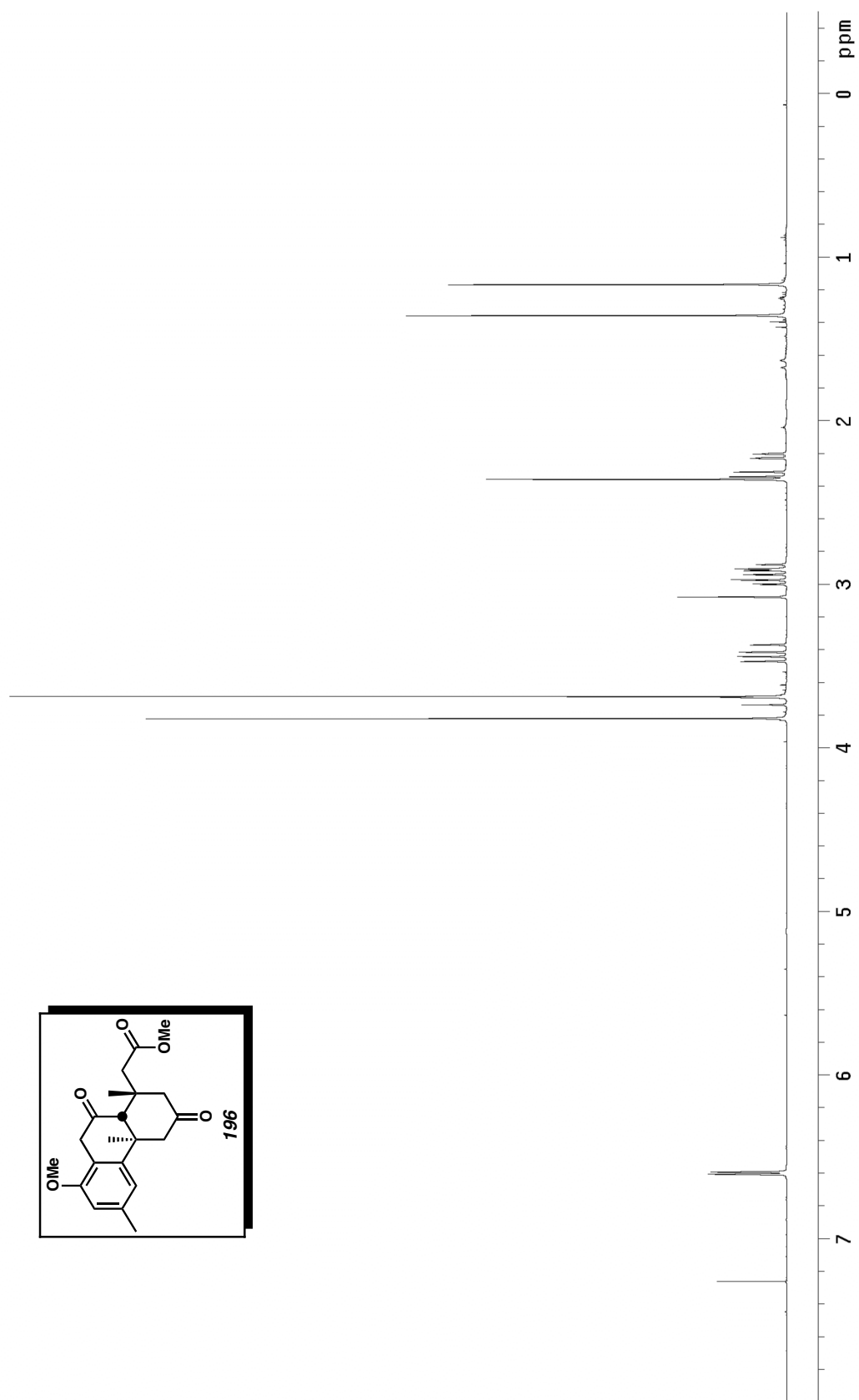


Figure A.64  $^1\text{H}$  NMR (500 MHz,  $\text{CDCl}_3$ ) of compound **196**.

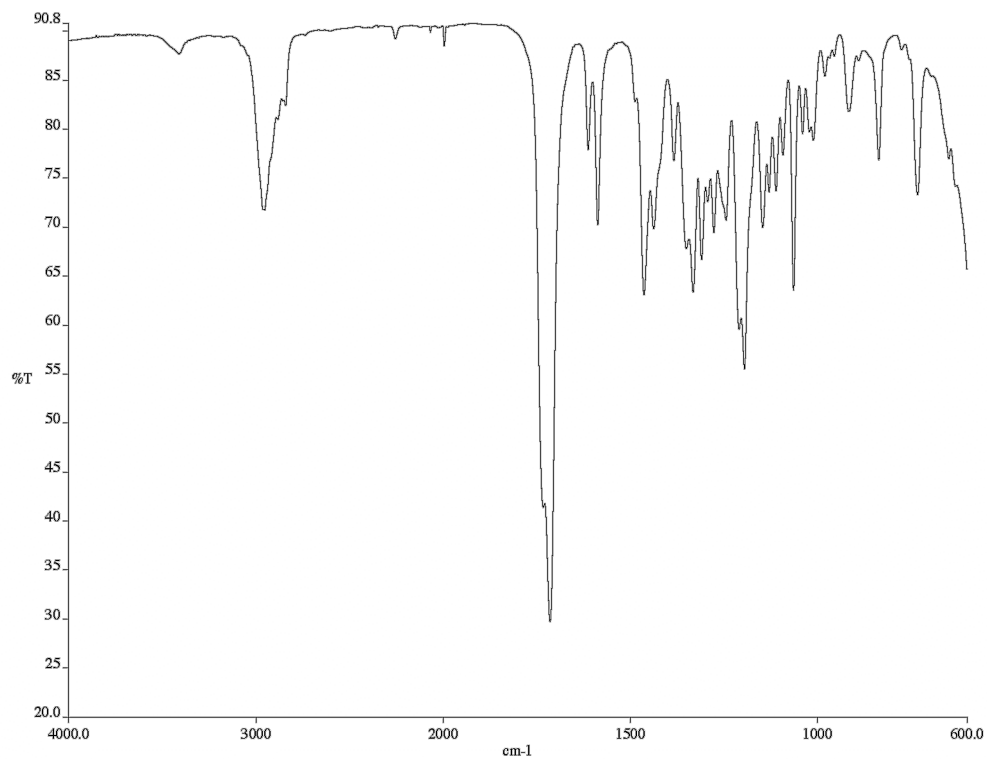


Figure A.65 Infrared spectrum (thin film/NaCl) of compound **196**.

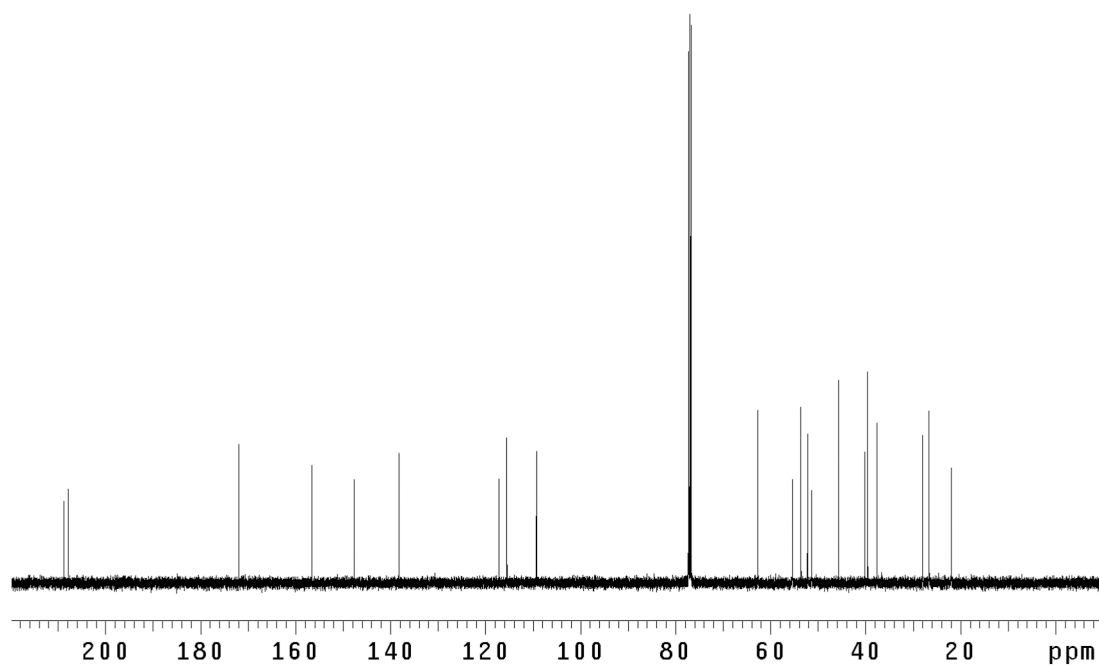


Figure A.66 <sup>13</sup>C NMR (125 MHz, CDCl<sub>3</sub>) of compound **196**.

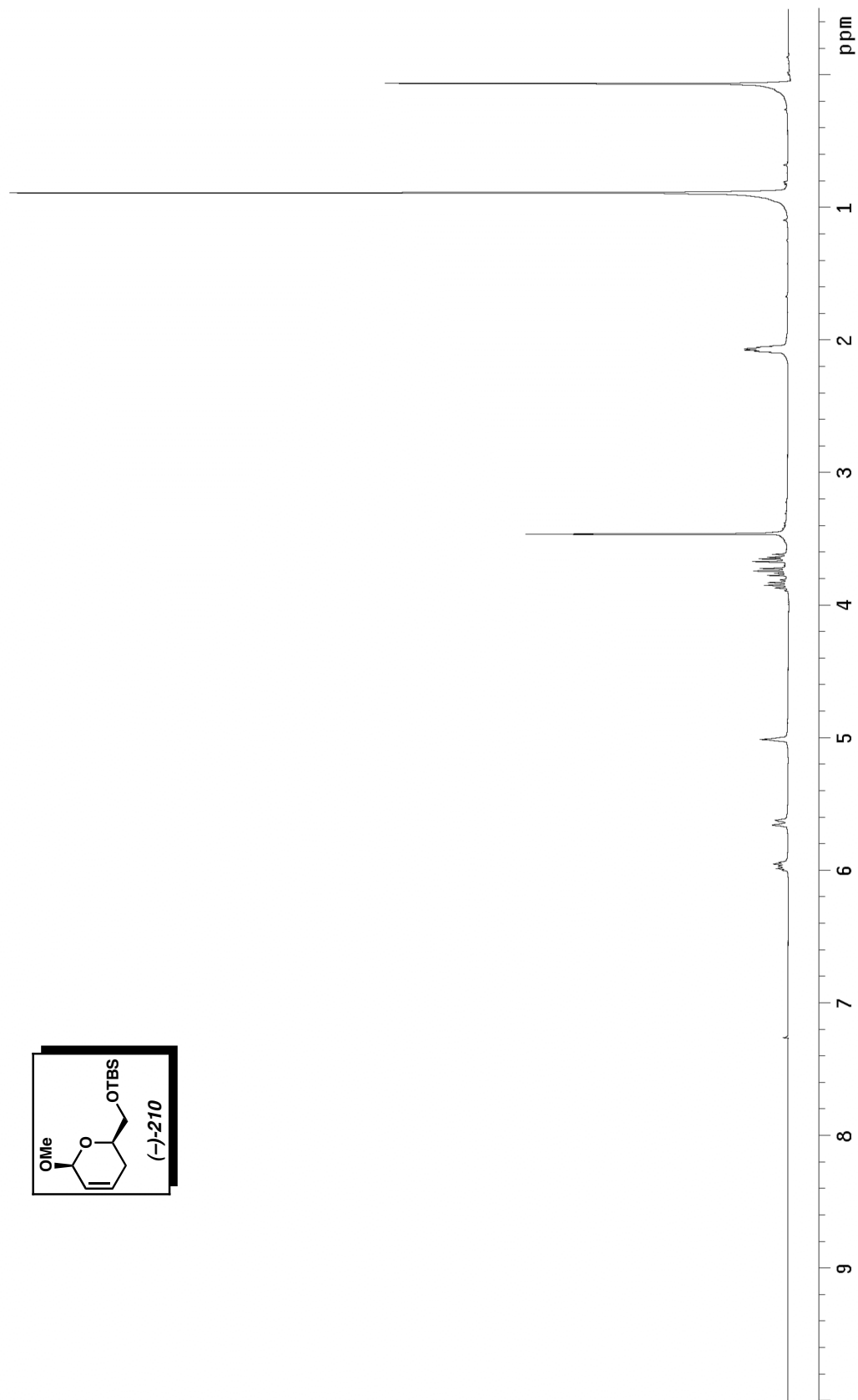
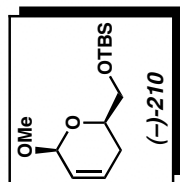


Figure A.67  $^1\text{H NMR}$  (300 MHz,  $\text{CDCl}_3$ ) of compound (-)-210.

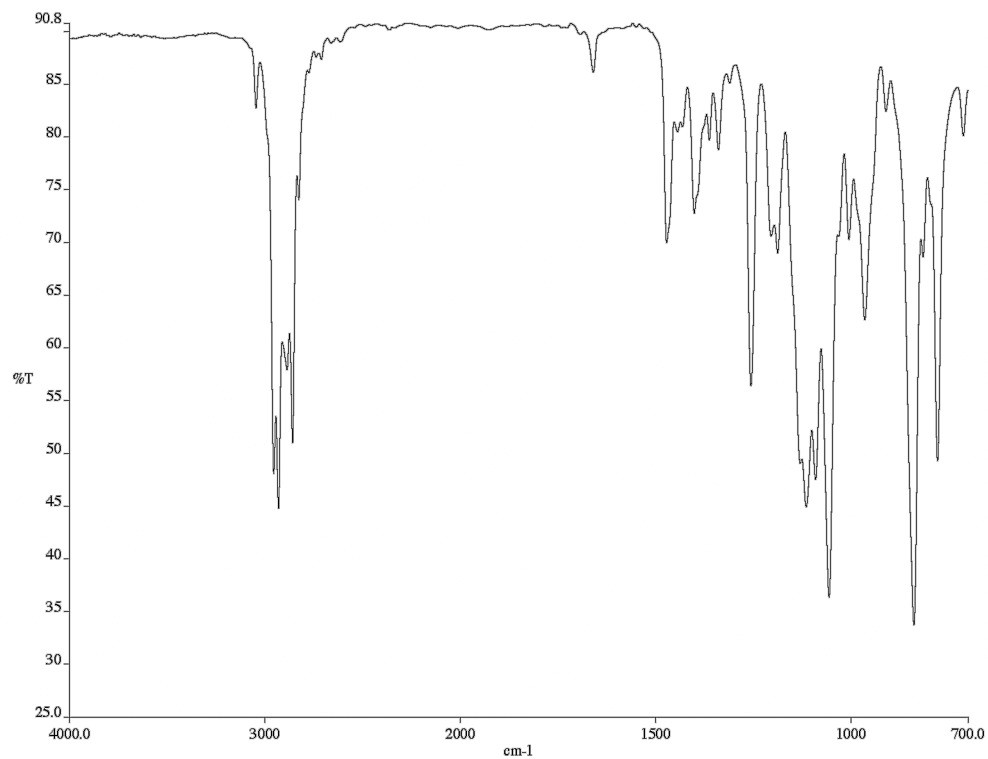


Figure A.68 Infrared spectrum (thin film/NaCl) of compound (-)-**210**.

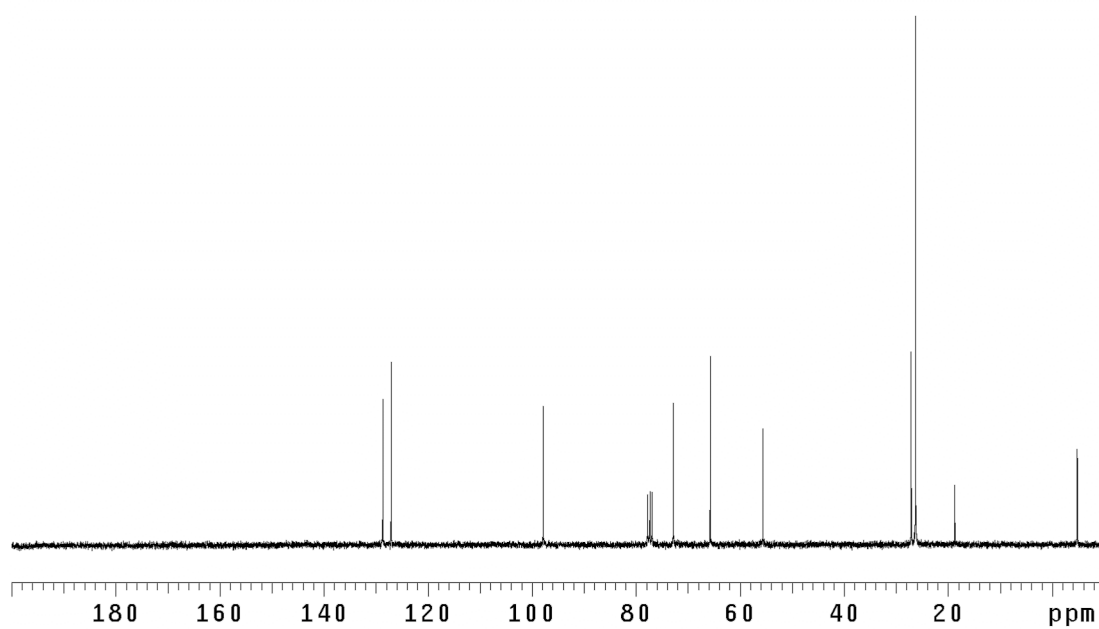


Figure A.69 <sup>13</sup>C NMR (75 MHz, CDCl<sub>3</sub>) of compound (-)-**210**.

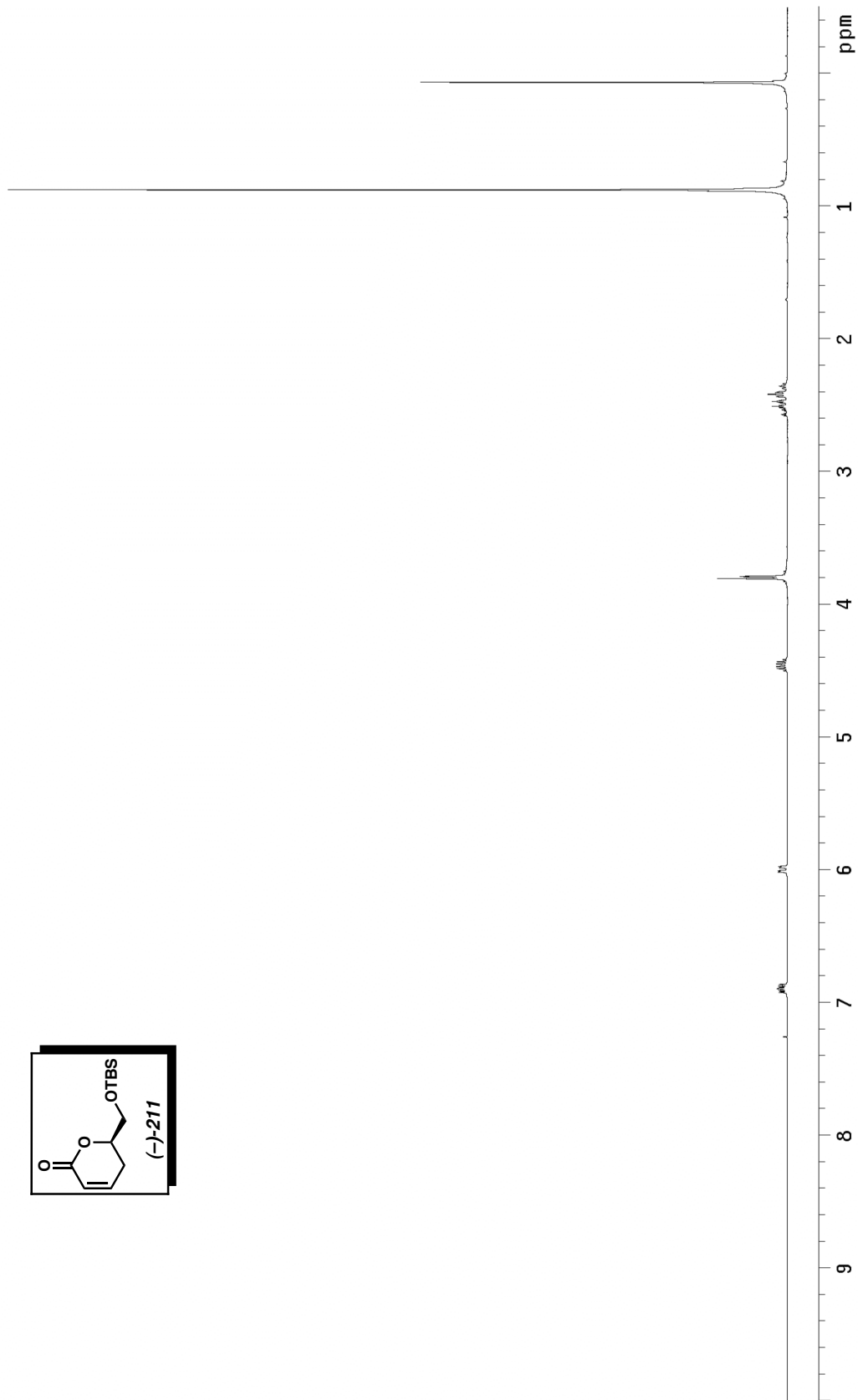
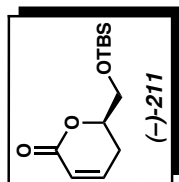


Figure A.70  $^1\text{H NMR}$  (300 MHz,  $\text{CDCl}_3$ ) of compound (-)-211.

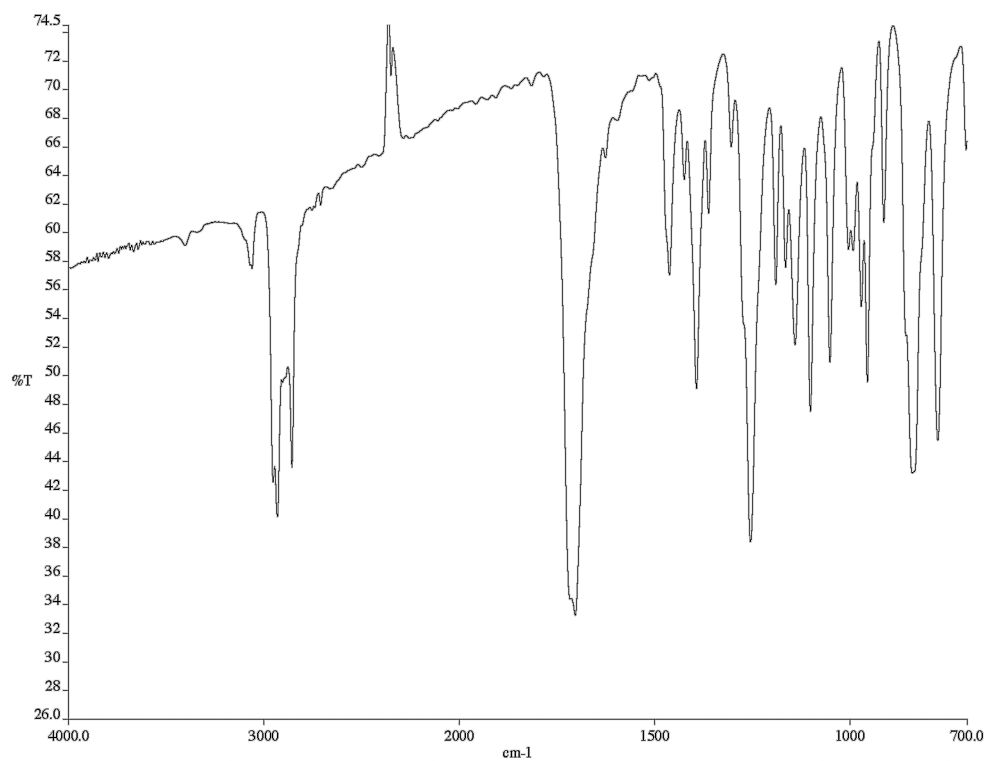


Figure A.71 Infrared spectrum (thin film/NaCl) of compound (-)-**211**.

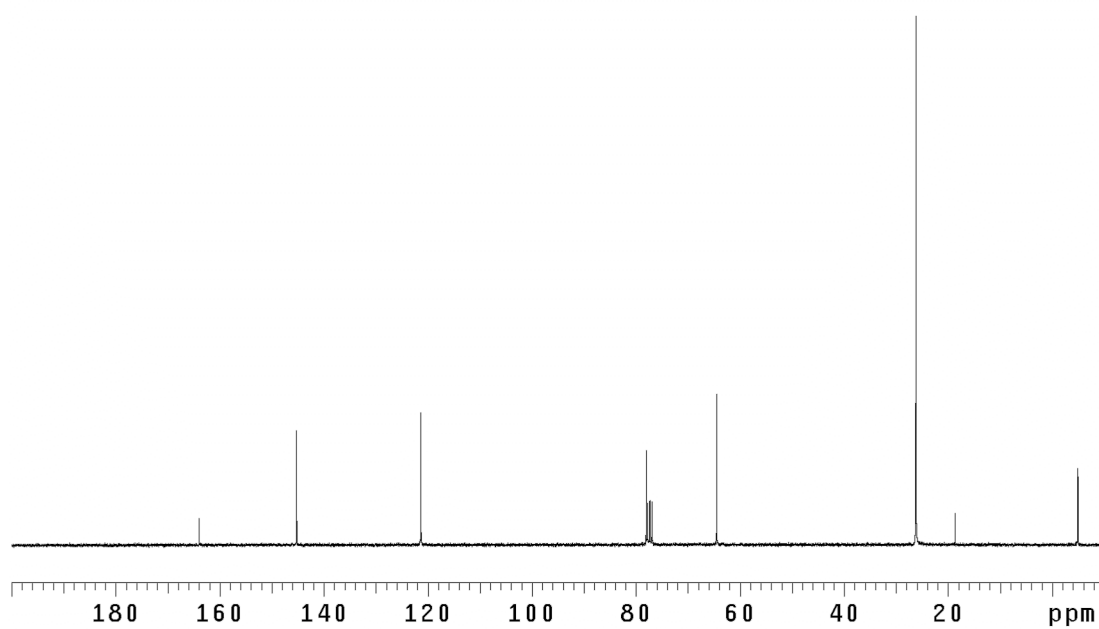


Figure A.72 <sup>13</sup>C NMR (75 MHz, CDCl<sub>3</sub>) of compound (-)-**211**.

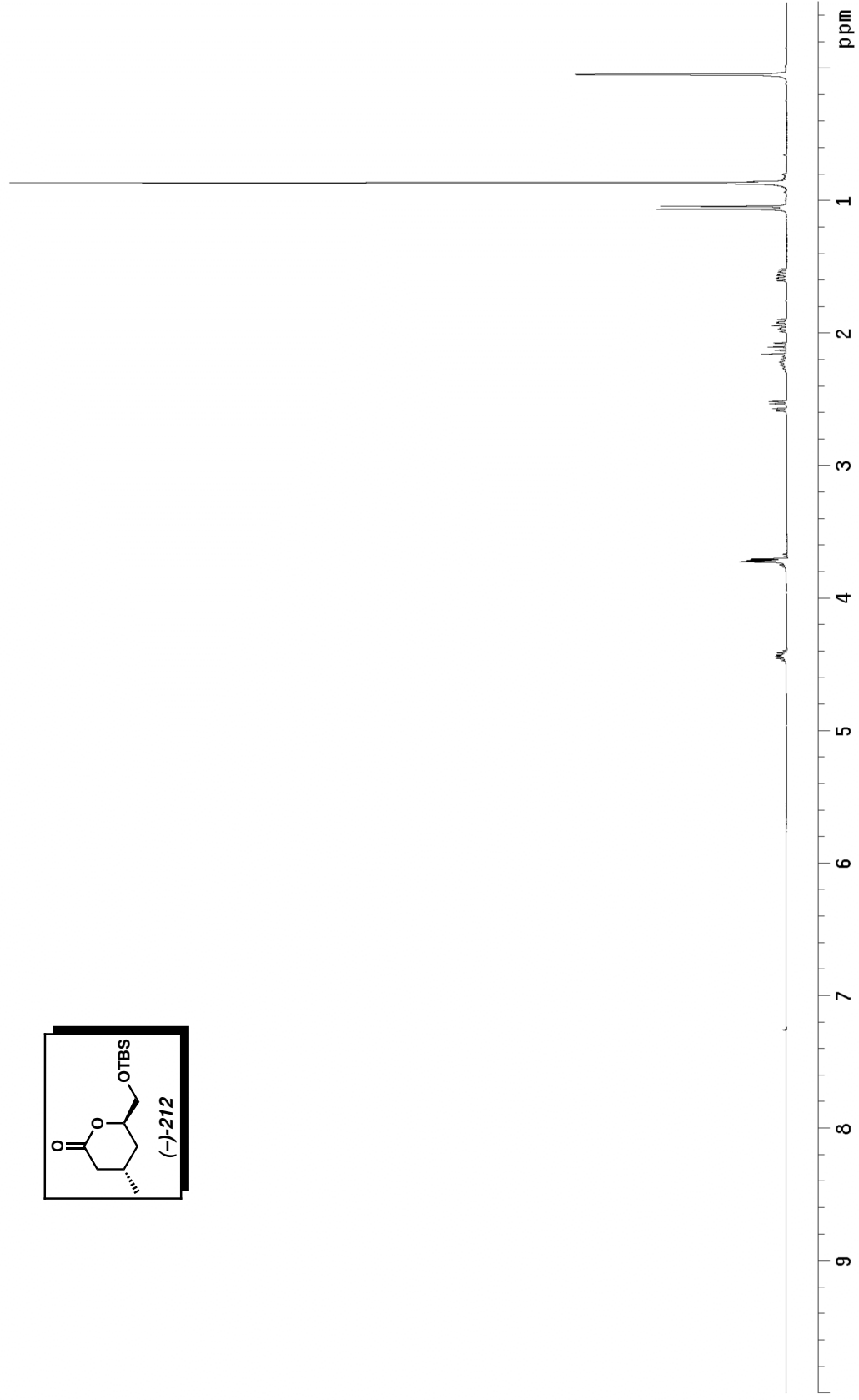
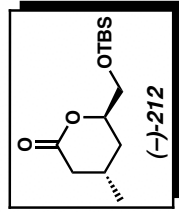


Figure A.73 <sup>1</sup>H NMR (300 MHz, CDCl<sub>3</sub>) of compound (-)-212.

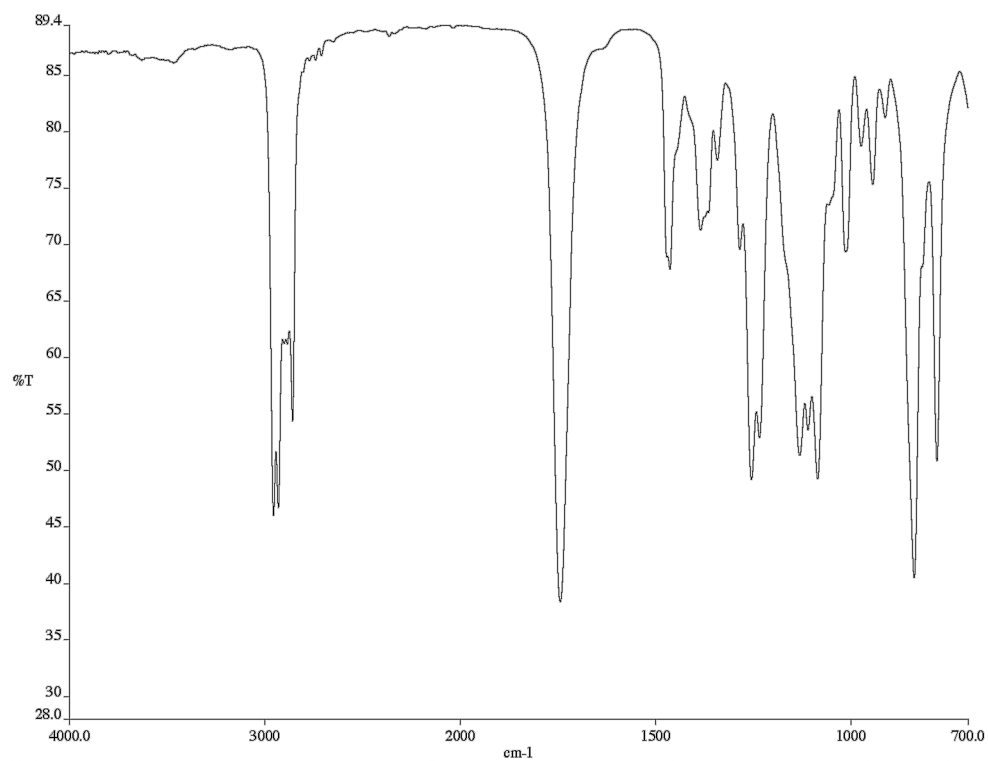


Figure A.74 Infrared spectrum (thin film/NaCl) of compound (-)-**212**.

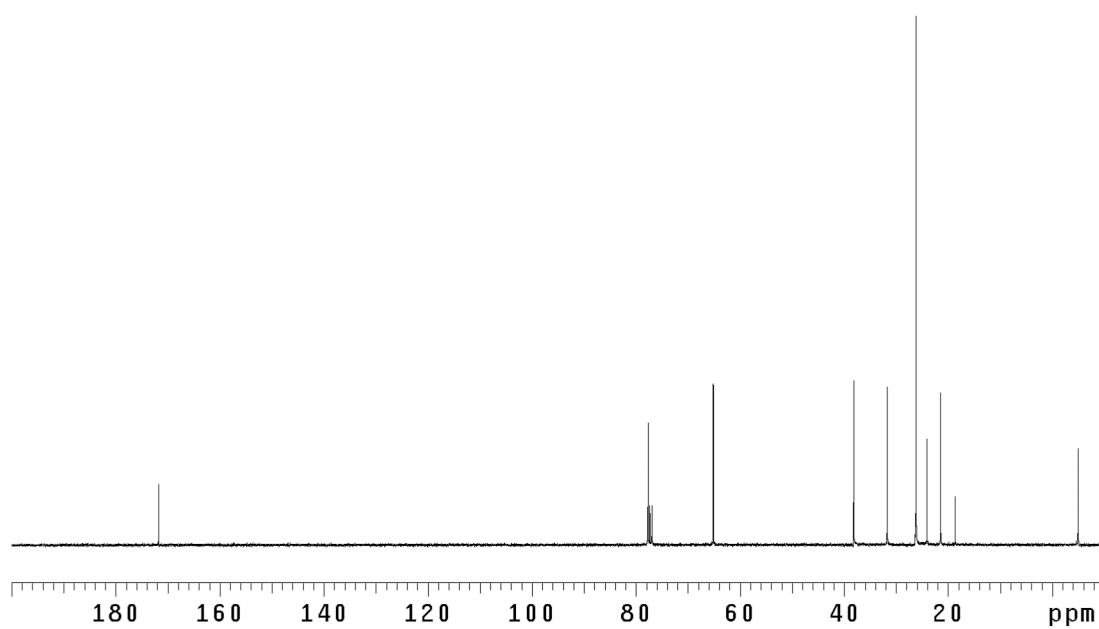


Figure A.75 <sup>13</sup>C NMR (75 MHz, CDCl<sub>3</sub>) of compound (-)-**212**.

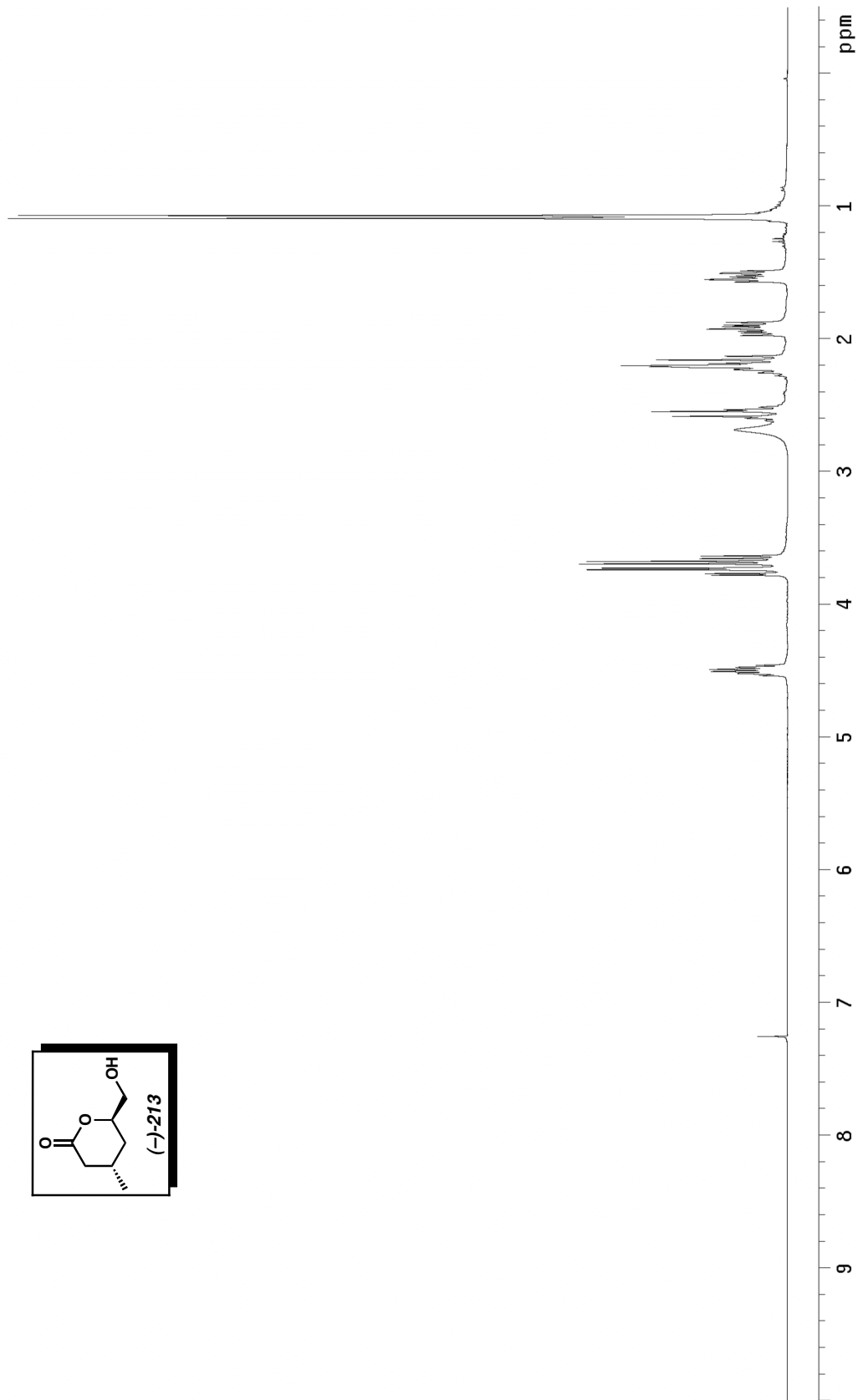
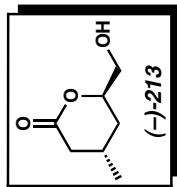


Figure A.76 <sup>1</sup>H NMR (300 MHz, CDCl<sub>3</sub>) of compound **213**.

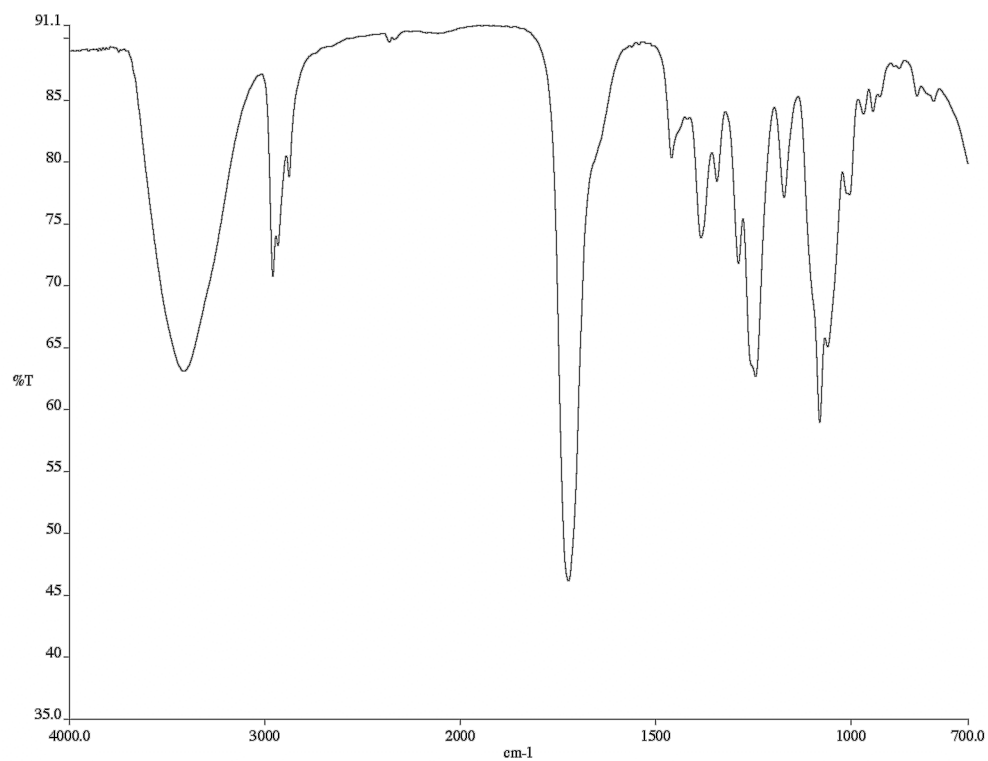


Figure A.77 Infrared spectrum (thin film/NaCl) of compound (-)-**213**.

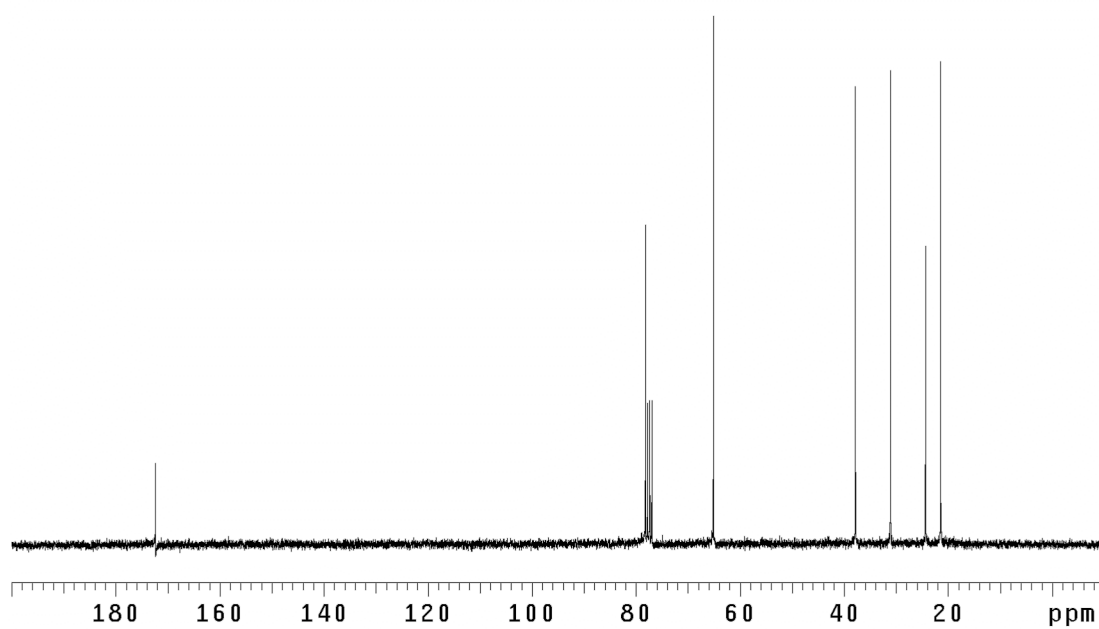


Figure A.78 <sup>13</sup>C NMR (75 MHz, CDCl<sub>3</sub>) of compound (-)-**213**.

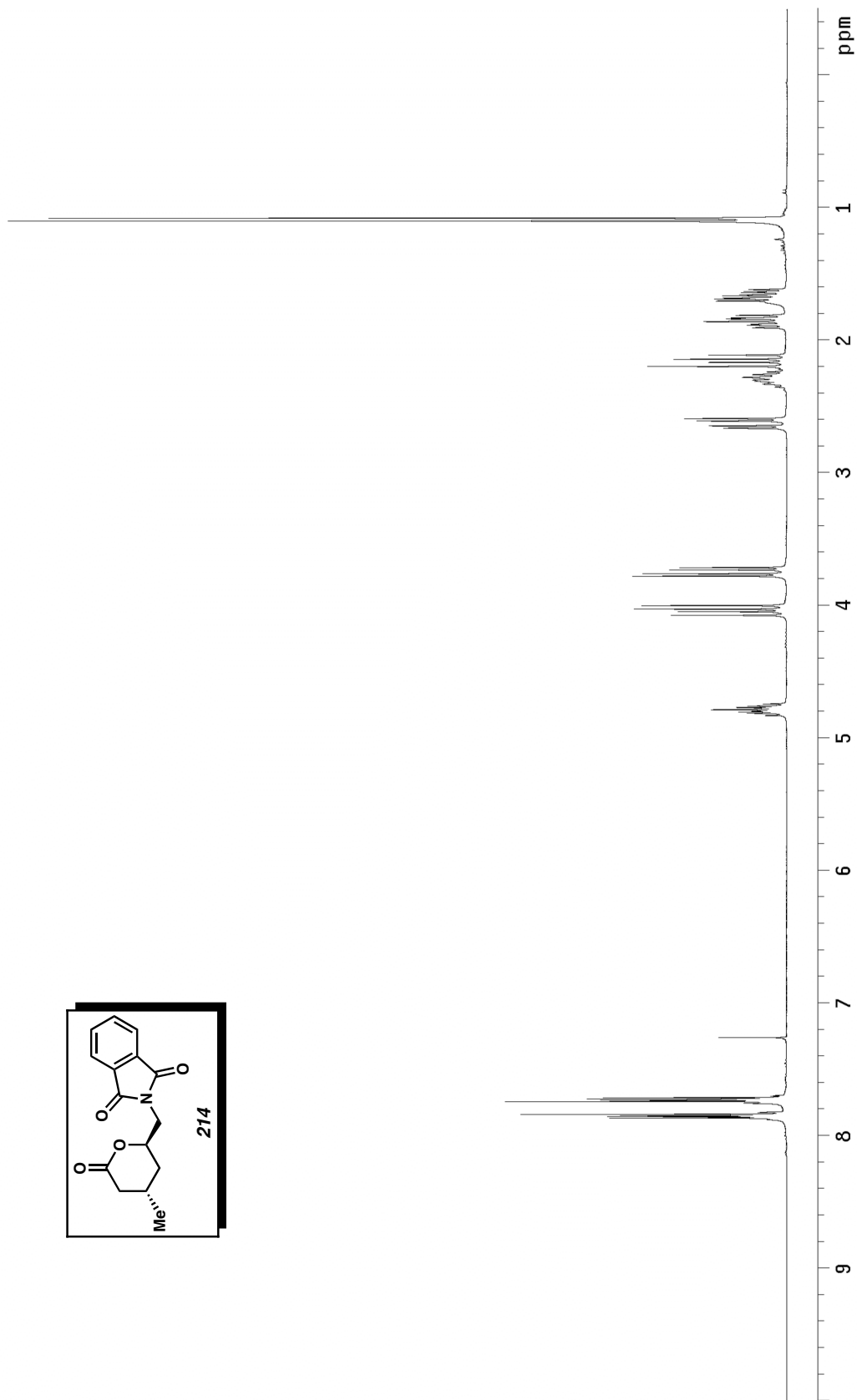
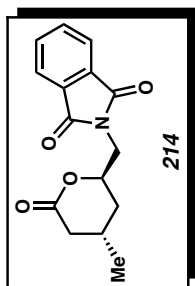


Figure A.79  $^1\text{H}$  NMR (300 MHz,  $\text{CDCl}_3$ ) of compound **214**.

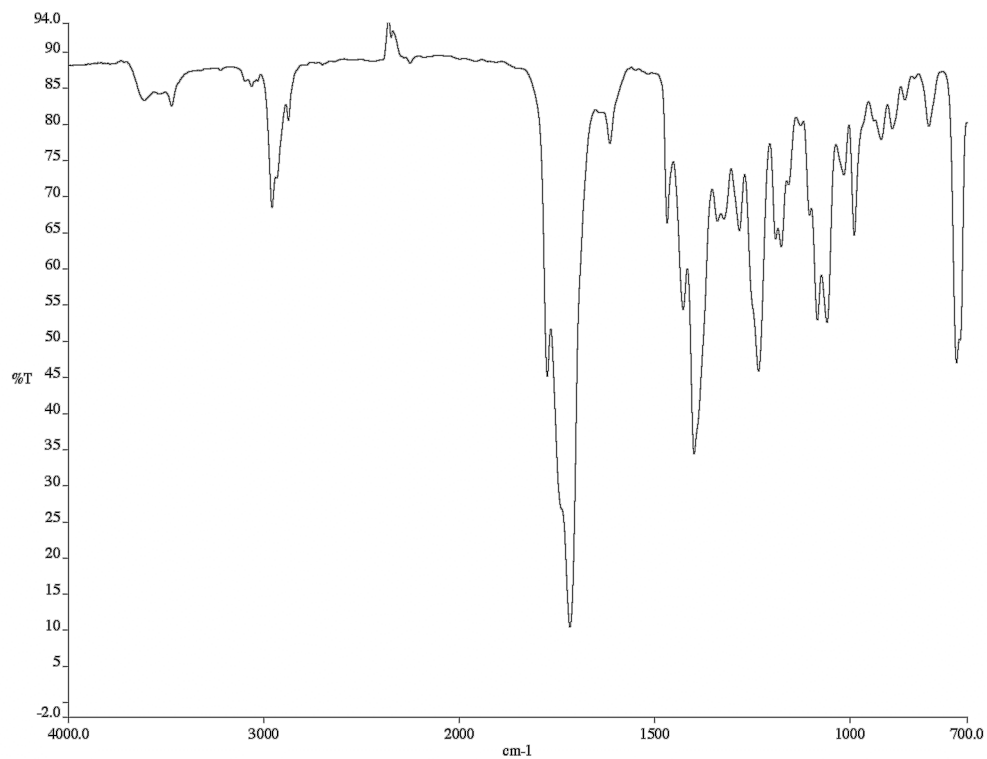


Figure A.80 Infrared spectrum (thin film/NaCl) of compound **214**.

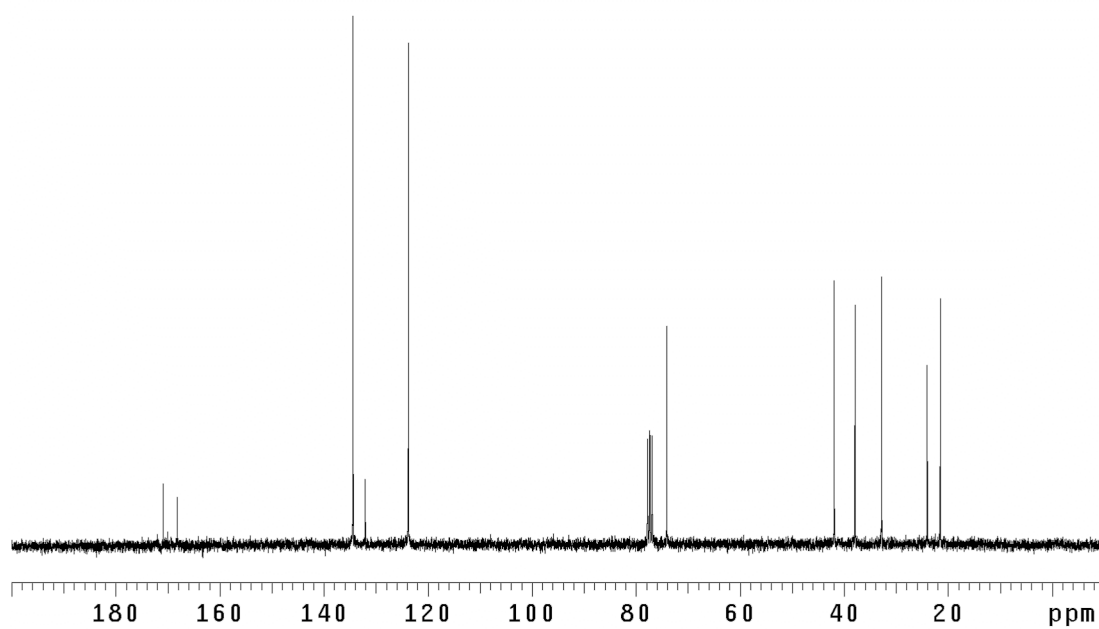


Figure A.81 <sup>13</sup>C NMR (75 MHz, CDCl<sub>3</sub>) of compound **214**.

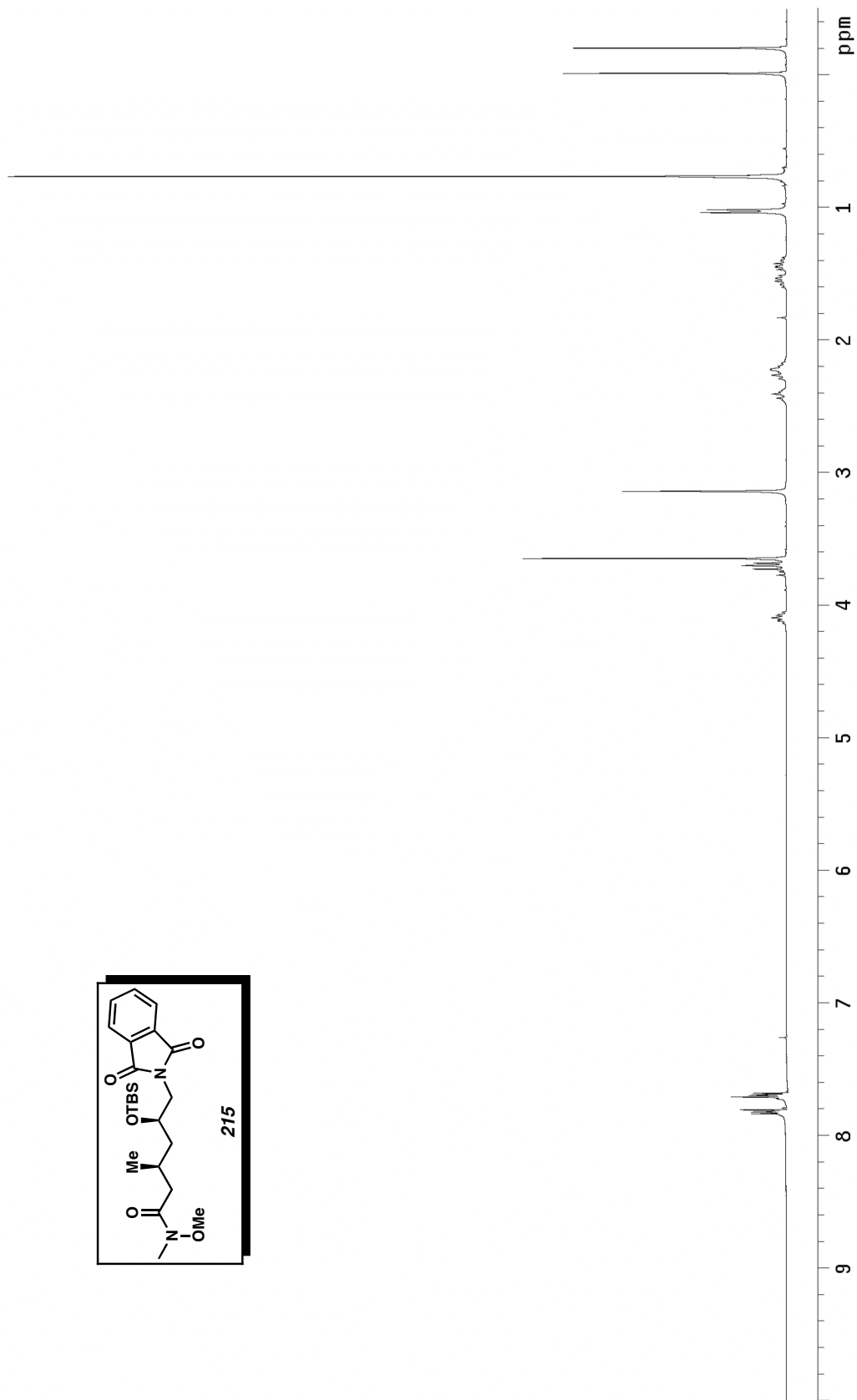
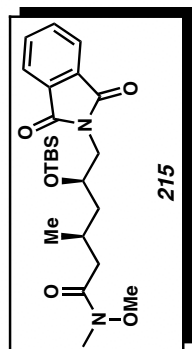


Figure A.82  $^1\text{H}$  NMR (300 MHz,  $\text{CDCl}_3$ ) of compound **215**.

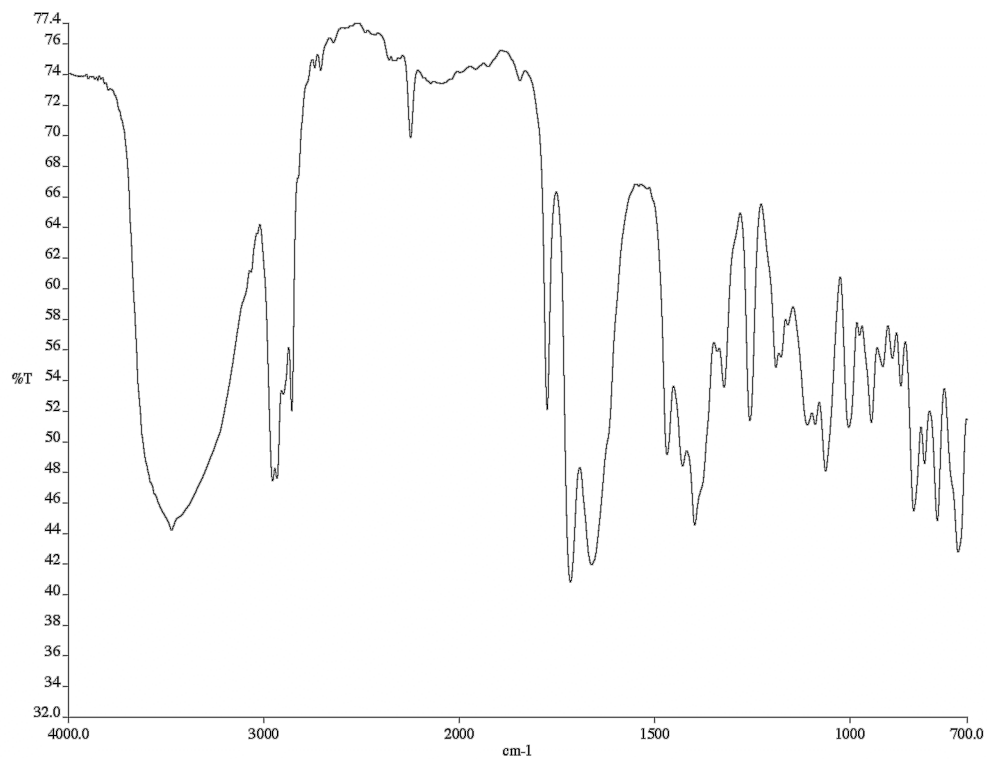


Figure A.83 Infrared spectrum (thin film/NaCl) of compound **215**.

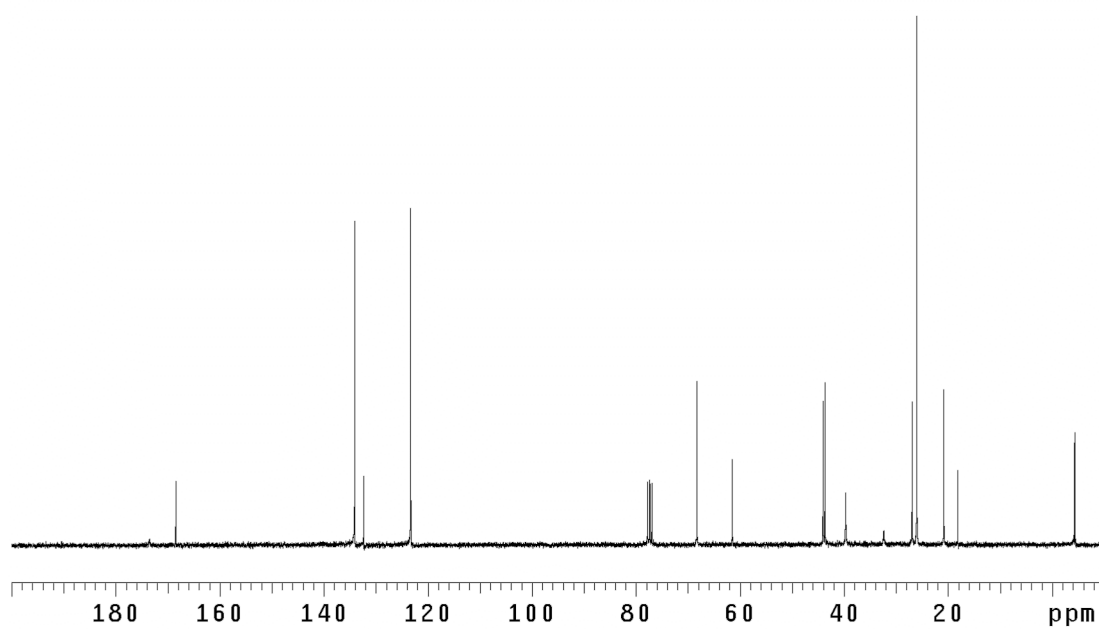


Figure A.84  $^{13}\text{C}$  NMR (75 MHz,  $\text{CDCl}_3$ ) of compound **215**.

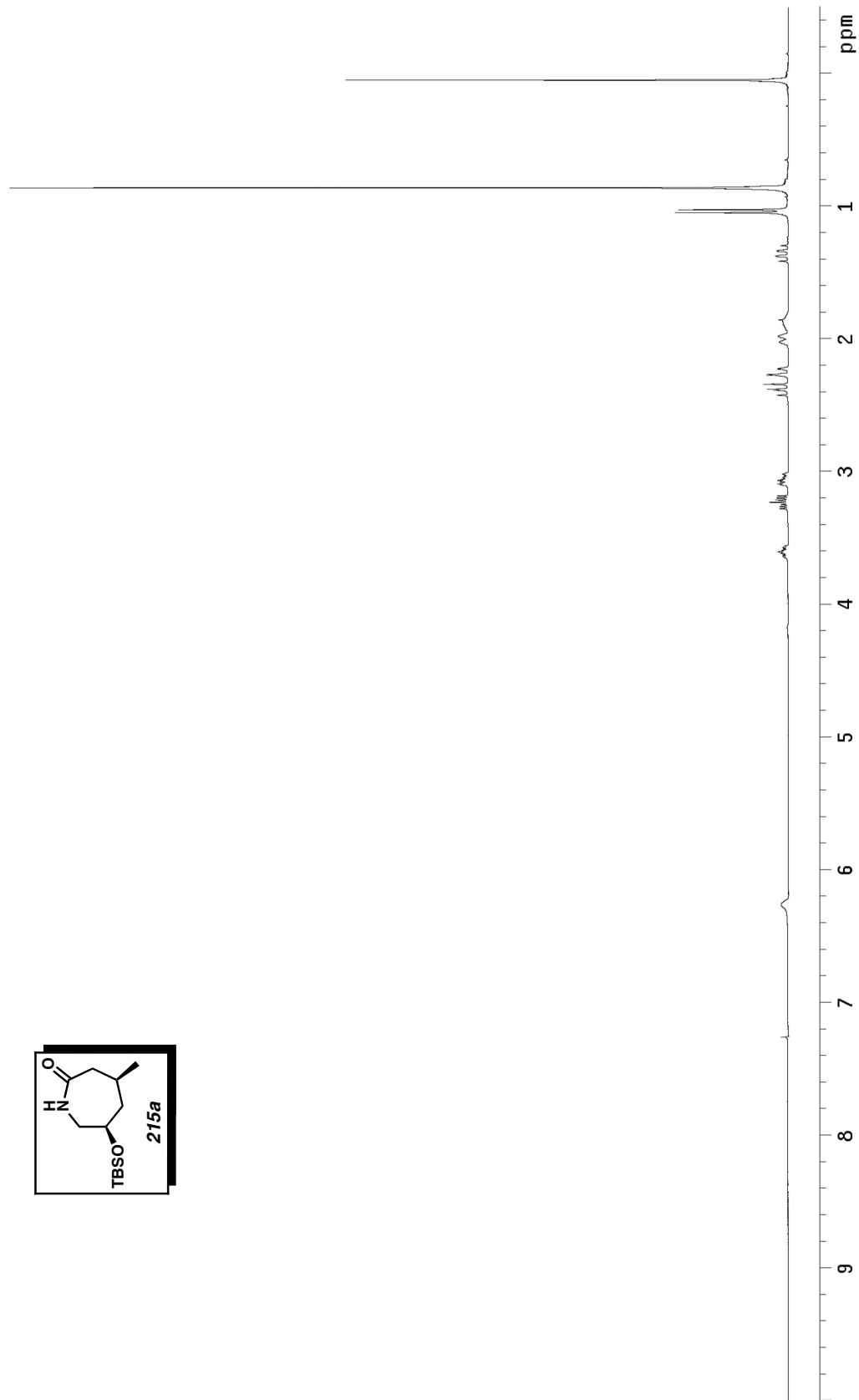
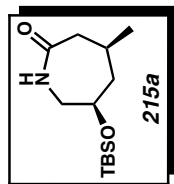


Figure A.85  $^1\text{H}$  NMR (300 MHz,  $\text{CDCl}_3$ ) of compound **215a**.

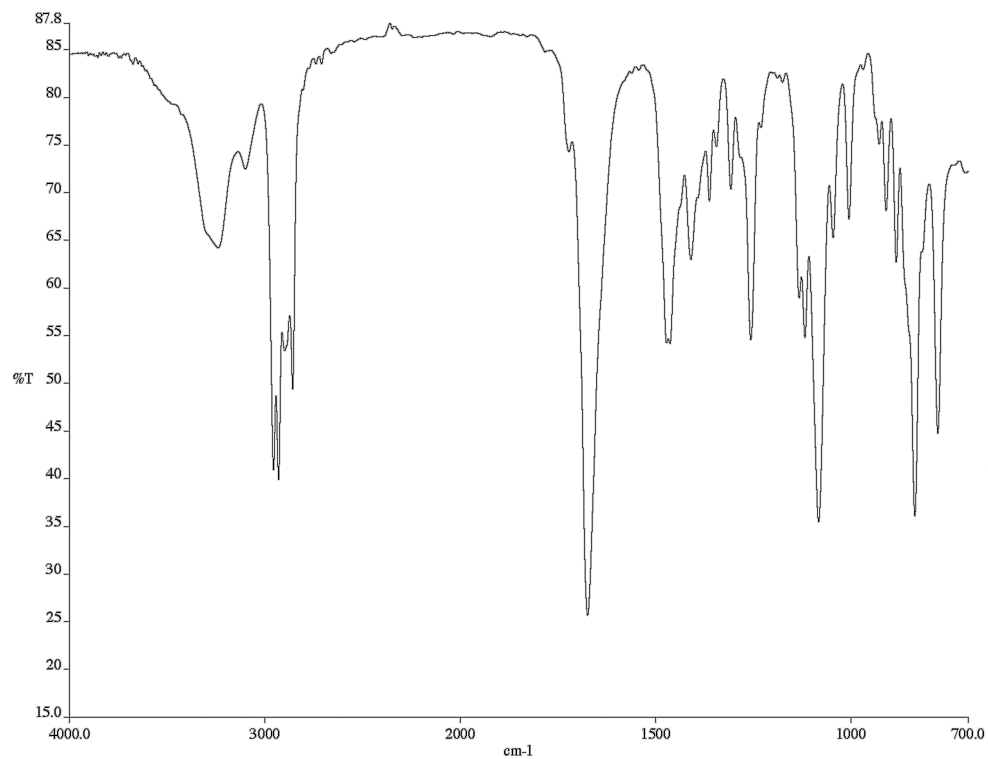


Figure A.86 Infrared spectrum (thin film/NaCl) of compound **215a**.

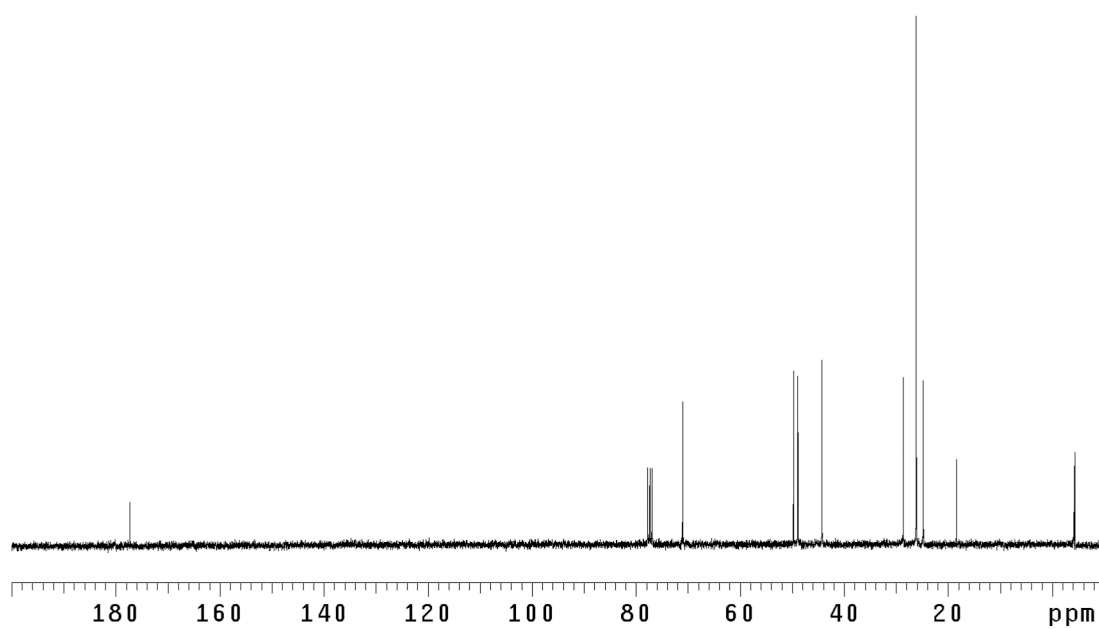


Figure A.87  $^{13}\text{C}$  NMR (75 MHz,  $\text{CDCl}_3$ ) of compound **215a**.

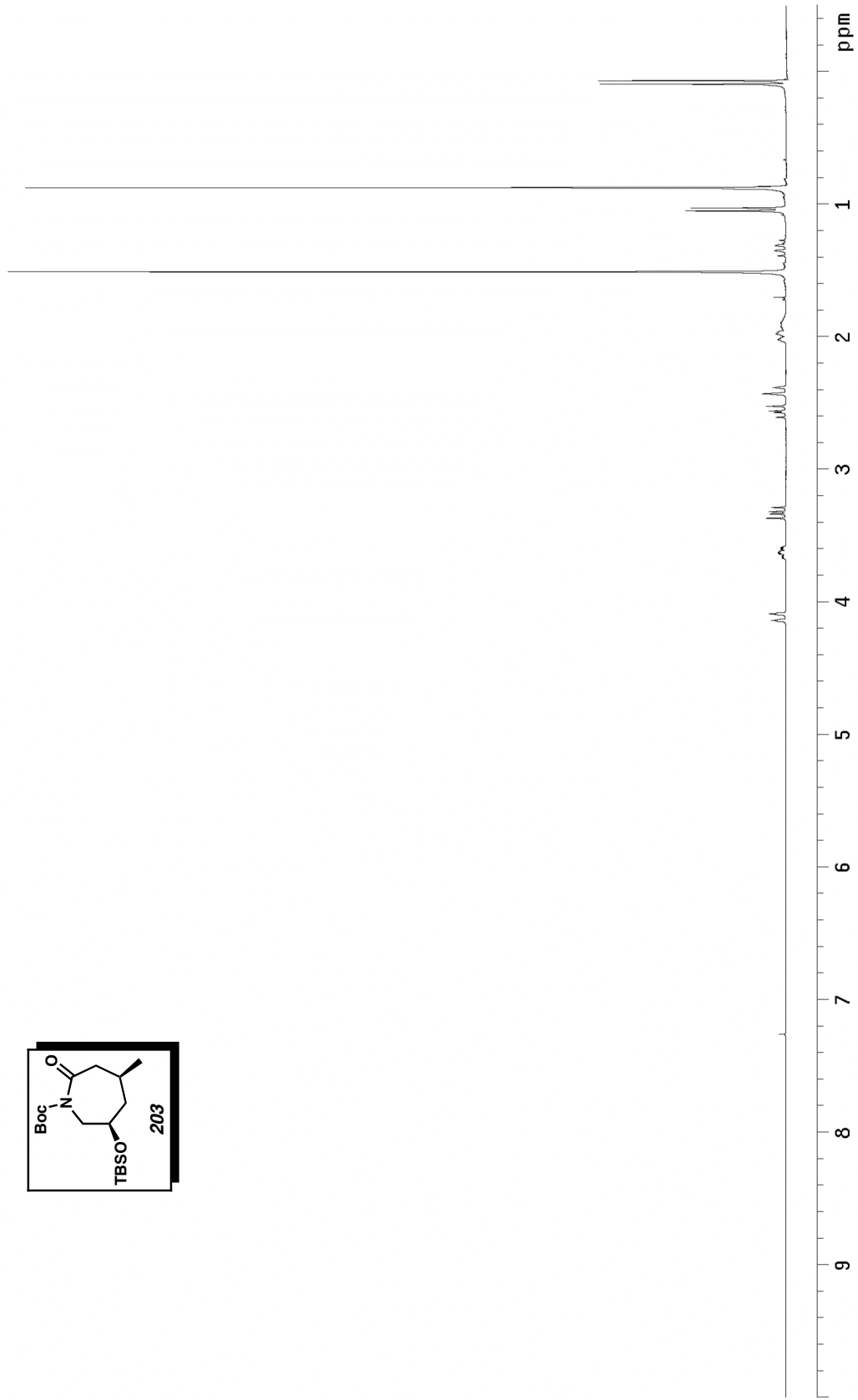
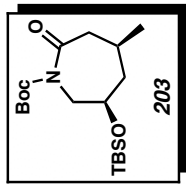


Figure A.88  $^1\text{H NMR}$  (300 MHz,  $\text{CDCl}_3$ ) of compound **203**.

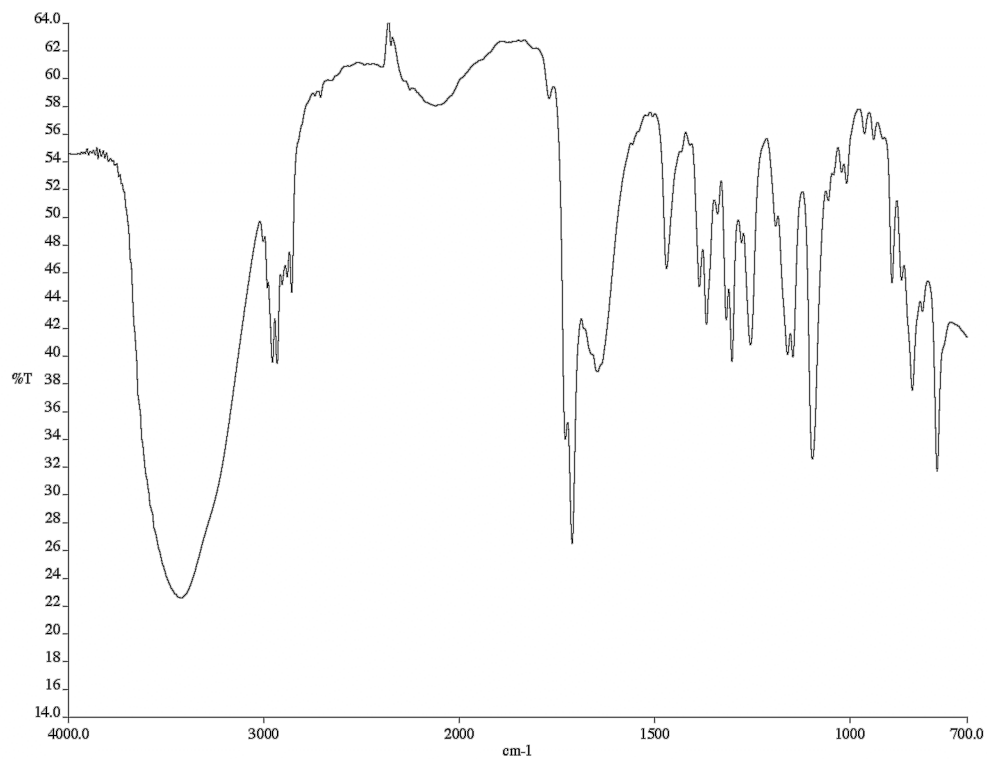


Figure A.89 Infrared spectrum (thin film/NaCl) of compound **203**.

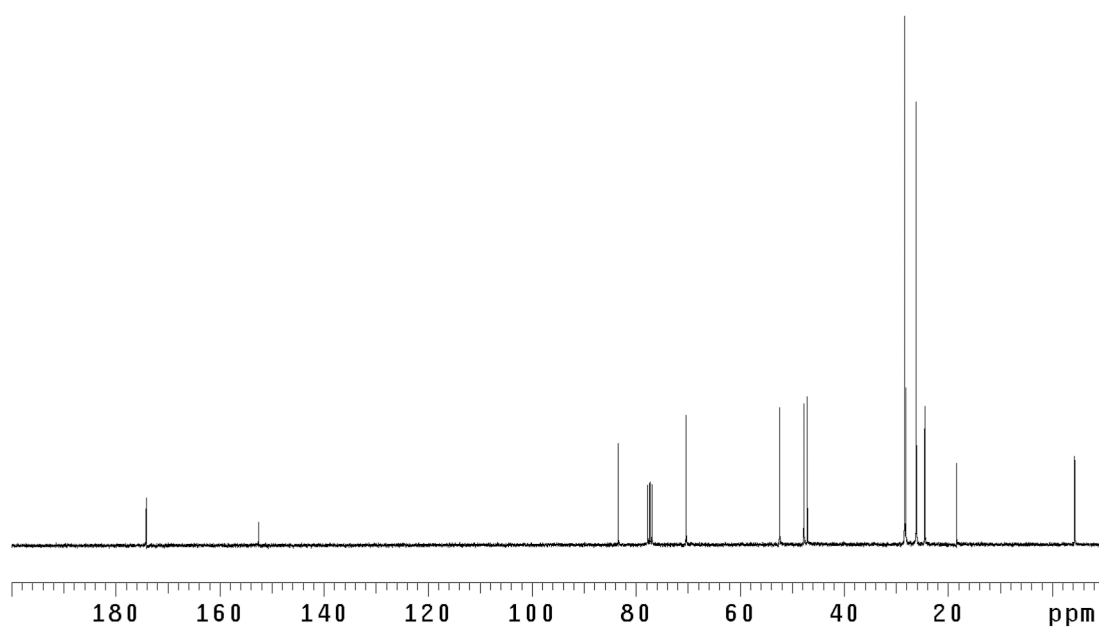


Figure A.90 <sup>13</sup>C NMR (75 MHz, CDCl<sub>3</sub>) of compound **203**.

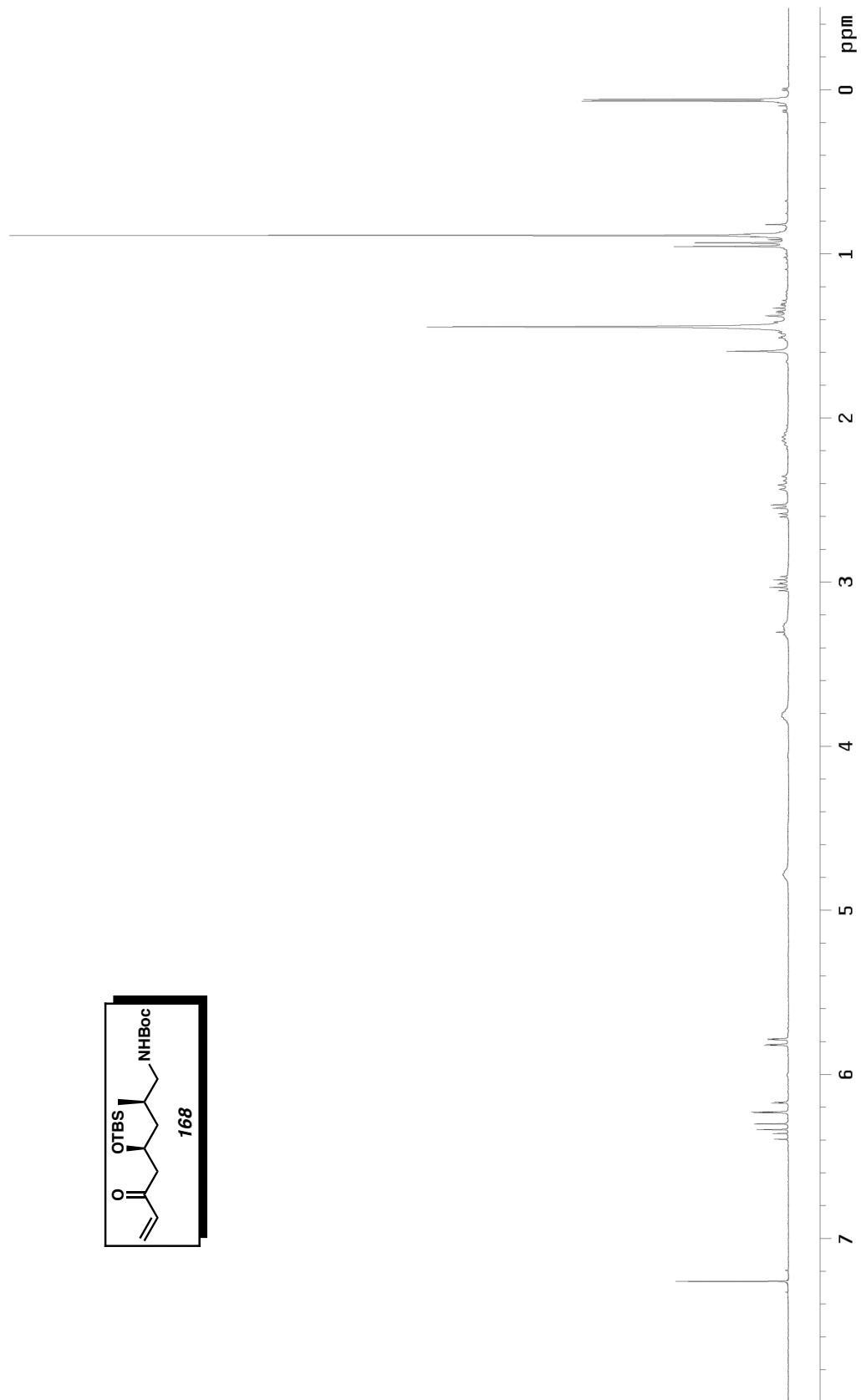
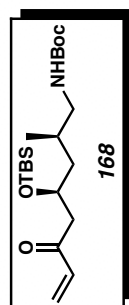


Figure A.91 <sup>1</sup>H NMR (500 MHz, CDCl<sub>3</sub>) of compound **168**.

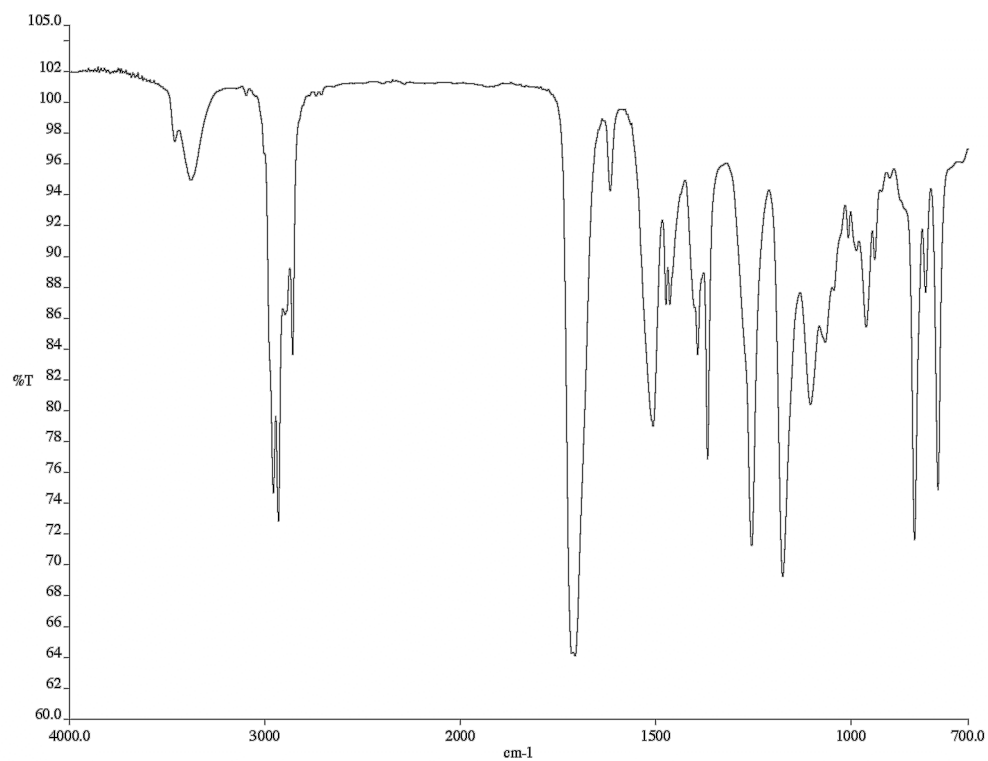


Figure A.92 Infrared spectrum (thin film/NaCl) of compound **168**.

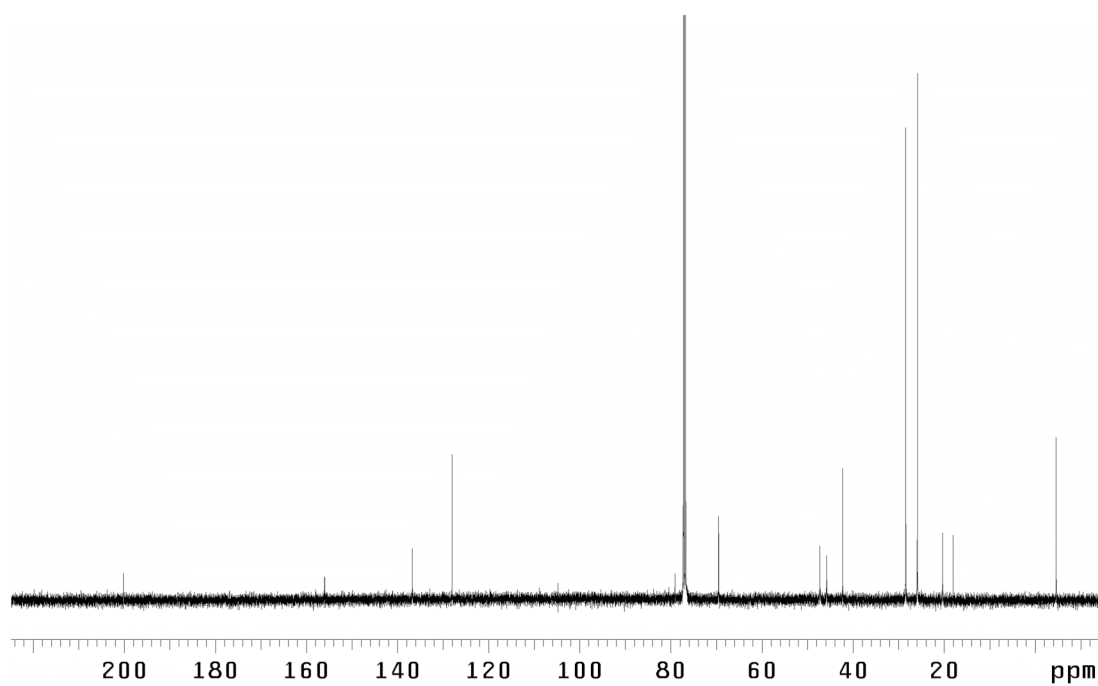


Figure A.93 <sup>13</sup>C NMR (125 MHz, CDCl<sub>3</sub>) of compound **168**.

CALIFORNIA INSTITUTE OF TECHNOLOGY  
BECKMAN INSTITUTE  
X-RAY CRYSTALLOGRAPHY LABORATORY

Crystal Structure Analysis of:

Lactone **184** (DCBo6)

(CCDC 175859)

Contents:

- Table 1. Crystal data
- Table 2. Atomic Coordinates
- Table 3. Full bond distances and angles (for deposit)
- Table 4. Anisotropic displacement parameters
- Table 5. Hydrogen atomic coordinates

Figure A.94 Representation of Lactone **184**

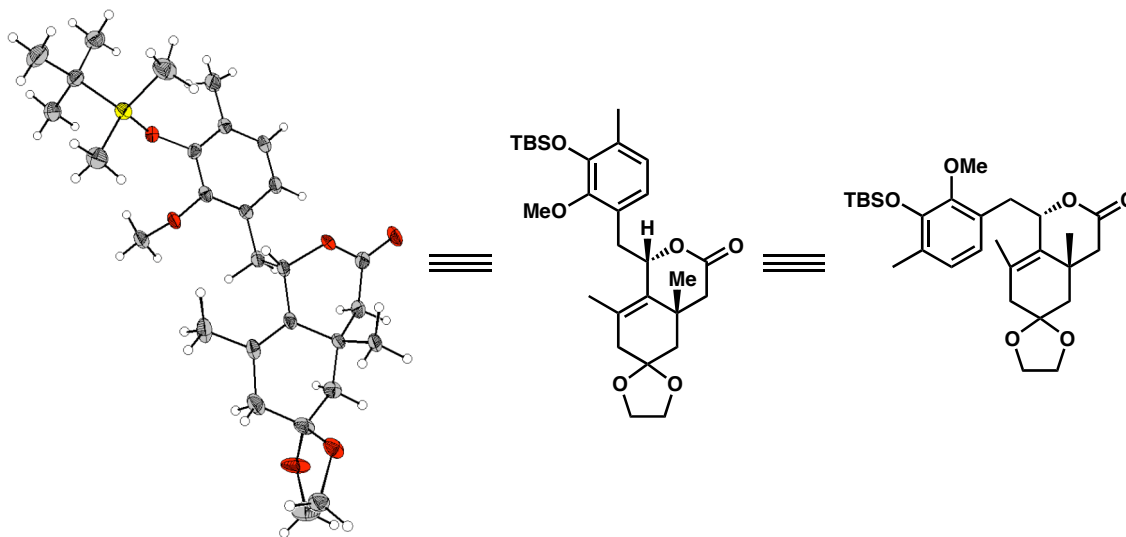


**Table 1.** Crystal data and structure refinement for DCB06\_(CCDC\_175859).

Empirical formula	C <sub>28</sub> H <sub>42</sub> O <sub>6</sub> Si
Formula weight	502.71
Crystallization Solvent	Hexanes
Crystal Habit	Block
Crystal size	0.33 x 0.17 x 0.14 mm <sup>3</sup>
Crystal color	Colorless

### Data Collection

Type of diffractometer	Bruker P4
Wavelength	0.71073 Å MoK $\alpha$
Data Collection Temperature	96(2) K
$\theta$ range for 8201 reflections used in lattice determination	2.79 to 26.49°
Unit cell dimensions	a = 29.220(3) Å b = 6.7215(8) Å c = 14.4249(17) Å
Volume	2833.0(6) Å <sup>3</sup>
Z	4
Crystal system	Monoclinic
Space group	P2 <sub>1</sub> /c
Density (calculated)	1.179 Mg/m <sup>3</sup>
F(000)	1088
Data collection program	Bruker SMART v5.054
$\theta$ range for data collection	1.39 to 28.38°
Completeness to $\theta = 28.38^\circ$	93.9 %
Index ranges	-37 $\leq$ h $\leq$ 38, -8 $\leq$ k $\leq$ 8, -19 $\leq$ l $\leq$ 19
Data collection scan type	$\omega$ scans at 5 $\phi$ settings
Data reduction program	Bruker SAINT v6.22
Reflections collected	38935
Independent reflections	6656 [R <sub>int</sub> = 0.0985]
Absorption coefficient	0.120 mm <sup>-1</sup>
Absorption correction	None
Max. and min. transmission	0.9829 and 0.9610

**Table 1 (cont.)**  
**Structure solution and Refinement**

Structure solution program	Bruker SHELXTL
Primary solution method	Direct methods
Secondary solution method	Difference Fourier map
Hydrogen placement	Difference Fourier map
Structure refinement program	Bruker SHELXTL
Refinement method	Full matrix least-squares on F <sup>2</sup>
Data / restraints / parameters	6656 / 0 / 484
Treatment of hydrogen atoms	Unrestrained
Goodness-of-fit on F <sup>2</sup>	1.403
Final R indices [I>2σ(I), 3988 reflections]	R <sub>1</sub> = 0.0584, wR <sub>2</sub> = 0.0804
R indices (all data)	R <sub>1</sub> = 0.1062, wR <sub>2</sub> = 0.0844
Type of weighting scheme used	Sigma
Weighting scheme used	w=1/σ <sup>2</sup> (F <sub>o</sub> <sup>2</sup> )
Max shift/error	0.001
Average shift/error	0.000
Largest diff. peak and hole	0.333 and -0.349 e.Å <sup>-3</sup>

### Special Refinement Details

Refinement of F<sup>2</sup> against ALL reflections. The weighted R-factor (wR) and goodness of fit (S) are based on F<sup>2</sup>, conventional R-factors (R) are based on F, with F set to zero for negative F<sup>2</sup>. The threshold expression of F<sup>2</sup> > 2σ(F<sup>2</sup>) is used only for calculating R-factors(gt) etc. and is not relevant to the choice of reflections for refinement. R-factors based on F<sup>2</sup> are statistically about twice as large as those based on F, and R-factors based on ALL data will be even larger.

All esds (except the esd in the dihedral angle between two l.s. planes) are estimated using the full covariance matrix. The cell esds are taken into account individually in the estimation of esds in distances, angles and torsion angles; correlations between esds in cell parameters are only used when they are defined by crystal symmetry. An approximate (isotropic) treatment of cell esds is used for estimating esds involving l.s. planes.

**Table 2.** Atomic coordinates ( $\times 10^4$ ) and equivalent isotropic displacement parameters ( $\text{\AA}^2 \times 10^3$ ) for DCBo6\_(CCDC\_175859).  $U(\text{eq})$  the trace of the orthogonalized  $U^{ij}$  tensor.

	x	y	z	$U_{\text{eq}}$
Si(1)	6142(1)	3545(1)	4087(1)	25(1)
O(1)	6571(1)	5169(2)	4135(1)	23(1)
O(2)	7293(1)	2606(2)	3725(1)	23(1)
O(3)	8211(1)	1108(2)	6169(1)	28(1)
O(4)	8640(1)	2202(2)	7317(1)	44(1)
O(5)	9414(1)	-4435(2)	4438(1)	30(1)
O(6)	9725(1)	-2363(2)	3364(1)	45(1)
C(1)	5665(1)	5006(3)	3527(1)	27(1)
C(2)	5841(1)	5905(4)	2608(2)	35(1)
C(3)	5260(1)	3633(5)	3329(2)	43(1)
C(4)	5503(1)	6694(4)	4154(2)	36(1)
C(5)	6282(1)	1358(4)	3362(2)	34(1)
C(6)	5995(1)	2734(5)	5291(2)	39(1)
C(7)	6962(1)	5171(3)	4672(1)	21(1)
C(8)	6990(1)	6481(3)	5429(1)	24(1)
C(9)	6595(1)	7823(4)	5660(2)	37(1)
C(10)	7397(1)	6526(4)	5928(1)	27(1)
C(11)	7762(1)	5352(3)	5700(1)	26(1)
C(12)	7740(1)	4049(3)	4942(1)	22(1)
C(13)	7334(1)	3973(3)	4446(1)	20(1)
C(14)	7349(1)	3475(4)	2815(1)	32(1)
C(15)	8145(1)	2785(3)	4670(1)	22(1)
C(16)	8169(1)	761(3)	5164(1)	22(1)
C(17)	8623(1)	1598(3)	6522(1)	28(1)
C(18)	9030(1)	1238(4)	5922(2)	26(1)
C(19)	8979(1)	-684(3)	5354(1)	19(1)
C(20)	8948(1)	-2437(4)	6036(1)	24(1)
C(21)	9394(1)	-899(3)	4715(1)	24(1)
C(22)	9349(1)	-2544(3)	4006(1)	28(1)
C(23)	9638(1)	-5668(3)	3767(2)	29(1)
C(24)	9927(1)	-4215(4)	3241(2)	39(1)
C(25)	8901(1)	-2427(4)	3480(2)	33(1)
C(26)	8502(1)	-1441(3)	3960(1)	24(1)
C(27)	8074(1)	-1401(5)	3388(2)	35(1)
C(28)	8545(1)	-548(3)	4787(1)	19(1)

**Table 3.** Bond lengths [Å] and angles [°] for DCBo6\_(CCDC\_175859).

Si(1)-O(1)	1.6629(15)	C(16)-C(28)	1.510(3)
Si(1)-C(5)	1.849(3)	C(16)-H(16)	0.995(16)
Si(1)-C(6)	1.872(2)	C(17)-C(18)	1.490(3)
Si(1)-C(1)	1.887(2)	C(18)-C(19)	1.538(3)
O(1)-C(7)	1.379(2)	C(18)-H(18A)	0.96(2)
O(2)-C(13)	1.392(2)	C(18)-H(18B)	0.96(2)
O(2)-C(14)	1.446(2)	C(19)-C(28)	1.512(3)
O(3)-C(17)	1.350(2)	C(19)-C(21)	1.531(3)
O(3)-C(16)	1.473(2)	C(19)-C(20)	1.538(3)
O(4)-C(17)	1.218(2)	C(20)-H(20A)	0.987(19)
O(5)-C(22)	1.428(2)	C(20)-H(20B)	1.016(18)
O(5)-C(23)	1.433(2)	C(20)-H(20C)	1.003(19)
O(6)-C(24)	1.389(3)	C(21)-C(22)	1.512(3)
O(6)-C(22)	1.443(2)	C(21)-H(21A)	0.99(2)
C(1)-C(4)	1.527(3)	C(21)-H(21B)	0.99(2)
C(1)-C(3)	1.528(3)	C(22)-C(25)	1.516(3)
C(1)-C(2)	1.545(3)	C(23)-C(24)	1.498(3)
C(2)-H(2A)	1.05(2)	C(23)-H(23A)	0.98(2)
C(2)-H(2B)	0.99(2)	C(23)-H(23B)	0.940(19)
C(2)-H(2C)	1.00(2)	C(24)-H(24A)	0.86(3)
C(3)-H(3A)	0.98(2)	C(24)-H(24B)	0.97(3)
C(3)-H(3B)	0.95(2)	C(25)-C(26)	1.509(3)
C(3)-H(3C)	1.04(2)	C(25)-H(25A)	0.99(2)
C(4)-H(4A)	0.99(2)	C(25)-H(25B)	0.98(2)
C(4)-H(4B)	0.99(2)	C(26)-C(28)	1.340(2)
C(4)-H(4C)	0.99(2)	C(26)-C(27)	1.498(3)
C(5)-H(5A)	0.97(2)	C(27)-H(27A)	0.95(2)
C(5)-H(5B)	1.01(2)	C(27)-H(27B)	0.97(2)
C(5)-H(5C)	0.98(2)	C(27)-H(27C)	1.06(2)
C(6)-H(6A)	1.03(3)		
C(6)-H(6B)	0.98(3)	O(1)-Si(1)-C(5)	112.26(10)
C(6)-H(6C)	0.98(2)	O(1)-Si(1)-C(6)	109.05(11)
C(7)-C(13)	1.392(3)	C(5)-Si(1)-C(6)	110.16(13)
C(7)-C(8)	1.405(3)	O(1)-Si(1)-C(1)	103.44(9)
C(8)-C(10)	1.389(3)	C(5)-Si(1)-C(1)	109.60(11)
C(8)-C(9)	1.503(3)	C(6)-Si(1)-C(1)	112.21(11)
C(9)-H(9A)	1.02(2)	C(7)-O(1)-Si(1)	130.34(12)
C(9)-H(9B)	0.92(2)	C(13)-O(2)-C(14)	113.73(17)
C(9)-H(9C)	0.95(2)	C(17)-O(3)-C(16)	118.89(15)
C(10)-C(11)	1.369(3)	C(22)-O(5)-C(23)	106.28(14)
C(10)-H(10)	0.98(2)	C(24)-O(6)-C(22)	109.25(17)
C(11)-C(12)	1.403(3)	C(4)-C(1)-C(3)	108.6(2)
C(11)-H(11)	0.965(19)	C(4)-C(1)-C(2)	108.7(2)
C(12)-C(13)	1.388(3)	C(3)-C(1)-C(2)	109.5(2)
C(12)-C(15)	1.508(3)	C(4)-C(1)-Si(1)	111.25(15)
C(14)-H(14A)	0.99(2)	C(3)-C(1)-Si(1)	109.77(18)
C(14)-H(14B)	1.00(2)	C(2)-C(1)-Si(1)	108.96(15)
C(14)-H(14C)	1.05(2)	C(1)-C(2)-H(2A)	113.2(11)
C(15)-C(16)	1.538(3)	C(1)-C(2)-H(2B)	109.5(13)
C(15)-H(15A)	1.047(18)	H(2A)-C(2)-H(2B)	106.4(17)
C(15)-H(15B)	0.950(18)	C(1)-C(2)-H(2C)	108.6(12)

H(2A)-C(2)-H(2C)	108.2(18)	H(14A)-C(14)-H(14C)	108.8(17)
H(2B)-C(2)-H(2C)	110.9(18)	H(14B)-C(14)-H(14C)	114.6(17)
C(1)-C(3)-H(3A)	110.1(14)	C(12)-C(15)-C(16)	114.35(16)
C(1)-C(3)-H(3B)	110.8(14)	C(12)-C(15)-H(15A)	112.3(10)
H(3A)-C(3)-H(3B)	108.4(19)	C(16)-C(15)-H(15A)	104.7(10)
C(1)-C(3)-H(3C)	113.7(12)	C(12)-C(15)-H(15B)	109.6(11)
H(3A)-C(3)-H(3C)	108.5(18)	C(16)-C(15)-H(15B)	108.4(11)
H(3B)-C(3)-H(3C)	105.0(19)	H(15A)-C(15)-H(15B)	107.1(14)
C(1)-C(4)-H(4A)	109.9(14)	O(3)-C(16)-C(28)	112.77(15)
C(1)-C(4)-H(4B)	112.8(12)	O(3)-C(16)-C(15)	108.69(16)
H(4A)-C(4)-H(4B)	110.7(17)	C(28)-C(16)-C(15)	112.34(16)
C(1)-C(4)-H(4C)	115.2(12)	O(3)-C(16)-H(16)	101.4(9)
H(4A)-C(4)-H(4C)	104.1(17)	C(28)-C(16)-H(16)	113.5(10)
H(4B)-C(4)-H(4C)	103.8(18)	C(15)-C(16)-H(16)	107.4(10)
Si(1)-C(5)-H(5A)	113.1(14)	O(4)-C(17)-O(3)	118.11(19)
Si(1)-C(5)-H(5B)	112.4(13)	O(4)-C(17)-C(18)	124.7(2)
H(5A)-C(5)-H(5B)	108(2)	O(3)-C(17)-C(18)	117.06(17)
Si(1)-C(5)-H(5C)	110.5(14)	C(17)-C(18)-C(19)	111.65(18)
H(5A)-C(5)-H(5C)	106.6(19)	C(17)-C(18)-H(18A)	109.4(12)
H(5B)-C(5)-H(5C)	106.0(18)	C(19)-C(18)-H(18A)	112.2(12)
Si(1)-C(6)-H(6A)	110.3(13)	C(17)-C(18)-H(18B)	111.5(11)
Si(1)-C(6)-H(6B)	114.0(13)	C(19)-C(18)-H(18B)	111.1(12)
H(6A)-C(6)-H(6B)	107(2)	H(18A)-C(18)-H(18B)	100.5(16)
Si(1)-C(6)-H(6C)	107.1(13)	C(28)-C(19)-C(21)	110.20(15)
H(6A)-C(6)-H(6C)	111.0(19)	C(28)-C(19)-C(18)	108.56(17)
H(6B)-C(6)-H(6C)	108(2)	C(21)-C(19)-C(18)	108.89(16)
O(1)-C(7)-C(13)	120.97(17)	C(28)-C(19)-C(20)	110.06(16)
O(1)-C(7)-C(8)	119.01(17)	C(21)-C(19)-C(20)	111.11(17)
C(13)-C(7)-C(8)	119.93(18)	C(18)-C(19)-C(20)	107.94(16)
C(10)-C(8)-C(7)	117.79(19)	C(19)-C(20)-H(20A)	111.0(10)
C(10)-C(8)-C(9)	121.9(2)	C(19)-C(20)-H(20B)	108.3(10)
C(7)-C(8)-C(9)	120.24(19)	H(20A)-C(20)-H(20B)	107.8(14)
C(8)-C(9)-H(9A)	109.2(13)	C(19)-C(20)-H(20C)	110.5(11)
C(8)-C(9)-H(9B)	112.5(13)	H(20A)-C(20)-H(20C)	104.4(15)
H(9A)-C(9)-H(9B)	111.6(18)	H(20B)-C(20)-H(20C)	114.8(14)
C(8)-C(9)-H(9C)	112.0(13)	C(22)-C(21)-C(19)	113.99(17)
H(9A)-C(9)-H(9C)	106.5(18)	C(22)-C(21)-H(21A)	107.4(12)
H(9B)-C(9)-H(9C)	104.8(19)	C(19)-C(21)-H(21A)	112.5(11)
C(11)-C(10)-C(8)	122.0(2)	C(22)-C(21)-H(21B)	107.6(10)
C(11)-C(10)-H(10)	120.2(12)	C(19)-C(21)-H(21B)	110.2(10)
C(8)-C(10)-H(10)	117.8(12)	H(21A)-C(21)-H(21B)	104.7(16)
C(10)-C(11)-C(12)	120.8(2)	O(5)-C(22)-O(6)	104.75(15)
C(10)-C(11)-H(11)	120.4(11)	O(5)-C(22)-C(21)	110.15(16)
C(12)-C(11)-H(11)	118.8(11)	O(6)-C(22)-C(21)	107.79(17)
C(13)-C(12)-C(11)	117.63(19)	O(5)-C(22)-C(25)	112.29(19)
C(13)-C(12)-C(15)	121.07(18)	O(6)-C(22)-C(25)	109.41(17)
C(11)-C(12)-C(15)	121.30(19)	C(21)-C(22)-C(25)	112.09(19)
C(12)-C(13)-C(7)	121.79(18)	O(5)-C(23)-C(24)	102.91(18)
C(12)-C(13)-O(2)	118.78(17)	O(5)-C(23)-H(23A)	110.8(11)
C(7)-C(13)-O(2)	119.39(17)	C(24)-C(23)-H(23A)	113.5(12)
O(2)-C(14)-H(14A)	107.7(11)	O(5)-C(23)-H(23B)	109.3(12)
O(2)-C(14)-H(14B)	103.7(13)	C(24)-C(23)-H(23B)	112.7(12)
H(14A)-C(14)-H(14B)	111.7(17)	H(23A)-C(23)-H(23B)	107.6(17)
O(2)-C(14)-H(14C)	109.9(11)	O(6)-C(24)-C(23)	106.3(2)

O(6)-C(24)-H(24A)	111(2)
C(23)-C(24)-H(24A)	121(2)
O(6)-C(24)-H(24B)	107.4(15)
C(23)-C(24)-H(24B)	109.6(15)
H(24A)-C(24)-H(24B)	101(2)
C(26)-C(25)-C(22)	117.35(18)
C(26)-C(25)-H(25A)	105.2(13)
C(22)-C(25)-H(25A)	103.6(13)
C(26)-C(25)-H(25B)	109.0(12)
C(22)-C(25)-H(25B)	108.3(12)
H(25A)-C(25)-H(25B)	113.4(18)
C(28)-C(26)-C(27)	124.0(2)
C(28)-C(26)-C(25)	122.27(19)
C(27)-C(26)-C(25)	113.50(18)
C(26)-C(27)-H(27A)	111.8(14)
C(26)-C(27)-H(27B)	110.0(13)
H(27A)-C(27)-H(27B)	108.2(19)
C(26)-C(27)-H(27C)	118.2(11)
H(27A)-C(27)-H(27C)	102.5(18)
H(27B)-C(27)-H(27C)	105.5(18)
C(26)-C(28)-C(16)	120.96(18)
C(26)-C(28)-C(19)	122.09(18)
C(16)-C(28)-C(19)	116.83(16)

---

**Table 4.** Anisotropic displacement parameters ( $\text{\AA}^2 \times 10^4$ ) for DCBo6\_(CCDC\_175859).  
The anisotropic displacement factor exponent takes the form:  
 $-2\pi^2 [ h^2 a^{*2} U^{11} + \dots + 2 h k a^* b^* U^{12} ]$

	U <sup>11</sup>	U <sup>22</sup>	U <sup>33</sup>	U <sup>23</sup>	U <sup>13</sup>	U <sup>12</sup>
Si(1)	252(3)	279(4)	224(3)	4(3)	10(3)	-5(3)
O(1)	223(8)	280(9)	195(7)	-17(6)	-35(6)	7(6)
O(2)	277(8)	286(9)	134(7)	-31(6)	-19(6)	-16(7)
O(3)	292(9)	444(10)	110(7)	15(7)	31(6)	67(7)
O(4)	623(12)	535(12)	148(8)	-121(7)	-86(7)	211(9)
O(5)	483(10)	221(9)	186(7)	34(7)	67(7)	24(7)
O(6)	607(11)	324(10)	426(9)	130(8)	373(8)	165(8)
C(1)	206(12)	327(14)	273(12)	19(10)	-8(10)	-14(10)
C(2)	339(16)	452(18)	257(13)	51(12)	-44(12)	55(14)
C(3)	243(15)	500(19)	547(18)	-31(17)	-58(13)	-29(14)
C(4)	287(15)	436(17)	370(15)	43(13)	11(12)	69(14)
C(5)	344(16)	311(15)	366(15)	-48(12)	17(12)	-74(14)
C(6)	465(18)	396(17)	313(14)	73(13)	77(13)	51(15)
C(7)	190(12)	250(13)	199(11)	50(9)	-14(9)	-7(10)
C(8)	254(12)	283(13)	190(10)	6(10)	-4(9)	29(10)
C(9)	400(17)	389(17)	309(15)	-133(14)	-63(12)	122(14)
C(10)	315(14)	336(14)	170(11)	-59(11)	-37(10)	-4(11)
C(11)	274(14)	329(14)	165(11)	3(10)	-41(10)	-10(11)
C(12)	225(12)	279(13)	143(10)	36(9)	23(9)	1(9)
C(13)	237(12)	217(13)	151(10)	13(9)	9(9)	-59(10)
C(14)	336(16)	453(16)	160(11)	-4(12)	-1(10)	-19(14)
C(15)	208(13)	273(13)	170(11)	13(10)	-15(9)	-33(10)
C(16)	202(12)	323(14)	128(10)	10(9)	-18(9)	-19(10)
C(17)	328(14)	308(14)	207(11)	3(10)	-45(10)	114(11)
C(18)	266(14)	297(15)	202(11)	-55(11)	-68(10)	5(11)
C(19)	191(11)	245(12)	126(10)	-11(9)	3(8)	-18(9)
C(20)	228(14)	356(15)	125(11)	21(11)	-11(10)	15(11)
C(21)	253(13)	218(14)	240(12)	33(10)	54(10)	-15(10)
C(22)	378(14)	250(13)	209(11)	52(10)	128(10)	45(11)
C(23)	364(15)	201(13)	292(13)	-18(11)	14(12)	51(12)
C(24)	351(17)	247(15)	576(18)	-68(13)	127(15)	-24(12)
C(25)	501(16)	330(16)	164(12)	6(12)	1(11)	53(13)
C(26)	318(13)	239(12)	150(10)	21(10)	-44(9)	-16(10)
C(27)	458(17)	310(16)	269(13)	-22(13)	-157(12)	-2(13)
C(28)	208(12)	244(13)	125(10)	42(9)	2(9)	-23(9)

**Table 5.** Hydrogen coordinates ( $\times 10^4$ ) and isotropic displacement parameters ( $\text{\AA}^2 \times 10^3$ ) for DCBo6\_(CCDC\_175859).

	x	y	z	$U_{\text{iso}}$
H(2A)	6133(7)	6800(30)	2693(13)	38(6)
H(2B)	5928(7)	4820(40)	2180(15)	49(7)
H(2C)	5594(8)	6750(40)	2334(15)	49(7)
H(3A)	5005(8)	4400(40)	3059(15)	54(8)
H(3B)	5343(7)	2620(40)	2906(15)	47(8)
H(3C)	5141(7)	2890(30)	3909(15)	48(7)
H(4A)	5371(7)	6140(40)	4734(15)	53(7)
H(4B)	5749(7)	7660(30)	4298(13)	29(6)
H(4C)	5256(7)	7520(30)	3897(14)	38(6)
H(5A)	6544(8)	620(40)	3588(15)	55(8)
H(5B)	6018(8)	410(40)	3306(15)	53(7)
H(5C)	6356(8)	1770(40)	2728(16)	53(7)
H(6A)	5864(8)	3910(40)	5662(16)	68(8)
H(6B)	5767(8)	1660(40)	5317(15)	60(8)
H(6C)	6278(8)	2230(30)	5577(15)	50(7)
H(9A)	6319(8)	6970(30)	5851(14)	47(7)
H(9B)	6667(7)	8740(30)	6106(14)	36(7)
H(9C)	6499(7)	8590(30)	5140(16)	48(7)
H(10)	7416(7)	7440(30)	6454(14)	36(6)
H(11)	8045(6)	5450(30)	6044(12)	27(6)
H(14A)	7663(7)	4000(30)	2774(12)	28(6)
H(14B)	7302(7)	2330(40)	2385(15)	49(7)
H(14C)	7118(7)	4650(30)	2727(13)	39(6)
H(15A)	8144(6)	2430(30)	3962(13)	27(5)
H(15B)	8421(6)	3490(30)	4792(11)	16(5)
H(16)	7859(6)	150(20)	5125(10)	8(4)
H(18A)	9081(6)	2380(30)	5535(13)	31(6)
H(18B)	9308(7)	1230(30)	6276(13)	31(6)
H(20A)	8897(6)	-3700(30)	5704(12)	18(5)
H(20B)	9252(6)	-2550(30)	6377(12)	21(5)
H(20C)	8673(7)	-2290(30)	6446(12)	26(5)
H(21A)	9683(7)	-1130(30)	5063(13)	34(6)
H(21B)	9448(6)	360(30)	4373(12)	24(5)
H(23A)	9815(7)	-6710(30)	4072(13)	34(6)
H(23B)	9417(6)	-6290(30)	3393(13)	24(6)
H(24A)	9995(11)	-4420(50)	2670(20)	112(14)
H(24B)	10229(9)	-4160(40)	3514(16)	64(9)
H(25A)	8972(7)	-1560(30)	2948(15)	51(7)
H(25B)	8812(7)	-3770(30)	3298(14)	39(7)
H(27A)	8088(8)	-420(40)	2917(16)	56(8)
H(27B)	8027(7)	-2690(40)	3096(15)	48(7)
H(27C)	7762(7)	-1060(30)	3722(13)	43(7)

CALIFORNIA INSTITUTE OF TECHNOLOGY  
BECKMAN INSTITUTE  
X-RAY CRYSTALLOGRAPHY LABORATORY

Crystal Structure Analysis of:

Acid **187**•CHCl<sub>3</sub> (DCBo5)

(CCDC 175588)

Contents:

- Table 1. Crystal data
- Table 2. Atomic Coordinates
- Table 3. Full bond distances and angles (for deposit)
- Table 4. Anisotropic displacement parameters
- Table 5. Hydrogen atomic coordinates
- Table 6. Hydrogen bonds

Figure A.95 Representation of Acid **187**•CHCl<sub>3</sub>

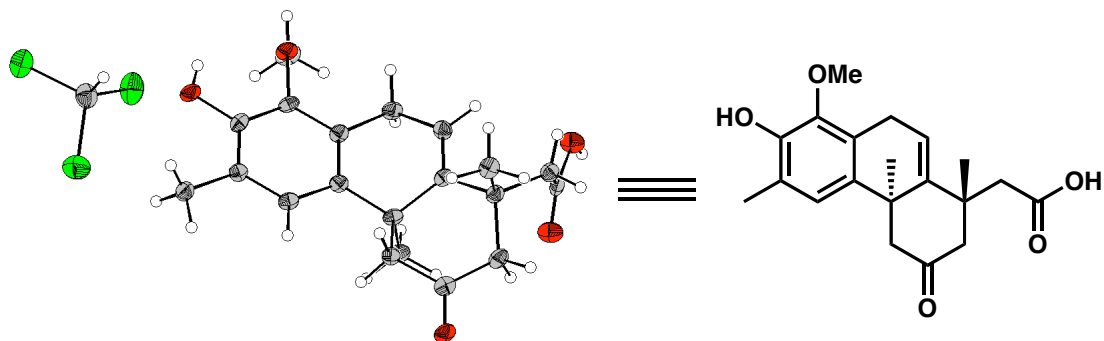


**Table 1.** Crystal data and structure refinement for DCBO<sub>5</sub> (CCDC 175588).

Empirical formula	C <sub>20</sub> H <sub>24</sub> O <sub>5</sub> · CHCl <sub>3</sub>
Formula weight	463.76
Crystallization Solvent	Chloroform
Crystal Habit	Fragment
Crystal size	0.22 x 0.15 x 0.15 mm <sup>3</sup>
Crystal color	Colorless

### Data Collection

Preliminary Photos	Rotation	
Type of diffractometer	Bruker SMART 1000	
Wavelength	0.71073 Å MoK $\alpha$	
Data Collection Temperature	98(2) K	
$\theta$ range for 4336 reflections used in lattice determination	2.47 to 25.80°	
Unit cell dimensions	a = 11.137(3) Å b = 13.282(3) Å c = 15.008(4) Å	$\beta = 98.762(4)^\circ$
Volume	2194.3(10) Å <sup>3</sup>	
Z	4	
Crystal system	Monoclinic	
Space group	P2 <sub>1</sub> /n	
Density (calculated)	1.404 Mg/m <sup>3</sup>	
F(000)	968	
Data collection program	Bruker SMART v5.054	
$\theta$ range for data collection	2.06 to 28.36°	
Completeness to $\theta = 28.36^\circ$	93.7 %	
Index ranges	-14 ≤ h ≤ 14, -17 ≤ k ≤ 17, -19 ≤ l ≤ 19	
Data collection scan type	$\omega$ scans at 5 $\phi$ settings	
Data reduction program	Bruker SAINT v6.22	
Reflections collected	32070	
Independent reflections	5144 [R <sub>int</sub> = 0.1503]	
Absorption coefficient	0.447 mm <sup>-1</sup>	
Absorption correction	None	
Max. and min. transmission	0.9368 and 0.9072	

**Table 1 (cont.)**  
**Structure solution and Refinement**

Structure solution program	SHELXS-97 (Sheldrick, 1990)
Primary solution method	Direct methods
Secondary solution method	Difference Fourier map
Hydrogen placement	Difference Fourier map
Structure refinement program	SHELXL-97 (Sheldrick, 1997)
Refinement method	Full matrix least-squares on F <sup>2</sup>
Data / restraints / parameters	5144 / 0 / 362
Treatment of hydrogen atoms	Unrestrained
Goodness-of-fit on F <sup>2</sup>	1.064
Final R indices [I > 2σ(I), 2718 reflections]	R <sub>1</sub> = 0.0468, wR <sub>2</sub> = 0.0744
R indices (all data)	R <sub>1</sub> = 0.1218, wR <sub>2</sub> = 0.0862
Type of weighting scheme used	Sigma
Weighting scheme used	w = 1/σ <sup>2</sup> (F <sub>o</sub> <sup>2</sup> )
Max shift/error	0.000
Average shift/error	0.000
Largest diff. peak and hole	0.402 and -0.348 e.Å <sup>-3</sup>

### Special Refinement Details

Refinement of F<sup>2</sup> against ALL reflections. The weighted R-factor (wR) and goodness of fit (S) are based on F<sup>2</sup>, conventional R-factors (R) are based on F, with F set to zero for negative F<sup>2</sup>. The threshold expression of F<sup>2</sup> > 2σ(F<sup>2</sup>) is used only for calculating R-factors(gt) etc. and is not relevant to the choice of reflections for refinement. R-factors based on F<sup>2</sup> are statistically about twice as large as those based on F, and R-factors based on ALL data will be even larger.

All esds (except the esd in the dihedral angle between two l.s. planes) are estimated using the full covariance matrix. The cell esds are taken into account individually in the estimation of esds in distances, angles and torsion angles; correlations between esds in cell parameters are only used when they are defined by crystal symmetry. An approximate (isotropic) treatment of cell esds is used for estimating esds involving l.s. planes.

**Table 2.** Atomic coordinates ( $\times 10^4$ ) and equivalent isotropic displacement parameters ( $\text{\AA}^2 \times 10^3$ ) for DCBo5 (CCDC 175588).  $U(\text{eq})$  is defined as the trace of the orthogonalized  $U^{ij}$  tensor.

	x	y	z	$U_{\text{eq}}$
O(1)	2996(2)	1246(2)	424(1)	23(1)
O(2)	3667(2)	289(1)	2011(1)	23(1)
O(3)	10816(2)	767(1)	809(1)	24(1)
O(4)	10340(2)	21(1)	3988(1)	28(1)
O(5)	9289(2)	-1153(1)	4583(1)	27(1)
C(1)	4196(2)	1102(2)	735(2)	20(1)
C(2)	4579(2)	649(2)	1547(2)	19(1)
C(3)	5789(2)	489(2)	1874(2)	19(1)
C(4)	6178(2)	-65(2)	2727(2)	22(1)
C(5)	7352(2)	-608(2)	2734(2)	20(1)
C(6)	8184(2)	-314(2)	2243(2)	18(1)
C(7)	9343(2)	-929(2)	2231(2)	20(1)
C(8)	9093(3)	-1750(2)	1504(2)	25(1)
C(9)	9748(3)	-1452(2)	3131(2)	22(1)
C(10)	9824(2)	-789(2)	3926(2)	21(1)
C(11)	10377(2)	-254(2)	2003(2)	23(1)
C(12)	10036(2)	410(2)	1214(2)	21(1)
C(13)	8738(2)	652(2)	926(2)	19(1)
C(14)	7993(2)	658(2)	1710(2)	18(1)
C(15)	8424(3)	1530(2)	2337(2)	22(1)
C(16)	6654(2)	805(2)	1345(2)	18(1)
C(17)	6244(2)	1260(2)	531(2)	19(1)
C(18)	5037(2)	1421(2)	199(2)	19(1)
C(19)	4615(3)	1892(3)	-688(2)	24(1)
C(20)	3502(3)	888(3)	2774(2)	28(1)
C(21)	1118(3)	3109(2)	603(2)	31(1)
Cl(1)	1475(1)	3147(1)	1778(1)	41(1)
Cl(2)	2089(1)	3910(1)	117(1)	45(1)
Cl(3)	-397(1)	3458(1)	263(1)	39(1)

**Table 3.** Bond lengths [Å] and angles [°] for DCB05 (CCDC 175588).

O(1)-C(1)	1.361(3)	C(21)-Cl(3)	1.749(3)
O(1)-H(1)	0.72(3)	C(21)-Cl(1)	1.749(3)
O(2)-C(2)	1.401(3)	C(21)-Cl(2)	1.753(3)
O(2)-C(20)	1.428(3)	C(21)-H(21)	0.91(3)
O(3)-C(12)	1.230(3)		
O(4)-C(10)	1.216(3)	C(1)-O(1)-H(1)	107(3)
O(5)-C(10)	1.319(3)	C(2)-O(2)-C(20)	113.6(2)
O(5)-H(5A)	0.97(4)	C(10)-O(5)-H(5A)	111.0(18)
C(1)-C(2)	1.368(4)	O(1)-C(1)-C(2)	121.6(2)
C(1)-C(18)	1.390(3)	O(1)-C(1)-C(18)	118.2(2)
C(2)-C(3)	1.378(3)	C(2)-C(1)-C(18)	120.3(2)
C(3)-C(16)	1.403(3)	C(1)-C(2)-C(3)	122.7(2)
C(3)-C(4)	1.483(4)	C(1)-C(2)-O(2)	116.2(2)
C(4)-C(5)	1.492(4)	C(3)-C(2)-O(2)	120.9(2)
C(4)-H(4A)	0.94(3)	C(2)-C(3)-C(16)	118.1(2)
C(4)-H(4B)	0.96(3)	C(2)-C(3)-C(4)	121.7(2)
C(5)-C(6)	1.328(3)	C(16)-C(3)-C(4)	120.1(2)
C(5)-H(5)	0.97(3)	C(3)-C(4)-C(5)	112.8(2)
C(6)-C(14)	1.516(4)	C(3)-C(4)-H(4A)	108.3(16)
C(6)-C(7)	1.529(3)	C(5)-C(4)-H(4A)	109.2(15)
C(7)-C(9)	1.525(4)	C(3)-C(4)-H(4B)	108.8(16)
C(7)-C(8)	1.538(4)	C(5)-C(4)-H(4B)	107.1(16)
C(7)-C(11)	1.539(3)	H(4A)-C(4)-H(4B)	111(2)
C(8)-H(8A)	0.95(3)	C(6)-C(5)-C(4)	122.6(3)
C(8)-H(8B)	1.02(3)	C(6)-C(5)-H(5)	119.0(14)
C(8)-H(8C)	1.03(3)	C(4)-C(5)-H(5)	118.4(14)
C(9)-C(10)	1.475(4)	C(5)-C(6)-C(14)	119.3(2)
C(9)-H(9A)	0.92(3)	C(5)-C(6)-C(7)	120.7(2)
C(9)-H(9B)	0.93(2)	C(14)-C(6)-C(7)	119.97(19)
C(11)-C(12)	1.478(4)	C(9)-C(7)-C(6)	111.69(19)
C(11)-H(11A)	0.99(3)	C(9)-C(7)-C(8)	107.6(2)
C(11)-H(11B)	1.00(3)	C(6)-C(7)-C(8)	109.0(2)
C(12)-C(13)	1.480(4)	C(9)-C(7)-C(11)	109.4(2)
C(13)-C(14)	1.541(3)	C(6)-C(7)-C(11)	110.7(2)
C(13)-H(13A)	0.94(2)	C(8)-C(7)-C(11)	108.4(2)
C(13)-H(13B)	1.00(2)	C(7)-C(8)-H(8A)	108.3(15)
C(14)-C(16)	1.520(4)	C(7)-C(8)-H(8B)	107.9(16)
C(14)-C(15)	1.523(4)	H(8A)-C(8)-H(8B)	109(2)
C(15)-H(15A)	1.00(2)	C(7)-C(8)-H(8C)	113.1(14)
C(15)-H(15B)	1.00(2)	H(8A)-C(8)-H(8C)	106(2)
C(15)-H(15C)	1.01(3)	H(8B)-C(8)-H(8C)	113(2)
C(16)-C(17)	1.378(4)	C(10)-C(9)-C(7)	114.7(2)
C(17)-C(18)	1.377(4)	C(10)-C(9)-H(9A)	111.5(15)
C(17)-H(17)	0.97(2)	C(7)-C(9)-H(9A)	114.9(16)
C(18)-C(19)	1.481(4)	C(10)-C(9)-H(9B)	105.6(15)
C(19)-H(19A)	0.94(3)	C(7)-C(9)-H(9B)	111.0(15)
C(19)-H(19B)	0.92(3)	H(9A)-C(9)-H(9B)	97(2)
C(19)-H(19C)	1.03(2)	O(4)-C(10)-O(5)	122.0(2)
C(20)-H(20A)	1.00(3)	O(4)-C(10)-C(9)	123.9(2)
C(20)-H(20B)	0.95(2)	O(5)-C(10)-C(9)	114.2(2)
C(20)-H(20C)	0.99(3)	C(12)-C(11)-C(7)	114.6(2)

C(12)-C(11)-H(11A)	106.0(16)
C(7)-C(11)-H(11A)	112.5(15)
C(12)-C(11)-H(11B)	113.7(14)
C(7)-C(11)-H(11B)	108.6(15)
H(11A)-C(11)-H(11B)	101(2)
O(3)-C(12)-C(11)	120.7(2)
O(3)-C(12)-C(13)	120.3(2)
C(11)-C(12)-C(13)	119.0(2)
C(12)-C(13)-C(14)	113.2(2)
C(12)-C(13)-H(13A)	109.8(13)
C(14)-C(13)-H(13A)	108.8(12)
C(12)-C(13)-H(13B)	110.1(13)
C(14)-C(13)-H(13B)	109.3(12)
H(13A)-C(13)-H(13B)	105.3(19)
C(6)-C(14)-C(16)	110.5(2)
C(6)-C(14)-C(15)	108.5(2)
C(16)-C(14)-C(15)	108.9(2)
C(6)-C(14)-C(13)	110.5(2)
C(16)-C(14)-C(13)	109.8(2)
C(15)-C(14)-C(13)	108.6(2)
C(14)-C(15)-H(15A)	109.5(14)
C(14)-C(15)-H(15B)	111.6(14)
H(15A)-C(15)-H(15B)	107.9(18)
C(14)-C(15)-H(15C)	116.1(16)
H(15A)-C(15)-H(15C)	111(2)
H(15B)-C(15)-H(15C)	100(2)
C(17)-C(16)-C(3)	118.0(2)
C(17)-C(16)-C(14)	123.4(2)
C(3)-C(16)-C(14)	118.6(2)
C(18)-C(17)-C(16)	124.3(2)
C(18)-C(17)-H(17)	117.2(15)
C(16)-C(17)-H(17)	118.6(15)
C(17)-C(18)-C(1)	116.7(2)
C(17)-C(18)-C(19)	123.3(2)
C(1)-C(18)-C(19)	120.0(2)
C(18)-C(19)-H(19A)	114.1(17)
C(18)-C(19)-H(19B)	111.4(17)
H(19A)-C(19)-H(19B)	109(2)
C(18)-C(19)-H(19C)	109.9(15)
H(19A)-C(19)-H(19C)	104(2)
H(19B)-C(19)-H(19C)	107(2)
O(2)-C(20)-H(20A)	111.9(14)
O(2)-C(20)-H(20B)	104.7(14)
H(20A)-C(20)-H(20B)	108(2)
O(2)-C(20)-H(20C)	112.1(16)
H(20A)-C(20)-H(20C)	108(2)
H(20B)-C(20)-H(20C)	111(2)
Cl(3)-C(21)-Cl(1)	110.32(16)
Cl(3)-C(21)-Cl(2)	110.32(17)
Cl(1)-C(21)-Cl(2)	109.98(17)
Cl(3)-C(21)-H(21)	109.2(19)
Cl(1)-C(21)-H(21)	105.5(19)
Cl(2)-C(21)-H(21)	111.4(16)

**Table 4.** Anisotropic displacement parameters ( $\text{\AA}^2 \times 10^4$ ) for DCBo5 (CCDC 175588).  
 The anisotropic displacement factor exponent takes the form:  
 $-2\pi^2 [ h^2 a^{*2} U^{11} + \dots + 2 h k a^* b^* U^{12} ]$

	U <sup>11</sup>	U <sup>22</sup>	U <sup>33</sup>	U <sup>23</sup>	U <sup>13</sup>	U <sup>12</sup>
O(1)	149(10)	334(13)	235(11)	33(9)	80(9)	-25(9)
O(2)	182(10)	311(11)	210(10)	7(9)	113(8)	-10(8)
O(3)	154(10)	348(11)	253(11)	24(9)	102(8)	-2(8)
O(4)	324(11)	318(12)	214(10)	-30(9)	98(9)	-60(9)
O(5)	325(11)	325(12)	182(11)	-13(10)	95(9)	-42(9)
C(1)	142(14)	230(15)	221(15)	-30(12)	23(11)	8(12)
C(2)	142(14)	248(15)	205(15)	-29(12)	82(11)	-27(11)
C(3)	174(15)	228(15)	167(14)	-8(12)	58(11)	4(11)
C(4)	183(15)	279(17)	222(16)	16(14)	92(12)	-9(13)
C(5)	223(15)	228(16)	165(15)	17(13)	41(12)	4(12)
C(6)	155(14)	222(15)	159(14)	-23(11)	31(11)	-4(11)
C(7)	164(14)	230(15)	198(15)	8(12)	36(11)	1(11)
C(8)	240(17)	298(18)	208(16)	-20(14)	47(13)	18(14)
C(9)	190(16)	242(16)	242(16)	20(13)	49(12)	24(14)
C(10)	148(14)	267(17)	208(15)	27(13)	-21(12)	41(12)
C(11)	150(15)	294(17)	243(16)	-13(14)	53(12)	15(13)
C(12)	216(15)	196(15)	230(16)	-72(12)	56(12)	-7(12)
C(13)	175(15)	235(16)	172(15)	24(13)	71(12)	9(12)
C(14)	158(14)	222(15)	186(14)	-19(12)	92(11)	-10(11)
C(15)	192(15)	254(16)	217(16)	-18(13)	85(12)	-7(13)
C(16)	169(14)	203(14)	180(14)	-3(11)	79(11)	13(11)
C(17)	176(14)	229(15)	194(15)	-22(12)	92(12)	-2(12)
C(18)	184(14)	216(15)	191(14)	-5(12)	67(11)	22(11)
C(19)	181(16)	298(18)	228(16)	44(15)	29(13)	-2(14)
C(20)	237(18)	400(20)	250(17)	-48(15)	140(15)	-19(15)
C(21)	345(18)	274(18)	296(17)	-15(15)	10(14)	23(15)
Cl(1)	443(5)	519(5)	245(4)	-55(4)	17(3)	122(4)
Cl(2)	415(5)	447(5)	491(5)	63(4)	117(4)	-38(4)
Cl(3)	331(4)	475(5)	339(4)	-10(4)	21(3)	69(4)

**Table 5.** Hydrogen coordinates ( $\times 10^4$ ) and isotropic displacement parameters ( $\text{\AA}^2 \times 10^3$ ) for DCBo5 (CCDC 175588).

	x	y	z	$U_{\text{iso}}$
H(1)	2670(30)	960(20)	710(20)	37(11)
H(4A)	6260(20)	400(20)	3203(17)	23(7)
H(4B)	5570(20)	-560(20)	2799(17)	29(7)
H(5)	7500(20)	-1210(20)	3098(17)	29(8)
H(5A)	9470(30)	-750(30)	5120(20)	60(10)
H(8A)	8480(20)	-2180(20)	1656(18)	30(8)
H(8B)	9870(30)	-2160(20)	1514(18)	40(8)
H(8C)	8770(20)	-1467(19)	875(19)	30(7)
H(9A)	9340(20)	-2040(20)	3214(16)	19(7)
H(9B)	10520(20)	-1729(19)	3152(16)	22(7)
H(11A)	10710(20)	190(20)	2508(19)	39(8)
H(11B)	11100(20)	-680(20)	1959(16)	29(7)
H(13A)	8666(18)	1287(17)	642(14)	3(6)
H(13B)	8370(20)	165(18)	456(16)	16(7)
H(15A)	8294(19)	2176(18)	1999(15)	11(6)
H(15B)	7970(20)	1565(18)	2856(17)	22(7)
H(15C)	9280(30)	1480(20)	2670(19)	39(8)
H(17)	6830(20)	1466(18)	154(16)	23(7)
H(19A)	4240(20)	2520(20)	-652(18)	31(8)
H(19B)	4110(20)	1470(20)	-1056(19)	33(8)
H(19C)	5350(20)	2042(19)	-1011(17)	32(7)
H(20A)	4260(30)	910(20)	3234(18)	29(8)
H(20B)	2880(20)	553(17)	3031(15)	14(6)
H(20C)	3270(20)	1590(20)	2602(19)	38(9)
H(21)	1220(20)	2450(20)	447(19)	39(9)

**Table 6.** Hydrogen bonds for DCBo5 (CCDC 175588) [ $\text{\AA}$  and  $^\circ$ ].

D-H...A	d(D-H)	d(H...A)	d(D...A)	$\angle$ (DHA)
O(1)-H(1)...O(3)#1	0.72(3)	2.10(3)	2.656(2)	135(3)
O(1)-H(1)...O(2)	0.72(3)	2.28(3)	2.703(3)	119(3)
O(5)-H(5A)...O(4)#2	0.97(4)	1.64(4)	2.600(3)	175(3)

Symmetry transformations used to generate equivalent atoms:

#1  $x-1, y, z$  #2  $-x+2, -y, -z+1$

CALIFORNIA INSTITUTE OF TECHNOLOGY  
BECKMAN INSTITUTE  
X-RAY CRYSTALLOGRAPHY LABORATORY

Crystal Structure Analysis of:

Diketone **196** (DCB11)

(CCDC 201187)

Contents:

- Table 1. Crystal data
- Table 2. Atomic Coordinates
- Table 3. Full bond distances and angles (for deposit)
- Table 4. Anisotropic displacement parameters
- Table 5. Hydrogen atomic coordinates

Figure A.96 Representation of Diketone **196**.

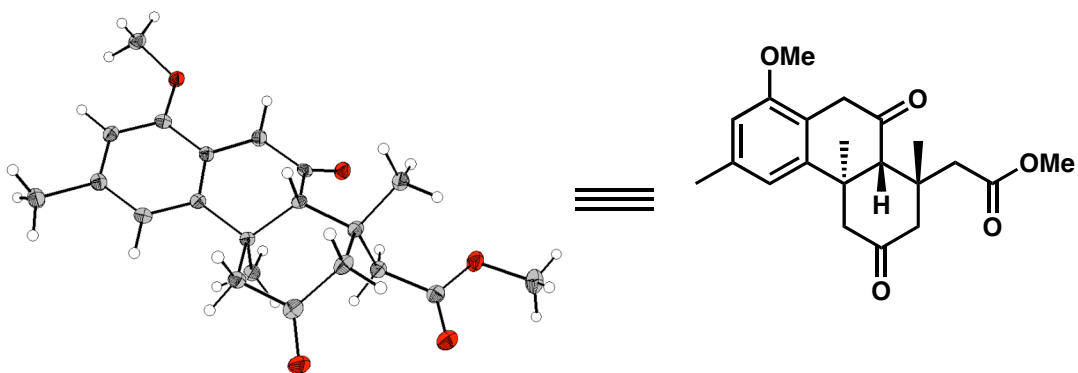


**Table 1.** Crystal data and structure refinement for DCB11 (CCDC 201187).

Empirical formula	C <sub>21</sub> H <sub>26</sub> O <sub>5</sub>
Formula weight	358.42
Crystallization Solvent	Acetone/heptane
Crystal Habit	Fragment
Crystal size	0.26 x 0.22 x 0.17 mm <sup>3</sup>
Crystal color	Colorless

### Data Collection

Preliminary Photos	Rotation	
Type of diffractometer	Bruker SMART 1000	
Wavelength	0.71073 Å MoK $\alpha$	
Data Collection Temperature	98(2) K	
$\theta$ range for 11980 reflections used in lattice determination	2.28 to 28.32°	
Unit cell dimensions	a = 9.0211(6) Å b = 11.3617(7) Å c = 17.9596(12) Å	$\beta$ = 97.5510(10)°
Volume	1824.8(2) Å <sup>3</sup>	
Z	4	
Crystal system	Monoclinic	
Space group	P2 <sub>1</sub> /n	
Density (calculated)	1.305 Mg/m <sup>3</sup>	
F(000)	768	
Data collection program	Bruker SMART v5.054	
$\theta$ range for data collection	2.13 to 28.32°	
Completeness to $\theta = 28.32^\circ$	93.0 %	
Index ranges	-11 $\leq$ h $\leq$ 11, -14 $\leq$ k $\leq$ 14, -23 $\leq$ l $\leq$ 23	
Data collection scan type	$\omega$ scans at 5 $\phi$ settings	
Data reduction program	Bruker SAINT v6.022	
Reflections collected	25862	
Independent reflections	4226 [R <sub>int</sub> = 0.0517]	
Absorption coefficient	0.092 mm <sup>-1</sup>	
Absorption correction	None	
Max. and min. transmission	0.9845 and 0.9764	

**Table 1 (cont.)**  
**Structure solution and Refinement**

Structure solution program	SHELXS-97 (Sheldrick, 1990)
Primary solution method	Direct methods
Secondary solution method	Difference Fourier map
Hydrogen placement	Difference Fourier map
Structure refinement program	SHELXL-97 (Sheldrick, 1997)
Refinement method	Full matrix least-squares on F <sup>2</sup>
Data / restraints / parameters	4226 / 0 / 339
Treatment of hydrogen atoms	Unrestrained
Goodness-of-fit on F <sup>2</sup>	2.153
Final R indices [I>2σ(I), 3426 reflections]	R1 = 0.0404, wR2 = 0.0704
R indices (all data)	R1 = 0.0511, wR2 = 0.0715
Type of weighting scheme used	Sigma
Weighting scheme used	w=1/σ <sup>2</sup> (F <sub>o</sub> <sup>2</sup> )
Max shift/error	0.001
Average shift/error	0.000
Largest diff. peak and hole	0.326 and -0.254 e.Å <sup>-3</sup>

### Special Refinement Details

Refinement of F<sup>2</sup> against ALL reflections. The weighted R-factor (wR) and goodness of fit (S) are based on F<sup>2</sup>, conventional R-factors (R) are based on F, with F set to zero for negative F<sup>2</sup>. The threshold expression of F<sup>2</sup> > 2σ(F<sup>2</sup>) is used only for calculating R-factors(gt) etc. and is not relevant to the choice of reflections for refinement. R-factors based on F<sup>2</sup> are statistically about twice as large as those based on F, and R-factors based on ALL data will be even larger.

All esds (except the esd in the dihedral angle between two l.s. planes) are estimated using the full covariance matrix. The cell esds are taken into account individually in the estimation of esds in distances, angles and torsion angles; correlations between esds in cell parameters are only used when they are defined by crystal symmetry. An approximate (isotropic) treatment of cell esds is used for estimating esds involving l.s. planes.

**Table 2.** Atomic coordinates ( $\times 10^4$ ) and equivalent isotropic displacement parameters ( $\text{\AA}^2 \times 10^3$ ) for DCB11 (CCDC 201187).  $U(\text{eq})$  is defined as the trace of the orthogonalized  $U^{\text{ij}}$  tensor.

	x	y	z	$U_{\text{eq}}$
O(1)	7731(1)	4507(1)	529(1)	19(1)
O(2)	4749(1)	8200(1)	472(1)	21(1)
O(3)	9216(1)	11345(1)	2166(1)	25(1)
O(4)	3377(1)	11397(1)	1288(1)	24(1)
O(5)	5418(1)	12446(1)	1710(1)	29(1)
C(1)	10631(1)	7158(1)	1330(1)	16(1)
C(2)	11220(1)	6047(1)	1256(1)	16(1)
C(3)	12869(2)	5814(1)	1455(1)	23(1)
C(4)	10262(1)	5133(1)	986(1)	16(1)
C(5)	8757(1)	5346(1)	789(1)	15(1)
C(6)	8217(2)	3305(1)	562(1)	20(1)
C(7)	8162(1)	6478(1)	851(1)	14(1)
C(8)	6510(1)	6650(1)	623(1)	18(1)
C(9)	5914(1)	7834(1)	811(1)	15(1)
C(10)	6851(1)	8484(1)	1442(1)	14(1)
C(11)	6098(1)	9579(1)	1751(1)	15(1)
C(12)	4682(1)	9175(1)	2071(1)	19(1)
C(13)	5708(1)	10548(1)	1148(1)	17(1)
C(14)	4865(1)	11569(1)	1417(1)	18(1)
C(15)	2478(2)	12330(1)	1540(1)	31(1)
C(16)	7204(1)	10084(1)	2400(1)	18(1)
C(17)	8678(1)	10359(1)	2139(1)	18(1)
C(18)	9450(1)	9319(1)	1844(1)	18(1)
C(19)	8466(1)	8626(1)	1220(1)	14(1)
C(20)	8500(2)	9259(1)	463(1)	19(1)
C(21)	9104(1)	7387(1)	1138(1)	14(1)

**Table 3.** Bond lengths [Å] and angles [°] for DCB11 (CCDC 201187).

O(1)-C(5)	1.3673(13)	C(20)-H(20A)	0.996(14)
O(1)-C(6)	1.4332(14)	C(20)-H(20B)	0.987(13)
O(2)-C(9)	1.2162(13)	C(20)-H(20C)	0.985(13)
O(3)-C(17)	1.2186(13)		
O(4)-C(14)	1.3457(14)	C(5)-O(1)-C(6)	117.41(9)
O(4)-C(15)	1.4438(16)	C(14)-O(4)-C(15)	115.32(10)
O(5)-C(14)	1.2036(14)	C(2)-C(1)-C(21)	121.54(11)
C(1)-C(2)	1.3828(16)	C(2)-C(1)-H(1)	118.7(7)
C(1)-C(21)	1.3997(16)	C(21)-C(1)-H(1)	119.8(7)
C(1)-H(1)	1.006(12)	C(1)-C(2)-C(4)	118.97(11)
C(2)-C(4)	1.3963(16)	C(1)-C(2)-C(3)	121.17(11)
C(2)-C(3)	1.5069(17)	C(4)-C(2)-C(3)	119.86(11)
C(3)-H(3A)	0.967(14)	C(2)-C(3)-H(3A)	109.9(8)
C(3)-H(3B)	0.963(16)	C(2)-C(3)-H(3B)	111.4(9)
C(3)-H(3C)	0.980(15)	H(3A)-C(3)-H(3B)	109.7(12)
C(4)-C(5)	1.3783(16)	C(2)-C(3)-H(3C)	111.9(9)
C(4)-H(4)	0.958(11)	H(3A)-C(3)-H(3C)	108.7(12)
C(5)-C(7)	1.4037(15)	H(3B)-C(3)-H(3C)	105.1(12)
C(6)-H(6A)	0.978(12)	C(5)-C(4)-C(2)	120.19(11)
C(6)-H(6B)	0.973(12)	C(5)-C(4)-H(4)	119.0(7)
C(6)-H(6C)	0.999(13)	C(2)-C(4)-H(4)	120.8(7)
C(7)-C(21)	1.3926(16)	O(1)-C(5)-C(4)	124.44(10)
C(7)-C(8)	1.5051(16)	O(1)-C(5)-C(7)	114.64(10)
C(8)-C(9)	1.5034(16)	C(4)-C(5)-C(7)	120.92(11)
C(8)-H(8A)	0.993(13)	O(1)-C(6)-H(6A)	105.1(7)
C(8)-H(8B)	0.996(13)	O(1)-C(6)-H(6B)	110.4(7)
C(9)-C(10)	1.5144(16)	H(6A)-C(6)-H(6B)	110.7(10)
C(10)-C(11)	1.5546(16)	O(1)-C(6)-H(6C)	111.8(7)
C(10)-C(19)	1.5679(16)	H(6A)-C(6)-H(6C)	110.0(10)
C(10)-H(10)	0.982(11)	H(6B)-C(6)-H(6C)	108.8(10)
C(11)-C(12)	1.5377(16)	C(5)-C(7)-C(21)	119.20(11)
C(11)-C(13)	1.5525(16)	C(5)-C(7)-C(8)	118.20(10)
C(11)-C(16)	1.5420(16)	C(21)-C(7)-C(8)	122.58(10)
C(12)-H(12A)	0.986(12)	C(7)-C(8)-C(9)	115.21(10)
C(12)-H(12B)	1.025(12)	C(7)-C(8)-H(8A)	112.9(8)
C(12)-H(12C)	0.993(12)	C(9)-C(8)-H(8A)	106.4(7)
C(13)-C(14)	1.5018(16)	C(7)-C(8)-H(8B)	109.6(8)
C(13)-H(13A)	0.986(12)	C(9)-C(8)-H(8B)	105.9(8)
C(13)-H(13B)	0.957(11)	H(8A)-C(8)-H(8B)	106.3(11)
C(15)-H(15A)	0.969(14)	O(2)-C(9)-C(10)	124.61(11)
C(15)-H(15B)	0.980(15)	O(2)-C(9)-C(8)	120.35(11)
C(15)-H(15C)	0.989(15)	C(10)-C(9)-C(8)	115.03(10)
C(16)-C(17)	1.4999(17)	C(9)-C(10)-C(11)	115.52(10)
C(16)-H(16A)	0.980(12)	C(9)-C(10)-C(19)	107.82(9)
C(16)-H(16B)	0.982(12)	C(11)-C(10)-C(19)	118.21(9)
C(17)-C(18)	1.5039(17)	C(9)-C(10)-H(10)	104.1(6)
C(18)-C(19)	1.5492(16)	C(11)-C(10)-H(10)	105.7(6)
C(18)-H(18A)	0.966(12)	C(19)-C(10)-H(10)	103.8(6)
C(18)-H(18B)	0.996(12)	C(12)-C(11)-C(10)	108.53(9)
C(19)-C(21)	1.5357(15)	C(12)-C(11)-C(13)	110.46(10)
C(19)-C(20)	1.5424(16)	C(10)-C(11)-C(13)	112.81(9)

C(12)-C(11)-C(16)	108.40(10)
C(10)-C(11)-C(16)	107.36(9)
C(13)-C(11)-C(16)	109.15(10)
C(11)-C(12)-H(12A)	109.5(7)
C(11)-C(12)-H(12B)	110.2(7)
H(12A)-C(12)-H(12B)	109.2(9)
C(11)-C(12)-H(12C)	109.5(7)
H(12A)-C(12)-H(12C)	108.7(10)
H(12B)-C(12)-H(12C)	109.7(9)
C(14)-C(13)-C(11)	113.64(10)
C(14)-C(13)-H(13A)	104.7(7)
C(11)-C(13)-H(13A)	110.9(7)
C(14)-C(13)-H(13B)	108.1(7)
C(11)-C(13)-H(13B)	109.4(7)
H(13A)-C(13)-H(13B)	110.0(10)
O(5)-C(14)-O(4)	122.87(11)
O(5)-C(14)-C(13)	125.55(12)
O(4)-C(14)-C(13)	111.58(10)
O(4)-C(15)-H(15A)	107.3(8)
O(4)-C(15)-H(15B)	109.3(9)
H(15A)-C(15)-H(15B)	110.0(12)
O(4)-C(15)-H(15C)	110.6(8)
H(15A)-C(15)-H(15C)	111.5(12)
H(15B)-C(15)-H(15C)	108.1(12)
C(17)-C(16)-C(11)	110.67(10)
C(17)-C(16)-H(16A)	108.5(7)
C(11)-C(16)-H(16A)	111.5(7)
C(17)-C(16)-H(16B)	108.4(7)
C(11)-C(16)-H(16B)	107.5(7)
H(16A)-C(16)-H(16B)	110.2(9)
O(3)-C(17)-C(18)	122.40(11)
O(3)-C(17)-C(16)	122.92(11)
C(18)-C(17)-C(16)	114.67(11)
C(17)-C(18)-C(19)	113.93(10)
C(17)-C(18)-H(18A)	109.0(7)
C(19)-C(18)-H(18A)	110.2(7)
C(17)-C(18)-H(18B)	105.8(7)
C(19)-C(18)-H(18B)	109.9(7)
H(18A)-C(18)-H(18B)	107.8(9)
C(21)-C(19)-C(20)	106.90(9)
C(21)-C(19)-C(18)	110.43(9)
C(20)-C(19)-C(18)	108.92(10)
C(21)-C(19)-C(10)	107.65(9)
C(20)-C(19)-C(10)	113.48(10)
C(18)-C(19)-C(10)	109.42(9)
C(19)-C(20)-H(20A)	108.7(7)
C(19)-C(20)-H(20B)	111.1(7)
H(20A)-C(20)-H(20B)	107.8(10)
C(19)-C(20)-H(20C)	112.4(7)
H(20A)-C(20)-H(20C)	107.0(10)
H(20B)-C(20)-H(20C)	109.7(10)
C(1)-C(21)-C(7)	119.14(11)
C(1)-C(21)-C(19)	121.02(10)
C(7)-C(21)-C(19)	119.82(10)

**Table 4.** Anisotropic displacement parameters ( $\text{\AA}^2 \times 10^4$ ) for DCB11 (CCDC 201187).  
 The anisotropic displacement factor exponent takes the form:  

$$-2\pi^2 [ h^2 a^{*2} U^{11} + \dots + 2 h k a^* b^* U^{12} ]$$

	U <sup>11</sup>	U <sup>22</sup>	U <sup>33</sup>	U <sup>23</sup>	U <sup>13</sup>	U <sup>12</sup>
O(1)	179(5)	129(4)	246(5)	-34(4)	5(4)	-8(3)
O(2)	175(5)	198(5)	252(5)	-10(4)	-23(4)	19(4)
O(3)	239(5)	164(5)	340(5)	-50(4)	-12(4)	-28(4)
O(4)	181(5)	202(5)	316(5)	-22(4)	1(4)	57(4)
O(5)	270(5)	197(5)	396(6)	-85(4)	44(4)	-6(4)
C(1)	170(6)	162(6)	152(6)	-5(5)	26(5)	-28(5)
C(2)	160(6)	188(7)	140(6)	12(5)	29(5)	5(5)
C(3)	165(7)	220(8)	302(8)	-28(7)	7(6)	13(6)
C(4)	189(7)	140(6)	158(6)	10(5)	43(5)	31(5)
C(5)	176(6)	159(6)	118(6)	-7(5)	29(5)	-31(5)
C(6)	223(8)	142(7)	237(7)	-9(6)	13(6)	-2(6)
C(7)	145(6)	157(6)	123(6)	7(5)	31(5)	4(5)
C(8)	162(7)	168(7)	209(7)	-33(6)	8(5)	0(5)
C(9)	142(6)	161(6)	161(6)	30(5)	48(5)	-18(5)
C(10)	151(6)	128(6)	143(6)	26(5)	21(5)	7(5)
C(11)	173(6)	128(6)	153(6)	1(5)	32(5)	14(5)
C(12)	202(7)	167(7)	216(7)	13(6)	73(6)	27(6)
C(13)	185(7)	159(7)	171(7)	4(5)	29(5)	13(5)
C(14)	209(7)	164(7)	163(6)	30(5)	19(5)	19(5)
C(15)	218(8)	287(9)	419(10)	-13(7)	64(7)	94(7)
C(16)	241(7)	145(7)	153(7)	-7(5)	26(5)	29(5)
C(17)	203(7)	172(7)	130(6)	-11(5)	-53(5)	9(5)
C(18)	158(7)	159(7)	206(7)	-1(5)	4(5)	-17(5)
C(19)	139(6)	125(6)	166(6)	0(5)	15(5)	-6(5)
C(20)	196(7)	182(7)	201(7)	18(5)	58(6)	0(6)
C(21)	162(6)	150(6)	114(6)	8(5)	37(5)	3(5)

**Table 5.** Hydrogen coordinates ( $\times 10^4$ ) and isotropic displacement parameters ( $\text{\AA}^2 \times 10^3$ ) for DCB11 (CCDC 201187).

	x	y	z	$U_{\text{iso}}$
H(1)	11324(13)	7813(10)	1530(6)	16(3)
H(3A)	13385(15)	6538(12)	1604(7)	35(4)
H(3B)	13289(17)	5469(13)	1039(9)	50(5)
H(3C)	13068(16)	5243(13)	1865(9)	48(5)
H(4)	10635(12)	4351(10)	941(6)	13(3)
H(6A)	7338(14)	2849(10)	357(7)	21(3)
H(6B)	8556(13)	3077(10)	1078(7)	18(3)
H(6C)	9048(14)	3171(10)	254(7)	19(3)
H(8A)	6202(14)	6529(11)	77(8)	29(4)
H(8B)	5944(15)	6062(11)	886(7)	33(4)
H(10)	6980(11)	7914(9)	1856(6)	9(3)
H(12A)	4310(12)	9821(10)	2363(6)	17(3)
H(12B)	3867(14)	8942(10)	1643(7)	22(3)
H(12C)	4927(13)	8491(11)	2410(7)	20(3)
H(13A)	6623(14)	10898(10)	997(6)	18(3)
H(13B)	5112(12)	10214(10)	719(6)	12(3)
H(15A)	1440(17)	12099(12)	1419(8)	38(4)
H(15B)	2664(16)	13060(13)	1277(8)	43(4)
H(15C)	2744(16)	12466(12)	2086(9)	44(4)
H(16A)	6816(13)	10804(10)	2604(6)	16(3)
H(16B)	7366(13)	9478(10)	2792(7)	18(3)
H(18A)	10357(14)	9583(10)	1663(6)	16(3)
H(18B)	9741(13)	8799(10)	2285(7)	22(3)
H(20A)	9509(15)	9153(10)	304(7)	26(3)
H(20B)	7759(14)	8917(10)	69(7)	22(3)
H(20C)	8331(13)	10112(11)	498(6)	21(3)

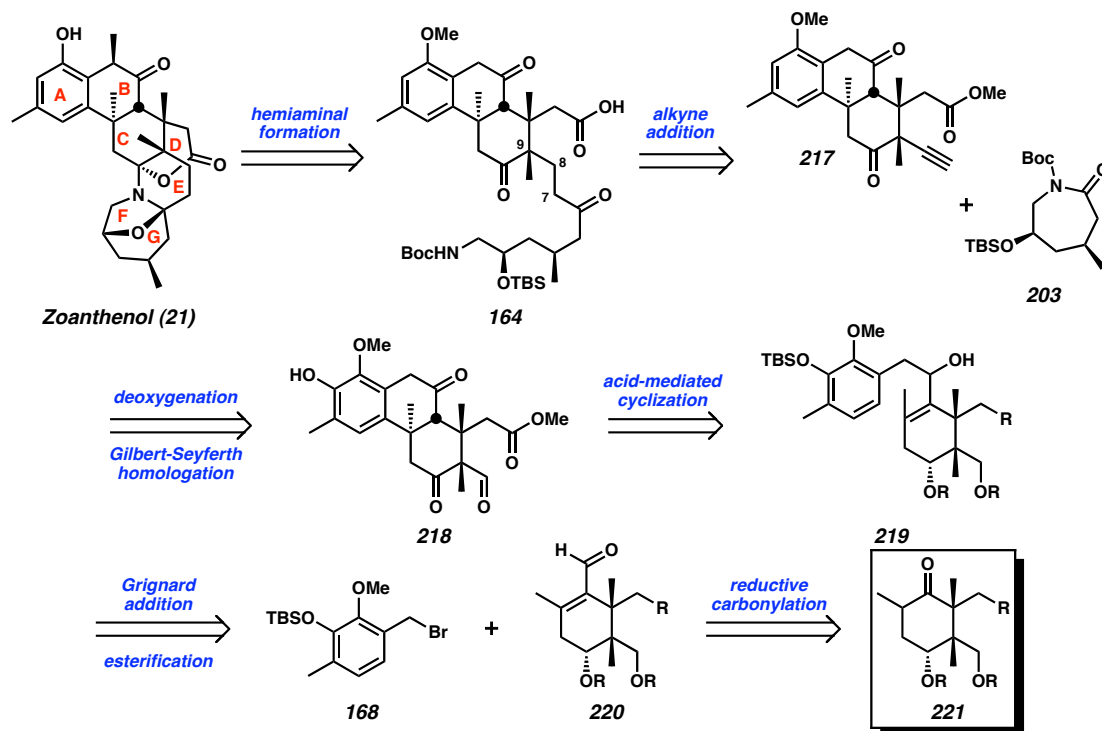
## CHAPTER THREE

Acid-Mediated Cyclization Approaches to the  
Densely Substituted Carbocyclic Core of Zoanthenol<sup>†</sup>*3.1.1 Revised Retrosynthetic Analysis*

Chapter 2 described an interesting acid-mediated S<sub>N</sub>'-type cyclization to construct the carbocyclic core of zoanthenol. Efforts to elaborate the product of this route were unsuccessful, thus the retrosynthetic analysis was altered to include the all-carbon quaternary stereocenter at C(9) prior to our key cyclization step. Disconnection of side-chain-appended intermediate **164** at the C(8)–C(9) bond, revealed tricyclic alkyne **217** and lactam **203** (Scheme 3.1.1). The alkyne was envisioned to arise from aldehyde **218**, which would be accessed via an acid-mediated cyclization of an allylic alcohol such as **218**. This tethered A–C ring system would in turn be derived from aryl bromide **168** and enal **220**. Enal **220** would be available from a ketone such as **221** by means of a reductive carbonylation as described in Chapter 2.

---

<sup>†</sup> This work was conducted in close collaboration with Dr. Douglas C. Behenna, a former graduate student in the Stoltz Group.



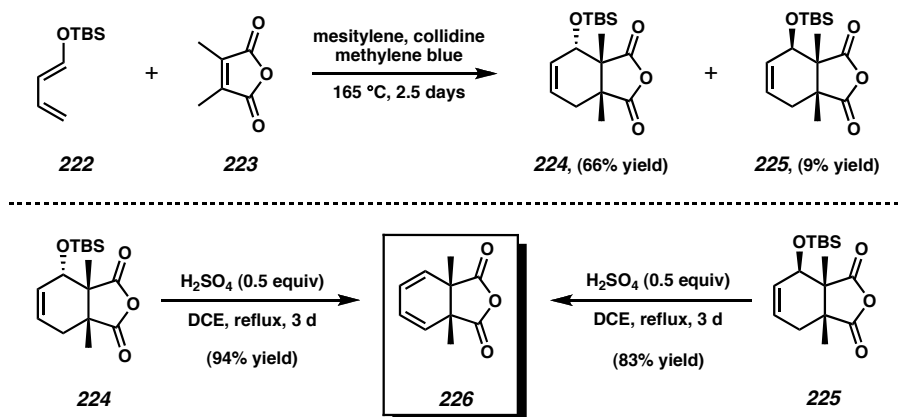
**Scheme 3.1.1** Revised retrosynthesis of zoanthenol.

### 3.2 Toward a Vicinal Quaternary Center-Containing C Ring Synthon

#### 3.2.1 Synthesis and Desymmetrization of a meso-Anhydride

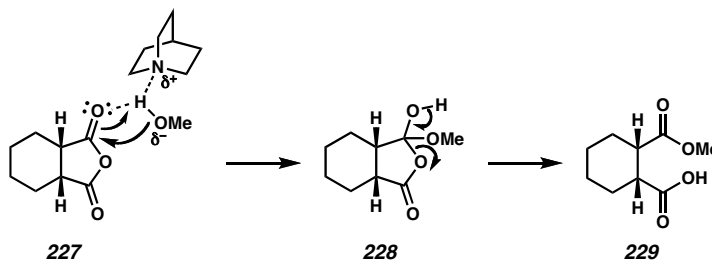
Given our previous difficulties installing the all-carbon quaternary stereocenter at C(9), we chose to tackle the synthesis of the vicinal quaternary centers first. Fortunately, an effective approach to a similar problem had recently been published.<sup>1</sup> In their total synthesis of merrilactone A, Danishefsky and coworkers treated electron-rich diene **222** and dimethyl maleic anhydride (**223**) with mesitylene, collidine, and methylene blue at 165 °C for 3 days to form cycloadduct **224** in 74% yield (Scheme 3.2.1).<sup>1</sup> The scalable nature of this reaction allowed access to quantities as large as 75.7 g (66% yield) of endo adduct **224** and 10.5 g of exo adduct **225** (9% yield) from a single large-scale reaction. It was envisioned that this Diels-Alder adduct could be advanced to a *meso*-symmetric compound, which could be treated with a chiral reagent to allow entry into an

enantioselective synthesis. We anticipated that employing a strong acid would induce desilylation followed by in situ dehydration. Gratifyingly, treatment of either the *endo* (**224**) or *exo* (**225**) Diels-Alder adduct with 0.5 equivalents of sulfuric acid in 0.1 M 1,2-dichloroethane produced anhydride **226** in excellent yield.<sup>2</sup>



**Scheme 3.2.1** Synthesis of vicinal all-carbon quaternary centers.

Several reports indicated the feasibility of a *meso*-anhydride desymmetrization as a viable entry into an enantioselective synthesis.<sup>3</sup> These reactions involve alcoholysis of an anhydride, catalyzed or mediated by a cinchona alkaloid or derivative. The alkaloid activates the alcohol by a hydrogen bond, forming a noncovalent adduct such as **227** (Scheme 3.2.2).<sup>3a</sup> This adduct preferentially activates one of the anhydride carbonyls, serving as both a Brønsted acid catalyst and a nucleophile. Thus, the carbonyl is activated via a developing hydrogen bond, while methoxide is delivered selectively to the same carbonyl. Collapse of tetrahedral intermediate **228** leads to half ester **229**.



**Scheme 3.2.2** Mechanism of *meso*-anhydride desymmetrization by cinchona alkaloids.

The desymmetrization of *meso*-anhydrides is known for a number of bicyclic and tricyclic systems (**232–238**, Figure 3.2.1).<sup>4</sup> Interestingly, Bolm and coworkers found that compounds **239–241** were completely unreactive. The authors hypothesize that steric interactions prevent reactivity, though these effects appear to be quite subtle.<sup>4</sup> This presumed steric constraint cast doubt on the likelihood of success in our own system because both of the carbonyls in anhydride **226** are neopentyl in nature. Nevertheless, we proceeded with our efforts to desymmetrize *meso* anhydride **226**.

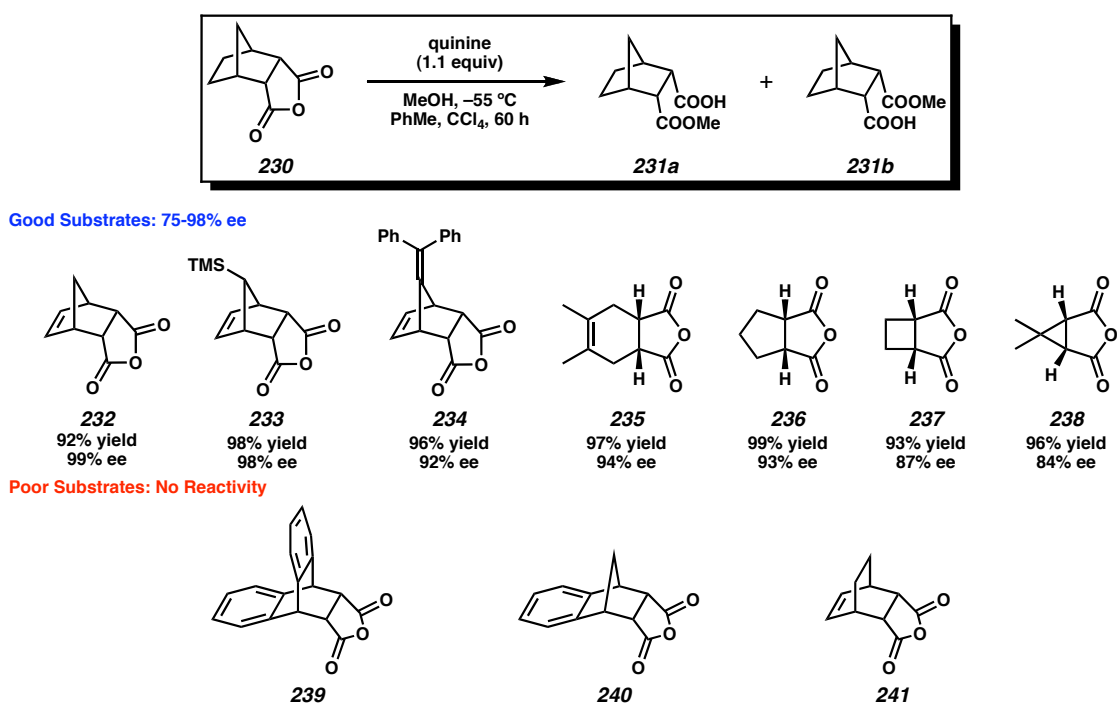


**Figure 3.2.1** Known *meso*-anhydride desymmetrization substrates.

At this point, we were poised to attempt the key desymmetrization step. To our delight, desymmetrization of anhydride **226** was accomplished at ambient temperature upon treatment with quinine and methanol in toluene to form half-ester **242** in > 99% yield and 50% ee (Entry 1, Table 3.2.1). Cooling the reaction to -50 °C increased the ee to 74% (Entry 2), and treatment of **226** with catalytic quinine (**243**), 1 equiv pentamethylpiperidine (pempidine) and methanol for 18 days at -50 °C provided half-ester **242** in 88% yield and 70% ee (Entry 3). The use of quinidine (**244**) resulted in the

formation of the opposite enantiomer of the half-ester in 70% ee (Entry 4). Quinine derivative **245** allowed access to the desymmetrized product in 72% ee at  $-25\text{ }^{\circ}\text{C}$  (Entry 5). The best enantioselectivities were observed upon treatment with menthyl-acetate-substituted quinidine derivative **246**.<sup>5</sup> In this case, subjecting anhydride **226** to **246**, MeOH, and PhMe at  $-50\text{ }^{\circ}\text{C}$  provided half-ester **242** in 85% ee (Entry 6). A number of alternative alcohols were also screened, but they did not show improved enantioselectivity in the reaction.<sup>6</sup> Interestingly, significant rate acceleration was observed for the menthyl acetate derivatives **245** and **246**. Although this effect has not been studied in detail, it is feasible that the alcohol moiety in the parent structures could intramolecularly hydrogen bond to the tertiary amine and compete with hydrogen bonding to methanol. Such competition would be prevented by use of menthyl acetate derivatives **245** and **246**. Importantly, this work represents the first example of a desymmetrization of a *meso* anhydride that simultaneously sets the absolute stereochemistry of vicinal all-carbon quaternary centers. Additionally, the ability to access either enantiomer of half-ester **242** has enabled important flexibility in our synthetic efforts.

$\xrightarrow[\text{PhMe, MeOH, temp}]{\text{chiral catalyst}}$

**226**
**242**

quinine (**243**)

quinidine (**244**)

O-(menthylacetate)-  
quinine (**245**)

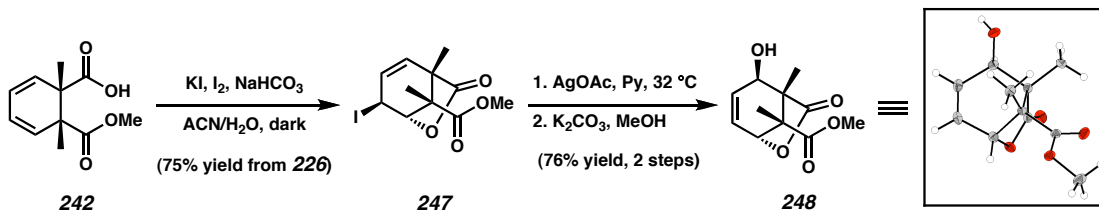
O-((-)-menthylacetate)-  
quinidine (**246**)

Entry	Chiral Controller (mol%)	Other Conditions	Temperature (°C)	Time (d)	Sign of Rotation	%ee (% yield)
1	243 (105)	MeOH (5 equiv)	22	0.3	–	50 (>99)
2	243 (105)	MeOH (5 equiv)	–50	0.3	–	74
3	243 (10)	MeOH (3 equiv) pempidine (1 equiv) 50% CCl <sub>4</sub> v/v	–50	18	–	70 (88)
4	244 (100)	MeOH (3 equiv)	–50	6	+	70
5	245 (105)	MeOH (10 equiv)	–25	3	–	72
6	246 (101)	MeOH (3 equiv)	–50	10	+	85

**Table 3.2.1** Optimized synthesis and desymmetrization of a C ring *meso*-anhydride.

### 3.2.2 Elaboration of the Half-Ester

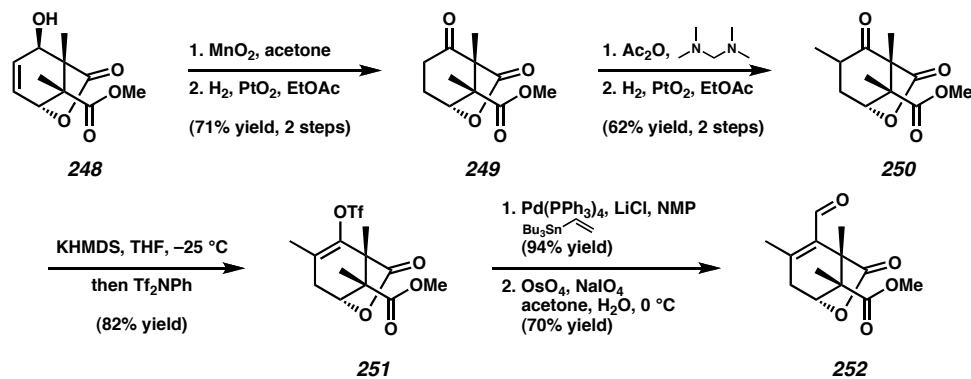
With our desymmetrized diene in hand, we sought to relay the stereochemical information into the C ring. We investigated several approaches toward this goal, including an Arndt-Eistert homologation,<sup>7</sup> a homologation/ $\pi$ -allyl sequence,<sup>8</sup> and a selenolactonization/oxidative rearrangement sequence.<sup>9</sup> Ultimately, we found that iodolactonization could be affected with good positional selectivity and yield (Scheme 3.2.3). Treatment of the iodolactone with silver acetate led to *syn*-periplanar attack of the incoming acetate nucleophile to provide, after methanolysis, allylic alcohol **248**. The connectivity and relative stereochemistry were proven by X-ray analysis of a single crystal.



**Scheme 3.2.3** C ring functionalization: iodolactonization and displacement.

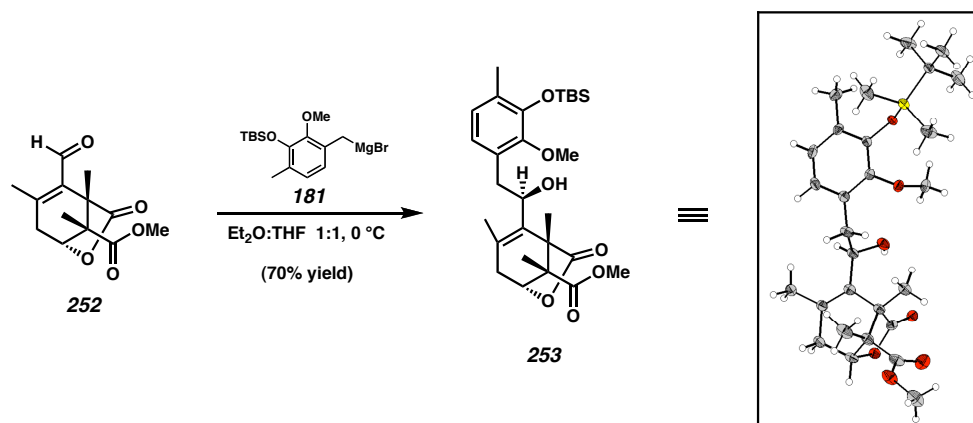
### 3.3.1 Toward a Lactone-Derived C Ring Synthon

Allylic alcohol **248** served as an ideal branch point for our synthetic investigations, ultimately allowing access to a variety of C ring synthons. Initially, it was advanced to a lactone-derived synthon, enabling quick access to cyclization substrates. Along these lines, a simple two-step protocol involving allylic oxidation with  $\text{MnO}_2$ <sup>10</sup> followed by hydrogenation with Adams' catalyst<sup>11</sup> was employed to provide ketone **249** (Scheme 3.3.1). Methylation of this substrate using simple LDA/MeI conditions afforded almost exclusively bis-alkylated products as a mixture with starting ketone. Thus, we chose to employ a 2-step protocol for the installation of the methyl group. Methylenation was accomplished with *N,N*-tetramethylmethylenediamine and acetic anhydride.<sup>12</sup> Hydrogenation once again occurred cleanly upon treatment with Adams' catalyst under a balloon of  $\text{H}_2$ , providing methyl ketone **250** as a mixture of diastereomers. Enolization and trapping with *N*-phenyl bis(trifluoromethanesulfonamide) provided enol triflate **251**. Stille coupling proceeded smoothly to provide a diene, which was oxidatively cleaved to provide enal **252**.



**Scheme 3.3.1** Synthesis of a lactone-derived C ring synthon.

In previous C ring synthons, we were able to increase the selectivity during our fragment coupling step by conducting the Grignard addition in a mixture of  $\text{CH}_2\text{Cl}_2$  and  $\text{Et}_2\text{O}$ . Unfortunately, enal **252** was insoluble in this mixture of solvents (Scheme 3.3.2). Thus, we turned to use of a combination of THF and  $\text{Et}_2\text{O}$ . Under these conditions, the reaction proceeded smoothly to provide allylic alcohol **253**. However, we observed complete selectivity for addition in the opposite sense from that of our previous substrate.<sup>13,14,15</sup>



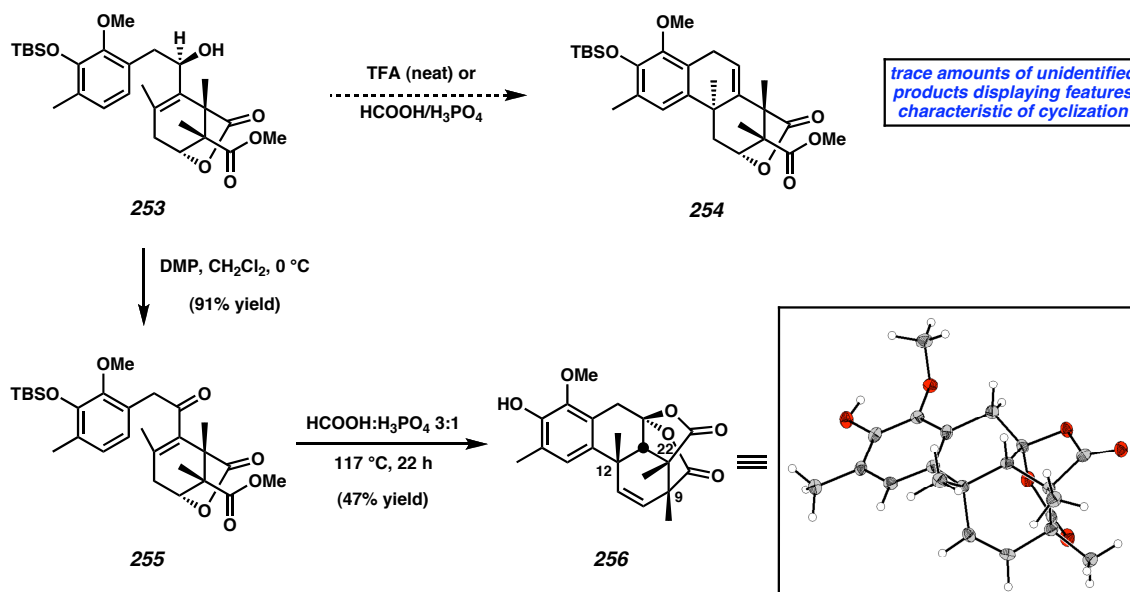
**Scheme 3.3.2** Grignard addition to synthon **252**.

### 3.3.2 Acid-Mediated Cyclizations of Lactone-Derived A–C Ring Systems

Owing to our success with allylic alcohol substrates in our early work, we subjected allylic alcohol **253** to neat trifluoroacetic acid at  $65^\circ\text{C}$  (Scheme 3.3.3). From these

conditions, we observed almost exclusive desilylation of the A ring, and only a trace amount of a cyclized product was observed. Treatment with a mixture of formic acid and 85% phosphoric acid led to substantial decomposition as well as a trace amount of a compound that appeared to be cyclized. Overall, we found that this system could not be efficiently cyclized.

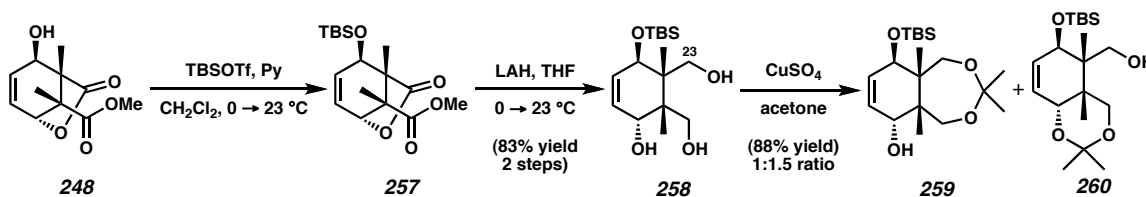
With the goal of increasing the reactivity of the system, we oxidized allylic alcohol **253** to the corresponding enone using Dess-Martin periodinane. Upon treatment with TFA at temperatures as high as 110 °C, with AlCl<sub>3</sub> in toluene at 100 °C, or with polyphosphoric acid at 100 °C, we only observed A-ring desilylation or decomposition. Interestingly, treatment with a 3:1 (v/v) ratio of formic acid and 85% phosphoric acid induced cyclization of enone **255** to afford the unusual caged bisacetoxycetal **256** in 47% yield. Unfortunately, X-ray crystallographic analysis of a single crystal revealed that pentacycle **256** did not possess the desired relative stereochemistry between the newly formed C(12) stereocenter and the C(9) and C(22) centers.



**Scheme 3.3.3** Lactone-derived A–C ring system cyclizations.

### 3.4.1 Functionalization of Allylic Alcohol **248**

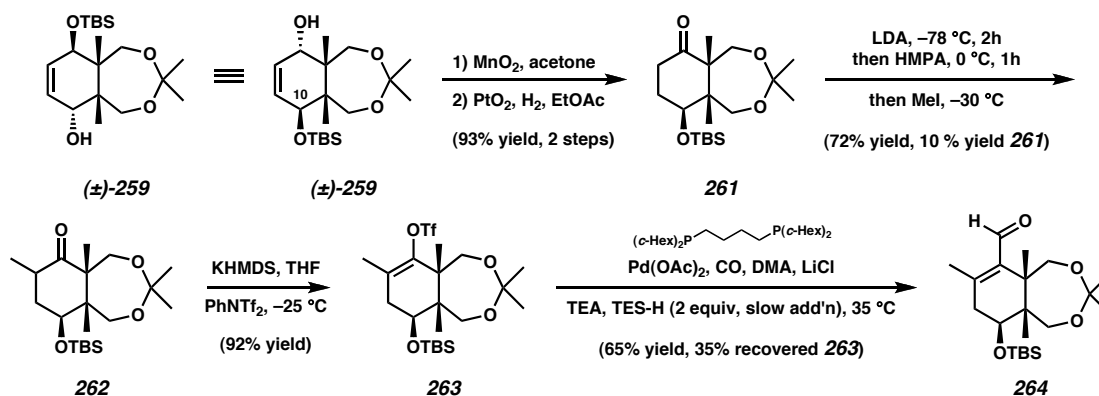
During the above investigations, we were also working to functionalize allylic alcohol **248** toward alternative C ring precursors. Accordingly, allylic alcohol **248** was smoothly silylated upon treatment with TBSOTf and pyridine to provide silyl ether **257** (Scheme 3.4.1).<sup>16</sup> At this point, we sought to differentiate the oxidation states of the lactone and methyl ester carbonyl carbons and selectively homologate C(23). Though several options were pursued, the most facile manner to accomplish this goal was to conduct a global reduction with lithium aluminum hydride, and then selectively constrain the 1,3-diol as a cyclic acetal. In the event, LAH reduction proceeded in good yield to provide triol **258**. Subsequent treatment of the triol with anhydrous copper(II) sulfate in acetone<sup>17</sup> afforded a mixture of acetal products **259** and **260**. Although we targeted selectivity for the 6-membered ring, we were aware of the competition that could exist between the 6 and 7-membered ring products.<sup>18</sup> The energy gained by formation of the more stable 6-membered ring is partially counteracted by the 1,3-diaxial interactions ( $H_{axial}/CH_{3axial}$ ) developed in the process. The greater conformational flexibility of the 7-membered ring avoids the diaxial interaction, but such a ring system is inherently less stable.<sup>18</sup> Although this mixture of products seemed like an obstacle at first, we were able to utilize it as another branching point for our synthetic efforts. Thus, we simply split our material to generate two different C ring synthons.<sup>19</sup>



**Scheme 3.4.1** Lactone reduction and triol differentiation.

### 3.5.1 Toward a 7-Membered Acetal-Derived C Ring

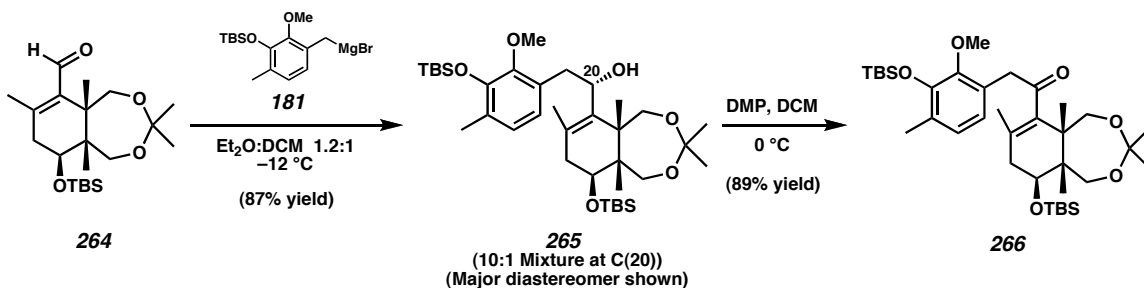
Because our desymmetrization strategy provided access to either enantiomer of all of our intermediates (see Section 3.1.1), we were able to utilize the 7-membered ring acetal product to access a C ring synthon with inverted stereochemistry at C(10) (Scheme 3.5.1). C ring synthons **252** (Scheme 3.3.1), **278** (Scheme 3.6.1), and **280** (Scheme 3.7.1) all feature an  $\alpha$ -disposed secondary alcohol at C(10). Access to a C ring synthon with a  $\beta$ -disposed alcohol derivative was of interest because we were uncertain about the role this stereocenter might play in both the acid-mediated cyclizations and radical conjugate addition reactions (see Chapter 4). Thus, oxidation of allylic alcohol **259** followed by hydrogenation with Adams' catalyst afforded ketone **261** in excellent yield over the two steps. The ketone was then methylated under standard conditions to provide methyl ketone **262** as a mixture of diastereomers. Enolization with KHMDS and trapping with *N*-phenyl bis(trifluoromethanesulfonamide) afforded enol triflate **263** in 92% yield. Treatment of enol triflate **263** under the reductive carbonylation conditions developed during our early work<sup>13</sup> led to formation of enal **264** in 65% yield with quantitative recovery of enol triflate **263**.



**Scheme 3.5.1** Synthesis of a 7-membered acetal-derived C ring.

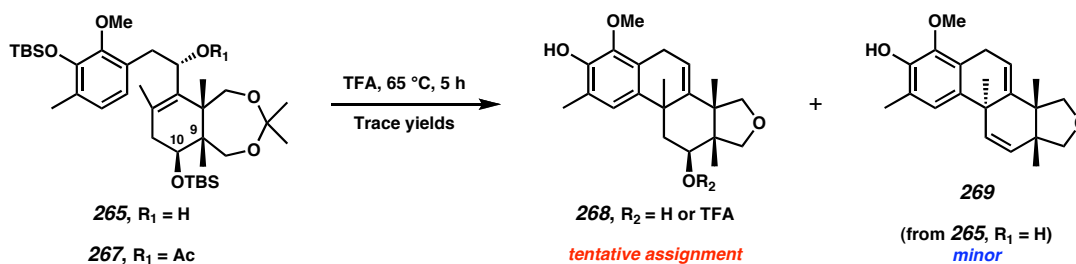
### 3.5.2 Acid-Mediated Cyclization of the 7-Membered Acetal Substrate

With enal **264** in hand, we employed our mixed-solvent Grignard conditions for fragment coupling, which gratifyingly afforded the desired stereochemistry of the C(20) alcohol in 87% yield with a 10:1 diastereomeric ratio (**265**, Scheme 3.5.2). Subsequent oxidation of this alcohol with Dess-Martin periodinane<sup>20</sup> provided the corresponding enone (**266**) in 89% yield.



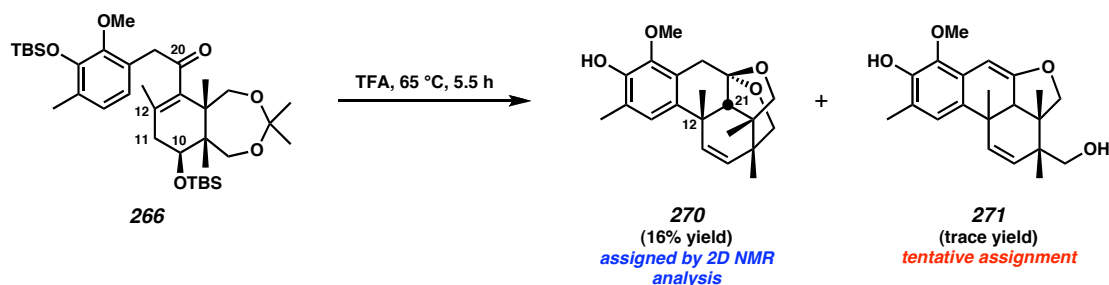
**Scheme 3.5.2** Grignard addition and oxidation to access cyclization substrates.

At this point, we were well poised to begin testing cyclization conditions for this system. Accordingly, allylic alcohol **265** was treated with neat trifluoroacetic acid, but provided only trace amounts of products that appeared to be cyclized (Scheme 3.5.3). The methylene coupling constants in the <sup>1</sup>H NMR for **268** indicated the presence of a tetrahydrofuran-type ring, and a methine signal in the <sup>1</sup>H NMR spectra indicated the presence of the C(10) alcohol functionality. Analysis of the <sup>19</sup>F NMR spectra for **268** indicated that in one case, the alcohol was substituted by a trifluoroacetate group. Tetracycle **269** was only isolated in trace amounts, but it was successfully assigned after it was isolated unexpectedly in a later reaction (see Section 3.7.2).

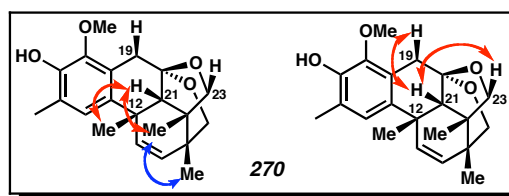


**Scheme 3.5.3** Cyclization of allylic alcohol **265**.

When enone **266** was subjected to TFA at 60 °C (Scheme 3.5.4), we were able to isolate 4 compounds that showed evidence of cyclization, with the major cyclized product having an intriguing set of spectral properties. We found that this compound possessed two olefinic resonances in its  $^1\text{H}$  NMR spectrum, and it did not display a carbonyl stretching frequency in the IR spectrum, nor could a carbonyl carbon be seen in its  $^{13}\text{C}$  NMR spectrum. Ultimately, by comparing the spectra with those observed for cyclization product **256**, we were able to determine that the product observed in this case must be **270**. The methylene coupling constants are also consistent with this assignment, and the C(12) and C(21) stereochemistry was initially assigned by analogy to **256** as well as by geometrical constraints. Ultimately, we were able to confirm this assignment by 2D NMR spectroscopy. Strong NOESY correlations were observed between the methine H at C(21) and the methyl groups at the C(12) and C(22) quaternary centers as well as the psuedoaxial Hs at C(19) and C(23). Furthermore, a substantial 3-bond coupling was observed between the equatorial H at C(19) and C(21).



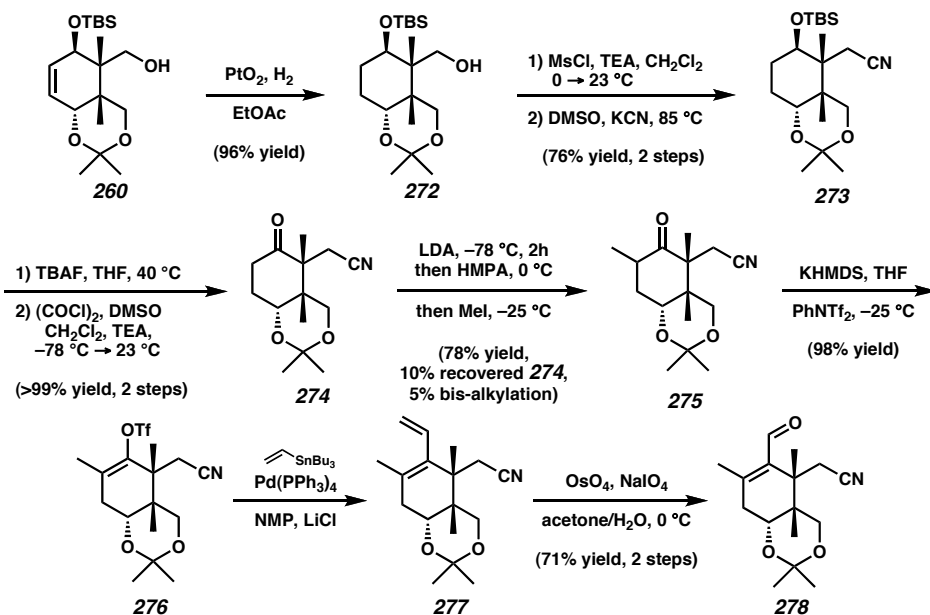
*NOESY correlations  
observed for acetal 270*



**Scheme 3.5.4** Cyclization of 7-membered acetal-derived enone substrate.

### 3.6.1 Synthesis of a Homologated C Ring Synthon

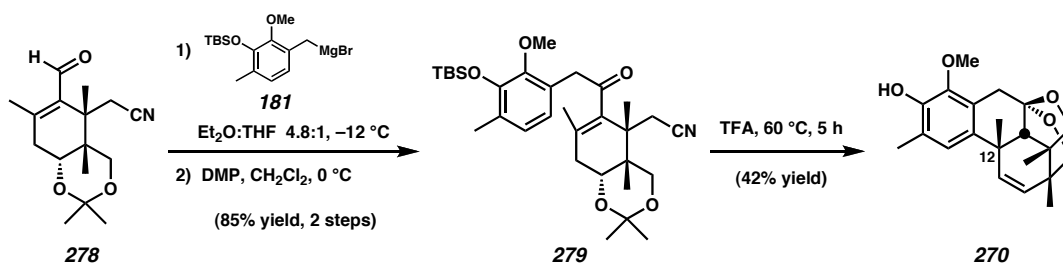
Concomitant with our investigations of the 7-membered acetal C ring, we were also exploring further functionalization of the 6-membered acetonide substrate. Our first goal in this system was to homologate the primary alcohol by one carbon. Although alcohol **260** could be readily oxidized to the corresponding aldehyde, we were unable to homologate this position using the methoxy methylene Wittig reagent.<sup>21</sup> Thus, we chose to hydrogenate the double bond (**272**), activate the primary alcohol by mesylation, and conduct a KCN displacement to form nitrile **273** (Scheme 3.6.1). Given the challenging nature of S<sub>N</sub>2 chemistry at neopentyl centers,<sup>22</sup> we were delighted to observe good yields over the homologation sequence. Desilylation was accomplished upon treatment with TBAF in THF at 40 °C to reveal a secondary alcohol, which was quantitatively converted to ketone **273** under Swern oxidation conditions. Ketone  $\alpha$ -methylation again resulted in formation of significant amounts of bis-methylation products. Presumably, the first methylation occurs with good selectivity for the equatorial product, owing to the bicyclic nature and conformational rigidity of the system. Thus, the remaining proton is likely the more acidic axial proton. We found it highly challenging to overcome the preference for the double methylation product. Ultimately, we found that reverse dropwise addition of the enolate solution into methyl iodide at -35 °C allowed formation of the mono-methyl product as the major product. In order to obtain this selectivity, the reaction was quenched before it reached complete conversion, and starting material was readily re-isolated. In the event, the desired methyl ketone **275** was obtained in 78% yield with 10% yield of recovered ketone **274** and only 5% over-alkylation. Methyl ketone **275** was then enolized and trapped with Tf<sub>2</sub>NPh to give enol triflate **276** in 97% yield. Stille coupling with vinyl tributylstannane proceeded smoothly and was followed by oxidative cleavage of the terminal olefin to provide enal **278** in good yield for the two steps.



**Scheme 3.6.1** Synthesis of a homologated C ring synthon.

### 3.6.2 Acid-Mediated Cyclizations of the Homologated A–C Ring System

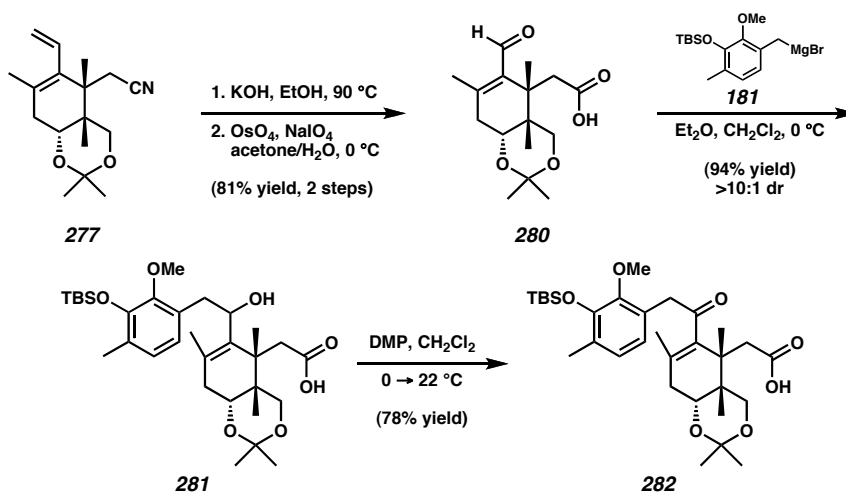
With our homologated C ring synthon in hand, we were excited to investigate the cyclization of the corresponding fragment-coupled product. We anticipated that the nitrile functionality in this substrate would prevent acetal formation in our enone cyclization. Addition of Grignard **181** occurred smoothly in a mixture of Et<sub>2</sub>O and THF to afford a 4.8:1 ratio of diastereomers (Scheme 3.6.2). This mixture was oxidized to enone **279** in 85% yield over the two steps. Much to our surprise, treatment of **279** with neat TFA again led to acetal **270** in 42% yield. The loss of the nitrile functionality was unexpected,<sup>23</sup> and a mechanism for this transformation will be discussed in Section 3.8.1.



**Scheme 3.6.2** Fragment coupling and cyclization of the nitrile-derived A–C system.

### 3.7.1 Modification of the Homologated A–C Ring System.

In order to access a system more similar to **183** (Scheme 2.2.4), nitrile **277** was hydrolyzed to the corresponding acid and oxidatively cleaved the terminal olefin to provide enal **280** (Scheme 3.7.1). Addition of Grignard **181** to a solution of enal **280** in Et<sub>2</sub>O and CH<sub>2</sub>Cl<sub>2</sub> provided allylic alcohol **281** in 94% yield and > 10:1 diastereomeric ratio.<sup>24</sup> The allylic alcohol could then be oxidized readily to provide enone **282**.

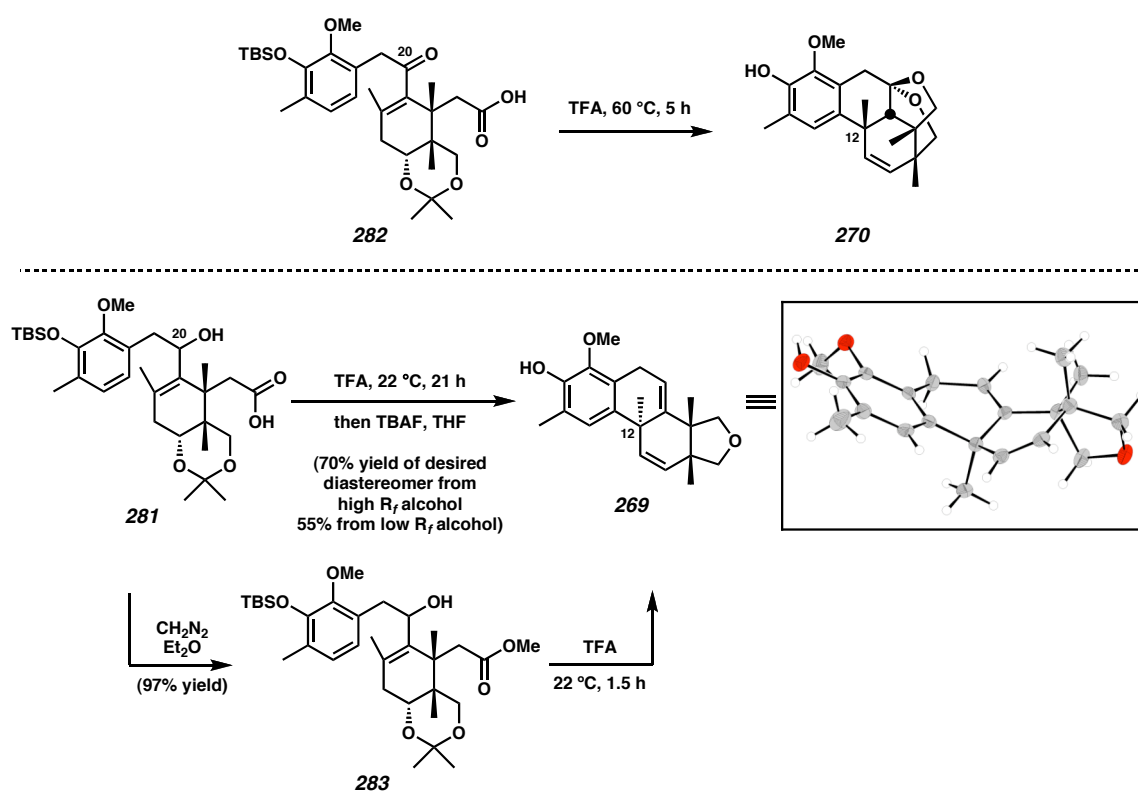


**Scheme 3.7.1** Synthesis of an acid-derived A–C ring system.

### 3.7.2 Acid-Mediated Cyclizations of Carboxylic Acid-Derived A–C Ring Systems

Cyclization precursors **281** and **282** held great promise for the acid-mediated cyclization because they represented the most similar substrates prepared to date when compared with our successful acid-cyclization system. Specifically, they possessed a homologated acid functionality on the C ring, as was present in allylic alcohol **183**.<sup>13</sup> Upon subjecting enone **282** to neat TFA, we were astounded to find that we had again formed acetal (**270**, Scheme 3.7.2). The repeated formation of this compound from significantly different substrates was perplexing. We were excited, however, about the prospects for allylic alcohol **281**, which was not expected to form such an acetal given the lower oxidation state at C(20). Indeed, upon treatment with neat TFA, now at ambient

temperature instead of 55–65 °C we observed the formation of a new compound displaying the desired relative stereochemistry at C(12). Unfortunately, upon examination of the  $^{13}\text{C}$  NMR and IR spectra, we found that there were no signals corresponding to the carboxylic acid or lactone functionalities that we would have anticipated. Thus, we assigned the observed product as **269**. X-Ray diffraction data obtained from a single crystal confirmed both the desired relative stereochemistry and our assignment of the fourth ring as a tetrahydrofuran-type ring.

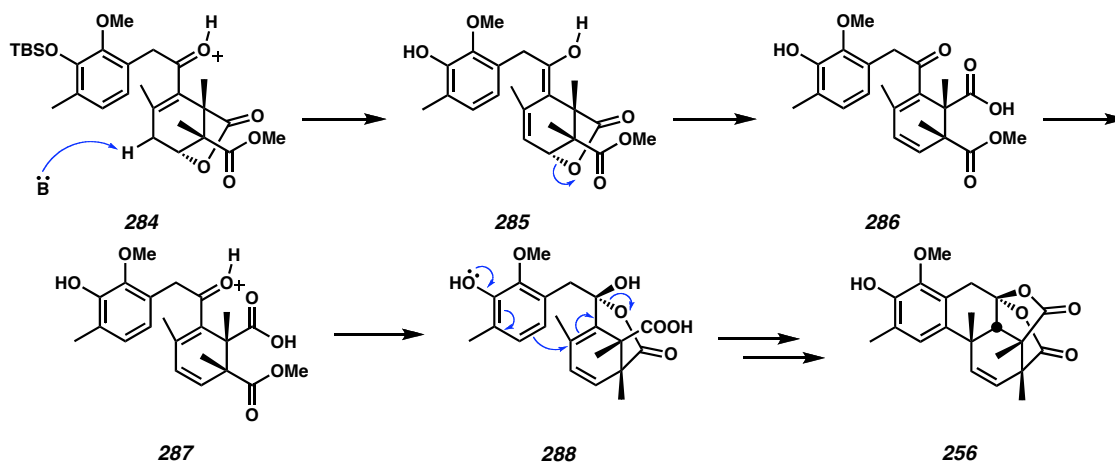


**Scheme 3.7.2** Cyclization of carboxylic acid-derived tethered A–C ring systems.

### 3.8.1 Mechanistic Hypotheses

Before discussing general mechanistic insights, we outline the proposed mechanism and potential interactions governing the stereoselectivity for each substrate type employed in the acid-mediated cyclization. In the lactone-derived C ring system, enone **255** (Scheme 3.3.3) may be activated by protonation, providing extended enol **285**

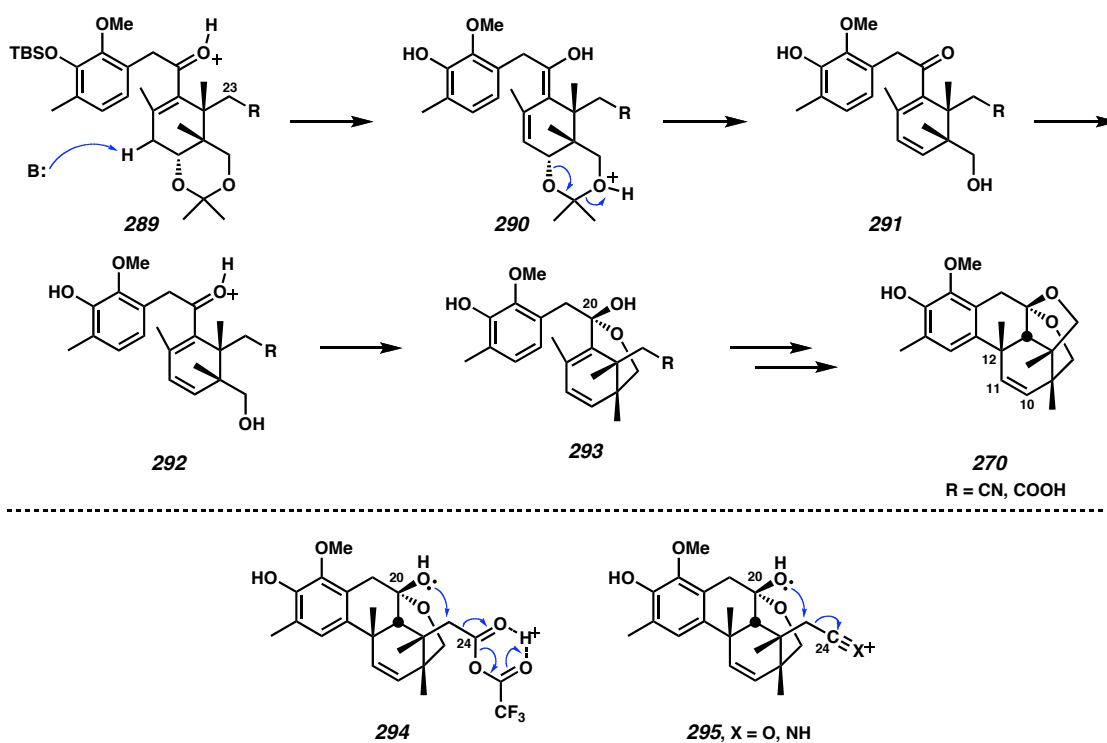
(Scheme 3.8.1). Regeneration of the enone and elimination of the lactone moiety would give carboxylic acid **286**. Subsequent enone protonation leads to resonance-stabilized cation **287**. Formation of hemi-acetal **288** leaves only the concave face of the olefin available for nucleophilic attack by the electron-rich A ring, thus yielding bis-lactone **256** after tautomerization and condensation.



**Scheme 3.8.1** Proposed mechanism for formation of bis-lactone **256**.

Cyclization of the enone versions of the 7-membered ring acetal (**266**), nitrile (**279**), and carboxylic acid (**282**) substrates led to the formation of acetal **270** (Scheme 3.8.2). In the latter two cases, we were surprised to observe loss of C(24). We propose that these substrates begin with a mechanism similar to that described above, wherein enone activation leads to deprotonation of **289** to form **290**. Subsequent reformation of the ketone again leads to elimination of the alcohol functionality at C(10) and formation of a C(10)–C(11) olefin. Protonation leads to a similar resonance stabilized cation **292**, which proceeds through hemiacetal **293**, ultimately providing acetal **270**. Attack by the A ring will occur from the concave face of hemiacetal **293** because the convex face is inaccessible. Intermediates **294** and **295** represent two potential mechanisms by which C(24) could be lost. In the case of the acid-derived substrate (**282**), a bifurcated hydrogen bond could be formed (**294**), which would activate C(23) for attack by the

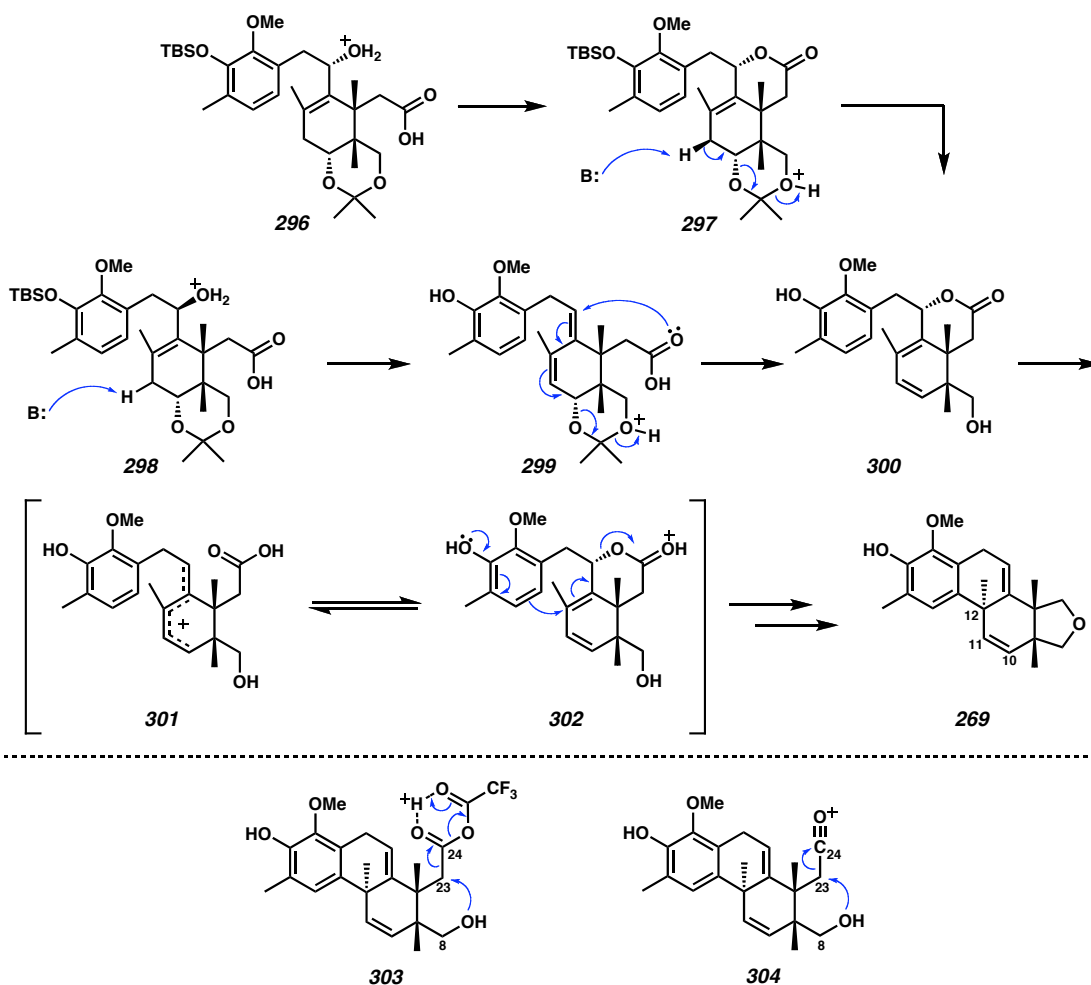
C(20) hemi-acetal. Concomitant liberation of CO and loss of TFA would provide the observed acetal. Alternatively, intermediate **294** could eliminate TFA directly to form acylium **295**. Attack by the C(20) hemi-acetal would then afford acetal **270**. Either of these intermediates could be accessed upon hydrolysis of the nitrile to form a carboxylic acid. Alternatively, protonation of the nitrile on N would form a nitrilium, resulting in elimination to form HCN and the acetal product.



**Scheme 3.8.2** Proposed mechanism for formation of acetal **270**.

For allylic alcohol substrate **281**, the  $\alpha$ -diastereomer likely forms lactone **297** very quickly (Scheme 3.8.3). Subsequent elimination of the C(10) acetal would then result in intermediate **300**. The  $\beta$ -diastereomer could undergo dehydration, forming diene **299**. Carboxylic acid attack would then lead to lactone **300**. Protonation of the lactone carbonyl would induce an equilibrium between highly stabilized carbocation **301** and **302**. We anticipate that protonated lactone **300** is the intermediate that actually undergoes cyclization, given the extraordinary selectivity observed for this system.

Furthermore, the stability of this intermediate likely aids in the formation of the product in the relatively high yields observed. Once again, we were surprised to observe loss of the C(24) carbonyl during the cyclization. We believe that the cyclization occurs much more quickly than the C(23)–C(24) bond cleavage. Thus, we propose similar intermediates to those described above, with the exception that it is the C(8) alcohol that attacks activated anhydride **303** or acylium **304** to release CO and form tetrahydrofuran-type product **269**.



**Scheme 3.8.3** Proposed mechanism for formation of tetracycle **269**.

### 3.8.2 Mechanistic Summary and Substrate Requirements

Taken together, these results provide a general outline for the development of new substrates for future investigations. In all cases where cyclized products were observed from an enone precursor, elimination of the C(10) alcohol occurred. We hypothesize that the elimination to form the C(10)–C(11) olefin stabilized the developing carbocation and lowered the energy of the transition state sufficiently to allow cyclization. Additionally, these substrates led to the formation of an acetal at C(20). The equilibrium between the ketone and the acetal states may be sufficiently deactivating to slow cyclization until the C(10)–C(11) olefin is formed. The structural rigidity of the system is such that the equilibrium between the acetal and ketone intermediates likely predisposes these substrates toward formation of the undesired stereochemistry at C(12). In all of the enone substrates, protonation occurs from the  $\beta$  face, leading to *syn* stereochemistry at the newly formed stereocenters. In fact, the desired stereochemistry at C(12) has only been observed for substrates possessing an allylic alcohol as the electrophile. The highest selectivities and yields are observed for substrates where the alcohol is already in the  $\alpha$  orientation (as depicted), allowing direct anti-periplanar attack via an  $S_N2'$ -type pathway. Additionally, the presence of a tethered carboxylic acid substantially improves both the selectivity and the yield of the cyclization. In the best case, the key directing lactone may be formed without initial loss of water, thus preventing decomposition pathways that may occur during intermediate steps.

Thus, any future substrates should display the following design elements. First, the electrophilic component of the substrate should be a secondary allylic alcohol, preferably with an  $\alpha$ -disposed alcohol (Figure 3.8.1). The substrate should incorporate a carboxylic acid group pendant from the C(22) quaternary center. It may be necessary to have already installed C(23) before the cyclization, although it remains unclear at this point whether  $\gamma$ -lactone formation is required or whether a  $\delta$ -lactone would direct the

cyclization equally well. If C(24) is present in the substrate, the R group at the C(9) quaternary center should not contain a nucleophilic moiety that can induce expulsion of CO from the carboxylic acid moiety. Furthermore, both C(8) and C(23) cannot be in the alcohol oxidation state, or a furan will be formed. Finally, in order to avoid excessive late-stage reinstallation of oxygenation, C(10) should be in the ketone oxidation state. In this way, the more activated intermediates with C(10)-C(11) olefination can be accessed (in the form of the enol tautomer) without loss of oxygenation.

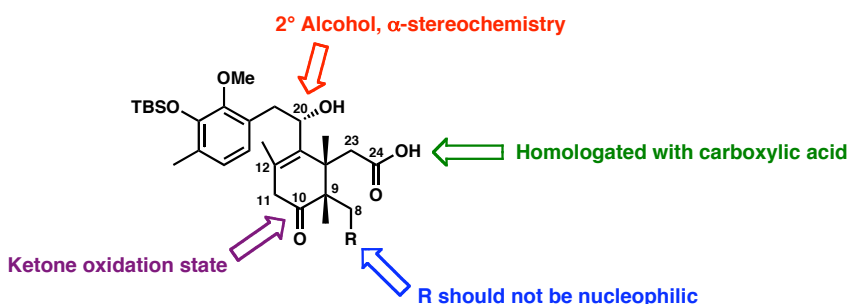


**Figure 3.8.1** Requirements for future acid cyclization substrates.

### 3.9.1 Summary of Brønsted Acid Cyclization Efforts.

In summary, we have synthesized and tested a host of different cyclization precursors for the acid-mediated cyclization of tethered A–C ring systems to form the carbocyclic core of zoanthanol. Despite the harsh nature of this system, we have been able to access highly complex systems in very good yields when the multi-step nature of the reaction is considered. For example, in the case of allylic alcohol **281**, a desilylation, alcohol/lactone elimination, acetone elimination, and CO elimination all occur in addition to the cyclization. In total, 6 reactions occur in one reaction flask, with one reagent, to form the desired diastereomer of a tetracyclic compound possessing three all-carbon quaternary centers in 70% yield (corresponding to an average 94% yield per reaction). Clearly, this method has presented a number of challenges. However, the

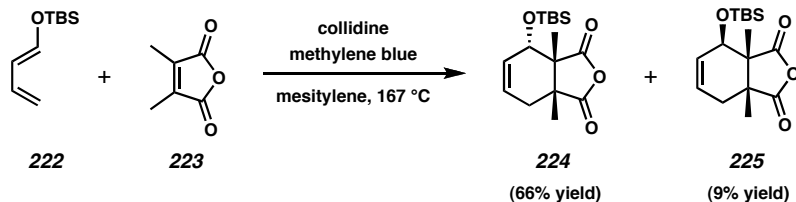
range of substrates that we have employed has helped us to develop a detailed grasp of the requirements of the system. Thus, we remain confident that this method is the most powerful of our current methods to form the C(12) quaternary center from a tethered A–C ring system.

### 3.10.1 Materials and Methods

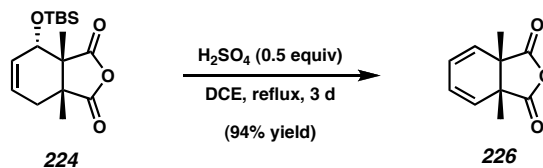
Unless otherwise stated, reactions were performed at ambient temperature (typically 19–24 °C) in flame-dried glassware under an argon or nitrogen atmosphere using dry, deoxygenated solvents. Solvents were dried by passage through an activated alumina column under argon. HMPA, TEA, DIPA, and pyridine were freshly distilled from CaH<sub>2</sub>. KHMDS (95%) was purchased from Aldrich and stored in a glovebox until use. Trifluoroacetic acid (99%) was purchased from Aldrich. LiCl was flame-dried under vacuum prior to use. Magnesium turnings were of 99.98% purity and purchased from Aldrich. TBSCl was purchased from Gelest. TBSOTf was freshly prepared as described by Corey.<sup>25</sup> All other commercially obtained reagents were used as received. Reaction temperatures were controlled by an IKAmag temperature modulator. Thin-layer chromatography (TLC) was performed using E. Merck silica gel 60 F254 precoated plates (0.25 mm) and visualized by UV fluorescence quenching, anisaldehyde, KMnO<sub>4</sub>, or CAM staining. ICN silica gel (particle size 0.032–0.063 mm) was used for flash chromatography. Optical rotations were measured with a Jasco P-1010 polarimeter at 589 nm. <sup>1</sup>H and <sup>13</sup>C NMR spectra were recorded on a Varian Mercury 300 (at 300 MHz and 75 MHz respectively), or a Varian Inova 500 (at 500 MHz and 125 MHz respectively) and are reported relative to Me<sub>4</sub>Si (δ 0.0). Data for <sup>1</sup>H NMR spectra are reported as follows: chemical shift (δ ppm) (multiplicity, coupling constant (Hz), integration). Multiplicities are reported as follows: s = singlet, d = doublet, t = triplet, q = quartet, sept. = septet, m = multiplet, comp. m = complex multiplet, app. = apparent, bs = broad

singlet. IR spectra were recorded on a Perkin Elmer Paragon 1000 spectrometer and are reported in frequency of absorption ( $\text{cm}^{-1}$ ). High-resolution mass spectra were obtained from the Caltech Mass Spectral Facility. Crystallographic analyses were performed at the California Institute of Technology Beckman Institute X-Ray Crystallography Laboratory. Crystallographic data have been deposited at the CCDC, 12 Union Road, Cambridge CB2 1EZ, UK and copies can be obtained on request, free of charge, from the CCDC by quoting the publication citation and the deposition number (see Appendix B for deposition numbers).

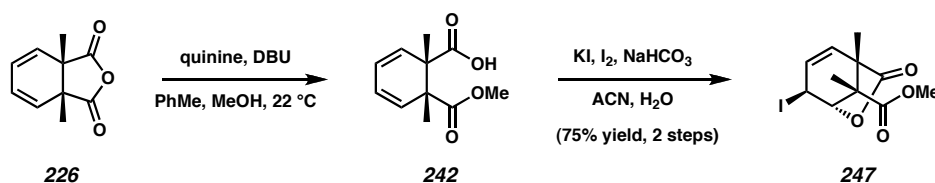
## 3.10.2 Preparation of Compounds



**Endo-Diels-Alder Adduct 224 and Exo-Diels-Alder Adduct 225.** A mixture of diene **222** (67.3 g, 367.2 mmol, 1.00 equiv), 2,3-dimethylmaleic anhydride (**223**, 46.3 g, 367.2 mmol, 1.00 equiv), collidine (2.91 mL, 22.0 mmol, 0.06 equiv), methylene blue (68.0 mg, 0.213 mmol, 0.000579 equiv), and mesitylene (80 mL) in a flamed-dried Ar filled Schlenk was sparged with Ar for 10 min, sealed, and heated to 167 °C for 3 d. Upon cooling, the reaction mixture was concentrated at 80 °C to give an oil, which was purified by flash chromatography on silica gel (1 to 10% EtOAc in hexanes) to give known *endo*-Diels-Alder adduct **224** (75.7 g, 66% yield) which solidified on standing:  $R_f$  0.42 (15% EtOAc in hexanes) and *exo*-Diels-Alder adduct **225** (10.5 g, 9% yield) as an amorphous solid:  $R_f$  0.58 (15% EtOAc in hexanes);  $^1\text{H}$  NMR (500 MHz,  $\text{CDCl}_3$ )  $\delta$  6.11 (m, 1H), 5.99 (m, 1H), 4.35 (d,  $J = 5.5$  Hz, 1H), 2.61 (dd,  $J = 6.3, 16.3$  Hz, 1H), 2.42 (app. dt,  $J = 3.3, 16.5$  Hz, 1H), 1.42 (s, 3H), 1.39 (s, 3H), 0.88 (s, 9H), 0.10 (s, 3H), 0.04 (s, 3H);  $^{13}\text{C}$  NMR (125 MHz,  $\text{CDCl}_3$ )  $\delta$  177.4, 175.1, 132.2, 129.8, 69.1, 53.8, 46.5, 34.2, 25.6, 21.6, 18.0, 17.6, -4.4, -5.2; IR (Neat film NaCl) 2952, 2930, 1774, 1250, 986, 1091, 986, 958, 914, 838, 778  $\text{cm}^{-1}$ ; HRMS (FAB+)  $[\text{M}+\text{H}]^+$   $m/z$  calc'd for  $[\text{C}_{16}\text{H}_{26}\text{SiO}_4+\text{H}]^+$ : 311.1679, found 311.1671.



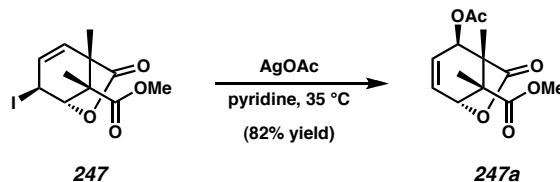
**Diene 226.** To a solution of *endo*-Diels-Alder adduct **224** (19.0 g, 61.4 mmol, 1.0 equiv) in DCE (614 mL) was added H<sub>2</sub>SO<sub>4</sub> (1.71 mL, 30.7 mmol, 0.50 equiv) and the resulting solution was refluxed for 3 d. Upon cooling the reaction mixture was washed with sat. aq. NaHCO<sub>3</sub> (2 x 300 mL) [*Caution: gas evolution!*] and extracted with CH<sub>2</sub>Cl<sub>2</sub> (2 x 120 mL). The combined organics from two such reactions were concentrated to give an oil and purified by flash chromatography on silica gel (1 to 10% EtOAc in hexanes) to give diene **226** (20.7 g, 94% yield) as a white solid: mp 61.5–62.5 °C; *R<sub>f</sub>* 0.33 (15% EtOAc in hexanes); <sup>1</sup>H NMR (500 MHz, CDCl<sub>3</sub>) δ 6.18–6.13 (m, 2H), 5.66–5.61 (m, 2H), 1.37 (s, 6H); <sup>13</sup>C NMR (125 MHz, CDCl<sub>3</sub>) δ 175.1, 126.3, 124.5, 49.9, 18.6; IR (Neat film NaCl) 2984, 2940, 2848, 1856, 1785, 1233, 1196, 962, 912 cm<sup>-1</sup>; HRMS (FAB+) [M+H]<sup>+</sup> *m/z* calc'd for [C<sub>16</sub>H<sub>26</sub>SiO<sub>4</sub>+H]<sup>+</sup>: 311.1679, found 311.1671.



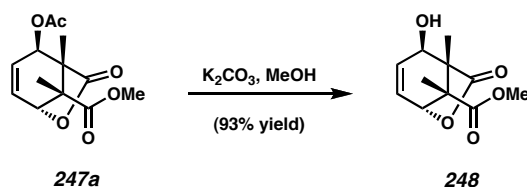
**Iodolactone 247.** To a solution of diene **226** (17.2 g, 96.6 mmol, 1.00 equiv), quinine (3.48 g, 9.66 mmol, 0.10 equiv), and DBU (15.9 mL, 106 mmol, 1.1 equiv) in toluene (483 mL) was added MeOH (39.1 mL, 966 mmol, 10.0 equiv). After 5 h, the reaction mixture was concentrated and the residue was diluted with EtOAc (1.00 L), washed with 2 M HCl (3 x 200 mL) and brine (1 x 200 mL), dried (MgSO<sub>4</sub>), and concentrated. Upon standing under vacuum, carboxylic acid **242** solidified and was typically used immediately in the next step without purification: *R<sub>f</sub>* 0.19 (30% acetone in hexanes); <sup>1</sup>H NMR (500 MHz, CDCl<sub>3</sub>) δ 5.80–5.45 (m, 4H), 3.66 (s, 3H), 1.46 (s, 3H), 1.45 (s, 3H); <sup>13</sup>C NMR (125 MHz,

$\text{CDCl}_3$ )  $\delta$  180.5, 175.1, 131.6, 131.5, 121.9, 121.8, 52.1, 48.4, 48.1, 20.2 (2C); IR (Neat film NaCl) 2985, 2954, 1731, 1700, 1258, 1240, 1132, 1102, 702  $\text{cm}^{-1}$ ; HRMS (EI)  $[\text{M}]^+$   $m/z$  calc'd for  $[\text{C}_{11}\text{H}_{14}\text{O}_4]^+$ : 210.0892, found 210.0898;  $[\alpha]_{\text{D}}^{26}$   $-10.94$  (c 1.03,  $\text{CHCl}_3$ , 50% ee) from reaction with stoichiometric quinine. HPLC analysis (Chirapak AD 4.6 x 25 mm, 5.0% IPA in 95% hexane with 0.1% TFA, 1.0 mL/min,  $\lambda$  = 254 nm) of the asymmetric reaction performed with a catalytic amount of menthol derivative **246** showed carboxylic acid **242** to be of 85% ee ( $t_{\text{fast}}$  = 10.11 min, major;  $t_{\text{slow}}$  = 12.13 min, minor).

The above residue containing carboxylic acid **242** (theoretical yield: 96.6 mmol, 1.00 equiv) was dissolved in ACN (380 mL) and  $\text{H}_2\text{O}$  (380 mL) and treated with  $\text{NaHCO}_3$  (24.3 g, 290 mmol, 3.00 equiv), KI (43.3 g, 261 mmol, 2.70 equiv), and  $\text{I}_2$  (66.2 g, 261 mmol, 2.70 equiv) and the flask was wrapped in foil to exclude light. After 10 h, the reaction mixture was quenched in the dark with sat. aq.  $\text{Na}_2\text{S}_2\text{O}_3$  until colorless, diluted with EtOAc (650 mL), extracted with EtOAc (2 x 300 mL), washed with brine (200 mL), dried ( $\text{MgSO}_4$ ), and concentrated to an oil, which was purified by flash chromatography on silica gel (10 to 20% EtOAc in hexanes) to provide iodolactone **247** (24.4 g, 75% yield, 2 steps) as an unstable solid (typically used immediately in the next step):  $R_f$  0.35 (50% EtOAc in hexanes);  $^1\text{H}$  NMR (300 MHz,  $\text{C}_6\text{D}_6$ )  $\delta$  5.33 (ddd,  $J$  = 1.5, 3.0, 9.3 Hz, 1H), 4.86 (dd,  $J$  = 1.5, 9.3 Hz, 1H), 4.63 (app. t,  $J$  = 2.1 Hz, 1H), 4.29 (m, 1H), 3.13 (s, 3H), 1.34 (s, 3H), 1.27 (s, 3H);  $^{13}\text{C}$  NMR (75 MHz,  $\text{C}_6\text{D}_6$ )  $\delta$  175.3, 173.0, 133.0, 130.1, 80.4, 53.6, 52.5, 47.0, 16.9, 16.0, 15.0; IR (Neat film NaCl) 2953, 1795, 1732, 1450, 1293, 1247, 1141, 1107, 1062, 969  $\text{cm}^{-1}$ ; HRMS (EI)  $[\text{M}]^+$   $m/z$  calc'd for  $[\text{C}_{11}\text{H}_{14}\text{O}_4\text{I}]^+$ : 336.9937, found 336.9930.

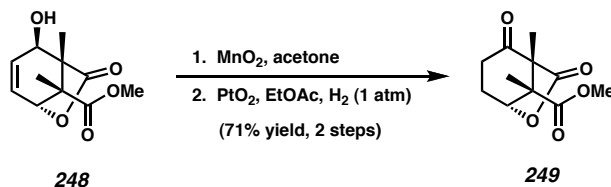


**Allylic Acetate 247a.** To a solution of iodolactone **247** (23.0 g, 68.5 mmol, 1.00 equiv) in pyridine (140 mL) was added AgOAc (34.3 g, 206 mmol, 3.00 equiv). The reaction mixture was wrapped in foil to exclude light and heated to 35 °C. After 3.5 d, the reaction mixture was concentrated (~ 5 torr at 50 °C), diluted with H<sub>2</sub>O (500 mL) and CH<sub>2</sub>Cl<sub>2</sub> (300 mL), and extracted with CH<sub>2</sub>Cl<sub>2</sub> (7 x 150 mL). The combined organics were dried (MgSO<sub>4</sub>), filtered, concentrated, and purified by flash chromatography on silica gel (15 to 35% EtOAc in hexanes) to provide allylic acetate **247a** (15.2 g, 82% yield) as an oil: *R<sub>f</sub>* 0.57 (50% EtOAc in hexanes); <sup>1</sup>H NMR (500 MHz, CDCl<sub>3</sub>) δ 6.33 (ddd, *J* = 1.0, 5.6, 9.1 Hz, 1H), 5.98 (ddd, *J* = 1.0, 3.5, 9.0 Hz, 1H), 5.35 (dd, *J* = 1.5, 3.5 Hz, 1H), 4.85 (dd, *J* = 1.0, 6.0 Hz, 1H), 3.75 (s, 3H), 2.11 (s, 3H), 1.46 (s, 3H), 1.34 (s, 3H); <sup>13</sup>C NMR (125 MHz, CDCl<sub>3</sub>) δ 177.2, 173.0, 169.6, 131.1, 129.5, 76.8, 69.9, 54.7, 52.7, 50.0, 20.7, 15.6, 13.6; IR (Neat film NaCl) 2986, 2953, 1788, 1735, 1373, 1257, 1219, 1024, 962 cm<sup>-1</sup>; HRMS (FAB+) [M+H]<sup>+</sup> *m/z* calc'd for [C<sub>13</sub>H<sub>16</sub>O<sub>6</sub>+H]<sup>+</sup>: 269.1025, found 269.1014.



**Allylic Alcohol 211.** To a solution of allylic acetate **210** (15.2 g, 56.2, 1.00 equiv) in MeOH (275 mL) was added K<sub>2</sub>CO<sub>3</sub> (1.55 g, 11.3 mmol, 0.20 equiv) and the reaction was vigorously stirred. After 10 min, TLC analysis indicated consumption of the starting material, and the reaction mixture was quenched with H<sub>2</sub>O (200 mL), brine (300 mL), and CH<sub>2</sub>Cl<sub>2</sub> (200 mL). The pH of the aqueous layer was adjusted to pH 7 with 3 M HCl

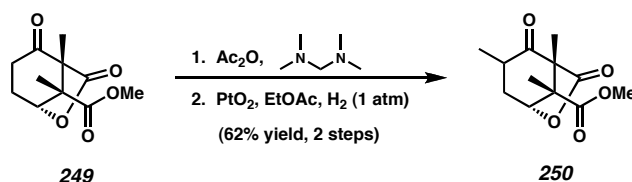
(~ 8 mL) [*Caution: gas evolution!*] and extracted with CH<sub>2</sub>Cl<sub>2</sub> (10 x 50 mL). The combined organics were washed with brine (100 mL), concentrated, and purified by flash chromatography on silica gel (25 to 35% EtOAc in hexanes) to provide allylic alcohol **211** (11.9 g, 93% yield) as a white solid. Crystals suitable for X-ray analysis were obtained by crystallization from Et<sub>2</sub>O/heptanes at ambient temperature: mp 94.5–95.5 °C (Et<sub>2</sub>O/heptane); *R<sub>f</sub>* 0.38 (50% EtOAc in hexanes); <sup>1</sup>H NMR (500 MHz, CDCl<sub>3</sub>) δ 6.22 (ddd, *J* = 1.5, 5.8, 9.3 Hz, 1H), 6.04 (ddd, *J* = 1.0, 3.3, 9.3 Hz, 1H), 4.79 (dd, *J* = 1.0, 5.5 Hz, 1H), 4.15 (dd, *J* = 1.0, 3.5 Hz, 1H), 3.72 (s, 3H), 1.43 (s, 3H), 1.41 (s, 3H); <sup>13</sup>C NMR (125 MHz, CDCl<sub>3</sub>) δ 179.3, 173.6, 134.8, 127.3, 77.4, 69.8, 54.7, 52.6, 50.8, 15.5, 13.7; IR (Neat film NaCl) 3484, 2954, 1773, 1731, 1454, 1259, 1137, 1110, 1049, 1031, 983, 955 cm<sup>-1</sup>; HRMS (FAB+) [M+H]<sup>+</sup> *m/z* calc'd for [C<sub>11</sub>H<sub>14</sub>O<sub>5</sub>+H]<sup>+</sup>: 227.0919, found 227.0924.



**Ketone 249.** To a solution of allylic alcohol **248** (2.23 g, 9.86 mmol, 1.00 equiv) in acetone (100 mL) was added activated MnO<sub>2</sub> (17.1 g, 197 mmol, 20.0 equiv) and the reaction mixture was stirred at ambient temperature for 1.25 h. The reaction mixture was filtered, washed with acetone, and concentrated to an oil.

To a solution of this crude material in EtOAc (60 mL) was added PtO<sub>2</sub> (67.1 mg, 0.296 mmol, 0.03 equiv), and the reaction mixture was sparged with H<sub>2</sub> (5 min) and stirred vigorously under an atmosphere of H<sub>2</sub> (balloon) for 1.5 h. The reaction mixture was flushed with N<sub>2</sub> and concentrated to an oil, which was purified by flash chromatography on silica gel (30 to 50% EtOAc in hexanes) to provide ketone **249** (1.59 g, 71% yield) as an amorphous solid: *R<sub>f</sub>* 0.38 (50% EtOAc in hexanes); <sup>1</sup>H NMR (300

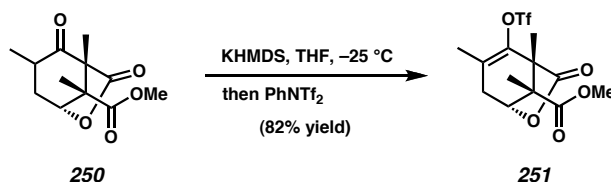
MHz, CDCl<sub>3</sub>) δ 4.89 (dd,  $J = 1.2, 3.9$  Hz, 1H), 3.75 (s, 3H), 2.62–2.56 (m, 2H), 2.47–2.37 (m, 1H), 2.15–2.01 (m, 1H), 1.23 (s, 3H), 1.20 (s, 3H); <sup>13</sup>C NMR (75 MHz, CDCl<sub>3</sub>) δ 200.0, 173.4, 171.3, 79.4, 62.4, 56.5, 53.0, 33.9, 24.9, 14.3, 9.3; IR (Neat film NaCl) 2989, 2955, 1790, 1732, 1343, 1267, 1227, 1152, 1089, 1018, 966 cm<sup>-1</sup>; HRMS (EI) [M]<sup>+</sup>  $m/z$  calc'd for [C<sub>11</sub>H<sub>14</sub>O<sub>5</sub>]<sup>+</sup>: 226.0841, found 226.0847.



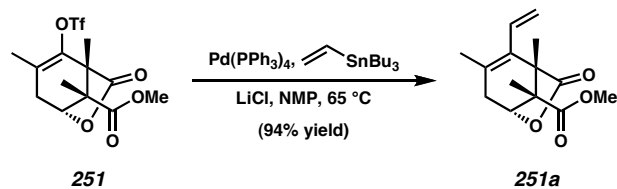
**Methyl ketone 250.** To a cooled (15 °C) solution of ketone **249** (1.31 g, 5.77 mmol, 1.00 equiv) and Ac<sub>2</sub>O (6.55 mL, 69.3 mmol, 12.0 equiv) was added *N,N,N',N'*-tetramethyldiaminomethane (4.73 mL, 34.6 mmol, 6.00 equiv) in a dropwise manner over 30 min. At the end of the addition, the reaction was allowed to come to ambient temperature. After 4 h, additional Ac<sub>2</sub>O (6.00 mL, 63.5 mmol, 11.0 equiv) and *N,N,N',N'*-tetramethyldiaminomethane (7.00 mL, 51.3 mmol, 8.89 equiv) were added and the reaction was warmed to 32 °C for 12 h. The reaction mixture was then cooled, concentrated in vacuo, quenched into water (40 mL), sat. aq. NaHCO<sub>3</sub> (20 mL), and ice (40 g), and extracted with CH<sub>2</sub>Cl<sub>2</sub> (4 x 40 mL). The combined organics were dried (Na<sub>2</sub>SO<sub>4</sub>) and concentrated to give a crude solid which was used immediately in the next step.

To a solution of the crude material in EtOAc (100 mL) was added PtO<sub>2</sub> (131 mg, 0.577 mmol, 0.10 equiv), and the reaction mixture was sparged with H<sub>2</sub> (5 min) and stirred vigorously under an atmosphere of H<sub>2</sub> (balloon) for 5.5 h. The reaction mixture was flushed with N<sub>2</sub> and concentrated to an oil, which was purified by flash chromatography on silica gel (20 to 40% EtOAc in hexanes) to provide a single diastereomer of methyl ketone **250** (854 mg, 62% yield) as an amorphous solid:  $R_f$  0.57, 0.29 (50% EtOAc in

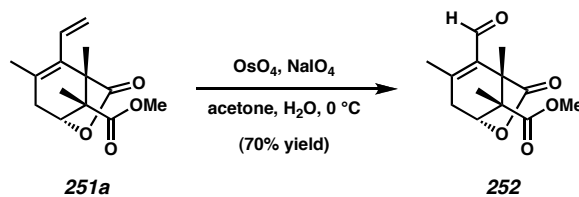
hexanes, 50% Et<sub>2</sub>O in hexanes developed twice); <sup>1</sup>H NMR (300 MHz, CDCl<sub>3</sub>) δ 4.87 (m, 1H), 3.75 (s, 3H), 2.75–2.56 (m, 2H), 1.82–1.66 (m, 1H), 1.27 (s, 3H), 1.14 (d, *J* = 6.3 Hz, 3H), 1.11 (s, 3H); <sup>13</sup>C NMR (75 MHz, CDCl<sub>3</sub>) δ 202.3, 174.1, 171.3, 79.4, 62.0, 57.3, 53.0, 38.9, 34.0, 14.7, 13.9, 9.6; IR (Neat film NaCl) 2987, 2954, 1788, 1726, 1259, 1154, 1077, 1038 cm<sup>-1</sup>; HRMS (EI) [M]<sup>+</sup> *m/z* calc'd for [C<sub>12</sub>H<sub>16</sub>O<sub>5</sub>]<sup>+</sup>: 240.0998, found 240.0996.



**Triflate 251.** To a cooled (-25 °C) solution of KHMDS (339 mg, 1.70 mmol, 1.20 equiv) in THF (12 mL) was added methyl ketone **250** (340 mg, 1.42 mmol, 1.00 equiv) in THF (10 mL) in a dropwise manner over 10 min. After 1.5 h at -25 °C, PhNTf<sub>2</sub> (708 mg, 1.98 mmol, 1.40 equiv) in THF (5 mL) was added, and the reaction was maintained for an additional 30 min at -25 °C. The reaction mixture quenched into half-saturated brine (40 mL) and EtOAc (40 mL), and extracted with EtOAc (4 x 15 mL). The combined organics were washed with brine (2 x 20 mL), dried (MgSO<sub>4</sub>), and concentrated to an oil, which was purified by flash chromatography on silica gel (15 to 40% EtOAc in hexanes) to provide triflate **251** (435 mg, 82% yield) as an oil: *R<sub>f</sub>* 0.20 (50% Et<sub>2</sub>O in hexanes developed twice); <sup>1</sup>H NMR (300 MHz, CDCl<sub>3</sub>) δ 4.59 (app. t, *J* = 2.7 Hz, 1H), 3.75 (s, 3H), 2.63–2.47 (m, 2H), 1.86 (s, 3H), 1.42 (s, 3H), 1.33 (s, 3H); <sup>13</sup>C NMR (75 MHz, CDCl<sub>3</sub>) δ 174.1, 172.1, 138.2, 128.2, 118.4 (app. d, *J*<sub>C-F</sub> = 319 Hz), 77.2, 54.6, 53.0, 50.4, 35.0, 17.2, 12.6, 10.0; IR (Neat film NaCl) 2956, 1790, 1727, 1408, 1208, 1138, 824 cm<sup>-1</sup>; HRMS (EI) [M+H]<sup>+</sup> *m/z* calc'd for [C<sub>13</sub>H<sub>15</sub>O<sub>7</sub>F<sub>3</sub>S+H]<sup>+</sup>: 373.0569, found 373.0550.

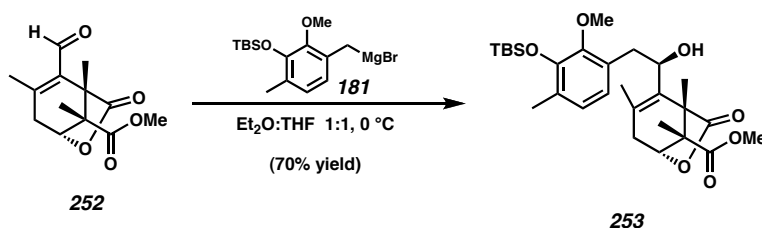


**Diene 251a.** To a solution of triflate **251** (865 mg, 2.32 mmol, 1.00 equiv), Pd(PPh<sub>3</sub>)<sub>4</sub> (134.2 mg, 0.116 mmol, 0.05 equiv), and LiCl (295 mg, 6.97 mmol, 3.00 equiv) in NMP (18 mL) was added tributyl(vinyl)tin (1.02 mL, 3.48 equiv, 1.50 equiv), and the mixture was heated to 65 °C for 9.5 h. The reaction mixture was cooled to ambient temperature, quenched with H<sub>2</sub>O (50 mL) and Et<sub>2</sub>O (50 mL), and extracted with Et<sub>2</sub>O (5 x 30 mL). The combined organics were washed with brine (2 x 20 mL), dried (MgSO<sub>4</sub>), and concentrated to an oil, which was purified by flash chromatography on silica gel (5 to 25% EtOAc in hexanes) to provide diene **251a** (545 mg, 94% yield) as an oil: *R<sub>f</sub>* 0.63, 0.80 (50% Et<sub>2</sub>O in hexanes developed thrice, 50% EtOAc in hexanes developed twice); <sup>1</sup>H NMR (300 MHz, CDCl<sub>3</sub>) δ 6.01 (ddd, *J* = 1.2, 11.3, 17.6 Hz, 1H), 5.34 (dd, *J* = 2.0, 11.3 Hz, 1H), 5.02 (dd, *J* = 2.3, 17.6 Hz, 1H), 4.53 (app. t, *J* = 2.7 Hz, 1H), 3.70 (s, 3H), 2.37 (s, 2H), 1.72 (s, 3H), 1.23 (s, 3H), 1.20 (s, 3H); <sup>13</sup>C NMR (75 MHz, CDCl<sub>3</sub>) δ 176.7, 173.7, 132.3, 131.5, 130.2, 120.6, 77.7, 53.6, 52.5, 49.3, 35.3, 20.0, 12.9, 12.5; IR (Neat film NaCl) 2985, 2951, 2911, 1782, 1730, 1267, 1198, 1144, 1089, 1035, 972 cm<sup>-1</sup>; HRMS (EI) [M]<sup>+</sup> *m/z* calc'd for [C<sub>14</sub>H<sub>18</sub>O<sub>4</sub>]<sup>+</sup>: 250.1205, found 250.1204.



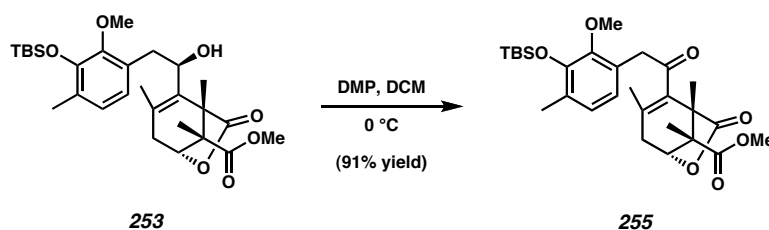
**Enal 252.** To a cooled (0 °C) solution of diene **251a** (271 mg, 1.08 mmol, 1.00 equiv) in acetone (8.00 mL) and H<sub>2</sub>O (8.00 mL) was added OsO<sub>4</sub> (27.5 mg, 0.108 mmol, 0.10 equiv) and NaIO<sub>4</sub> (511 mg, 2.38 mmol, 2.20 equiv). After 8.5 h at 0 °C, the reaction

mixture was quenched with brine (30 mL) and EtOAc (30 mL), and extracted with EtOAc (5 x 30 mL). The combined organics were dried (Na<sub>2</sub>SO<sub>4</sub>) and concentrated to an oil, which was purified by flash chromatography on silica gel (25 to 50% EtOAc in hexanes) to provide enal **252** (191 mg, 70% yield) as a solid: *R<sub>f</sub>* 0.48 (50% EtOAc in hexanes developed twice); <sup>1</sup>H NMR (300 MHz, CDCl<sub>3</sub>) δ 9.88 (s, 1H), 4.54 (app. t, *J* = 2.4 Hz, 1H), 3.72 (s, 3H), 2.57 (d, *J* = 1.8 Hz, 2H), 2.07 (s, 3H), 1.49 (s, 2H), 1.21 (s, 3H); <sup>13</sup>C NMR (75 MHz, CDCl<sub>3</sub>) δ 189.9, 176.0, 172.8, 151.0, 131.6, 76.7, 53.9, 52.7, 48.2, 37.5, 19.2, 12.5, 12.3; IR (Neat film NaCl) 2952, 1786, 1729, 1681, 1333, 1273, 1250, 1201, 1136, 1082, 1034, 969 cm<sup>-1</sup>; HRMS (EI) [M]<sup>+</sup> *m/z* calc'd for [C<sub>13</sub>H<sub>16</sub>O<sub>5</sub>]<sup>+</sup>: 252.0998, found 252.0984.



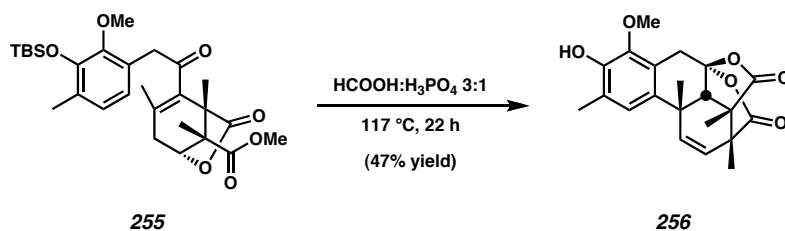
**Allylic alcohol 252.** A flame-dried two-neck round bottom flask equipped with a reflux condenser and septum was charged with magnesium turnings (1.03 g, 42.4 mmol, 32.4 equiv) and Et<sub>2</sub>O (12 mL) under an N<sub>2</sub> atmosphere and heated to reflux. To this mixture was added 1,2-dibromoethane (150 μL, 1.74 mmol, 1.33 equiv) in a dropwise manner [*Caution: gas evolution!*]. When gas evolution ceased, a solution of benzyl bromide **151** (677 mg, 1.96 mmol, 1.50 equiv) in Et<sub>2</sub>O (7.0 mL) was added in a dropwise manner over 30 min and heating was continued for an additional 30 min. The Grignard reagent was then cooled (0 °C) and added to a cooled (0 °C) solution of enal **252** (330 mg, 1.31 mmol, 1.00 equiv) in Et<sub>2</sub>O (10 mL) and THF (30 mL). After 1 h at 0 °C, the reaction mixture was allowed to come to ambient temperature, and after an additional 30 min, the reaction was quenched with ice-cold H<sub>2</sub>O (50 mL), 2 M HCl (2.0 mL), and

Et<sub>2</sub>O (20 mL), and extracted with Et<sub>2</sub>O (4 x 40 mL). The combined organics were washed with brine (2 x 30 mL), dried (MgSO<sub>4</sub>), and concentrated to an oil, which was purified by flash chromatography on silica gel (15 to 50% EtOAc in hexanes) to give allylic alcohol **253** (477 mg, 70% yield) as a white solid. Crystals suitable for X-ray analysis were obtained by crystallization from EtOAc/heptanes at ambient temperature: mp 154–155 °C (EtOAc/heptane); *R<sub>f</sub>* 0.50 (35% EtOAc in hexanes developed twice); <sup>1</sup>H NMR (300 MHz, CDCl<sub>3</sub>) δ 6.83 (d, *J* = 7.7 Hz, 1H), 6.71 (d, *J* = 7.5 Hz, 1H), 4.75 (bs, 1H), 4.52 (app. t, *J* = 2.6 Hz, 1H), 3.74 (s, 3H), 3.72 (s, 3H), 3.00–2.80 (m, 2H), 2.76–2.54 (bs, 1H), 2.36 (m, 2H), 2.20 (s, 3H), 1.78 (s, 3H), 1.50 (s, 3H), 1.29 (s, 3H), 1.02 (s, 9H), 0.15 (m, 6H); <sup>13</sup>C NMR (75 MHz, CDCl<sub>3</sub>) δ 177.7, 173.8, 149.4, 147.1, 132.5, 131.8, 129.8, 129.6, 126.3, 123.5, 123.3, 72.0, 60.1, 54.4, 52.6, 50.0, 37.4, 37.0, 26.0, 19.4, 18.6, 17.1, 13.1, 12.9, –4.1; IR (Neat film NaCl) 3519, 2953, 2930, 2858, 1777, 1731, 1462, 1419, 1259, 1073, 840 cm<sup>-1</sup>; HRMS (FAB+) [M+Na]<sup>+</sup> *m/z* calc'd for [C<sub>28</sub>H<sub>42</sub>SiO<sub>7</sub>+Na]<sup>+</sup>: 541.2598, found 541.2571.



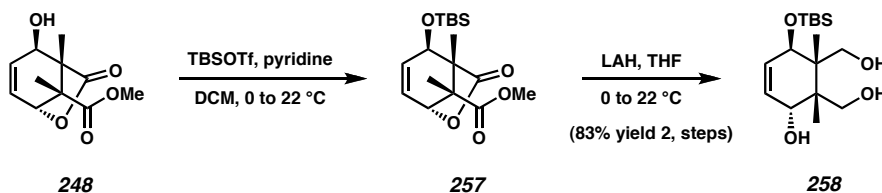
**Enone 255.** To a cooled (0 °C) solution of allylic alcohol **253** (129 mg, 0.248 mmol, 1.00 equiv) in CH<sub>2</sub>Cl<sub>2</sub> (20 mL) was added Dess-Martin periodinane (210 mg, 0.496 mmol, 2.00 equiv) and the resulting mixture was stirred for 1 h. The reaction mixture was diluted with Et<sub>2</sub>O (75 mL), filtered, and concentrated to an oil, which was purified by gradient flash chromatography on silica gel (15 to 40% EtOAc in hexanes) to give enone **255** (117 mg, 91% yield) as a foam: *R<sub>f</sub>* 0.57 (35% EtOAc in hexanes developed twice); <sup>1</sup>H NMR (300 MHz, CDCl<sub>3</sub>) δ 6.83 (d, *J* = 7.8 Hz, 1H), 6.64 (d, *J* = 8.1 Hz, 1H), 4.61 (app. t,

$J = 2.4$  Hz, 1H), 3.94 (d,  $J = 17.7$  Hz, 1H), 3.76 (d,  $J = 17.7$  Hz, 1H), 3.75 (s, 3H), 3.65 (s, 3H), 2.46 (dd,  $J = 2.7, 18.9$  Hz, 1H), 2.35 (dd,  $J = 1.5, 18.9$  Hz, 1H), 2.20 (s, 3H), 1.66 (s, 3H), 1.29 (s, 3H), 1.28 (s, 3H), 1.02 (s, 9H), 0.15 (s, 6H);  $^{13}\text{C}$  NMR (75 MHz,  $\text{CDCl}_3$ )  $\delta$  203.3, 176.2, 173.1, 150.0, 146.9, 135.4, 130.6, 130.0, 125.7, 124.4, 123.3, 77.8, 59.8, 53.5, 52.7, 47.8, 46.2, 34.3, 26.0, 18.8, 18.4, 17.0, 12.5, 11.7, -4.3; IR (Neat film NaCl) 2953, 2930, 2858, 1785, 1732, 1463, 1421, 1286, 1252, 1236, 840  $\text{cm}^{-1}$ ; HRMS (FAB+)  $[\text{M}+\text{H}]^+$   $m/z$  calc'd for  $[\text{C}_{28}\text{H}_{40}\text{SiO}_7+\text{H}]^+$ : 517.2622, found 517.2631.



**Bisacetoxycetal 256.** A solution of enone **255** (58.5 mg, 0.113 mmol, 1.00 equiv) in formic acid (2.40 mL) and 85%  $\text{H}_3\text{PO}_4$  (800  $\mu\text{L}$ ) was fitted with a reflux condenser and heated at 117 °C for 22 h. The reaction mixture was cooled to ambient temperature, diluted with ice cold  $\text{H}_2\text{O}$  (60 mL) and extracted with  $\text{Et}_2\text{O}$  (5 x 15 mL). The combined organics were dried ( $\text{MgSO}_4$ ) and concentrated to an oil, which was purified by flash chromatography on silica gel (10 to 40%  $\text{EtOAc}$  in hexanes) to give bisacetoxycetal **256** (19.6 mg, 47% yield) as a white solid. Crystals suitable for X-ray analysis were obtained by crystallization from  $\text{Et}_2\text{O}$ /hexanes at ambient temperature: mp 185–190 °C decomp. ( $\text{Et}_2\text{O}$ /hexanes);  $R_f$  0.32 (35%  $\text{EtOAc}$  in hexanes);  $^1\text{H}$  NMR (300 MHz,  $\text{CDCl}_3$ )  $\delta$  6.92 (s, 1H), 6.14 (dd,  $J = 0.9, 9.3$  Hz, 1H), 5.62 (bs, 1H), 5.42 (d,  $J = 9.3$  Hz, 1H), 3.77 (s, 3H), 3.61 (d,  $J = 15.9$  Hz, 1H), 3.02 (dd,  $J = 0.9, 15.9$  Hz, 1H), 2.48 (s, 1H), 2.52 (s, 3H), 1.47 (s, 3H), 1.43 (s, 3H), 1.41 (s, 3H);  $^{13}\text{C}$  NMR (75 MHz,  $\text{CDCl}_3$ )  $\delta$  175.6, 169.5, 145.9, 144.4, 137.4, 130.8, 126.0, 124.9, 124.7, 121.8, 105.7, 60.9, 53.0, 45.9, 38.0, 32.2, 31.5, 16.3,

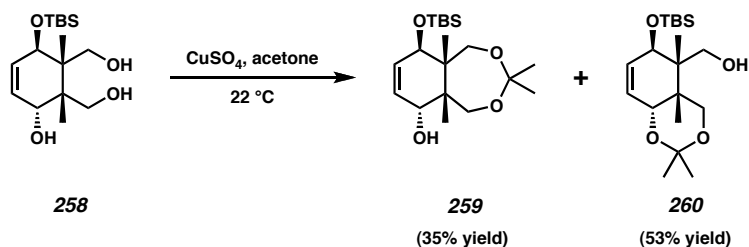
16.2, 15.8; IR (Neat film NaCl) 3468, 2978, 2942, 1801, 1757, 1360, 1213, 1057, 937, 914, 732  $\text{cm}^{-1}$ ; HRMS (EI)  $[\text{M}]^+$   $m/z$  calc'd for  $[\text{C}_{21}\text{H}_{22}\text{O}_6]^+$ : 370.1416, found 370.1410.



**Triol 258.** To cooled (0 °C) solution of allylic alcohol **248** (4.37 g, 19.3 mmol, 1.00 equiv) and pyridine (3.12 mL, 38.7 mmol, 2.00 equiv) in  $\text{CH}_2\text{Cl}_2$  (19 mL) was added TBSOTf (6.66 mL, 29.0 mmol, 1.50 equiv) in a dropwise manner. At the end of the addition, the reaction was allowed to warm to ambient temperature and stirred for 15 h. The reaction mixture was diluted with  $\text{CH}_2\text{Cl}_2$  (200 mL), quenched with sat. aq.  $\text{NH}_4\text{Cl}$  (75 mL), and extracted with  $\text{CH}_2\text{Cl}_2$  (4 x 50 mL). The combined organics were dried ( $\text{MgSO}_4$ ) and concentrated to give crude silyl ether **257**, which was typically used without purification in the next step:  $R_f$  0.69 (50% EtOAc in hexanes);  $^1\text{H}$  NMR (500 MHz,  $\text{CDCl}_3$ )  $\delta$  6.19 (ddd,  $J = 1.0, 6.0, 9.0$  Hz, 1H), 5.89 (ddd,  $J = 1.0, 3.5, 9.0$  Hz, 1H), 4.78 (d,  $J = 5.5$  Hz, 1H), 4.08 (dd,  $J = 1.0, 3.5$  Hz, 1H), 3.72 (s, 3H), 1.44 (s, 3H), 1.35 (s, 3H), 0.88 (s, 9H), 0.11 (s, 3H), 0.09 (s, 3H);  $^{13}\text{C}$  NMR (125 MHz,  $\text{CDCl}_3$ )  $\delta$  178.9, 173.7, 134.8, 126.9, 77.3, 70.5, 54.9, 52.5, 51.3, 25.6, 17.9, 15.7, 14.7, -4.5, -5.1; IR (Neat film NaCl) 2952, 2933, 2857, 1779, 1737, 1725, 1454, 1374, 1254, 1095, 1065, 957, 841, 780  $\text{cm}^{-1}$ ; HRMS (FAB+)  $[\text{M}+\text{H}]^+$   $m/z$  calc'd for  $[\text{C}_{17}\text{H}_{28}\text{SiO}_5+\text{H}]^+$ : 341.1784, found 341.1781.

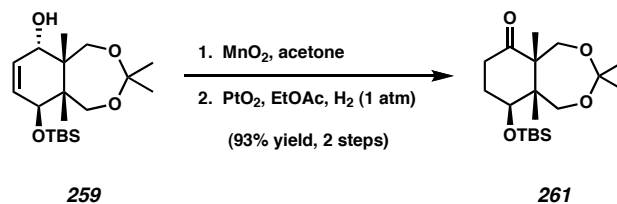
The above residue containing silyl ether **257** (theoretical yield: 19.3 mmol, 1.00 equiv) was dissolved in THF (193 mL), cooled (0 °C), and treated with LAH (2.20 g, 58.0 mmol, 3.00 equiv) in portions. At the end of the addition, the reaction was allowed to come to ambient temperature, and stirred for 18 h. The cooled (0 °C) reaction mixture was quenched by the careful dropwise addition of EtOAc (66 mL) until out gassing ceased, addition of Celite (7.0 g), and finally careful addition of sat. aq.  $\text{Na}_2\text{SO}_4$  (33 mL).

The resulting slurry was filtered, dried ( $\text{Na}_2\text{SO}_4$ ), and concentrated to give triol **258** (5.05 g, 83% yield, 2 steps) as a white solid of ~ 95% purity. Analytically pure material could be obtained by recrystallization from 1% EtOAc in benzene: mp 130.5–132.0 °C (EtOAc/benzene);  $R_f$  0.22 (30% acetone in hexanes);  $^1\text{H}$  NMR (500 MHz,  $\text{CDCl}_3$ )  $\delta$  5.68–5.62 (m, 2H), 4.45 (s, 1H), 4.20 (s, 1H), 3.91 (d,  $J = 11.5$  Hz, 1H), 3.76 (d,  $J = 11.5$  Hz, 1H), 3.69 (d,  $J = 11.5$  Hz, 1H), 3.50 (d,  $J = 12.0$  Hz, 1H), 1.15 (s, 3H), 0.89 (s, 9H), 0.84 (s, 3H), 0.11 (s, 3H), 0.10 (s, 3H);  $^{13}\text{C}$  NMR (125 MHz,  $\text{CDCl}_3$ )  $\delta$  131.3, 129.1, 73.6, 69.3, 65.6, 63.7, 46.1, 45.2, 25.8, 18.0, 16.2, 13.6, -4.0, -5.0; IR (Neat film NaCl) 3255, 2955, 2929, 2886, 2857, 1472, 1253, 1076, 1049, 1026, 880, 835  $\text{cm}^{-1}$ ; HRMS (FAB+)  $[\text{M}+\text{H}]^+$   $m/z$  calc'd for  $[\text{C}_{16}\text{H}_{32}\text{SiO}_4+\text{H}]^+$ : 317.2148, found 317.2162.



**1,3-Dioxepane 259 and Acetonide 260.** To a solution of triol **258** (3.75 g, 11.9 mmol, 1.00 equiv) in acetone (120 mL) was added anhydrous  $\text{CuSO}_4$  (9.46 g, 59.3 mmol, 5.00 equiv), and the reaction mixture was stirred for 40 min. An additional portion of  $\text{CuSO}_4$  (1.89 g, 11.9 mmol, 1.00 equiv) was added to the reaction mixture, and after an additional 3 h of stirring, a final portion of  $\text{CuSO}_4$  (1.00 g, 6.27 mmol, 0.53 equiv) was added. After 30 min, the reaction mixture was filtered, concentrated, and purified by flash chromatography on silica gel (5 to 15% EtOAc in hexanes) to give 1,3-dioxepane **259** (1.48 g, 35% yield) as a waxy solid:  $R_f$  0.66 (35% EtOAc in hexanes);  $^1\text{H}$  NMR (300 MHz,  $\text{CDCl}_3$ )  $\delta$  5.57 (dt,  $J = 2.1, 10.2$  Hz, 1H), 5.49 (dt,  $J = 2.1, 10.2$  Hz, 1H), 4.99 (s, 1H), 4.23 (app. q,  $J = 2.4$  Hz, 1H), 3.73 (d,  $J = 12.3$  Hz, 1H), 3.58 (d,  $J = 12.6$  Hz, 1H), 3.56 (d,  $J = 12.6$  Hz, 1H), 3.19 (d,  $J = 12.6$  Hz, 1H), 1.33 (s, 3H), 1.30 (s, 3H), 0.90 (s, 9H), 0.71 (s,

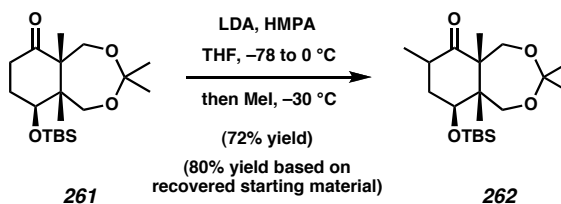
3H), 0.10 (s, 3H), 0.09 (s, 3H);  $^{13}\text{C}$  NMR (75 MHz,  $\text{C}_6\text{D}_6$ )  $\delta$  131.7, 129.2, 101.8, 73.5, 68.1, 63.8, 63.0, 46.9, 46.3, 26.5, 25.7, 25.4, 18.8, 18.7, 11.7, -3.7, -4.5; IR (Neat film NaCl) 3446, 2983, 2954, 2858, 1472, 1372, 1253, 1221, 1085, 1070, 1044, 835, 775  $\text{cm}^{-1}$ ; HRMS (FAB+)  $[\text{M}-\text{H}_2+\text{H}]^+$  calc'd for  $[\text{C}_{19}\text{H}_{35}\text{SiO}_4]^+$ :  $m/z$  355.2305, found 355.2317 and acetone **260** (2.25 g, 53% yield) as an oil:  $R_f$  0.76 (35% EtOAc in hexanes);  $^1\text{H}$  NMR (300 MHz,  $\text{CDCl}_3$ )  $\delta$  5.93 (dd,  $J = 4.4, 9.6$  Hz, 1H), 5.69 (dd,  $J = 4.8, 9.9$  Hz, 1H), 4.12 (d,  $J = 4.5$  Hz, 1H), 4.01 (d,  $J = 12.9$  Hz, 1H), 3.91 (s, 1H), 3.76 (d,  $J = 10.2$  Hz, 1H), 3.64 (d,  $J = 10.2$  Hz, 1H), 3.56 (d,  $J = 12.9$  Hz, 1H), 1.49 (s, 3H), 1.43 (s, 3H), 1.04 (s, 3H), 0.98 (s, 3H), 0.88 (s, 9H), 0.09 (s, 3H), 0.08 (s, 3H);  $^{13}\text{C}$  NMR (75 MHz,  $\text{CDCl}_3$ )  $\delta$  133.5, 124.4, 98.6, 71.7, 70.9, 68.9, 65.2, 43.8, 35.1, 28.4, 25.7, 20.9, 20.0 (bs), 17.9, 15.3, -4.1, -5.1; IR (Neat film NaCl) 3451, 2955, 2931, 2886, 2858, 1379, 1256, 1104, 1056, 836, 775  $\text{cm}^{-1}$ ; HRMS (FAB+)  $[\text{M}+\text{H}]^+$   $m/z$  calc'd for  $[\text{C}_{19}\text{H}_{36}\text{SiO}_4+\text{H}]^+$ : 357.2461, found 357.2478.



**Ketone 261.** To a solution of 1,3-dioxepane **259** (798 mg, 2.24 mmol, 1.00 equiv) in acetone (23 mL) was added activated  $\text{MnO}_2$  (3.89 g, 44.7 mmol, 20.0 equiv), and the reaction mixture was stirred at ambient temperature for 1.5 h. The reaction mixture was filtered, washed with acetone, and concentrated to an oil.

To a solution of this crude material in EtOAc (28 mL) was added  $\text{PtO}_2$  (16.0 mg, 67.2  $\mu\text{mol}$ , 0.03 equiv), and the reaction mixture was sparged with  $\text{H}_2$  (5 min) and stirred vigorously under an atmosphere of  $\text{H}_2$  (balloon) for 1.5 h. The reaction mixture was flushed with  $\text{N}_2$  and concentrated to an oil, which was purified by flash chromatography on silica gel (2.5 to 10% EtOAc in hexanes) to provide ketone **261** (744 mg, 93% yield, 2

steps) as an amorphous solid:  $R_f$  0.52 (20% EtOAc in hexanes);  $^1\text{H}$  NMR (300 MHz,  $\text{CDCl}_3$ )  $\delta$  4.59 (bs, 1H), 4.15 (bs, 1H), 3.40 (bs, 2H), 2.99 (bs, 1H), 2.31 (m, 2H), 2.10–1.70 (m, 2H), 1.33 (s, 3H), 1.32 (s, 3H), 1.09 (s, 3H), 0.89 (s, 9H), 0.64 (bs, 3H), 0.11 (s, 3H), 0.10 (s, 3H);  $^{13}\text{C}$  NMR (75 MHz,  $\text{CDCl}_3$ )  $\delta$  212.7, 101.8, 67.3, 65.1, 64.0, 57.1, 47.2, 37.9, 29.4, 25.8, 24.8, 24.4, 18.0, 15.8, 11.5, -4.4, -5.1; IR (Neat film NaCl) 2954, 2857, 1709, 1220, 1096, 1073, 884, 836  $\text{cm}^{-1}$ ; HRMS (FAB+)  $[\text{M}+\text{H}]^+$   $m/z$  calc'd for  $[\text{C}_{19}\text{H}_{36}\text{O}_4\text{Si}+\text{H}]^+$ : 357.2461, found 357.2473.

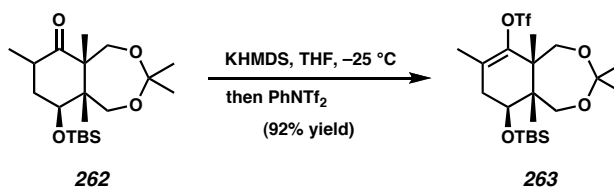


**Methyl Ketones 262.** A solution of LDA in THF was prepared by dropwise addition of 2.45 M *n*-BuLi solution in hexanes (1.21 mL, 2.96 mmol, 1.20 equiv) to diisopropylamine (519  $\mu\text{L}$ , 3.70 mmol, 1.50 equiv) in THF (30.0 mL) at 0  $^\circ\text{C}$ , followed by stirring for 1 h. Upon cooling the solution to -78  $^\circ\text{C}$ , a solution of ketone **261** (879 mg, 2.47 mmol, 1.00 equiv) in THF (30.0 mL) was added in a dropwise manner, and the reaction mixture was stirred at -78  $^\circ\text{C}$  for 30 min. HMPA (1.07 mL, 6.17 mmol, 2.50 equiv) was added and the reaction mixture brought to 0  $^\circ\text{C}$  for 1 h. After cooling again to -78  $^\circ\text{C}$ , the reaction mixture was treated with MeI (200  $\mu\text{L}$ , 3.21 mmol, 1.30 equiv), and after 15 min allowed to warm to -30  $^\circ\text{C}$ . The reaction was allowed to warm to 0  $^\circ\text{C}$  slowly over 10 h, quenched with  $\text{H}_2\text{O}$  (150 mL) and EtOAc (75 mL), and extracted with EtOAc (4 x 50 mL). The combined organics were washed with brine (50 mL), dried ( $\text{Na}_2\text{SO}_4$ ), and concentrated to an oil, which was purified by flash chromatography on silica gel (2.5 to 10% EtOAc in hexanes) to give recovered ketone **261** (90.9 mg, 10% yield), methyl ketone **262a** (219

mg, 24% yield, high  $R_f$  diastereomer), and methyl ketone **262b** (436 mg, 48% yield, low  $R_f$  diastereomer) as an oil.

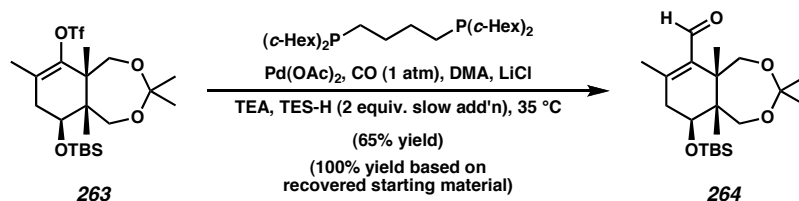
**High  $R_f$  diastereomer 262a:**  $R_f$  0.65 (10% EtOAc in hexanes developed 2 times);  $^1\text{H}$  NMR (300 MHz,  $\text{CDCl}_3$ )  $\delta$  4.70 (dd,  $J = 4.7, 12.2$  Hz, 1H), 4.22 (d,  $J = 12.0$  Hz, 1H), 3.49 (d,  $J = 12.6$  Hz, 1H), 3.34 (d,  $J = 12.3$  Hz, 1H), 2.93 (d,  $J = 11.7$  Hz, 1H), 2.41 (dq,  $J = 6.3, 19.8$  Hz, 1H), 1.98 (dt,  $J = 5.1, 12.9$  Hz, 1H), 1.53 (d,  $J = 13.2$  Hz, 1H), 1.34 (s, 3H), 1.10 (s, 3H), 1.01 (d,  $J = 6.6$  Hz, 3H), 0.89 (s, 9H), 0.55 (s, 3H), 0.12 (s, 6H);  $^{13}\text{C}$  NMR (75 MHz,  $\text{CDCl}_3$ )  $\delta$  213.4, 101.9, 67.0, 65.5, 63.9, 56.8, 48.1, 41.0, 38.6, 25.8, 24.8, 24.5, 18.0, 15.7, 14.7, 11.3, -4.3, -5.1; IR (Neat film NaCl) 2984, 2955, 2935, 2858, 1709, 1220, 1095, 1072, 1044, 868, 837, 776  $\text{cm}^{-1}$ ; HRMS (FAB+)  $[\text{M}+\text{H}]^+$  calc'd for  $[\text{C}_{20}\text{H}_{38}\text{O}_4\text{Si}+\text{H}]^+$ :  $m/z$  371.2618, found 371.2607.

**High  $R_f$  diastereomer 262b:**  $R_f$  0.36 (10% EtOAc in hexanes developed 2 times);  $^1\text{H}$  NMR (300 MHz,  $\text{CDCl}_3$ )  $\delta$  3.80 (d,  $J = 12.6$  Hz, 1H), 3.60 (d,  $J = 12.0$  Hz, 1H), 3.58 (bs, 1H), 3.41 (d,  $J = 12.6$  Hz, 1H), 3.02–2.80 (m, 2H), 1.91 (ddd,  $J = 4.2, 5.6, 14.0$  Hz, 1H), 1.58 (m, 1H), 1.30 (s, 3H), 1.24 (s, 3H), 1.08 (s, 3H), 1.07 (s, 3H), 1.05 (s, 3H), 0.92 (s, 9H), 0.11 (s, 3H), 0.09 (s, 3H);  $^{13}\text{C}$  NMR (75 MHz,  $\text{CDCl}_3$ )  $\delta$  214.6, 101.2, 73.0, 67.8, 64.3, 54.4, 47.0, 37.7, 35.3, 25.8, 25.0, 23.9, 19.4, 18.1, 16.9, 14.7, -4.6, -5.0; IR (Neat film NaCl) 2933, 2858, 1709, 1255, 1222, 1078, 1046, 838, 775  $\text{cm}^{-1}$ ; HRMS (FAB+)  $[\text{M}+\text{H}]^+$   $m/z$  calc'd for  $[\text{C}_{20}\text{H}_{38}\text{O}_4\text{Si}+\text{H}]^+$ : 371.2618, found 371.2625.



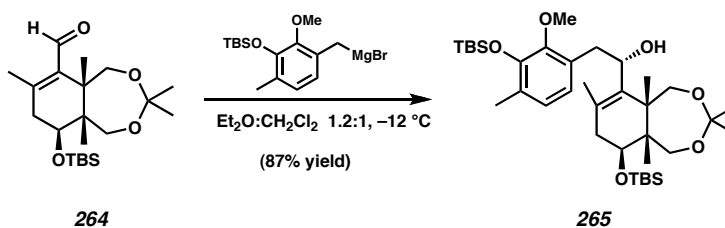
**Triflate 263.** To a cooled ( $-25\text{ }^\circ\text{C}$ ) solution of KHMDS (668 mg, 3.35 mmol, 1.20 equiv) in THF (40 mL) was added the low  $R_f$  diastereomer methyl ketone **262b** (1.04 g,

2.79 mmol, 1.00 equiv) in THF (20 mL) in a dropwise manner over 10 min. After 2 h at  $-25\text{ }^{\circ}\text{C}$ ,  $\text{PhNTf}_2$  (1.30 g, 3.63 mmol, 1.30 equiv) in THF (20 mL) was added, and the reaction was maintained for an additional 30 min at  $-25\text{ }^{\circ}\text{C}$ . The reaction mixture was quenched into half-saturated  $\text{NaHCO}_3$  (50 mL) and EtOAc (50 mL), and extracted with EtOAc (5 x 50 mL). The combined organics were washed with brine (1 x 50 mL), dried ( $\text{Na}_2\text{SO}_4$ ), and concentrated to an oil, which was purified by flash chromatography on silica gel (0 to 10% EtOAc in hexanes) to provide triflate **263** (1.30 g, 92% yield) as an oil:  $R_f$  0.69 (10% Et<sub>2</sub>O in hexanes);  $^1\text{H}$  NMR (300 MHz,  $\text{C}_6\text{D}_6$ )  $\delta$  4.18 (dd,  $J = 6.3, 9.9$  Hz, 1H), 3.79 (d,  $J = 12.3$  Hz, 1H), 3.65 (d,  $J = 12.9$  Hz, 1H), 3.41 (d,  $J = 12.3$  Hz, 1H), 3.33 (d,  $J = 12.6$  Hz, 1H), 2.08 (dd,  $J = 6.5, 17.6$  Hz, 1H), 1.91 (ddd,  $J = 1.1, 9.9, 17.6$  Hz, 1H), 1.61 (s, 3H), 1.20 (s, 3H), 1.17 (s, 3H), 1.16 (s, 3H), 0.98 (s, 9H), 0.49 (s, 3H), 0.15 (s, 3H), 0.05 (s, 3H);  $^{13}\text{C}$  NMR (75 MHz,  $\text{C}_6\text{D}_6$ )  $\delta$  145.9, 127.1, 119.7 (q,  $J_{\text{C-F}} = 318$  Hz), 102.0, 65.4, 65.2, 62.7, 47.4, 45.9, 38.2, 26.5, 25.0, 24.9, 18.6, 18.3, 17.0, 11.0,  $-3.8, -4.6$ ; IR (Neat film NaCl) 2988, 2954, 2858, 1405, 1213, 1141, 1078, 879  $\text{cm}^{-1}$ ; HRMS (FAB+)  $[\text{M}+\text{H}]^+$   $m/z$  calc'd for  $[\text{C}_{21}\text{H}_{37}\text{SSiO}_6\text{F}_3+\text{H}]^+$ : 503.2110, found 503.2094.



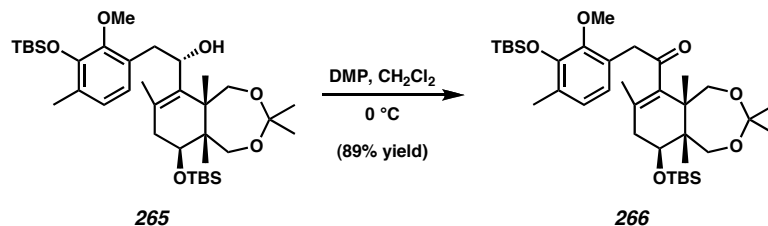
**Enal 264.** A solution of flame-dried LiCl (433 mg, 10.2 mmol, 3.0 equiv),  $\text{Pd(OAc)}_2$  (153 mg, 0.680 mmol, 0.20 equiv), and 1,4-bis-(dicyclohexylphosphino)butane (306 mg, 0.680 mmol, 0.20 equiv) in DMA (16 mL) was sparged with CO and warmed to  $85\text{ }^{\circ}\text{C}$  until a color change from red/orange to pale yellow was observed, at which point the reaction mixture was cooled to  $40\text{ }^{\circ}\text{C}$ . To the homogenous reaction mixture was added TEA (1.89 mL, 13.6 mmol, 4.00 equiv) and enol triflate **263** (1.71 g, 3.40 mmol, 1.00

equiv) in DMA (20 mL). A solution of  $\text{Et}_3\text{SiH}$  (1.09 mL, 6.80 mmol, 2.0 equiv) in DMA (10.0 mL) was added by syringe pump to the reaction over 10 h. After an additional 14 h at 40 °C, the reaction mixture was cooled to ambient temperature, poured into  $\text{H}_2\text{O}$  (100 mL) and  $\text{Et}_2\text{O}$  (100 mL), and extracted with  $\text{Et}_2\text{O}$  (5 x 50 mL). The combined organic layers were washed with  $\text{H}_2\text{O}$  (20 mL), brine (2 x 20 mL), dried ( $\text{Na}_2\text{SO}_4$ ), and concentrated to give an oil, which was purified by flash chromatography on silica gel (2 to 10%  $\text{EtOAc}$  in hexanes) to give recovered triflate **263** (606 mg, 35% yield) and enal **264** (841 mg, 65% yield) as a pale yellow oil:  $R_f$  0.50, 0.55 (10%  $\text{EtOAc}$  in hexanes developed twice, 25%  $\text{Et}_2\text{O}$  in hexanes);  $^1\text{H}$  NMR (300 MHz,  $\text{CDCl}_3$ )  $\delta$  10.06 (s, 1H), 4.19 (dd,  $J = 7.1, 9.2$  Hz, 1H), 3.73 (d,  $J = 12.3$  Hz, 1H), 3.60 (d,  $J = 12.0$  Hz, 1H), 3.57 (d,  $J = 12.3$  Hz, 1H), 3.34 (d,  $J = 12.3$  Hz, 1H), 2.32–2.22 (m, 2H), 2.09 (s, 3H), 1.31 (s, 3H), 1.24 (s, 6H), 0.89 (s, 9H), 0.53 (s, 3H), 0.08 (s, 6H);  $^{13}\text{C}$  NMR (75 MHz,  $\text{CDCl}_3$ )  $\delta$  192.7, 154.2, 135.2, 101.0, 65.2, 65.0, 61.4, 45.2, 43.7, 41.3, 25.8, 24.6, 19.6, 18.0, 17.5, 10.7, -4.4, -5.1; IR (Neat film NaCl) 2986, 2953, 2888, 2857, 1677, 1371, 1221, 1101, 1073, 870, 837, 780  $\text{cm}^{-1}$ ; HRMS (FAB+)  $[\text{M}-\text{H}_2+\text{H}]^+$   $m/z$  calc'd for  $[\text{C}_{20}\text{H}_{37}\text{O}_5]^+$ : 385.2410, found 385.2412.



**Allylic alcohol 265.** A flame-dried two-neck round bottom flask equipped with a reflux condenser and septum was charged with magnesium turnings (3.00 g, 123 mmol, 56.1 equiv) and  $\text{Et}_2\text{O}$  (45 mL) under an  $\text{N}_2$  atmosphere and heated to reflux. To this mixture was added 1,2-dibromoethane (75.0  $\mu\text{L}$ , 0.870 mmol, 0.40 equiv) in a dropwise manner. [*Caution: gas evolution!*] When gas evolution ceased, a solution of benzyl bromide **151** (1.37 g, 3.96 mmol, 1.80 equiv) in  $\text{Et}_2\text{O}$  (18.0 mL) was added in a dropwise manner over

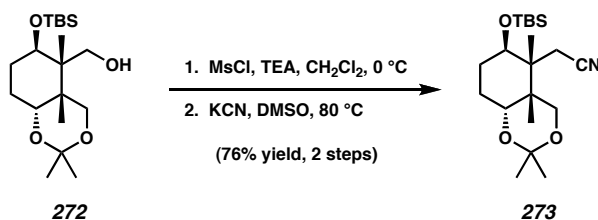
30 min and heating was continued for an additional 30 min. The Grignard reagent was then cooled (0 °C), and added to a cooled (-12 °C) solution of enal **264** (841 mg, 2.20 mmol, 1.00 equiv) in Et<sub>2</sub>O (45 mL) and CH<sub>2</sub>Cl<sub>2</sub> (90 mL). After 1 h at -12 °C, the reaction was quenched with H<sub>2</sub>O (150 mL), 2 M citric acid (20 mL), brine (20 mL), and EtOAc (50 mL), and extracted with EtOAc (4 x 50 mL). The combined organics were washed with brine (2 x 50 mL), dried (Na<sub>2</sub>SO<sub>4</sub>), and concentrated to an oil, which was purified by flash chromatography on silica gel (2.5 to 12.5% Et<sub>2</sub>O in hexanes) to give allylic alcohol **265** (1.24 g, 87% yield) as a foam consisting of a 10:1 mixture diastereomers. Only the major component (stereochemistry shown above) could be isolated in pure form: *R<sub>f</sub>* 0.41, 0.29 (25% Et<sub>2</sub>O in hexanes, 10% EtOAc in hexanes); <sup>1</sup>H NMR (300 MHz, CDCl<sub>3</sub>) δ 6.84 (d, *J* = 7.5 Hz, 1H), 6.70 (d, *J* = 7.5 Hz, 1H), 4.46 (d, *J* = 10.2 Hz, 1H), 4.16 (dd, *J* = 7.1, 9.5 Hz, 1H), 3.71 (s, 3H), 3.62 (d, *J* = 12.6 Hz, 1H), 3.53 (d, *J* = 12.3 Hz, 1H), 3.39 (d, *J* = 12.3 Hz, 1H), 3.32 (bs, 1H), 3.27 (dd, *J* = 10.7, 14.0 Hz, 1H), 2.59 (dd, *J* = 3.0, 14.1 Hz, 1H), 2.46 (s, 1H), 2.20 (s, 3H), 2.10–2.00 (m, 2H), 1.98 (s, 3H), 1.31 (s, 3H), 1.26 (s, 3H), 1.21 (s, 3H), 1.03 (s, 9H), 0.90 (s, 9H), 0.56 (s, 3H), 0.19 (s, 3H), 0.16 (s, 3H), 0.10 (s, 6H); <sup>13</sup>C NMR (75 MHz, CDCl<sub>3</sub>) δ 149.5, 147.2, 134.6, 132.2, 130.8, 129.4, 126.4, 123.1, 100.8, 72.6, 66.1, 65.7, 62.2, 60.0, 47.1, 43.6, 40.0, 38.4, 26.0, 25.9, 24.7(2C), 20.9, 18.6, 18.1, 17.8, 17.0, 10.9, -4.0, -4.2, -4.3, -5.1; IR (Neat film NaCl) 3479, 2955, 2931, 2858, 1463, 1253, 1221, 1074, 838, 780 cm<sup>-1</sup>; HRMS (FAB+) [M-H<sub>2</sub>+H]<sup>+</sup> *m/z* calc'd for [C<sub>36</sub>H<sub>63</sub>Si<sub>2</sub>O<sub>6</sub>]<sup>+</sup>: 647.4163, found 647.4156.



**Enone 266.** To a cooled (0 °C) solution of allylic alcohol **265** (1.24 g, 1.91 mmol, 1.00 equiv) in CH<sub>2</sub>Cl<sub>2</sub> (120 mL) was added Dess-Martin periodinane (1.21 g, 2.86 mmol, 1.50 equiv) and the resulting mixture was stirred for 2 h. The reaction mixture was concentrated to ~ 40 mL, diluted with Et<sub>2</sub>O (250 mL), filtered, and concentrated to an oil, which was purified by gradient flash chromatography on silica gel (2.5 to 5% EtOAc in hexanes) to give enone **266** (1.10 g, 89% yield) as a foam: *R<sub>f</sub>* 0.43, 0.69 (10% EtOAc in hexanes, 10% Et<sub>2</sub>O in hexanes); <sup>1</sup>H NMR (300 MHz, CDCl<sub>3</sub>) δ 6.83 (d, *J* = 7.5 Hz, 1H), 6.63 (d, *J* = 7.8 Hz, 1H), 4.28 (dd, *J* = 7.1, 9.5 Hz, 1H), 3.92 (d, *J* = 18.3 Hz, 1H), 3.80 (d, *J* = 18.0 Hz, 1H), 3.75 (d, *J* = 11.4 Hz, 1H), 3.64 (s, 3H), 3.52 (d, *J* = 12.6 Hz, 1H), 3.39 (d, *J* = 12.3 Hz, 1H), 2.20 (s, 3H), 2.12–1.98 (m, 2H), 1.72 (s, 3H), 1.31 (s, 3H), 1.27 (s, 3H), 1.13 (s, 3H), 1.02 (s, 9H), 0.90 (s, 9H), 0.66 (s, 3H), 0.15 (s, 6H), 0.09 (s, 3H), 0.08 (s, 6H); <sup>13</sup>C NMR (75 MHz, CDCl<sub>3</sub>) δ 208.1, 150.1, 147.0, 138.2, 129.9 (2C), 125.8, 125.3, 123.2, 101.1, 65.9, 65.5, 61.5, 60.0, 47.1, 45.3, 42.9, 37.9, 26.1, 25.9, 24.7 (2C), 20.7, 18.6, 18.1, 17.1, 11.1, -4.2 (2C), -4.4, -5.1; IR (Neat film NaCl) 2954, 2930, 2858, 1699, 1463, 1252, 1221, 1099, 1073, 864, 836, 780 cm<sup>-1</sup>; HRMS (FAB+) [M+H]<sup>+</sup> *m/z* calc'd for [C<sub>36</sub>H<sub>63</sub>Si<sub>2</sub>O<sub>6</sub>+H]<sup>+</sup>: 647.4163, found 647.4140.



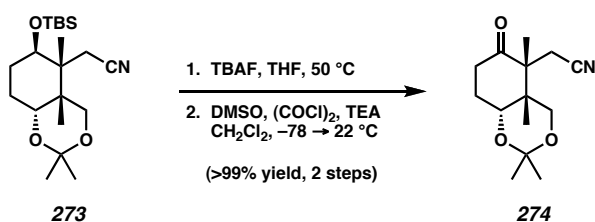
alcohol **272** (5.47 g, 96% yield) as an oil:  $R_f$  0.76 (35% EtOAc in hexanes);  $^1\text{H}$  NMR (500 MHz,  $\text{CDCl}_3$ )  $\delta$  4.43 (dd,  $J = 5.5, 12.0$  Hz, 1H), 3.98 (dd,  $J = 5.0, 10.3$  Hz, 1H), 3.88 (d,  $J = 13.0$  Hz, 1H), 3.79 (app. t,  $J = 3.0$  Hz, 1H), 3.45 (s, 1H), 3.32 (d,  $J = 12.0$  Hz, 1H), 3.04 (app. t,  $J = 11.0$  Hz, 1H), 2.12 (app. tt,  $J = 3.8, 14.3$  Hz, 1H), 1.86 (app. tt,  $J = 3.0, 14.0$  Hz, 1H), 1.48 (s, 3H), 1.47–1.37 (m, 1H), 1.42 (s, 3H), 0.97 (s, 3H), 0.93 (s, 3H), 0.90 (s, 9H), 0.05 (s, 3H), 0.04 (s, 3H);  $^{13}\text{C}$  NMR (125 MHz,  $\text{CDCl}_3$ )  $\delta$  98.5, 75.0, 74.4, 69.5, 66.8, 43.5, 35.0, 29.5, 25.9, 25.1, 21.9, 20.2, 18.8, 18.0, 17.2, -4.6, -5.0; IR (Neat film NaCl) 3497, 2953, 2936, 2883, 2858, 1472, 1379, 1257, 1196, 1083, 1060, 1034, 1005, 866, 834, 774  $\text{cm}^{-1}$ ; HRMS (FAB+)  $[\text{M}+\text{H}]^+$   $m/z$  calc'd for  $[\text{C}_{19}\text{H}_{38}\text{SiO}_4+\text{H}]^+$ : 359.2618, found 359.2632.



**Nitrile 273.** To a cooled (0 °C) solution of alcohol **272** (880 mg, 2.45 mmol, 1.00) and TEA (1.02 mL, 7.36 mmol, 3.00 equiv) in  $\text{CH}_2\text{Cl}_2$  (25 mL) was added methanesulfonyl chloride (228  $\mu\text{L}$ , 2.95 mmol, 1.20 equiv) in a dropwise manner. After 30 min at 0 °C, the reaction mixture was diluted with  $\text{CH}_2\text{Cl}_2$  (40 mL), ice cold  $\text{H}_2\text{O}$  (50 mL), and brine (25 mL), and extracted with  $\text{CH}_2\text{Cl}_2$  (3 x 35 mL). The combined organics were washed with brine (30 mL), dried ( $\text{Na}_2\text{SO}_4$ ), and concentrated to a waxy solid that was used in the next step immediately.

The above residue was dissolved in DMSO (25 mL) and treated with KCN (400 mg, 6.14 mmol, 2.50 equiv) at 80 °C for 4 h. The reaction mixture was cooled to ambient temperature, diluted with EtOAc (50 mL) and  $\text{H}_2\text{O}$  (150 mL), and extracted with EtOAc (7 x 40 mL). The combined organics were washed with brine (30 mL), dried ( $\text{Na}_2\text{SO}_4$ ),

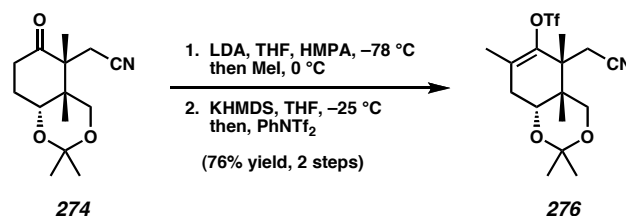
concentrated, and purified by flash chromatography on silica gel (2.5 to 10% EtOAc in hexanes) to provide nitrile **273** (682 mg, 76% yield) as a solid :  $R_f$  0.42 (20% EtOAc in hexanes);  $^1\text{H}$  NMR (300 MHz,  $\text{CDCl}_3$ )  $\delta$  4.07 (d,  $J = 8.7$  Hz, 1H), 3.83 (d,  $J = 8.4$  Hz, 1H), 3.70–3.60 (m, 2H), 3.49 (d,  $J = 8.1$  Hz, 1H), 3.46 (d,  $J = 8.7$  Hz, 1H), 2.18–2.04 (m, 1H), 1.74–1.45 (m, 3H), 1.55 (s, 6H), 1.14 (s, 3H), 0.90 (s, 3H), 0.87 (s, 9H), 0.06 (s, 3H), 0.05 (s, 3H);  $^{13}\text{C}$  NMR (75 MHz,  $\text{CDCl}_3$ )  $\delta$  121.7, 78.8, 76.1, 74.8, 71.0, 70.1, 50.8, 48.8, 28.8 (2C), 27.6 (2C), 25.8, 22.6, 18.0, 9.5, -3.9, -5.0; IR (Neat film NaCl) 2956, 2934, 2882, 2860, 1460, 1254, 1183, 1080, 1047, 916, 868, 835, 772  $\text{cm}^{-1}$ ; HRMS (FAB+)  $[\text{M}-\text{H}_2+\text{H}]^+$   $m/z$  calc'd for  $[\text{C}_{20}\text{H}_{36}\text{NO}_3\text{Si}]^+$ : 366.2464, found 366.2459.



**Ketone 274.** To a solution of nitrile **273** (889.8 mg, 2.421 mmol, 1.00 equiv) in THF (14.5 mL) was added a 1.0 M solution of TBAF (7.26  $\mu\text{L}$ , 7.262 mmol, 3.00 equiv) in THF, and the reaction mixture was heated to 50  $^\circ\text{C}$  for 12 h. The reaction mixture was cooled to ambient temperature, quenched with sat.  $\text{NH}_4\text{Cl}$  aq. (75 mL) and diluted with  $\text{CH}_2\text{Cl}_2$  (125 mL). The aqueous layer was further extracted with  $\text{CH}_2\text{Cl}_2$  (3 x 20 mL), dried over  $\text{MgSO}_4$ , and concentrated into an oil, which was used without further purification.

A solution of DMSO (1.37 mL, 19.4 mmol, 8.0 equiv) in  $\text{CH}_2\text{Cl}_2$  (100 mL) was cooled to -78  $^\circ\text{C}$  and oxalyl chloride (1.48 mL, 16.9 mmol, 7.00 equiv) was added in a dropwise manner. After 30 min at -78  $^\circ\text{C}$ , a solution of the crude alcohol generated above in  $\text{CH}_2\text{Cl}_2$  (10 mL, + 2 x 2 mL rinse) was added in a dropwise manner down the wall of the flask. After 1.5 h at -78  $^\circ\text{C}$ , TEA 6.75 mL, 48.4 mmol, 20.0 equiv) was added and the

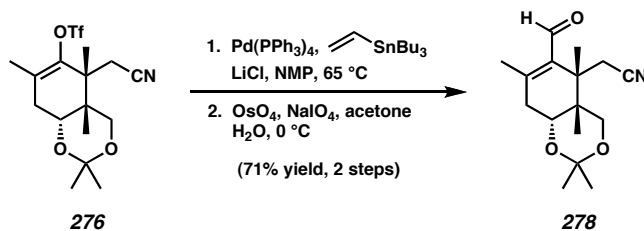
reaction mixture was allowed to warm slowly to ambient temperature, diluted with half-saturated  $\text{NH}_4\text{Cl}$  (100 mL), and extracted with  $\text{CH}_2\text{Cl}_2$  (4 x 50 mL). The combined organics were washed with saturated  $\text{NaHCO}_3$  (75 mL), dried ( $\text{MgSO}_4$ ), concentrated to an oil, and purified by flash chromatography on silica gel (20 to 35% EtOAc in hexanes) to provide ketone **274** (617 mg, 2.45 mmol, > 99% yield, 2 steps) as an oil:  $R_f$  0.49 (50% EtOAc in hexanes);  $^1\text{H}$  NMR (300 MHz,  $\text{CDCl}_3$ )  $\delta$  4.53 (d,  $J$  = 8.7 Hz, 1H), 4.01 (dd,  $J$  = 4.4, 10.7 Hz, 1H), 3.95 (d,  $J$  = 9.3 Hz, 1H), 3.50 (d,  $J$  = 9.3 Hz, 1H), 3.41 (d,  $J$  = 8.1 Hz, 1H), 2.68–2.41 (m, 2H), 2.41–2.24 (m, 1H), 2.10–1.90 (m, 1H), 1.61 (s, 6H), 1.23 (s, 3H), 1.14 (s, 3H), 0.87 (s, 9H), 0.06 (s, 3H), 0.05 (s, 3H);  $^{13}\text{C}$  NMR (75 MHz,  $\text{CDCl}_3$ )  $\delta$  210.6, 121.3, 77.5, 75.0, 74.1, 70.7, 58.0, 50.4, 35.6, 28.6, 27.7, 27.5, 21.4, 16.7; IR (Neat film NaCl) 2983, 2881, 2254, 1714, 1387, 1373, 1171, 1052, 907, 729, 651  $\text{cm}^{-1}$ ; HRMS (EI)  $[\text{M}]^+$   $m/z$  calc'd for  $[\text{C}_{14}\text{H}_{21}\text{NO}_3]^+$ : 251.1521, found 251.1518.



**Triflate 276.** A solution of LDA in THF was prepared by dropwise addition of 2.50 M *n*-BuLi solution in hexanes (580  $\mu\text{L}$ , 1.45 mmol, 1.05 equiv) to diisopropylamine (252  $\mu\text{L}$ , 1.79 mmol, 1.30 equiv) in THF (15.0 mL) at 0  $^\circ\text{C}$ , followed by stirring for 30 min. Upon cooling the solution to  $-78\text{ }^\circ\text{C}$ , a solution of ketone **274** (347 mg, 1.38 mmol, 1.00 equiv) in THF (15.0 mL) was added in a dropwise manner, and the reaction mixture was stirred at  $-78\text{ }^\circ\text{C}$  for 2 h. HMPA (552  $\mu\text{L}$ , 3.18 mmol, 2.30 equiv) was added and the reaction mixture was brought to 0  $^\circ\text{C}$  for 1 h. After cooling again to  $-78\text{ }^\circ\text{C}$ , the solution containing the enolate was added to a solution of MeI (258  $\mu\text{L}$ , 4.14 mmol, 3.00 equiv) in THF (4.00 mL) at  $-30\text{ }^\circ\text{C}$  in a dropwise manner over 25 min. After 6 h at  $-25\text{ }^\circ\text{C}$ , the

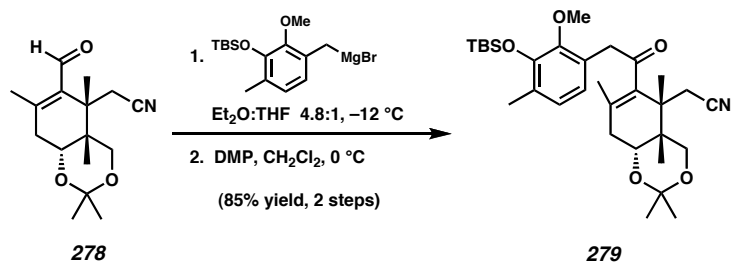
reaction mixture was quenched with H<sub>2</sub>O (30 mL) and CH<sub>2</sub>Cl<sub>2</sub> (30 mL), and extracted with CH<sub>2</sub>Cl<sub>2</sub> (5 x 30 mL). The combined organics were washed, dried (MgSO<sub>4</sub>), and concentrated to an oil, which was purified by flash chromatography on silica gel (10 to 25% EtOAc in hexanes) to give to an inseparable mixture of diastereomeric methyl ketones (286 mg, 78% yield).

To a cooled (-25 °C) solution of KHMDS (300 mg, 1.50 mmol, 1.40 equiv) in THF (17 mL) was added the above mixture of methyl ketones (286 mg, 1.07 mmol, 1.00 equiv) in THF (15 mL) in a dropwise manner over 10 min. After 2.5 h at -25 °C, PhNTf<sub>2</sub> (614 mg, 1.72 mmol, 1.60 equiv) in THF (10.7 mL) was added, and the reaction maintained for an additional 30 min at -25 °C. The reaction mixture was quenched into half-saturated NaHCO<sub>3</sub> (100 mL) and extracted with EtOAc (4 x 70 mL). The combined organics were dried (Na<sub>2</sub>SO<sub>4</sub>) and concentrated to an oil, which was purified by flash chromatography on silica gel (15 to 25% Et<sub>2</sub>O in hexanes) to provide triflate **276** (420 mg, 98% yield, 76% yield for 2 steps) as an oil: *R<sub>f</sub>* 0.41 (50% Et<sub>2</sub>O in hexanes); <sup>1</sup>H NMR (300 MHz, C<sub>6</sub>D<sub>6</sub>) δ 4.16 (d, *J* = 8.7 Hz, 1H), 3.95 (d, *J* = 9.3 Hz, 1H), 3.52 (dd, *J* = 6.2, 8.6 Hz, 1H), 3.46 (d, *J* = 9.0 Hz, 1H), 3.36 (d, *J* = 9.0 Hz, 1H), 2.17 (dd, *J* = 6.0, 18.0 Hz, 1H), 1.95 (dd, *J* = 8.1, 18.0 Hz, 1H), 1.50 (s, 3H), 1.01 (s, 3H), 0.97 (s, 3H), 0.90 (s, 3H), 0.88 (s, 3H); <sup>13</sup>C NMR (75 MHz, C<sub>6</sub>D<sub>6</sub>) δ 145.7, 125.1, 121.5, 119.5 (app. d, *J<sub>C-F</sub>* = 296 Hz), 75.2, 74.7, 74.3, 71.0, 51.2, 50.4, 36.1, 28.2, 27.4, 21.6, 18.1, 16.4; IR (Neat film NaCl) 2988, 2942, 2884, 1403, 1211, 1141, 1053, 990, 874 cm<sup>-1</sup>; HRMS (EI) [M]<sup>+</sup> *m/z* calc'd for [C<sub>16</sub>H<sub>22</sub>NO<sub>5</sub>F<sub>3</sub>S]<sup>+</sup>: 397.1171, found 397.1179.



**Enal 278.** To a solution of triflate **276** (1.41 g, 3.54 mmol, 1.00 equiv), Pd(PPh<sub>3</sub>)<sub>4</sub> (307 mg, 0.266 mmol, 0.075 equiv), and LiCl (450 mg, 10.6 mmol, 3.00 equiv) in NMP (59 mL) was added tributyl(vinyl)stannane (1.55 mL, 5.31 equiv, 1.50 equiv), and the mixture was heated to 65 °C for 0.5 h. The reaction mixture was cooled to ambient temperature, quenched with H<sub>2</sub>O (300 mL) and Et<sub>2</sub>O (200 mL), and extracted with Et<sub>2</sub>O (4 x 125 mL). The combined organics were washed with brine (170 mL), dried (MgSO<sub>4</sub>), and concentrated to an oil, which was purified by flash chromatography on silica gel (2.5 to 10% EtOAc in hexanes) to provide the intermediate diene (1.04 g, quantitative yield) as a viscous oil containing a small amount of solvent.

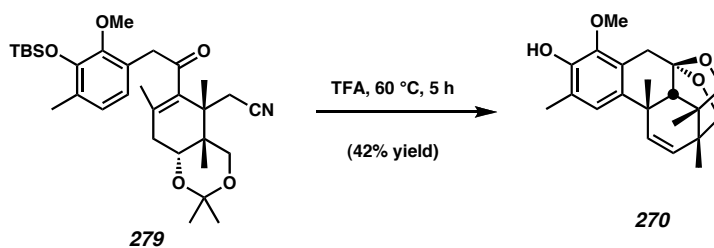
To a cooled (0 °C) solution of the intermediate diene (116.7 mg, 0.42 mmol, 1.00 equiv) in acetone (5.30 mL) and H<sub>2</sub>O (5.30 mL) was added OsO<sub>4</sub> (10.8 mg, 42.3 μmol, 0.10 equiv) and NaIO<sub>4</sub> (227 mg, 1.06 mmol, 2.50 equiv). After 3.5 h at 0 °C, the reaction mixture was diluted with H<sub>2</sub>O (35 mL) and EtOAc (35 mL), and extracted with EtOAc (5 x 15 mL). The combined organics from four such reactions were washed with brine (200 mL), dried (MgSO<sub>4</sub>), and concentrated to an oil, which was purified by flash chromatography on silica gel (20 to 35% EtOAc in hexanes) to provide enal **278** (332 mg, 71% yield, 2 steps) as an oil: *R*<sub>f</sub> 0.28 (35% EtOAc in hexanes); <sup>1</sup>H NMR (300 MHz, CDCl<sub>3</sub>) δ 10.10 (s, 1H), 4.21 (d, *J* = 9.0 Hz, 1H), 3.87 (d, *J* = 9.3 Hz, 1H), 3.85 (d, *J* = 8.4 Hz, 1H), 3.70 (d, *J* = 9.0 Hz, 1H), 3.51 (d, *J* = 8.7 Hz, 1H), 2.78 (dd, *J* = 6.0, 19.8 Hz, 1H), 2.49 (dd, *J* = 9.0, 19.8 Hz, 1H), 2.16 (s, 3H), 1.60 (s, 3H), 1.59 (s, 3H), 1.20 (s, 3H), 1.16 (s, 3H); <sup>13</sup>C NMR (75 MHz, CDCl<sub>3</sub>) δ 191.0, 153.2, 136.8, 121.5, 76.0, 74.2, 74.1, 70.4, 48.7, 48.0, 38.7, 28.7, 27.3, 20.7, 19.0, 18.0; IR (Neat film NaCl) 2982, 2938, 2880, 1671, 1628, 1386, 1177, 1050 cm<sup>-1</sup>; HRMS (EI) [M]<sup>+</sup> *m/z* calc'd for [C<sub>16</sub>H<sub>23</sub>NO<sub>3</sub>]<sup>+</sup>: 277.1678, found 277.1677.



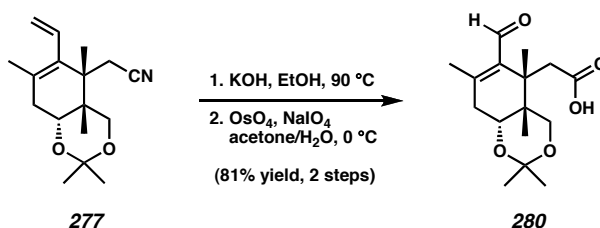
**Enone 279.** A flame-dried two-neck round bottom flask equipped with a reflux condenser and septum was charged with magnesium turnings (1.66 g, 68.4 mmol, 57.0 equiv) and  $\text{Et}_2\text{O}$  (27 mL) under an  $\text{N}_2$  atmosphere and heated to reflux. To this mixture was added 1,2-dibromoethane (120  $\mu\text{L}$ , 1.39 mmol, 1.16 equiv) in a dropwise manner. [*Caution: gas evolution!*] When gas evolution ceased, a solution of benzyl bromide **151** (1.24 g, 3.60 mmol, 3.00 equiv) in  $\text{Et}_2\text{O}$  (8.0 mL) was added in a dropwise manner over 30 min, and heating was continued for an additional 20 min. The Grignard reagent was then cooled ( $0\text{ }^\circ\text{C}$ ), and added to a cooled ( $0\text{ }^\circ\text{C}$ ) solution of enal **278** (332 mg, 1.20 mmol, 1.00 equiv) in THF (12 mL). After 1 h at  $0\text{ }^\circ\text{C}$ , the reaction was quenched with 0.5 M citric acid (40 mL), and  $\text{EtOAc}$  (40 mL), and extracted with  $\text{EtOAc}$  (5 x 25 mL). The combined organics were dried ( $\text{Na}_2\text{SO}_4$ ) and concentrated to an oil, which was purified by flash chromatography on silica gel (10 to 25%  $\text{EtOAc}$  in hexanes) to give a separable 3:1 mixture of diastereomeric allylic alcohols (533.3 mg, 85% yield).

To a cooled ( $0\text{ }^\circ\text{C}$ ) solution of the above allylic alcohol (76.0 mg, 0.140 mmol, 1.00 equiv) in  $\text{CH}_2\text{Cl}_2$  (5.0 mL) was added Dess-Martin periodinane (89.1 mg, 0.211 mmol, 1.50 equiv) and the resulting mixture was stirred for 2 h. The reaction mixture was diluted with  $\text{Et}_2\text{O}$  (35 mL), filtered, concentrated to an oil, and purified by flash chromatography on silica gel (5 to 20%  $\text{EtOAc}$  in hexanes) to give enone **279** (75.7 mg, 100% yield, 85% yield 2 steps) as an oil:  $R_f$  0.47 (25%  $\text{EtOAc}$  in hexanes);  $^1\text{H NMR}$  (300 MHz,  $\text{CDCl}_3$ )  $\delta$  6.85 (d,  $J = 7.8$  Hz, 1H), 6.64 (d,  $J = 7.8$  Hz, 1H), 4.16 (d,  $J = 8.7$  Hz, 1H), 4.08 (d,  $J = 9.0$  Hz, 1H), 3.87 (dd,  $J = 6.0, 8.4$  Hz, 1H), 3.86 (s, 2H), 3.64 (s, 3H), 3.53

(d,  $J = 8.7$  Hz, 1H), 3.52 (d,  $J = 9.0$  Hz, 1H), 2.54 (dd,  $J = 6.0, 17.7$  Hz, 1H), 2.30 (dd,  $J = 8.3, 18.2$  Hz, 1H), 2.21 (s, 3H), 1.79 (s, 3H), 1.62 (s, 3H), 1.61 (s, 3H), 1.17 (s, 3H), 1.15 (s, 3H), 1.02 (s, 9H), 0.16 (s, 6H);  $^{13}\text{C}$  NMR (75 MHz,  $\text{CDCl}_3$ )  $\delta$  207.4, 150.0, 147.0, 138.7, 130.0, 128.2, 125.8, 125.2, 123.3, 121.6, 75.5 (2C), 75.2, 70.5, 59.9, 49.7, 47.2, 47.1, 35.5, 28.7, 27.6, 26.0, 21.1, 20.8, 18.5, 18.2, 17.1, -4.2; IR (Neat film NaCl) 2932, 2859, 1699, 1464, 1422, 1286, 1073, 1047, 856, 841  $\text{cm}^{-1}$ ; HRMS (FAB+)  $[\text{M}+\text{H}]^+$   $m/z$  calc'd for  $[\text{C}_{31}\text{H}_{47}\text{NSiO}_5+\text{H}]^+$ : 542.3302, found 542.3296.



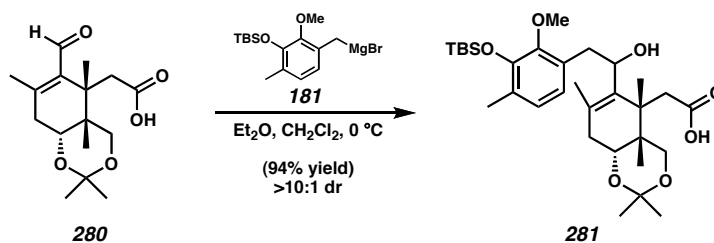
**Acetal 270.** A solution of enone **279** (29.9 mg, 55.2  $\mu\text{mol}$ , 1.00 equiv) in trifluoroacetic acid (4.00 mL) was heated to 60  $^\circ\text{C}$  for 5 h. The reaction mixture was then cooled to ambient temperature, concentrated to an oil, and purified by flash chromatography on silica gel (5 to 50% EtOAc in hexanes) to give acetal **270** (7.9 mg, 23.1  $\mu\text{mol}$ , 42% yield) as an off-white solid.



**Enal 280.** To a stirred solution of nitrile **277** (370.3 mg, 1.35 mmol, 1 equiv) in EtOH (26.9 mL, 0.05 M) was added KOH aq. (26.9 mL, 5 wt% in  $\text{H}_2\text{O}$ , 0.05 M). The reaction was then heated to 80  $^\circ\text{C}$  for 44 hours. The reaction was then cooled to ambient temperature and the EtOH was removed by rotary evaporation. The resulting aqueous

solution was diluted with 60 mL CH<sub>2</sub>Cl<sub>2</sub>, 26.9 mL HCl (2M), and further extracted with CH<sub>2</sub>Cl<sub>2</sub> (5 x 40 mL). The organic layers were dried over MgSO<sub>4</sub> and concentrated to an oil (406.7 mg, 1.38 mmol, > 99% yield), which was carried on to the next step without further purification.

To a solution of the carboxylic acid intermediate (133.2 mg, 0.4525 mmol, 1 equiv) in acetone (5.7 mL, 0.08 M) and water (5.7 mL, 0.08 M) at 0 °C was added OsO<sub>4</sub> (11.5 mg, 45.25 μmol, 0.1 M) and NaIO<sub>4</sub> (241.7 mg, 1.13 mmol, 2.5 equiv). The reaction mixture was stirred at 0 °C for 1 h then diluted with H<sub>2</sub>O (25 mL), EtOAc (25 mL), further extracted with EtOAc (3 x 15 mL), dried over MgSO<sub>4</sub>, and concentrated to an oil. Purification by flash chromatography (30% to 60% acetone/hexanes, with 3 drops AcOH per 100 mL eluent during the last half of the column) afforded enal **280** (111.5 mg, 0.3762 mmol, 83% yield) as a white amorphous solid. *R<sub>f</sub>* 0.28 (40% EtOAc in hexanes); <sup>1</sup>H NMR (500 MHz, CDCl<sub>3</sub>) δ 10.14 (s, 1H), 4.06 (d, *J* = 9.0 Hz, 1H), 4.01 (d, *J* = 9.0 Hz, 1H), 3.89 (d, *J* = 9.0 Hz, 1H), 3.88 (t, *J* = 3.7 Hz, 1H), 3.76 (d, *J* = 9.3 Hz, 1H), 2.63 (comp. m, 1H), 2.27 (dd, *J* = 19.3, 4.0 Hz, 1 H), 2.18 (s, 3H), 1.53 (s, 3H), 1.46 (s, 3H), 1.26 (s, 3H), 1.01 (s, 3H); <sup>13</sup>C NMR (125 MHz, CDCl<sub>3</sub>) δ 190.6, 175.9 150.1, 138.5, 80.9, 78.2, 76.2, 74.2, 47.4, 45.2, 38.1, 26.8, 23.0, 21.7, 19.3, 18.2; IR (Neat film NaCl) 3600–2500, 2981, 2939, 2882, 1731, 1668, 1385, 1175, 1154, 1049, 918 cm<sup>-1</sup>; MS (FAB+) [M+H]<sup>+</sup> *m/z* calc'd for [C<sub>16</sub>H<sub>24</sub>O<sub>5</sub>+H]<sup>+</sup>: 297.1702, found 297.1697.



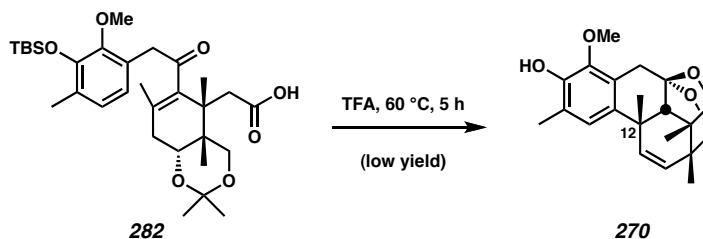
**Allylic alcohol 281.** A flame-dried two-neck round bottom flask equipped with a reflux condenser and septum was charged with magnesium turnings (1.03 g, 42.4 mmol,

32.4 equiv) and Et<sub>2</sub>O (12 mL) under an N<sub>2</sub> atmosphere and heated to reflux. To this mixture was added 1,2-dibromoethane (150 μL, 1.74 mmol, 1.33 equiv) in a dropwise manner [*Caution: gas evolution!*]. When gas evolution ceased, a solution of benzyl bromide **151** (677 mg, 1.96 mmol, 1.50 equiv) in Et<sub>2</sub>O (7.0 mL) was added in a dropwise manner over 30 min and heating was continued for an additional 30 min. The Grignard reagent was then cooled to 0 °C and 3 equivalents were added dropwise to a cooled (0 °C) solution of enal **280** (100 mg, 0.337 mmol, 1.00 equiv) in Et<sub>2</sub>O (3.8 mL) and CH<sub>2</sub>Cl<sub>2</sub> (7.4 mL) (1:2 ratio, 0.03 M overall). After 15 min at 0 °C, the reaction was quenched with H<sub>2</sub>O (5 mL) and 2 M citric acid (2.0 mL) and allowed to come to ambient temperature. The mixture was diluted with H<sub>2</sub>O (30 mL) and Et<sub>2</sub>O (30 mL), and extracted with Et<sub>2</sub>O (50 mL then 3 x 10 mL). The combined organics were washed with brine (30 mL), dried over Na<sub>2</sub>SO<sub>4</sub>, and concentrated to an oil. Purification by flash chromatography on silica gel (15 to 65% EtOAc in hexanes with 3 drops AcOH per 100 mL eluent for last half of column) provided allylic alcohol **281** (178.3 mg, 0.3168 mmol, 94% yield, > 10:1 dr) as a partially separated mixture of two diastereomers **281a** and **281b**.

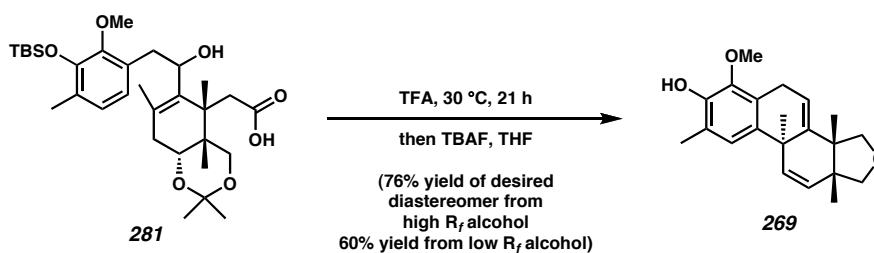
**High R<sub>f</sub> diastereomer 281a:** R<sub>f</sub> 0.72 (50% acetone in hexanes); <sup>1</sup>H NMR (500 MHz, CDCl<sub>3</sub>) δ 6.86 (d, *J* = 7.8 Hz, 1H), 6.72 (d, *J* = 7.8 Hz, 1H), 4.56 (d, *J* = 9.3 Hz, 1H), 4.04 (d, *J* = 8.5 Hz, 1H), 3.89 (app. t, *J* = 8.8 Hz, 2H), 3.81 (t, *J* = 4.2 Hz, 1H), 3.78 (d, *J* = 8.8 Hz, 1H), 3.72 (s, 3H), 3.09 (dd, *J* = 13.9, 10.5 Hz, 1H), 2.79 (dd, *J* = 13.9, 2.4 Hz, 1H), 2.41 (dd, *J* = 18.1, 3.9 Hz, 1H), 2.21 (s, 3H), 2.05 (dd, *J* = 18.1, 4.2 Hz, 1H), 1.52 (s, 3H), 1.03 (s, 9H), 1.01 (s, 3H), 0.19 (s, 3H), 0.17 (s, 3H); <sup>13</sup>C NMR (125 MHz, CDCl<sub>3</sub>) δ 176.5, 149.4, 147.3, 135.9, 130.4, 129.8, 126.4, 123.2, 78.0, 76.4, 75.0, 73.6, 60.0, 47.3, 39.2, 36.7, 26.7, 26.0, 23.1, 20.6, 18.6, 17.0, -4.0, -4.1; IR (Neat film NaCl) 3426, 2956, 2932, 2859, 1731, 1464, 1419, 1286, 1253, 1178, 1074, 1046, 918, 840, 782, 733 cm<sup>-1</sup>; MS (FAB+) [M+H-H<sub>2</sub>]<sup>+</sup> calc'd for [C<sub>31</sub>H<sub>49</sub>O<sub>7</sub>Si]<sup>+</sup>: *m/z* 561.3248, found 561.3253.



123.3, 80.6, 78.3, 76.5, 74.8, 59.9, 46.8, 35.4, 26.8, 26.1, 23.1, 21.9, 21.2, 18.5, 17.7, 17.1, -4.19, -4.22; IR (Neat film NaCl) 3695–2398, 2932, 2859, 1735, 1699, 1464, 1421, 1286, 1073, 919, 840, 782, 733  $\text{cm}^{-1}$ ; MS (FAB+)  $[\text{M}+\text{H}]^+$   $m/z$  calc'd for  $[\text{C}_{31}\text{H}_{48}\text{O}_7\text{Si}+\text{H}]^+$ : 561.3248, found 561.3220.



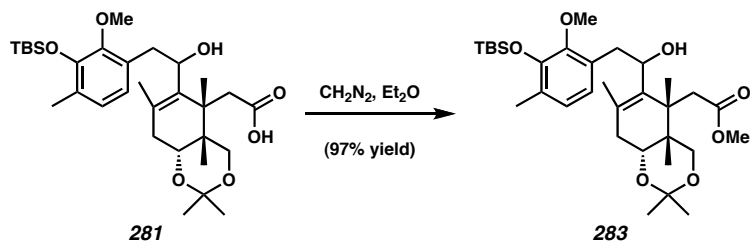
**Acetal 270 from enone 282:** A solution of enone **282** (20.4 mg, .036 mmol, 1.0 equiv) in TFA (2.0 mL, 0.018 M) was heated to 65 °C for 5 h, then cooled to ambient temperature. The solvent was removed by rotary evaporation and benzene was added and removed by rotary evaporation (3x). The crude oil was purified by preparative thin-layer chromatography (30% EtOAc/hexanes) to afford a small amount of acetal **270**.



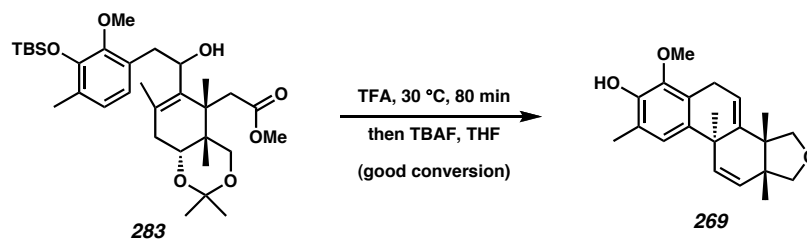
**Tetracycle 269.** A solution of allylic alcohol **281a** (30 mg, 0.053 mmol, 1.0 equiv) in TFA (3 mL, 10 mg/mL) was warmed to 30 °C and stirred for 21 h (reaction times as low as 30 min provide similar results) before cooling to ambient temperature. TFA was removed by rotary evaporation, diluted with benzene and concentrated to an oil (3x) then redissolved in THF (2 mL, 0.025 M). A solution of TBAF (54  $\mu\text{L}$ , 0.106 mmol, 2.0 equiv) in THF (2.0 M) was added, and the reaction mixture was stirred for 3 h, quenched

with H<sub>2</sub>O (20 mL), extracted with CH<sub>2</sub>Cl<sub>2</sub> (5 x 20 mL), dried over MgSO<sub>4</sub>, and purified by flash chromatography (10 to 20% EtOAc in hexanes) to provide tetracycle **269** (13.3 mg, 0.041 mmol, 76% yield) as a yellow solid.

A solution of allylic alcohol **281b** (30 mg, 0.053 mmol, 1.0 equiv) in TFA (3 mL, 10 mg/mL) was warmed to 30 °C and stirred for 21 h (reaction times as low as 30 min provide similar results) before cooling to ambient temperature. TFA was removed by rotary evaporation, diluted with benzene and concentrated to an oil (3x) then redissolved in THF (2 mL, 0.025 M). A solution of TBAF (54 μL, 0.106 mmol, 2.0 equiv) in THF (2.0 M) was added, and the reaction mixture was stirred for 3 h, quenched with H<sub>2</sub>O (20 mL), extracted with CH<sub>2</sub>Cl<sub>2</sub> (5 x 20 mL), dried over MgSO<sub>4</sub>, and purified by flash chromatography (10 to 20% EtOAc in hexanes) to provide tetracycle **269** (10.4 mg, 0.032 mmol, 60% yield) as a yellow solid. Crystals suitable for X-ray analysis were obtained by crystallization from Et<sub>2</sub>O/heptanes at ambient temperature: mp 150–153 °C (Et<sub>2</sub>O/heptane); *R<sub>f</sub>* 0.39 (30% acetone in hexanes); <sup>1</sup>H NMR (300 MHz, CDCl<sub>3</sub>) δ 6.86 (s, 1H), 6.18 (d, *J* = 10.3 Hz, 1H), 6.14 (d, *J* = 6.4 Hz, 1H), 5.69 (d, *J* = 10.3 Hz, 1H), 5.54 (s, 1H), 4.33 (d, *J* 7.6 Hz, 1H), 3.86 (s, 2H), 3.63 (dd, *J* = 19.9, 7.0 Hz, 3.49 (d, *J* = 7.3 Hz, 1H), 3.16 (d, *J* = 19.6 Hz, 1H), 2.24 (s, 3H), 1.26 (s, 3H), 1.20 (s, 3H), 0.76 (s, 3H) ; <sup>13</sup>C NMR (75 MHz, CDCl<sub>3</sub>) δ 144.3, 143.4, 143.1 138.8, 134.1, 131.4, 125.8, 123.9, 121.8, 120.7, 80.1, 78.1, 77.2, 60.9, 48.7, 46.6, 39.0, 28.9, 25.0, 20.6, 17.1, 15.8; IR (Neat film NaCl) 3368, 2961, 2925, 1871, 1485, 1462, 1421, 1320, 1211, 1070, 907, 733 cm<sup>-1</sup>; MS (FAB+) [M+H-H<sub>2</sub>]<sup>+</sup> *m/z* calc'd for [C<sub>21</sub>H<sub>25</sub>O<sub>3</sub>]<sup>+</sup>: 325.1799, found 325.1804.



**Methyl ester 283.** To a solution of acid **281** (10 mg, 0.018 mmol, 1.0 equiv) in Et<sub>2</sub>O (0.5 mL) was added CH<sub>2</sub>N<sub>2</sub> in Et<sub>2</sub>O (2 mL, ~ 1–2 M). The solution was stirred, open to air, until no further yellow color was visible. The solvent was removed by rotary evaporation to provide pure methyl ester **283** (9.9 mg, 0.017 mmol, 97% yield) as a clear oil: *R<sub>f</sub>* 0.47 (30% EtOAc in hexanes); <sup>1</sup>H NMR (300 MHz, CDCl<sub>3</sub>) δ 6.85 (d, *J* = 7.9 Hz, 1H), 6.74 (d, *J* = 7.7 Hz, 1H), 4.21 (d, *J* = 9.4 Hz, 1H), 4.07 (d, *J* = 9.1 Hz, 1H), 4.02 (d, *J* = 8.2 Hz, 1H), 3.77 (d, *J* = 7.9 Hz, 1H), 3.72 (s, 3H), 3.71 (s, 3H), 3.58 (d, *J* = 5.6 Hz, 1H), 3.55 (d, *J* = 5.0 Hz, 1H), 3.16 (dd, *J* = 14.1, 10.5 Hz, 1H), 2.79 (dd, *J* = 14.1, 1.8 Hz, 1H), 2.44 (br s, 1H), 2.21 (s, 3H), 2.17 (d, *J* = 8.2 Hz, 1H), 1.97 (s, 3H), 1.42 (s, 3H), 1.25 (s, 3H), 1.11 (s, 3H), 1.07 (s, 9H), 0.17 (app. d, *J* = 1.8 Hz, 6H); <sup>13</sup>C NMR (75 MHz, CDCl<sub>3</sub>) δ 174.8, 149.5, 147.3, 135.1, 130.8, 129.6, 129.2, 126.4, 76.7, 74.8, 74.2, 73.6, 71.8, 60.0, 51.9, 51.7, 47.3, 38.2, 37.9, 26.3, 26.0, 24.3, 21.1, 21.0, 18.6, 17.8, 17.0, -4.1, -4.06; IR (Neat film NaCl) 3444, 2931, 2858, 1734, 1464, 1285, 1142, 1044, 1004, 919, 840, 782, 732 cm<sup>-1</sup>; MS (FAB+) [M+H]<sup>+</sup> *m/z* calc'd for [C<sub>32</sub>H<sub>52</sub>O<sub>7</sub>Si+H]<sup>+</sup>: 577.3561, found 577.3544.

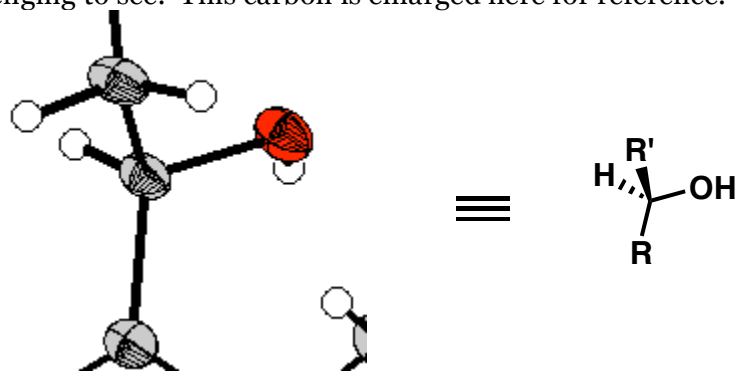


**Tetracycle 269 from methyl ester 283.** A solution of allylic alcohol **283** (9.9 mg, 17.7 μmol, 1.0 equiv) in TFA (700 μL, 0.025 M) was warmed to 30 °C and stirred for 80 min before cooling to ambient temperature. TFA was removed by rotary evaporation,

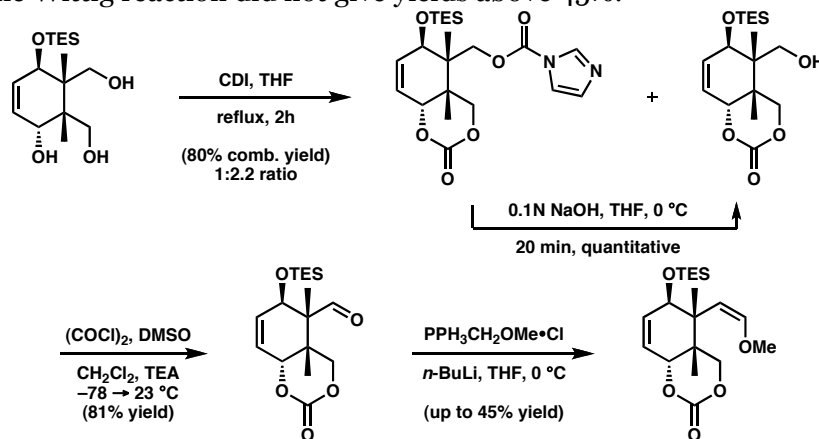
diluted with benzene and concentrated to an oil (3x).  $^1\text{H}$  NMR analysis indicated the formation of tetracycle **269** as the major product.



10. Ball, S.; Goodwin, T. W.; Morton, R. A., *Biochem. J.* **1948**, *42*, 516–523.  
 11. Evans, D. A.; Mitch, C. H.; Thomas, R. C.; Zimmerman, D. M.; Robey, R. L. *J. Am. Chem. Soc.* **1980**, *102*, 5955–5956.  
 12. Bhattacharya, A.; Segmuller, B.; Y. A. *Synth. Commun.* **1996**, *26*, 1775–1784.  
 13. See Chapter 2 for details.  
 14. When the ORTEP image was shrunk, the stereochemistry at the center of interest became challenging to see. This carbon is enlarged here for reference.

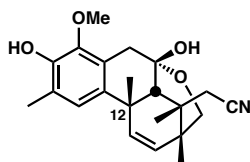


15. Attempts were made to access the opposite alcohol diastereomer. Mitsunobu attempts led either to recovered starting alcohol or to decomposition. Additionally, enone **255** was reduced under Luche conditions, but led to the same diastereomer of allylic alcohol **253**.  
 16. Silylation with TBSCl, DMAP, Imidazole, and DMF only proceeded to 10% conversion upon heating for extensive time scales.  
 17. Miljkovic, M.; Hagel, P. *Carbohydr. Res.* **1983**, *111*, 319–324. b) Morgenlie, S. *Carbohydr. Res.* **1975**, *41*, 77–83.  
 18. Brewster, A. G.; Leach, A. *Tetrahedron Lett.* **1986**, *27*, 2539–2542.  
 19. The 7-membered acetal can be accessed exclusively via selective oxidation of the secondary alcohol to the enone followed by acetal formation. The 7-membered acetal can be converted to the 6-membered acetal with 50% conversion and 100% mass recovery.  
 20. Dess, D. B.; Martin, J. C. *J. Am. Chem. Soc.* **1991**, *113*, 7277–7278.  
 21. A similar strategy was conducted in the below system. Once again, the methoxy methylene Wittig reaction did not give yields above 45%.



22. a) Okamoto, Y.; Yano, T. *Tetrahedron Lett.* **1971**, 4285–4287. b) Fraser, G. M.; Hoffmann, H. M. R. *Chem. Commun.* **1967**, 561–563.

23. The structure of this compound has been verified by extensive 2D NMR analysis. It should be noted that the compound was originally reported in D. Behenna's thesis as the following hemiacetal:

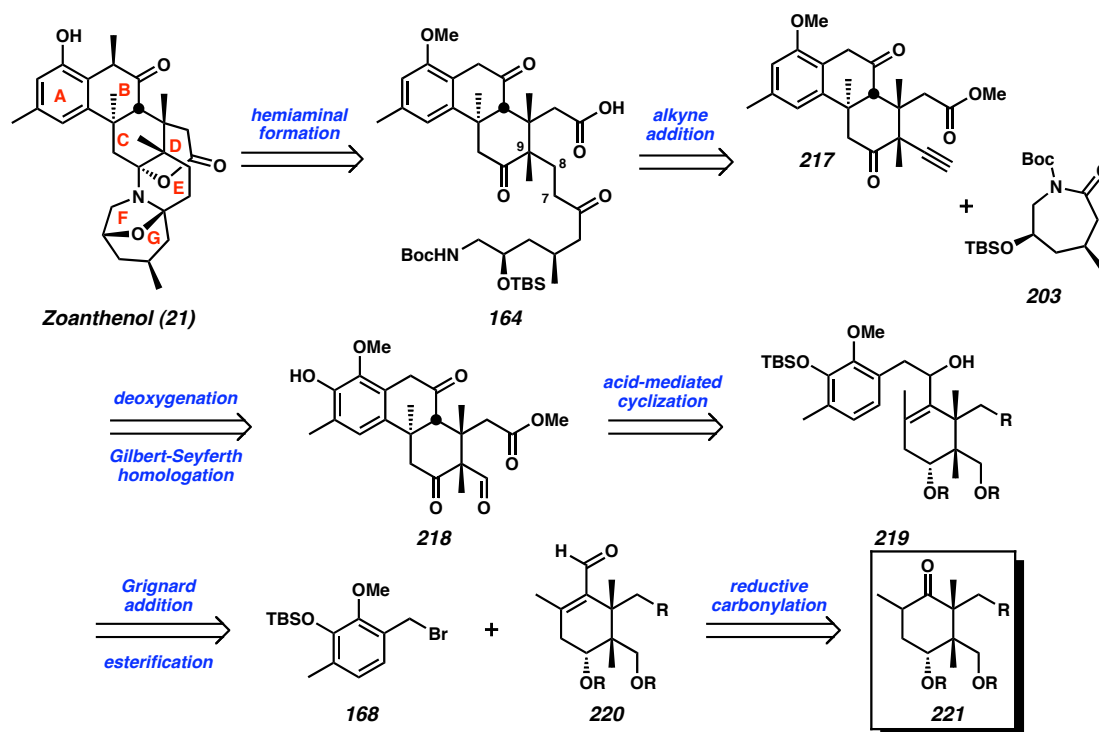


24. Efforts to determine the stereochemistry of the major isomer are ongoing.
25. Corey, E. J.; Cho, H.; Rucker, C.; Hua, D. H. *Tetrahedron Lett.* **1981**, 22, 3455–3458.

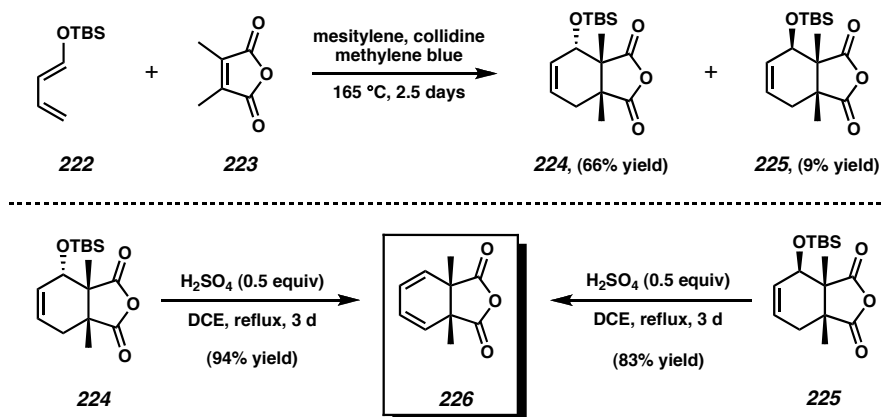
## SYNTHETIC SUMMARY

## Acid-Mediated Cyclization Approaches to the Densely Substituted Carbocyclic Core of Zoanthanol

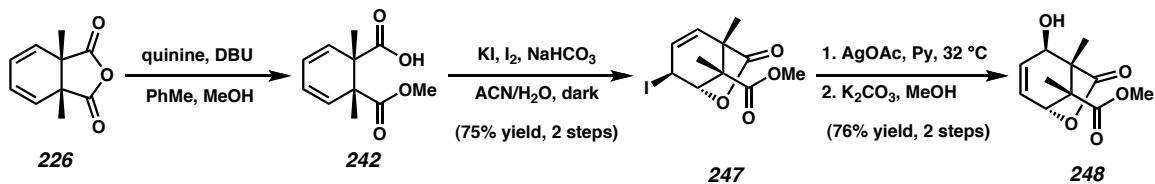
Scheme S3.1 Revised retrosynthetic analysis



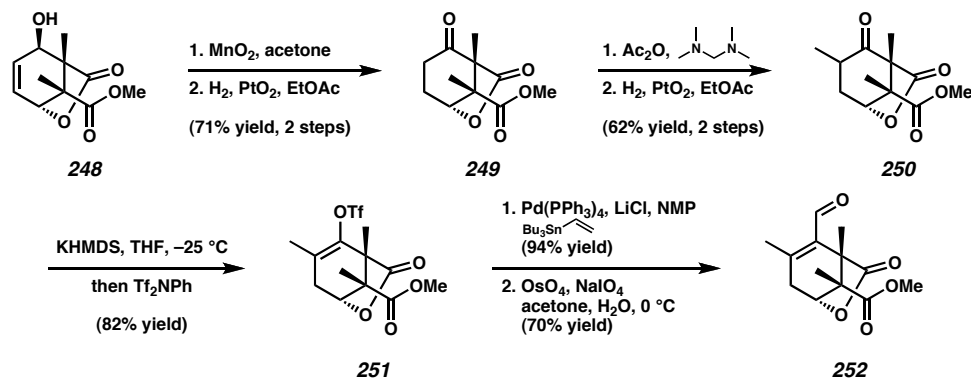
Scheme S3.2 Access to a meso anhydride



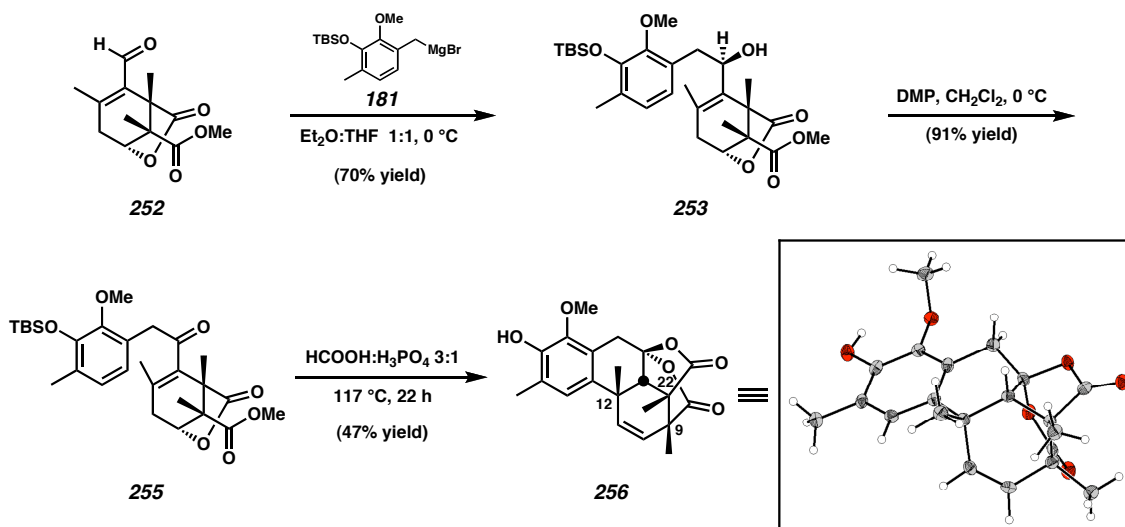
## Scheme S3.2 Desymmetrization and elaboration of a meso anhydride

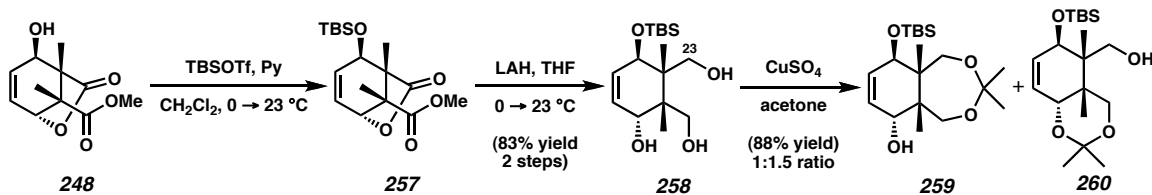


## Scheme S3.3 Synthesis of a lactone-derived C ring synthon

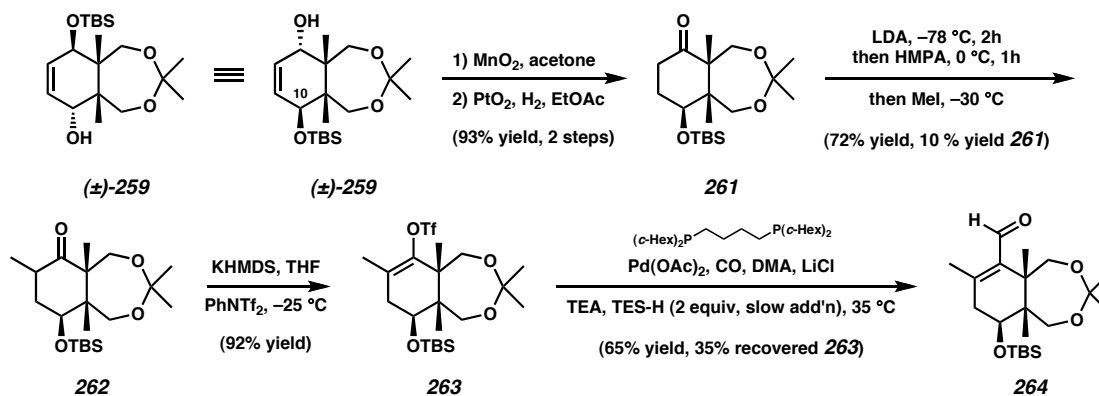


## Scheme S3.4 Fragment coupling and cyclization of the A and lactone-derived C rings

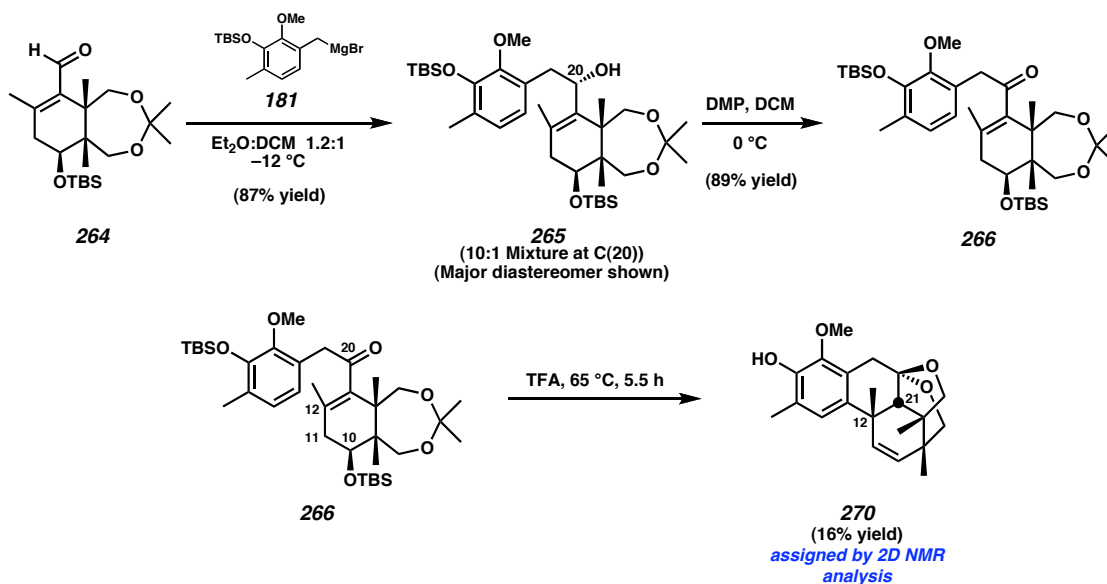


Scheme S3.5 Elaboration of lactone **248**

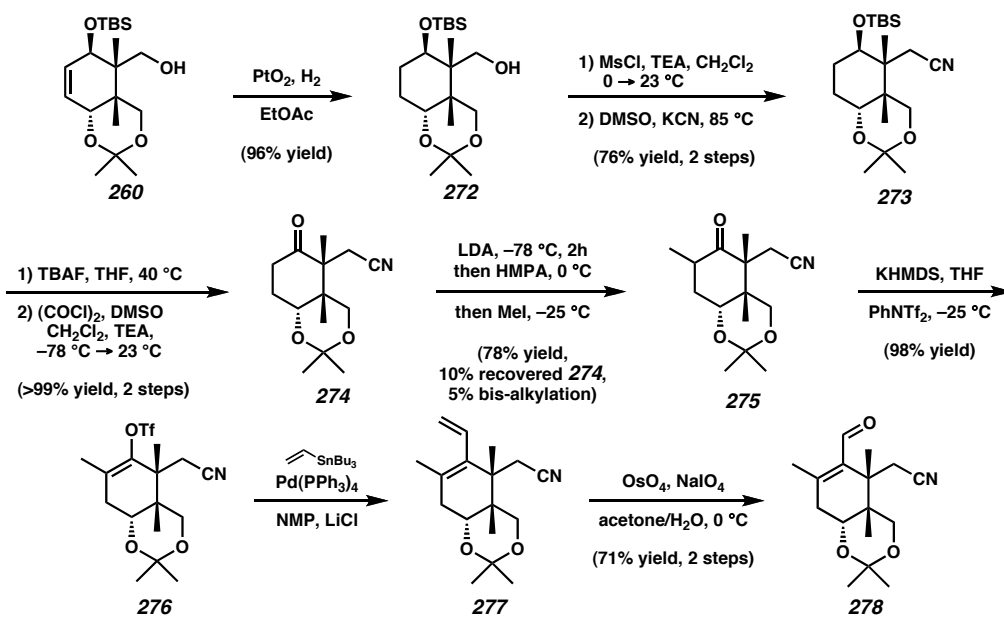
## Scheme S3.6 Synthesis of a 7-membered acetal-derived C ring synthon



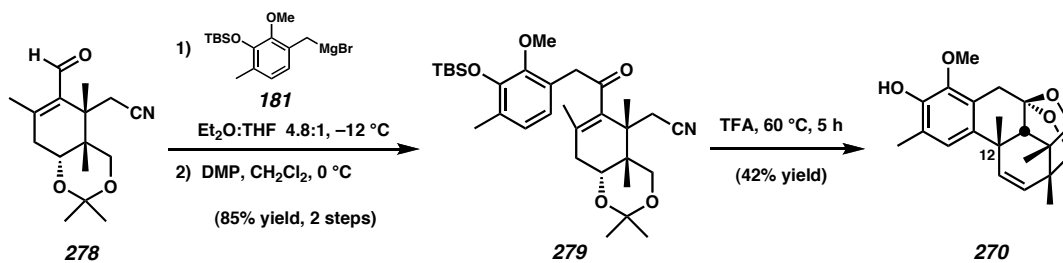
## Scheme S3.7 Fragment coupling and cyclization of the A and 7-membered acetal-derived C rings



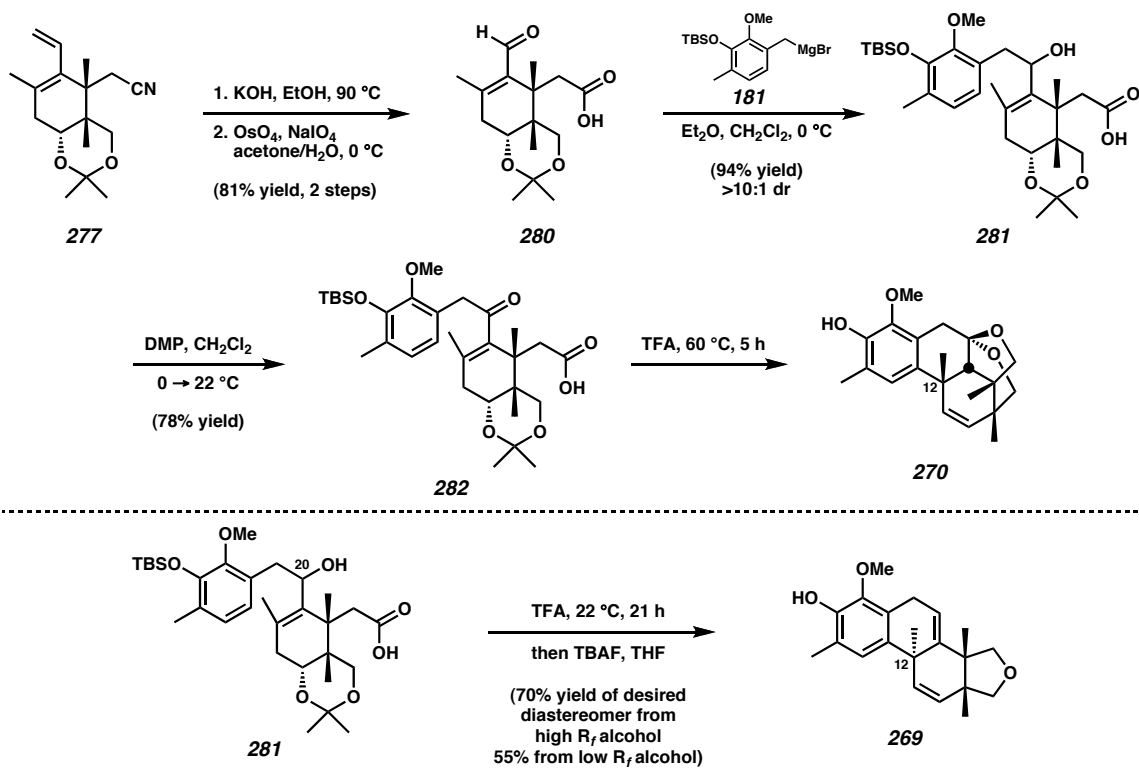
Scheme S3.8 Synthesis of a homologated nitrile-derived C ring synthon



Scheme S3.9 Fragment coupling and cyclization of the A and homologated nitrile-derived C rings



*Scheme S3.10 Synthesis, fragment coupling, and cyclization of the A and homologated carboxylic acid-derived C rings*



**APPENDIX B**

**Spectra and X-Ray Crystallographic Data:  
Acid-Mediated Cyclization Approaches to the  
Densely Substituted Carbocyclic Core of Zoanthenol**

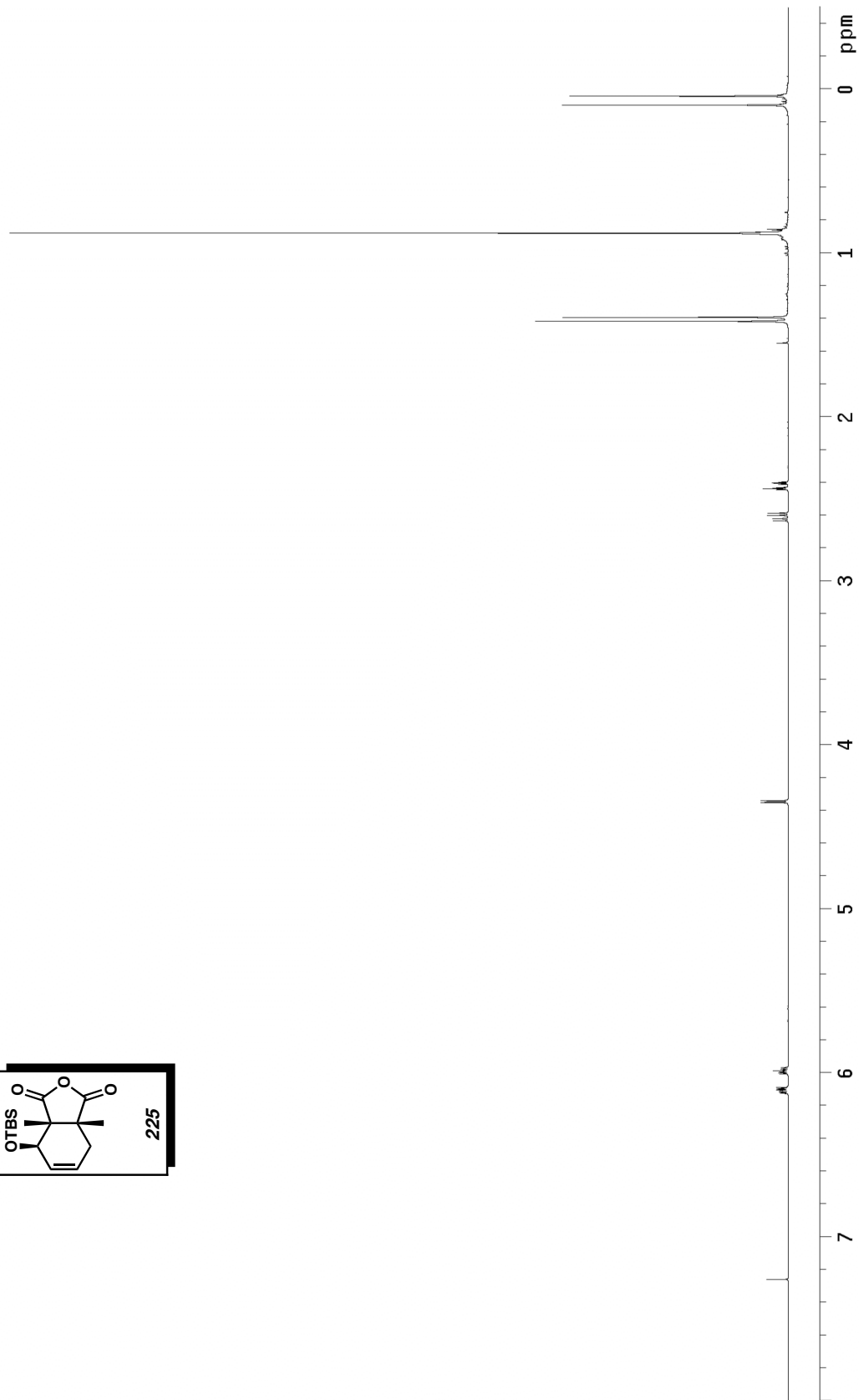
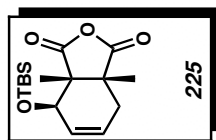


Figure B.1  $^1\text{H}$  NMR (500 MHz,  $\text{CDCl}_3$ ) of compound 225.

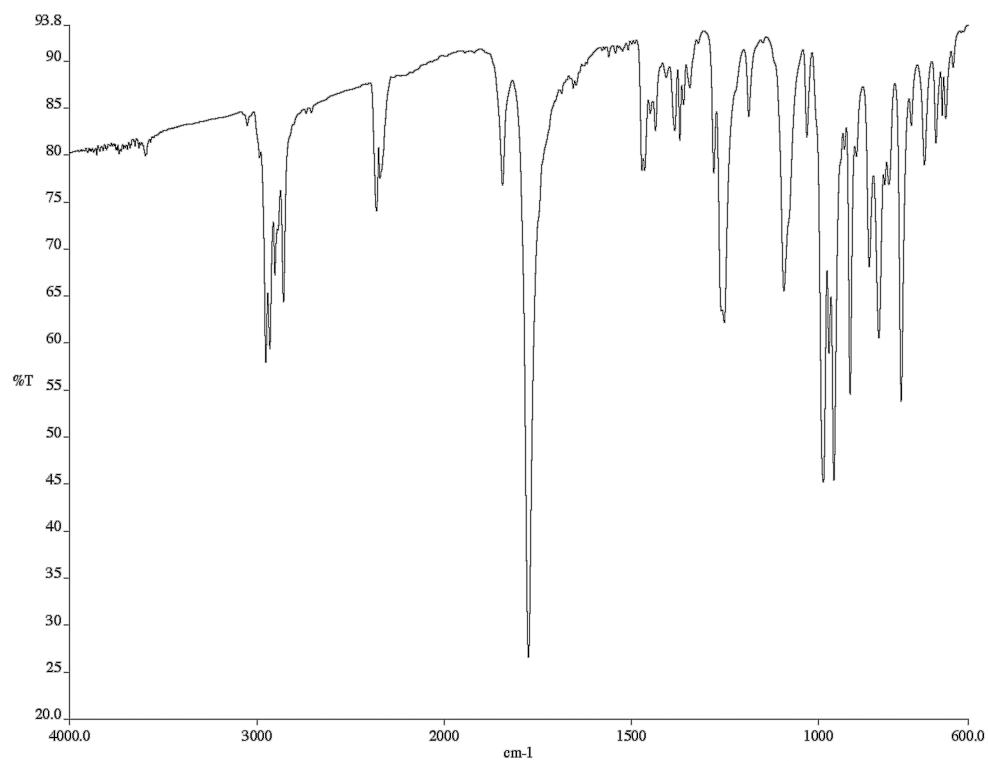


Figure B.2 Infrared spectrum (thin film/NaCl) of compound **225**.

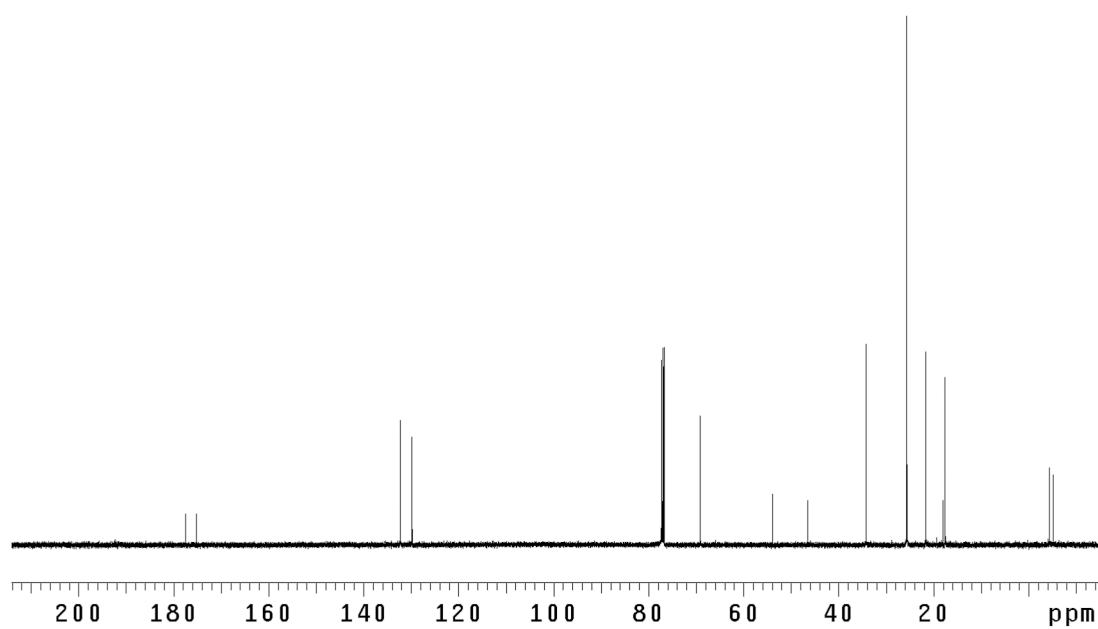


Figure B.3 <sup>13</sup>C NMR (125 MHz, CDCl<sub>3</sub>) of compound **225**.

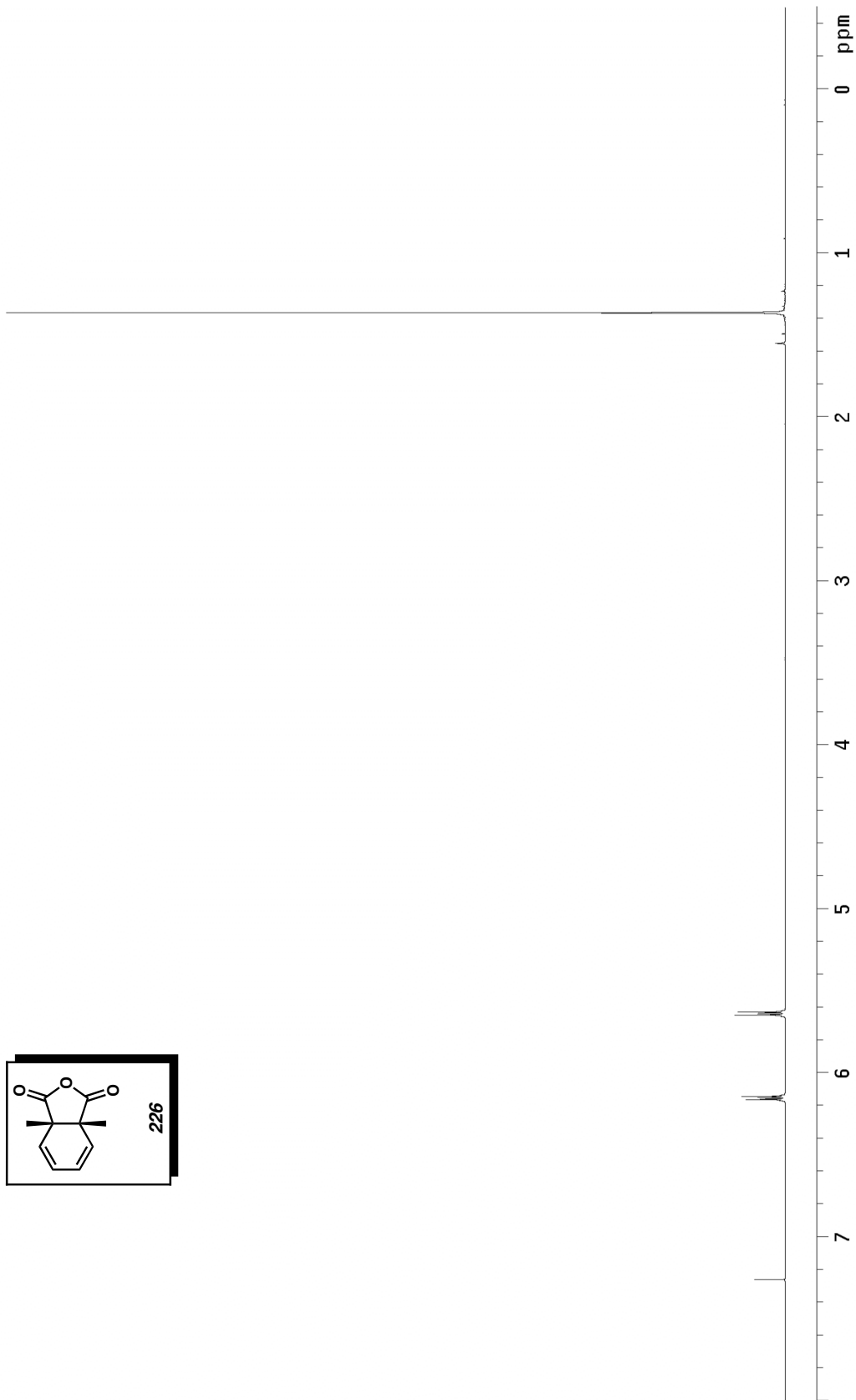
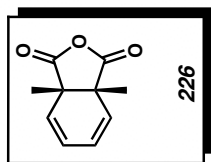


Figure B.4  $^1\text{H}$  NMR (500 MHz,  $\text{CDCl}_3$ ) of compound **226**.

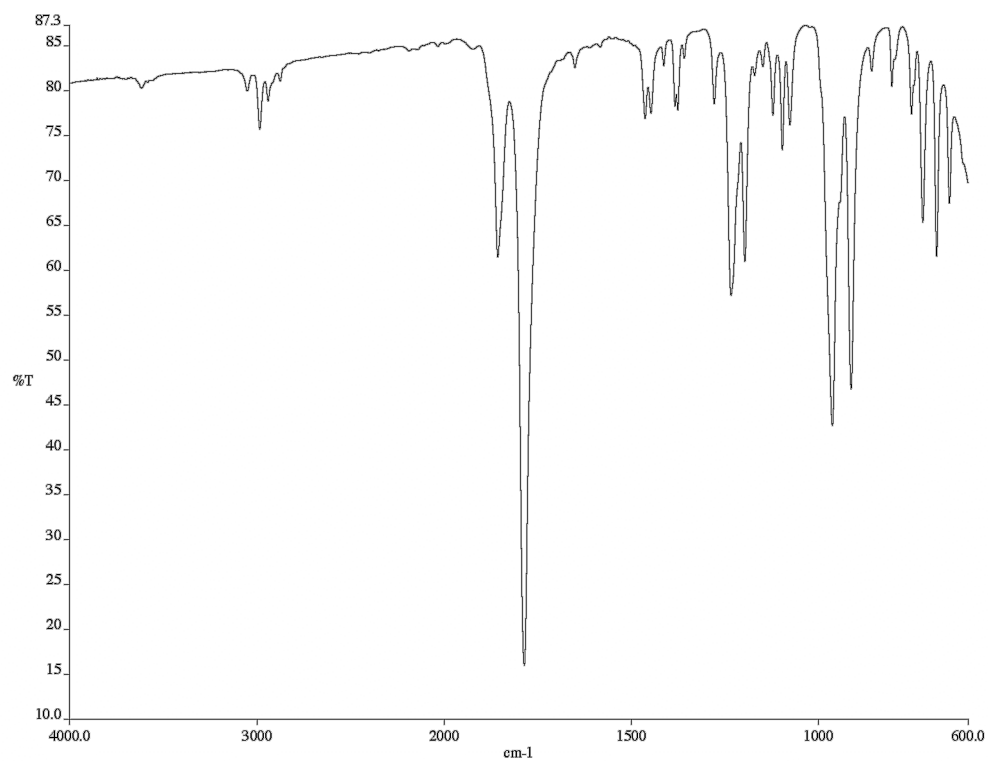


Figure B.5 Infrared spectrum (thin film/NaCl) of compound **226**.

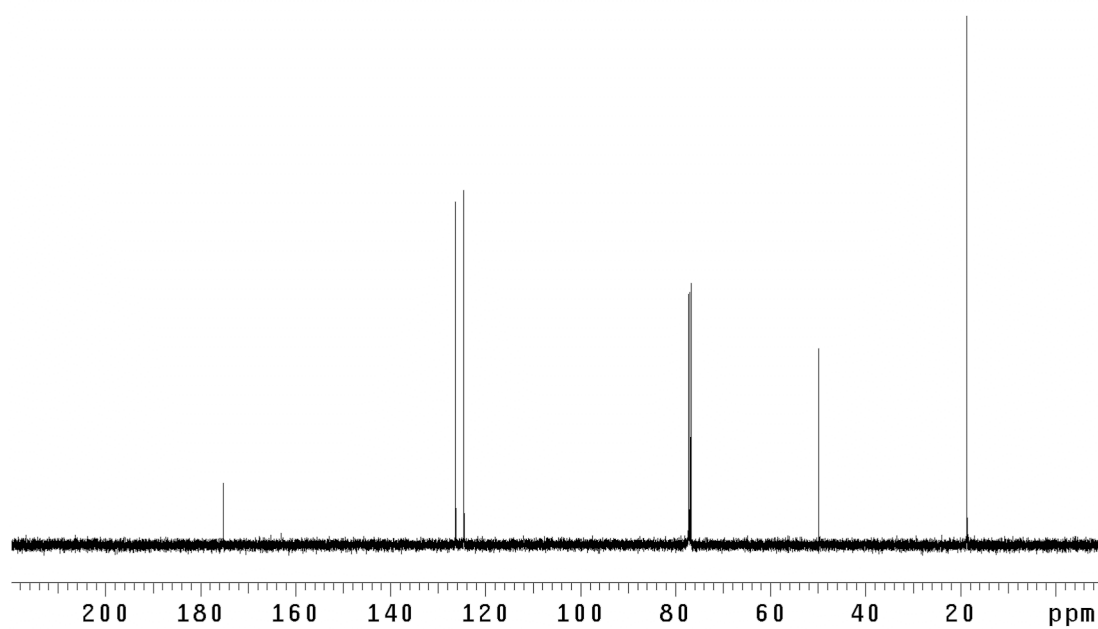


Figure B.6 <sup>13</sup>C NMR (125 MHz, CDCl<sub>3</sub>) of compound **226**.



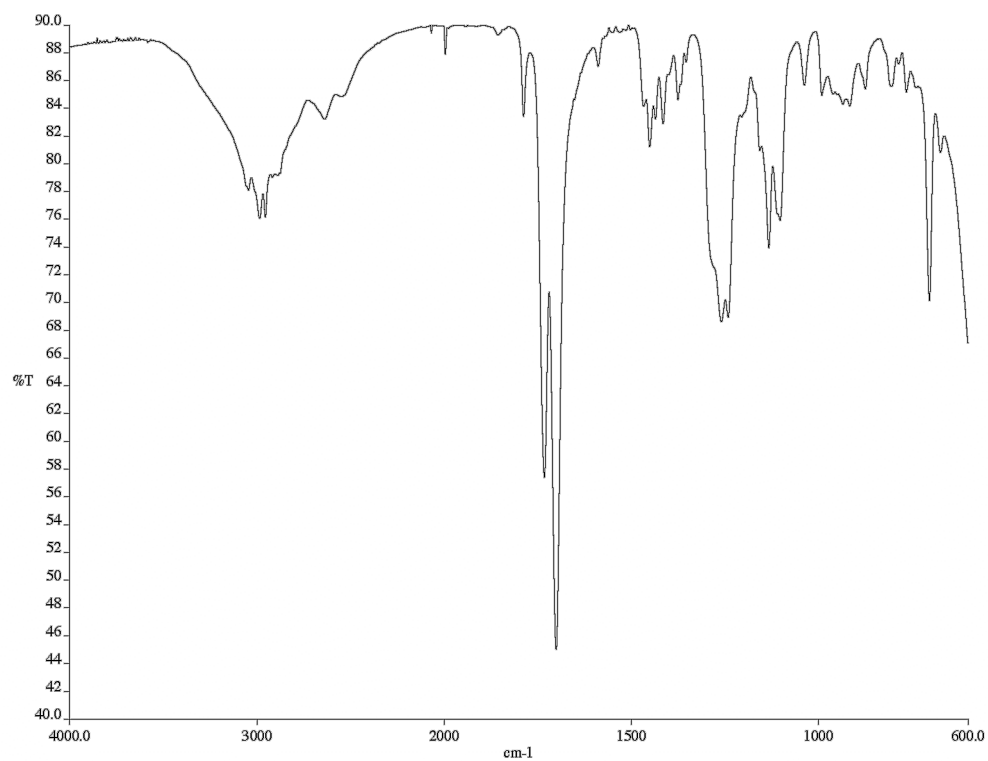


Figure B.8 Infrared spectrum (thin film/NaCl) of compound **242**.

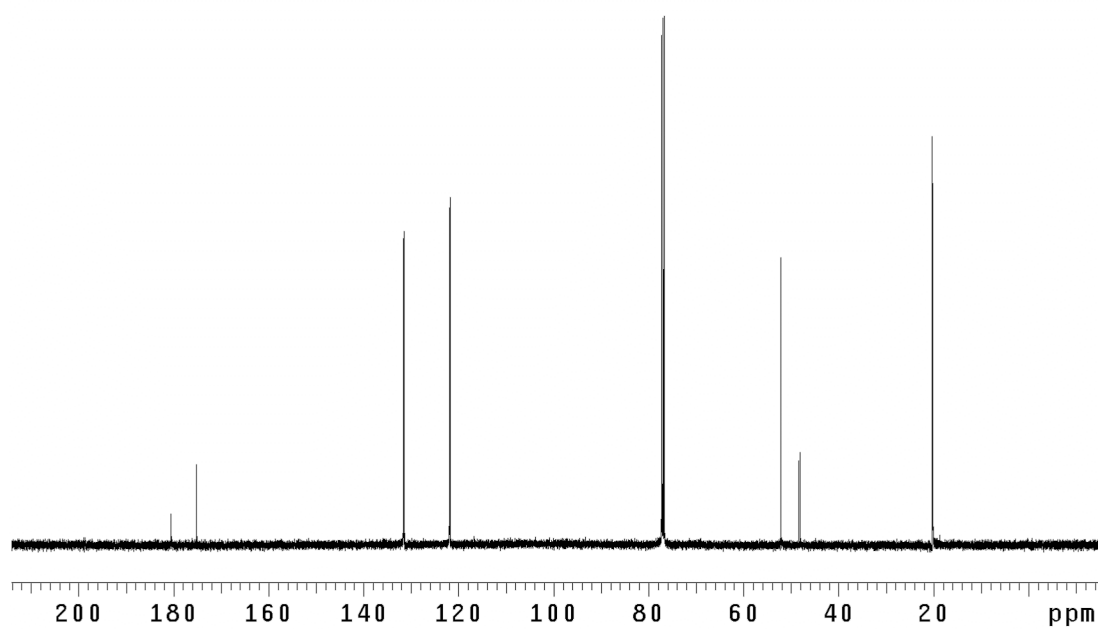


Figure B.9 <sup>13</sup>C NMR (125 MHz, CDCl<sub>3</sub>) of compound **242**.

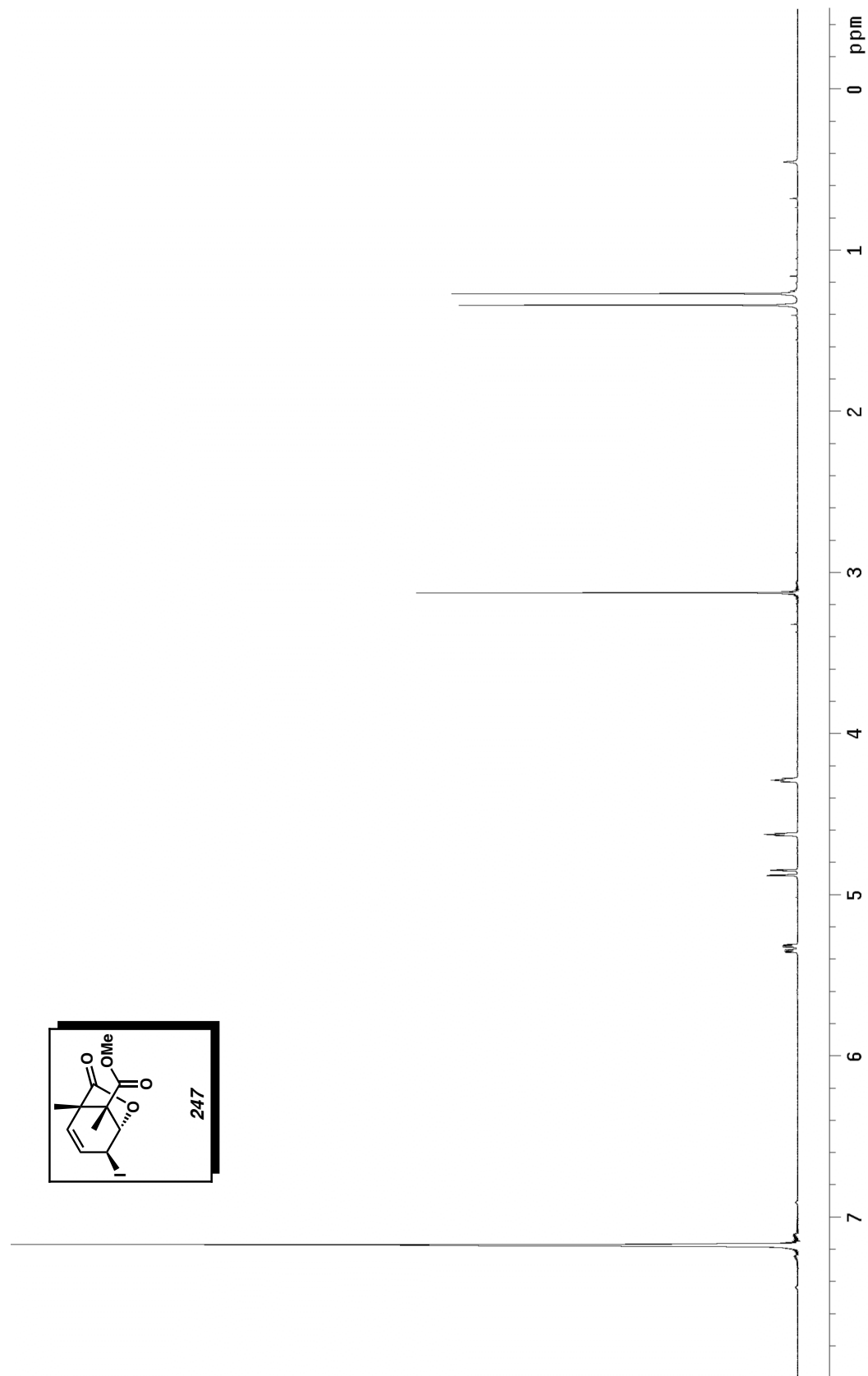


Figure B.10  $^1\text{H}$  NMR (300 MHz,  $\text{C}_6\text{D}_6$ ) of compound **247**.

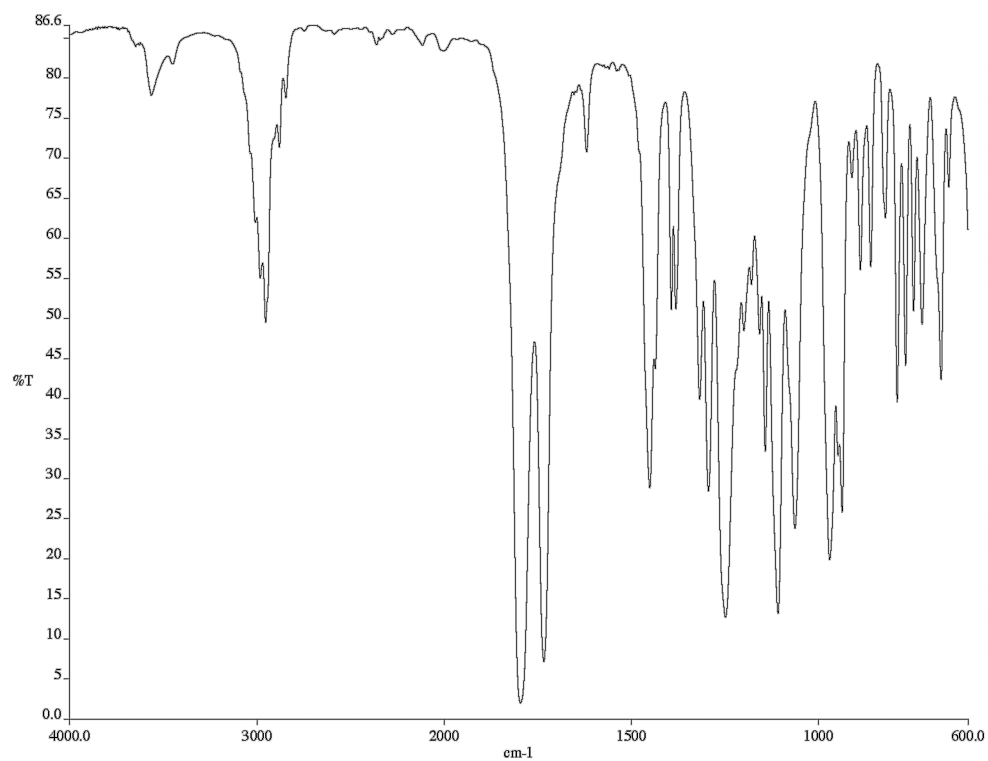


Figure B.11 Infrared spectrum (thin film/NaCl) of compound **247**.

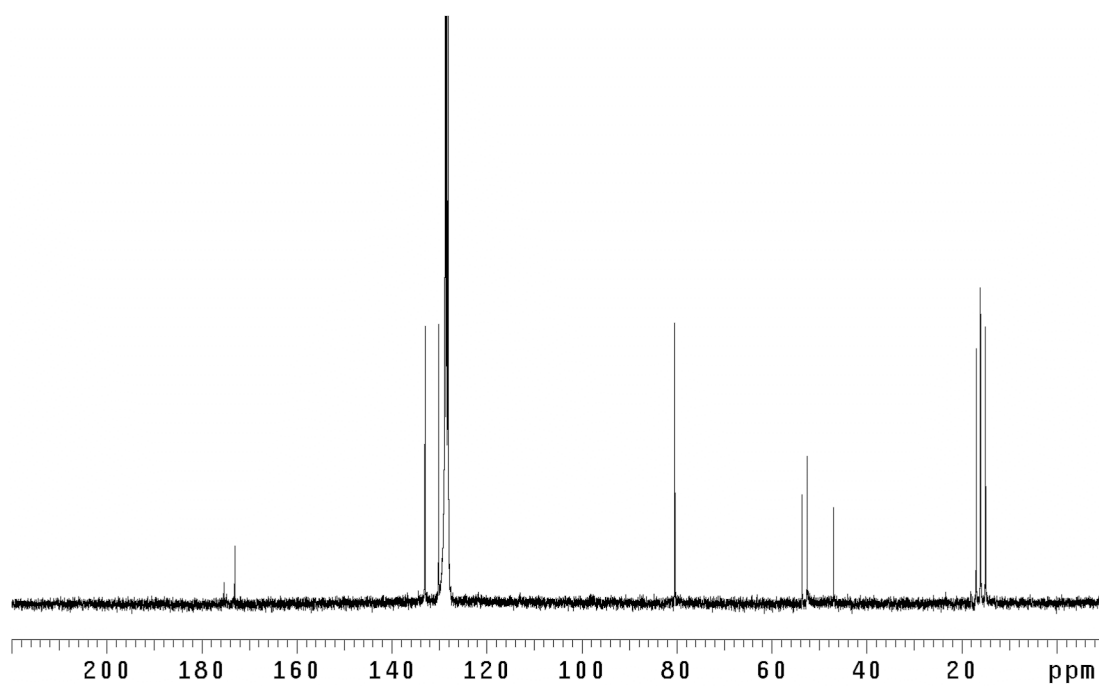


Figure B.12 <sup>13</sup>C NMR (75 MHz, C<sub>6</sub>D<sub>6</sub>) of compound **247**.

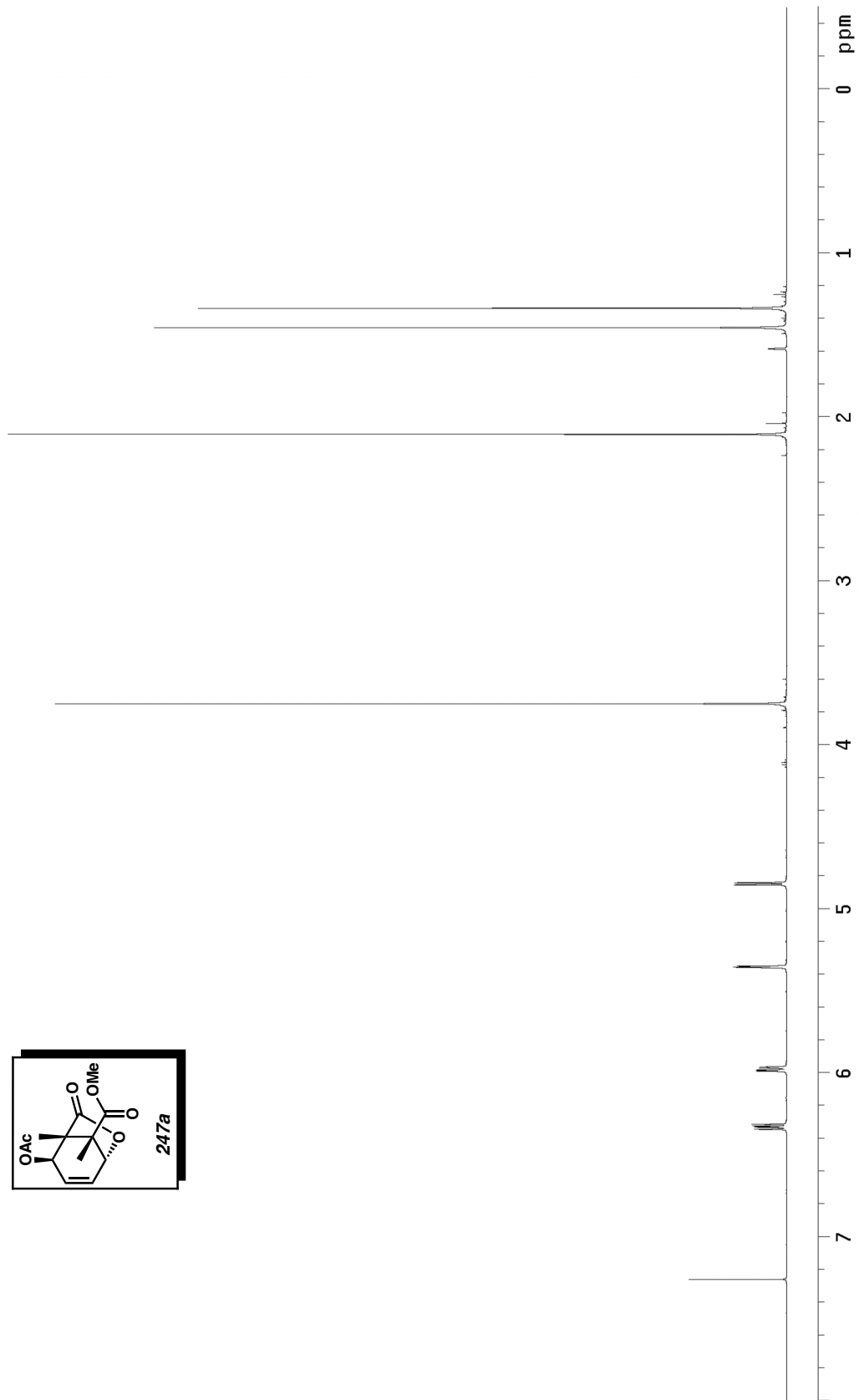
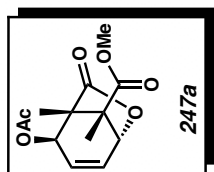


Figure B.13  $^1\text{H NMR}$  (500 MHz,  $\text{CDCl}_3$ ) of compound **247a**.

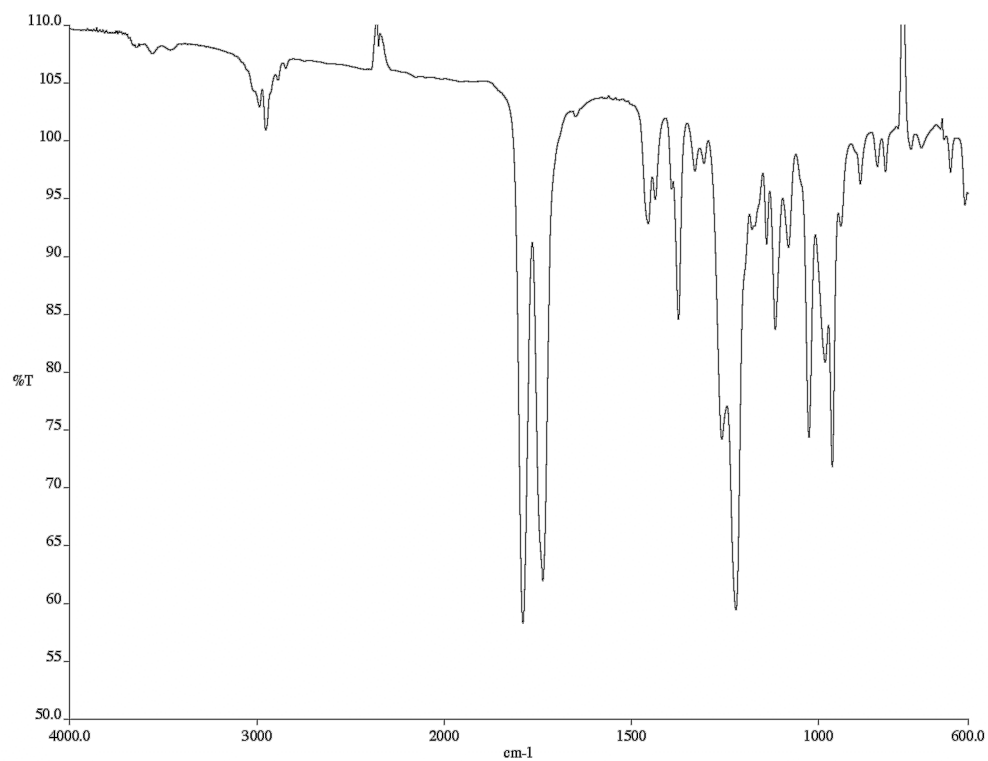


Figure B.14 Infrared spectrum (thin film/NaCl) of compound **247a**.

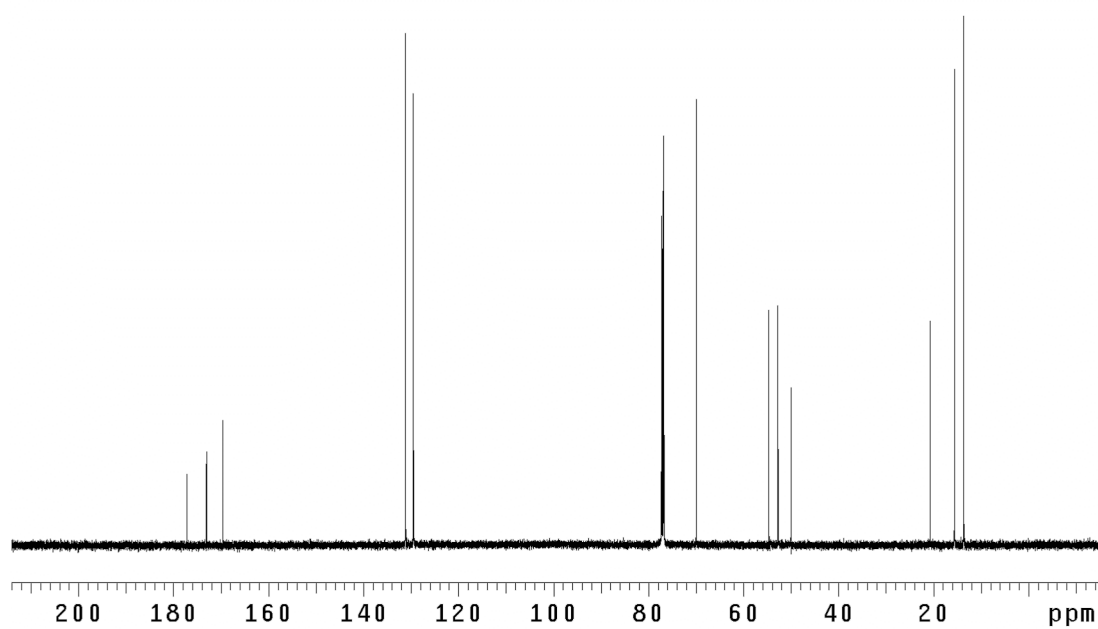


Figure B.15 <sup>13</sup>C NMR (125 MHz, CDCl<sub>3</sub>) of compound **247a**.

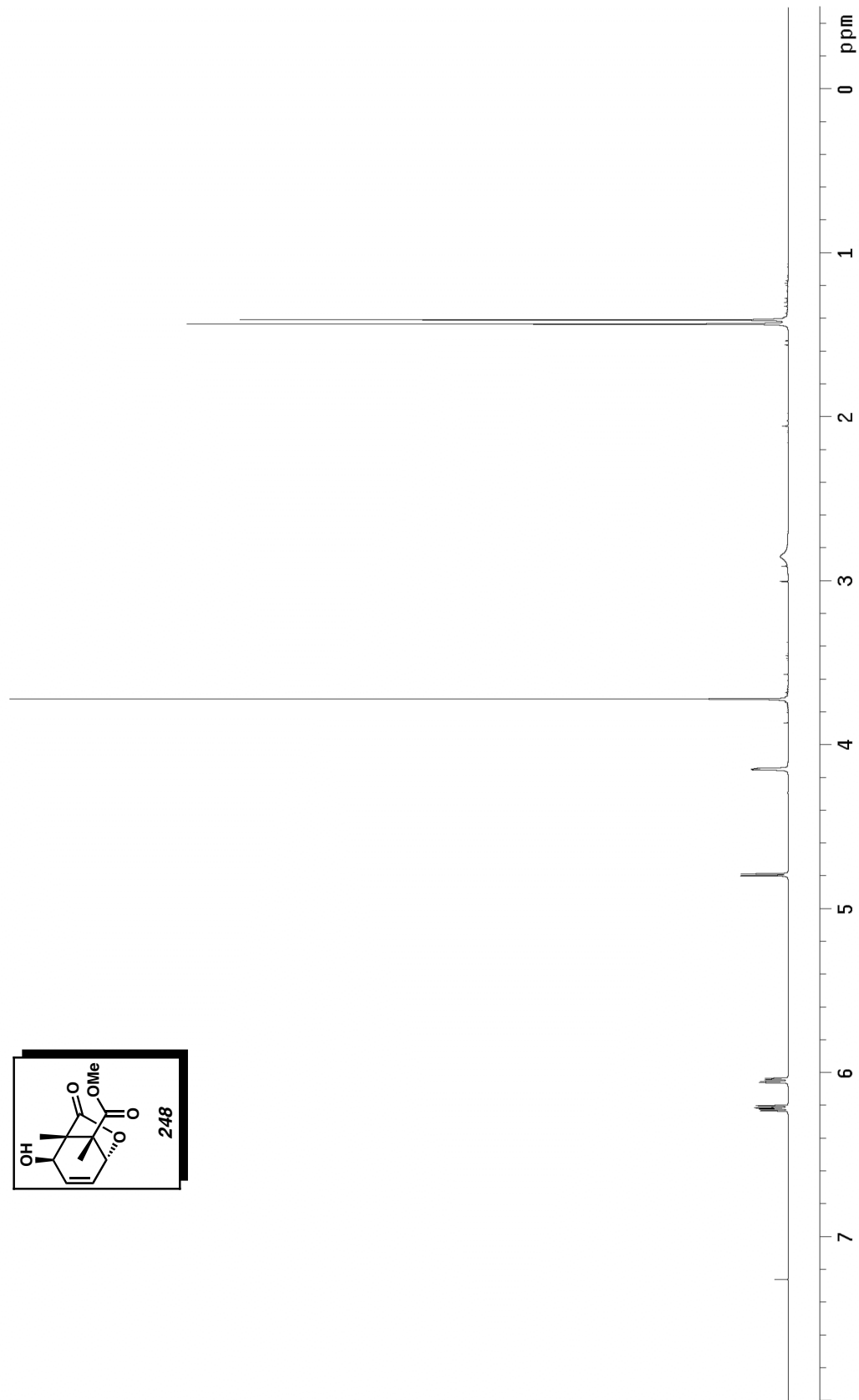
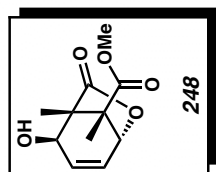


Figure B.16  $^1\text{H}$  NMR (500 MHz,  $\text{CDCl}_3$ ) of compound 248.

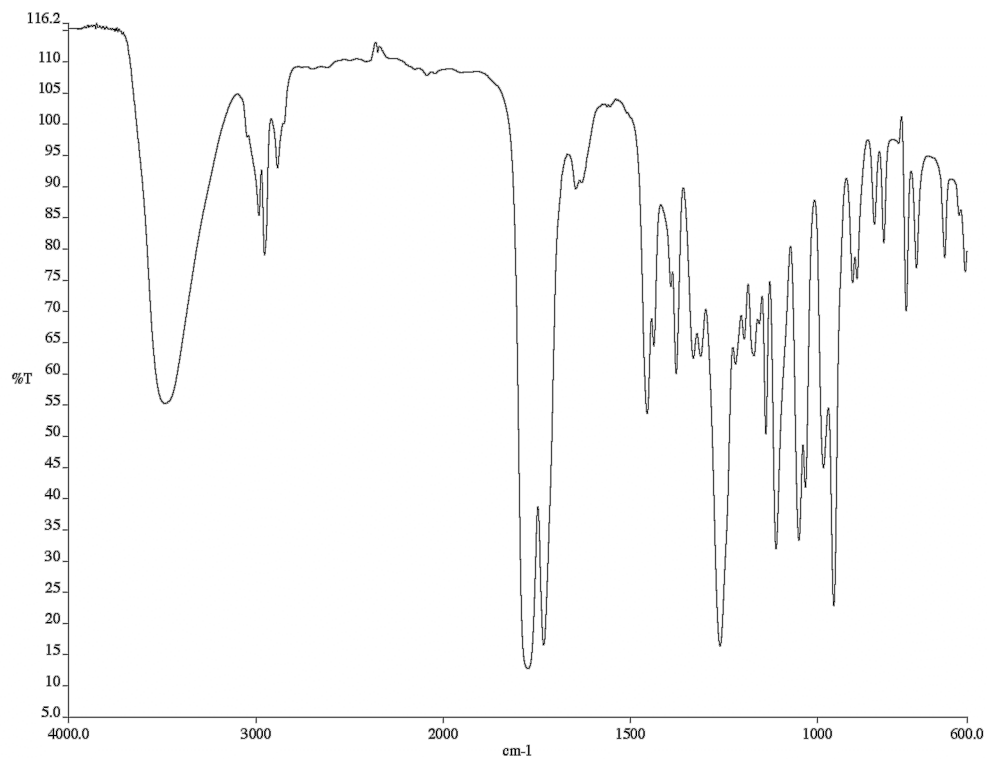


Figure B.17 Infrared spectrum (thin film/NaCl) of compound **248**.

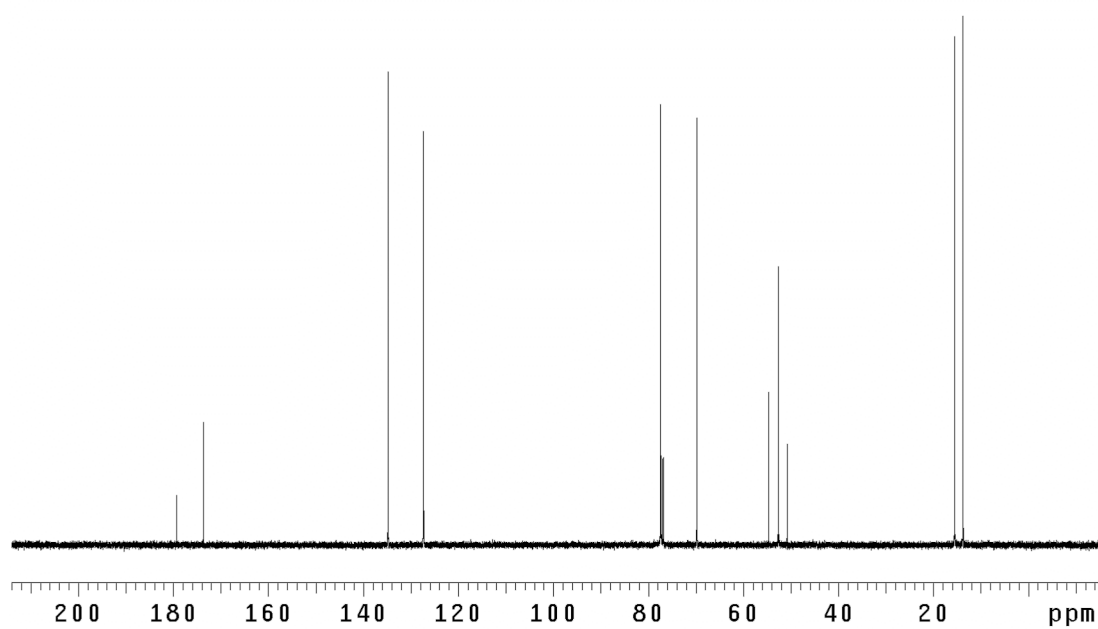


Figure B.17 <sup>13</sup>C NMR (125 MHz, CDCl<sub>3</sub>) of compound **248**.

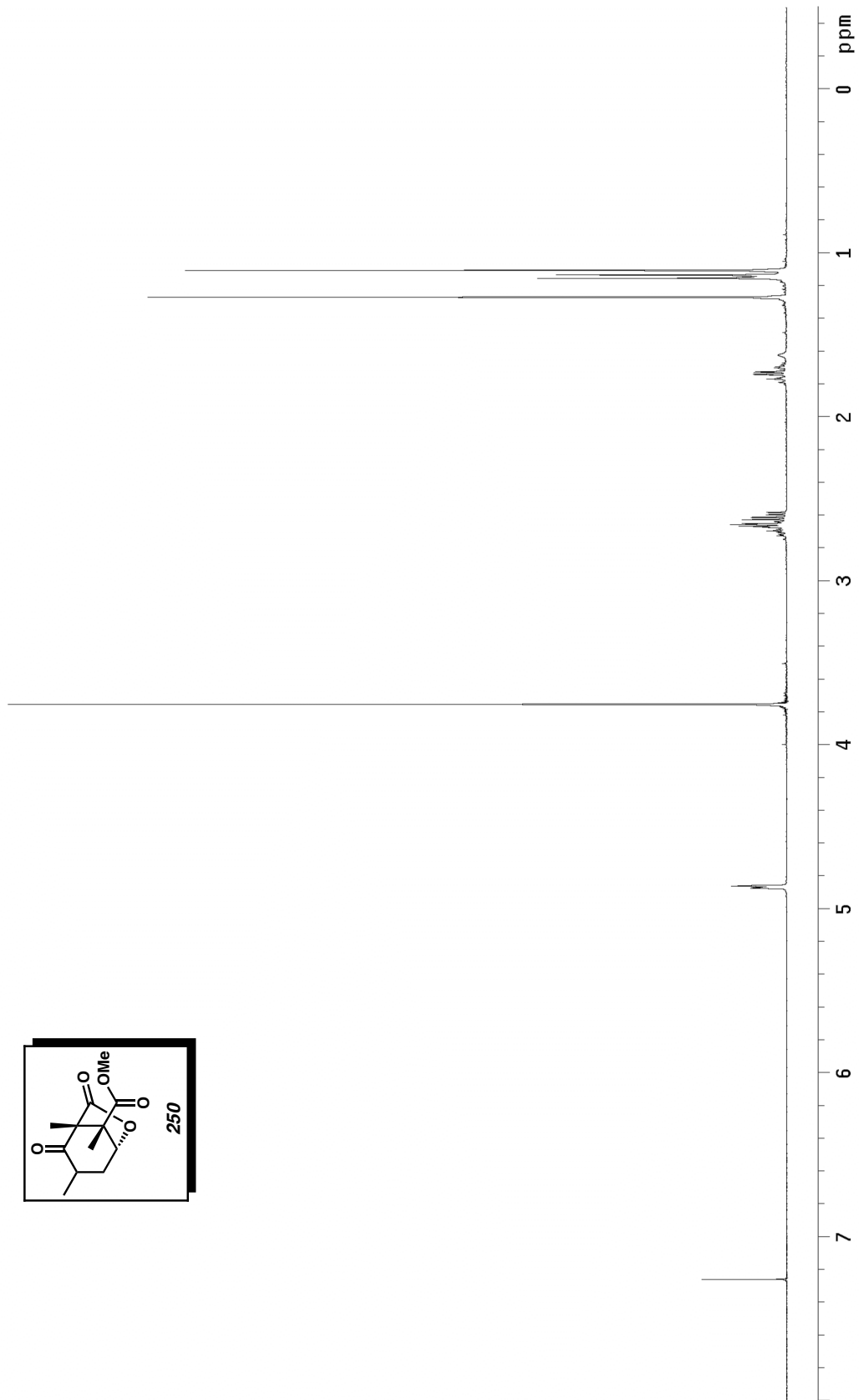
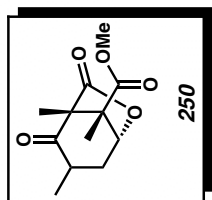


Figure B.19  $^1\text{H}$  NMR (300 MHz,  $\text{CDCl}_3$ ) of compound **250**.

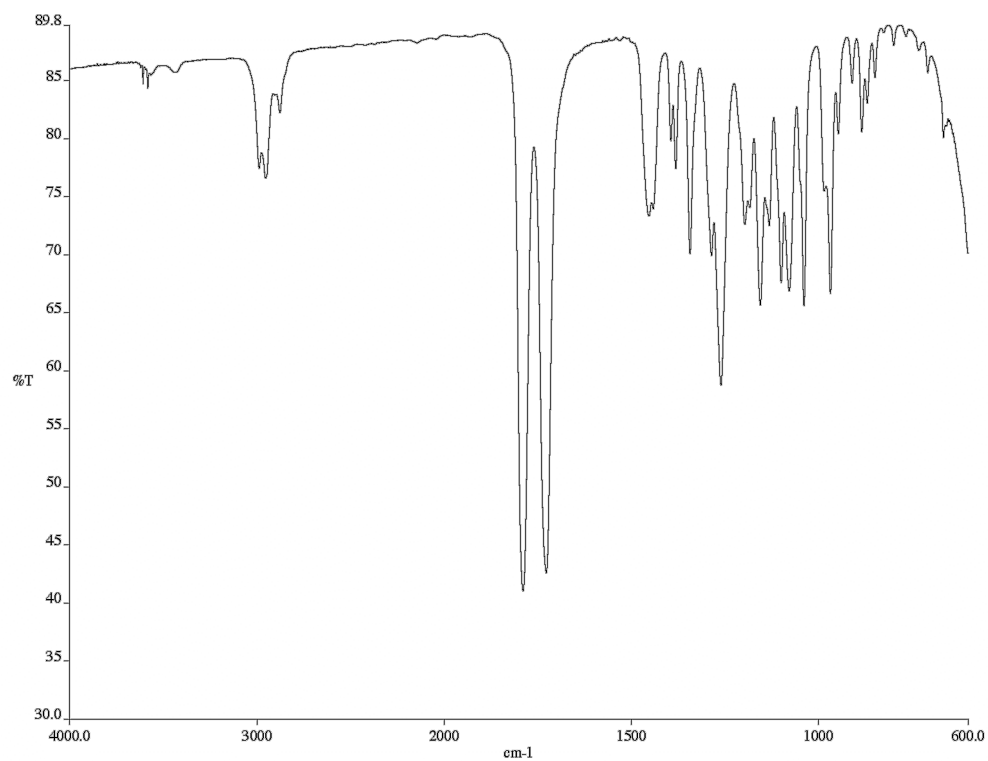


Figure B.20 Infrared spectrum (thin film/NaCl) of compound **250**.

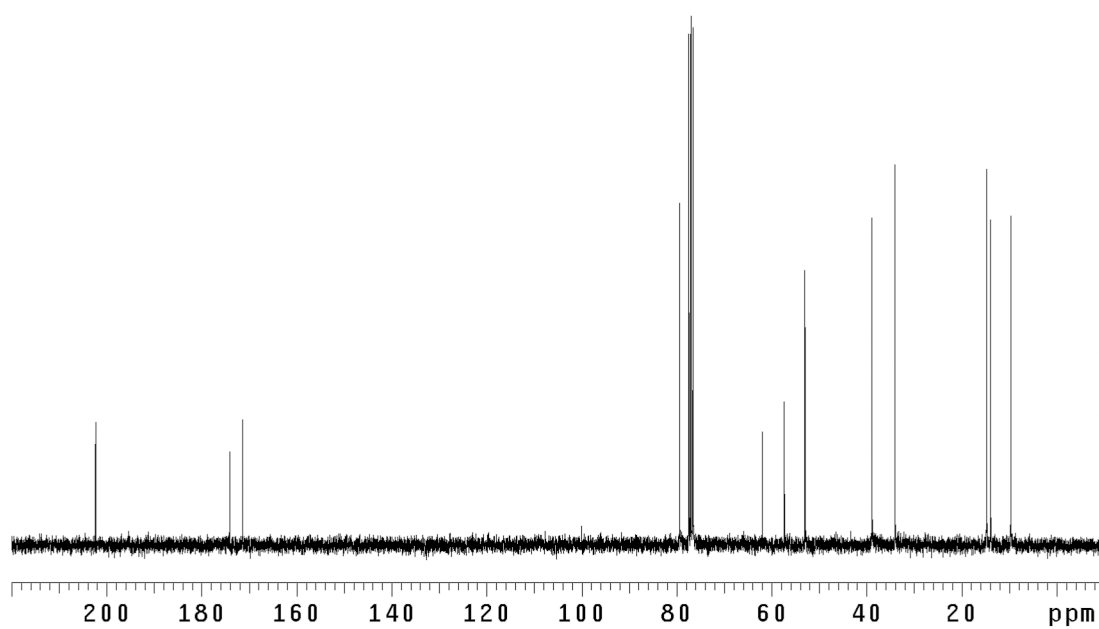


Figure B.21 <sup>13</sup>C NMR (75 MHz, CDCl<sub>3</sub>) of compound **250**.

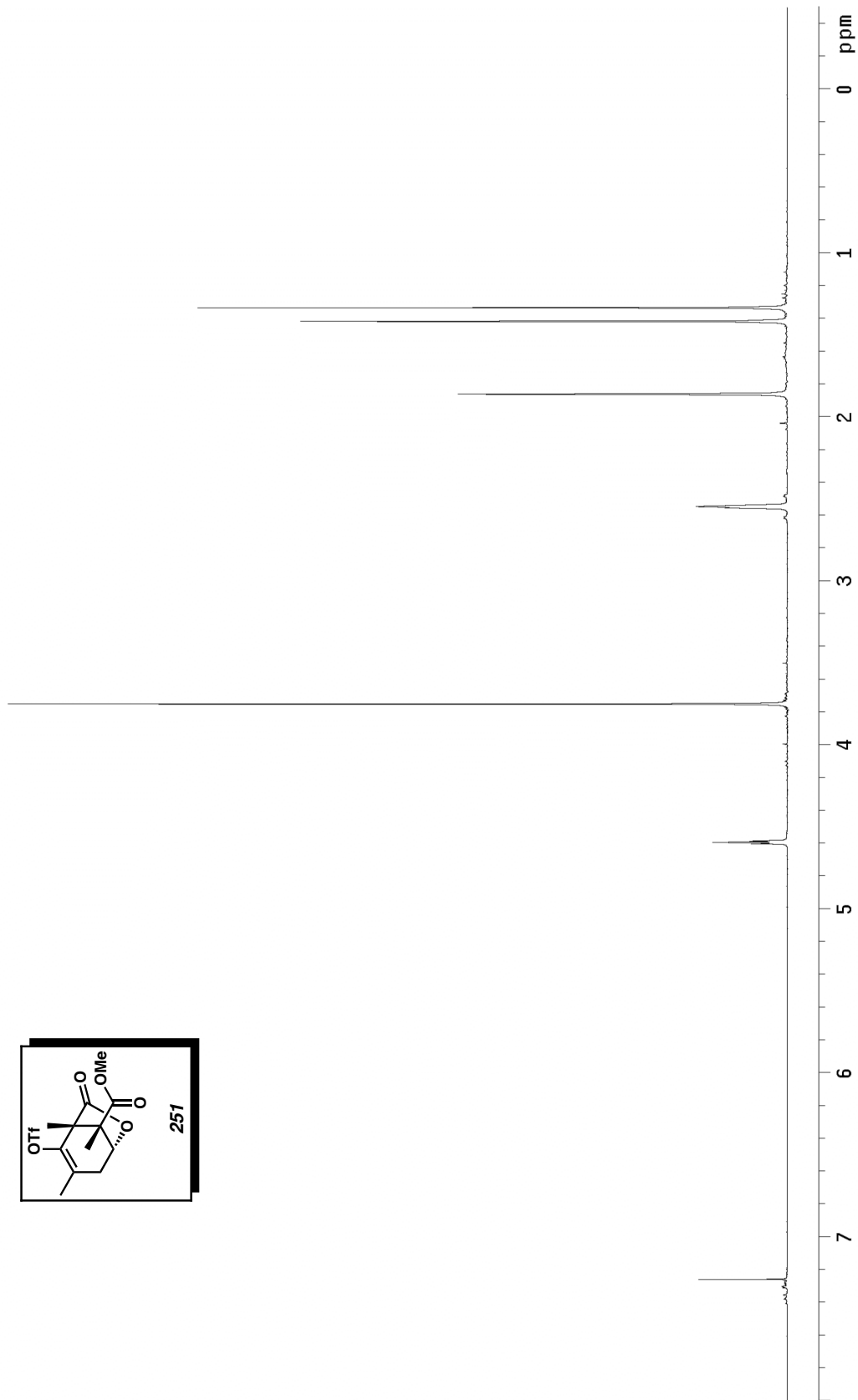
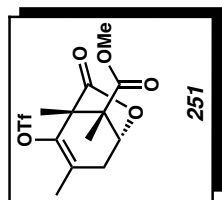


Figure B.22  $^1\text{H}$  NMR (300 MHz,  $\text{CDCl}_3$ ) of compound **251**.

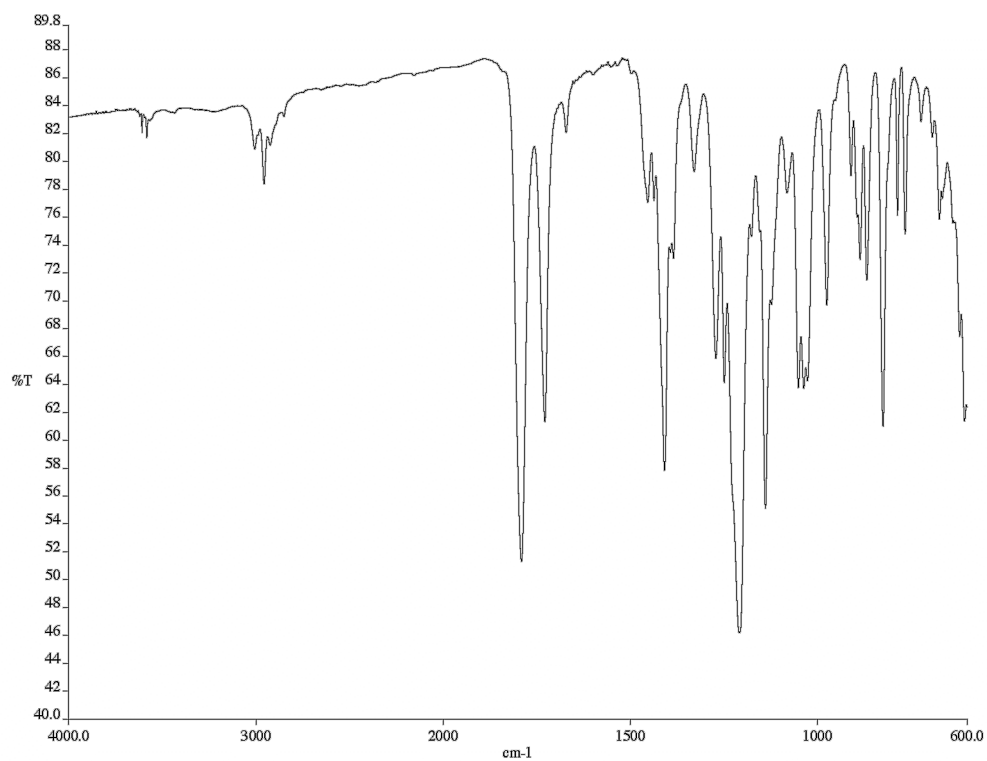


Figure B.23 Infrared spectrum (thin film/NaCl) of compound **251**.

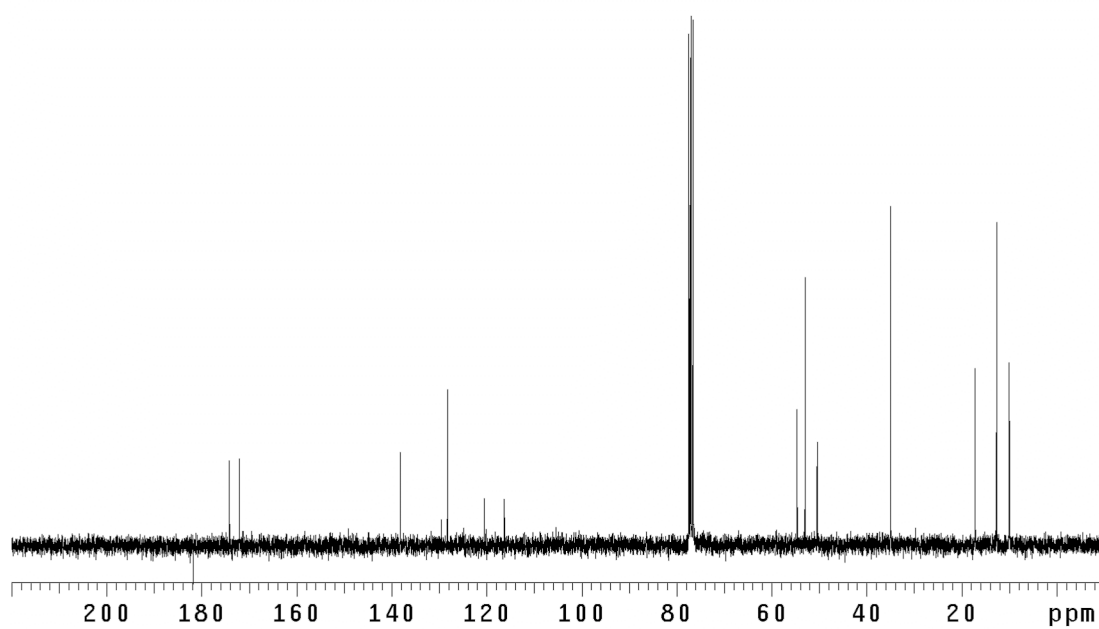


Figure B.24 <sup>13</sup>C NMR (75 MHz, CDCl<sub>3</sub>) of compound **251**.

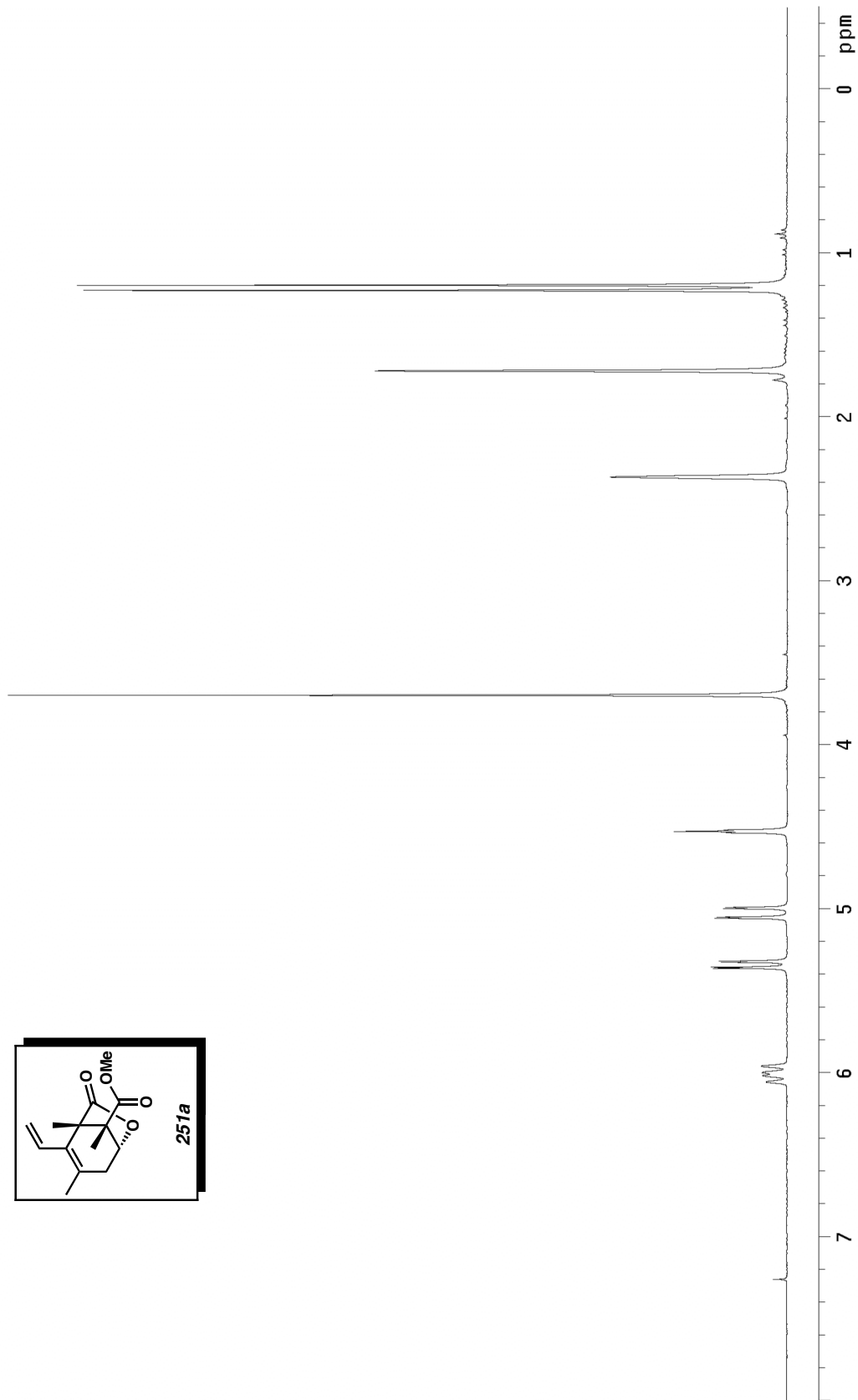
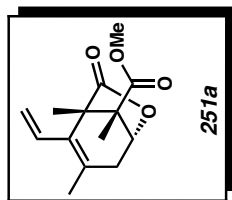


Figure B.25  $^1\text{H}$  NMR (300 MHz,  $\text{CDCl}_3$ ) of compound **251a**.

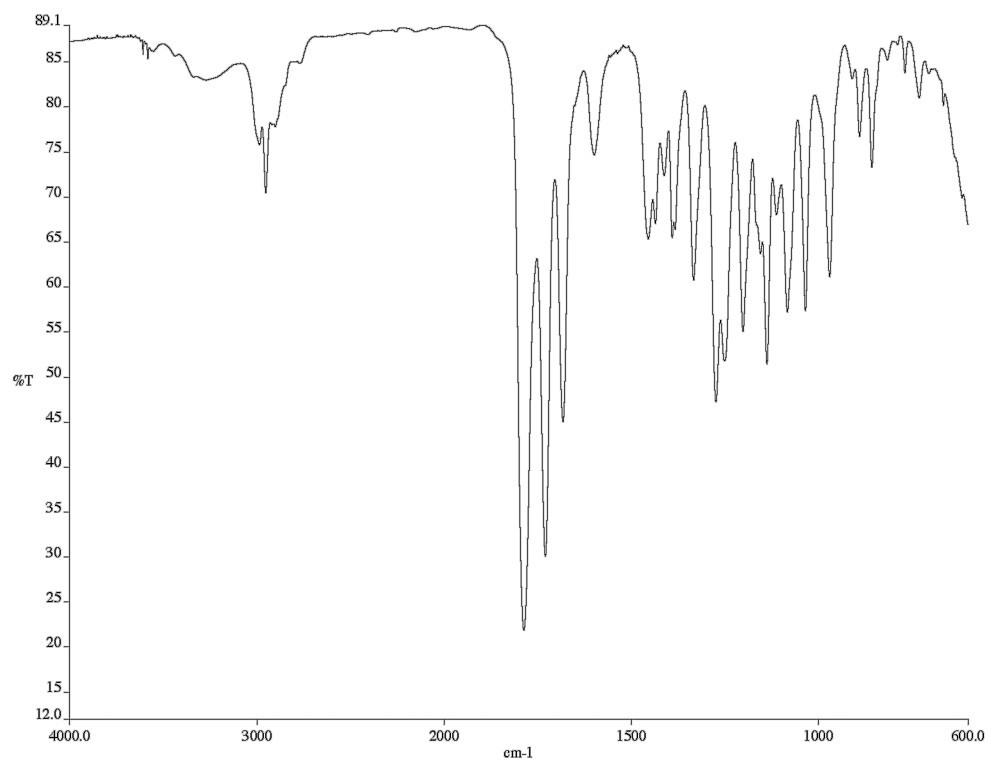


Figure B.28 Infrared spectrum (thin film/NaCl) of compound **252**.

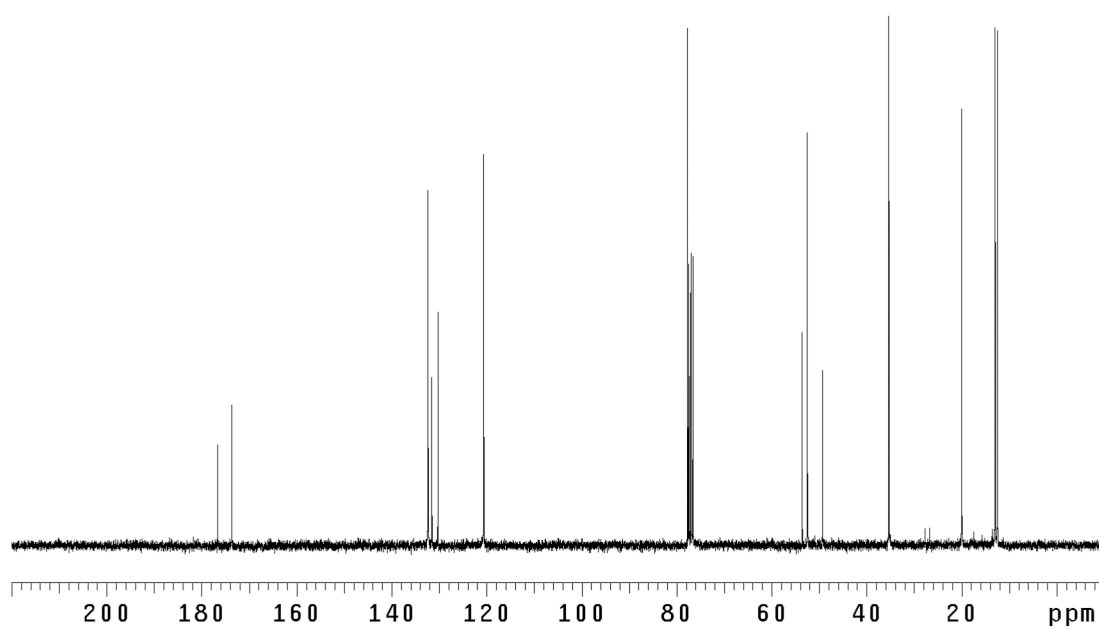


Figure B.29 <sup>13</sup>C NMR (75 MHz, CDCl<sub>3</sub>) of compound **252**.

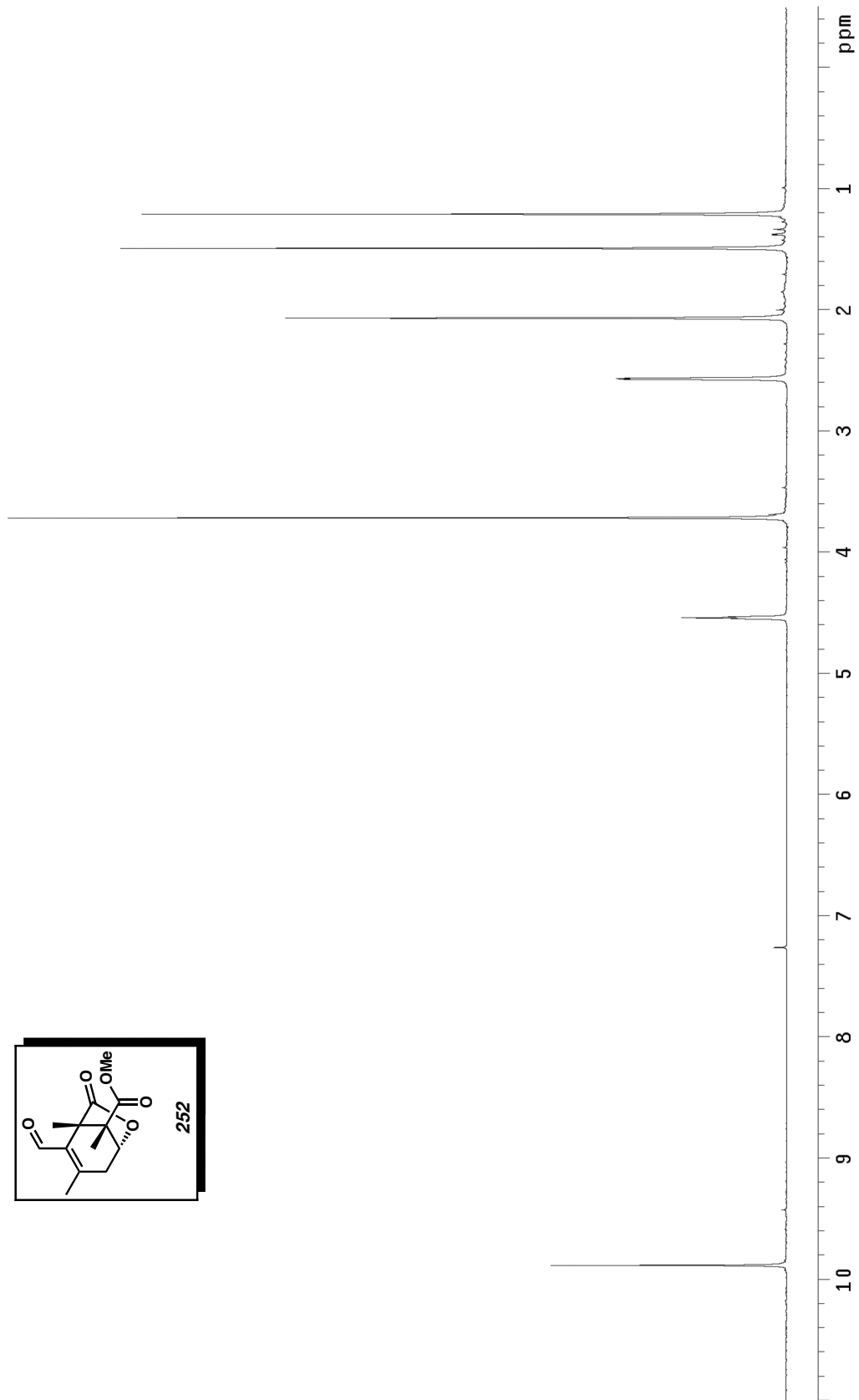
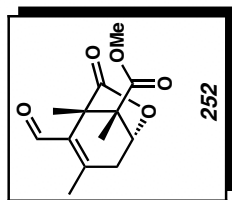


Figure B.28  $^1\text{H}$  NMR (300 MHz,  $\text{CDCl}_3$ ) of compound **252**.

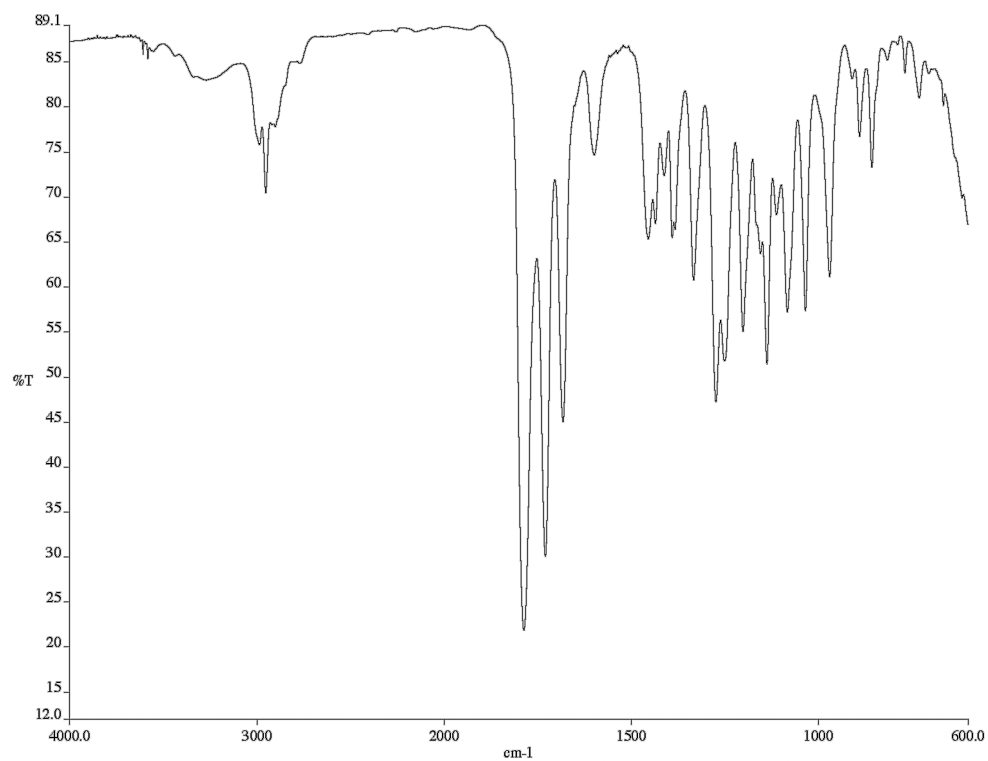


Figure B.29 Infrared spectrum (thin film/NaCl) of compound **252**.

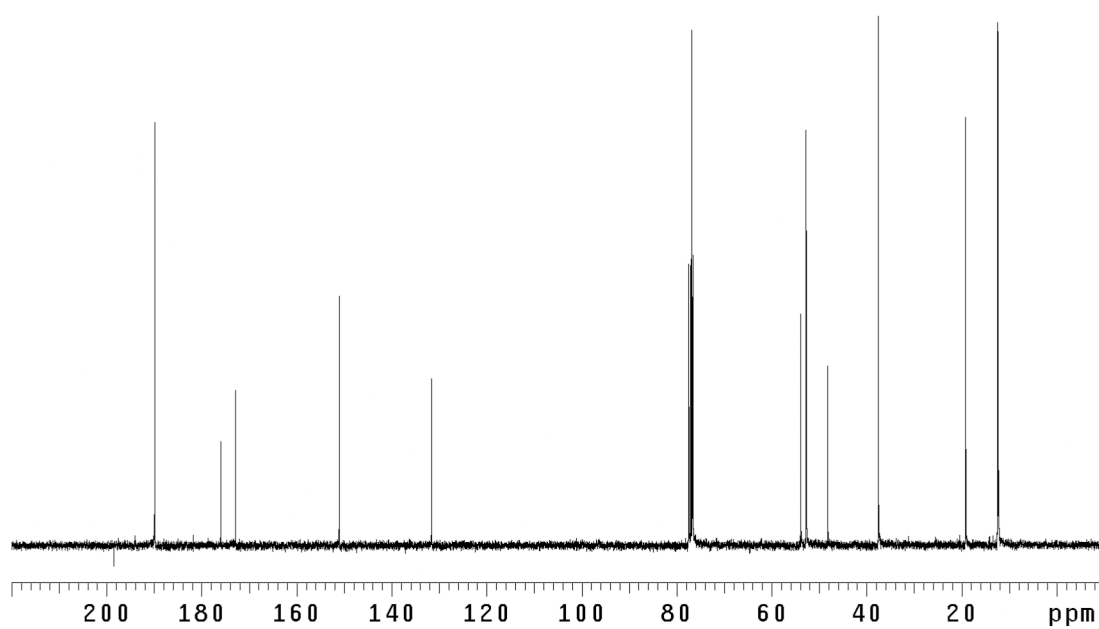


Figure B.30 <sup>13</sup>C NMR (75 MHz, CDCl<sub>3</sub>) of compound **252**.

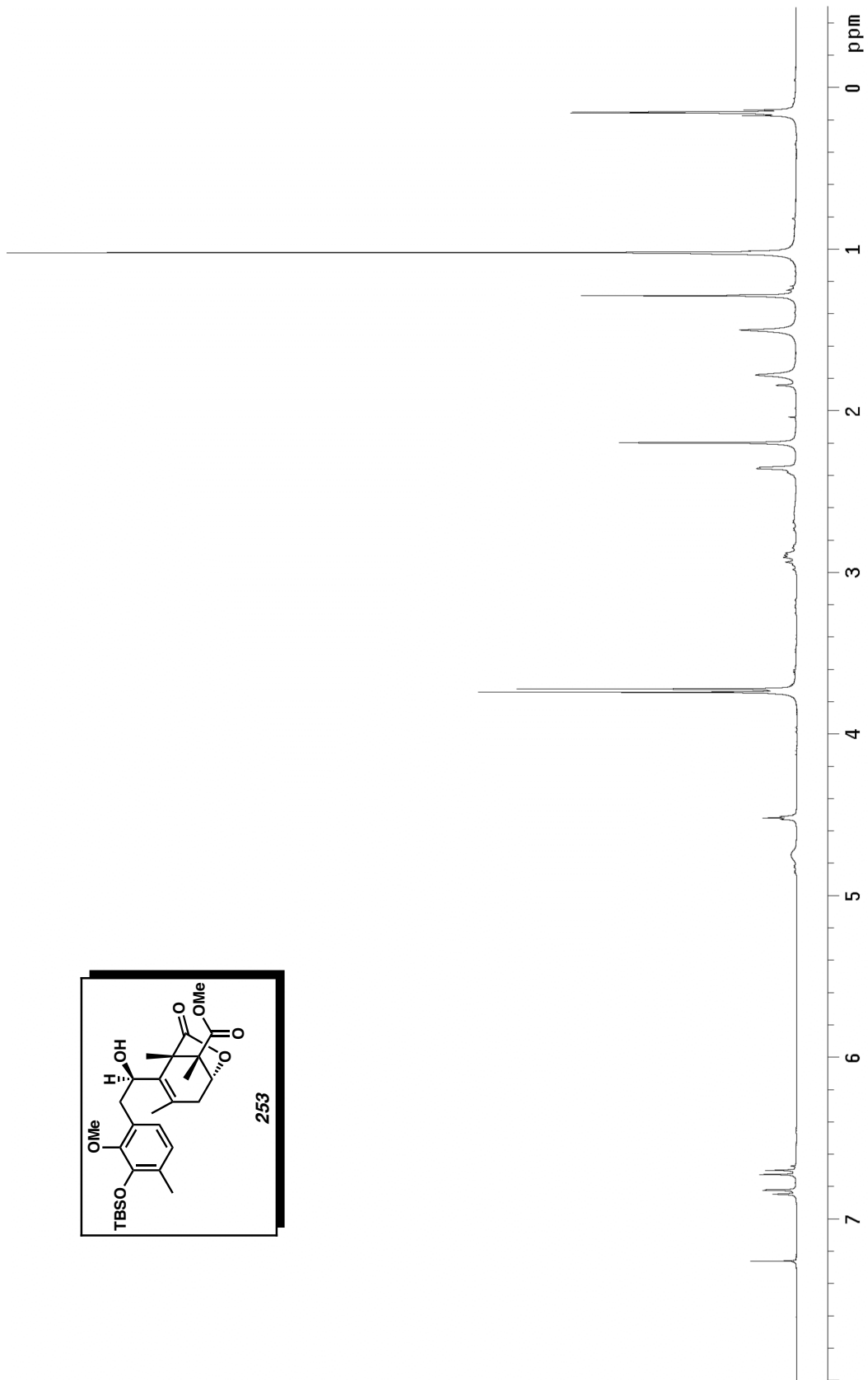
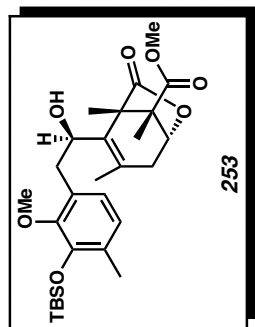


Figure B.31  $^1\text{H NMR}$  (300 MHz,  $\text{CDCl}_3$ ) of compound **253**.

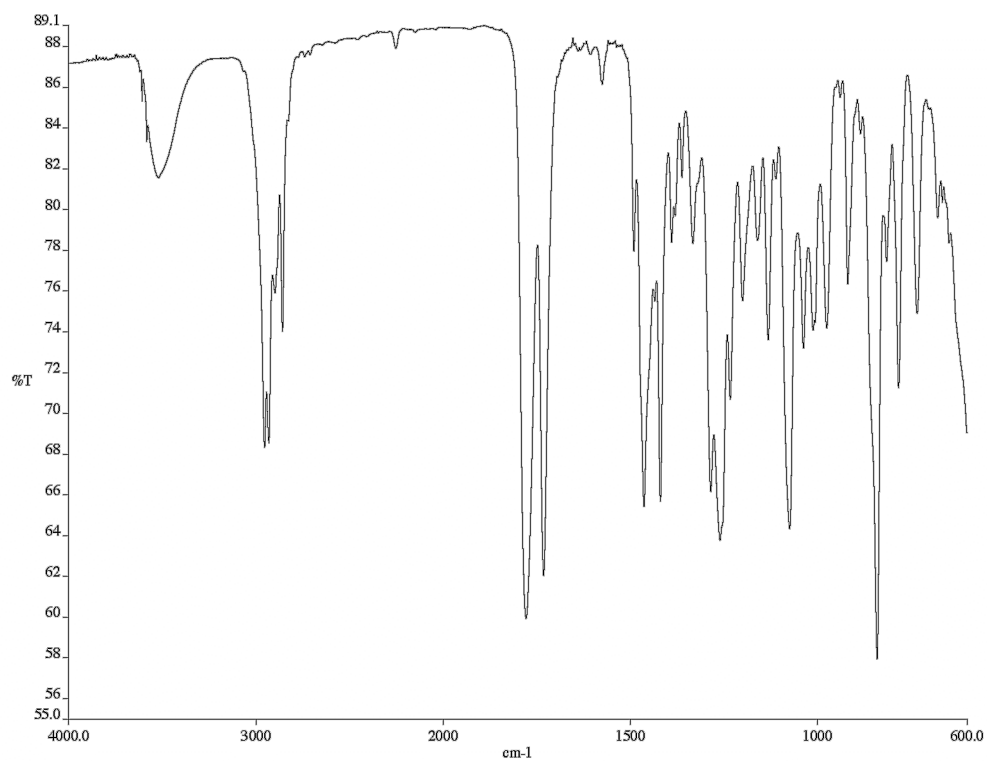


Figure B.32 Infrared spectrum (thin film/NaCl) of compound **253**.

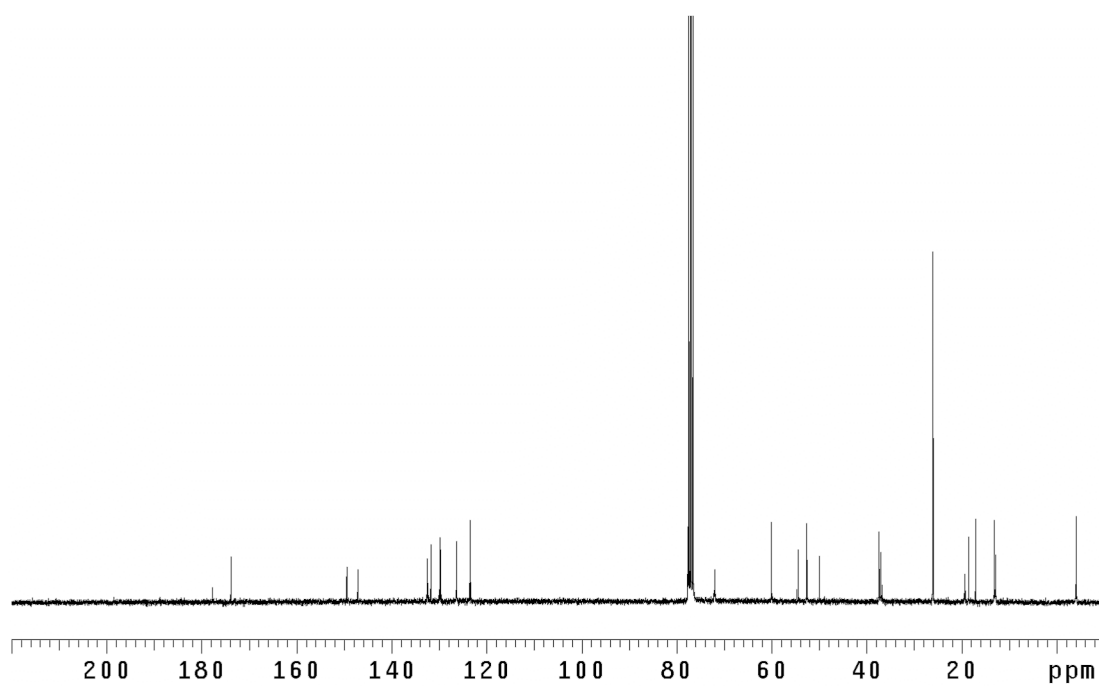


Figure B.33 <sup>13</sup>C NMR (75 MHz, CDCl<sub>3</sub>) of compound **253**.

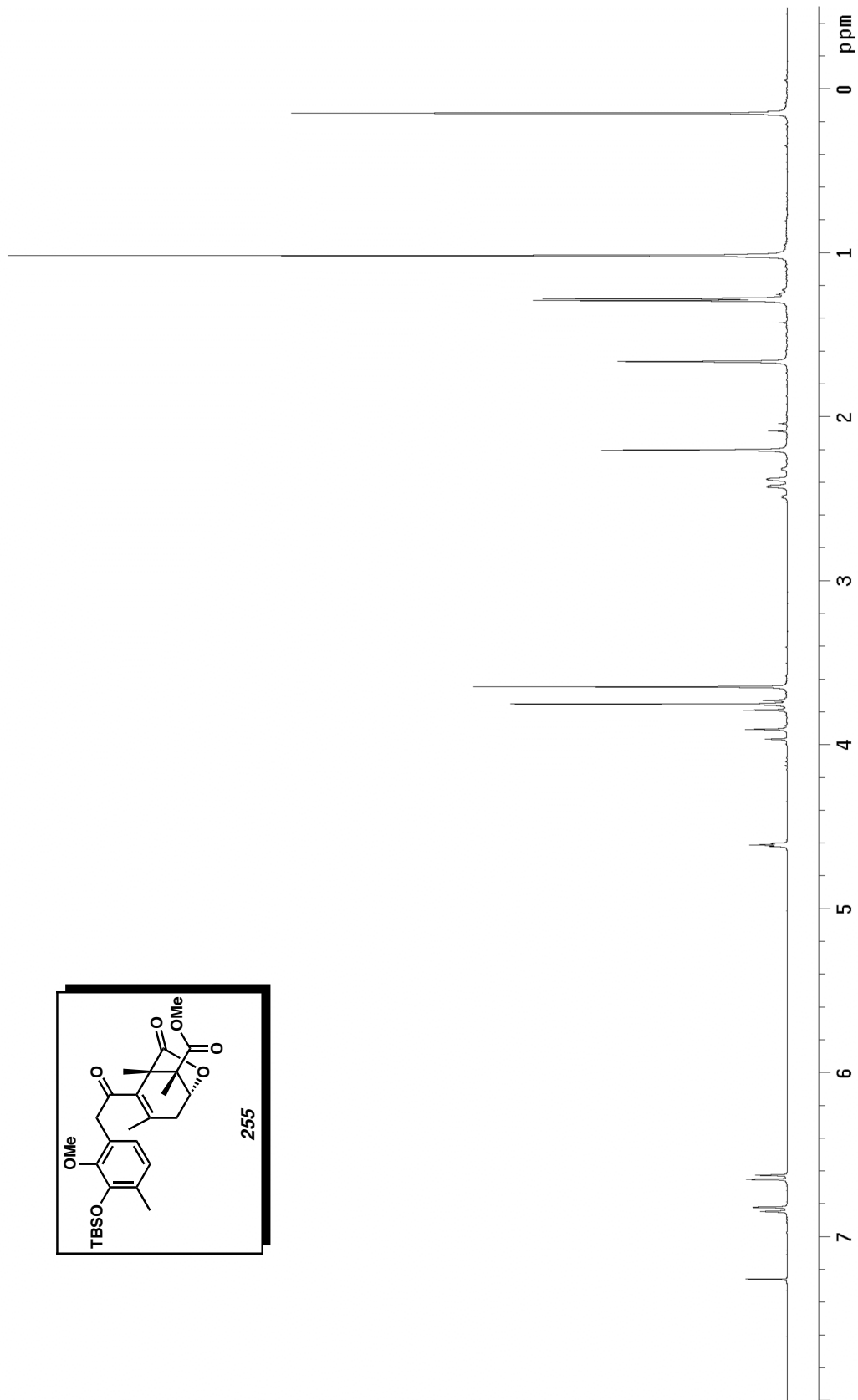
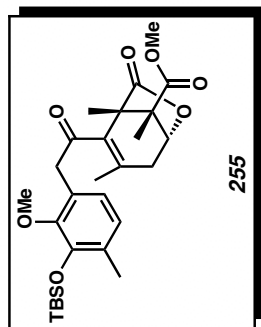


Figure B.34  $^1\text{H}$  NMR (300 MHz,  $\text{CDCl}_3$ ) of compound 255.

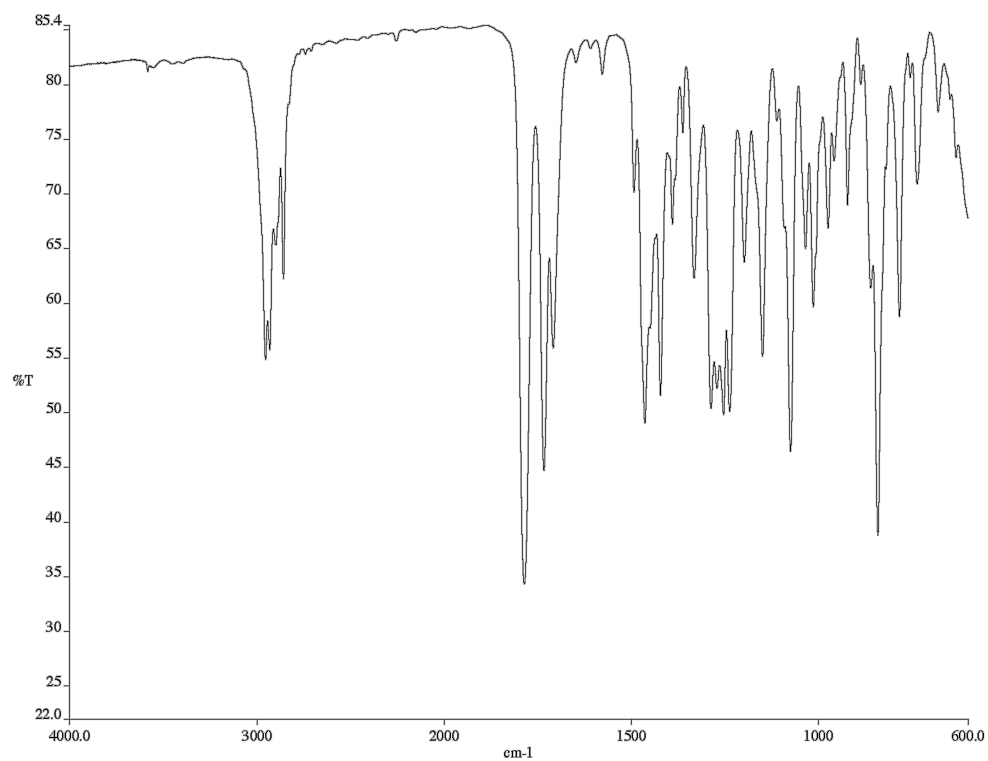


Figure B.35 Infrared spectrum (thin film/NaCl) of compound **255**.

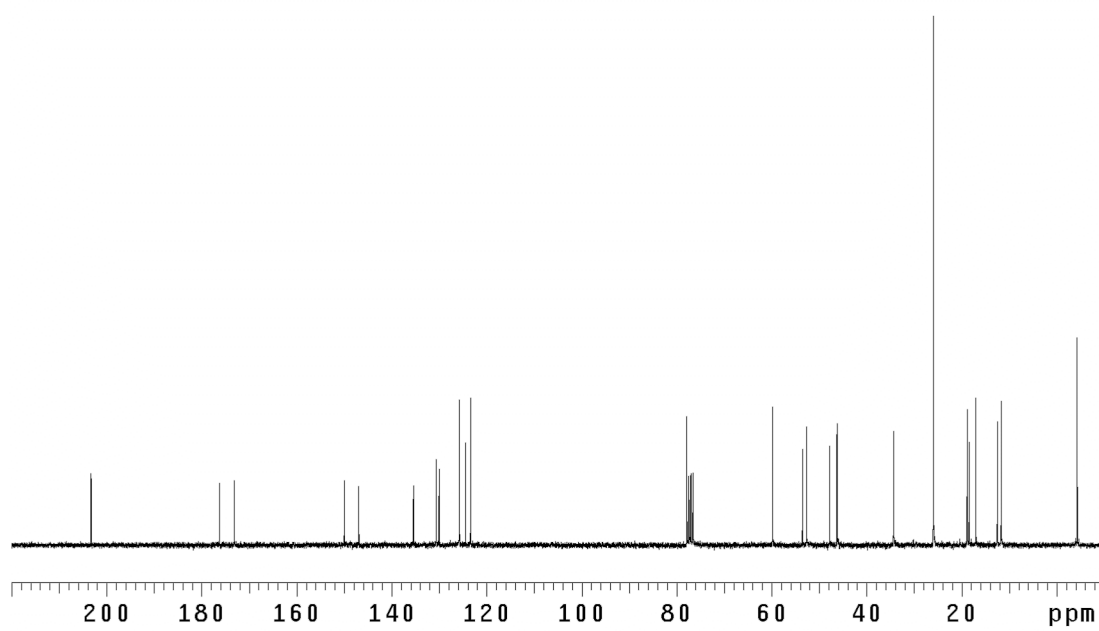


Figure B.36 <sup>13</sup>C NMR (75 MHz, 255) of compound **255**.

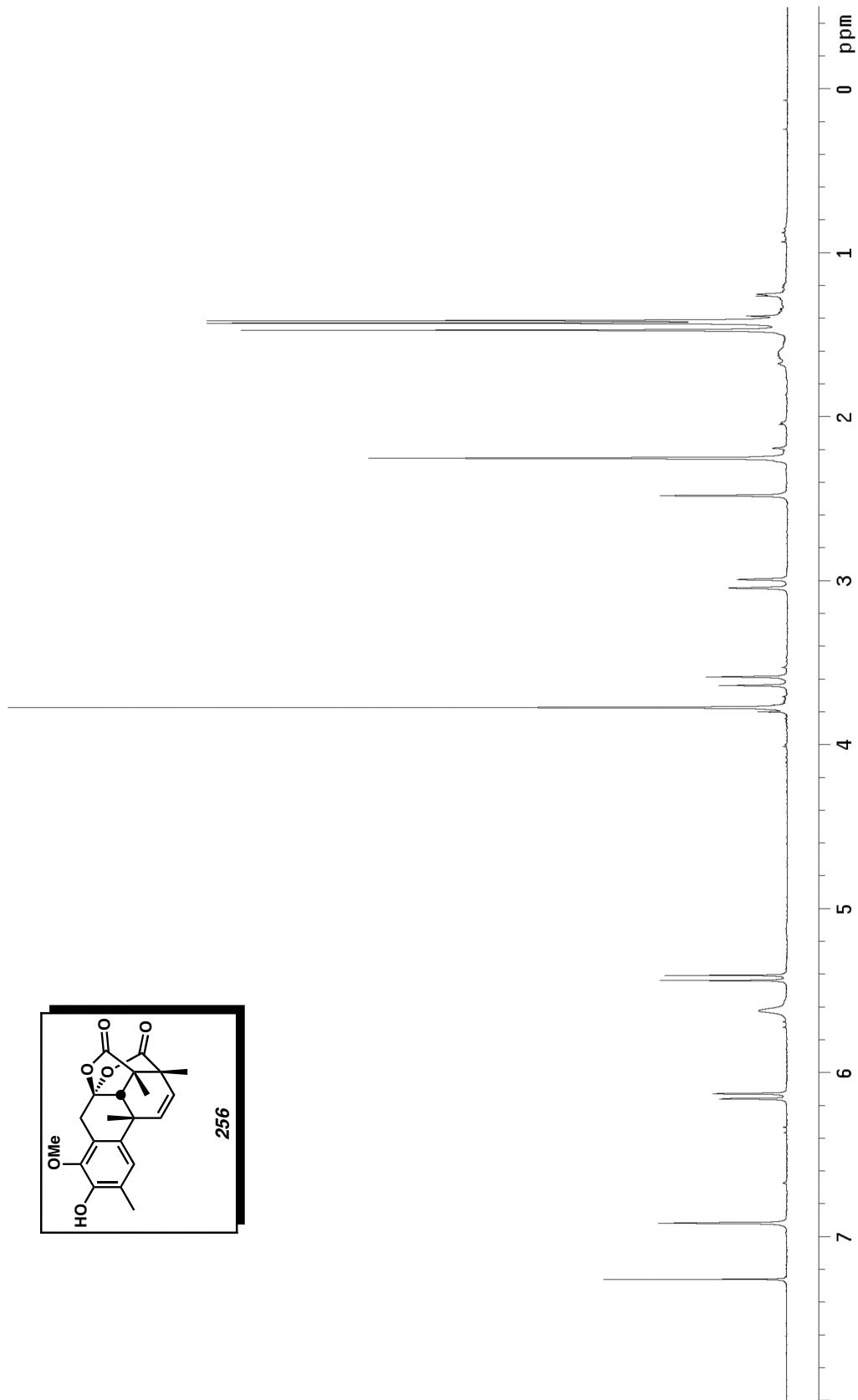
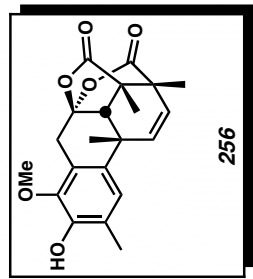


Figure B.37  $^1\text{H}$  NMR (500 MHz,  $\text{CDCl}_3$ ) of compound **256**.

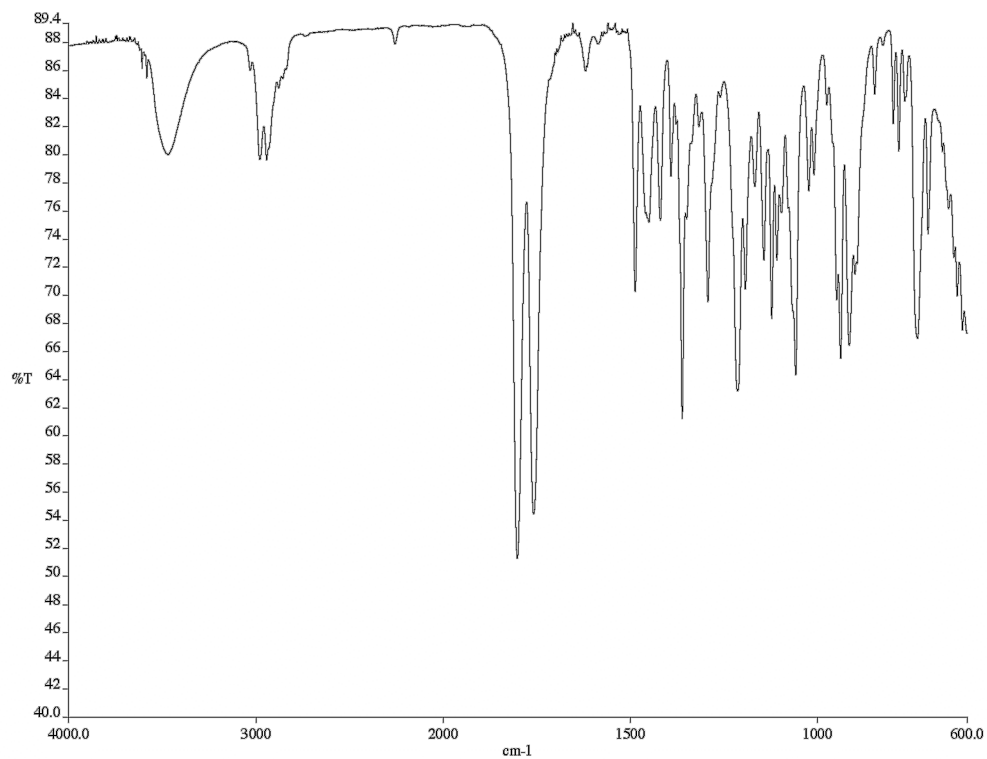


Figure B.38 Infrared spectrum (thin film/NaCl) of compound **256**.

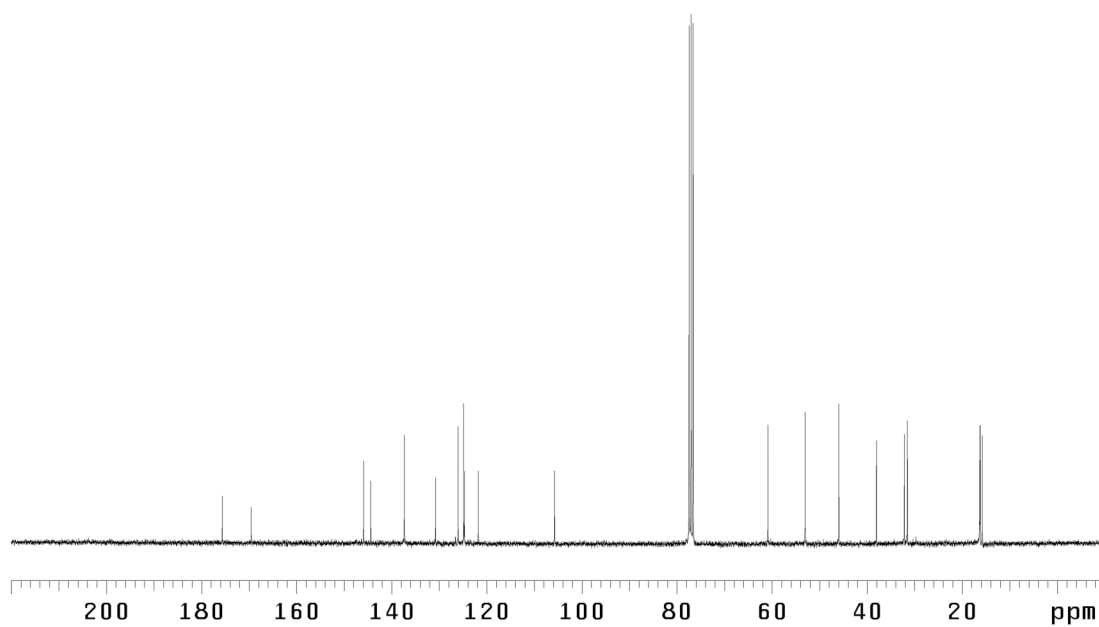


Figure B.39 <sup>13</sup>C NMR (75 MHz, CDCl<sub>3</sub>) of compound **256**.

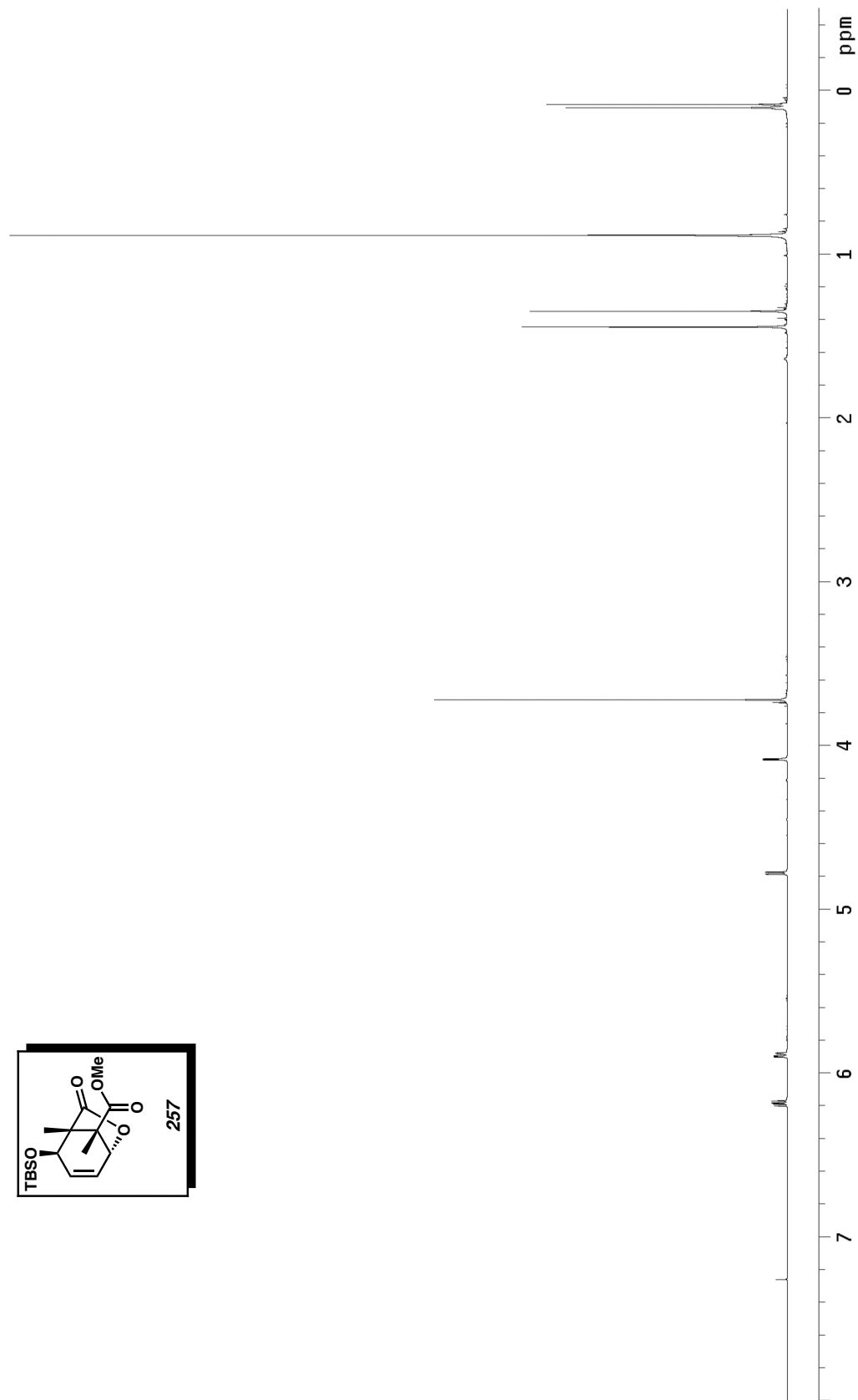
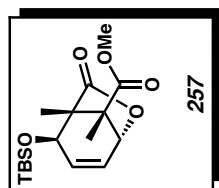


Figure B.40  $^1\text{H}$  NMR (500 MHz,  $\text{CDCl}_3$ ) of compound **257**. 275

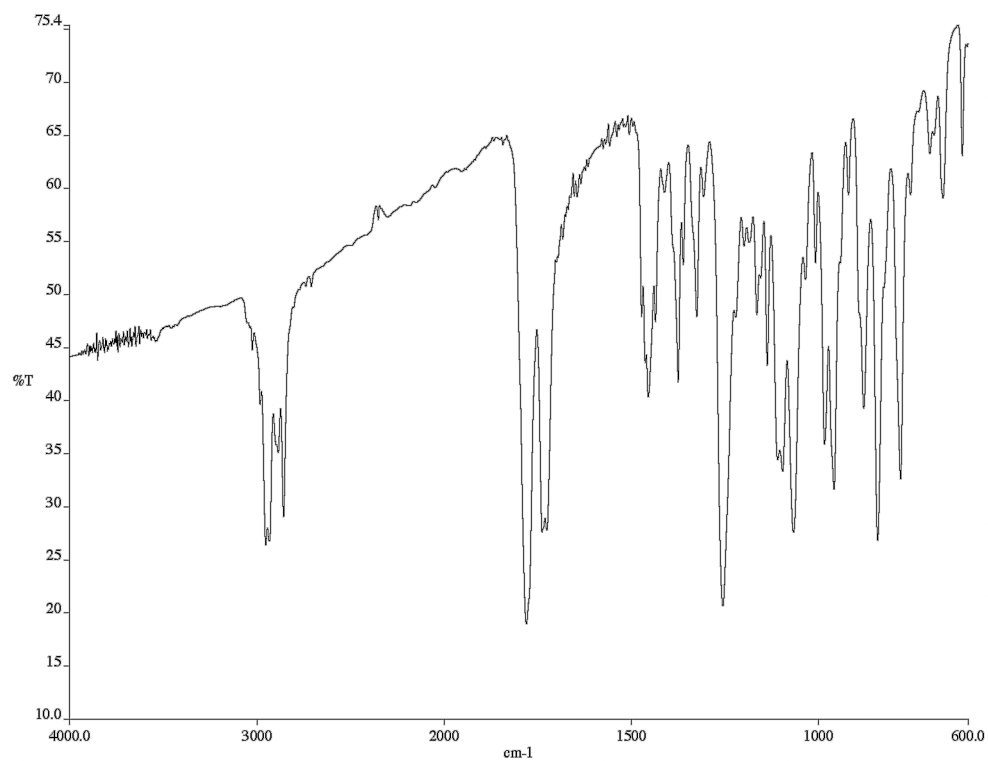


Figure B.41 Infrared spectrum (thin film/NaCl) of compound **257**.

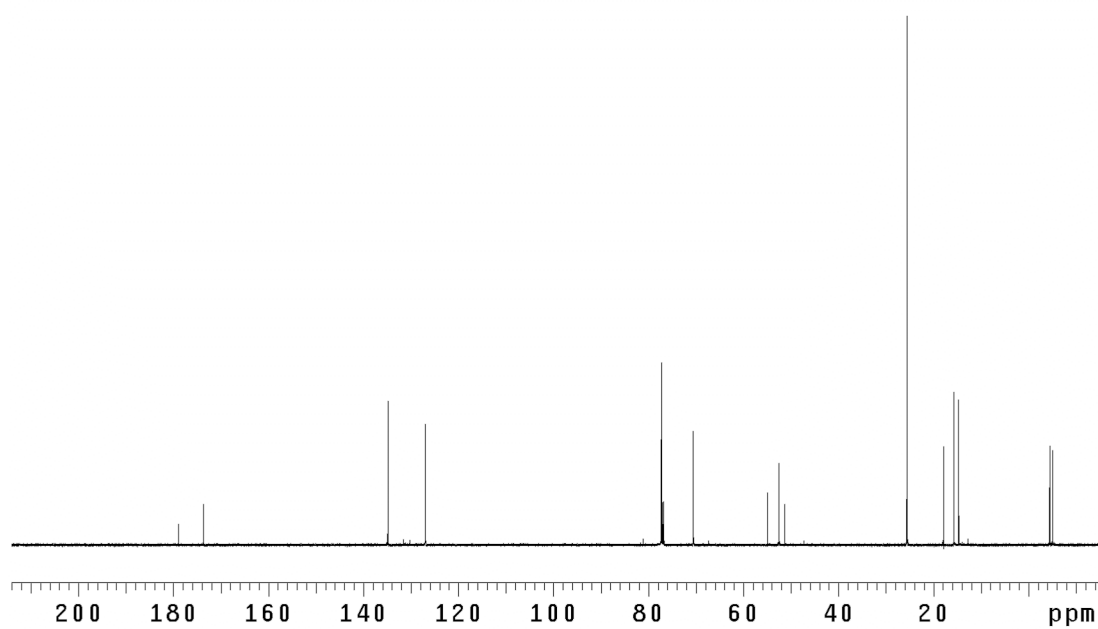


Figure B.42 <sup>13</sup>C NMR (125 MHz, CDCl<sub>3</sub>) of compound **257**.

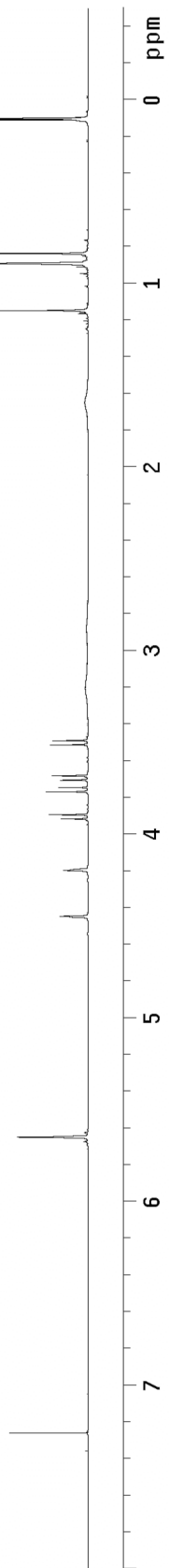
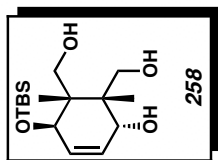


Figure B.43  $^1\text{H}$  NMR (300 MHz,  $\text{CDCl}_3$ ) of compound 258.

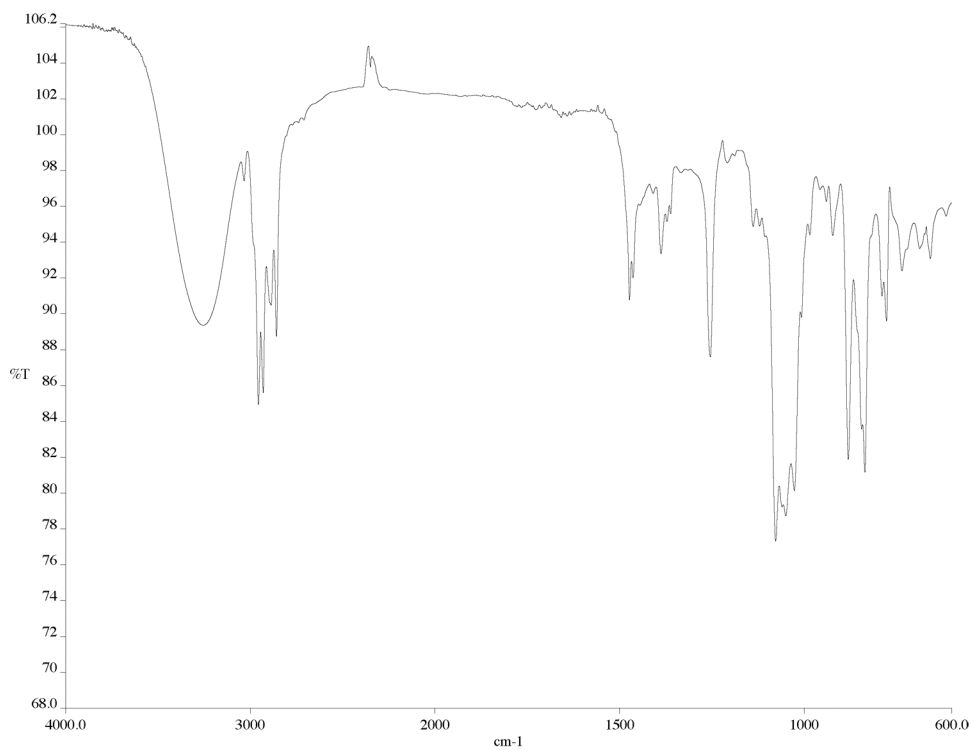


Figure B.44 Infrared spectrum (thin film/NaCl) of compound **258**.

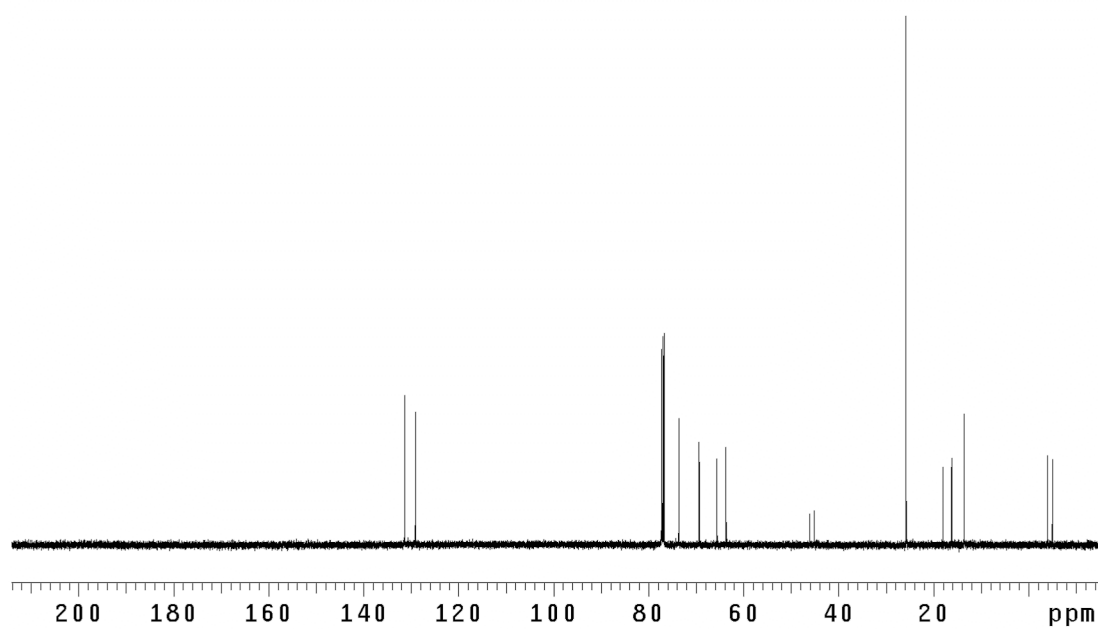


Figure B.45  $^{13}\text{C}$  NMR (125 MHz,  $\text{CDCl}_3$ ) of compound **258**.

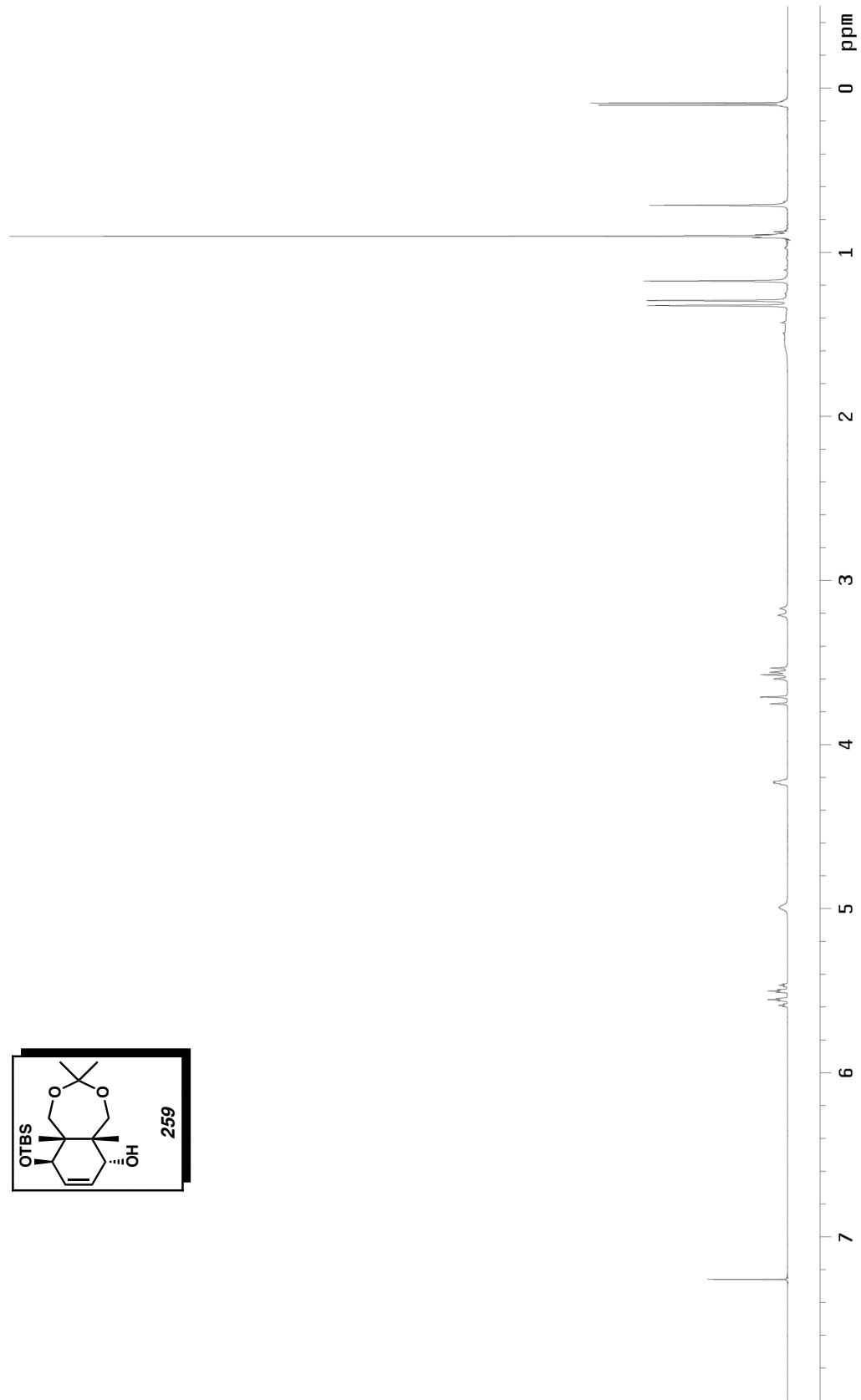
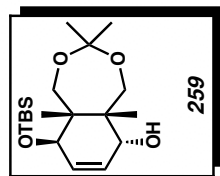


Figure B.46  $^1\text{H}$  NMR (300 MHz,  $\text{CDCl}_3$ ) of compound **259**.

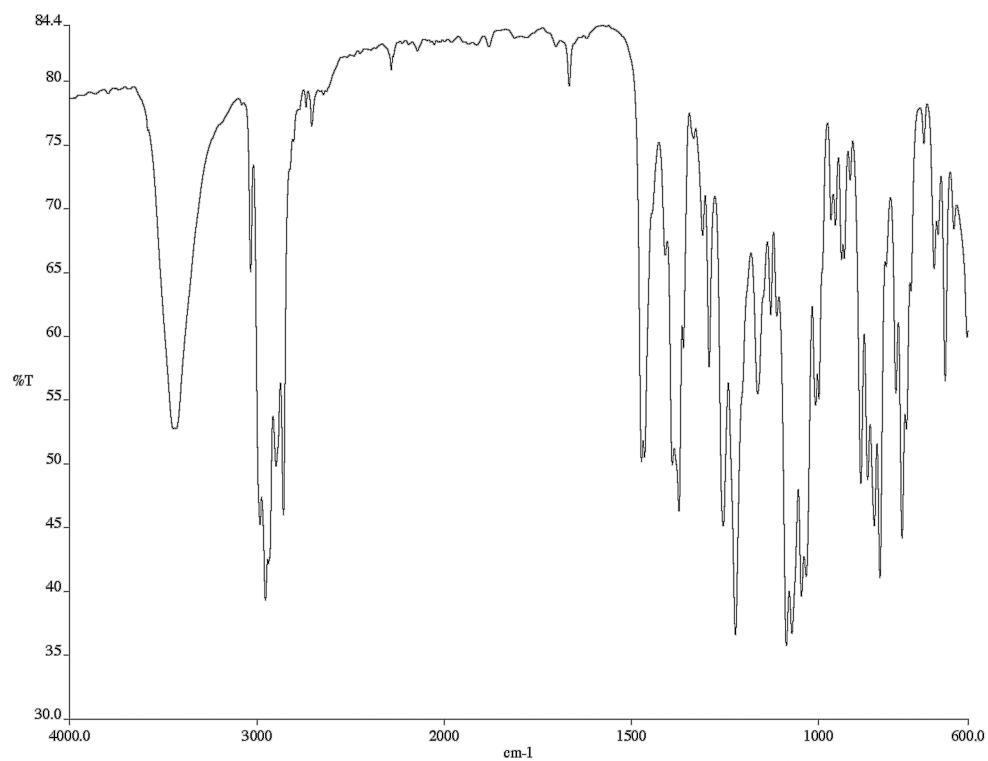


Figure B.47 Infrared spectrum (thin film/NaCl) of compound **259**.

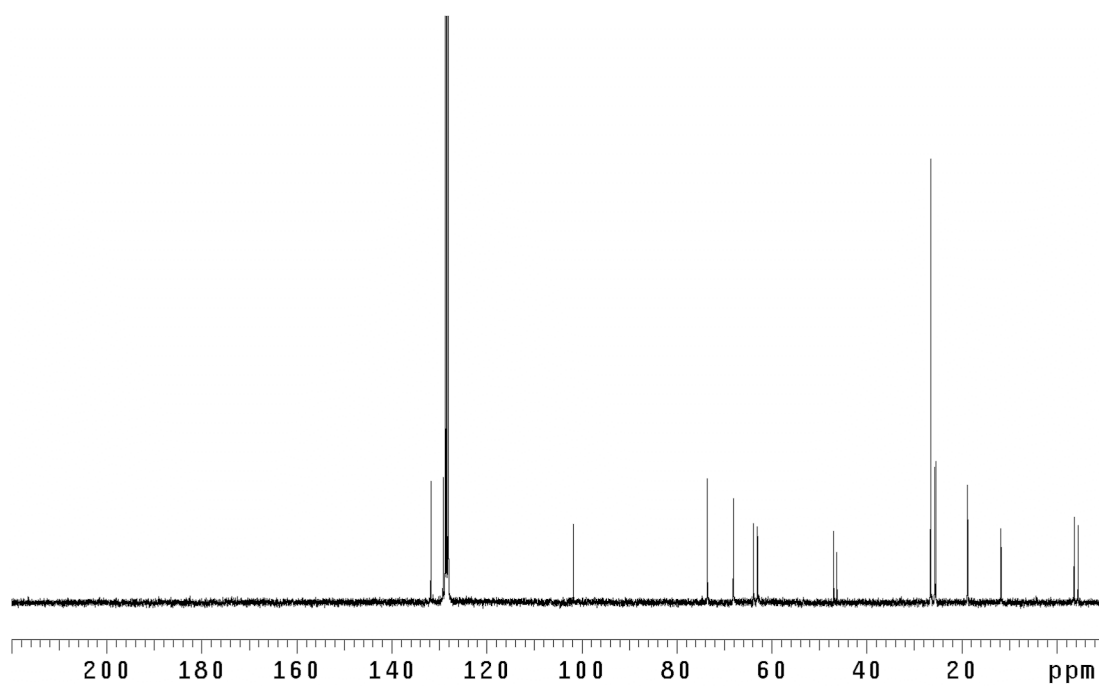


Figure B.48 <sup>13</sup>C NMR (75 MHz, CDCl<sub>3</sub>) of compound **259**.

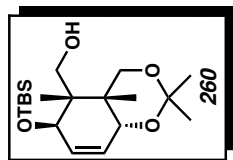


Figure B.49  $^1\text{H}$  NMR (300 MHz,  $\text{CDCl}_3$ ) of compound **260**.

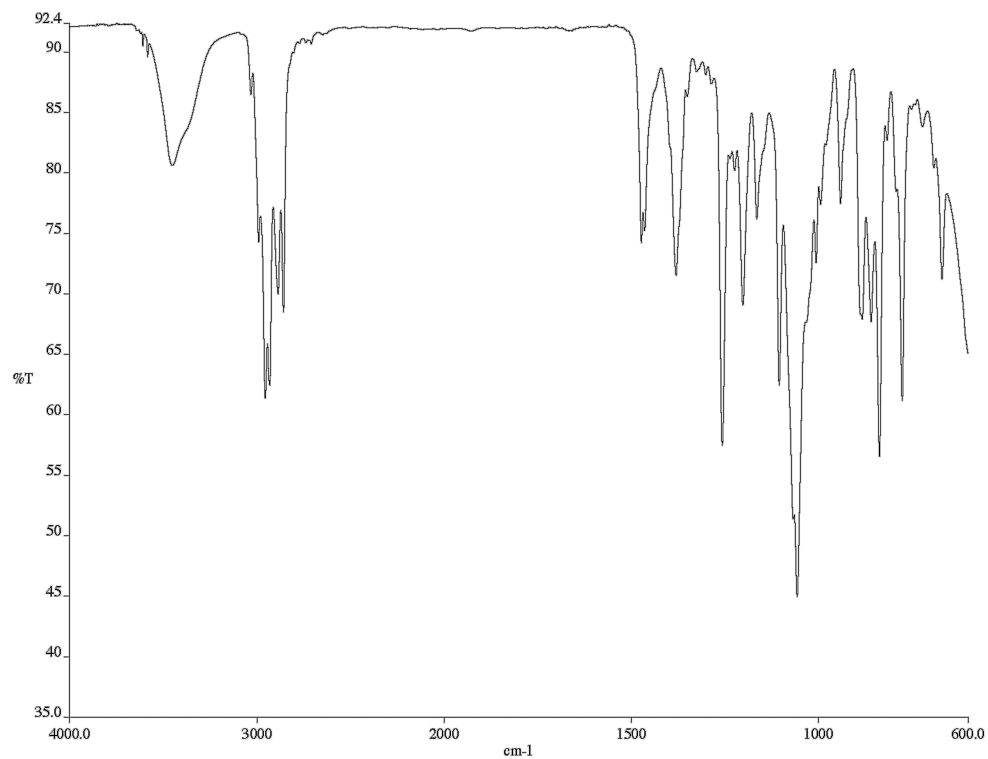


Figure B.50 Infrared spectrum (thin film/NaCl) of compound **260**.

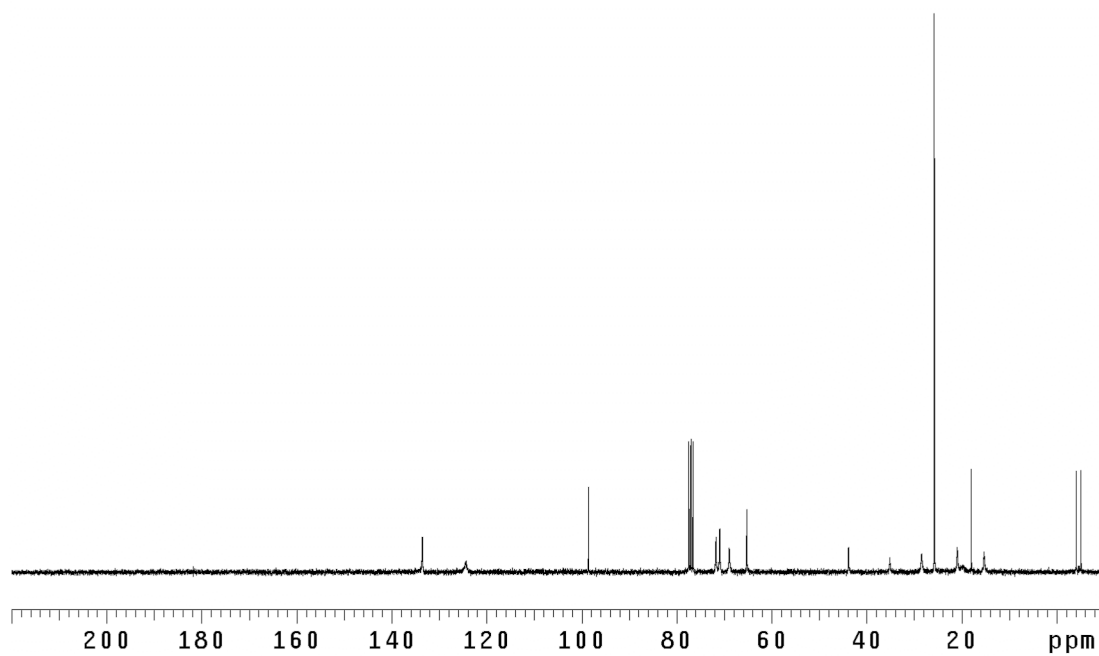


Figure B.51  $^{13}\text{C}$  NMR (75 MHz,  $\text{CDCl}_3$ ) of compound **260**.

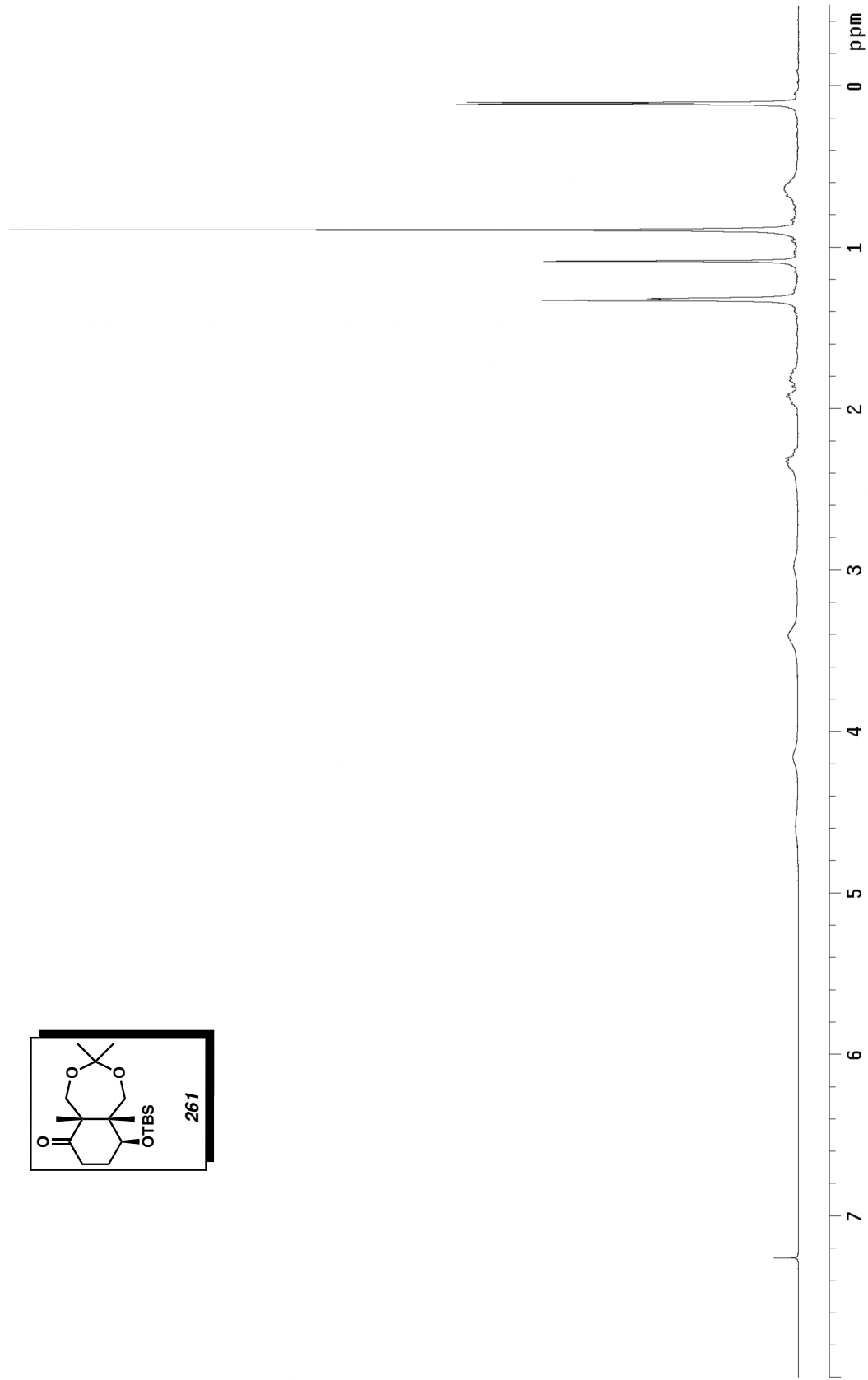
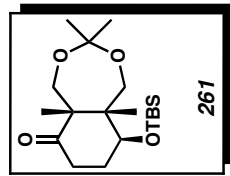


Figure B.52 <sup>1</sup>H NMR (300 MHz, CDCl<sub>3</sub>) of compound **261**.

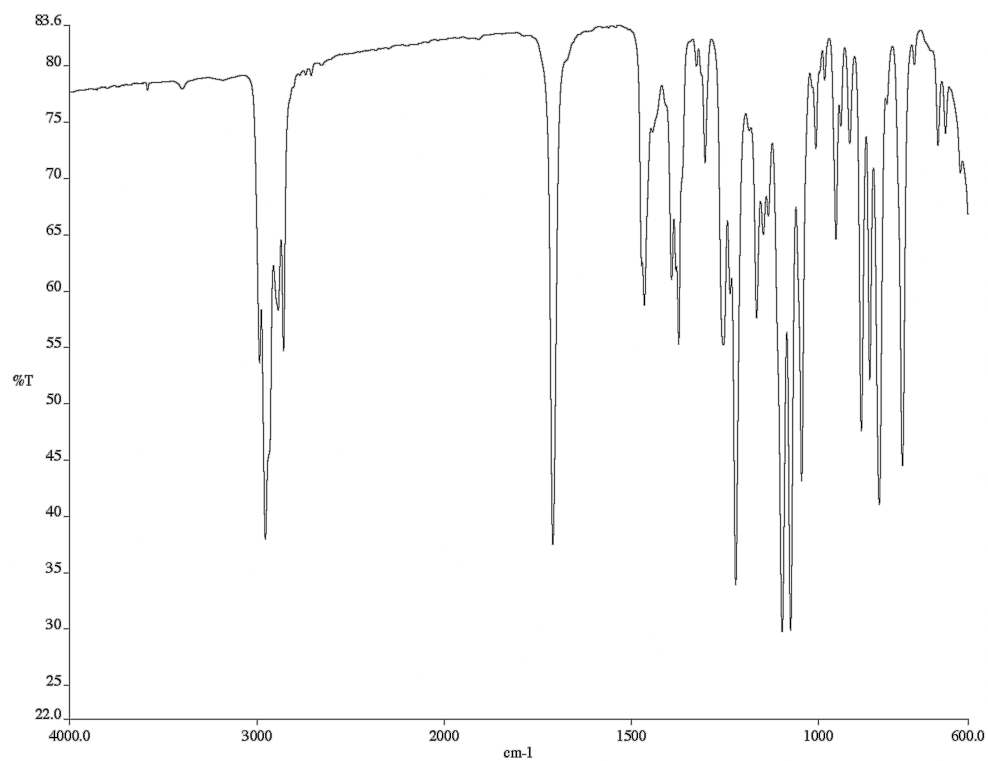


Figure B.53 Infrared spectrum (thin film/NaCl) of compound **261**.

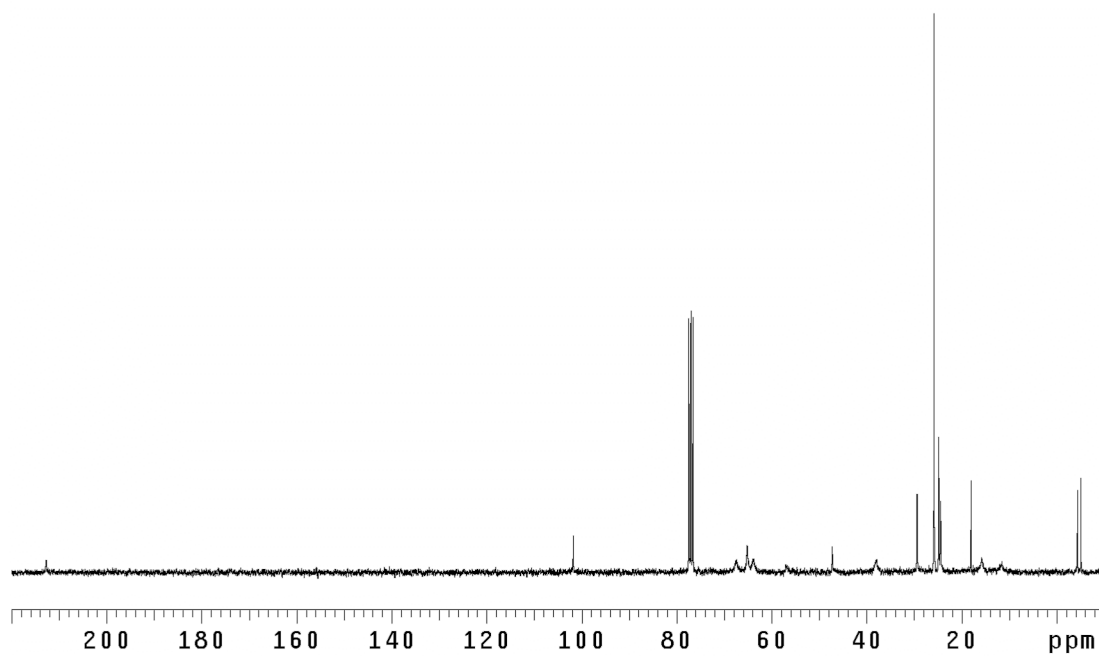


Figure B.54 <sup>13</sup>C NMR (75 MHz, CDCl<sub>3</sub>) of compound **261**.

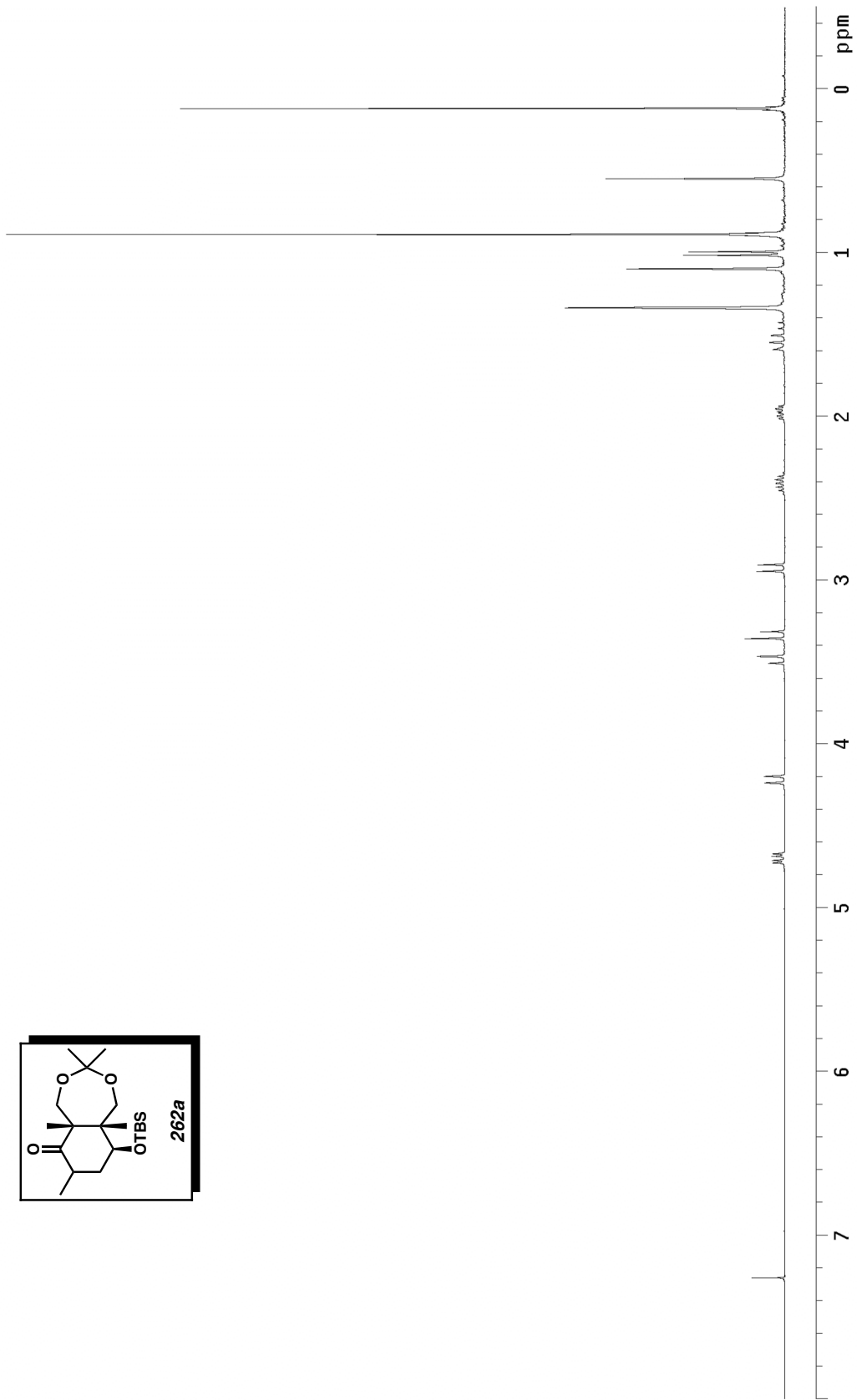
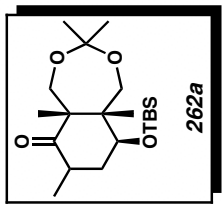


Figure B.55  $^1\text{H}$  NMR (300 MHz,  $\text{CDCl}_3$ ) of compound **262a**.

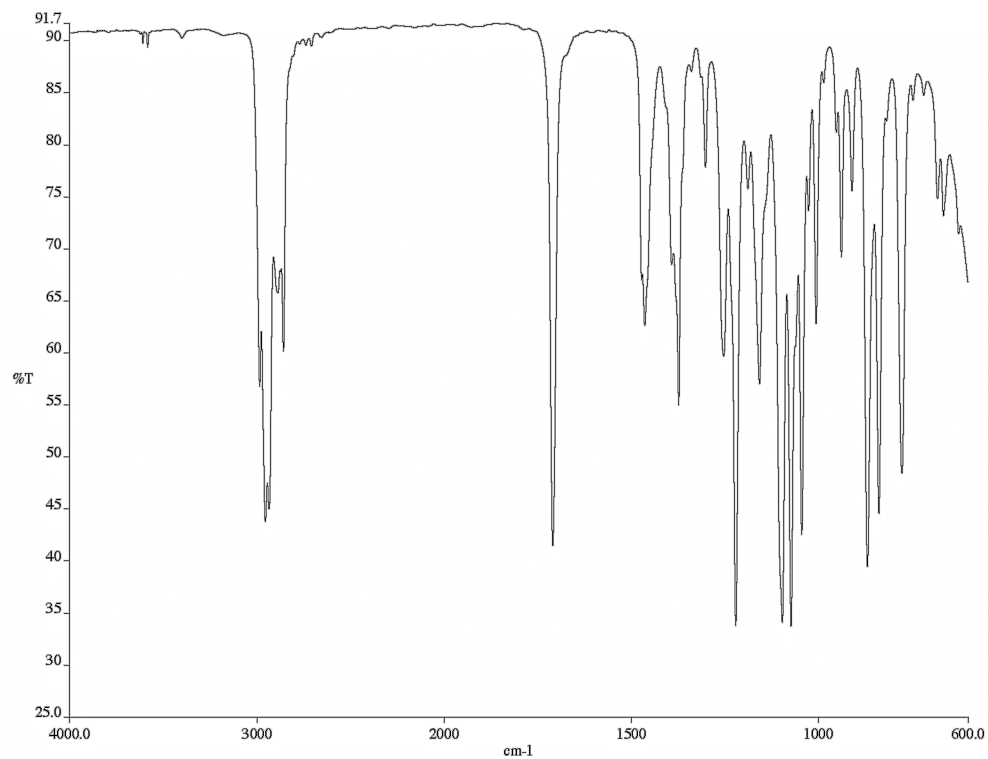


Figure B.56 Infrared spectrum (thin film/NaCl) of compound **262a**.

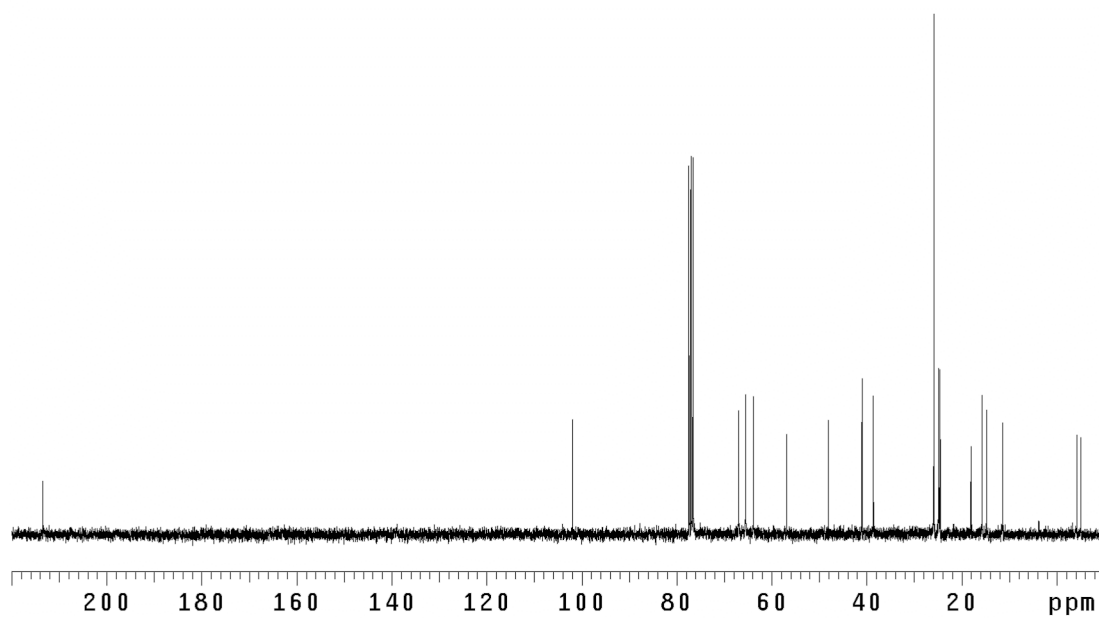


Figure B.57 <sup>13</sup>C NMR (75 MHz, CDCl<sub>3</sub>) of compound **262a**.

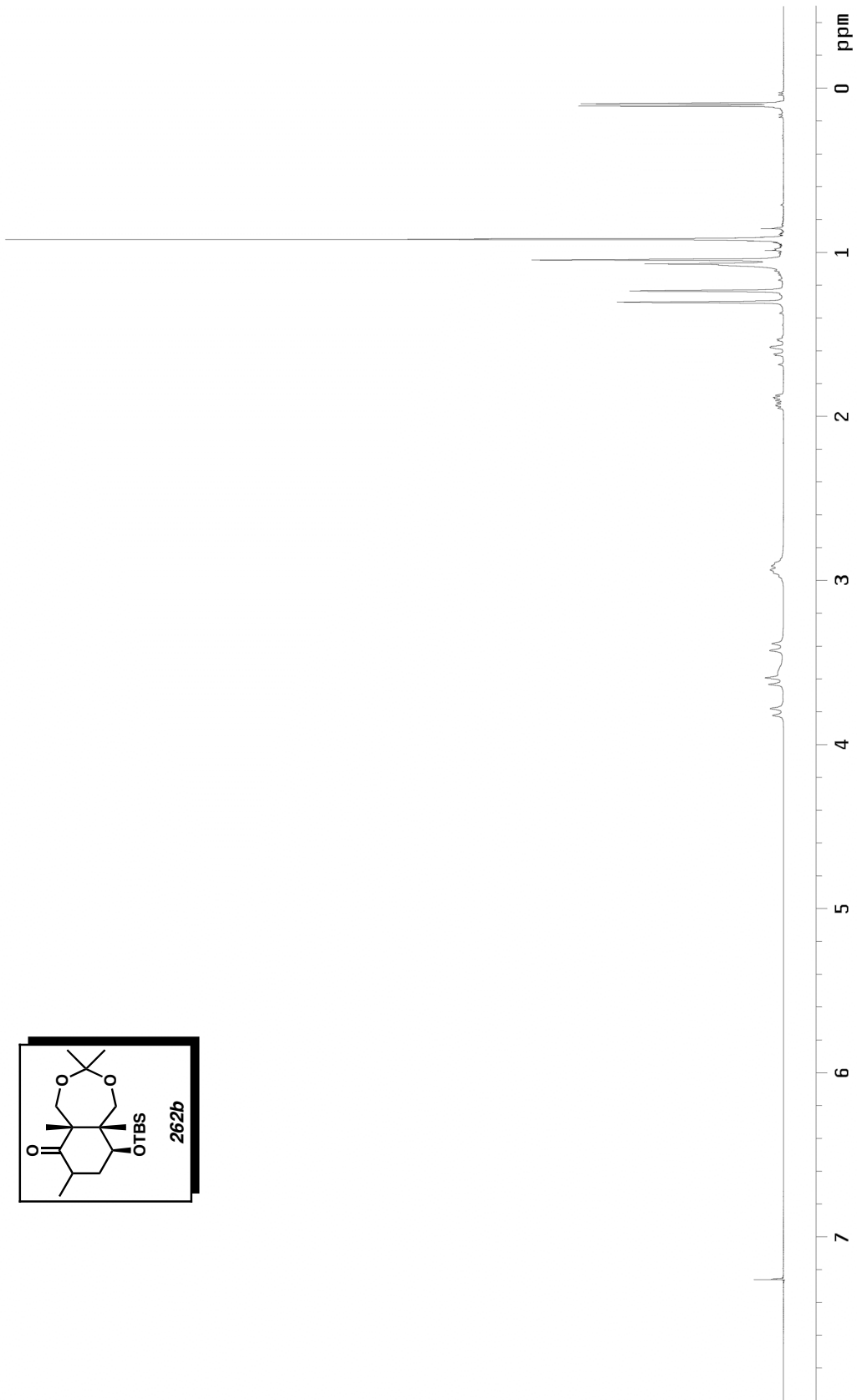
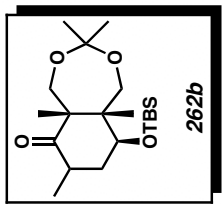


Figure B.58  $^1\text{H}$  NMR (300 MHz,  $\text{CDCl}_3$ ) of compound **262b**.

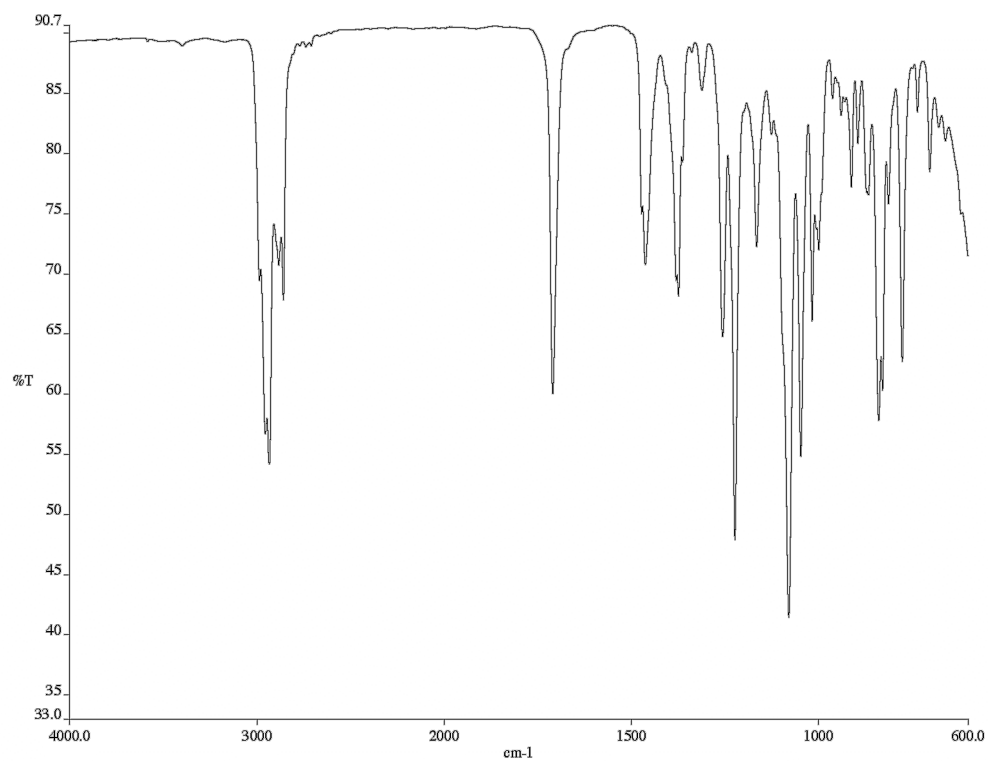


Figure B.59 Infrared spectrum (thin film/NaCl) of compound **262b**.

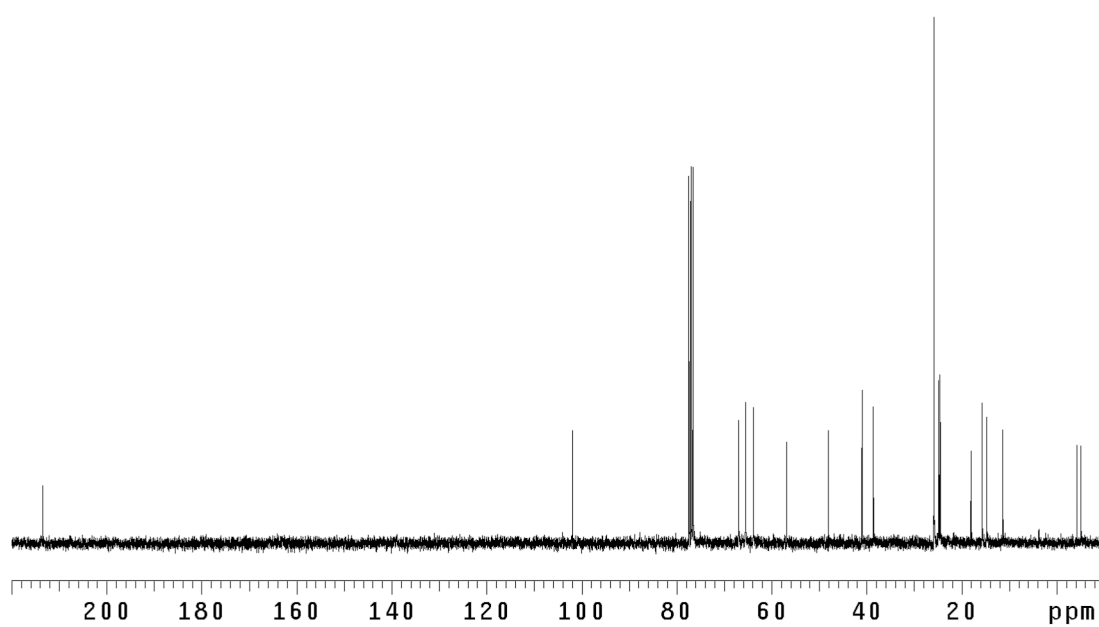


Figure B.60 <sup>13</sup>C NMR (75 MHz, CDCl<sub>3</sub>) of compound **262b**.

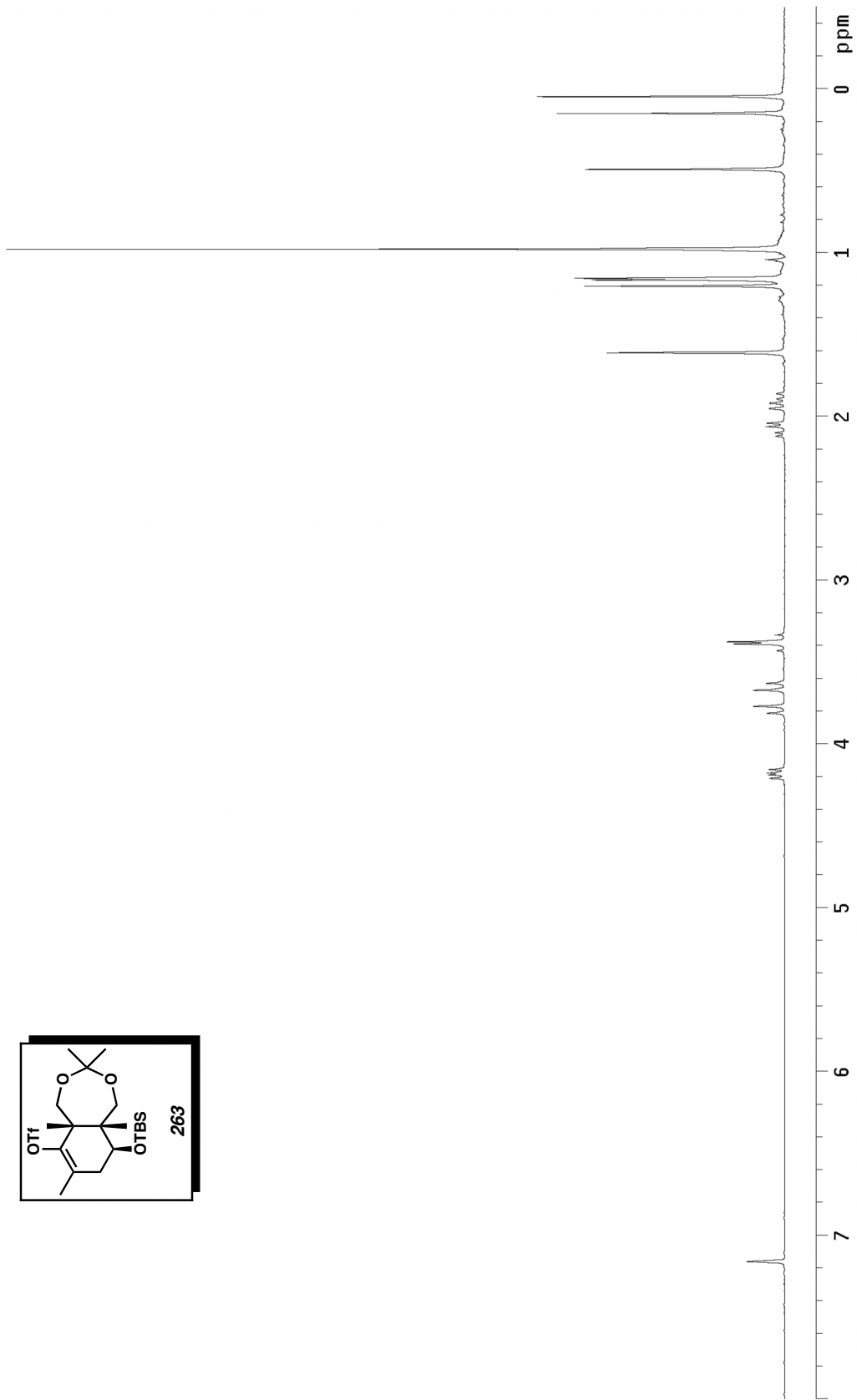
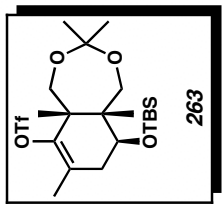


Figure B.61  $^1\text{H}$  NMR (300 MHz,  $\text{C}_6\text{D}_6$ ) of compound **263**.

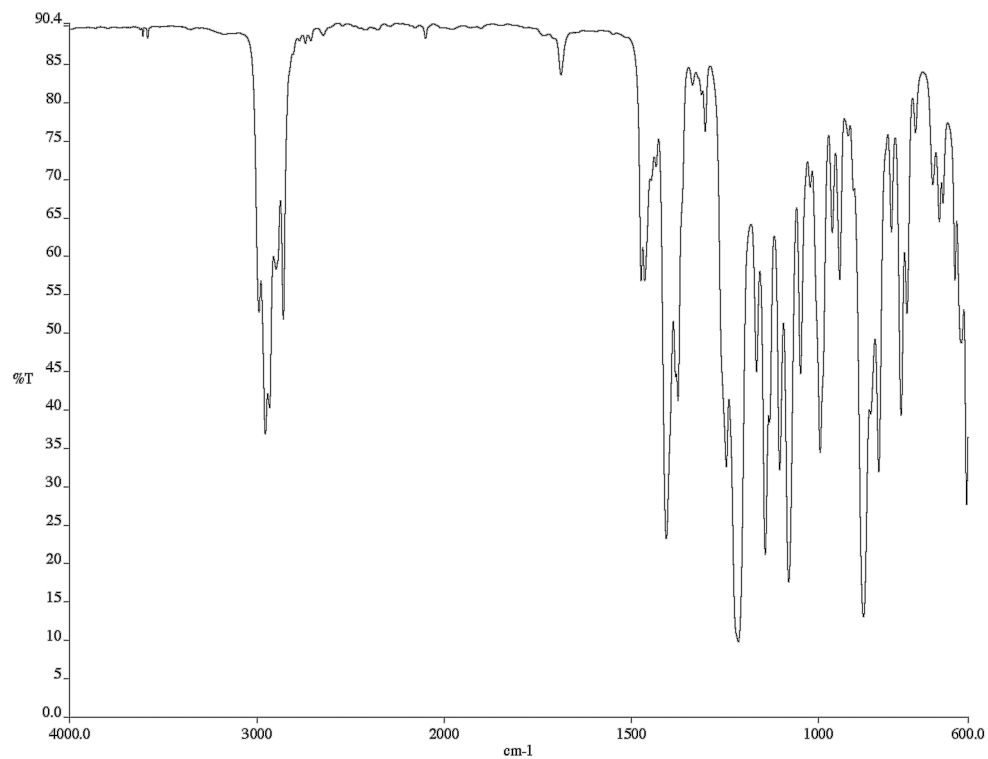


Figure B.62 Infrared spectrum (thin film/NaCl) of compound **263**.

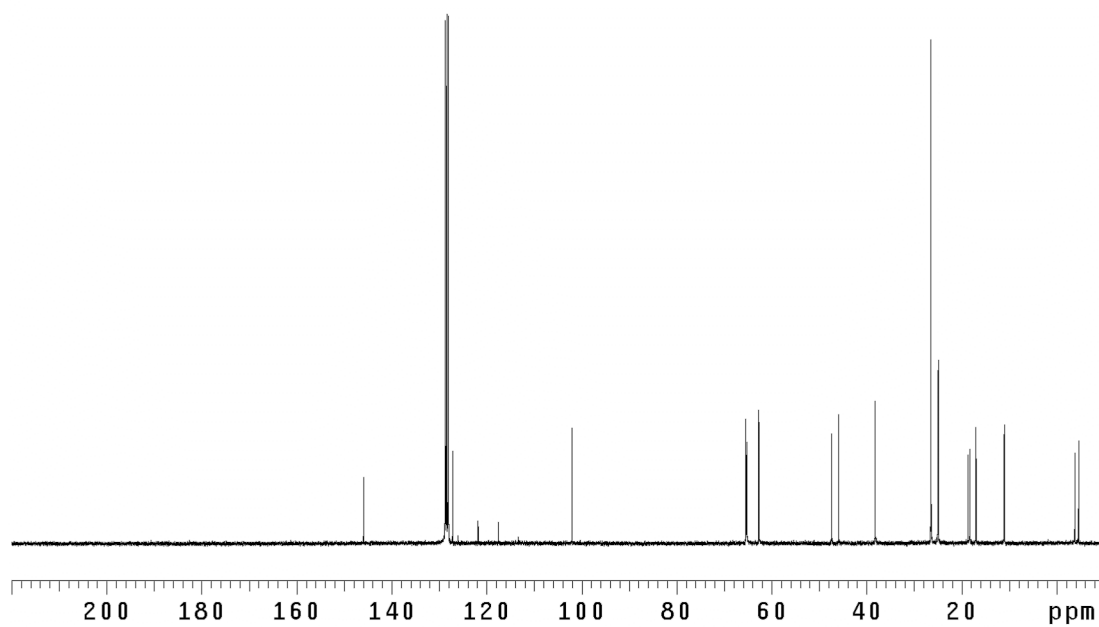


Figure B.63  $^{13}\text{C}$  NMR (300 MHz,  $\text{C}_6\text{D}_6$ ) of compound **263**.

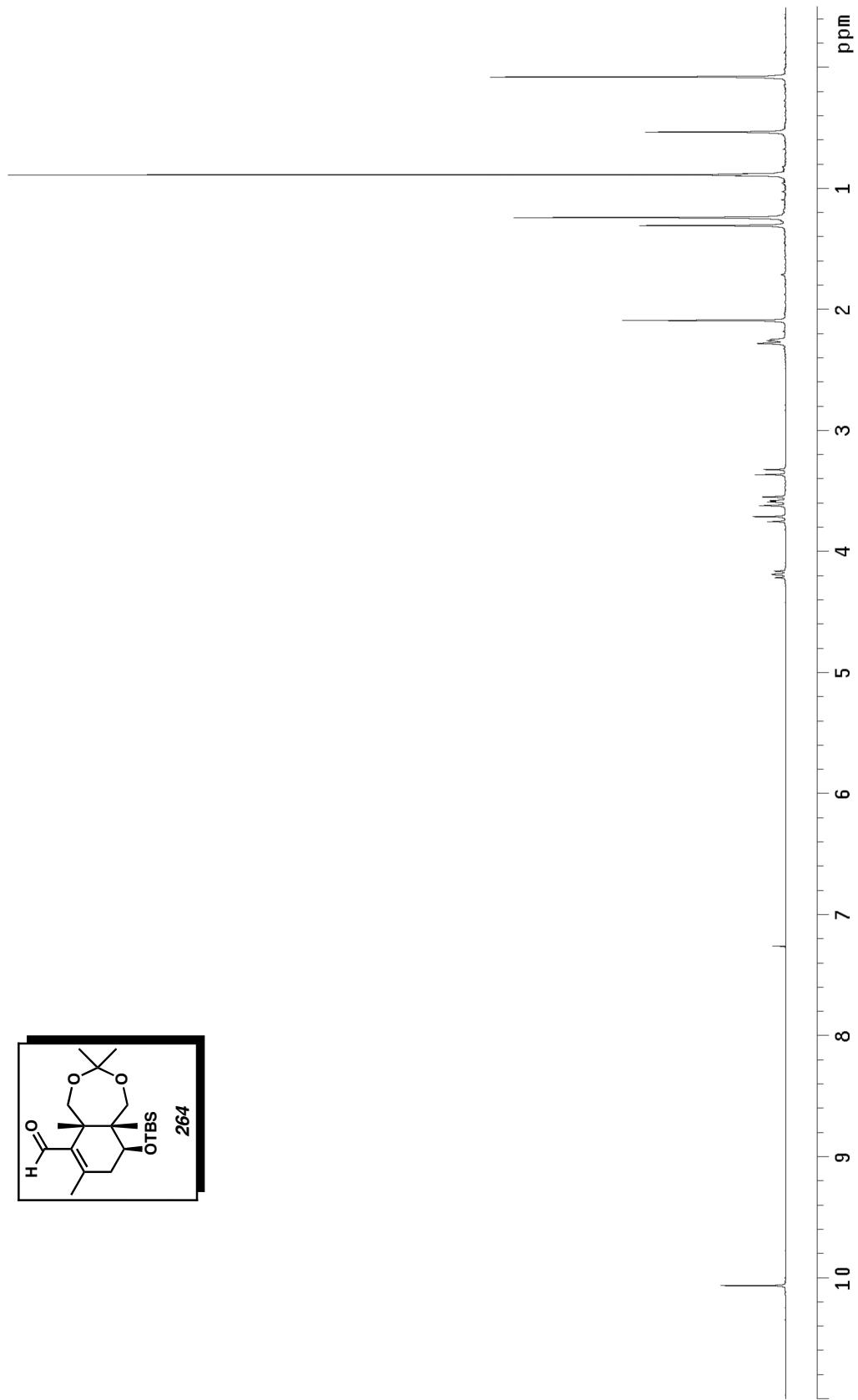
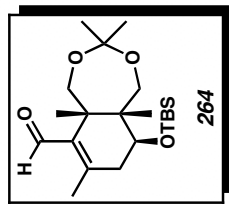


Figure B.64  $^1\text{H}$  NMR (300 MHz,  $\text{CDCl}_3$ ) of compound **264**.

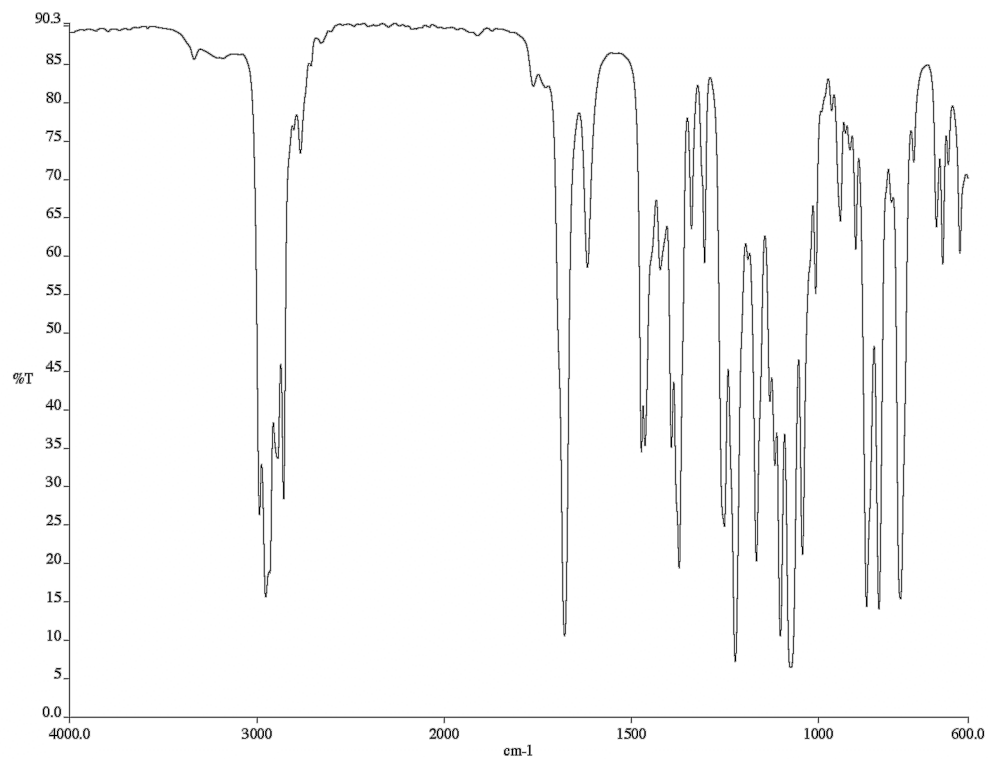


Figure B.65 Infrared spectrum (thin film/NaCl) of compound **264**.

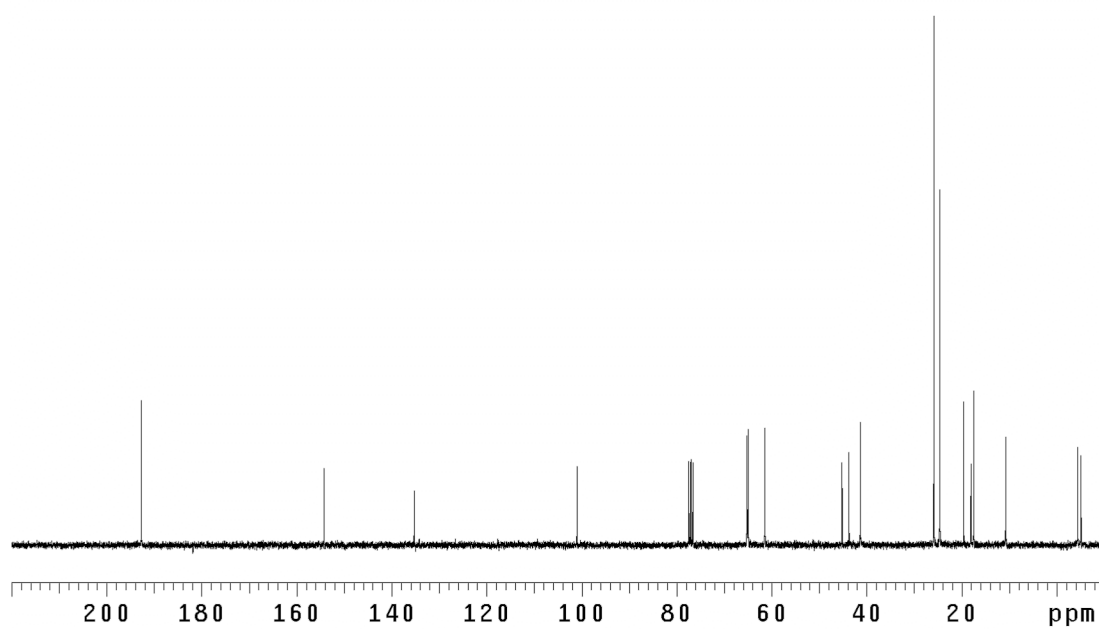


Figure B.66 <sup>13</sup>C NMR (75 MHz, CDCl<sub>3</sub>) of compound **264**.

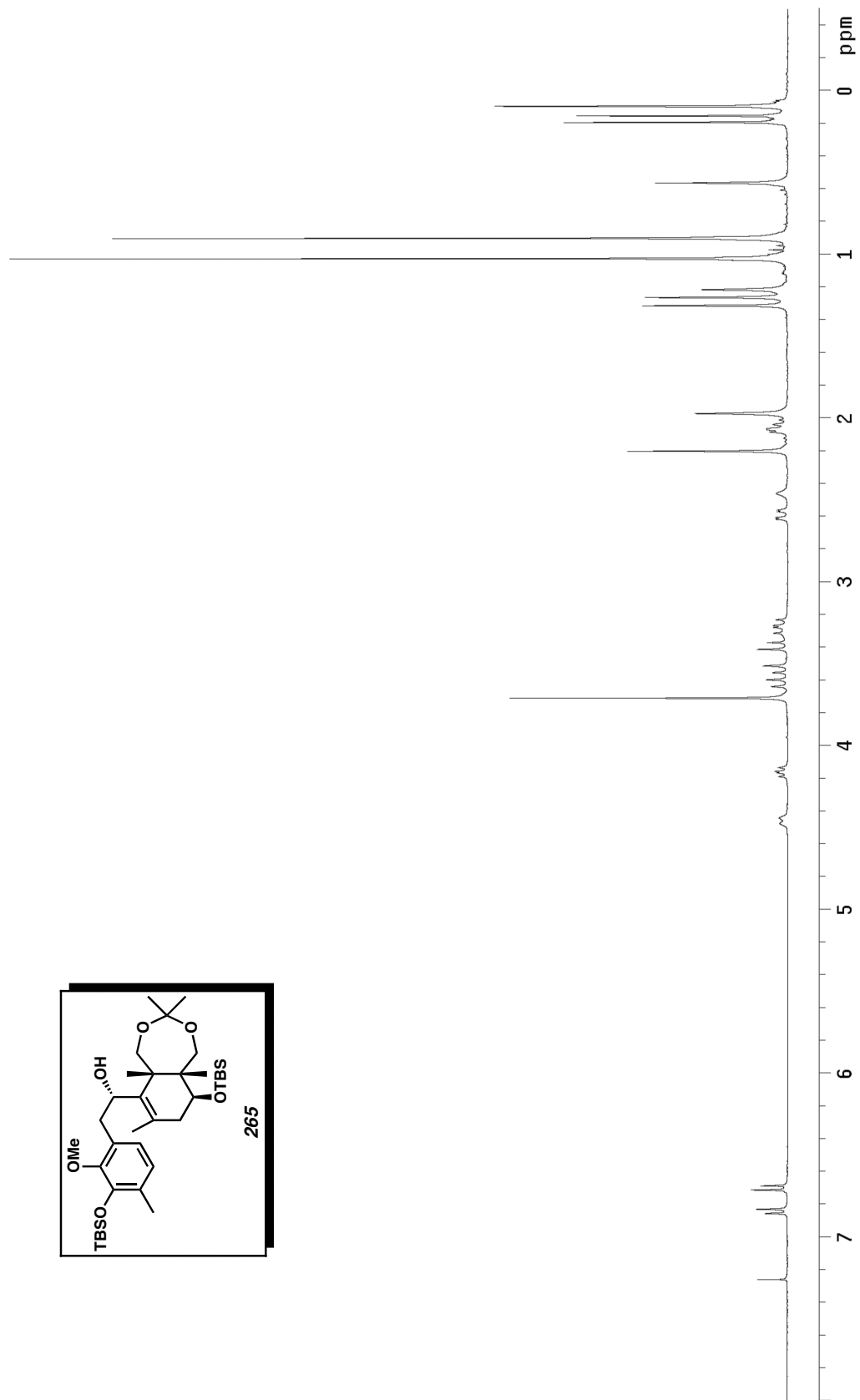
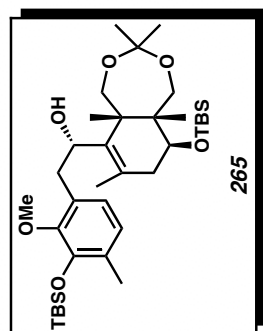


Figure B.67  $^1\text{H}$  NMR (300 MHz,  $\text{CDCl}_3$ ) of compound **265**.

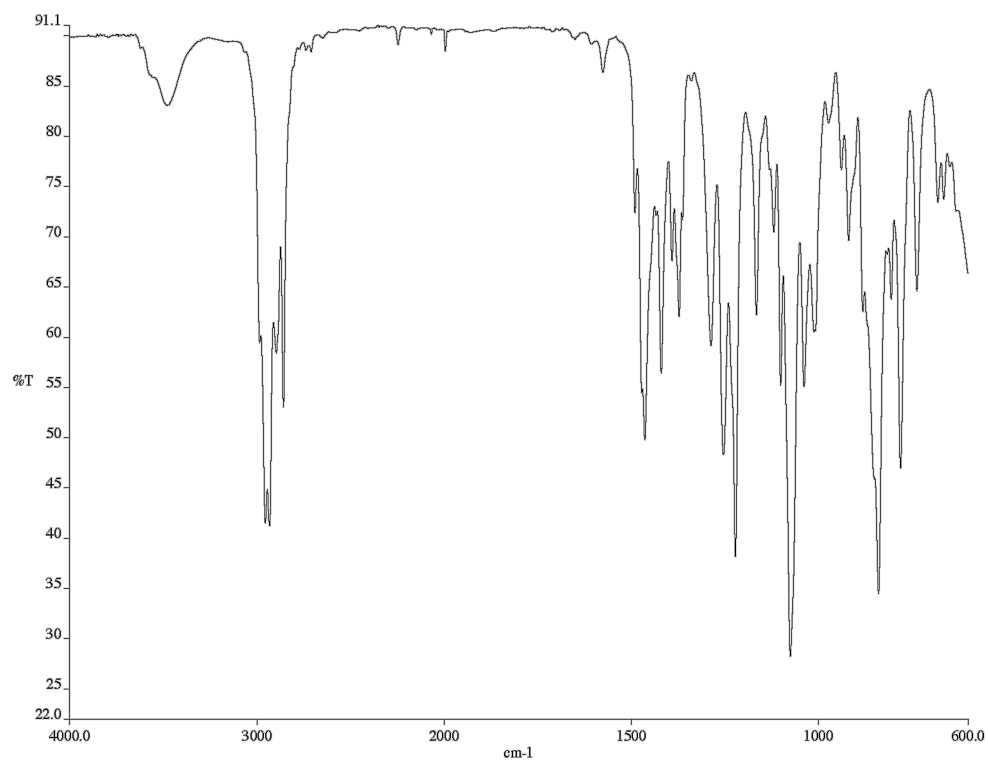


Figure B.68 Infrared spectrum (thin film/NaCl) of compound **265**.

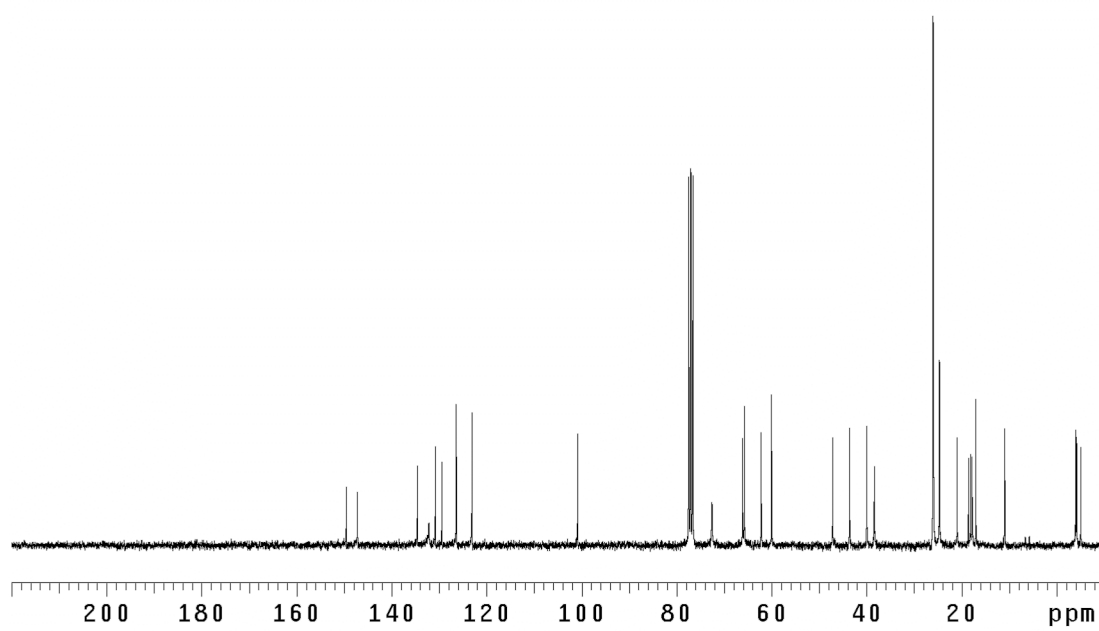


Figure B.69 <sup>13</sup>C NMR (75 MHz, CDCl<sub>3</sub>) of compound **265**.

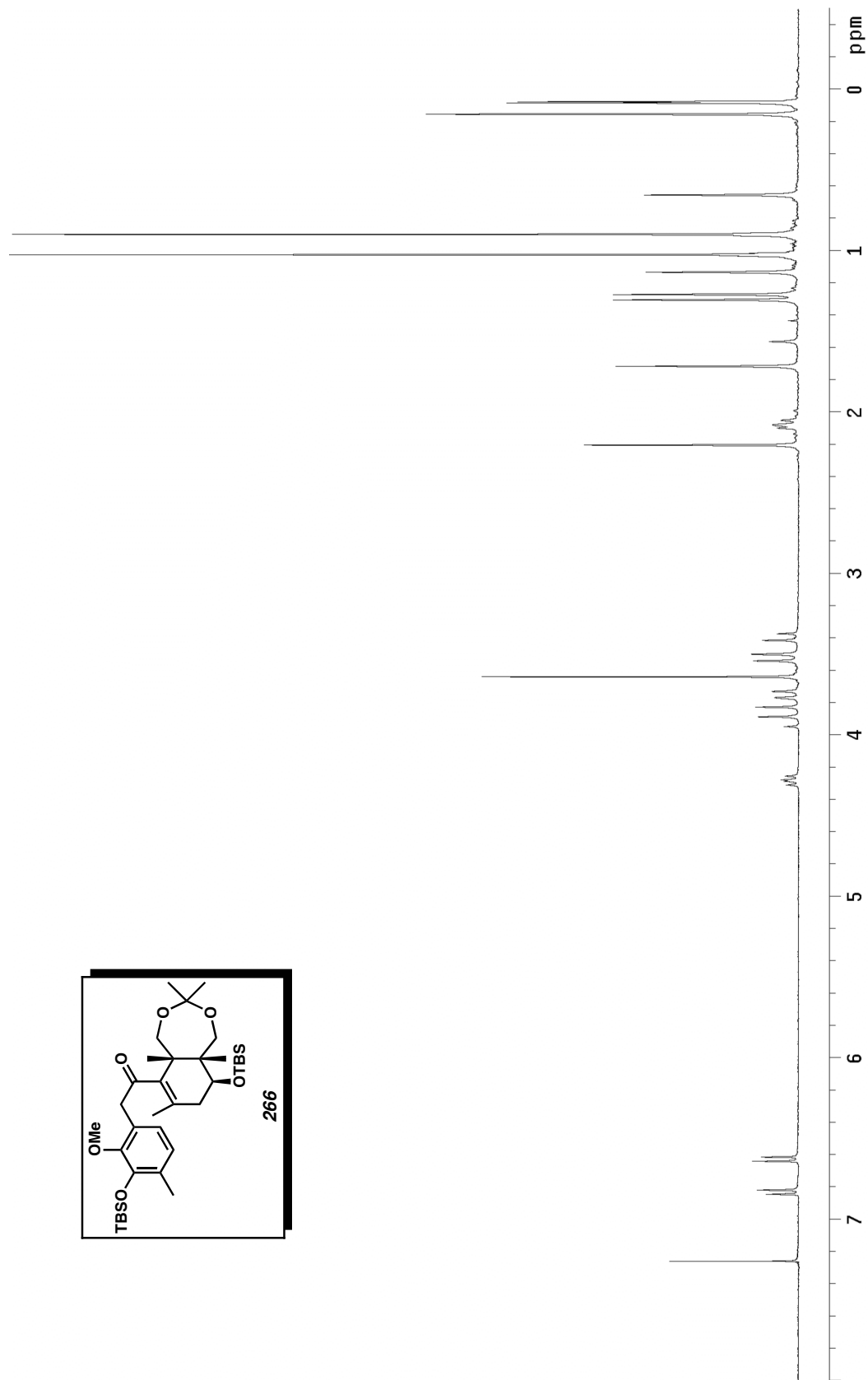
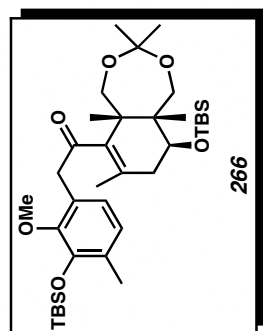


Figure B.70  $^1\text{H}$  NMR (300 MHz,  $\text{CDCl}_3$ ) of compound **266**.

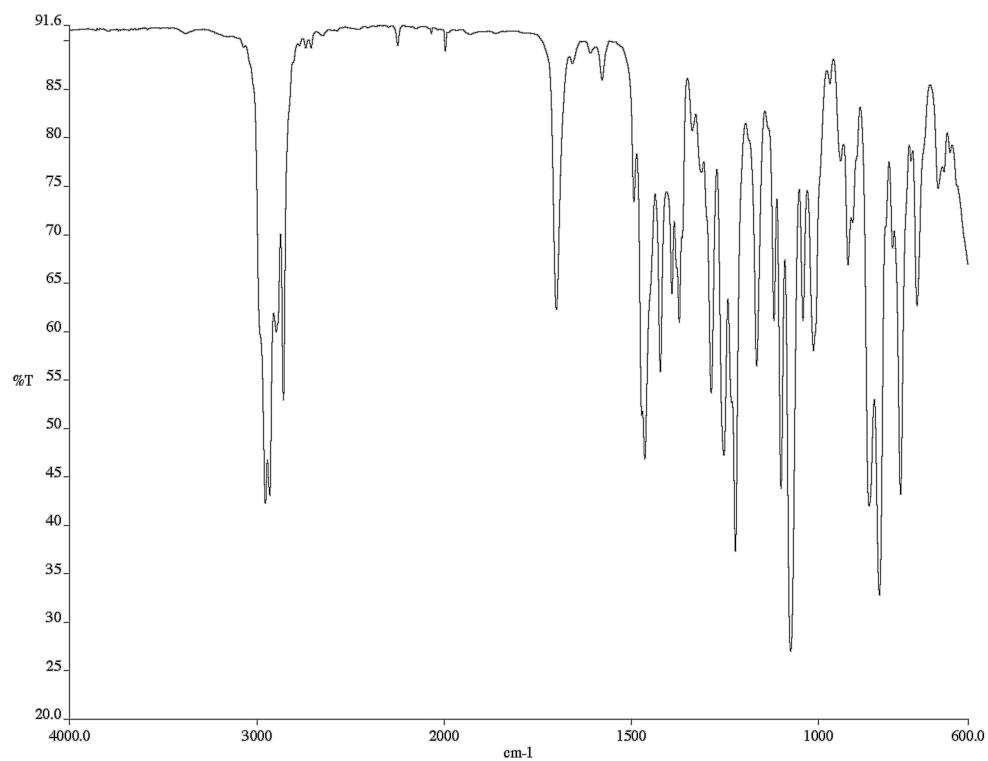


Figure B.71 Infrared spectrum (thin film/NaCl) of compound **266**.

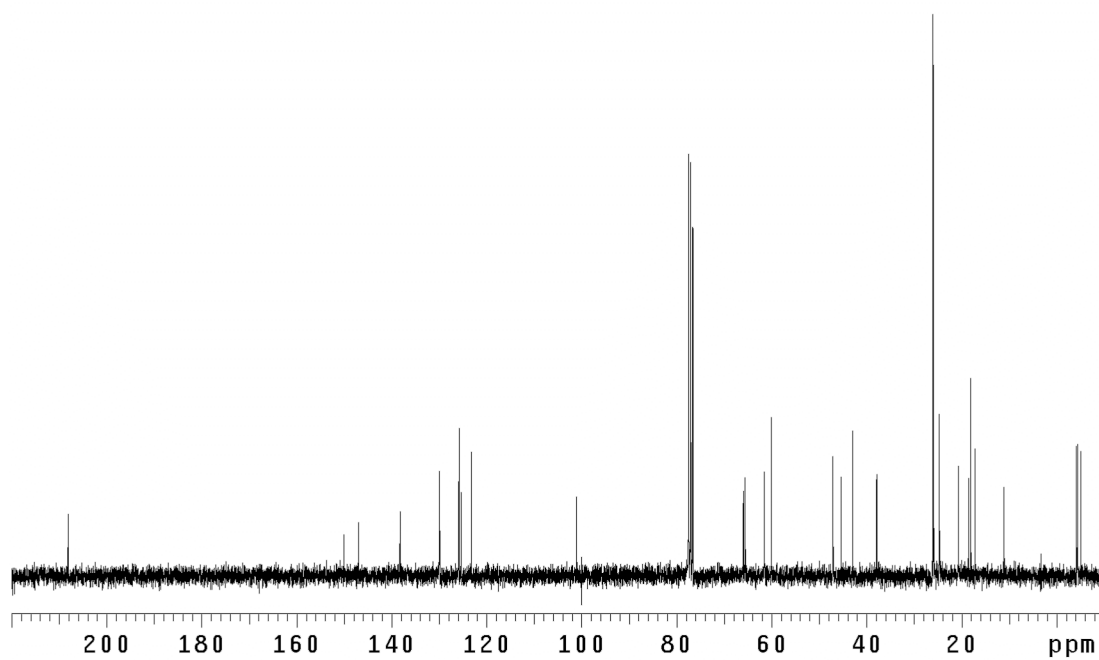


Figure B.72 <sup>13</sup>C NMR (75 MHz, CDCl<sub>3</sub>) of compound **266**.

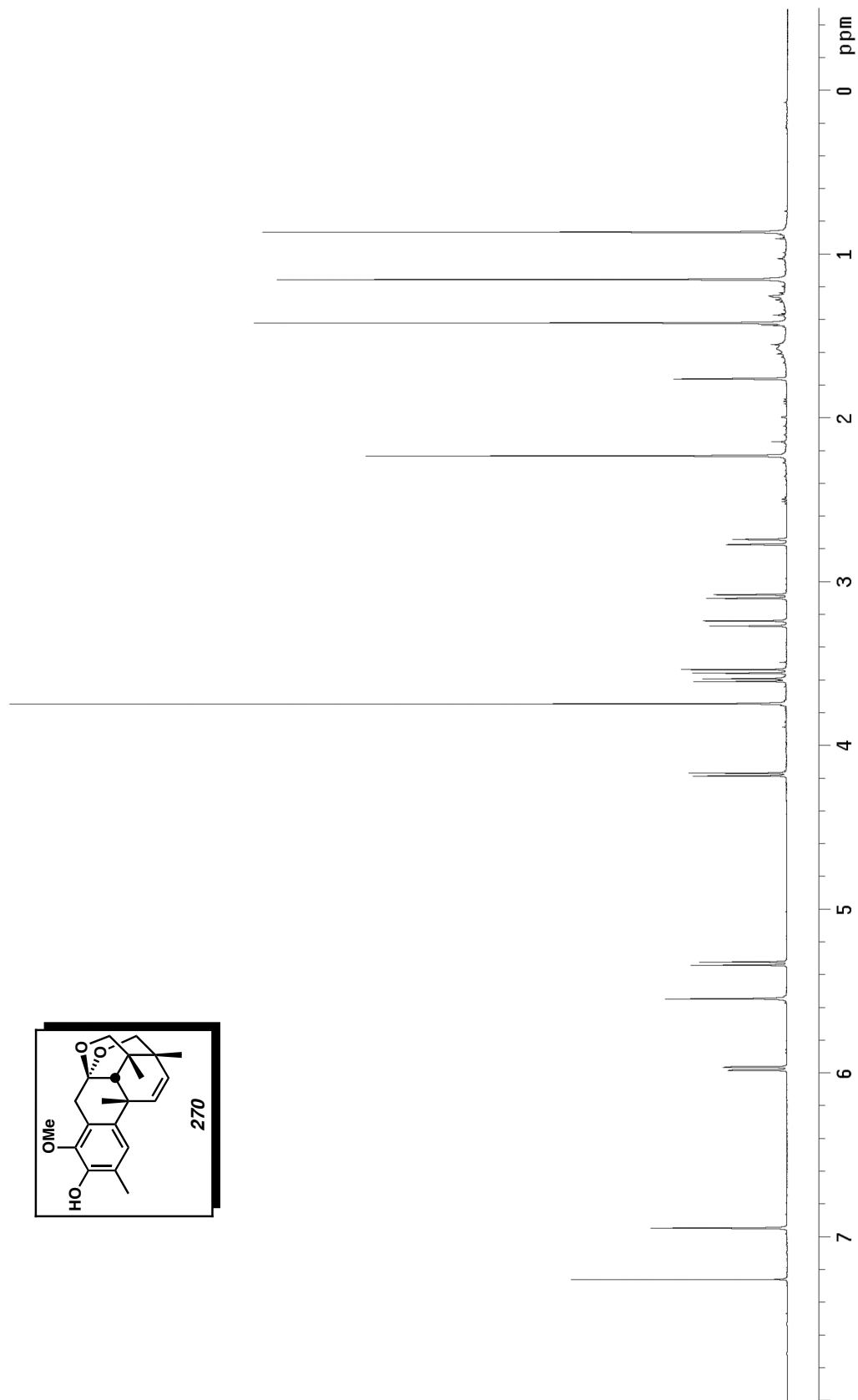
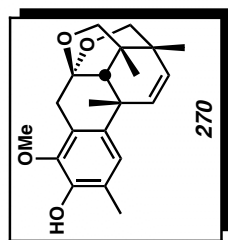


Figure B.73  $^1\text{H}$  NMR (500 MHz,  $\text{CDCl}_3$ ) of compound 270.

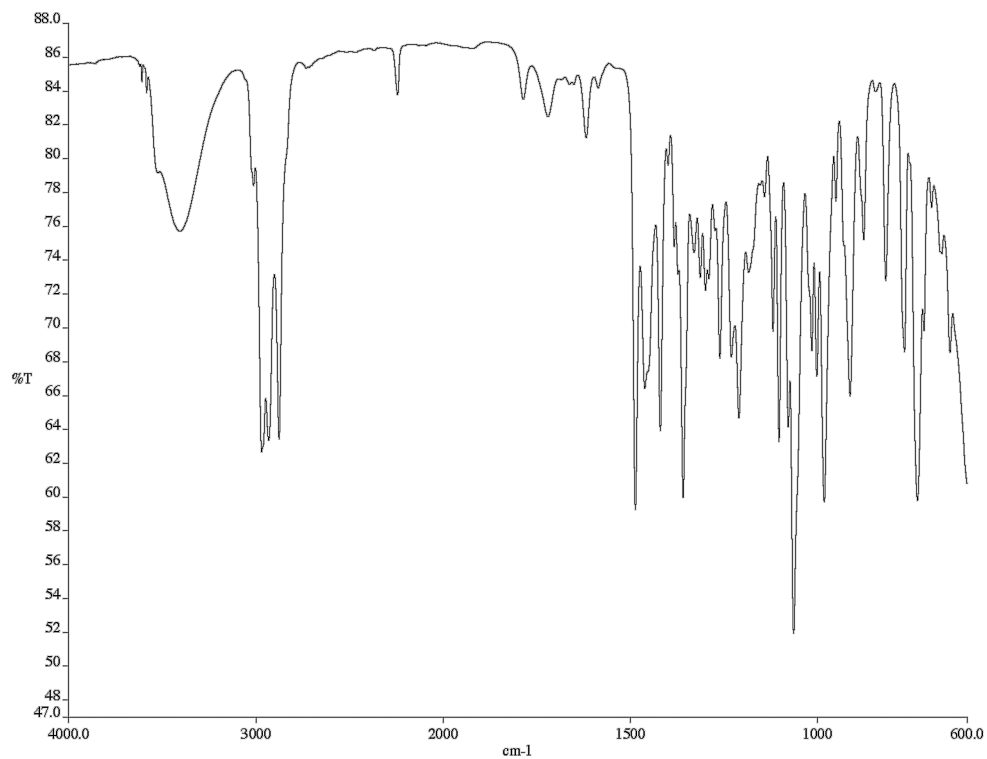


Figure B.73 Infrared spectrum (thin film/NaCl) of compound **270**.

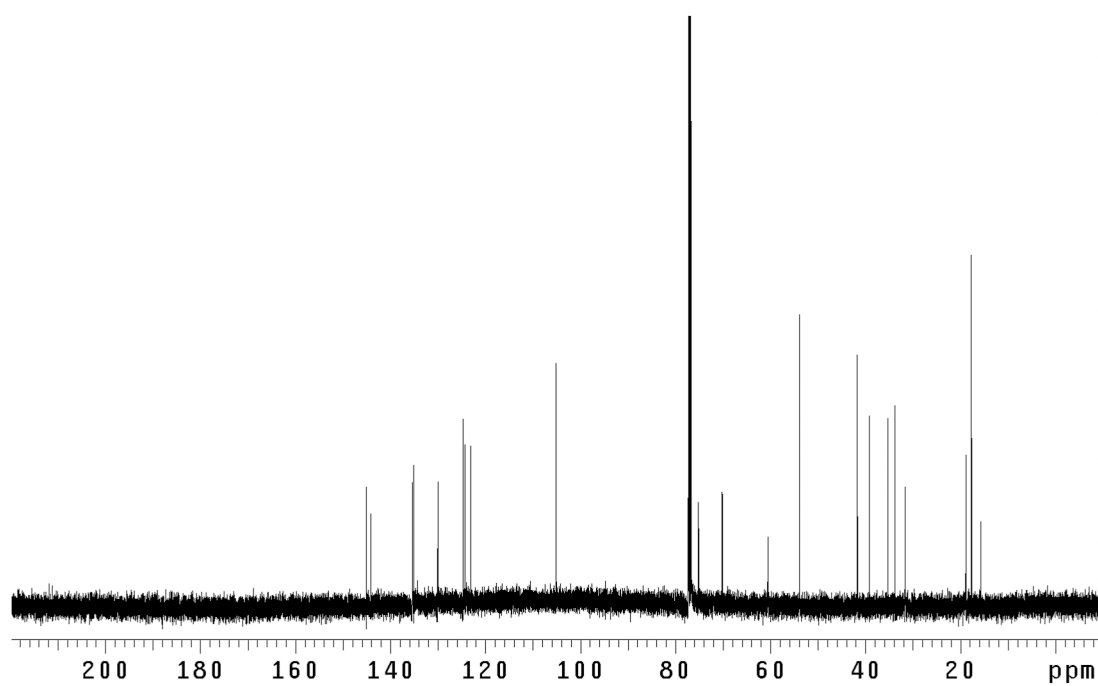


Figure B.74  $^{13}\text{C}$  NMR (125 MHz,  $\text{CDCl}_3$ ) of compound **270**.

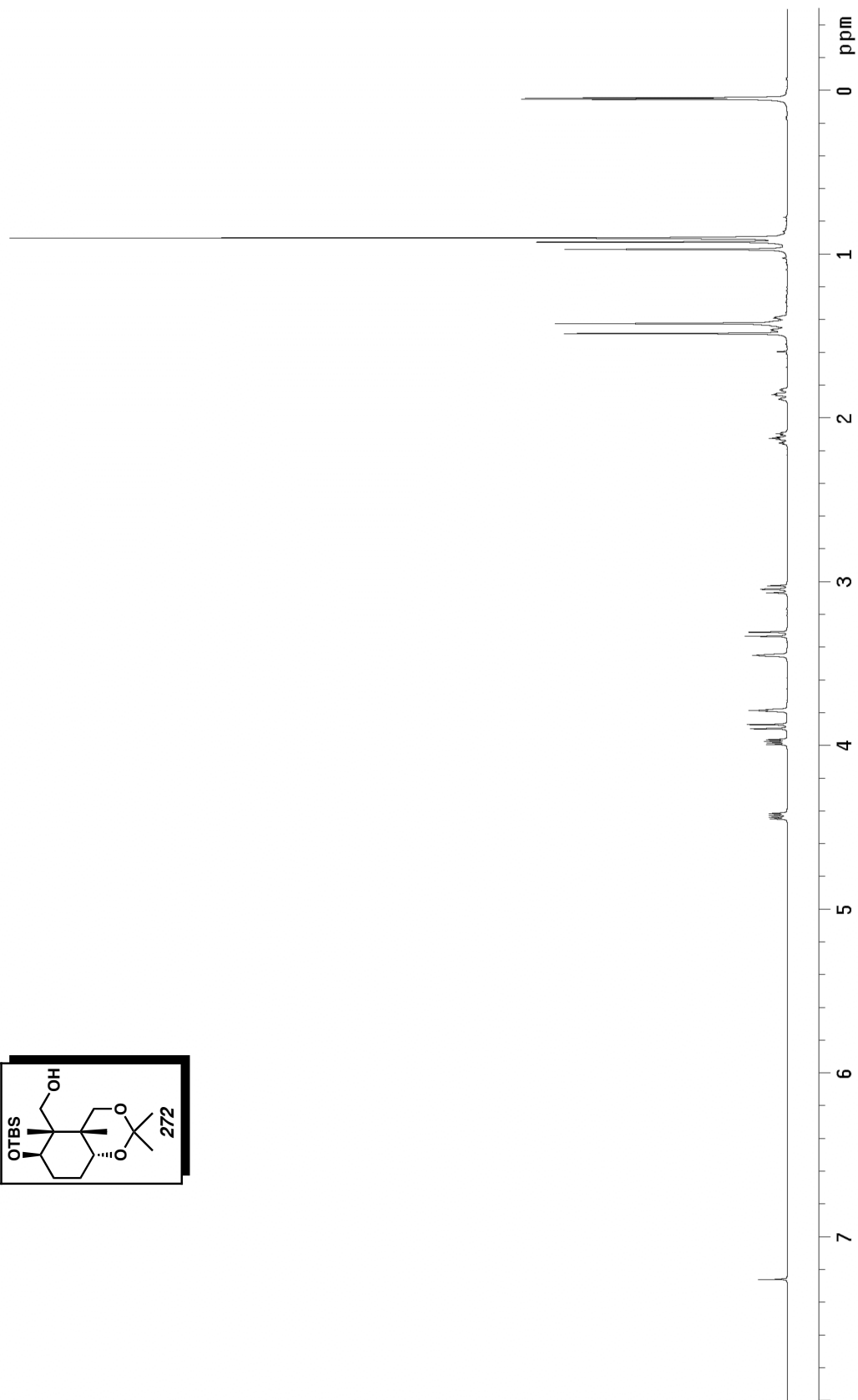
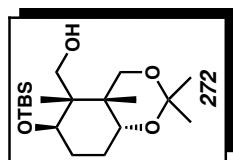


Figure B.76  $^1\text{H}$  NMR (500 MHz,  $\text{CDCl}_3$ ) of compound 272.

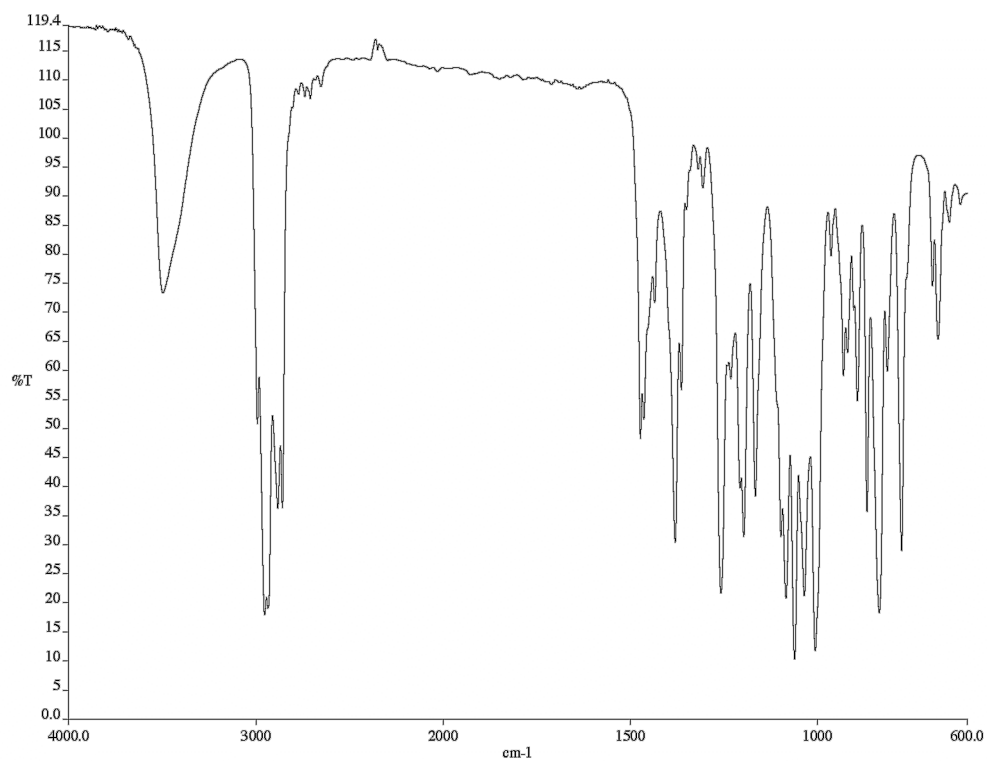


Figure B.77 Infrared spectrum (thin film/NaCl) of compound **272**.

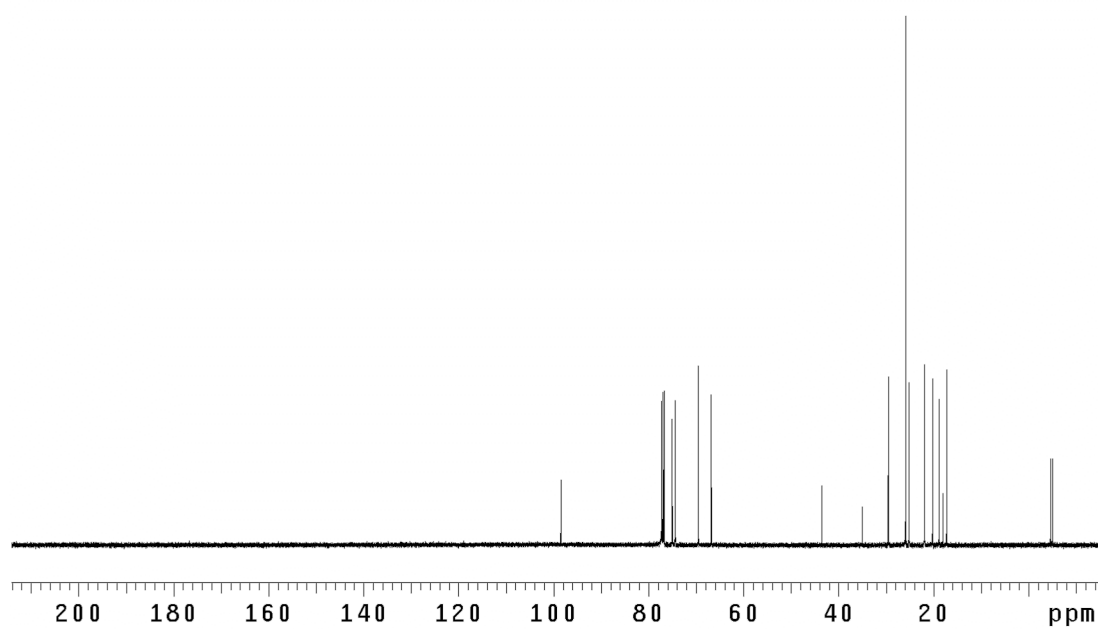


Figure B.78  $^{13}\text{C}$  NMR (125 MHz,  $\text{CDCl}_3$ ) of compound **272**.

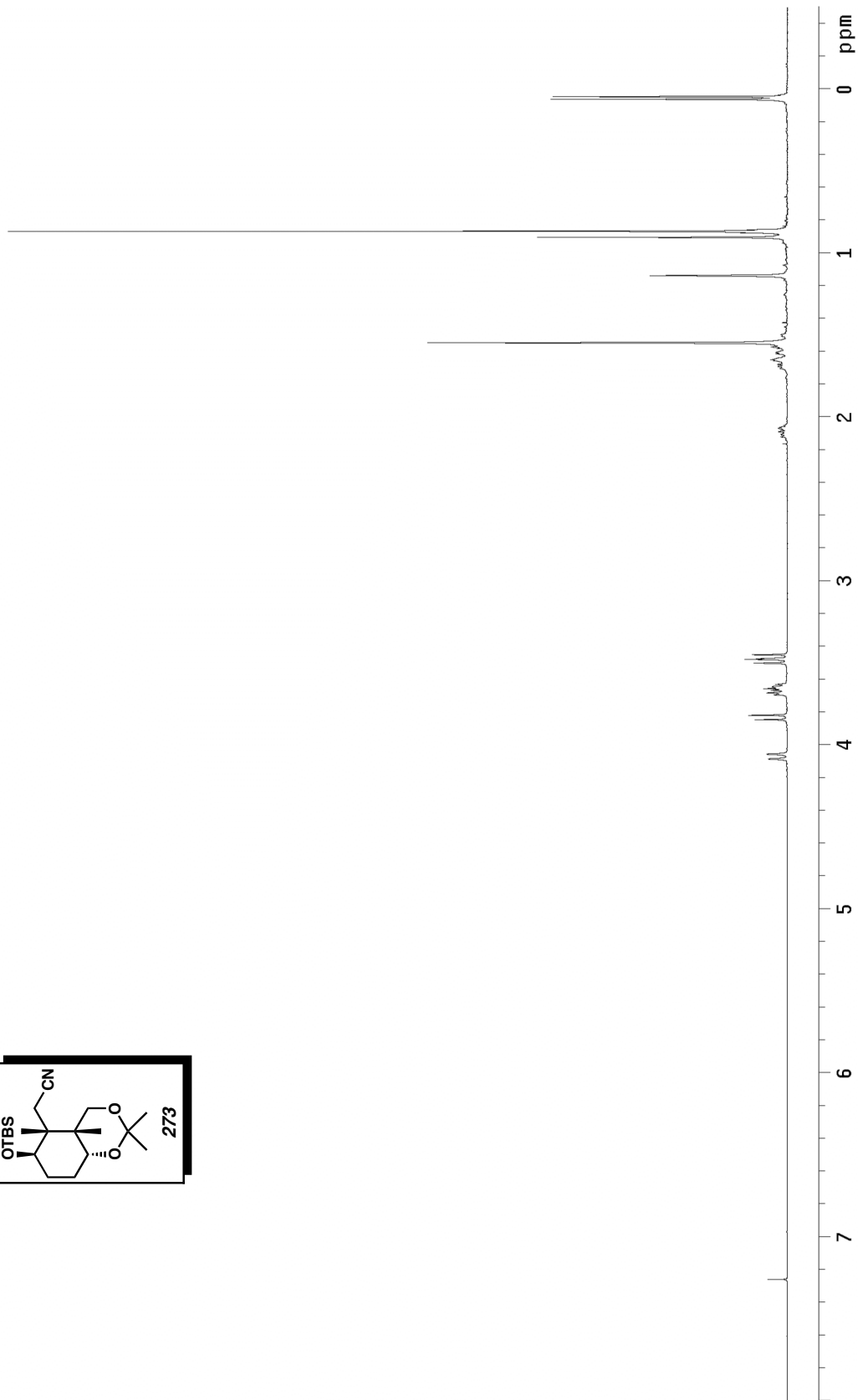
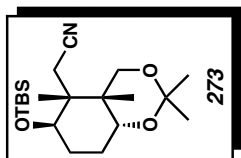


Figure B.79  $^1\text{H}$  NMR (300 MHz,  $\text{CDCl}_3$ ) of compound **273**.

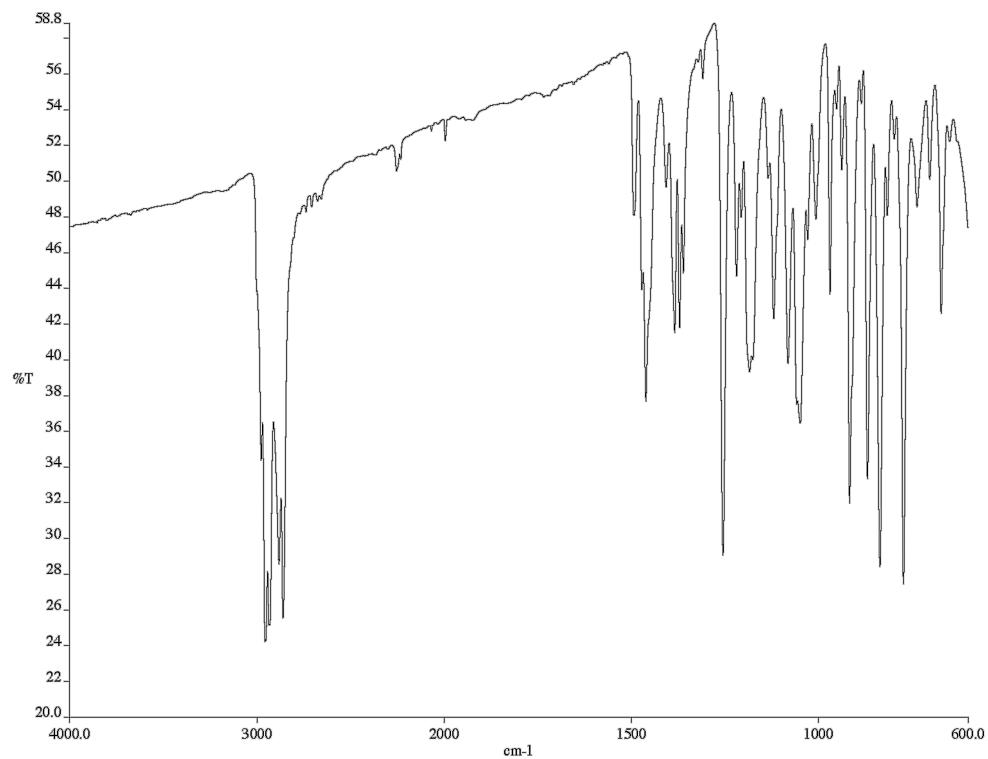


Figure B.80 Infrared spectrum (thin film/NaCl) of compound **273**.

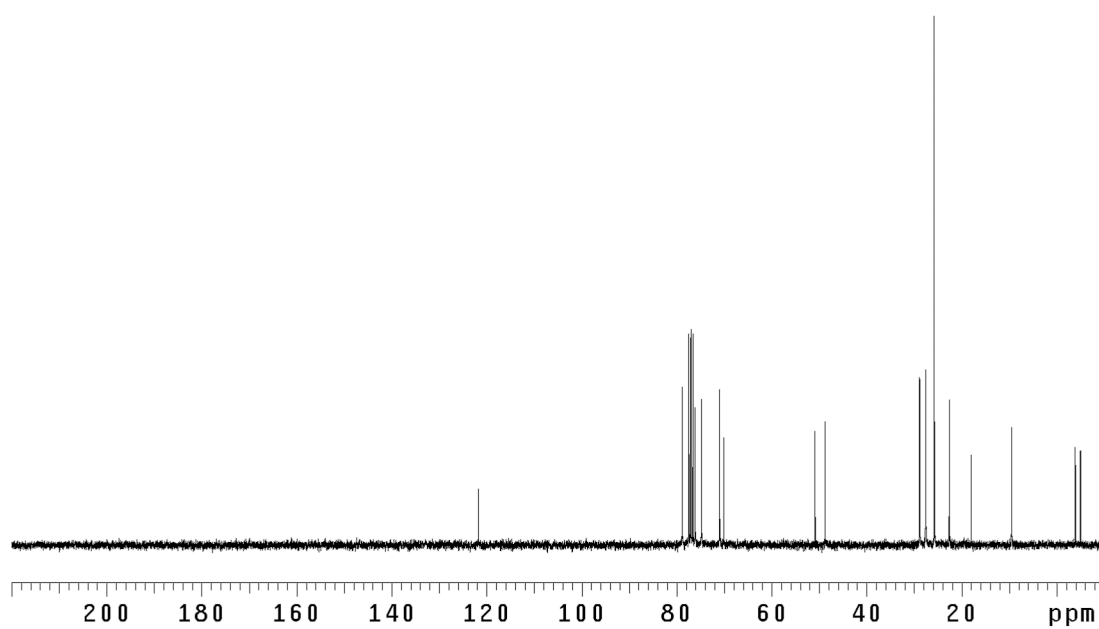


Figure B.81 <sup>13</sup>C NMR (75 MHz, CDCl<sub>3</sub>) of compound **273**.

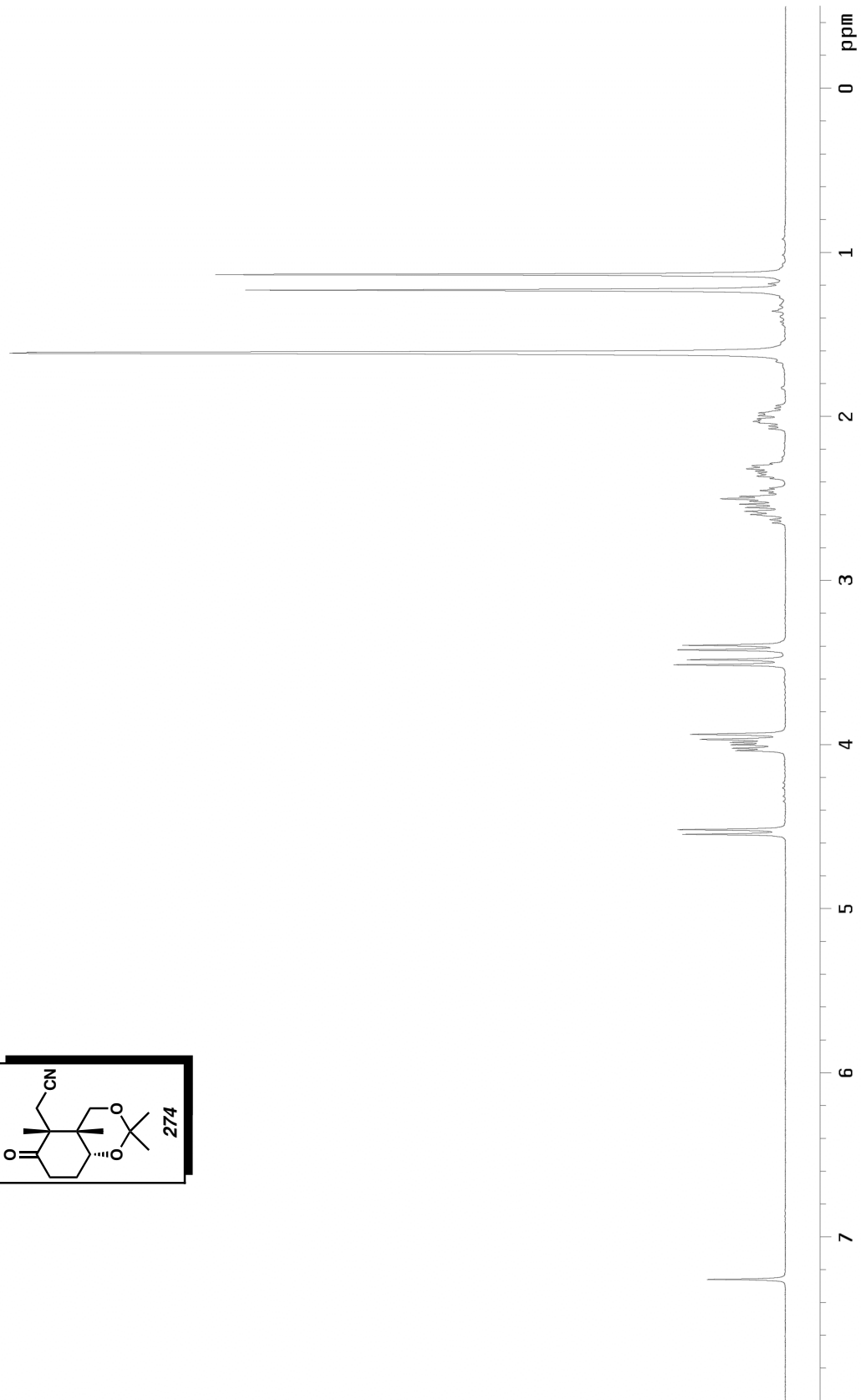
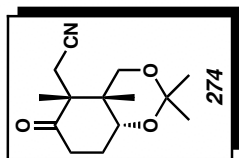


Figure B.82 <sup>1</sup>H NMR (300 MHz, CDCl<sub>3</sub>) of compound 274.

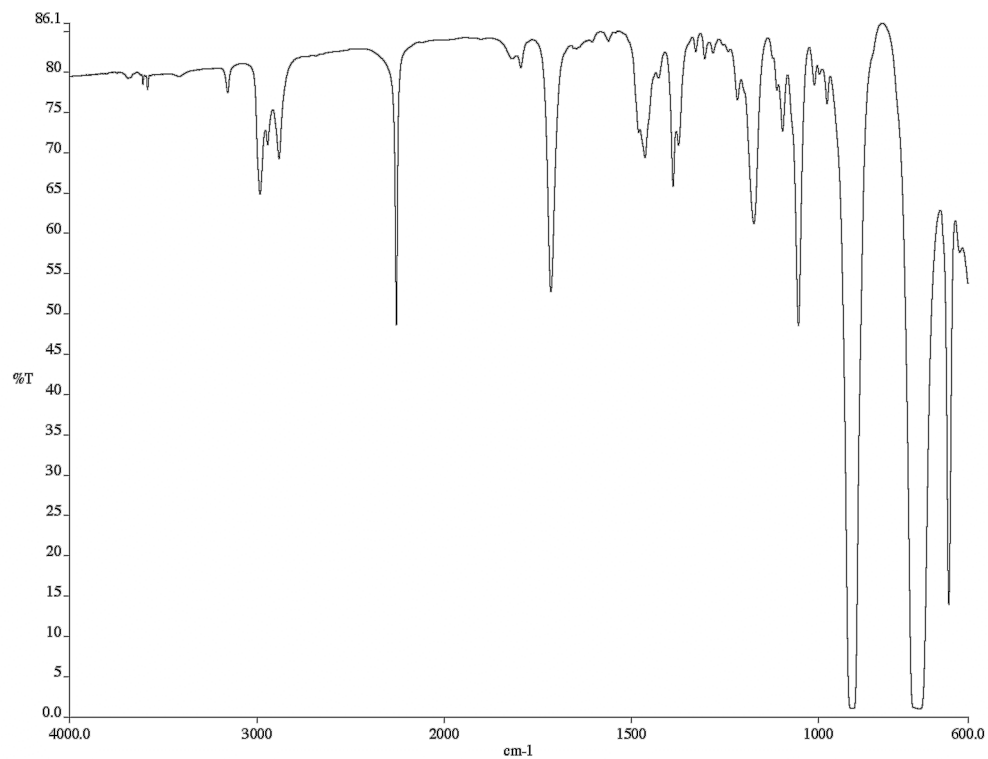


Figure B.83 Infrared spectrum (thin film/NaCl) of compound **274**.

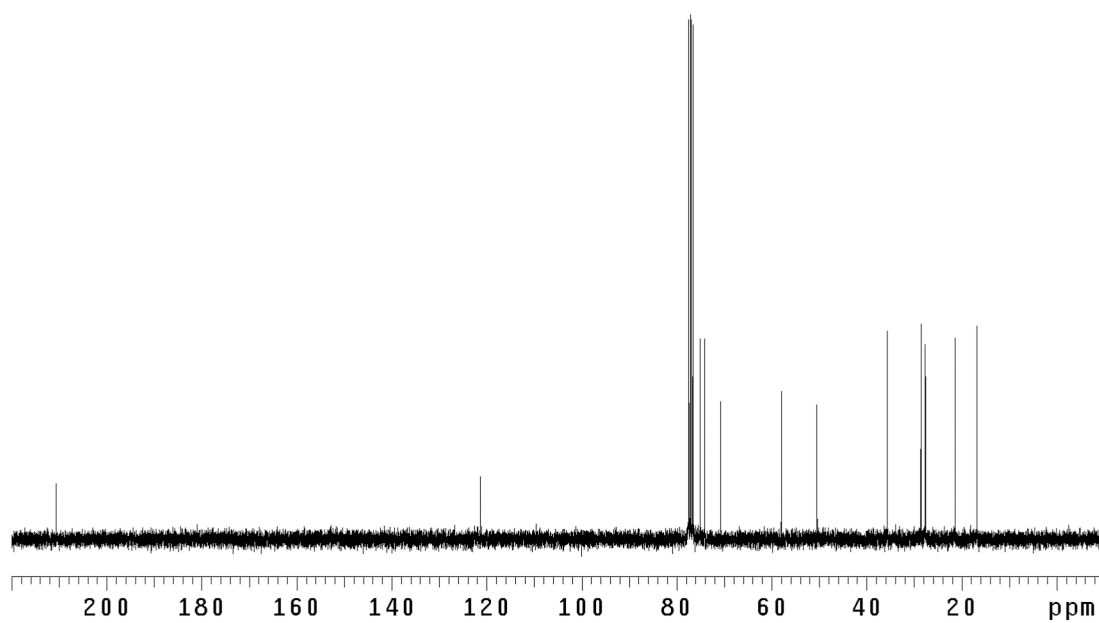
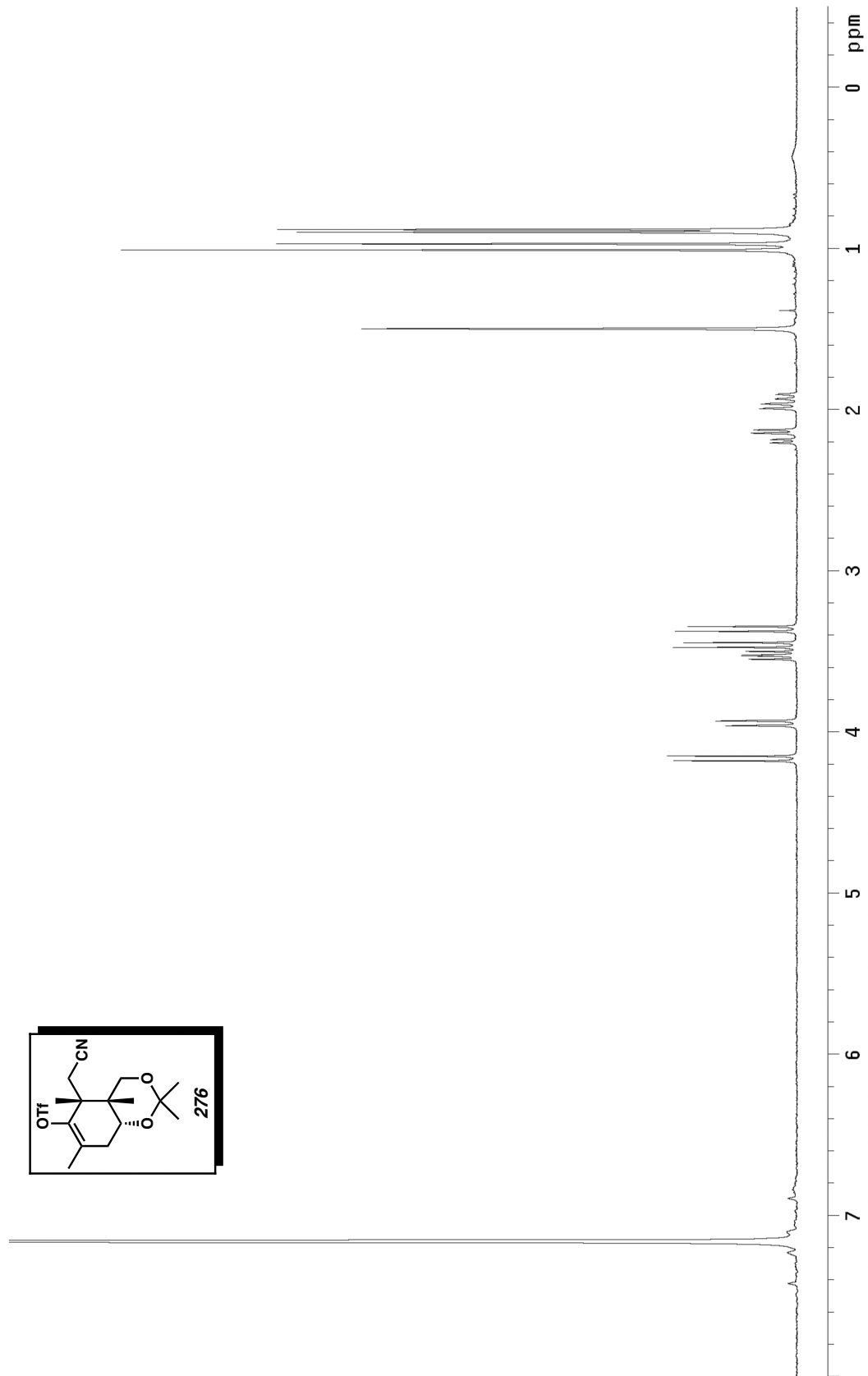


Figure B.84 <sup>13</sup>C NMR (75 MHz, CDCl<sub>3</sub>) of compound **274**.



305  
*Figure B.85*  $^1\text{H}$  NMR (300 MHz,  $\text{C}_6\text{D}_6$ ) of compound **276**.

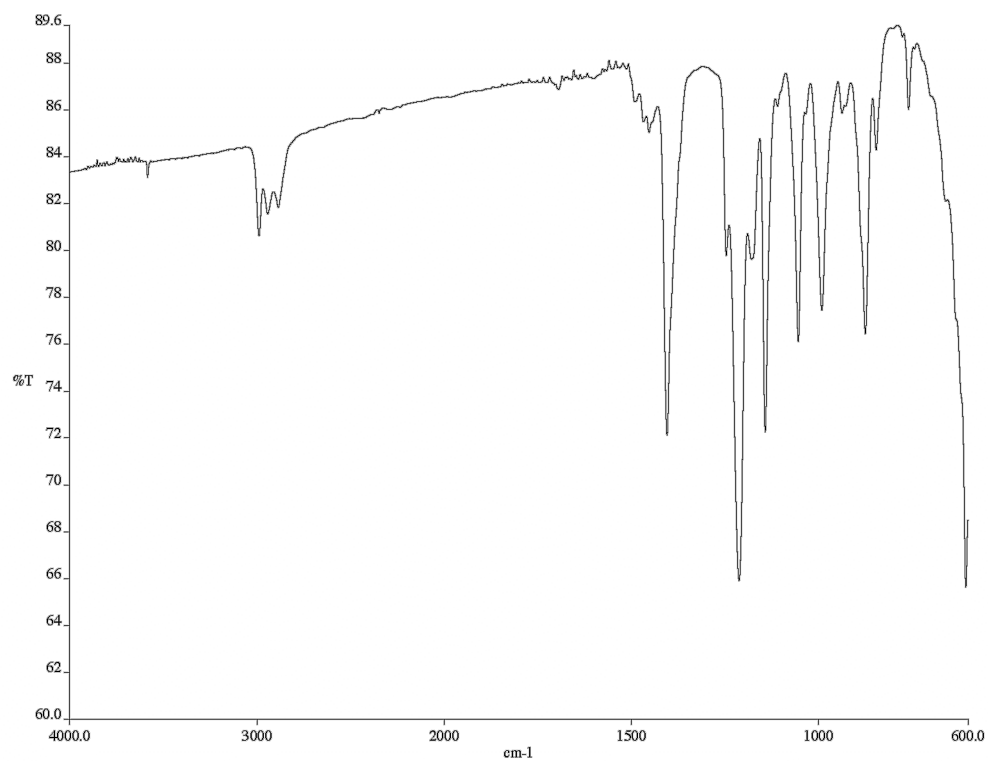


Figure B.86 Infrared spectrum (thin film/NaCl) of compound **276**.

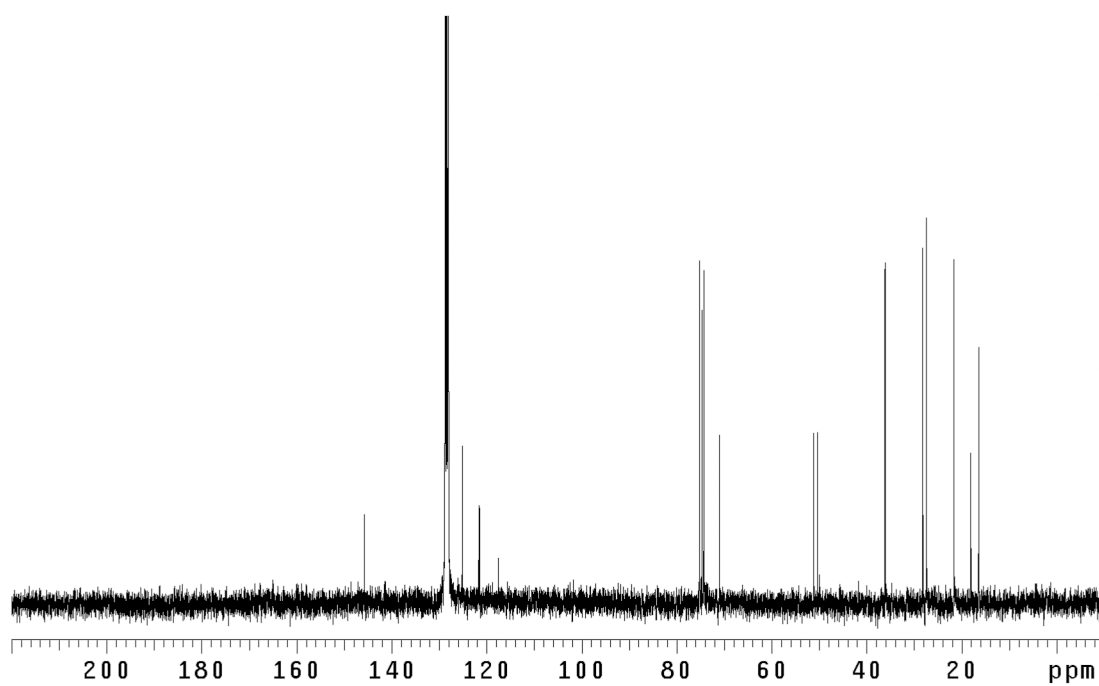


Figure B.87 <sup>13</sup>C NMR (75 MHz, C<sub>6</sub>D<sub>6</sub>) of compound **276**.

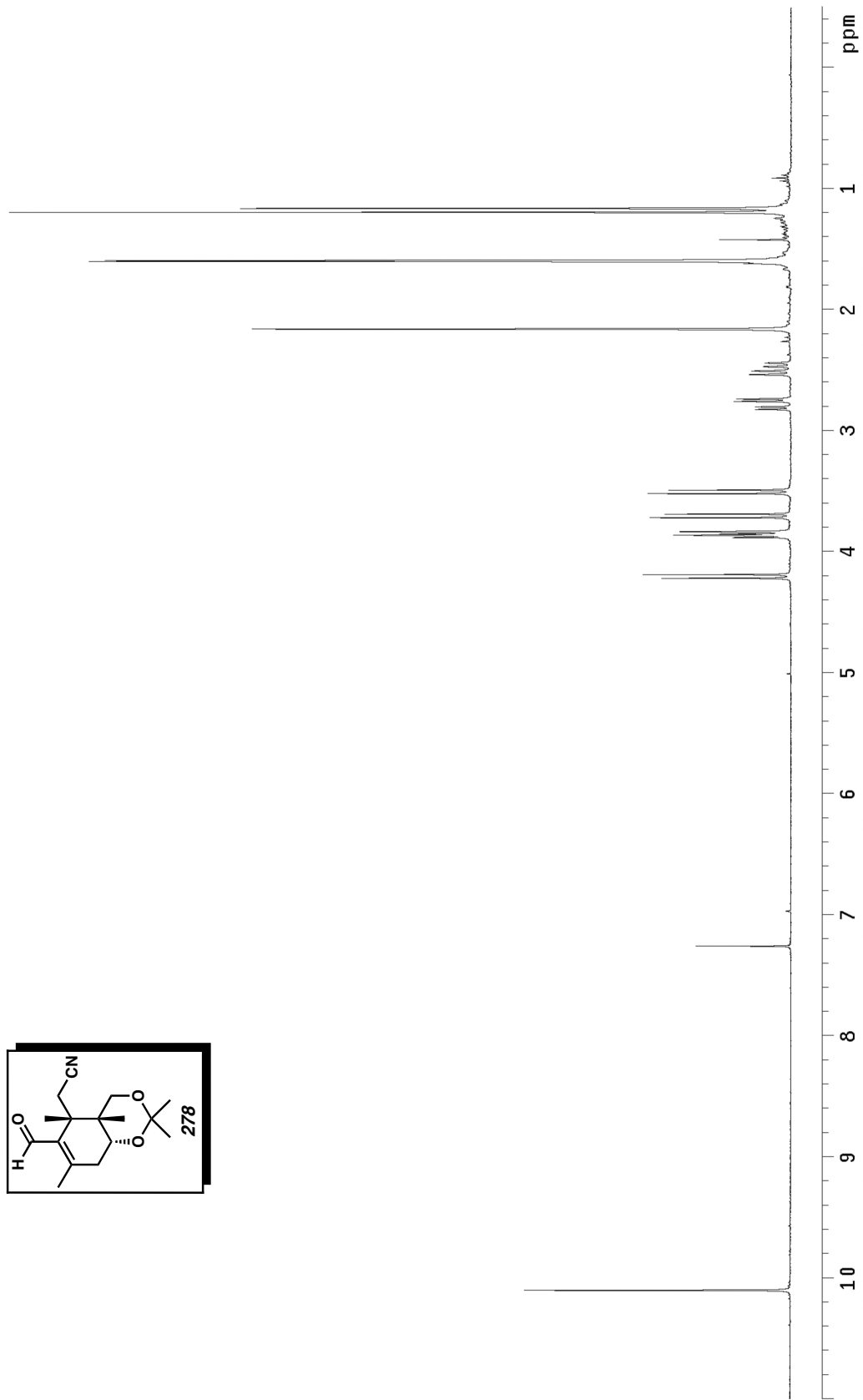
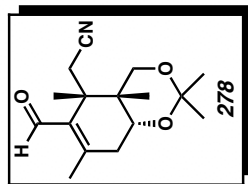


Figure B.88 <sup>1</sup>H NMR (300 MHz, CDCl<sub>3</sub>) of compound **278**.

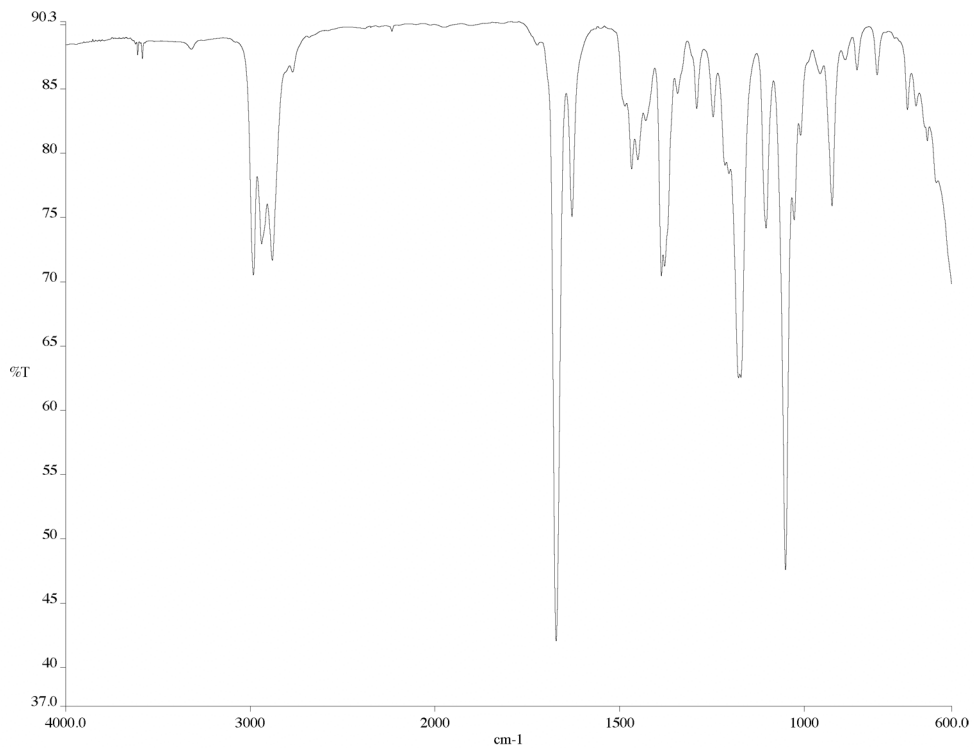


Figure B.89 Infrared spectrum (thin film/NaCl) of compound **278**.

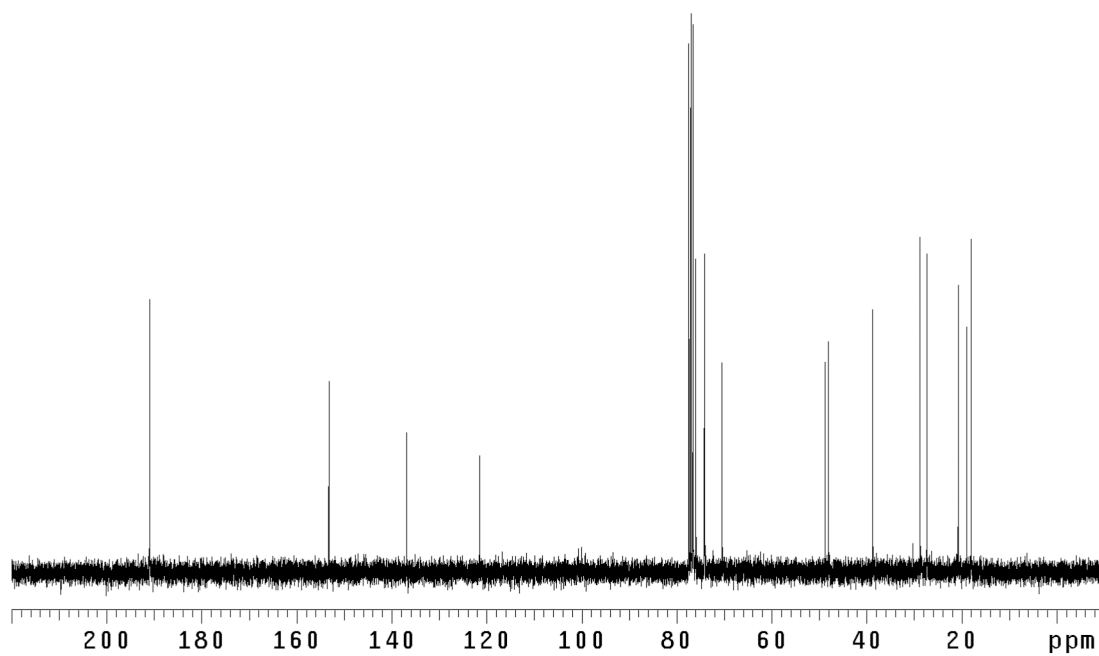


Figure B.90 <sup>13</sup>C NMR (75 MHz, CDCl<sub>3</sub>) of compound **278**.

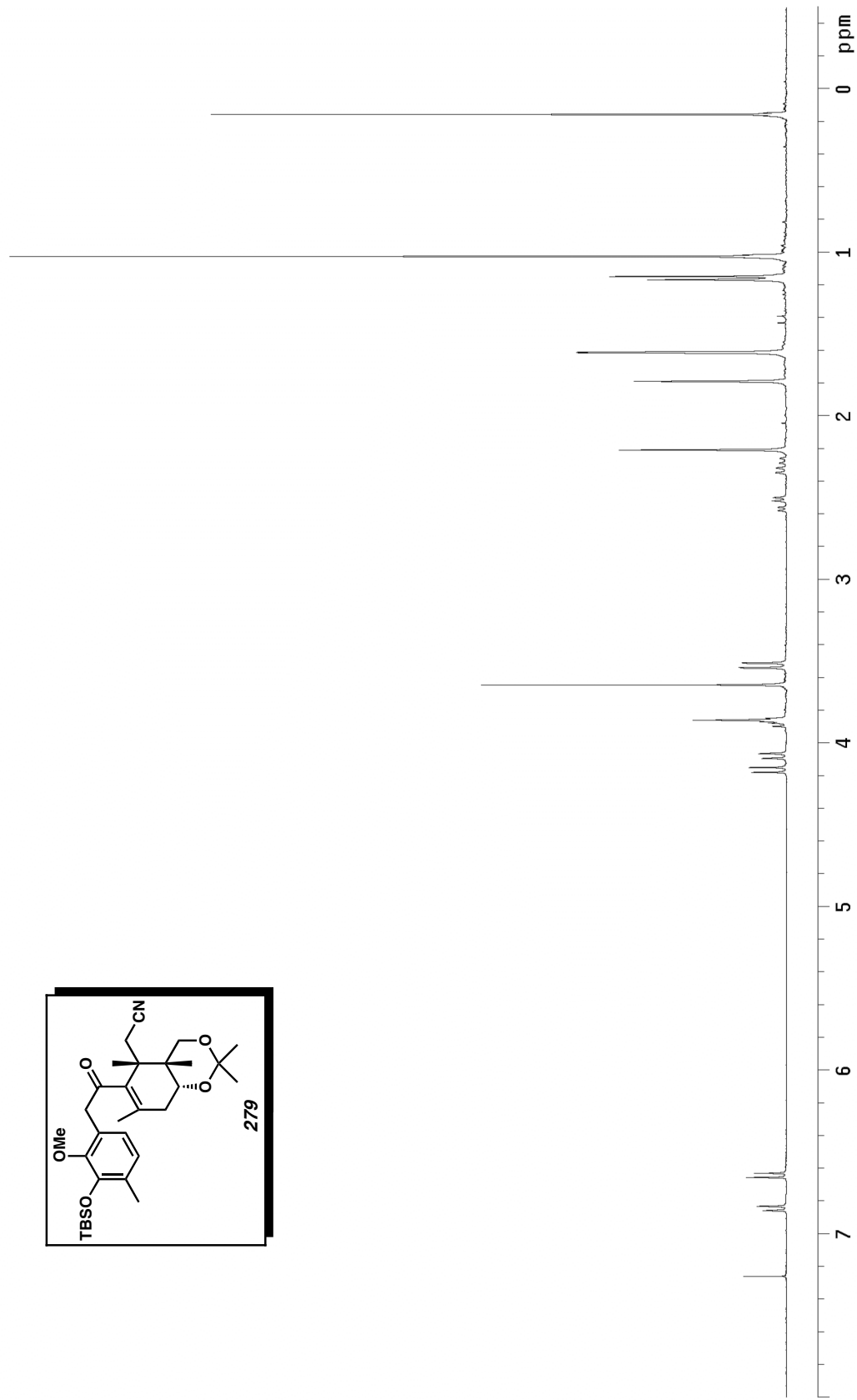
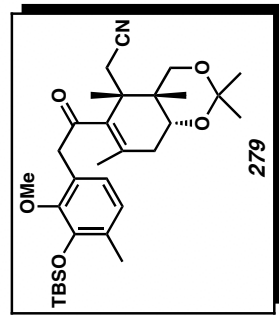


Figure B.91  $^1\text{H NMR}$  (300 MHz,  $\text{CDCl}_3$ ) of compound **279**.

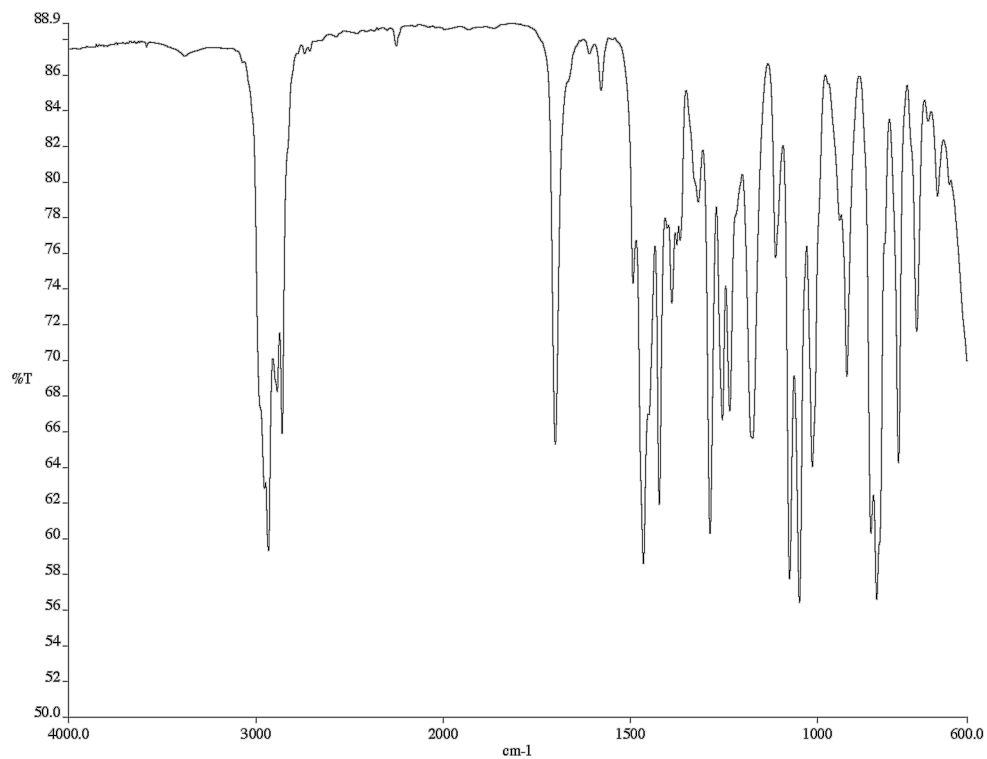


Figure B.92 Infrared spectrum (thin film/NaCl) of compound **279**.

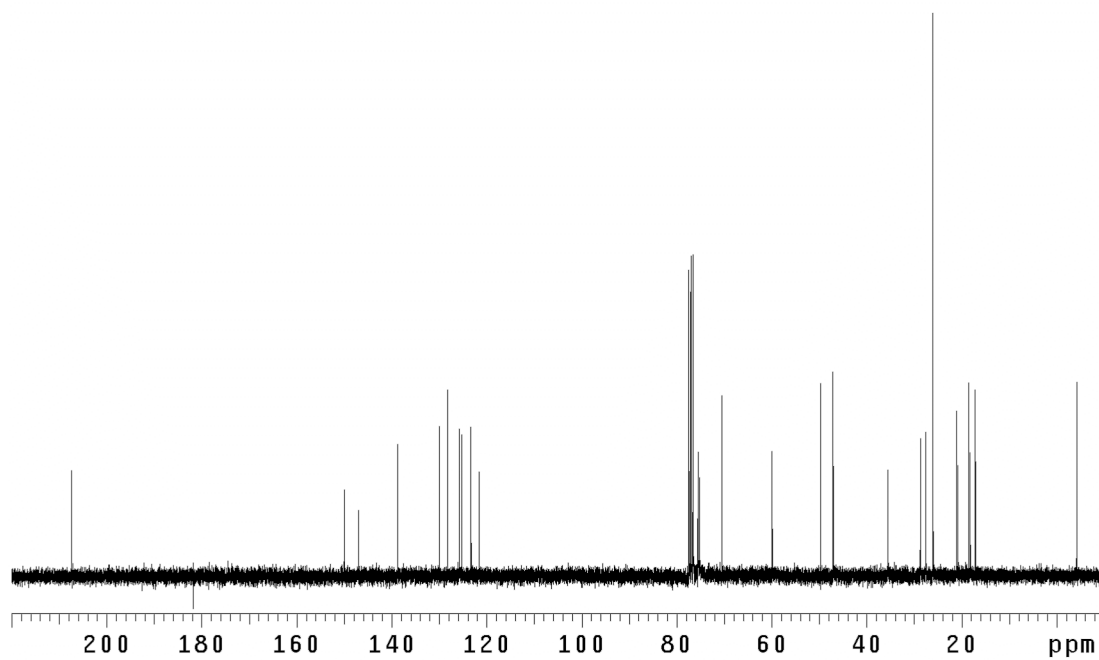


Figure B.93 <sup>13</sup>C NMR (75 MHz, CDCl<sub>3</sub>) of compound **279**.



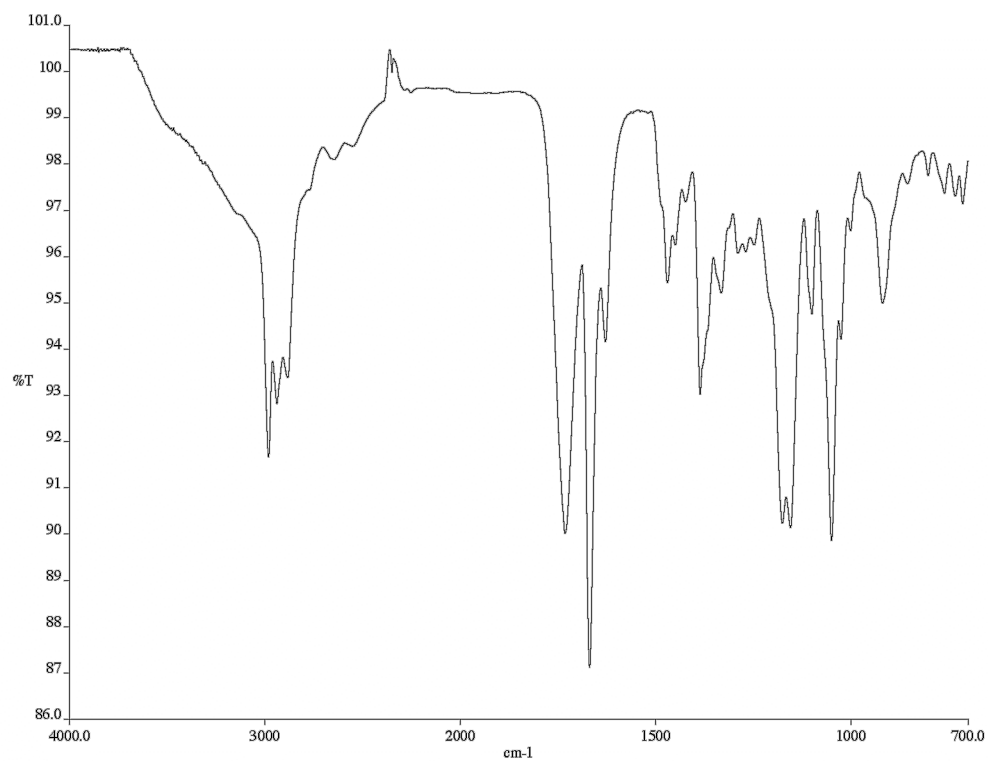


Figure B.95 Infrared spectrum (thin film/NaCl) of compound **280**.

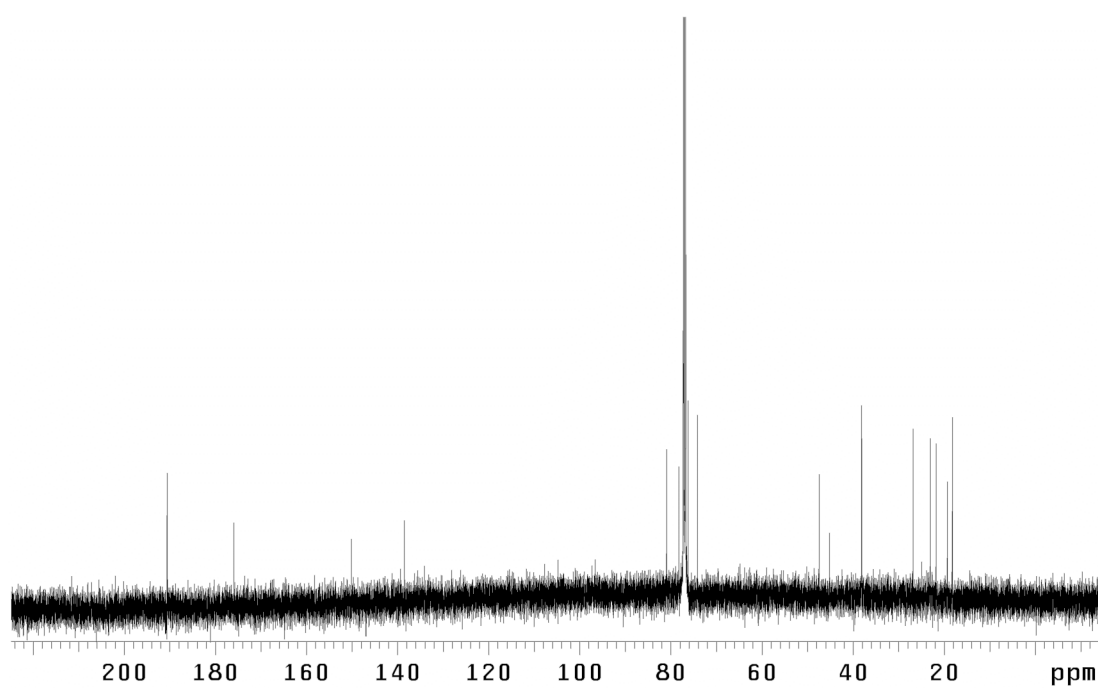


Figure B.96  $^{13}\text{C}$  NMR (125 MHz,  $\text{CDCl}_3$ ) of compound **280**.

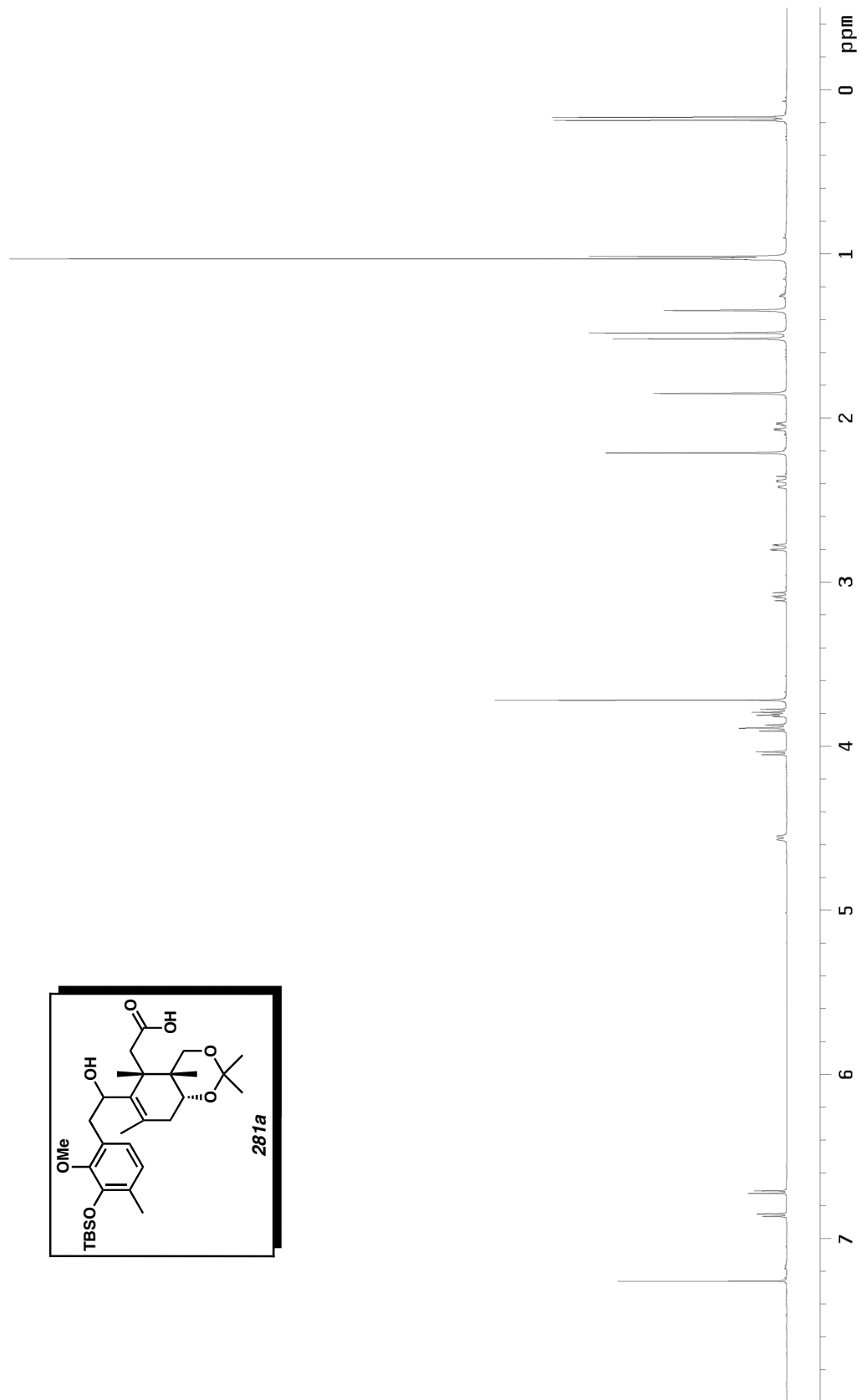
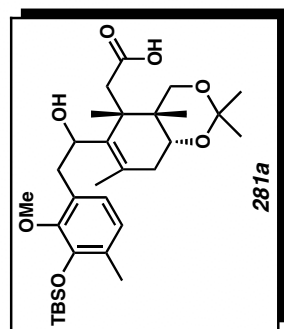


Figure B.97  $^1\text{H}$  NMR (500 MHz,  $\text{CDCl}_3$ ) of compound **281a**.

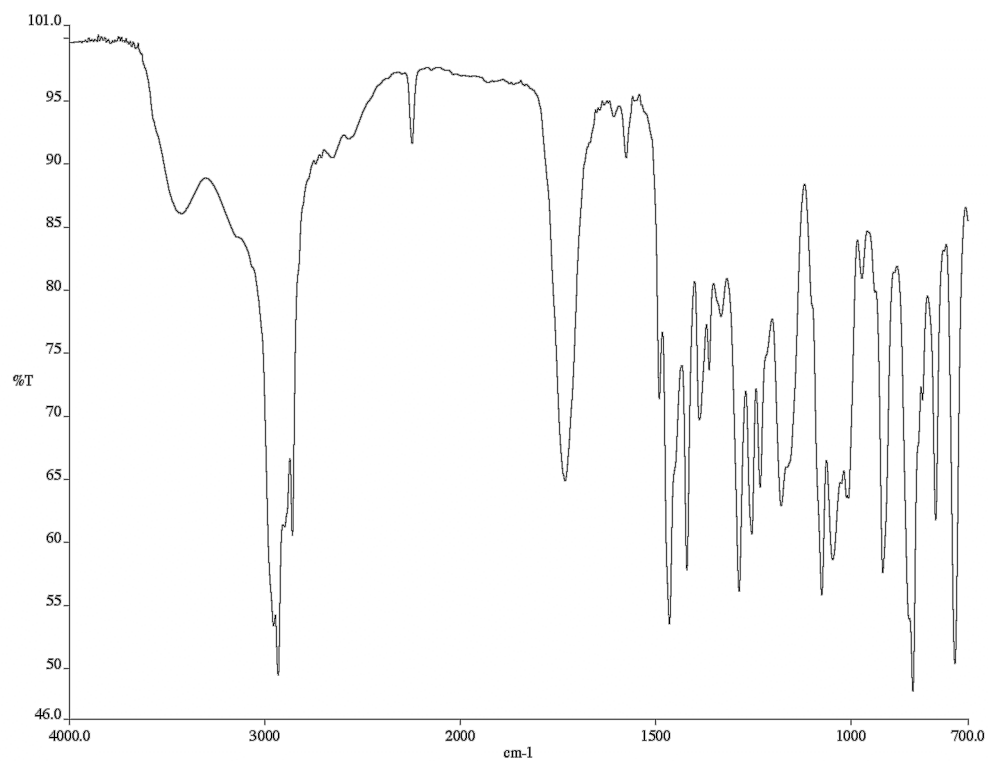


Figure B.98 Infrared spectrum (thin film/NaCl) of compound **281a**.

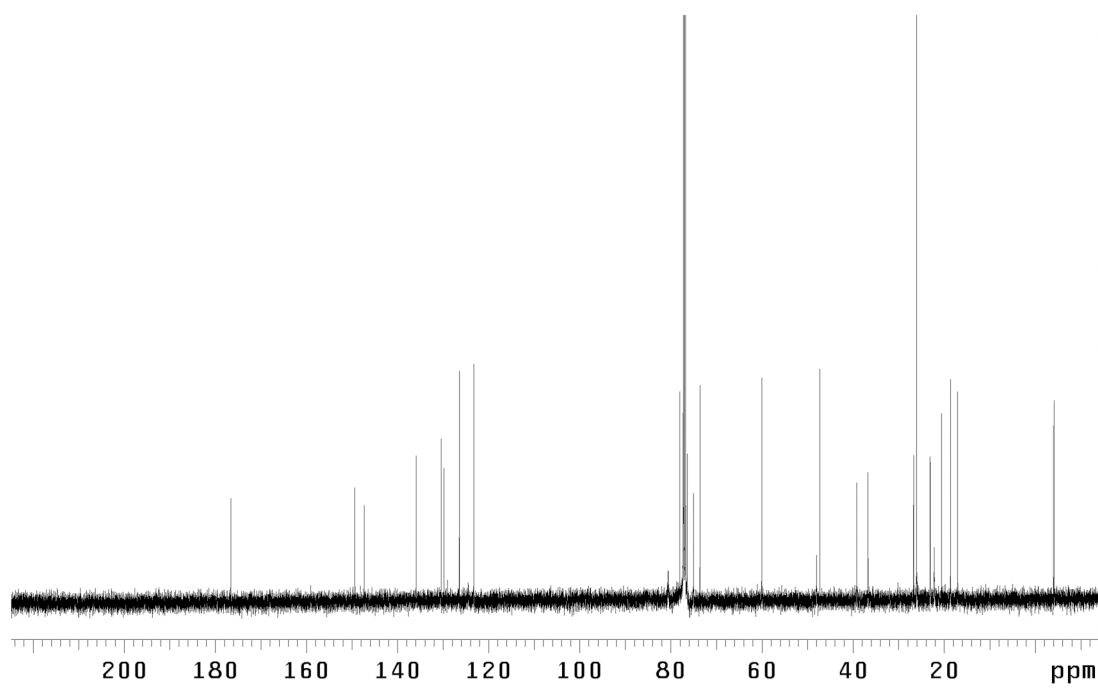


Figure B.99 <sup>13</sup>C NMR (125 MHz, CDCl<sub>3</sub>) of compound **281a**.

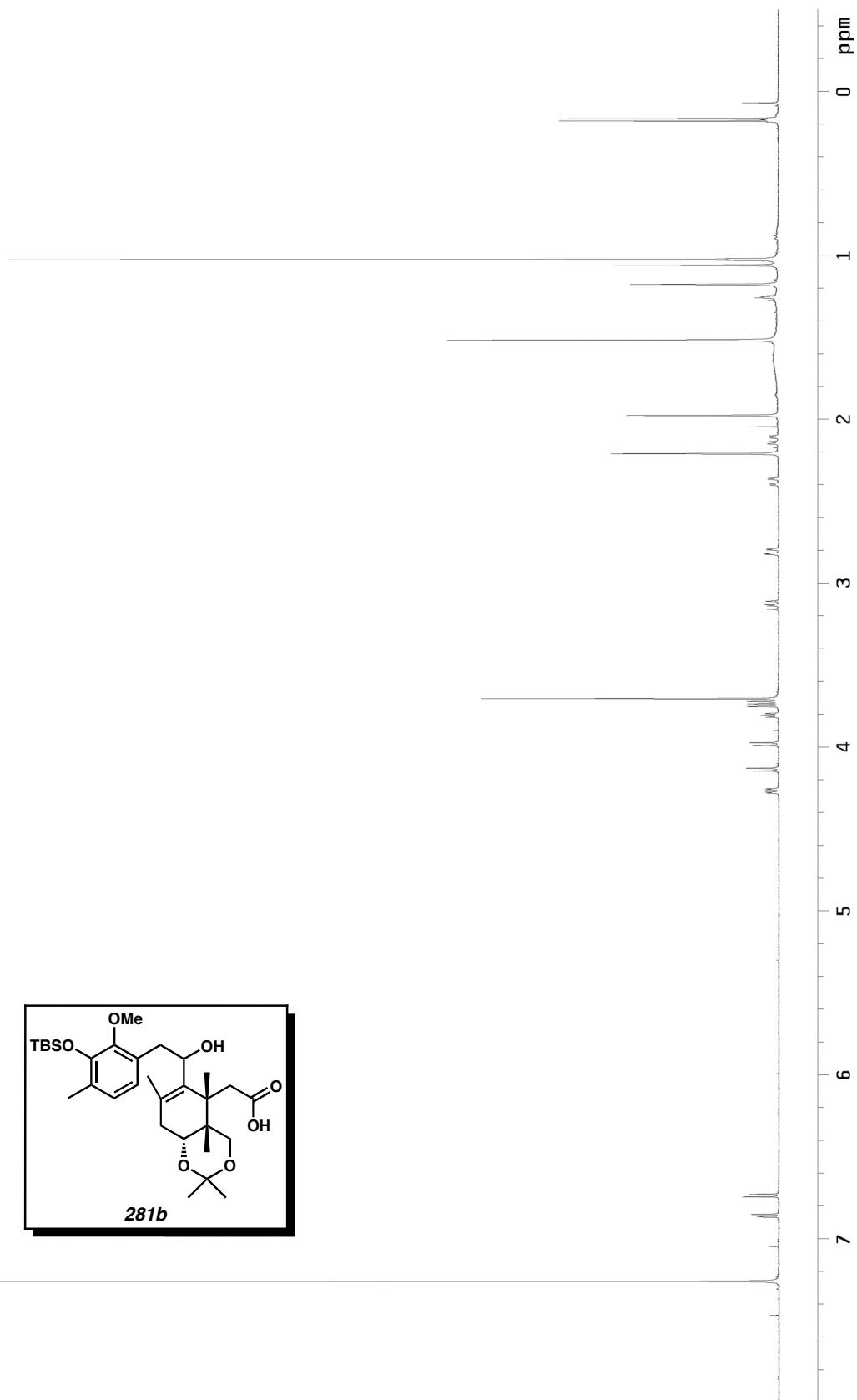
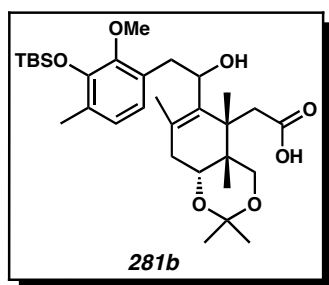


Figure B.100  $^1\text{H}$  NMR (500 MHz,  $\text{CDCl}_3$ ) of compound **281b**.

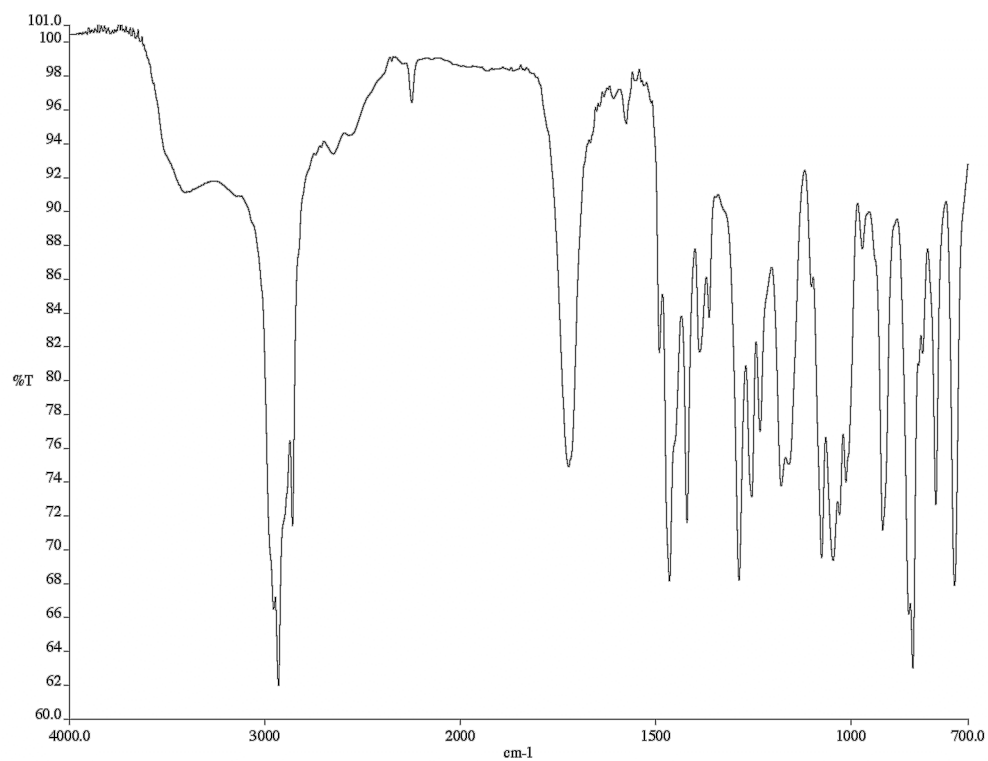


Figure B.101 Infrared spectrum (thin film/NaCl) of compound **281b**.

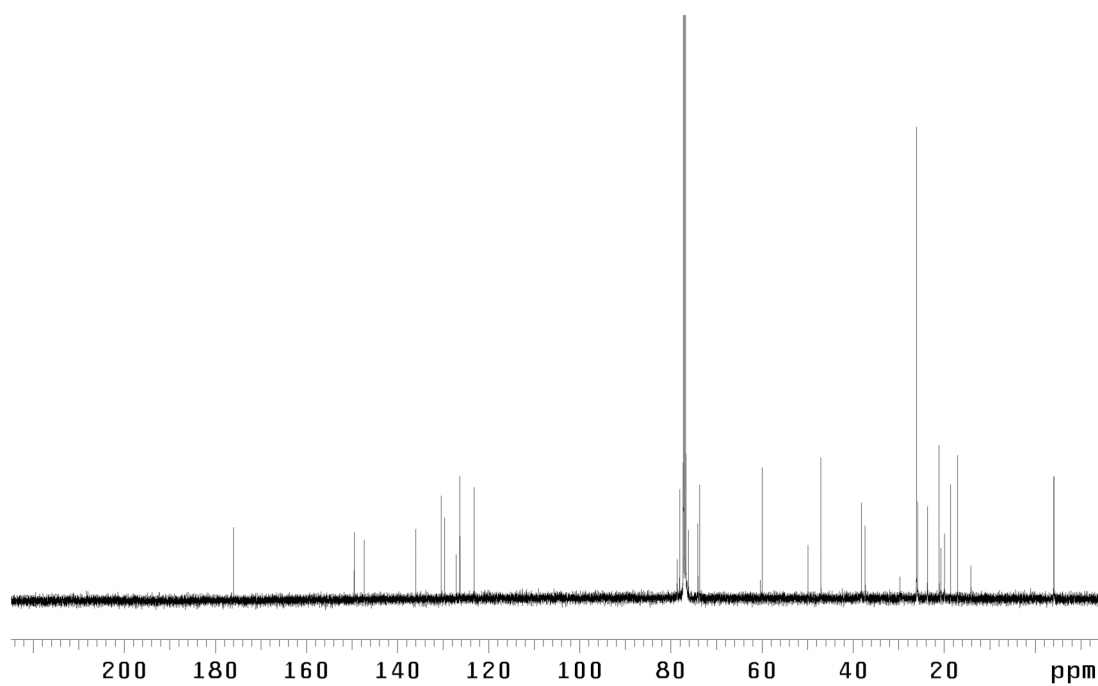


Figure B.102  $^{13}\text{C}$  NMR (125 MHz,  $\text{CDCl}_3$ ) of compound **281b**.

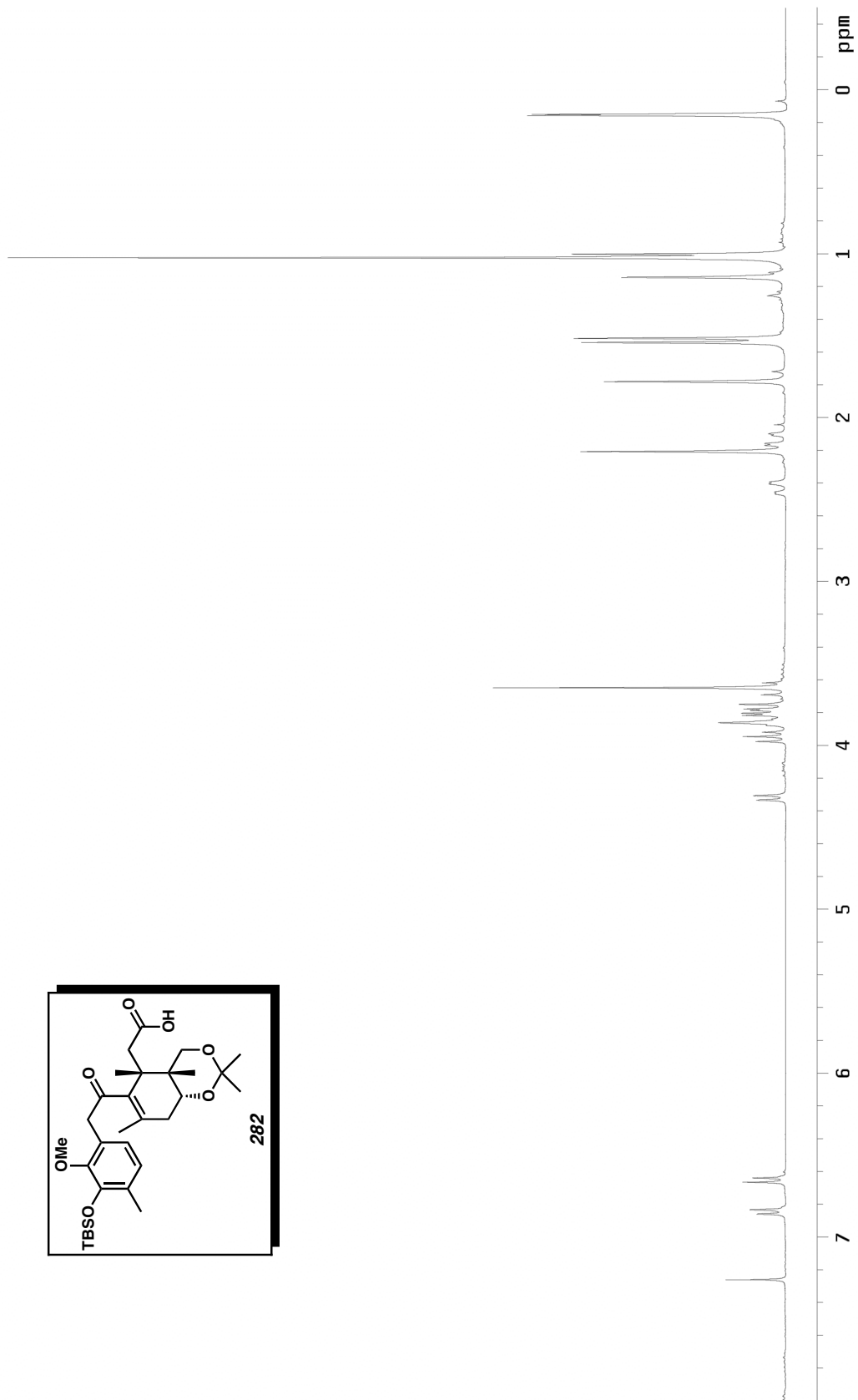
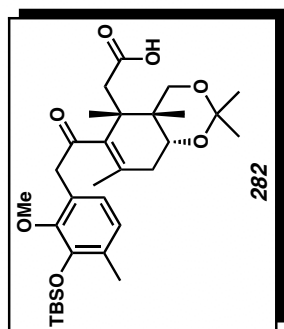


Figure B.103  $^1\text{H}$  NMR (300 MHz,  $\text{CDCl}_3$ ) of compound **282**.

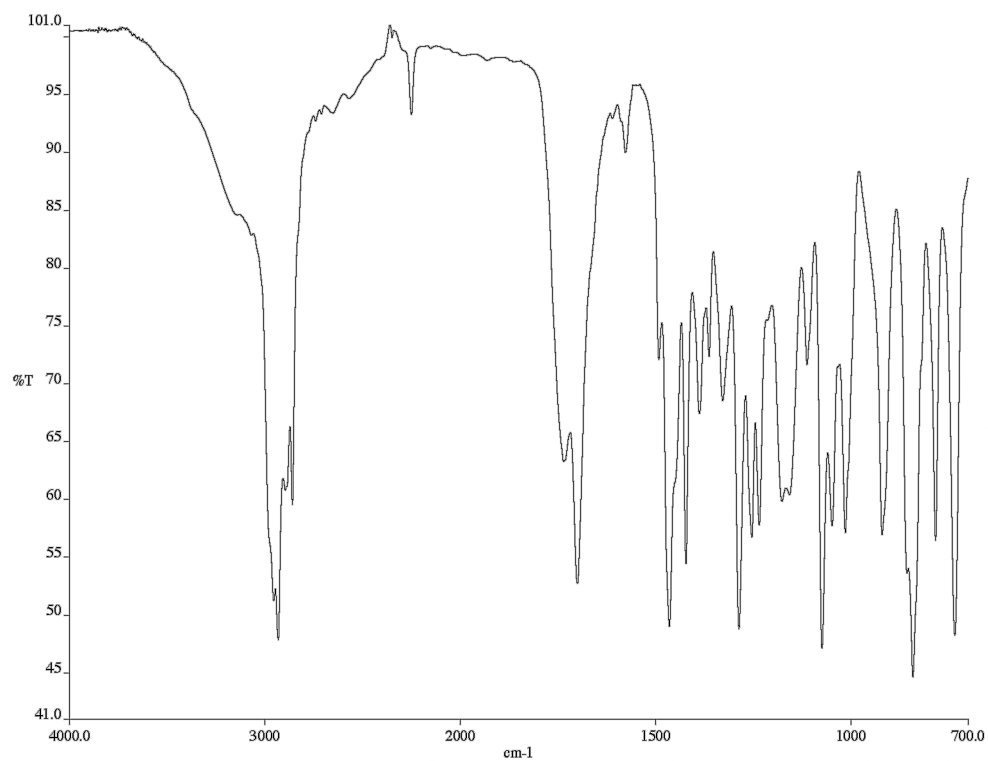


Figure B.104 Infrared spectrum (thin film/NaCl) of compound **282**.

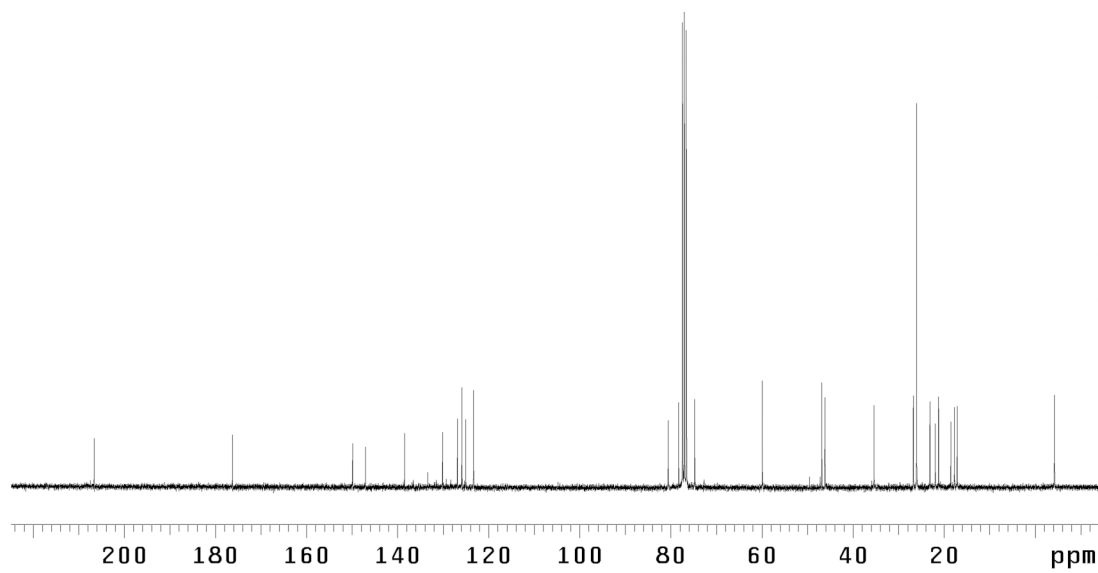


Figure B.105 <sup>13</sup>C NMR (75 MHz, CDCl<sub>3</sub>) of compound **282**.

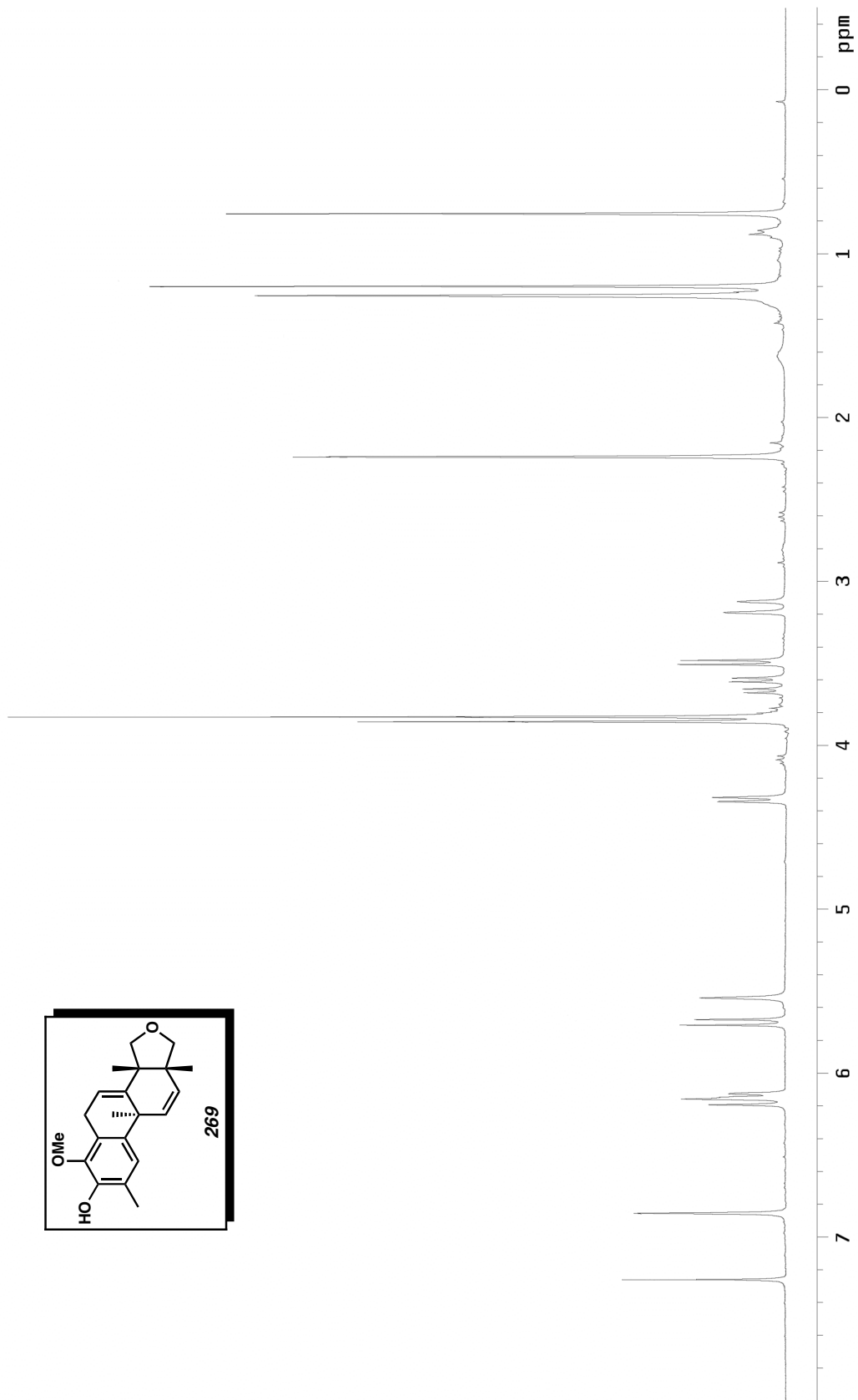
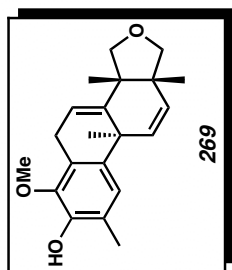


Figure B.106  $^1\text{H}$  NMR (300 MHz,  $\text{CDCl}_3$ ) of compound **269**.

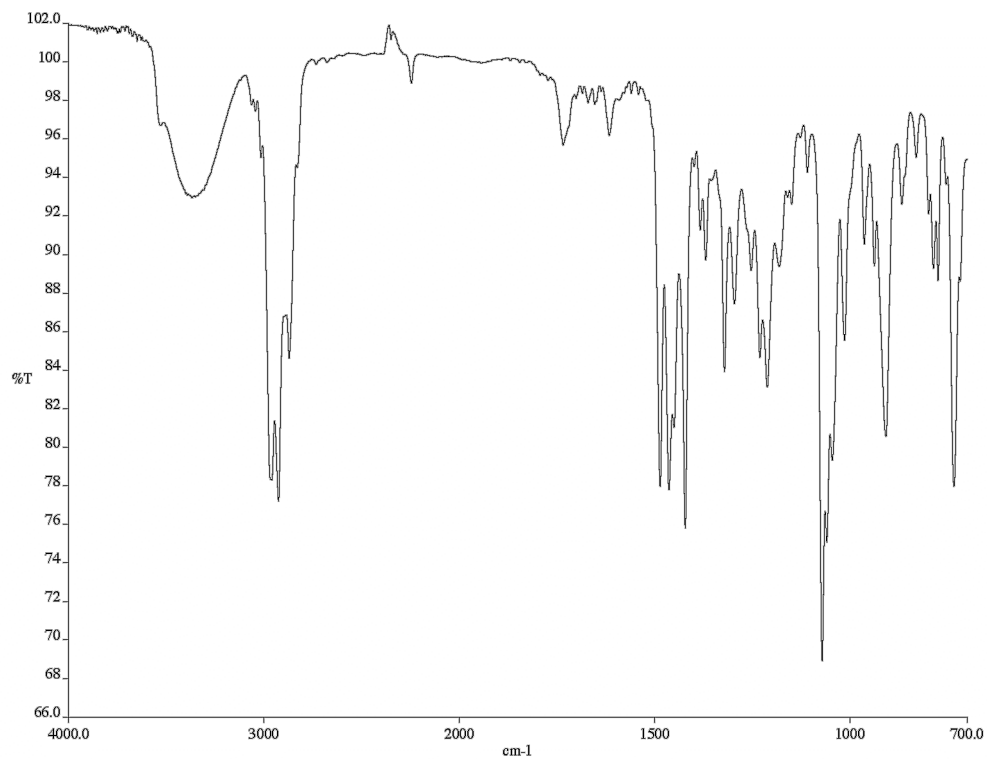


Figure B.107 Infrared spectrum (thin film/NaCl) of compound **269**.

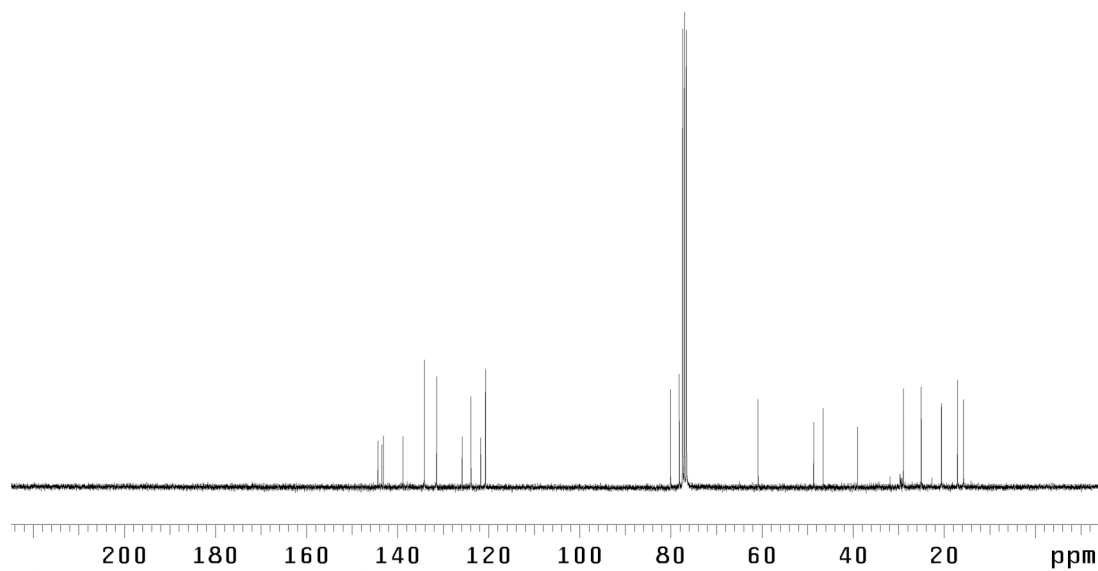


Figure B.108 <sup>13</sup>C NMR (75 MHz, CDCl<sub>3</sub>) of compound **269**.

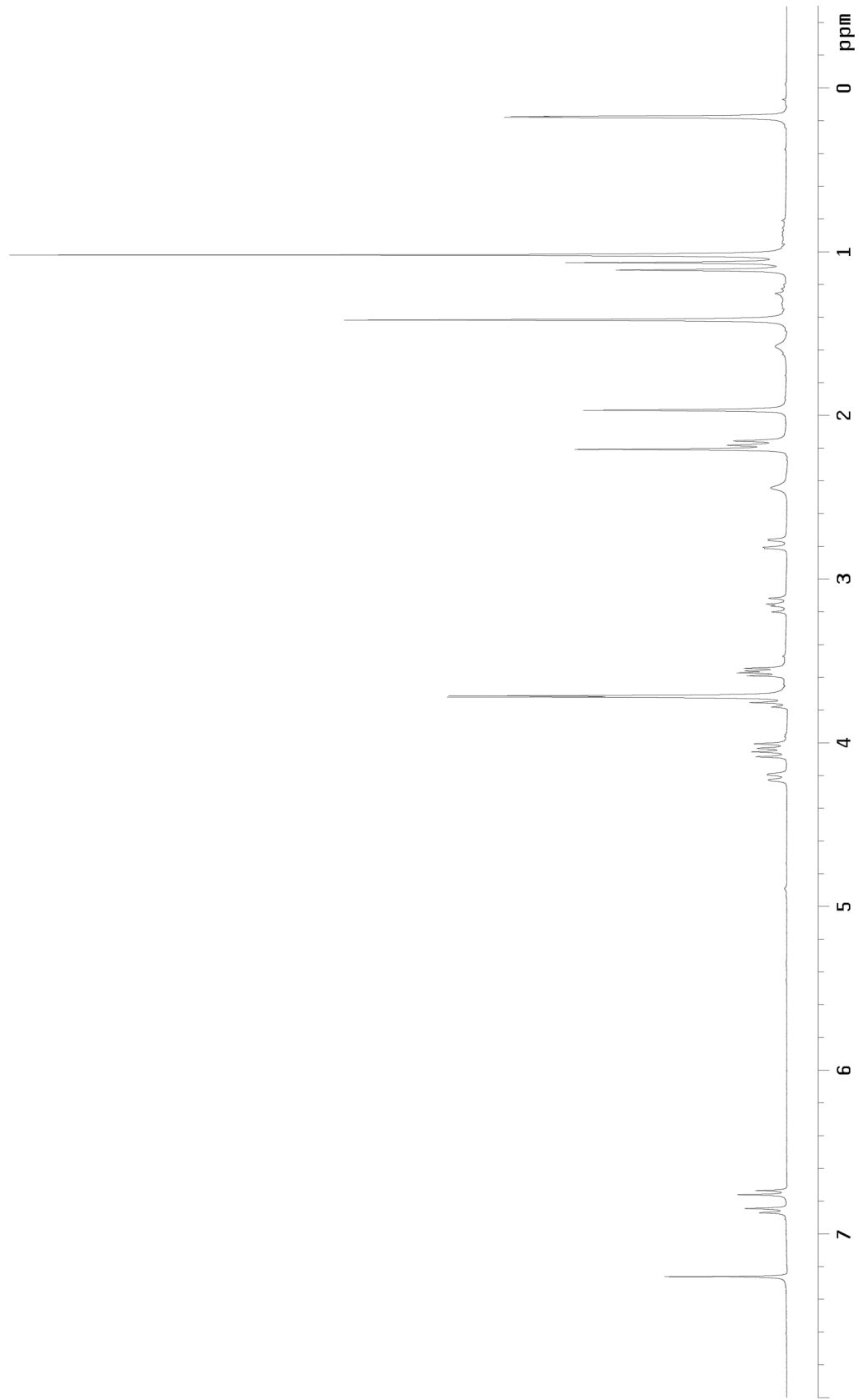


Figure B.109  $^1\text{H}$  NMR (300 MHz,  $\text{CDCl}_3$ ) of compound **283**.

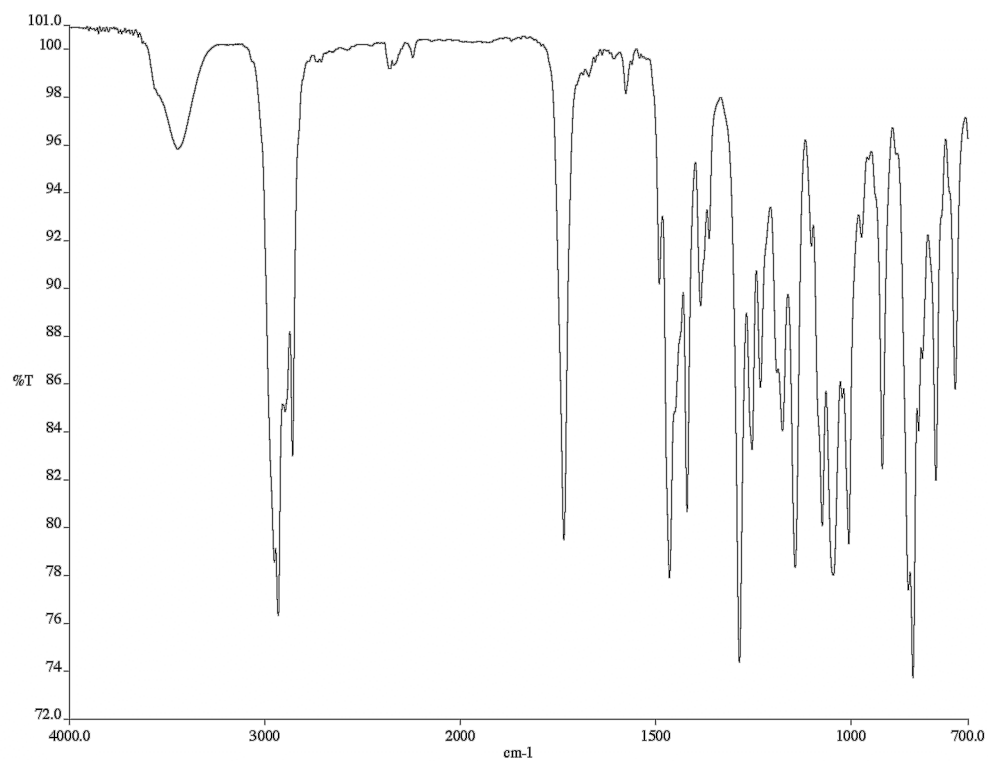


Figure B.110 Infrared spectrum (thin film/NaCl) of compound **283**.

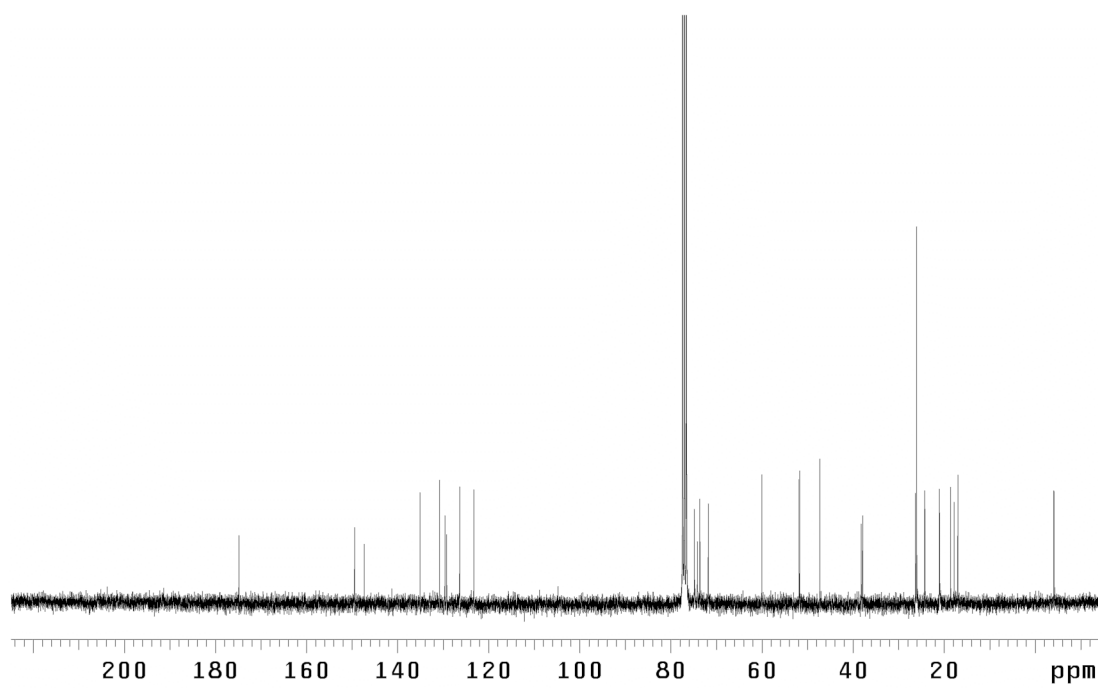


Figure B.111  $^{13}\text{C}$  NMR (75 MHz,  $\text{CDCl}_3$ ) of compound **283**.

CALIFORNIA INSTITUTE OF TECHNOLOGY  
BECKMAN INSTITUTE  
X-RAY CRYSTALLOGRAPHY LABORATORY

Crystal Structure Analysis of:  
Allylic Alcohol **248** (DCB30)  
(CCDC 277462)

Contents:

- Table 1. Crystal data
- Table 2. Atomic coordinates
- Table 3. Full bond distances and angles
- Table 4. Anisotropic displacement parameters
- Table 5. Hydrogen atomic coordinates
- Table 6. Hydrogen bond distances and angles

Figure B.112 Representation of Allylic Alcohol **248**

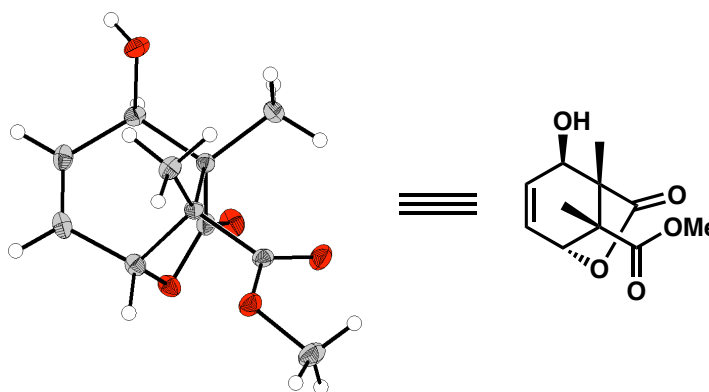


**Table 1.** Crystal data and structure refinement for DCB30 (CCDC 277462).

Empirical formula	C <sub>11</sub> H <sub>14</sub> O <sub>5</sub>
Formula weight	226.22
Crystallization Solvent	Heptane/diethylether
Crystal Habit	Fragment
Crystal size	0.41 x 0.24 x 0.16 mm <sup>3</sup>
Crystal color	Colorless

### Data Collection

Type of diffractometer	Bruker SMART 1000
Wavelength	0.71073 Å MoK $\alpha$
Data Collection Temperature	100(2) K
$\theta$ range for 8068 reflections used in lattice determination	2.74 to 39.14°
Unit cell dimensions	a = 8.5469(4) Å b = 8.7203(4) Å c = 14.1988(6) Å
Volume	1058.26(8) Å <sup>3</sup>
Z	4
Crystal system	Orthorhombic
Space group	P2 <sub>1</sub> 2 <sub>1</sub> 2 <sub>1</sub>
Density (calculated)	1.420 Mg/m <sup>3</sup>
F(000)	480
Data collection program	Bruker SMART v5.630
$\theta$ range for data collection	2.74 to 40.70°
Completeness to $\theta = 40.70^\circ$	92.3 %
Index ranges	-15 $\leq$ h $\leq$ 13, -15 $\leq$ k $\leq$ 15, -25 $\leq$ l $\leq$ 23
Data collection scan type	$\omega$ scans at 5 $\phi$ settings
Data reduction program	Bruker SAINT v6.45A
Reflections collected	19516
Independent reflections	6114 [ $R_{\text{int}} = 0.0607$ ]
Absorption coefficient	0.113 mm <sup>-1</sup>
Absorption correction	None
Max. and min. transmission	0.9822 and 0.9553

**Table 1** (cont.)**Structure Solution and Refinement**

Structure solution program	Bruker XS v6.12
Primary solution method	Direct methods
Secondary solution method	Difference Fourier map
Hydrogen placement	Difference Fourier map
Structure refinement program	Bruker XL v6.12
Refinement method	Full matrix least-squares on F <sup>2</sup>
Data / restraints / parameters	6114 / 0 / 201
Treatment of hydrogen atoms	Unrestrained
Goodness-of-fit on F <sup>2</sup>	1.304
Final R indices [ $I > 2\sigma(I)$ , 4485 reflections]	R1 = 0.0415, wR2 = 0.0690
R indices (all data)	R1 = 0.0621, wR2 = 0.0715
Type of weighting scheme used	Sigma
Weighting scheme used	$w=1/\sigma^2(F_0^2)$
Max shift/error	0.001
Average shift/error	0.000
Absolute structure determination configuration	Not possible to reliably determine absolute configuration
Absolute structure parameter	-0.2(6)
Largest diff. peak and hole	0.427 and -0.273 e.Å <sup>-3</sup>

**Special Refinement Details**

Refinement of F<sup>2</sup> against ALL reflections. The weighted R-factor ( $wR$ ) and goodness of fit ( $S$ ) are based on F<sup>2</sup>, conventional R-factors ( $R$ ) are based on F, with F set to zero for negative F<sup>2</sup>. The threshold expression of  $F^2 > 2\sigma(F^2)$  is used only for calculating R-factors(gt) etc. and is not relevant to the choice of reflections for refinement. R-factors based on F<sup>2</sup> are statistically about twice as large as those based on F, and R-factors based on ALL data will be even larger.

All esds (except the esd in the dihedral angle between two l.s. planes) are estimated using the full covariance matrix. The cell esds are taken into account individually in the estimation of esds in distances, angles and torsion angles; correlations between esds in cell parameters are only used when they are defined by crystal symmetry. An approximate (isotropic) treatment of cell esds is used for estimating esds involving l.s. planes.

**Table 2.** Atomic coordinates ( $\times 10^4$ ) and equivalent isotropic displacement parameters ( $\text{\AA}^2 \times 10^3$ ) for DCB30 (CCDC 277462).  $U(\text{eq})$  is defined as the trace of the orthogonalized  $U^{ij}$  tensor.

	x	y	z	$U_{\text{eq}}$
O(1)	1165(1)	11191(1)	7918(1)	16(1)
O(2)	1872(1)	13004(1)	8946(1)	21(1)
O(3)	4173(1)	9617(1)	8803(1)	21(1)
O(4)	3237(1)	7678(1)	7931(1)	18(1)
O(5)	-878(1)	9680(1)	10618(1)	19(1)
C(1)	-1241(1)	9774(1)	8195(1)	17(1)
C(2)	492(1)	9626(1)	8002(1)	15(1)
C(3)	1380(1)	8989(1)	8868(1)	12(1)
C(4)	1180(1)	10414(1)	9520(1)	12(1)
C(5)	-565(1)	10628(1)	9813(1)	14(1)
C(6)	-1706(1)	10259(1)	9031(1)	17(1)
C(7)	1471(1)	11701(1)	8802(1)	14(1)
C(8)	2214(1)	10544(1)	10395(1)	16(1)
C(9)	763(1)	7465(1)	9253(1)	16(1)
C(10)	3095(1)	8815(1)	8558(1)	14(1)
C(11)	4809(1)	7460(1)	7566(1)	23(1)

**Table 3.** Bond lengths [Å] and angles [°] for DCB30 (CCDC 277462).

O(1)-C(7)	1.3559(11)	C(8)-C(4)-C(7)	113.05(7)
O(1)-C(2)	1.4855(11)	C(8)-C(4)-C(3)	118.58(7)
O(2)-C(7)	1.2050(11)	C(7)-C(4)-C(3)	99.84(6)
O(3)-C(10)	1.2082(11)	C(8)-C(4)-C(5)	109.06(7)
O(4)-C(10)	1.3387(11)	C(7)-C(4)-C(5)	104.16(7)
O(4)-C(11)	1.4519(12)	C(3)-C(4)-C(5)	111.03(7)
O(5)-C(5)	1.4350(11)		
O(5)-H(5A)	0.783(13)	O(5)-C(5)-C(6)	110.00(7)
C(1)-C(6)	1.3223(13)	O(5)-C(5)-C(4)	108.75(7)
C(1)-C(2)	1.5115(13)	C(6)-C(5)-C(4)	113.26(7)
C(1)-H(1)	0.973(11)	O(5)-C(5)-H(5)	109.9(6)
C(2)-C(3)	1.5486(12)	C(6)-C(5)-H(5)	108.8(6)
C(2)-H(2)	0.989(9)		
C(3)-C(9)	1.5301(12)	C(4)-C(5)-H(5)	106.0(6)
C(3)-C(10)	1.5380(13)	C(1)-C(6)-C(5)	122.26(8)
C(3)-C(4)	1.5586(12)	C(1)-C(6)-H(6)	120.8(6)
C(4)-C(8)	1.5294(12)	C(5)-C(6)-H(6)	116.9(6)
C(4)-C(7)	1.5365(12)	O(2)-C(7)-O(1)	121.44(8)
C(4)-C(5)	1.5600(12)	O(2)-C(7)-C(4)	128.47(8)
C(5)-C(6)	1.5120(13)	O(1)-C(7)-C(4)	110.07(7)
C(5)-H(5)	0.994(11)	C(4)-C(8)-H(8A)	108.8(6)
C(6)-H(6)	0.951(10)	C(4)-C(8)-H(8B)	108.5(7)
C(8)-H(8A)	1.025(12)	H(8A)-C(8)-H(8B)	109.1(9)
C(8)-H(8B)	0.977(11)	C(4)-C(8)-H(8C)	112.1(7)
C(8)-H(8C)	0.976(12)	H(8A)-C(8)-H(8C)	105.7(10)
C(9)-H(9A)	0.987(11)	H(8B)-C(8)-H(8C)	112.6(10)
C(9)-H(9B)	0.952(11)	C(3)-C(9)-H(9A)	110.7(6)
C(9)-H(9C)	0.952(12)	C(3)-C(9)-H(9B)	111.9(7)
C(11)-H(11A)	0.967(12)	H(9A)-C(9)-H(9B)	104.0(9)
C(11)-H(11B)	0.940(13)	C(3)-C(9)-H(9C)	110.2(7)
C(11)-H(11C)	0.962(12)	H(9A)-C(9)-H(9C)	108.6(9)
		H(9B)-C(9)-H(9C)	111.2(10)
C(7)-O(1)-C(2)	107.57(7)	O(3)-C(10)-O(4)	123.45(8)
C(10)-O(4)-C(11)	114.73(8)	O(3)-C(10)-C(3)	125.99(8)
C(5)-O(5)-H(5A)	104.1(10)	O(4)-C(10)-C(3)	110.48(7)
C(6)-C(1)-C(2)	119.00(8)	O(4)-C(11)-H(11A)	107.9(7)
C(6)-C(1)-H(1)	122.2(6)	O(4)-C(11)-H(11B)	106.0(8)
C(2)-C(1)-H(1)	118.8(6)	H(11A)-C(11)-H(11B)	111.7(10)
O(1)-C(2)-C(1)	108.39(7)	O(4)-C(11)-H(11C)	108.7(7)
O(1)-C(2)-C(3)	101.75(7)	H(11A)-C(11)-H(11C)	111.6(9)
C(1)-C(2)-C(3)	111.51(7)	H(11B)-C(11)-H(11C)	110.6(10)
O(1)-C(2)-H(2)	105.7(6)		
C(1)-C(2)-H(2)	112.9(6)		
C(3)-C(2)-H(2)	115.6(5)		
C(9)-C(3)-C(10)	110.19(7)		
C(9)-C(3)-C(2)	115.23(8)		
C(10)-C(3)-C(2)	105.96(7)		
C(9)-C(3)-C(4)	116.29(7)		
C(10)-C(3)-C(4)	110.65(7)		
C(2)-C(3)-C(4)	97.55(7)		

**Table 4.** Anisotropic displacement parameters ( $\text{\AA}^2 \times 10^4$ ) for DCB3o (CCDC 277462). The anisotropic displacement factor exponent takes the form:  $-2\pi^2 [ h^2 a^{*2} U^{11} + \dots + 2 h k a^* b^* U^{12} ]$

	U <sup>11</sup>	U <sup>22</sup>	U <sup>33</sup>	U <sup>23</sup>	U <sup>13</sup>	U <sup>12</sup>
O(1)	203(3)	149(3)	142(3)	30(2)	-26(3)	-27(3)
O(2)	239(4)	146(3)	239(3)	28(3)	-42(3)	-47(3)
O(3)	154(3)	239(4)	236(3)	-25(3)	30(3)	-54(3)
O(4)	154(3)	204(3)	196(3)	-37(3)	29(3)	16(3)
O(5)	178(3)	213(3)	185(3)	47(3)	60(3)	34(3)
C(1)	159(4)	156(4)	203(4)	11(3)	-58(3)	-11(4)
C(2)	167(4)	130(4)	149(4)	-4(3)	-18(3)	-17(4)
C(3)	129(4)	116(4)	122(3)	8(3)	3(3)	-2(3)
C(4)	120(4)	119(4)	124(3)	11(3)	-4(3)	0(3)
C(5)	147(4)	127(4)	144(4)	9(3)	21(3)	14(3)
C(6)	129(4)	162(4)	230(4)	24(3)	-19(3)	10(4)
C(7)	118(4)	149(4)	157(4)	18(3)	-10(3)	3(3)
C(8)	163(4)	190(5)	138(4)	6(3)	-24(3)	-5(4)
C(9)	154(4)	117(4)	201(4)	11(3)	21(4)	-5(4)
C(10)	148(4)	151(4)	120(4)	32(3)	18(3)	10(4)
C(11)	191(5)	259(6)	230(5)	-5(4)	75(4)	52(4)

**Table 5.** Hydrogen coordinates ( $\times 10^4$ ) and isotropic displacement parameters ( $\text{\AA}^2 \times 10^3$ ) for DCB30 (CCDC 277462).

	x	y	z	$U_{\text{iso}}$
H(5A)	-1603(15)	10067(15)	10856(9)	35(4)
H(1)	-1977(13)	9484(13)	7703(7)	18(3)
H(2)	719(11)	9112(11)	7397(7)	6(2)
H(5)	-680(12)	11727(13)	9986(7)	15(3)
H(6)	-2786(12)	10404(12)	9164(7)	14(3)
H(8A)	1942(13)	11540(14)	10742(8)	23(3)
H(8B)	1993(13)	9673(14)	10807(7)	23(3)
H(8C)	3321(14)	10627(15)	10235(8)	29(3)
H(9A)	1386(12)	7128(12)	9800(8)	17(3)
H(9B)	-271(13)	7561(12)	9496(8)	17(3)
H(9C)	815(14)	6693(14)	8779(8)	27(3)
H(11A)	5491(14)	7243(13)	8093(8)	20(3)
H(11B)	4748(14)	6625(15)	7148(9)	29(3)
H(11C)	5121(13)	8376(14)	7239(8)	20(3)

**Table 6.** Hydrogen bonds for DCB30 (CCDC 277462) [ $\text{\AA}$  and  $^\circ$ ].

D-H...A	d(D-H)	d(H...A)	d(D...A)	<(DHA)
O(5)-H(5A)...O(2)#1	0.783(13)	2.147(13)	2.8567(10)	151.0(13)

Symmetry transformations used to generate equivalent atoms:

#1  $x-1/2, -y+5/2, -z+2$

CALIFORNIA INSTITUTE OF TECHNOLOGY  
BECKMAN INSTITUTE  
X-RAY CRYSTALLOGRAPHY LABORATORY

Crystal Structure Analysis of:

Allylic Alcohol **253** (DCB31)

(CCDC 283708)

Contents:

- Table 1. Crystal data
- Table 2. Atomic coordinates
- Table 3. Full bond distances and angles
- Table 4. Anisotropic displacement parameters
- Table 5. Hydrogen atomic coordinates
- Table 6. Hydrogen-bond distances and angles

Figure B.113 Representation of Allylic Alcohol **253**

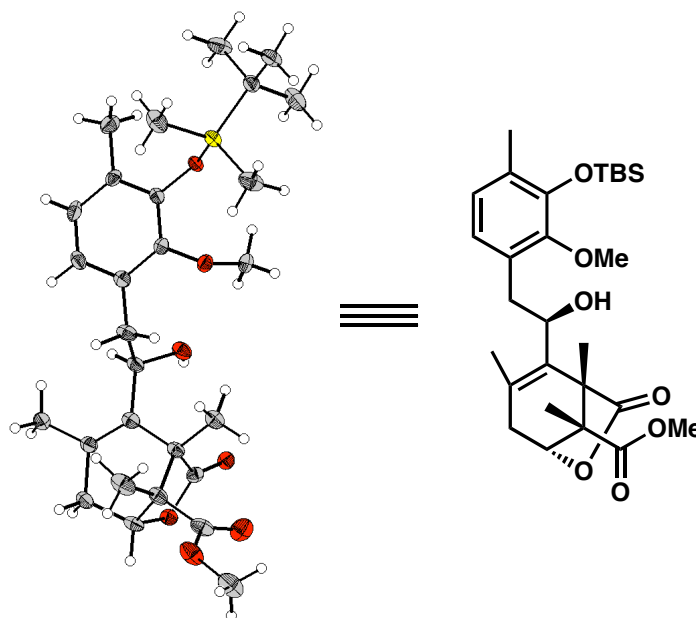


**Table 1.** Crystal data and structure refinement for DCB31 (CCDC 283708).

Empirical formula	C <sub>28</sub> H <sub>42</sub> O <sub>7</sub> Si
Formula weight	518.71
Crystallization Solvent	EtOAc/heptane
Crystal Habit	Block
Crystal size	0.32 x 0.31 x 0.22 mm <sup>3</sup>
Crystal color	Colorless

### Data Collection

Type of diffractometer	Bruker SMART 1000	
Wavelength	0.71073 Å MoK $\alpha$	
Data Collection Temperature	100(2) K	
$\theta$ range for 15772 reflections used in lattice determination	2.32 to 28.21°	
Unit cell dimensions	a = 12.6604(8) Å b = 15.4100(10) Å c = 15.7147(10) Å	$\alpha$ = 81.0750(10)° $\beta$ = 66.6280(10)° $\gamma$ = 87.6100(10)°
Volume	2779.6(3) Å <sup>3</sup>	
Z	4	
Crystal system	Triclinic	
Space group	P-1	
Density (calculated)	1.240 Mg/m <sup>3</sup>	
F(000)	1120	
Data collection program	Bruker SMART v5.630	
$\theta$ range for data collection	1.75 to 28.27°	
Completeness to $\theta = 28.27^\circ$	92.1 %	
Index ranges	-16 $\leq$ h $\leq$ 16, -20 $\leq$ k $\leq$ 19, -20 $\leq$ l $\leq$ 20	
Data collection scan type	$\omega$ scans at 7 $\phi$ settings	
Data reduction program	Bruker SAINT v6.45A	
Reflections collected	56601	
Independent reflections	12691 [R <sub>int</sub> = 0.0626]	
Absorption coefficient	0.127 mm <sup>-1</sup>	
Absorption correction	None	
Max. and min. transmission	0.9725 and 0.9604	

**Table 1** (cont.)**Structure solution and Refinement**

Structure solution program	SHELXS-97 (Sheldrick, 1990)
Primary solution method	Direct methods
Secondary solution method	Difference Fourier map
Hydrogen placement	Difference Fourier map
Structure refinement program	SHELXL-97 (Sheldrick, 1997)
Refinement method	Full matrix least-squares on $F^2$
Data / restraints / parameters	12691 / 0 / 985
Treatment of hydrogen atoms	Unrestrained
Goodness-of-fit on $F^2$	1.502
Final R indices [ $I > 2\sigma(I)$ , 7901 reflections]	$R_1 = 0.0455$ , $wR_2 = 0.0721$
R indices (all data)	$R_1 = 0.0839$ , $wR_2 = 0.0763$
Type of weighting scheme used	Sigma
Weighting scheme used	$w = 1/\sigma^2(F_0^2)$
Max shift/error	0.003
Average shift/error	0.000
Largest diff. peak and hole	0.492 and -0.382 e.Å <sup>-3</sup>

**Special Refinement Details**

Refinement of  $F^2$  against ALL reflections. The weighted R-factor ( $wR$ ) and goodness of fit ( $S$ ) are based on  $F^2$ , conventional R-factors ( $R$ ) are based on  $F$ , with  $F$  set to zero for negative  $F^2$ . The threshold expression of  $F^2 > 2\sigma(F^2)$  is used only for calculating R-factors(gt) etc. and is not relevant to the choice of reflections for refinement. R-factors based on  $F^2$  are statistically about twice as large as those based on  $F$ , and R-factors based on ALL data will be even larger.

All esds (except the esd in the dihedral angle between two l.s. planes) are estimated using the full covariance matrix. The cell esds are taken into account individually in the estimation of esds in distances, angles and torsion angles; correlations between esds in cell parameters are only used when they are defined by crystal symmetry. An approximate (isotropic) treatment of cell esds is used for estimating esds involving l.s. planes.

**Table 2.** Atomic coordinates ( $\times 10^4$ ) and equivalent isotropic displacement parameters ( $\text{\AA}^2 \times 10^3$ ) for DCB31 (CCDC 283708).  $U(\text{eq})$  is defined as the trace of the orthogonalized  $U^{ij}$  tensor.

	x	y	z	$U_{\text{eq}}$
Si(1)	-42(1)	510(1)	2060(1)	21(1)
O(1A)	816(1)	1084(1)	2346(1)	19(1)
O(2A)	1297(1)	2515(1)	937(1)	23(1)
O(3A)	3033(1)	4131(1)	770(1)	26(1)
O(4A)	3980(1)	6315(1)	-2542(1)	37(1)
O(5A)	2422(1)	7069(1)	-2515(1)	38(1)
O(6A)	4208(1)	6810(1)	-903(1)	21(1)
O(7A)	4924(1)	5456(1)	-917(1)	22(1)
C(1A)	646(1)	1925(1)	2572(1)	18(1)
C(2A)	899(1)	2648(1)	1864(1)	18(1)
C(3A)	719(1)	3501(1)	2073(1)	21(1)
C(4A)	306(2)	3607(1)	3011(1)	27(1)
C(5A)	107(2)	2895(1)	3709(1)	26(1)
C(6A)	276(1)	2039(1)	3508(1)	20(1)
C(7A)	81(2)	1260(1)	4263(1)	29(1)
C(8A)	2448(2)	2186(2)	597(2)	28(1)
C(9A)	166(2)	811(2)	810(2)	38(1)
C(10A)	-1553(2)	709(2)	2806(2)	35(1)
C(11A)	375(1)	-659(1)	2268(1)	22(1)
C(12A)	-338(2)	-1258(1)	1990(2)	30(1)
C(13A)	1656(2)	-771(2)	1691(2)	37(1)
C(14A)	138(2)	-938(1)	3311(1)	34(1)
C(15A)	999(2)	4291(1)	1317(1)	25(1)
C(16A)	2140(1)	4736(1)	1130(1)	21(1)
C(17A)	2349(1)	5629(1)	503(1)	20(1)
C(18A)	2866(1)	5673(1)	-583(1)	20(1)
C(19A)	2473(1)	6519(1)	-1042(1)	24(1)
C(20A)	3079(2)	7190(1)	-749(1)	24(1)
C(21A)	2454(2)	7262(1)	276(1)	24(1)
C(22A)	2158(1)	6374(1)	879(1)	22(1)
C(23A)	1640(2)	6435(1)	1910(1)	29(1)
C(24A)	2706(2)	4851(1)	-947(1)	25(1)
C(25A)	4114(2)	5923(1)	-833(1)	20(1)
C(26A)	1171(2)	6613(2)	-701(2)	35(1)
C(27A)	3055(2)	6601(1)	-2107(1)	28(1)
C(28A)	2900(3)	7207(2)	-3527(2)	44(1)
Si(2)	5149(1)	9590(1)	2638(1)	21(1)
O(1B)	4218(1)	9004(1)	2444(1)	20(1)
O(2B)	3743(1)	7599(1)	3860(1)	24(1)
O(3B)	1918(1)	5944(1)	4116(1)	26(1)
O(4B)	1344(1)	3774(1)	7408(1)	34(1)
O(5B)	2918(1)	2985(1)	7232(1)	32(1)
O(6B)	863(1)	3261(1)	5877(1)	21(1)
O(7B)	126(1)	4607(1)	5934(1)	23(1)
C(1B)	4350(1)	8159(1)	2224(1)	17(1)
C(2B)	4097(1)	7444(1)	2943(1)	18(1)

C(3B)	4225(1)	6587(1)	2749(1)	21(1)
C(4B)	4584(1)	6466(1)	1817(1)	24(1)
C(5B)	4779(1)	7171(1)	1112(1)	24(1)
C(6B)	4666(1)	8032(1)	1295(1)	19(1)
C(7B)	4854(2)	8801(1)	525(1)	26(1)
C(8B)	2574(2)	7893(1)	4228(1)	29(1)
C(9B)	5680(2)	8968(1)	3484(2)	29(1)
C(10B)	6404(2)	9919(2)	1510(2)	33(1)
C(11B)	4327(2)	10573(1)	3092(1)	25(1)
C(12B)	5122(2)	11175(1)	3282(2)	32(1)
C(13B)	3289(2)	10289(2)	4020(2)	46(1)
C(14B)	3894(2)	11088(2)	2385(2)	46(1)
C(15B)	3966(2)	5805(1)	3514(1)	25(1)
C(16B)	2821(1)	5350(1)	3733(1)	19(1)
C(17B)	2636(1)	4457(1)	4354(1)	19(1)
C(18B)	2219(1)	4416(1)	5438(1)	19(1)
C(19B)	2690(1)	3582(1)	5839(1)	22(1)
C(20B)	2018(2)	2897(1)	5624(1)	22(1)
C(21B)	2507(2)	2827(1)	4603(1)	22(1)
C(22B)	2764(1)	3713(1)	3988(1)	20(1)
C(23B)	3189(2)	3634(1)	2963(1)	26(1)
C(24B)	2419(2)	5244(1)	5771(1)	23(1)
C(25B)	955(2)	4150(1)	5785(1)	19(1)
C(26B)	3999(2)	3506(2)	5394(2)	29(1)
C(27B)	2231(2)	3484(1)	6908(1)	25(1)
C(28B)	2541(2)	2794(2)	8236(1)	35(1)

---

**Table 3.** Bond lengths [Å] and angles [°] for DCB31 (CCDC 283708).

Si(1)-O(1A)	1.6602(11)	C(17A)-C(22A)	1.342(2)
Si(1)-C(10A)	1.847(2)	C(17A)-C(18A)	1.559(2)
Si(1)-C(9A)	1.860(2)	C(18A)-C(25A)	1.520(2)
Si(1)-C(11A)	1.8719(17)	C(18A)-C(24A)	1.519(2)
O(1A)-C(1A)	1.3834(18)	C(18A)-C(19A)	1.552(2)
O(2A)-C(2A)	1.3854(18)	C(19A)-C(26A)	1.525(2)
O(2A)-C(8A)	1.440(2)	C(19A)-C(27A)	1.525(2)
O(3A)-C(16A)	1.4266(19)	C(19A)-C(20A)	1.538(2)
O(3A)-H(3A)	0.92(2)	C(20A)-C(21A)	1.506(2)
O(4A)-C(27A)	1.203(2)	C(20A)-H(20A)	1.015(16)
O(5A)-C(27A)	1.337(2)	C(21A)-C(22A)	1.505(2)
O(5A)-C(28A)	1.442(2)	C(21A)-H(21A)	0.976(15)
O(6A)-C(25A)	1.3611(19)	C(21A)-H(21B)	1.002(16)
O(6A)-C(20A)	1.4637(19)	C(22A)-C(23A)	1.505(2)
O(7A)-C(25A)	1.2020(18)	C(23A)-H(23A)	0.95(2)
C(1A)-C(2A)	1.394(2)	C(23A)-H(23B)	0.963(19)
C(1A)-C(6A)	1.393(2)	C(23A)-H(23C)	0.98(2)
C(2A)-C(3A)	1.392(2)	C(24A)-H(24A)	0.973(16)
C(3A)-C(4A)	1.389(2)	C(24A)-H(24B)	1.022(16)
C(3A)-C(15A)	1.508(2)	C(24A)-H(24C)	0.984(16)
C(4A)-C(5A)	1.378(2)	C(26A)-H(26A)	1.042(16)
C(4A)-H(4A)	0.933(16)	C(26A)-H(26B)	0.994(18)
C(5A)-C(6A)	1.392(2)	C(26A)-H(26C)	0.944(18)
C(5A)-H(5A)	0.918(15)	C(28A)-H(28A)	0.96(2)
C(6A)-C(7A)	1.504(2)	C(28A)-H(28B)	1.00(2)
C(7A)-H(7A1)	0.978(19)	C(28A)-H(28C)	0.95(2)
C(7A)-H(7A2)	0.991(17)	Si(2)-O(1B)	1.6614(12)
C(7A)-H(7A3)	0.977(17)	Si(2)-C(9B)	1.844(2)
C(8A)-H(8A1)	0.96(2)	Si(2)-C(10B)	1.864(2)
C(8A)-H(8A2)	0.96(2)	Si(2)-C(11B)	1.8712(17)
C(8A)-H(8A3)	0.980(18)	O(1B)-C(1B)	1.3842(18)
C(9A)-H(9A1)	0.96(2)	O(2B)-C(2B)	1.3868(18)
C(9A)-H(9A2)	0.99(2)	O(2B)-C(8B)	1.441(2)
C(9A)-H(9A3)	1.04(2)	O(3B)-C(16B)	1.4298(19)
C(10A)-H(10A)	1.032(18)	O(3B)-H(3B)	0.98(3)
C(10A)-H(10B)	0.95(2)	O(4B)-C(27B)	1.2025(19)
C(10A)-H(10C)	0.91(2)	O(5B)-C(27B)	1.3347(19)
C(11A)-C(13A)	1.530(2)	O(5B)-C(28B)	1.441(2)
C(11A)-C(14A)	1.537(2)	O(6B)-C(25B)	1.3590(19)
C(11A)-C(12A)	1.539(2)	O(6B)-C(20B)	1.4668(19)
C(12A)-H(12A)	0.995(16)	O(7B)-C(25B)	1.2030(18)
C(12A)-H(12B)	1.002(16)	C(1B)-C(6B)	1.396(2)
C(12A)-H(12C)	0.939(17)	C(1B)-C(2B)	1.396(2)
C(13A)-H(13A)	0.986(18)	C(2B)-C(3B)	1.389(2)
C(13A)-H(13B)	0.990(17)	C(3B)-C(4B)	1.391(2)
C(13A)-H(13C)	1.072(16)	C(3B)-C(15B)	1.509(2)
C(14A)-H(14A)	1.043(18)	C(4B)-C(5B)	1.378(2)
C(14A)-H(14B)	1.016(17)	C(4B)-H(4B)	0.941(15)
C(14A)-H(14C)	0.982(18)	C(5B)-C(6B)	1.391(2)
C(15A)-C(16A)	1.525(2)	C(5B)-H(5B)	0.956(15)
C(15A)-H(15A)	0.967(16)	C(6B)-C(7B)	1.508(2)
C(15A)-H(15B)	1.012(16)	C(7B)-H(7B1)	0.984(18)
C(16A)-C(17A)	1.529(2)	C(7B)-H(7B2)	0.973(18)
C(16A)-H(16A)	1.032(13)	C(7B)-H(7B3)	0.959(18)

C(8B)-H(8B1)	0.994(16)	C(10A)-Si(1)-C(11A)	112.83(9)
C(8B)-H(8B2)	0.949(17)	C(9A)-Si(1)-C(11A)	109.35(9)
C(8B)-H(8B3)	0.976(19)	C(1A)-O(1A)-Si(1)	126.87(10)
C(9B)-H(9B1)	1.021(19)	C(2A)-O(2A)-C(8A)	112.94(13)
C(9B)-H(9B2)	0.968(18)	C(16A)-O(3A)-H(3A)	109.0(14)
C(9B)-H(9B3)	0.910(18)	C(27A)-O(5A)-C(28A)	116.14(17)
C(10B)-H(10D)	0.929(19)	C(25A)-O(6A)-C(20A)	108.79(12)
C(10B)-H(10E)	0.972(19)	O(1A)-C(1A)-C(2A)	119.97(14)
C(10B)-H(10F)	1.041(19)	O(1A)-C(1A)-C(6A)	119.17(14)
C(11B)-C(14B)	1.529(3)	C(2A)-C(1A)-C(6A)	120.77(16)
C(11B)-C(12B)	1.537(3)	O(2A)-C(2A)-C(3A)	119.27(15)
C(11B)-C(13B)	1.541(3)	O(2A)-C(2A)-C(1A)	119.52(15)
C(12B)-H(12D)	0.961(18)	C(3A)-C(2A)-C(1A)	121.17(15)
C(12B)-H(12E)	0.976(16)	C(4A)-C(3A)-C(2A)	117.57(16)
C(12B)-H(12F)	1.036(18)	C(4A)-C(3A)-C(15A)	120.43(17)
C(13B)-H(13D)	0.99(2)	C(2A)-C(3A)-C(15A)	121.96(16)
C(13B)-H(13E)	0.97(2)	C(5A)-C(4A)-C(3A)	121.26(18)
C(13B)-H(13F)	0.988(19)	C(5A)-C(4A)-H(4A)	120.0(10)
C(14B)-H(14D)	1.009(19)	C(3A)-C(4A)-H(4A)	118.7(10)
C(14B)-H(14E)	0.99(2)	C(4A)-C(5A)-C(6A)	121.60(17)
C(14B)-H(14F)	1.010(19)	C(4A)-C(5A)-H(5A)	120.6(10)
C(15B)-C(16B)	1.526(2)	C(6A)-C(5A)-H(5A)	117.8(10)
C(15B)-H(15C)	0.983(16)	C(5A)-C(6A)-C(1A)	117.47(16)
C(15B)-H(15D)	0.969(15)	C(5A)-C(6A)-C(7A)	121.95(16)
C(16B)-C(17B)	1.527(2)	C(1A)-C(6A)-C(7A)	120.58(16)
C(16B)-H(16B)	1.061(14)	C(6A)-C(7A)-H(7A1)	113.2(11)
C(17B)-C(22B)	1.336(2)	C(6A)-C(7A)-H(7A2)	110.5(10)
C(17B)-C(18B)	1.562(2)	H(7A1)-C(7A)-H(7A2)	109.8(14)
C(18B)-C(24B)	1.519(2)	C(6A)-C(7A)-H(7A3)	111.4(10)
C(18B)-C(25B)	1.524(2)	H(7A1)-C(7A)-H(7A3)	105.1(15)
C(18B)-C(19B)	1.545(2)	H(7A2)-C(7A)-H(7A3)	106.4(13)
C(19B)-C(27B)	1.528(2)	O(2A)-C(8A)-H(8A1)	109.8(11)
C(19B)-C(26B)	1.530(2)	O(2A)-C(8A)-H(8A2)	107.6(11)
C(19B)-C(20B)	1.538(2)	H(8A1)-C(8A)-H(8A2)	113.2(16)
C(20B)-C(21B)	1.494(2)	O(2A)-C(8A)-H(8A3)	111.8(10)
C(20B)-H(20B)	0.966(15)	H(8A1)-C(8A)-H(8A3)	106.8(15)
C(21B)-C(22B)	1.511(2)	H(8A2)-C(8A)-H(8A3)	107.7(15)
C(21B)-H(21C)	1.005(15)	Si(1)-C(9A)-H(9A1)	110.4(11)
C(21B)-H(21D)	0.945(15)	Si(1)-C(9A)-H(9A2)	110.6(11)
C(22B)-C(23B)	1.505(2)	H(9A1)-C(9A)-H(9A2)	107.4(16)
C(23B)-H(23D)	1.002(18)	Si(1)-C(9A)-H(9A3)	112.4(11)
C(23B)-H(23E)	0.977(19)	H(9A1)-C(9A)-H(9A3)	108.1(16)
C(23B)-H(23F)	0.991(17)	H(9A2)-C(9A)-H(9A3)	107.9(16)
C(24B)-H(24D)	0.991(16)	Si(1)-C(10A)-H(10A)	108.2(10)
C(24B)-H(24E)	0.985(17)	Si(1)-C(10A)-H(10B)	108.1(11)
C(24B)-H(24F)	0.994(16)	H(10A)-C(10A)-H(10B)	104.5(15)
C(26B)-H(26D)	1.02(2)	Si(1)-C(10A)-H(10C)	108.5(13)
C(26B)-H(26E)	1.022(17)	H(10A)-C(10A)-H(10C)	115.9(16)
C(26B)-H(26F)	0.902(18)	H(10B)-C(10A)-H(10C)	111.3(17)
C(28B)-H(28D)	0.973(19)	C(13A)-C(11A)-C(14A)	108.50(17)
C(28B)-H(28E)	1.01(2)	C(13A)-C(11A)-C(12A)	109.27(16)
C(28B)-H(28F)	1.005(18)	C(14A)-C(11A)-C(12A)	108.78(16)
		C(13A)-C(11A)-Si(1)	110.65(13)
O(1A)-Si(1)-C(10A)	108.83(9)	C(14A)-C(11A)-Si(1)	110.17(12)
O(1A)-Si(1)-C(9A)	112.73(9)	C(12A)-C(11A)-Si(1)	109.44(13)
C(10A)-Si(1)-C(9A)	108.59(12)	C(11A)-C(12A)-H(12A)	110.6(9)
O(1A)-Si(1)-C(11A)	104.53(7)	C(11A)-C(12A)-H(12B)	110.9(9)

H(12A)-C(12A)-H(12B)	109.3(13)	C(21A)-C(22A)-C(23A)	112.67(16)
C(11A)-C(12A)-H(12C)	109.0(11)	C(22A)-C(23A)-H(23A)	115.5(12)
H(12A)-C(12A)-H(12C)	110.9(14)	C(22A)-C(23A)-H(23B)	108.7(11)
H(12B)-C(12A)-H(12C)	106.0(14)	H(23A)-C(23A)-H(23B)	102.7(15)
C(11A)-C(13A)-H(13A)	109.7(10)	C(22A)-C(23A)-H(23C)	113.8(11)
C(11A)-C(13A)-H(13B)	111.0(9)	H(23A)-C(23A)-H(23C)	108.7(17)
H(13A)-C(13A)-H(13B)	106.6(14)	H(23B)-C(23A)-H(23C)	106.5(16)
C(11A)-C(13A)-H(13C)	107.1(9)	C(18A)-C(24A)-H(24A)	112.1(10)
H(13A)-C(13A)-H(13C)	113.9(14)	C(18A)-C(24A)-H(24B)	110.3(9)
H(13B)-C(13A)-H(13C)	108.6(13)	H(24A)-C(24A)-H(24B)	107.2(13)
C(11A)-C(14A)-H(14A)	111.0(10)	C(18A)-C(24A)-H(24C)	111.6(9)
C(11A)-C(14A)-H(14B)	108.8(9)	H(24A)-C(24A)-H(24C)	107.9(13)
H(14A)-C(14A)-H(14B)	107.3(14)	H(24B)-C(24A)-H(24C)	107.4(13)
C(11A)-C(14A)-H(14C)	110.1(10)	O(7A)-C(25A)-O(6A)	121.67(15)
H(14A)-C(14A)-H(14C)	111.2(14)	O(7A)-C(25A)-C(18A)	129.29(16)
H(14B)-C(14A)-H(14C)	108.3(14)	O(6A)-C(25A)-C(18A)	108.93(14)
C(3A)-C(15A)-C(16A)	112.34(15)	C(19A)-C(26A)-H(26A)	110.5(9)
C(3A)-C(15A)-H(15A)	110.7(9)	C(19A)-C(26A)-H(26B)	107.7(10)
C(16A)-C(15A)-H(15A)	105.5(9)	H(26A)-C(26A)-H(26B)	107.1(13)
C(3A)-C(15A)-H(15B)	110.2(9)	C(19A)-C(26A)-H(26C)	109.7(11)
C(16A)-C(15A)-H(15B)	110.8(9)	H(26A)-C(26A)-H(26C)	109.4(14)
H(15A)-C(15A)-H(15B)	107.2(13)	H(26B)-C(26A)-H(26C)	112.4(15)
O(3A)-C(16A)-C(15A)	107.75(15)	O(4A)-C(27A)-O(5A)	123.21(17)
O(3A)-C(16A)-C(17A)	112.97(13)	O(4A)-C(27A)-C(19A)	125.58(16)
C(15A)-C(16A)-C(17A)	113.83(14)	O(5A)-C(27A)-C(19A)	111.16(16)
O(3A)-C(16A)-H(16A)	99.6(7)	O(5A)-C(28A)-H(28A)	110.6(12)
C(15A)-C(16A)-H(16A)	112.7(7)	O(5A)-C(28A)-H(28B)	103.5(13)
C(17A)-C(16A)-H(16A)	109.1(7)	H(28A)-C(28A)-H(28B)	109.6(18)
C(22A)-C(17A)-C(16A)	120.51(15)	O(5A)-C(28A)-H(28C)	110.8(11)
C(22A)-C(17A)-C(18A)	119.78(15)	H(28A)-C(28A)-H(28C)	112.4(17)
C(16A)-C(17A)-C(18A)	119.58(15)	H(28B)-C(28A)-H(28C)	109.6(17)
C(25A)-C(18A)-C(24A)	114.37(15)	O(1B)-Si(2)-C(9B)	112.15(8)
C(25A)-C(18A)-C(19A)	100.28(13)	O(1B)-Si(2)-C(10B)	109.07(9)
C(24A)-C(18A)-C(19A)	113.17(14)	C(9B)-Si(2)-C(10B)	108.51(10)
C(25A)-C(18A)-C(17A)	101.39(12)	O(1B)-Si(2)-C(11B)	104.44(7)
C(24A)-C(18A)-C(17A)	116.05(14)	C(9B)-Si(2)-C(11B)	111.62(9)
C(19A)-C(18A)-C(17A)	109.92(14)	C(10B)-Si(2)-C(11B)	111.00(9)
C(26A)-C(19A)-C(27A)	112.09(16)	C(1B)-O(1B)-Si(2)	127.35(10)
C(26A)-C(19A)-C(20A)	114.62(16)	C(2B)-O(2B)-C(8B)	112.18(13)
C(27A)-C(19A)-C(20A)	106.69(14)	C(16B)-O(3B)-H(3B)	107.7(14)
C(26A)-C(19A)-C(18A)	114.66(15)	C(27B)-O(5B)-C(28B)	116.43(15)
C(27A)-C(19A)-C(18A)	109.97(14)	C(25B)-O(6B)-C(20B)	108.58(13)
C(20A)-C(19A)-C(18A)	97.74(13)	O(1B)-C(1B)-C(6B)	119.68(14)
O(6A)-C(20A)-C(21A)	109.08(14)	O(1B)-C(1B)-C(2B)	119.45(14)
O(6A)-C(20A)-C(19A)	103.63(13)	C(6B)-C(1B)-C(2B)	120.76(16)
C(21A)-C(20A)-C(19A)	110.94(15)	O(2B)-C(2B)-C(3B)	119.92(14)
O(6A)-C(20A)-H(20A)	107.1(9)	O(2B)-C(2B)-C(1B)	118.93(15)
C(21A)-C(20A)-H(20A)	112.5(9)	C(3B)-C(2B)-C(1B)	121.12(15)
C(19A)-C(20A)-H(20A)	113.0(9)	C(2B)-C(3B)-C(4B)	117.72(16)
C(22A)-C(21A)-C(20A)	112.11(15)	C(2B)-C(3B)-C(15B)	121.99(16)
C(22A)-C(21A)-H(21A)	108.0(9)	C(4B)-C(3B)-C(15B)	120.27(17)
C(20A)-C(21A)-H(21A)	111.1(9)	C(5B)-C(4B)-C(3B)	121.15(17)
C(22A)-C(21A)-H(21B)	111.3(9)	C(5B)-C(4B)-H(4B)	119.8(9)
C(20A)-C(21A)-H(21B)	107.9(9)	C(3B)-C(4B)-H(4B)	119.0(9)
H(21A)-C(21A)-H(21B)	106.3(13)	C(4B)-C(5B)-C(6B)	121.71(17)
C(17A)-C(22A)-C(21A)	121.63(16)	C(4B)-C(5B)-H(5B)	120.8(10)
C(17A)-C(22A)-C(23A)	125.70(16)	C(6B)-C(5B)-H(5B)	117.5(10)

C(5B)-C(6B)-C(1B)	117.39(16)	O(3B)-C(16B)-C(17B)	112.54(13)
C(5B)-C(6B)-C(7B)	121.52(16)	O(3B)-C(16B)-C(15B)	108.21(14)
C(1B)-C(6B)-C(7B)	121.08(16)	C(17B)-C(16B)-C(15B)	114.24(14)
C(6B)-C(7B)-H(7B1)	113.2(10)	O(3B)-C(16B)-H(16B)	98.2(7)
C(6B)-C(7B)-H(7B2)	112.6(10)	C(17B)-C(16B)-H(16B)	110.5(8)
H(7B1)-C(7B)-H(7B2)	104.5(15)	C(15B)-C(16B)-H(16B)	112.1(7)
C(6B)-C(7B)-H(7B3)	111.5(11)	C(22B)-C(17B)-C(16B)	120.84(15)
H(7B1)-C(7B)-H(7B3)	109.7(14)	C(22B)-C(17B)-C(18B)	119.74(14)
H(7B2)-C(7B)-H(7B3)	104.8(14)	C(16B)-C(17B)-C(18B)	119.31(14)
O(2B)-C(8B)-H(8B1)	110.8(9)	C(24B)-C(18B)-C(25B)	113.84(15)
O(2B)-C(8B)-H(8B2)	107.1(10)	C(24B)-C(18B)-C(19B)	113.46(14)
H(8B1)-C(8B)-H(8B2)	110.8(14)	C(25B)-C(18B)-C(19B)	100.43(13)
O(2B)-C(8B)-H(8B3)	109.1(11)	C(24B)-C(18B)-C(17B)	116.12(14)
H(8B1)-C(8B)-H(8B3)	107.0(14)	C(25B)-C(18B)-C(17B)	102.22(12)
H(8B2)-C(8B)-H(8B3)	112.0(14)	C(19B)-C(18B)-C(17B)	109.14(13)
Si(2)-C(9B)-H(9B1)	110.4(11)	C(27B)-C(19B)-C(26B)	112.00(15)
Si(2)-C(9B)-H(9B2)	109.6(10)	C(27B)-C(19B)-C(20B)	105.71(14)
H(9B1)-C(9B)-H(9B2)	106.8(15)	C(26B)-C(19B)-C(20B)	114.79(16)
Si(2)-C(9B)-H(9B3)	109.9(11)	C(27B)-C(19B)-C(18B)	110.73(14)
H(9B1)-C(9B)-H(9B3)	110.6(15)	C(26B)-C(19B)-C(18B)	114.56(14)
H(9B2)-C(9B)-H(9B3)	109.6(15)	C(20B)-C(19B)-C(18B)	97.96(13)
Si(2)-C(10B)-H(10D)	109.2(11)	O(6B)-C(20B)-C(21B)	108.63(14)
Si(2)-C(10B)-H(10E)	110.5(10)	O(6B)-C(20B)-C(19B)	103.56(13)
H(10D)-C(10B)-H(10E)	107.8(15)	C(21B)-C(20B)-C(19B)	111.22(14)
Si(2)-C(10B)-H(10F)	113.3(10)	O(6B)-C(20B)-H(20B)	107.2(9)
H(10D)-C(10B)-H(10F)	108.2(15)	C(21B)-C(20B)-H(20B)	112.0(9)
H(10E)-C(10B)-H(10F)	107.7(14)	C(19B)-C(20B)-H(20B)	113.7(9)
C(14B)-C(11B)-C(12B)	109.06(17)	C(20B)-C(21B)-C(22B)	112.67(15)
C(14B)-C(11B)-C(13B)	108.9(2)	C(20B)-C(21B)-H(21C)	110.0(8)
C(12B)-C(11B)-C(13B)	108.43(17)	C(22B)-C(21B)-H(21C)	110.7(8)
C(14B)-C(11B)-Si(2)	111.31(14)	C(20B)-C(21B)-H(21D)	108.8(9)
C(12B)-C(11B)-Si(2)	108.80(13)	C(22B)-C(21B)-H(21D)	110.2(9)
C(13B)-C(11B)-Si(2)	110.29(13)	H(21C)-C(21B)-H(21D)	104.2(12)
C(11B)-C(12B)-H(12D)	110.8(11)	C(17B)-C(22B)-C(23B)	126.52(16)
C(11B)-C(12B)-H(12E)	111.3(10)	C(17B)-C(22B)-C(21B)	121.36(15)
H(12D)-C(12B)-H(12E)	105.1(14)	C(23B)-C(22B)-C(21B)	112.11(15)
C(11B)-C(12B)-H(12F)	112.8(10)	C(22B)-C(23B)-H(23D)	115.8(10)
H(12D)-C(12B)-H(12F)	105.8(14)	C(22B)-C(23B)-H(23E)	113.2(10)
H(12E)-C(12B)-H(12F)	110.6(14)	H(23D)-C(23B)-H(23E)	108.1(14)
C(11B)-C(13B)-H(13D)	109.3(12)	C(22B)-C(23B)-H(23F)	108.3(9)
C(11B)-C(13B)-H(13E)	110.6(12)	H(23D)-C(23B)-H(23F)	104.7(13)
H(13D)-C(13B)-H(13E)	108.2(17)	H(23E)-C(23B)-H(23F)	105.9(14)
C(11B)-C(13B)-H(13F)	108.0(10)	C(18B)-C(24B)-H(24D)	113.2(9)
H(13D)-C(13B)-H(13F)	110.4(16)	C(18B)-C(24B)-H(24E)	110.4(10)
H(13E)-C(13B)-H(13F)	110.3(16)	H(24D)-C(24B)-H(24E)	108.6(13)
C(11B)-C(14B)-H(14D)	109.6(10)	C(18B)-C(24B)-H(24F)	110.5(9)
C(11B)-C(14B)-H(14E)	110.8(12)	H(24D)-C(24B)-H(24F)	108.5(13)
H(14D)-C(14B)-H(14E)	105.5(15)	H(24E)-C(24B)-H(24F)	105.3(13)
C(11B)-C(14B)-H(14F)	108.6(12)	O(7B)-C(25B)-O(6B)	121.65(16)
H(14D)-C(14B)-H(14F)	115.0(16)	O(7B)-C(25B)-C(18B)	129.16(16)
H(14E)-C(14B)-H(14F)	107.3(17)	O(6B)-C(25B)-C(18B)	109.13(14)
C(3B)-C(15B)-C(16B)	112.59(15)	C(19B)-C(26B)-H(26D)	109.0(11)
C(3B)-C(15B)-H(15C)	108.3(10)	C(19B)-C(26B)-H(26E)	109.2(9)
C(16B)-C(15B)-H(15C)	110.0(9)	H(26D)-C(26B)-H(26E)	111.8(14)
C(3B)-C(15B)-H(15D)	110.1(9)	C(19B)-C(26B)-H(26F)	110.8(11)
C(16B)-C(15B)-H(15D)	107.5(9)	H(26D)-C(26B)-H(26F)	105.9(15)
H(15C)-C(15B)-H(15D)	108.3(13)	H(26E)-C(26B)-H(26F)	110.2(15)

O(4B)-C(27B)-O(5B)	123.36(17)
O(4B)-C(27B)-C(19B)	125.61(16)
O(5B)-C(27B)-C(19B)	110.94(15)
O(5B)-C(28B)-H(28D)	112.0(11)
O(5B)-C(28B)-H(28E)	107.3(11)
H(28D)-C(28B)-H(28E)	117.1(16)
O(5B)-C(28B)-H(28F)	112.6(10)
H(28D)-C(28B)-H(28F)	96.4(14)
H(28E)-C(28B)-H(28F)	111.3(15)

**Table 4.** Anisotropic displacement parameters ( $\text{\AA}^2 \times 10^4$ ) for DCB31 (CCDC 283708). The anisotropic displacement factor exponent takes the form:  $-2\pi^2 [h^2 a^{*2} U^{11} + \dots + 2 h k a^* b^* U^{12}]$

	U <sup>11</sup>	U <sup>22</sup>	U <sup>33</sup>	U <sup>23</sup>	U <sup>13</sup>	U <sup>12</sup>
Si(1)	246(3)	166(3)	247(3)	-46(2)	-122(2)	20(2)
O(1A)	218(7)	140(6)	209(6)	-42(5)	-89(5)	25(5)
O(2A)	235(7)	253(7)	173(6)	-30(5)	-67(5)	39(6)
O(3A)	198(7)	203(7)	373(8)	-42(6)	-118(6)	22(6)
O(4A)	350(8)	465(9)	301(8)	4(7)	-165(6)	64(7)
O(5A)	562(9)	293(8)	437(9)	-82(7)	-372(7)	140(7)
O(6A)	189(7)	196(7)	260(7)	-20(5)	-99(5)	-15(5)
O(7A)	170(7)	244(7)	230(7)	-32(5)	-82(5)	31(6)
C(1A)	140(9)	163(10)	236(10)	-59(8)	-64(8)	2(8)
C(2A)	125(9)	219(10)	200(10)	-34(8)	-58(7)	3(8)
C(3A)	99(9)	196(10)	304(11)	-37(8)	-44(8)	0(8)
C(4A)	175(10)	184(11)	378(12)	-115(10)	-14(9)	-18(8)
C(5A)	205(10)	327(12)	211(11)	-121(9)	0(8)	-51(9)
C(6A)	156(9)	238(11)	176(10)	-32(8)	-27(8)	-46(8)
C(7A)	308(13)	319(13)	205(11)	-27(9)	-78(9)	-47(11)
C(8A)	227(12)	296(13)	235(12)	-65(10)	4(9)	37(10)
C(9A)	642(18)	241(13)	365(13)	-23(10)	-322(13)	-22(12)
C(10A)	281(12)	289(13)	538(16)	-137(12)	-195(11)	40(10)
C(11A)	254(10)	188(10)	231(10)	-56(8)	-103(8)	11(8)
C(12A)	390(14)	169(12)	358(13)	-41(10)	-182(11)	1(10)
C(13A)	351(13)	250(13)	550(16)	-136(11)	-187(12)	57(10)
C(14A)	506(15)	206(12)	379(13)	22(10)	-264(12)	-19(11)
C(15A)	157(10)	174(11)	395(13)	2(9)	-100(9)	-11(8)
C(16A)	163(10)	150(10)	287(11)	-20(8)	-78(8)	13(8)
C(17A)	116(9)	190(10)	297(10)	-27(8)	-78(8)	-11(8)
C(18A)	178(10)	160(10)	270(10)	-26(8)	-103(8)	10(8)
C(19A)	222(10)	189(10)	341(11)	-43(8)	-145(9)	34(8)
C(20A)	242(11)	139(10)	339(11)	8(9)	-143(9)	4(8)
C(21A)	213(11)	162(10)	324(11)	-52(9)	-93(9)	17(9)
C(22A)	140(9)	178(10)	300(11)	-25(8)	-48(8)	10(8)
C(23A)	272(12)	208(12)	307(12)	-50(10)	-27(10)	10(10)
C(24A)	238(12)	217(11)	321(12)	-52(9)	-141(10)	12(9)
C(25A)	220(10)	213(11)	163(9)	-8(8)	-94(8)	-19(8)
C(26A)	263(12)	263(13)	599(16)	-47(12)	-252(12)	52(10)
C(27A)	365(12)	184(11)	394(12)	-14(9)	-269(10)	-28(9)
C(28A)	750(20)	329(15)	444(15)	-103(12)	-428(14)	111(14)
Si(2)	224(3)	166(3)	247(3)	-30(2)	-96(2)	14(2)
O(1B)	223(7)	140(7)	237(7)	-21(5)	-98(5)	13(5)
O(2B)	255(7)	269(7)	176(7)	0(6)	-64(5)	-3(6)
O(3B)	237(8)	179(7)	385(8)	-45(6)	-133(6)	34(6)
O(4B)	300(8)	425(9)	267(7)	-10(6)	-100(6)	72(7)
O(5B)	431(8)	303(8)	273(7)	-35(6)	-207(6)	95(6)
O(6B)	175(7)	173(7)	257(7)	-21(5)	-58(5)	-15(5)
O(7B)	179(7)	243(7)	246(7)	-58(6)	-74(5)	33(6)
C(1B)	149(9)	135(9)	218(10)	-21(8)	-63(8)	1(7)
C(2B)	141(9)	212(10)	167(9)	1(8)	-48(7)	7(8)

C(3B)	121(9)	188(10)	273(10)	15(8)	-54(8)	-24(8)
C(4B)	182(10)	150(11)	346(12)	-63(9)	-58(9)	-11(8)
C(5B)	171(10)	289(12)	213(11)	-96(9)	-15(8)	-23(8)
C(6B)	149(9)	212(10)	178(9)	-1(8)	-37(7)	-24(8)
C(7B)	294(12)	270(12)	189(11)	31(9)	-89(9)	-29(10)
C(8B)	303(13)	269(13)	222(12)	-62(10)	-26(9)	15(10)
C(9B)	321(13)	249(12)	356(13)	-55(10)	-177(11)	25(10)
C(10B)	290(12)	329(13)	334(13)	-78(11)	-82(10)	-43(11)
C(11B)	242(10)	183(10)	341(11)	-73(8)	-111(9)	19(8)
C(12B)	332(13)	219(12)	412(14)	-126(10)	-134(11)	19(10)
C(13B)	329(14)	304(14)	624(18)	-215(13)	7(12)	17(12)
C(14B)	586(17)	253(13)	755(19)	-156(13)	-461(16)	154(13)
C(15B)	181(11)	171(11)	348(12)	48(9)	-92(9)	-14(9)
C(16B)	171(10)	135(10)	264(10)	2(8)	-92(8)	-13(8)
C(17B)	128(9)	179(10)	227(10)	0(8)	-58(8)	-16(8)
C(18B)	186(10)	141(10)	236(10)	-8(8)	-88(8)	-2(8)
C(19B)	231(10)	186(10)	232(10)	-4(8)	-93(8)	9(8)
C(20B)	213(10)	139(10)	267(11)	27(8)	-74(8)	0(8)
C(21B)	215(11)	154(10)	265(11)	-55(8)	-66(9)	22(9)
C(22B)	169(10)	174(10)	218(10)	-17(8)	-50(8)	-14(8)
C(23B)	279(12)	219(12)	218(11)	-32(9)	-31(9)	14(10)
C(24B)	243(12)	193(11)	284(12)	-45(9)	-124(9)	-5(9)
C(25B)	231(10)	207(10)	142(9)	-28(8)	-79(8)	-4(9)
C(26B)	214(11)	284(13)	350(13)	20(10)	-119(10)	53(10)
C(27B)	272(11)	193(10)	312(11)	-10(9)	-156(9)	-17(9)
C(28B)	468(15)	337(13)	264(12)	-40(10)	-188(11)	62(12)

---

**Table 5.** Hydrogen coordinates ( $\times 10^4$ ) and isotropic displacement parameters ( $\text{\AA}^2 \times 10^3$ ) for DCB31 (CCDC 283708).

	x	y	z	$U_{\text{iso}}$
H(3A)	3688(19)	4314(14)	814(14)	78(8)
H(4A)	201(13)	4175(11)	3162(11)	30(5)
H(5A)	-132(13)	2974(10)	4325(11)	25(5)
H(7A1)	-544(16)	867(12)	4330(12)	46(6)
H(7A2)	-69(13)	1455(11)	4872(12)	32(5)
H(7A3)	760(15)	894(11)	4127(11)	40(6)
H(8A1)	2967(16)	2594(13)	644(12)	53(7)
H(8A2)	2642(16)	2081(13)	-37(14)	60(7)
H(8A3)	2505(14)	1627(12)	968(12)	41(6)
H(9A1)	45(16)	1427(14)	673(13)	59(7)
H(9A2)	-397(16)	488(13)	676(13)	58(7)
H(9A3)	985(18)	670(14)	351(14)	71(8)
H(10A)	-1676(14)	505(12)	3497(13)	46(6)
H(10B)	-2032(17)	324(13)	2692(13)	55(7)
H(10C)	-1708(17)	1284(14)	2659(14)	66(8)
H(12A)	-171(13)	-1113(10)	1309(12)	28(5)
H(12B)	-1181(15)	-1199(10)	2360(11)	29(5)
H(12C)	-170(14)	-1847(12)	2143(11)	33(5)
H(13A)	1874(15)	-1379(12)	1840(12)	45(6)
H(13B)	2135(14)	-385(11)	1849(11)	29(5)
H(13C)	1796(13)	-581(11)	968(12)	34(5)
H(14A)	-721(16)	-845(12)	3734(12)	49(6)
H(14B)	627(14)	-554(11)	3490(11)	31(5)
H(14C)	355(14)	-1552(12)	3421(12)	43(6)
H(15A)	425(13)	4736(10)	1503(10)	25(5)
H(15B)	998(13)	4120(11)	721(11)	30(5)
H(16A)	2236(11)	4803(8)	1738(9)	3(4)
H(20A)	3219(13)	7783(11)	-1165(11)	34(5)
H(21A)	2915(13)	7589(10)	494(10)	21(5)
H(21B)	1745(13)	7611(10)	350(10)	26(5)
H(23A)	1387(17)	5894(14)	2315(14)	64(7)
H(23B)	941(17)	6760(13)	2048(12)	54(7)
H(23C)	2132(17)	6743(13)	2117(13)	60(7)
H(24A)	3128(14)	4891(11)	-1621(12)	33(5)
H(24B)	1857(15)	4754(10)	-810(11)	32(5)
H(24C)	2960(13)	4324(11)	-645(11)	28(5)
H(26A)	782(14)	6455(11)	27(12)	33(5)
H(26B)	880(14)	6179(12)	-967(11)	39(6)
H(26C)	997(14)	7196(12)	-883(12)	40(6)
H(28A)	3459(16)	7683(14)	-3771(13)	55(7)
H(28B)	2220(20)	7377(15)	-3685(15)	87(9)
H(28C)	3208(16)	6680(13)	-3761(13)	53(7)
H(3B)	1220(20)	5723(16)	4087(17)	114(10)
H(4B)	4665(12)	5890(10)	1672(10)	19(5)
H(5B)	5010(13)	7083(10)	475(11)	26(5)
H(7B1)	5590(16)	9117(12)	338(12)	44(6)
H(7B2)	4273(15)	9247(12)	709(12)	45(6)

H(7B3)	4798(14)	8624(11)	-15(12)	39(6)
H(8B1)	2458(13)	8392(11)	3792(11)	29(5)
H(8B2)	2434(13)	8067(11)	4816(12)	32(5)
H(8B3)	2056(16)	7416(13)	4285(12)	51(6)
H(9B1)	5015(17)	8795(12)	4117(14)	58(7)
H(9B2)	6204(15)	9337(12)	3590(11)	43(6)
H(9B3)	6052(15)	8483(12)	3257(12)	41(6)
H(10D)	6756(15)	9418(13)	1273(12)	47(6)
H(10E)	6969(15)	10252(12)	1610(12)	45(6)
H(10F)	6179(15)	10302(12)	1002(13)	52(6)
H(12D)	4742(15)	11708(12)	3470(12)	43(6)
H(12E)	5801(14)	11364(11)	2713(12)	30(5)
H(12F)	5359(15)	10891(12)	3820(13)	47(6)
H(13D)	3564(17)	9949(14)	4480(14)	66(8)
H(13E)	2761(17)	9917(13)	3923(13)	60(7)
H(13F)	2901(15)	10825(12)	4254(12)	44(6)
H(14D)	3408(15)	11588(12)	2666(12)	48(6)
H(14E)	3379(17)	10716(13)	2251(13)	62(7)
H(14F)	4577(18)	11267(13)	1777(14)	62(8)
H(15C)	3961(13)	6006(11)	4080(11)	29(5)
H(15D)	4563(13)	5374(10)	3328(10)	20(5)
H(16B)	2690(11)	5298(9)	3116(10)	13(4)
H(20B)	1938(12)	2330(10)	6009(10)	21(5)
H(21C)	1972(13)	2468(10)	4457(10)	21(5)
H(21D)	3183(13)	2494(10)	4462(10)	19(5)
H(23D)	3419(14)	4199(12)	2518(12)	43(6)
H(23E)	2648(16)	3318(12)	2812(12)	47(6)
H(23F)	3899(15)	3285(11)	2794(11)	34(5)
H(24D)	2117(13)	5778(11)	5512(10)	26(5)
H(24E)	3246(15)	5340(11)	5603(11)	34(5)
H(24F)	2058(13)	5180(10)	6467(12)	29(5)
H(26D)	4364(16)	3949(13)	5623(12)	55(7)
H(26E)	4271(14)	3613(11)	4680(12)	42(6)
H(26F)	4218(15)	2973(12)	5585(12)	39(6)
H(28D)	2178(16)	3296(13)	8539(13)	51(6)
H(28E)	3210(17)	2533(13)	8372(13)	60(7)
H(28F)	1846(15)	2391(12)	8536(12)	41(6)

---

**Table 6.** Hydrogen bonds for DCB31 (CCDC 283708) [ $\text{\AA}$  and  $^\circ$ ].

D-H...A	d(D-H)	d(H...A)	d(D...A)	$\angle$ (DHA)
O(3A)-H(3A)...O(7A)#1	0.92(2)	1.88(2)	2.7946(17)	173(2)
O(3B)-H(3B)...O(7B)#2	0.98(3)	1.81(3)	2.7910(17)	176(2)

Symmetry transformations used to generate equivalent atoms:

#1 -x+1,-y+1,-z

#2 -x,-y+1,-z+1

CALIFORNIA INSTITUTE OF TECHNOLOGY  
BECKMAN INSTITUTE  
X-RAY CRYSTALLOGRAPHY LABORATORY

Crystal Structure Analysis of:  
Bisacetoxyacetal **256** (DCB32)  
(CCDC 289914)

Contents:

- Table 1. Crystal data
- Table 2. Atomic coordinates
- Table 3. Full bond distances and angles
- Table 4. Anisotropic displacement parameters
- Table 5. Hydrogen atomic coordinates
- Table 6. Hydrogen bond distances and angles

Figure B.114 Representation of Bisacetoxyacetal **256**

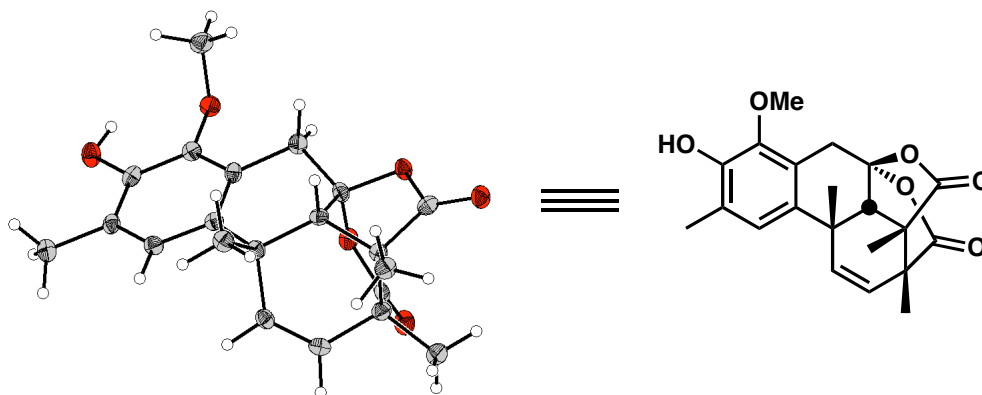


**Table 1.** Crystal data and structure refinement for DCB32 (CCDC 289914).

Empirical formula	C <sub>21</sub> H <sub>22</sub> O <sub>6</sub>
Formula weight	370.39
Crystallization Solvent	Et <sub>2</sub> O/hexanes
Crystal Habit	Needle
Crystal size	0.39 x 0.22 x 0.19 mm <sup>3</sup>
Crystal color	Colorless

### Data Collection

Type of diffractometer	Bruker SMART 1000
Wavelength	0.71073 Å MoK $\alpha$
Data Collection Temperature	100(2) K
$\theta$ range for 13215 reflections used in lattice determination	2.27 to 28.03°
Unit cell dimensions	a = 21.9617(16) Å b = 8.5236(6) Å c = 19.6358(14) Å
Volume	3675.7(5) Å <sup>3</sup>
Z	8
Crystal system	Orthorhombic
Space group	Pbcn
Density (calculated)	1.339 Mg/m <sup>3</sup>
F(000)	1568
Data collection program	Bruker SMART v5.630
$\theta$ range for data collection	1.85 to 28.38°
Completeness to $\theta = 28.38^\circ$	94.2 %
Index ranges	-28 $\leq$ h $\leq$ 28, -11 $\leq$ k $\leq$ 11, -24 $\leq$ l $\leq$ 26
Data collection scan type	$\omega$ scans at 5 $\phi$ settings
Data reduction program	Bruker SAINT v6.45A
Reflections collected	50823
Independent reflections	4344 [R <sub>int</sub> = 0.0809]
Absorption coefficient	0.098 mm <sup>-1</sup>
Absorption correction	None
Max. and min. transmission	0.9816 and 0.9628

**Table 1** (cont.)**Structure Solution and Refinement**

Structure solution program	Bruker XS v6.12
Primary solution method	Direct methods
Secondary solution method	Difference Fourier map
Hydrogen placement	Difference Fourier map
Structure refinement program	Bruker XL v6.12
Refinement method	Full matrix least-squares on $F^2$
Data / restraints / parameters	4344 / 0 / 332
Treatment of hydrogen atoms	Unrestrained
Goodness-of-fit on $F^2$	1.880
Final R indices [ $I > 2\sigma(I)$ , 3001 reflections]	$R_1 = 0.0466$ , $wR_2 = 0.0611$
R indices (all data)	$R_1 = 0.0778$ , $wR_2 = 0.0633$
Type of weighting scheme used	Sigma
Weighting scheme used	$w = 1/\sigma^2(F_o^2)$
Max shift/error	0.001
Average shift/error	0.000
Largest diff. peak and hole	0.331 and -0.276 e.Å <sup>-3</sup>

**Special Refinement Details**

Refinement of  $F^2$  against ALL reflections. The weighted R-factor ( $wR$ ) and goodness of fit ( $S$ ) are based on  $F^2$ , conventional R-factors ( $R$ ) are based on  $F$ , with  $F$  set to zero for negative  $F^2$ . The threshold expression of  $F^2 > 2\sigma(F^2)$  is used only for calculating R-factors(gt) etc. and is not relevant to the choice of reflections for refinement. R-factors based on  $F^2$  are statistically about twice as large as those based on  $F$ , and R-factors based on ALL data will be even larger.

All esds (except the esd in the dihedral angle between two l.s. planes) are estimated using the full covariance matrix. The cell esds are taken into account individually in the estimation of esds in distances, angles and torsion angles; correlations between esds in cell parameters are only used when they are defined by crystal symmetry. An approximate (isotropic) treatment of cell esds is used for estimating esds involving l.s. planes.

**Table 2.** Atomic coordinates ( $\times 10^4$ ) and equivalent isotropic displacement parameters ( $\text{\AA}^2 \times 10^3$ ) for DCB32 (CCDC 289914).  $U(\text{eq})$  is defined as the trace of the orthogonalized  $U^{ij}$  tensor.

	x	y	z	$U_{\text{eq}}$
O(1)	2750(1)	8498(1)	11657(1)	20(1)
O(2)	3463(1)	6194(1)	12216(1)	22(1)
O(3)	4347(1)	12923(1)	9814(1)	24(1)
O(4)	3652(1)	11114(1)	10020(1)	19(1)
O(5)	2849(1)	12317(1)	8276(1)	22(1)
O(6)	2812(1)	11335(1)	9329(1)	18(1)
C(1)	3243(1)	8168(2)	10565(1)	16(1)
C(2)	3171(1)	7737(2)	11243(1)	16(1)
C(3)	3539(1)	6609(2)	11548(1)	17(1)
C(4)	3993(1)	5863(2)	11174(1)	17(1)
C(5)	4067(1)	6316(2)	10500(1)	17(1)
C(6)	3705(1)	7443(2)	10182(1)	16(1)
C(7)	3834(1)	7839(2)	9427(1)	15(1)
C(8)	3386(1)	9079(2)	9173(1)	15(1)
C(9)	3172(1)	10217(2)	9710(1)	17(1)
C(10)	2832(1)	9437(2)	10272(1)	18(1)
C(11)	2149(1)	7822(2)	11619(1)	25(1)
C(12)	4388(1)	4633(2)	11498(1)	24(1)
C(13)	3759(1)	6327(2)	8998(1)	20(1)
C(14)	4480(1)	8405(2)	9339(1)	18(1)
C(15)	4634(1)	9789(2)	9089(1)	19(1)
C(16)	4175(1)	11058(2)	8904(1)	18(1)
C(17)	3586(1)	10261(2)	8630(1)	15(1)
C(18)	4452(1)	12247(2)	8416(1)	23(1)
C(19)	3652(1)	9638(2)	7907(1)	21(1)
C(20)	4062(1)	11828(2)	9598(1)	19(1)
C(21)	3057(1)	11422(2)	8689(1)	17(1)

**Table 3.** Bond lengths [Å] and angles [°] for DCB32 (CCDC 289914).

O(1)-C(2)	1.3917(16)	C(2)-O(1)-C(11)	113.13(12)
O(1)-C(11)	1.4405(18)	C(3)-O(2)-H(2)	108.0(13)
O(2)-C(3)	1.3695(17)	C(20)-O(4)-C(9)	117.64(11)
O(2)-H(2)	0.887(19)	C(21)-O(6)-C(9)	107.19(11)
O(3)-C(20)	1.2002(16)	C(2)-C(1)-C(6)	118.61(13)
O(4)-C(20)	1.3677(17)	C(2)-C(1)-C(10)	118.79(13)
O(4)-C(9)	1.4373(16)	C(6)-C(1)-C(10)	122.58(13)
O(5)-C(21)	1.2031(16)	C(1)-C(2)-C(3)	121.92(13)
O(6)-C(21)	1.3697(16)	C(1)-C(2)-O(1)	120.79(13)
O(6)-C(9)	1.4462(16)	C(3)-C(2)-O(1)	117.17(13)
C(1)-C(2)	1.3899(19)	O(2)-C(3)-C(2)	121.36(13)
C(1)-C(6)	1.4059(19)	O(2)-C(3)-C(4)	118.33(13)
C(1)-C(10)	1.521(2)	C(2)-C(3)-C(4)	120.30(13)
C(2)-C(3)	1.3915(19)	C(5)-C(4)-C(3)	117.36(14)
C(3)-C(4)	1.3917(19)	C(5)-C(4)-C(12)	122.04(14)
C(4)-C(5)	1.388(2)	C(3)-C(4)-C(12)	120.60(14)
C(4)-C(12)	1.503(2)	C(4)-C(5)-C(6)	123.54(14)
C(5)-C(6)	1.3954(19)	C(4)-C(5)-H(5)	118.2(7)
C(5)-H(5)	0.960(12)	C(6)-C(5)-H(5)	118.2(7)
C(6)-C(7)	1.546(2)	C(5)-C(6)-C(1)	118.25(14)
C(7)-C(14)	1.5080(19)	C(5)-C(6)-C(7)	118.43(13)
C(7)-C(8)	1.5268(19)	C(1)-C(6)-C(7)	123.32(13)
C(7)-C(13)	1.548(2)	C(14)-C(7)-C(8)	110.30(12)
C(8)-C(9)	1.5086(19)	C(14)-C(7)-C(6)	110.57(12)
C(8)-C(17)	1.5300(19)	C(8)-C(7)-C(6)	110.27(12)
C(8)-H(8)	0.966(13)	C(14)-C(7)-C(13)	107.68(12)
C(9)-C(10)	1.490(2)	C(8)-C(7)-C(13)	109.33(12)
C(10)-H(10A)	1.027(14)	C(6)-C(7)-C(13)	108.64(12)
C(10)-H(10B)	0.976(14)	C(9)-C(8)-C(7)	114.69(12)
C(11)-H(11A)	1.018(15)	C(9)-C(8)-C(17)	98.80(11)
C(11)-H(11B)	0.941(14)	C(7)-C(8)-C(17)	119.94(12)
C(11)-H(11C)	1.017(15)	C(9)-C(8)-H(8)	106.2(8)
C(12)-H(12A)	0.965(18)	C(7)-C(8)-H(8)	107.8(8)
C(12)-H(12B)	0.994(18)	C(17)-C(8)-H(8)	108.4(8)
C(12)-H(12C)	0.989(17)	O(4)-C(9)-O(6)	105.61(11)
C(13)-H(13A)	1.003(14)	O(4)-C(9)-C(10)	106.90(12)
C(13)-H(13B)	0.988(15)	O(6)-C(9)-C(10)	113.83(12)
C(13)-H(13C)	0.996(14)	O(4)-C(9)-C(8)	114.14(12)
C(14)-C(15)	1.323(2)	O(6)-C(9)-C(8)	103.46(11)
C(14)-H(14)	0.975(13)	C(10)-C(9)-C(8)	112.83(13)
C(15)-C(16)	1.523(2)	C(9)-C(10)-C(1)	107.47(13)
C(15)-H(15)	0.987(11)	C(9)-C(10)-H(10A)	107.7(7)
C(16)-C(18)	1.520(2)	C(1)-C(10)-H(10A)	113.2(8)
C(16)-C(20)	1.533(2)	C(9)-C(10)-H(10B)	111.0(8)
C(16)-C(17)	1.5582(19)	C(1)-C(10)-H(10B)	110.6(8)
C(17)-C(19)	1.523(2)	H(10A)-C(10)-H(10B)	106.9(11)
C(17)-C(21)	1.530(2)	O(1)-C(11)-H(11A)	111.2(8)
C(18)-H(18A)	0.989(14)	O(1)-C(11)-H(11B)	104.9(8)
C(18)-H(18B)	0.977(15)	H(11A)-C(11)-H(11B)	109.5(11)
C(18)-H(18C)	1.001(16)	O(1)-C(11)-H(11C)	111.2(8)
C(19)-H(19A)	0.956(14)	H(11A)-C(11)-H(11C)	110.5(12)
C(19)-H(19B)	1.006(15)	H(11B)-C(11)-H(11C)	109.4(12)
C(19)-H(19C)	0.974(17)	C(4)-C(12)-H(12A)	112.6(11)
		C(4)-C(12)-H(12B)	111.6(10)

H(12A)-C(12)-H(12B)	104.8(14)
C(4)-C(12)-H(12C)	112.2(10)
H(12A)-C(12)-H(12C)	108.5(14)
H(12B)-C(12)-H(12C)	106.7(14)
C(7)-C(13)-H(13A)	109.3(8)
C(7)-C(13)-H(13B)	111.2(8)
H(13A)-C(13)-H(13B)	109.6(11)
C(7)-C(13)-H(13C)	108.8(8)
H(13A)-C(13)-H(13C)	110.4(11)
H(13B)-C(13)-H(13C)	107.5(11)
C(15)-C(14)-C(7)	124.68(14)
C(15)-C(14)-H(14)	118.8(8)
C(7)-C(14)-H(14)	116.5(7)
C(14)-C(15)-C(16)	123.55(14)
C(14)-C(15)-H(15)	119.1(7)
C(16)-C(15)-H(15)	117.2(7)
C(18)-C(16)-C(15)	111.10(13)
C(18)-C(16)-C(20)	109.81(13)
C(15)-C(16)-C(20)	101.49(11)
C(18)-C(16)-C(17)	113.92(13)
C(15)-C(16)-C(17)	108.83(12)
C(20)-C(16)-C(17)	111.00(12)
C(19)-C(17)-C(21)	111.62(12)
C(19)-C(17)-C(8)	116.54(13)
C(21)-C(17)-C(8)	99.01(11)
C(19)-C(17)-C(16)	113.21(12)
C(21)-C(17)-C(16)	108.81(12)
C(8)-C(17)-C(16)	106.55(11)
C(16)-C(18)-H(18A)	107.5(8)
C(16)-C(18)-H(18B)	111.6(8)
H(18A)-C(18)-H(18B)	110.3(12)
C(16)-C(18)-H(18C)	108.8(9)
H(18A)-C(18)-H(18C)	111.5(12)
H(18B)-C(18)-H(18C)	107.2(12)
C(17)-C(19)-H(19A)	107.7(8)
C(17)-C(19)-H(19B)	110.6(8)
H(19A)-C(19)-H(19B)	111.7(12)
C(17)-C(19)-H(19C)	113.5(9)
H(19A)-C(19)-H(19C)	104.7(12)
H(19B)-C(19)-H(19C)	108.6(12)
O(3)-C(20)-O(4)	118.39(14)
O(3)-C(20)-C(16)	124.22(14)
O(4)-C(20)-C(16)	117.06(13)
O(5)-C(21)-O(6)	120.27(13)
O(5)-C(21)-C(17)	130.33(14)
O(6)-C(21)-C(17)	109.40(12)

**Table 4.** Anisotropic displacement parameters ( $\text{\AA}^2 \times 10^4$ ) for DCB32 (CCDC 289914). The anisotropic displacement factor exponent takes the form:  $-2\pi^2 [ h^2 a^{*2} U^{11} + \dots + 2 h k a^* b^* U^{12} ]$

	$U^{11}$	$U^{22}$	$U^{33}$	$U^{23}$	$U^{13}$	$U^{12}$
O(1)	219(6)	189(6)	191(6)	-17(5)	52(5)	31(5)
O(2)	300(7)	204(6)	154(6)	14(5)	13(5)	46(5)
O(3)	273(6)	157(6)	288(7)	-25(5)	-80(5)	-20(5)
O(4)	233(6)	155(6)	172(6)	-15(5)	-14(5)	-8(5)
O(5)	248(6)	236(6)	179(6)	56(5)	-2(5)	32(5)
O(6)	215(6)	187(6)	141(6)	24(5)	18(5)	52(5)
C(1)	198(9)	125(8)	164(8)	-5(7)	-11(7)	-4(7)
C(2)	186(8)	133(8)	168(9)	-39(7)	23(7)	0(7)
C(3)	227(9)	148(9)	130(9)	-8(7)	-8(7)	-46(7)
C(4)	201(9)	112(8)	200(9)	-4(7)	-20(7)	-16(7)
C(5)	172(9)	147(8)	204(9)	-35(7)	31(7)	20(7)
C(6)	172(8)	139(8)	166(8)	-26(7)	1(7)	-13(7)
C(7)	156(8)	139(8)	161(8)	-18(7)	3(7)	18(7)
C(8)	136(8)	152(8)	162(9)	-18(7)	-2(7)	-18(7)
C(9)	166(8)	156(8)	183(8)	15(7)	-40(7)	20(7)
C(10)	211(9)	175(9)	157(9)	1(7)	36(8)	24(7)
C(11)	232(10)	239(10)	269(11)	-6(9)	92(9)	14(8)
C(12)	245(10)	208(10)	272(11)	45(8)	2(8)	35(8)
C(13)	221(10)	182(9)	205(10)	-34(8)	4(8)	11(8)
C(14)	179(9)	198(9)	159(9)	-11(7)	3(7)	40(7)
C(15)	141(8)	234(9)	180(9)	-23(7)	3(7)	0(7)
C(16)	168(8)	170(8)	188(9)	-1(7)	3(7)	-14(7)
C(17)	167(8)	146(8)	148(8)	-11(7)	10(7)	7(7)
C(18)	228(10)	218(10)	249(10)	30(8)	2(8)	-26(8)
C(19)	239(10)	241(10)	159(9)	7(8)	3(8)	-8(9)
C(20)	178(9)	154(9)	228(9)	32(7)	-44(7)	41(7)
C(21)	188(9)	169(8)	159(9)	-30(7)	-2(7)	-52(7)

**Table 5.** Hydrogen coordinates ( $\times 10^4$ ) and isotropic displacement parameters ( $\text{\AA}^2 \times 10^3$ ) for DCB32 (CCDC 289914).

	x	y	z	$U_{\text{iso}}$
H(2)	3183(9)	6820(20)	12395(10)	66(7)
H(5)	4383(6)	5822(14)	10239(6)	7(3)
H(8)	3027(6)	8542(15)	9011(6)	11(4)
H(10A)	2434(6)	9003(15)	10073(7)	16(4)
H(10B)	2719(6)	10191(17)	10624(7)	21(4)
H(11A)	1959(6)	8003(17)	11152(8)	27(4)
H(11B)	1921(6)	8358(16)	11952(7)	15(4)
H(11C)	2158(6)	6658(19)	11731(7)	26(4)
H(12A)	4187(8)	3630(20)	11532(9)	59(6)
H(12B)	4495(7)	4910(20)	11975(9)	56(6)
H(12C)	4777(8)	4488(19)	11252(8)	49(5)
H(13A)	4066(6)	5529(17)	9151(7)	26(4)
H(13B)	3815(6)	6542(16)	8508(8)	22(4)
H(13C)	3338(7)	5917(15)	9061(7)	22(4)
H(14)	4801(6)	7679(15)	9475(6)	12(4)
H(15)	5070(5)	10055(15)	9044(6)	9(4)
H(18A)	4804(6)	12732(16)	8649(7)	23(4)
H(18B)	4157(7)	13051(17)	8286(7)	29(4)
H(18C)	4578(6)	11692(17)	7990(8)	32(5)
H(19A)	3300(6)	9017(16)	7809(7)	20(4)
H(19B)	4038(7)	9014(17)	7859(7)	30(5)
H(19C)	3650(6)	10458(19)	7561(8)	36(5)

**Table 6.** Hydrogen bonds for DCB32 (CCDC 289914) [ $\text{\AA}$  and  $^\circ$ ].

D-H...A	d(D-H)	d(H...A)	d(D...A)	<(DHA)
O(2)-H(2)...O(5)#1	0.887(19)	2.02(2)	2.7848(15)	144.2(17)
O(2)-H(2)...O(1)	0.887(19)	2.248(19)	2.7418(14)	114.8(15)

Symmetry transformations used to generate equivalent atoms:

#1 x,-y+2,z+1/2

CALIFORNIA INSTITUTE OF TECHNOLOGY  
BECKMAN INSTITUTE  
X-RAY CRYSTALLOGRAPHY LABORATORY

Crystal Structure Analysis of:

Tetracycline **269** (JLS03)

(CCDC 701799)

Contents:

- Table 1. Crystal data
- Table 2. Atomic coordinates
- Table 3. Full bond distances and angles
- Table 4. Anisotropic displacement parameters

Figure B.115 Representation of Tetracycline **269**

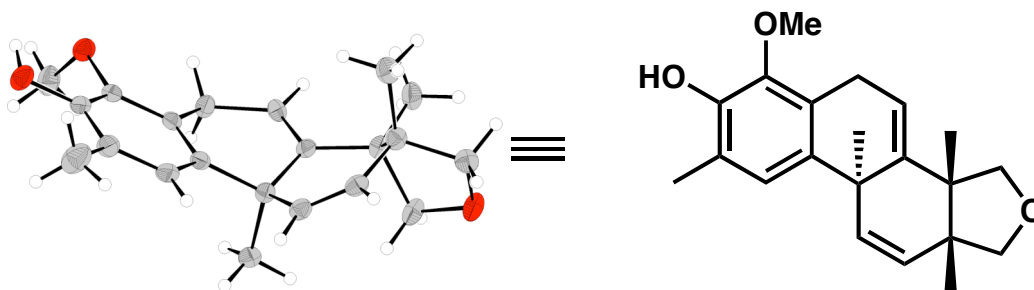


**Table 1.** Crystal data and structure refinement for JLS03 (CCDC 701799).

Empirical formula	C <sub>21</sub> H <sub>26</sub> O <sub>3</sub>
Formula weight	326.42
Crystallization Solvent	Acetone/heptane
Crystal Habit	Fragment
Crystal size	0.26 x 0.24 x 0.14 mm <sup>3</sup>
Crystal color	Colorless

### Data Collection

Type of diffractometer	Bruker SMART 1000	
Wavelength	0.71073 Å MoK $\alpha$	
Data Collection Temperature	100(2) K	
$\theta$ range for 11684 reflections used in lattice determination	2.24 to 28.20°	
Unit cell dimensions	a = 14.7511(11) Å b = 20.2786(15) Å c = 18.3704(14) Å	$\beta$ = 102.6820(10)°
Volume	5361.1(7) Å <sup>3</sup>	
Z	12	
Crystal system	Monoclinic	
Space group	P2 <sub>1</sub> /c	
Density (calculated)	1.213 Mg/m <sup>3</sup>	
F(000)	2112	
Data collection program	Bruker SMART v5.630	
$\theta$ range for data collection	1.41 to 28.49°	
Completeness to $\theta$ = 28.49°	92.3 %	
Index ranges	-19 ≤ h ≤ 18, -26 ≤ k ≤ 26, -24 ≤ l ≤ 23	
Data collection scan type	$\omega$ scans at 4 $\phi$ settings	
Data reduction program	Bruker SAINT v6.45A	
Reflections collected	59115	
Independent reflections	12523 [R <sub>int</sub> = 0.0934]	
Absorption coefficient	0.080 mm <sup>-1</sup>	
Absorption correction	None	
Max. and min. transmission	0.9890 and 0.9796	

**Table 1** (cont.)**Structure Solution and Refinement**

Structure solution program	SHELXS-97 (Sheldrick, 2008)
Primary solution method	Direct methods
Secondary solution method	Difference Fourier map
Hydrogen placement	Geometric positions
Structure refinement program	SHELXL-97 (Sheldrick, 2008)
Refinement method	Full matrix least-squares on F <sup>2</sup>
Data / restraints / parameters	12523 / 0 / 667
Treatment of hydrogen atoms	Riding
Goodness-of-fit on F <sup>2</sup>	1.353
Final R indices [ $I > 2\sigma(I)$ , 7169 reflections]	R <sub>1</sub> = 0.0549, wR <sub>2</sub> = 0.0886
R indices (all data)	R <sub>1</sub> = 0.1055, wR <sub>2</sub> = 0.0944
Type of weighting scheme used	Sigma
Weighting scheme used	$w=1/\sigma^2(Fo^2)$
Max shift/error	0.001
Average shift/error	0.000
Largest diff. peak and hole	0.822 and -0.258 e.Å <sup>-3</sup>

**Special Refinement Details**

Crystals were mounted on a glass fiber using Paratone oil then placed on the diffractometer under a nitrogen stream at 100K.

There are three molecules in the asymmetric unit. Molecules B and C have the same stereochemistry and are the enantiomer of molecule A.

Refinement of F<sup>2</sup> against ALL reflections. The weighted R-factor (wR) and goodness of fit (S) are based on F<sup>2</sup>, conventional R-factors (R) are based on F, with F set to zero for negative F<sup>2</sup>. The threshold expression of  $F^2 > 2\sigma(F^2)$  is used only for calculating R-factors(gt) etc. and is not relevant to the choice of reflections for refinement. R-factors based on F<sup>2</sup> are statistically about twice as large as those based on F, and R-factors based on ALL data will be even larger.

All esds (except the esd in the dihedral angle between two l.s. planes) are estimated using the full covariance matrix. The cell esds are taken into account individually in the estimation of esds in distances, angles and torsion angles; correlations between esds in cell parameters are only used when they are defined by crystal symmetry. An approximate (isotropic) treatment of cell esds is used for estimating esds involving l.s. planes.

**Table 2.** Atomic coordinates ( $\times 10^4$ ) and equivalent isotropic displacement parameters ( $\text{\AA}^2 \times 10^3$ ) for JLSO<sub>3</sub> (CCDC 701799).  $U(\text{eq})$  is defined as the trace of the orthogonalized  $U^{ij}$  tensor.

	x	y	z	$U_{\text{eq}}$
O(1A)	7781(1)	4925(1)	6261(1)	33(1)
O(2A)	3817(1)	3682(1)	9705(1)	26(1)
O(3A)	3532(1)	4840(1)	8912(1)	22(1)
C(1A)	7309(1)	4309(1)	6048(1)	33(1)
C(2A)	6651(1)	4205(1)	6577(1)	27(1)
C(3A)	7175(1)	3880(1)	7279(1)	27(1)
C(4A)	7116(1)	4047(1)	7961(1)	26(1)
C(5A)	6523(1)	4595(1)	8155(1)	22(1)
C(6A)	5787(1)	4327(1)	8556(1)	20(1)
C(7A)	5871(1)	3722(1)	8924(1)	21(1)
C(8A)	5218(1)	3497(1)	9307(1)	21(1)
C(9A)	4454(1)	3898(1)	9322(1)	20(1)
C(10A)	4350(1)	4496(1)	8943(1)	20(1)
C(11A)	5016(1)	4720(1)	8573(1)	20(1)
C(12A)	4887(1)	5369(1)	8160(1)	27(1)
C(13A)	5309(1)	5343(1)	7494(1)	26(1)
C(14A)	6046(1)	4976(1)	7457(1)	23(1)
C(15A)	6414(1)	4931(1)	6749(1)	26(1)
C(16A)	7376(1)	5241(1)	6813(1)	30(1)
C(17A)	5815(1)	3774(1)	6218(1)	39(1)
C(18A)	7169(1)	5056(1)	8716(1)	29(1)
C(19A)	5309(1)	2835(1)	9693(1)	27(1)
C(20A)	3616(1)	5376(1)	9436(1)	30(1)
C(21A)	5758(1)	5245(1)	6074(1)	37(1)
O(1B)	12026(1)	934(1)	4456(1)	28(1)
O(2B)	6313(1)	3047(1)	1644(1)	32(1)
O(3B)	6616(1)	2908(1)	3181(1)	25(1)
C(1B)	11457(1)	485(1)	3938(1)	26(1)
C(2B)	10545(1)	848(1)	3619(1)	21(1)
C(3B)	10667(1)	1254(1)	2963(1)	22(1)
C(4B)	10390(1)	1869(1)	2834(1)	22(1)
C(5B)	9884(1)	2269(1)	3311(1)	19(1)
C(6B)	8916(1)	2466(1)	2862(1)	19(1)
C(7B)	8730(1)	2542(1)	2092(1)	24(1)
C(8B)	7869(1)	2738(1)	1681(1)	26(1)
C(9B)	7166(1)	2865(1)	2056(1)	24(1)
C(10B)	7346(1)	2803(1)	2827(1)	21(1)
C(11B)	8217(1)	2606(1)	3236(1)	20(1)
C(12B)	8385(1)	2533(1)	4068(1)	23(1)
C(13B)	9119(1)	2026(1)	4345(1)	21(1)
C(14B)	9799(1)	1877(1)	4008(1)	19(1)
C(15B)	10478(1)	1318(1)	4276(1)	21(1)
C(16B)	11504(1)	1527(1)	4509(1)	25(1)
C(17B)	9724(1)	376(1)	3380(1)	28(1)
C(18B)	10430(1)	2920(1)	3536(1)	25(1)
C(19B)	7689(2)	2784(1)	845(1)	42(1)
C(20B)	6617(1)	3554(1)	3491(1)	34(1)
C(21B)	10244(1)	942(1)	4932(1)	29(1)

O(1C)	5389(1)	7929(1)	3000(1)	32(1)
O(2C)	10400(1)	4690(1)	3474(1)	29(1)
O(3C)	10726(1)	5860(1)	4260(1)	25(1)
C(1C)	5614(1)	7760(1)	2303(1)	27(1)
C(2C)	6458(1)	7307(1)	2485(1)	22(1)
C(3C)	6132(1)	6619(1)	2589(1)	24(1)
C(4C)	6524(1)	6214(1)	3128(1)	24(1)
C(5C)	7376(1)	6367(1)	3715(1)	24(1)
C(6C)	8184(1)	5918(1)	3627(1)	21(1)
C(7C)	8054(1)	5326(1)	3225(1)	24(1)
C(8C)	8788(1)	4917(1)	3158(1)	23(1)
C(9C)	9682(1)	5097(1)	3526(1)	22(1)
C(10C)	9818(1)	5682(1)	3931(1)	21(1)
C(11C)	9084(1)	6096(1)	3975(1)	22(1)
C(12C)	9262(1)	6763(1)	4346(1)	29(1)
C(13C)	8545(1)	7252(1)	3983(1)	26(1)
C(14C)	7671(1)	7088(1)	3671(1)	23(1)
C(15C)	6974(1)	7584(1)	3257(1)	24(1)
C(16C)	6134(1)	7713(1)	3605(1)	29(1)
C(17C)	7024(1)	7318(1)	1881(1)	27(1)
C(18C)	7178(2)	6225(1)	4497(1)	37(1)
C(19C)	8632(1)	4304(1)	2687(1)	32(1)
C(20C)	11013(1)	5618(1)	5010(1)	34(1)
C(21C)	7424(1)	8253(1)	3168(1)	32(1)

---

**Table 3.** Bond lengths [Å] and angles [°] for JLSO<sub>3</sub> (CCDC 701799).

O(1A)-C(16A)	1.435(2)	C(14B)-C(15B)	1.521(2)
O(1A)-C(1A)	1.441(2)	C(15B)-C(21B)	1.529(3)
O(2A)-C(9A)	1.365(2)	C(15B)-C(16B)	1.538(2)
O(3A)-C(10A)	1.383(2)	O(1C)-C(1C)	1.433(2)
O(3A)-C(20A)	1.440(2)	O(1C)-C(16C)	1.449(2)
C(1A)-C(2A)	1.532(3)	O(2C)-C(9C)	1.362(2)
C(2A)-C(3A)	1.502(3)	O(3C)-C(10C)	1.391(2)
C(2A)-C(17A)	1.537(3)	O(3C)-C(20C)	1.435(2)
C(2A)-C(15A)	1.560(3)	C(1C)-C(2C)	1.525(3)
C(3A)-C(4A)	1.318(3)	C(2C)-C(3C)	1.501(3)
C(4A)-C(5A)	1.504(3)	C(2C)-C(17C)	1.527(3)
C(5A)-C(14A)	1.530(3)	C(2C)-C(15C)	1.560(3)
C(5A)-C(6A)	1.540(3)	C(3C)-C(4C)	1.319(3)
C(5A)-C(18A)	1.554(3)	C(4C)-C(5C)	1.497(3)
C(6A)-C(7A)	1.392(2)	C(5C)-C(14C)	1.533(3)
C(6A)-C(11A)	1.395(2)	C(5C)-C(6C)	1.536(3)
C(7A)-C(8A)	1.388(2)	C(5C)-C(18C)	1.554(3)
C(8A)-C(9A)	1.395(3)	C(6C)-C(11C)	1.388(2)
C(8A)-C(19A)	1.510(2)	C(6C)-C(7C)	1.401(3)
C(9A)-C(10A)	1.389(2)	C(7C)-C(8C)	1.390(3)
C(10A)-C(11A)	1.389(2)	C(8C)-C(9C)	1.392(3)
C(11A)-C(12A)	1.509(2)	C(8C)-C(19C)	1.502(3)
C(12A)-C(13A)	1.491(3)	C(9C)-C(10C)	1.392(3)
C(13A)-C(14A)	1.331(2)	C(10C)-C(11C)	1.386(3)
C(14A)-C(15A)	1.519(3)	C(11C)-C(12C)	1.512(3)
C(15A)-C(16A)	1.533(3)	C(12C)-C(13C)	1.496(3)
C(15A)-C(21A)	1.534(3)	C(13C)-C(14C)	1.332(3)
O(1B)-C(16B)	1.442(2)	C(14C)-C(15C)	1.518(3)
O(1B)-C(1B)	1.445(2)	C(15C)-C(21C)	1.535(3)
O(2B)-C(9B)	1.369(2)	C(15C)-C(16C)	1.537(3)
O(3B)-C(10B)	1.391(2)	C(16A)-O(1A)-C(1A)	109.14(15)
O(3B)-C(20B)	1.428(2)	C(10A)-O(3A)-C(20A)	114.02(14)
C(1B)-C(2B)	1.533(2)	O(1A)-C(1A)-C(2A)	106.45(16)
C(2B)-C(3B)	1.502(3)	C(3A)-C(2A)-C(1A)	109.07(16)
C(2B)-C(17B)	1.531(3)	C(3A)-C(2A)-C(17A)	109.39(17)
C(2B)-C(15B)	1.558(2)	C(1A)-C(2A)-C(17A)	111.47(17)
C(3B)-C(4B)	1.318(2)	C(3A)-C(2A)-C(15A)	109.67(17)
C(4B)-C(5B)	1.506(2)	C(1A)-C(2A)-C(15A)	101.46(16)
C(5B)-C(14B)	1.535(3)	C(17A)-C(2A)-C(15A)	115.44(17)
C(5B)-C(6B)	1.537(2)	C(4A)-C(3A)-C(2A)	124.98(19)
C(5B)-C(18B)	1.556(2)	C(3A)-C(4A)-C(5A)	125.32(19)
C(6B)-C(7B)	1.389(2)	C(4A)-C(5A)-C(14A)	111.02(17)
C(6B)-C(11B)	1.389(2)	C(4A)-C(5A)-C(6A)	111.13(15)
C(7B)-C(8B)	1.386(3)	C(14A)-C(5A)-C(6A)	109.66(15)
C(8B)-C(9B)	1.389(3)	C(4A)-C(5A)-C(18A)	107.35(16)
C(8B)-C(19B)	1.504(3)	C(14A)-C(5A)-C(18A)	110.74(15)
C(9B)-C(10B)	1.388(3)	C(6A)-C(5A)-C(18A)	106.84(15)
C(10B)-C(11B)	1.396(2)	C(7A)-C(6A)-C(11A)	118.66(18)
C(11B)-C(12B)	1.500(2)	C(7A)-C(6A)-C(5A)	123.12(17)
C(12B)-C(13B)	1.499(2)	C(11A)-C(6A)-C(5A)	118.18(17)
C(13B)-C(14B)	1.325(2)	C(8A)-C(7A)-C(6A)	122.53(18)

C(7A)-C(8A)-C(9A)	118.11(18)	C(6B)-C(11B)-C(10B)	119.17(18)
C(7A)-C(8A)-C(19A)	122.05(17)	C(6B)-C(11B)-C(12B)	120.61(17)
C(9A)-C(8A)-C(19A)	119.84(17)	C(10B)-C(11B)-C(12B)	120.21(17)
O(2A)-C(9A)-C(10A)	121.73(17)	C(13B)-C(12B)-C(11B)	111.08(16)
O(2A)-C(9A)-C(8A)	118.26(17)	C(14B)-C(13B)-C(12B)	124.23(18)
C(10A)-C(9A)-C(8A)	120.00(18)	C(13B)-C(14B)-C(15B)	122.10(17)
O(3A)-C(10A)-C(9A)	117.39(17)	C(13B)-C(14B)-C(5B)	118.75(17)
O(3A)-C(10A)-C(11A)	121.25(17)	C(15B)-C(14B)-C(5B)	119.13(16)
C(9A)-C(10A)-C(11A)	121.24(17)	C(14B)-C(15B)-C(21B)	112.37(16)
C(10A)-C(11A)-C(6A)	119.40(17)	C(14B)-C(15B)-C(16B)	115.01(15)
C(10A)-C(11A)-C(12A)	120.44(17)	C(21B)-C(15B)-C(16B)	107.24(16)
C(6A)-C(11A)-C(12A)	120.10(17)	C(14B)-C(15B)-C(2B)	110.76(15)
C(13A)-C(12A)-C(11A)	110.63(16)	C(21B)-C(15B)-C(2B)	111.63(15)
C(14A)-C(13A)-C(12A)	123.67(19)	C(16B)-C(15B)-C(2B)	99.10(14)
C(13A)-C(14A)-C(15A)	121.84(18)	O(1B)-C(16B)-C(15B)	105.02(15)
C(13A)-C(14A)-C(5A)	118.05(18)	C(1C)-O(1C)-C(16C)	109.10(14)
C(15A)-C(14A)-C(5A)	120.11(16)	C(10C)-O(3C)-C(20C)	112.42(14)
C(14A)-C(15A)-C(16A)	114.14(17)	O(1C)-C(1C)-C(2C)	106.71(15)
C(14A)-C(15A)-C(21A)	112.67(16)	C(3C)-C(2C)-C(1C)	108.54(16)
C(16A)-C(15A)-C(21A)	107.48(17)	C(3C)-C(2C)-C(17C)	110.42(15)
C(14A)-C(15A)-C(2A)	111.58(16)	C(1C)-C(2C)-C(17C)	112.50(16)
C(16A)-C(15A)-C(2A)	99.14(15)	C(3C)-C(2C)-C(15C)	108.92(16)
C(21A)-C(15A)-C(2A)	111.01(17)	C(1C)-C(2C)-C(15C)	101.13(15)
O(1A)-C(16A)-C(15A)	106.47(16)	C(17C)-C(2C)-C(15C)	114.85(16)
C(16B)-O(1B)-C(1B)	109.14(13)	C(4C)-C(3C)-C(2C)	125.08(18)
C(10B)-O(3B)-C(20B)	113.18(14)	C(3C)-C(4C)-C(5C)	124.87(19)
O(1B)-C(1B)-C(2B)	106.45(14)	C(4C)-C(5C)-C(14C)	111.29(16)
C(3B)-C(2B)-C(17B)	109.82(16)	C(4C)-C(5C)-C(6C)	110.47(16)
C(3B)-C(2B)-C(1B)	108.71(16)	C(14C)-C(5C)-C(6C)	108.89(16)
C(17B)-C(2B)-C(1B)	112.45(16)	C(4C)-C(5C)-C(18C)	109.14(16)
C(3B)-C(2B)-C(15B)	109.02(15)	C(14C)-C(5C)-C(18C)	109.82(16)
C(17B)-C(2B)-C(15B)	115.07(16)	C(6C)-C(5C)-C(18C)	107.13(15)
C(1B)-C(2B)-C(15B)	101.36(15)	C(11C)-C(6C)-C(7C)	118.14(18)
C(4B)-C(3B)-C(2B)	125.12(18)	C(11C)-C(6C)-C(5C)	118.87(17)
C(3B)-C(4B)-C(5B)	125.37(18)	C(7C)-C(6C)-C(5C)	122.97(17)
C(4B)-C(5B)-C(14B)	110.38(16)	C(8C)-C(7C)-C(6C)	122.59(18)
C(4B)-C(5B)-C(6B)	110.43(15)	C(7C)-C(8C)-C(9C)	118.30(18)
C(14B)-C(5B)-C(6B)	110.24(15)	C(7C)-C(8C)-C(19C)	121.33(18)
C(4B)-C(5B)-C(18B)	108.57(15)	C(9C)-C(8C)-C(19C)	120.36(18)
C(14B)-C(5B)-C(18B)	110.42(15)	O(2C)-C(9C)-C(8C)	118.38(18)
C(6B)-C(5B)-C(18B)	106.73(15)	O(2C)-C(9C)-C(10C)	122.08(18)
C(7B)-C(6B)-C(11B)	118.64(17)	C(8C)-C(9C)-C(10C)	119.54(18)
C(7B)-C(6B)-C(5B)	121.87(17)	C(11C)-C(10C)-O(3C)	120.57(17)
C(11B)-C(6B)-C(5B)	119.41(17)	C(11C)-C(10C)-C(9C)	121.64(18)
C(8B)-C(7B)-C(6B)	122.58(19)	O(3C)-C(10C)-C(9C)	117.69(17)
C(7B)-C(8B)-C(9B)	118.58(19)	C(10C)-C(11C)-C(6C)	119.74(18)
C(7B)-C(8B)-C(19B)	120.58(19)	C(10C)-C(11C)-C(12C)	120.45(17)
C(9B)-C(8B)-C(19B)	120.79(18)	C(6C)-C(11C)-C(12C)	119.63(17)
O(2B)-C(9B)-C(10B)	122.40(18)	C(13C)-C(12C)-C(11C)	110.87(16)
O(2B)-C(9B)-C(8B)	118.09(18)	C(14C)-C(13C)-C(12C)	123.30(19)
C(10B)-C(9B)-C(8B)	119.51(18)	C(13C)-C(14C)-C(15C)	122.37(18)
C(9B)-C(10B)-O(3B)	117.92(17)	C(13C)-C(14C)-C(5C)	118.35(17)
C(9B)-C(10B)-C(11B)	121.49(18)	C(15C)-C(14C)-C(5C)	119.26(17)
O(3B)-C(10B)-C(11B)	120.50(17)	C(14C)-C(15C)-C(21C)	112.13(16)

C(14C)-C(15C)-C(16C)	115.08(16)
C(21C)-C(15C)-C(16C)	107.55(16)
C(14C)-C(15C)-C(2C)	111.01(15)
C(21C)-C(15C)-C(2C)	110.98(16)
C(16C)-C(15C)-C(2C)	99.40(15)
O(1C)-C(16C)-C(15C)	106.10(15)

**Table 4.** Anisotropic displacement parameters ( $\text{\AA}^2 \times 10^4$ ) for JLSO<sub>3</sub> (CCDC 701799). The anisotropic displacement factor exponent takes the form:  $-2\pi^2 [ h^2 a^{*2} U^{11} + \dots + 2 h k a^* b^* U^{12} ]$

	U <sup>11</sup>	U <sup>22</sup>	U <sup>33</sup>	U <sup>23</sup>	U <sup>13</sup>	U <sup>12</sup>
O(1A)	307(9)	288(8)	454(10)	-52(7)	217(7)	-26(7)
O(2A)	231(8)	299(8)	262(8)	46(7)	69(7)	0(6)
O(3A)	206(8)	206(7)	243(8)	-56(6)	54(6)	12(6)
C(1A)	290(13)	321(13)	414(15)	-52(11)	124(11)	-40(10)
C(2A)	197(12)	307(12)	342(13)	-44(10)	125(10)	-21(10)
C(3A)	207(12)	197(11)	445(15)	-19(10)	132(11)	1(9)
C(4A)	201(12)	195(11)	386(14)	33(10)	70(10)	18(9)
C(5A)	170(11)	209(11)	284(13)	6(9)	51(9)	3(9)
C(6A)	189(11)	186(10)	213(12)	-34(9)	25(9)	-37(9)
C(7A)	159(11)	208(11)	253(12)	-55(9)	-5(9)	9(9)
C(8A)	217(12)	207(11)	178(11)	-23(9)	1(9)	-34(9)
C(9A)	179(11)	236(11)	173(11)	-39(9)	35(9)	-64(9)
C(10A)	171(11)	204(11)	210(12)	-49(9)	29(9)	-15(9)
C(11A)	187(11)	170(10)	239(12)	-16(9)	43(9)	-15(9)
C(12A)	242(12)	235(11)	352(14)	70(10)	112(10)	42(9)
C(13A)	233(12)	231(11)	336(13)	82(10)	86(10)	18(9)
C(14A)	187(11)	199(11)	315(13)	14(9)	76(10)	-24(9)
C(15A)	217(12)	280(12)	305(13)	26(10)	105(10)	41(9)
C(16A)	309(13)	236(12)	401(14)	-1(10)	188(11)	21(10)
C(17A)	334(14)	408(14)	450(15)	-97(12)	145(12)	-83(11)
C(18A)	232(12)	261(12)	382(14)	12(10)	88(10)	-28(9)
C(19A)	252(12)	269(12)	267(12)	42(10)	1(10)	-15(9)
C(20A)	282(13)	302(12)	327(13)	-132(10)	89(10)	0(10)
C(21A)	332(14)	480(15)	337(14)	53(12)	164(11)	63(11)
O(1B)	233(8)	282(8)	309(9)	-63(7)	0(7)	71(6)
O(2B)	204(8)	471(9)	279(9)	128(7)	39(7)	32(7)
O(3B)	217(8)	266(8)	284(8)	-18(6)	81(7)	26(6)
C(1B)	257(12)	244(12)	264(12)	-35(9)	40(10)	14(9)
C(2B)	183(11)	217(11)	232(12)	-26(9)	62(9)	25(9)
C(3B)	187(11)	280(12)	213(12)	-75(9)	56(9)	-14(9)
C(4B)	211(12)	273(12)	191(11)	9(9)	62(9)	3(9)
C(5B)	186(11)	217(11)	185(11)	19(9)	53(9)	9(9)
C(6B)	189(11)	169(10)	216(12)	12(9)	44(9)	-25(8)
C(7B)	224(12)	281(12)	234(12)	42(10)	83(10)	-28(9)
C(8B)	234(12)	309(12)	224(12)	60(10)	45(10)	-18(10)
C(9B)	186(11)	233(11)	269(13)	66(9)	0(10)	-19(9)
C(10B)	185(11)	184(10)	263(12)	15(9)	73(9)	-24(9)
C(11B)	215(12)	158(10)	213(12)	5(9)	37(9)	-24(8)
C(12B)	191(11)	271(12)	220(12)	16(9)	51(9)	25(9)
C(13B)	233(12)	235(11)	170(11)	32(9)	38(9)	31(9)
C(14B)	178(11)	193(11)	204(11)	-31(9)	26(9)	-15(9)
C(15B)	197(11)	220(11)	216(12)	-2(9)	53(9)	33(9)
C(16B)	206(12)	278(12)	248(12)	-64(9)	33(9)	70(9)
C(17B)	288(13)	266(12)	307(13)	-19(10)	85(10)	12(10)
C(18B)	207(11)	245(11)	278(12)	31(9)	25(9)	-21(9)
C(19B)	296(13)	685(17)	274(14)	90(12)	69(11)	-5(12)
C(20B)	301(13)	327(13)	399(15)	-37(11)	77(11)	101(10)

C(21B)	307(13)	272(12)	302(13)	39(10)	94(10)	89(10)
O(1C)	242(8)	444(9)	254(9)	-78(7)	31(7)	90(7)
O(2C)	236(8)	248(8)	376(9)	6(7)	71(7)	32(6)
O(3C)	210(8)	319(8)	207(8)	35(6)	24(6)	24(6)
C(1C)	240(12)	306(12)	263(13)	-48(10)	58(10)	8(10)
C(2C)	188(11)	247(11)	214(12)	-46(9)	32(9)	20(9)
C(3C)	183(11)	276(12)	240(12)	-72(10)	35(9)	-15(9)
C(4C)	195(11)	252(11)	304(13)	-14(10)	87(10)	-16(9)
C(5C)	217(12)	304(12)	216(12)	23(10)	84(9)	34(9)
C(6C)	232(12)	236(11)	178(11)	43(9)	80(9)	18(9)
C(7C)	232(12)	250(11)	231(12)	79(9)	60(9)	-37(9)
C(8C)	255(12)	202(11)	242(12)	53(9)	84(10)	2(9)
C(9C)	256(12)	209(11)	217(12)	81(9)	100(10)	63(9)
C(10C)	197(11)	286(12)	156(11)	52(9)	40(9)	-4(9)
C(11C)	227(12)	260(11)	172(11)	19(9)	61(9)	11(9)
C(12C)	241(12)	362(13)	243(12)	-86(10)	15(10)	70(10)
C(13C)	278(13)	268(12)	230(12)	-91(10)	23(10)	67(10)
C(14C)	247(12)	276(12)	185(11)	-75(9)	68(9)	49(9)
C(15C)	209(11)	261(12)	243(12)	-66(9)	32(9)	32(9)
C(16C)	252(12)	346(13)	257(12)	-89(10)	20(10)	90(10)
C(17C)	227(12)	295(12)	268(13)	-38(10)	31(10)	2(9)
C(18C)	339(14)	501(15)	309(14)	92(11)	161(11)	111(11)
C(19C)	307(13)	245(12)	410(15)	12(10)	87(11)	-16(10)
C(20C)	282(13)	435(14)	257(13)	35(11)	-11(10)	23(11)
C(21C)	297(13)	271(12)	349(14)	-78(10)	-16(11)	54(10)

---

**Table 5.** Hydrogen bonds for JLSO<sub>3</sub> (CCDC 701799) [Å and °].

D-H...A	d(D-H)	d(H...A)	d(D...A)	<(DHA)
O(2A)-H(2A)...O(1B)#1	0.84	1.91	2.6954(18)	155.0
O(2A)-H(2A)...O(3A)	0.84	2.31	2.7465(17)	112.3
O(2B)-H(2B)...O(1C)#2	0.84	1.97	2.7397(19)	152.2
O(2B)-H(2B)...O(3B)	0.84	2.37	2.7747(18)	110.5
O(2C)-H(2C)...O(1A)#3	0.84	1.94	2.7345(19)	158.5
O(2C)-H(2C)...O(3C)	0.84	2.34	2.7633(18)	111.5

Symmetry transformations used to generate equivalent atoms:

#1  $x-1, -y+1/2, z+1/2$

#2  $-x+1, y-1/2, -z+1/2$

#3  $-x+2, -y+1, -z+1$

## CHAPTER FOUR

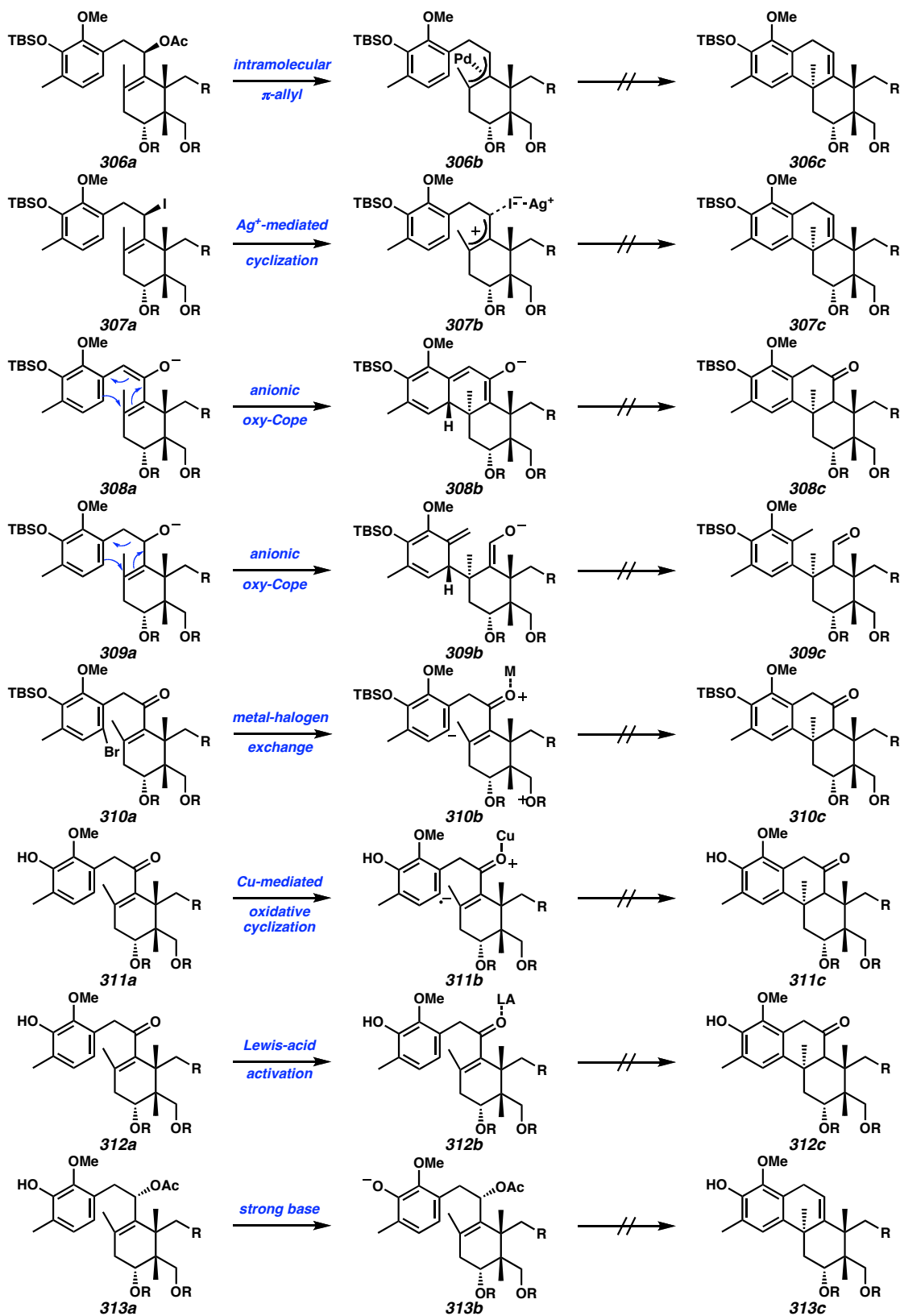
Radical Cyclization Approaches Toward  
the Tricyclic Core of Zoanthenol<sup>†</sup>

## 4.1.1 Introduction

The acid-mediated cyclization chemistry detailed in Chapter 3 is a powerful method for the formation of the carbocyclic core of zoanthenol. Unfortunately, the utility of these cyclizations is limited by the sensitivity of the system to the substrate, the harsh conditions required, and the loss of functionality during cyclization. With these issues in mind, other strategies were explored to form the B ring from the available tethered A–C ring systems. Among these, several methods displayed no reactivity for the tested substrates (Scheme 4.1.1). Such cyclization methods included intramolecular  $\pi$ -allyl reactions<sup>1</sup> of allylic acetates (**306a**  $\rightarrow$  **306b**  $\rightarrow$  **306c**), reductive Heck reactions of enones, silver-mediated cyclizations of allylic iodides (**307a**  $\rightarrow$  **307b**  $\rightarrow$  **307c**), anionic oxy-Cope electrocyclizations<sup>2</sup> of enones (**308a**  $\rightarrow$  **308b**  $\rightarrow$  **308c**) or allylic alcohols (**309a**  $\rightarrow$  **309b**  $\rightarrow$  **309c**), aryl anion additions (**310a**  $\rightarrow$  **310b**  $\rightarrow$  **310c**), Lewis-acid enone activation (**311a**  $\rightarrow$  **311b**  $\rightarrow$  **311c**), copper-mediated arene/enone oxidative cyclizations<sup>3</sup> (**312a**  $\rightarrow$  **312b**  $\rightarrow$  **312c**), and strong base-mediated cyclization of allylic acetates (**313a**  $\rightarrow$  **313b**  $\rightarrow$  **313c**).

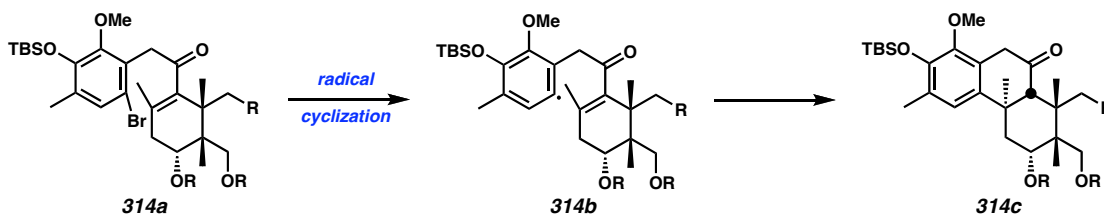
---

<sup>†</sup> This work was conducted in close collaboration with Dr. Douglas C. Behenna, a former graduate student in the Stoltz Group.



**Scheme 4.1.1** Failed methods for cyclization of tethered A-C ring systems.

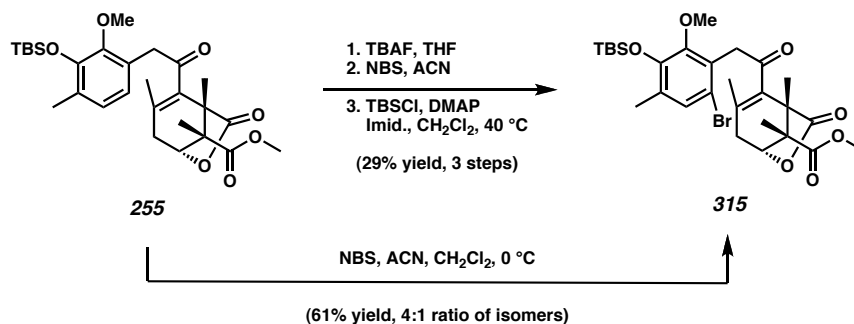
However, one cyclization method held some promise: the conjugate radical addition of an aryl radical to our enone substrates (Scheme 4.1.2). Although this type of reaction has substantial precedence, *endo* radical conjugate addition cyclization reactions are much less common than *exo* reactions.<sup>4</sup> However, we were inspired by a report of an arene radical conjugate addition that built a quaternary center while closing a six-membered ring.<sup>5</sup> In this chapter, we detail efforts toward the application of radical conjugate additions for the synthesis of zoanthenol's tricyclic core.



**Scheme 4.1.2** Radical-induced cyclization of a tethered A–C ring system.

#### 4.2.1 Synthesis and Cyclization of a Lactone-Derived Precursor

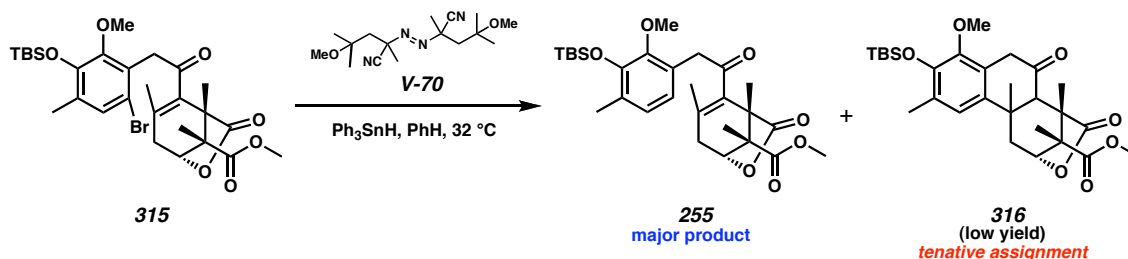
The radical cyclization substrate required a selective bromination of the A ring *para* to the silyl ether. While bromination with *N*-bromosuccinimide (NBS) was well known to occur *para* to electron releasing groups,<sup>6</sup> there was little precedent for *para*-directing preference of silyl ethers versus methyl ethers. There was significant evidence that phenols were superior to methyl ethers in their directing ability.<sup>7</sup> Thus, we began by executing a selective synthesis of the desired aryl bromide over three steps (Scheme 4.2.1). Desilylation of **255** provided a phenol, which was treated with NBS in acetonitrile to afford a single bromide isomer. Resilylation provided **315** in 29% yield over the three steps.<sup>8</sup> Subsequently, direct bromination of enone **255** led to a 4:1 mixture of bromide positional isomers favoring the desired aryl bromide.



#### Scheme 4.2.1 Synthesis of lactone-derived radical cyclization precursor

We initially tested a number of conditions for cyclization. The most effective conditions employed V-70 initiator in benzene at 32 °C with triphenyltin hydride. The V-70 initiator decomposes more readily ( $t_{1/2} = \sim 10$  h at 30 °C) than AIBN ( $t_{1/2} = \sim 10$  h at 80 °C), and it enables initiation of the radical reaction at lower temperatures. Additionally, the lower temperature reduces the amount of debrominated enone recovered. For all substrates tested, these are the conditions used.

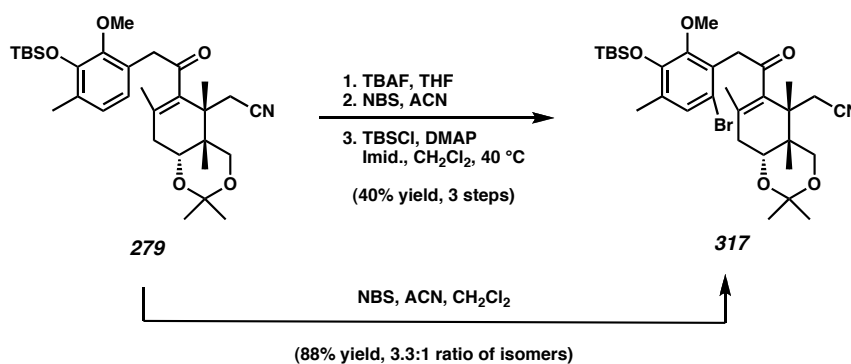
Treatment of aryl bromide **315** led to the formation of a 1:1 mixture of two diastereomers of cyclized product **316** as well as reisolation of debrominated precursor **255**. This result was very promising, but we were only able to isolate small amounts of the cyclized material, which was produced as a 1:1 ratio of diastereomers. Thus, we ventured forward to explore cyclizations of more synthetically advanced A–C ring systems.



#### Scheme 4.2.2 Attempted cyclization of lactone-derived A–C ring system

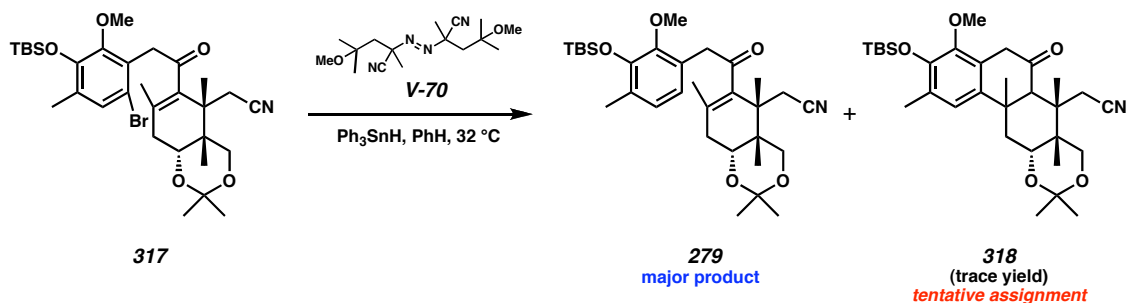
### 4.3.1 Synthesis and Cyclization of a Homologated Nitrile-Derived Cyclization Precursor

Having established the selectivity of the bromination for arene **313**, it was anticipated that similar bromination selectivity would allow preparation of the desired bromide isomer. Nevertheless, an independent synthesis of **317** was conducted as confirmation for the product assignments. Accordingly, enone **279** was desilylated with TBAF, treated with NBS in acetonitrile and methylene chloride, and finally resilylated to afford a cyclization precursor **317** in 40% yield over the three steps (Scheme 4.3.1). The one-step procedure was accomplished by treating enone **279** with NBS in acetonitrile at ambient temperature and led to the formation of a favorable 3.3:1 mixture of bromide isomers in 88% combined yield.



**Scheme 4.3.1** Synthesis of homologated nitrile-derived radical cyclization precursor.

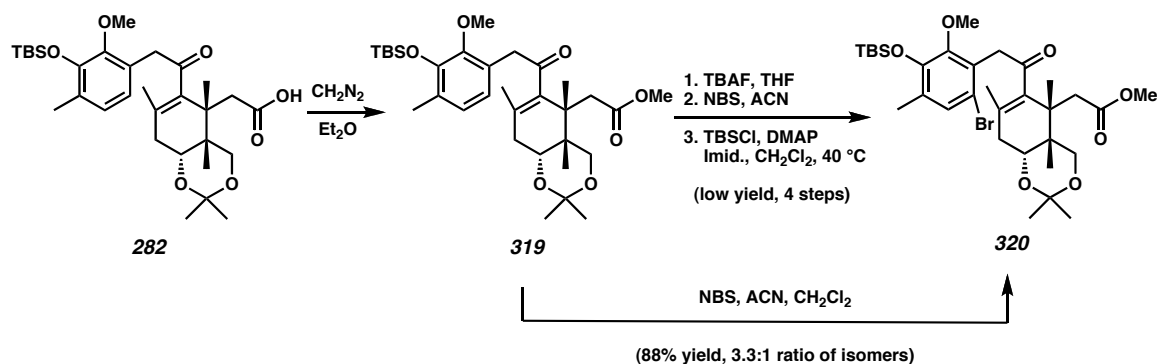
Treatment of cyclization precursor **317** with the standard cyclization conditions once again yielded mainly reductive debromination product **279** (Scheme 4.3.2). However, we were also able to obtain spectra for what appeared to be two diastereomers of cyclized products, tentatively assigned as a 1:1 mixture of diastereomers of **318**.



**Scheme 4.3.2** Attempted cyclization of nitrile-derived A-C ring system.

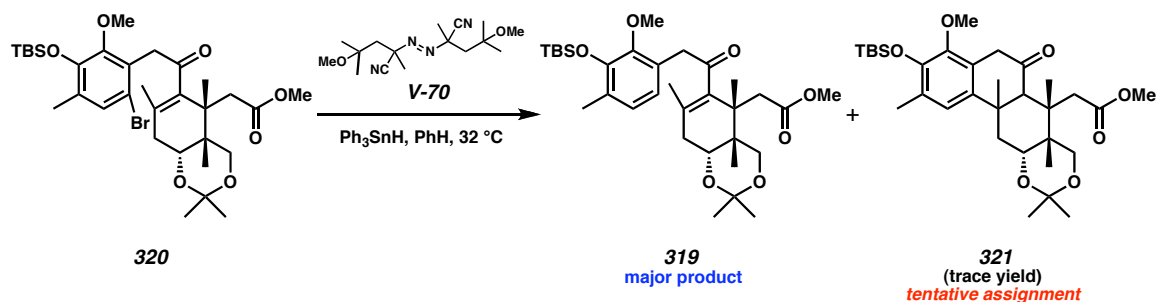
#### 4.4.1 Synthesis and Cyclization of a Homologated Ester-Derived Cyclization Precursor

Owing to concerns that the nitrile moiety was interfering with the cyclization, the corresponding methyl ester-derived substrate was targeted. Thus, carboxylic acid **282**<sup>9</sup> was treated with diazomethane to afford the corresponding ester, **319** (Scheme 4.4.1). Desilylation, bromination, and resilylation afforded aryl bromide **320** in < 20% overall yield.<sup>10</sup> In the one-step procedure, bromination of methyl ester **319** led directly to 88% yield of radical cyclization precursor **320** in a 3.3:1 dr.



**Scheme 4.4.1** Synthesis of homologated ester-derived radical cyclization precursor.

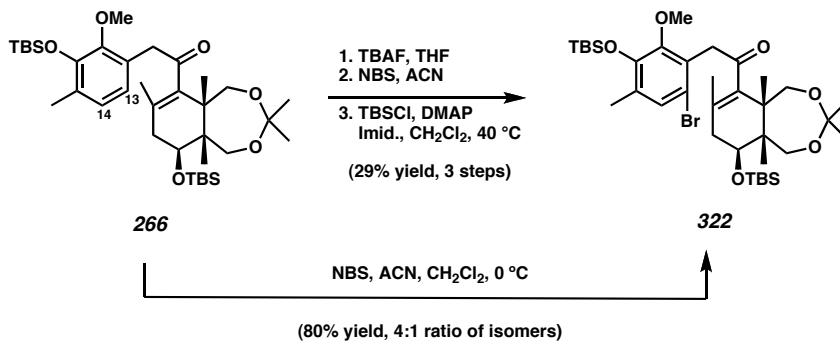
Aryl bromide **320** was subjected to the radical cyclization conditions to afford trace amounts of a mixture of diastereomeric cyclized products as well as a substantial amount of enone **319** (Scheme 4.4.2).



**Scheme 4.4.2** Attempted cyclization of ester-derived A–C ring system.

#### 4.5.1 Synthesis and Cyclization of a 7-Membered Acetal-Derived Cyclization Precursor

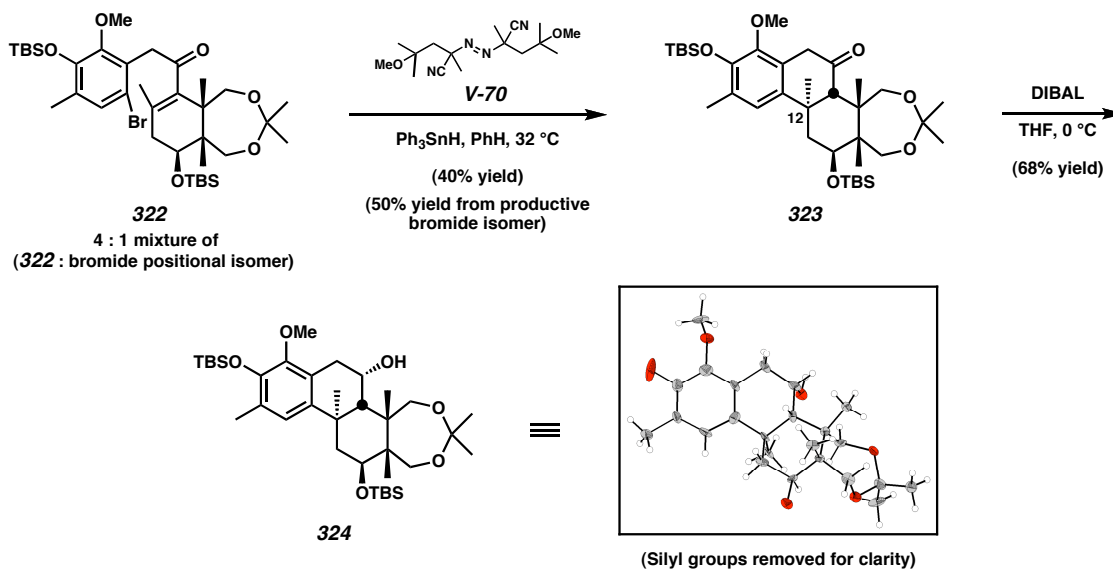
To this point, the C(10) oxygen functionality of all substrates tested was  $\alpha$ -disposed. These substrates were initially targeted due to their bicyclic nature, with the expectation that this would bias the formation of the desired stereochemistry at the new quaternary center. To explore the impact of the C(10) stereocenter, we assembled the aryl bromide derivative of enone **266**. Direct bromination afforded a 4:1 mixture of isomers in 80% yield, while the three-step procedure confirmed the identity of the major product with a 29% yield of **322** over the 3 steps (Scheme 4.5.1).<sup>8</sup>



**Scheme 4.5.1** Synthesis of 7-membered acetal-derived radical cyclization precursor.

Aryl bromide **322** was treated under the standard cyclization conditions. Much to our delight, significant amounts of cyclization product **323** were observed (Scheme 4.5.2). As in other cyclization attempts, debrominated enone **266** was also obtained. The relative stereochemistry at the newly formed stereocenter was confirmed by X-ray

structure analysis of alcohol **324**, obtained by DIBAL reduction of **323**.<sup>11</sup> While the yield of ketone **323** was modest, many reaction parameters remain to be optimized, such as amounts of reagents, temperature, and rate of triphenyltin hydride addition, as well as the possibility of activating the system further by employing Lewis acids.<sup>12</sup>

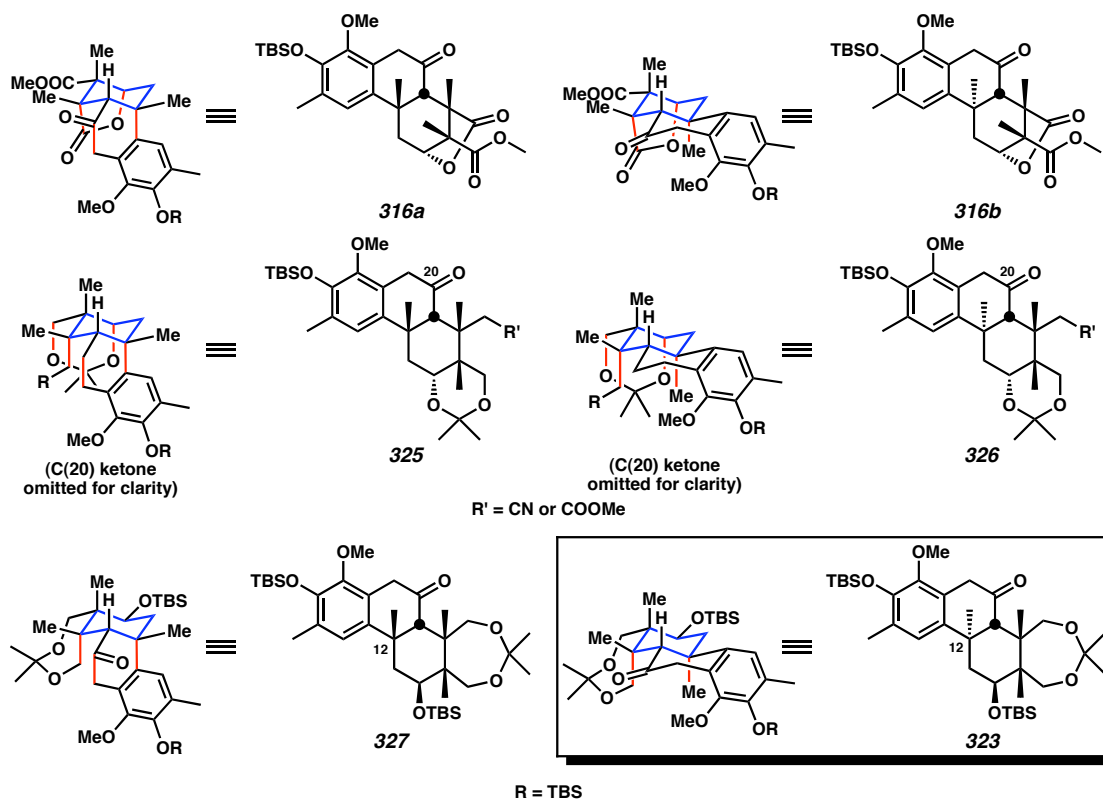


**Scheme 4.5.2** Cyclization of 7-membered acetal-derived A–C ring system.

#### 4.6.1 Substrate Requirements and Limits of System

Radical cyclizations of aryl bromides **315**, **317**, and **320** lead primarily to reductive debromination as well as trace yields of cyclized products as mixtures of diastereomers at C(12). However, in the case of aryl bromide **322**, the desired diastereomer was isolated as the exclusive cyclized product. Although all of the substrates tested possess a bicyclic framework, the facial bias provided by the 6–7 bicycle in aryl bromide **324** is expected to be the least substantial. Additionally, this system is the most structurally flexible. Thus, the observed selectivity must be derived from a different feature of the 7-membered acetal substrate. Analysis of the two most likely product structures for each case provided insight into the selectivity of the transformation. Scheme 4.6.1 outlines the key 1,3-diaxial interactions experienced by each product. In accessing the desired

diastereomer, a minimal number of destabilizing interactions are formed. In all cases, the desired diastereomer (**316b**, **326**, and **323**) exhibits one fewer diaxial interaction than the alternative diastereomer. Additionally, **316b** and **326** possess one and two additional diaxial interactions, respectively, when compared with **323**. It is reasonable to assume that, at the reaction temperature (32 °C), the additional destabilizing energy imparted by an extra diaxial interaction is sufficient to guide selectivity toward the desired case for **323** versus **327** or to almost completely prevent reactivity in the more hindered cases (**316a**, **316b**, **325**, and **326**). All of these arguments are dependent on the 6-membered ring depicted in blue occupying the chair conformation shown. For the lactone and 6-membered acetonide substrates, this conformation is locked by the bicycle. However, in the 7-membered acetal substrate, there is more conformational flexibility, and it is the equatorial disposition of the C(10) alcohol that favors the chair conformation illustrated below.

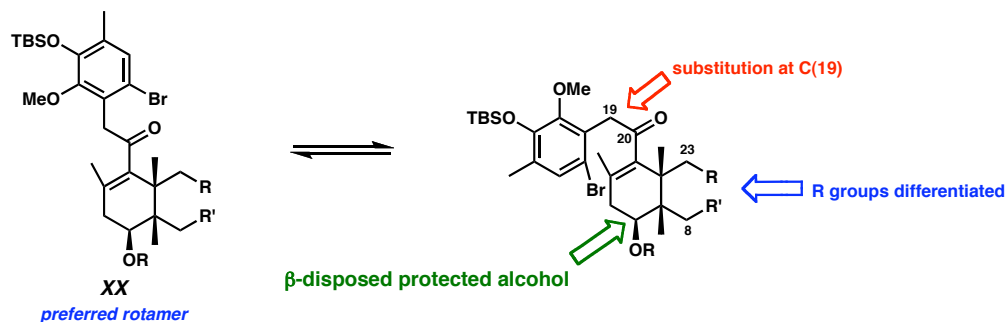


**Scheme 4.6.1** 3D representations of cyclization products. (1,3-Diaxial interactions are depicted in red.)

In addition to these considerations, it is important to note that the major non-productive pathway in these cyclizations is reductive debromination. We hypothesize that this by-product is observed in such high quantities because of the slow rotation about the C(19)-C(20) bond (Figure 4.6.2), combined with a strong conformational preference for the substrate to orient itself in a more linear arrangement to reduce steric interactions. One possibility to improve the outcome of the reaction is to functionalize the molecule at C(19) with the goal of decreasing the energetic advantage of occupying the linear conformation relative to the reactive conformation.<sup>13,14</sup>

Any future substrates should possess substitution at C(19) to increase the reactivity. Owing to the harsh conditions required in other systems for the differentiation and homologation of C(23) and C(8), these groups should be differentiated and, ideally, homologated. Finally, the alcohol functionality at C(10) should be  $\beta$ -disposed. This

substituent will occupy the equatorial position, thus setting the preferred chair conformation and enabling the selectivity arguments presented above to occur as expected.



**Scheme 4.6.2** Structural requirements for future radical cyclization products.

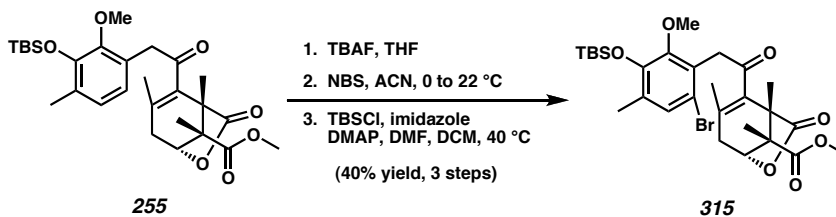
#### 4.7.1 Summary

In summary, we believe that this radical cyclization strategy provides a novel, functional group tolerant method to form the key C(12) quaternary stereocenter and to close the B ring. Although cyclization products are observed in all cases, substantial amounts of the product are only isolable in the case of the 7-membered acetal-derived substrate (**322**  $\rightarrow$  **323**). Additionally, this substrate is the only one to display selectivity for the desired relative stereochemistry of the product. Unique to this substrate is a  $\beta$ -disposed silyl ether at C(10), which is thought to be instrumental in the stereochemical outcome of the reaction.

#### 4.8.1 Materials and Methods

Unless otherwise stated, reactions were performed at ambient temperature (typically 19–24 °C) in flame-dried glassware under an argon or nitrogen atmosphere using dry, deoxygenated solvents. Solvents were dried by passage through an activated alumina column under argon. *N*-Bromosuccinimide was recrystallized before use. TBSCl was purchased from Gelest. V-70 was purchased from Waco Chemicals. All other commercially obtained reagents were used as received. Reaction temperatures were controlled by an IKAmag temperature modulator. Thin-layer chromatography (TLC) was performed using E. Merck silica gel 60 F254 precoated plates (0.25 mm) and visualized by UV fluorescence quenching, anisaldehyde, KMnO<sub>4</sub>, or CAM staining. ICN silica gel (particle size 0.032–0.063 mm) was used for flash chromatography. Optical rotations were measured with a Jasco P-1010 polarimeter at 589 nm. <sup>1</sup>H and <sup>13</sup>C NMR spectra were recorded on a Varian Mercury 300 (at 300 MHz and 75 MHz respectively), or a Varian Inova 500 (at 500 MHz and 125 MHz respectively) and are reported relative to Me<sub>4</sub>Si (δ 0.0). Data for <sup>1</sup>H NMR spectra are reported as follows: chemical shift (δ ppm) (multiplicity, coupling constant (Hz), integration). Multiplicities are reported as follows: s = singlet, d = doublet, t = triplet, q = quartet, sept. = septet, m = multiplet, comp. m = complex multiplet, app. = apparent, bs = broad singlet. IR spectra were recorded on a Perkin Elmer Paragon 1000 spectrometer and are reported in frequency of absorption (cm<sup>-1</sup>). High-resolution mass spectra were obtained from the Caltech Mass Spectroscopy Facility. Crystallographic analyses were performed at the California Institute of Technology Beckman Institute X-Ray Crystallography Laboratory. Crystallographic data have been deposited at the CCDC, 12 Union Road, Cambridge CB2 1EZ, UK and copies can be obtained on request, free of charge, from the CCDC by quoting the publication citation and the deposition number (see Appendix C for deposition numbers).

## 4.8.2 Preparation of Compounds

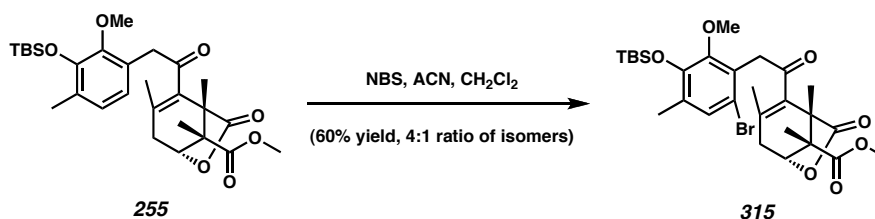


**Aryl bromide 315.** Enone **255** (58.8 mg, 0.114 mmol, 1.0 equiv) was treated with a 1.0 M solution of TBAF in THF (314  $\mu$ L, 0.341 mmol, 3.0 equiv) for 40 min at ambient temperature. The reaction mixture was then diluted with H<sub>2</sub>O (15 mL) and EtOAc (15 mL). The aqueous layer was extracted with EtOAc (3 x 10 mL). The combined organics were washed with brine (20 mL), dried over MgSO<sub>4</sub>, and concentrated to an oil, which was purified by flash chromatography (20 to 50% EtOAc in Hexanes) to provide phenol **255a** (28 mg, 0.070 mmol, 61% yield).  $R_f$  0.25 (50% EtOAc in hexanes); <sup>1</sup>H NMR (500 MHz, CDCl<sub>3</sub>)  $\delta$  6.85 (d,  $J$  = 7.8 Hz, 1H) 6.59 (d,  $J$  = 7.9 Hz, 1H), 5.53 (s, 1H), 4.62 (t,  $J$  = 2.7 Hz, 1H), 3.98 (d,  $J$  = 17.8, 1H), 3.77 (s, 3H), 3.77 (d,  $J$  = 17.6 Hz, 1H), 3.76 (s, 3H), 2.45 (dd,  $J$  = 19.0, 2.2 Hz, 1H), 2.36 (ddd,  $J$  = 19.0, 2.2, 0.98 Hz, 1H), 2.23 (s, 3H), 1.63 (s, 3H), 1.29 (s, 3H), 1.27 (s, 3H); <sup>13</sup>C NMR (125 MHz, CDCl<sub>3</sub>)  $\delta$  203.0, 176.3, 173.1, 147.2, 145.4, 135.5, 130.9, 126.4, 124.6, 123.5, 122.0, 77.9, 61.2, 53.6, 52.8, 47.9, 45.6, 34.4, 19.0, 15.5, 12.6, 11.9; IR (Neat film NaCl) 3446, 2951, 1779, 1731, 1706, 1465, 1425, 1333, 1272, 1239, 1200, 1150, 1063, 732 cm<sup>-1</sup>; HRMS (FAB+) [M+H]<sup>+</sup> calc'd for [C<sub>22</sub>H<sub>26</sub>O<sub>7</sub>+H]<sup>+</sup>:  $m/z$  403.1757, found 403.1766.

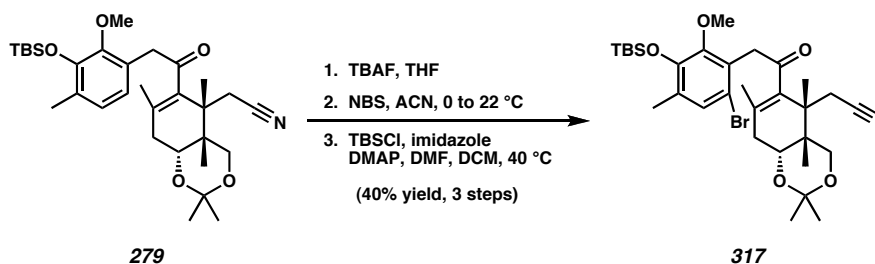
To a solution of the above phenol (**255a**, 27.8 mg, 0.691 mmol, 1.0 equiv) in ACN (1.4 mL, 0.05 M) was added *N*-Bromosuccinimide (13.5 mg, 0.0760 mmol, 1.1 equiv). The solution was stirred at ambient temperature for 6 h then quenched with H<sub>2</sub>O (10 mL) and diluted with EtOAc (20 mL) and H<sub>2</sub>O (10 mL). The aqueous layer was extracted with EtOAc (3 x 20 mL), dried over MgSO<sub>4</sub>, and concentrated to an oil, which was

purified by flash chromatography (20 to 60% EtOAc in hexanes) to provide aryl bromide **255b** (20.1 mg, 0.042 mmol, 61% yield) as an oil.  $R_f$  0.33 (50% EtOAc in hexanes);  $^1\text{H}$  NMR (500 MHz,  $\text{CDCl}_3$ )  $\delta$  7.15 (s, 1H), 5.47 (s, 1H), 4.63 (t,  $J = 2.2$  Hz, 1H), 4.26 (d,  $J = 19.0$  Hz, 1H), 3.91 (d,  $J = 19.0$  Hz, 1H), 3.78 (s, 3H), 3.76 (s, 3H), 2.49 (dd,  $J = 19.0, 2.2$  Hz, 1H), 2.39 (app. d,  $J = 18.8$  Hz, 1H), 2.22 (s, 3H), 1.82 (s, 3H), 1.34 (s, 3H), 1.26 (s, 3H);  $^{13}\text{C}$  NMR (125 MHz,  $\text{CDCl}_3$ )  $\delta$  201.2, 176.4, 173.2, 146.6, 146.2, 135.3, 131.3, 129.9, 126.4, 124.2, 114.8, 78.0, 61.3, 53.6, 52.8, 48.1, 46.4, 34.5, 19.2, 15.4, 12.6, 11.6; IR (Neat film NaCl) 3441, 2951, 2255, 1780, 1730, 1708, 1141, 1271, 1240, 1150, 1073, 912, 731  $\text{cm}^{-1}$ ; HRMS (FAB+)  $[\text{M}+\text{H}]^+$  calc'd for  $[\text{C}_{22}\text{H}_{25}\text{O}_7\text{Br}+\text{H}]^+$ :  $m/z$  481.0862, found 481.0869.

To a solution of aryl bromide **255b** (19.0 mg, 0.039 mmol, 1.0 equiv) in  $\text{CH}_2\text{Cl}_2$  (1 mL, 0.04 M) were added TBSCl (11.9 mg, 0.079 mmol, 2.0 equiv), DMAP (4.8 mg, 0.039 mmol, 1.0 equiv), and imidazole (8.1 mg, 0.118 mmol, 3.0 equiv). Stirred at 40 °C for 1.5 d before adding TBSCl (11.9 mg, 0.079 mmol, 2.0 equiv), DMAP (4.8 mg, 0.039 mmol, 1.0 equiv), and imidazole (8.1 mg, 0.118 mmol, 3.0 equiv). Upon completion, the reaction was quenched with  $\text{NH}_4\text{Cl}$  (5 mL), extracted with  $\text{CH}_2\text{Cl}_2$  (4 x 5 mL), dried over  $\text{MgSO}_4$ , concentrated to an oil, and purified by flash chromatography (10 to 50% EtOAc in Hexanes) to provide isomerically pure aryl bromide **315** (18.6 mg, mmol, 79% yield, 29% yield over 3 steps) as an oil.  $R_f$  0.63 (50% EtOAc in Hexanes);  $^1\text{H}$  NMR (500 MHz,  $\text{CDCl}_3$ )  $\delta$  7.13 (s, 1H), 4.618 (t,  $J = 2.4$  Hz, 1H), 4.25 (d,  $J = 19.0$  Hz, 1H), 3.90 (d,  $J = 19.0$  Hz, 1H), 3.76 (s, 3H), 3.65 (s, 3H), 2.48 (dd,  $J = 19.0, 2.4$  Hz, 1H), 2.38 (dd,  $J = 18.8, 1.2$  Hz, 1H), 2.19 (s, 3H), 1.81 (s, 3H), 1.36 (s, 3H), 1.29 (s, 3H), 1.00 (s, 9H), 1.40 (app. d,  $J = 3.9$  Hz, 6H);  $^{13}\text{C}$  NMR (125 MHz,  $\text{CDCl}_3$ )  $\delta$  201.7, 176.4, 173.3, 150.8, 146.5, 135.5, 131.5, 131.1, 129.4, 125.3, 116.3, 77.9, 60.1, 53.7, 52.8, 48.1, 46.9, 34.6, 26.0, 19.1, 18.5, 16.9, 12.7, 11.6, -4.26, -4.28; IR (Neat film NaCl) 2954, 2932, 2859, 1784, 1732, 1710, 1470, 1405, 1237, 1149, 1084, 1017, 841, 784, 733  $\text{cm}^{-1}$ ; HRMS (FAB+)  $[\text{M}+\text{H}]^+$  calc'd for  $[\text{C}_{28}\text{H}_{39}\text{O}_7\text{BrSi}+\text{H}]^+$ :  $m/z$  595.1727, found 595.1719.



**Aryl bromide 315** directly from enone **255**. To a solution of enone **255** (39.7 mg, 0.077 mmol, 1.00 equiv) in ACN (1.5 mL, 0.05 M) and CH<sub>2</sub>Cl<sub>2</sub> (0.59 mL, 0.13 M) was added NBS (13.7 mg, 0.127 mmol, 1.01 equiv). After 12 h, the reaction was diluted with EtOAc (10 mL), washed with sat. NH<sub>4</sub>Cl (5 mL), dried over MgSO<sub>4</sub>, concentrated, and purified by flash chromatography on silica gel (10 to 50% EtOAc in hexanes) to give aryl bromide **315** (27.3 mg, mmol, 60% yield) as a 4:1 mixture of bromide isomers favoring the desired aryl bromide **315**.

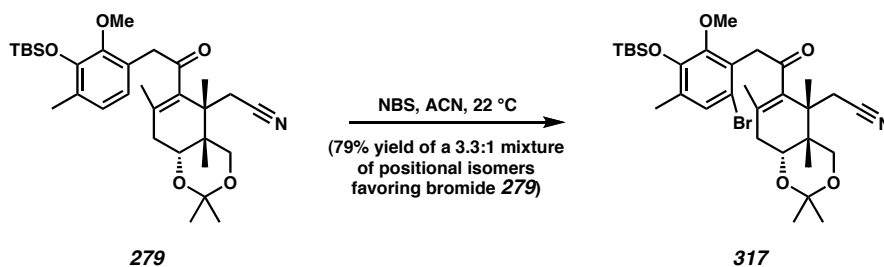


**Aryl bromide 317**. To a solution of enone **279** (60.0 mg, 0.111 mmol, 1.00 equiv) in THF (3.7 mL) was added a 1.0 M solution of TBAF (166  $\mu$ L, 0.166 mmol, 1.50 equiv) in THF. After 15 min, the reaction mixture was diluted with EtOAc (15 mL), H<sub>2</sub>O (5 mL), and saturated aqueous NH<sub>4</sub>Cl (5 mL), and extracted with EtOAc (5 x 20 mL). The combined organics were dried (MgSO<sub>4</sub>), concentrated, and purified by flash chromatography on silica gel (20 to 30% EtOAc in hexanes) to give the intermediate phenol (40.0 mg, 85% yield).

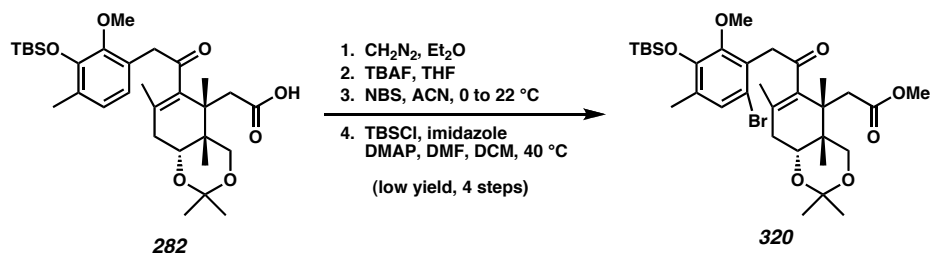
To a cooled (0 °C) solution of intermediate phenol (33.7 mg, 78.8  $\mu$ mol, 1.00 equiv) in ACN (1.6 mL) was added NBS (15.4 mg, 86.7  $\mu$ mol, 1.10 equiv) and the reaction

mixture was allowed to come to ambient temperature. After 5 h, the reaction was diluted with H<sub>2</sub>O (10 mL) and EtOAc (20 mL), and extracted with EtOAc (5 x 10 mL). The combined organics were dried (MgSO<sub>4</sub>), concentrated and used without further purification in the next step.

To a solution of the above crude material (theory: 78.8 μmol, 1.00 equiv), imidazole (16.1 mg, 0.236 mmol, 3.00 equiv), TBSCl (17.8 mg, 0.118 mmol, 1.50 equiv) in DMF (200 μL) and CH<sub>2</sub>Cl<sub>2</sub> (200 μL) was added DMAP (9.6 mg, 78.8 μmol, 1.00 equiv) and the reaction was stirred at ambient temperature for 24 h and then at 30 °C for 18 h. An additional portion of DMAP (10.0 mg, 81.9 μmol, 1.04 equiv) and TBSCl (20.0 mg, 132.7 μmol, 1.69 equiv) were added and the reaction mixture was heated at 40 °C for 4 h. The reaction was diluted with EtOAc (10 mL), washed with saturated aqueous NH<sub>4</sub>Cl (3 x 5 mL), and extracted with EtOAc (3 x 10 mL). The combined organics were concentrated and purified by flash chromatography on silica gel (5 to 15% Et<sub>2</sub>O in hexanes) to give isomerically pure bromide **317** (23.0 mg, 47% yield, 40% yield for three steps) as an amorphous white solid: *R<sub>f</sub>* 0.43 (20% EtOAc in hexanes); <sup>1</sup>H NMR (500 MHz, CDCl<sub>3</sub>) δ 7.13 (s, 1H), 4.29 (d, *J* = 8.5 Hz, 1H), 4.10 (d, *J* = 7.0 Hz, 1H), 4.07 (d, *J* = 7.0 Hz, 1H), 4.06 (d, *J* = 4.0 Hz, 1H), 3.88 (dd, *J* = 6.3, 8.8 Hz, 1H), 3.62 (s, 3H), 3.54 (app. t, *J* = 9.3 Hz, 1H), 2.55 (dd, *J* = 6.3, 17.8 Hz, 1H), 2.32 (dd, *J* = 8.5, 18.0 Hz, 1H), 2.18 (s, 3H), 1.87 (s, 3H), 1.62 (s, 3H), 1.61 (s, 3H), 1.21 (s, 3H), 1.17 (s, 3H), 1.01 (s, 9H), 0.14 (s, 6H); <sup>13</sup>C NMR (125 MHz, CDCl<sub>3</sub>) δ 205.4, 150.9, 146.4, 138.3, 131.4, 129.3, 128.7, 126.0, 121.5, 116.3, 75.5, 75.3, 75.2, 70.5, 60.0, 49.7, 47.7, 47.2, 35.7, 28.7, 27.6, 26.0, 21.0, 20.8, 18.1, 16.8, -4.3; IR (Neat film NaCl) 2932, 2860, 2252, 1699, 1470, 1404, 1234, 1171, 1083, 1047, 853, 842, 734 cm<sup>-1</sup>; HRMS (FAB+) [M+H]<sup>+</sup> calc'd for [C<sub>31</sub>H<sub>46</sub> O<sub>5</sub>NSiBr+H]<sup>+</sup>: *m/z* 620.2407, found 620.2394.



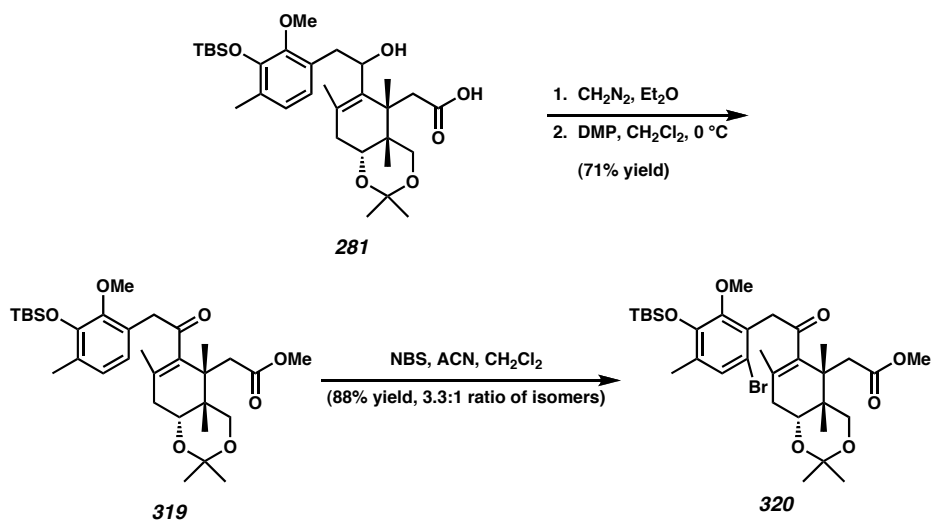
**Aryl bromide 317** directly from enone **279**. To a solution of enone **279** (74.7 mg, 0.138 mmol, 1.00 equiv) in ACN (1.4 mL, 0.1 M) was added NBS (27.0 mg, 0.1517 mmol, 1.1 equiv). After 2 h, the reaction was diluted with H<sub>2</sub>O (10 mL) and EtOAc (10 mL), and extracted with EtOAc (4 x 5 mL). The combined organics were washed with brine (10 mL), dried over MgSO<sub>4</sub>, concentrated, and purified by flash chromatography on silica gel (5 to 30% Et<sub>2</sub>O in hexanes) to give aryl bromide **317** (67.5 mg, 79% yield) as a 3.3:1 mixture of bromide isomers favoring the desired aryl bromide **317**.



**Aryl bromide 320**. To a solution of enone **282** (27.1 mg, 0.048 mmol, 1.0 equiv) in Et<sub>2</sub>O (1 mL, 0.05 M) was added CH<sub>2</sub>N<sub>2</sub> (2 mL, 1–2 M in Et<sub>2</sub>O). The reaction was stirred uncovered until no further yellow color was observed, and then it was concentrated to an oil and redissolved in THF (1.6 mL, 0.03 M). A 1.0 M solution of TBAF (72.5 μL, 0.073 mmol, 1.5 equiv) in THF was added, and the reaction was stirred at ambient temperature 25 min, quenched with H<sub>2</sub>O (5 mL) and brine (5 mL), and diluted with EtOAc (10 mL). The aqueous layer was extracted with EtOAc (5 x 10 mL), and the combined organics were dried over MgSO<sub>4</sub> and concentrated to an oil, which was carried on without further purification.

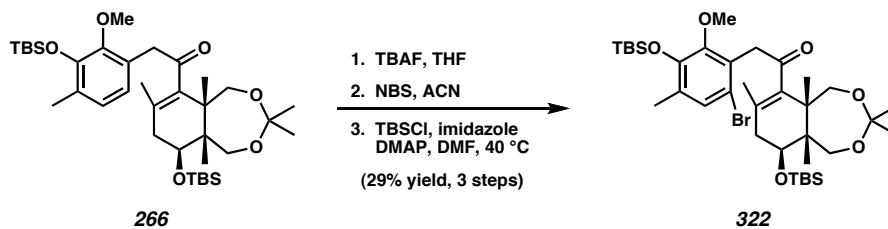
To a solution of the intermediate phenol **282a** in ACN (1 mL, 0.05 M) at 0 °C was added *N*-bromosuccinimide (9.4 mg, 0.053 mmol, 1.1 equiv). The reaction was then stirred at ambient temperature 10 h, diluted with H<sub>2</sub>O (15 mL) and EtOAc (10 mL), and extracted with EtOAc (5 x 10 mL). The combined organics were dried over MgSO<sub>4</sub> and concentrated to an oil.

The intermediate aryl bromide **282b** was redissolved in DMF (0.2 mL, 0.25 M) and CH<sub>2</sub>Cl<sub>2</sub> (0.2 mL, 0.25 M) and TBSCl (11.0 mg, mmol, equiv), DMAP (5.9 mg, mmol, equiv), and imidazole (9.9 mg, mmol, equiv) were added. The reaction was stirred at 40 °C for 24 h then diluted with sat. NH<sub>4</sub>Cl (5 mL), H<sub>2</sub>O (5 mL), and EtOAc (5 mL), and extracted with EtOAc (4 x 5 mL). The combined organics were dried over MgSO<sub>4</sub>, concentrated, and purified by flash chromatography (5 to 10% EtOAc in hexanes) to provide a small amount of aryl bromide **320** as a single positional isomer (plus impurities unrelated to the product). <sup>1</sup>H NMR (500 MHz, CDCl<sub>3</sub>) δ 7.13 (d, *J* = 0.6 Hz, 1H), 4.28 (d, *J* = 9.0 Hz, 1H), 4.11 (d, *J* = 8.5 Hz, 1H), 4.06 (s, 2H), 3.77 (m, 1H), 3.74 (s, 3H), 3.61 (s, 3H), 3.55 (d, *J* = 8.8 Hz, 1H), 3.53 (d, *J* = 9.1 Hz, 1H), 2.19 (s, 3H), 1.83 (s, 3H), 1.55 (s, 9H), 1.44 (s, 6H), 1.16 (s, 3H), 1.11 (s, 3H), 1.01 (s, 3H), 0.14 (s, 6H); <sup>13</sup>C NMR (125 MHz, CDCl<sub>3</sub>) δ 205.8, 174.8, 150.9, 146.4, 138.2, 131.4, 129.4, 129.1, 126.1, 116.4, 75.2, 74.9, 72.3, 60.0, 51.9, 49.8, 47.8, 35.9, 29.7, 26.4, 26.0, 24.2, 21.1, 20.8, 18.5, 17.9, 16.9, -4.3; IR (Neat film NaCl) 2928, 2857, 1733, 1670, 1470, 1404, 1290, 1234, 1142, 1083, 1048, 936, 841, 783, 735 cm<sup>-1</sup>; HRMS (FAB+) [M+H]<sup>+</sup> calc'd for [C<sub>32</sub>H<sub>49</sub>O<sub>7</sub>SiBr+H]<sup>+</sup>: *m/z* 653.2509, found 653.2510.



**Aryl bromide 320** directly from enone **319**. To a solution of allylic alcohol **281a** (24.3 mg, 0.043 mmol, 1.0 equiv) in Et<sub>2</sub>O (2 mL) was added CH<sub>2</sub>N<sub>2</sub> (1 mL, 1–2 M in Et<sub>2</sub>O). The reaction was stirred uncovered until no yellow color remained. The solvents were removed by rotary evaporation, and the intermediate methyl ester was redissolved in CH<sub>2</sub>Cl<sub>2</sub> (1.5 mL, 0.03 M). The solution was cooled to 0 °C, and DMP (27.9 mg, 0.065 mmol 1.5 equiv) was added. The reaction was stirred at 0 °C for 4 h then diluted with Et<sub>2</sub>O (20 mL). The solids were removed by filtration thru #2 Whatman paper, the solution was concentrated to an oil then purified by flash chromatography (5 to 15% EtOAc in hexanes) to provide enone **319** (17.5 mg, 0.030 mmol, 71% yield).

To a solution of enone **319** (50.9 mg, 0.089 mmol, 1.00 equiv) in ACN (1.8 mL, 0.05 M) and CH<sub>2</sub>Cl<sub>2</sub> (0.68 mL, 0.13 M) was added NBS (15.9 mg, 0.089 mmol, 1.01 equiv). After 3 h, the reaction was diluted with H<sub>2</sub>O (25 mL) and EtOAc (25 mL), and the aqueous layer was extracted with EtOAc (2 x 25 mL). The combined organics were washed with brine (25 mL), dried over MgSO<sub>4</sub>, concentrated, and purified by flash chromatography on silica gel (5 to 10% EtOAc in hexanes) to give aryl bromide **320** (51.2 mg, 88% yield) as a 3.3:1 mixture of bromide isomers favoring the desired aryl bromide **320**.

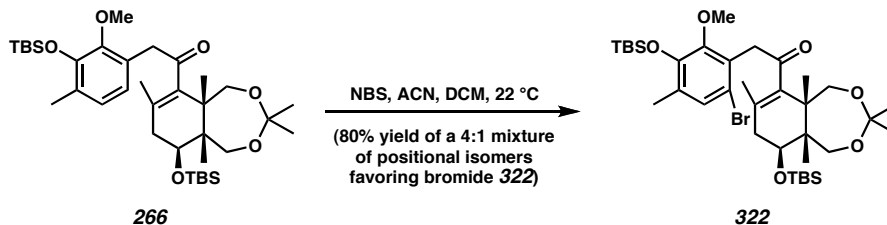


**Aryl bromide 322.** To a solution of enone **266** (114 mg, 0.176 mmol, 1.00 equiv) in THF (8.0 mL) was added a 1.0 M solution of TBAF (176  $\mu$ L, 0.176 mmol, 1.00 equiv) in THF. After 5 min, the reaction mixture was diluted with H<sub>2</sub>O (50 mL) and CH<sub>2</sub>Cl<sub>2</sub> (50 mL), and extracted with CH<sub>2</sub>Cl<sub>2</sub> (4 x 25 mL). The combined organics were dried (Na<sub>2</sub>SO<sub>4</sub>), concentrated, and purified by flash chromatography on silica gel (5 to 25% EtOAc in hexanes) to give the intermediate phenol (91 mg, 97% yield).

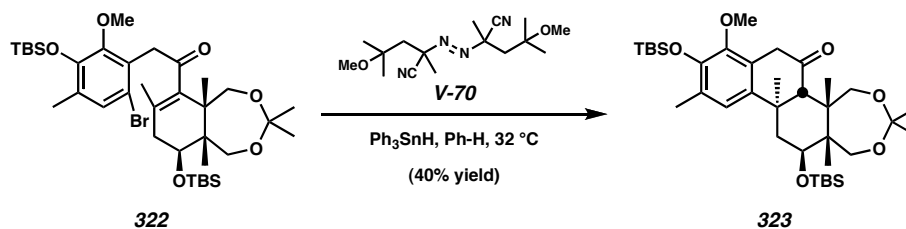
To a solution of intermediate phenol (36.0 mg, 67.6  $\mu$ mol, 1.00 equiv) in ACN (2.0 mL) was added NBS (18.0 mg, 101  $\mu$ mol, 1.50 equiv). After 2.5 h, the reaction was diluted with H<sub>2</sub>O (8 mL) and EtOAc (8 mL), and extracted with EtOAc (4 x 5 mL). The combined organics were dried (Na<sub>2</sub>SO<sub>4</sub>), concentrated, and purified by flash chromatography on silica gel (2.5 to 15% EtOAc in hexanes) to give the intermediate bromide (14.4 mg, 35% yield).

To a solution of intermediate bromide (14.4 mg, 23.5  $\mu$ mol, 1.00 equiv), imidazole (36.0 mg, 0.530 mmol, 22.5 equiv), and TBSCl (26.6 mg, 0.177 mmol, 7.50 equiv) in DMF (2.5 mL) was added DMAP (21.5 mg, 0.176 mmol, 7.50 equiv) and the reaction was warmed to 40  $^\circ$ C. After 36 h, the reaction was diluted with H<sub>2</sub>O (8 mL) and EtOAc (8 mL), and extracted with EtOAc (4 x 5 mL). The combined organics were dried (Na<sub>2</sub>SO<sub>4</sub>), concentrated, and purified by flash chromatography on silica gel (1 to 5% Et<sub>2</sub>O in hexanes) to give isomerically pure bromide **322** (14.5 mg, 85% yield, 29% yield for three steps) as a white foam:  $R_f$  0.76, 0.79 (10% Et<sub>2</sub>O in hexanes, 25% Et<sub>2</sub>O in hexanes); <sup>1</sup>H NMR (300 MHz, CDCl<sub>3</sub>)  $\delta$  7.13 (s, 1H), 4.29 (dd,  $J$  = 7.1, 9.5 Hz, 1H), 4.11 (d,  $J$  = 18.6 Hz, 1H), 4.00 (d,  $J$  = 18.6 Hz, 1H), 3.77 (d,  $J$  = 12.3 Hz, 1H), 3.62 (s, 3H), 3.55 (d,  $J$  = 12.9 Hz,

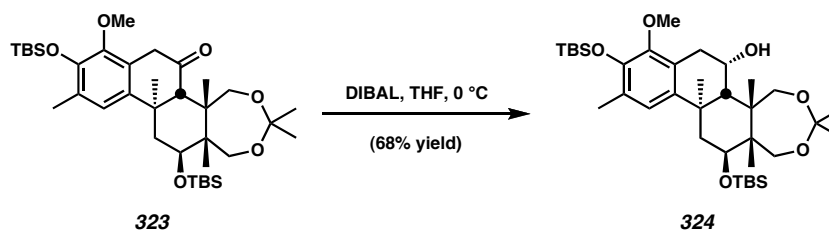
1H), 3.54 (d,  $J = 12.6$  Hz, 1H), 3.39 (d,  $J = 12.3$  Hz, 1H), 2.19 (s, 3H), 2.14–2.04 (m, 2H), 1.82 (s, 3H), 1.31 (s, 3H), 1.28 (s, 3H), 1.23 (s, 3H), 1.01 (s, 9H), 0.90 (s, 9H), 0.67 (s, 3H), 0.15 (s, 6H), 0.14 (s, 3H), 0.09 (s, 3H), 0.08 (s, 3H);  $^{13}\text{C}$  NMR (75 MHz,  $\text{CDCl}_3$ )  $\delta$  206.1, 151.0, 146.4, 137.8, 131.4, 130.9, 129.4, 126.0, 116.4, 101.1, 66.0, 65.5, 61.5, 60.0, 48.0, 45.5, 43.0, 38.1, 26.0, 25.9, 24.7 (2C), 20.7, 18.5, 18.2, 18.1, 16.9, 11.1, -4.2, -4.3, -4.4, -5.1; IR (Neat film NaCl) 2954, 2930, 2858, 1700, 1471, 1404, 1233, 1220, 1099, 1075, 855, 837, 779  $\text{cm}^{-1}$ ; HRMS (FAB+)  $[\text{M}-\text{H}_2+\text{H}]^+$  calc'd for  $[\text{C}_{36}\text{H}_{60}\text{Si}_2\text{O}_6\text{Br}]^+$ :  $m/z$  723.3112, found 723.3128.



**Aryl bromide 322** directly from enone **266**. To a solution of enone **266** (200 mg, 0.309 mmol, 1.00 equiv) in ACN (8.0 mL) and  $\text{CH}_2\text{Cl}_2$  (1.2 mL) was added NBS (66.0 mg, 0.371 mmol, 1.20 equiv). After 2.5 h, the reaction was diluted with  $\text{H}_2\text{O}$  (30 mL) and EtOAc (15 mL), and extracted with EtOAc (5 x 15 mL). The combined organics were washed with brine (10 mL), dried ( $\text{Na}_2\text{SO}_4$ ), concentrated, and purified by flash chromatography on silica gel (1 to 5%  $\text{Et}_2\text{O}$  in hexanes) to give aryl bromide **322** (179 mg, 80% yield) as a 4:1 mixture of bromide isomers favoring the desired aryl bromide **322**.



**Cyclized ketone 323.** To a solution of aryl bromide **322** (25.0 mg, 34.4  $\mu\text{mol}$ , 1.00 equiv of a 4:1 mixture of isomers) and initiator **V-70** (15.9 mg, 51.7  $\mu\text{mol}$ , 1.50 equiv) in benzene (2.0 mL) at  $32\text{ }^\circ\text{C}$  was added a solution of  $\text{Ph}_3\text{SnH}$  (24.2 mg, 68.8  $\mu\text{mol}$ , 2.00 equiv) in benzene (0.5 mL) by syringe pump over 5 h. At the end of the addition, the reaction was cooled to ambient temperature, concentrated, and purified by flash chromatography on silica gel (2 to 7.5%  $\text{Et}_2\text{O}$  in hexanes) to give ketone **323** (8.9 mg, 40% yield, 50% yield based on the correct isomer of the starting material) as an oil:  $R_f$  0.52 (25%  $\text{Et}_2\text{O}$  in hexanes);  $^1\text{H}$  NMR (500 MHz,  $\text{CDCl}_3$ )  $\delta$  6.77 (s, 1H), 4.53 (d,  $J = 12.0$  Hz, 1H), 4.43 (dd,  $J = 4.5, 12.5$  Hz, 1H), 3.97 (d,  $J = 12.5$  Hz, 1H), 3.66 (d,  $J = 22.0$  Hz, 1H), 3.64 (s, 3H), 3.55 (d,  $J = 12.5$  Hz, 1H), 3.39 (d,  $J = 22.0$  Hz, 1H), 3.33 (d,  $J = 12.5$  Hz, 1H), 2.84 (s, 1H), 2.22 (s, 3H), 2.18 (dd,  $J = 4.5, 12.5$  Hz, 1H), 1.92 (app. t,  $J = 12.5$  Hz, 1H), 1.33 (s, 3H), 1.31 (s, 3H), 1.16 (s, 3H), 1.14 (s, 3H), 1.03 (s, 9H), 0.94 (s, 9H), 0.57 (s, 3H), 0.19 (s, 6H), 0.18 (s, 3H), 0.15 (s, 3H), 0.14 (s, 3H);  $^{13}\text{C}$  NMR (125 MHz,  $\text{CDCl}_3$ )  $\delta$  209.3, 147.8, 145.1, 141.5, 129.0, 123.8, 120.8, 100.9, 65.8, 62.2, 62.1, 59.3, 58.8, 44.7, 43.5, 42.5, 41.2, 41.0, 27.4, 26.0 (2C), 24.8, 24.6, 20.0, 18.6, 18.2, 17.6, 10.1, -4.0, -4.2 (2C), -4.9; IR (Neat film NaCl) 2954, 2929, 2857, 1715, 1472, 1462, 1254, 1221, 1088, 1071, 838  $\text{cm}^{-1}$ ; HRMS (FAB+)  $[\text{M}-\text{H}_2+\text{H}]^+$  calc'd for  $[\text{C}_{36}\text{H}_{61}\text{Si}_2\text{O}_6]^+$ :  $m/z$  645.4007, found 645.4007.



**Alcohol 324.** To a cooled (0 °C) solution of ketone **323** (19.9 mg, 30.8 μmol, 1.00 equiv) in THF (5.0 mL) was added a 1.0 M solution of DIBAL-H (250 μL, 0.250 mmol, 8.12 equiv) in toluene. After 4 h, an additional portion of DIBAL-H (100 μL, 0.100 mmol, 3.25 equiv) in toluene was added. After an additional 1 h at 0 °C, the reaction mixture was quenched with Na<sub>2</sub>SO<sub>4</sub>•10H<sub>2</sub>O (300 mg) in a portionwise manner, filtered, washed (CH<sub>2</sub>Cl<sub>2</sub>), concentrated, and purified by flash chromatography on silica gel (10 to 40% Et<sub>2</sub>O in hexanes) to give alcohol **324** (13.6 mg, 68% yield) as a white solid. Crystals suitable for X-ray analysis were obtained by crystallization from CH<sub>2</sub>Cl<sub>2</sub> at ambient temperature: mp 185–190 °C decomp. (CH<sub>2</sub>Cl<sub>2</sub>); *R<sub>f</sub>* 0.21 (25% Et<sub>2</sub>O in hexanes); <sup>1</sup>H NMR (500 MHz, CDCl<sub>3</sub>) δ 6.78 (s, 1H), 4.68 (s, 1H), 4.47 (dd, *J* = 3.8, 12.3 Hz, 1H), 4.28 (d, *J* = 12.5 Hz, 1H), 3.93 (d, *J* = 13.0 Hz, 1H), 3.65 (s, 3H), 3.53 (d, *J* = 12.0 Hz, 1H), 3.37 (d, *J* = 12.5 Hz, 1H), 2.95 (s, 1H), 2.94 (s, 1H), 2.20 (s, 3H), 2.07 (dd, *J* = 4.0, 12.5 Hz, 1H), 1.66 (s, 1H), 1.62 (d, *J* = 12.0 Hz, 1H), 1.58 (s, 3H), 1.33 (s, 3H), 1.32 (s, 3H), 1.20 (bs, 1H), 1.11 (s, 3H), 1.03 (s, 9H), 0.92 (s, 9H), 0.57 (s, 3H), 0.19 (s, 3H), 0.17 (s, 6H), 0.14 (s, 3H); <sup>13</sup>C NMR (125 MHz, CDCl<sub>3</sub>) δ 148.6, 144.4, 141.8, 128.3, 122.8, 122.1, 100.9, 66.4, 65.4, 65.3, 63.0, 59.2, 48.6, 45.7, 45.4, 44.6, 37.5, 36.7, 29.6, 26.1, 26.0, 25.0, 24.6, 22.2, 18.6, 18.1, 17.5, 10.4, -4.0 (2C), -4.1, -4.9; IR (Neat film NaCl) 3454, 2954, 2930, 2858, 1473, 1252, 1220, 1089, 1061, 836 cm<sup>-1</sup>; HRMS (FAB+) [M-H<sub>2</sub>+H]<sup>+</sup> calc'd for [C<sub>36</sub>H<sub>63</sub>Si<sub>2</sub>O<sub>6</sub>]<sup>+</sup>: *m/z* 647.4163, found 647.4162.

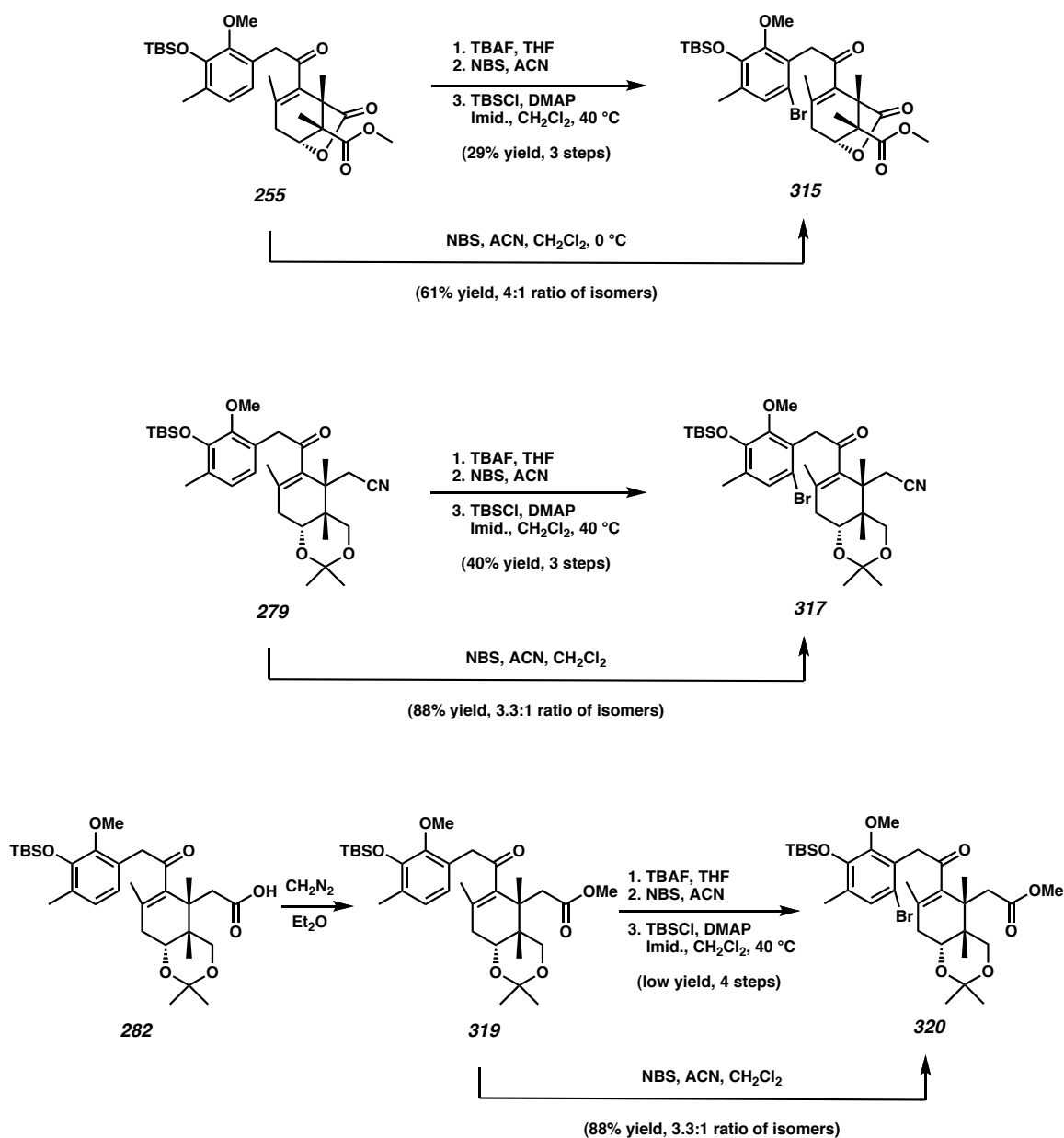
## References

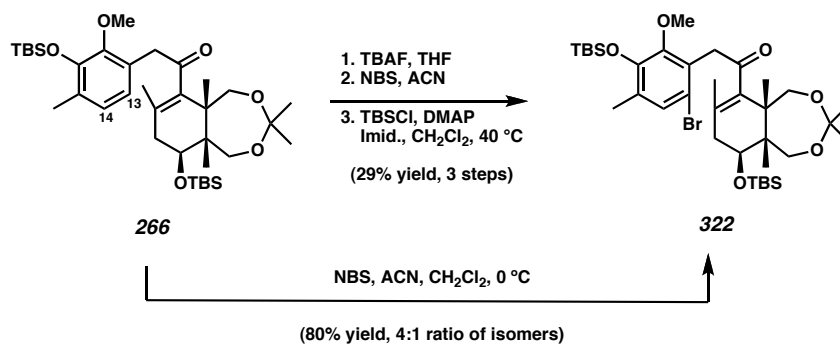
1. Satoh, T.; Ikeda, M.; Miura, M.; Nomura, M. *J. Org. Chem.*, **1997**, *62*, 4877–4879.
2. Jung, M. E.; Hudspeth, J. P. *J. Am. Chem. Soc.* **1980**, *102*, 2463–2464.
3. Li, X.; Hewgley, J. B.; Mulrooney, C. A.; Yang, J.; Kozlowski, M. C. *J. Org. Chem.*, **2003**, *68*, 5500–5511.
4. For an excellent review of intramolecular radical conjugate addition, see: Zhang, W. *Tetrahedron* **2001**, *57*, 7237–7262. Also see: Srikanth, G. S. C.; Castle, S. L. *Tetrahedron* **2005**, *61*, 10377–10441.
5. Rajamannar, T.; Balasubramanian, K. K. *J. Chem. Soc., Chem. Commun.* **1994**, 25–26.
6. a) Carreno, M. C.; Ruano, J. L. G.; Sanz, G.; Toledo, M. A.; Urbano, A. *J. Org. Chem.* **1995**, *60*, 5328–5331. b) Berthelot, J.; Guette, C.; Desbène, P.-J.; Basselier, J.-J. *Can. J. Chem.* **1989**, *67*, 2061–2066.
7. Carreno, M. C.; Ruano, J. L. G.; Sanz, G.; Toledo, M. A.; Urbano, A. *Synlett.* **1997**, 1241–1242.
8. The yields for this sequence were low for several substrates. Depending on the substrate, the desilylation and bromination steps led to significant decomposition if stirred for too long or at too high of a temperature. Generally, we found the mixture of bromide isomers sufficient for investigation of cyclizations. Thus, the three-step procedure was not optimized in most cases.
9. See Chapter 3 for details.
10. The exact yield for this sequence was not calculated owing to impurity of the product. An analytically pure sample was ultimately obtained by repetitive preparative methods.
11. TBS groups removed from the figure for clarity.
12. Lewis acids have been used numerous times to promote radical conjugate additions, see: a) Sibi, M. P.; Ji, J.; Sausker, J. B.; Jasperse, C. P. *J. Am. Chem. Soc.* **1999**, *121*, 7517–7526; b) Iserloh, U.; Curran, D. P.; Kanemasa, S. *Tetrahedron: Asymmetry* **1999**, *10*, 2417–2428; c) Murakata, M.; Tsutsui, H.; Hoshino, O. *Org. Lett.* **2001**, *3*, 299–302. d) Sibi, M. P.; Manyem, S. *Org. Lett.* **2002**, *4*, 2929–2932.
13. a) Beesley, R. M.; Ingold, C. K.; Thorpe, J. F. *J. Chem. Soc.* **1915**, *107*, 1080–1106. b) Ingold, C. K. *J. Chem. Soc.* **1921**, *119*, 305–329.
14. a) Bruice, T. C.; Pandit, U. K. *J. Am. Chem. Soc.* **1960**, *82*, 5858–5865. b) Jung, M. E.; Gervay, J. *J. Am. Chem. Soc.* **1991**, *113*, 224–232. c) Jung, M. E.; Kiankarimi, M. *J. Org. Chem.* **1998**, *63*, 2968–2974.

## SYNTHETIC SUMMARY

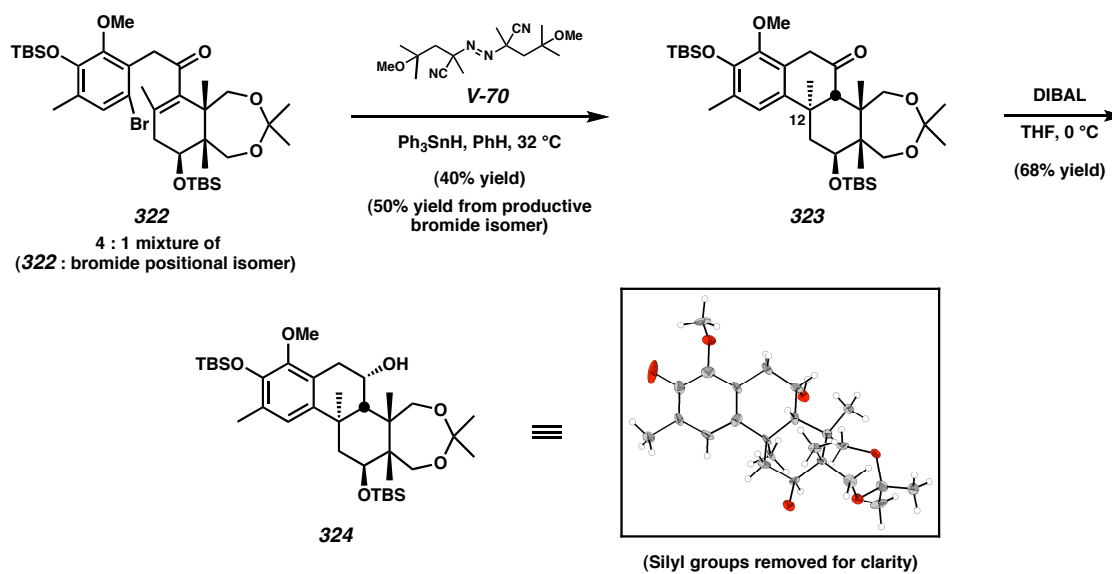
## Radical Cyclization Approaches Toward the Tricyclic Core of Zoanthanol

Scheme S4.1 Synthesis of brominated radical cyclization precursors





*Scheme S4.2 Radical cyclization of a 7-membered acetal-derived cyclization precursor*



## APPENDIX C

Spectra and X-Ray Crystallographic Data:  
Radical Cyclization Approaches Toward  
the Tricyclic Core of Zoanthenol

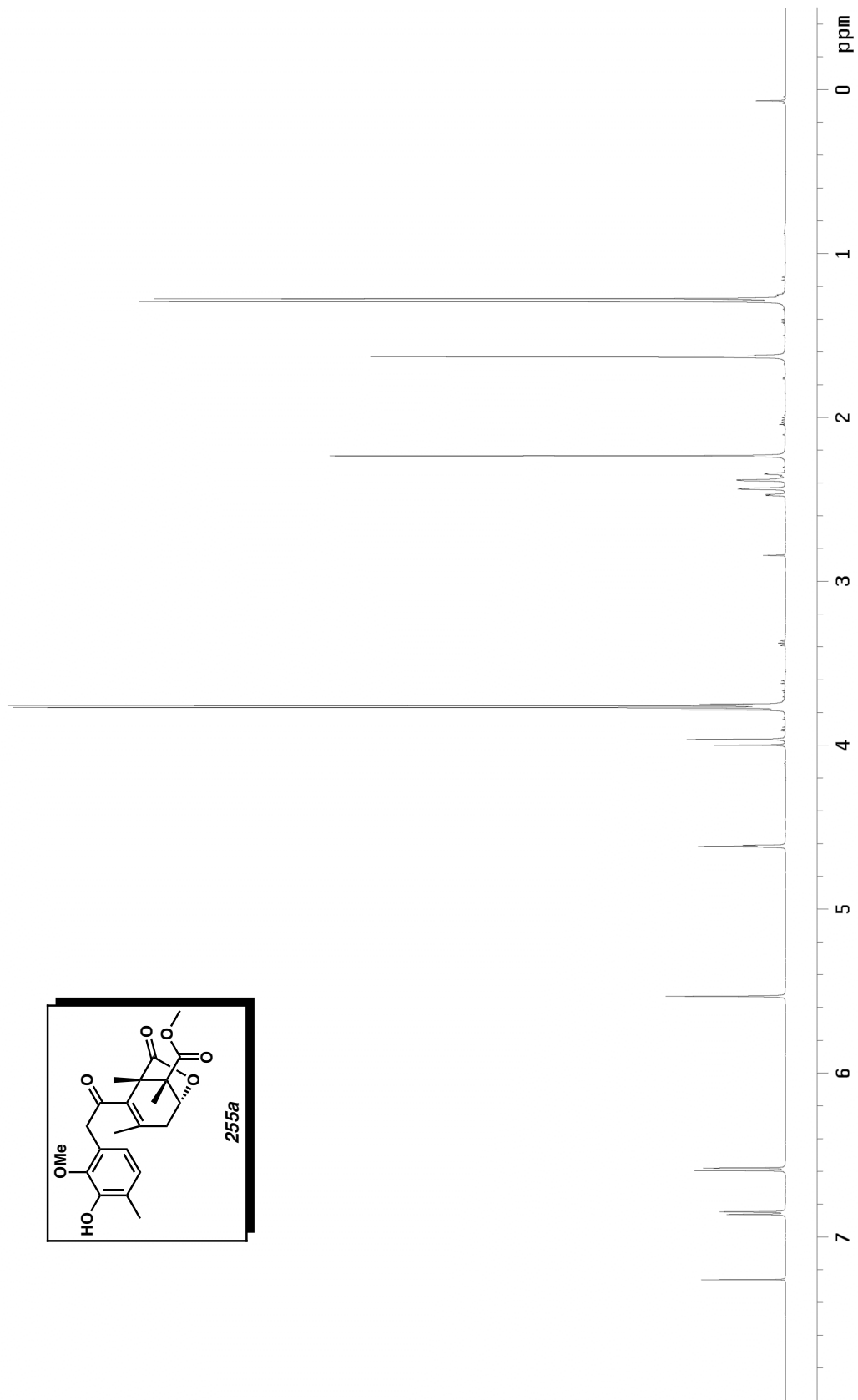
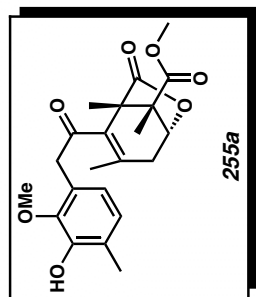


Figure C.1  $^1\text{H}$  NMR (500 MHz,  $\text{CDCl}_3$ ) of compound **255a**.

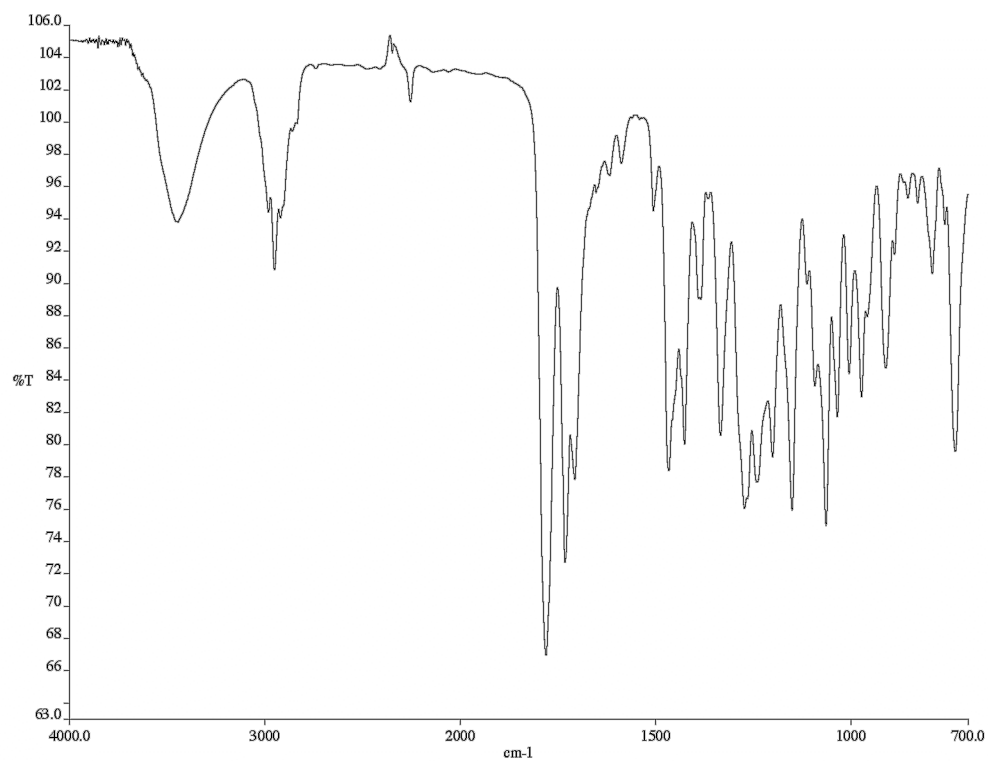


Figure C.2 Infrared spectrum (thin film/NaCl) of compound **255a**.

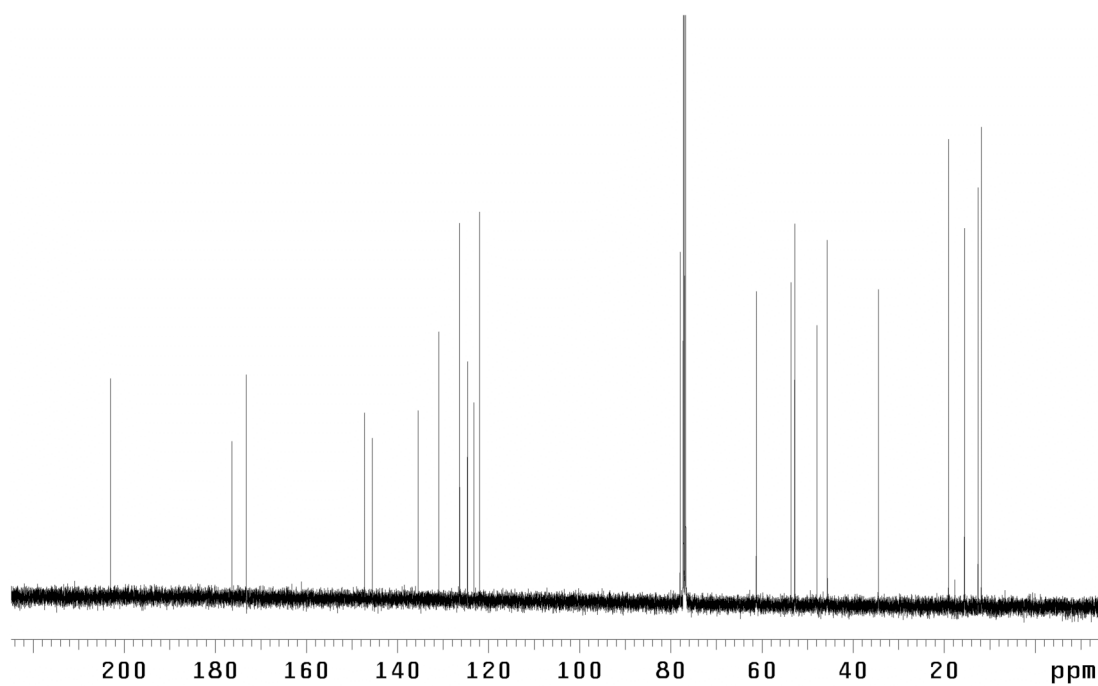


Figure C.3  $^{13}\text{C}$  NMR (125 MHz,  $\text{CDCl}_3$ ) of compound **255a**.

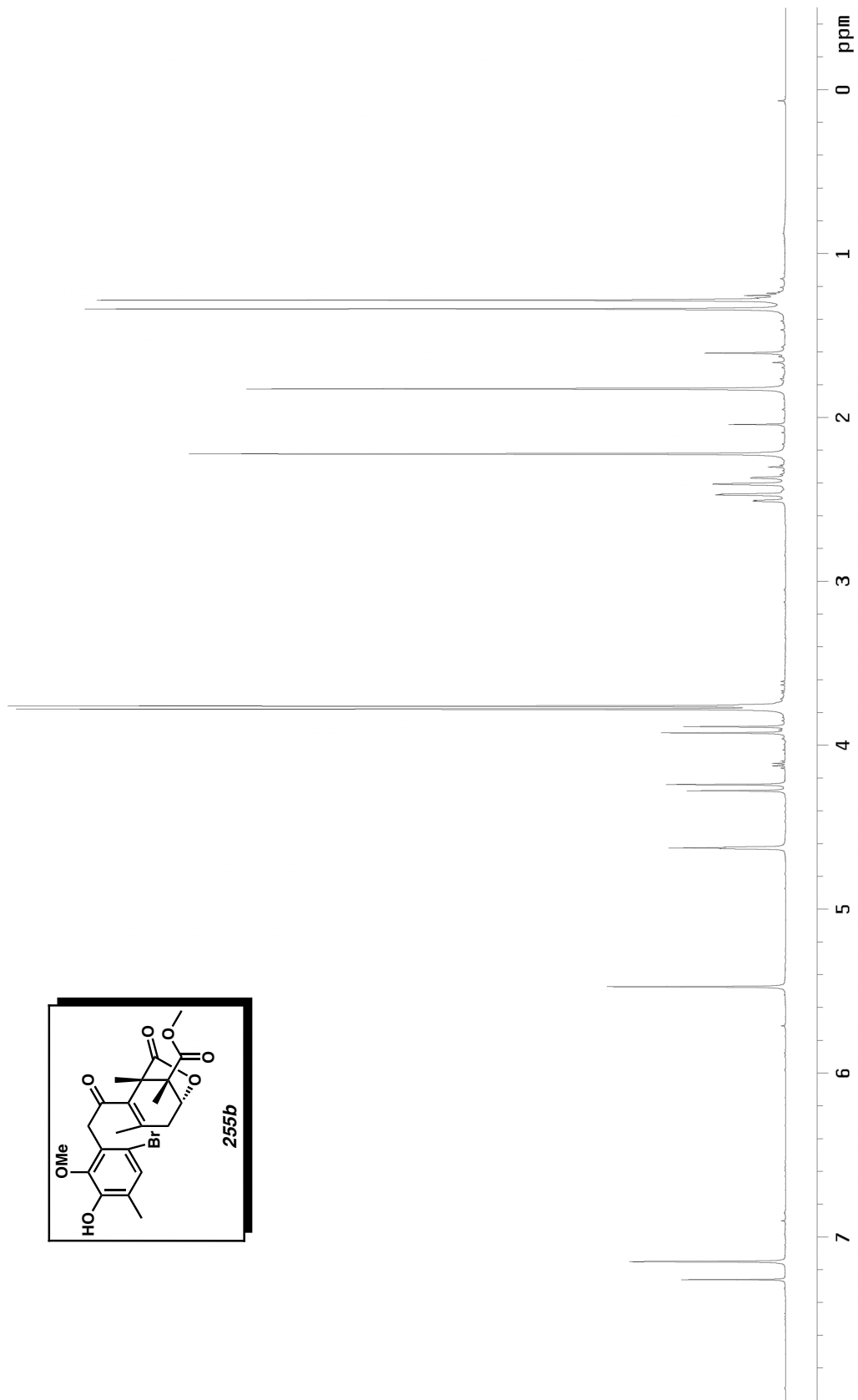
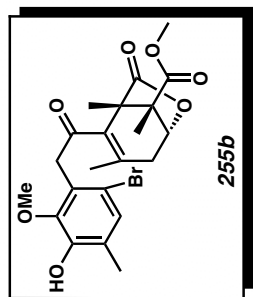


Figure C.4  $^1\text{H}$  NMR (500 MHz,  $\text{CDCl}_3$ ) of compound **255b**.

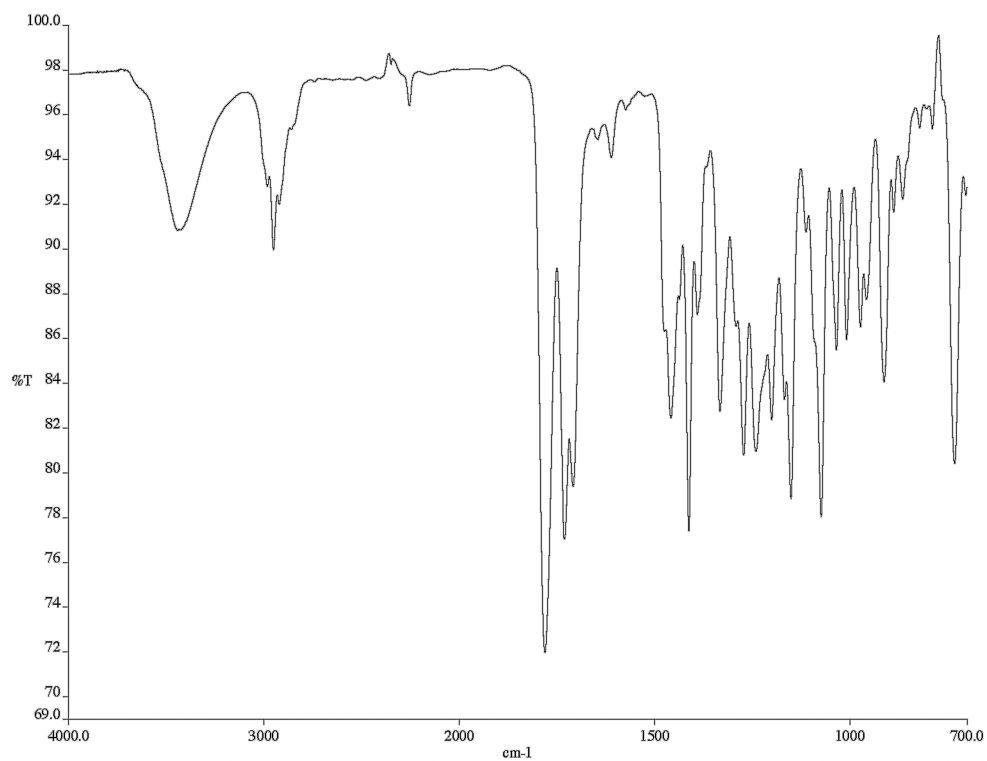


Figure C.5 Infrared spectrum (thin film/NaCl) of compound **255b**.

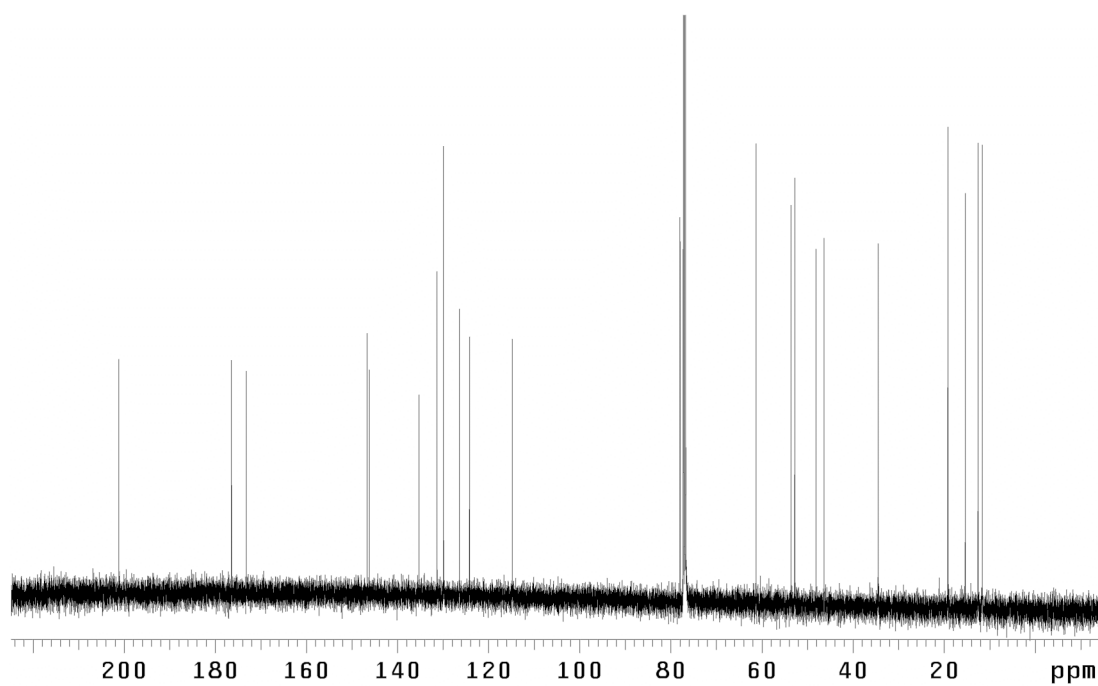


Figure C.6  $^{13}\text{C}$  NMR (125 MHz,  $\text{CDCl}_3$ ) of compound **255b**.

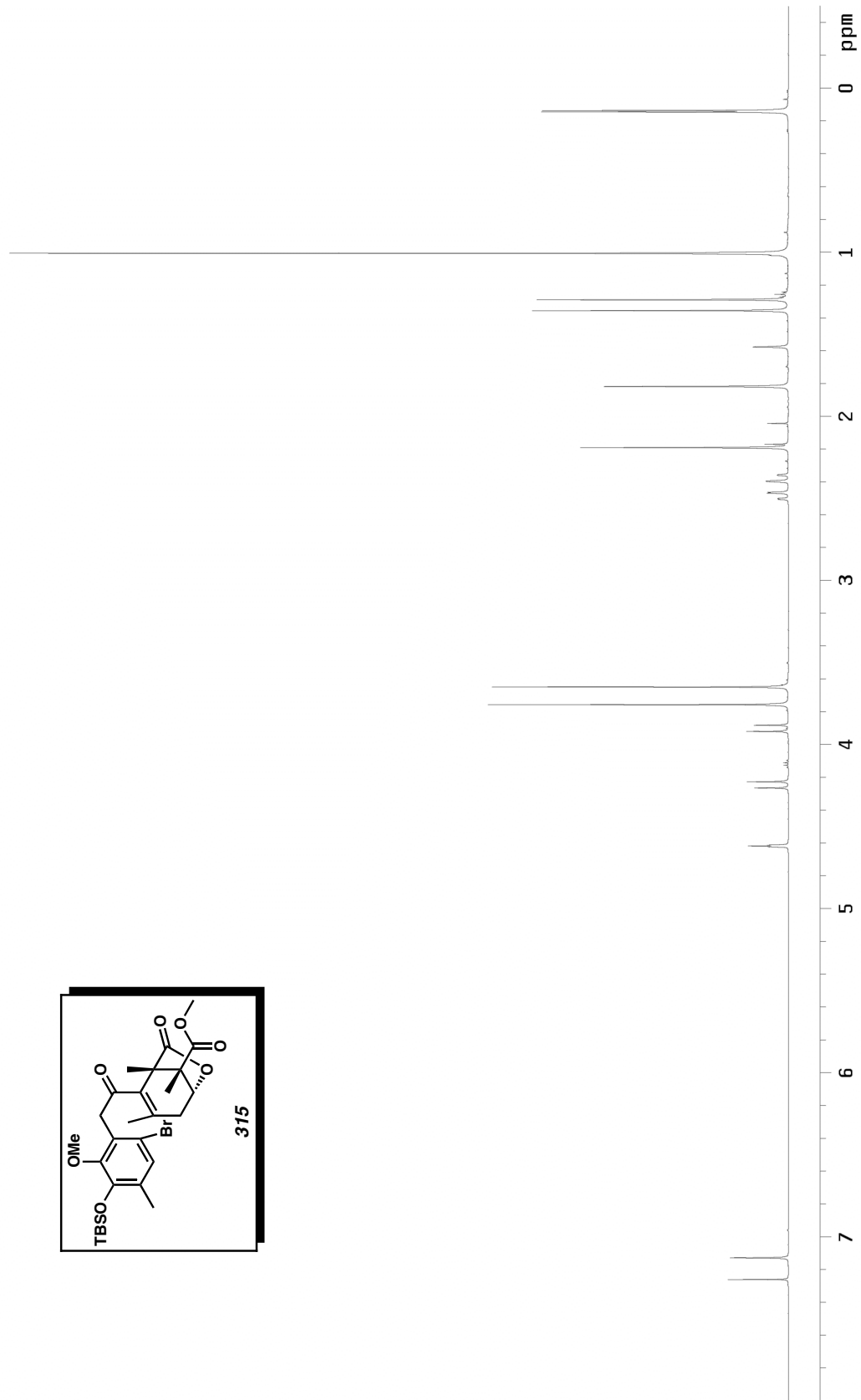
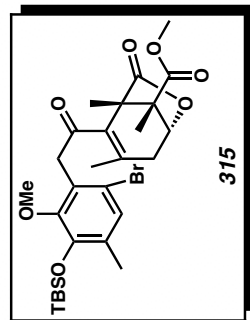


Figure C.7  $^1\text{H}$  NMR (500 MHz,  $\text{CDCl}_3$ ) of compound **315**.

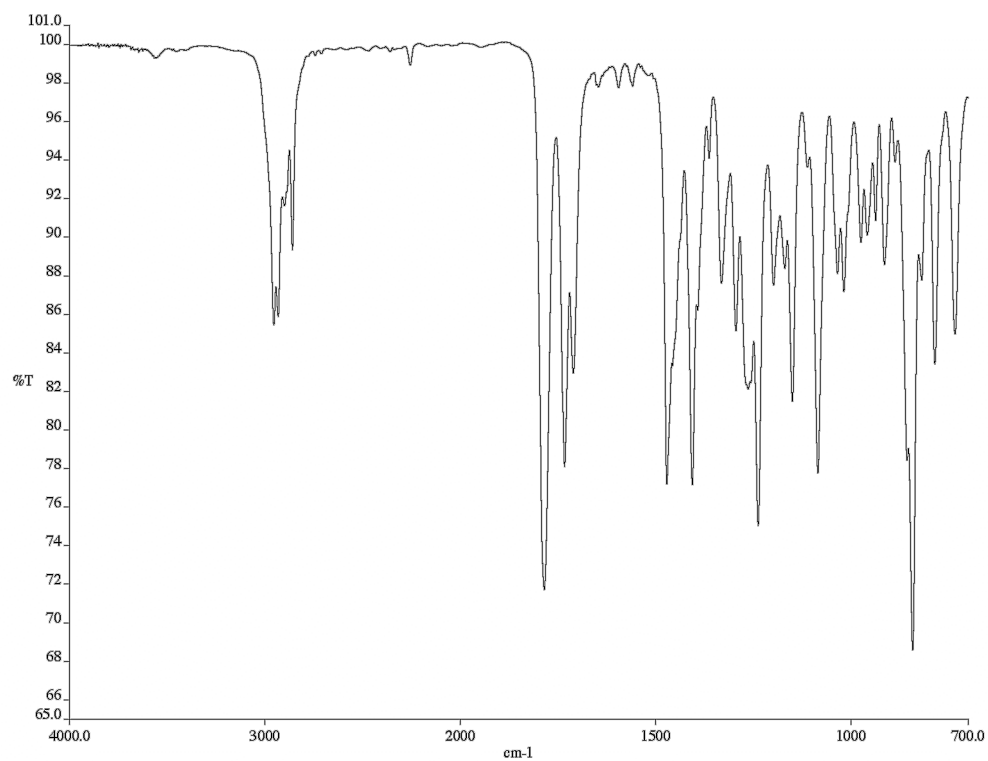


Figure C.8 Infrared spectrum (thin film/NaCl) of compound **315**.

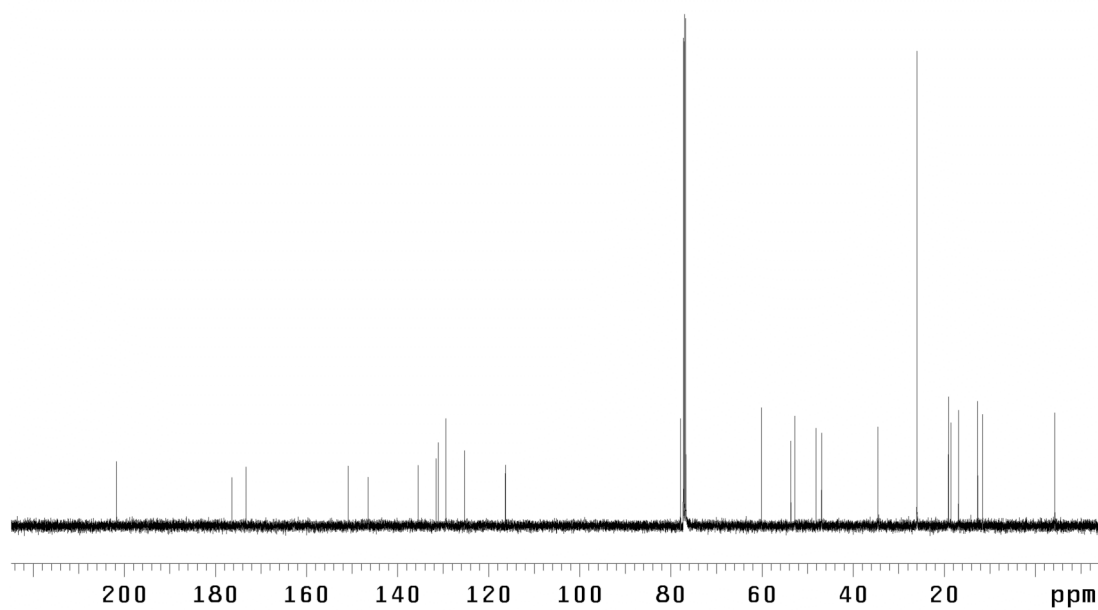


Figure C.9 <sup>13</sup>C NMR (125 MHz, CDCl<sub>3</sub>) of compound **315**.

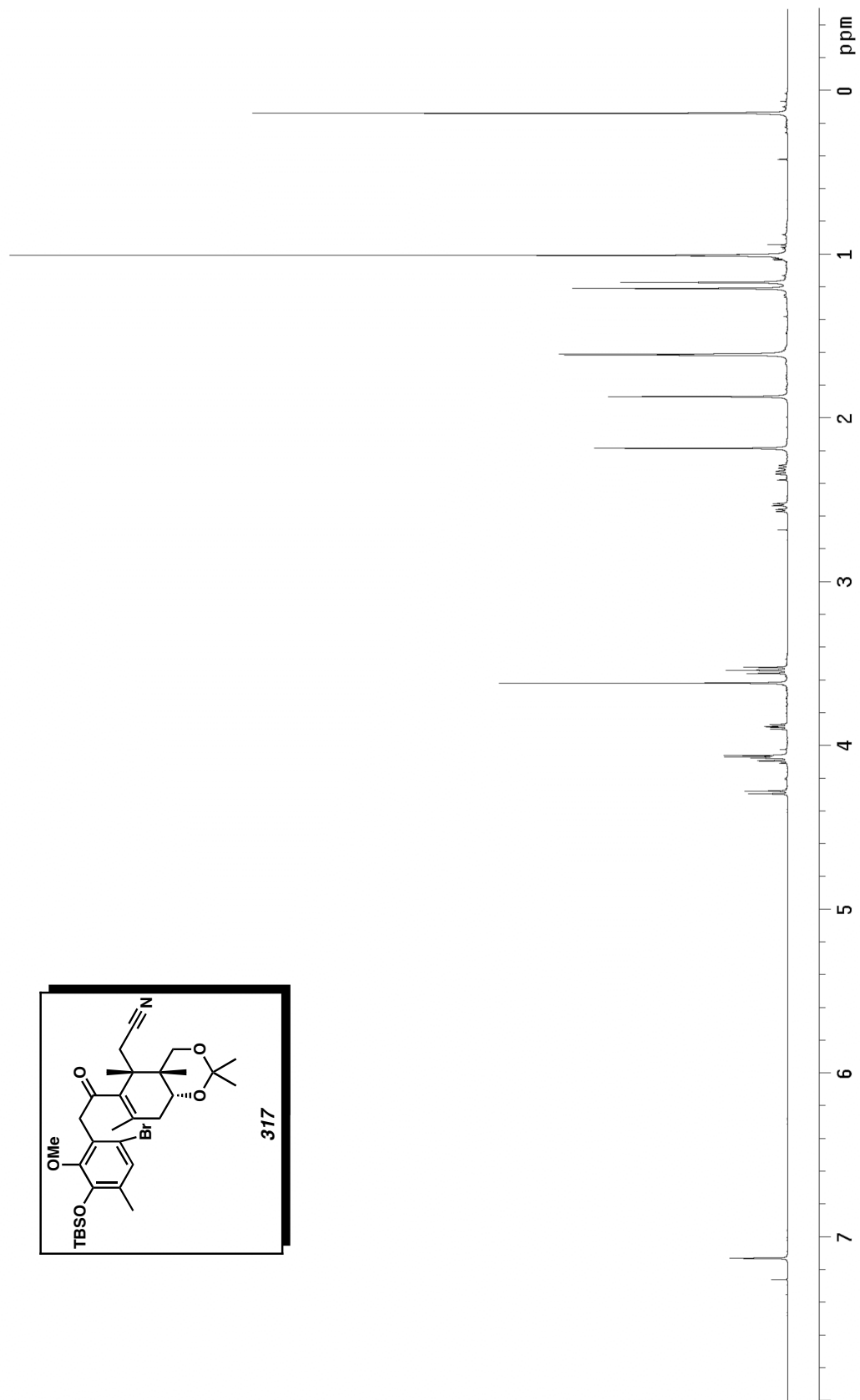
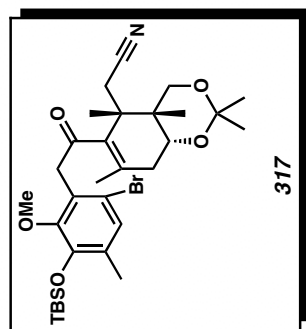


Figure C.10  $^1\text{H}$  NMR (500 MHz,  $\text{CDCl}_3$ ) of compound **317**.

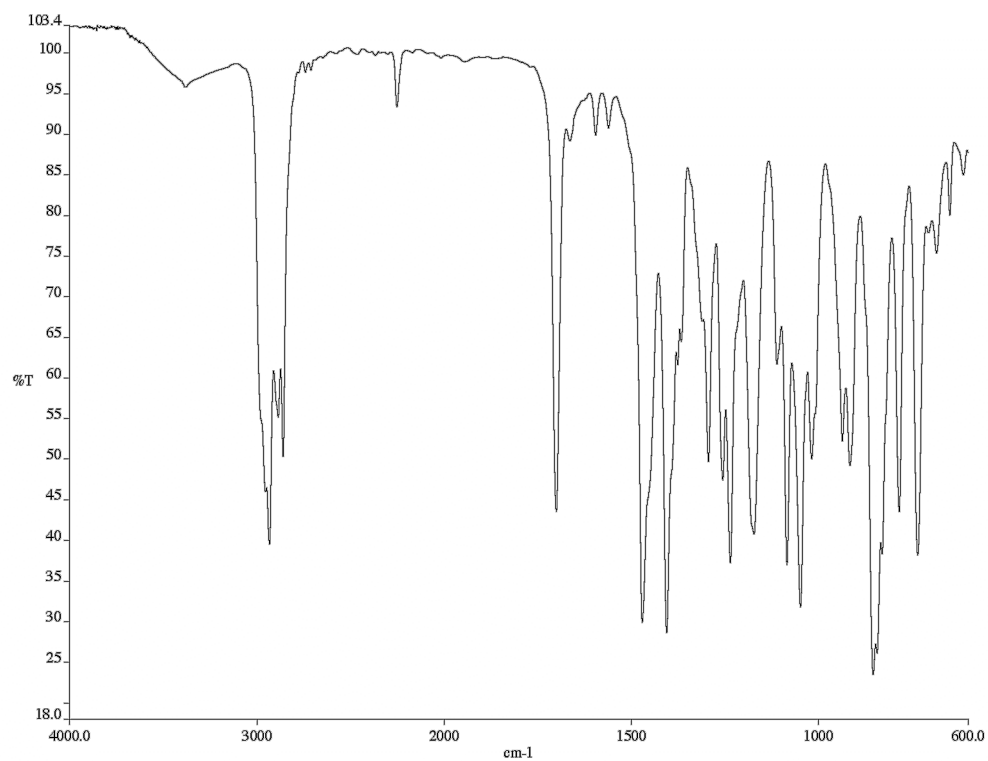


Figure C.11 Infrared spectrum (thin film/NaCl) of compound **317**.

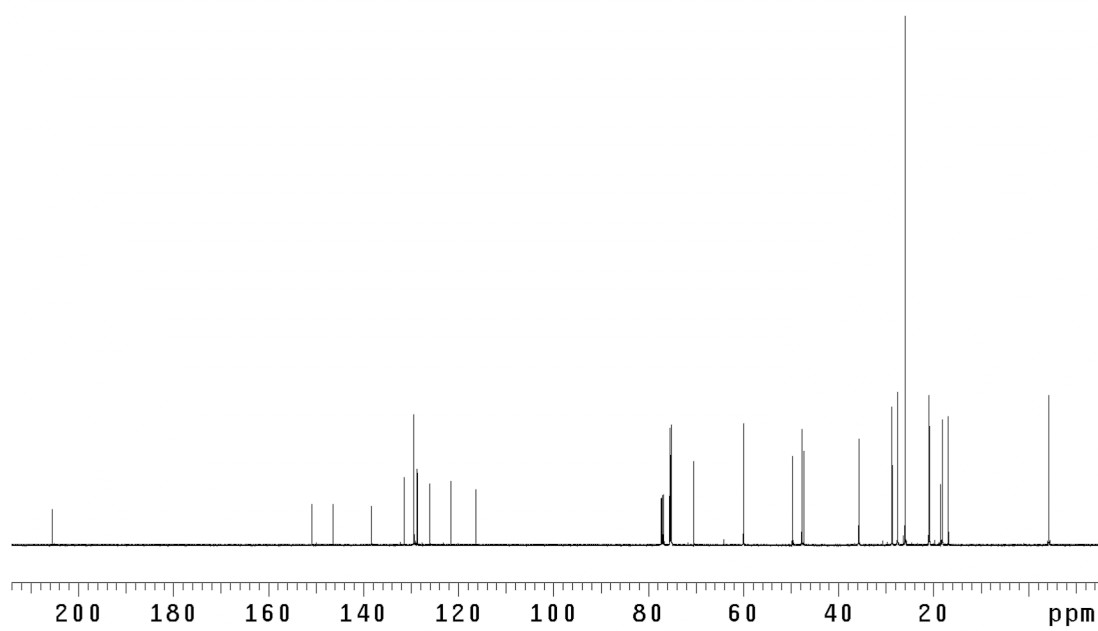


Figure C.12 <sup>13</sup>C NMR (125 MHz, CDCl<sub>3</sub>) of compound **317**.

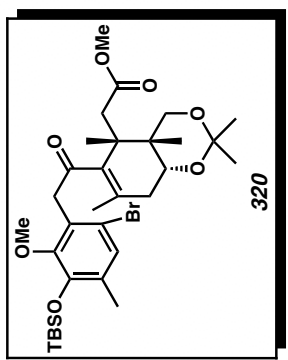
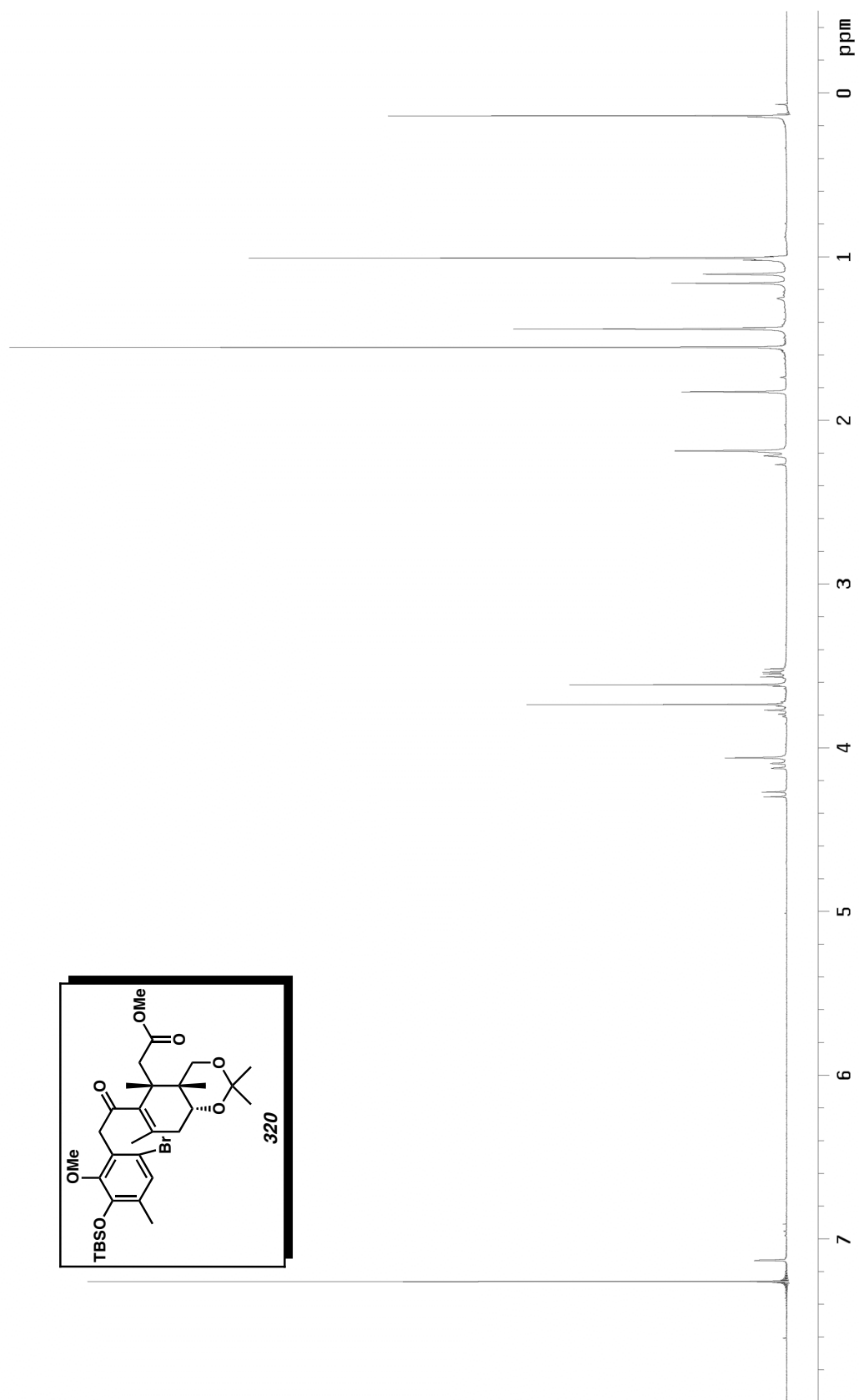


Figure C.13 <sup>1</sup>H NMR (300 MHz, CDCl<sub>3</sub>) of compound **320**.

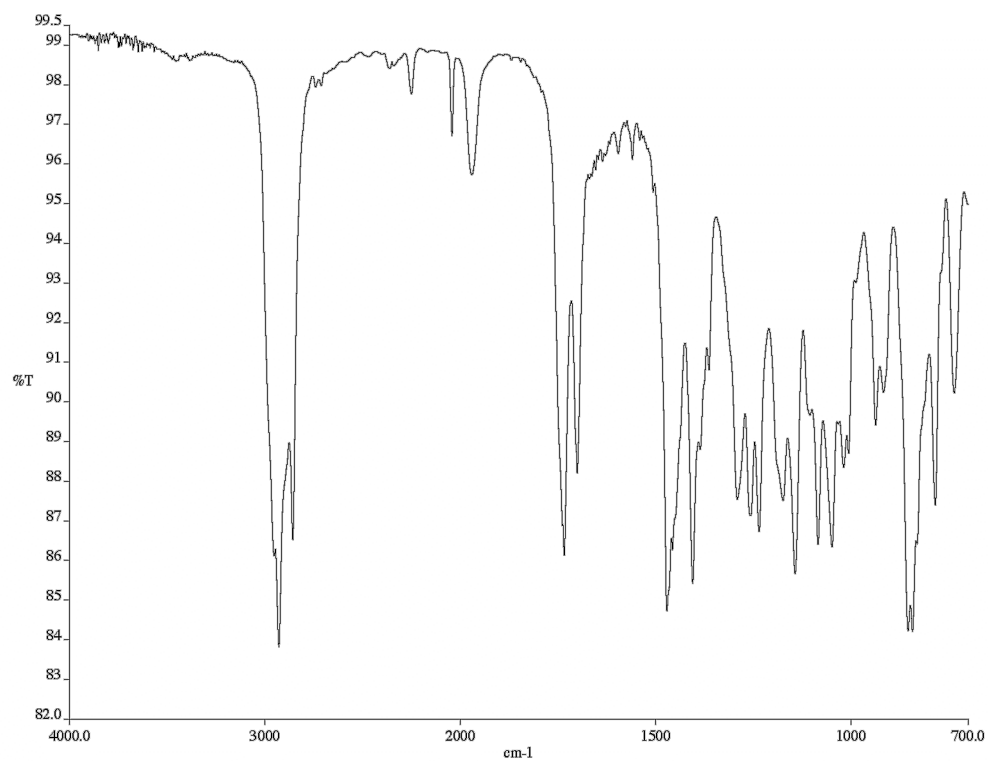


Figure C.14 Infrared spectrum (thin film/NaCl) of compound **320**.

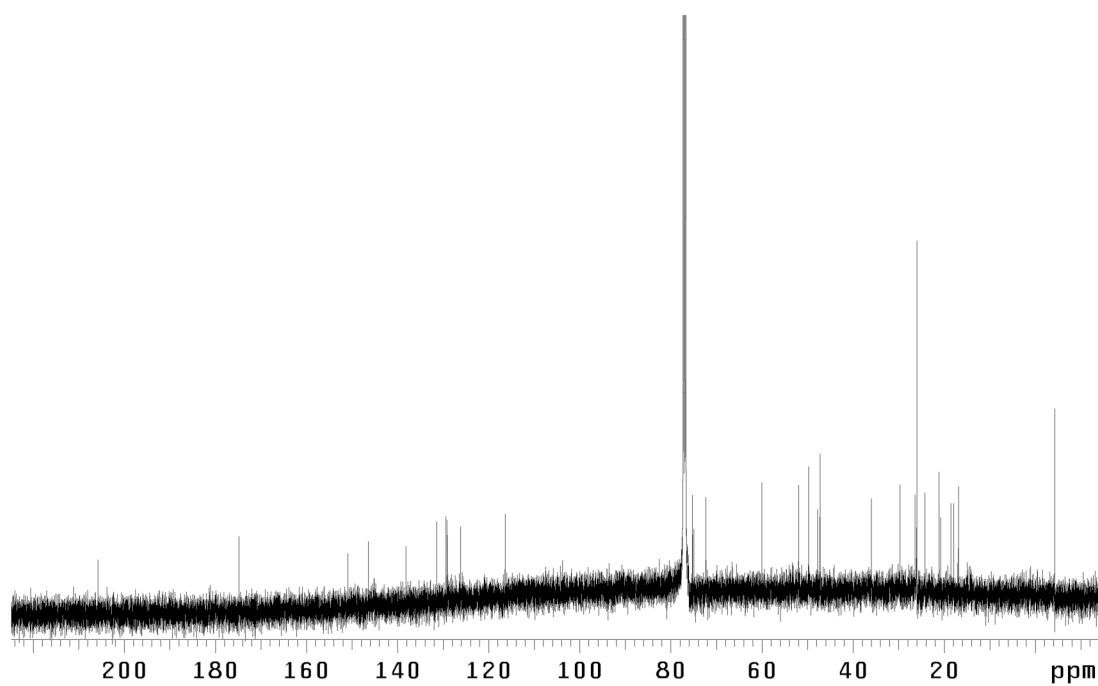


Figure C.15 <sup>13</sup>C NMR (75 MHz, CDCl<sub>3</sub>) of compound **320**.

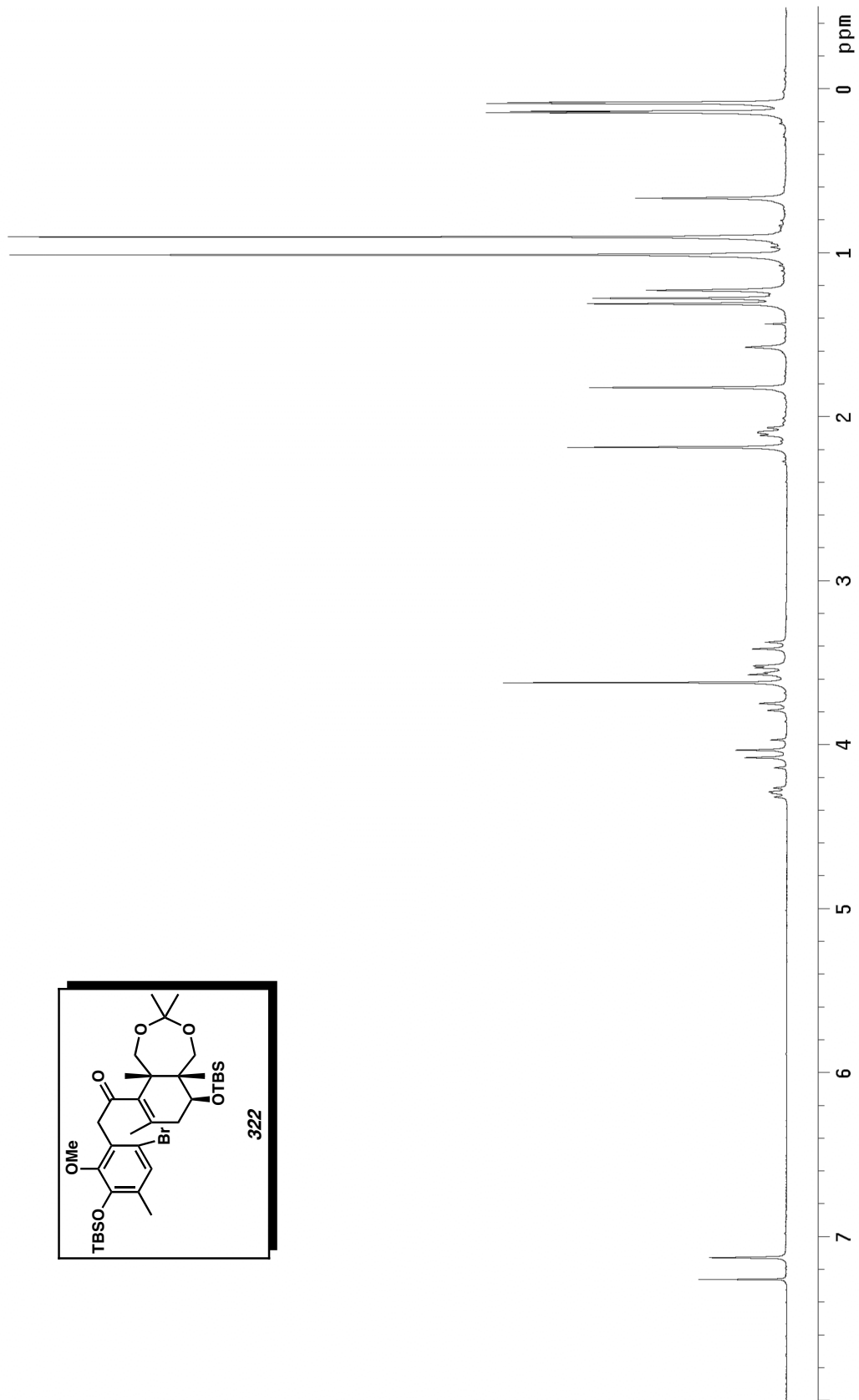
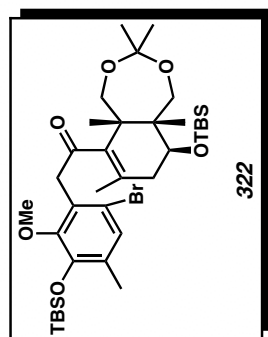


Figure C.16  $^1\text{H NMR}$  (300 MHz,  $\text{CDCl}_3$ ) of compound **322**.

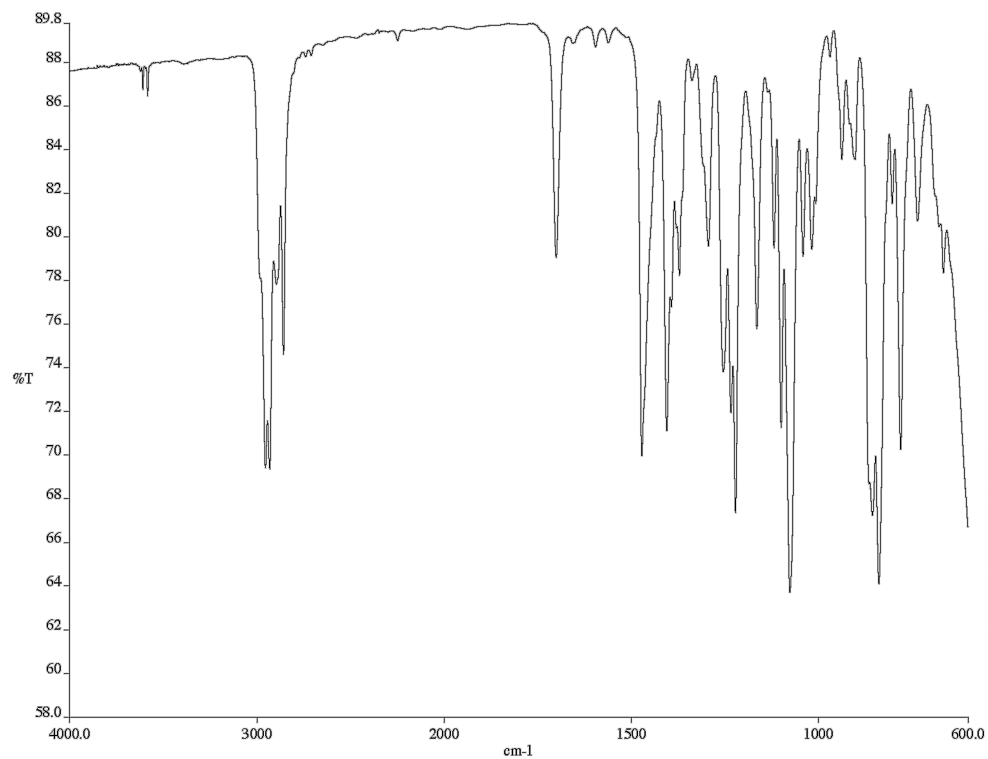


Figure C.17 Infrared spectrum (thin film/NaCl) of compound **322**.

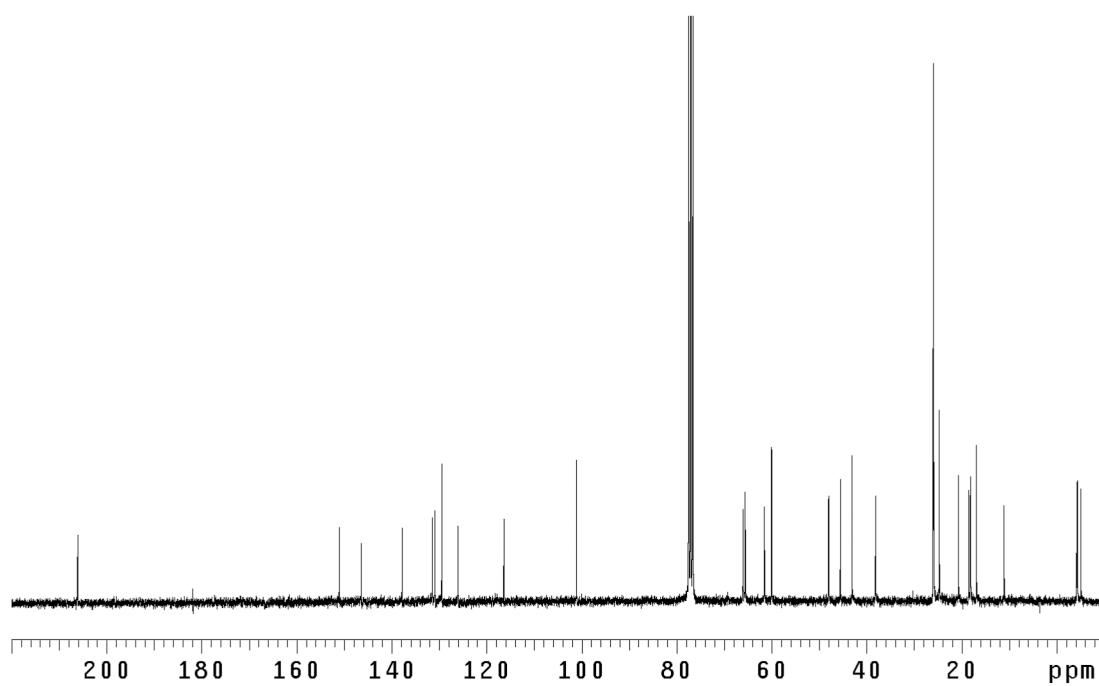


Figure C.18 <sup>13</sup>C NMR (75 MHz, CDCl<sub>3</sub>) of compound **322**.

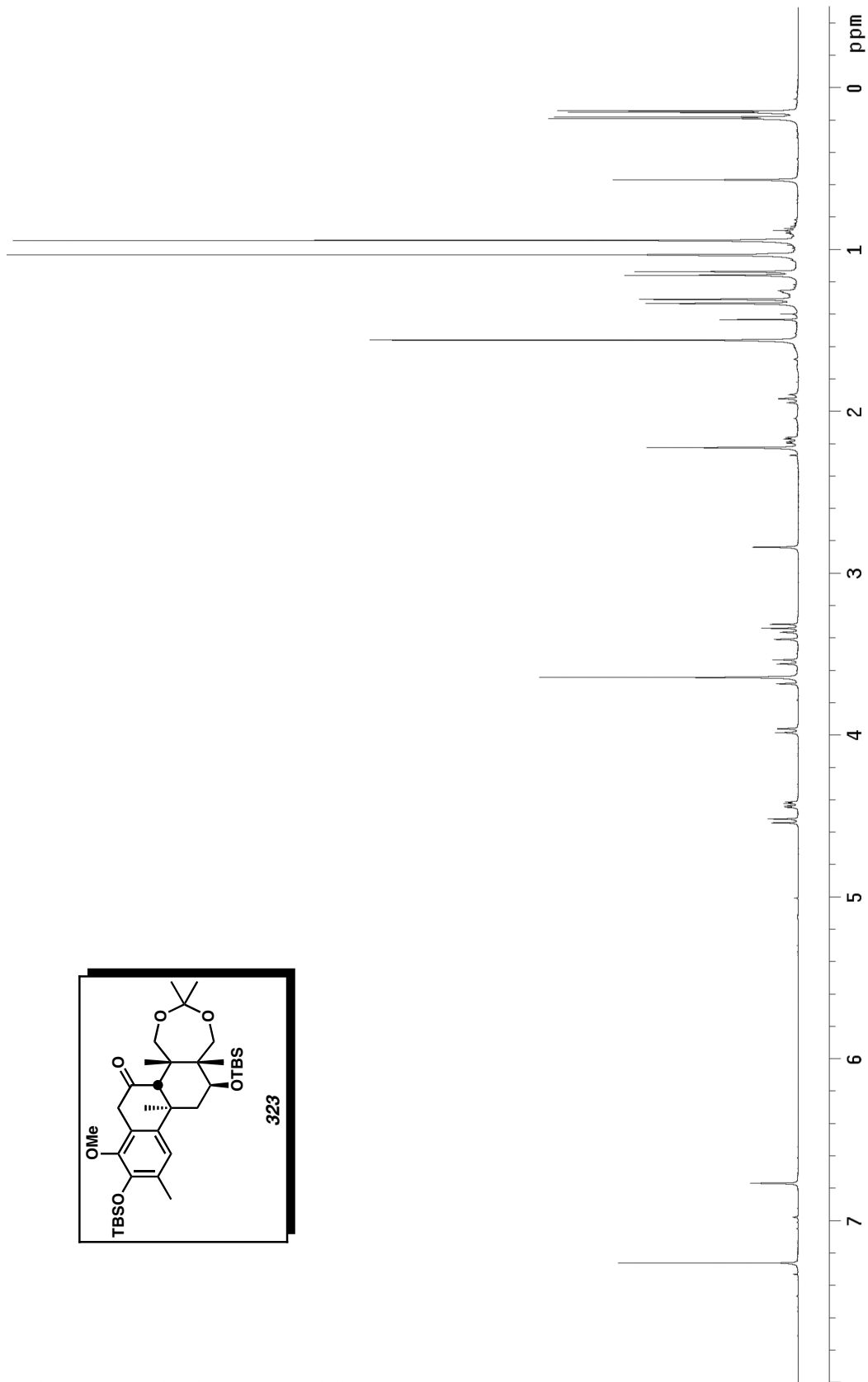
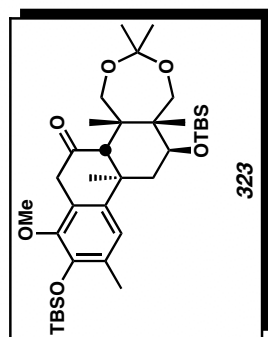


Figure C.19  $^1\text{H NMR}$  (500 MHz,  $\text{CDCl}_3$ ) of compound **323**.

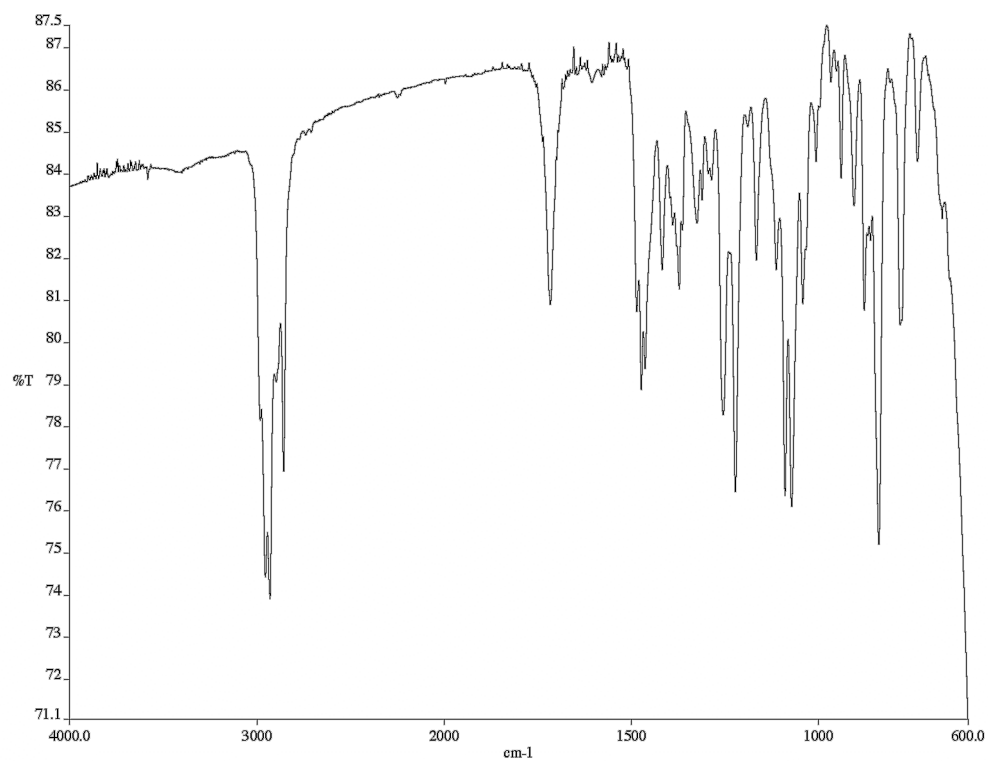


Figure C.20 Infrared spectrum (thin film/NaCl) of compound **323**.

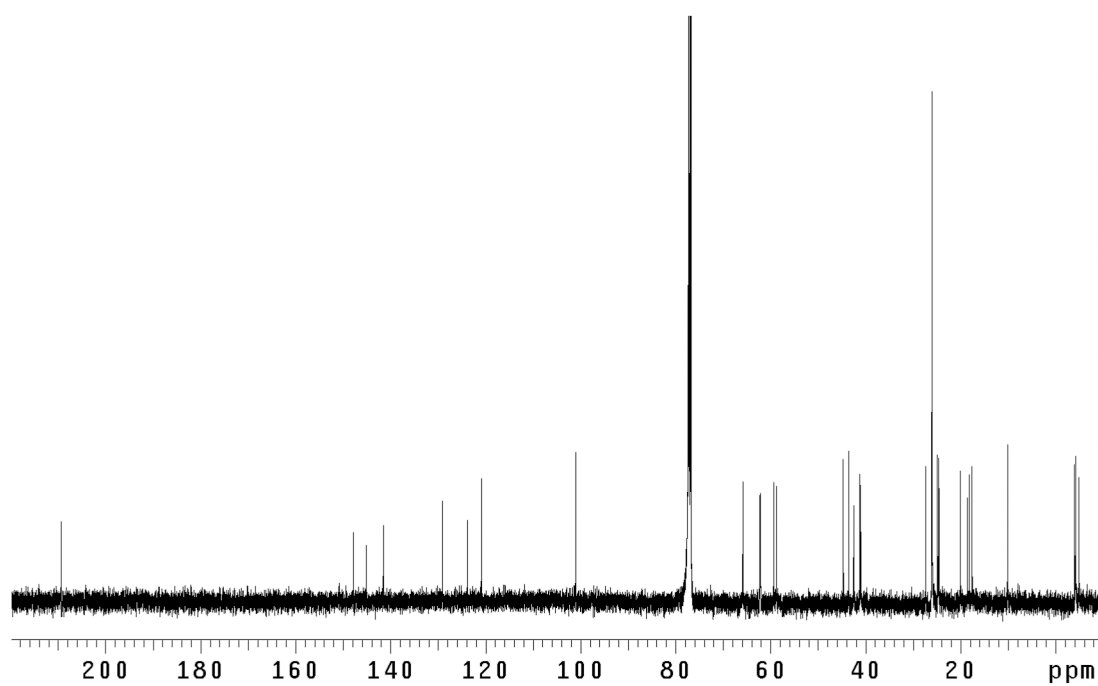


Figure C.21 <sup>13</sup>C NMR (125 MHz, CDCl<sub>3</sub>) of compound **323**.

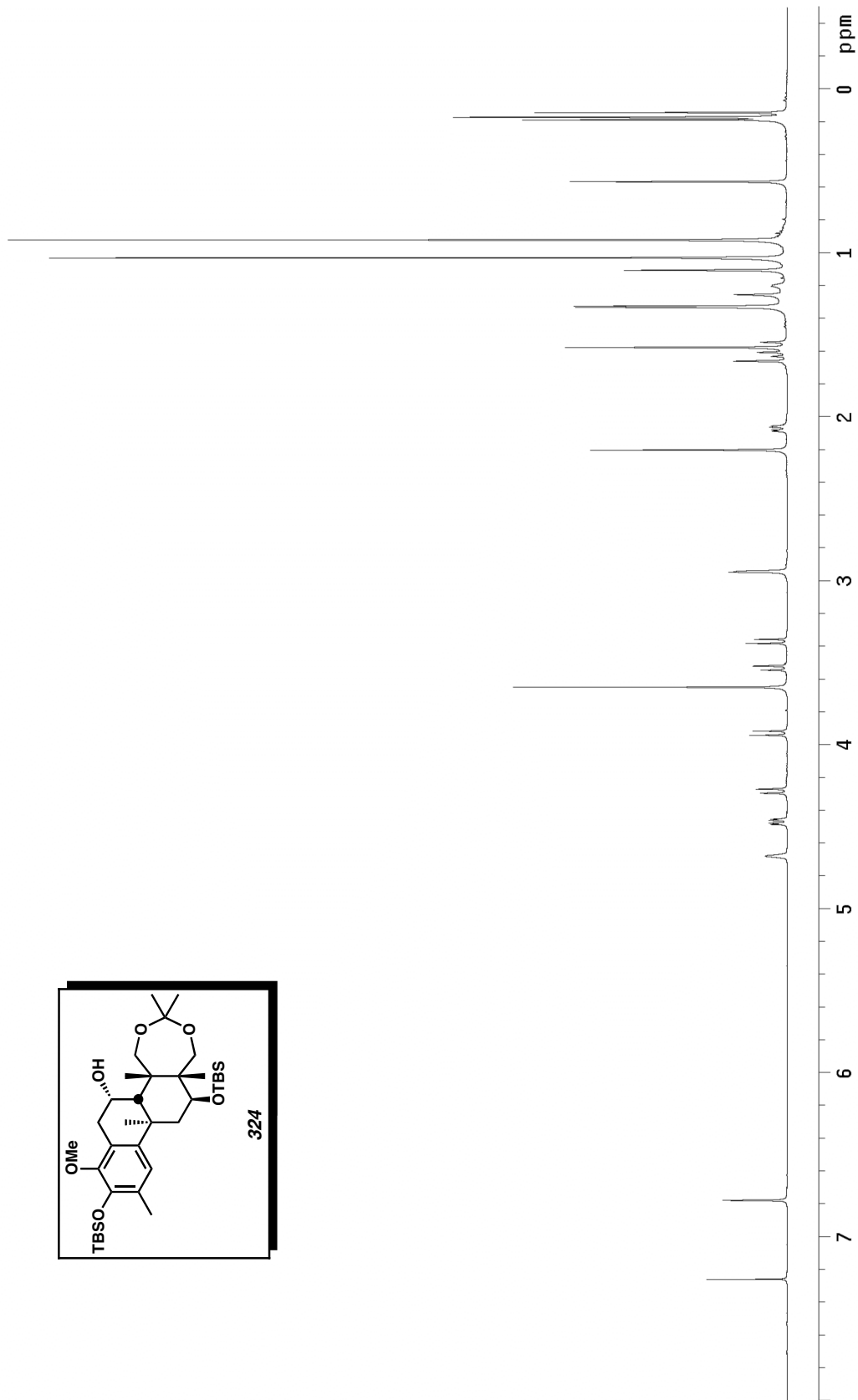
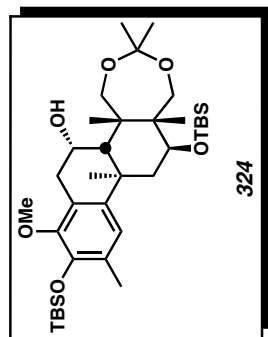


Figure C.22  $^1\text{H}$  NMR (500 MHz,  $\text{CDCl}_3$ ) of compound 324.

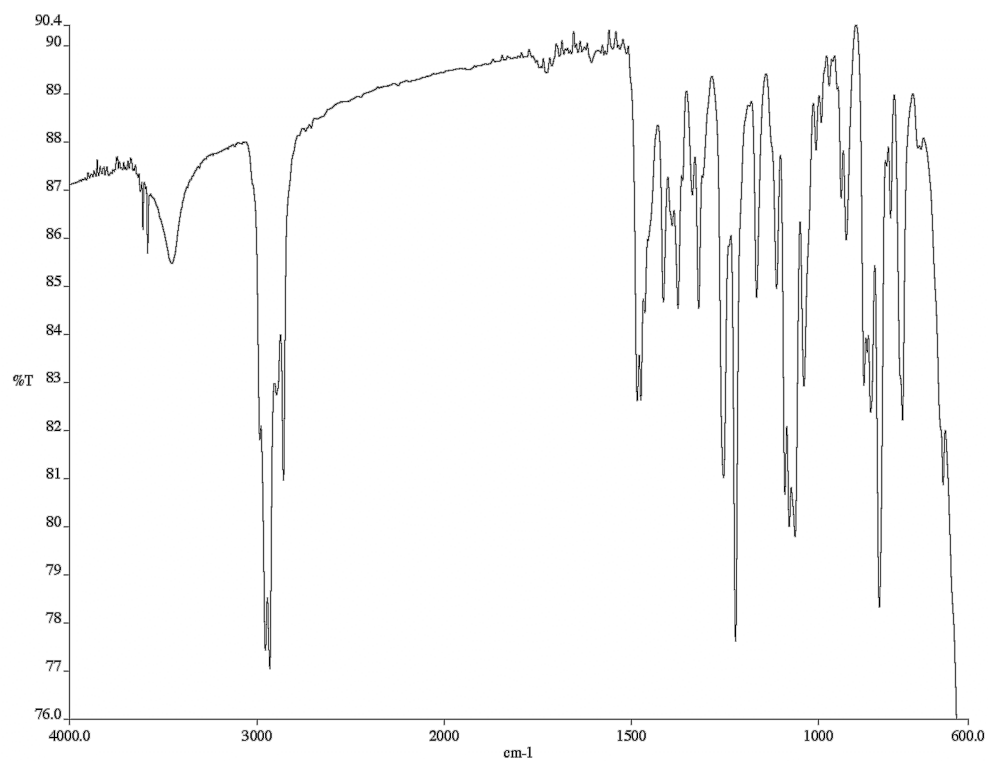


Figure C.23 Infrared spectrum (thin film/NaCl) of compound **324**.

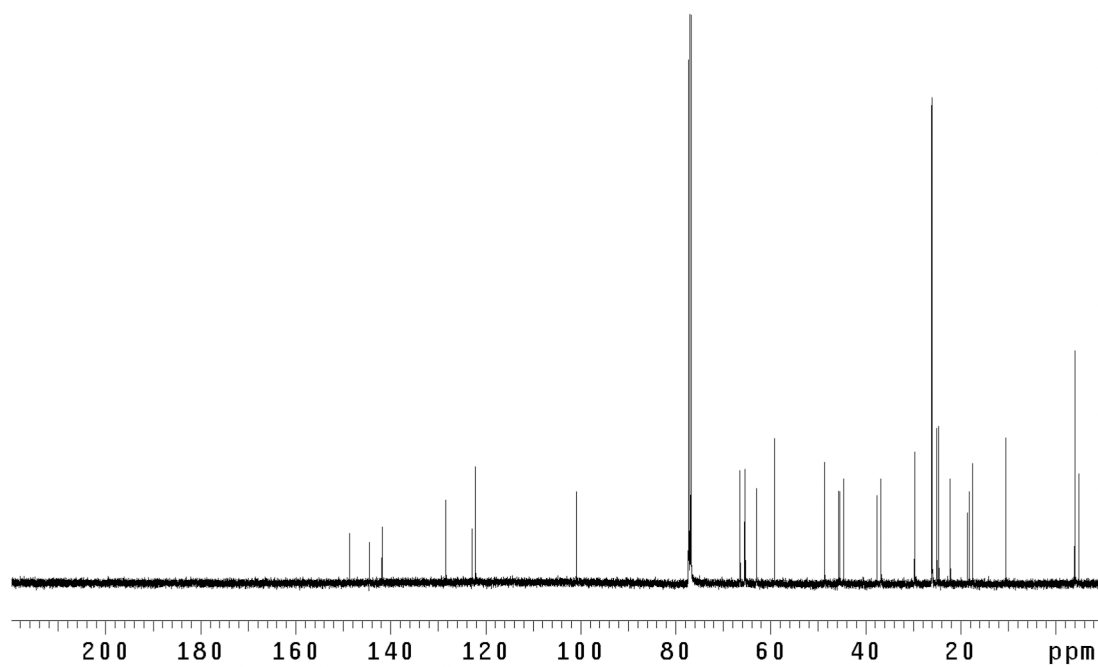


Figure C.24  $^{13}\text{C}$  NMR (125 MHz,  $\text{CDCl}_3$ ) of compound **324**.

CALIFORNIA INSTITUTE OF TECHNOLOGY  
BECKMAN INSTITUTE  
X-RAY CRYSTALLOGRAPHY LABORATORY

Crystal Structure Analysis of:  
Alcohol **324** (DCB34)

Contents:

- Table C.1 Crystal data.  
Table C.2 Atomic coordinates.  
Table C.3 Full bond distances and angles.

**Figure C.25** Representation of Alcohol **324**.

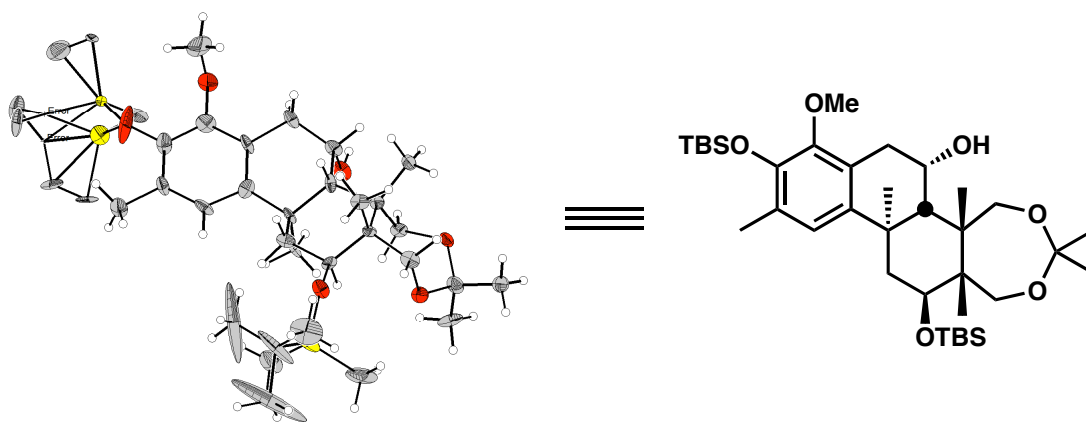


**Table C.1** Crystal data and structure refinement for dcb34.

Empirical formula	C <sub>36</sub> H <sub>49</sub> O <sub>6</sub> Si <sub>2</sub>
Formula weight	633.93
Crystallization Solvent	Methylene Chloride
Crystal Habit	Fragment
Crystal size	0.45 x 0.20 x 0.19 mm <sup>3</sup>
Crystal color	Colorless

### Data Collection

Preliminary Photos		
Type of diffractometer	Bruker SMART 1000	
Wavelength	0.71073 Å MoK $\alpha$	
Data Collection Temperature	100(2) K	
$\theta$ range for 2391 reflections used in lattice determination	2.25 to 25.75°	
Unit cell dimensions	a = 8.012(3) Å b = 12.103(5) Å c = 21.064(8) Å	$\alpha$ = 104.652(5)° $\beta$ = 92.405(7)° $\gamma$ = 98.610(6)°
Volume	1947.0(12) Å <sup>3</sup>	
Z	2	
Crystal system	Triclinic	
Space group	P-1	
Density (calculated)	1.081 Mg/m <sup>3</sup>	
F(000)	682	
$\theta$ range for data collection	1.76 to 27.12°	
Completeness to $\theta = 27.12^\circ$	78.9 %	
Index ranges	-10 <= h <= 8, -15 <= k <= 15, -26 <= l <= 12	
Data collection scan type	scans at 3 settings	
Reflections collected	8155	
Independent reflections	6807 [R <sub>int</sub> = 0.0961; GOF <sub>merge</sub> = ]	
Absorption coefficient	0.129 mm <sup>-1</sup>	
Absorption correction	None	

**Table C.1** (cont.)**Structure Solution and Refinement**

Structure solution program	SHELXS-97 (Sheldrick, 1990)
Primary solution method	direct
Secondary solution method	difmap
Hydrogen placement	geom
Structure refinement program	SHELXL-97 (Sheldrick, 1997)
Refinement method	Full-matrix least-squares on F <sup>2</sup>
Data / restraints / parameters	6807 / 0 / 456
Treatment of hydrogen atoms	mixed
Goodness-of-fit on F <sup>2</sup>	2.722
Final R indices [I > 2σ(I), 4077 reflections]	R1 = 0.1484, wR2 = 0.1836
R indices (all data)	R1 = 0.2120, wR2 = 0.1890
Type of weighting scheme used	calc
Weighting scheme used	calc
	$w=1/[\sigma^2(F_o^2)+(0.0000P)^2+0.0000P]$ where $P=(F_o^2+2F_c^2)/3$
Max shift/error	1.254
Average shift/error	0.004
Largest diff. peak and hole	0.655 and -0.594 e.Å <sup>-3</sup>

**Table C.2** Atomic coordinates (  $\times 10^4$ ) and equivalent isotropic displacement parameters ( $\text{\AA}^2 \times 10^3$ ) for dcb34.  $U(\text{eq})$  is defined as the trace of the orthogonalized  $U^{ij}$  tensor.

	x	y	z	$U_{\text{eq}}$	Occ
Si(2A)	11898(6)	1267(5)	4132(2)	15(2)	0.480(9)
Si(2B)	12395(6)	2036(5)	4004(2)	32(2)	0.520(9)
O(6)	2561(6)	4434(4)	2066(2)	26(1)	1
O(4)	3040(6)	1577(4)	-102(2)	21(1)	1
O(3)	7053(6)	620(4)	947(2)	27(1)	1
O(5)	2281(6)	3355(4)	432(2)	24(1)	1
O(1A)	10070(40)	1775(16)	4115(16)	23(7)	0.480(9)
C(1)	2380(8)	2466(5)	1362(3)	16(2)	1
O(2)	8803(7)	-67(4)	2989(3)	41(2)	1
C(2)	4738(9)	3387(6)	2278(3)	23(2)	1
C(3)	4299(8)	1754(6)	459(3)	21(2)	1
C(4)	4798(8)	1409(6)	1584(3)	20(2)	1
C(5)	5795(9)	384(6)	1376(3)	23(2)	1
C(6)	5952(8)	2528(5)	1996(3)	19(2)	1
C(7)	7591(9)	3162(6)	3129(4)	25(2)	1
C(8)	7268(8)	3098(6)	1588(3)	21(2)	1
C(9)	3425(8)	1492(6)	1051(3)	16(2)	1
C(10)	3552(8)	3555(5)	1752(3)	19(2)	1
C(11)	8602(9)	3023(6)	3647(3)	24(2)	1
C(12)	6986(9)	2280(7)	2562(3)	24(2)	1
C(13)	7315(8)	1161(6)	2542(3)	22(2)	1
C(14)	1097(8)	2053(6)	1829(3)	20(2)	1
C(15)	1296(8)	2793(6)	853(3)	22(2)	1
C(16)	8395(9)	1028(6)	3049(4)	30(2)	1
C(17)	9097(10)	1930(7)	3580(4)	30(2)	1
C(18)	976(8)	2272(6)	-653(3)	25(2)	1
C(19)	2236(8)	320(5)	817(3)	23(2)	1
C(20)	6564(9)	111(6)	1978(3)	24(2)	1
C(21)	9165(10)	4017(6)	4246(3)	38(2)	1
C(22)	2536(10)	2627(6)	-208(4)	28(2)	1
C(23)	5312(9)	6404(7)	2242(4)	45(2)	1
C(24)	3956(9)	3325(6)	-466(4)	34(2)	1
C(25)	2088(11)	6074(7)	1347(5)	71(3)	1
C(26)	26(11)	6041(8)	2774(4)	64(3)	1
C(27)	2062(17)	7851(9)	2892(9)	241(12)	1
C(28)	1911(11)	6533(7)	2886(6)	80(4)	1
C(29)	2709(15)	6347(16)	3472(5)	225(13)	1
C(30)	7871(15)	-666(8)	3383(5)	95(5)	1
C(34)	15112(10)	2027(7)	4889(4)	39(2)	1
C(33)	12570(10)	2764(7)	5392(3)	43(2)	1
C(32)	13620(60)	2710(70)	4690(20)	330(60)	0.480(9)
O(1B)	10270(40)	1780(20)	4019(18)	67(10)	0.520(9)
C(37)	13940(30)	3570(18)	4427(13)	49(8)	0.480(9)
C(38)	12530(30)	502(17)	4794(9)	62(7)	0.520(9)
C(39)	13340(30)	2090(30)	4776(15)	42(7)	0.520(9)
C(42)	12884(10)	1006(6)	3290(3)	33(2)	1
C(40)	11720(20)	-94(12)	4414(8)	21(4)	0.480(9)

C(41)	13220(20)	3598(12)	3960(8)	30(4)	0.520(9)
Si(1)	2960(3)	5826(2)	2116(1)	36(1)	1

---

**Table C.3** Bond lengths [ $\text{\AA}$ ] and angles [ $^\circ$ ] for dcb34.

Si(2A)-O(1A)	1.68(3)	C(14)-H(14A)	0.9800
Si(2A)-C(40)	1.876(15)	C(14)-H(14B)	0.9800
Si(2A)-C(42)	1.943(8)	C(14)-H(14C)	0.9800
Si(2A)-C(32)	2.11(7)	C(15)-H(15A)	0.9900
Si(2B)-O(1B)	1.69(3)	C(15)-H(15B)	0.9900
Si(2B)-C(39)	1.75(3)	C(16)-C(17)	1.381(10)
Si(2B)-C(42)	1.793(8)	C(17)-O(1B)	1.35(3)
Si(2B)-C(41)	1.934(15)	C(18)-C(22)	1.470(9)
O(6)-C(10)	1.464(7)	C(18)-H(18A)	0.9800
O(6)-Si(1)	1.643(5)	C(18)-H(18B)	0.9800
O(4)-C(22)	1.456(8)	C(18)-H(18C)	0.9800
O(4)-C(3)	1.471(7)	C(19)-H(19A)	0.9800
O(3)-C(5)	1.426(8)	C(19)-H(19B)	0.9800
O(3)-H(3)	0.8400	C(19)-H(19C)	0.9800
O(5)-C(15)	1.441(7)	C(20)-H(20A)	0.9900
O(5)-C(22)	1.454(8)	C(20)-H(20B)	0.9900
O(1A)-C(17)	1.41(3)	C(21)-H(21A)	0.9800
C(1)-C(15)	1.516(9)	C(21)-H(21B)	0.9800
C(1)-C(10)	1.520(9)	C(21)-H(21C)	0.9800
C(1)-C(14)	1.567(9)	C(22)-C(24)	1.516(9)
C(1)-C(9)	1.572(8)	C(23)-Si(1)	1.892(8)
O(2)-C(16)	1.388(8)	C(23)-H(23A)	0.9800
O(2)-C(30)	1.403(11)	C(23)-H(23B)	0.9800
C(2)-C(10)	1.502(8)	C(23)-H(23C)	0.9800
C(2)-C(6)	1.554(8)	C(24)-H(24A)	0.9800
C(2)-H(2A)	0.9900	C(24)-H(24B)	0.9800
C(2)-H(2B)	0.9900	C(24)-H(24C)	0.9800
C(3)-C(9)	1.535(9)	C(25)-Si(1)	1.847(8)
C(3)-H(3A)	0.9900	C(25)-H(25A)	0.9800
C(3)-H(3B)	0.9900	C(25)-H(25B)	0.9800
C(4)-C(6)	1.551(9)	C(25)-H(25C)	0.9800
C(4)-C(5)	1.556(8)	C(26)-C(28)	1.523(11)
C(4)-C(9)	1.570(9)	C(26)-H(26A)	0.9800
C(4)-H(4)	1.0000	C(26)-H(26B)	0.9800
C(5)-C(20)	1.519(9)	C(26)-H(26C)	0.9800
C(5)-H(5)	1.0000	C(27)-C(28)	1.578(15)
C(6)-C(12)	1.540(9)	C(27)-H(27A)	0.9800
C(6)-C(8)	1.576(9)	C(27)-H(27B)	0.9800
C(7)-C(11)	1.391(9)	C(27)-H(27C)	0.9800
C(7)-C(12)	1.397(9)	C(28)-C(29)	1.449(17)
C(7)-H(7)	0.9500	C(28)-Si(1)	1.923(9)
C(8)-H(8A)	0.9800	C(29)-H(29A)	0.9800
C(8)-H(8B)	0.9800	C(29)-H(29B)	0.9800
C(8)-H(8C)	0.9800	C(29)-H(29C)	0.9800
C(9)-C(19)	1.537(9)	C(30)-H(30A)	0.9800
C(10)-H(10)	1.0000	C(30)-H(30B)	0.9800
C(11)-C(17)	1.412(10)	C(30)-H(30C)	0.9800
C(11)-C(21)	1.505(9)	C(34)-C(39)	1.45(3)
C(12)-C(13)	1.410(9)	C(34)-C(32)	1.65(5)
C(13)-C(16)	1.402(9)	C(33)-C(39)	1.55(3)
C(13)-C(20)	1.528(8)	C(33)-C(32)	1.73(5)

C(32)-C(37)	1.29(9)	C(4)-C(6)-C(8)	113.9(5)
C(38)-C(39)	1.94(4)	C(2)-C(6)-C(8)	109.6(5)
O(1A)-Si(2A)-C(40)	113.4(11)	C(11)-C(7)-C(12)	124.2(7)
O(1A)-Si(2A)-C(42)	112.9(13)	C(11)-C(7)-H(7)	117.9
C(40)-Si(2A)-C(42)	108.8(5)	C(12)-C(7)-H(7)	117.9
O(1A)-Si(2A)-C(32)	103.6(15)	C(6)-C(8)-H(8A)	109.5
C(40)-Si(2A)-C(32)	117(2)	C(6)-C(8)-H(8B)	109.5
C(42)-Si(2A)-C(32)	100.4(15)	H(8A)-C(8)-H(8B)	109.5
O(1B)-Si(2B)-C(39)	109.1(16)	C(6)-C(8)-H(8C)	109.5
O(1B)-Si(2B)-C(42)	106.2(11)	H(8A)-C(8)-H(8C)	109.5
C(39)-Si(2B)-C(42)	119.3(11)	H(8B)-C(8)-H(8C)	109.5
O(1B)-Si(2B)-C(41)	112.0(12)	C(3)-C(9)-C(19)	108.6(5)
C(39)-Si(2B)-C(41)	99.8(12)	C(3)-C(9)-C(4)	109.4(5)
C(42)-Si(2B)-C(41)	110.5(6)	C(19)-C(9)-C(4)	108.9(5)
C(10)-O(6)-Si(1)	126.8(4)	C(3)-C(9)-C(1)	110.8(5)
C(22)-O(4)-C(3)	115.3(5)	C(19)-C(9)-C(1)	109.7(5)
C(5)-O(3)-H(3)	109.5	C(4)-C(9)-C(1)	109.4(5)
C(15)-O(5)-C(22)	116.3(5)	O(6)-C(10)-C(2)	107.6(5)
C(17)-O(1A)-Si(2A)	130(2)	O(6)-C(10)-C(1)	110.2(5)
C(15)-C(1)-C(10)	107.9(5)	C(2)-C(10)-C(1)	115.2(6)
C(15)-C(1)-C(14)	104.9(5)	O(6)-C(10)-H(10)	107.9
C(10)-C(1)-C(14)	108.9(5)	C(2)-C(10)-H(10)	107.9
C(15)-C(1)-C(9)	113.1(6)	C(1)-C(10)-H(10)	107.9
C(10)-C(1)-C(9)	110.7(5)	C(7)-C(11)-C(17)	117.5(7)
C(14)-C(1)-C(9)	111.1(5)	C(7)-C(11)-C(21)	120.5(6)
C(16)-O(2)-C(30)	112.3(6)	C(17)-C(11)-C(21)	122.0(7)
C(10)-C(2)-C(6)	112.6(5)	C(7)-C(12)-C(13)	117.3(6)
C(10)-C(2)-H(2A)	109.1	C(7)-C(12)-C(6)	120.7(6)
C(6)-C(2)-H(2A)	109.1	C(13)-C(12)-C(6)	121.9(6)
C(10)-C(2)-H(2B)	109.1	C(16)-C(13)-C(12)	118.3(6)
C(6)-C(2)-H(2B)	109.1	C(16)-C(13)-C(20)	120.0(6)
H(2A)-C(2)-H(2B)	107.8	C(12)-C(13)-C(20)	121.7(6)
O(4)-C(3)-C(9)	110.2(5)	C(1)-C(14)-H(14A)	109.5
O(4)-C(3)-H(3A)	109.6	C(1)-C(14)-H(14B)	109.5
C(9)-C(3)-H(3A)	109.6	H(14A)-C(14)-H(14B)	109.5
O(4)-C(3)-H(3B)	109.6	C(1)-C(14)-H(14C)	109.5
C(9)-C(3)-H(3B)	109.6	H(14A)-C(14)-H(14C)	109.5
H(3A)-C(3)-H(3B)	108.1	H(14B)-C(14)-H(14C)	109.5
C(6)-C(4)-C(5)	112.0(5)	O(5)-C(15)-C(1)	113.0(6)
C(6)-C(4)-C(9)	119.5(6)	O(5)-C(15)-H(15A)	109.0
C(5)-C(4)-C(9)	115.5(5)	C(1)-C(15)-H(15A)	109.0
C(6)-C(4)-H(4)	102.2	O(5)-C(15)-H(15B)	109.0
C(5)-C(4)-H(4)	102.2	C(1)-C(15)-H(15B)	109.0
C(9)-C(4)-H(4)	102.2	H(15A)-C(15)-H(15B)	107.8
O(3)-C(5)-C(20)	111.5(6)	C(17)-C(16)-O(2)	119.7(7)
O(3)-C(5)-C(4)	111.1(6)	C(17)-C(16)-C(13)	123.3(7)
C(20)-C(5)-C(4)	110.5(6)	O(2)-C(16)-C(13)	117.0(7)
O(3)-C(5)-H(5)	107.9	O(1B)-C(17)-C(16)	120.7(14)
C(20)-C(5)-H(5)	107.9	O(1B)-C(17)-O(1A)	11(3)
C(4)-C(5)-H(5)	107.9	C(16)-C(17)-O(1A)	123.0(10)
C(12)-C(6)-C(4)	110.9(6)	O(1B)-C(17)-C(11)	120.6(14)
C(12)-C(6)-C(2)	110.1(5)	C(16)-C(17)-C(11)	118.6(7)
C(4)-C(6)-C(2)	105.8(5)	O(1A)-C(17)-C(11)	117.5(11)
C(12)-C(6)-C(8)	106.6(6)	C(22)-C(18)-H(18A)	109.5

C(22)-C(18)-H(18B)	109.5	C(28)-C(27)-H(27B)	109.5
H(18A)-C(18)-H(18B)	109.5	H(27A)-C(27)-H(27B)	109.5
C(22)-C(18)-H(18C)	109.5	C(28)-C(27)-H(27C)	109.5
H(18A)-C(18)-H(18C)	109.5	H(27A)-C(27)-H(27C)	109.5
H(18B)-C(18)-H(18C)	109.5	H(27B)-C(27)-H(27C)	109.5
C(9)-C(19)-H(19A)	109.5	C(29)-C(28)-C(26)	112.9(11)
C(9)-C(19)-H(19B)	109.5	C(29)-C(28)-C(27)	113.7(11)
H(19A)-C(19)-H(19B)	109.5	C(26)-C(28)-C(27)	106.1(9)
C(9)-C(19)-H(19C)	109.5	C(29)-C(28)-Si(1)	110.7(7)
H(19A)-C(19)-H(19C)	109.5	C(26)-C(28)-Si(1)	107.6(6)
H(19B)-C(19)-H(19C)	109.5	C(27)-C(28)-Si(1)	105.4(8)
C(5)-C(20)-C(13)	115.6(6)	C(28)-C(29)-H(29A)	109.5
C(5)-C(20)-H(20A)	108.4	C(28)-C(29)-H(29B)	109.5
C(13)-C(20)-H(20A)	108.4	H(29A)-C(29)-H(29B)	109.5
C(5)-C(20)-H(20B)	108.4	C(28)-C(29)-H(29C)	109.5
C(13)-C(20)-H(20B)	108.4	H(29A)-C(29)-H(29C)	109.5
H(20A)-C(20)-H(20B)	107.5	H(29B)-C(29)-H(29C)	109.5
C(11)-C(21)-H(21A)	109.5	O(2)-C(30)-H(30A)	109.5
C(11)-C(21)-H(21B)	109.5	O(2)-C(30)-H(30B)	109.5
H(21A)-C(21)-H(21B)	109.5	H(30A)-C(30)-H(30B)	109.5
C(11)-C(21)-H(21C)	109.5	O(2)-C(30)-H(30C)	109.5
H(21A)-C(21)-H(21C)	109.5	H(30A)-C(30)-H(30C)	109.5
H(21B)-C(21)-H(21C)	109.5	H(30B)-C(30)-H(30C)	109.5
O(5)-C(22)-O(4)	107.4(5)	C(39)-C(34)-C(32)	30(4)
O(5)-C(22)-C(18)	112.5(6)	C(39)-C(33)-C(32)	28(3)
O(4)-C(22)-C(18)	107.1(6)	C(37)-C(32)-C(34)	123(4)
O(5)-C(22)-C(24)	105.3(6)	C(37)-C(32)-C(33)	124(4)
O(4)-C(22)-C(24)	111.1(6)	C(34)-C(32)-C(33)	96(4)
C(18)-C(22)-C(24)	113.4(7)	C(37)-C(32)-Si(2A)	116(3)
Si(1)-C(23)-H(23A)	109.5	C(34)-C(32)-Si(2A)	99(4)
Si(1)-C(23)-H(23B)	109.5	C(33)-C(32)-Si(2A)	93(3)
H(23A)-C(23)-H(23B)	109.5	C(17)-O(1B)-Si(2B)	127(3)
Si(1)-C(23)-H(23C)	109.5	C(34)-C(39)-C(33)	113.8(18)
H(23A)-C(23)-H(23C)	109.5	C(34)-C(39)-Si(2B)	123(2)
H(23B)-C(23)-H(23C)	109.5	C(33)-C(39)-Si(2B)	117(2)
C(22)-C(24)-H(24A)	109.5	C(34)-C(39)-C(38)	95.0(19)
C(22)-C(24)-H(24B)	109.5	C(33)-C(39)-C(38)	100.8(16)
H(24A)-C(24)-H(24B)	109.5	Si(2B)-C(39)-C(38)	98.6(14)
C(22)-C(24)-H(24C)	109.5	Si(2B)-C(42)-Si(2A)	32.6(2)
H(24A)-C(24)-H(24C)	109.5	O(6)-Si(1)-C(25)	108.9(3)
H(24B)-C(24)-H(24C)	109.5	O(6)-Si(1)-C(23)	111.8(3)
Si(1)-C(25)-H(25A)	109.5	C(25)-Si(1)-C(23)	109.2(4)
Si(1)-C(25)-H(25B)	109.5	O(6)-Si(1)-C(28)	104.3(4)
H(25A)-C(25)-H(25B)	109.5	C(25)-Si(1)-C(28)	113.9(5)
Si(1)-C(25)-H(25C)	109.5	C(23)-Si(1)-C(28)	108.8(4)
H(25A)-C(25)-H(25C)	109.5		
H(25B)-C(25)-H(25C)	109.5		
C(28)-C(26)-H(26A)	109.5		
C(28)-C(26)-H(26B)	109.5		
H(26A)-C(26)-H(26B)	109.5		
C(28)-C(26)-H(26C)	109.5		
H(26A)-C(26)-H(26C)	109.5		
H(26B)-C(26)-H(26C)	109.5		
C(28)-C(27)-H(27A)	109.5		

## APPENDIX D

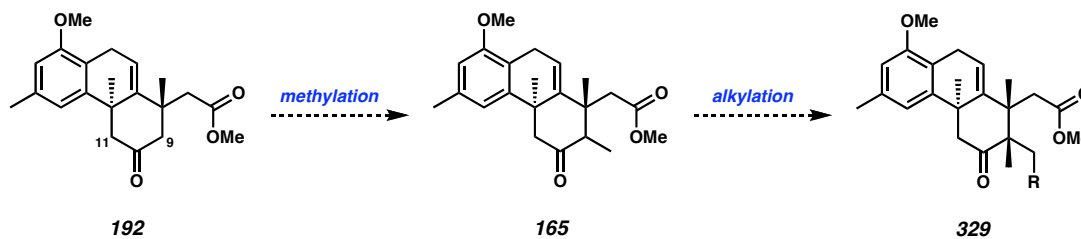
## Current and Future Investigations Toward Zoanthenol

*D.1 Introduction*

In the preceding chapters, we described our attempts to advance C ring synthons containing vicinal quaternary stereocenters toward zoanthenol via acid-mediated cyclization approaches or conjugate radical cyclization approaches. Here, we suggest methods for utilizing intermediates developed in our early work as well as possible avenues for further exploration using our more advanced C ring synthons.

*D.2 Proposed Methods for the Utilization of Tricycle 192*

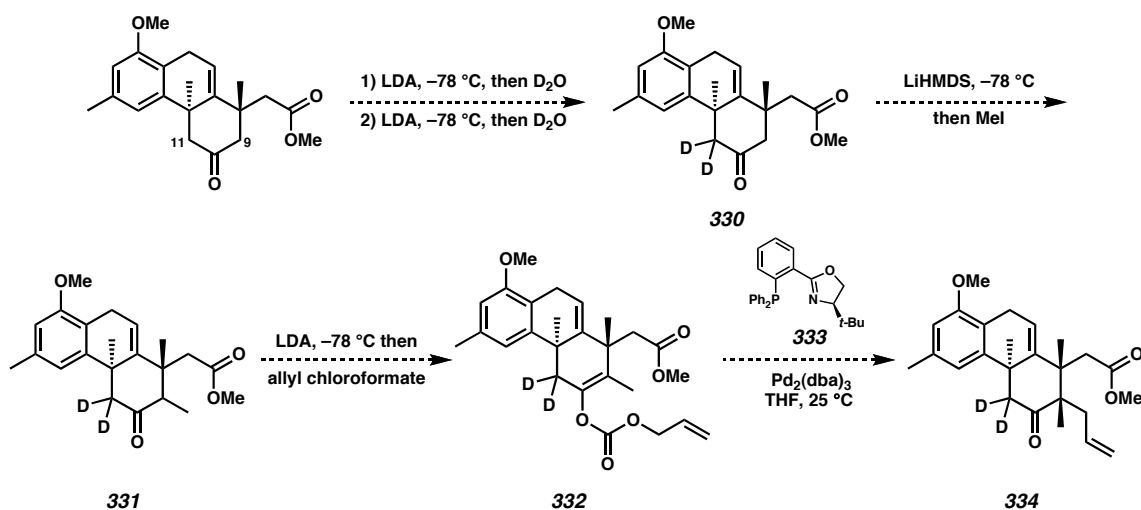
In our early work, we synthesized the key tricycle **192** but were unable to functionalize the C(9) position for further elaboration toward the natural product due to the preference for enolization to occur at C(11) instead of C(9) (Scheme D.2.1).



**Scheme D.2.1** Plan for functionalization of C(9).

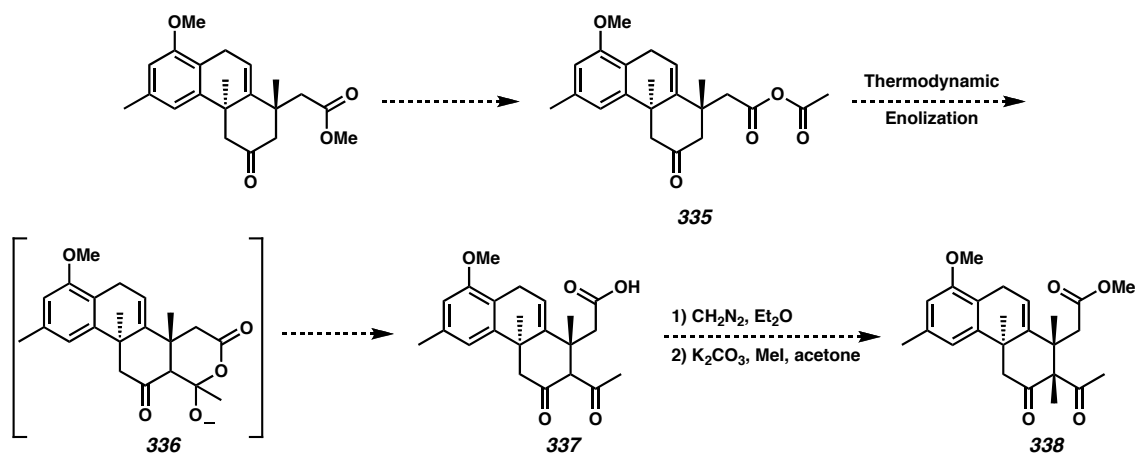
One potential method to overcome this challenge would be to take advantage of the inherent selectivity of the system to deuterate at C(11), allowing selective enolization by deprotonation instead of de-deuteration.<sup>1</sup> Held and Xie have measured the deuterium isotope effect for enolization of 2,2-d<sub>2</sub>-3-pentanone with LDA, LITA, and LiHMDS.<sup>2</sup> They find  $k_{\text{H}}/k_{\text{D}}$  values of 2.3, 5.2, and 6.6, respectively, for these bases. As illustrated in Scheme D.2.2, tricycle **192** will be enolized, resulting in selective deuteration at C(11) upon addition of 1.0 equivalents of D<sub>2</sub>O. A second enolization and quenching with D<sub>2</sub>O

should lead to di-deutero ketone **330**. Treatment with lithium hexamethyldisilazide will result in selective enolization at the desired C(9) position. Trapping this enolate with methyl iodide will furnish methyl ketone **331**. Enolization and trapping with allyl chloroformate will provide allyl enol carbonate **332**. A decarboxylative alkylation event would then provide the desired  $\alpha,\beta,\beta'$ -quaternary ketone **334**. The deuteration at C(11) will be removed upon treatment with aqueous acid.



**Scheme D.2.2** Deuteration to functionalize C(9) by alkylation.

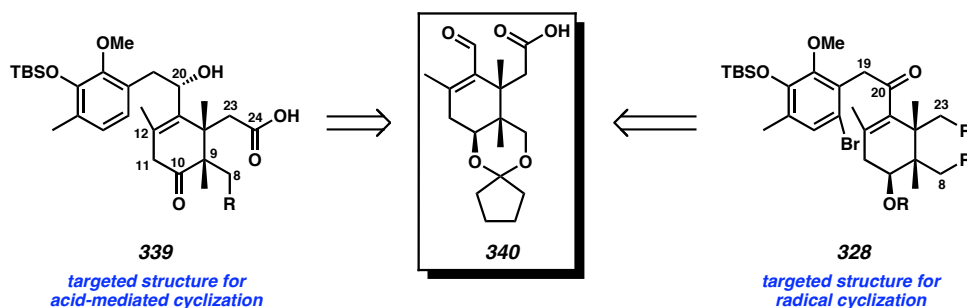
Another possible route by which to advance tricyclic **192** would be via an intramolecular acylation. Conversion of ester **192** to anhydride **335** would provide a substrate for thermodynamic enolization (Scheme D.2.3). By utilizing thermodynamic enolization conditions, an equilibrium between the two enolate isomers should be established. When an enolate is generated at C(9), it can be trapped by the anhydride moiety to provide intermediate **336**, which will ultimately furnish acid **337** as the product of the alkylation. At this point, enolization at the central carbon of the  $\beta$ -diketone **337** will lead to the desired C(9)-quaternary ketone **338**.



**Scheme D.2.3** Thermodynamic deprotonation to functionalize C(9) by acylation.

### D.3.1 Development and Cyclization of a 6-Membered Acetal-Derived A–C Ring System with Inverted C(10) Stereochemistry

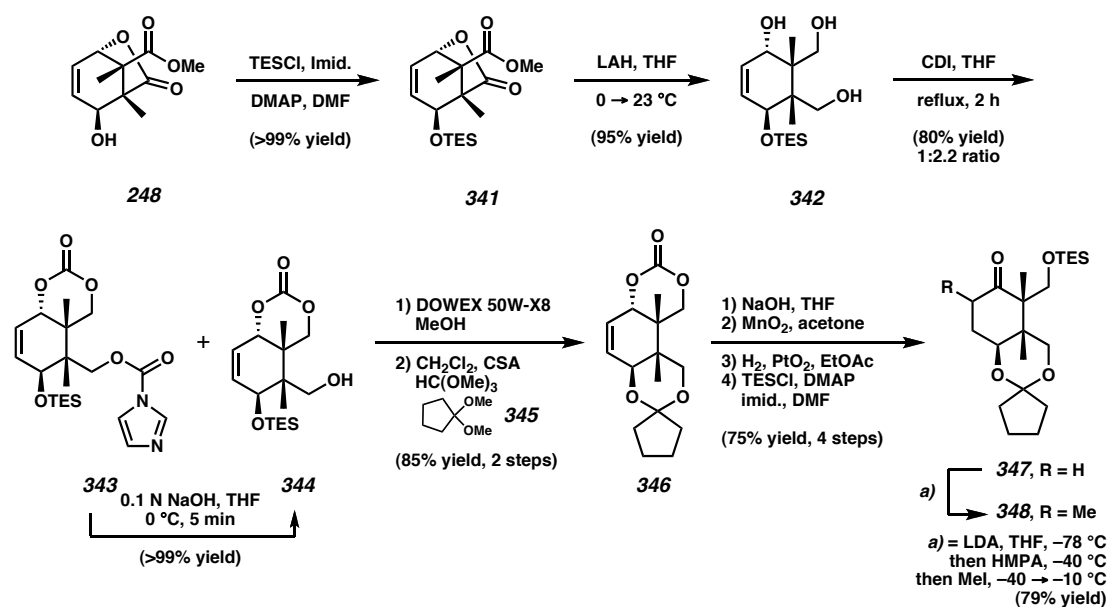
Recent efforts have been focused on the synthesis of new substrates for the acid- and radical-mediated cyclizations (**339** and **328**, respectively, Scheme D.3.1). For these substrates, we needed to develop a final C ring synthon that would allow us to access the structural features described in Chapters 3 and 4.<sup>3</sup> Of particular note is the stereochemistry at C(10) for the radical cyclization substrate (**328**), which is hypothesized to be critical for the stereoselectivity of the cyclization.



**Scheme D.3.1** Common intermediate for acid-mediated and radical cyclizations.

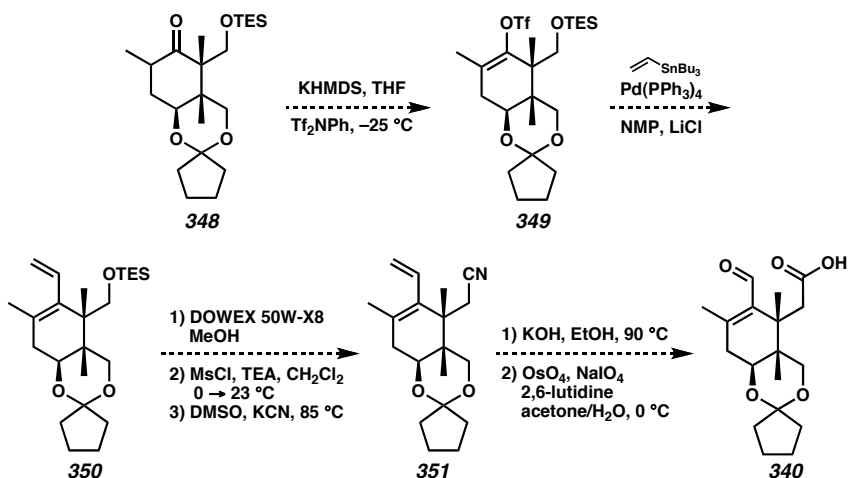
Efforts toward intermediate **340** began with silylation of allylic alcohol **248** to **341** then global reduction to form triol **342** (Scheme D.3.2). For this system, a triethylsilyl group was incorporated at C(10) in order to facilitate its later removal. Triol **342** was

treated with carbonyl diimidazole in refluxing THF to afford a mixture of carbamate **343** and carbonate **344**. Brief exposure of carbamate **343** to dilute sodium hydroxide converted it quantitatively to carbonate **344**. Desilylation with DOWEX resin and cyclopentylidene acetal formation<sup>4</sup> led to tetracycle **346**. The cyclopentylidene acetal was chosen with the goal of improving the efficiency of acetal removal.<sup>3</sup> A four-step sequence of carbonate saponification, allylic oxidation, hydrogenation, and primary alcohol silylation provided ketone **346**. Enolization of ketone **347** and trapping with MeI led to methyl ketone **348** in 79% yield.



**Scheme D.3.2** Toward an optimal C ring synthon.

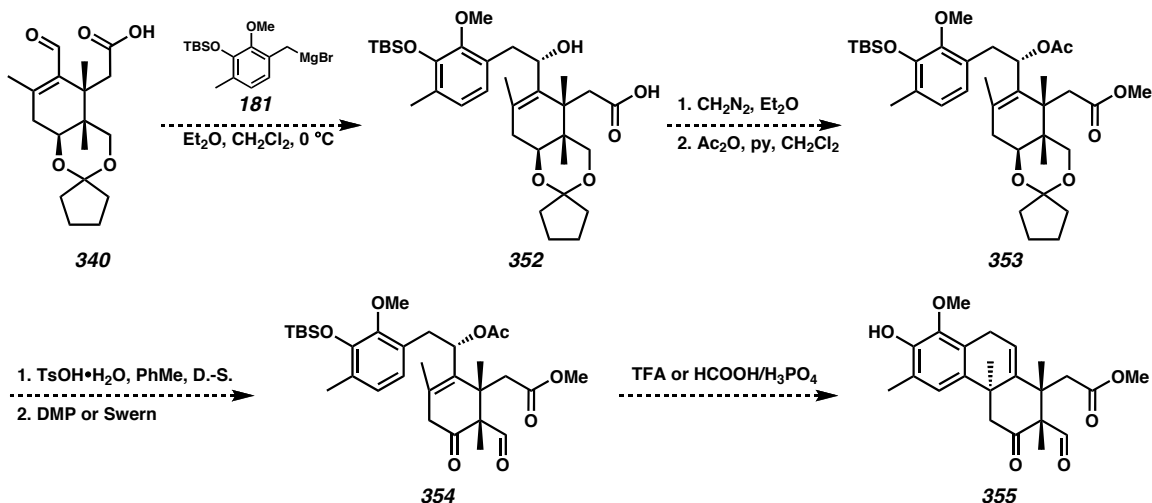
Enolization of **347** with KHMDS and trapping should provide enol triflate **349** (Scheme D.3.3). Stille coupling of enol triflate **349** with vinyl(tributyl)stannane will yield **350**. A three-step sequence of desilylation, mesylation, and nitrile displacement will provide diene **351**. Nitrile hydrolysis and oxidative cleavage should generate C ring synthon **340**.



**Scheme D.3.3** Preparation of a C ring synthon with inverted C(10) stereochemistry.

### D.3.2 Advancement of Cyclopentylidene-Derived C Ring Synthon for Acid-Mediated Cyclization

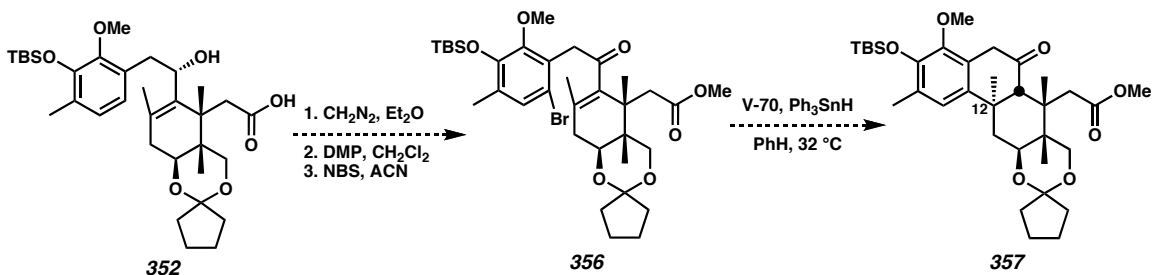
In order to advance this new C ring synthon to the acid-mediated cyclization precursor, we will need to conduct a fragment coupling with the A ring synthon (**168**, Scheme 2.1.1). Treatment of enal **340** with the Grignard reagent formed from **181** will provide alcohol **352** (Scheme D.3.4). Subsequently, treatment with diazomethane followed by acetylation of the secondary alcohol will lead to ester **353**. Acetal removal and oxidation will then produce keto-aldehyde **354**. At this point, cyclization conditions will be tested, yielding tricycle **355**.



**Scheme D.3.4** Acid-mediated cyclization of cyclopentylidene-derived C ring synthon.

### D.3.3 Advancement of Cyclopentylidene-Derived C Ring for Radical Cyclization

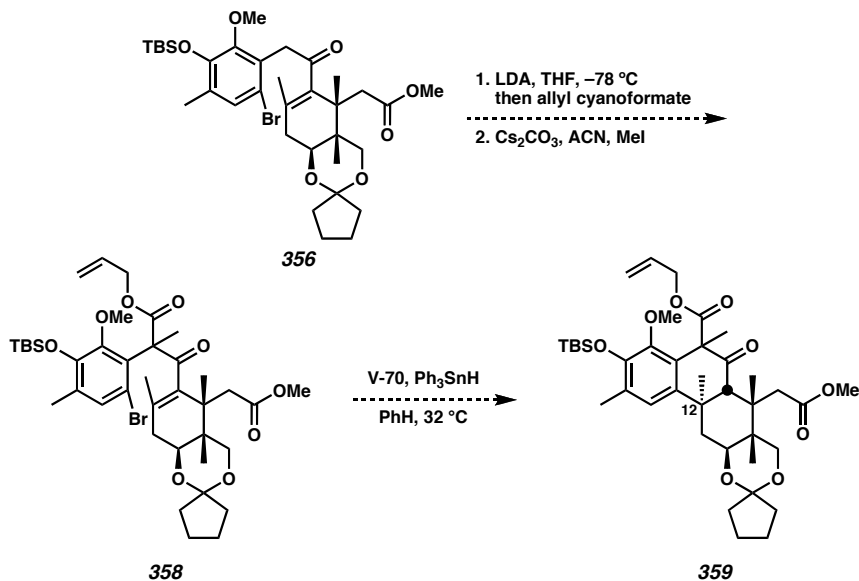
We envision accessing the substrate for radical cyclization beginning from the Grignard product described above. Esterification of **352** followed by oxidation and bromination will yield cyclization precursor **356** (Scheme D.3.5). Treatment with radical conditions should lead to formation of cyclization product **357**, with all three quaternary centers installed in a system readily advanced toward the natural product.



**Scheme D.3.5** Radical cyclization of cyclopentylidene-containing precursor.

Additionally, we propose an alternative radical cyclization substrate that would take advantage of a reactive rotamer<sup>5</sup> variation of the Thorpe-Ingold<sup>6</sup> effect to improve yields of the desired product relative to the debrominated starting material. Scheme D.3.6 outlines a method for functionalization of enone **356**. Enolization and trapping with

allyl cyanofornate followed by methylation will provide cyclization precursor **358**. This precursor will be subjected to the standard radical conditions<sup>7</sup> to determine the effect of substitution at C(19) on the efficacy of the cyclization, which is expected to yield **359**.



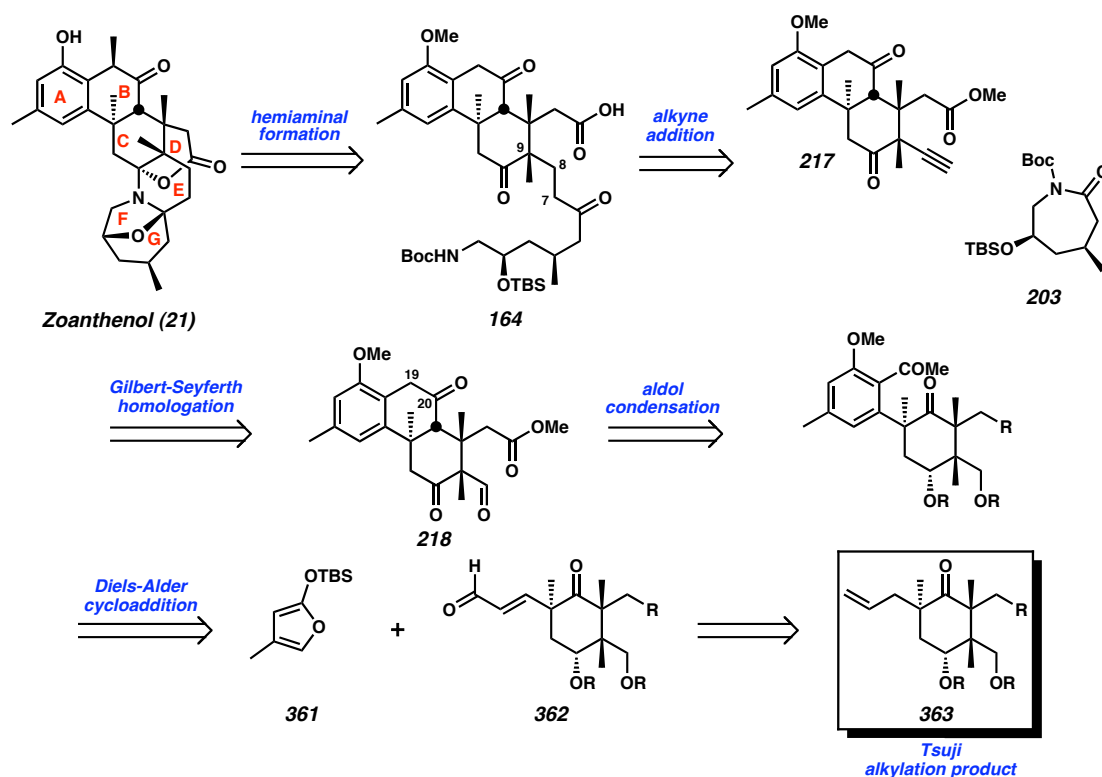
**Scheme D.3.6** Radical cyclization of C(19)-substituted cyclization precursor.

#### D.4.1 Alternative Approaches to the Tricyclic Core of Zoanthenol

In addition to our plans to access a substrate that will allow our acid-mediated and radical-based cyclization reactions to occur, we have begun efforts toward installation of the C(12) quaternary center at an earlier stage in the synthesis. Toward this end, we have identified two potential approaches that might enable this position to be functionalized prior to B ring closure: an alkylation/Diels-Alder/aldol cyclization approach and an  $\alpha$ -arylation/alkylation/aldol cyclization approach.

### D.4.2 Allylation/Diels-Alder Approach

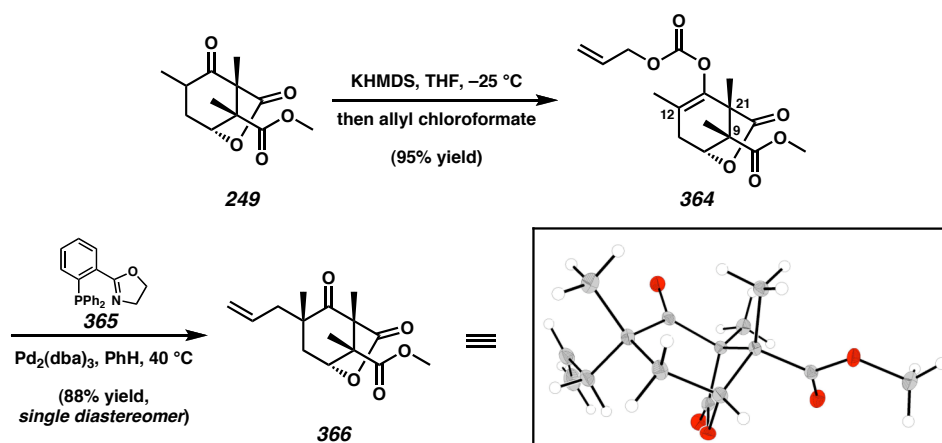
Our first alternative approach disconnects the B ring at the C(19)–C(20) bond of intermediate **218** via retro-aldol condensation to reveal retron **360**, representing a change in strategy wherein the challenging third quaternary center is constructed prior to B ring closure (Scheme D.4.1). The A ring is then disconnected by a retro-Diels-Alder cycloaddition to give synthons **361** and **362**. Enal **362** can be accessed from allyl ketone **363**, the product of a diastereoselective Tsuji alkylation.



**Scheme D.4.1** Revised retrosynthesis for allylation/Diels-Alder approach.

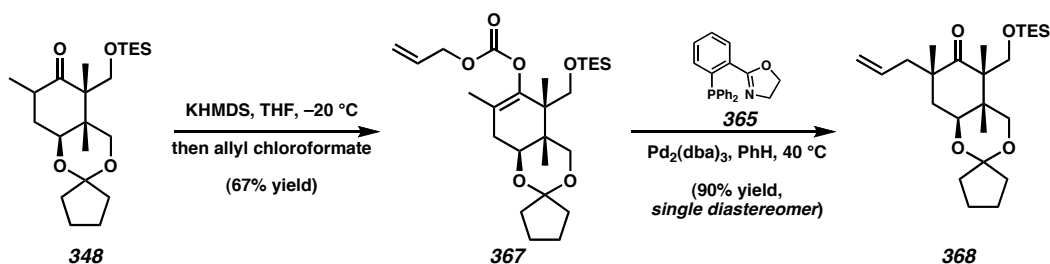
In order to access allyl ketone **363**, intermediate ketone **249** was intercepted. Its potassium enolate was trapped with allyl chloroformate to access allyl enol carbonate in 95% yield (Scheme D.4.2). Subjecting this compound to achiral glycine-derived PHOX ligand **365** led to the formation of a single diastereomer of undesired  $\alpha,\alpha',\beta$ -quaternary ketone **366** in 88% yield. Interestingly treatment with the enantioselective version of the catalyst,<sup>8</sup> utilizing the (*S*)-*t*-butyl PHOX ligand, provided the identical product, but at

an extremely reduced rate. Since this enantiomer of the chiral ligand is expected to provide the desired stereochemistry at C(12), it is clear that substrate control is the exclusive source of selectivity in this transformation. The C(12)–C(21) olefin is blocked on the convex face by the protruding methyl group from the C(9) quaternary center, leading to the observed allyl attack from the  $\alpha$ -face of the substrate. This stereochemistry was confirmed by X-ray crystallographic analysis of a single crystal of **366**.<sup>9</sup>



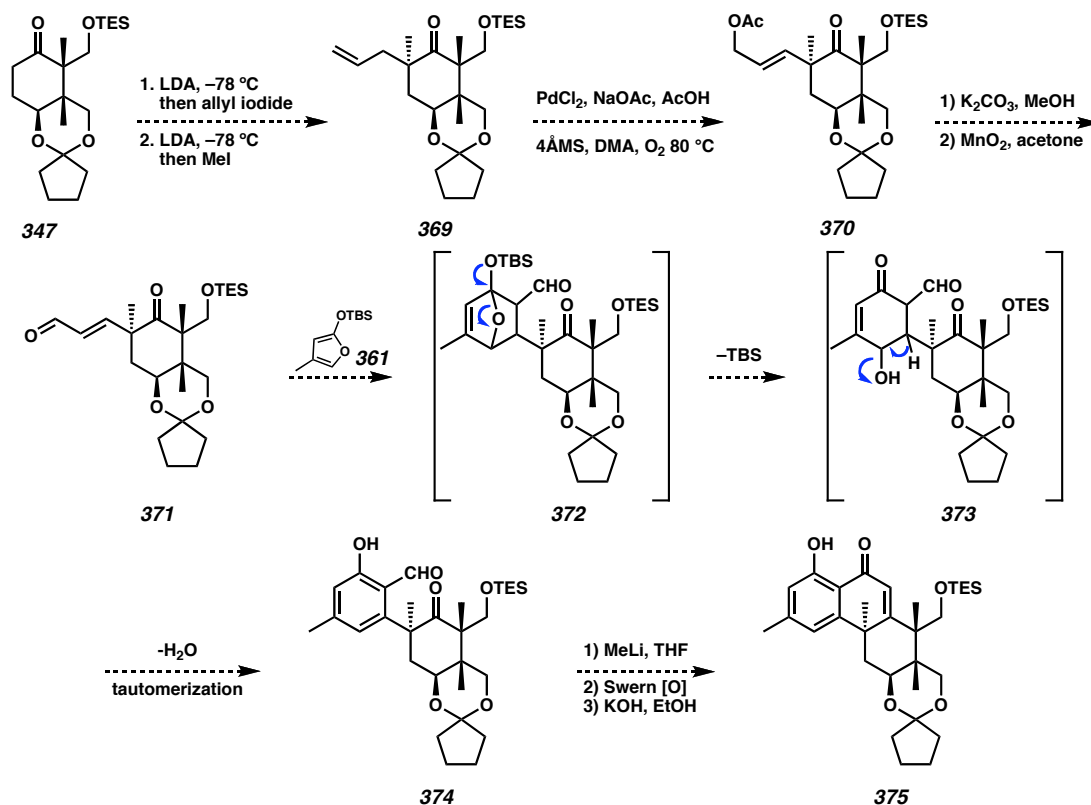
**Scheme D.4.2** Palladium-catalyzed alkylation of lactone **366**.

Given the inability of the catalyst to override the substrate control of the diastereoselectivity for the alkylation of lactone **364**, an alternative substrate possessing a substantially different ring system was targeted. Thus, enolization of methyl ketone **348** and trapping with allyl chloroformate led to allyl enol carbonate **367** (Scheme D.4.3). Treatment with achiral PHOX ligand **365** provided a single diastereomer of alkylation product **368** in 90% yield, as determined by 2D NMR analysis.



**Scheme D.4.3** Alkylation of a cyclopentylidene-containing ketone.

Although the Tsuji alkylation approach resulted in exclusive formation of the undesired diastereomer in the above cases, the desired product should be accessible by reversing the order of the alkylation steps. Thus, ketone **347** may be converted to allyl methyl ketone **369** by alkylation with allyl iodide then methylation (Scheme D.4.4). In analogy to some model systems we have studied, the allyl functionality will be oxidized with allylic transposition to provide **370** using conditions developed by Kaneda.<sup>9,10</sup> Subsequent methanolysis and oxidation will lead to desired enal **371**. With enal **371** in hand, we will begin exploring conditions for a possible Diels-Alder cycloaddition with silyl ether substituted furan **361**. Upon [4+2] cycloaddition, intermediate **372** will be generated. Upon acidic workup, we anticipate that desilylation will occur, forming enone **373**. Further protonation of the secondary alcohol will result in dehydration, and subsequent spontaneous tautomerization will provide the desired zoanthenol A rinD. Addition of methyl lithium into the aldehyde, oxidation to the ketone, and aldol cyclized the B ring to form **375**, the carbocyclic core of zoanthenol.

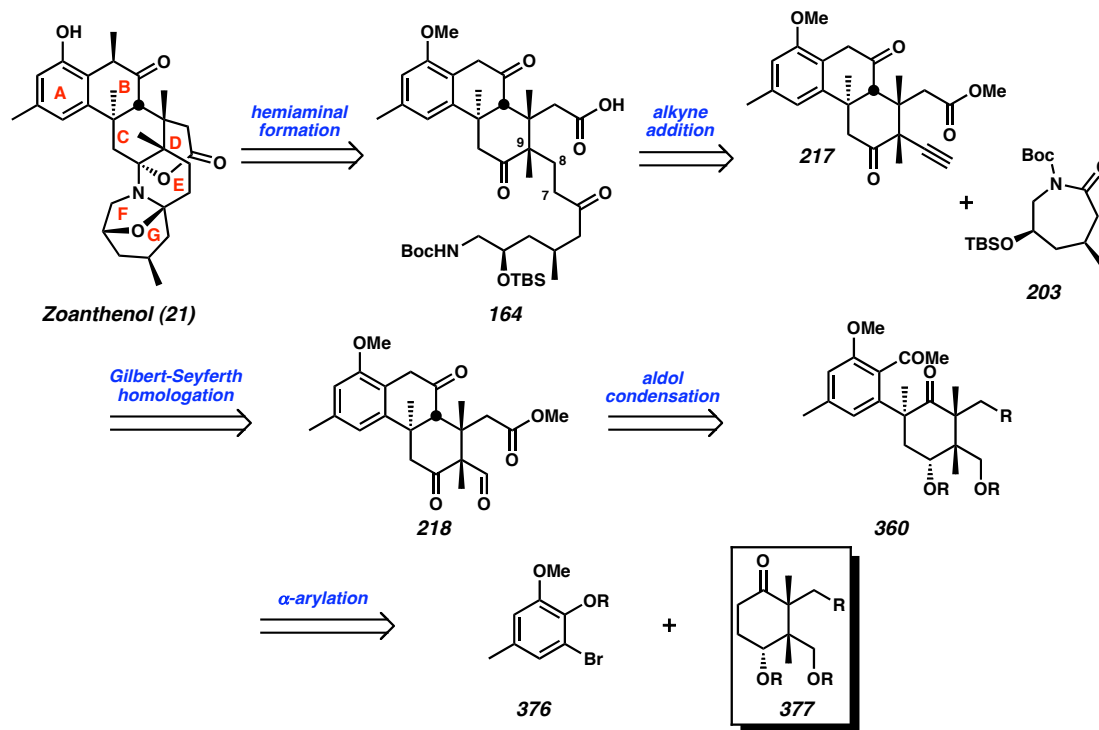


**Scheme D.4.4** Alternative alkylation and advancement of ketone **347**.

#### D.4.3 $\alpha$ -Arylation Approach<sup>†</sup>

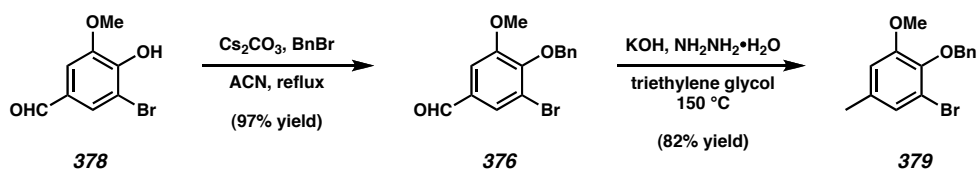
An alternative method by which the C(12) quaternary center might be disconnected involves a retro diastereoselective methylation and  $\alpha$ -arylation<sup>11</sup> of retron **360** to reveal synthons **376** and **377** (Scheme D.4.5).

<sup>†</sup> The work in this subsection was conducted by Dr. Andrew McClory, a postdoctoral researcher in the Stoltz Group.



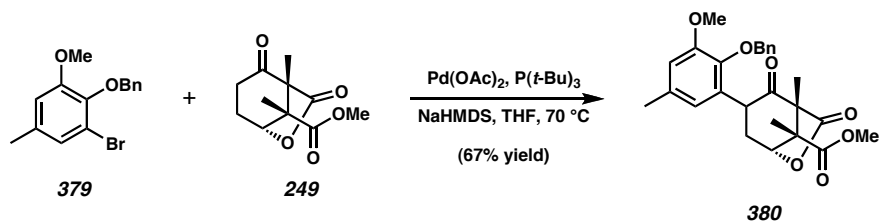
**Scheme D.4.5** Revised retrosynthesis for  $\alpha$ -arylation approach.

In order to investigate the viability of such an approach, a suitable A ring synthon was prepared. Known bromo-phenol **378**<sup>12</sup> was etherified with benzyl bromide to provide aryl bromide **376** (Scheme D.4.6). Wolff-Kischner reduction of the aldehyde then provided A ring synthon **379**.



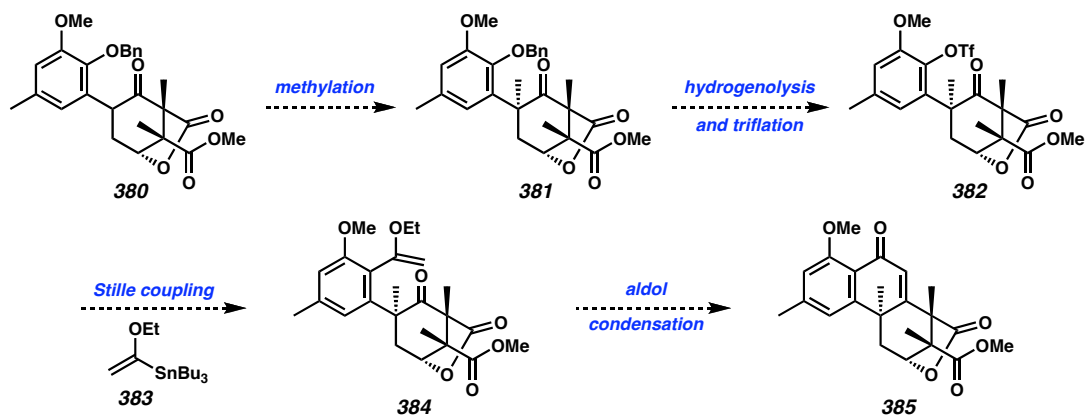
**Scheme D.4.6** Synthesis of aryl bromide **379**

Initial studies show that arylation is a viable method to append the A ring. Treatment of ketone **249** with aryl bromide **379**, Pd(OAc)<sub>2</sub>, P(*t*-Bu)<sub>3</sub>, and NaHMDS in THF at 70 °C provided A–C ring adduct **380** in 67% yield (Scheme D.4.7).



**Scheme D.4.7**  $\alpha$ -Arylation to form A–C ring adduct **380**.

Adduct **380** may be advanced to a tricycle through a number of potential routes. We detail one of these in Scheme D.4.8 below. Efforts to methylate **380** have proved challenging to date.<sup>13</sup> However, careful screening may lead to successful methylation at the C(12) position. Subsequent hydrogenolysis of the benzyl ether and triflation will provide enol triflate **382**. Stille coupling with (1-ethoxyvinyl)tributylstannane (**383**) will provide **384**, which, upon treatment with acidic conditions will undergo global deprotection and aldol condensation under acidic conditions to provide **385**.



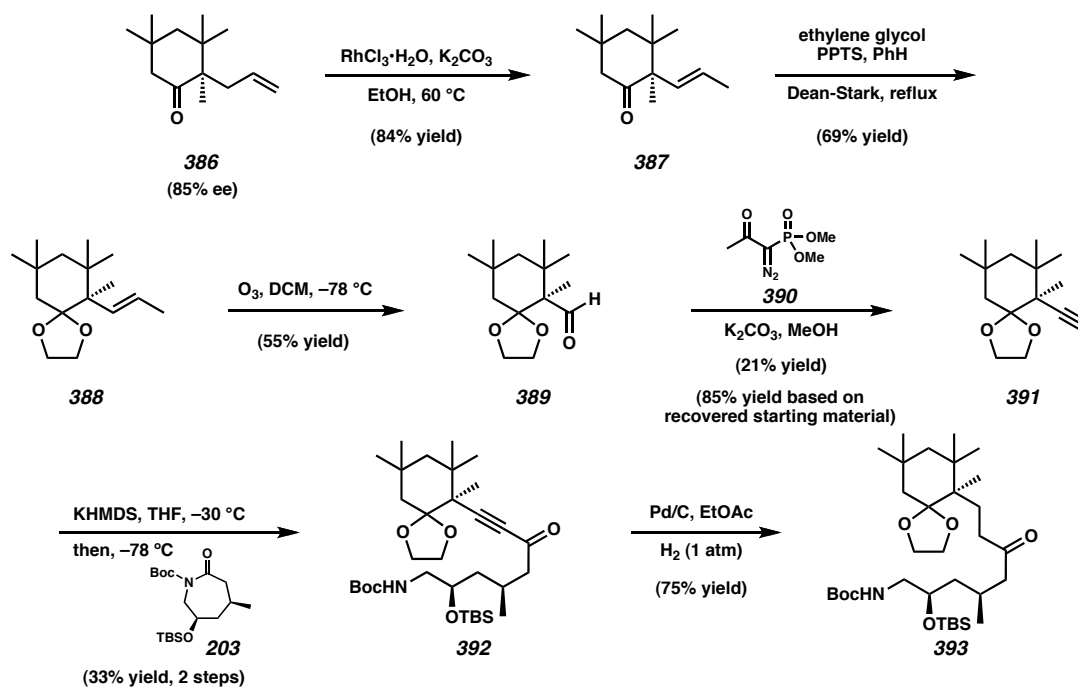
**Scheme D.4.8** B ring closure of  $\alpha$ -arylation product **380**.

### D.5.1 Precedence for Planned Late-Stage Side Chain Couplings

The retrosynthetic approaches outlined for our vicinal quaternary center-containing C ring synthons require a late-stage side chain attachment to an alkyne or aldehyde moiety. Some initial model studies have been conducted to test the viability of each of these routes, and they are outlined below.

### D.5.2 Alkyne Addition into Enantiopure Lactam Synthon

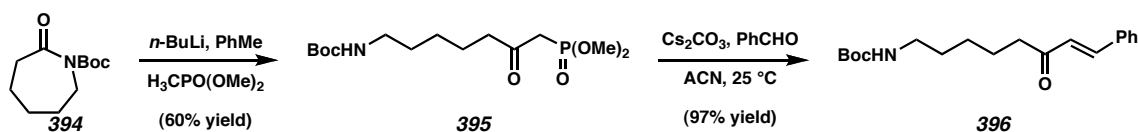
In order to determine the feasibility of an alkyne addition into lactam **203**, alkyne **391** was synthesized from a readily available asymmetric alkylation product (**386**).<sup>8a</sup> Allyl ketone **386** was smoothly isomerized to ketone **387**, which was then ketalized to provide olefin **388** (Scheme D.5.1). Ozonolysis with mild reductive workup allowed access to the desired model aldehyde **389**. Treatment with the Ohira-Bestman reagent (**390**)<sup>14</sup> proceeded sluggishly to afford alkyne **391** along with a substantial amount of recovered starting material. Deprotonation of the alkyne with KHMDS and trapping with caprolactam **203** provided alkynone **392**. Hydrogenation of the alkyne readily provided the final side-chain-appended model product **393**. This sequence of steps functions as a proof of principle that our retrosynthetic plan is viable and will ultimately allow coupling of the side chain. Yields in this section are unoptimized, and it is anticipated that they will be improved before undertaking such a coupling strategy in the fully functionalized system.



**Scheme D.5.1** Side chain functionalization of a model ketone.

### D.5.3 Synthesis of a Horner-Wadsworth-Emmons Reagent for Side Chain Synthesis<sup>†</sup>

In addition to the alkyne coupling strategy, we have recently undertaken investigations toward a Horner-Wadsworth-Emmons coupling strategy that would allow us to use a C(8) aldehyde directly rather than first homologating to an alkyne. Deprotonation of dimethyl methylphosphonate and addition to Boc-protected caprolactam **394** resulted in formation of Horner-Wadsworth-Emmons reagent **395** (Scheme D.5.2). The viability of this reagent in olefinations was tested by treatment with benzaldehyde and cesium carbonate, providing an excellent yield of enone **396**. This approach remains to be tested with fully functionalized lactam **203** or with a more hindered aldehyde such as **389**.



**Scheme D.5.2** Horner-Wadsworth-Emmons coupling strategy.

### D.6.1 Summary

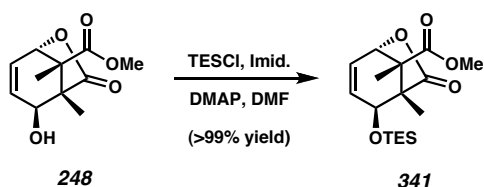
In summary, we have outlined a number of remaining potential approaches to the carbocyclic core of zoanthenol. These strategies include the utilization of early acid-mediated cyclization product **192**, the synthesis of new substrates for vicinal quaternary center-containing systems for acid-mediated and radical cyclization approaches, and finally, the installation of the C(12) quaternary center prior to B-ring formation by alkylation or arylation. Additionally, we have outlined two potential methods for the late-stage coupling of the heterocyclic synthon to the carbocyclic core of zoanthenol.

<sup>†</sup> The work in this subsection was primarily conducted by Dr. Andrew McClory, a postdoctoral researcher in the Stoltz Group.

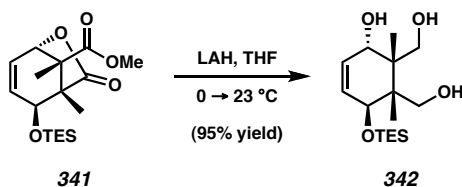
### D.7.1 Materials and Methods

Unless otherwise stated, reactions were performed at ambient temperature (typically 19–24 °C) in flame-dried glassware under an argon or nitrogen atmosphere using dry, deoxygenated solvents. Solvents were dried by passage through an activated alumina column under argon. *N*-Bromosuccinimide was recrystallized before use. TESC1 and TBSC1 were purchased from Gelest. Metal salts were purchased from Strem. All other commercially obtained reagents were purchased from Aldrich or Acros and used as received. Reaction temperatures were controlled by an IKAmag temperature modulator. Thin-layer chromatography (TLC) was performed using E. Merck silica gel 60 F254 precoated plates (0.25 mm) and visualized by UV fluorescence quenching, anisaldehyde, KMnO<sub>4</sub>, or CAM staining. ICN silica gel (particle size 0.032–0.063 mm) was used for flash chromatography. Optical rotations were measured with a Jasco P-1010 polarimeter at 589 nm. <sup>1</sup>H and <sup>13</sup>C NMR spectra were recorded on a Varian Mercury 300 (at 300 MHz and 75 MHz, respectively), or a Varian Inova 500 (at 500 MHz and 125 MHz, respectively) and are reported relative to Me<sub>4</sub>Si (δ 0.0). Data for <sup>1</sup>H NMR spectra are reported as follows: chemical shift (δ ppm) (multiplicity, coupling constant (Hz), integration). Multiplicities are reported as follows: s = singlet, d = doublet, t = triplet, q = quartet, sept. = septet, m = multiplet, comp. m = complex multiplet, app. = apparent, bs = broad singlet. IR spectra were recorded on a Perkin Elmer Paragon 1000 spectrometer and are reported in frequency of absorption (cm<sup>-1</sup>). High-resolution mass spectra were obtained from the Caltech Mass Spectroscopy Facility. Crystallographic analyses were performed at the California Institute of Technology Beckman Institute X-Ray Crystallography Laboratory. Crystallographic data have been deposited at the CCDC, 12 Union Road, Cambridge CB2 1EZ, UK and copies can be obtained on request, free of charge, from the CCDC by quoting the publication citation and the deposition number (see Appendix E for deposition numbers).

## D.7.2 Preparation of Compounds

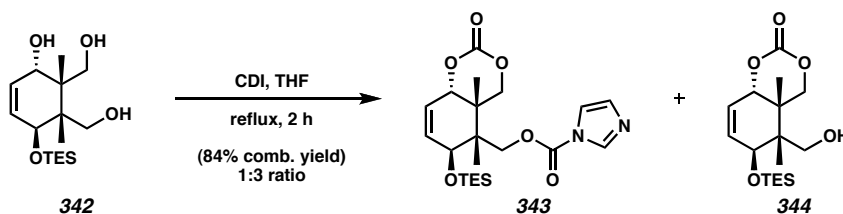


**Silyl ether 341.** To a solution of allylic alcohol **248** (2.078 g, 9.185 mmol, 1.0 equiv) in DMF (4.59 mL, 2.0 M) were added imidazole (1.88 g, 27.56 mmol, 3.0 equiv), DMAP (280.5 mg, 2.296 mmol, 0.25 equiv), and TESCl (2.0 mL, 11.94 mmol, 1.3 equiv). The reaction was stirred at ambient temperature 7h before diluting with EtOAc (500 mL). The solution was washed with sat.  $\text{NH}_4\text{Cl}$  (3 x 150 mL), and the combined aqueous layers were extracted with EtOAc (4 x 150 mL). The combined organics were then dried over  $\text{MgSO}_4$ , concentrated to an oil, and purified by flash chromatography (5 to 10% EtOAc in hexanes) to provide pure lactone **341** (3.121 g, 9.167 mmol, > 99% yield) as an oil.  $R_f$  0.8 (35% EtOAc in hexanes);  $^1\text{H}$  NMR (500 MHz,  $\text{CDCl}_3$ )  $\delta$  6.19 (ddd,  $J = 9.5, 5.9, 1.0$  Hz, 1H), 5.91 (ddd,  $J = 9.3, 3.2, 0.7$  Hz, 1H), 4.78 (dd,  $J = 5.9, 0.7$  Hz, 1H), 4.13 (dd,  $J = 3.4, 1.0$  Hz, 1H), 3.73 (s, 3H), 1.45 (s, 3H) 1.38 (s, 3H), 0.97 (t,  $J = 8.1$  Hz, 9H), 0.63 (q,  $J = 8.1$  Hz, 6H);  $^{13}\text{C}$  NMR (125 MHz,  $\text{CDCl}_3$ )  $\delta$  179.0, 173.8, 135.0, 126.8, 77.3, 70.6, 54.9, 52.5, 51.3, 15.7, 14.5, 6.8, 4.9; IR (Neat film NaCl) 2956, 2878, 1787, 1733, 1255, 1066, 959, 726  $\text{cm}^{-1}$ ; HRMS (FAB+)  $[\text{M}+\text{H}]^+$  calc'd for  $[\text{C}_{17}\text{H}_{28}\text{O}_5+\text{H}]^+$ :  $m/z$  341.1784, found 341.1798.



**Triol 342.** To a cooled (0 °C) solution of LAH (680.7 mg, 17.04 mmol, 4.0 equiv) in THF (40 mL) was added lactone **341** (1.4506 g, 4.26 mmol, 1.0 equiv) in THF (10 mL).

The ice bath was allowed to melt, bringing the solution gradually to ambient temperature and stirred 5 h. The solution was cooled again to 0 °C and slowly quenched with EtOAc until no further bubbles were observed. Celite (1.5 g) was added, and the reaction was further quenched with sat. Na<sub>2</sub>SO<sub>4</sub> (10 mL) in a dropwise manner. The reaction was further diluted with EtOAc (30 mL), allowed to warm to ambient temperature, then filtered through a pad of celite. The pad was rinsed with EtOAc (2 x 25 mL), the combined organics were dried over Na<sub>2</sub>SO<sub>4</sub> and concentrated to an oil (**342**, 1.200 g, 3.791 mmol, 89% yield) of sufficient purity for use in the next reaction. *R<sub>f</sub>* 0.13 (35% EtOAc in hexanes); <sup>1</sup>H NMR (300 MHz, CDCl<sub>3</sub>) δ 5.66 (app. s, 2H), 4.51 (d, *J* = 2.8 Hz, 1H), 4.21 (bs, 1H), 3.91 (d, *J* = 11.4 Hz, 1H), 3.75 (d, *J* = 11.4 Hz, 1H), 3.72 (d, *J* = 11.4 Hz, 1H), 3.53 (d, *J* = 11.4 Hz, 1H), 2.97 (bs, 1H), 2.68 (bs, 1H), 1.16 (s, 3H), 0.97 (t, *J* = 7.9 Hz, 9H), 0.87 (s, 3H), 0.64 (q, *J* = 7.9 Hz, 6H); <sup>13</sup>C NMR (125 MHz, CDCl<sub>3</sub>) δ 131.3, 129.3, 73.8, 69.9, 65.8, 63.7, 46.1, 45.2, 15.9, 13.2, 6.9, 5.2; IR (Neat film NaCl) 3282, 2955, 2915, 2879, 1458, 1078, 1026, 845, 727 cm<sup>-1</sup>; HRMS (ESI) [M+H]<sup>+</sup> calc'd for [C<sub>16</sub>H<sub>32</sub>O<sub>4</sub>Si+H]<sup>+</sup>: *m/z* 317.2148, found 317.2147.

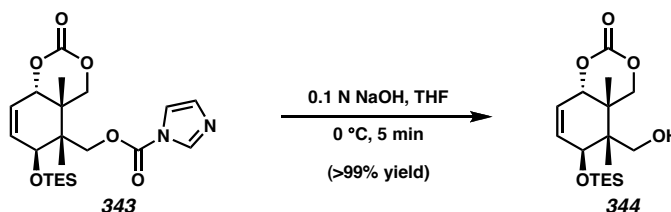


**Carbamate 343 and Alcohol 344.** To a solution of triol **342** (2.449 g, 7.74 mmol, 1.0 equiv) in THF (50 mL, 0.15 M) was added carbonyl diimidazole (2.01 g, 12.38 mmol, 1.6 equiv). The solution was heated to reflux 22 h before cooling to ambient temperature. Silica gel was added to the solution to generate a slurry, and the solvent was removed by careful rotary evaporation. The resulting powder was loaded onto a flash column for

purification (10 to 50% EtOAc in hexanes), providing carbamate **343** (707.2 mg, 21% yield) as a white powder and alcohol **344** (1.664 g, 63% yield) as a white powder.

**Carbamate 343.**  $R_f$  0.18 (35% EtOAc in hexanes);  $^1\text{H NMR}$  (500 MHz,  $\text{CDCl}_3$ )  $\delta$  8.11 (s, 1H), 7.36 (s, 1H), 7.14 (d,  $J = 0.7$  Hz, 1H), 5.89 (dt  $J = 10.5, 2.2$  Hz, 1H), 5.79 (dt,  $J = 10.5, 1.7$  Hz, 1H), 4.75 (ddd,  $J = 4.9, 4.1, 2.0$  Hz, 1H), 4.57 (d,  $J = 10.7$  Hz, 1H), 4.48 (comp. m, 2H), 4.37 (d,  $J = 11.7$  Hz, 1H), 4.22 (dd,  $J = 10.7, 2.0$  Hz, 1H), 1.39 (s, 3H), 1.01 (s, 3H), 0.92 (t,  $J = 8.1$  Hz, 9H), 0.58 (comp. m, 6H);  $^{13}\text{C NMR}$  (125 MHz,  $\text{CDCl}_3$ )  $\delta$  147.9, 147.4, 136.8, 132.0, 131.5, 125.6, 116.7, 81.4, 70.8, 68.1, 66.5, 45.8, 37.6, 16.2, 11.8, 6.7, 4.9; IR (Neat film NaCl) 2956, 2907, 2877, 1755 (br), 1391, 1290, 1241, 1078, 1003, 832, 744  $\text{cm}^{-1}$ ; HRMS (FAB+)  $[\text{M}+\text{H}]^+$  calc'd for  $[\text{C}_{21}\text{H}_{22}\text{O}_6\text{SiN}_2+\text{H}]^+$ :  $m/z$  437.2108, found 437.2104.

**Alcohol 344.**  $R_f$  0.6 (35% EtOAc in hexanes);  $^1\text{H NMR}$  (500 MHz,  $\text{CDCl}_3$ )  $\delta$  5.80 (dt,  $J = 10.5, 2.2$  Hz, 1H), 5.74 (dt,  $J = 10.5, 1.7$  Hz, 1H), 4.68 (ddd,  $J = 4.9, 4.2, 2.0$  Hz, 1H), 4.59 (dd,  $J = 11.2, 2.0$  Hz, 1H), 4.59 (m, 1H), 4.45 (d,  $J = 11.5$  Hz, 1H), 3.66 (d,  $J = 2.2$  Hz, 1H), 1.32 (s, 3H), 0.97 (t,  $J = 7.8$  Hz, 9H), 0.79 (s, 3H), 0.64 (comp. m, 6H);  $^{13}\text{C NMR}$  (125 MHz,  $\text{CDCl}_3$ )  $\delta$  148.5, 133.0, 125.3, 82.0, 71.8, 66.2, 63.6, 47.0, 37.8, 15.6, 11.6, 6.8, 5.0; IR (Neat film NaCl) 3472, 2954, 2915, 2879, 1737, 1713, 1478, 1424, 1370, 1287, 1243, 1199, 1045, 842, 727  $\text{cm}^{-1}$ ; HRMS (FAB+)  $[\text{M}+\text{H}]^+$  calc'd for  $[\text{C}_{17}\text{H}_{30}\text{O}_5\text{Si}+\text{H}]^+$ :  $m/z$  343.1941, found 343.1953.



**Alcohol 344 from carbamate 343.** To a cooled (0 °C) solution of carbamate **344** (942.3 mg, 2.158 mmol, 1.0 equiv) in THF (43 mL, 0.05 M) was added a cooled (0 °C) 0.1

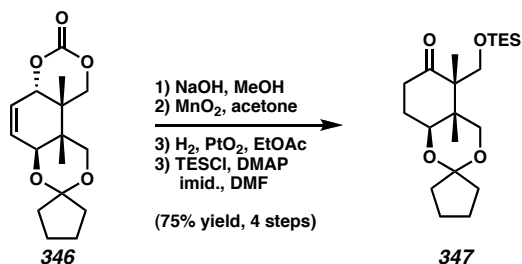
N solution of NaOH (21.58 mL, 2.158 mmol, 1.0 equiv). The reaction was stirred 5 min then quenched by addition of HCl (2.16 mL, 1.0 M) and allowed to warm to ambient temperature. The reaction mixture was diluted with H<sub>2</sub>O (75 mL) and EtOAc (50 mL). The aqueous layer was extracted with EtOAc (4 x 25 mL), then the combined organic layers were washed with brine (75 mL), dried over MgSO<sub>4</sub>, and concentrated to an oil, which was purified by flash chromatography (10 to 50% EtOAc in hexanes) to provide carbonate **343** (741.9 mg, 2.166 mmol, > 99% yield) as a white solid.



**Acetal 346.** To a solution of alcohol **344** (250.6 mg, 0.730 mmol, 1.0 equiv) in MeOH (7.3 mL, 0.1 M) was added DOWEX 50W-X8 resin (270 mg). The suspension was stirred at ambient temperature for 3 h, filtered, concentrated, and redissolved in CH<sub>2</sub>Cl<sub>2</sub> (7.3 mL, 0.1M). Acetal **345**<sup>\*,15</sup> (475 mg, 3.65 mmol, 5 equiv), camphor sulfonic acid (5.1 mg, 0.022 mmol, 0.03 equiv) were added, and the solution was stirred at ambient temperature for 12 h. Additional acetal **345**<sup>\*</sup> (200 mg, 1.54 mmol, 2.1 equiv) was added, and the reaction was stirred an additional 1 h before quenching by dropwise addition of sat NaHCO<sub>3</sub> until no further bubbling was observed. The reaction was diluted with H<sub>2</sub>O (25 mL) and CH<sub>2</sub>Cl<sub>2</sub> (18 mL), the aqueous layer was extracted with CH<sub>2</sub>Cl<sub>2</sub> (3 x 25 mL), dried over MgSO<sub>4</sub>, and concentrated to an oil before purification by flash chromatography (10 to 50% EtOAc in hexanes) to provide acetal **346** (170.6 mg, 0.580 mmol, 79% yield) as an oil. *R<sub>f</sub>* 0.7 (50% acetone in hexanes); <sup>1</sup>H NMR (500 MHz, CDCl<sub>3</sub>)

\* Acetal **345** contained 10 mol% HC(OMe)<sub>3</sub>, as determined by <sup>1</sup>H NMR.

$\delta$  5.84 (dt,  $J = 10.5, 2.4$  Hz, 1H), 5.79 (dt,  $J = 11.7, 1.2$  Hz, 1H), 4.78 (ddd,  $J = 5.4, 4.2, 2.2$  Hz, 1H), 4.48 (d,  $J = 10.5$  Hz, 1H), 4.35 (dd,  $J = 4.4, 2.9$  Hz, 1H), 4.04 (dd,  $J = 10.7, 2.2$  Hz, 1H), 3.72 (d,  $J = 10.7$  Hz, 1H), 3.62 (d,  $J = 10.7$  Hz, 1H), 2.01 (m, 1H), 1.89 (m, 1H), 1.8–1.61 (comp. m, 4H), 1.23 (s, 3H), 1.21 (app. d,  $J = 0.5$  Hz, 3H);  $^{13}\text{C}$  NMR (125 MHz,  $\text{CDCl}_3$ )  $\delta$  148.2, 130.5, 125.7, 111.9, 83.0, 71.5, 69.3, 66.3, 40.4, 39.9, 36.4, 30.9, 24.3, 22.5, 15.1, 12.4; IR (Neat film NaCl) 2961, 2873, 1756, 1185, 1122, 1084  $\text{cm}^{-1}$ ; HRMS (FAB+)  $[\text{M}+\text{H}]^+$  calc'd for  $[\text{C}_{16}\text{H}_{22}\text{O}_5+\text{H}]^+$ :  $m/z$  295.1545, found 295.1533.



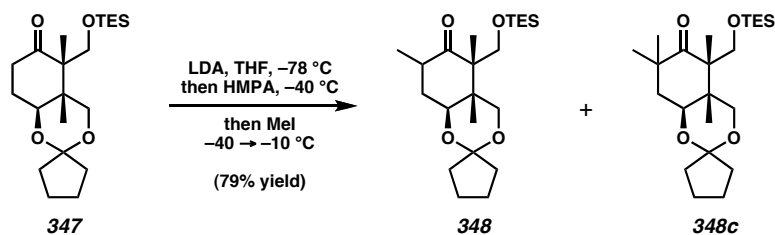
**Ketone 347.** To a solution of carbonate **346** (1.214 g, 4.123 mmol, 1.0 equiv) in MeOH (65 mL, 0.06 M) was added 0.2 M NaOH (41 mL, 8.25 mmol, 2.0 equiv), and the solution was stirred at ambient temperature 70 min. The MeOH was removed by rotary evaporation, and the resulting solution was brought to pH 7 by addition of solid  $\text{NH}_4\text{Cl}$ , diluted with EtOAc (50 mL), and the aqueous layer was extracted with EtOAc (3 x 50 mL). The combined organics were dried over  $\text{MgSO}_4$  and concentrated.

The crude diol was redissolved in acetone (137 mL, 0.03 M),  $\text{MnO}_2$  (12.65 g, 123.7 mmol, 30 equiv) was added, and the resulting suspension was stirred 2.5 h, filtered through #2 Whatman paper, and concentrated to an oil.

The crude enone was dissolved in EtOAc (260 mL, 0.016 M),  $\text{PtO}_2$  (93.6 mg, 0.412 mmol, 0.1 equiv) was added, and the suspension was sparged with  $\text{H}_2$  until it turned from brown to black. The reaction mixture was then stirred under  $\text{H}_2$  (1 atm) 10.5 h,

filtered through #2 Whatman paper, and concentrated to an oil, which was carried on without further purification.

The primary alcohol was then dissolved in DMF (3 mL, 1 M) and DMAP (365.3 mg, 2.99 mmol, 1.0 equiv), imidazole (610.7 mg, 8.97 mmol, 3.0 equiv), and TESCl (653.1  $\mu$ L, 3.89 mmol, 1.3 equiv) were added. The mixture was stirred at ambient temperature for 17 h, then additional TESCl (300  $\mu$ L, 1.79 mmol, 0.6 equiv) was added. The reaction was stirred an additional 3 h then diluted with sat.  $\text{NH}_4\text{Cl}$  (100 mL) and extracted with EtOAc (5 x 25 mL). The combined organics were washed with brine (25 mL), dried over  $\text{MgSO}_4$ , and concentrated to an oil. The crude product was purified by flash chromatography (10 to 40% EtOAc in hexanes) to provide silyl ether **347** (863 mg, 3.081 mmol, 75% yield over 4 steps) as an oil.  $R_f$  0.56 (25% acetone in hexanes);  $^1\text{H}$  NMR (300 MHz,  $\text{CDCl}_3$ )  $\delta$  4.67 (dd,  $J = 11.7, 5.0$  Hz, 1H), 4.02 (d,  $J = 10.8$  Hz, 1H), 3.91 (d,  $J = 10.0$  Hz, 1H), 3.52 (d,  $J = 10.8$  Hz, 1H), 3.51 (d,  $J = 10.0$  Hz, 1H), 2.59 (m, 1H), 2.44 (ddd,  $J = 14.9, 5.0, 1.8$  Hz, 1H), 2.08–1.61 (m, 10H), 1.03 (s, 3H), 0.94 (t,  $H$  8.2 Hz, 9H), 0.93 (s, 3H), 0.59 (app. dd,  $J = 15.8, 7.6$  Hz, 6H);  $^{13}\text{C}$  NMR (125 MHz,  $\text{CDCl}_3$ )  $\delta$  211.7, 110.8, 70.5, 68.0, 66.3, 55.5, 40.2, 39.9, 38.2, 31.0, 27.3, 24.3 22.5, 14.8, 14.0, 6.7, 4.2; IR (Neat film NaCl) 2956, 2879, 1721, 1336, 1118, 1084, 1008, 977, 813, 747  $\text{cm}^{-1}$ ; HRMS (FAB+)  $[\text{M}]^+$  calc'd for  $[\text{C}_{21}\text{H}_{38}\text{O}_4\text{Si}]^+$ :  $m/z$  382.2539, found 382.2543.



**Methyl ketone 348.** To a solution of DIPA (97.6  $\mu$ L, 0.696 mmol, 1.3 equiv) in THF (5.0 mL, 0.1 M to *n*-BuLi) at  $0\text{ }^\circ\text{C}$  was added *n*-butyllithium (245  $\mu$ L, 2.16 M, 0.530 mmol, 0.99 equiv) dropwise. The solution was stirred at  $0\text{ }^\circ\text{C}$  30 min, then cooled to  $-78$

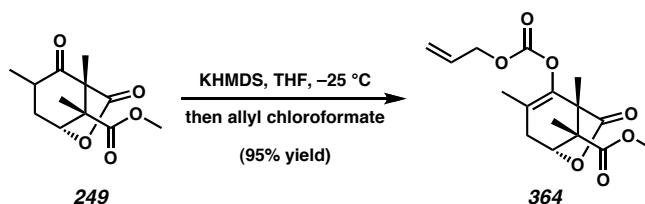
°C. Ketone **347** (204.9 mg, 0.5355 mmol, 1.0 equiv) was added as a solution in THF (5.5 mL, 0.1 M) dropwise, then stirred at  $-78$  °C 2 h. HMPA (279.5  $\mu$ L, 1.607 mmol, 3.0 equiv) was added and stirred 20 min. The solution was then warmed to  $-40$  °C and MeI (667  $\mu$ L, 10.71 mmol, 20 equiv) was added all at once. The reaction was stirred an additional 90 min, while slowly warming to  $-10$  °C, then was quenched with H<sub>2</sub>O (1 mL) and allowed to come to ambient temperature. Brine (25 mL) was added, and the mixture was extracted with EtOAc (5 x 20 mL), dried over MgSO<sub>4</sub>, concentrated to an oil, and purified by flash chromatography (0 to 10% Et<sub>2</sub>O in hexanes, slow gradient) to provide a mixture of partially separable methyl ketones **348** (168.6 mg, 0.425 mmol, 79% yield) as well as a small amount of bis-methylated ketone **348c**. (Use of  $> 0.99$  equiv *n*-BuLi resulted in significant formation of this undesired product.)

**Methyl ketone 348a.** (high *R<sub>f</sub>* diastereomer) *R<sub>f</sub>* 0.39 (20% Et<sub>2</sub>O in hexanes); <sup>1</sup>H NMR (500 MHz, CDCl<sub>3</sub>)  $\delta$  4.65 (dd, *J* = 12.0, 4.6 Hz, 1H), 3.97 (d, *J* = 11.0 Hz, 1H), 3.96 (d, *J* = 10.0 Hz, 1H), 3.52 (d, *J* = 10.0 Hz, 1H), 3.51 (d, *J* = 10.7 Hz, 1H), 2.68 (m, 1H), 2.06–1.97 (comp. m, 2H), 1.94–1.81 (comp. m, 3H), 1.77–1.61 (comp. m, 5H), 1.05 (d, *J* = 6.3 Hz, 3H), 0.97 (s, 3H), 0.93 (t, *J* = 7.8 Hz, 9H), 0.57 (comp. m, 6H); <sup>13</sup>C NMR (125 MHz, CDCl<sub>3</sub>)  $\delta$  212.2, 110.8, 70.4, 68.1, 66.0, 55.4, 40.89, 40.87, 39.9, 36.3, 31.0, 24.3, 22.5, 14.8, 14.6, 14.2, 6.7, 4.2; IR (Neat film NaCl) 2956, 2876, 1718, 1458, 1335, 1109, 1084, 1003, 816, 745 cm<sup>-1</sup>; HRMS (FAB+) [M]<sup>+</sup> calc'd for [C<sub>22</sub>H<sub>40</sub>O<sub>4</sub>Si]: *m/z* 396.2696, found 396.2690.

**Methyl ketone 348b.** (low *R<sub>f</sub>* diastereomer) *R<sub>f</sub>* 0.30 (20% Et<sub>2</sub>O in hexanes); <sup>1</sup>H NMR (500 MHz, CDCl<sub>3</sub>)  $\delta$  4.61 (dd, *J* = 11.5, 5.9 Hz, 1H), 4.07 (d, *J* = 11.0 Hz, 1H), 3.67 (d, *J* = 10.0 Hz, 1H), 3.57 (d, *J* = 10.0 Hz, 1H), 3.43 (d, *J* = 10.7 Hz, 1H), 2.64 (m, 1H), 2.00–1.85 (comp. m, 3H), 1.80 (t, *J* = 7.1 Hz, 1H), 1.68–1.54 (comp. m., 5H), 1.13 (d, *J* = 7.6 Hz, 1H), 1.09 (s, 3H), 0.88 (t, *J* = 7.8 Hz, 9 H), 0.85 (s, 3H), 0.53 (q, *J* = 7.8 Hz, 6H); <sup>13</sup>C NMR (125 MHz, CDCl<sub>3</sub>)  $\delta$  216.1, 110.6, 68.4, 68.0, 67.0, 54.7, 41.1, 40.0, 39.0, 33.2, 31.2, 24.2,

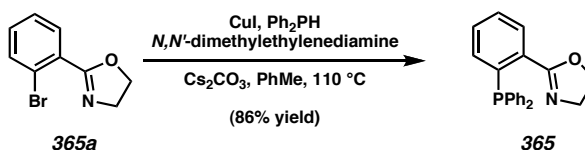
22.6, 18.7, 16.6, 15.8, 6.8, 4.1; IR (Neat film NaCl) 2955, 2979, 1706, 1456, 1336, 1114, 1083, 1006, 812, 745  $\text{cm}^{-1}$ ; HRMS (FAB+)  $[\text{M}]^+$  calc'd for  $[\text{C}_{22}\text{H}_{40}\text{O}_4\text{Si}]$ :  $m/z$  396.2696, found 396.2681.

**Bis-methyl ketone 348c.**  $R_f$  0.47 (20%  $\text{Et}_2\text{O}$  in hexanes);  $^1\text{H}$  NMR (300 MHz,  $\text{CDCl}_3$ )  $\delta$  4.70 (dd,  $J = 5.0, 4.7$  Hz, 1H), 4.74 (d,  $J = 11.1$  Hz, 1H), 3.66 (app. dd,  $J = 12.3, 10.0$  Hz, 2H), 3.49 (d,  $J = 11.1$  Hz, 1H), 2.00 (comp. m, 2H), 1.86 (comp. m, 2H), 1.77–1.62 (comp. m, 6H), 1.55 (s, 3H), 1.20 (s, 3H), 1.05 (s, 3H), 0.943 (t,  $J = 8.2$  Hz, 9H), 0.59 (q,  $J = 7.9$  Hz, 6H);  $^{13}\text{C}$  NMR (125 MHz,  $\text{CDCl}_3$ )  $\delta$  217.5, 110.6, 68.2, 67.9, 67.4, 55.8, 44.3, 40.7, 40.1, 39.4, 31.1, 28.5, 27.9, 24.3, 22.6, 16.5, 16.1, 6.8, 4.1; IR (Neat film NaCl) 2956, 2876, 1696, 1461, 1335, 1117, 1084, 1016, 815, 745  $\text{cm}^{-1}$ ; HRMS (FAB+)  $[\text{M}]^+$  calc'd for  $[\text{C}_{23}\text{H}_{42}\text{O}_4\text{Si}]$ :  $m/z$  410.2852, found 410.2870.



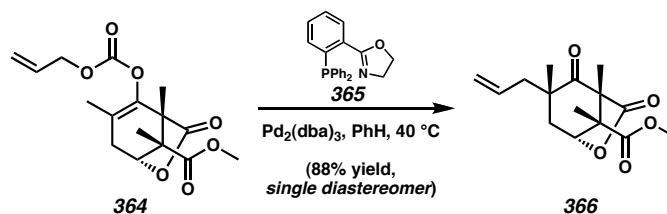
**Allyl methyl ketone 364.** To a solution of KHMDS (546.1 mg, 2.737 mmol, 1.3 equiv) in THF (27 mL, 0.1 M) at  $-25$   $^\circ\text{C}$  was added a solution of ketone **249** (505.9 mg, 2.106 mmol, 1.0 equiv) in THF (20 mL + 2 x 0.5 mL rinse). The solution was stirred at  $-25$   $^\circ\text{C}$  for 2 h then allyl chloroformate (314.6  $\mu\text{L}$ , 2.948 mmol, 1.4 equiv) was added and stirred at  $-20$   $^\circ\text{C}$  an additional 1 h. The reaction was quenched with sat.  $\text{NaHCO}_3$  (25 mL) and allowed to warm to ambient temperature. Further dilution with  $\text{H}_2\text{O}$  (25 mL) was followed by extraction with  $\text{EtOAc}$  (50, 3 x 20 mL). The combined organics were washed with brine (25 mL), dried over  $\text{MgSO}_4$ , and concentrated to an oil, which was purified by flash chromatography (25 to 55%  $\text{EtOAc}$  in hexanes) to provide allyl enol carbonate **364** (646.8 mg, 1.994 mmol, 95% yield) as a clear oil.  $R_f$  0.50 (50%  $\text{EtOAc}$  in hexanes);  $^1\text{H}$

NMR (500 MHz, CDCl<sub>3</sub>) δ 5.93 (dddd,  $J = 17.1, 10.5, 5.9, 5.6$  Hz, 1H), 5.39 (ddd,  $J = 17.1, 2.7, 1.5$  Hz, 1H), 5.30 (ddd,  $J = 10.5, 2.4, 1.2$  Hz, 1H), 4.67 (ddd,  $J = 4.6, 2.2, 1.0$  Hz, 1H), 4.58 (app. t,  $J = 2.7$  Hz, 1H), 3.73 (s, 3H), 2.44 (app. t,  $J = 1.22$  Hz, 1H), 1.61 (s, 3H), 1.37 (s, 3H), 1.29 (s, 3H); <sup>13</sup>C NMR (125 MHz, CDCl<sub>3</sub>) δ 175.1, 172.8, 152.8, 138.7, 130.9, 122.1, 119.4, 77.7, 69.3, 54.4, 52.7, 50.1, 33.7, 15.3, 12.7, 8.9; IR (Neat film NaCl) 2989, 2953, 1790, 1761, 1732, 1454, 1252, 1225, 1200, 1159, 1075, 1033, 976, 782 cm<sup>-1</sup>; HRMS (FAB+) [M+H]<sup>+</sup> calc'd for [C<sub>16</sub>H<sub>20</sub>O<sub>7</sub>+H]<sup>+</sup>:  $m/z$  325.1287, found 325.1272.



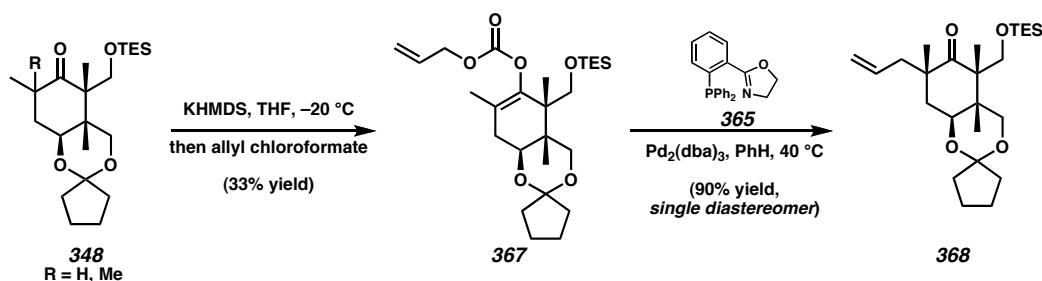
**Phosphine 365:** A 250-mL Schlenk flask was charged with CuI (66.7 mg, 0.35 mmol), Ph<sub>2</sub>PH (4.12g, 3.85 mL, 22.1 mmol) and then *N,N'*-dimethylethylenediamine (156 mg, 191 μL, 1.77 mmol) followed by toluene (18 mL). The solution was stirred at 23 °C for 20 min. Oxazole **365a** (4.0 g, 17.7 mmol) was azeotroped with toluene (2 x 5 mL) under reduced pressure, then dissolved in toluene (18 mL) and transferred quantitatively to the Schlenk flask by use of positive pressure cannulation. Cs<sub>2</sub>CO<sub>3</sub> (8.65 g, 26.5 mmol) was added in one portion, and the flask was evacuated and backfilled with Ar (x 3). The Teflon valve was sealed and the yellow heterogenous reaction mixture was placed in an oil bath, heated to 110 °C, and stirred vigorously. After 20 h stirring at 110 °C, the mixture was allowed to cool to ambient temperature and filtered through a pad of celite using CH<sub>2</sub>Cl<sub>2</sub> (2 x 50 mL). The filtrate was concentrated under reduced pressure to afford a clear orange oil. The crude oil was flushed through a plug of silica gel (5.0 x 10 cm SiO<sub>2</sub>, hexanes → 10% Et<sub>2</sub>O in CH<sub>2</sub>Cl<sub>2</sub>) to afford **365** (5.03 g, 86% yield) as a colorless viscous oil that crystallized upon standing;  $R_f = 0.50$  (30% EtOAc in hexanes); <sup>31</sup>P NMR (121 MHz, CDCl<sub>3</sub>) δ -3.99 (s); <sup>1</sup>H NMR (500 MHz, CDCl<sub>3</sub>) δ 7.85 (dd,  $J = 7.6, 3.4$  Hz, 1H),

7.37–7.26 (comp. m, 12H), 6.89 (dd,  $J = 7.6, 4.1$  Hz, 1H), 4.08 (t,  $J = 9.5$  Hz, 2H), 3.78 (t,  $J = 9.5$  Hz, 2H);  $^{13}\text{C}$  NMR (125 MHz,  $\text{CDCl}_3$ )  $\delta$  164.5 (d,  $J_{\text{CP}} = 2.8$  Hz), 139.1 (d,  $J_{\text{CP}} = 24.9$  Hz), 138.0 (d,  $J_{\text{CP}} = 11.5$  Hz), 134.1 (d,  $J_{\text{CP}} = 20.7$  Hz), 133.7 (d,  $J_{\text{CP}} = 1.8$  Hz), 131.9 (d,  $J_{\text{CP}} = 18.9$  Hz), 130.5, 129.9 (d,  $J_{\text{CP}} = 2.8$  Hz), 128.7, 128.5 (d,  $J_{\text{CP}} = 7.4$  Hz), 128.1, 67.2, 55.0; IR (Neat Film NaCl) 3053, 3000, 2971, 2901, 2876, 1650, 1585, 1562, 1478, 1434, 1354, 1326, 1248, 1133, 1089, 1070, 1041, 974, 942, 898, 743  $\text{cm}^{-1}$ ; HRMS (FAB+)  $[\text{M}]^+$   $m/z$  calc'd for  $[\text{C}_{21}\text{H}_{19}\text{NOP}]^+$ : 332.1204, found 332.1218; mp = 99–101 °C.



**Allyl methyl ketone 366.** To a 50-mL round-bottomed flask in the glovebox was added  $\text{Pd}_2(\text{dba})_3$  (35.3 mg, 0.0385 mmol, 0.05 equiv) and PHOX ligand<sup>16</sup> **365** (56.2 mg, 0.1696 mmol, 0.22 equiv). The flask was removed from the glovebox, purged for 5 min under vacuum and refilled with  $\text{N}_2$  (3x). Benzene (25.7 mL, 0.03 M, sparged with argon 30 min) was added via cannula, and the pre-catalyst mixture was heated to 40 °C for 30 min (a color change from red to orange was observed). A solution of allyl enol carbonate **364** (250 mg, 0.7708 mmol, 1.0 equiv) in benzene (1 mL, sparged with argon 5 min) was transferred via cannula to the catalyst solution (a color change from orange to green was observed after 5 min). The reaction was stirred at 40 °C for 4 h then cooled to ambient temperature. The reaction mixture was concentrated then loaded directly onto a flash column and purified (10 to 40% EtOAc in hexanes), yielding allyl methyl ketone **366** (191 mg, 0.681 mmol, 88% yield) as a white solid. m.p. 77–78 °C;  $R_f$  0.62 (50% EtOAc in hexanes);  $^1\text{H}$  NMR (500 MHz,  $\text{CDCl}_3$ )  $\delta$  5.60 (dddd,  $J = 16.8, 10.2, 7.8, 7.0$  Hz, 1H), 5.12 (dd,  $J = 11.0, 0.7$  Hz, 1H), 5.06 (dd,  $J = 16.8, 1.22$  Hz, 1H), 4.90 (dd,  $J = 3.7, 2.0$  Hz, 1H),

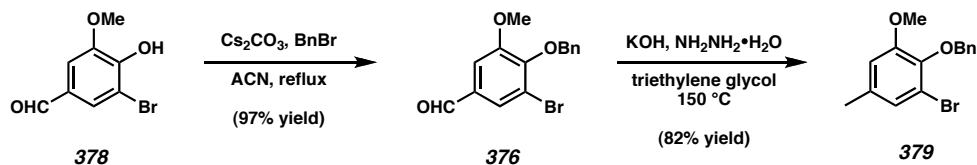
3.76 (s, 3H), 2.46 (dd,  $J = 15.4, 3.7$  Hz, 1H), 2.33 (dd,  $J = 14.2, 7.1$  Hz, 1H), 2.22 (dd,  $J = 13.9, 7.8$  Hz, 1H), 1.77 (dd,  $J = 15.4, 2.0$  Hz, 1H), 1.28 (s, 3H), 1.19 (app. s, 6H);  $^{13}\text{C}$  NMR (125 MHz,  $\text{CDCl}_3$ )  $\delta$  204.0, 173.2, 171.6, 131.8, 120.1, 80.4, 61.7, 57.4, 53.0, 47.4, 46.7, 36.5, 24.5, 15.0, 10.3; IR (Neat film NaCl) 3079, 2985, 2954, 1789, 1732, 1715, 1640, 1440, 1342, 1261, 1228, 1157, 1094, 976  $\text{cm}^{-1}$ ; HRMS (FAB+)  $[\text{M}+\text{H}]^+$  calc'd for  $[\text{C}_{15}\text{H}_{20}\text{O}_5+\text{H}]^+$ :  $m/z$  281.1389, found 281.1376. Stereochemistry assigned via X-ray crystallographic analysis.



**Allyl methyl ketone 368.** To a solution of KHMDS (33.2 mg, 0.1665 mmol, 1.3 equiv) in THF (2.0 mL, 0.08 M) at  $-20\text{ }^\circ\text{C}$  was added a solution of ketone **348**\* (50.8 mg, 0.1281 mmol, 1.0 equiv) in THF (1 mL + 2 x 0.5 mL rinse). The solution was stirred at  $-20\text{ }^\circ\text{C}$  2 h then allyl chloroformate (19.1  $\mu\text{L}$ , 0.1793 mmol, 1.4 equiv) was added and stirred an additional 1.5 h. The reaction was quenched with  $\text{H}_2\text{O}$  (1 mL), diluted with EtOAc (1 mL) and allowed to warm to ambient temperature. Further dilution with  $\text{H}_2\text{O}$  (20 mL) was followed by extraction with EtOAc (4 x 15 mL). The combined organics were washed with brine (25 mL), dried over  $\text{MgSO}_4$ , and concentrated to an oil, which was purified by flash chromatography (0 to 10% EtOAc in hexanes, slow gradient) to provide allyl enol carbonate **367** (20.5 mg, 0.0427 mmol, 33% yield) as well as recovered bis-methyl ketone **348c** (17.8 mg, 0.0434 mmol, 34% yield).

\* The sample was a mixture of methyl ketone **348** and bis-methyl ketone **348c**.

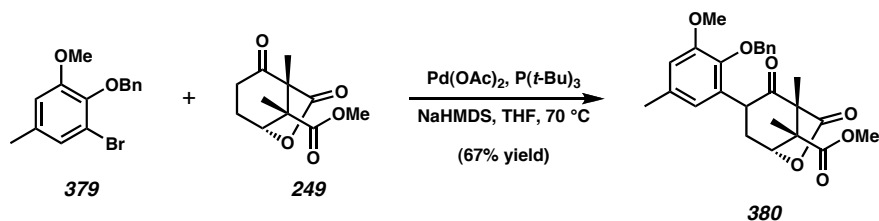
To a 20-mL vial containing allyl enol carbonate **367** (20.5 mg, 0.0427 mmol, 1.0 equiv) was added a flame-dried stirbar and it was cycled into the glovebox and benzene (0.4 mL) was added. In a separate 1-dram vial in the glovebox, Pd<sub>2</sub>(dba)<sub>3</sub>, PHOX ligand **365**, and benzene (1 mL) were combined, sealed, and heated to 40 °C for 30 min (a color change from red to orange was observed). At this point, it was transferred via syringe to the vial containing allyl enol carbonate **367**, sealed, and removed from the glovebox (a color change from orange to green was observed). The reaction was stirred at 40 °C 6.5 h (a color change from green to brown was observed), then cooled to ambient temperature. The reaction mixture was loaded directly onto a flash column and purified (0 to 10% EtOAc in hexanes, slow gradient), yielding allyl methyl ketone **368** (16.7 mg, 0.0391 mmol, 90% yield) as a clear oil. <sup>1</sup>H NMR (500 MHz, CDCl<sub>3</sub>) δ 5.68 (m, 1H), 5.10 (m, 1H), 5.03 (ddd, *J* = 17.2, 3.4, 2.2 Hz, 1H), 4.68 (dd, *J* = 12.2, 4.9 Hz, 1H), 4.11 (d, *J* = 11.0 Hz, 1H), 3.68 (d, *J* = 10.0 Hz, 1H), 3.62 (d, *J* = 10.0 Hz, 1H), 3.49 (d, *J* = 11.0 Hz, 1H), 2.34 (dd, *J* = 13.7, 8.1 Hz, 1H), 2.28 (dd, *J* = 13.9, 6.6 Hz, 1H), 1.98 (comp. m, 2H), 1.87–1.60 (comp. m, 10 H), 1.07 (s, 3H), 1.05 (s, 3H), 0.97 (s, 3H), 0.94 (comp. m, 9H), 0.60 (q, *J* = 8.1 Hz, 6H); <sup>13</sup>C NMR (125 MHz, CDCl<sub>3</sub>) δ 217.1, 133.6, 118.5, 110.6, 67.89, 67.88, 67.6, 55.8, 47.5, 42.5, 40.0, 39.3, 37.5, 31.2, 25.2, 24.3, 22.5, 16.8, 16.3, 6.8, 4.1; IR (Neat film NaCl) 2957, 2877, 1694, 1460, 1336, 1117, 1084, 1006, 813, 745 cm<sup>-1</sup>; HRMS (FAB+) [M]<sup>+</sup> calc'd for [C<sub>25</sub>H<sub>44</sub>O<sub>4</sub>Si]: *m/z* 436.3009, found 436.2993. Stereochemistry assigned using a combination of HSQC, HMBC, COSY, and NOESY 2D experiments.



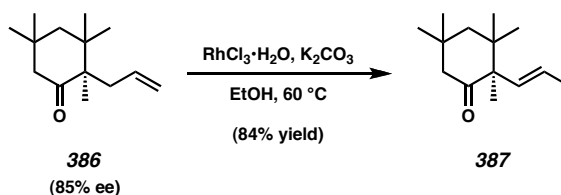
**Aryl Bromide 379.** To a flask equipped with a reflux condenser and containing a mixture of phenol **378** (2.00 g, 8.66 mmol, 1.0 equiv) and Cs<sub>2</sub>CO<sub>3</sub> (3.53 g, 10.8 mmol,

1.25 equiv) was added ACN (34.6 mL) followed by benzyl bromide (1.13 mL, 9.53 mmol, 1.1 equiv). The reaction was stirred at 85 °C (reflux) for 1 h then cooled to ambient temperature. The mixture was diluted with H<sub>2</sub>O (100 mL) and extracted with EtOAc (3 x 25 mL). The combined organics were washed with brine (25 mL), dried over MgSO<sub>4</sub>, and concentrated. The crude product was purified by flash chromatography (10 to 50% Et<sub>2</sub>O in petroleum ether) to give benzyl ether **376** (2.70 g, 8.4 mmol, 97% yield) as a slightly yellow powder. m.p. 48–48.5 °C; *R<sub>f</sub>* 0.4 (25% EtOAc in pet. ether).

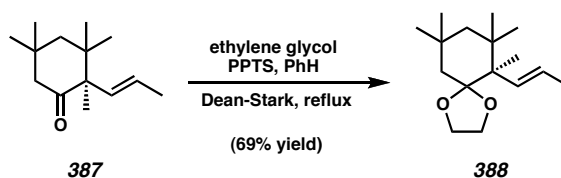
To a flask equipped with a reflux condenser and containing a solution of aldehyde **376** (1.99 g, 6.2 mmol, 1.0 equiv) in triethylene glycol (12.4 mL) was added hydrazine monohydrate (752 μL, 15.5 mmol, 2.5 equiv). The resulting mixture was heated to 110 °C and to the resulting clear solution was added KOH pellets (1.74 g, 31.0 mmol, 5.0 equiv) one-by-one through the condenser over 20 min. The mixture was then heated to 150 °C and stirred for 30 min. The solution was cooled to ambient temperature then to 0 °C, then diluted with 1 M HCl (aq., 40 mL) followed by H<sub>2</sub>O (40 mL), and extracted with EtOAc (4 x 20 mL). The combined organics were washed with brine (25 mL), dried over MgSO<sub>4</sub>, and concentrated to an oil, which was purified by flash chromatography (5 to 10% EtOAc in pet. ether) to provide aryl bromide **379** (1.56 g, 5.8 mmol, 82% yield) as a clear, nonviscous oil. *R<sub>f</sub>* 0.33 (10% EtOAc in pet. ether); <sup>1</sup>H NMR (500 MHz, CDCl<sub>3</sub>) δ 7.56 (comp. m, 2H), 7.38 (comp m, 2H), 7.33 (m, 1H), 6.97 (dd, *J* = 2.0, 0.7 Hz, 1H), 6.68 (d, *J* = 1.7 Hz, 1H), 4.99 (s, 2H), 3.84 (s, 3H), 2.30 (s, 3H); <sup>13</sup>C NMR (125 MHz, CDCl<sub>3</sub>) δ 153.5, 143.0, 137.3, 135.2, 128.5, 128.3, 128.0, 117.6, 112.7, 74.7, 56.0, 21.0; IR (Neat film NaCl) 3032, 2938, 2868, 1597, 1568, 1485, 1456, 1406, 979, 830, 728, 696 cm<sup>-1</sup>; HRMS (FAB+) [M+H]<sup>+</sup> calc'd for [C<sub>15</sub>H<sub>15</sub>O<sub>2</sub>Br+H]<sup>+</sup>: *m/z* 307.0334, found 307.0325.



**Aryl ketone 380.** To a vial containing aryl bromide **379** (62 mg, 0.201 mmol, 1.0 equiv) and ketone **249** (50 mg, 0.221 mmol, 1.1 equiv) was added Pd(OAc)<sub>2</sub> (4.5 mg, 0.020 mmol, 0.1 equiv). The mixture was brought into the glovebox under vacuum. NaHMDS (5.5 mg, 0.302 mmol, 1.5 equiv), THF (0.8 mL, 0.25 M), and P(*t*-Bu)<sub>3</sub> (5.1 mg, 0.025 mmol, 1.25 equiv) were added. The vial was sealed, removed from the glovebox, and heated to 70 °C for 5 h. The reaction was cooled to ambient temperature and extracted from 1M NaHSO<sub>4</sub> (aq, 10 mL) with Et<sub>2</sub>O (3 x 5 mL). The combined organics were washed with brine, dried over MgSO<sub>4</sub>, and concentrated to an oil. Purification by flash chromatography (15 to 33% EtOAc in hexanes) provided aryl ketone **380** (61 mg, mmol, 67% yield). *R<sub>f</sub>* ~ 0.3 (33% EtOAc in hexanes); <sup>1</sup>H NMR (500 MHz, CDCl<sub>3</sub>) δ 7.33 (comp. m, 5H), 6.73 (s, 1H), 6.40 (s, 1H), 4.95 (s, 2H), 4.85 (d, *J* = 3.7 Hz, 1H), 4.16 (app. t, *J* = 9.6 Hz, 1H), 3.88 (s, 3H), 3.75 (s, 3H), 2.35 (m, 1H), 2.30 (s, 3H), 2.19 (dd, *J* = 13.9, 11.0 Hz, 1H), 1.29 (s, 3H), 1.21 (s, 3H); <sup>13</sup>C NMR (125 MHz, CDCl<sub>3</sub>) δ 199.5, 173.9, 171.6, 152.3, 143.7, 137.1, 129.1, 128.8, 128.5, 128.1, 121.2, 113.1, 79.3, 74.7, 62.3, 57.7, 55.7, 53.0, 45.8, 33.1, 21.4, 14.3, 9.9; IR (Neat film NaCl) 2951, 1790, 1732, 1488, 1465, 1254, 1153, 1077, 1016, 734 cm<sup>-1</sup>; HRMS (FAB+) [M+H]<sup>+</sup> calc'd for [C<sub>26</sub>H<sub>27</sub>O<sub>7</sub>+H]<sup>+</sup>: *m/z* 452.1825, found 452.1852.

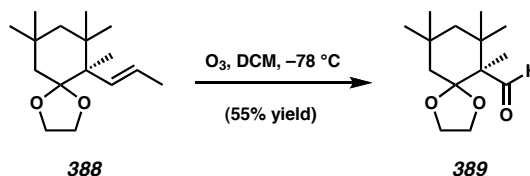


**Vinyl ketone 387.** To a solution of allyl ketone **386** (905 mg, 4.35 mmol, 1.00 equiv) in EtOH (45 mL) in a sealable Schlenk flask (100 mL) was added  $K_2CO_3$  (601 mg, 4.35 mmol, 1.00 equiv) and  $RhCl_3 \cdot H_2O$  (49.4 mg, 0.218 mmol, 0.05 equiv). The reaction mixture was sparged with Ar for 10 min, sealed and heated to 60 °C for 12 h. After cooling to ambient temperature, the reaction mixture was filtered, washed with EtOH, concentrated, and purified by flash chromatography on silica gel (7.5 to 10% Et<sub>2</sub>O in pentane) to give vinyl ketone **387** (759 mg, 84% yield of a 10:1 mixture containing allyl ketone **386** as the minor component) as an amorphous solid.  $R_f$  0.67, 0.46 (25% Et<sub>2</sub>O in hexanes, 5% Et<sub>2</sub>O in hexanes developed twice); <sup>1</sup>H NMR (300 MHz, CDCl<sub>3</sub>) δ 5.88 (dq,  $J = 1.8, 15.5$  Hz, 1H), 5.42 (dq,  $J = 15.3, 6.3$  Hz, 1H), 2.53 (d,  $J = 13.2$  Hz, 1H), 2.11 (dd,  $J = 13.5, 1.8$  Hz, 1H), 1.85 (d,  $J = 14.4$  Hz, 1H), 1.71 (dd,  $J = 6.5, 1.7$  Hz, 3H), 1.42 (dd,  $J = 14.4, 1.8$  Hz, 1H), 1.09 (s, 3H), 1.04 (s, 3H), 1.01 (s, 3H), 0.90 (s, 6H); <sup>13</sup>C NMR (75 MHz, CDCl<sub>3</sub>) δ 214.1, 132.5, 126.2, 56.4, 50.7, 49.6, 40.6, 35.4, 33.7, 30.2, 26.9, 26.8, 18.6, 15.6; IR (Neat film NaCl) 2957, 1707, 1458, 1391, 1370, 1283, 977 cm<sup>-1</sup>; HRMS (EI) [M]<sup>+</sup> calc'd for [C<sub>14</sub>H<sub>24</sub>O]<sup>+</sup>:  $m/z$  208.1827, found 208.1820;  $[\alpha]_D^{25} -59.07$  (c 1.04, CHCl<sub>3</sub>, 85% ee).

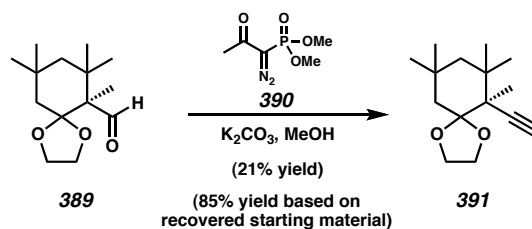


**Ketal 388.** A solution of the vinyl ketone **387** (700 mg, 3.36 mmol, 1.00 equiv), ethylene glycol (1.30 mL, 23.5 mmol, 7.00 equiv), and pyridinium *p*-toluenesulfonate (211 mg, 0.84 mmol, 0.25 equiv) in benzene (70 mL) was fitted with a Dean-Stark apparatus and refluxed at 100 °C for 30 h. The reaction mixture was cooled to ambient temperature, diluted with saturated aqueous NaHCO<sub>3</sub> (40 mL), and extracted with Ph-H (3 x 30 mL). The combined organics were washed with brine (20 mL), dried (Na<sub>2</sub>SO<sub>4</sub>), concentrated, and purified by flash chromatography on silica gel (1 to 2% Et<sub>2</sub>O in

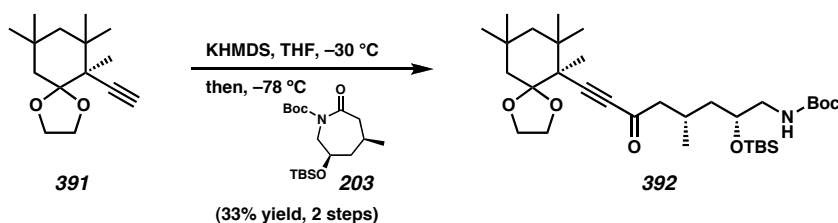
hexane) to give acetal **388** (585 mg, 70% yield) as an oil:  $R_f$  0.61, 0.67 (5% Et<sub>2</sub>O in hexanes developed twice, 25% Et<sub>2</sub>O in hexanes); <sup>1</sup>H NMR (300 MHz, CDCl<sub>3</sub>) δ 5.74 (dq,  $J$  = 15.8, 1.5 Hz, 1H), 5.44 (dq,  $J$  = 15.8, 6.3 Hz, 1H), 3.92–3.78 (m, 4H), 1.72 (dd,  $J$  = 6.5, 1.7 Hz, 3H), 1.52 (s, 2H), 1.37 (d,  $J$  = 14.1 Hz, 1H), 1.30 (d,  $J$  = 14.1 Hz, 1H), 1.03 (s, 6H), 1.02 (s, 3H), 0.96 (s, 3H), 0.95 (s, 3H); <sup>13</sup>C NMR (75 MHz, CDCl<sub>3</sub>) δ 133.7, 124.3, 113.8, 64.6, 64.4, 49.8, 48.6, 42.2, 38.0, 32.3, 32.0, 31.5, 28.3, 27.7, 18.7, 14.2; IR (Neat film NaCl) 2952, 1455, 1388, 1225, 1146, 1124, 1078, 981 cm<sup>-1</sup>; HRMS (EI) [M]<sup>+</sup> calc'd for [C<sub>16</sub>H<sub>28</sub>O]<sup>+</sup>:  $m/z$  252.2089, found 252.2090;  $[\alpha]_D^{24}$  +1.51 (c 1.11, CHCl<sub>3</sub>, 85% ee).



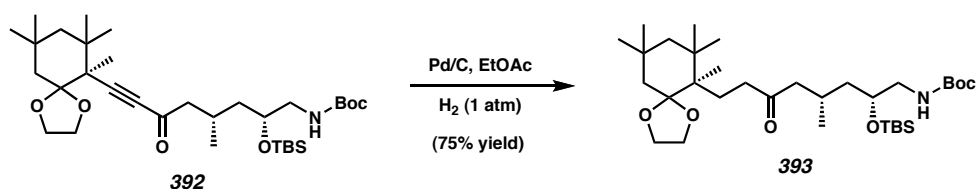
**Aldehyde 389.** Through a cooled (−78 °C) solution of acetal **388** (252 mg, 1.00 mmol, 1.00 equiv) in CH<sub>2</sub>Cl<sub>2</sub> (25 mL) was bubbled a stream of ozone until the reaction mixture turned blue. The reaction mixture was quenched with dimethyl sulfide (0.20 mL), allowed to warm to ambient temperature, concentrated to an oil, and purified by flash chromatography on silica gel (2.5 to 10% Et<sub>2</sub>O in hexane) to give aldehyde **389** (132 mg, 55% yield) as an oil:  $R_f$  0.41, 0.29 (25% Et<sub>2</sub>O in hexanes, 5% Et<sub>2</sub>O in hexanes developed twice); <sup>1</sup>H NMR (300 MHz, CDCl<sub>3</sub>) δ 9.93 (s, 1H), 3.98–3.85 (m, 4H), 1.69 (d,  $J$  = 14.4 Hz, 3H), 1.57 (dd,  $J$  = 14.4, 1.2 Hz, 1H), 1.50 (d,  $J$  = 14.4 Hz, 1H), 1.37 (dd,  $J$  = 14.4, 1.2 Hz, 1H), 1.08 (s, 3H), 1.07 (s, 3H), 1.06 (s, 3H), 1.04 (s, 3H), 1.03 (s, 3H); <sup>13</sup>C NMR (75 MHz, CDCl<sub>3</sub>) δ 206.2, 112.1, 64.5, 64.3, 58.0, 50.3, 43.0, 38.1, 32.9, 31.6, 30.6, 27.8, 27.7, 11.1; IR (Neat film NaCl) 2954, 2899, 1722, 1241, 1110, 1075, 964 cm<sup>-1</sup>; HRMS (EI) [M]<sup>+</sup> calc'd for [C<sub>14</sub>H<sub>24</sub>O<sub>3</sub>]<sup>+</sup>:  $m/z$  240.1726, found 240.1720;  $[\alpha]_D^{24}$  −39.53 (c 0.385, CHCl<sub>3</sub>, 85% ee).



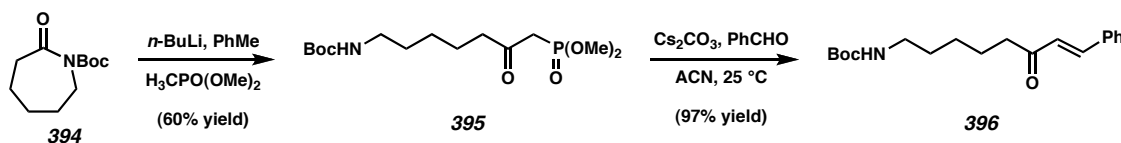
**Alkyne 391.** To a solution of aldehyde **389** (75.0 mg, 0.312 mmol, 1.00 equiv), and  $\text{K}_2\text{CO}_3$  (108 mg, 0.780 mmol, 2.50 equiv) in MeOH (3.10 mL) was added diazoketone **390** (89.9 mg, 0.468 mmol, 1.5 equiv). After 1 h, an additional portion of  $\text{K}_2\text{CO}_3$  (214 mg, 1.56 mmol, 5.00 equiv) and of diazoketone **390** (150 mg, 0.780 mmol, 2.5 equiv) were added. After a further 4 h, a final portion of  $\text{K}_2\text{CO}_3$  (200 mg, 1.45 mmol, 4.65 equiv) and of diazoketone **390** (200 mg, 1.05 mmol, 3.37 equiv) were added. After stirring for 20 h, the reaction mixture was diluted with  $\text{H}_2\text{O}$  (10 mL), extracted with  $\text{CH}_2\text{Cl}_2$  (8 x 5 mL), dried ( $\text{MgSO}_4$ ), concentrated, and purified by flash chromatography on silica gel (1 to 7%  $\text{Et}_2\text{O}$  in hexanes) to give recovered aldehyde **389** (55.6 mg, 74% yield) and alkyne **391** (15.5 mg, 21% yield, 85% yield based on recovered aldehyde **389**) as an oil:  $R_f$  0.40 (5%  $\text{Et}_2\text{O}$  in hexanes developed twice);  $^1\text{H}$  NMR (300 MHz,  $\text{C}_6\text{D}_6$ )  $\delta$  3.62–3.40 (m, 4H), 2.01 (d,  $J = 14.1$  Hz, 1H), 1.93 (s, 1H), 1.72 (d,  $J = 14.1$  Hz, 1H), 1.47 (dd,  $J = 13.8, 1.8$  Hz, 1H), 1.36 (s, 3H), 1.34 (s, 3H), 1.22 (s, 3H), 1.17 (dd,  $J = 14.3, 1.7$  Hz, 1H), 1.10 (s, 3H), 1.04 (s, 3H);  $^{13}\text{C}$  NMR (75 MHz,  $\text{CDCl}_3$ )  $\delta$  112.5, 89.1, 76.6, 70.7, 65.5, 64.2, 49.8, 47.3, 42.5, 38.0, 34.6, 31.4, 29.8, 28.8, 24.9, 16.2; IR (Neat film NaCl) 3309, 2954, 2911, 2111, 1454, 1390, 1367, 1235, 1148, 1088, 1073, 984  $\text{cm}^{-1}$ ; HRMS (EI)  $[\text{M}]^+$  calc'd for  $[\text{C}_{15}\text{H}_{24}\text{O}_2]^+$ :  $m/z$  236.1776, found 236.1786;  $[\alpha]_{\text{D}}^{26} -20.35$  ( $c$  1.25,  $\text{CH}_2\text{Cl}_2$ , 85% ee).



**Ynone 392.** To a cooled ( $-30\text{ }^{\circ}\text{C}$ ) solution of KHMDS (24.1 mg, 0.121 mmol, 2.20 equiv) in THF (1.00 mL) was added alkyne **391** (13.0 mg, 0.055 mmol, 1.00 equiv) in THF (1.00 mL). The solution was maintained for 30 min each at  $-30\text{ }^{\circ}\text{C}$ ,  $0\text{ }^{\circ}\text{C}$ , and  $22\text{ }^{\circ}\text{C}$ . The alkyne anion was cooled to  $-78\text{ }^{\circ}\text{C}$ , and caprolactam **203** (23.6 mg, 0.066 mmol, 1.2 equiv) in THF (1.00 mL) was added. After 1 h, additional KHMDS (12.0 mg, 0.061 mmol, 1.10 equiv) in THF (0.50 mL) was added. After a further 5 h, the reaction mixture was quenched with saturated aqueous  $\text{NaHCO}_3$  (0.50 mL), diluted with  $\text{H}_2\text{O}$  (2 mL), brine (4 mL), and  $\text{Et}_2\text{O}$  (4 mL), and extracted with  $\text{Et}_2\text{O}$  (6 x 4 mL) and  $\text{CH}_2\text{Cl}_2$  (2 x 2 mL). The combined organics were dried ( $\text{Na}_2\text{SO}_4$ ), and concentrated to an oil, which was purified by flash chromatography on silica gel (2.5 to 15%  $\text{EtOAc}$  in hexanes) to give ynone **392** (10.9 mg, 33% yield) as an oil:  $R_f$  0.24, 0.50 (10%  $\text{EtOAc}$  in hexanes developed twice, 20%  $\text{EtOAc}$  in hexanes);  $^1\text{H}$  NMR (500 MHz,  $\text{CDCl}_3$ )  $\delta$  4.78 (s, 1H), 4.07–4.02 (m, 1H), 4.00–3.94 (m, 3H), 3.84 (bs, 1H), 3.38–3.30 (m, 1H), 2.97 (dt,  $J = 14.5, 6.0$  Hz, 1H), 2.58 (dd,  $J = 15.5, 5.5$  Hz, 1H), 2.38 (dd,  $J = 15.5, 8.0$  Hz, 1H), 2.26–2.16 (m, 1H), 1.76 (d,  $J = 14.0$  Hz, 1H), 1.62–1.44 (comp. m, 4H), 1.46 (s, 9H), 1.40–1.30 (m, 1H), 1.26 (s, 3H), 1.17 (s, 3H), 1.14 (s, 3H), 1.07 (s, 3H), 1.01 (s, 3H), 1.00 (s, 3H), 0.91 (s, 9H), 0.09 (s, 3H), 0.08 (s, 3H);  $^{13}\text{C}$  NMR (125 MHz,  $\text{CDCl}_3$ )  $\delta$  187.2, 155.9, 112.1, 98.7, 83.7, 79.1, 69.4, 65.5, 64.6, 53.2, 49.8, 48.1, 45.9, 43.0, 42.2, 38.7, 33.8, 31.4, 29.7, 29.6, 28.4, 28.0, 26.3, 25.9, 25.6, 20.2, 18.0,  $-4.5, -4.6$ ; IR (Neat film NaCl) 3383, 2955, 2930, 2208, 1716, 1673, 1504, 1391, 1366, 1252, 1171, 1090, 836  $\text{cm}^{-1}$ ; HRMS (FAB+)  $[\text{M}+\text{H}]^+$  calc'd for  $[\text{C}_{33}\text{H}_{59}\text{NO}_6\text{Si}+\text{H}]^+$ :  $m/z$  594.4190, found 594.4208;  $[\alpha]_{\text{D}}^{26} -36.12$  ( $c$  0.545,  $\text{EtOAc}$ ).



**Ketone 393.** To a solution of ynone **392** (10.9 mg, 18.3  $\mu\text{mol}$ , 1.00 equiv) in EtOAc (6 mL) was added 10% Pd/C (4.0 mg), and the reaction mixture was sparged with  $\text{H}_2$  (5 min). After 18 h of vigorous stirring under an atmosphere of  $\text{H}_2$  (balloon), the reaction mixture was concentrated, and purified by flash chromatography on silica gel (5 to 10% EtOAc in hexanes). NMR analysis of the chromatographed product indicated the presence of some partially hydrogenated material. A solution of this material in EtOAc (5 mL) was treated again with 10% Pd/C (5.0 mg) under an atmosphere of  $\text{H}_2$  (balloon) for 4 h. The reaction mixture was concentrated to an oil and purified by flash chromatography on silica gel (5 to 10% EtOAc in hexanes) to give ketone **393** (8.2 mg, 75% yield) as a oil:  $R_f$  0.53 (20% EtOAc in hexanes);  $^1\text{H}$  NMR (500 MHz,  $\text{CDCl}_3$ )  $\delta$  4.79 (s, 1H), 3.96 (app. t,  $J = 6.8$  Hz, 1H), 3.83 (app. q,  $J = 7.0$  Hz, 1H), 3.79 (bs, 1H), 3.74 (app. q,  $J = 7.0$  Hz, 1H), 3.34–3.26 (m, 1H), 2.98 (dt,  $J = 13.5, 6.5$  Hz, 1H), 2.60–2.50 (m, 1H), 2.48–2.36 (m 2H), 2.20 (dd,  $J = 16.3, 7.8$  Hz, 1H), 2.12–2.02 (m, 1H), 2.00–1.92 (m, 1H), 1.56–1.24 (comp. m, 9H), 1.44 (s, 9H), 1.15 (d,  $J = 14.0$  Hz, 1H), 1.11 (s, 3H), 1.05 (s, 3H), 0.96 (s, 3H), 0.92–0.89 (m, 6H), 0.89 (s, 9H), 0.07 (s, 3H), 0.06 (s, 3H);  $^{13}\text{C}$  NMR (125 MHz,  $\text{CDCl}_3$ )  $\delta$  211.9, 156.2, 115.2, 79.3, 69.8, 64.9, 62.6, 50.6, 50.5, 46.2, 44.2, 42.7, 41.4, 40.9, 39.1, 34.7, 31.5, 30.0, 29.4, 28.7, 28.3, 26.8, 26.1, 26.0, 24.4, 20.6, 18.3, 16.8,  $-4.3$ ; IR (Neat film NaCl) 3391, 2953, 2930, 1714, 1503, 1366, 1253, 1173, 1076, 836, 776  $\text{cm}^{-1}$ ; HRMS (FAB+)  $[\text{M}+\text{H}]^+$  calc'd for  $[\text{C}_{33}\text{H}_{63}\text{NO}_6\text{Si}+\text{H}]^+$ :  $m/z$  598.4503, found 598.4489;  $[\alpha]_{\text{D}}^{26}$  9.33 ( $c$  0.105,  $\text{CH}_2\text{Cl}_2$ ).



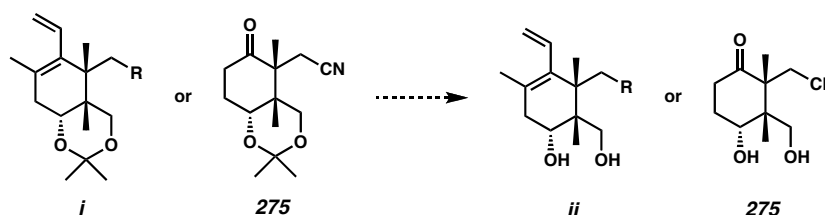
**Enone 396.** To a solution of dimethyl methylphosphonate (285  $\mu\text{L}$ , 2.63 mmol, 1.05 equiv) in toluene (12.5 mL) at  $-78^\circ\text{C}$  was added  $n$ -butyllithium (1.47 mL, 2.63 mmol, 1.05 equiv). The solution was stirred at  $-78^\circ\text{C}$  for 20 min then transferred dropwise via

cannula (20 gauge) over 30 min to a cooled ( $-78\text{ }^{\circ}\text{C}$ ) solution of Boc-caprolactam **394**<sup>17</sup> in toluene (12.5 mL). The reaction was stirred an additional 1 h at  $-78\text{ }^{\circ}\text{C}$  then warmed to ambient temperature over 30 min and quenched with  $\text{KH}_2\text{PO}_4$  (1 M, aq., 20 mL) and extracted with EtOAc (3 x 20 mL). The combined organics were washed with brine (20 mL), dried over  $\text{MgSO}_4$ , and concentrated to an oil. The crude product was purified by flash chromatography to provide phosphonate **395** (0.507 g, 1.5 mmol, 60% yield) as a clear viscous oil.

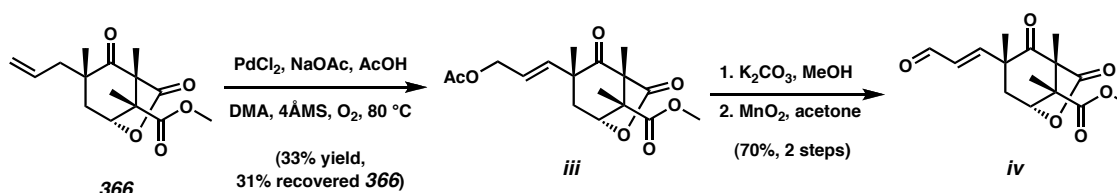
To a solution of phosphonate **395** (103 mg, 0.305 mmol, 1.0 equiv) in ACN (3.1 mL, 0.1 M) was added benzaldehyde (31  $\mu\text{L}$ , 0.305 mmol, 1.0 equiv) followed by  $\text{Cs}_2\text{CO}_3$  (124 mg, 0.381 mmol, 1.25 equiv). The heterogeneous mixture was stirred vigorously for 4 h at  $25\text{ }^{\circ}\text{C}$  then extracted from  $\text{KH}_2\text{PO}_4$  (1 M, aq., 5 mL) with EtOAc (3 x 5 mL). The combined organics were washed with brine (5 mL), dried over  $\text{MgSO}_4$ , and concentrated. The crude product was dissolved in a minimal amount of  $\text{Et}_2\text{O}$ , loaded onto a flash column, and purified (10 to 25% EtOAc in pet. ether) to give enone **396** (94 mg, 0.296 mmol, 97% yield) as a white solid. m.p.  $62\text{--}64.5\text{ }^{\circ}\text{C}$ ;  $R_f$  0.29 (25% EtOAc in pet. ether);  $^1\text{H}$  NMR (300 MHz,  $\text{CDCl}_3$ )  $\delta$  7.55 (comp. m, 3H), 7.39 (comp. m, 3H), 6.73 (d,  $J = 16.2$  Hz, 1H), 4.55 (bs, 1H), 3.15 (d,  $J = 6.6$  Hz, 1H), 3.10 (d,  $J = 6.6$  Hz, 1H), 2.67 (app. t,  $J = 7.4$  Hz, 2H), 1.70 (comp. m, 2H), 1.51 (comp. m, 2H), 1.44 (s, 9H), 1.37 (comp. m, 2H);  $^{13}\text{C}$  NMR (75 MHz,  $\text{CDCl}_3$ )  $\delta$  200.3, 155.9, 142.4, 134.5, 130.4, 128.9, 128.2, 126.1, 40.6, 40.4, 28.4, 26.4, 23.8; IR (Neat film NaCl) 3381, 2979, 2946, 2867, 1688, 1527, 1364, 1251, 1178, 988, 742, 689  $\text{cm}^{-1}$ ; HRMS (FAB+)  $[\text{M}+\text{H}]^+$  calc'd for  $[\text{C}_{19}\text{H}_{27}\text{O}_3\text{N}+\text{H}]^+$ :  $m/z$  318.2069, found 318.2066.

## References

1. For a similar strategy, see: Miyashita, M.; Sasaki, M.; Hattori, I.; Sakai, M.; Tanino, K. *Science* **2004**, *305*, 495–499.
2. Held, D.; Xie, L. *Microchem. J.* **1997**, *55*, 261–269.
3. We were unable to deprotect the 6-membered acetonide in order to access a homologated substrate with C(10) in the ketone oxidation state.

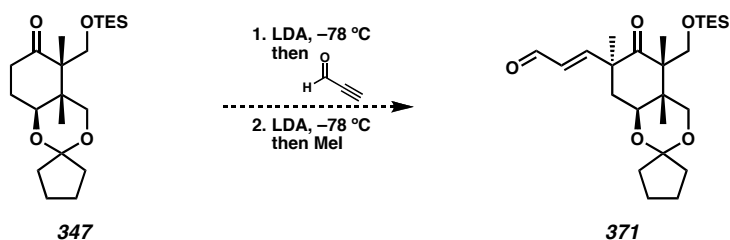


4. Hampton, A.; Fratantoni, J. C.; Carroll, P. M.; Wang, S. *J. Am. Chem. Soc.* **1965**, *87*, 5481–5487.
5. a) Beesley, R. M.; Ingold, C. K.; Thorpe, J. F. *J. Chem. Soc.* **1915**, *107*, 1080–1106. b) Ingold, C. K. *J. Chem. Soc.* **1921**, *119*, 305–329.
6. a) Bruice, T. C.; Pandit, U. K. *J. Am. Chem. Soc.* **1960**, *82*, 5858–5865. b) Jung, M. E.; Gervay, J. *J. Am. Chem. Soc.* **1991**, *113*, 224–232. c) Jung, M. E.; Kiankarimi, M. *J. Org. Chem.* **1998**, *63*, 2968–2974.
7. See Chapter 4.
8. a) Behenna, D. C.; Stoltz, B. M. *J. Am. Chem. Soc.* **2004**, *126*, 15044–15045; b) Mohr, J. T.; Behenna, D. C.; Harned, A. M.; Stoltz, B. M. *Angew. Chem. Int. Ed.* **2005**, *44*, 6924–6927; c) McFadden, R. M.; Stoltz, B. M. *J. Am. Chem. Soc.* **2006**, *128*, 7738–7739; d) Mohr, J. T.; Nishimata, T.; Behenna, D. C.; Stoltz, B. M. *J. Am. Chem. Soc.* **2006**, *128*, 11348–11349; e) Keith, J. A.; Behenna, D. C.; Mohr, J. T.; Ma, S.; Marinescu, S. C.; Oxgaard, J.; Stoltz, B. M.; Goddard, W. A., III *J. Am. Chem. Soc.* **2007**, *129*, 11876–11877; f) Mohr, J. T.; Stoltz, B. M. *Chem. Asian J.* **2007**, *2*, 1476–1491; g) White, D. E.; Stewart, I. C.; Grubbs, R. H.; Stoltz, B. M. *J. Am. Chem. Soc.* **2008**, *130*, 810–811; h) Marinescu, S. C.; Nishimata, T.; Mohr, J. T.; Stoltz, B. M. *Org. Lett.* **2008**, *10*, 1039–1042; i) Enquist, J. A., Jr.; Stoltz, B. M. *Nature* **2008**, *453*, 1228–1231; j) Seto, M.; Roizen, J. L.; Stoltz, B. M. *Angew. Chem. Int. Ed.* **2008**, *47*, 6873–6876.
9. We took advantage of this product in order to test our ideas for functionalization of the allyl group, and we found that the allyl group can be converted to the corresponding enone over a three-step sequence in good yield. Treatment of **366** with Pd(OAc)<sub>2</sub>, NaOAc, AcOH, and DMA in the presence of 4Å molecular sieves led to oxidation with transposition of the olefin to provide **iii**. Methanolysis of the acetate and oxidation provided enal **iv**.



First step from: Mitsudome, T.; Umetani, T.; Nosaka, N.; Mori, K.; Mizugaki, T. Ebitani, K.; Kaneda, K. *Angew. Chem. Int. Ed.* **2006**, *45*, 481–485.

10. An alternative method to access enal **371** would be to add the enolate of ketone **347** directly to formyl acetylene then methylate the intermediate enal.



11. a) Culkin D. A.; Hartwig, J. F. *Acc. Chem. Res.* **2003**, *36*, 234–245. b) Palucki, M.; Buchwald, S. L. *J. Am. Chem. Soc.* **1997**, *119*, 11108–11109.
12. Yang, Z.; Liu, H. B.; Lee, C. M.; Chang, H. M. Wong, H. N. C. *J. Org. Chem.* **1992**, *57*, 7248–7257.
13. Thus far, only *O*-alkylated products have been observed.
14. a) Müller, S.; Liepold, B.; Roth, D.; Bestmann, H. J. *Synlett* **1996**, 521–522. b) Müller, S.; Liepold, B.; Roth, D.; Bestmann, H. J. *Synthesis* **2004**, 59–62.
15. Kumar, R.; Chakraborti, A. K. *Tetrahedron Lett.* **2005**, *46*, 8319–8323.
16. Synthesized according to: Tani, K.; Behenna, D. C.; McFadden, R. M.; Stoltz, B. M. *Org. Lett.* **2007**, *9*, 2529–2531.
17. Prepared according to: Lepifre, F.; Clavier, S.; Bouyssou, P.; Coudert, D. *Tetrahedron* **2001**, *57*, 6969–6975.

## APPENDIX E

Spectra and X-Ray Crystallographic Data:  
Current and Future Investigations Toward Zoanthenol

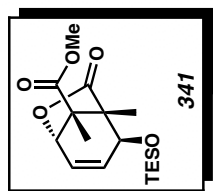
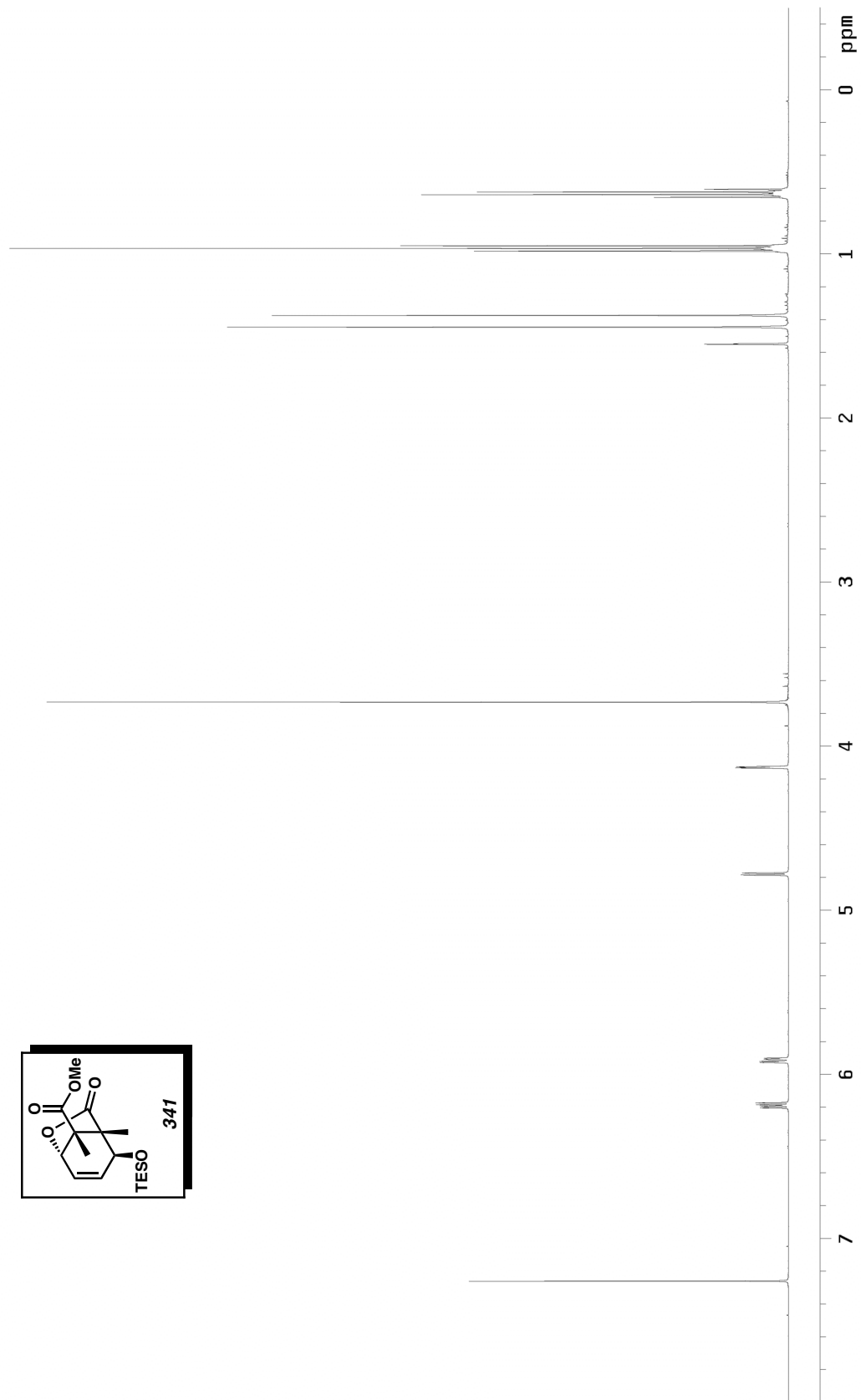


Figure E.1  $^1\text{H}$  NMR (500 MHz,  $\text{CDCl}_3$ ) of compound **341**.

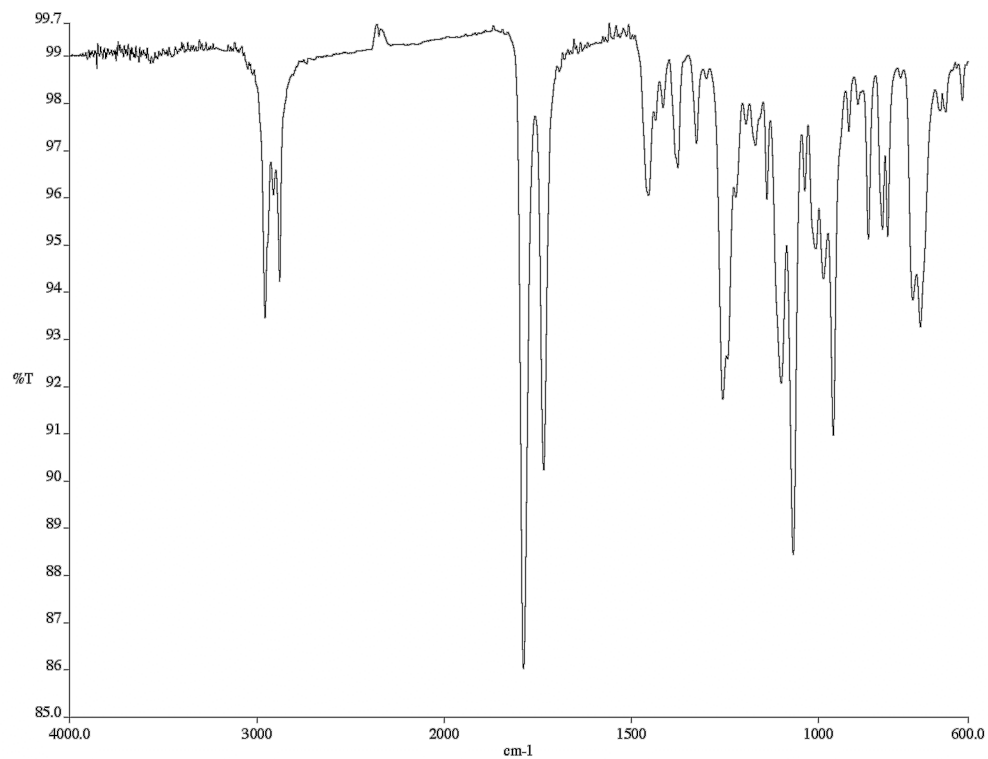


Figure E.2 Infrared spectrum (thin film/NaCl) of compound **341**.

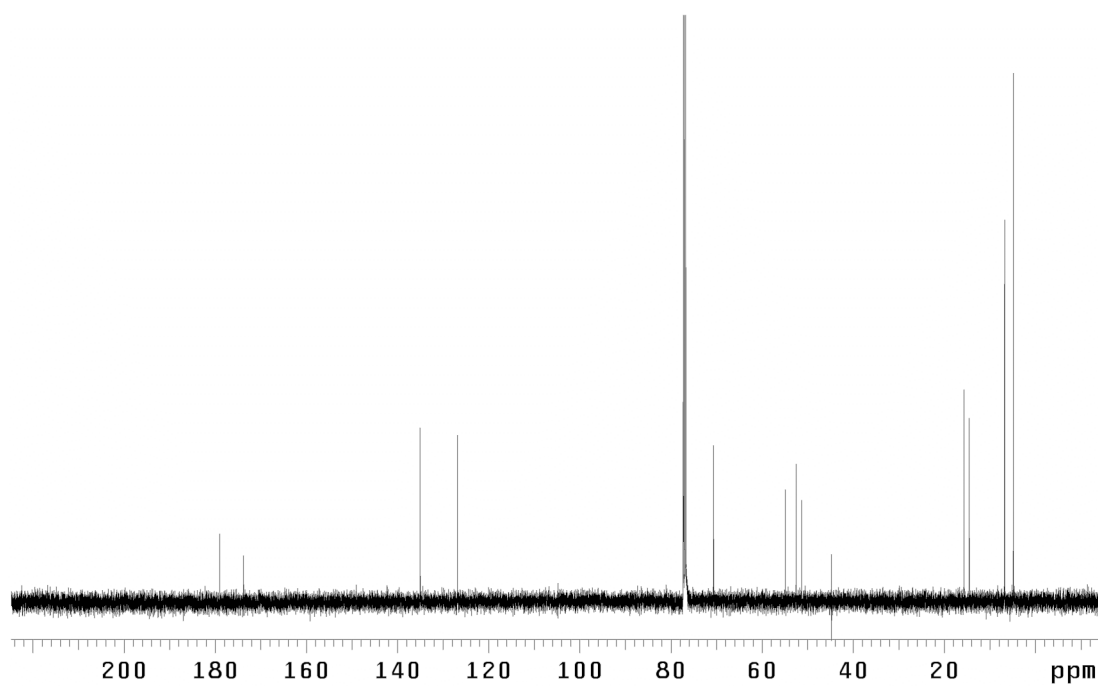
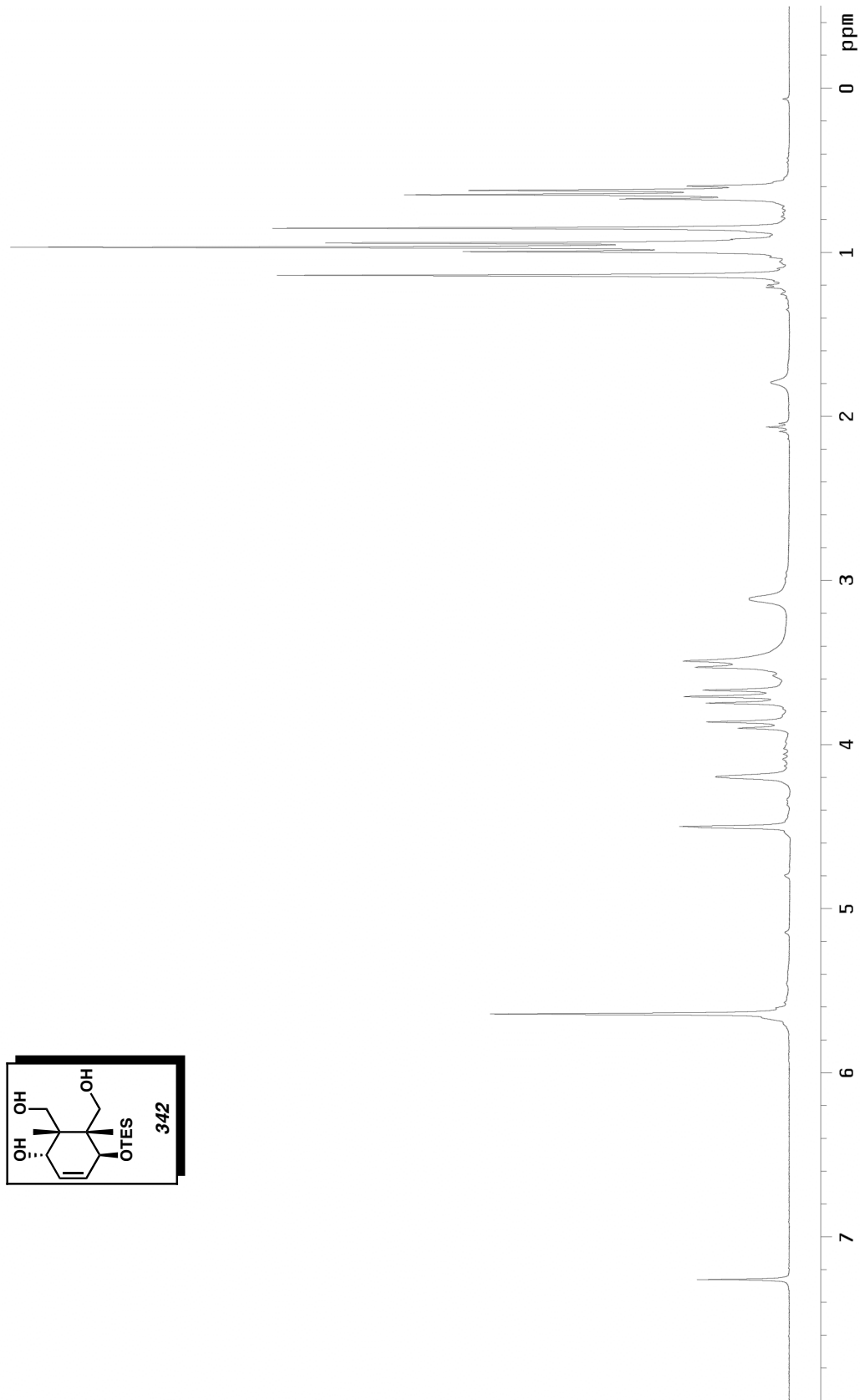
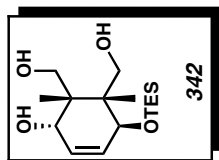


Figure E.3 <sup>13</sup>C NMR (125 MHz, CDCl<sub>3</sub>) of compound **341**.



459  
Figure E.4  $^1\text{H}$  NMR (300 MHz,  $\text{CDCl}_3$ ) of compound 342.

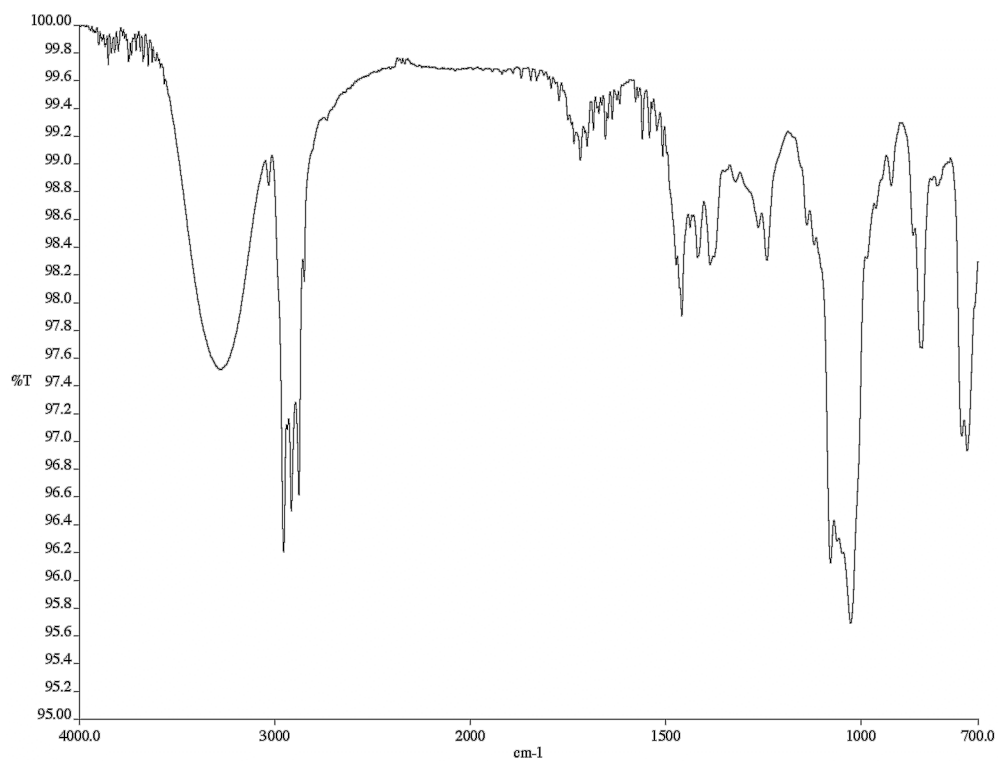


Figure E.5 Infrared spectrum (thin film/NaCl) of compound **342**.

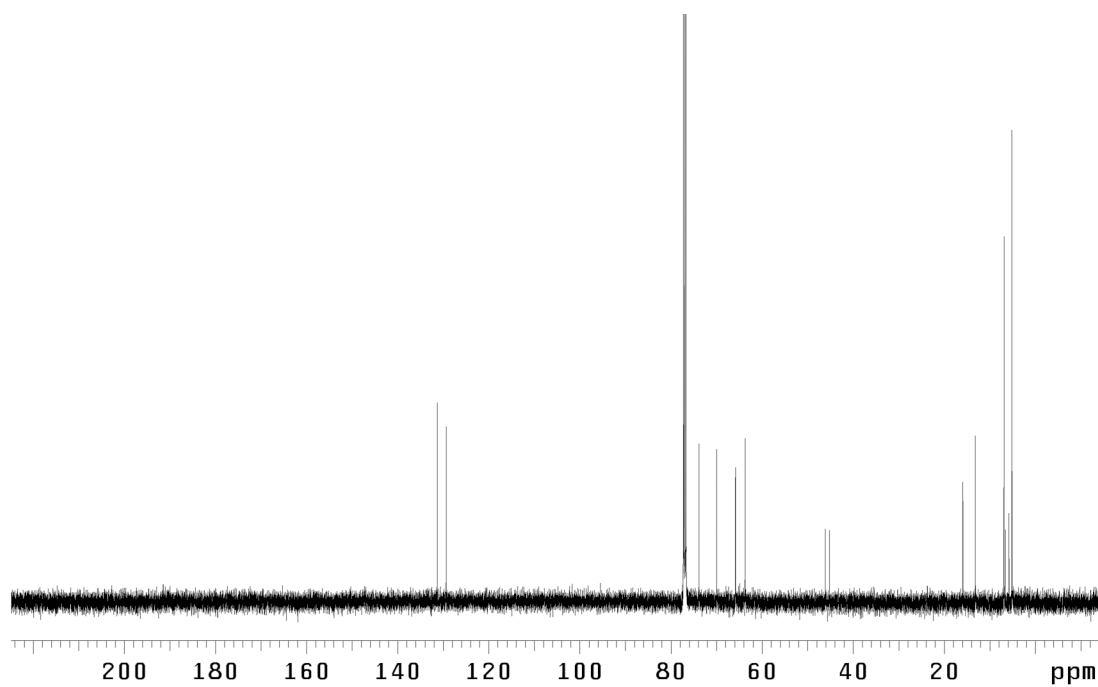


Figure E.6 <sup>13</sup>C NMR (125 MHz, CDCl<sub>3</sub>) of compound **342**.

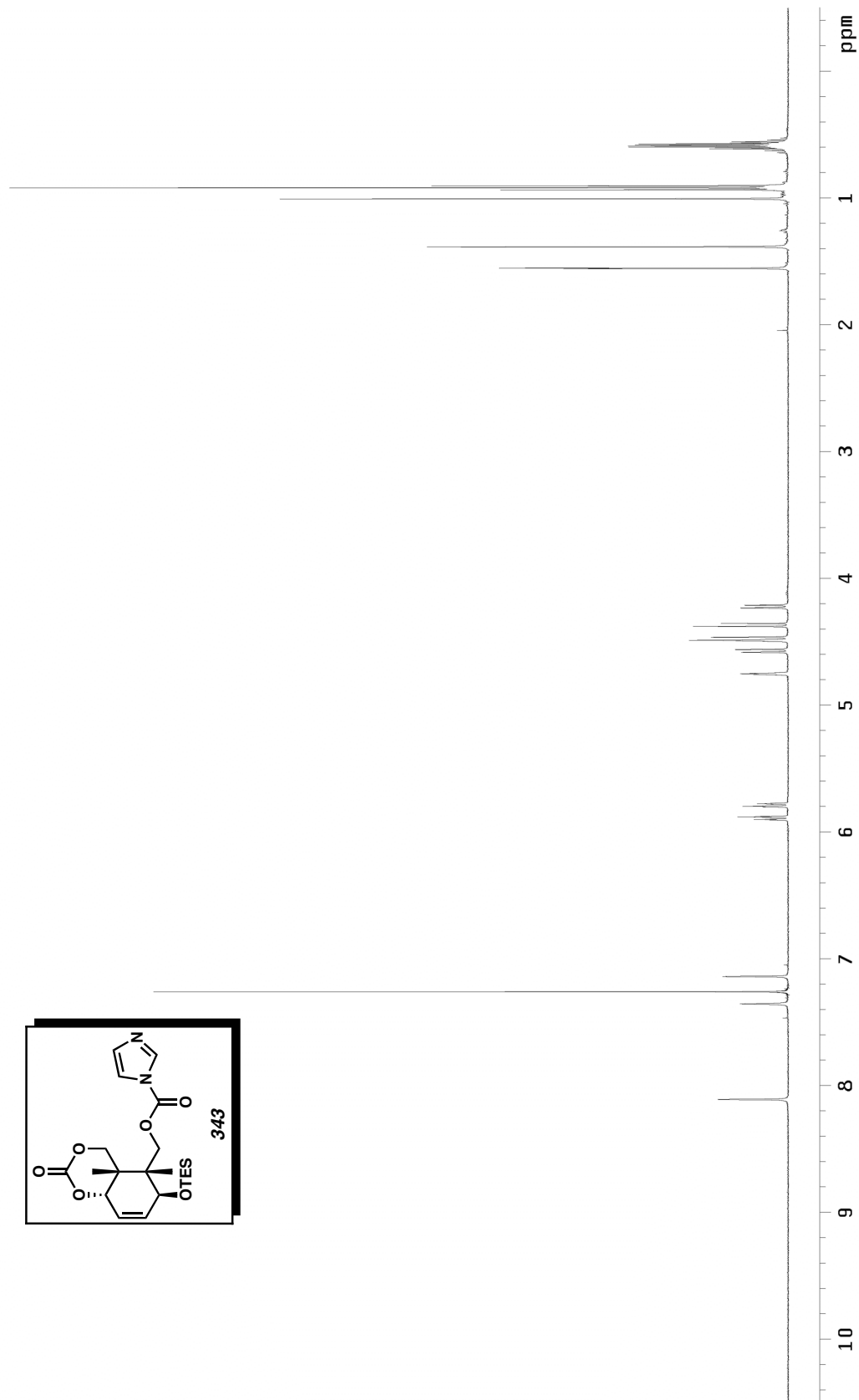
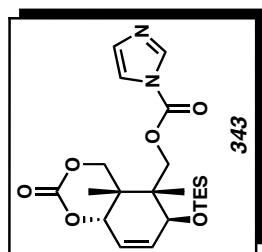


Figure E.7  $^1\text{H}$  NMR (500 MHz,  $\text{CDCl}_3$ ) of compound 343.

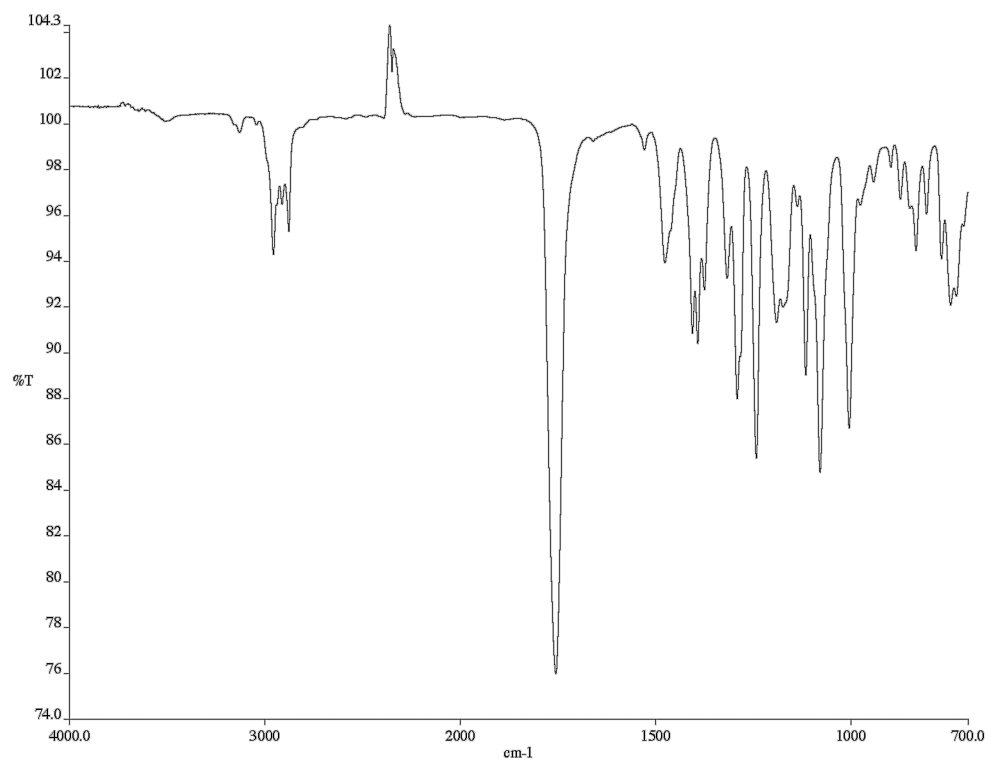


Figure E.8 Infrared spectrum (thin film/NaCl) of compound **343**.

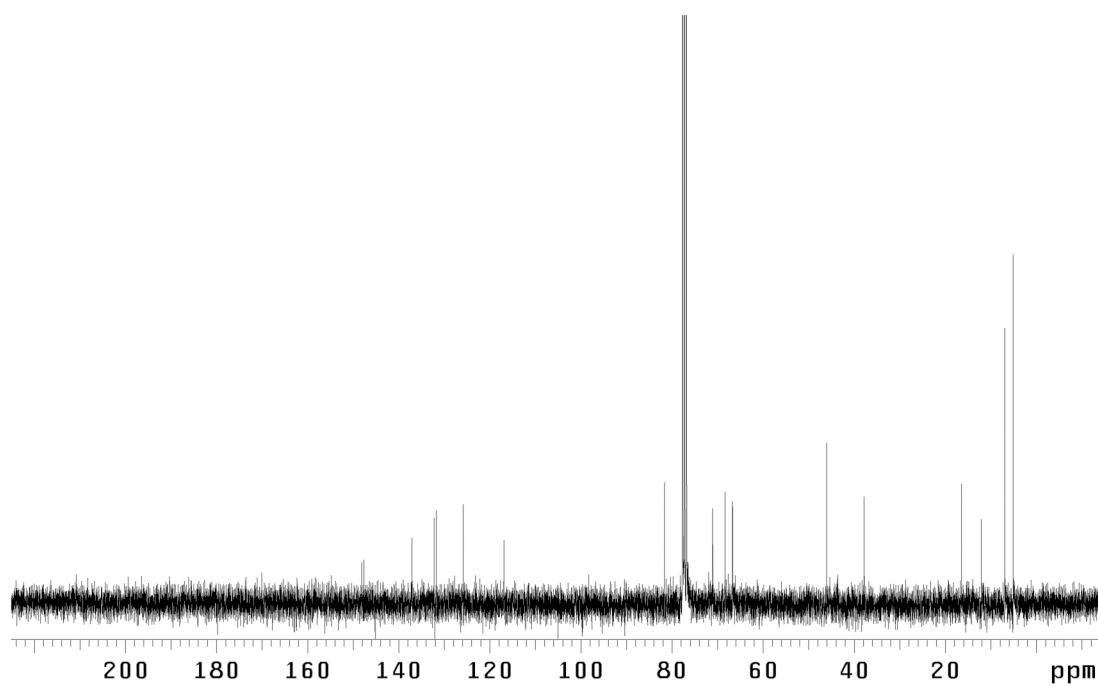


Figure E.9 <sup>13</sup>C NMR (75 MHz, CDCl<sub>3</sub>) of compound **343**.

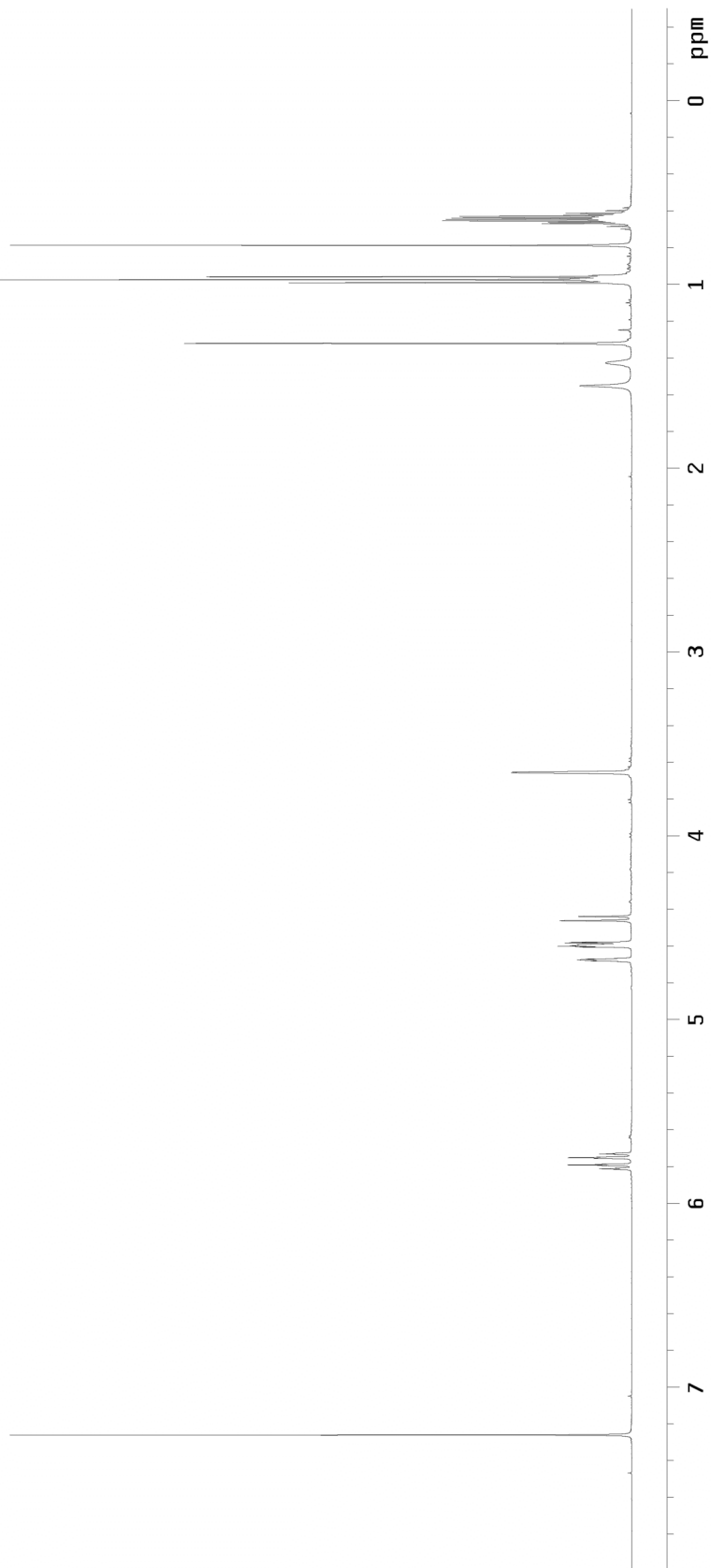
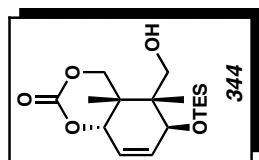


Figure E.10  $^1\text{H NMR}$  (500 MHz,  $\text{CDCl}_3$ ) of compound 344.

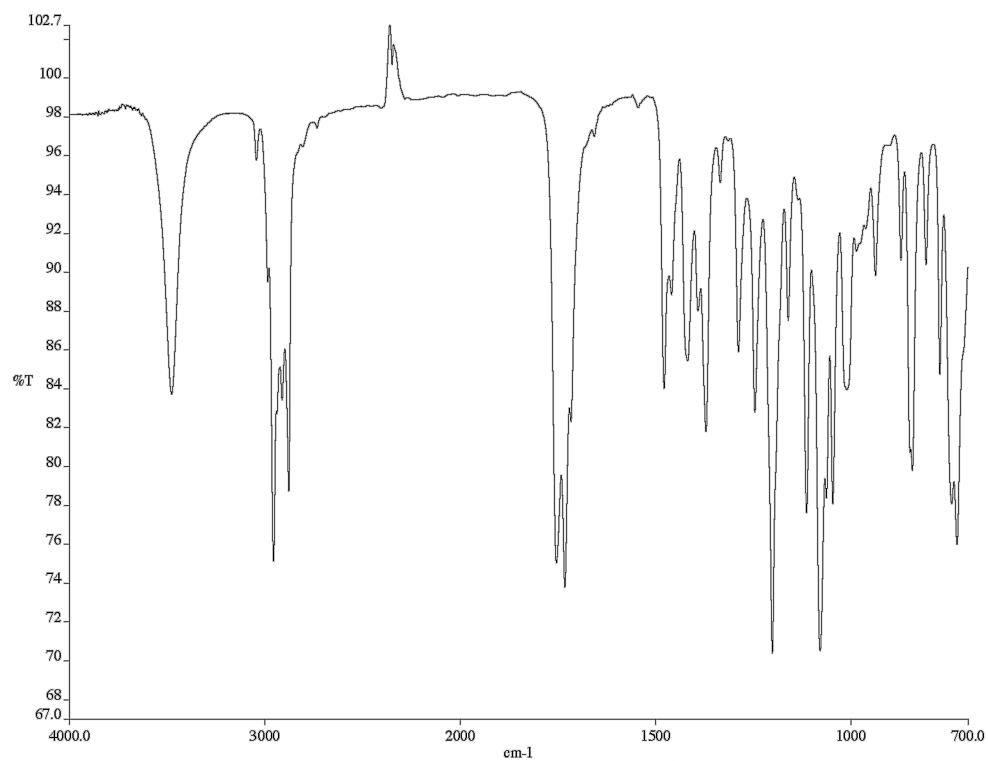


Figure E.11 Infrared spectrum (thin film/NaCl) of compound **344**.

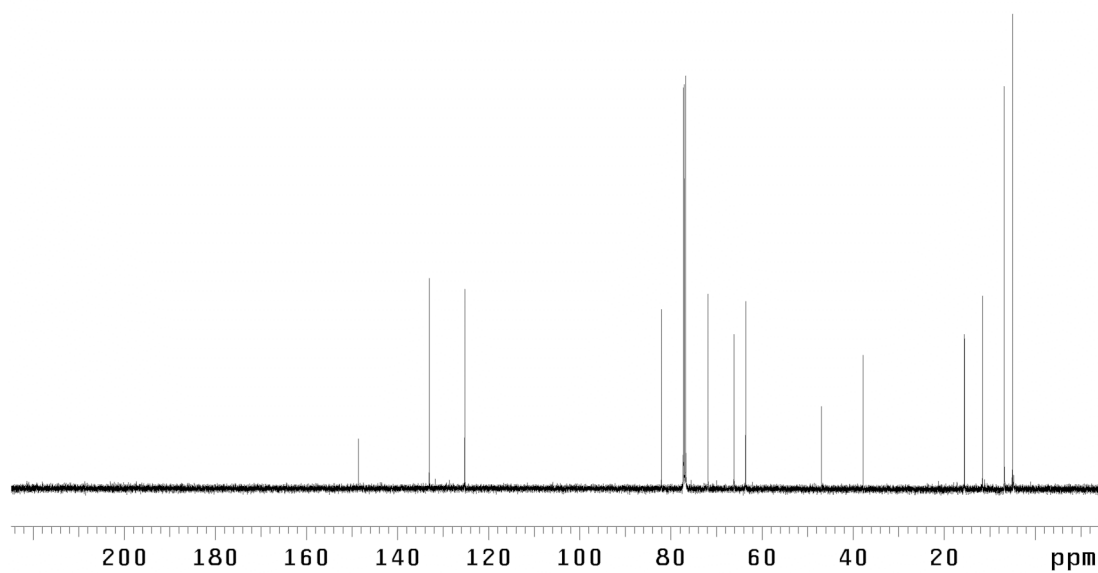


Figure E.12 <sup>13</sup>C NMR (125 MHz, CDCl<sub>3</sub>) of compound **344**.

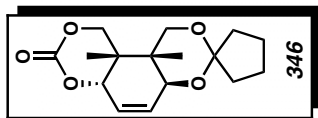


Figure E.13  $^1\text{H NMR}$  (500 MHz,  $\text{CDCl}_3$ ) of compound **346**.

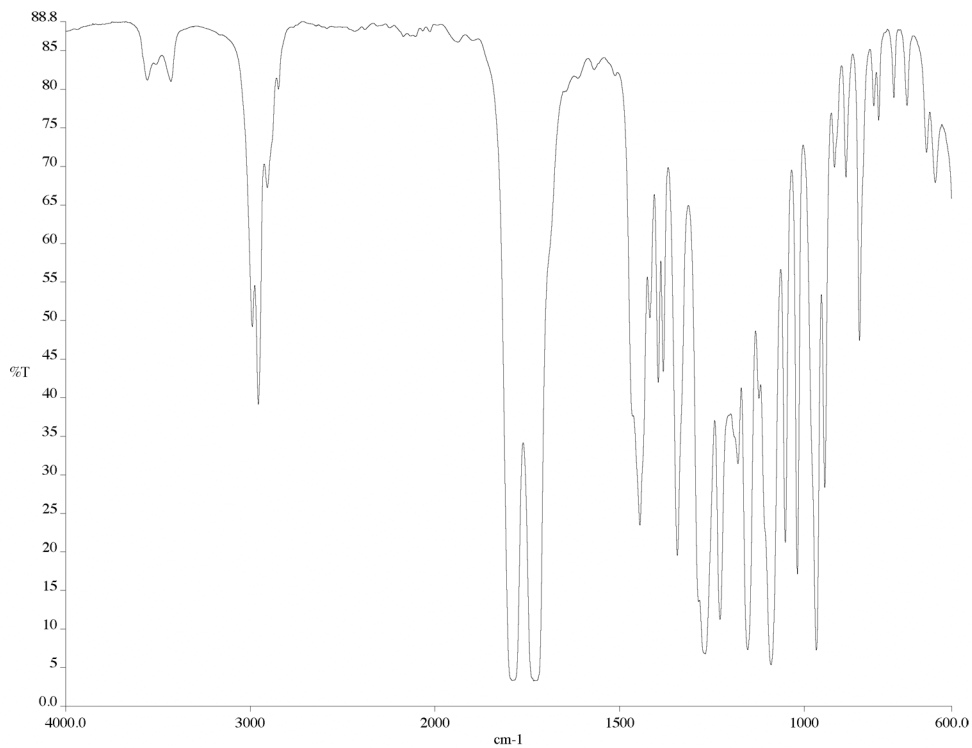


Figure E.14 Infrared spectrum (thin film/NaCl) of compound **346**.

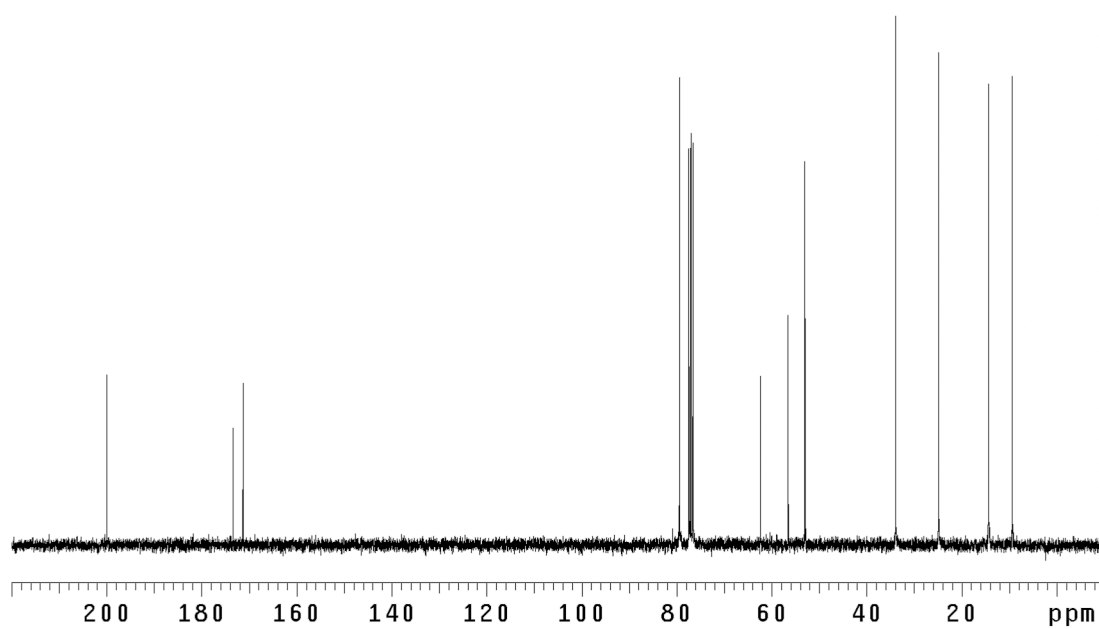


Figure E.15  $^{13}\text{C}$  NMR (125 MHz,  $\text{CDCl}_3$ ) of compound **346**.

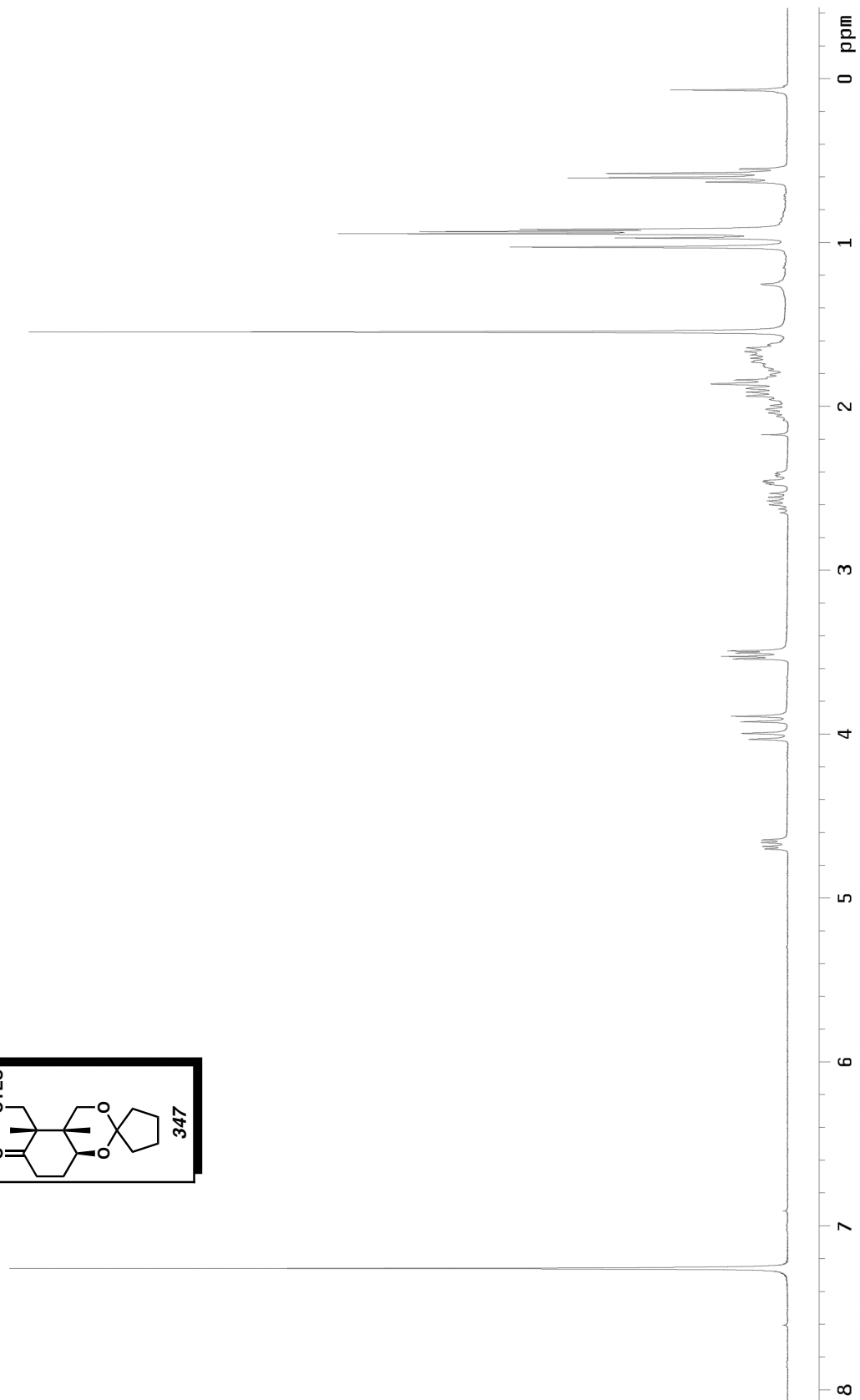
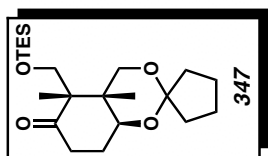


Figure E.16  $^1\text{H}$  NMR (500 MHz,  $\text{CDCl}_3$ ) of compound **347**.

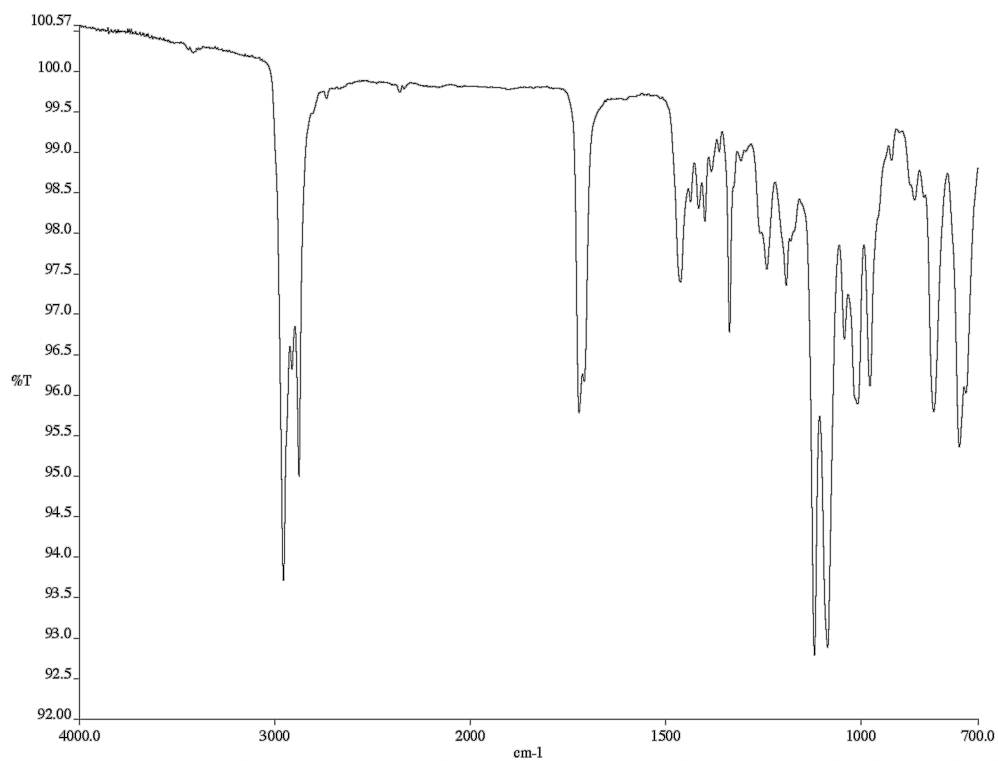


Figure E.17 Infrared spectrum (thin film/NaCl) of compound **347**.

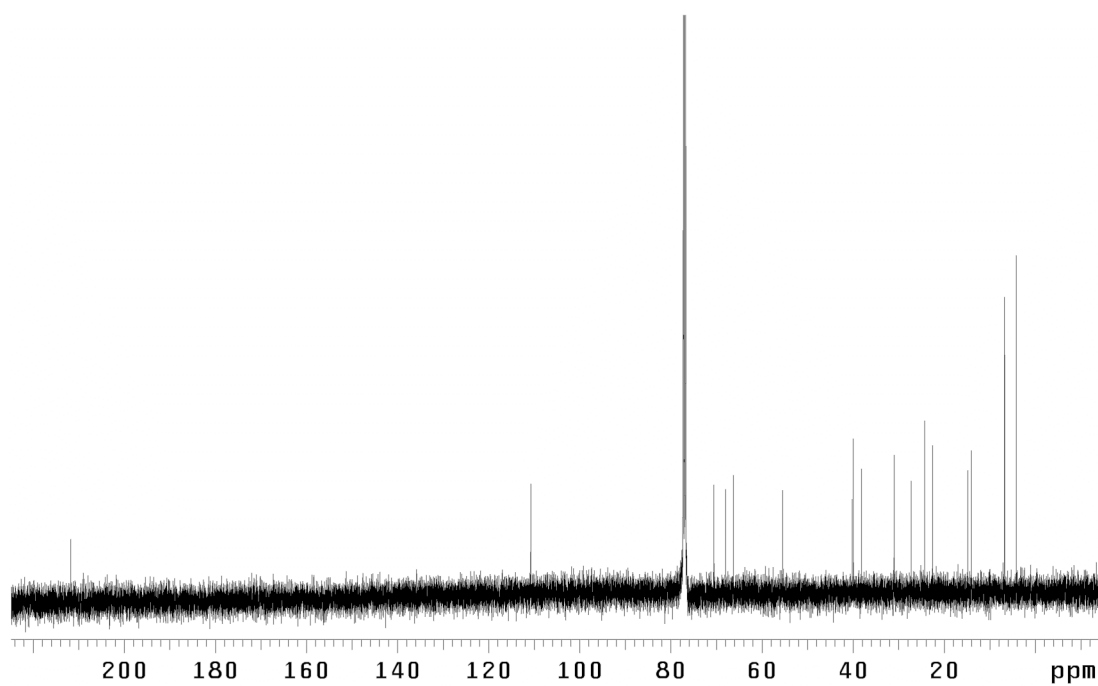


Figure E.18 <sup>13</sup>C NMR (125 MHz, CDCl<sub>3</sub>) of compound **347**.

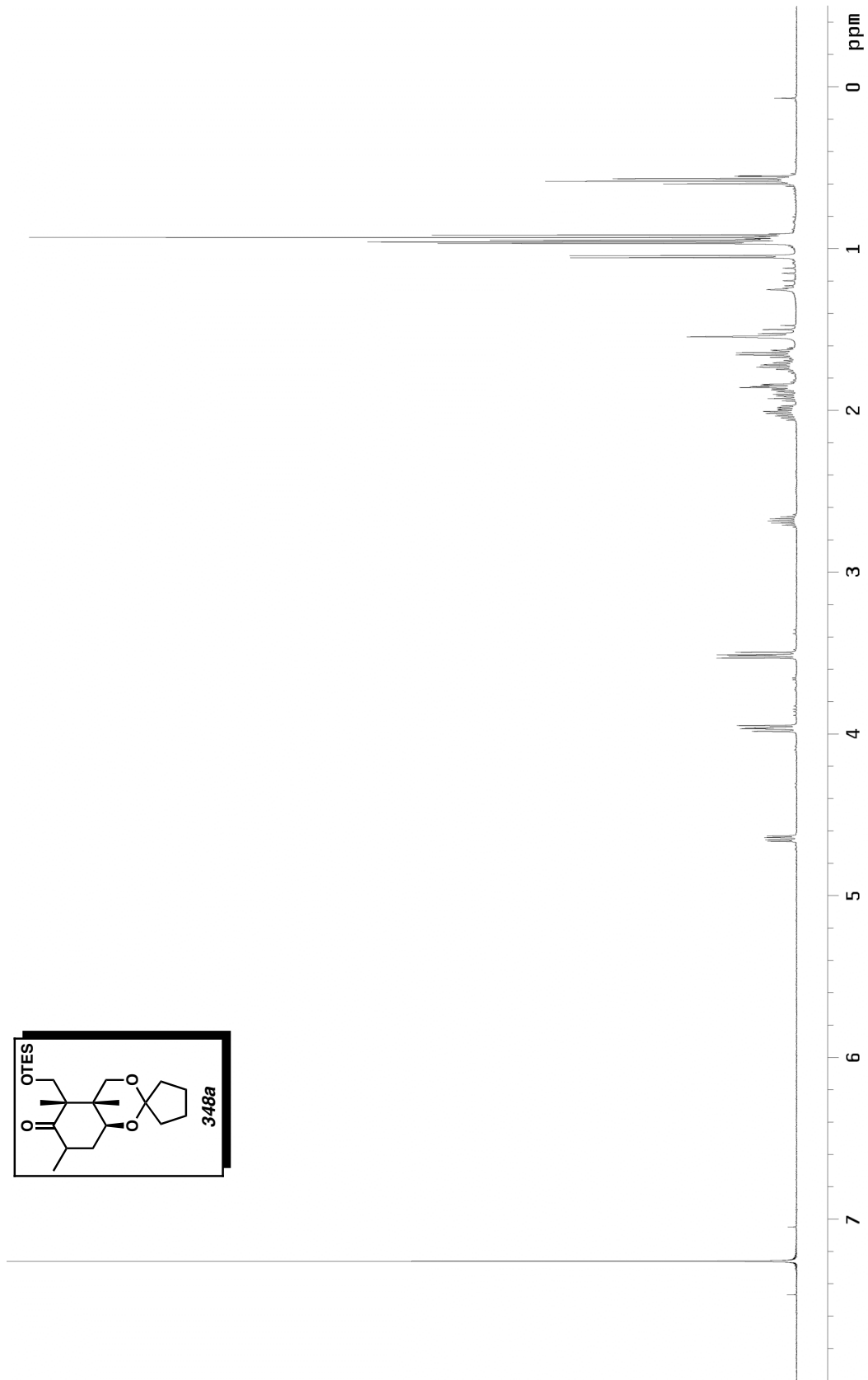
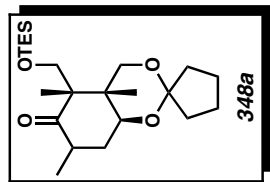


Figure E.19  $^1\text{H}$  NMR (300 MHz,  $\text{CDCl}_3$ ) of compound 348a.

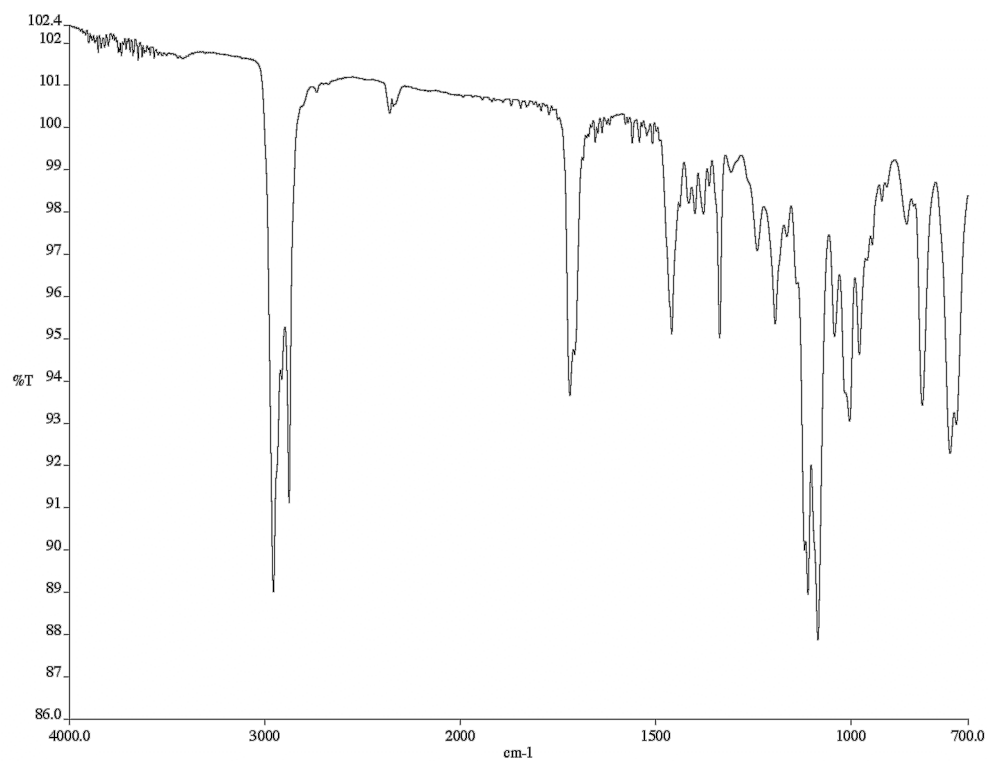


Figure E.20 Infrared spectrum (thin film/NaCl) of compound **348a**.

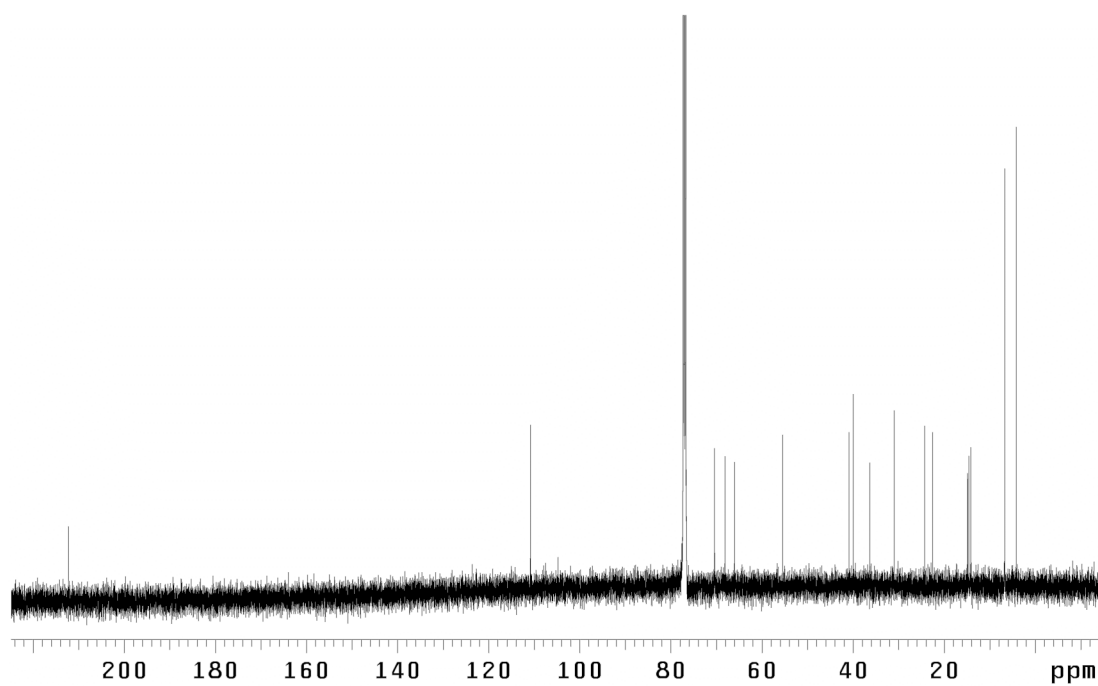


Figure E.20 <sup>13</sup>C NMR (125 MHz, CDCl<sub>3</sub>) of compound **348a**.

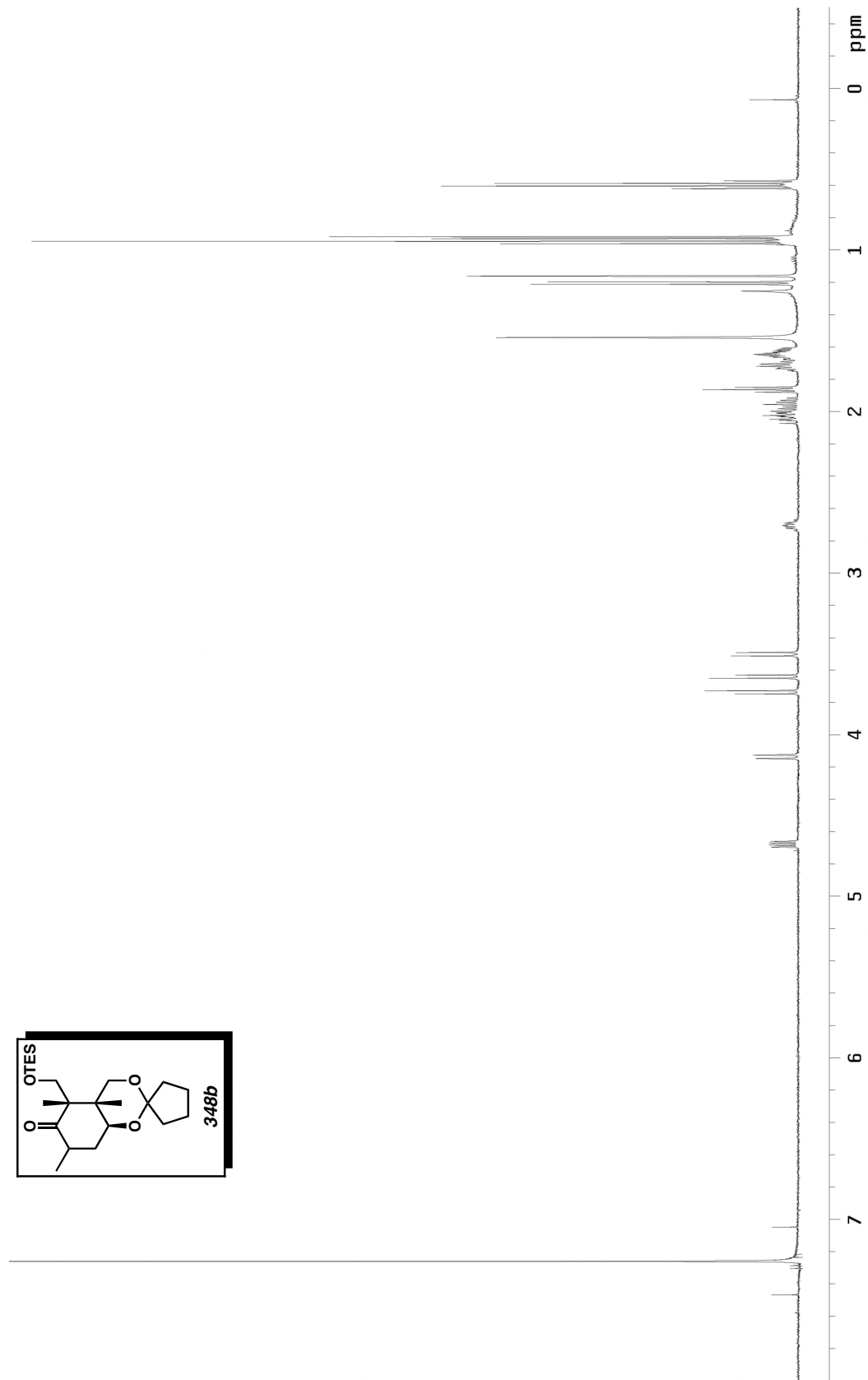
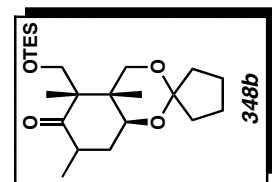


Figure E.22 <sup>1</sup>H NMR (500 MHz, CDCl<sub>3</sub>) of compound **348b**.

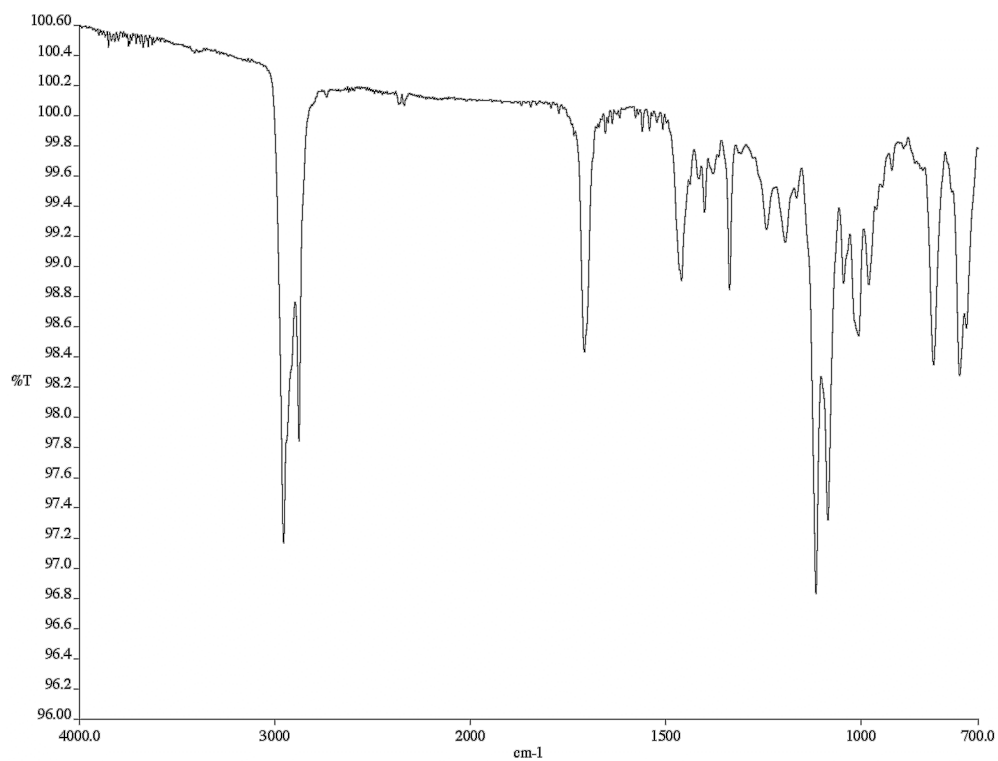


Figure E.23 Infrared spectrum (thin film/NaCl) of compound **348b**.

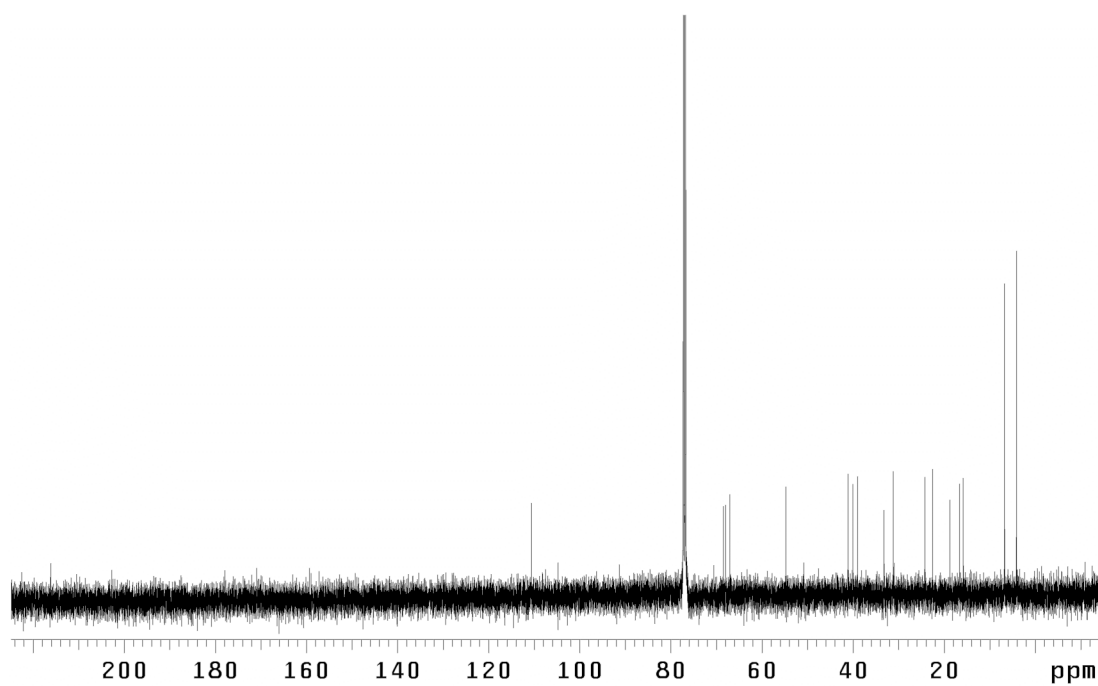


Figure E.24 <sup>13</sup>C NMR (125 MHz, CDCl<sub>3</sub>) of compound **348b**.

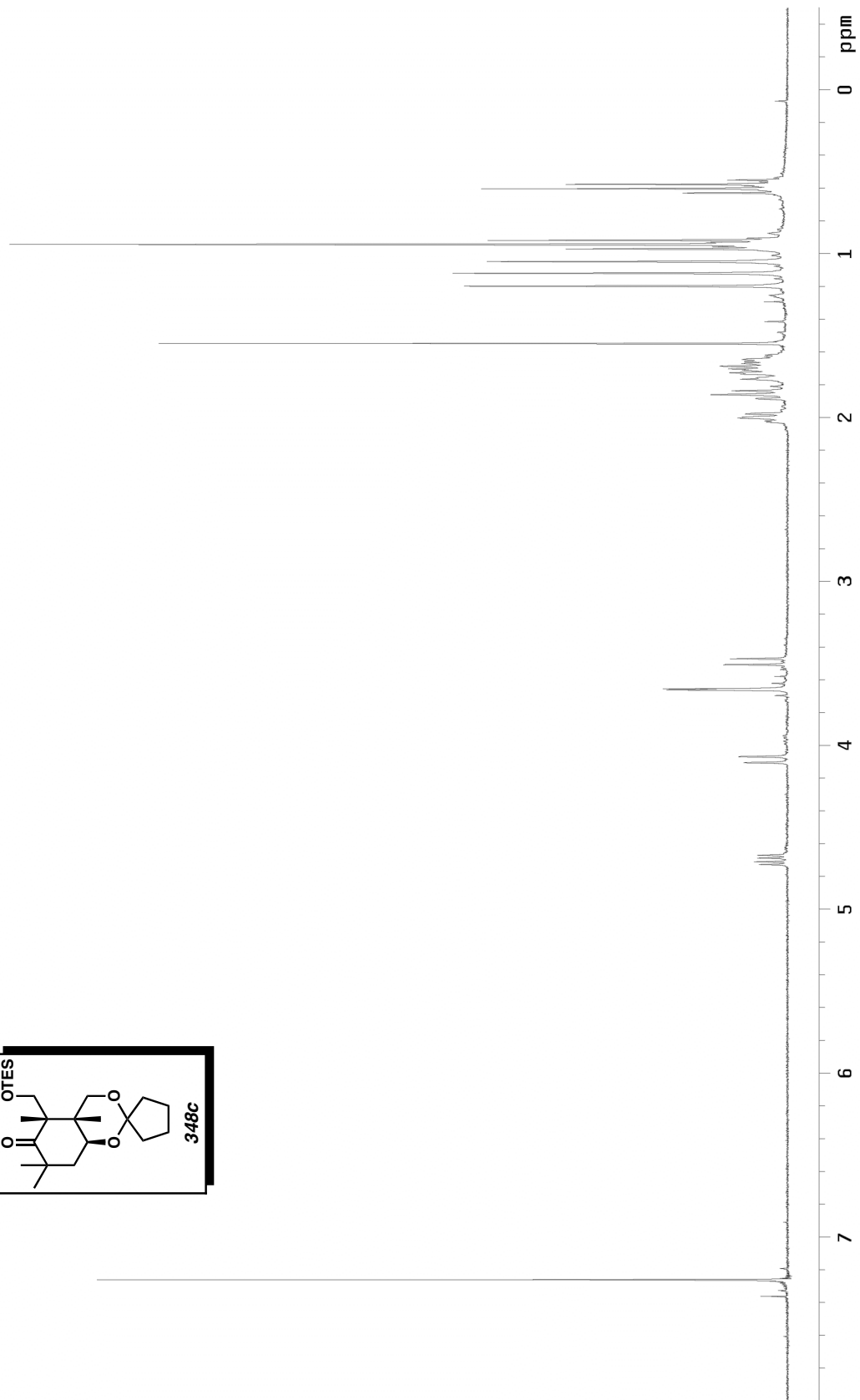
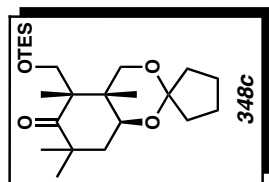


Figure E.25  $^1\text{H}$  NMR (300 MHz,  $\text{CDCl}_3$ ) of compound **348c**.

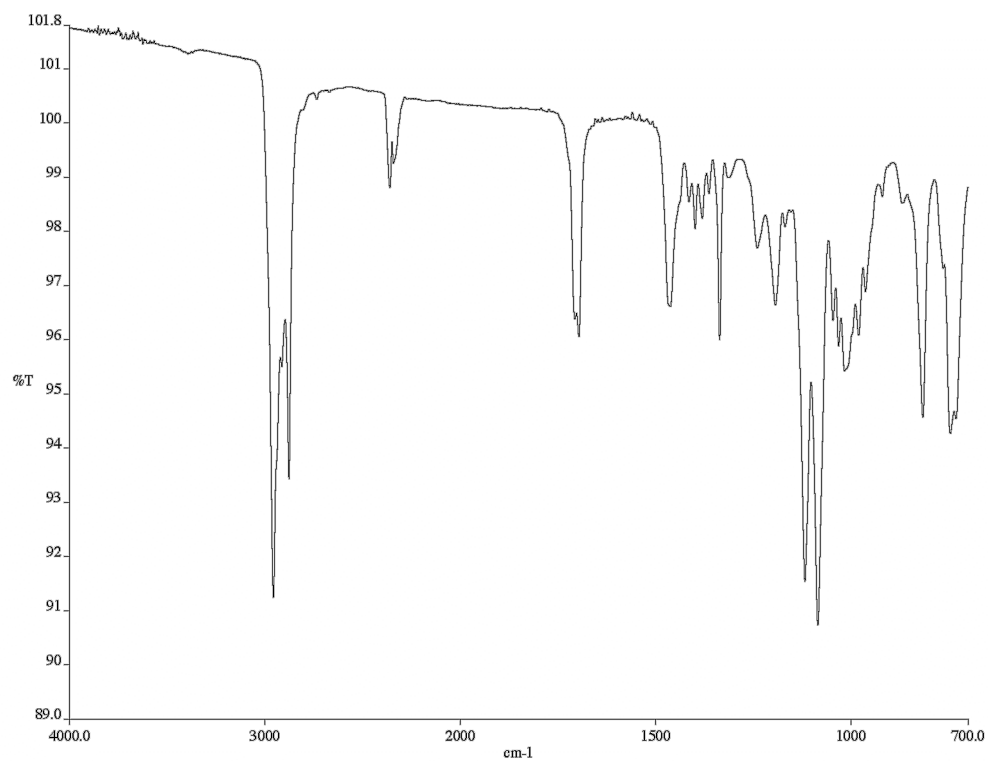


Figure E.26 Infrared spectrum (thin film/NaCl) of compound **348c**.

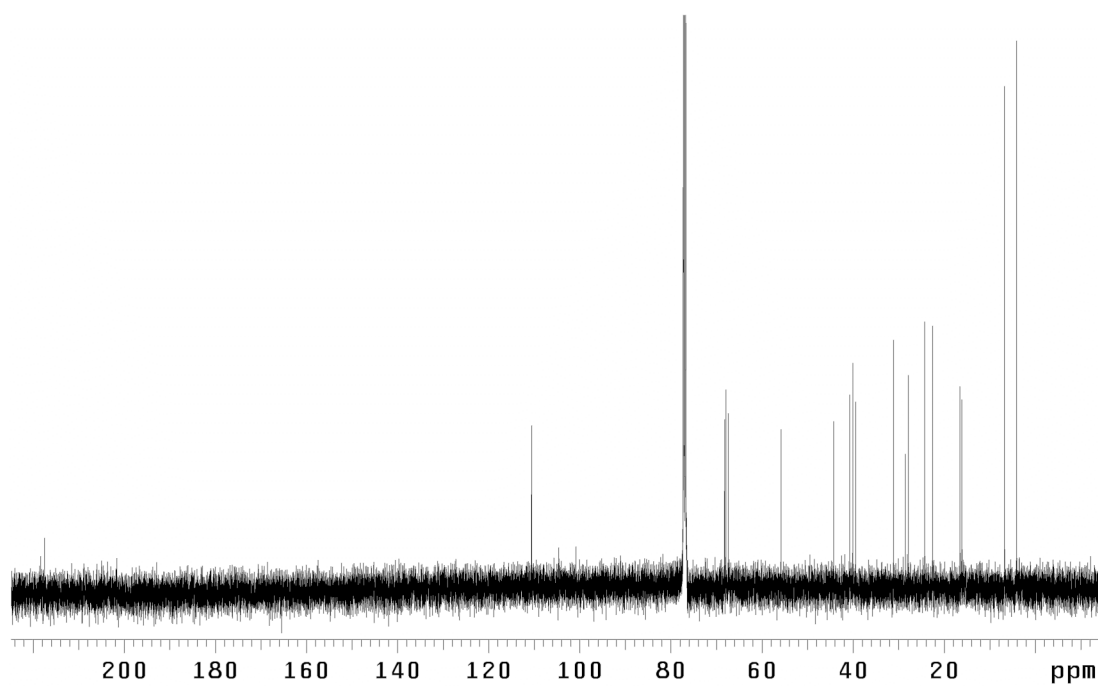


Figure E.27 <sup>13</sup>C NMR (125 MHz, CDCl<sub>3</sub>) of compound **348c**.

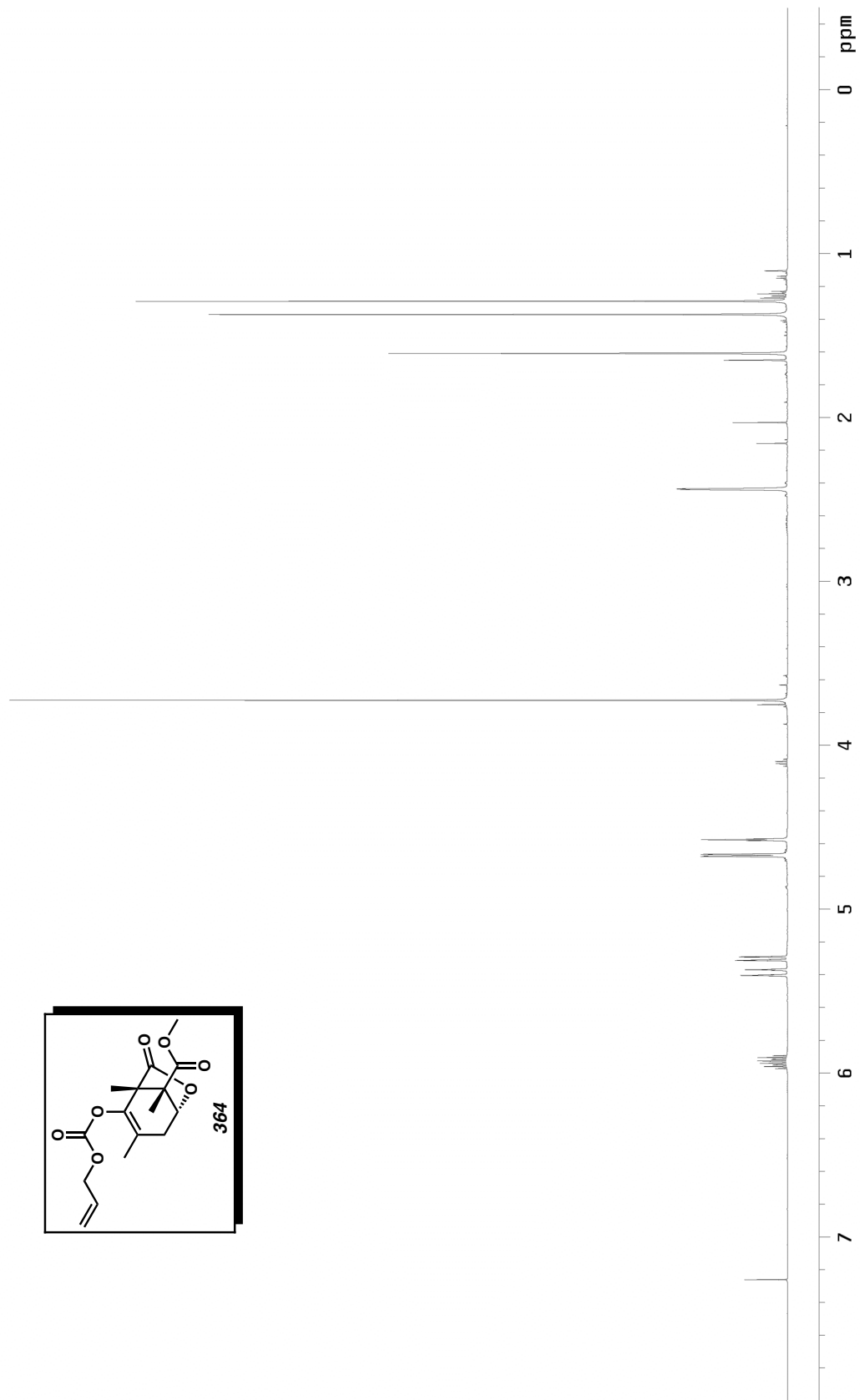
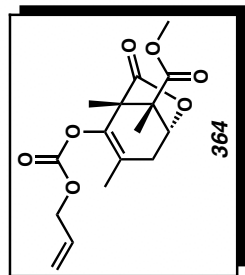


Figure E.28  $^1\text{H NMR}$  (500 MHz,  $\text{CDCl}_3$ ) of compound 364.

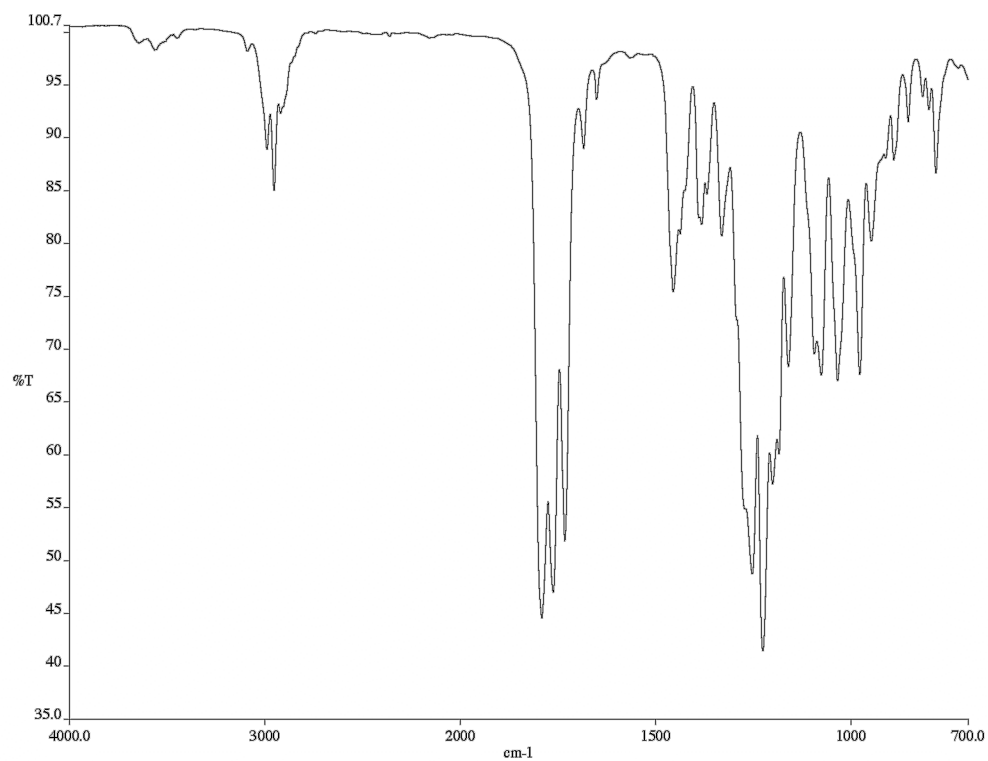


Figure E.29 Infrared spectrum (thin film/NaCl) of compound **364**.

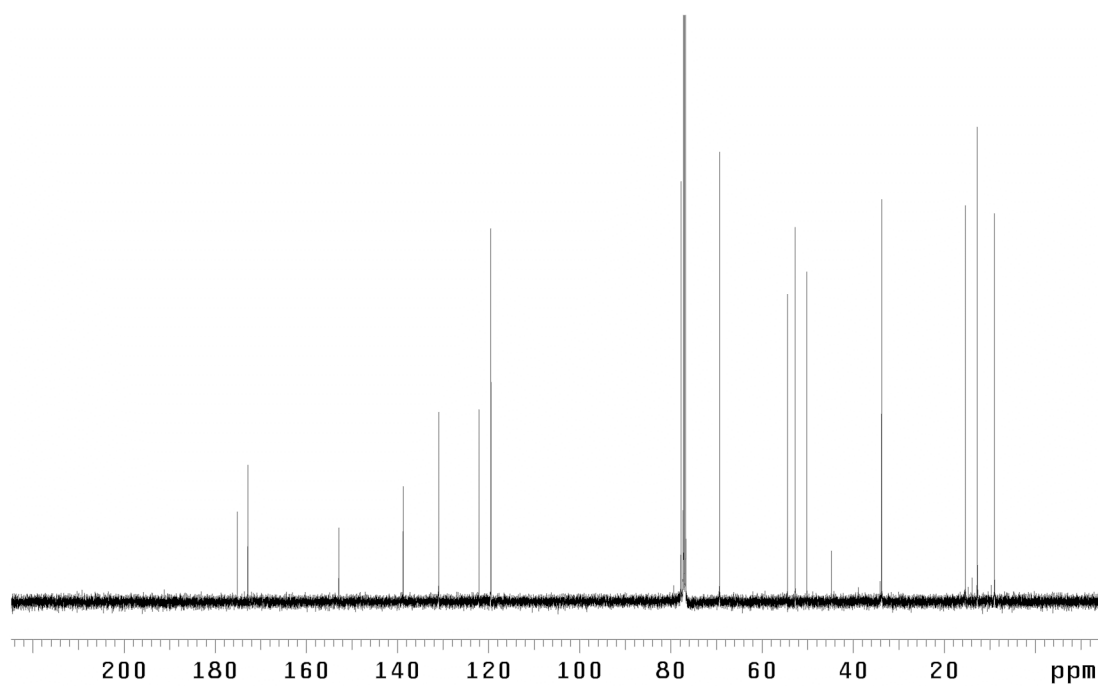


Figure E.30 <sup>13</sup>C NMR (500 MHz, CDCl<sub>3</sub>) of compound **364**.

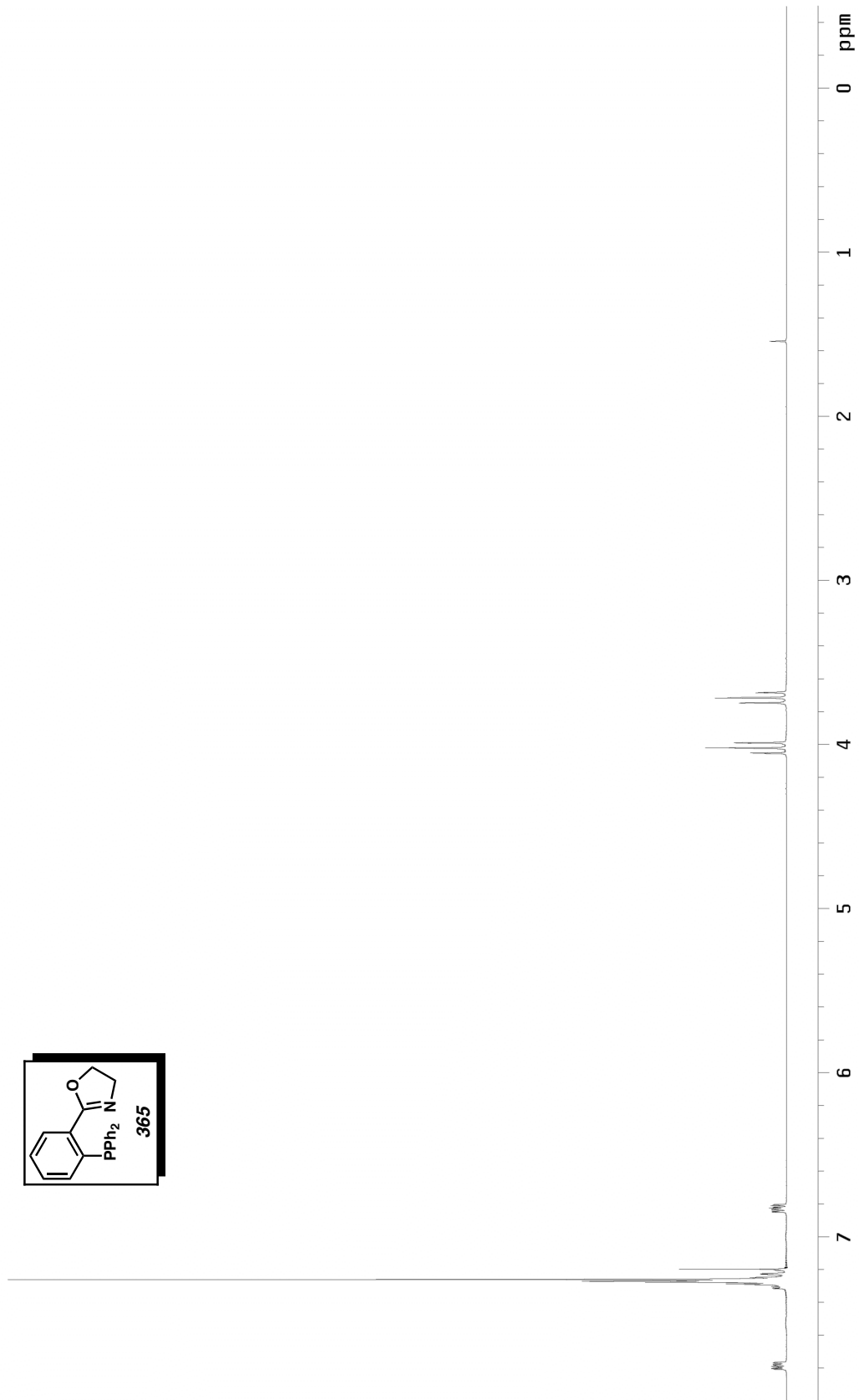
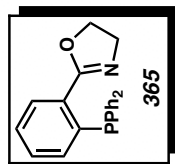


Figure E.31 <sup>1</sup>H NMR (500 MHz, CDCl<sub>3</sub>) of compound 365.

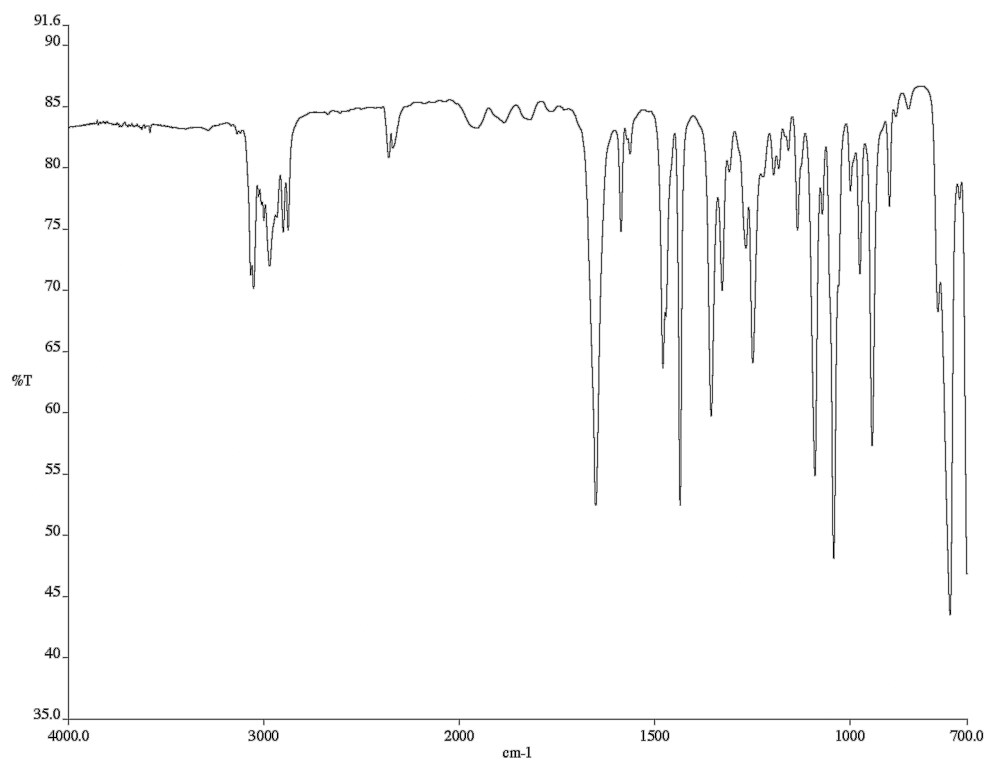


Figure E.32 Infrared spectrum (thin film/NaCl) of compound **365**.

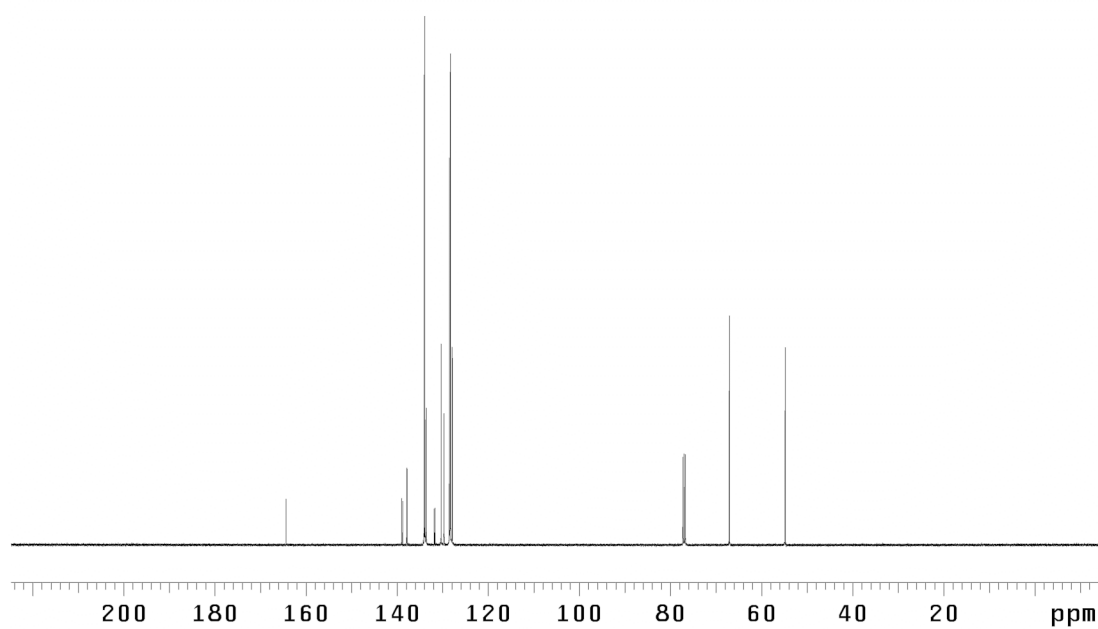
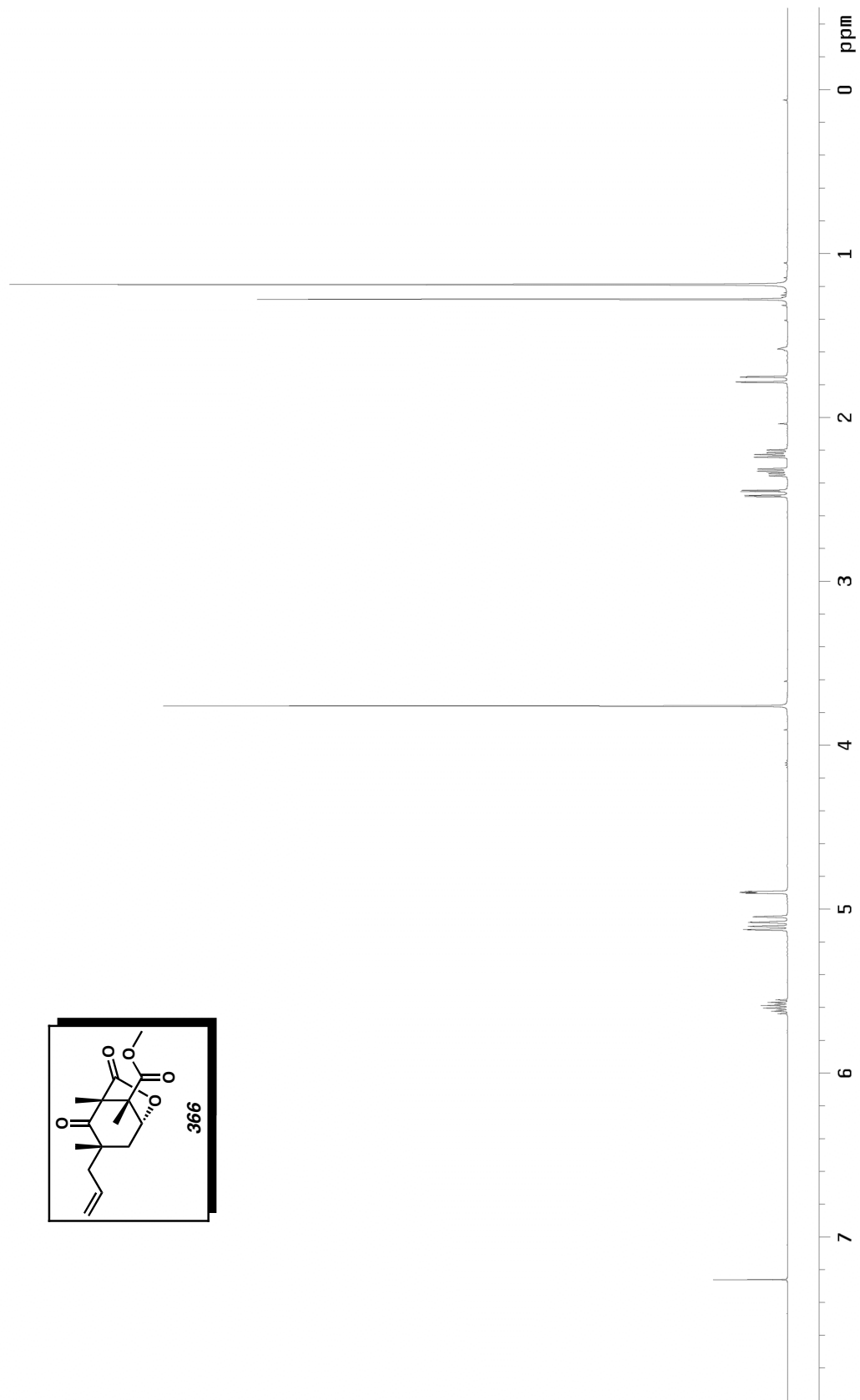
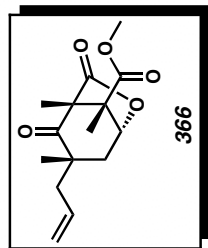


Figure E.33 <sup>13</sup>C NMR (125 MHz, CDCl<sub>3</sub>) of compound **365**.



479  
*Figure E.34*  $^1\text{H}$  NMR (500 MHz,  $\text{CDCl}_3$ ) of compound **366**.

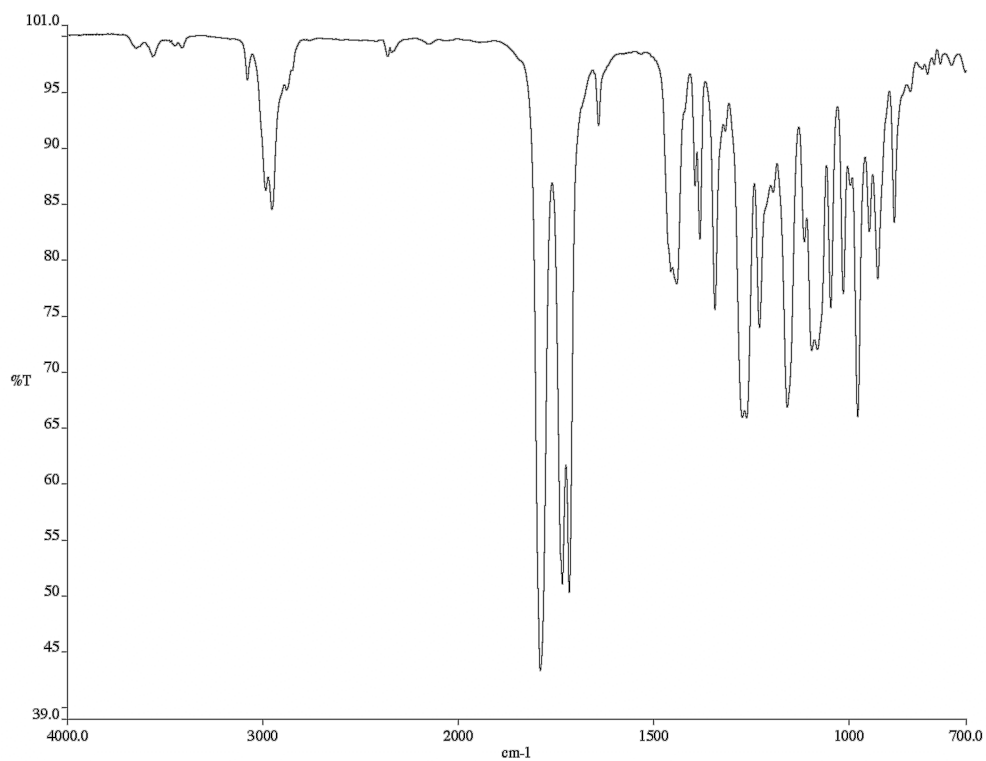


Figure E.35 Infrared spectrum (thin film/NaCl) of compound **366**.

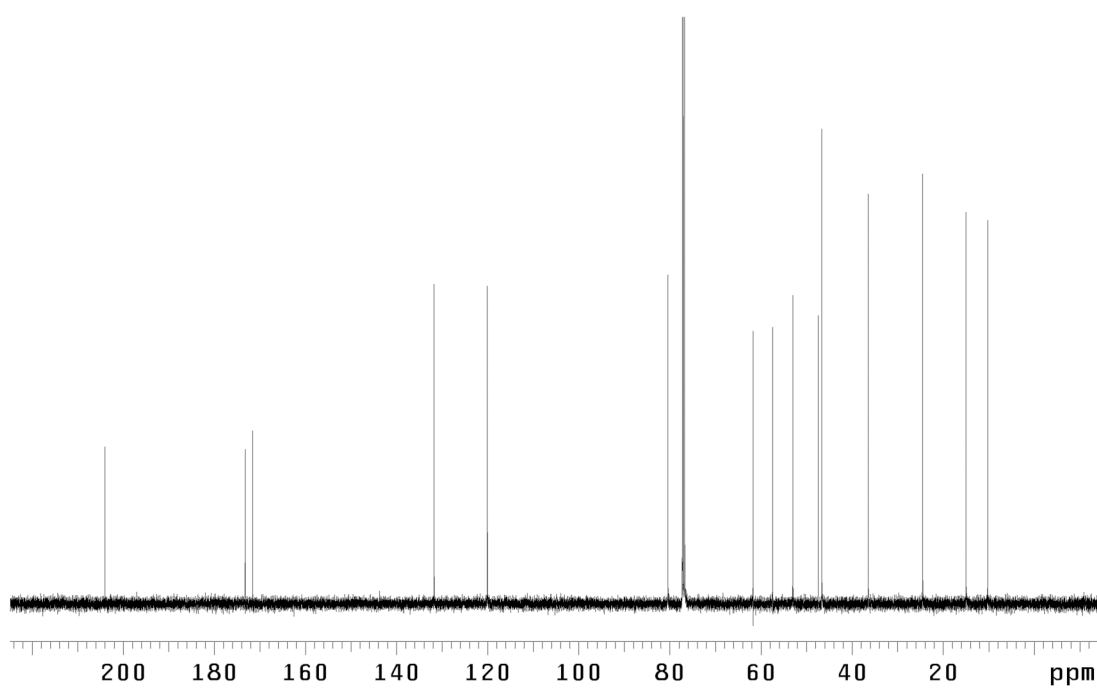


Figure E.36 <sup>13</sup>C NMR (125 MHz, CDCl<sub>3</sub>) of compound **366**.

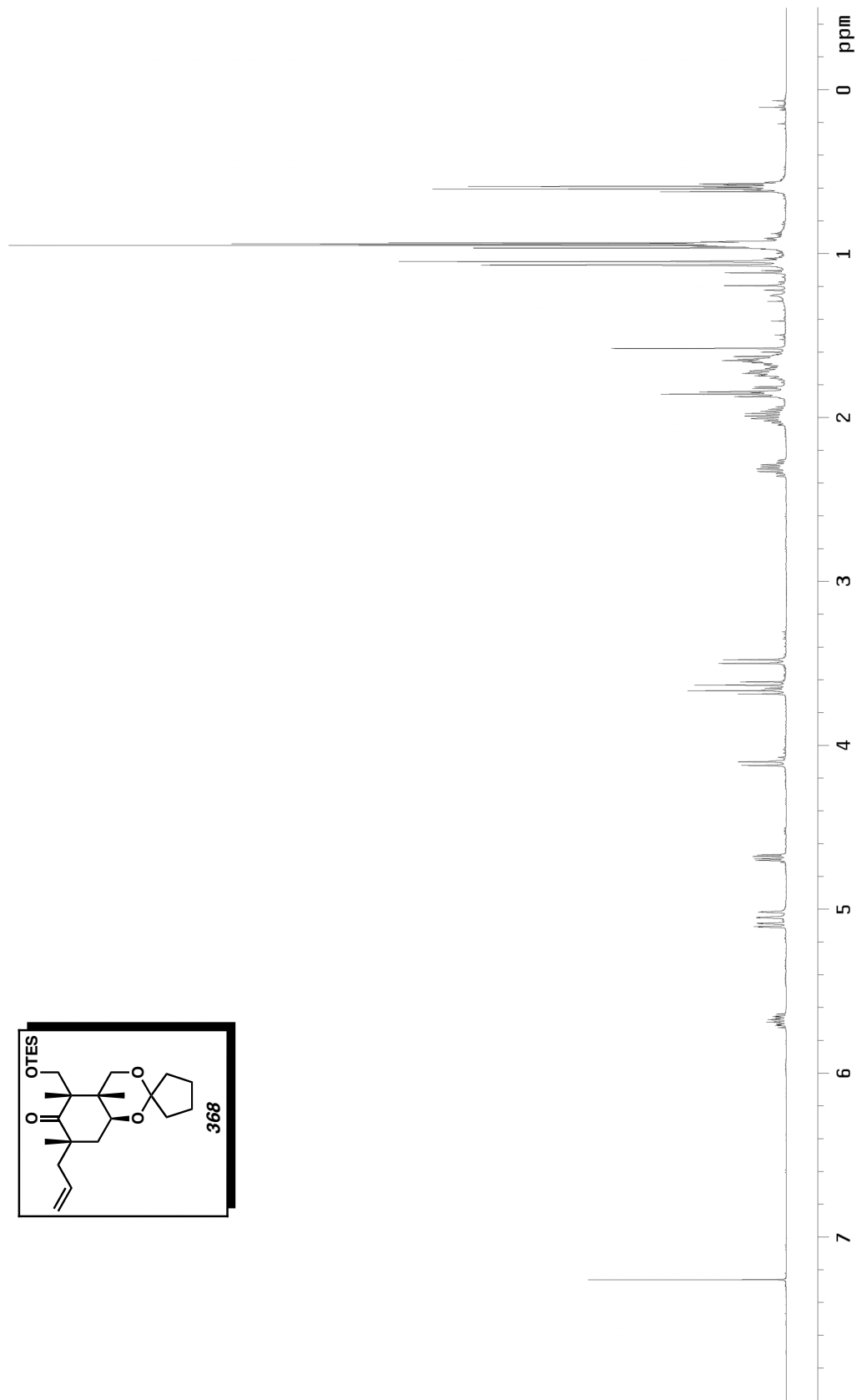
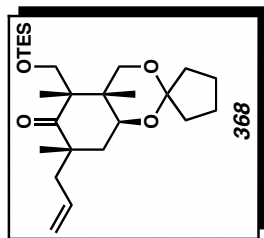


Figure E.37  $^1\text{H}$  NMR (500 MHz,  $\text{CDCl}_3$ ) of compound 368.

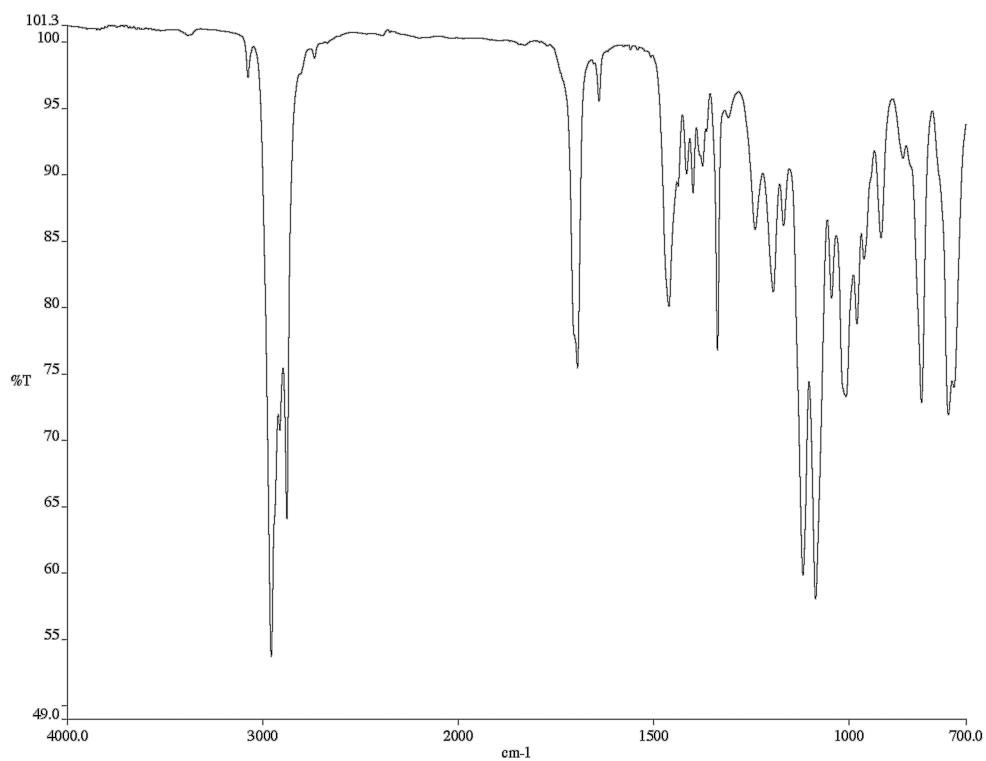


Figure E.38 Infrared spectrum (thin film/NaCl) of compound **368**.

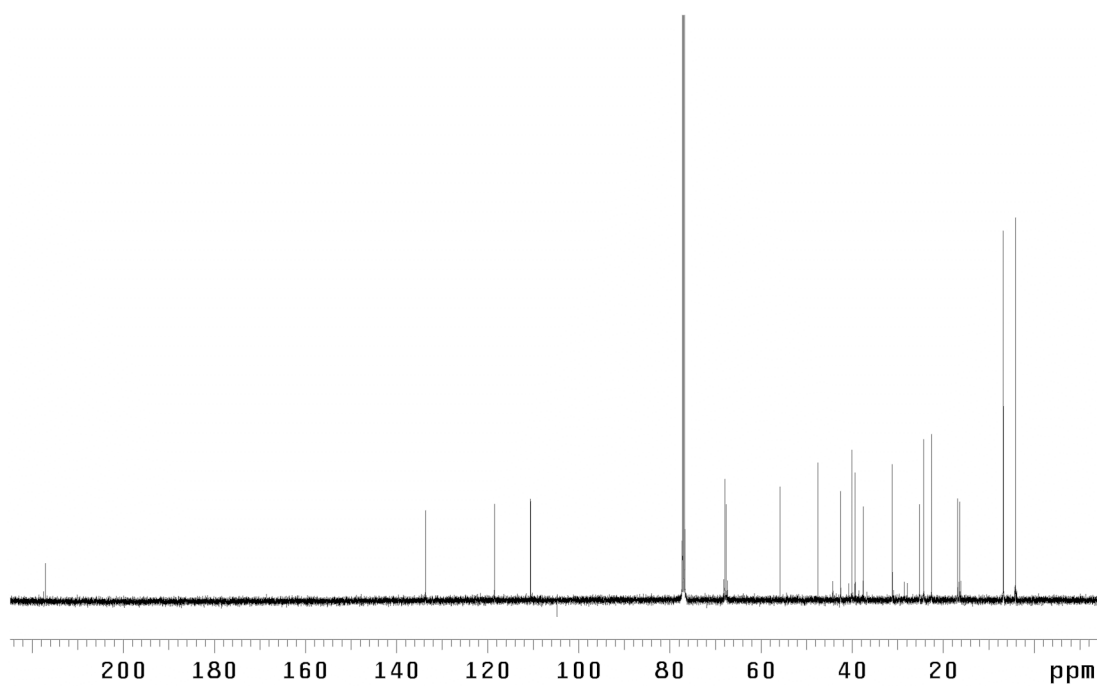


Figure E.39 <sup>13</sup>C NMR (125 MHz, CDCl<sub>3</sub>) of compound **368**.

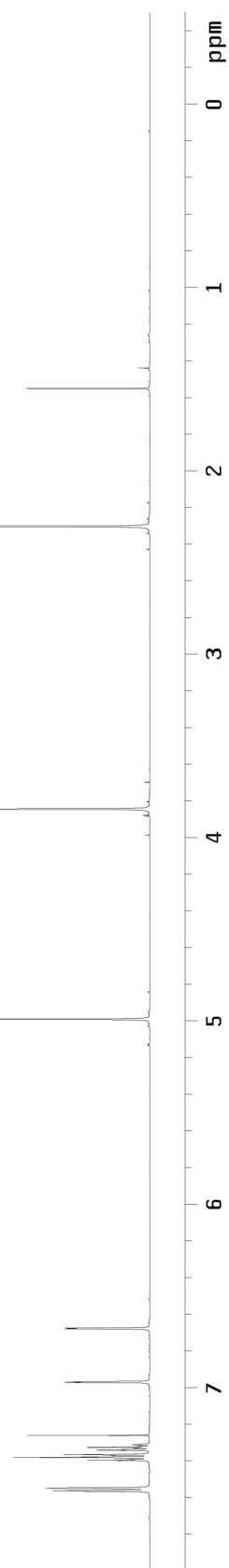
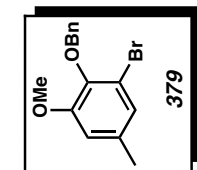


Figure E.40  $^1\text{H}$  NMR (500 MHz,  $\text{CDCl}_3$ ) of compound 379.

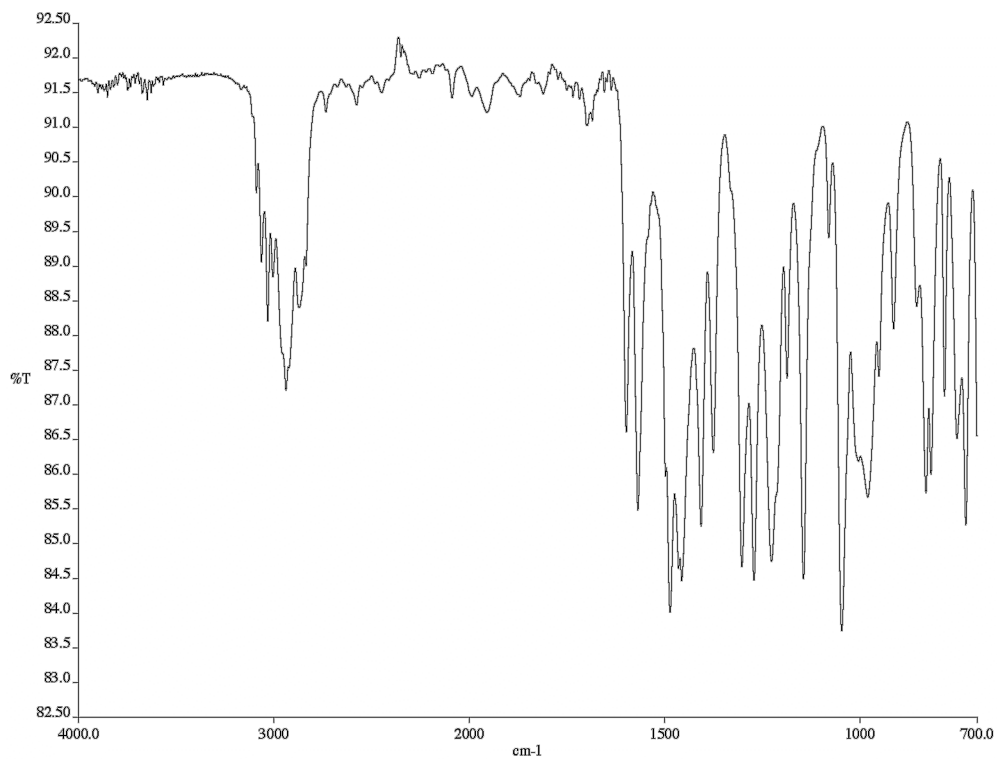


Figure E.41 Infrared spectrum (thin film/NaCl) of compound **370**.

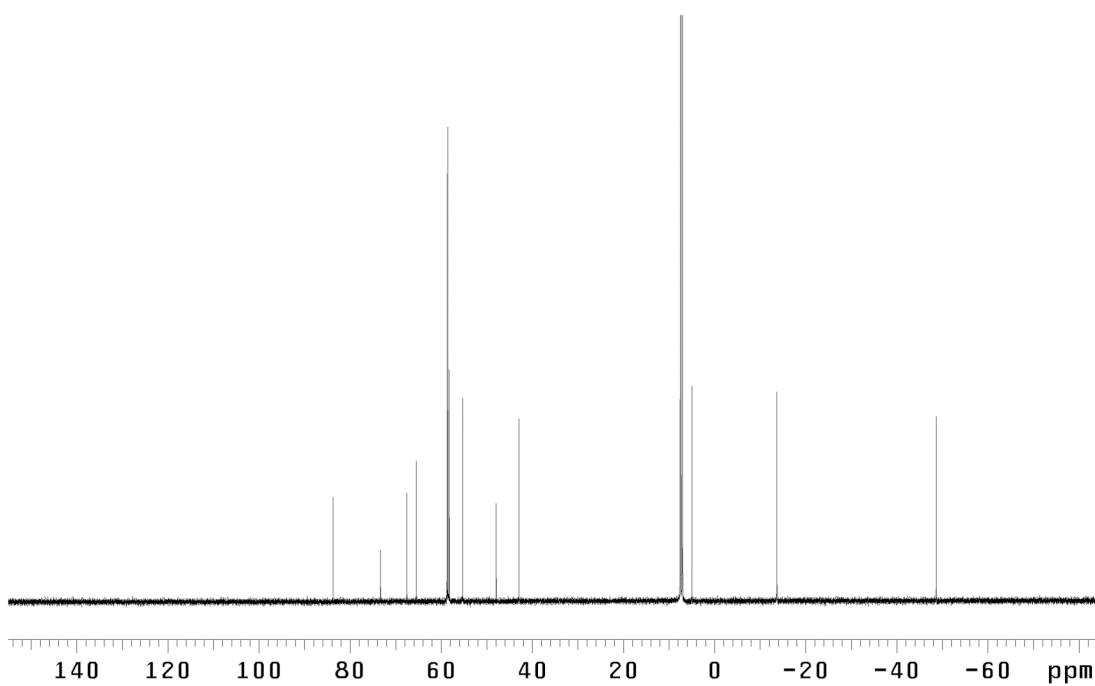


Figure E.42 <sup>13</sup>C NMR (125 MHz, CDCl<sub>3</sub>) of compound **379**.

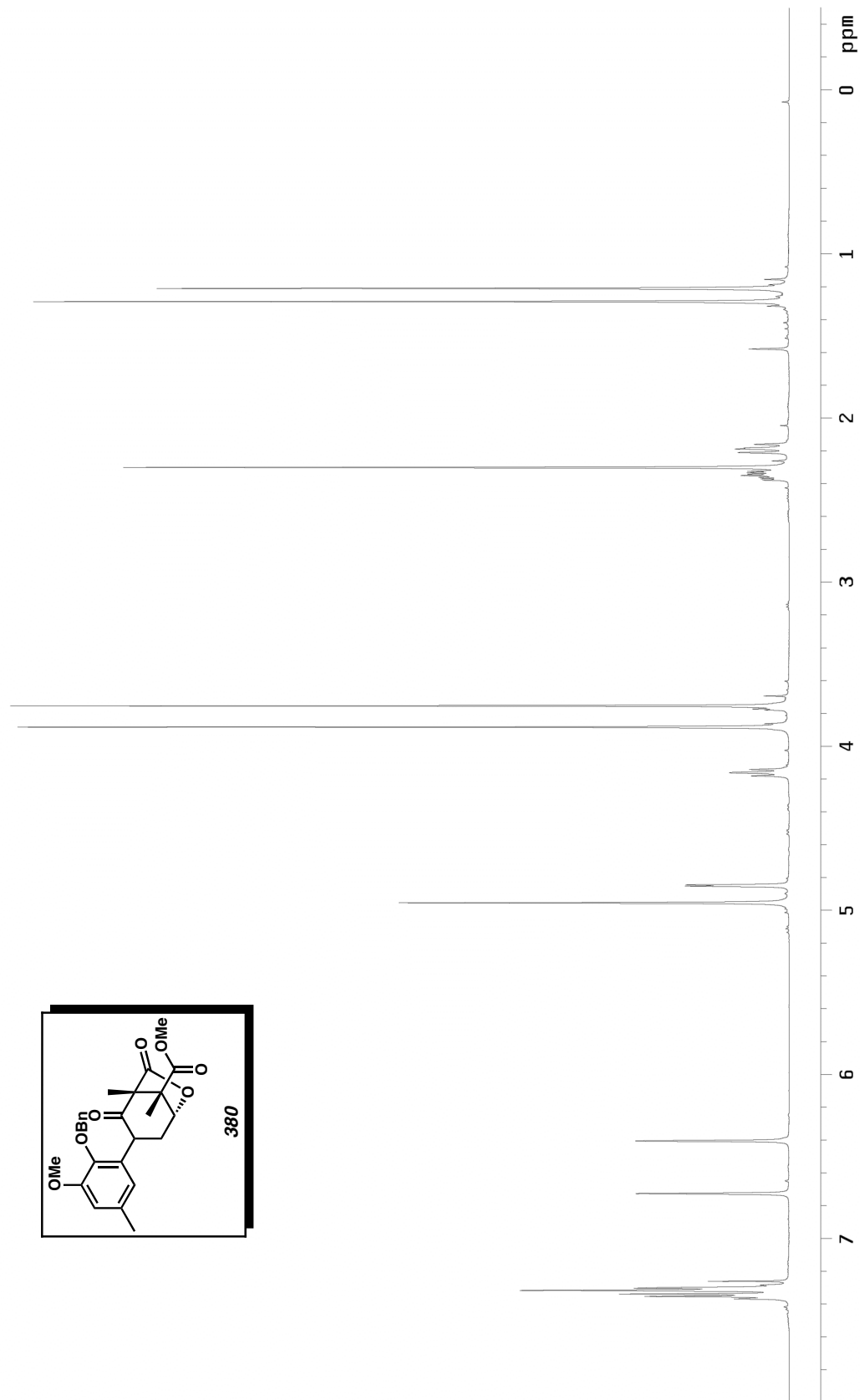


Figure E.43  $^1\text{H}$  NMR (300 MHz,  $\text{CDCl}_3$ ) of compound **380**.

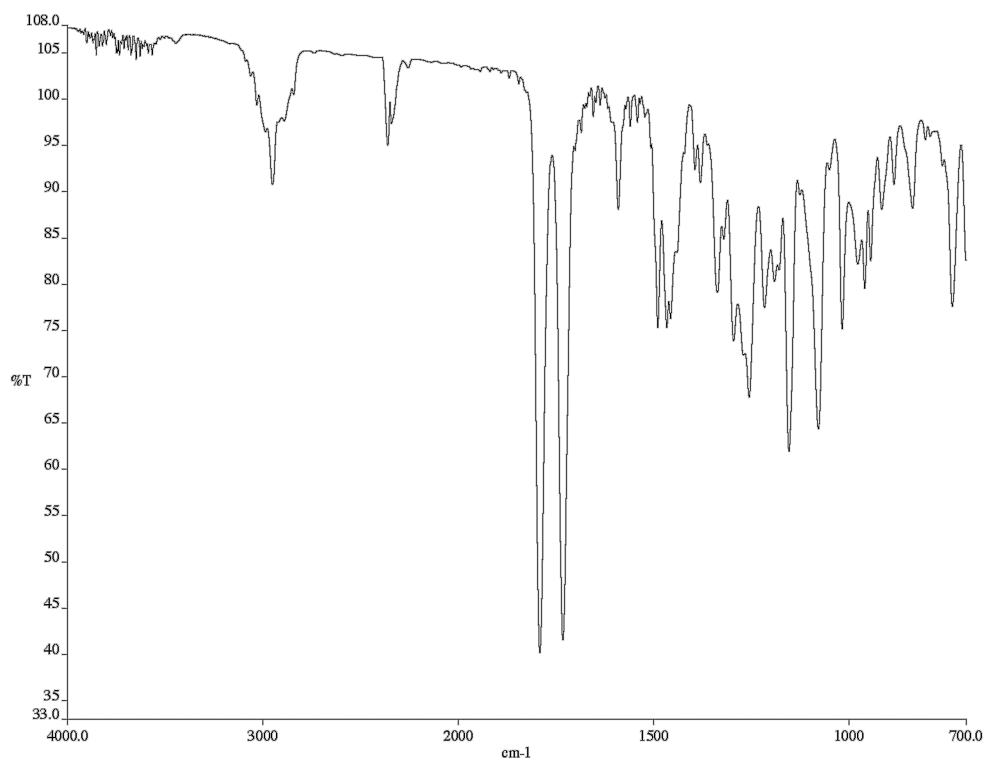


Figure E.44 Infrared spectrum (thin film/NaCl) of compound **380**.

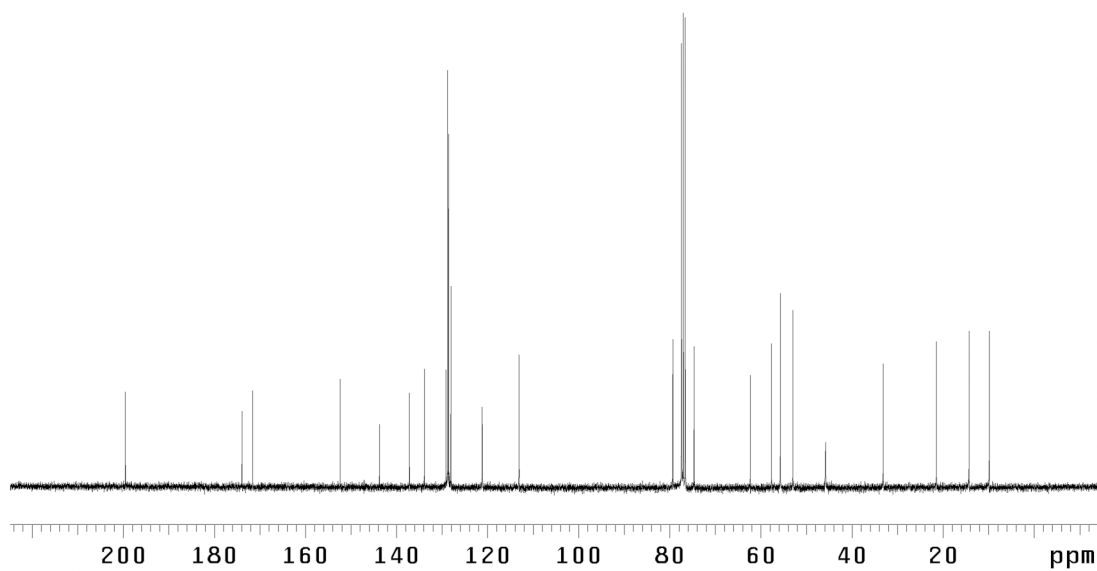


Figure E.45 <sup>13</sup>C NMR (75 MHz, CDCl<sub>3</sub>) of compound **380**.

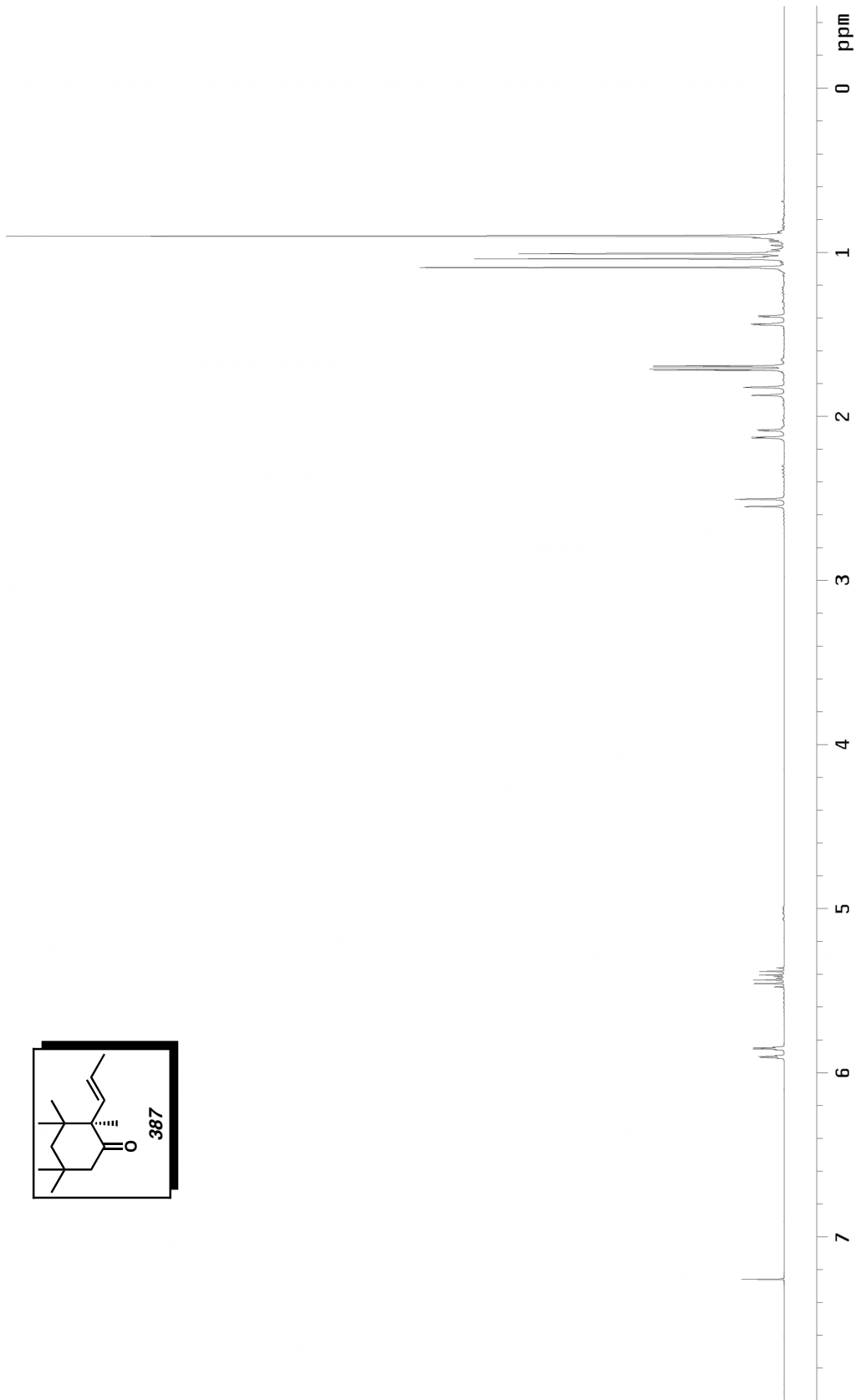
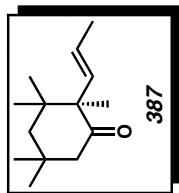


Figure E.46  $^1\text{H}$  NMR (300 MHz,  $\text{CDCl}_3$ ) of compound 387.

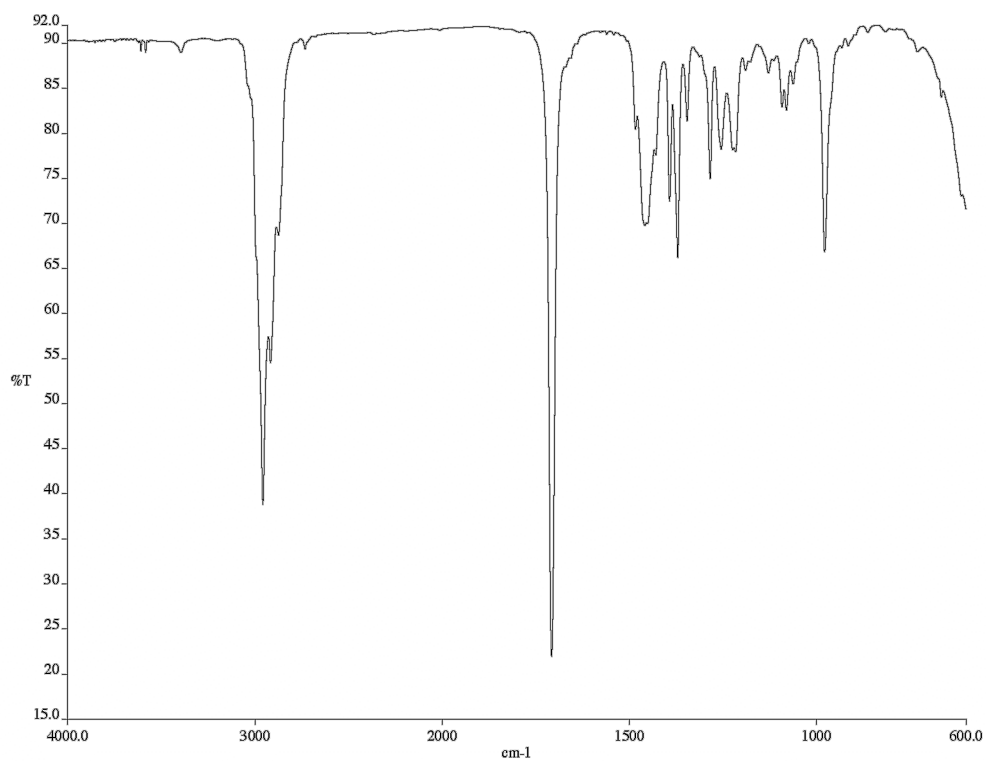


Figure E.47 Infrared spectrum (thin film/NaCl) of compound **387**.

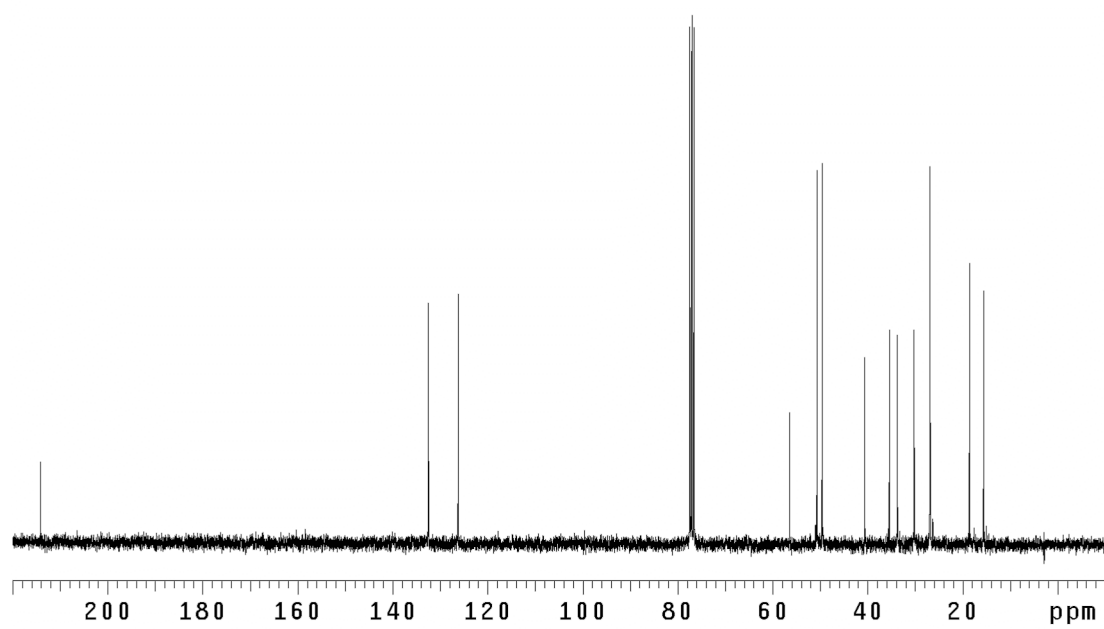


Figure E.48 <sup>13</sup>C NMR (75 MHz, CDCl<sub>3</sub>) of compound **387**.

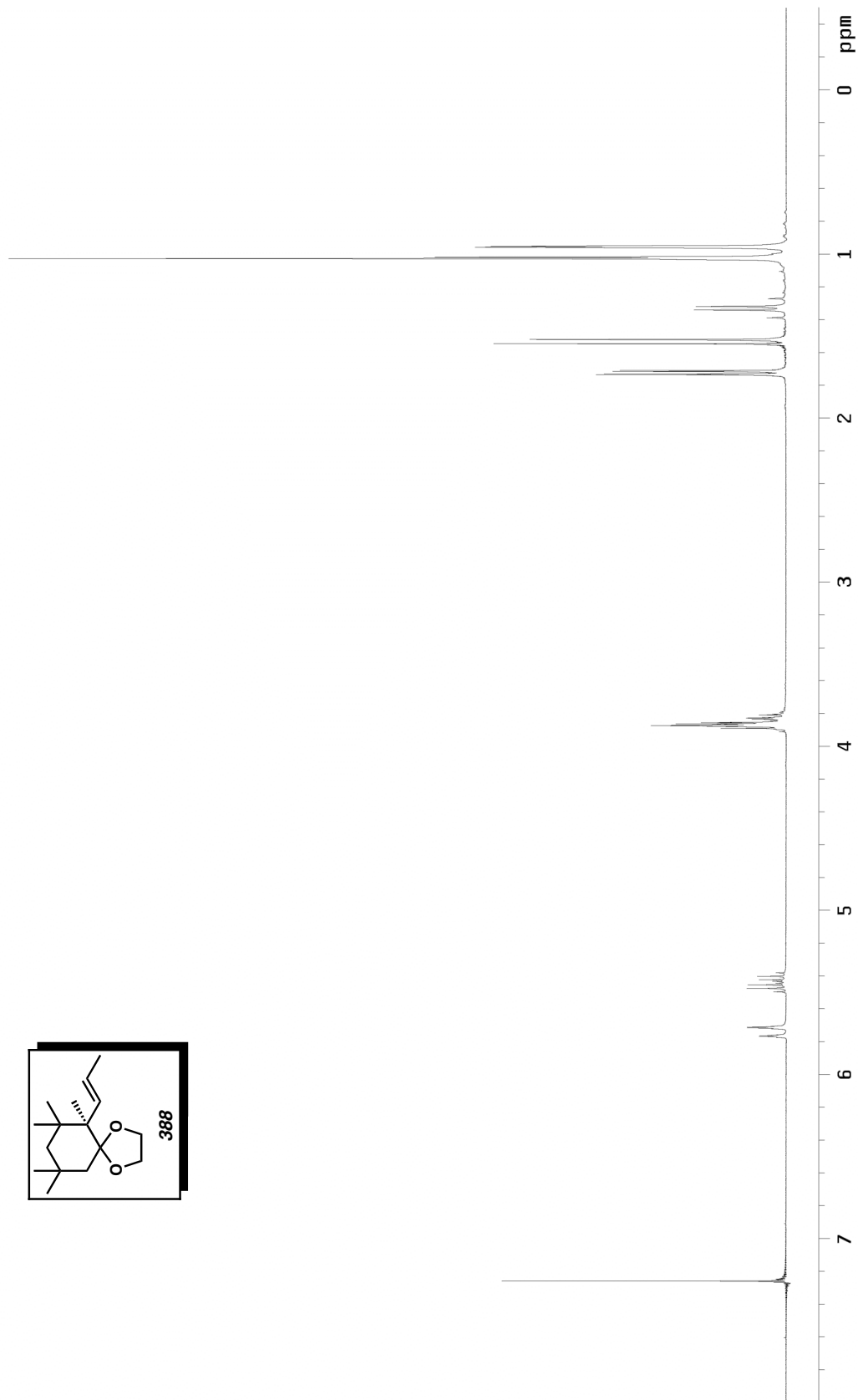
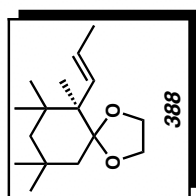


Figure E.49  $^1\text{H}$  NMR (300 MHz,  $\text{CDCl}_3$ ) of compound 388.

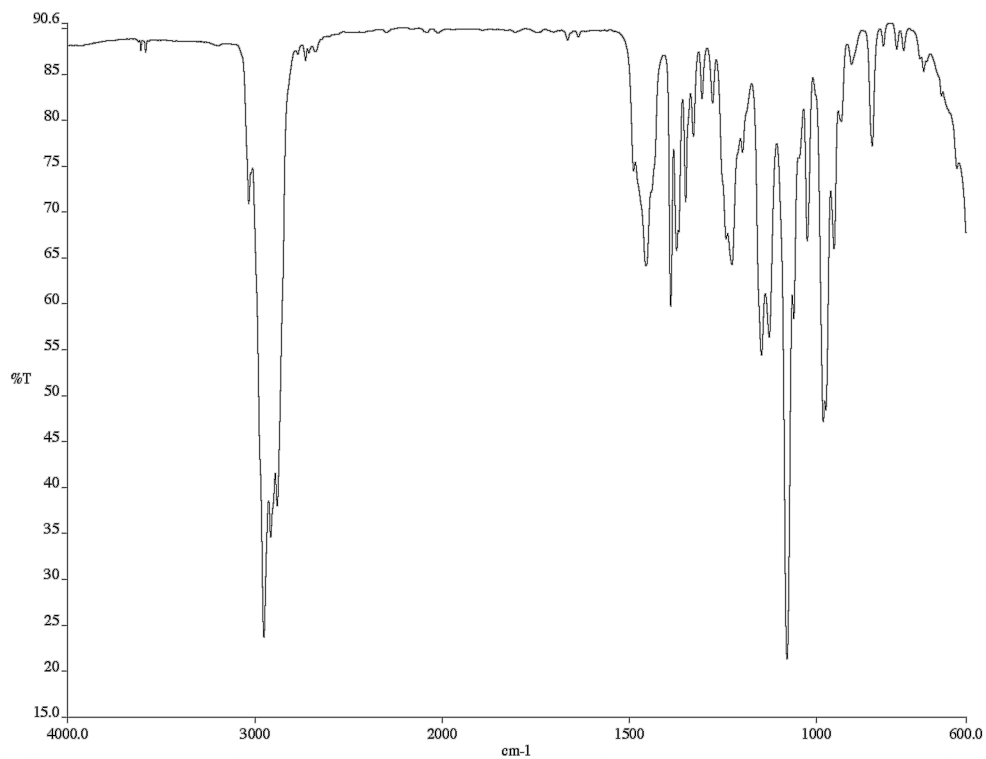


Figure E.50 Infrared spectrum (thin film/NaCl) of compound **388**.

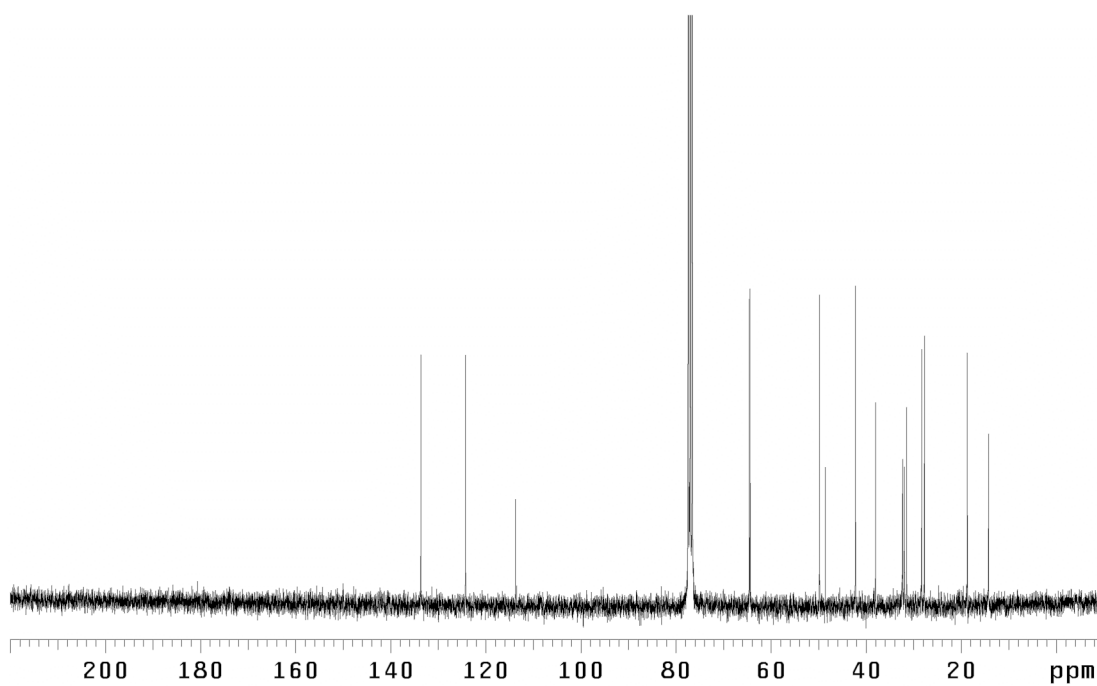


Figure E.51 <sup>13</sup>C NMR (75 MHz, CDCl<sub>3</sub>) of compound **380**.

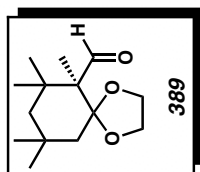
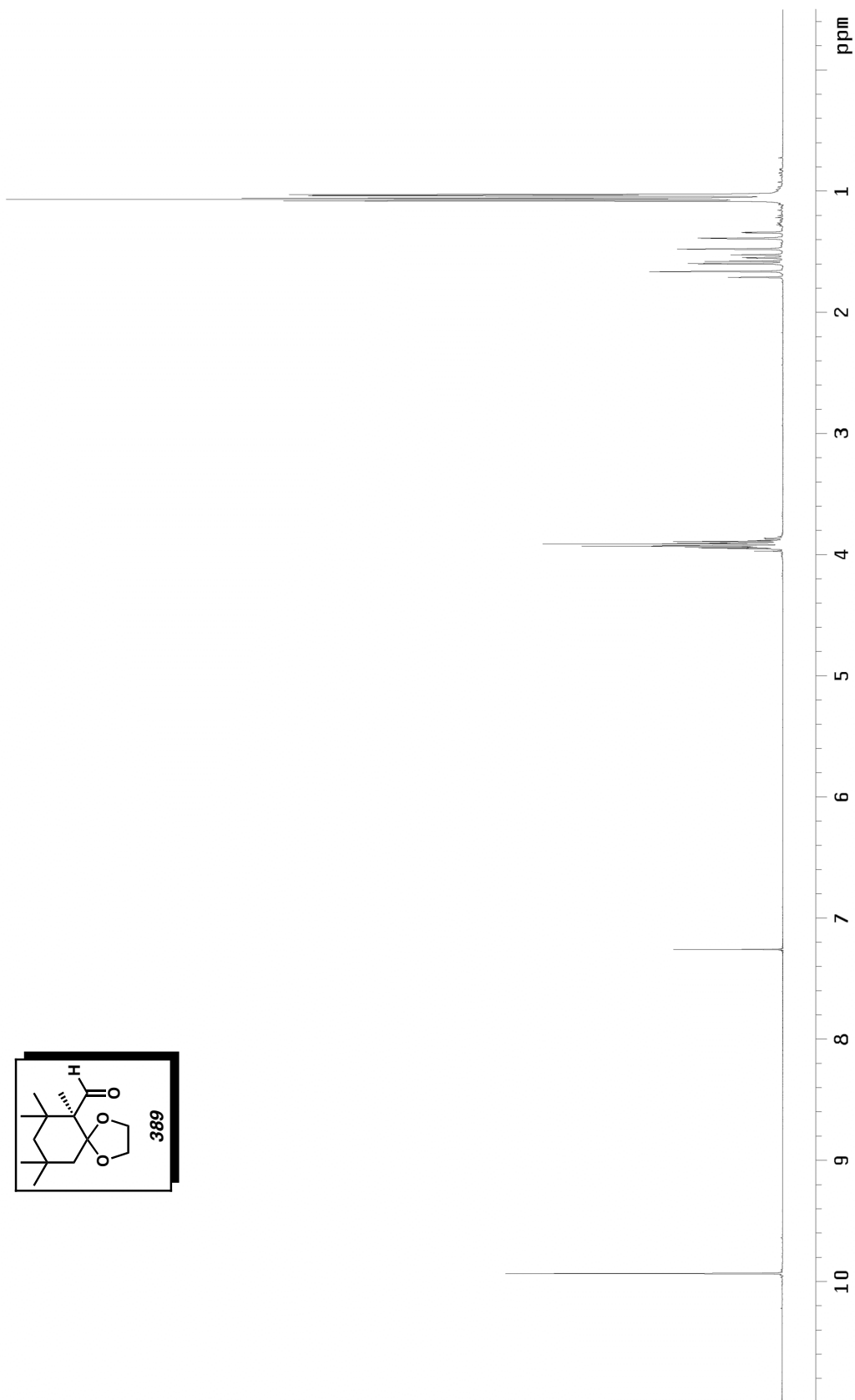


Figure E.52  $^1\text{H}$  NMR (300 MHz,  $\text{CDCl}_3$ ) of compound **389**.

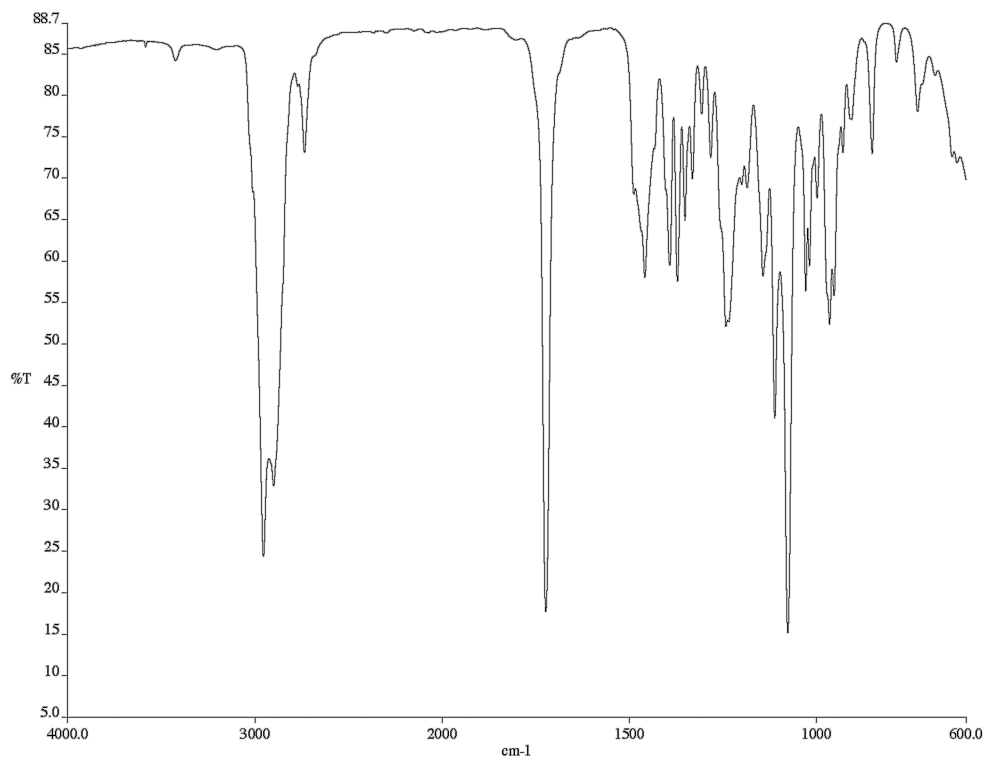


Figure E.53 Infrared spectrum (thin film/NaCl) of compound **389**.

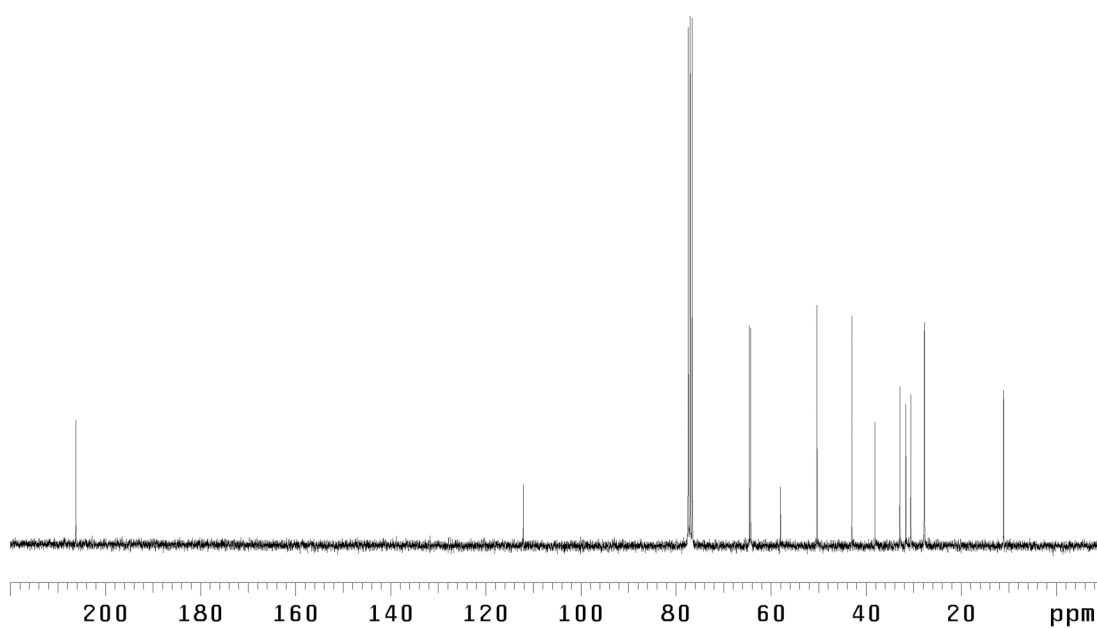


Figure E.54 <sup>13</sup>C NMR (75 MHz, CDCl<sub>3</sub>) of compound **389**.

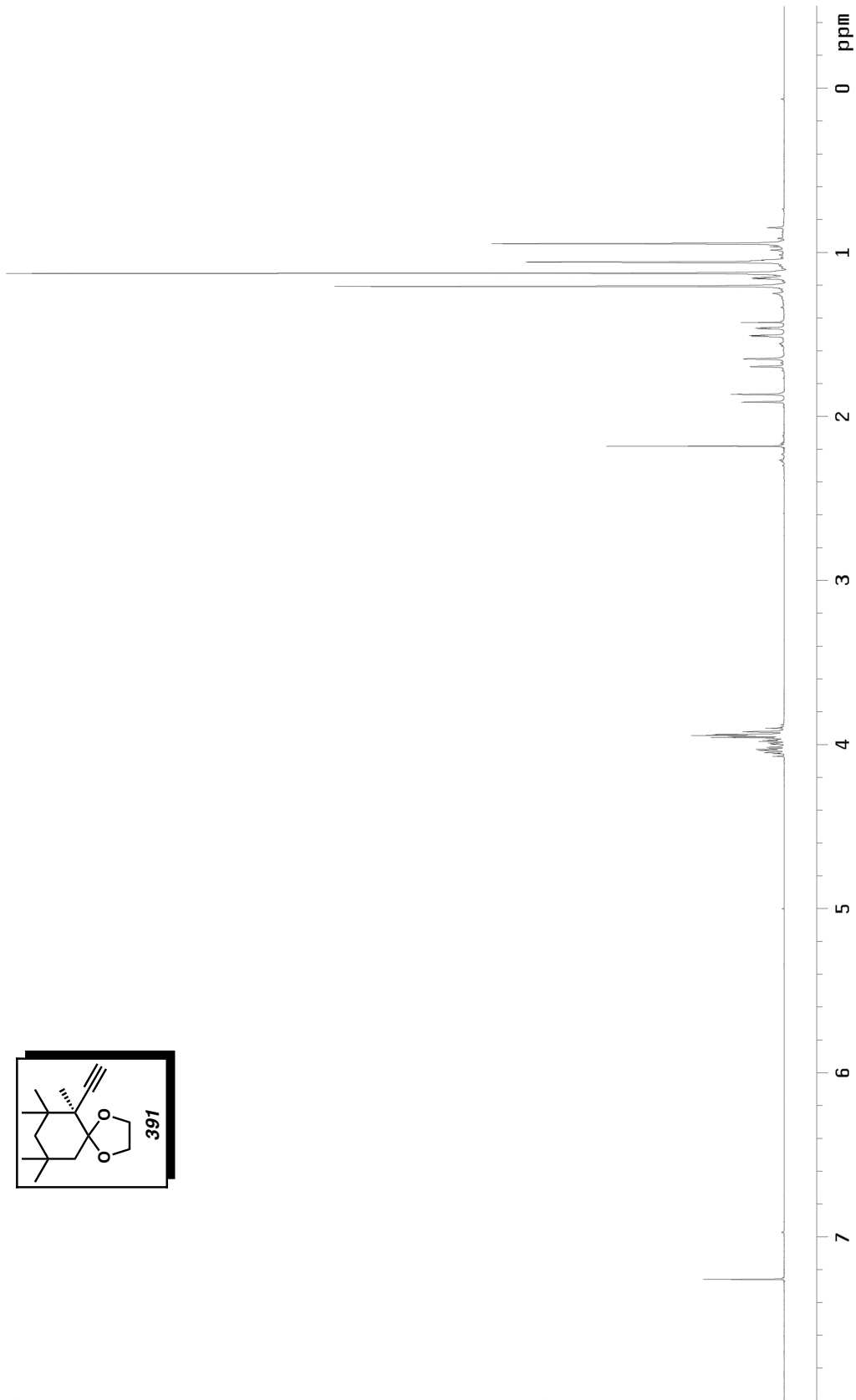
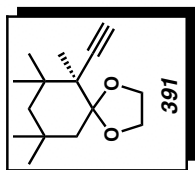


Figure E.55  $^1\text{H}$  NMR (300 MHz,  $\text{CDCl}_3$ ) of compound **391**.

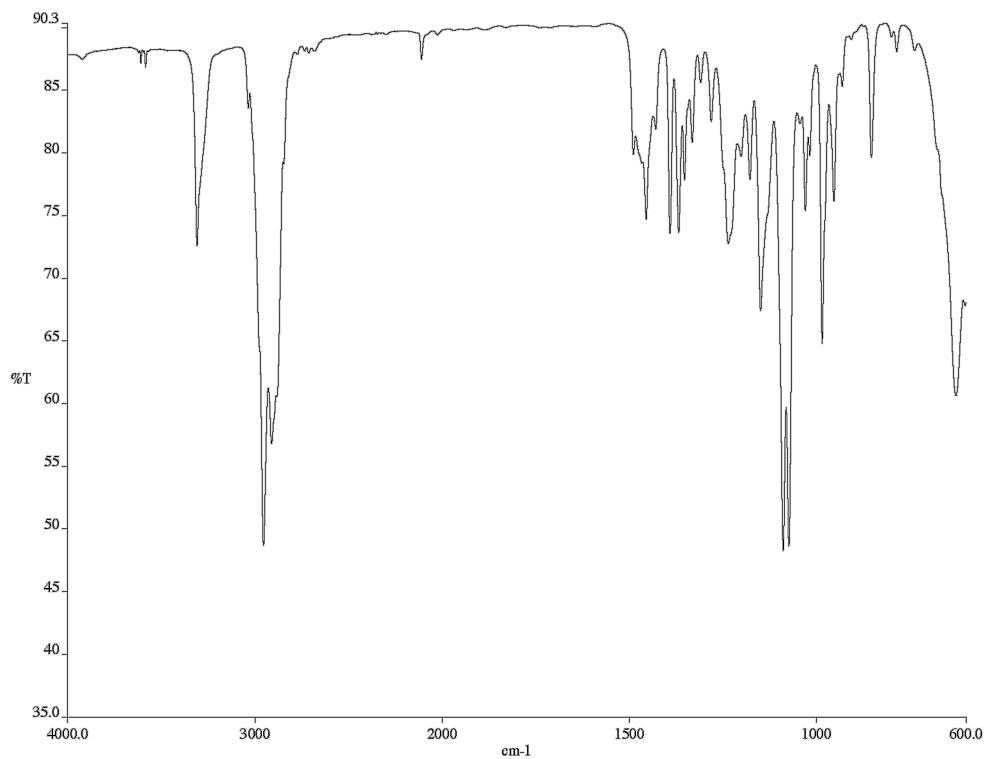


Figure E.56 Infrared spectrum (thin film/NaCl) of compound **391**.

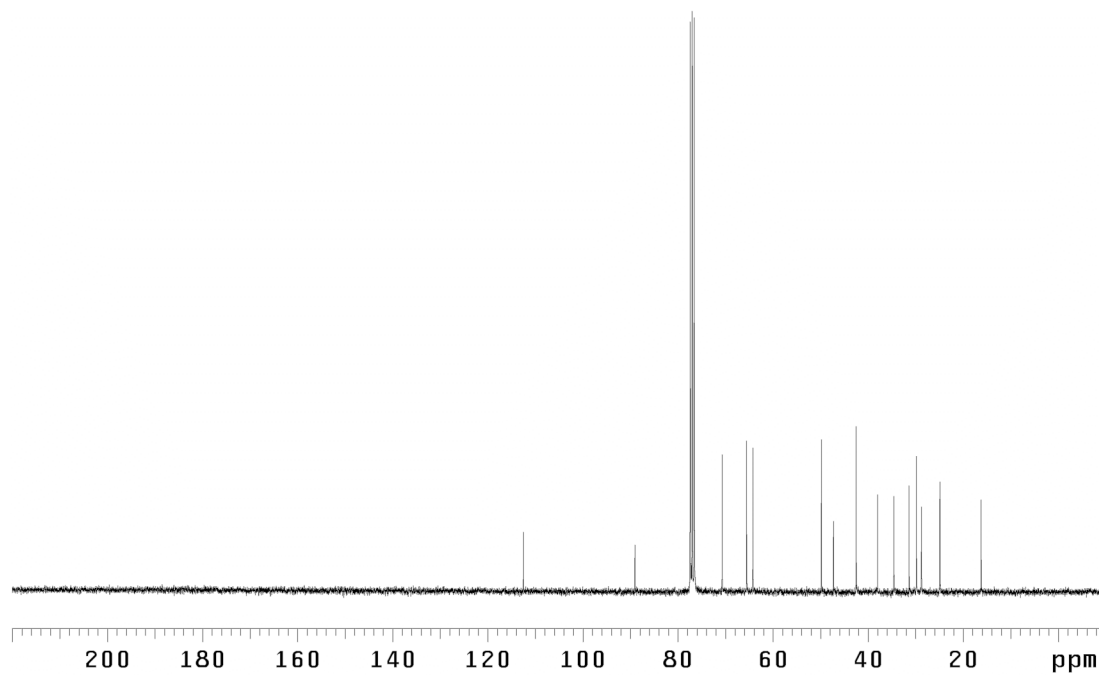


Figure E.57 <sup>13</sup>C NMR (75 MHz, CDCl<sub>3</sub>) of compound **391**.

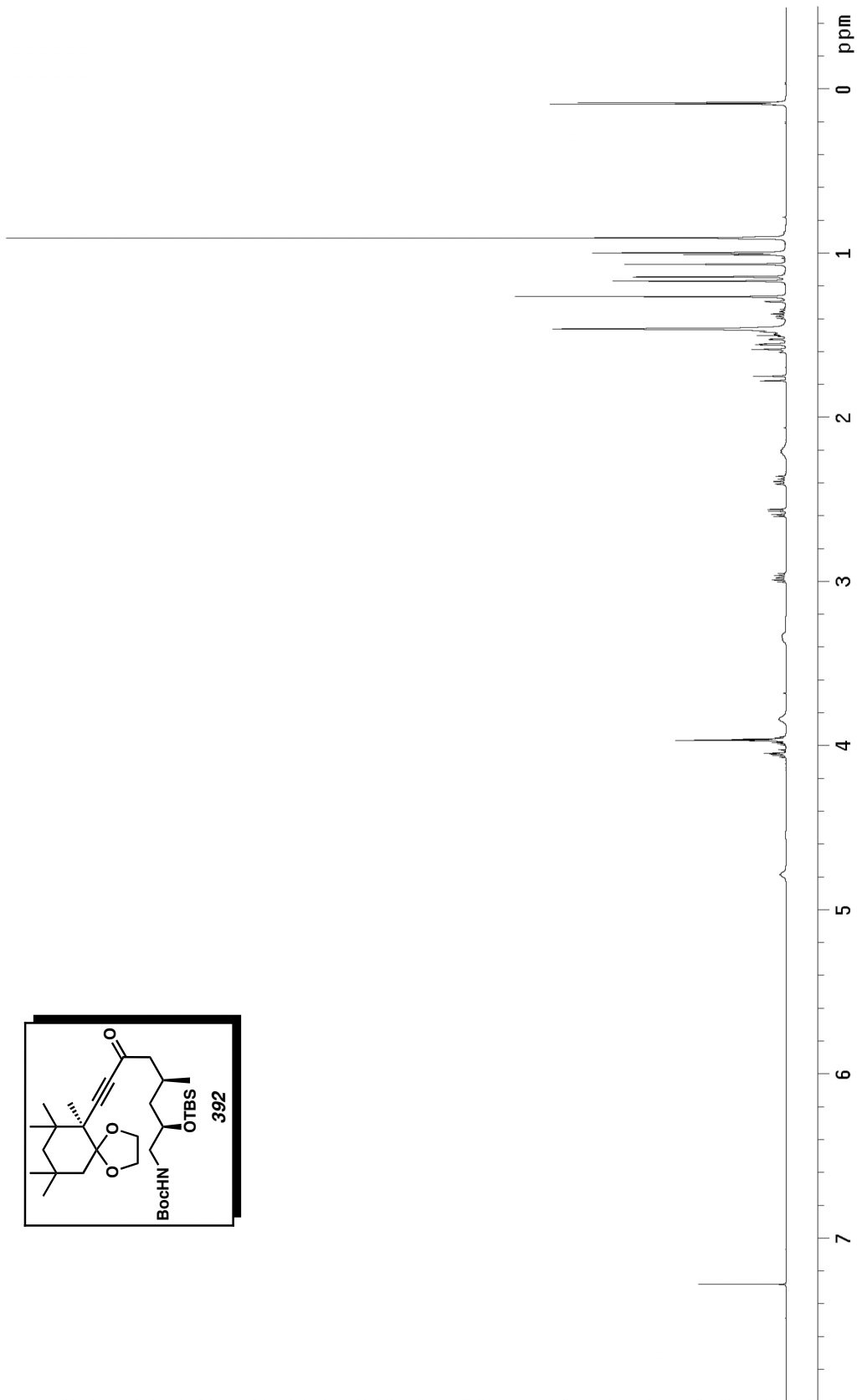


Figure E.58  $^1\text{H}$  NMR (500 MHz,  $\text{CDCl}_3$ ) of compound **392**.

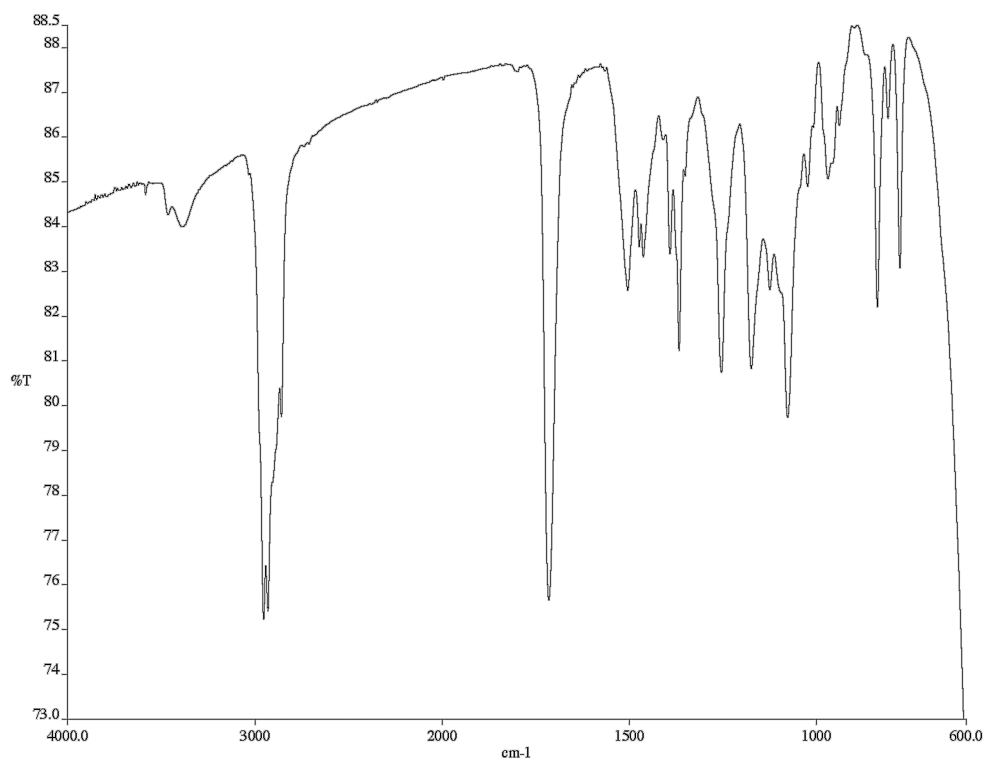


Figure E.59 Infrared spectrum (thin film/NaCl) of compound **392**.

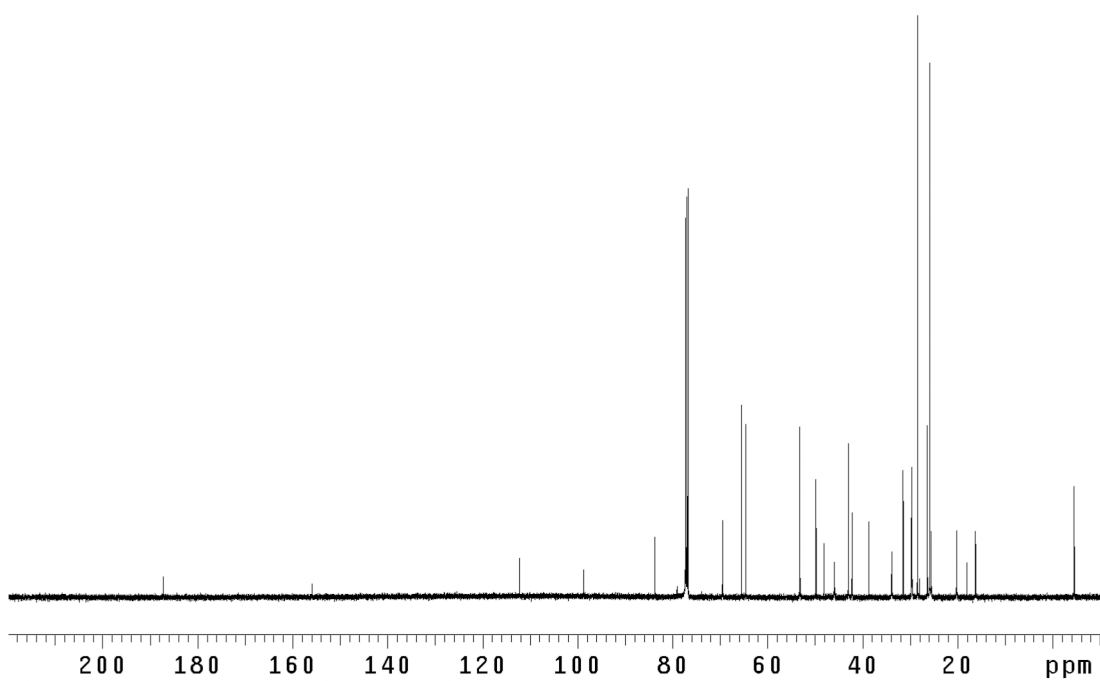


Figure E.60 <sup>13</sup>C NMR (125 MHz, CDCl<sub>3</sub>) of compound **392**.

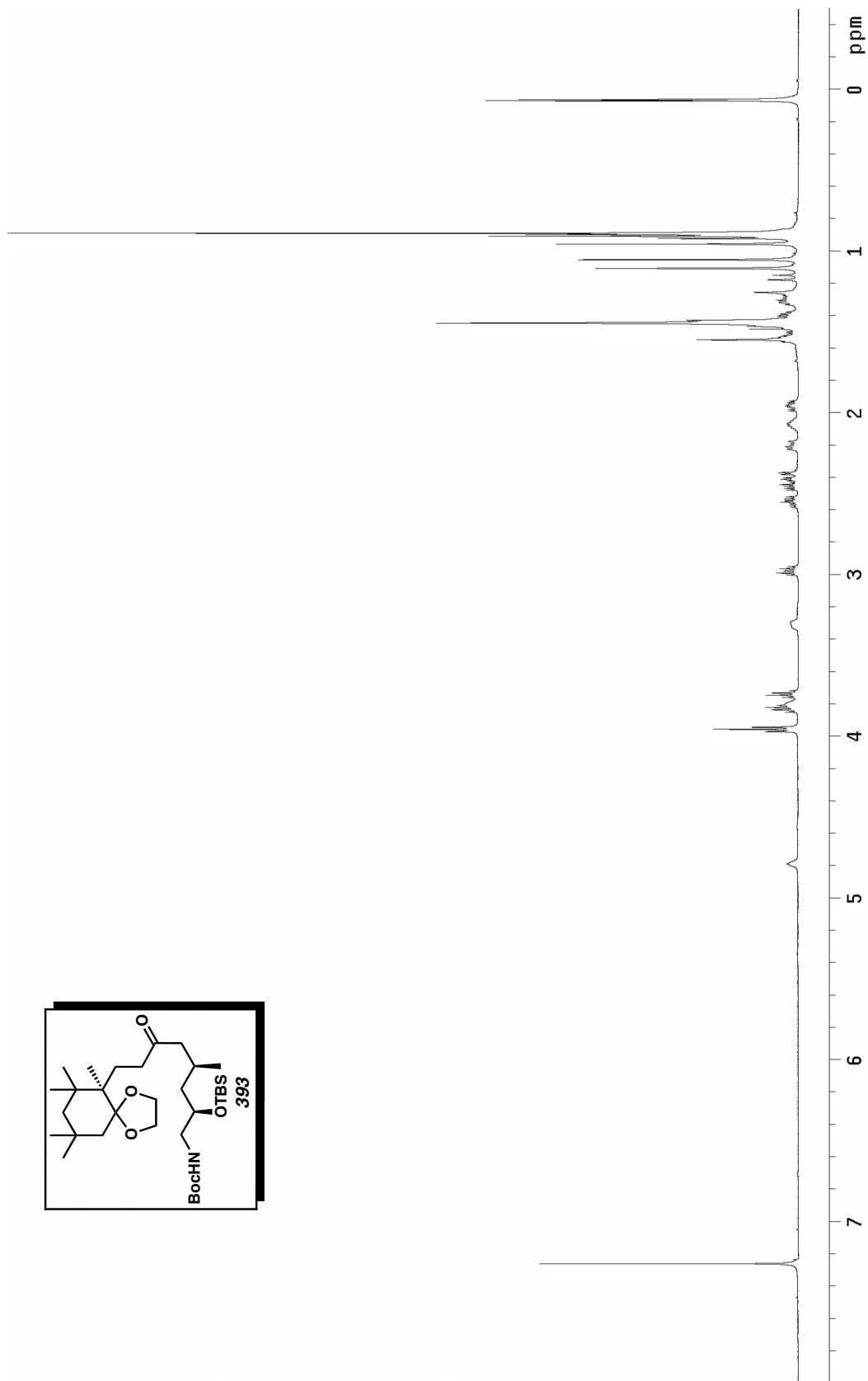


Figure E.61  $^1\text{H}$  NMR (500 MHz,  $\text{CDCl}_3$ ) of compound **393**.

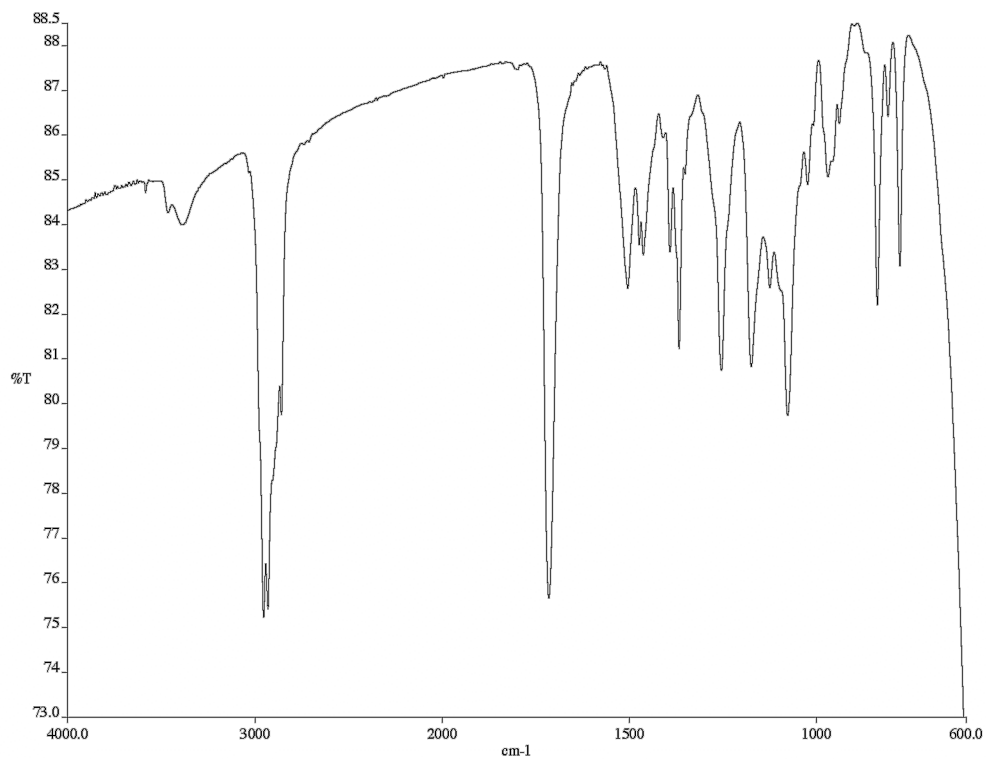


Figure E.62 Infrared spectrum (thin film/NaCl) of compound **393**.

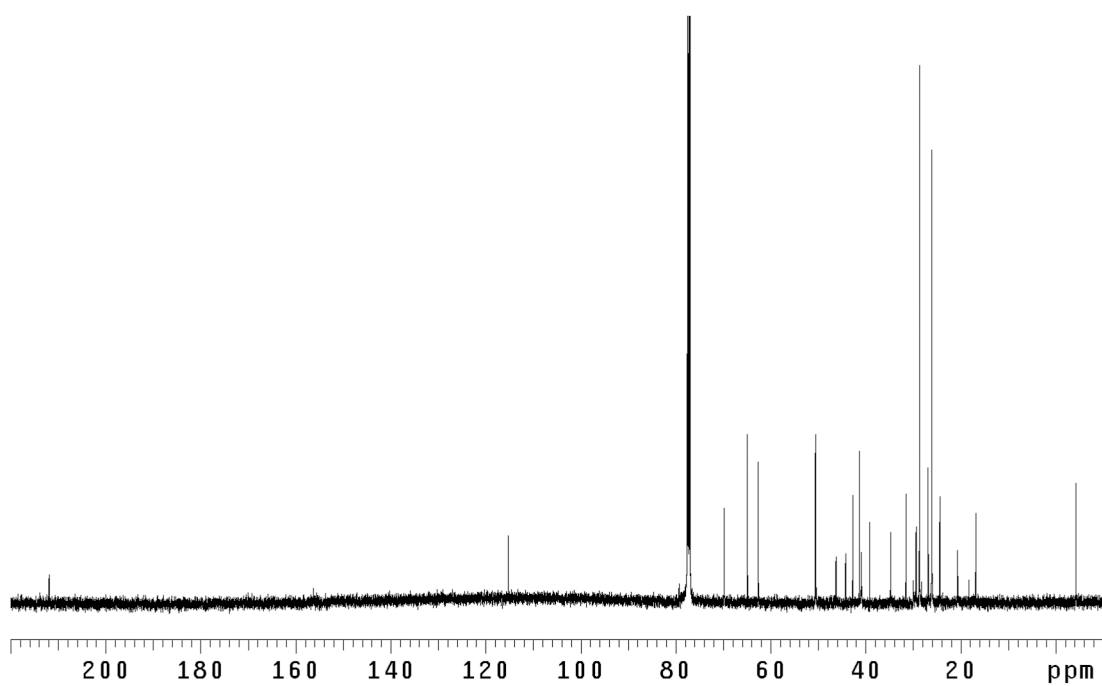


Figure E.63 <sup>13</sup>C NMR (125 MHz, CDCl<sub>3</sub>) of compound **393**.

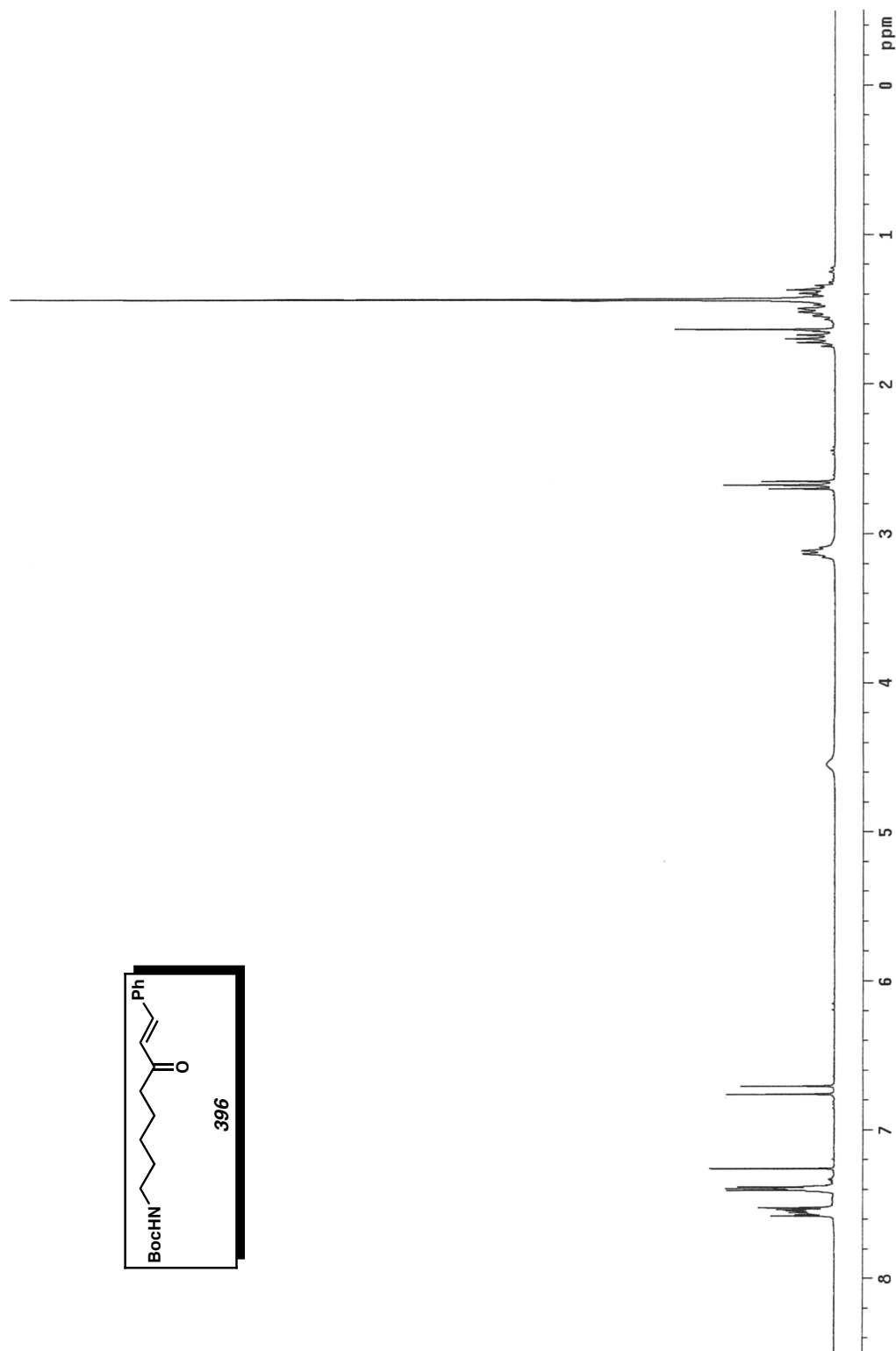


Figure E.64  $^1\text{H}$  NMR (300 MHz,  $\text{CDCl}_3$ ) of compound **396**.

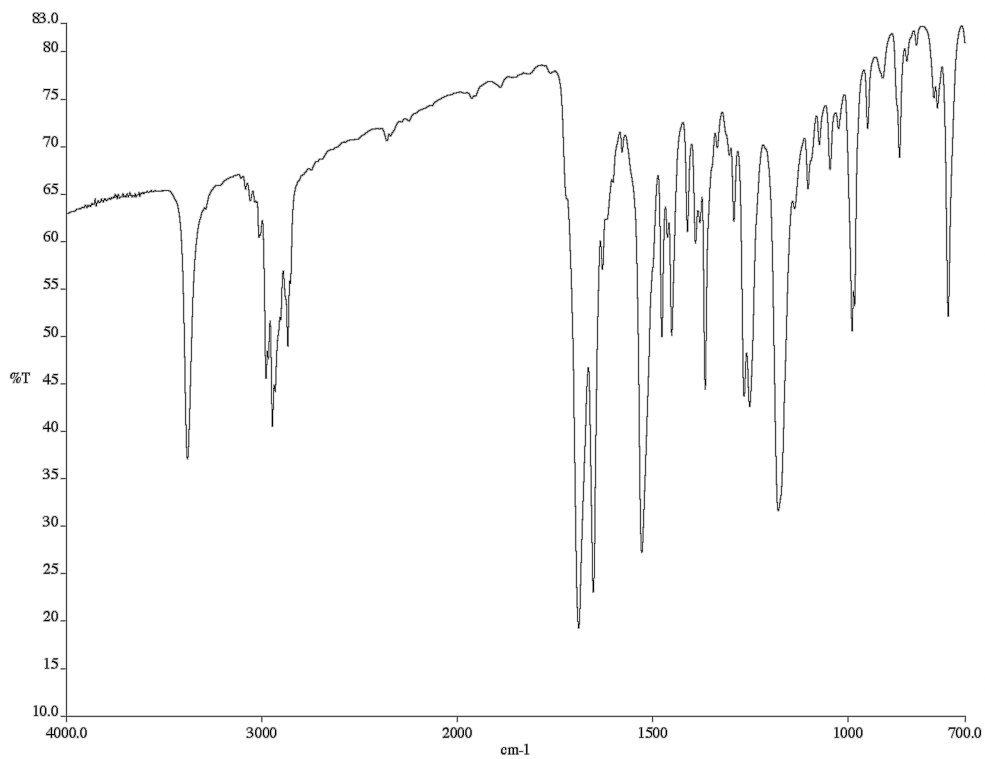


Figure E.65 Infrared spectrum (thin film/NaCl) of compound **396**.

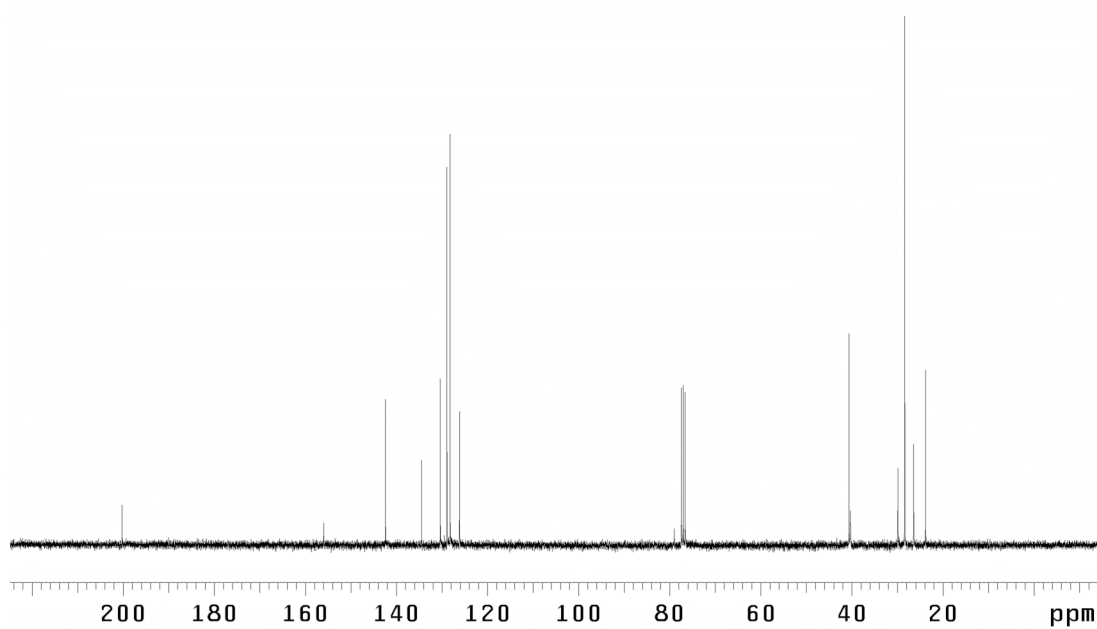


Figure E.66 <sup>13</sup>C NMR (75 MHz, 75) of compound **396**.

CALIFORNIA INSTITUTE OF TECHNOLOGY  
BECKMAN INSTITUTE  
X-RAY CRYSTALLOGRAPHY LABORATORY

Crystal Structure Analysis of:

Allyl ketone **366** (JLSO4)

(CCDC 701675)

Contents:

Table E.1	Crystal data.
Table E.2	Atomic coordinates.
Table E.3	Full bond distances and angles.
Table E.4	Anisotropic displacement parameters.
Table E.5	Hydrogen atomic coordinates.

**Figure E.67** Representation of Allyl ketone **366**.

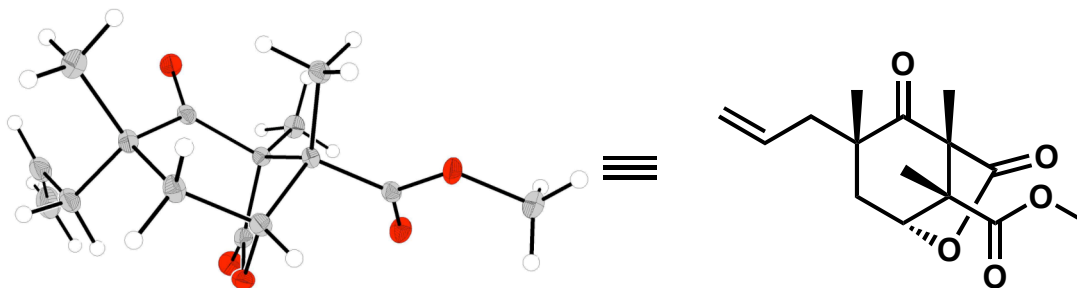


**Table E.1** Crystal data and structure refinement for JLS04 (CCDC 701675).

Empirical formula	C <sub>15</sub> H <sub>20</sub> O <sub>5</sub>
Formula weight	280.31
Crystallization Solvent	Diethylether/heptane
Crystal Habit	Block
Crystal size	0.33 x 0.17 x 0.17 mm <sup>3</sup>
Crystal color	Colorless



### Data Collection

Type of diffractometer	Bruker KAPPA APEX II
Wavelength	0.71073 Å MoK $\alpha$
Data Collection Temperature	100(2) K
$\theta$ range for 9397 reflections used in lattice determination	2.29 to 34.60°
Unit cell dimensions	a = 8.5338(4) Å b = 11.6571(5) Å c = 14.1940(6) Å $\beta$ = 103.172(2)°
Volume	1374.86(10) Å <sup>3</sup>
Z	4
Crystal system	Monoclinic
Space group	P2 <sub>1</sub> /c
Density (calculated)	1.354 Mg/m <sup>3</sup>
F(000)	600
Data collection program	Bruker APEX2 v2.1-0
$\theta$ range for data collection	2.29 to 35.00°
Completeness to $\theta$ = 35.00°	92.9 %
Index ranges	-13 ≤ h ≤ 13, -18 ≤ k ≤ 18, -22 ≤ l ≤ 21
Data collection scan type	$\omega$ scans; 19 settings
Data reduction program	Bruker SAINT-Plus v7.34A
Reflections collected	56123
Independent reflections	5626 [R <sub>int</sub> = 0.0566]
Absorption coefficient	0.101 mm <sup>-1</sup>
Absorption correction	None
Max. and min. transmission	0.9830 and 0.9674

**Table E.1** (cont.)**Structure Solution and Refinement**

Structure solution program	SHELXS-97 (Sheldrick, 2008)
Primary solution method	Direct methods
Secondary solution method	Difference Fourier map
Hydrogen placement	Difference Fourier map
Structure refinement program	SHELXL-97 (Sheldrick, 2008)
Refinement method	Full matrix least-squares on $F^2$
Data / restraints / parameters	5626 / 0 / 261
Treatment of hydrogen atoms	Unrestrained
Goodness-of-fit on $F^2$	3.518
Final R indices [ $I > 2\sigma(I)$ , 4781 reflections]	$R_1 = 0.0391$ , $wR_2 = 0.0840$
R indices (all data)	$R_1 = 0.0464$ , $wR_2 = 0.0844$
Type of weighting scheme used	Sigma
Weighting scheme used	$w = 1/\sigma^2(F_o^2)$
Max shift/error	0.001
Average shift/error	0.000
Largest diff. peak and hole	0.473 and -0.278 e. $\text{\AA}^{-3}$

**Special Refinement Details**

Crystals were mounted on a glass fiber using Paratone oil then placed on the diffractometer under a nitrogen stream at 100K.

Refinement of  $F^2$  against ALL reflections. The weighted R-factor ( $wR$ ) and goodness of fit ( $S$ ) are based on  $F^2$ , conventional R-factors ( $R$ ) are based on  $F$ , with  $F$  set to zero for negative  $F^2$ . The threshold expression of  $F^2 > 2\sigma(F^2)$  is used only for calculating R-factors(gt) etc. and is not relevant to the choice of reflections for refinement. R-factors based on  $F^2$  are statistically about twice as large as those based on  $F$ , and R-factors based on ALL data will be even larger.

All esds (except the esd in the dihedral angle between two l.s. planes) are estimated using the full covariance matrix. The cell esds are taken into account individually in the estimation of esds in distances, angles and torsion angles; correlations between esds in cell parameters are only used when they are defined by crystal symmetry. An approximate (isotropic) treatment of cell esds is used for estimating esds involving l.s. planes.

**Table E.2** Atomic coordinates ( $\times 10^4$ ) and equivalent isotropic displacement parameters ( $\text{\AA}^2 \times 10^3$ ) for JLSO4 (CCDC 701675).  $U(\text{eq})$  is defined as the trace of the orthogonalized  $U^{ij}$  tensor.

	x	y	z	$U_{\text{eq}}$
O(1)	8256(1)	3008(1)	5023(1)	20(1)
O(2)	6441(1)	4468(1)	2454(1)	23(1)
O(3)	6792(1)	2677(1)	1977(1)	16(1)
O(4)	9995(1)	3728(1)	1801(1)	20(1)
O(5)	11377(1)	2075(1)	2019(1)	17(1)
C(1)	3966(1)	3880(1)	4264(1)	28(1)
C(2)	4624(1)	2860(1)	4446(1)	21(1)
C(3)	5025(1)	2097(1)	3689(1)	17(1)
C(4)	6786(1)	1622(1)	3915(1)	14(1)
C(5)	7908(1)	2654(1)	4200(1)	13(1)
C(6)	8593(1)	3265(1)	3408(1)	12(1)
C(7)	9404(1)	2307(1)	2926(1)	11(1)
C(8)	7852(1)	1714(1)	2354(1)	13(1)
C(9)	7081(1)	988(1)	3008(1)	15(1)
C(10)	6997(1)	778(1)	4764(1)	21(1)
C(11)	9596(1)	4297(1)	3823(1)	17(1)
C(12)	7173(1)	3583(1)	2580(1)	15(1)
C(13)	10277(1)	2809(1)	2193(1)	13(1)
C(14)	12227(1)	2420(1)	1297(1)	22(1)
C(15)	10529(1)	1524(1)	3643(1)	14(1)

**Table E.3** Bond lengths [Å] and angles [°] for JLSO4 (CCDC 701675).

O(1)-C(5)	1.2099(9)	C(2)-C(3)-H(3A)	105.9(6)
O(2)-C(12)	1.1981(9)	C(4)-C(3)-H(3A)	112.0(7)
O(3)-C(12)	1.3519(9)	C(2)-C(3)-H(3B)	111.6(6)
O(3)-C(8)	1.4647(9)	C(4)-C(3)-H(3B)	103.5(6)
O(4)-C(13)	1.2059(9)	H(3A)-C(3)-H(3B)	108.3(8)
O(5)-C(13)	1.3341(9)	C(5)-C(4)-C(10)	109.95(6)
O(5)-C(14)	1.4403(11)	C(5)-C(4)-C(9)	112.52(6)
C(1)-C(2)	1.3145(13)	C(10)-C(4)-C(9)	109.46(7)
C(1)-H(1A)	0.986(13)	C(5)-C(4)-C(3)	106.81(6)
C(1)-H(1B)	0.976(12)	C(10)-C(4)-C(3)	108.84(7)
C(2)-C(3)	1.4934(12)	C(9)-C(4)-C(3)	109.16(6)
C(2)-H(2)	0.957(11)	O(1)-C(5)-C(4)	121.58(7)
C(3)-C(4)	1.5646(11)	O(1)-C(5)-C(6)	119.52(6)
C(3)-H(3A)	0.974(11)	C(4)-C(5)-C(6)	118.90(6)
C(3)-H(3B)	0.947(11)	C(11)-C(6)-C(12)	112.63(6)
C(4)-C(5)	1.5339(10)	C(11)-C(6)-C(7)	118.25(7)
C(4)-C(10)	1.5343(11)	C(12)-C(6)-C(7)	100.99(5)
C(4)-C(9)	1.5539(11)	C(11)-C(6)-C(5)	110.77(6)
C(5)-C(6)	1.5534(11)	C(12)-C(6)-C(5)	107.73(6)
C(6)-C(11)	1.5160(10)	C(7)-C(6)-C(5)	105.58(6)
C(6)-C(12)	1.5290(9)	C(13)-C(7)-C(15)	110.60(6)
C(6)-C(7)	1.5526(10)	C(13)-C(7)-C(8)	107.75(6)
C(7)-C(13)	1.5276(11)	C(15)-C(7)-C(8)	114.45(6)
C(7)-C(15)	1.5312(10)	C(13)-C(7)-C(6)	111.12(6)
C(7)-C(8)	1.5495(9)	C(15)-C(7)-C(6)	114.28(6)
C(8)-C(9)	1.5134(11)	C(8)-C(7)-C(6)	97.94(6)
C(8)-H(8)	0.960(9)	O(3)-C(8)-C(9)	109.52(6)
C(9)-H(9A)	0.964(10)	O(3)-C(8)-C(7)	103.47(5)
C(9)-H(9B)	0.992(10)	C(9)-C(8)-C(7)	111.55(6)
C(10)-H(10A)	1.000(11)	O(3)-C(8)-H(8)	105.8(5)
C(10)-H(10B)	0.959(11)	C(9)-C(8)-H(8)	113.1(6)
C(10)-H(10C)	0.988(11)	C(7)-C(8)-H(8)	112.7(5)
C(11)-H(11A)	0.950(12)	C(8)-C(9)-C(4)	114.65(6)
C(11)-H(11B)	0.995(10)	C(8)-C(9)-H(9A)	108.3(7)
C(11)-H(11C)	0.998(11)	C(4)-C(9)-H(9A)	108.8(6)
C(14)-H(14A)	0.929(12)	C(8)-C(9)-H(9B)	108.6(6)
C(14)-H(14B)	0.998(12)	C(4)-C(9)-H(9B)	108.0(6)
C(14)-H(14C)	0.949(10)	H(9A)-C(9)-H(9B)	108.4(8)
C(15)-H(15A)	0.981(11)	C(4)-C(10)-H(10A)	109.3(6)
C(15)-H(15B)	0.985(11)	C(4)-C(10)-H(10B)	109.3(6)
C(15)-H(15C)	0.974(10)	H(10A)-C(10)-H(10B)	106.8(9)
		C(4)-C(10)-H(10C)	112.4(6)
C(12)-O(3)-C(8)	109.13(5)	H(10A)-C(10)-H(10C)	105.6(8)
C(13)-O(5)-C(14)	116.25(6)	H(10B)-C(10)-H(10C)	113.2(9)
C(2)-C(1)-H(1A)	118.5(8)	C(6)-C(11)-H(11A)	110.7(6)
C(2)-C(1)-H(1B)	122.5(6)	C(6)-C(11)-H(11B)	110.4(6)
H(1A)-C(1)-H(1B)	118.8(10)	H(11A)-C(11)-H(11B)	108.4(9)
C(1)-C(2)-C(3)	123.75(9)	C(6)-C(11)-H(11C)	109.6(6)
C(1)-C(2)-H(2)	119.3(6)	H(11A)-C(11)-H(11C)	108.9(9)
C(3)-C(2)-H(2)	116.9(6)	H(11B)-C(11)-H(11C)	108.8(8)
C(2)-C(3)-C(4)	115.50(6)	O(2)-C(12)-O(3)	122.43(6)

O(2)-C(12)-C(6)	128.19(7)
O(3)-C(12)-C(6)	109.37(6)
O(4)-C(13)-O(5)	123.97(8)
O(4)-C(13)-C(7)	125.29(7)
O(5)-C(13)-C(7)	110.72(6)
O(5)-C(14)-H(14A)	109.1(7)
O(5)-C(14)-H(14B)	103.7(7)
H(14A)-C(14)-H(14B)	113.6(9)
O(5)-C(14)-H(14C)	108.5(6)
H(14A)-C(14)-H(14C)	109.7(9)
H(14B)-C(14)-H(14C)	111.9(9)
C(7)-C(15)-H(15A)	111.6(5)
C(7)-C(15)-H(15B)	111.3(6)
H(15A)-C(15)-H(15B)	108.5(8)
C(7)-C(15)-H(15C)	109.6(5)
H(15A)-C(15)-H(15C)	106.1(8)
H(15B)-C(15)-H(15C)	109.6(8)

**Table E.4** Anisotropic displacement parameters ( $\text{\AA}^2 \times 10^4$ ) for JLSO4 (CCDC 701675). The anisotropic displacement factor exponent takes the form:  $-2\pi^2 [h^2 a^{*2} U^{11} + \dots + 2 h k a^* b^* U^{12}]$ .

	$U^{11}$	$U^{22}$	$U^{33}$	$U^{23}$	$U^{13}$	$U^{12}$
O(1)	187(3)	267(3)	135(3)	-37(2)	41(2)	-38(2)
O(2)	215(3)	215(3)	253(3)	43(2)	57(2)	93(2)
O(3)	131(2)	201(3)	132(2)	-3(2)	11(2)	25(2)
O(4)	222(3)	171(3)	212(3)	46(2)	90(2)	13(2)
O(5)	160(3)	204(3)	168(3)	2(2)	88(2)	27(2)
C(1)	246(4)	260(4)	381(5)	-62(4)	141(4)	-20(4)
C(2)	134(3)	294(4)	205(4)	-36(3)	59(3)	-18(3)
C(3)	111(3)	230(4)	180(4)	-18(3)	42(3)	-14(3)
C(4)	117(3)	167(3)	148(3)	0(3)	40(3)	-20(3)
C(5)	98(3)	158(3)	138(3)	-4(3)	27(2)	18(3)
C(6)	117(3)	115(3)	124(3)	-12(2)	30(3)	8(2)
C(7)	100(3)	106(3)	132(3)	-9(2)	33(2)	-1(2)
C(8)	119(3)	142(3)	137(3)	-29(3)	27(3)	0(2)
C(9)	133(3)	149(3)	182(4)	-32(3)	51(3)	-29(3)
C(10)	211(4)	211(4)	205(4)	41(3)	71(3)	-20(3)
C(11)	199(4)	135(3)	195(4)	-33(3)	58(3)	-34(3)
C(12)	134(3)	177(3)	142(3)	20(3)	47(3)	22(3)
C(13)	111(3)	148(3)	132(3)	-22(3)	26(2)	-13(3)
C(14)	186(4)	333(5)	164(4)	5(3)	88(3)	-2(3)
C(15)	126(3)	140(3)	157(4)	19(3)	31(3)	12(3)

**Table E.5** Hydrogen coordinates ( $\times 10^4$ ) and isotropic displacement parameters ( $\text{\AA}^2 \times 10^3$ ) for JLSO4 (CCDC 701675).

	x	y	z	$U_{\text{iso}}$
H(1A)	3788(16)	4183(11)	3599(9)	49(4)
H(1B)	3733(14)	4372(10)	4771(8)	34(3)
H(2)	4851(13)	2572(9)	5094(8)	29(3)
H(3A)	4773(13)	2536(9)	3090(8)	28(3)
H(3B)	4383(13)	1425(9)	3601(7)	24(3)
H(8)	8014(11)	1306(8)	1796(6)	12(2)
H(9A)	7765(13)	335(9)	3217(7)	24(3)
H(9B)	6029(12)	706(8)	2628(7)	22(2)
H(10A)	8136(14)	503(9)	4934(7)	31(3)
H(10B)	6335(13)	116(9)	4567(7)	32(3)
H(10C)	6809(13)	1141(9)	5357(7)	25(3)
H(11A)	9975(14)	4689(10)	3332(8)	31(3)
H(11B)	10542(13)	4054(8)	4333(7)	24(3)
H(11C)	8929(13)	4836(9)	4114(7)	30(3)
H(14A)	11493(15)	2516(9)	709(8)	35(3)
H(14B)	13007(14)	1783(9)	1296(7)	35(3)
H(14C)	12756(13)	3127(8)	1492(7)	22(3)
H(15A)	10863(12)	854(9)	3318(7)	26(3)
H(15B)	10012(12)	1252(9)	4155(7)	22(2)
H(15C)	11512(12)	1937(8)	3933(6)	18(2)

## COMPREHENSIVE BIBLIOGRAPHY

1. Ager, D. J.; Prakash, I.; Schaad, D. R. *Aldrichimica Acta* **1997**, *30*, 3–12.
2. Atta-ur-Rahman; Alvi, K. A.; Abbas, S. A.; Choudhary, M. I.; Clardy, J. *Tetrahedron Lett.* **1989**, *30*, 6825–6828.
3. Ball, S.; Goodwin, T. W.; Morton, R. A., *Biochem. J.* **1948**, *42*, 516–523.
4. Barnard, C. F. J. *Organometallics*, **2008**, *27*, 5402–5422 and references therein.
5. Beesley, R. M.; Ingold, C. K.; Thorpe, J. F. *J. Chem. Soc.* **1915**, *107*, 1080–1106.
6. Behenna, D. C.; Stockdill, J. L.; Stoltz, B. M. *Angew. Chem. Int. Ed.* **2007**, *46*, 4077–4079.
7. Behenna, D. C.; Stockdill, J. L.; Stoltz, B. M. *Angew. Chem. Int. Ed.* **2008**, *47*, 2365–2386.
8. Behenna, D. C.; Stoltz, B. M. *J. Am. Chem. Soc.* **2004**, *126*, 15044–15045.
9. Benowitz, N. L. *Progress in Cardiovascular Diseases* **2003**, *46*, 91–111.
10. Berthelot, J.; Guette, C.; Desbène, P.-J.; Basselier, J.-J. *Can. J. Chem.* **1989**, *67*, 2061–2066.
11. Bhattacharya, A.; Segmuller, B.; Y. A. *Synth. Commun.* **1996**, *26*, 1775–1784.
12. Birman, V. B.; Danishefsky, S. J., *J. Am. Chem. Soc.* **2002**, *124*, 2080–2081.
13. Bodine, P. V. N.; Harris, H. A.; Komm, B. S. *Endocrinology* **1999**, *140*, 2439–2451.
14. Bolm, C.; Schiffrers, I.; Dinter, C. L.; Gerlach, A., *J. Org. Chem.* **2000**, *65*, 6984–6991.
15. Brewster, A. G.; Leach, A. *Tetrahedron Lett.* **1986**, *27*, 2539–2542.
16. Bruice, T. C.; Pandit, U. K. *J. Am. Chem. Soc.* **1960**, *82*, 5858–5865.
17. Buchschacher, P.; Fürst, A.; Gutzwiller, *J. Org. Synth.* **1985**, *63*, 37–43.
18. Carreno, M. C.; Ruano, J. L. G.; Sanz, G.; Toledo, M. A.; Urbano, A. *J. Org. Chem.* **1995**, *60*, 5328–5331.

19. Carreno, M. C.; Ruano, J. L. G.; Sanz, G.; Toledo, M. A.; Urbano, A. *Synlett.* **1997**, 1241-1242.
20. Cha, J. K.; Christ, W. J.; Finan, J. M.; Fujioka, H.; Kishi, Y.; Klein, L. L.; Ko, S. S.; Leder, J.; McWhorter, W. W.; Pfaff, K.-P.; Yonaga, M.; Uemura, D.; Hirata, Y. *J. Am. Chem. Soc.* **1982**, *104*, 7369-7371.
21. Chen, Y.; McDaid, P.; Deng, L. *Chem. Rev.* **2003**, *103*, 2965-2983.
22. Corey, E. J.; Cho, H.; Rucker, C.; Hua, D. H. *Tetrahedron Lett.* **1981**, *22*, 3455-3458.
23. Culkin D. A.; Hartwig, J. F. *Acc. Chem. Res.* **2003**, *36*, 234-245.
24. d'Angelo, J.; Desmaële, D.; Dumas, F.; Guingant, A. *Tetrahedron: Asymmetry* **1992**, *3*, 459-505.
25. Daranas, A. H.; Fernández, J. J.; Gavín, J. A.; Norte, M. *Tetrahedron* **1998**, *54*, 7891-7896.
26. Daranas, A. H.; Fernández, J. J.; Gavín, J. A.; Norte, M. *Tetrahedron* **1999**, *55*, 5539-5546.
27. Dess, D. B.; Martin, J. C. *J. Am. Chem. Soc.* **1991**, *113*, 7277-7278.
28. Enquist, J. A., Jr.; Stoltz, B. M. *Nature* **2008**, *453*, 1228-1231.
29. Evans, D. A.; Mitch, C. H.; Thomas, R. C.; Zimmerman, D. M.; Robey, R. L. *J. Am. Chem. Soc.* **1980**, *102*, 5955-5956.
30. Fattorusso, E.; Romano, A.; Taglialatela-Scafati, O.; Achmad, M. J.; Bavestrello, G.; Cerrano, C. *Tetrahedron Lett.* **2008**, *49*, 2189-2192.
31. Fernández, J. J.; Souto, M. L.; Daranas, A. H.; Norte, M. *Curr. Top. Phytochem.* **2000**, *4*, 106-119.
32. Franck-Neumann, M.; Miesch, M.; Barth, F. *Tetrahedron* **1993**, *49*, 1409-1420.
33. Fraser, G. M.; Hoffmann, H. M. R. *Chem. Commun.* **1967**, 561-563.

34. Fukuzawa, S.; Hayashi, Y.; Uemura, D. Nagatsu, A.; Yamada, K.; Ijuin, Y. *Heterocyc. Commun.* **1995**, *1*, 207–214.
35. Gawley, R. E. *Synthesis* **1976**, 777–794.
36. Ghosh, S.; Rivas, F.; Fischer, D.; González, M. A.; Theodorakis, E. A. *Org. Lett.* **2004**, *6*, 941–944.
37. Hampton, A.; Fratantoni, J. C.; Carroll, P. M.; Wang, S. *J. Am. Chem. Soc.* **1965**, *87*, 5481–5487.
38. Han, C.; Qi, J.; Shi, X.; Sakagami, Y.; Shibata, T.; Uchida, K.; Ojika, M. *Biosci. Biotechnol. Biochem.* **2006**, *70*, 706–711.
39. Han, X.; Stoltz, B. M.; Corey, E. J. *J. Am. Chem. Soc.* **1999**, *121*, 7600–7605.
40. Heck, R. F. *Acc. Chem. Res.* **1979**, *12*, 146–151.
41. Heck, R. F. *Org. React.* **1982**, *27*, 345–390.
42. Heck, R. F.; Nolley, J. P. *J. Am. Chem. Soc.* **1968**, *90*, 5518–5526.
43. Held, D.; Xie, L. *Microchem. J.* **1997**, *55*, 261–269.
44. Hickmott, P. W. *Tetrahedron* **1984**, *40*, 2989–3051.
45. Hikage, N.; Furukawa, H.; Takao, K.; Kobayashi, S. *Chem. Pharm. Bull.* **2000**, *48*, 1370–1372.
46. Hikage, N.; Furukawa, H.; Takao, K.; Kobayashi, S. *Tetrahedron Lett.* **1998**, *39*, 6237–6240.
47. Hikage, N.; Furukawa, H.; Takao, K.; Kobayashi, S. *Tetrahedron Lett.* **1998**, *39*, 6241–6244.
48. Hirai, G.; Koizumi, Y.; Moharram, S. M.; Oguri, H.; HIRAMA, M. *Org. Lett.* **2002**, *4*, 1627–1630.
49. Hirai, G.; Oguri, H.; Hayashi, M.; Koyama, K.; Koizumi, Y.; Moharram, S. M.; HIRAMA, M. *Bioorg. Med. Chem. Lett.* **2004**, *14*, 2647–2651.
50. Hirai, G.; Oguri, H.; HIRAMA, M. *Chem. Lett.* **1999**, *28*, 141–142.

51. Hirai, G.; Oguri, H.; Moharram, S. M.; Koyama, K.; Hirama, M. *Tetrahedron Lett.* **2001**, *42*, 5783–5787.
52. Ingold, C. K. *J. Chem. Soc.* **1921**, *119*, 305–329.
53. Irifune, T.; Ohashi, T.; Ichino, T.; Sakia, E.; Suenaga, K.; Uemura, D. *Chem. Lett.* **2005**, *34*, 1058–1059.
54. Iserloh, U.; Curran, D. P.; Kanemasa, S. *Tetrahedron: Asymmetry* **1999**, *10*, 2417–2428.
55. Jackson, S. P.; Schoenwalder, S. M. *Nature Rev.* **2003**, *2*, 1–15.
56. Juhl, M.; Monrad, R.; Søtofte, I.; Tanner, D. *J. Org. Chem.* **2007**, *72*, 4644–4654.
57. Juhl, M.; Nielsen, T. E.; Le Quement, S.; Tanner, D. *J. Org. Chem.* **2006**, *71*, 265–280.
58. Jung, M. E.; Gervay, J. *J. Am. Chem. Soc.* **1991**, *113*, 224–232.
59. Jung, M. E.; Hudspeth, J. P. *J. Am. Chem. Soc.* **1980**, *102*, 2463–2464.
60. Jung, M. E.; Kiankarimi, M. *J. Org. Chem.* **1998**, *63*, 2968–2974.
61. Keith, J. A.; Behenna, D. C.; Mohr, J. T.; Ma, S.; Marinescu, S. C.; Oxgaard, J.; Stoltz, B. M.; Goddard, W. A., III *J. Am. Chem. Soc.* **2007**, *129*, 11876–11877.
62. Kita, M.; Uemura, D. *Chem. Lett.* **2005**, *34*, 454–459.
63. Kumar, R.; Chakraborti, A. K. *Tetrahedron Lett.* **2005**, *46*, 8319–8323.
64. Kuramoto, K.; Yamaguchi, K.; Tsuji, T.; Uemura, D. in *Drugs from the Sea*, (Ed.: Fusetani, N.), Karger, Basel, **2000**, pp. 98–106.
65. Kuramoto, M.; Arimoto, H.; Hayashi, K.; Hayakawa, I.; Uemura, D.; Chou, T.; Yamada, K.; Tsuji, T.; Yamaguchi, K.; Yazawa, K. Symposium Papers, 38th Symposium on the Chemistry of Natural Products **1996**, 79–84.
66. Kuramoto, M.; Arimoto, H.; Uemura, D. *J. Synth. Org. Chem. Jpn.* **2003**, *61*, 59–65.
67. Kuramoto, M.; Arimoto, H.; Uemura, D. *Mar. Drugs* **2004**, *1*, 39–54.

68. Kuramoto, M.; Hayashi, K.; Fujitani, Y.; Yamaguchi, K.; Tsuji, T.; Yamada, K.; Ijuin, Y.; Uemura, D. *Tetrahedron Lett.* **1997**, *38*, 5683–5686.
69. Kuramoto, M.; Hayashi, K.; Yamaguchi, K.; Yada, M.; Tsuji, T.; Uemura, D. *Bull. Chem. Soc. Jpn.* **1998**, *71*, 771–779.
70. Lepifre, F.; Clavier, S.; Bouyssou, P.; Coudert, D. *Tetrahedron* **2001**, *57*, 6969–6975.
71. Li, X.; Hewgley, J. B.; Mulrooney, C. A.; Yang, J.; Kozlowski, M. C. *J. Org. Chem.*, **2003**, *68*, 5500–5511.
72. Liebeskind, L. S.; Chidambaram, R. Nimkar, S.; Liotta, D. *Tetrahedron Lett.* **1990**, *31*, 3723–3726.
73. Ling, T.; Chowdhury, C.; Kramer, B. A.; Vong, B. G.; Palladino, M. A.; Theodorakis, E. A. *J. Org. Chem.* **2001**, *66*, 8843–8853.
74. Ling, T.; Kramer, B. A.; Palladino, M. A.; Theodorakis, E. A. *Org. Lett.* **2000**, *2*, 2073–2076.
75. Ma, S.; Zhang, J. *Tetrahedron Lett.* **2002**, *43*, 3435–3438.
76. Marinescu, S. C.; Nishimata, T.; Mohr, J. T.; Stoltz, B. M. *Org. Lett.* **2008**, *10*, 1039–1042.
77. Matsumoto, T.; Ohmura, T. *Chem. Lett.* **1977**, 335–338.
78. Matsumoto, T.; Usui, S. *Chem. Lett.* **1978**, 897–900.
79. Matsumoto, T.; Usui, S.; Morimoto, T. *Bull. Chem. Soc. Jpn.* **1977**, *50*, 1575–1579.
80. McFadden, R. M.; Stoltz, B. M. *J. Am. Chem. Soc.* **2006**, *128*, 7738–7739.
81. Miljkovic, M.; Hagel, P. *Carbohydr. Res.* **1983**, *111*, 319–324.
82. Mitsudome, T.; Umetani, T.; Nosaka, N.; Mori, K.; Mizugaki, T. Ebitani, K.; Kaneda, K. *Angew. Chem. Int. Ed.* **2006**, *45*, 481–485.
83. Miyashita, M. *Pure Appl. Chem.* **2007**, *79*, 651–665.

84. Miyashita, M.; Sasaki, M.; Hattori, I.; Sakai, M.; Tanino, K. *Science* **2004**, *305*, 495–499.
85. Moharram, S. M.; Hirai, G.; Koyama, K.; Oguri, H.; Hirama, M. *Tetrahedron Lett.* **2000**, *41*, 6669–6673.
86. Moharram, S. M.; Oguri, H.; Hirama, M. *Egypt. J. Pharm. Sci.* **2003**, *44*, 177–193.
87. Mohr, J. T.; Behenna, D. C.; Harned, A. M.; Stoltz, B. M. *Angew. Chem. Int. Ed.* **2005**, *44*, 6924–6927.
88. Mohr, J. T.; Nishimata, T.; Behenna, D. C.; Stoltz, B.M. *J. Am. Chem. Soc.* **2006**, *128*, 11348–11349.
89. Mohr, J. T.; Stoltz, B. M. *Chem. Asian J.* **2007**, *2*, 1476–1491.
90. Morgenlie, S. *Carbohydr. Res.* **1975**, *41*, 77–83.
91. Müller, S.; Liepold, B.; Roth, D.; Bestmann, H. J. *Synlett* **1996**, 521–522.
92. Müller, S.; Liepold, B.; Roth, D.; Bestmann, H. J. *Synthesis* **2004**, 59–62.
93. Murakata, M.; Tsutsui, H.; Hoshino, O. *Org. Lett.* **2001**, *3*, 299–302.
94. Nakamura, H.; Kawase, Y.; Maruyama, K.; Muria, A. *Bull. Chem. Soc. Jpn.* **1998**, *71*, 781–787.
95. Naqvi, S. M.; Horwitz, J. P.; Filler, R. *J. Am. Chem. Soc.* **1957**, *79*, 6283–6286.
96. Naqvi, S. M.; Horwitz, J. P.; Filler, R. *J. Am. Chem. Soc.* **1957**, *79*, 6283–6286.
97. Nielsen, T. E.; Le Quement, S.; Juhl, M.; Tanner, D. *Tetrahedron* **2005**, *61*, 8013–8024.
98. Nielsen, T. E.; Tanner, D. *J. Org. Chem.* **2002**, *67*, 6366–6371.
99. Okamoto, Y.; Yano, T. *Tetrahedron Lett.* **1971**, 4285–4287.
100. Ono, S.; Reimer, J. D.; Tsukahara, J. *Zool. Sci.* **2005**, *22*, 247–255.
101. Palucki, M.; Buchwald, S. L. *J. Am. Chem. Soc.* **1997**, *119*, 11108–11109.
102. Pinnick, H. W. *Org. React.* **1990**, *38*, 655–792.
103. R. E. Moore, P. J. Scheuer, *Science* **1971**, *172*, 495–498.

104. Rajamannar, T.; Balasubramanian, K. K. *J. Chem. Soc., Chem. Commun.* **1994**, 25-26.
105. Rivas, F.; Ghosh, S.; Theodorakis, E. A. *Tetrahedron Lett.* **2005**, 46, 5281-5284.
106. Roa, C. B.; Anjaneyula, A. S. R.; Sarma, N. S.; Venkateswarlu, Y. *J. Org. Chem.* **1985**, 50, 3757-3760.
107. Roa, C. B.; Anjaneyulu, A. S. R.; Sarma, N. S.; Venkateswarlu, Y.; Rosser, R. M.; Faulkner, D. J.; Chen, M. H. M.; Clardy, J. *J. Am. Chem. Soc.* **1984**, 106, 7983-7984.
108. Roa, C. B.; Roa, D. V.; Raju, V. S. N. *Heterocycles* **1989**, 28, 103-106.
109. Ryland, J. S. *Invert. Rep. Develop.* **1997**, 31, 177-188.
110. Saá, J. M.; Dopico, M.; Martorell, G.; García-Raso, A. G. *J. Org. Chem.* **1990**, 55, 991-995.
111. Sakai, M.; Sasaki, M.; Tanino, K.; Miyashita, M. *Tetrahedron Lett.* **2002**, 43, 1705-1708.
112. Satoh, T.; Ikeda, M.; Miura, M.; Nomura, M. *J. Org. Chem.*, **1997**, 62, 4877-4879.
113. Schmidt, C.; Thazhuthaveetil, *Can. J. Chem.* **1973**, 51, 3620-3624.
114. Sepcic, K.; Turk, T.; Macek, P. *Toxicon* **1998**, 36, 93-940.
115. Seto, M.; Roizen, J. L.; Stoltz, B. M. *Angew. Chem. Int. Ed.* **2008**, 47, 6873-6876.
116. Shigemori, H.; Sato, Y.; Kagata, T.; Kobayashi, J. *J. Nat. Prod.* **1999**, 62, 372-374.
117. Sibi, M. P.; Ji, J.; Sausker, J. B.; Jasperse, C. P. *J. Am. Chem. Soc.* **1999**, 121, 7517-7526.
118. Sibi, M. P.; Manyem, S. *Org. Lett.* **2002**, 4, 2929-2932.
119. Sinniger, F.; Montoya-Burgos, J. I.; Chevaldonné, P.; Pawlowski, J. *Mar. Biol.* **2005**, 147, 1121-1128.
120. Sonogashira, K.; Tohdo, Y.; Hagihara, N. *Tetrahedron Lett.* **1975**, 16, 4467-4470.
121. Srikanth, G. S. C.; Castle, S. L. *Tetrahedron* **2005**, 61, 10377-10441.

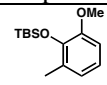
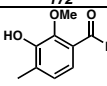
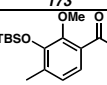
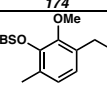
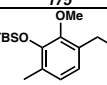
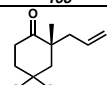
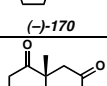
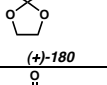
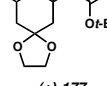
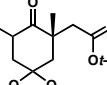
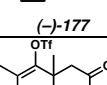
122. Starr, J. T.; Koch, G.; Carreira, E. M. *J. Am. Chem. Soc.* **2000**, *122*, 8793-8794.
123. Stevens, R. V.; Bisacchi, G. S. *J. Org. Chem.* **1982**, *47*, 2396-2399.
124. Stork, G.; Mook, R.; Biller, S. A.; Rychnovsky, S. D. *J. Am. Chem. Soc.* **1983**, *105*, 3741-3742.
125. Stork, G.; Sher, P. M. *J. Am. Chem. Soc.* **1983**, *105*, 6765-6766.
126. Sugano, N.; Koizumi, Y.; Oguri, H.; Kobayashi, S.; Yamashita, S.; Hiramama, M. *Chem. Asian J.* **2008**, *3*, 1549-1557.
127. Suh, E. M.; Kishi, Y. *J. Am. Chem. Soc.* **1994**, *116*, 11205-11206.
128. Suksamrarn, A.; Jankam, A.; Tarnchompoo, B.; Putchakarn, S. *J. Nat. Prod.* **2002**, *65*, 1194-1197.
129. T. J. Chambers, *J. Cell Sci.* **1982**, *57*, 247-260.
130. Tani, K.; Behenna, D. C.; McFadden, R. M.; Stoltz, B. M. *Org. Lett.* **2007**, *9*, 2529-2531.
131. Tanner, D.; Anderson, P. G.; Tedenborg, L.; Somfai, P. *Tetrahedron* **1994**, *50*, 9135-9144.
132. Tanner, D.; Tedenborg, L.; Somfai, P. *Acta Chem. Scand.* **1997**, *51*, 1217-1223.
133. Trench, R. K. *Pure Appl. Chem.* **1981**, *53*, 819-835.
134. Uemura, D. *Chem. Rec.* **2006**, *6*, 235-248.
135. Venkateswarlu, Y.; Reddy, N. S.; Ramesh, P.; Reddy, P. S.; Jamil, K. *Heterocyc. Commun.* **1998**, *4*, 575-580.
136. Villar, R. M.; Gil-Longo, J.; Daranas, A. H.; Souto, M. L.; Fernández, J. J.; Peixinho, S.; Barral, M. A.; Santafé, G.; Rodríguez, J.; Jiménez, C. *Bioorg. Med. Chem.* **2003**, *11*, 2301-2306.
137. Weiland, P.; Miescher, K. *Helv. Chim. Acta* **1950**, *33*, 2215-2228.
138. White, D. E.; Stewart, I. C.; Grubbs, R. H.; Stoltz, B. M. *J. Am. Chem. Soc.* **2008**, *130*, 810-811.

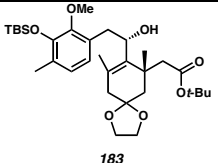
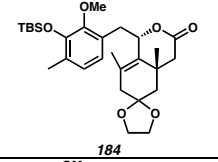
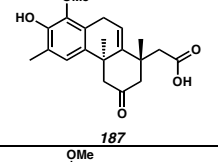
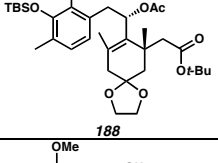
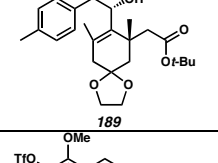
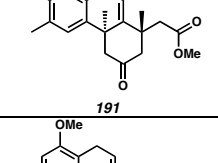
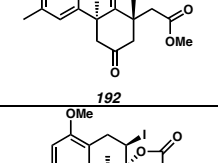
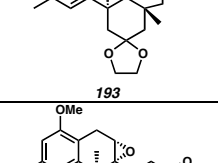
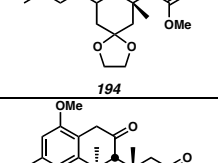
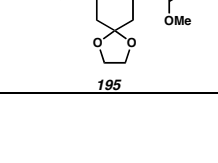
139. Williams, D. R.; Brugel, T. A. *Org. Lett.* **2000**, *2*, 1023–1026.
140. Williams, D. R.; Cortez, G. A. *Tetrahedron Lett.* **1998**, *39*, 2675–2678.
141. Williams, D. R.; Ihle, D. C.; Brugel, T. A.; Patanaik, S. *Heterocycles*, **2006**, *70*, 77–82.
142. Yamada, K.; Kuramoto, M.; Uemura, D. *Recent Res. Devel. Pure & App. Chem.* **1999**, *3*, 245–254.
143. Yamaguchi, K.; Yada, M.; Tsuji, T.; Kuramoto, M.; Uemura, D. *Biol. Pharm. Bull.* **1999**, *22*, 920–924.
144. Yang, Z.; Liu, H. B.; Lee, C. M.; Chang, H. M. Wong, H. N. C. *J. Org. Chem.* **1992**, *57*, 7248–7257.
145. Zhang, W. *Tetrahedron* **2001**, *57*, 7237–7262.

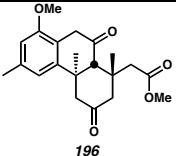
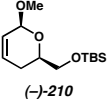
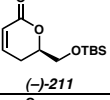
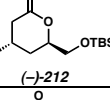
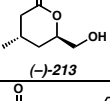
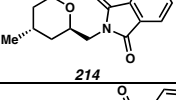
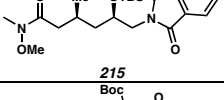
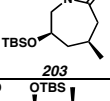
## NOTEBOOK CROSS-REFERENCES

The following notebook cross-references have been included to facilitate access to the original spectroscopic data obtained for the compounds presented in this thesis. For each compound, both hard copy and electronic versions of the original  $^1\text{H}$  NMR,  $^{13}\text{C}$  NMR,  $^{19}\text{F}$  NMR,  $^{31}\text{P}$  NMR, and IR spectra are stored in the Stoltz group archives.

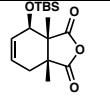
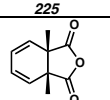
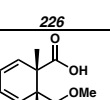
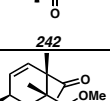
### *Compounds from Chapter 2 - Early Efforts Toward the Synthesis of Zoanthenol*

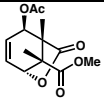
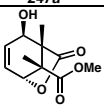
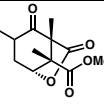
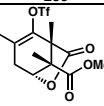
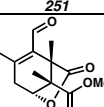
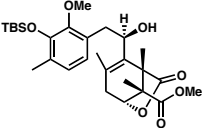
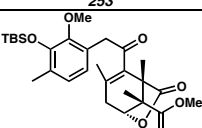
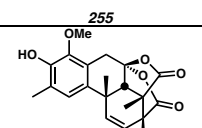
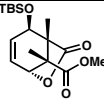
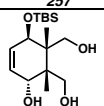
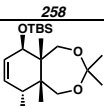
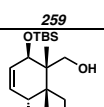
Compound	Procedure	$^1\text{H}$ NMR	$^{13}\text{C}$ NMR	IR
	DCBX_339	DCBXII_239_H	DCBXII_239_C	DCBXII_239
	DCBX_299	DCBXI_Benzaldehyde_H	DCBXI_Benzaldehyde_C	DCBXXVI_93_HighRf
	DCBX_299	DCBXXVI_93_LowRf_H	DCBXXVI_93_LowRf_C	DCBXXVI_93_LowRf
	DCBXXVIII_225	DCBXXVIII_225_H	DCBXXVIII_225_C	DCBXXVIII_225
	DCBXII_217	DCBXII_217_H	DCBXII_217_C	DCBXII_217
	DCBXXIII_97	DCBXXIII_97_H	DCBXXIII_97_C	DCBXXIII_97
	DCBXXV_101	DCBXXV_99_41_H	DCBXXV_99_C	DCBXXV_99
	DCBXXV_103	DCBXXV_103_HighRf_H	DCBXXV_103_HighRf_C	DCBXXV_103_HighRf
	DCBXXV_103	DCBXXV_103_LowRf_H	DCBXXV_103_LowRf_C	DCBXXV_103_LowRf
	DCBX_175	DCBXXVIII_235_H	DCBXXVIII_235_C	DCBXXVIII_235
	DCBXI_59	DCBXXVIII_237_H	DCBXXVIII_237_C	DCBXXVIII_237

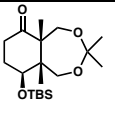
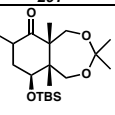
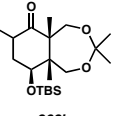
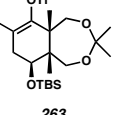
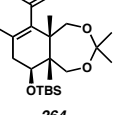
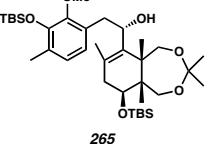
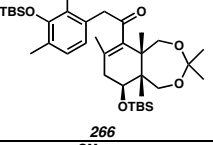
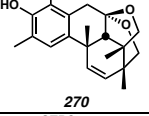
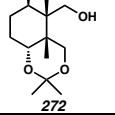
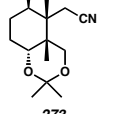
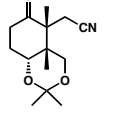
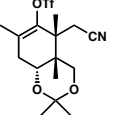
 <p>183</p>	DCBXI_67	BBG_Grignard_H	BBG_Grignard_Pdt_C	BBG_Grignard_Pdt
 <p>184</p>	DCBXXVIII_227	DCBXXVIII_227_H	DCBXXVIII_227_C	DCBXXVIII_227
 <p>187</p>	DCBXI_99	DCBXXVIII_241_H	DCBXXVIII_241_CD2CL2_C	DCBXXVIII_241
 <p>188</p>	DCBVII_189	DCBVII_189_H	DCBVII_189_C	DCBVII_189
 <p>189</p>	DCBX_281-285	DCBX_185_H	DCBX_185_C	DCBX_185
 <p>191</p>	DCBXII_93	DCBXXVIII_Tf_H	DCBXXVIII_Tf_C	DCBXXVIII_Tf
 <p>192</p>	DCBX_235	DCBVIII_115_H	DCBVIII_115_C	DCBVIII_115
 <p>193</p>	DCBVIII_223,227,231	DCBXXVIII_257_final_H	DCBXXVIII_257_C	DCBXXVIII_257
 <p>194</p>	DCBIX_69	DCBXXVIII_259_CDCl3_H	DCBXXVIII_259A_C	DCBXXVIII_259
 <p>195</p>	DCBIX_131	DCBXXVIII_261_H	DCBXXVIII_261_C	DCBXXVIII_261

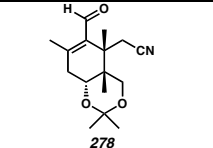
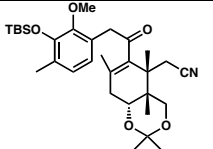
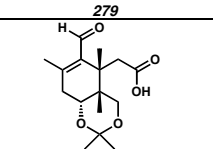
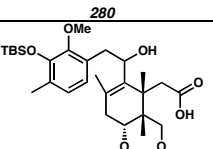
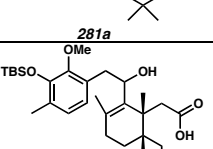
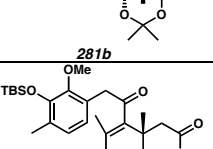
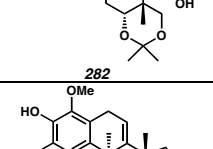
 196	DCBXXXVIII_269	DCBXXXVIII_269_H	DCBXXXVIII_269_C	DCBXXXVIII_269
 (-)-210	JTBIII_71	JTB-A-HNMR	JTB-A-CNMR	JTB-A-IR
 (-)-211	JTBI_289	JTB-B-HNMR	JTB-B-CNMR	JTB-B-IR
 (-)-212	JTBI_243	JTB-C-HNMR	JTB-C-CNMR	JTB-C-IR
 (-)-213	JTBIII_53	JTB-D-HNMR	JTB-D-CNMR	JTB-D-IR
 214	JTBIII_57	JTB-E-HNMR	JTB-E-CNMR	JTB-E-IR
 215	JTBI_227	JTB-F-HNMR	JTB-F-CNMR	JTB-F-IR
 203	JTBI_295	JTB-G-HNMR	JTB-G-CNMR	JTB-G-IR
 168	JTBIII_49	JTB-H-HNMR	JTB-H-CNMR	JTB-H-IR

*Compounds from Chapter 3 - Acid-Mediated Cyclization Approaches to the Densely Substituted Carbocyclic Core of Zoanthanol*

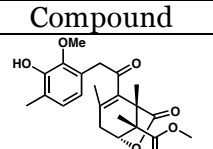
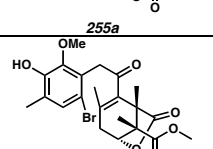
Compound	Procedure	<sup>1</sup> H NMR	<sup>13</sup> C NMR	IR
 225	DCBXXXVI-77	ThesisChar1_1Hredo	ThesisChar1_13C	ThesisChar1
 226	JLSIX_155	Diene_H	Diene_C	JLSX_295
 242	JLSXI_25	ThesisChar9_1H	ThesisChar9_13C	JLSVII_73
 247	JLSXI_27	JLSV_87_1	IodoLact_C	JLSV_153

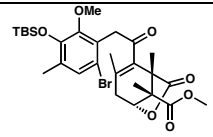
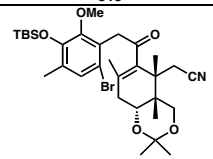
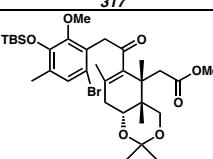
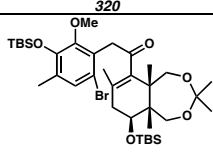
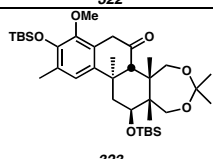
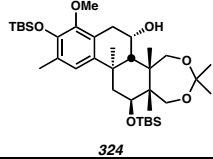
 247a	DCBXXVIII_14 3	ThesisChar2_1H	ThesisChar2_13C	ThesisChar2
 248	DCBXXVIII_15 1	ThesisChar3_1H	ThesisChar3_13C	ThesisChar3
 250	DCBXXVI_ 149	DCBXXVI_149_H	DCBXXVI_149_ C	DCBXXVI_149
 251	DCBXXVI_ 191	DCBXXVI_191_H	DCBXXVI_191_C	DCBXXVI_191
 252	DCBXXVI_ 199	DCBXXVI_199_H	DCBXXVI_199_ C	DCBXXVI_199
 253	DCBXXVI_ 147	DCBXXVI_101_2 4_H	DCBXXVI_147_ C	DCBXXVI_147
 255	DCBXXVI_ 189	DCBXXVI_189_H	DCBXXVI_189_ C	DCBXXVI_189
 256	DCBXXVI_ 193	DCBXXVI_193_H	DCBXXVI_193_ C	DCBXXVI_193
 257	JLSVIII_299	ThesisChar4_1H	ThesisChar4_13C	ThesisChar4
 258	JLSVIII_303	ThesisChar5_1H	ThesisChar5_13C	ThesisChar5
 259	JLSX_49	DCBXXVII_157_L S	JLSIX_47_2_C	JLSIX_47_2
 260	JLSX_49	DCBXXVII_161TS	JLSIX- 47_1_CDCL3_C	JLSIX-47_1

 261	DCBXXVII_215	JLSIX_25_1_H	JLSIX_25_1_C	JLSIX_25_1
 262a	DCBXXVII_225	DCBXXVII_225_HighRf_H	DCBXXVII_225_HighRf_C	DCBXXVII_225_HighRf
 262b	DCBXXVII_225	DCBXXVII_211_39	DCBXXVIII_33_LowRf_C	DCBXXVIII_33_LowRf
 263	DCBXXVII_219	DCBXXVII_243_SM_H	DCBXXVII_243_SM_C	DCBXXVII_243_SM
 264	DCBXXVIII_239	DCBXXVIII_51_H	DCBXXVIII_51_C	DCBXXVIII_51
 265	DCBXXVIII_243	DCBXXVIII_243_H	DCBXXVIII_243_C	DCBXXVIII_243
 266	DCBXXVIII_247	DCBXXVIII_95_H	DCBXXVIII_95_C	DCBXXVIII_95
 270	DCBXXVIII_99	DCBXXVIII_99_48_H	DCBXXVIII_99_48_C	DCBXXVIII_99_48
 272	JLSIX_213	ThesisChar6_1HRedo	ThesisChar6_13CRedo	ThesisChar6
 273	DCBXXVII_217	DCBXXVII_217_H	DCBXXVII_217_C	DCBXXVII_217
 274	JLSIX_105	DCBXXVII_145SM_H	DCBXXVII_145SM_C	DCBXXVII_145SM
 276	JLS IX_101 JLS IX_107	DCBXXVII_153C6D6_H	DCBXXVII_153C6D6_C	DCBXXVII_153

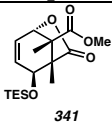
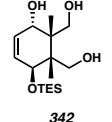
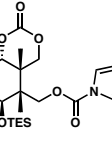
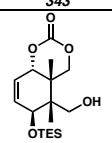
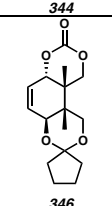
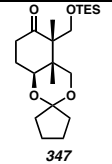
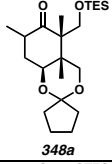
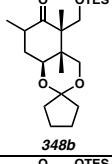
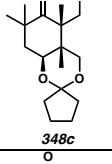
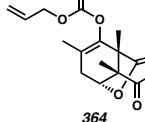
 278	JLSX_21 JLSIX_179	DCBXXVII_163_ H	DCBXXVII_163_ C	DCBXXVII_16 3
 279	JLSIX_193 JLSIX_211	DCBXXVIII_97_ H	DCBXXVIII_97_ C	DCBXXVIII_97
 280	JLSXVII71	JLSXVII71_1a_1H	JLSXVII71_1a_1 3C	JLSXVII71-1a
 281a	JLSXVII89	JLSXVII89_1_1H	JLSXVII89_1_13 C	JLSXVII89-1
 281b	JLSXVII75	JLSXVII75_2a_1 H	JLSXVII75_2a_1 3C	JLSXVII75-2a
 282	JLSXVII91	JLSXVII91_1_1H	JLSXVII91_1_13 C	JLSXVII91-1
 269	JLSXIII61	JLSXIII61_1_1H	JLSXIII61_1_13C	JLSXIII61-1

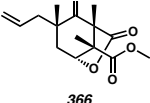
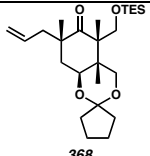
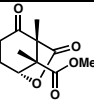
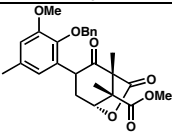
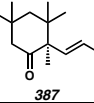
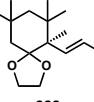
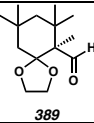
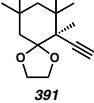
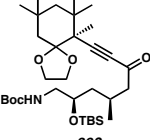
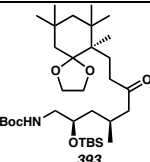
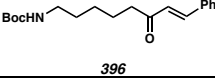
*Compounds from Chapter 4 – Radical Cyclization Approaches to the Tricyclic Core of Zoanthanol*

Compound	Procedure	<sup>1</sup> H NMR	<sup>13</sup> C NMR	IR
 255a	DCBXXVI_ 189	DCBXXVI_189_H	DCBXXVI_189_ C	DCBXXVI_189
 255b	JLSXVI115	JLSXVI115_2_1H	JLSXVI115_2_13 C	JLSXVI115b

 <p>315</p>	JLSXVI119	JLSXVI119_1_1H	JLSXVI119_1_13 C	JLSXVI119a
 <p>317</p>	JLSX_31 JLSX_121 JLSX_135	ThesisChar7_1Hb	ThesisChar7_13C	ThesisChar7
 <p>320</p>	JLSX299	JLSXVII 85_4b2_1H	JLSXVII 85_4b2_13C	JLSXVII85-4b2
 <p>322</p>	DCBXXVIII_ 251	DCBXXVIII_ 159_H	DCBXXVIII_ 159_C	DCBXXVIII_ 159
 <p>323</p>	DCBXXIX_49	DCBXXIX57_H	DCBXXVIII_ 255_C	DCBXXVIII_ 163_29B
 <p>324</p>	DCBXXIX_59	DCBXXIX_59_H	DCBXXIX_59_C	DCBXXIX_55

## Compounds from Appendix D – Current and Future Investigations Toward Zoanthol

Compound	Procedure	<sup>1</sup> H NMR	<sup>13</sup> C NMR	IR
 341	JLSXV303	JLSXV303-1_1H	JLSXV303_1_13C	JLSXV303a
 342	JLSVII39	JLSXV125-1_1H	JLSVII-39_13C	JLSVII39
 343	JLSXVII49	JLSXVII49-2_1H	JLSXVII49-2_13C	JLSXVII49-2
 344	JLSXV263	JLSXV263-1_1H	JLSXV263-1_13C	JLSXV263-1
 346	JLSXVII53	JLSXVII53-1_1H	JLSXVII53-1_13C	JLSXVII53-1
 347	JLSXV253	JLSXV253-1a_1H	JLSXV253-1a_13C	JLSXV253-1
 348a	JLSXVII45	JLSXVII45-1a3_1H	JLSXVII45-1a3_13C	JLSXVII45-1a3
 348b	JLSXVII45	JLSXVII45-2b3_1H	JLSXVII45-2b3_13C	JLSXVII45-2b3
 348c	JLSXVII45	JLSXVII45-1a_1H	JLSXVII45-1a_13C	JLSXVII45-1a
 364	JLSXVI159	JLSXVI159-1_1H	JLSXVI159-1_13C	JLSXVI159a

 365	TJ-I-263	TJ-PHOX-1H	TJ-PHOX-13C	TJ-I-263a
 366	JLSXVI147	JLSXVI147-1_1H	JLSXVI147-1_13C	JLSXVI147a
 368	JLSXVI231	JLSXVI231-1_1H	JLSXVI231-1_13C	JLSXVI231-1a
 379	AM-II-125	AM-II-125_1H	AM-II-125_13C	AM-II-125
 249	DCBXXVI_163	DCBXXVI_163_H	DCBXXVI_163_C	DCBXXVI_163
 380	AM-II-265	AM-II-265_prepTLC_1H	AM-II-265_prepTLC_13C	AM-II-265_prepTLC
 387	DCBXXV_31	DCBXXIV_249_19_H	DCBXXIV_249_19_C	DCBXXIV_249_19
 388	DCBXXV_39	DCBXXV_39_19_H	DCBXXV_39_19_C	DCBXXV_39
 389	DCBXXV_77	DCBXXV_77_37_H	DCBXXV_77_C	DCBXXV_77
 391	DCBXXV_79	DCBXXV_83_H	DCBXXV_83_C	DCBXXV_83
 392	DCBXXV_113	DCBChar11_H	DCBXXIX_Char11_C	DCBXXV_113
 393	DCBXXV_115	DCBthesisChar10_H	DCBthesisChar10_C	DCBXXIX_the sisChar10
 396	AM-I-199	AM-I-199_1H	AM-I-199_13C	AM-I-199

## ABOUT THE AUTHOR

Jenn Stockdill was born on the 17<sup>th</sup> of August, 1981 in Mankato, Minnesota to Dave and Lucy Stockdill. She was the youngest of three children, and as such benefited both from her parents' exhaustion and her siblings' guidance. The Stockdills moved to King George County, Virginia when Jenn was 2. When she was 5, they moved to Stafford County, where she then spent her formative years. Jenn spent her childhood exploring nature, and it is this background in combination with the (occasionally long-winded) descriptive answers that her parents gave to her questions that shaped her mind scientifically. The attraction to science became irreversible in eighth grade owing to an especially gifted teacher and family friend, M. A. Robinson.

After graduating from Stafford Senior High School, Jenn went to Virginia Polytechnic Institute and State University to pursue a degree in Chemistry. Ultimately, it was Richard Gandour's Organic Chemistry class that sealed Jenn's fate as an organic chemist. Professor Gandour's enthusiasm and rigorous teaching style led to a fantastic learning environment. After one term of organic chemistry, Jenn decided to conduct undergraduate research in the area with Professor Felicia Etzkorn. And just to be sure, she also spent a few summers working in a physical chemistry lab with Professor Alan Esker.

Upon completion of a Bachelor of Science degree at Virginia Tech, Jenn sought an increase in population density and moved to the California Institute of Technology to pursue her doctorate with Professor Brian Stoltz. She has spent the last five and half years there, working toward the total synthesis of the marine natural product zoanthenol. After her defense, Jenn will move to the Big Apple to conduct postdoctoral studies with Professor Sam Danishefsky at the Memorial Sloan-Kettering Cancer Center.